Ashok Vaseashta
Nimet Bölgen *Editors*

Electrospun Nanofibers

Principles, Technology and Novel Applications

Springer

Electrospun Nanofibers

Ashok Vaseashta · Nimet Bölgen
Editors

Electrospun Nanofibers

Principles, Technology and Novel Applications

Springer

Editors
Ashok Vaseashta
International Clean Water Institute
Manassas, VA, USA

Nimet Bölgen
Department of Chemical Engineering
Mersin University
Mersin, Turkey

ISBN 978-3-030-99957-5 ISBN 978-3-030-99958-2 (eBook)
https://doi.org/10.1007/978-3-030-99958-2

© The Editor(s) (if applicable) and The Author(s), under exclusive license to Springer Nature Switzerland AG 2022
This work is subject to copyright. All rights are solely and exclusively licensed by the Publisher, whether the whole or part of the material is concerned, specifically the rights of translation, reprinting, reuse of illustrations, recitation, broadcasting, reproduction on microfilms or in any other physical way, and transmission or information storage and retrieval, electronic adaptation, computer software, or by similar or dissimilar methodology now known or hereafter developed.
The use of general descriptive names, registered names, trademarks, service marks, etc. in this publication does not imply, even in the absence of a specific statement, that such names are exempt from the relevant protective laws and regulations and therefore free for general use.
The publisher, the authors, and the editors are safe to assume that the advice and information in this book are believed to be true and accurate at the date of publication. Neither the publisher nor the authors or the editors give a warranty, expressed or implied, with respect to the material contained herein or for any errors or omissions that may have been made. The publisher remains neutral with regard to jurisdictional claims in published maps and institutional affiliations.

Disclaimer: The opinions, recommendations, and propositions presented in various chapters represent the findings, views, and opinions of the authors and may not coincide with the position(s) of the editors. The editors do not promote, endorse, or express their dissent against any product and/or commercial entities mentioned in any of the chapters. Although due precautions are exercised before publication, the editors, however, do not take any responsibility for infringement by authors of any copyrighted material of either their own or copied from elsewhere.

This Springer imprint is published by the registered company Springer Nature Switzerland AG
The registered company address is: Gewerbestrasse 11, 6330 Cham, Switzerland

Foreword

One-dimensional nanomaterials in the form of nanofibers present a wide-ranging spectrum of research and commercial applications, due to their exceptional physicochemical properties and characteristics. These nanofibers with cross-sectional diameters ranging from tens to hundreds of manometers possess large surface area and surface area-to-volume ratio, form networks of highly porous mesh with remarkable interconnectivity between their pores, and high surface energy, thus making them scientifically interesting for a multitude of innovative applications. The nanofibers materials include natural polymers, synthetic polymers, carbon-based materials, semiconducting materials, and composite materials and can be produced by electrospinning—a versatile and promising method for the production of nanofibrous materials for a wide variety of applications in the biomedical and engineering area. Electrospinning has become a very efficient and specialized method to produce nanofibers with desired diameter and morphology, tunable characteristics, and with specific patterns and 3D structures.

The book *Electrospun Nanofibers—Principles, Technology, and Novel Applications* is a collection of chapters with up-to-date information, original research, reviews, and discussions by several authors from different parts of the world, presenting the development of electrospun materials, fundamental principles of electrospinning process, controlling parameters, electrospinning strategies, and electrospun nanofibrous structures with specific properties for applications in tissue engineering and regenerative medicine, textile, water treatment, sensor, and energy fields. With a strong focus on fundamental materials science and engineering, this book provides systematic and comprehensive coverage of the manufacture, properties, recent developments, applications, and future perspectives of electrospun materials.

Undoubtedly, this book addresses topics that are not only timely and relevant but will need to be revisited soon due to the fast-changing field of nanotechnology. In this respect, I foresee that the editors will be busy again in near future to prepare an updated version of this book in the coming years. This book is important to a wide, interdisciplinary variety of students and researchers involved in nanotechnology, nanoscience, advanced manufacturing, biomedical sciences, and related subjects, as well as to people in health care, industry, and pharmaceuticals. Many books have

been published in the past decade drawing attention to the topic of electrospinning; however, this edited book is a collection of articles from researchers, practitioners in the field, experts, and medical professionals that cover topics comprehensively for a broad readership. Such an approach in this field is refreshing, as it combines field knowledge with mathematics, modeling, process engineering, microbiology, physics, additive processing, and biomedical technology in a balanced way, providing theoretical and fundamental information to the extent required for the solution of practical problems, regularly demonstrated by one or more examples. This book will make a major contribution toward better addressing the subject to bridging the gap between science and technology and their real-world practical applications. This approach adopted in this book is surprisingly direct and transparent, and the knowledge is genuinely shared. The usefulness of this book to all stakeholders in the field is genuine, and it will be used by its intended audience and, even, may become compulsory, "must have", an item for the collection for nanoscience and nanotechnology scientists and professionals.

I am delighted to note that Prof. Dr. Acad. Ashok Vaseashta, whom I have known personally for many years and who also serves as Chaired Professor at the D. Ghitu Institute of Electronic Engineering and Nanotechnologies, Ministry of Education, Culture, and Research, for his admirable efforts to prepare this edited book, with his colleague Prof. Nimet Bölgen, Mersin University, Turkey. The book was subjected to comprehensive peer review, and consequently, the material in this book represents the type of interdisciplinary knowledge that is urgently needed to transfer it from the laboratory to real-world applications. I am delighted that the editors and authors have made such a tremendous effort to create this perfect book.

I wish everyone well and hope that you find this book interesting and useful.



January 2022

Prof. Dr. Acad. Anatoli Sidorenko
D. Ghitu Institute of Electronic Engineering
and Nanotechnologies
Ministry of Education, Culture, and Research
Chisinau, Republic of Moldova

Preface

The process of electrospinning is over a century old, as the first patent for this process was filed by J. F. Cooley in 1902. Anton Formhals filed the first patent on yarn fabrication using the electrospinning process in 1934, while around 1940, a commercial application of the electrospun fiber filter, known as the "Petryanov filter", was introduced in the, now, Russian Federation. Through the mid-1970s, there were several other notable achievements, including the first known application of electrospun fibers for wound dressing by Martin and Cockshott in 1974. The first recorded study of electrospun fibers as implantable vascular graft was reported in 1978, by Annis et al., which spurred additional momentum for many other biomedical applications. Resulting from new and innovative methodologies of fiber fabrication down to nanoscale by Darrell et al. in 1996, and later with the addition of nanomaterials in polymeric solutions, spurred a significant increase in research innovations in the field of electrospinning, especially in the last two decades.

One-dimensional nanomaterials in the form of nanofibers have a wide-ranging spectrum of research and commercial applications, due to their exceptional physicochemical properties and characteristics. These nanofibers with cross-sectional diameters ranging from tens to hundreds of nanometers possess high surface energy, large surface area, and surface area-to-volume ratio. Furthermore, they can form networks of highly porous mesh with remarkable interconnectivity between their pores, making them attractive for a multitude of innovative applications. The nanofibers materials include natural polymers, synthetic polymers, carbon-based materials, semiconducting materials, and composite materials. Many scientists working in the fields of physics and chemistry, as well as engineering, materials, polymers, biomedicine, pharmaceutics, food, environment, and textile, have contributed to many additional research applications of electrospinning. Many of such contributions of different disciplines and their complementarity were led by significant developments in the modification of the electrospinning process. Significant improvement has also been

achieved in the development of electrospun nanofibrous matrices, which includes tailoring compositions of polymers and active agents, surface functionalization with nanoparticles, and encapsulation of functional materials within the nanofibers.

This can be easily understood from the availability of a large number of books review and research articles published on electrospinning, especially in the last two decades. Electrospinning has received significant attention not only in the academic field but also at the commercial level in a variety of applications from biomedical to energy storage and other technologies such as defense and security, environmental, e-textile, automobile, aviation, and handicrafts. This book provides coverage of advancements in electrospinning technology, the latest applications of nanofibers in various fields, and emerging applications that can be used in advanced manufacturing combining electrospinning and 3D printing.

This book can broadly be divided into three parts: The first part comprises basic principles of electrospinning process, general requirements of electrospun materials, and advancement in electrospinning technology; the second part describes the applications of electrospun materials in different fields and future prospects, while the third part uses this technology as a springboard for advanced manufacturing, such as 3D printing. Hence, this book consists of chapters that cover topics ranging from fundamentals of electrospinning and advances in electrospun nanofiber technology to applications and a combination of electrospinning with advanced manufacturing. The book begins with a brief overview on the electrospinning technique, advancements in electrospinning technology, and functionalization routes to add nanofibers several features for a wide variety of applications (Bölgen et al.). Fabrication of multifunctional electrospun structures by multi-axial electrospinning methods and side-by-side electrospinning for preparing multifunctional and more complex fibers and their implementation in different applications are discussed (Okan et al.). In another chapter, the progress of solvent-free electrospinning, which provides an eco-friendly process, is comprehensively summarized (Long et al.). An extrusion-based advanced manufacturing technique, melt electrospinning writing, its process parameters, and challenges/limitations are described in the following chapter (Aytac, Wang). One of the chapters focuses on the co-electrohydrodynamic forming of hollow polymeric materials by electrospinning and their use as test objects for diffusion magnetic resonance imaging by mimicking the microstructure of tissues (Zhou, Parker). As there is growing interest in the scientific community among researchers and readers, one of the chapters describes a combination of electrospinning and microfluidic spinning and hybrid technologies engineered by the integration of electrospun fibers within a microfluidic chip (Neves et al.). Several applications of electrospun materials were discussed in this book, including drug delivery, wound dressing, tissue engineering, wastewater treatment, energy storage, food packaging, sensing and detection, and catalysis, to name a few. In the current COVID-19 pandemic, many regulatory authorities recommended using face masks for the general public to avoid spreading the

respiratory droplets. In one of the chapters of this book, the role of electrospun fibers in protective facemasks has been highlighted (Abid et al.). Also covered in this book is the description of applications that can be used in advanced manufacturing based on conjoining electrospinning and 3D printing, and three chapters are devoted to using electrospinning in conjunction with 3D printing. One of the chapters highlights electrospinning and 3D printing in bio-fabrication (Ashammakhi et al.), while a chapter discusses hierarchical integration of 3D printing and electrospinning for rapid prototyping (Vaseashta et al.). As the versatility grows, the use of handheld electrospinning, especially for medical applications, appears attractive (Long et al.). Despite all the advancements in the electrospinning area, there are still challenges to be addressed and overcome for nanofiber technology to move toward technology maturation and readiness level.

This book is expected to serve as a valuable resource for students, lecturers, scientists, and engineers to broaden their knowledge in the field of electrospun nanofiber fabrication, advancements, and applications. We envision that this book will serve as a platform to identify further progress in the development of nanofiber synthesis strategies and identification of new and innovative applications of nanofibers to move this field beyond its current state. Hence, a vast spectrum of synthesis techniques, applications aspects, and projection toward advanced manufacturing renders this book quite useful to a vast readership. The book is oriented toward researchers, students, and scientists and may serve not only as a reference but also for their class instructions and hence will be a valuable resource for materials scientists, engineers, postgraduate students, and industry professionals wishing to broaden their knowledge in the field of electrospun nanofibers, applications in different fields, and advancing the technology for advanced manufacturing. The contents will also be useful for courses, such as nanoscience and nanomaterials, biomedical sciences, water sciences, environmental sciences, and materials synthesis and characterization. The editors acknowledge excellent contributions from several scientists, technologists, and medical practitioners for their chapters. We hope that information provided by the authors in this book guides them for their research, new discoveries, and many directions, yet undiscovered.

We express our deep appreciation for the reviewers, who provided comments to ensure novelty, accuracy, and continuity of chapters. Our deep appreciation is also toward the publishers, especially to Ms. Annelies Kersbergen and Dr. Christoph Bauman for their constant support, response to questions, and encouragement. We deeply appreciate the help and coordination of Dr. Didem Demir. Of course, every endeavor of preparing any book takes a lot of time away from our families and pets.

One of the editors (AV) owes a lot of missed playtime to his pet dog Isabella—an avid frisbee and ballplayer.

Prof. Dr. Acad. Ashok Vaseashta
International Clean Water Institute
Manassas, VA, USA

Faculty of Civil Engineering
Universitatea Transilvania din Braşov
Braşov, Romania

D. Ghitu Institute of Electronic Engineering
and Nanotechnologies
Ministry of Education, Culture, and Research, Academy
of Sciences of Moldova
Chisinau, Republic of Moldova

Prof. Dr. Nimet Bölgen
Biomaterials, Nanofibers, and Tissue Engineering Laboratory
Department of Chemical Engineering, Faculty of Engineering
Institute of Medical Sciences
Mersin University
Mersin, Turkey

Contents

Part I Fundamentals of Electrospinning

1 Introduction and Fundamentals of Electrospinning 3
Nimet Bölgen, Didem Demir, Müge Aşık, Burcu Sakım, and Ashok Vaseashta

2 Fabrication Methodologies of Multi-layered and Multi-functional Electrospun Structures by Co-axial and Multi-axial Electrospinning Techniques 35
Marjan Hezarkhani, Nargiz Aliyeva, Yusuf Ziya Menceloglu, and Burcu Saner Okan

3 Solvent-Free Electrospinning—Application in Wound Dressing 67
Yun-Ze Long, Jun Zhang, Xiao-Fei Liu, Zhong Liu, Miao Yu, and Seeram Ramakrishna

4 Melt Electrospinning Writing 93
Zeynep Aytac and Xinzhu Wang

5 Co-electrohydrodynamic Forming of Biomimetic Polymer Materials for Diffusion Magnetic Resonance Imaging 121
Feng-Lei Zhou and Geoff J. M. Parker

6 Polysuccinimide and Polyaspartamide for Functional Fibers: Synthesis, Characterization, and Properties 135
Kristof Molnar, Eniko Krisch, and Judit E. Puskas

Part II Applications of Electrospun Nanofibers

7 Electrospun Fibers in Drug Delivery 159
V. Umayangana Godakanda, Karolina Dziemidowicz, Rohini M. de Silva, K. M. Nalin de Silva, and Gareth R. Williams

8 Suitability of Electrospun Nanofibers for Specialized Biomedical Applications 183
Havva Başkan and Hale Karakaş

9 Biopolymeric Electrospun Nanofibers for Wound Dressings in Diabetic Patients 207
Paola I. Campa-Siqueiros, Maria M. Castillo-Ortega, Jaime López-Cervantes, Jesús Fernando Ayala-Zavala, David Servin de la Mora-López, and Tomas J. Madera-Santana

10 Biomedical Applications of Fibers Produced by Electrospinning, Microfluidic Spinning and Combinations of Both 251
Filipa Vasconcelos, Rui L. Reis, Albino Martins, and Nuno M. Neves

11 Multifunctional Wound Dressings Based on Electrospun Nanofibers 297
Kelcilene B. R. Teodoro, Danilo M. Santos, Camilo A. S. Ballesteros, Paulo A. M. Chagas, Vittor P. V. Costa, Rodrigo Schneider, and Daniel S. Correa

12 Incorporating Poorly Soluble Drugs into Electrospun Nanofibers for Improved Solubility and Dissolution Profile 331
Taha Umair Wani, Taseen Aamir Wani, Anjum Hamid Rather, Rumysa Saleem Khan, Mushtaq A. Beigh, and Faheem A. Sheikh

13 Electrospun Nanofibers based Electrodes and Electrolytes for Supercapacitors 351
Dheeraj Kumar Maurya and Subramania Angaiah

14 Energy Harvesting Solutions Based on Piezoelectric Textiles Structures from Macro Nano Approach 391
Zhongchen He, Elham Mohsenzadeh, François Rault, Maryline Lewandowski, and Fabien Salaün

15 Morphological and Mechanical Properties of Electrospun Polyurethane Nanofibers—Air-Filtering Application 417
Parian Mohamadi, Elham Mohsenzadeh, Cedric Cochrane, and Vladan Koncar

16 Electrospun Polymeric Nanofibers: An Innovative Application for Preservation of Fruits and Vegetables 451
Juliana Botelho Moreira, Jorge Alberto Vieira Costa, Michele Greque de Morais, and Eliezer Avila Gandra

17 Encapsulation of Bioactive Compounds in Electrospun Nanofibers for Food Packaging 473
Michele Greque de Morais, Suelen Goettems Kuntzler, Ana Claudia Araujo de Almeida, Ana Gabrielle Pires Alvarenga, and Jorge Alberto Vieira Costa

18 Application of Electrospun Polyaniline (PANI) Based Composites Nanofibers for Sensing and Detection 491
Nayana D. Sonwane, Sanchit S. Kondawar, Pitambar V. Gayakwad, and Subhash B. Kondawar

19 Protective Facemask Made of Electrospun Fibers 519
Sonia Javed, Misbah Hameed, Ahsan Nazir, Tanveer Hussain, Nabyl Khenoussi, and Sharjeel Abid

Part III Advanced Manufacturing

20 Electrospinning and Three-Dimensional (3D) Printing for Biofabrication 555
Nureddin Ashammakhi, Maryam Tavafoghi, Arman Jafari, Sumama Nuthana Kalva, Robin Augustine, Anwarul Hasan, Houman Savoji, Yavuz Nuri Ertas, and Song Li

21 Application of Hand-Held Electrospinning Devices in Medicine 605
Yun-Ze Long, Jun Zhang, Zhong Liu, Bing-Chang Wang, Miao Yu, and Seeram Ramakrishna

22 Hierarchical Integration of 3D Printing and Electrospinning of Nanofibers for Rapid Prototyping 631
Ashok Vaseashta, Didem Demir, Burcu Sakım, Müge Aşık, and Nimet Bölgen

23 Integration of Electrospinning and 3D Printing Technology 657
Zhaoxu Zhang, Wei Zhang, Xiaoli Peng, Xindan Zhang, Yunpeng Wang, Bing Yu, Ming Tian, Liqun Zhang, Jiajia Xue, and Yunqian Dai

24 Electrospun Nanofibers for Industrial and Energy Applications 693
Narayanan Vimalasruthi, Ganesan Vigneshkumar, Shanmugasundaran Esakkimuthu, Krishnamoorthy Sivakumar, and Thambusamy Stalin

25 Electrospun Nanofibers for Energy Harvesting 721
Mina Abbasipour and Ramin Khajavi

26 Development of Micro/Nano Channels Using Electrospinning for Neural Differentiation of Cells 737
Zahra Hesari

Author Index 761

Subject Index 763

About the Editors



Prof. Dr. Ashok Vaseashta is CEO/CTO and Executive Director for research with the International Clean Water Institute in Virginia, USA. He also serves as Professor at Riga Technical University, Chaired Professor of Nanotechnology at the Academy of Sciences of Moldova, Academician at Euro-Mediterranean Academy of Arts and Sciences, and Senior Strategic Research Advisor for several organizations. Inspired by nature and guided by societal necessities, he strives for technological innovations to address the global challenges of the twenty-first century. His research interests include CBRN defense, critical infrastructure safety and security, and environmental sustainability—all using nexus of advanced technological solution platforms. He is a scholar, visionary, strategist, and dedicated futurist providing strategic leadership to promote and advance research initiatives and priorities using data-driven decisions. He received Ph.D. from the Virginia Polytechnic Institute and State University, Blacksburg, VA, in 1990 followed by Kobe postdoctoral fellowship. Following his Ph.D., he served as Professor and Researcher at Virginia Tech and Marshall University. He also served as Director of Research at the Institute for Advanced Sciences Convergence and International Clean Water Institute for Norwich University Applied Research Institutes, Vice-Provost (Rector) for Research in South Carolina, Visiting Professor at the 3 Nano-SAE Research Center, University of Bucharest, Romania, and Visiting Scientist at the Helen and Martin Kimmel Center of Nanoscale Science at the Weizmann Institute of Science, Israel. He served

the U.S. Department of State in two rotations, as Strategic S&T Advisor in the Bureau of International Security and Nonproliferation, Office of Weapons of Mass Destruction and Terrorism, and US Diplomat. His research interests span foresight, nanotechnology, environmental/ecological science, and critical infrastructure safety and security. He is Author/Editor of 13 books and has published over 300 articles in scientific journals, chapters, and conferences. He serves on editorial boards of several international journals and is an active member of various professional organizations.



Prof. Dr. Nimet Bölgen received B.S. degree in Chemical Engineering at Ankara University, Turkey, in 2002, and M.S. degree in Chemical Engineering at Hacettepe University, Turkey, in 2004. She received Ph.D. degree in Bioengineering at Hacettepe University, Turkey, in 2008. She was Visiting Scientist at Sabancı University, Turkey; Lund University, Sweden; Institute of Polymer Science and Technology, Spain; and Keele University, UK. She has been working at Chemical Engineering Department, Mersin University, Turkey, since 2009. She is Author of 13 chapters, 45 articles, and more than 100 proceedings. Her research is focused on the development of biomaterials for tissue engineering and regenerative medicine, drug delivery systems from natural and synthetic polymers, cryogels, and electrospun nanofibers for biomedical applications.

Symbols and Abbreviations

$(BA)_3$	Benzoic acid
AgNPs	Silver nanoparticles
$Al(NO_3)_3$	Aluminum nitrate
AUC	Area under plasma drug concentration–time curve
CA	Cellulose acetate
CAD	Computer-aided design
CF	Carbon fiber
CIP	Ciprofloxacin
Cisplatin	Cis-diammineplatinum (II) dichloride
CNT	Carbon nanotubes
CSA	Camphoric acid
DCM DMAc	Dichloromethane N,N-dimethylacetamide
DFT	Density function theory
DLP	Digital light processing
DMF	Dimethylformamide
DSC	Differential scanning calorimetry
EC	Ethyl cellulose
EDS	Energy dispersive X-ray spectrometry
Fe_3O_4	Iron oxide
FePt	Iron–platinum
FIB-FESEM	Focused ion beam–field emission scanning electron microscopy
FTIR	Fourier transform infrared
g/mL	Gram/milliliter
GNP	Graphene nanoplatelet
GO	Graphene oxide
HFP	Hexafluoro-2-propanaol
HPLC	High performance liquid chromatography
KET	Ketoprofen
MD	Molecular dynamics
Mn_3O_4	Manganese oxide
$MnCl_2$	Manganese chloride

MPa	Mega pascal
mV/s	Millivolts/second
NMMO.H_2O	N-methylmorpholine N-oxide
P(VDF-HFP)	Poly (vinylidene fluoride-cohexafluoropropylene)
P(VDF-TrFE)	Poly(vinylidene fluoride-trifluroethylene)
PA11	Polyamide 11
PAAm	Polyacrylamide
PAN	Polyacrylonitrile
PANI	Polyaniline
PBA	Polybenzoxazine
PCL	Poly(ε-caprolactone)
PCL	Polycaprolactone
PDMAEMA	Poly(dimethylaminoethyl methacrylate)
PDMS	Polydimethylsiloxane
PDT	Poly(dodecylthiophene)
PEDOT	Poly(3,4-ethyl-enedioxythiophene)
PEO	Poly(ethylene oxide)
PET	Polyethylene terephthalate
PFM	Piezoresponse force microscopy
Phen	1,10-phenanthroline
PI	Polyimide
PLA	Poly(lactic) acid
PLA	Polylactic acid
PLG	Poly(d,l-lactide-co-glycolide)
PLGA	Poly (DL-lactide-co-glycolide)
PLGA	Poly(lactic-co-glycolic acid)
PMAA	Poly(methacrylic acid)
PMMA	Poly(methyl methacrylate)
PP	Polypropylene
PPy	Polypyrrole
PS	Polystyrene
PSS	Poly(styrene sulfonate)
PSU	Polysulfone
PTA	Polythioaniline
PU	Polyurethane
PUMVS	Poly(ureamethylvinyl)silazane
PVA	Polyvinyl alcohol
PVC	Polyvinyl chloride
PVDF	Poly(vinylidene fluoride)
PVP	Polyvinylpyrrolidone
SARS-nCOV2	Severe acute respiratory syndrome novel coronavirus 2
SBS	Styrene–butadiene–styrene
SEM	Scanning electron microscopy
SHM	Structural health monitoring
$SnCl_2 \cdot 2H_2O$	Stannous chloride dihydrate

SnO_2	Stannic oxide
SOF	System on fiber
TEGO	Thermally exfoliated graphene oxide
TEM	Transmission electron microscopy
TFE	Trifluoroethanol
THF	Tetrahydrofuran
$Ti(OBu)_4$	Titanium butoxide
$Ti(OiPr)_4$	Titanium isopropoxide
TiO_2	Titanium oxide
TPU	Thermoplastic polyurethane
UV–vis	Ultraviolet–visible
$V(acac)_3$	Vanadium(III) acetylacetonate
XRD	X-ray diffraction

Part I
Fundamentals of Electrospinning

Chapter 1
Introduction and Fundamentals of Electrospinning



Nimet Bölgen, Didem Demir, Müge Aşık, Burcu Sakım, and Ashok Vaseashta

Abstract Electrospinning is an effective and versatile technique used to produce continuous fibers from submicron down to nanometer diameters. The produced nanofibers from polymer solutions or melts have been a focus of interest as they have many potential applications in energy conversion and storage, environmental, biomedical, and pharmacological area. In addition, new application areas are created by functionalizing the produced nanofibers with different features as antimicrobial, conductive, responsive to stimulus, and biomimetic properties. Conventional electrospinning setup can be modified for large-scale and continuous production by integration with developing technologies. In this chapter, firstly, history, process theory, and basic principles of electrospinning are summarized. Then, the latest developed technologies related to electrospinning, functionalization routes to add superior features to the nanofibrous materials, and remarkable application areas of electrospun nanofibers are presented. Finally, future trends in the electrospinning area are discussed.

N. Bölgen (✉) · D. Demir · M. Aşık · B. Sakım
Chemical Engineering Department, Engineering Faculty, Mersin University, 33343 Mersin, Turkey
e-mail: nimet@mersin.edu.tr

D. Demir
e-mail: didemdemir@tarsus.edu.tr

M. Aşık
e-mail: 1702120171002@mersin.edu.tr

B. Sakım
e-mail: 1902120171002@mersin.edu.tr

D. Demir
Department of Chemistry and Chemical Process Technologies, Vocational School of Technical Sciences at Mersin Tarsus Organized Industrial Zone, Tarsus University, 33100 Mersin, Turkey

A. Vaseashta
International Clean Water Institute, Manassas, VA, USA
e-mail: prof.vaseashta@ieee.org

Faculty of Civil Engineering, Transylvania University of Brasov, Brasov, Romania

© The Author(s), under exclusive license to Springer Nature Switzerland AG 2022

A. Vaseashta and N. Bölgen (eds.), *Electrospun Nanofibers*,
https://doi.org/10.1007/978-3-030-99958-2_1

Keywords Electrospinning · Modified techniques · Electrospun nanofibers · Functional nanofibers · Application areas

1.1 Historical Background of the Electrospinning Process

One-dimensional nanostructures including wires, ribbons, tubes, belts, filaments, rings, and fibers are new-generation materials that have attracted great attention in the scientific field as the most promising building blocks for applications in different areas. Among these materials, fibers have been involved in numerous studies and applications due to their unique features such as lightness, porosity, large surface area, high functionality, mechanical strength, and superior electrical properties. Different methods based on electrostatic and mechanical forces such as two-component extrusion, self-assembly, template synthesis, thermally induced phase separation, melt blowing, drawing, electrospinning, and centrifugal spinning can be used for the production of nanofibers [1]. Electrospinning, also called electrostatic spinning, is a process in which the electrostatic force is used for the formation of fibers, is the simplest and the only method of choice for the large-scale preparation over other available methods. In general, the fibers manufactured via electrospinning are defined as cylindrical structures, with typical cross-sectional dimensions that can be ranged from 1 nm to 1 μm. The approach of electrospinning enables the creation of fibers with continuous length, tunable diameter, aligned direction, diverse and controllable composition by changing the electrospinning conditions. In addition, the fibers can be generated from different polymer solutions or melts, and hence have different physical properties and application potentials.

As shown in Fig. 1.1, almost 24,400 scientific documents, including conference papers, articles, reviews, and book chapters, on electrospun nanofibers have been published and continue to be published at an increasing rate over the past years. Over the course of nearly 20 years, this versatile synthesis technique has been applied in a wide variety of research areas, including energy conversion and storage, environmental, biomedical, and pharmacology applications.

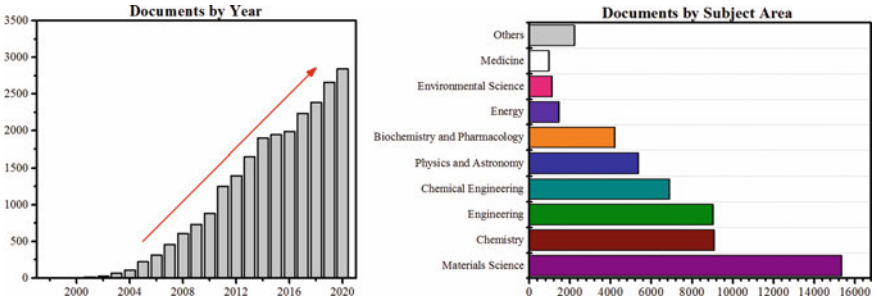


Fig. 1.1 The number of documents and their subject area related to electrospun nanofibers published in Scopus-indexed scientific sources from 2000 to 2020

The motion of a liquid under an electrostatic field, which is the basis of the electrospinning method, was first observed by William Gilbert in 1600s. Charles Vernon Boys described the production of nanofibers in an article published in 1887. It was patented by John Francis Cooley in 1900 and the electrospinning process continued to be used in the production of a series of artificial fibers throughout the nineteenth century [2]. The theoretical foundation of electrospinning began between 1964 and 1969 by Sir Geoffrey Ingram Taylor, when he mathematically modeled the shape of a (Taylor) cone formed by a liquid droplet under the influence of an electric field. Subsequently, in the early 1990s, electrospun nanofibers were demonstrated by some research groups, and Reneker (known as the person who popularized the name electrospinning) [2, 3]. Since then, the number of investigations on electrospinning has been growing exponentially every year.

1.2 Micro and Nanofibers Produced by Electrospinning

The electrospinning method is the only method that allows continuous fiber production with many different lengths and diameter (micro or nano) sizes. Both micro/nanofibers produced by electrospinning generally show solid interior and smooth surface properties. The traditional setup used has been modified in various ways to be able to control the electrospinning process and specifically to adapt the structure of the micro/nanofibers. Moreover, by changing parameters including solution properties (viscosity and solvent type) and process variables (flow rate, the internal needle diameter, the distance from the needle to the collector, and the applied voltage) fibers with different diameters can be produced. Fibers with ultra-fine diameters are very interesting both from a technological and scientific point of view. It is possible to produce nano-sized thin films by electrospinning, and in one of the studies, ultra-thin nanofibers with a diameter of 1.6 nm have successfully been produced at low polymer concentrations, by using Nylon-4,6. In that study, it has been found that the concentration of polymer solution is the main factor influencing the fiber diameter [4].

Current studies include the preparation of fibers with sub-nanometer diameter from inorganic materials and the investigation of their properties. Besides, there are few reports on the production of fibers with sub-nanometer diameter using organic polymers. These fibers, produced in sub-nanometer diameters, are consist of only a single polymer chain. Jian et al. prepared polyamic acid (PAA) fibers with diameters ranging from hundreds of nanometers to sub-nanometers by electrospinning. The morphologies of the electrospun ultrafine nanofibers were demonstrated by microscopic images as shown in TEM images in Fig. 1.2. They showed for the first time that a sub-nanometer fiber of about 0.17–0.63 nm, containing only one molecular chain, was produced by electrospinning from ultra-dilute PAA solutions [5].

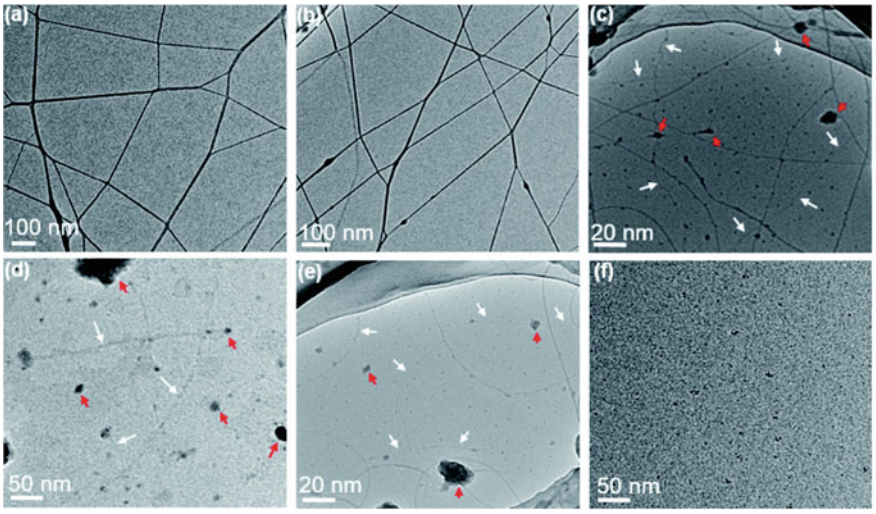


Fig. 1.2 TEM images of PAA nanofibers obtained from PAA solutions with different concentrations of 0.5 (**a**), 0.3 (**b**), 0.1 (**c**), 0.06 (**d**), 0.03 (**e**) and 0.02 (**f**) (wt%). White arrows indicate the sub-nanometer fibers and red arrows indicate the polymer droplets

1.3 Basic Apparatus of Electrospinning and Recent Advances in Manufacturing Techniques

To understand the electrospinning technique, it is necessary to investigate the basic equipment and the mechanism behind the process. This technology is based on the creation of fibers that are reduced in diameter down to nano-size by pulling a polymer-based solution under electrical force. The required experimental setup is very simple and accessible. It consists of a pump to feed the solution placed in a needle tip syringe, a grounding conductive collector, and a high-voltage power supply as basically illustrated in Fig. 1.3 [6]. As a result of the high voltage applied during the electrospinning process, the polymer solution droplet at the needle tip is deformed into a cone shape called the "Taylor cone" under electrostatic forces [7].

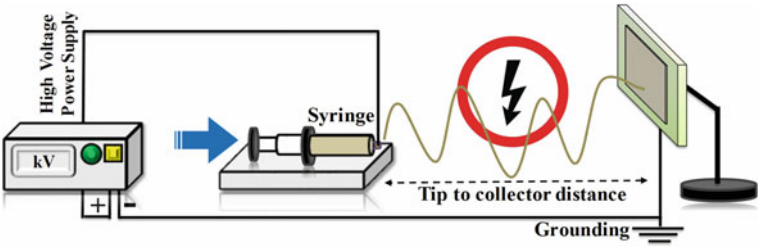


Fig. 1.3 Schematic diagram of an electrospinning process with basic apparatus

Under this strong electrostatic field force, which is the driving force to initiate the electrospinning process, the charged solution jet at the tip of the needle changes its size to maintain force balance. With increasing electrostatic field density, induction charges on the surface repel each other and generate shear stresses. These repulsive forces act in the opposite direction of the surface tension, causing the solution to expand towards a Taylor cone. When the electrostatic field reaches the critical voltage value, the driving forces are out of balance and thus a charged jet is ejected from the tip of the cone droplet. The fibers elongated by the jetting of the jet are deposited on the collector as solid ultrafine fibers after evaporation of the solvent. A thin nonwoven film with a fibrous structure is formed by the continuous accumulation of fibers on the collector [8].

With the advancing technology and increasing demand, besides the traditional electrospinning method presented above, many special techniques have been developed that can serve to manufacture fibers with different properties in large quantities. This greatly enriches the production of electrospun fibers and expands the application range of electrospun fibers. In the following sections, the latest designs of electrospinning setups developed by modification of collectors and spinnerets will be discussed.

1.3.1 Melt Electrospinning

In the electrospinning process, fiber production can be achieved by using polymer solutions as well as polymer melts. This technology, called melt electrospinning, is an important branch of electrospinning that prevents the occurrence of disadvantages such as low mechanical strength, low density, and potential environmental pollution that can be caused by the solvents used in the preparation of polymer solutions. Moreover, the method makes it possible to produce nanofibers from polyolefins that do not have a suitable solvent at room temperature (polyethylene and polypropylene) or from multicomponent polymer blends in which it is difficult to find a common solvent [9, 10]. The most important factor limiting the application of this method is that the fibers obtained have larger diameters compared to the fibers produced in solution electrospinning. Therefore, studies with melt electrospinning have been limited [11].

In melt electrospinning, the polymer is melted using a heating assembly to obtain a suitable viscosity for electrospinning (Fig. 1.4a). The heating assembly as a reservoir for molten polymer can be created using various sources such as heating elements, heating guns, laser heating, and ultrasound heating [9]. Similar to solution electrospinning, a high voltage is applied between the polymer and the collector. The melt starts to be pushed to a spinneret. The applied charge overcomes the surface tension of the suspended drop and the molten jet is diverted to the collector. Finally, the polymeric fibers deposited in the collector are formed as a result of the solidification of the polymer melt after cooling [12]. Recent studies demonstrated the manufacturability of single- or multi-layer fibers with high surface area using melt electrospinning.

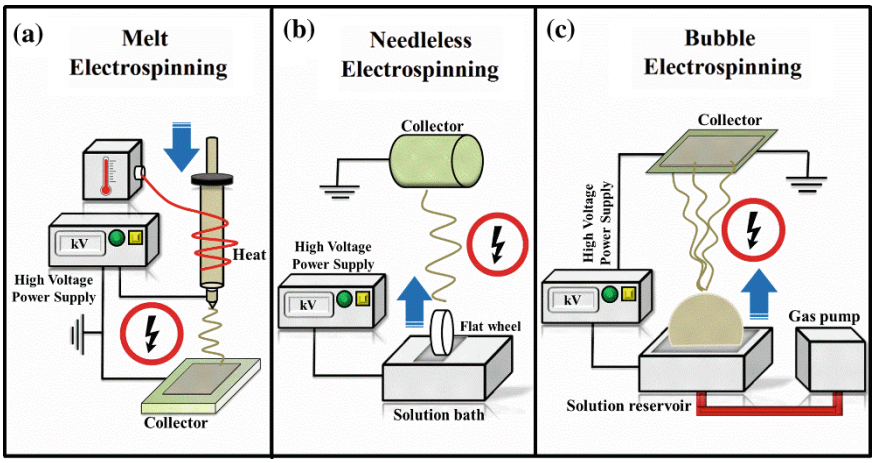


Fig. 1.4 Basic set-up illustrations of some types of electrospinning. **a** Melt electrospinning, **b** needleless electrospinning and **c** bubble electrospinning

The prepared fibers can have potential applications in many areas such as membrane filtration, sensors, solar and fuel cells for energy storage, enzyme carriers for biological processes, catalyst carriers for chemical reactions, drug release, wound healing, tissue engineering, and sound absorbers [13].

1.3.2 Needleless Electrospinning

When using conventional needle electrospinning, nanofibers are produced at low production rates (typically less than 0.3 g/h). This situation prevents commercialization by the inability to provide high quantities and rapid production [14, 15]. Needleless electrospinning has emerged with the need for efficient, continuous, and high mass production of fibers, especially for industrial production. The spinning process as shown in Fig. 1.4b can be summarized as follows: The set-up consists of a solution bath/reservoir with a disc (flat wheel) placed inside, a high-voltage power supply, and a collector. With the rotation of the disc, a thin layer of the polymer solution is loaded onto the disc surface and as a result of this rotation conical spikes are created on the surface of the solution layer. When high voltage is applied, the liquid around the spikes is attracted and Taylor cones are formed. Once the electric force is large enough, these fine solution jets exit the ends of the Taylor cones and deposit on the collector plate.

The first needleless electrospinning system using a ring as the spinneret was patented in 1979. In 2005, Jirsak et al. patented a needleless electrospinning setup that consists of a rotating cylindrical roller as the spinneret and then Elmarco Ltd. (Liberec, Czech Republic) has commercialized it with a brand name “Nanospider”

[16, 17]. Studies conducted so far show that the spinneret type is of great importance in terms of efficiency and determination of fiber morphology in needleless electrospinning. Therefore, researchers have focused on many techniques with different geometrical designs in the spinneret systems such as rotating cylinder, ball and disc [18], conical wire coil [19], double-ring slit [20], twisted wire [21], linear flume [21] and mace shaped [22].

1.3.3 Bubble Electrospinning

Bubble electrospinning technology, invented in 2007, mainly depends on the size of the geometrically generated bubbles that occur on the surface of polymer solution [23]. The basic working principle of this method, which is accepted as one of the methods in needleless electrospinning technology, is to create polymer bubbles instead of the Taylor cone observed in the classical method and to create polymeric fibers by overcoming the surface tension of this bubble. Figure 1.4c shows the equipment used for a general bubble electrospinning setup. Here, the polymeric bubbles can be obtained with the high air force generated using a gas pump, while the electrical force obtained by the high voltage power supply is used to overcome the surface tension of the bubbles. When the voltage reaches a threshold, multiple jets are ejected from the bubbles and a collector is used to deposit the fibers on [24]. The problem that can be encountered in this method is to control the number, size, geometry, and stability of bubbles formed on the surface of the polymer solution. To overcome these undesirable situations, researchers have proposed a new method called "critical bubble spinning" [25]. The purpose of critical bubble electrospinning is to utilize a single independent and stable bubble by constructing a theoretical model. Using this method Li et al. produced nanofibers from different polymers including polyvinyl alcohol (PVA), polyethersulfone (PES), and polyvinylpyrrolidone (PVP) in their recent study [26].

1.3.4 Coaxial Electrospinning

Coaxial electrospinning, which has a similar working procedure as conventional electrospinning, can be used to produce hollow nanofibers or nanotubes in core–shell structures through a single spinneret of two polymer solutions (Fig. 1.5). Like in conventional electrospinning, the morphology of fibers can be adjusted by varying the solution parameters and processing conditions. Especially, the properties of the selected polymers and their solutions (solution viscosity, concentration, and conductivity, solvent vapor pressure, solvent/solution miscibility, and incompatibility) have an important role in controlling the core–shell morphology and structure of the fibers produced [27, 28].

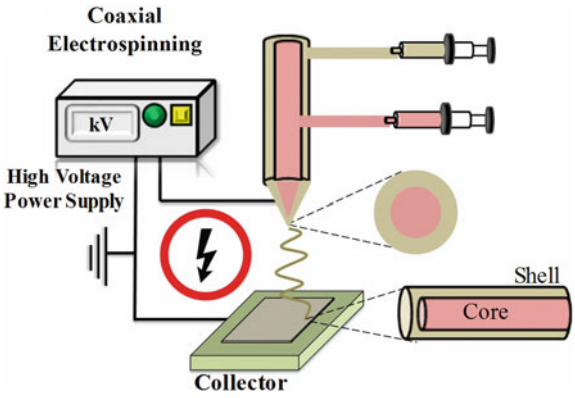


Fig. 1.5 Basic set-up for coaxial electrospinning process to produce core–shell nanofibers

Consisting of an outer sheath and an inner core with different compositions produced by coaxial electrospinning, nanofibers have the potential to be used as sensors, photocatalysts, batteries, membranes for filtration, nanoelectronics, scaffolds, and release systems. Studies conducted in recent years especially aim to investigate the encapsulation of drugs, essential oils, growth factors, and active compounds in the core of the fibers for the enhancement of a sustainable and long-term release. In this regard, Davani et al. synthesized a core–shell nanofibrous drug release system containing vancomycin and imipenem/cilastatin by coaxial electrospinning for the treatment of diabetic foot ulcer infections. The release profiles of the drugs showed a faster release of the drug-loaded in the shell while the sustained release of the drug-loaded in the core [29]. In another study, Rojas et al. developed curcumin and quercetin loaded-cellulose acetate/polycaprolactone core/shell electrospun nanofibers for use as food packaging. They showed that the coaxial structure of fibers effectively reduced the diffusion of active compounds throughout the fibers based on the type of food simulant. They also concluded that while the core of the fibers enables the release, the shell layer provides the barrier and mechanical properties of the packaging material [30].

1.3.5 3D Electrospinning Technologies

Conventional electrospinning plays an important role in the construction of two-dimensional (2D) nanofiber mats/membranes for many applications. Besides, with developing and modifying the traditional method, electrospinning holds a great promise to produce three-dimensional (3D) nanofibrous structures with superior features. Up to now, different methods for the preparation of 3D electrospun

nanofibers have been reported, such as wet electrospinning [31], coaxial-wet electrospinning [32], template-assisted electrospinning [33], porogen-incorporated electrospinning [34], cold-plate electrospinning [35], emulsion electrospinning [36], and centrifugal spinning [17].

3D structures enable the material to acquire features such as higher surface area, more interconnected channels, and higher porosity due to a larger third axis they offer. Thus, it is aimed to increase the performance of nanofibers for applications requiring a third dimension such as tissue engineering, filtration, and isolation [37]. For instance, 2D fibrous scaffolds produced for tissue engineering applications are usually too dense which may result in non-uniform cellular distribution and prevent both cell infiltration, migration and growth, and diffusion of nutrients and metabolites [37, 38]. Sheikh et al. performed a comparison study of 3D scaffold and 2D nanofiber sheet in terms of morphology, cell culture studies, and histological results. In this work, they introduced the production of 3D fibrous scaffolds with cold-plate electrospinning. The resultant network exhibited better cell infiltration due to its more regular pore structure, higher porosity, and water-binding abilities compared with 2D nanofibers produced using conventional electrospinning [35].

On the other hand, the attachment and viability of different cell types may also vary according to the material topography. Related to this, Vocetkova et al. examined the proliferation of keratinocytes and fibroblasts on core/shell 2D and 3D fibrous scaffolds. Lyophilised platelets loaded 2D and 3D coaxial scaffolds were prepared using poly-ε-caprolactone and two different technologies; needleless emulsion electrospinning and centrifugal spinning (forcespinning). The results showed that epithelial cells (keratinocytes) prefer the electrospun 2D structure, while dermal cells (fibroblasts) prefer forcespun 3D samples [39].

In a study by Bagheri et al., the extracting performance of chlorobenzenes from aquatic media was compared using polyamide-based 3D nanofibrous scaffolds and 2D nanofiber mats as needle trap devices. 3D and 2D nanostructures were produced using wet and conventional electrospinning, respectively. The resulting 3D structure provided a more appropriate environment for the isolation of analytes, with higher porosity and extraction efficiency for chlorobenzenes compared to 2D nanofiber mats [31].

1.4 Composite Nanofibers—Materials and Properties

A variety of materials such as organic polymers, small molecules, colloidal particles, composites, organic/inorganic, and organic/organic systems have been successfully electrospun into nonwoven mats using different modified techniques. Among them, the most commonly used materials are organic polymers. Mixtures formed by incorporating nanoscale components of different sizes and morphologies (such as nanoparticles, nanorods, nanowires, nanotubes, and nanosheets) into polymeric solutions have also been used in electrospinning [40].

Studies to date showed the production of a wide variety of polymeric nanofibers, including industrial, biodegradable, synthetic, and natural polymers. Generally, these high molecular weight polymers are electrospun after dissolving in a suitable solvent or in molten form. Collagen, gelatin, chitosan, fibrinogen, hyaluronic acid, chitosan, and silk as natural polymers have been used due to their biocompatibility, biodegradability, and low immune response. They have significant importance in medical applications, especially due to their biological origins, although they have some disadvantages such as low mechanical properties, difficulty in processing, and the need for cross-linking. On the other hand, synthetic polymers such as polyurethanes, polyesters, polyethers, and functionalized polyolefins are frequently used due to their advantages such as high mechanical strength, easy processability, and functionalizability. However, their low bioactivity limits their use. To take advantage of both synthetic and natural polymers, researchers produce composite fibrous structures combining the good physical properties of synthetic polymers and the high bioactivity of natural ones [41].

1.5 Functionalized Nanofibers

Electrospun nanofibrous structures are considered to be promising substrates for a wide range of applications due to their configurations that provide a high surface-to-volume ratio with high porosity. Moreover, the fiber properties including porosity, orientation, and dimension can be easily tailored by changing the solution characteristic (polymer and solvent type, viscosity, molecular weight, and conductivity), environmental conditions (temperature and humidity), and process parameters (voltage, feed rate, tip-to-collector distance, and collector and spinneret type). However, in some applications such as targeted drug delivery, biomimetic scaffolds for tissue engineering, antimicrobial materials, active food packaging, and adsorption, separation, and purification for water treatment, nanofibers may need to be functionalized with different strategies in addition to their previously mentioned features. Surface functionalized nanofibers continue to attract attention due to their improved active functions compared to traditional nanofibers.

1.5.1 Physical and Chemical Functionalization Methods

Electrospun nanofibers offer many advantages for application areas due to their proneness to surface functionalization. To make nanofibers more useful and compatible with the purpose, the surface of electrospun fibrils can be functionalized by physical (non-covalent) adsorption or chemical (covalent) immobilization of different bioactive molecules, nanoparticles, and drugs (Fig. 1.6). The techniques of wet chemical or plasma treatment, surface graft polymerization induced by plasma or radiation, encapsulation by co-electrospinning, layer-by-layer assembly, and adsorption can be

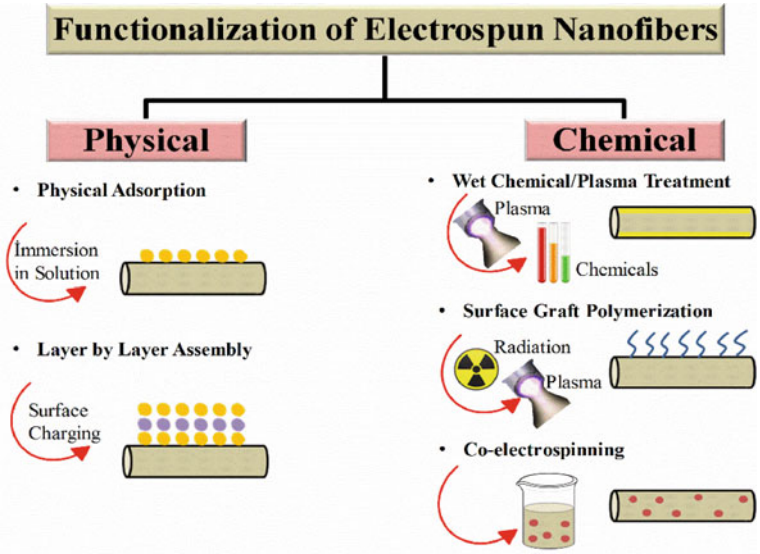


Fig. 1.6 Physical (adsorption and layer-by-layer assembly) and chemical (wet chemical/plasma treatment, surface graft polymerization and co-electrospinning) surface functionalization methods of electrospun nanofibers

used for the functionalization [42]. The simplest and uncomplicated way among these methods is the physical adsorption of bioactive compounds to the surface of the fibers using electrostatic interaction, hydrogen bonding, hydrophobic interaction, and Van der Waals interaction forces. Because of the high surface ratio of nanofibers, a wide range of bioactive compounds have been successfully immobilized on the surface of fibers [43]. Despite the advantages, physical functionalization has some disadvantages. For example, some viscous bioactive agents can fill the pores, significantly changing the morphology of the fibers. In addition, the bioactive compounds can be easily removed from the surface when exposed to polar solvents or cell culture media due to the weak physical bonds. For a more stable and irreversible structure, the use of chemical methods is essential. Since immobilized molecules are covalently bound to nanofibers, they cannot easily leak from surface-modified nanofibers when incubated in any environment [42].

Using different methods, it is possible to improve the surface properties of nanofibers such as electrostatic interactions, wettability, biomineralization, surface energy, cell attachment, and proliferation. In a recent study about to increase the biomineralization capability of scaffolds, polyurethane (PU) fibrous scaffolds were produced using electrospinning and the obtained nanofibers were modified by depositing polydopamine (PDA) on the activated surface under oxygen plasma treatment. The effect of the modification process on the homogeneous surface coating and the changes in the physicochemical and biological properties were evaluated. When PDA coating was applied to the surface of nanofibers, it was observed that

there was a remarkable improvement in the interaction of scaffolds with water molecules. It was found that PDA has mineralization ability and the amount of hydroxyapatite deposited increases as a function of PDA content. In vitro evaluation of constructs showed great improvements in cell-scaffold interactions, biocompatibility, and alkaline phosphatase activity after coating of PDA on plasma modified matrix. These results show that PDA coating, especially after oxygen plasma treatment, improves the physicochemical and in vitro properties of PU scaffolds for bone tissue engineering applications [44]. In another study, Chen et al. synthesized silica nanofibers (SNF2) by electrospinning using an optimized ratio of tetraethyl orthosilicate (TEOS) to polyvinyl pyrrolidone (PVP). They then worked to attach Laminin to the matrix (EXM) surface through a series of chemical reactions. The SNF2-AP-S-L (laminin modified SNF2) substrate was characterized and the results reported that the modified electrospun structures are promising for tissue engineering with their biocompatibility, bioactivity, and biodegradability properties [45].

1.5.2 Functional Nanofibers with Desired Properties

With the rapid development of nanotechnology in the last two decades, great advances have been made not only in the preparation and characterization of nanoscale materials but also in their functional applications. Membranes formed from nanofibers have an extremely high specific surface area due to their small diameter and are highly porous with excellent pore connections. In addition to these unique properties, it is possible to produce nanofibers with many desirable properties for advanced applications with their own functionality and surface modifications of the polymers used. By using polymers alone or in combination, natural and synthetic polymer-based nanofibers can be produced. Depending on the chemical structure and composition of the polymers used, different properties can be given to the produced nanofibers, and new application areas can be created. For example, polymer nanofibers with high thermal conductivity and good thermal stability have applications in thermal management, heat exchangers, and energy storage [46]. On the other hand, it is possible to develop biocompatible nanofibers by using natural and biodegradable polymers for use in medical applications. In addition, by blending polymers while production of nanofibers, conductivity can be increased for sensor applications, or biodegradation rate can be tailored for tissue engineering applications [47]. Apart from combining the polymer with another polymer, it is also possible to improve the features of polymeric nanofibers by adding nanoparticles or bioactive agents with variable properties [48]. In this section, different functional properties of nanofibers depending on the type of polymers used in nanofiber production, surface modification, surface coating, and additives added to polymer solutions before the electrospinning process will be discussed.

1.5.2.1 Conductive Nanofibers

The use of self-conducting polymers in the electrospinning method is gaining more and more popularity due to its sustainable, easy of synthesis and altering, lightweight and flexible structure. In addition, thanks to all these features, conductive nanofibers are used as an electromagnetic shield, sensors, multifunctional textile surfaces, organic photovoltaic, or biomedical applications.

While nanofibers can be obtained from pure or mixed polymers by electrospinning, it is often more difficult to produce conductive nanofibers. Conductive polymers are difficult to dissolve in co-solvents due to their low molecular weight and there is the challenge of integrating the conductive nanofiller, which needs evaporation of the non-conductive matrix required for the electrospinning process. This makes them difficult to electrospin. Conductive coatings disrupt the morphology and porosity of the surface and cause problems such as biocompatibility and degradation of the properties of the fibers. Therefore, approaches based on the production of conductive polymers by the electrospinning method attracted attention [49, 50].

Polymers such as polypyrrole (PPy), polyaniline (PANI), polythiophene (PT), and Poly (3,4-ethylene-dioxythiophene) (PEDOT) were generally used in the literature to provide conductivity in electrospun due to their high tunable wettability, biocompatibility, redox stability properties [51]. In a recent study performed by Bhattacharya et al., PANI, a self-conducting polymer, was used to prepare conductive nanofibers by electrospinning. They also added a secondary additive, m-cresol, to the structure and formed fibers with higher conductivity. Due to the low volatility of secondary additives, electrospinning with a secondary additive is not available in the literature and was reported for the first time by Bhattacharya et al. The conductive electrospun nanofibers showed a conductivity value of 1.73 S/cm, which is higher than the average values in the literature. Conductive nanofibers were shown to have a specific capacitance as high as 3121 F/g when tested as supercapacitors [50].

FDA-approved synthetic and non-conductive PCL generally provides poor cell adhesion, migration, and proliferation. Maharjan et al. used polypyrrole (PPy), a biocompatible conjugated conductive polymer, to improve the properties of PCL due to the ability of PPy to support cell growth, proliferation, and adhesion, the high-energy storage potential, simple polymerization process, and structural tunability. They carried out in-situ polymerization of polypyrrole nanoparticles in PCL polymeric solution and formed fibers from this solution by electrospinning. PCL/PPy conductive nanofibers supported better binding of MC3T3-E1 cells [51].

1.5.2.2 Antimicrobial Nanofibers

Multi-functional electrospun nanofibers, which have antibacterial, antiviral, and anti-infective properties, are in high demand in the food industry, filtration, wound-dressing, protective textiles, tissue engineering scaffolds, and biomedical devices applications. The antimicrobial property gained by the functionalization of nanofibers is provided by adding substances that exhibit microbial activity to the solution before

the electrospinning process or by modifying the surface of the produced fibers. The commonly used active agents are antibiotics, biocides (triclosan, chlorhexidine, QACs), silver nanoparticles, and metal oxide nanoparticles (zinc oxide and titanium dioxide nanoparticles) [52]. The test used for the determination of the antimicrobial activities of electrospun nanofibers is minimum inhibitory concentrations, diffusion (agar well diffusion, agar disc diffusion, bioautography and epsilometry testing), dilution (agar dilution and broth micro/microdilution), qualitative or quantitative assay methods against model organisms and metabolic based assay methods [53].

In a recent study performed by Karagoz et al., they decorated the polymethyl methacrylate (PMMA) electrospun materials with silver nanoparticles and ZnO nanorods on the nonwoven fabric mats. Multifunctional mats, which have protective properties with antibacterial agents, provided inhibition against Gram-negative and Gram-positive bacteria, inhibition against viruses such as COVID-19 and influenza, and protection against organic pollutants with its self-cleaning photocatalytic properties under UV light [54].

1.5.2.3 Biomimetic Nanofibers

To make conditions more favorable for cells, a chemical modification can be performed by attaching biological molecules to nanofibers to form a complex, mimicking the surface structure of the extracellular matrix (ECM) and the biological functions of cells on the ECM surface. A surface that can provide cell affinity, adhesion, proliferation, and viability are very important. Developing scaffolds that mimic tissue architecture, especially at the nanoscale, is one of the biggest challenges in tissue engineering. Electrospinning is a very suitable technique in terms of preparing fibrous materials that can imitate the architecture of natural human tissues at nanoscale by providing all these features along with the ratio of volume and surface, transport of nutrients, surface porosity and mimicking structure [55, 56]. Various structures resembling natural objects such as lotus leaf, silver ragwort leaf, rice leaf, honeycomb, polar bear fur, spider webs, soap bubbles and ECM have been successfully bio-mimicked by utilizing fibers that can be easily prepared in the desired composition and shape by adjusting the electrospinning parameters (Fig. 1.7).

In addition to chemical modification, biomimetic nanofibers can be prepared in different forms by changing the process parameters. These forms are aligned, tubular conduit scaffolds and spiral-structured nanofibrous scaffolds [57]. For example, electrospun nanofibrous scaffolds with various axial, thread, or radial alignments have been reported to exhibit superior capacity in shaping cell morphology, guiding cell migration, and influencing cell differentiation compared to other types of scaffolds both in vitro and in vitro [58, 59].

Coating biomaterials with nanofibers and then coating to simulate it is another approach for enhancement of the biomimicry properties. As an example of this approach, Saniei et al. used the surface modification method to improve the bioactivity and cell affinity of the PLA screw implant they produced with a bio-3D printer.

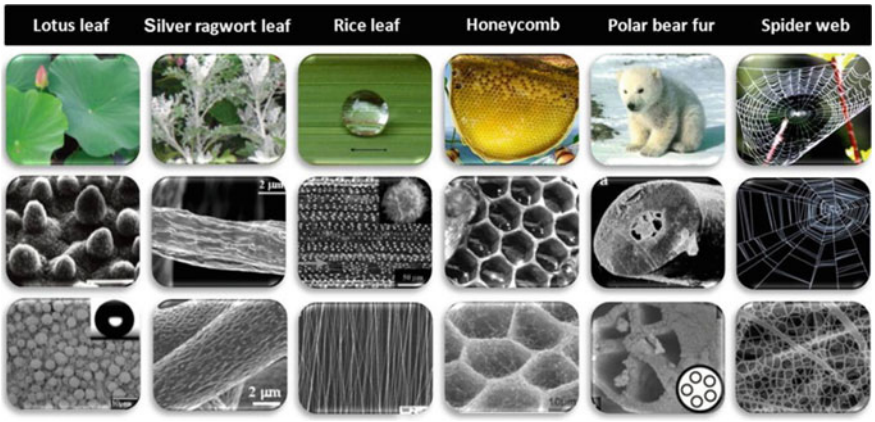


Fig. 1.7 Various biomimetic electrospun nanofibrous structures resemble natural objects such as lotus leaf, silver ragwort leaf, rice leaf, honeycomb, polar bear fur, and spider webs

For this, PLA implants were coated with poly(vinyl alcohol) (PVA)-nano Hydroxyapatite (nHA) nanofibers using the electrospinning method. They immersed the nanofiber-coated screws in body fluid and investigated its bioactivity. The results showed that the adhesion and cell growth of MC3T3-E1 cells on implants coated with PVA-nHA nanofiber was much better than the negative control, and they observed that nHA nanofibers accelerated the formation of an apatite layer on the sample surface [60].

1.5.2.4 Essential Oil Loaded Nanofibers

In the use of antibiotics, the pathogen's ability to mutate and our immunization have turned attention to other innovative approaches. Antibiotic resistance caused by synthetic drugs led to the trend towards bioactive products derived from natural plants, especially essential oils. Essential oils are volatile, easily degradable, and have antibacterial activity, which is derived from aromatic plants, consisting of phenols, terpenoids, fragrant and aliphatic components. Hence, for this reason, it is important to use them with nanocarriers to increase their stability and improve their activity [61].

To accomplish this, essential oils can be integrated into electrospun nanofibers to protect them from rapid degradation and evaporation, boost their stability and solubility, and hide their strong aroma. Nowadays, essential oil-loaded fibers have attracted a lot of attention as a wound dressing material in tissue engineering applications and active packaging in the food industry [62]. These essential oils are extracted from flowers (rosemary, chamomile, and lavender), fruits/berries (black pepper, juniper berry, and May chang), buds (clove), leaves (thyme, eucalyptus, and

rosemary), roots (ginger, angelica), seeds (coriander, cardamom, and fennel) and bark (cassia and cinnamon) of aromatic plants.

In a study published by Ullah et al., they used the essential oil obtained from the medicinal plant Blumea balsamifera, which has a long history in Southeast Asian countries. They showed that Blumea oil-loaded cellulose acetate nanofibers present antibacterial properties against *Escherichia coli* and *Staphylococcus aureus.* The oil-loaded-nanofibers exhibited antioxidant activity against DPPH solution and showed 92% cell viability for NIH 3T3 cells [61]. El Aassar et al. aimed to produce a non-antibiotic combination to enhance wound healing and reduce microbial invasion. In that study, novel antibiotic-free fibrils of hyaluronic acid/polyvinyl alcohol/polyethylene oxide mixture and ZnONPs/cinnamon essential oil (CEO) combination were produced by electrospinning method. Hyaluronic acid is known for its excellent biocompatibility, biodegradability, and wound healing properties. In addition, ZnO is one of the valuable compounds that have antimicrobial activity and physical effects that provide rupture of the bacterial cell envelope and it has been reported to accelerate wound healing. The CEO and its valuable cinnamaldehyde and eugenol components increase the permeability of the cell membrane and facilitate the passage of cellular nutrients, contributing to wound healing due to its antioxidant and anti-inflammatory effects. Functionalized novel NFs showed good physicochemical properties, cytocompatibility, antibacterial activity, and improved healing in the surgical incision wound of the bone prominence inoculated with *S. aureus* in the back of the rat [63].

Essential oil-loaded nanofibers are in demand in the field of food packaging, as well as being used in medical and wound dressing applications due to their antibacterial, antiviral and anti-inflammatory properties [64]. Zhou et al. produced gelatin nanofibers containing encapsulated angelica essential oil (AEO) using the electrospinning method for use as a natural food packaging with bioactivities that could extend the shelf life of foods. AEO/Gelatin electrospun non-cytotoxic nanofibers, exhibited strong immune properties and antioxidant activities against gram-negative and gram-positive bacteria. Also, AEO increased the fiber diameter of gelatin nanofibers and contributed to the improvement of the hydrophobicity of gelatin nanofibers [64].

1.6 Application Areas

1.6.1 Tissue Engineering

Tissue engineering is a constantly evolving multidisciplinary field that aims to regenerate damaged or lost tissues/organs in living organisms as a result of an accident or disease using a combination of cells and polymeric scaffolds [65]. Electrospun nanofibers have great advantages for tissue engineering applications as scaffolds owing to their large and specific surface area, high porosity enabling the interaction

of ECM signaling molecules, good biocompatibility while ensuring cell adhesion, proliferation, and differentiation. Electrospun nanofibers can be loaded with many bioactive agents needed for tissue repairs, such as proteins, peptides, stem cells, small molecule drugs and antibiotics [66].

To date, scientists have investigated a considerable number of fabricated structures of electrospun fibers and their corresponding functions for tissue engineering, including the generation of skin, bone, muscle, cartilage, and blood vessels [67]. In wound dressing applications, the high surface area of electrospun fibrous scaffolds allows oxygen permeability at the wound site, making these scaffolds suitable substrates for wound healing. In bone tissue engineering, electrospinning has been used as a successful nanofabrication technique to try to replicate the ECM, which consists of multilayered, fibrous and porous architecture [68]. It is also a very successful method in the production of blood vessel scaffolds, as it allows the fabrication of tubular fibrous membranes and favorable elasticity.

1.6.2 Drug Delivery

The use of electrospun fibers in drug delivery applications is also one of the most popular approaches. Electrospun fibers allow targeted drug release for different treatments to be carried out simultaneously with different active pharmaceutical ingredients in the same carrier. It even enables multiple drug releases, provides more accurate and realistic results for real and complex in vivo environments of biomedical applications, and creates the potential for clinical challenges. By using nano/microfibers, anticancer drugs, antibacterial and antiviral components, antibiotics, proteins, and living cells, DNA and RNA transport are carried out [69–71].

Qin et al. developed chitosan/pullulan (C/P) nanofiber oral films that dissolve in water in 30 s. The ratio of chitosan/pullulan in the electrospun solution affected the porosity and surface morphology of the film, and thermal stability increased as the ratio of chitosan in the solution increased. Chitosan/pullulan electrospun oral films were loaded with aspirin, as a model drug. The results showed that nanofibers can be used as an effective release system [70].

Liu et al. developed a triaxial electrospinning process with 3 different fluids. They developed a structure in which the central fluid forms electro-bendable fibers, while the outer two layers consist of non-electrospinning fluid. To prepare drug-loaded electrospun fibers, a system consisting of the core fluid consisting of ferulic acid-loaded protein (gliadin), a thin layer polymer (cellulose acetate) as the shell, and a solvent mixture of the third fluid was established. They showed that by adjusting the flow rate of cellulose acetate, which is the medium fluid of the electrospinning solution, the thickness of the coating can be changed and thus the oscillation rate can be adjusted. In addition, drug absorption and bioavailability were increased by examining the sustained release of ferulic acid, which can reduce the risk for many types of cancer and is promising for diabetes by bringing blood sugar to normal levels [72].

Protein-based electrospun fibers were formed by electrospinning α-lactalbumin and poly(ethylene oxide), an important milk protein used in nutrition and pharmacy, by Stie et al. Protein-based nanofibers contained up to 84% protein. TR146 human buccal epithelium and NIH 3T3 of electrospun nanofibers showed excellent in vitro biocompatibility, while murine fibroblast cells were unaffected by exposure. In addition, α-lactalbumin-based nanofibers were loaded with up to 6% (w/w) of ampicillin, an antibiotic component, and the drug-loaded fibers successfully inhibited Gram-negative bacteria [73].

1.6.3 Textile Industry

Fibers are the building units of textile and textile has been very important to us since ancient times. The potential and importance of nano and micro sized electrospun fibers are increasing day by day. Due to its production efficiency and high porosity, it can be used as functionalized fabric materials or protective clothing in the textile industries. Fiber textiles, which can also be used to filter aerosol particles, have the potential to neutralize chemicals that are impermeable to air and water [74, 75]. Masks, a textile product, are the sum of active layers of very fine fibers that form complex paths with fine microscopic sieves. When a particle, virus or bacterium is inhaled with air, it has to pass through these complex pathways and be absorbed into the interlayers [76].

The use of masks has become a necessity due to the COVID-19 pandemic, which started in 2019, continues today, and is facing the whole world. For this, the development of 3-layer antiviral masks is of great importance. It is very important that waste masks are biodegradable not to harm the environment. In the preparation of these 3-layer masks, at least one layer must be consisted of fibers. A recent study similar to this phenomenon, Patil et al. obtained a 3-layer antiviral, antibacterial and breathable PLA mask containing phytochemical-based plant extracts encapsulated in the inner filtration layer. The lower and upper layers consist of cotton, while the middle layer consists of a PLA layer functionalized with Indian herbal extracts that neutralize the effect of bacteria and viruses. The fiber mask they obtained showed 35.78 Pa/cm^2 differential pressure and 97.9% bacterial filtration efficiency. In addition, due to the PLA biopolymer, the mask showed biodegradable properties [75].

In another increasingly important applications of fibers is their use as protective dressing material against volatile organic compounds such as acetone, toluene, benzene, chloroform, etc.. Protective textiles are the last protective barrier designed to protect the user from various harmful substances as well as environments. Bhuiyan and his colleagues developed a new flexible and thermally protected protective clothing by integrating the electrospun PAN/silica aerogel nanofibrous membrane into the middle layer of the nonwoven fabric [77].

1.6.4 Food Packaging Industry

Packaging industry, has become an important part of the global industry to extend the shelf life of foods, protect product safety, reduce environmental problems and ensure cost efficiency [78]. Packages with moisture absorbing antioxidant or odor absorbing properties are in demand in the food industry. Functional packaging materials must be degradable, renewable and environmentally friendly, super hydrophobic and antibacterial. Micro and nano structures such as fibers have a large surface area/volume ratio, so they have a high potential to gain these properties. Electrospun nanofibers can be an excellent food packaging source due to their high surface/volume ratio, porous structure with interconnected pores and good adhesion properties. In addition, electrospun nanofibers are suitable for encapsulating active agents that can provide desired properties in food packaging [79].

In a study by Amjadi et al. In 2020, they used the zein protein as food packaging because of its good flexibility, low cost, hydrophilic properties, and non-toxicity. Along with these advantages, there are also disadvantages such as weak mechanical properties and rapid dissolution of zein electrospun materials which restricts their utilization in food packaging area. But the nanofibers obtained by the addition of carrageenan and active agents exhibited good thermal and mechanical properties along with high surface hydrophobicity [80].

In another study, they activated the system by adding ZnO nanoparticles, known for their strong antimicrobial properties and non-toxicity, to electrospun nanofibers, so the electrospun materials showed inhibition activity against *S. aureus* and *E. coli* bacteria. In addition, using Rosemary essential oil as a natural food preservative due to its powerful antioxidant and antimicrobial activity contributed to the inhibitory activity of bacteria.

Zou and colleagues used the chlorogenic acid (CGA), a bioactive compound that occurs naturally in plants for using it in the food packaging system that could extend the shelf life of foods, for its antimicrobial and antioxidant properties. They produced chitosan (CS)/polycaprolactone (PCL) electrospun fibers loaded with halloysite nanotubes (HNTs) which are carrier for the chlorogenic acid's long-term sustained release by electrospun method. The incorporation of CGA@HNTs into electrospun fibers improved thermal stability caused by the formation of hydrogen bonds, and the property of a hydrophilic surface and water vapor barrier, but negatively affected the mechanical properties of the fibers. Nanofibers containing 2%, 4%, and 6% CGA@HNTs exhibited 34.7%, 41.4%, 51.3% long term release at 240 h, respectively. They aimed that continuous homogeneous fibers with an average diameter of 159–166 nm can be used as an inner layer bonding to packaging surfaces owing to the fact that they show antioxidant and antimicrobial activities [81].

There is an intense research of cellulose, which is used for many purposes in almost all production areas and is one of the most common raw materials in the world. Chitin is the second most abundant raw material found on earth, obtained from the shell of crustaceans, and since it is biocompatible, biodegradable and non-toxic, there is a lot of research in the literature about its use in the fields of textiles, medicine,

sensors and food. Related to this, Hai and his colleagues created a nanocomposite by blending chitin and bamboo nanofibers without using chemical solvents for use in food packaging. Since bamboo cellulose has good mechanical properties, and chitin has excellent biodegradability and biocompatibility, these raw materials are suitable for use in food packaging. The nanocomposite they created for use in the food packaging industry could biodegrade for up to 1 week. In addition, as the concentration of bamboo cellulose fibers in the nanocomposite increased, the tensile strength and Young's modulus of the composite increased 3 and 1.3 times, respectively. Chitin/bamboo fiber nanocomposites, showing better stability than nanocomposite made from pure bamboo cellulose fiber, have good mechanical properties, thermal stability for food packaging [82].

In the food industry, nanofibers developed by the electrospinning method to prevent foodborne infections have attracted increasing attention. An example to this object, Shi et al. evaluated the protective properties of multifunctional nanofibers containing Oktyl Galate (OG), known by the number E311, used as a food additive with preservative and an antioxidant property on the Chinese Taihu icefish, to both foodborne pathogenic against Gram-negative (G–) *E. coli* and Gram-positive *S. aureus* (G+) as model microorganisms. The food packaging system they developed using encapsulated OG nanofibers produced by electrospinning showed strong antibacterial property and synergistic sterilization effect on the microbial load of the Chinese Taihu icefish [83].

1.6.5 Separation and Filtration Applications

Recently, the use of electrospun nanofiber membranes in separation and purification has become increasingly widespread. Electrospun membranes can be an excellent material for this task as they can be easily functionalized. Superhydrophilic materials are an effective source for separating effective oil/water mixtures and are gaining increasing attention. However, it is still a great challenge to perform this process with environmentally friendly multifunctional materials with superhydrophilicity. Several studies have proven that titanium dioxide (TiO_2) has good photocatalytic and self-cleaning properties. They combined the usability of TiO_2 in antifouling superhydrophilic materials and the PLA membrane as a biodegradable separation material, which has been recently demonstrated in novel publications. A research group enhanced the PLA membrane's superhydrophilicity with a Gallic acid modified TiO_2 coating. GA-TiO_2 coated PLA membranes showed superhydrophilicity and underwater superoleophobicity in saturated saline, acid solution ($pH = 1$) and corrosive organic solutions. PLA membranes were given superhydrophilicity properties with excellent oil resistance, thus showing the expected results in the separation of oil-containing water mixtures with antifouling properties. Due to the self-cleaning with strong photocatalytic property of the TiO_2 coating, the coated membranes performed effective and efficient oil/water separation under UV irradiation [84].

Wastewater consisting large amounts of toxic and synthetic dye wastes and impurities is a big challenge in the textile industry. Various dyes such as acid, basic, reactive, disperse are used for dyeing in the textile industry. Ghanavati et al. evaluated the adsorption of Acid Blue 74 with electrospun PA-6/ Modified zeolite nanofibrous composite and electrospun nanofibers were used as a filtration system to adsorb acid Blue 74 dye.

1.6.6 Sensor Applications

Advanced and functionalized electrospun nanofibers can react highly precisely in the light and low pressure range and therefore they are suitable for sensor applications. The applications of electrospun fibers in potential smart devices and next generation motion and pressure sensor wearable textile products are increasingly attracting attention.

Ahmed et al. developed a conductive and transparent PVDF-TrFE based fiber electrode for the piezoelectric pressure sensor using electrospinning method. And to form the electrode, they deposited reduced PEDOT that contained graphene oxide (rGO) and multi-walled carbon nanotubes (rGO-MCNTs) on the surface via spray coating [85]. Another important application area of electrospun sensor nanofibers is wearable clothing that can breathe, have high flexibility and stretchability, anticorrosive, and can detect body movements. Gao et al. synthesized superhydrophobic and conductive nanofiber composites by inducing SiO_2 nanoparticles and graphene shells on polyurethane (PU) electrospun nanofibers. The addition of graphene and SiO_2 nanoparticles to the PU nanofibrous membrane improved the elongation at break and tensile strength of the structure [86].

1.6.7 Battery Materials

Due to the rapid depletion of fossil fuel resources, there is an urgent need to find new sources of renewable energy that are cheaper for energy production and are harmless to the environment. Rapidly depleting fossil fuel resources led to searching for new resources for energy production, cheaper and environmentally friendly renewable energy [87]. Electrodes, which are an important part of the battery, provide reaction areas for redox reactions and are often used as electrodes as graphite mats provide a large specific surface and wide operating range. However, the electrochemical kinetics of graphite felt is limiting for battery performance. Recently, carbon nanofiber (CNF) prepared by electrospinning method was used to increase battery performance.

Electrospun nanostructures have great potential to be used as rechargeable secondary batteries in battery systems due to their high surface area/volume ratio

and good mechanical stability [88]. He et al., produced nitrogen doped polyacrylonitrile nanofibers using urea by electrospinning method. The results showed that nitrogen doped fibers can effectively increase the reaction rate of the $V2^{+}/V3^{+}$ redox couple. And in this way, fibers with superior electrochemical properties offered better energy efficiency and higher discharge capacity [88].

Zeng and colleagues produced MnO-carbon hybrid nanofibers using electrospinning technology, using polyvinyl alcohol (PVA) and manganese acetylacetonate. Manganese monoxide (MnO) is widely used in batteries due to its lower electrochemical motivation force, low cost, and environmentally harmless. Carbonaceous materials with high electrical conductivity and elastic properties are generally used as matrices for metal oxides to reduce the stress caused by the volumetric change during the liquefaction process. The use of easily synthesized MnO/CNF electrospun materials as anodes in lithium-ion batteries created potential due to their stable electrochemical properties [89].

1.6.8 Protection Against Chemical and Biological Agents

Fibers have great protection potential against chemical and biological warfare agents due to their high penetration resistance, breathability content, low weight, low pressure drop, surface functionalization potential and simple processing equipment requirement [90].

Factors such as nerve agents, threats from the release of chemical and biological toxic agents with their ineffective delivery, bring along the concern about the increasing use of pesticides and new, harmless and novel searches. Nanofiber innovations developed against harmful effects of chemical and biological toxic wastes, increasingly needed requirement and interested in areas such as health, agriculture and military [91]. Compared to other fibers, electrospun nanofibers have a larger effective surface area (up to 40 m^2/g) depending on the fiber diameter and have higher efficiency due to their homogeneous porosity. The average pore size of the fibrous scaffold varies with the average fiber diameter, so electrospun membranes cannot filter out very small objects such as viruses, toxic ions and organic matter. Therefore, in the fibrous membrane, a component that acts as an adsorbent is often used to treat contamination [92]. Also, it is possible to incorporate bioactive, antimicrobial and antiviral agents into electrospun nanofiber [93].

Wang and colleagues developed ultrafine cellulose nanofibers with a fibrous scaffold, one layer of nanoscale polyacrylonitrile (PAN) and the other layer of microscale polyethylene terephthalate (PET). Due to its double layer, these membranes could remove bacteria, viruses and toxic heavy metal ions simultaneously [92].

In a study performed by Farias et al., electrospun cellulose diacetate (CDA) nanofibers were directly coated on the soybean seeds. The coating showed no detrimental effects on seed germination and water dissolution studies showed that the nanofibers retained their integrity for more than 2 weeks. They tested using

fluopiram-loaded nanofibers as coatings and observed successful activity against a plant pathogen, *Alternaria linearіae* [94].

Pesticide exposure varies with wind, method, type of activity, and duration of application. However, worker hygiene and exposure time should also be considered. More than 16,000 pesticide products are used in the United States alone. Pesticides classified as extremely hazardous and Class IA can cause serious toxic effects in humans, but are also very harmful to the environment. Kumar and colleagues developed a highly comfortable agricultural protective suit to protect the human body from harmful pesticide liquids. They coated electrospun polyurethane and polyacrylonitrile nanofibers on 100% polypropylene spun-bond nonwoven fabric, which has good mechanical, thermal and chemical resistance properties [95].

1.6.9 Optical Cloaking

After 1999, more than 50 articles about transparent electrospun membranes have been published so far. This issue shows that it has attracted the attention of researchers in recent years. If the luminous flux coming to a surface is well transmitted or the light is less refracted, the transmittance will be high. And the transmissivity of materials varies according to their molecular bonding, microstructure and difference in properties [96]. Oppositely, optical cloaking is possible by the total scattering of electromagnetic waves around an object at all angles and polarizations over a wide frequency range, independently of the environment. The metamaterials that provide these properties are based on the method of designing a new class of periodically arranged macroscopic atoms that can impart desired properties, rather than chemically altering the structure. Metamaterials can provide exciting applications by enabling different light-matter interactions, such as when light coming into an object bypasses it and acts as an optical cloak [97].

Woo Kim et al. created high clarity transparent electrode-based Ag metal electrospun wires with a diameter of 300–1800 nm that are invisible in the wide band range. The absorbing Ag_2O shell, with a dielectric coating, led to the cancellation of multipolar electric moments in the Ag wires. Therefore, it greatly suppressed the scattering in the visible region range and the Ag wires were not visible. They also used Ag wires for high permeability and fast defrosting in automobile windshields [98]. Vaseashta et al. reported optical cloaking using metamaterials embedded in nanofibers for defense applications to protect military assets in the battlefield [99].

1.6.10 Water Contamination Mitigation

The development of production technology along with inefficient environmental policy has begun to threaten the fresh water and other water resources of the world and this has become a global problem. Therefore, all over the world, there is an

urgent need to conserve water and to improve the quality of wastewater by treating it. The World Health Organization announced that 2 million people use polluted water sources for drinking water. Bacteria, viruses, biological pollutants or chemical pollutants containing toxic heavy metal ions are some of the substances that cause water pollution. There are currently methods in water treatment like active carbon filtration systems, distillations, electrochemical oxidation, photocatalysis and various physicochemical ways. Electrospinning, the most effective way to prepare nanofibers used for water treatment in recent years, is used to produce micro or nanofiber web-like nonwoven ultrafine fibers from different types of polymers [100].

Blanco and colleagues used polyamide 6 (PA6), a polymer commonly used in water treatment, to remove organic contaminants and bacteria. For this, polyamide 6 spun fibers were modified with titanium dioxide nanoparticles to form a hybrid membrane that provides photocatalytic activity under UV light irradiation [101]. In addition to the mixing of all harmful bacteria and wastes into water sources, heavy metals detected in water recently have become a major problem and it has been reported that heavy metals can cause health problems such as poisoning, seizures, nerve, skin and blood diseases. B. Dela Pena et al. developed a Fe-doped and nanoclay filled electrospun PCL adsorbent sheet for the dynamic removal of arsenic, a heavy metal, from wastewater [93].

The photocatalytic method is another effective method which uses sunlight, cheap and which has a continuous source. For this method, in the presence of photocatalysts, harmful pollutants are removed from the environment by using the energy of sunlight [102]. Due to the discharge of industrial, agricultural and domestic wastes into water bodies, phenolic compounds are formed in water bodies. And these compounds are known to have long-term and serious negative effects on living things. Norouzi et al. synthesized Ag/TiO_2 nanofibers using the electrospinning method and studied the photocatalytic degradation of phenol under visible light using the fibers and modeled them depending on pH and catalyst dosage. And with the least amount of catalyst they used, they achieved the highest degradation value of phenol, 82.65% [102].

1.7 Future Trends and Conclusions

Electrospinning technique, which is a technique that allows the production of nano/micro scale fibers from polymer solutions or melts, is frequently used to obtain fibers with many applications from medicine to engineering. Compared to other methods used in fiber synthesis, it is an easy-to-use, versatile and low-cost method suitable for continuous fiber production. Nanofibers produced by electrospinning have many advantages such as extraordinary surface area/volume ratio, controllable pore structure, high porosity, flexible surface properties, high functionality and superior mechanical properties. In addition, with this technique it is possible to obtain fibers in various forms by modifying the general electrospinning set-up. With this method, both natural and synthetic polymers and combinations of them with other materials can produced in nanofibrous form. When studies carried out in recent years

are evaluated, the electrospinning method comes to the fore when the ease of production technique, reproducibility and scale-up steps are considered. As a result, it is possible to obtain fibers with different morphologies by using various parameters with the electrospinning method for various applications. Since the fibers produced by the electrospinning method are used in many fields, it can be said that this method is a technology worth working with today and also promising for the future.

Conflict of Interest Statement The authors declare no conflict of interest. Due to commercial interest in this technology, any commercial name or product displayed or described in this chapter is coincidental and in no way, should be treated as an endorsement of that product. The chapter did not require collection of any personal data and hence the Institutional Review Board policy related to involvement of human subjects is not applicable.

References

1. Alghoraibi, I., & Alomari, S. (2019). *Handbook of nanofibers*. Epub ahead of print 2019. http://doi.org/10.1007/978-3-319-42789-8
2. Tucker, N., Stanger, J. J., Staiger, M. P., et al. (2012). *The history of the science and technology of electrospinning from 1600 to 1995*, http://www.jeffjournal.org. Accessed 25 February 2021.
3. Ghosal, K., Agatemor, C., Tucker, N., et al. (2018). Electrical spinning to electrospinning: A brief history. In *RSC soft matter* (pp. 1–23). Royal Society of Chemistry.
4. Huang, C., Chen, S., Lai, C., et al. (2006). Electrospun polymer nanofibres with small diameters. *Nanotechnology, 17*, 1558–1563.
5. Jian, S., Zhu, J., Jiang, S., et al. (2018). Nanofibers with diameter below one nanometer from electrospinning. *RSC Advances, 8*, 4794–4802.
6. Santangelo, S. (2019). Electrospun nanomaterials for energy applications: Recent advances. *Applied Sciences (Switzerland), 9*, 1049.
7. Taylor, G. I. (1969). Electrically driven jets. *Proceedings of the Royal Society of London A. Mathematical and Physical Sciences, 313*, 453–475.
8. Long, Y. Z., Yan, X., Wang, X. X., et al. (2018). Electrospinning: The setup and procedure. In *Electrospinning: Nanofabrication and applications* (pp. 21–52). Elsevier.
9. Nayak, R. (2017). Review of literature: Melt electrospinning. In *Polypropylene nanofibers* (pp. 9–39). Springer.
10. Zakaria, M., Shibahara, K., & Nakane, K. (2020). Melt-electrospun polyethylene nanofiber obtained from polyethylene/polyvinyl butyral blend film. *Polymers (Basel), 12*, 457.
11. Brown, T. D., Dalton, P. D., & Hutmacher, D. W. (2016). Melt electrospinning today: An opportune time for an emerging polymer process. *Progress in Polymer Science, 56*, 116–166.
12. Muerza-Cascante, M. L., Haylock, D., Hutmacher, D. W., et al. (2015). Melt electrospinning and its technologization in tissue engineering. *Tissue Engineering Part B: Reviews, 21*, 187–202.
13. Nayak, R., Padhye, R., & Arnold, L. (2017). Melt-electrospinning of nanofibers. In *Electrospun nanofibers* (pp. 11–40). Elsevier Inc.
14. Niu, H., Wang, X., & Li, T. (2011). Needleless electrospinning: Developments and performances. In *Nanofibers—Production, properties and functional applications*. InTech. Epub ahead of print 14 November 2011. http://doi.org/10.5772/24999
15. Niu, H., & Lin, T. (2012). Fiber generators in needleless electrospinning. *Journal of Nanomaterials*. Epub ahead of print 2012. http://doi.org/10.1155/2012/725950
16. Lin, T. (2012). Needleless electrospinning: A practical way to mass production of nanofibers. *Journal of Textile Science and Engineering,* 2. Epub ahead of print 2012. http://doi.org/10.4172/2165-8064.1000e109

17. Rihova, M., Ince, A. E., Cicmancova, V., et al. (2021). Water-born 3D nanofiber mats using cost-effective centrifugal spinning: Comparison with electrospinning process: A complex study. *Journal of Applied Polymer Science, 138*, 49975.
18. Niu, H., Lin, T., & Wang, X. (2009). Needleless electrospinning. I. A comparison of cylinder and disk nozzles. *Journal of Applied Polymer Science, 114*, 3524–3530.
19. Wang, X., Niu, H., Lin, T., et al. (2009). Needleless electrospinning of nanofibers with a conical wire coil. *Polymer Engineering & Science, 49*, 1582–1586.
20. Wei, L., Qiu, Q., Wang, R., et al. (2018). Influence of the processing parameters on needleless electrospinning from double ring slits spinneret using response surface methodology. *Journal of Applied Polymer Science, 135*, 46407.
21. Holopainen, J., Penttinen, T., Santala, E., et al. (2015). Needleless electrospinning with twisted wire spinneret. *Nanotechnology, 26*. Epub ahead of print 16 January 2015. http://doi.org/10.1088/0957-4484/26/2/025301
22. Ali, U., Niu, H., Khurshid, M. F., et al. (2019). Electrospinning behavior of needleless spinneret with a popular mace shape. *Journal of the Textile Institute, 110*, 349–357.
23. Yang, R., He, J., Xu, L., et al. (2009). Bubble-electrospinning for fabricating nanofibers. *Polymer (Guildf), 50*, 5846–5850.
24. Chen, R. X., Li, Y., & He, J. H. (2014). Mini-review on Bubbfil spinning process for mass-production of nanofibers. *Review Materials, 19*, 325–344.
25. Li, Y., & He, J. H. (2019). Fabrication and characterization of ZrO_2 nanofibers by critical bubble electrospinning for high-temperature-resistant adsorption and separation. *Adsorption Science & Technology, 37*, 425–437.
26. Li, Y., Dong, A., & He, J. (2020). Innovation of critical bubble electrospinning and its mechanism. *Polymers (Basel), 12*, 304.
27. Qin, X. (2017). Coaxial electrospinning of nanofibers. In *Electrospun nanofibers* (pp. 41–71). Elsevier Inc.
28. Li, M., Zheng, Y., Xin, B., et al. (2020). Coaxial electrospinning: Jet motion, core-shell fiber morphology, and structure as a function of material parameters. *Industrial and Engineering Chemistry Research, 59*, 6301–6308.
29. Davani, F., Alishahi, M., Sabzi, M., et al. (2021). Dual drug delivery of vancomycin and imipenem/cilastatin by coaxial nanofibers for treatment of diabetic foot ulcer infections. *Materials Science and Engineering: C, 123*, 111975.
30. Rojas, A., Velásquez, E., Piña, C., et al. (2021). Designing active mats based on cellulose acetate/polycaprolactone core/shell structures with different release kinetics. *Carbohydrate Polymers, 261*. Epub ahead of print 1 June 2021. http://doi.org/10.1016/j.carbpol.2021.117849
31. Bagheri, H., Manshaei, F., & Rezvani, O. (2018). Three-dimensional nanofiber scaffolds are superior to two-dimensional mats in micro-oriented extraction of chlorobenzenes. *Microchimica Acta, 185*, 1–10.
32. Rafiei, M., Jooybar, E., Abdekhodaie, M. J., et al. (2020). Construction of 3D fibrous PCL scaffolds by coaxial electrospinning for protein delivery. *Materials Science and Engineering: C, 113*, 110913.
33. Miguel, S. P., Cabral, C. S. D., Moreira, A. F., et al. (2019). Production and characterization of a novel asymmetric 3D printed construct aimed for skin tissue regeneration. *Colloids Surfaces B Biointerfaces, 181*, 994–1003.
34. Kim, T. G., Chung, H. J., & Park, T. G. (2008). Macroporous and nanofibrous hyaluronic acid/collagen hybrid scaffold fabricated by concurrent electrospinning and deposition/leaching of salt particles. *Acta Biomaterialia, 4*, 1611–1619.
35. Sheikh, F. A., Ju, H. W., Lee, J. M., et al. (2015). 3D electrospun silk fibroin nanofibers for fabrication of artificial skin. *Nanomedicine Nanotechnology, Biology and Medicine, 11*, 681–691.
36. Liu, M., Hao, X., Wang, Y., et al. (2020). A biodegradable core-sheath nanofibrous 3D hierarchy prepared by emulsion electrospinning for sustained drug release. *Journal of Materials Science, 55*, 16730–16743.

37. Dilamian, M., Joghataei, M., Ashrafi, Z., et al. (2021). From 1D electrospun nanofibers to advanced multifunctional fibrous 3D aerogels. *Applied Materials Today, 22*, 100964.
38. Keirouz, A., Chung, M., Kwon, J., et al. (2020). 2D and 3D electrospinning technologies for the fabrication of nanofibrous scaffolds for skin tissue engineering: A review. *WIREs Nanomedicine and Nanobiotechnology, 12*, e1626.
39. Vocetkova, K., Buzgo, M., Sovkova, V., et al. (2017). A comparison of high throughput core-shell 2D electrospinning and 3D centrifugal spinning techniques to produce platelet lyophilisate-loaded fibrous scaffolds and their effects on skin cells. *RSC Advances, 7*, 53706–53719.
40. Xue, J., Wu, T., Dai, Y., et al. (2019). Electrospinning and electrospun nanofibers: Methods, materials, and applications. *Chemical Reviews, 119*, 5298.
41. Nemati, S., Kim, S., Shin, Y. M., et al. (2019). Current progress in application of polymeric nanofibers to tissue engineering. *Nano convergence, 61*, 1–16.
42. Yoo, H. S., Kim, T. G., & Park, T. G. (2009). Surface-functionalized electrospun nanofibers for tissue engineering and drug delivery. *Advanced Drug Delivery Reviews, 61*, 1033–1042.
43. Zhang, C., Li, Y., Wang, P., et al. (2020). Electrospinning of nanofibers: Potentials and perspectives for active food packaging. *Comprehensive Reviews in Food Science and Food Safety, 19*, 479–502.
44. Ghorbani, F., Zamanian, A., & Torabinejad, B. (2020). The effect of oxygen plasma pretreatment on the properties of mussel-inspired polydopamine-decorated polyurethane nanofibers. *Journal of Polymer Engineering, 40*, 109–119.
45. Chen, W. S., Guo, L. Y., Tang, C. C., et al. (2018). The effect of laminin surface modification of electrospun silica nanofiber substrate on neuronal tissue engineering. http://doi.org/10.3390/nano8030165
46. Asmatulu, R., & Khan, W. S. (2019). Electrospun nanofibers for photonics and electronics applications. In *Synthesis and applications of electrospun nanofibers* (pp. 239–256). Elsevier.
47. Zahmatkeshan, M., Adel, M., Bahrami, S., et al. (2018). Polymer based nanofibers: Preparation, fabrication, and applications. In *Handbook of nanofibers* (pp. 1–47).
48. Thamer, B. M., Aldalbahi, A., Moydeen A. M., Rahaman, M., & El-Newehy, M. H. (2020). Modified electrospun polymeric nanofibers and their nanocomposites as nanoadsorbents for toxic dye removal from contaminated waters: A review. *Polymers, 13*, 20.
49. Blachowicz, T., Ehrmann, A. (2020). Conductive electrospun nanofiber mats. Materials, 13, 1, 152. https://doi.org/10.3390/ma13010152
50. Bhattacharya, S., Roy, I., Tice, A., et al. (2020). High-conductivity and high-capacitance electrospun fibers for supercapacitor applications. Epub ahead of print 2020. http://doi.org/10.1021/acsami.9b21696
51. Maharjan, B., Krishnamoorthi, V., & Rim, S. (2020). In-situ polymerized polypyrrole nanoparticles immobilized poly (ε-caprolactone) electrospun conductive scaffolds for bone tissue engineering. *Materials Science & Engineering C, 114*, 111056.
52. Gao, Y., Truong, Y. B., Zhu, Y., et al. (2014). Electrospun antibacterial nanofibers: Production, activity, and in vivo applications. *Journal of Applied Polymer Science, 131*, 9041–9053.
53. Song, K., Wu, Q., Qi, Y., et al. (2017). Electrospun nanofibers with antimicrobial properties. *Electrospun Nanofibers*; 551–569.
54. Karagoz, S., Kiremitler, N. B., Sarp, G., et al. (2021). Antibacterial, antiviral, and self-cleaning mats with sensing capabilities based on electrospun nano fibers decorated with ZnO nanorods and Ag nanoparticles for protective clothing applications. Epub ahead of print 2021. http://doi.org/10.1021/acsami.0c15606
55. Jiang, J., Xie, J., Ma, B., et al. (2014). Mussel-inspired protein-mediated surface functionalization of electrospun nanofibers for pH-responsive drug delivery. *Acta Biomaterialia, 10*, 1324–1332.
56. Sang, H., Gyoung, T., & Gwan, T. (2009). Surface-functionalized electrospun nano fibers for tissue engineering and drug delivery. *Advanced Drug Delivery Reviews, 61*, 1033–1042.
57. Wang, X., Ding, B., & Li, B. (2013). Biomimetic electrospun nanofibrous structures for tissue engineering. *Materials Today, 16*, 229–241.

58. Ls, W., & Zk, X. (2009). Polymer surfaces structured with random or aligned electrospun nanofibers to promote the adhesion of blood platelets. *Journal of Biomedical Materials Research. Part A, 89*, 168–175.
59. Xie, J., MacEwan, M. R., Ray, W. Z., et al. (2010). Radially aligned, electrospun nanofibers as dural substitutes for wound closure and tissue regeneration applications. *ACS Nano, 4*, 5027–5036.
60. Saniei, H., & Mousavi, S. (2020). Surface modification of PLA 3D-printed implants by electrospinning with enhanced bioactivity and cell affinity. *Polymer, 196*, 122467.
61. Ullah, A., Saito, Y., Ullah, S., et al. (2021). Bioactive Sambong oil-loaded electrospun cellulose acetate nano fibers: Preparation, characterization, and in-vitro biocompatibility. *International Journal of Biological Macromolecules, 166*, 1009–1021.
62. Rather, A. H., Wani, T. U., Khan, R. S., et al. (2021). Prospects of polymeric nanofibers loaded with essential oils for biomedical and food-packaging applications. *International Journal of Molecular Sciences, 22*. Epub ahead of print 2 April 2021. http://doi.org/10.3390/IJMS22084017
63. El-aassar, M. R., El-beheri, N. G., Agwa, M. M., et al. (2021). Antibiotic-free combinational hyaluronic acid blend nano fibers for wound healing enhancement. *International Journal of Biological Macromolecules, 167*, 1552–1563.
64. Zhou, Y., Miao, X., Lan, X., et al. (2020). Angelica essential oil loaded electrospun gelatin nanofibers for active food packaging application. Polymers, 12, 2, 299. https://doi.org/10.3390/polym12020299
65. Ceylan, S., Göktürk, D., Demir, D., et al. (2017). Comparison of additive effects on the PVA/starch cryogels: Synthesis, characterization, cytotoxicity, and genotoxicity studies. *International Journal of Polymeric Materials and Polymeric Biomaterials,* 1–10.
66. Ye, K., Kuang, H., You, Z., et al. (2019). Electrospun nanofibers for tissue engineering with drug loading and release, 1–17.
67. Jun, I., Han, H.-S., Edwards, J. R., et al. (2018). Electrospun fibrous scaffolds for tissue engineering: viewpoints on architecture and fabrication. *International Journal of Molecular Sciences, 19*. Epub ahead of print 6 March 2018. http://doi.org/10.3390/IJMS19030745
68. Gouma, P.-I., & Ramachandran, K. (2008). Electrospinning for bone tissue engineering. *Recent Patents on Nanotechnology, 2*, 1–7.
69. Ding, Y., Li, W., Zhang, F., et al. (2019). Electrospun fibrous architectures for drug delivery. *Tissue Engineering and Cancer Therapy, 1802852*, 1–35.
70. Qin, Z., Jia, X., Liu, Q., et al. (2019). Fast dissolving oral films for drug delivery prepared from chitosan/pullulan electrospinning nano fibers. *International Journal of Biological Macromolecules, 137*, 224–231.
71. Islam, A., Begum, H. A., Shahid, A., et al. (2020). Antibacterial electrospun nanofibers from poly (vinyl alcohol) and Mikania micrantha with augmented moisture properties: Formation and evaluation. *The Journal of The Textile Institute*, 1–9.
72. Liu, X., Yang, Y., Yu, D., et al. (2019). Tunable zero-order drug delivery systems created by modified triaxial electrospinning. *Chemical Engineering Journal, 356*, 886–894.
73. Stie, M. B., Corezzi, M., Bombin, A. D. J., et al. (2020). Waterborne electrospinning of α-lactalbumin generates tunable and biocompatible nano fibers for drug delivery. Epub ahead of print 2020. http://doi.org/10.1021/acsanm.9b02557
74. Andleeb, A., & Yar, M. (2020). Application of electrospun materials in industrial applications (pp. 215–242).
75. Avinash, N., Macchindra, P., Jaya, N., et al. (2021). Needleless electrospun phytochemicals encapsulated nanofibre based 3-ply biodegradable mask for combating COVID-19 pandemic. *Chemical Engineering Journal, 416*, 129152.
76. Tebyetekerwa, M., Xu, Z., Yang, S., et al. (2020). Electrospun nanofibers-based face masks. *Advanced Fiber Materials, 2*, 161–166.
77. Anjuman, Z., Tanushree, A., & Shanks, R. A. (2020). Electrospun polyacrylonitrile–silica aerogel coating on viscose nonwoven fabric for versatile protection and thermal comfort. *Cellulose, 27*, 10501–10517.

78. Topuz, F., & Uyar, T. (2020). Antioxidant, antibacterial and antifungal electrospun nano fibers for food packaging applications. *Food Research International, 130*, 108927.
79. Zhao, L., Duan, G., Zhang, G., et al. (2020). Electrospun functional materials toward food packaging applications: A review. *Nanomaterials, 10*(1), 150.
80. Amjadi, S., Almasi, H., Ghorbani, M., et al. (2020). Reinforced ZnONPs/rosemary essential oil-incorporated zein electrospun nano fibers by κ-carrageenan. *Carbohydrate Polymers, 232*, 115800.
81. Zou, Y., Zhang, C., Wang, P., et al. (2020). Electrospun chitosan/polycaprolactone nanofibers containing chlorogenic acid-loaded halloysite nanotube for active food packaging. *Carbohydrate Polymers, 247*, 116711.
82. Hai, L., Sik, E., Zhai, L., et al. (2020). Green nanocomposite made with chitin and bamboo nano fibers and its mechanical, thermal and biodegradable properties for food packaging. *International Journal of Biological Macromolecules, 144*, 491–499.
83. Shi, Y., Zhang, R., Zhu, C., et al. (2021). Antimicrobial mechanism of alkyl gallates against Escherichia coli and Staphylococcus aureus and its combined effect with electrospun nanofibers on Chinese Taihu icefish preservation. *Food Chemistry, 346*, 128949.
84. Zhang, Z., Gan, Z., Bao, R., et al. (2020). Green and robust superhydrophilic electrospun stereocomplex polylactide membranes: Multifunctional oil/water separation and self-cleaning. *Journal of Membrane Science, 593*, 117420.
85. Ahmed, A., Jia, Y., Huang, Y., et al. (2019). Preparation of PVDF-TrFE based electrospun nanofibers decorated with PEDOT-CNT/rGO composites for piezo-electric pressure sensor. *Journal of Materials Science: Materials in Electronics, 30*, 14007–14021.
86. Gao, J., Li, B., Huang, X., et al. (2019). Electrically conductive and fluorine free superhydrophobic strain sensors based on SiO_2/graphene-decorated electrospun nanofibers for human motion monitoring. *Chemical Engineering Journal, 373*, 298–306.
87. Singh, A. (2019). Electrospun nanostructures for conversion type cathode (S, Se) based lithium and sodium batteries. *Journal of Materials Chemistry A,* 11613–11650.
88. He, Z., Li, M., Li, Y., et al. (2019). Applied surface science electrospun nitrogen-doped carbon nanofiber as negative electrode for vanadium redox flow battery. *Applied Surface Science, 469*, 423–430.
89. Zeng, S., Zhao, R., Li, A., et al. (2019). Applied surface science MnO/carbon fibers prepared by an electrospinning method and their properties used as anodes for lithium ion batteries. *Applied Surface Science, 463*, 211–216.
90. Nurfaizey, A. H., Tucker, N., Stanger, J., et al. *Functional nanofibers in clothing for protection against chemical and biological hazards.* Woodhead Publishing Limited. http://doi.org/10.1533/9780857095640.2.236
91. Baji, A., Agarwal, K., & Oopath, S. V. (2020). Emerging developments in the use of electrospun fibers and membranes for protective clothing applications. *Polymers, 12*(2), 492.
92. Wang, R., Guan, S., Sato, A., et al. (2013). Nano fibrous micro filtration membranes capable of removing bacteria, viruses and heavy metal ions. *Journal of Membrane Science, 446*, 376–382.
93. May, E., Dela, P. B., Araño K., et al. (2021). The design of a bench-scale adsorbent column based on loaded electrospun fiber membrane for the removal of arsenic in wastewater, 1–6.
94. Khan, S. A. (2019). Electrospun polymer nano fibers as seed coatings for crop protection. Epub ahead of print 2019. http://doi.org/10.1021/acssuschemeng.9b05200
95. Kubera, S., Kumar, S., & Prakash, C. (2021). Characterization of electrospun polyurethane/polyacrylonitrile nanofiber for protective textiles. *Iranian Polymer Journal*. Epub ahead of print 2021. http://doi.org/10.1007/s13726-021-00961-6
96. Xiao, Y., Luo, H., Tang, R., Hou, J. (2021). Preparation and applications of electrospun optically transparent fibrous membrane. Polymers (Basel), 13, 4, 506. https://doi.org/10.3390/polym13040506
97. Lee, K., Ji, C., Iizuka, H., et al. (2021). Optical cloaking and invisibility: From fiction toward a technological reality. *Journal of Applied Physics, 129*(23), 1–18.

98. Kim, S., An, B. W., Cho, E., et al. (2018). A full-visible-spectrum invisibility cloak for mesoscopic metal wires. Epub ahead of print 2018. http://doi.org/10.1021/acs.nanolett.8b01157
99. Vaseashta, A. (2013). Ecosystem of innovations in nanomaterials based CBRNE sensors and threat mitigation. In A. Vaseashta, & S. Khudaverdyan (Eds.), *Advanced sensors for safety and security. NATO Science for Peace and Security Series B: Physics and Biophysics* (pp. 3–25). Springer. http://doi.org/10.1007/978-94-007-7003-4_1
100. Fahimirad, S., Fahimirad, Z., & Sillanpää, M. (2021) Science of the total environment efficient removal of water bacteria and viruses using electrospun nano fibers, 751. Epub ahead of print 2021. http://doi.org/10.1016/j.scitotenv.2020.141673
101. Blanco, M., Monteser, C., Ana, P., et al. (2019). TiO2-doped electrospun nanofibrous membrane for photocatalytic water treatment, Polymers (Basel), 11, 5, 747. https://doi.org/10.3390/polym11050747
102. Norouzi, M., Fazeli, A., & Tavakoli, O. (2020). Phenol contaminated water treatment by photocatalytic degradation on electrospun Ag/TiO_2 nano fibers: Optimization by the response surface method. *Journal of Water Process Engineering, 37*, 101489.



Nimet Bölgen received B.S. degree in Chemical Engineering at Ankara University, Turkey in 2002, and M.S. degree in Chemical Engineering at Hacettepe University, Turkey in 2004. She received Ph.D. degree in Bioengineering at Hacettepe University, Turkey in 2008. She was visiting scientist at Sabancı University, Turkey; Lund University, Sweden; Institute of Polymer Science and Technology, Spain; and Keele University, United Kingdom. She has been working at Chemical Engineering Department, Mersin University, Turkey since 2009. She is the author of 13 book chapters, 45 articles, and more than 100 proceedings. Prof. Bölgen's research is focused on the development of biomaterials for tissue engineering and regenerative medicine, drug delivery systems from natural and synthetic polymers, cryogels, and electrospun nanofibers for biomedical applications.



Didem Demir was born in İstanbul, Turkey, in 1988. She received the B.S. and M.S. degrees in Chemical Engineering from the Fırat University, Turkey, in 2011 and Mersin University, Turkey, in 2014, respectively. She received a Ph.D. degree in Chemical Engineering at Mersin University, in 2021. She is working as Assistant Professor at the Chemistry and Chemical Processes Technologies Department of Tarsus University, Mersin, Turkey. Mrs. Demir's proficiency in the development and characterization of biomaterials including gels, nanofibers, and micro-and nanoparticles for tissue engineering applications such as tissue regeneration, wound healing, and drug release. Her research interests also include the extraction of natural polymers and the fabrication of polymeric materials for wastewater treatment. Up to now, she published 20 articles, 6 book chapters and 50 proceedings.



Müge Aşık was born in Adana in 1995. She received the B.S. degree in chemical engineering from the University of Mersin, Mersin, Turkey in 2017 and the M.S. degree in chemical engineering from the University of Mersin, Mersin, Turkey in 2019. She is currently pursuing a Ph.D. degree in chemical engineering at Mersin University, Mersin, Turkey. From 2017 to 2019, she was a researcher with the TUBITAK industry-focused research project about developing the drug nano formula that supports the immune system in Mersin University and Izmir High Technology Institute. Her research interests include the development of nanoformulations for biomaterials using green and sustainable methods and their applications in tissue engineering and the development of innovative applications with electrospinning methods for tissue engineering.



Burcu Sakım was born in Mersin, Turkey in 1994. She graduated from Eskişehir Osmangazi University, Faculty of Engineering and Architecture, Department of Chemical Engineering in 2018. Since 2019, She has been doing her master's degree in Chemical Engineering at Mersin University, Institute of Science. Her research interests are the production of multi-layer tissue scaffolds in tissue engineering, cryogel production by cryogelation method, and nanofiber production technology by electrospinning method.



Ashok Vaseashta is CEO/CTO and Executive Director for research with the International Clean Water Institute in Virginia, USA. He also serves as a Professor at Riga Technical University, Chaired Professor of Nanotechnology at the Academy of Sciences of Moldova, Academician at Euro-Mediterranean Academy of Arts and Sciences, and a Senior Strategic Research Advisor for several organizations. Inspired by nature and guided by societal necessities, he strives for technological innovations to address the global challenges of the twenty-first century. His research interests include CBRN defense, critical infrastructure safety and security, and environmental sustainability—all using nexus of advanced technological solution platforms. He is a scholar, visionary, strategist, and dedicated futurist providing strategic leadership to promote and advance research initiatives and priorities using data-driven decisions. He received Ph.D. from the Virginia Polytechnic Institute and State University, Blacksburg, VA in 1990 followed by Kobe post-doctoral fellowship. Following his Ph.D., he served as a professor and researcher at Virginia Tech and Marshall University. He also served as the Director of Research at the Institute for Advanced Sciences Convergence and International Clean Water Institute for Norwich University Applied Research Institutes, Vice-Provost (Rector) for Research in South Carolina, Visiting

Professor at the 3 Nano-SAE Research Centre, University of Bucharest, Romania and Visiting Scientist at the Helen and Martin Kimmel Center of Nanoscale Science at the Weizmann Institute of Science, Israel. He served the U.S. Department of State in two rotations, as strategic S&T advisor in the Bureau of International Security and Nonproliferation, Office of Weapons of Mass Destruction and Terrorism, and U.S. diplomat. His research interests span foresight, nanotechnology, environmental/ecological science, and critical infrastructure safety and security. He is the author/editor of 11 books and has published over 300 articles in scientific journals, book chapters, and conferences. He serves on editorial boards of several international journals and is an active member of various professional organizations.

Chapter 2
Fabrication Methodologies of Multi-layered and Multi-functional Electrospun Structures by Co-axial and Multi-axial Electrospinning Techniques



Marjan Hezarkhani, Nargiz Aliyeva, Yusuf Ziya Menceloglu, and Burcu Saner Okan

Abstract Electrospinning emerges as a simple, cost-effective, and highly versatile method used for mass fabrication of continuous ultrafine fibers with the diameter changing from micron- to nanoscale using various polymer types and their blends. Recently, multi-axial electrospinning technique incorporating additional walls in electrospun fiber structures in a single-step process resulted in new generation fibers with unique architecture and morphology. The arrangement of multi-axial spinneret consequences the development of multi-material fibers and other dimensional structures with core/shell, a hollow and side-by-side skeleton which have an uncountable preponderance compared to monolithic structures obtained by conventional electrospinning. These nonwoven multifunctional electrospun structures can gain extra functionality, porosity, chemical stability, and mechanical robustness by adding core and sheath materials, in various applications such as tissue engineering, drug delivery, filtration, smart textiles, energy storage, and conversion systems. This chapter covers the procurement of multiple core-sheath electrospun fibers and other dimensional structures by co-axial, tri-axial, and side-by-side electrospinning techniques with emphasizing fiber development comprehensively. By providing current developments in the aspect of used techniques, this chapter also provides an understanding of a suitable selection of ideal composition and adjustment of the dimension and configuration of structures during the electrospinning process by considering the end application.

M. Hezarkhani · N. Aliyeva · Y. Z. Menceloglu · B. Saner Okan (✉)
Integrated Manufacturing Technologies Research and Application Center, Composite Technologies Center of Excellence, Sabanci University, Teknopark Istanbul, 34906 Pendik, Istanbul, Turkey
e-mail: burcu.saner@sabanciuniv.edu

N. Aliyeva · Y. Z. Menceloglu · B. Saner Okan
Faculty of Engineering and Natural Sciences, Sabanci University, Orhanli, 34956 Tuzla, Istanbul, Turkey

© The Author(s), under exclusive license to Springer Nature Switzerland AG 2022

A. Vaseashta and N. Bölgen (eds.), *Electrospun Nanofibers*,
https://doi.org/10.1007/978-3-030-99958-2_2

Keywords Core/shell electrospinning · Multifunctionality · Multi-axial electrospun structures · Hollow fibers · Janus fibers

2.1 Introduction

The electrospinning technique is a system based on the use of electrostatic forces to generate continuous nonwoven fibers [1]. In the late 1890s, the electrospraying process was turned into an electrospinning [2]. To build a basic electrospinning set-up on a laboratory scale, there are three main components a syringe pump, a high voltage supply, and the collector as simply as a sheet of aluminum foil. In this simple set-up, a polymer solution spins out of the tip of the syringe while high voltage is applied, and a fiber mat is deposited randomly on top of the collector. In addition to the electrospinning apparatus designed for research purposes in the laboratories, pilot devices for industrial applications can be found in the market for mass production of electrospun fibers [1].

In addition to a conventional electrospinning system, there is possibility to increase nozzle and needle number. This provides to produce multifunctional and multi-materials nano- and micron-scale structures for various applications. In multi-axial needle, two or more different concentric needles with different diameters are located one into another. By using a multi-axial nozzle, electrospun fibers can be formed as core/shell, hollow fiber, and side-by-side formed fibers. Multi-walled nonwoven fibers and hollow fibers in the scale of micron and nano-size cannot be produced through conventional methods such as single-axial electrospinning [1]. The spinning process of nanofibers produced by the electrospinning technique allows a planned formation of pores in the web structure and gives fibers with an exceptionally large active surface area on fibers. The hollowness and fiber structures of multi-axial electrospun nano/micron size fibers with different inner and outer diameters can be controlled by using several polymer solutions and different layers of polymers to control the fiber structure. In other words, nano- and micron-size hollow fibers with a multi-layer complex structure such as multifluid, core/shell, side-by-side fiber are possible to produce by co-axial and multi-axial electrospinning. Table 2.1 summarizes types of polymers, additives and electrospinning techniques used to fabricate of different types of structures. In general, the fabrication of individual fiber networks or webs with the planned or random fiber arrangement as well as nanoparticle doped fibers is possible by using either single or multi-axial electrospinning [2]. Also, natural or synthetic polymers and copolymers can be used for fiber or spherical structure production. These produced electrospun structures can be utilized in different fields such as textile industry [3] for producing shielding fiber, agrotextiles, most of all medical textiles [4] and membrane development for water treatment [5]. This approach can also be used in the production of photovoltaic cells and batteries [6].

Table 2.1 Summary of different types of electrospun structures by applying various types of electrospinning methods

Polymers	Solvent system	Additives	Electrospinning technique	Structure type	Refs.
PEO/PEO PEO/PDT PEO/PSU	Water + ethanol Water + ethanol/chloroform Water + ethanol/chloroform	Bromo-phenol and palladium(II) acetate	Co-axial	Core/shell fiber	[7]
Chitosan/PEO	Aqueous acetic acid	–	Co-axial	Core/shell fiber	[8]
Cellulose/PEO CA/PEO	NMMO.H_2O/DMF Acetone + DMAc/water	Cisplatin, NaCl and propyl gallate	Co-axial	Core/shell fiber	[9]
PI-b-PDMAEMA/PAN	Hexane/DMF	–	Co-axial	Helical core/shell fiber	[10]
PCL/PCL	TFE + hexane	FePt	Co-axial	Core/shell fiber	[11]
PAN/PAN:PS	DMF	Si and C	Co-axial	Core/shell fiber	[12]
CA	Ethanol + acetone + DMAc	Acyclovir	Tri-axial	Tri-layer fiber	[13]
CA/PVP:KET CA:KET/CA/PVP:KET	Ethanol + acetone + DMAc	Methylene blue	Co-axial and tri-axial	Core/shell and tri-layer Core/shell fiber	[14]
Gelatin/PCL/Gelatin	TFE/water	–	Tri-axial	Tri-layer fiber	[15]
PLGA Gelatin/PLGA PCL/Gelatin/PLGA	HFP	Rhodamine-b and fluorescein isothiocyanate	Single axial Co-axial Tri-axial	Mono-layer Core/shell Tri-layer fiber	[16]
PS TPU PS/TPU PS/TPU/PS	DMF THF DMF/THF DMF/THF/DMF	–	Single e-spin Single e-spin Co-axial Tri-axial	Mono-layer Mono-layer Core/shell Tri-layer fiber	[17]

(continued)

Table 2.1 (continued)

Polymers	Solvent system	Additives	Electrospinning technique	Structure type	Refs.
PAN	DMF	–	Co-axial	Hollow fiber	[18]
PAN	DMF	$Al(NO_3)_3$	Single axial	Mono-layer Porous hollow fiber	[19]
PVP	Ethanol	$Ti(OiPr)_4$	Co-axial	Hollow fiber	[20]
PVP	Ethanol + DMF	$SnCl_2 \cdot 2H_2O$	Co-axial	Core/shell Hollow fiber	[21]
PVP	Ethanol	Silicalite-1	Co-axial	Hollow fiber	[22]
PAAm/PS PAAm/PMMA	DMF/THF/EA	–	Tri-axial	Multi-layer hollow fiber	[23]
PU/PAN	THF/DMF	–	Side-by-side	Janus fiber	[24]
PVP	Ethanol	Fe_3O_4 and $Tb(BA)_3phen$	Side-by-side	Janus fiber	[25, 26]
PAN/PVP	DMF/ethanol	Rhodamine-b and Coumarin-6	Side-by-side	Janus fiber	[27]
PVP/EC	Ethanol + acetic acid	CIP and AgNP	Side-by-side	Janus fiber	[28]
PVP/PMAA-co-PMMA	Ethanol + DMAc	Rhodamine-b and 8-Anilinonaphthalene-1-sulfonic acid	Side-by-side	Janus fiber	[29]
PVP	Ethanol + acetic acid	$Ti(OBu)_4$, $V(acac)_3$ and $Sn[CH_3(CH_2)_3CH(C_2H_5)CO_2]_2$	Side-by-side	Janus fiber	[30]
PPy/PVP	Ethanol + DMF	$FeCl_3$	Side-by-side	Janus fiber	[31]

(continued)

Table 2.1 (continued)

Polymers	Solvent system	Additives	Electrospinning technique	Structure type	Refs.
PEO/PVP PVP/PEO:PANI PEO/PVP:PANI PEO/PEO:PANI PVP/PVP:PANI PEO:PANI/PVP:PANI	Chloroform + DMF	–	Side-by-side	Janus fiber	[32]
PLG	DCM	Rhodamine-b	Spraying	Sphere	[33]
PEO	Distilled water	NaCl	Single-axial	Beaded fiber	[34]
PAN	DMF	Pt deposited TEGO	Co-axial electrospinning and electrospraying	Foam, fibers, and spheres	[35]
PAN	DMF	Si	Electrospinning and electrospraying	Sphere and fiber	[36]
PAN PS PMMA	DMF	TEGO	Tri-axial and core/shell electrospraying	Sphere	[37]
PS	THF	–	Single-axial	Beads	[38]
PS/PCL PMMA/PCL	Chloroform	Coumarin-6 and Rhodamine-b	Co-axial	Core/shell sphere	[39]
PS	DMF	–	Electrospraying	Sphere	[40]

2.2 Electrospinning Techniques for the Fabrication of Multi-material and Hollow Fibers

Multi-axial electrospinning offers to control the hollowness, wall number and size of the structures [41]. The multi-walled structure, surface morphology, and diameter of the fibers are tailored by controlling needle number and its diameter, polymer and solvent types, solution concentration, miscibility, and its evaporation rate. In addition, also system parameters like voltage, flow rate, working distance, humidity and pressure are effective parameters [4]. In co-axial and multi-axial electrospinning process, two types of spinnable polymer solutions as outer and inner layers of fibers with different viscosities and different polarities are adjusted in order to prevent the diffusion of each electrospun solution into each other and get a well-ordered electrospun structure. On the other hand, side-by-side electrospinning set-up having a nozzle consisting of split outlets running side-by-side provides the coverage of two different materials running from two different nozzles at the nozzle outlet and this process can be advantageous over the core/shell or tri-axial processes due to its capability to interact with surrounding equally. In this chapter, the main development of electrospinning from mono-axial fiber formation to double-fluid by using co-axial and side-by-side, and to tri-fluidic by using tri-axial electrospinning techniques are discussed in detail.

2.2.1 Multi-axial Electrospinning Methods

For the production of 3D multi-walled hollow fibers through a single-step process, there are multi-axial electrospinning set-ups such as co-axial and tri-axial methods to provide gives the possibility of inserting any spacer between the layers without applying any post-treatment [7]. Having a multi-walled structure consolidates the framework of the fiber by preventing from its deformation. A successful formation of two-walled fibers is possible by tailoring polymer solution and processing parameters intently [42].

One of the main distinctions between single- and multi-axial electrospinning set-up is the shape of their spinneret. Multi-axial spinneret contains two (co-axial) or more (tri-axial) nested needles placed into each other by changing diameter size. Figures 2.1 and 2.2 show the schematic representations of co- and tri-axial electrospinning spinnerets, respectively. The multi-axial nozzle gives the possibility of core/shell and hollow fiber formation. Moreover, using of three different polymer solutions with a nozzle with three nested needles increases the functionality of the electrospun fibers having a unique morphology and architecture [41].

The working principle of multi-liquid electrospinning is mostly similar to single-liquid electrospinning since the factors such as polymer molecular weight, solution concentration, flow rate, applied voltage, and the distance between nozzle and collector are needed to optimize during the process [43]. There are a variety of

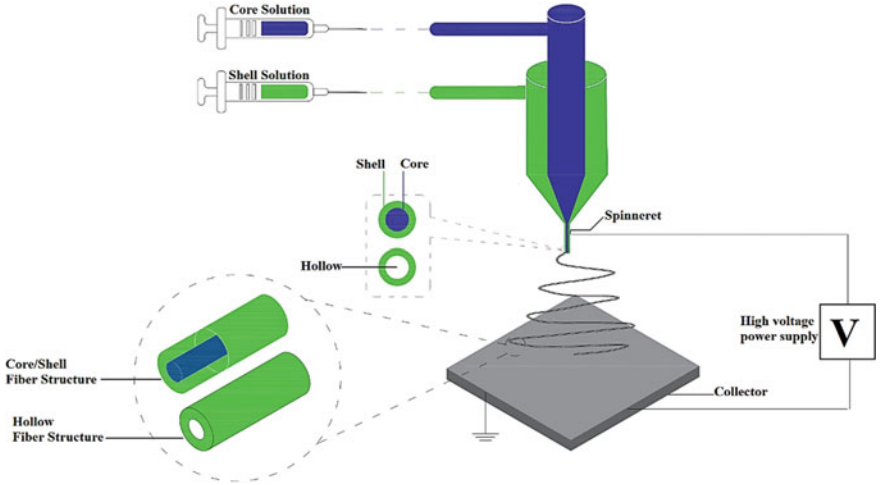


Fig. 2.1 Schematic representation of co-axial electrospinning set-up

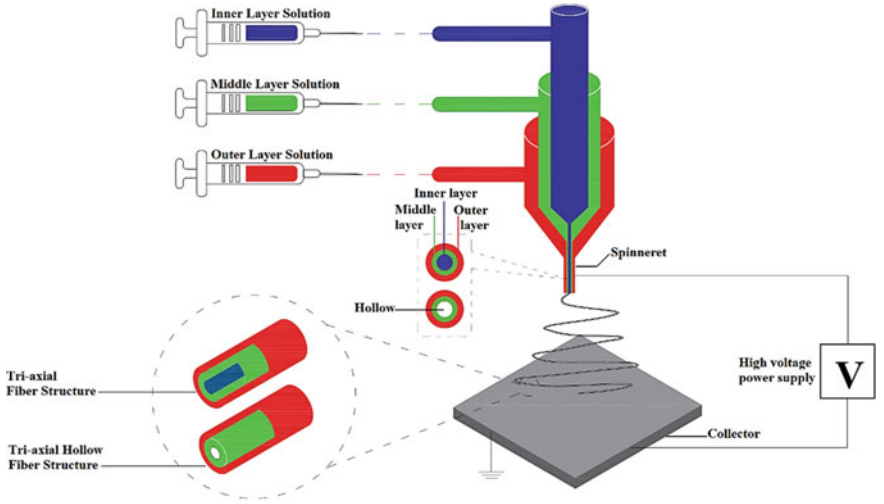


Fig. 2.2 Schematic representation of tri-axial electrospinning set-up

synthetic and natural polymers used for the fabrication of electrospun nanofibers. For instance, Dror et al. [44] fabricated bio-based microtubes fiber by using co-electrospun biocompatible and biodegradable polymers such as poly(ethylene oxide) (PEO) and poly(ε-caprolactone) (PCL). The polymer type and its solvent are essential in adjusting the fiber composition by using two different liquids. In a multi-axial electrospinning set-up, there are two fluid interfaces: the liquid–liquid interface between two polymer solutions, and the liquid–gas interface between air and sheath solution.

Also, it is important to select ideal solvent systems for the multi-axial process and prevent their diffusion through each other during electrospinning process. Therefore, the rate of evaporation or solvent solidification is taken into consideration designing the solvent systems. If two solvents have similar solidification rate or just sheath liquid system is electrospinnable, a stable co-flow spinning can be achieved [43]. There is a possibility of needle clogging or separation of the two liquids if one of the solvents evaporates much faster than the other solvent due to not having a similar rate of solidification leads to the separation of core and shell layers of fibers. The properties of the sheath and core chosen solvents confirm the charge distribution in the electrospinning jet of the multi-axial equipment [45]. In multi-axial electrospinning, the charge is located at the interface of air, and the charge in liquid forming the Taylor cone triangle at the tip of the nozzle. Furthermore, the conical shape (Taylor cone phenomenon) of the sheath droplet is due to the charge-charge repulsions resulting in stretching and elongations of the droplet on the tip of nozzle. Since the accumulated charge reaches a certain level by increasing the applied voltage, a suitable jet extends out of the cone, thereby generating stress on the outer layer solution on the tip of the multi-axial nozzle that shears the core solution due to the contact fraction and the viscose dragging and thus the conical formation at the nozzle tip [42]. The hollowness and core/shell fiber formation achieved by using the tri-axial nozzle were monitored by the generation of Taylor cone under different applied voltages changing in the range of 0–30 kV by using high-speed camera which is illustrated in Fig. 2.3. In this fiber structure, polyacrylamide (PAAm) polymer solution was selected as a middle layer and polymethyl methacrylate (PMMA) solution was used for the sheath material and the structural integrity was attained by getting an ideal voltage [46].

Optimization of the interfacial compatibility between two different solvents is an essential part of co-axial and multi-axial electrospinning process to obtain the desired structure and provide nano and micro size homogenous core/shell fibers [47]. At this point, the flow rate is another parameter that is needed to adjust homogenous structures. For instance, the slower flow rate of shell solution can lead to the formation of larger core diameter [48]. On the other hand, high flow rates used in core solution causes the deformation in the structure and prevents the coverage of sheath material and also encapsulation. To conclude, adjusting of flow rate ratios for a designed experiment brings about the production of core and shell parts [49].

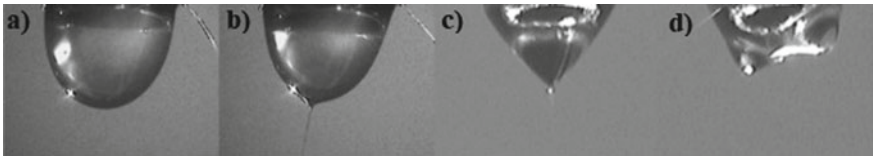


Fig. 2.3 Taylor cone formation consists of PAAm as a middle layer and PMMA as an outer recorded by a high-speed camera **a** no voltage, **b** 10 kV, **c** 20 kV, and **d** 30 kV [46]. Reproduced with permission of Elsevier

2.2.2 Side-by-Side Electrospinning Technique

One of the widely used electrospinning techniques for the fabrication of nano/micro-scale is side-by-side system. In this technique, the obtained fiber is called Janus the name of the ancient Greek God having two faces peering into the past and future. As Janus God, Janus fibers have two different polymers on two sides [50]. Side-by-side electrospinning method used for manufacturing Janus fibers is shown in Fig. 2.4 schematically. The split nozzle used in this method consists of a separate outlet working side-by-side. The nozzle has two syringes arranged in a side-by-side configuration for electrospinning the solutions. Electric field and the distance between nozzle tip and the collector are two major factors in creating Janus fibers. While electric field strength is insufficient at a long distance, two separate Taylor cones are formed at a very close distance [51]. Therefore, the main challenge in this electrospinning set-up is to make two fluids that move simultaneously under the same electric field [52]. An optimum distance between the nozzle tip and the collector is needed to maintain a steady single electrospinning jet. It is possible to produce Janus fibers with various widths and interface areas by controlling the electrospinning parameters while utilizing different spinneret design [53]. The desired properties of the fibers are attained by selecting suitable spinneret as well as controlling the behavior of the fluids under the electrical field [54]. The main advantage of these kinds of fibers is the direct contact with the medium of each component [55]. Consequently, there are several advantages of side-by-side technique including easy control over geometry and the channel dimensions, fabrication flexibility, and the potential of multiplexed nanofiber within a single microfluidic electrospinning device.

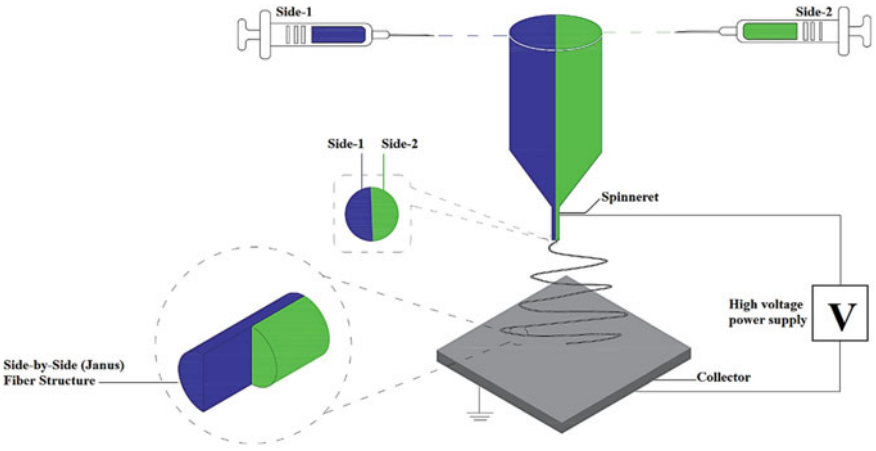


Fig. 2.4 Schematic representation of side-by-side electrospinning set-up

2.3 Development of Nano/Micro and Multi-material Electrospun Hollow Fiber Structures

Controlling fiber diameter and hollowness are managed to control the characteristics of electrospun structures. The multi-fluid electrospinning technique was introduced by Sun et al. [7] for the first time in 2003 to increase the mechanical and chemical properties of single-layer formed nanofibers using PEO in dimethylformamide (DMF) and poly(dodecylthiophene) (PDT) in chloroform. This technology gives the possibility of manufacturing 3D core/shell and hollow fibers made of different pairs of polymers and doped nanomaterials [56]. Multi-fluidic electrospinning can encapsulate the non-spinnable materials such as polymers, copolymers, and nanoparticles by using a spinnable shell polymer to form spheres or continuous fibers. The production of continuous nanotubes is even possible with this approach [57, 58]. In the literature, there are different attempts to fabricate the core/shell, hollow and Janus fibers by applying co-axial, tri-axial and side-by-side electrospinning techniques. All the details in terms of materials, method and structure type are discussed in this section. The schematic image of the development of electrospun core/shell, hollow and Janus fibers from monolithic to multi-layer processes is given in Fig. 2.5.

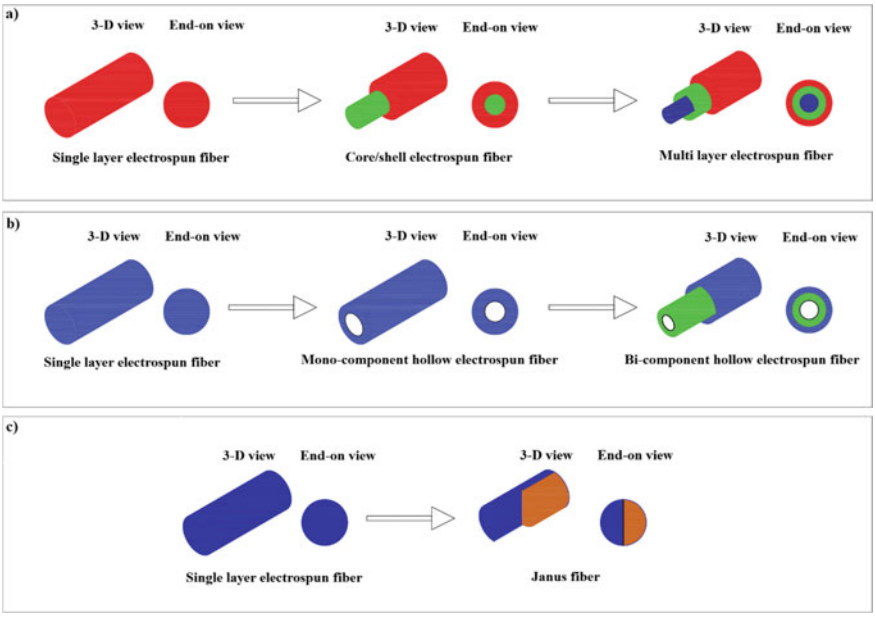


Fig. 2.5 Schematic representations of electrospun fibers formation development **a** from a single-layer to multi-layer core/shell fiber, **b** from a single-layer to multi-walled hollow fiber, and **c** from a single-layer to Janus fiber

2.3.1 Fabrication of Core/Shell Fibers

Core/shell fibers are developed by using multiple needles at the spinneret and ejecting several solutions simultaneously by using custom design co- and multi-axial electrospinning systems. In this section, the development of multi-fluid core/shell fibers produced by co- and tri-axial processes is discussed by evaluating the recent studies.

2.3.1.1 Multi-fluidic Core/Shell Fibers Produced by Co-axial Technique

Recently, co-axial electrospinning has made significant progress and attracted great attention to produce core/shell 3D structures with numerous functionalities to modify fiber characteristics such as isolating and releasing substances, and to improve its mechanical properties [42]. The co-axial electrospinning method is superior to fiber structures fabricated by using a regular single-axial electrospinning technique [7]. As mentioned before, co-axial nozzle set-up contains two concentrated tubes the inner and the outer shell of the spinning nozzle. The two different polymer solutions flow through these tubes under high voltage condition applied between the polymer solution droplet at the tip of the nozzle and the collector [42].

After the first introduction of core/shell fiber production using electrospinning, there is intense research on these developments. For instance, Basavaraja et al. [59] fabricated core/shell composite nanofibers for Li-ion batteries as an anode electrode by using reduced graphene oxide and polyacrylonitrile (PAN) solution as the fiber shell and zinc oxide with PMMA as the fiber core solution. Moreover, several investigations have shown that electrospun membranes possess attractive properties such as good tensile strength, high surface area and high porosity due to their porous structure making them suitable for filtration applications [60–62]. In another work, Kao et al. [63] fabricated core/shell PAN/polybenzoxazine (PBA) electrospun nanofibers with uniform fiber size and improved their physical and chemical properties by tailoring the diameters in the range of 250–1290 nm through varying core solution concentration (PAN/DMF) between 8 and 12 wt%. Furthermore, Pakravan et al. [8] produced a simple core/shell nanofiber with a diameter of 150–190 nm from PEO and chitosan dissolved in aqueous acetic acid solvent, as the inner and outer layer, respectively, to be used in the purification of blood in biomedical field. The structure of the nanofibers confirmed by transmission electron microscopy (TEM) is shown in Fig. 2.6.

Although most of the produced electrospun nanofibers have a simple linear fibrous shape, there are few attempts to generate distinct types of fibers. In one of the studies, Absar et al. [9] synthesized hierarchically branched fibers by using an anti-cancer drug named cis-diammineplatinum (II) dichloride (cisplatin) as the core material into three different shell structures namely, cellulose, cellulose acetate (CA), and PEO. As seen in Fig. 2.7, Kamperman et al. [10] manufactured a continuous core/shell electrospun nanofibers using poly(isoprene-block-dimethylamino ethyl methacrylate) (PI-b-PDMAEMA) block copolymer as the core and PAN as the shell. The chemical structure of the core suing PI-b-(PDMAEMA/poly(ureamethylvinyl)silazane

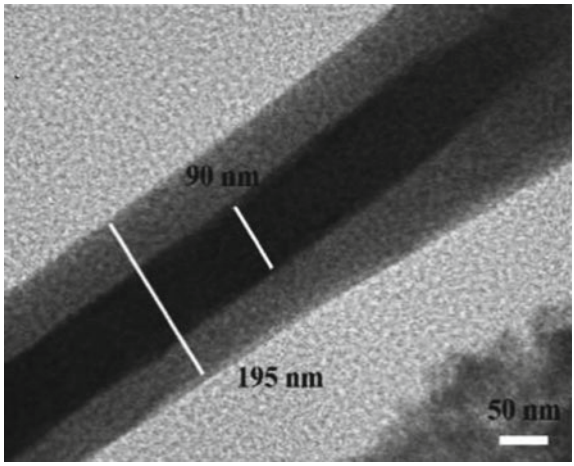


Fig. 2.6 TEM image of PEO/chitosan nanofiber produced by co-axial electrospinning [8]. Reproduced by the permission of American Chemical Society

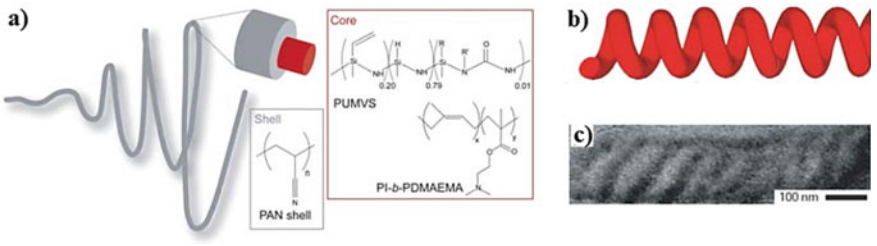


Fig. 2.7 **a** A schematic representation of the chemical structure of core (PI-b-PDMAEMA/PUMVS) and shell (PAN) layers, **b** a schematic representation of a helical morphology of core/shell electrospun nanofiber, and **c** TEM image of nanofiber cut parallel to the fiber axis consistent with a helical morphology [10]. Reproduced with the permission of The Royal Society of Chemistry

(PUMVS)) and the shell (PAN) layer, and the helical shape and ordered morphology of the produced fibers are given in Fig. 2.7. It is not possible to produce these kinds of helical forms by using bulk polymerization or other chemical techniques.

Incorporating of non-polymeric nanoparticles such as ceramic, metallic, metal oxides, and carbon materials into nanofibers have been investigated for different applications. In a research, the mechanical, and magnetic properties of the nanofibers were improved by the combination of iron–platinum (FePt) nanoparticle as the core and PCL as the shell via co-axial electrospinning technique [11]. In another work, Zhang et al. demonstrated the fabrication of core–shell silicon/carbon (Si/C) fibers with internal honeycomb-like carbon structures by a double coaxial electrospinning technique used as anode electrode of lithium-ion batteries [12]. PAN was used in both inner and shell parts of fibers, and calcination and carbonization steps were applied to increase the conductivity of the designed structure. The structural design of hierarchical porous core/shell Si/C composite fibers by indicating charge and

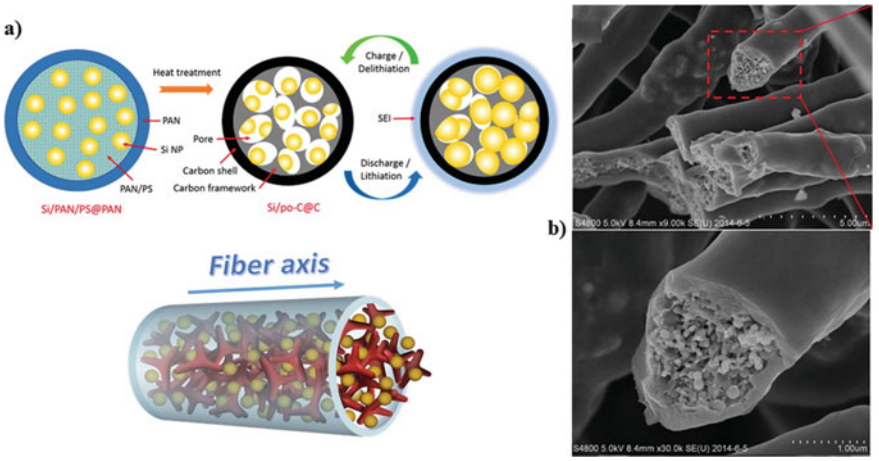


Fig. 2.8 **a** Structural formation and transformation of Si/porous C@C during heat treatment and cycling process, respectively, and **b** SEM images of cross-sectional core/shell Si/C fibers [12]. Reproduced with the permission of Royal Society of Chemistry

discharge processes is given in Fig. 2.8 by providing SEM images of cross-sectional core/shell Si/C fibers [12].

2.3.1.2 Multi-fluidic Core/Shell Fibers Produced by Tri-axial Technique

The major focus of the tri-axial electrospinning method is to encapsulate functional materials as an extra intermediate layer, and thereby preserving the encapsulated materials and increasing their lifetime. By utilizing the tri-axial electrospinning technique, multifunctional core/shell nanostructures are produced for various applications such as drug delivery, catalysts, filtration, and energy storage [64]. Especially most of the studies are focused on drug delivery. In one of the studies, Wang et al. produced core–shell nanofibers having drug reservoirs with an improved drug sustained release profile by applying tri-axial electrospinning process was successfully conducted to build into the for producing tri-layer nano depots [13]. Figure 2.9a depicts pumping a pure drug solution as an inner fluid to get a drug reservoir encapsulated in tri-axial fibers schematically. TEM images in Fig. 2.9b, c show the differences of core/shell and triaxial fibers in terms of elements, density and thickness. As seen in SEM images in Fig. 2.9d, e, after the drug release test, gaps appeared in the fiber structure, thereby indicating a successful release of the intended drug. In a similar study belonging to Yang et al. [14], tri-layer core/shell nanofibers were developed with discrete drug distributions by using cellulose acetate as a key filament-forming polymeric matrix and ketoprofen (KET) as a model drug in order to provide dual-stage release of the loaded drug.

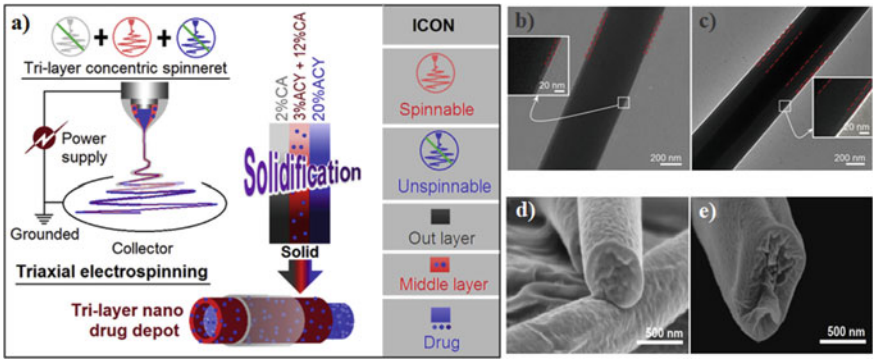


Fig. 2.9 **a** Schematic presentation of the preparation of tri-layer nanodepot fiber, TEM images of **b** core/shell fibers and **c** tri-layer nanodepots, and SEM images of **d** nanodepot nanofiber and **e** nanodepot residue after drug-releasing performance [13]. Reproduced with the permission of Elsevier

Kalra et al. [65] applied a tri-axial electrospinning technique to produce fibers with an intermediate layer of block-copolymers with self-assembly functionality flanked between the shell layers of thermally stable silica and the core. This hierarchy allowed the post-fabrication annealing of the fibers to obtain equilibrium self-assembly without destroying the initial morphology of the fibers. In another study, tri-axial nozzle electrospinning was used to produce biodegradable core/shell nanofibers where outer and inner walls were made of poly(ε-caprolactone), and gelatin was utilized as the middle wall to provide sufficient strength to support developing tissues. The microstructural comparison of tri-axial electrospun nanofibers with core/shell structures revealed that the presence of a third layer allowed the development and improvement of functional tissue scaffolds for wound healing and drug delivery applications. Moreover, it was shown that a sustainable drug release for long-term treatments and a quick-release for short-term treatments could be obtained simultaneously due to the core and outer walls, respectively [15]. FIB-SEM images of the tri-axial core/shell form of the produced nanofibers in this study are represented in Fig. 2.10.

In addition to drug delivery applications, core/shell structures are promising materials as an electrode used in energy storage and conversion applications and also higher capacitance values can be achieved by the integrating of carbon nanoparticles in the electrode structure [66–68]. Herein, graphene is a widely preferred 2D carbon material owing to its fast electron mobility and high electrical conductivity. For instance, Haghighi Poudeh et al. [69] attained 3D urchin-shaped free-standing composite electrodes by incorporating single- and multi-layer graphene oxide and manganese oxide (Mn_3O_4) in the presence of PAN polymer during the core/shell electrospinning process and then carried out carbonization and coating by polyaniline (PANI) processes to get higher capacitance. The stepwise procedure for single graphene nanoplatelets (GNP) is given in Fig. 2.11a. Each step for carbon composite

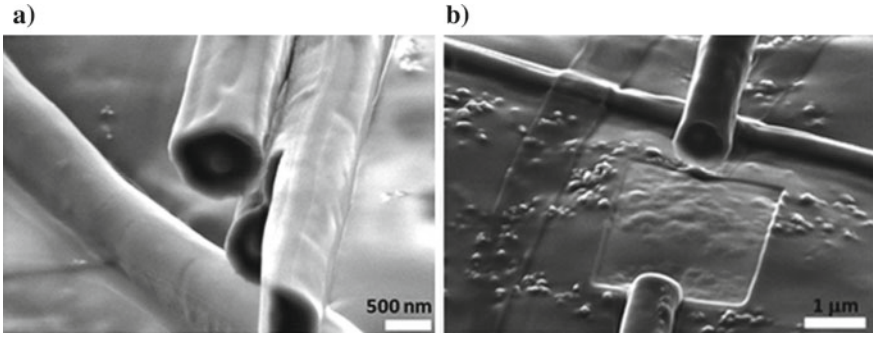


Fig. 2.10 **a** and **b** FIB-FESEM images of triaxial electrospun nanofibers at two disparate magnifications [15]. Reproduced with permission of American Chemical Society

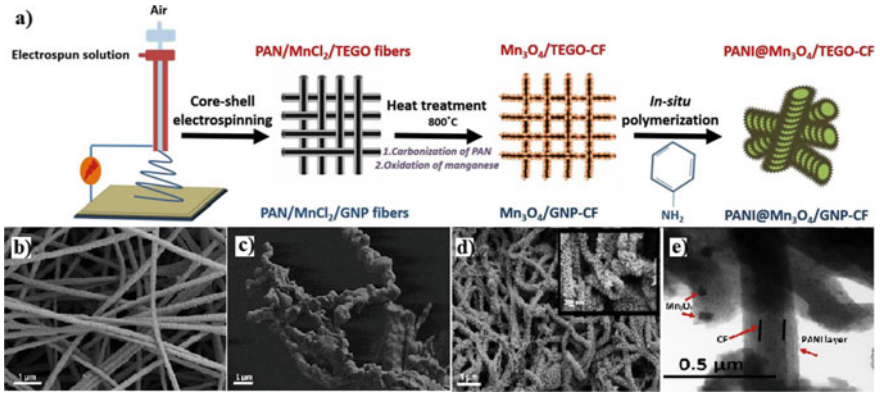


Fig. 2.11 **a** Preparation route of PANI coated Mn_3O_4/graphene embedded CF, SEM images of **b** electrospun PAN/$MnCl_2$/GNP fiber and **c** carbonized Mn_3O_4/GNP-CF fiber, **d** SEM image and **e** TEM image of PANI@Mn_3O_4/GNP-CF after PANI coating [69]. Reproduced by the permission of Wiley

electrode formation was monitored by SEM and TEM analysis as seen in Fig. 2.11b–e. Regarding the morphological results, GNP-based fibers led to more a uniform structure since inner and outer layers were detected by TEM analysis and structural integrity was provided by using core/shell electrospinning.

Additional layers in electrospun structures can improve their mechanical properties and increase their stiffness. In one of the work done by Nagiah et al. [16], tripolymeric triaxially electrospun fibrous scaffolds were fabricated by using PCL as a core material, a 50:50 poly (lactic-co-glycolic acid) (PLGA) as a sheath material and gelatin as an intermediate material. According to DMA analysis, a sharp increase in elastic modulus was achieved with this composition, the elastic modulus of tri-axial electrospun fiber (89.66 MPa) was increased when compared to that of uniaxial PLGA (50:50) (21.16 MPa) and coaxial PLGA (50:50) (sheath)-gelatin (core)

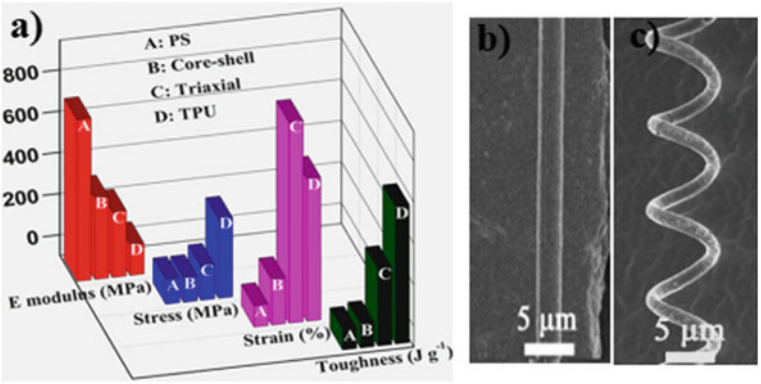


Fig. 2.12 **a** Tensile test results of PS, PS/TPU, PS/TPU/PS and TPU fibers, SEM images of **b** tri-layer fiber during elongation and **c** its spring morphology after the tensile test [17]. Reproduced with the permission of American Chemical Society

fibers (13.78 MPa). Moreover, Jiang et al. [17] reported the formation of tri-layered one-dimensional polymeric fibers by using elastomeric thermoplastic polyurethane (TPU) as an intermediate layer and attained the toughness of >270 J g^{-1} and 300% elongation without any cracks of this tri-axial structure in comparison to toughness of <0.5 J g^{-1} and elongation at break of <5% of single polystyrene (PS) fibers. Tensile test results of these produced fibers were compared by considering modulus, stress, strain and toughness parameters as seen in Fig. 2.12a. Morphological changes of triaxial fiber during elongation and its spring morphology after the tensile test are observed using SEM images given in Fig. 2.12b, c. Consequently, a multi-layer structure obtained by tri-axial electrospinning process is gained multifunctionality and enhanced the characteristics regarding the targeted applications.

2.3.2 Hollow Fibers Produced by Multi-axial Techniques

Nano and micron-scale hollow structured fibers with exceptional properties such as high specific surface area, tunable structure, and low-density properties have found considerable in the applications related to the pervaporation, water filtration, gas separations, and dialysis [18] in the membrane development industry [70] as well as in catalysis [71], photonics [72] and drug delivery [73]. Multiaxial concentric electrospinning provides the possibility of producing hollow fibers with the diameter range changing from a few micrometers to a nanometer (less than 100 nm) [18]. It is possible to produce hollow fibers by conventional and multi-axial electrospinning processes. Bognitzki et al. [74] reported the fabrication of a template polymeric nanofiber material by conventional electrospinning followed by a coating with a wall material through a deposition technique, and then removing the template material by a suitable solvent to obtain hollow fibrous structures. This procedure works properly

for manufacturing hollow fibers of alumina [19], silica [75], and titanium dioxide [58]. However, this method has some drawbacks due to its limiting factors such as the selection of ideal material systems, coating, and the removal of the template.

On the other hand, the multi-axial (co-axial and tri-axial) electrospinning process can to produce hollow structures in a direct manner [46]. The principal mechanism behind the formation of hollow fibers is based on the evaporation of the inner solution (core solution) out of the shell layer. An immiscible or poorly miscible solvent pumps through the inner nozzle which prevents mixing of the polymer solution and combining the outer shell of the hollow fiber while electrospinning [42, 76]. The solidification or gelation polymerization that occurs at the interface of immiscible solvent in the core part of the structure and its adjacent outer layer ensures the production of a hollow fiber. Some works are focusing on the using of innocuous solvents like olive oil, paraffin and glycerol as a core liquid encapsulated by polymeric shells [57, 77, 78]. For instance, Di et al. [22] used two immiscible solutions a suspension of PVP and zeolite nanoparticles in an ethanol solution as an outer fluid and paraffin oil as a core material, and obtained zeolite hollow fibers with a hierarchical structure. In another study, paraffin was pumped as an inner fluid and a solution of PVP polymer and stannous chloride dihydrate ($SnCl_2 \cdot 2H_2O$) was used as an outer fluid to obtain stannic oxide (SnO_2) hollow fibers. The fibers' diameters were reported in the range of 400–750 nm [21]. In a similar work, Li and Xia [20] employed co-electrospinning of PVP and titanium tetraisopropoxide solution in ethanol as a shell fluid and mineral oil as a core material. The subsequent extraction of oil by octane followed by the calcination process was resulted in the formation of hollow titania fibers. TEM images of the hollow fibers doped TiO_2, and SEM images of the uniaxial array of hollow fibers electrospun via co-axial technique are represented in Fig. 2.13.

Besides the techniques mentioned above for single-layer hollow fiber formation, novel hollow carbon nanotubes were fabricated by removing of the core material from core/shell PMMA/PAN electrospun fibers. In this method, the elimination of core material was accomplished by the degradation of PMMA followed by carbonization of PAN by applying heat treatment under an inert atmosphere at 1000 °C [57].

Instead of the coaxial electrospinning process, it is also possible to attain multi-wall hollow fibers by using tri-axial nozzle system. With these three or more layered fibers, the hollowness and functionality of electrospun structures can be managed

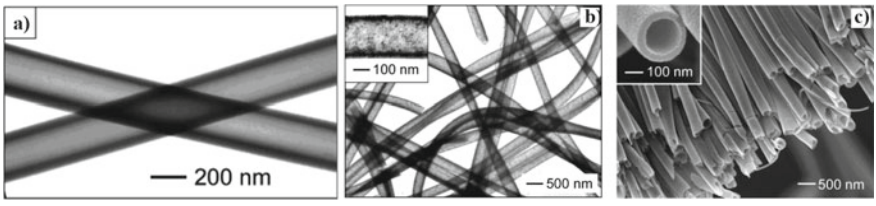


Fig. 2.13 TEM images of electrospun hollow fibers **a** after oily core extraction with octane, and **b** doped TiO_2, and **c** SEM image of a uniaxially array of hollow fibers [20]. Reproduced with permission of American Chemical Society

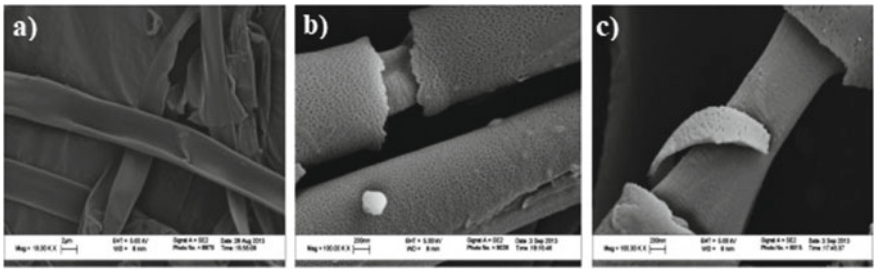


Fig. 2.14 SEM images of multi-walled hollow fibers with PMMA-*co*-PS as an outer layer and PAAm as an inner layer prepared by using different solvents **a** ethyl acetate, **b** and **c** THF [46]. Reproduced with permission of Elsevier

such as gaining multi-functionality and getting high mechanical integrity with the addition of electrospun polymer layer [41]. Zanjani et al. adjusted the hydrophilicity of inner and outer layers' solutions by using various solvent systems to obtain a two-walled/layered hollow fiber structure with a sharp interface through a direct, one-step tri-axial electrospinning process [46]. In this study, they used poly(methyl methacrylate-co-styrene) as an outer layer by dissolving in EA/THF and PAAm as a middle layer and stated that EA caused the separation of layers whereas THF led to the elongation of the fibers and provided a proper connection between outer and inner layers as seen in Fig. 2.14. These hollow two-walled electrospun fibers can be used as promising materials in structural composites [35], dialysis membranes [70], catalysis [71], photonics [72], and drug delivery [73] technologies. In one of the published studies, two-walled tri-axial hollow fibers were utilized as primary and secondary reinforcements in epoxy composites with or without primary glass fiber reinforcement to achieve high mechanical performance in laminated composites [23].

Despite the presence of numerous studies on hollow fiber fabrication, process modification and potential applications, there appear to be gaps for the improvement of their properties concerning to intended usage and practical demonstration of these hollow fibrous materials.

2.3.3 Side-by-Side Oriented Nanofiber Production (Janus Fibers)

Side-by-side electrospinning approach is one of the noticeable systems to produce bi-component fibers. These fibers can carry the characteristic properties of each component concurrently. The first set-up was built in 2003 by Wilkes and Gupta [51] by utilizing a parallel spinneret to prepare side-by-side fibers of polyvinyl chloride/polyvinylidene fluoride (PVC/PVDF) and PVC/segmented polyurethane. Then, the side-by-side morphology of polyurethane(PU)/PAN Janus fibers was analyzed

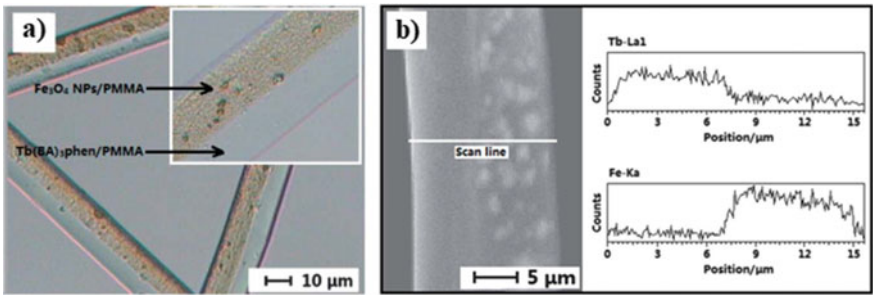


Fig. 2.15 **a** Optic image of side-by-side Janus fibers, and **b** EDS line scan analyses of electrospun PMMA based fiber containing Fe_3O_4 and Tb [81]. Reproduced with the permission of Royal Society of Chemistry

by Lin et al. [24] in 2005. Bi-functionality and other unique properties of Janus fibers such as magnetic, antibacterial, electrical, photoluminescence, and absorbability make them promising materials in various industries [25, 26, 79, 80]. For instance, Srivastava et al. [31] generated biphasic Polypyrrole (PPy)/PVP nanofibers by combining conductive and non-conductive properties. Moreover, Ma et al. [81] fabricated bifunctional Janus nanobelts consisting of PMMA with iron oxide (Fe_3O_4) and terbium (Tb) providing high electrical and magnetic properties. In this fiber design, one side of the fibers has Fe_3O_4 magnetic particles and the transparent side containing Tb particles monitored by optical microscopy and supported by Energy Dispersive X-ray Spectrometry (EDS) line scan analyses are shown in Fig. 2.15.

Light-emitting electrospun fiber based film can be used in sensor applications such as optical sensors and fluorescent probes [82, 83]. In one of the studies, white light-emitting Janus nanofibers were produced by pumping two different solutions of PVP with red and blue emission dyes and PAN with red and blue emission dyes by side-by-side electrospinning technique [27]. In addition to this work, Yang and coworkers [28] fabricated bactericidal cylindrical Janus fiber for tissue engineering and wound dressing applications using PVP/ciprofloxacin (CIP) and ethyl cellulose (EC)/silver nanoparticles (AgNPs) solutions. Schematic representation of Janus fiber production with its TEM and SEM images, and the images of antibacterial activities in the presence and absence of nanoparticles, are presented in Fig. 2.16.

Like the other electrospinning methods, one of the major requirements to achieve an ideal Janus fiber production is the optimization of electrospinning parameters. This design method can produce Janus nanofibers with multiple functionalities and different physical properties by adjusting the process parameters. For instance, Chen et al. [29] indicated that interfacial line in the center of Janus fibers, referring to its side-by-side structure became narrower by increasing the spinneret angle during parallel spinning an anionic copolymer and PVP/rhodamine-b solutions. In another study, Liu et al. [30] fabrication photocatalytic Janus fibers consisting of PVP doped TiO_2 and SnO_2 with the average fiber diameter of 100 nm SEM image shows the

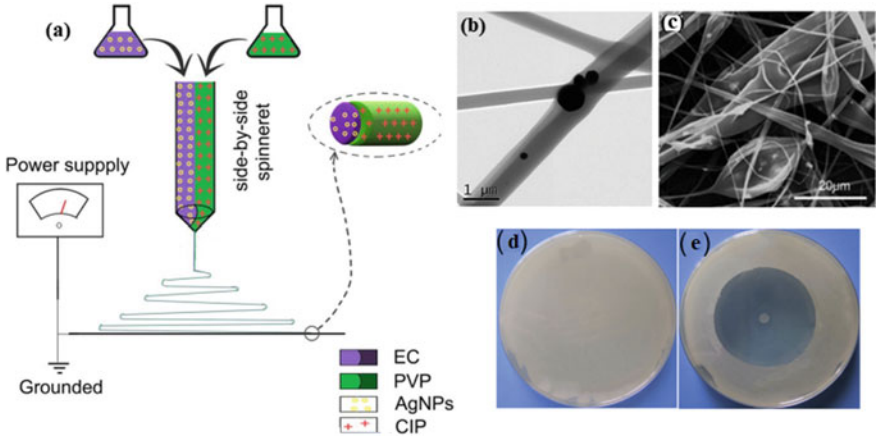


Fig. 2.16 **a** Schematic representation of fiber formation via side-by-side spinneret, **b** TEM image and **c** SEM image of the fibers, and antibacterial test results of the Janus fibers **d** without and **e** with CIP and AgNPs particles [28]. Reproduced with the permission of Elsevier

interface between these two fibers and EDS analysis confirms the presence of TiO_2 and SnO_2 particles in both fibers as seen in Fig. 2.17.

Side-by-side electrospinning can also be operated on a template-assisted fabrication system for continuous fiber formation from non-spinnable materials with noticeable physical and chemical properties [84, 85]. In this manner, a spinnable polymeric compound referring to a template helps to grow non-spinnable material as a continuous fiber. After completing the fabrication process the used template can be removed from the fiber backbone via chemical or physical treatments [86]. For instance, Jiang et al. [87] handled a template-assisted set-up by using side-by-side spinneret to get fiber formation of coumarin functionalized non-spinnable block copolymer with low

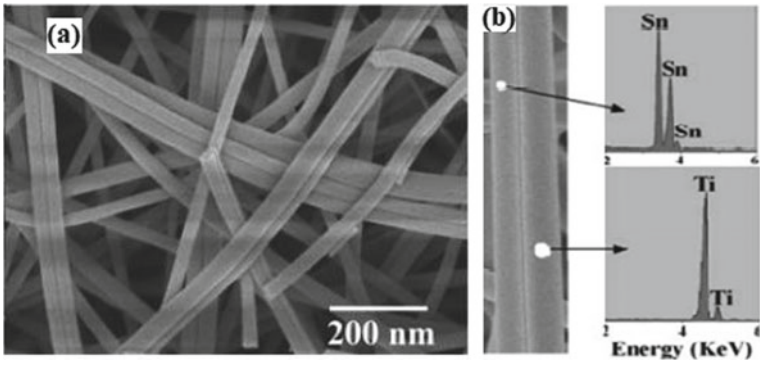


Fig. 2.17 **a** SEM image and **b** EDS microanalysis results of electrospun TiO_2/SnO_2 PVP based side-by-side nanofibers [30]. Reproduced with the permission of American Chemical Society

molecular weight using spinnable PEO as the template. The removal of the water-soluble PEO template with the washing process revealed the fibrous formation of non-spinnable coumarin functionalized copolymer used in biomedical applications.

While early efforts for side-by-side electrospinning techniques were aimed to produce Janus fibers suitable for structural utilization, recent studies have attempted to adapt Janus fibers to end use products. Accordingly, a successful approach was reported on the preparation and characterization of multicomponent conductive Janus nanofibers for sensor application in smart textiles, where one side of the nanofiber consisted of conductive camphoric acid doped polyaniline (PANI-CSA) mixed with one non-conductive polymer (PEO or PVP) and the other side was either PEO or PVP [32]. In another study, Cai et al. [55] applied heat treatment up to 230 °C on PVDF/polyimide (PI) electrospun Janus nanofibers to obtain more interfacial bonding by thermal fusing PVDF resulting in an increase in tensile strength from 7.28 to 15.49 MPa suitable for medium and high temperature filtrating applications. Consequently, these fibers can be tailorable by applying different chemical and thermal modifications techniques and adjusting the process parameters during the spinning process. Thus these structures can be easily adapted to disruptive technologies.

2.4 Miscellaneous Electrospun Structures by Co- and Multi-axial Electrospinning Techniques

As mentioned in previous sections, electrospinning is one of the widely used techniques to produce nano and micron size core/shell, layer-by-layer and hollow structural fibers. Furthermore, the production of hollow 3D polymeric bead, sphere, and foam structures with the diameter range changing from micrometer to nanometer is also possible by applying electrospinning approaches. Previously, traditional methods such as emulsion and suspension polymerizations have been utilized to produce of polymer-based micron and nano size particles [88]. In addition to the named traditional techniques, spraying polymer solution, solvent evaporation and emulsification techniques have also been investigated to attain spherical particles [33]. However, these mentioned methods have drawbacks such as nonuniform particle shape and inhomogeneous size distribution. Earlier in the seventeenth century, the appearance of a phenomenon named electrohydrodynamic atomization was observed and introduced to the world by Nollet. He described a fascinating circumstance that if a person's body electrified via connecting to a high-voltage generator and if the person cut himself/herself, his/her wound would not bleed normally, "blood would spray out from the person wound in the form of droplet" [34]. After that, Zeleny reported different possible electrospraying methods by using a nozzle in 1914 [89], and then Taylor defined the cone shape mathematically at the capillary tip of the electrospraying spinneret in 1964, and then electrospraying was established for industrial applications [90]. The electrospraying approach allows the control of

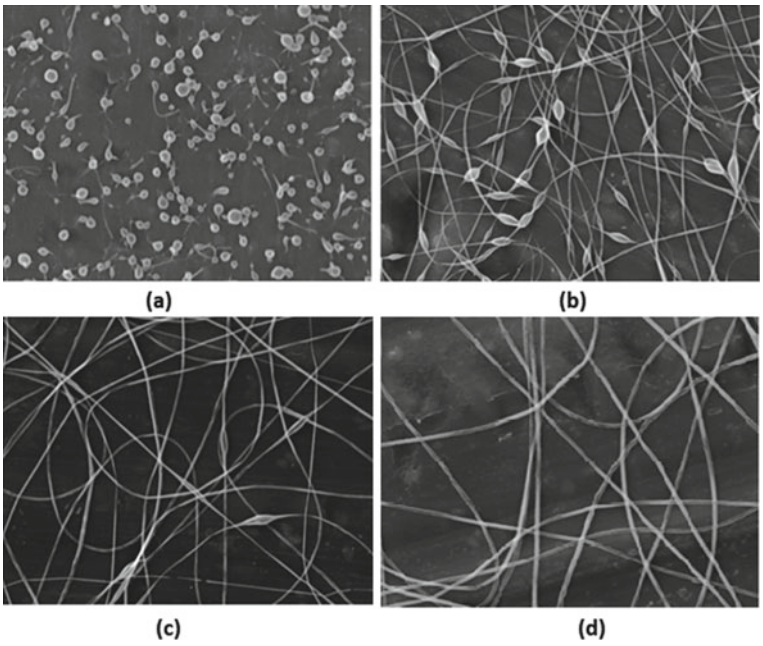


Fig. 2.18 SEM images of beads, beaded fibers, and continuous fibers as a function of different solution viscosities of **a** 13, **b** 160, **c** 527 and **d** 1835 centipoise. The scale bar of each SEM image is 20 μm [34]. Reproduced with the permission of Elsevier

sphere size and structure by adjusting the polymer solution viscosity and surface tension of the droplet by modifying the electric field [91]. Fong et al. investigated the bead formation using PEO solution with different viscosity conforming that the electrospun structure was affected by the capillary forces that occurred during the electrospinning jets changed by surface tension in the presence of electrical forces [34]. SEM images are given in Fig. 2.18 shows how beaded fibers' morphology changes with solution viscosity under the electric field of 0.7 kV/cm.

Recently, there have been several studies on electrospraying techniques used to fabricate polymer-based spheres with micro and nanospheres size. For instance, Haghighi Poudeh et al. fabricated several forms of multi-layer graphene doped PAN-based fiber, sphere, and foam by tailoring polymer molecular weight and polymer concentration by applying electrospinning/electrospraying technique weight [35]. There is a study about the importance of polymer solution concentration and polymer type forming foam, fiber, and sphere. In this study, they stated that PAN had a molecular weight of 50.000 g/mol keeping the concentration as 1 wt% led to the fabrication of foam structures; in contrast, whereas the content of PAN with the molecular weight of 45.000 g/mol concentration increased up to 5 wt% resulting in the generation of fibrous structures. Figure 2.19 shows SEM images of electrospun PAN/graphene-based foam, fiber, and spheres.

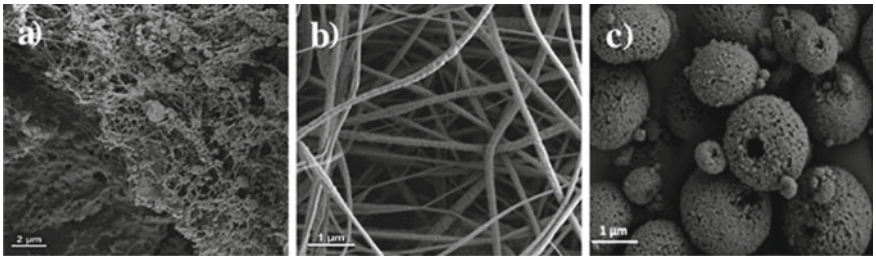


Fig. 2.19 SEM images of **a** PAN-based foam, **b** PAN-based fibers, and **c** PAN-based spheres [35]. Reproduced with the permission of American Chemical Society

Since the electrospraying technique allows the fabrication of homogenous nano or micron size particles, the studies have focused on the preparing polymeric bead structures and core/shell microcapsules and their morphological changing through tailoring electrospinning parameters [38, 92]. For instance, one of the works compared the processability of nonspinnable PEO based amphiphilic block copolymers and spinnable PEO and nonspinnable polymers under various process conditions led to spherical nanoparticles with uniform morphology [87]. It is also possible to integrate nanomaterials in these electrospun spherical structures by conducting a detailed optimization study. Haghighi Poudeh et al. converted thermally exfoliated graphene oxide (TEGO) sheets into 3D hollow and filled microspheres by using PS, PMMA and PAN polymers as carriers with different loading ratios by applying core–shell electrospraying technique [37]. Schematic representation of core–shell electrospraying and SEM images of hollow spheres before and after carbonization are given in Fig. 2.20. The aggregations and crumbling of graphene sheets were prevented in 3D composite structures by providing homogeneous distribution of graphene under

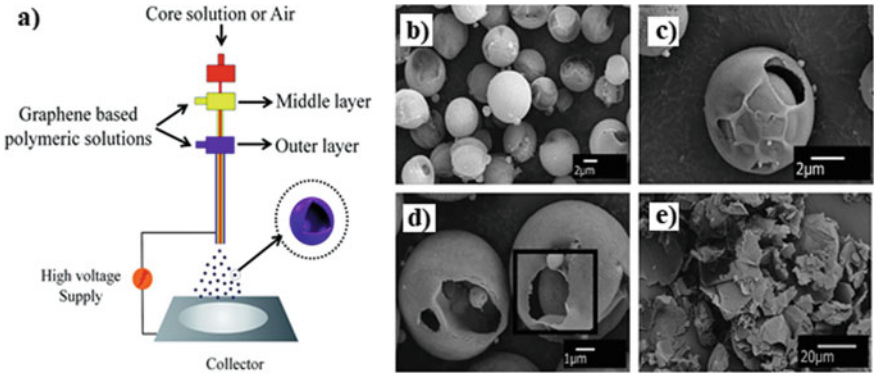


Fig. 2.20 **a** Schematic representation of graphene based spherical electrospun structures formation by tri-axial electrospraying technique, SEM images of hollow spheres consisting of 3.5 wt% PAN-0.05 wt% TEGO before (**b**, **d**) and after carbonization (**c**, **e**), respectively [37]. Reproduced with permission of Royal Society of Chemistry

an electric field. This study also indicated that ideal polymer concentration and molecular weight in solvent systems could be elaborated with the diagram showing the entanglement concentration vs average polymer molecular weight derived from Mark–Houwink–Sakurada equations.

Another work focused on the fabrication of PS based micron and nanospheres by using the electrospraying technique to investigate the fundamental effect of polymer solution concentration and the role of polymer molecular weight on the morphology of beads for getting smooth surfaces and uniform dimensions [40]. Within this work, the non-fiber forming concentration of PS polymer was investigated. They revealed that PS having high molecular weight usage caused a large amount of solvent evaporation and thus irregular and rough bead formation. To sum up, the electrospraying technique can provide the deposition of micron and nano size of particle production, thin-film formation, and capsule fabrication potentially used in several biotechnology and nanotechnology based industrial applications due to the advantages of uniform droplet formation [93].

2.5 Potential Applications and Future Outlook

Multi-axial approaches developed by co-axial [7], tri-axial [41], and side-by-side electrospinning/electrospraying techniques [50] are suitable for the producing core/shell, multi-material, hollow and Janus formed fibers and spheres. The co-axial electrospinning technique allows to fabricate multi-layer core/shell structural fibers [8] and single-layer hollow fibers [20]. Also, the number of walls increases by increasing the nozzle number in electrospinning system like tri-axial electrospinning. Adding extra layer can change the structural, and physical properties of the produced structures. Regarding the type of materials used in layers, these electrospun fibers or spherical structures can gain multi-functionality [13]. Furthermore, side-by-side electrospinning for the fabrication of Janus fibers allows spinning non-electrospinnable materials as continuous fibers and fibers containing encapsulated microparticles.

Surface structure and the characteristics of electrospun structures can be tailored by selecting suitable polymer types and applying a systematic optimization process. These electrospun structures carry a potential to be used in countless applications such as membrane development for water treatment application [5], textile [3] for producing agrotextiles and shielding fibers, and drug delivery systems for pharmaceutical applications [4] as well as electrode and membranes for energy storage and conversion systems (e.g. fuel cells, batteries, supercapacitor and producing photovoltaics) [6]. For instance, the polymer carrier has a conducting property that becomes advantageous in energy applications. On the other hand, biodegradable spinnable polymers [e.g. PCL, polylactic acid (PLA)] are widely used in biomedical and pharmaceutical applications such as tissue engineering [28] and drug delivery [46]. It is also possible to integrate nanomaterials such as graphene, carbon nanotubes

and metal nanoparticles into an electrospun solution to enhance the properties of electrospun structures.

Despite the mentioned properties and limitless advantages of multi-material electrospun fibers, there are still challenges that need to be considered such as the relatively slow collection speed of the electrospun mat [52]. Moreover, mass production of co-axial and tri-axial electrospun structures still has challenges. The projects based on process and system development are required to increase technology readiness and manufacturing levels to show the proof-of-concept of the proposed technologies. To conclude, core/shell bicomponent nanofibers, hollow fibers, fibers electrospun from non-electrospinnable materials, fibers containing encapsulated microparticles, Janus fibers, and spheres have been expanded the scope of electrospinning technology regarding the market needs and technological advancements in next generation materials.

2.6 Conclusions

This chapter summarizes the concept of producing multi-layered and multifunctional electrospun structures using co-axial and multi-axial electrospinning techniques and their implementation in different applications. It covers the published works comprehensively by providing a detailed discussion about multi-material electrospinning methodologies by giving specific examples of co- and tri-axial electrospinning/electrospraying research methods and side-by-side electrospinning. The utility and importance of preparing multifunctional and more complex biphasic nano and micron size fibers for a considerable number of applications in industries such as textile, biomedical, pharmaceutical, water treatment are explained how to get an ideal structure and meet the requirements in the target field. The essential parameters for the optimizing of all explained electrospinning approaches such as polymer molecular weight, solution concentration, the relation between two spinnable solvents, fluid flow rate, applied voltage, and the distance between nozzle and collector have been described thoroughly. This chapter also continues the discussions about the genesis pathway of fibers, bead-like structures, spheres and electrospun fiber based mat formation and the fabrication methodologies of nanomaterial integrated electrospun structures. Finally, the physical and chemical properties of the mentioned electrospun structures are explained in terms of material properties and used techniques.

Consequently, this chapter explicitly states that multi-axial electrospinning, side-by-side electrospinning or electrospraying techniques are provided to generate intricate nano and micron size structures concomitantly with controlled hollowness properties and also other functional properties such as mechanical and biodegradable properties to be used in a wide range of applications. The complexity in electrospinning systems directly depends on the number of spinnable solutions and nozzles and the prevention of their diffusion during the spinning process. Longer optimization process and tailoring process and system parameters for more than one material at the same time are main barriers in the mass production and commercialization of

these kinds of multi-functional core–shell electrospun structures and technological developments are still required for the enhancement of the used set-ups and adaptation to the natural environment tests. In addition, the demands of the market are constantly increasing in order to see the system/subsystem models and prototypes and transfer these co-axial and tri-axial experiments from laboratory scale to mass scale.

References

1. Kurecic, M., & Smole, M. S. (2013). Electrospinning: Nanofibre production method. *Tekstilec, 56*.
2. Thenmozhi, S., Dharmaraj, N., Kadirvelu, K., & Kim, H. Y. (2017). Electrospun nanofibers: New generation materials for advanced applications. *Materials Science and Engineering B, 217*, 36–48.
3. Bedford, N. M., & Steckl, A. J. (2010). Photocatalytic self cleaning textile fibers by coaxial electrospinning. *ACS Applied Materials & Interfaces, 2*, 2448–2455.
4. Mirjalili, M., & Zohoori, S. (2016). Review for application of electrospinning and electrospun nanofibers technology in textile industry. *Journal of Nanostructure in Chemistry, 6*, 207–213.
5. Ray, S. S., Chen, S.-S., Li, C.-W., Nguyen, N. C., & Nguyen, H. T. (2016). A comprehensive review: Electrospinning technique for fabrication and surface modification of membranes for water treatment application. *RSC Advances, 6*, 85495–85514.
6. Jung, J.-W., Lee, C.-L., Yu, S., & Kim, I.-D. (2016). Electrospun nanofibers as a platform for advanced secondary batteries: A comprehensive review. *Journal of Materials Chemistry A, 4*, 703–750.
7. Sun, Z., Zussman, E., Yarin, A. L., Wendorff, J. H., & Greiner, A. (2003). Compound core-shell polymer nanofibers by co-electrospinning. *Advanced Materials, 15*, 1929–1932.
8. Pakravan, M., Heuzey, M.-C., & Ajji, A. (2012). Core/shell structured PEO-chitosan nanofibers by coaxial electrospinning. *Biomacromolecules, 13*, 412–421.
9. Absar, S., Khan, M., Edwards, K., & Neumann, J. (2015). Investigation of synthesis and processing of cellulose, cellulose acetate and poly (ethylene oxide) nanofibers incorporating anti-cancer/tumor drug cis-diammineplatinum (II) dichloride using electrospinning techniques. *Journal of Polymer Engineering, 35*, 867–878.
10. Kamperman, M., et al. (2010). Nanomanufacturing of continuous composite nanofibers with confinement-induced morphologies. *Polymer Chemistry, 1*, 1001–1004.
11. Song, T., Zhang, Y. Z., & Zhou, T. J. (2006). Fabrication of magnetic composite nanofibers of poly(ε-caprolactone) with FePt nanoparticles by coaxial electrospinning. *Journal of Magnetism and Magnetic Materials, 303*, e286–e289.
12. Zhang, H., et al. (2015). Electrospun core–shell silicon/carbon fibers with an internal honeycomb-like conductive carbon framework as an anode for lithium ion batteries. *Journal of Materials Chemistry A, 3*, 7112–7120.
13. Wang, M., et al. (2020). Electrospun tri-layer nanodepots for sustained release of acyclovir. *Journal of Alloys and Compounds, 846*, 156471.
14. Yang, Y., Chang, S., Bai, Y., Du, Y., & Yu, D.-G. (2020). Electrospun triaxial nanofibers with middle blank cellulose acetate layers for accurate dual-stage drug release. *Carbohydrate Polymers,* 116477.
15. Liu, W., Ni, C., Chase, D. B., & Rabolt, J. F. (2013). Preparation of multilayer biodegradable nanofibers by triaxial electrospinning. *ACS Macro Letters, 2*, 466–468.
16. Nagiah, N., Murdock, C. J., Bhattacharjee, M., Nair, L., & Laurencin, C. T. (2020). Development of tripolymeric triaxial electrospun fibrous matrices for dual drug delivery applications. *Science and Reports, 10*, 1–11.

17. Jiang, S., Duan, G., Zussman, E., Greiner, A., & Agarwal, S. (2014). Highly flexible and tough concentric triaxial polystyrene fibers. *ACS Applied Materials & Interfaces, 6*, 5918–5923.
18. Anka, F. H., & Balkus, K. J., Jr. (2013). Novel nanofiltration hollow fiber membrane produced via electrospinning. *Industrial and Engineering Chemistry Research, 52*, 3473–3480.
19. Liu, P., et al. (2013). Preparation of continuous porous alumina nanofibers with hollow structure by single capillary electrospinning. *Colloids and Surfaces A: Physicochemical and Engineering Aspects, 436*, 489–494.
20. Li, D., & Xia, Y. (2004). Direct fabrication of composite and ceramic hollow nanofibers by electrospinning. *Nano Letters, 4*, 933–938.
21. Cao, J., Zhang, T., Li, F., Yang, H., & Liu, S. (2013). Enhanced ethanol sensing of SnO_2 hollow micro/nanofibers fabricated by coaxial electrospinning. *New Journal of Chemistry, 37*, 2031–2036.
22. Di, J., et al. (2008). Fabrication of zeolite hollow fibers by coaxial electrospinning. *Chemistry of Materials, 20*, 3543–3545.
23. Zanjani, J. S. M., Saner Okan, B., Menceloglu, Y. Z., & Yildiz, M. (2015). Design and fabrication of multi-walled hollow nanofibers by triaxial electrospinning as reinforcing agents in nanocomposites. *Journal of Reinforced Plastics and Composites, 34*, 1273–1286.
24. Lin, T., Wang, H., & Wang, X. (2005). Self-crimping bicomponent nanofibers electrospun from polyacrylonitrile and elastomeric polyurethane. *Advanced Materials, 17*, 2699–2703.
25. Wang, G., et al. (2019). Janus nanofiber array pellicle: Facile conjugate electrospinning construction, structure and bifunctionality of enhanced green fluorescence and adjustable magnetism. *RSC Advances, 9*, 206–214.
26. Wang, L., et al. (2015). One-pot facile electrospinning construct of flexible Janus nanofibers with tunable and enhanced magnetism–photoluminescence bifunctionality. *Journal of Nanoparticle Research, 17*, 91.
27. Qin, Z., et al. (2019). Electrospun Janus nanofibers for white-light emission through efficient spatial isolation to control two-step energy transfer. *Journal of Materials Chemistry C, 7*, 1065–1071.
28. Yang, J., et al. (2020). Electrospun Janus nanofibers loaded with a drug and inorganic nanoparticles as an effective antibacterial wound dressing. *Materials Science and Engineering: C,* 110805.
29. Chen, G., et al. (2015). Structure-tunable Janus fibers fabricated using spinnerets with varying port angles. *Chemical Communications, 51*, 4623–4626.
30. Liu, Z., Sun, D. D., Guo, P., & Leckie, J. O. (2007). An efficient bicomponent TiO_2/SnO_2 nanofiber photocatalyst fabricated by electrospinning with a side-by-side dual spinneret method. *Nano Letters, 7*, 1081–1085.
31. Srivastava, Y., Marquez, M., & Thorsen, T. (2009). Microfluidic electrospinning of biphasic nanofibers with Janus morphology. *Biomicrofluidics, 3*, 12801.
32. Liu, W., Zhong, T., Liu, T., Zhang, J., & Liu, H. (2020). Preparation and characterization of electrospun conductive Janus nanofibers with polyaniline. *ACS Applied Polymer Materials, 2*(7), 2819–2829.
33. Berkland, C., Kim, K. K., & Pack, D. W. (2001). Fabrication of PLG microspheres with precisely controlled and monodisperse size distributions. *Journal of Controlled Release, 73*, 59–74.
34. Fong, H., Chun, I., & Reneker, D. H. (1999). Beaded nanofibers formed during electrospinning. *Polymer (Guildf), 40*, 4585–4592.
35. Haghighi Poudeh, L., et al. (2018). Design of Pt-supported 1D and 3D multilayer graphene-based structural composite electrodes with controlled morphology by core-shell electrospinning/electrospraying. *ACS Omega, 3*, 6400–6410.
36. Xu, Y. H., Zhu, Y. J., Han, F. D., Luo, C., & Wang, C. S. (2015). Si/C fiber paper electrodes fabricated using a combined electrospray/electrospinning technique for Li ion batteries. *Advanced Energy Materials, 5*, 1400753.
37. Poudeh, L. H., Okan, B. S., Zanjani, J. S. M., Yildiz, M., & Menceloglu, Y. (2015). Design and fabrication of hollow and filled graphene-based polymeric spheres via core–shell electrospraying. *RSC Advances, 5*, 91147–91157.

38. Eda, G., & Shivkumar, S. (2006). Bead structure variations during electrospinning of polystyrene. *Journal of Materials Science, 41*, 5704–5708.
39. Hwang, Y. K., Jeong, U., & Cho, E. C. (2008). Production of uniform-sized polymer core-shell microcapsules by coaxial electrospraying. *Langmuir, 24*, 2446–2451.
40. Fantini, D., Zanetti, M., & Costa, L. (2006). Polystyrene microspheres and nanospheres produced by electrospray. *Macromolecular Rapid Communications, 27*, 2038–2042.
41. Chen, H., et al. (2010). Nanowire-in-microtube structured core/shell fibers via multifluidic coaxial electrospinning. *Langmuir, 26*, 11291–11296.
42. Moghe, A. K., & Gupta, B. S. (2008). Co-axial electrospinning for nanofiber structures: Preparation and applications. *Polymer Reviews, 48*, 353–377.
43. Chou, S.-F., Carson, D., & Woodrow, K. A. (2015). Current strategies for sustaining drug release from electrospun nanofibers. *Journal of Controlled Release, 220*, 584–591.
44. Dror, Y., et al. (2007). One-step production of polymeric microtubes by co-electrospinning. *Small, 3*, 1064–1073.
45. Bazilevsky, A. V, Yarin, A. L., & Megaridis, C. M. (2007). Co-electrospinning of core-shell fibers using a single-nozzle technique. *Langmuir, 23*, 2311–2314.
46. Zanjani, J. S. M., Okan, B. S., Letofsky-Papst, I., Yildiz, M., & Menceloglu, Y. Z. (2015). Rational design and direct fabrication of multi-walled hollow electrospun fibers with controllable structure and surface properties. *European Polymer Journal, 62*, 66–76.
47. Tiwari, S. K., & Venkatraman, S. S. (2012). Importance of viscosity parameters in electrospinning: Of monolithic and core-shell fibers. *Materials Science and Engineering C, 32*, 1037–1042.
48. Chakraborty, S., Liao, I.-C., Adler, A., & Leong, K. W. (2009). Electrohydrodynamics: A facile technique to fabricate drug delivery systems. *Advanced Drug Delivery Reviews, 61*, 1043–1054.
49. Illangakoon, U. E., Yu, D.-G., Ahmad, B. S., Chatterton, N. P., & Williams, G. R. (2015). 5-fluorouracil loaded Eudragit fibers prepared by electrospinning. *International Journal of Pharmaceutics, 495*, 895–902.
50. Xi, X., et al. (2014). Janus nanofiber: A new strategy to achieve simultaneous enhanced magnetic-photoluminescent bifunction. *Journal of Materials Science: Materials in Electronics, 25*, 4024–4032.
51. Gupta, P., & Wilkes, G. L. (2003). Some investigations on the fiber formation by utilizing a side-by-side bicomponent electrospinning approach. *Polymer (Guildf), 44*, 6353–6359.
52. Wang, C., et al. (2019). Fabrication of electrospun polymer nanofibers with diverse morphologies. *Molecules, 24*, 834.
53. Yu, D.-G., Li, J.-J., Zhang, M., & Williams, G. R. (2017). High-quality Janus nanofibers prepared using three-fluid electrospinning. *Chemical Communications, 53*, 4542–4545.
54. Zhao, Y., Cao, X., & Jiang, L. (2007). Bio-mimic multichannel microtubes by a facile method. *Journal of the American Chemical Society, 129*, 764–765.
55. Cai, M., et al. (2019). Efficient synthesis of PVDF/PI side-by-side bicomponent nanofiber membrane with enhanced mechanical strength and good thermal stability. *Nanomaterials, 9*, 39.
56. Yarin, A. L. (2011). Coaxial electrospinning and emulsion electrospinning of core-shell fibers. *Polymers for Advanced Technologies, 22*, 310–317.
57. Zussman, E., Yarin, A. L., Bazilevsky, A. V., Avrahami, R., & Feldman, M. (2006). Electrospun polyaniline/poly (methyl methacrylate)-derived turbostratic carbon micro-/nanotubes. *Advanced Materials, 18*, 348–353.
58. Qiu, Y., & Yu, J. (2008). Synthesis of titanium dioxide nanotubes from electrospun fiber templates. *Solid State Communications, 148*, 556–558.
59. Basavaraja, B. M., Majumder, S. B., Sharma, A., et al. (2015). Electrospun hollow glassy carbon-reduced graphene oxide nanofibers with encapsulated ZnO nanoparticles: a free standing anode for Li-ion batteries. *Journal of Materials Chemistry A*, *3*, 5344–5351.
60. Yoon, K., et al. (2006). High flux ultrafiltration membranes based on electrospun nanofibrous PAN scaffolds and chitosan coating. *Polymer (Guildf), 47*, 2434–2441.

61. Hinds, B. J., et al. (2004). Aligned multiwalled carbon nanotube membranes. *Science, 303*, 62–65.
62. Gopal, R., et al. (2006). Electrospun nanofibrous filtration membrane. *Journal of Membrane Science, 281*, 581–586.
63. Kao, T.-H., Cheng, C.-C., Huang, C.-F., & Chen, J.-K. (2015). Using coaxial electrospinning to fabricate core/shell-structured polyacrylonitrile–polybenzoxazine fibers as nonfouling membranes. *RSC Advances, 5*, 58760–58771.
64. Wu, J., Wang, N., Zhao, Y., & Jiang, L. (2013). Electrospinning of multilevel structured functional micro-/nanofibers and their applications. *Journal of Materials Chemistry A, 1*, 7290–7305.
65. Kalra, V., Lee, J. H., Park, J. H., Marquez, M., & Joo, Y. L. (2009). Confined assembly of asymmetric block-copolymer nanofibers via multiaxial jet electrospinning. *Small (Weinheim an der Bergstrasse, Germany), 5*, 2323–2332.
66. Hosseini, M. G., & Shahryari, E. (2016). Synthesis, characterization and electrochemical study of graphene oxide-multi walled carbon nanotube-manganese oxide-polyaniline electrode as supercapacitor. *Journal of Materials Science and Technology, 32*, 763–773.
67. Chen, W., et al. (2016). Hydrothermal synthesis of graphene-MnO_2-polyaniline composite and its electrochemical performance. *Journal of Materials Science: Materials in Electronics, 27*, 6816–6822.
68. Ke, Q., & Wang, J. (2016). Graphene-based materials for supercapacitor electrodes—A review. *Journal of Materials, 2*, 37–54.
69. Haghighi Poudeh, L., et al. (2019). Facile synthesis of single-and multi-layer graphene/Mn_3O_4 integrated 3D urchin-shaped hybrid composite electrodes by core-shell electrospinning. *ChemNanoMat, 5*, 792–801.
70. Ou, K.-L., et al. (2011). Membranes of epitaxial-like packed, super aligned electrospun micron hollow poly (l-lactic acid)(PLLA) fibers. *European Polymer Journal, 47*, 882–892.
71. Müller, G. F. J., Stürzel, M., & Mülhaupt, R. (2014). Core/shell and hollow ultra high molecular weight polyethylene nanofibers and nanoporous polyethylene prepared by mesoscopic shape replication catalysis. *Advanced Functional Materials, 24*, 2860–2864.
72. Niu, L., et al. (2014). A chemical vapor sensor based on Rayleigh scattering effect in simplified hollow-core photonic crystal fibers. *Optics Communication, 313*, 243–247.
73. Hong, Y., et al. (2010). Fabrication and drug delivery of ultrathin mesoporous bioactive glass hollow fibers. *Advanced Functional Materials, 20*, 1503–1510.
74. Bognitzki, M., et al. (2000). Polymer, metal, and hybrid nano-and mesotubes by coating degradable polymer template fibers (TUFT process). *Advanced Materials, 12*, 637–640.
75. Huang, Z., Chen, Y., Zhou, W., Nie, H., & Hu, Y. (2009). Preparation of silica hollow fibers by surface-initiated atom transfer radical polymerization from electrospun fiber templates. *Materials Letters, 63*, 1803–1806.
76. Zhao, T., et al. (2010). Multichannel TiO_2 hollow fibers with enhanced photocatalytic activity. *Journal of Materials Chemistry, 20*, 5095–5099.
77. Loscertales, I. G., et al. (2004). Electrically forced coaxial nanojets for one-step hollow nanofiber design. *Journal of the American Chemical Society, 126*, 5376–5377.
78. Li, D., McCann, J. T., & Xia, Y. (2005). Use of electrospinning to directly fabricate hollow nanofibers with functionalized inner and outer surfaces. *Small (Weinheim an der Bergstrasse, Germany), 1*, 83–86.
79. Xi, X., et al. (2018). Flexible special-structured Janus nanofiber synchronously endued with tunable trifunctionality of enhanced photoluminescence, electrical conductivity and superparamagnetism. *Journal of Materials Science: Materials in Electronics, 29*, 7119–7129.
80. Wang, Q., et al. (2018). Novel magnetic-fluorescent bifunctional Janus nanofiber membrane. *Nanotechnology, 29*, 135702.
81. Ma, Q., Yu, W., Dong, X., Wang, J., & Liu, G. (2014). Janus nanobelts: Fabrication, structure and enhanced magnetic–fluorescent bifunctional performance. *Nanoscale, 6*, 2945–2952.
82. Qin, Z., et al. (2018). Coaxial electrospinning for flexible uniform white-light-emitting porous fibrous membrane. *Materials and Design, 147*, 175–181.

83. Moran-Mirabal, J. M., et al. (2007). Electrospun light-emitting nanofibers. *Nano Letters, 7*, 458–463.
84. Wang, W., et al. (2011). Au-doped polyacrylonitrile-polyaniline core–shell electrospun nanofibers having high field-effect mobilities. *Small (Weinheim an der Bergstrasse, Germany), 7*, 597–600.
85. Huczko, A. (2000). Template-based synthesis of nanomaterials. *Applied Physics A, 70*, 365–376.
86. Wang, X.-X., et al. (2020). Conductive polymer ultrafine fibers via electrospinning: Preparation, physical properties and applications. *Progress in Materials Science,* 100704.
87. Jiang, S., Jin, Q., & Agarwal, S. (2014). Template assisted change in morphology from particles to nanofibers by side-by-side electrospinning of block copolymers. *Macromolecular Materials and Engineering, 299*, 1298–1305.
88. Hidalgo-Alvarez, R., et al. (1996). Electrokinetic properties, colloidal stability and aggregation kinetics of polymer colloids. *Advances in Colloid and Interface Science, 67*, 1–118.
89. Zeleny, J. (1914). The electrical discharge from liquid points, and a hydrostatic method of measuring the electric intensity at their surfaces. *Physical Review, 3*, 69.
90. Taylor, G. I. (1964). Disintegration of water drops in an electric field. *Proceedings of the Royal Society of London. Series A. Mathematical and Physical Sciences, 280*, 383–397.
91. Xu, Y., Zhu, Y., Han, F., Luo, C., & Wang, C. (2014). 3D Si/C fiber paper electrodes fabricated using a combined electrospray/electrospinning technique for Li-ion batteries. *Advanced Energy Materials*, 1–7.
92. Yoon, K. H., Unyong, J., & Eun, C. C. (2008). Production of uniform-sized polymer core-shell microcapsules by coaxial electrospraying. *Langmuir, 24*, 2446–2451.
93. Alehosseini, A., Ghorani, B., Sarabi-Jamab, M., & Tucker, N. (2018). Principles of electrospraying: A new approach in protection of bioactive compounds in foods. *Critical Reviews in Food Science and Nutrition, 58*, 2346–2363.



Marjan Hezarkhani received her B.Sc. degree in Textile Engineering/Textile Chemistry and Fiber Science from Arak Azad University, Iran, in 2010. She completed her Master and Doctorate degree in Chemistry from Eastern Mediterranean University, North Cyprus in 2015 and 2019, respectively. She worked in Eastern Mediterranean University—Institute of Graduate Studies and Research as a research assistant for six years from 2013 to 2019. She started to work as a Postdoctoral researcher at Sabanci University Integrated Manufacturing Research and Application Center (SU IMC), Istanbul-Turkey, in 2020. Her research focused on polymer chemistry, nanoscience, and nanotechnology. She has expertise in graphene-like materials synthesis and modification techniques, films and xerogels formation, electrospinning/spraying methods, and polymer nanocomposites. She successfully delivered several academic and industrial projects during her Doctorate and Postdoctoral research. Besides, she has published articles related to her work and attended international conferences.



Nargiz Aliyeva received the B.S. degree in Metallurgical and Materials Engineering in 2017 and completed her M.S. in Polymer Science and Technology in 2019 from Istanbul Technical University (ITU), Istanbul, Turkey. She is currently pursuing a Ph.D. degree in Material Science and Nanoengineering at Sabanci University, Istanbul, Turkey. Her research interest focused on polymeric materials and nanocomposites, surface modification of the natural fiber injection overmolding process.



Yusuf Ziya Menceloglu received the B.S. degree in Chemistry from Karadeniz Technical University, Trabzon, Turkey, in 1983. He completed his Master and Doctorate degree in Polymer Science from Istanbul Technical University 1987 and 1991, respectively. He worked as visiting scientist at Tokyo Institute of Technology 1988–1989 and University of North Carolina-Chapel Hill, 1991–1994, and he moved to industry (Textile Performance Chemicals) and served there six years before joining the Sabanci University. Prof. Menceloglu currently works as the Faculty Member of Engineering and Natural Sciences (FENS) Faculty at Sabanci University and is affiliated with SU IMC. He is also the founder and partner of technology-based startup companies and serves on the boards of associations and civic societies. Prof. Menceloglu has been working in polymer science since 1984 and in nanoscience and nanotechnology since 1991. Prof. Menceloğlu is author or co-author of more than 100 peer-reviewed papers/proceedings and four book chapters on polymers and nanosize materials. Inventor and co-inventor of 35 patents. Prof. Menceloğlu has diverse research experience in nanosize materials, polymers, composites, and reactions/processing in liquid/supercritical carbon dioxide. Prof. Menceloğlu teaches courses in polymeric materials, textile fibers and polymer science.



Burcu Saner Okan received B.S. degree in Chemistry at Middle East Technical University (METU), Turkey in 2005. Dr. Saner Okan received MS degree in 2007 and a Ph.D. degree in 2011 in Materials Science and Engineering programme at Sabanci University. Currently, she has been working as a research and application-oriented faculty member and acting as an academic director at Sabanci University Integrated Manufacturing Technologies Research and Application Center. Dr. Saner Okan is also co-founder of NANOGRAFEN Nano Technological Products Company, an official supplier of Renault. Nanografen produces a large volume of graphene nanoplatelets from waste tires by recycling and upcycling technology by decreasing manufacturing costs. Dr. Saner Okan develops cost-effective and lightweight automotive composites parts reinforced by waste tire-derived Graphene NanoPlatelet with part producers and leading OEM partners. Dr. Saner Okan has expertise in graphene, polymer nanocomposites, compounding, surface chemistry, and electrospinning. She has 40 articles published in international journals, 7 book chapters, 2 patents, and more than 50 conference papers in these fields.

Chapter 3
Solvent-Free Electrospinning—Application in Wound Dressing



Yun-Ze Long, Jun Zhang, Xiao-Fei Liu, Zhong Liu, Miao Yu, and Seeram Ramakrishna

Abstract Electrospinning is a versatile and relatively simple way for producing micro-/nanofibers from a variety of materials including synthetic/natural polymers, ceramics, and composites. However, most of the published papers describe conventional solution electrospinning that makes polymer solutions into continuous long nanofibers with a relatively low precursor utilization (generally in the range of 8–20 wt%). In order to avoid solvent evaporation into air and achieve higher precursor utilization (for example, more than 90 wt% and even 100 wt%), a few research groups have paid attention to solvent-free electrospinning such as melt electrospinning. Furthermore, solvent-free electrospun fibers that without any residual solvent provide opportunities in some important fields such as tissue engineering and wound dressings. In this chapter, the recent progress and future trends of solvent-free electrospinning have been summarized and discussed, for example, melt electrospinning, supercritical CO_2-aided electrospinning, UV-curing electrospinning, thermocuring electrospinning, anion-induced-curing electrospinning, and two-component electrospinning, etc. These solvent-free electrospinning methods may be further developed into an efficient and ecofriendly technique for the fabrication of micro-/nanofibers. Compared to conventional solution electrospinning, solvent-free electrospinning is a hopeful method and offers promising applications in wound dressings and tissue engineering, which may open the doors to new boundaries in modeling electrospinning without any risk of solvent residue in as-spun fibers, solvent emission into air, and high cost for organic solvent recycling.

Y.-Z. Long (✉) · J. Zhang · X.-F. Liu · Z. Liu · M. Yu
Collaborative Innovation Center for Nanomaterials and Devices, College of Physics, Qingdao University, Qingdao, China
e-mail: yunze.long@qdu.edu.cn

Y.-Z. Long
State Key Laboratory of Bio-Fibers and Eco-Textiles, Collaborative Innovation Center for Eco-Textiles of Shandong Province, Qingdao, China

M. Yu
Junada (Qingdao) Technology Co. Ltd., Qingdao International Academician Park, Qingdao, China

S. Ramakrishna
Department of Mechanical Engineering, Center for Nanofibers and Nanotechnology, National University of Singapore, Singapore 117574, Singapore

© The Author(s), under exclusive license to Springer Nature Switzerland AG 2022

A. Vaseashta and N. Bölgen (eds.), *Electrospun Nanofibers*,
https://doi.org/10.1007/978-3-030-99958-2_3

Keywords Solvent-free · Electrospinning · Wound-dressing · Thermocuring

3.1 Introduction of Solvent-Free Electrospinning

In this chapter, solvent-free electrospinning is defined as an electrospinning method that never uses conventional organic solvent or the precursor almost converts into ultrafine fibers so that only very few materials in the precursor enter air via evaporation, and thus the precursor utilization can reach more than 90 wt% and even 100 wt%. Similar to the conventional solution electrospinning mechanism, a solvent-free electrospun fiber is processed as the electrified polymer jet is continuously stretched by the electrostatic repulsions between the fiber surface charges. Compared to conventional solution electrospinning, the most outstanding characteristic of the solvent-free electrospinning process is that the ultrathin fibers are generated in the absence of common solvents and without obvious whipping instabilities due to the relatively higher viscosity of the precursor (Table 3.1).

3.1.1 Melt Electrospinning

Over the past forty years, melt electrospinning have emerged to cover the conventional solution electrospinning disadvantages of solvent accumulation, retention and toxicity [11–14], which have a strong impact on mass production of ultrathin fibers and design of biomaterials. As early as 1981s, Larrondo et al. reported melt electrospinning for the first time [11–13]. In their works, polyethylene (PE) and polypropylene (PP) melt directly acted as precursor to generate ultrafine fibers by melt electrospinning. Figure 3.1 exhibits the basic setup for melt electrospinning, which mainly consists of a high-voltage power supply, a spinneret, a collector and a heating unit.

Compared with conventional solution electrospinning setup, melt electrospinning needs a separate heating unit to melt polymers. So far, many remarkable heating units have been reported, for instance, electrical heater to melt electrospinning [11], circulating fluids or heated air to melt electrospinning [14, 15], and a laser melting device to melt electrospinning [16].

The forming mechanism of melt electrospun fibers is similar to conventional solution electrospinning except that the absence of common solvent emission and without apparent whipping instabilities owing to relative higher viscosity of the jet. However, melt electrospinning has typically leaded to fibers with large diameters of tens of microns or several microns, which has limited the wide potential applications of melt electrospun fibers. The diameters of melt electrospun fibers are influenced by many parameters, for instance, spinning voltage, collection distance, precursor temperature, molecular weight of polymers, etc. From our experiences, without the presence of the common solvent emission and the absence of strong whipping instability take the primary responsibility for larger average diameters of melt electrospun

Table 3.1 A summary of the benefits and disadvantages of conventional solution electrospinning and solvent-free electrospinning techniques

Electrospinning method		Advantage	Disadvantage	Refs.
Conventional solution electrospinning		Simple and inexpensive device, easy operation	Air pollution, organic solvent recovery	[1–3]
Solvent-free electrospinning	Melt electrospinning	Environment friendly, safety, biomedical applications, high efficient	Larger fiber diameter, limited electrospinning materials	[3–5]
	Two-component electrospinning			[6]
	Supercritical CO_2-aided electrospinning			[7]
	Anion-induced curing electrospinning			[8]
	UV-curing electrospinning			[9]
	Thermocuring electrospinning			[10]

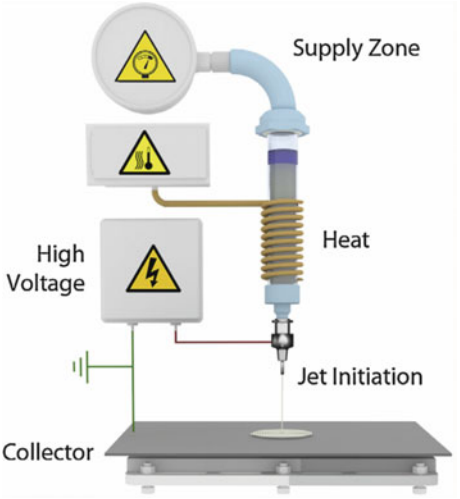


Fig. 3.1 Schematic diagram of a melt electrospinning setup [3]

fibers. Lyons et al. have systematically explored the influence of melt-electrospinning parameters on the morphology, structure and fiber diameter [17]. It is found that the molecular weight plays an important role in the diameter of melt electrospun fibers, the average fiber diameter increased with the increasing of molecular weight. Zhou et al. have also studied the thermal effects on melt electrospinning of polylactic acid (PLA), when the precursor temperature is below the glass transition temperature, jet whipping is suppressed by the fast solidification in the spinning region, resulting in a larger fiber diameter [18]. As shown in Fig. 3.2, the spinning temperature influences the viscosity of the precursor and then results in different fiber diameters. Our group demonstrated that the structures of PLA via melt electrospinning could be controlled from microfibers to microspheres by increasing the spinning temperature [19]. We

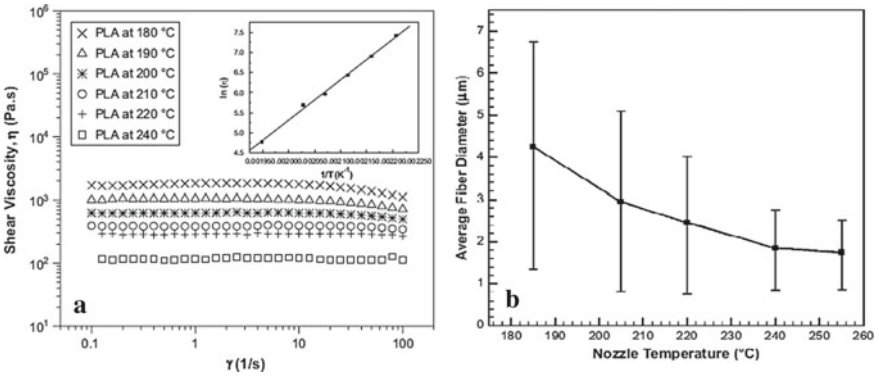


Fig. 3.2 Effects of spinning temperature in melt electrospinning on viscosity of precursor (**a**) and average fiber diameter (**b**) [18]

also reported that the average fiber diameter decreased with the increase of spinning voltage, as while as increased with the increase of spinning distance.

A lot of efforts have been paid to reduce the average diameter of melt electrospun fibers. The melt-electrospun fiber diameter has been successfully decreased to 292 ± 38 nm by using a single collector and 270 ± 100 nm by using a dual collector [10, 15]. In the past twenty years, the rapid development of biomaterials and tissue engineering has obviously promoted the exploration and innovation of solvent-free electrospinning, which resulting in extensive interest in melt electrospinning. By now, many polymer melts have been melt electrospun into ultrafine fibers.

In addition, because of the rigorous use requirements, the spinneret becomes a bottleneck of the conventional melt electrospinning. To overcome this limitation, bubble melt electrospinning, a metal needle-free method, has attracted much attention. Our group suggested a bubble melt electrospinning for generating polymer microfibers [20]. Compressed air was introduced into the polymer melt, many bubbles were produced on the surface quickly. When the bubbles were subjected to the strong electrostatic field between the collector and the polymer melt, the bubbles burst, and polymer jets were generated from the "Taylor cones" of the ruptured bubbles. The collector was then covered by as-spun polymer microfibers, as shown in Fig. 3.3. The research results suggest that bubble melt electrospinning might be a hopeful approach for needleless manufacturing in melt electrospinning.

Although the absence of solvent evaporation and strong whipping instability for solvent-free electrospinning led to fabricate larger fibers than conventional solution electrospinning, it provides an important contribution to generate controllably deposited fibers and obtain considerably uniform fiber diameter [21]. For example, melt electrospinning presents the advantage to obtain the amount of layers as a result of lesser charge accumulation effects on as-spun fibers than conventional solution electrospinning [22]. Just like 3D printing, the combination between melt electrospinning and direct writing has been considered as a promising method to design and

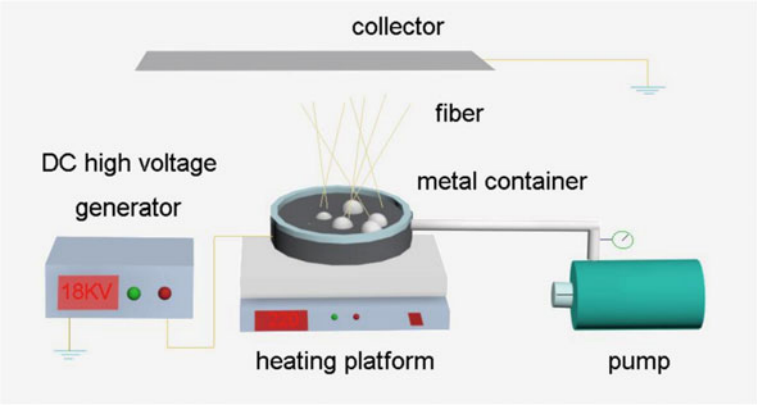


Fig. 3.3 Schematic diagram of the bubble melt electrospinning device [20]

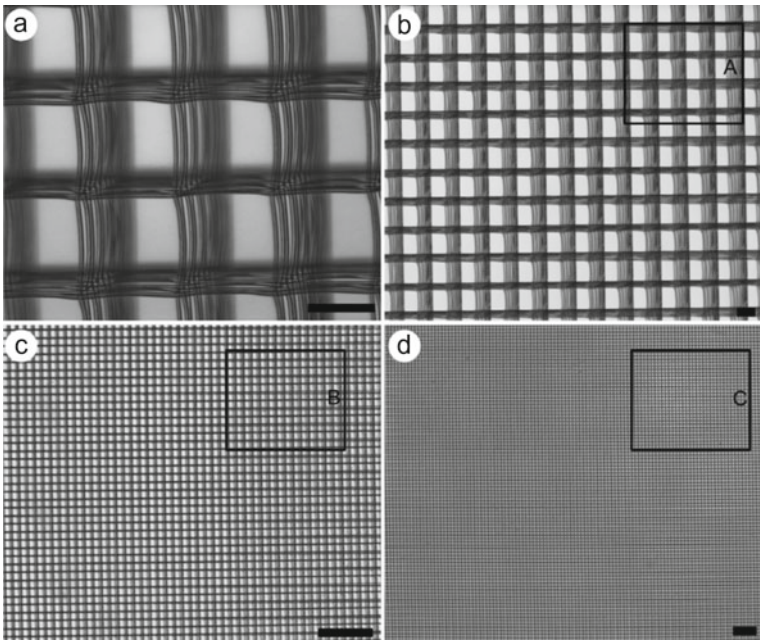


Fig. 3.4 Optical microscope pictures of a melt electrospun PCL 3D scaffold with high ordered arrangement [3]. Scale bar is 100 μm for (**a**) and (**b**), and 1 mm for (**c**) and (**d**)

produce fibrous scaffolds for tissue engineering applications. Recently, Brown et al. have systematically explored the direct writing by the way of melt electrospinning [23]. As shown in Fig. 3.4, substantial fibers with high ordered arrangement have been successfully melt electrospun.

3.1.2 Supercritical CO_2-Aided Electrospinning

Melt electrospinning, as a typical solvent-free electrospinning technique, has attracted a lot of attention due to its unique advantages. However, it also generates some other problems, e.g., relatively complicated setups, high viscosity of polymer melt, and relatively low spinning efficiency [24]. In order to solve these problems, there are still many research works need to do. Supercritical fluid is a substance for which both temperature and pressure are above the critical point. Due to the special combination of gas-like viscosity and liquid-like density of a supercritical fluid, supercritical fluid has been considered as an significant solvent for a wide variety of applications [25]. There are many kinds of supercritical fluids, CO_2 is the most popular supercritical solvent, which has been used in the many applications such as metal cation extraction, essential oil extraction, particle nucleation and polymer

synthesis. CO_2 supercritical solvent has many prominent features such as non-toxic, readily available and controllable supercritical operation at relatively low pressures (~7.38 MPa) and near room temperature (~31.06 °C) [26–28].

In 2004, Levit et al. firstly reported the supercritical CO_2 solvent-aided electrospinning. In this case, polydimethylsiloxane (PDMS) and PLA fibers were fabricated by using only electrostatic forces and with the use of supercritical CO_2 solvent instead of conventional liquid solvent [7]. High molecular weight PDMS and PLA were generated into ultrafine fibers using supercritical CO_2 solvent-aided electrospinning because the supercritical CO_2 solvent reduces the polymer viscosity sufficiently and thus the polymer jets can be electrostatically pulled from an un-dissolved bulk polymer sample. However, there are several disadvantages for this method. For example, the as-spun fiber diameter is too thick (~100–350 μm), and the fiber length is short (less than 1 cm). In addition, the electrospinning equipment is extremely more complicated than the conventional ones due to the use of high pressure vessel to control the supercritical step, which also makes problematic to use moving collector [29].

3.1.3 Anion-Induced-Curing Electrospinning

In recent years, biosensor, drug delivery, tissue engineering, regenerative medicine, have dramatically drawn much attention in the world. Electrospinning has been recognized as an excellent method to fabricate nanobiomaterials due to its unique and exceptional features. Many approaches for fabricating biomedical ultrafine fibers using electrospinning have been reported [30–32]. However, accumulation and retention of the organic solvent in the nanofibers will be harmful to physical health. Consequently, our group reported an interesting solventless electrospinning method for the generation of ultrafine fibers by using only two components of ethyl-2-cyanoacrylate (ECA) and polymethylmethacrylate (PMMA) [8]. In this case, more than 90 wt% of the precursor was electrospun into ultrafine fibers after undergoing a novel curing mechanism (as shown in Fig. 3.5, fast polymerization of the ECA monomer in the presence of hydroxide ions (water vapor) in air) at room temperature which is completely different from conventional solvent electrospinning or melt electrospinning. Here, it is worthy to note that the role of PMMA is only to increase the viscosity of the precursor. Since cyanoacrylate is the main component of a medical glue, this anion-induced-curing electrospinning can be used in rapid hemostasis (please see the following section).

3.1.4 UV-Curing Electrospinning

At present, melt electrospinning, as a relatively mature solvent-free electrospinning, has been interestingly applied to fabricate ultrafine fibers directly onto cells, a hand

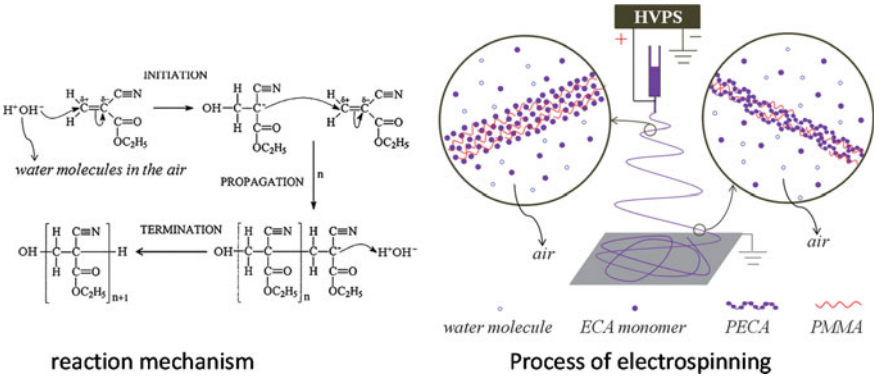


Fig. 3.5 Schematic diagram of the curing mechanism for the anion-induced-curing electrospinning [8]

or wound [14, 33]. However, the equipment used in melt electrospinning is relatively complicated than conventional ones. Photopolymerization has stimulated wide interest because of its many important applications in coatings, inks, photoresists to pressure-sensitive adhesives [34]. Among the several different techniques of photocuring (e.g., UV light, visible light, electron beam and laser-curing), UV-cuing has attracted extensive attention for fast reaction rate, low cost, high chemical stability, and solvent-free curing at ambient temperatures [35]. According to this information, our research group reported an interesting UV-curing electrospinning. In this method, UV curable materials were used as the precursor, all the precursor was electrospun into ultrafine fibers successfully without solvent evaporation in a box filled with N_2 and under UV light radiation [9]. For example, DR-U301 polyurethane acrylate as an UV curable material was used in the precursor and a homemade electrospinning device (as shown in Fig. 3.6a) was applied to fabricate ultrafine fibers.

As shown in Fig. 3.6b, the curing solidification mechanism of the UV-curing electrospun fibers was also studied. The curing mechanism could be attributed to the

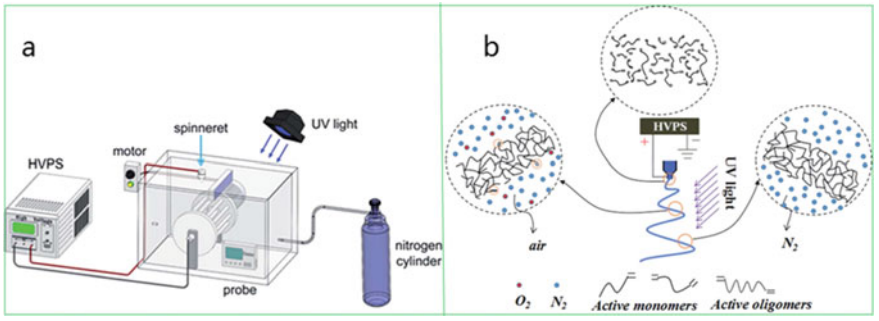


Fig. 3.6 Schematic diagram of the UV curing electrospinning device (**a**) and the curing mechanism of the precursor during the electrospinning process (**b**) [9]

acrylate bonds in the precursor jet undergoing a fast curing process under the UV light radiation and without oxygen inhibition in the nitrogen condition. Recently, our group prepared electromagnetic functionalized polyaniline/PUA/Fe_3O_4 microribbons by this UV-curing solvent-free electrospinning [36]. Solvent evaporation was avoided during the preparation, and the as-spun functionalized ribbons exhibited good electrical and magnetic properties.

3.1.5 Thermocuring Electrospinning

Polyurethane (PU) is an important synthetic polymer and has been widely used in coatings, plastics, elastic foaming material, fibers, adhesives and biomedical materials (e.g., artificial esophagus and artificial blood vessel) [37, 38]. PU fibers, also well-known as Spandex, were industrialized by the DuPont company in 1959 [39]. PU fibers were applied broadly in the clothing fabric due to its good elasticity and wearing comfort, which were fabricated mainly by conventional wet spinning or melt spinning techniques. The production equipment in a factory is usually huge and the process is very complex.

Over the past decade, PU ultrafine fibers via electrospinning method have also drawn a lot of attention. The electrospun PU fibers or composite fibers have micro-/nanoscale diameters and multi-functionalities, which extend their potential applications in fields of water-proof fabrics [40], wound dressing [41], and regenerative medicine [42], etc. These PU micro-/nanofibers could be prepared by conventional solution electrospinning or melt electrospinning of thermoplastic PU (TPU). In general, there are two stages for the synthesis of PU. At first, multi-isocyanate reacts with polyols (molecular weight in the range of 1000–2000) to prepare prepolymers in highly polar solvents with high boiling point, for example, dimethylsulfoxide or *N*, *N*-dimethyl formamide, and then the prepolymer chains are extended by feeding small molecule polyalcohols or amine. However, the viscosity of the prepolymers and its mixture with extender without any solvent is usually very high, this precursor is difficult to be electrospun.

Recently, our research group proposed a solvent-free thermocuring electrospinning technique to prepare PU fibers [43]. A homemade electrospinning setup consists of a high-voltage power supply, a syringe pump, a modified rotating disk collector, and a thermal radiation lamp was applied for solvent-free electrospinning, as shown in Fig. 3.7a. Figure 3.7b shows the curing and solidification mechanism of the electrospun PU micro-/nanofibers under thermal radiation.

3.1.6 Two-Component Electrospinning

In a conventional solution electrospinning, the charged polymer solution jet is stretched under the action of a high-voltage electrostatic field and further refined

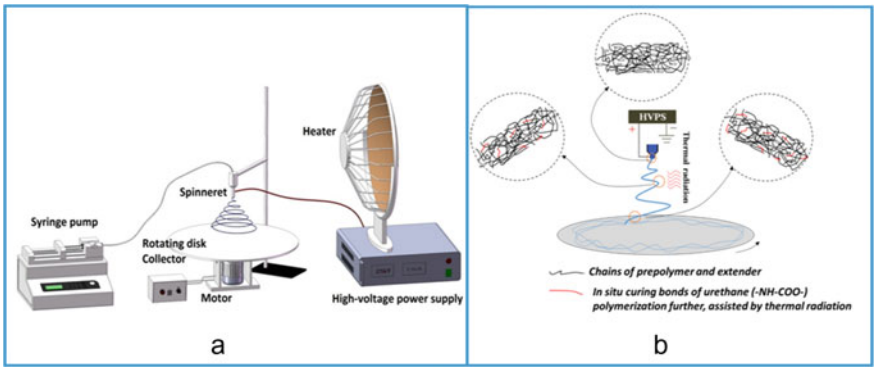


Fig. 3.7 Schematic diagram of the thermal-curing solvent-free electrospinning device (**a**), and the curing mechanism of the PU fibers during electrospinning process under thermal radiation (**b**) [43]

with splitting and/or whipping, at last the polymer jets become nanofibers with the solvent volatilizing. Namely, the curing or solidification mechanism of the solution electrospun fibers is mainly ascribed to the solvent evaporation. It is noted that the organic solvents used in conventional solution electrospinning, for instance, acetone, chloroform, tetrahydrofuran, *N*, *N*-dimethylformamide (DMF) and formic acid etc., are toxic or corrosive. The existence of these solvents in electrospun fibers seriously influences the application of electrospinning in biomedicine, followed by the emergence of solvent-free electrospinning technology has significantly reversed this situation. Recently, with the development of solvent-free electrospinning technology, multitude of electrospinning machines have been proposed [44–46]. These methods usually suffer, whereas, from tedious processing, high cost and low efficiency. Some reductant and oxidant produce radicals when they meet, and initiate polymerization of reactive monomers. To exemplify, our group suggested a new solvent-free electrospinning technique for fabricating ultrathin fibers based on a two-component adhesive system with a facile operation [6]. Meanwhile, this system just relies on a simple device (Fig. 3.8a) and has mild reaction conditions (Fig. 3.8b), which is more suitable for ideal solvent-free electrospinning.

3.2 Advantages and Challenges of Solvent-Free Electrospinning

Conventional solution electrospinning has been widely used in a variety of fields. However, some unconquerable points have limited its further exploitation, for example, (1) only about 8–20 wt% polymers in the spinning precursor was electrospun into nanofibers [47], the rest of the precursor emits into air; (2) the evaporated organic solvents may be toxic, flammable or highly corrosive; (3) some organic solvents are very expensive and difficult to recycle resulting in air pollution problem;

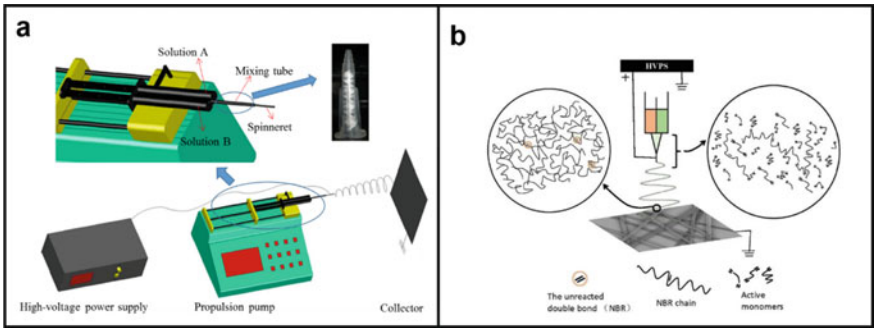


Fig. 3.8 Schematic diagram of the solvent-free two-component electrospinning device (**a**), and the solidification mechanism of electrospun fibers (**b**) [6]

(4) for scaffolds application, the electrospun membrane pore size is too small to cultivate cells [23]; (5) some widely used polymers such as polyethylene, polypropylene, and poly(ethylene terephthalate) (PET) are difficult to dissolve in an appropriate solvent. The advent of solvent-free electrospinning, as an interesting method for generating micro-/nanofibers with many unique benefits compared to conventional solution electrospinning, has compensated the disadvantages of the solution one.

3.2.1 High Efficient Utilization of Precursor

In spite of conventional solution electrospinning has tremendous promising applications, there are still some difficulties to realize large-scale commercial production. The main reasons are its ultralow efficient utilization of precursor and an abundance of expensive solvents hard to recycle. In a conventional solution electrospinning process, usually more than 80 wt% solvents were applied to dissolve/blend the polymer to achieve a uniform and viscoelastic precursor, and then almost all of the solvents emit into air during the process of electrospinning, which leading to a very low efficient precursor utilization. Besides the waste of organic solvents, electrospun fibers that with much residual solvent hardly provide opportunities in some areas, e.g., wound dressings and tissue engineering. For comparison, solvent-free electrospinning can achieve high efficient precursor utilization owing to this electrospinning method does not need common organic solvent to dissolve the polymer and the precursor almost converts into micro-/nanofibers, so that a very high yield is achieved (more than 90 wt% or even 100 wt%). Melt electrospinning, as the most typical solvent-free electrospinning technique, could realize 100 wt% precursor utilization since most polymers are dissolved in solvents. In anion-induced-curing electrospinning, the spinning solution was almost all of it (~90 wt%) was electrospun into ultrafine fibers at room temperature [8]. It is noted that the electrospinning precursor

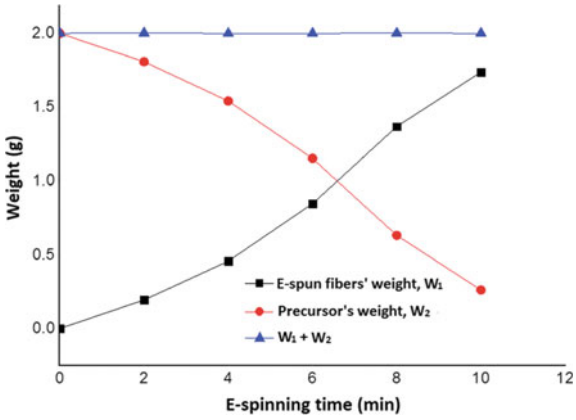


Fig. 3.9 Weight balance (electrospun fibers' weight W1 + precursor's weight W2, blue triangle) of precursor (W2, red circle) and the electrospun fibers (W1, black square) [9]

can be almost electrospun into fibers in the UV-induced-curing electrospinning (as shown in Fig. 3.9) [9].

3.2.2 Ecofriendly Electrospinning Process

Thus far, conventional solution electrospinning has been extensively used for generation of nanofibers in lab. In conventional solution electrospinning, organic solvents play a very important role in the full spinning process and the property of the solvent affects the feasibility of the electrospinning [48]. So far, the solvent accumulation from rapidly emission during the electrospinning process is a big challenge for mass fabrication of nanofibers, and thus causes serious environment pollution problem [8]. Based on the guiding principle of solvent toxicity established by the International Conference on Harmonization of Requirements for Registration Pharmaceuticals for Human Use, some commonly used solvents can be divided into three classes: (1) the first class solvents might cause cancer and do intense harm to human; (2) the second class solvents do not have genotoxic effect, but exhibit carcinogenicity to animal in some degree; (3) the third class solvents present slight toxicity, but long-term chronic toxicity is still unclear. Table 3.2 shows some typical solvents used in solution electrospinning process and their classes of toxicity and boiling points.

Most organic solvents used in conventional solution electrospinning, such as DMF, chloroform, and methanol, are toxic. Hence, solvent-free electrospinning is competent for mass fabrication of electrospun fibers, since entire solvent participates in the electrospinning process, so that the whole process is ecofriendly. Usually, solvent-free electrospinning has been considered as a safer and "greener" method compared with conventional solution electrospinning due to no risk of solvent emission and no residual organic solvent in the fibers [49]. Particularly, the absence of toxic solvent in the as-spun fibers makes it an interesting way for direct coating of functional

Table 3.2 Toxicity of some typical solvents used in conventional solution electrospinning

Solvents	Classes of toxicity (class)	Boiling point (°C)
Dichloro methane	Second	40
Dimethyl formamide (DMF)	Second	153
Acetic acid	Third	118.1
Acetone	Third	56.1
Methanol	Second	64.5
Tetrahydrofuran	Third	66
Formic acid	Third	100
Chloroform	Second	61.6
Ethanol	Third	78.3

fibers on the wound or skin without further treatment, which expands the promising applications of nanofibers in wound dressings [5].

3.2.3 Challenges in Solvent-Free Electrospinning

In spite of the solvent-free electrospinning has a lot of advantages, e.g., high efficient precursor utilization, controllable deposition of electrospun ultrafine fibers, and ecofriendly electrospinning process, its research is still not widely compared to conventional solution electrospinning [50–52]. There are still some challenges for solvent-free electrospinning technique: first, the average diameter of solvent-free electrospun fibers is much larger due to high viscosity and low conductivity of the precursor [2, 51, 53, 54]; second, the setup of solvent-free electrospinning is relatively complicated (e.g., a heater is needed in melt electrospinning, N_2 is used in UV-curing electrospinning); third, systematic theoretical studies are still needed for solvent-free electrospinning [55–57]. To realize the promising applications in various fields and mass fabrication, further researches are needed to investigate the mechanism of solvent-free electrospinning, reduce average fiber diameters, and improve solvent-free electrospinning devices.

At last, it is worthy to note that the deposition or coating of solvent-free electrospun fibers (e.g., melt electrospun fibers) could be precisely controlled. As we know, the mechanism of the electrospinning (e.g., whipping instability) is complicated, especially the motion track of the electrospun jet. Until 1999, high-speed photography was used to reveal the process of the polymer jet whipping. It is found that in most cases there is only a single, rapidly bending or whipping thread during the electrospinning process (Fig. 3.10a, b) [58].

As shown in Fig. 3.10c, it has been considered that the solvent-free electrospinning (e.g., melt electrospinning) presents a visible and rather straight polymer jet

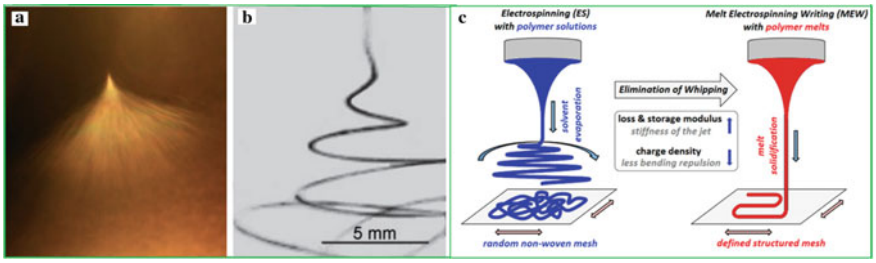


Fig. 3.10 **a** Photograph of a PEO solution jet during electrospinning process. **b** High-speed photograph of whipping instability of a jet [58]. **c** Comparison of different processes between a solution jet and a melt jet in electrospinning processes [59]

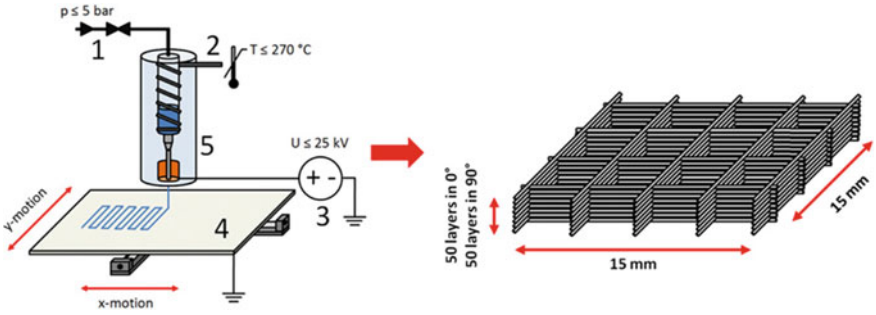


Fig. 3.11 Schematic diagram of direct writing via melt electrospinning and electrospun 3D fibrous scaffold [59]

between the spinneret and collector with very weak whipping instabilities [53, 59]. Usually, the stable jet formation is beneficial to fabricate controllable electrospun fibers. Moreover, the number of the deposited fiber layers also is controllable for melt electrospinning owing to low charges in the jet surface and the fibers easily fused together compared with conventional solvent electrospinning. The latter is limited by the charge accumulation effects on jet surface [23, 53, 55]. Due to these controllable feature, solvent-free electrospinning (e.g., melt electrospinning) has achieve direct writing to produce fibrous 3D scaffolds, as shown in Fig. 3.11 [59–62].

3.3 Biomedical Applications of Solvent-Free Electrospinning

Electrospinning has attracted a great deal of interest in the field of biomedicine [63–66]. As far, most of nanofibers were generated by conventional solution electrospinning. These solution electrospun nanofibers often are bio-incompatible and easily

result in undesirable host response due to residues of organic solvents [5]. As demonstrated above, solvent-free electrospinning (e.g., melt electrospinning), emerged as an alternative ultrafine fibers fabricating method, is a controllable, high efficient and environment friendly technique compared to conventional solution electrospinning. Particularly, solvent-free electrospinning allows for direct deposition of ultrafine fibers on wound or skin. In recent years, several research groups have studied the possible applications of solvent-free electrospinning due to its many unique advantages. By now, several articles have reviewed the applications of melt electrospinning [3–5]. In this chapter, we only present some representative biomedical applications of solvent-free electrospun fibers.

3.3.1 Tissue Engineering

As we know, tissue engineering uses scaffolds to develop functional substitutes for damaged tissues and organs [65]. These scaffolds work as natural extracellular matrix, providing a comfortable cell microenvironment. In the past twenty years, Mikos et al. has found electrospun scaffold with micro-/nanopores can promote cell invasion and growth. This research group also found that an increase in fiber diameter could increase pore size and interconnectivity. Solvent-free electrospinning can meet the requirements of scaffold owing to its advantages in fabrication of layered tissue constructs for tissue engineering compared to conventional solution electrospinning. As shown in Fig. 3.12, Dalton et al. have directly melt electrospun a blend of PEO-block-PCL with PCL in vitro cultured fibroblasts as the collector [14].

Our group found that PLA and PCL could be directly melt electrospun onto a pig liver as a potential wound dressing [33]. Figure 3.13 shows the schematic illustration of direct melt electrospinning onto the pig liver, and the melt electrospun membranes

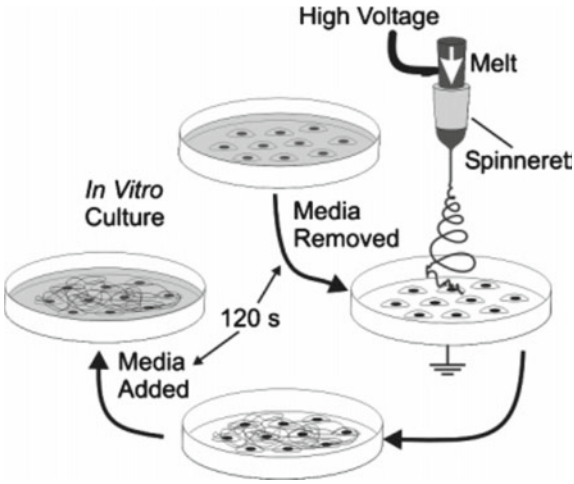


Fig. 3.12 Schematic diagram of direct in vitro melt electrospinning [14]

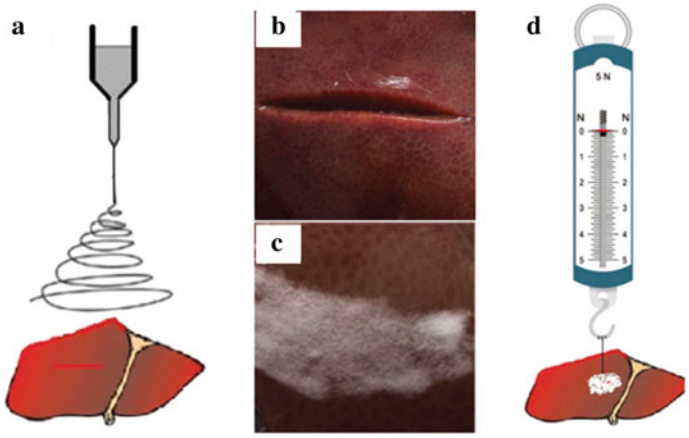


Fig. 3.13 **a** Schematic diagram of direct melt electrospinning of polymer fibers onto a pig liver; **b** optical image of a piece of pig liver with a long gash; **c** melt electrospun PCL fibers deposited on the pig liver, covering the gash; **d** schematic diagram of the adhesive power measurement [33]

exhibited an excellent mechanical property. Recently, our group also proposed an in situ precise solvent-free electrospinning (anion induced curing electrospinning) of medical glue fibers onto dural wound for improving sealing capability and avoiding tissue adhesion in the simulation experiment [44].

Subsequent research led to a breakthrough in the design of a hand-held in-situ melt electrospinning setup that only uses AAA dry batteries for working [67]. Figure 3.14 shows the structure of the setup, it is worthy to note that our group also suggested a heat preservation antistatic interference tubule with excellent thermal conductivity to avoid electromagnetic interference, making the whole setup compact and hand-held. This handheld melt electrospinning setup can be applied in wound dressing or hemostasis by a versatile method of replacing with some medical materials.

In addition, melt electrospun patterned scaffold also was reported by Dalton et al. for tissue engineering [21]. In this case, melt electrospun fibers were collected in focused spots as a patterning and drawing of a cell adhesive scaffold. The prepared scaffolds are mainly 2D structure, which cannot meet the requirement of engineering functional tissue. The latter needs effective organization of cells into tissue with morphological and physiological characteristics resembling those in vivo [68]. Namely, 3D scaffold mimicked the natural extracellular matrix is more suitable for cell growth, shape, migration, and differentiation than 2D one. According to the above viewpoints, 3D scaffolds based on electrospinning have emerged. Brown et al. have combined direct writing with solvent-free electrospinning (e.g., melt electrospinning) to fabricate 3D fibrous scaffold deposited accurately [23, 60]. It is found that melt electrospinning writing technique can successfully design and produce fibrous tubes, which is considered as a promising scaffold for tissue engineering (e.g., artificial blood vessel). As shown in Fig. 3.15, the fibrous tube consists of 20 μm diameter poly(ε-caprolactone) (PCL) fibers with controllable micropatterns and mechanical

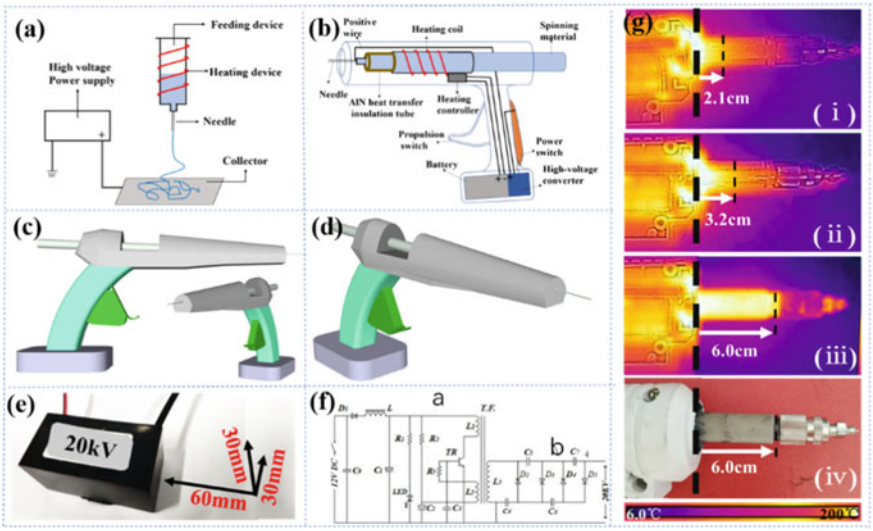


Fig. 3.14 Pictures of homemade hand-held melt electrospinning setup. Schematic illustrations of **a** a conventional melt electrospinning setup using a high voltage power supply connected to collector (cannot directly receive electrospun fibers with wound or skin) and **b** a battery-operated homemade hand-held melt electrospinning setup which can operate outdoors and directly receive electrospun fibers with wound or skin. **c**, **d** 3D model illustrations of the hand-held melt electrospinning setup. High voltage conversion unit: **e** a high voltage converter picture, and **f** schematic of the high voltage converter circuit. **g** High heat transfer insulation unit: (i) quartz tube; (ii) CaO tube; (iii) AlN tube; (iv) picture of the AlN tube [67]

property. Melt electrospinning writing, as a new additive manufacturing approach to produce porous fibrous scaffolds, has also attracted much attention of other research groups [59, 61, 62, 69, 70]. For example, Farrugia et al. combined melt electrospinning technology with a programmable x–y bench to prepare controllably oriented porous PCL scaffolds, and owing to the high porosity and interconnectivity of the resulting scaffolds, the top seeding approach was sufficient to achieve downward penetration of fibroblasts, allowing cells to exist on the surface and inside of the scaffolds [71].

3.3.2 Drug Sustained-Release Material

Traditional drug administrations, for example, oral administration and intravenous injection, generally resulted in burst release in body, and most of the medicine was cleared from the body as metabolites. There are many obvious disadvantages for these drug delivery systems, for instance, potential poisonous side effects, compromising therapeutic efficacy, and increasing extra pressure on metabolic system. So, there is much interest in developing new drug delivery system. Many research groups

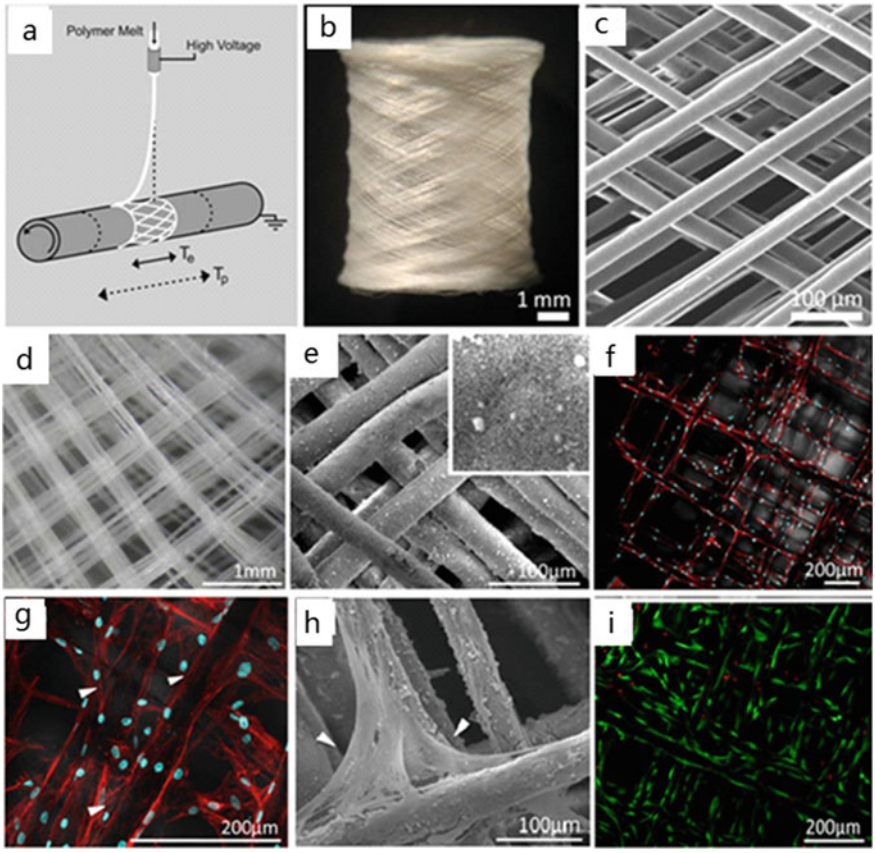


Fig. 3.15 **a** Schematic diagram showing production of a porous fibrous tube by melt electrospinning. **b** Picture of the resulting porous fibrous tube. **c** SEM picture showing the uniform and ordered PCL fibers interwoven. **d** Picture showing PCL fibers prior to CaP coating. **e** SEM picture showing the CaP coated PCL fibers. **f** 3D projection of hOBs cultured on the CaP/PCL scaffold for 2 weeks. Cells were fixed and stained for f-actin (red) and nuclei (blue). **g** Enlarged 3D projection in (**f**). **h** SEM picture showing hOBs after 2 weeks of culture. Arrows in (**g**) and (**h**) indicate fiber crossovers where hOBs start to span neighboring fibers. **i** Live/dead assay showed that after 2 weeks of culture more than 90% of the hOBs were still alive [60]

have shown that drug safety and efficacy can be apparently improved when a pharmaceutical agent is embedded within or attached to a polymer, and thus new therapies are possible [72, 73]. Conventional solution electrospinning has made an important contribution to improve drug delivery owing to its high surface area and multiporous feature [74–76]. However, only few publications have been reported about the application of drug delivery for solvent-free electrospinning [52]. Recently, Nagy et al. [49] firstly reported melt electrospinning for fabrication of fast dissolving drug delivery system with fast release of carvedilol, which is a drug with poor water solubility. This work demonstrated that melt electrospinning combined the advantages

of extrudate and conventional solution electrospinning is a promising method for the fabrication of drug delivery systems with improved dissolution. Furthermore, our group also studied the drug delivery of solvent-free electrospun ultrafine fibers [46]. It is found that the fibrous membranes via anion-induced curing electrospinning incorporated medical glue n-octyl-2-cyanoacrylate (NOCA) can significantly improve operational performance and safety (e.g., reducing inflammation and avoiding tissue adhesion) by precise deposition onto a wound, as well as reduce the dosage of medical glue NOCA by almost 80%. Figure 3.16 shows the comparison illustration of two methods (in situ precision electrospinning and common air spraying) for delivery the medical glue NOCA. Schneider et al. prepared functional fibrous mats by melt electrospinning, doping growth factor (EGF) into the fibrous mats and achieving slow release, releasing 25% of EGF after 170 h, reducing wound closure time by 90% [77]. These fibrous mats have great potential to promote wound recovery. Recently, Nagy et al. doped a poorly water-soluble drug into a melt electrospun cationic methacrylate copolymer, which improved the release of the drug [49]. Additionally, numerous experiments have demonstrated that wound dressings prepared by melt electrospinning can modulate their drug release behavior by changing their chemical composition and geometric structure. He and co-workers successfully prepared wound dressings with different geometries composed of different ratios PCL, polyethylene glycol (PEG) and ciprofloxacin using melt electrospinning method and studied the release behavior [78]. The drug release behavior can be controlled by adding polyethylene glycol and changing its geometry according to the different requirements of the trauma dressing.

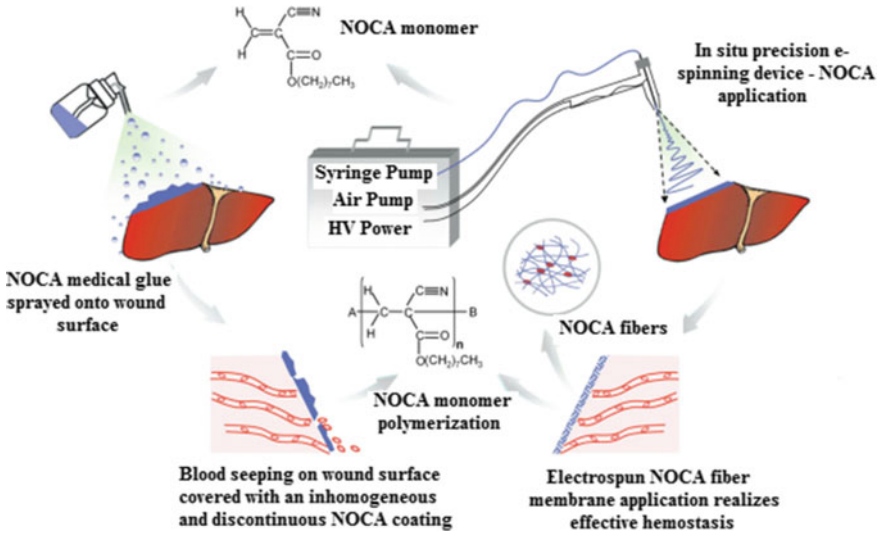


Fig. 3.16 Schematic illustration of two methods (conventional spraying and in situ electrospinning) for delivery medical glue NOCA [46]

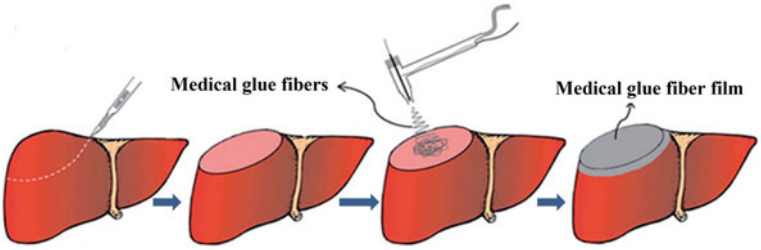


Fig. 3.17 Procedure of rapid hemostasis by in situ direct deposition of medical glue fibers on the liver wound [79]

3.3.3 Fast Hemostasis

Solvent-free electrospinning not only improves the precursor utilization but also is ecofriendly and nontoxic. According to these features, our research group studied the potential application of this promisingly solvent-free electrospinning (e.g., anion induced curing electrospinning) in fast stopping bleeding [79]. It is well known that fast stopping bleeding of visceral organs is still a challenge in surgical operation or after major trauma. By using solvent-free in situ electrospinning and a portable electrospinning setup, our group has precisely deposited an electrospun medical glue fiber membrane on a wound surface to realize stopping bleeding in less than 40 s, reducing the usage amount of medical glue and the toxicity caused by solvent retention in the fibers. Figure 3.17 shows the procedure of stopping bleeding by in situ rapid deposition of medical glue fibers on the pig liver wound.

3.4 Conclusion and Perspective

In summary, solvent-free electrospinning has been considered as an alternative micro-/nanofibers fabricating method due to many advantages such as high precursor utilization, ecofriendly electrospinning process, producing ultrafine fibers using some insoluble polymers (e.g., polypropylene and polyethylene) which are difficult to dissolve in vast majority of solvent for conventional solvent electrospinning, no toxic solvent residue, avoiding high cost for solvent recovery, and a high precursor utilization (typically more than 90 wt% and even 100 wt%). In addition, the absence of toxic organic solvent in the as-spun fibers makes it possible for direct deposition of functional fibers on skin or wound without further treatment. The emergence of solvent-free electrospinning has obviously extended the interesting application of electrospun fibers in the field of wound dressing.

However, there are still some challenges for solvent-free electrospinning. For instance, compared with conventional solution electrospinning, the requirement for solvent-free electrospinning setup or precursor is high owing to relative higher

viscosity of the precursor. The solvent-free electrospun fibers always have relatively larger diameters ascribed to no solvent evaporation and weak electrical bending instabilities than conventional solution electrospun nanofibers. In addition, there are only few reports on solvent-free electrospinning setups for large-scale fabrication. This is another challenge for solvent-free electrospinning. We hope that, based on this chapter where we highlight the unique advantages of solvent-free electrospinning, this promisingly efficient fibers generating technique should obtain much more attention to deepen the basic research, expand possible applications and realize practical uses.

Acknowledgements This work was financially supported by the National Key Research and Development Project of China (2019YFC0121402), the National Natural Science Foundation of China (51973100 and 11904193), and the State Key Laboratory of Bio-Fibers and Eco-Textiles, Qingdao University (RZ2000003334 and ZDKT202108).

References

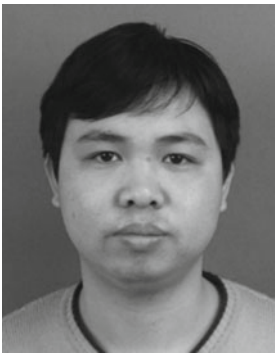
1. Li, D., & Xia, Y. (2004). Electrospinning of nanofibers: Reinventing the wheel? *Advanced Materials, 16*, 1151–1170.
2. Greiner, A., & Wendorff, J. H. (2007). Electrospinning: A fascinating method for the preparation of ultrathin fibers. *Angewandte Chemie, 46*, 5670–5703. https://doi.org/10.1002/anie.200604646
3. Brown, T. D., Dalton, P. D., & Hutmacher, D. W. (2016). Melt electrospinning today: An opportune time for an emerging polymer process. *Progress in Polymer Science, 56*, 116–166. https://doi.org/10.1016/j.progpolymsci.2016.01.001
4. Hutmacher, D. W., & Dalton, P. D. (2011). Melt electrospinning. *Chemistry, An Asian Journal, 6*, 44–56. https://doi.org/10.1002/asia.201000436
5. Góra, A., Sahay, R., Thavasi, V., & Ramakrishna, S. (2011). Melt-electrospun fibers for advances in biomedical engineering, clean energy, filtration, and separation. *Polymer Reviews, 51*, 265–287. https://doi.org/10.1080/15583724.2011.594196
6. Zhao, Y.-T., et al. (2018). Solvent-free two-component electrospinning of ultrafine polymer fibers. *New Journal of Chemistry, 42*, 11739–11745. https://doi.org/10.1039/c8nj01513a
7. Levit, N., & Tepper, G. (2004). Supercritical CO_2-assisted electrospinning. *The Journal of Supercritical Fluids, 31*, 329–333. https://doi.org/10.1016/j.supflu.2003.12.008
8. Liu, S.-L., et al. (2013). Solventless electrospinning of ultrathin polycyanoacrylate fibers. *Polymer Chemistry, 4*, 5696–5700.
9. He, H.-W., et al. (2016). Solvent-free electrospinning of UV curable polymer microfibers. *RSC Advances, 6*, 29423–29427.
10. He, H. W., Zhang, B., Yan, X., Dong, R. H., Jia, X. S., Yu, G. F., Ning, X., Xia, L. H., & Long, Y. Z. (2016). A solvent-free thermal assisted electrospinning to fabricate polyurethane microfibers with high conductivity by in-situ polymerization of polyaniline. *RSC Advances, 6*(108), 106945–106950.
11. Larrondo, L., & St. John Manley, R. (1981). Electrostatic fiber spinning from polymer melts. I. Experimental observations on fiber formation and properties. *Journal of Polymer Science: Polymer Physics Edition, 19*, 909–920.
12. Larrondo, L., & St, John Manley, R. (1981). Electrostatic fiber spinning from polymer melts. II. Examination of the flow field in an electrically driven jet. *Journal of Polymer Science: Polymer Physics Edition, 19*, 921–932.

13. Larrondo, L., & St. John Manley, R. (1981). Electrostatic fiber spinning from polymer melts. III. Electrostatic deformation of a pendant drop of polymer melt. *Journal of Polymer Science: Polymer Physics Edition, 19*, 933–940.
14. Dalton, P. D., Klinkhammer, K., Salber, J., Klee, D., & Möller, M. (2006). Direct in vitro electrospinning with polymer melts. *Biomacromolecules, 7*, 686–690. Dalton, P. D., Lleixà Calvet, J., Mourran, A., Klee, D., & Möller, M. (2006). Melt electrospinning of poly-(ethylene glycol-block-ϵ-caprolactone). *Biotechnology Journal, 1*, 998–1006.
15. McKee, M. G., Wilkes, G. L., Colby, R. H., & Long, T. E. (2004). Correlations of solution rheology with electrospun fiber formation of linear and branched polyesters. *Macromolecules, 37*, 1760–1767.
16. Haghi, A., & Akbari, M. (2007). Trends in electrospinning of natural nanofibers. *Physica Status Solidi (A), 204*, 1830–1834.
17. Fong, H., Chun, I., & Reneker, D. (1999). Beaded nanofibers formed during electrospinning. *Polymer, 40*, 4585–4592.
18. Deitzel, J., Kleinmeyer, J., Harris, D., & Tan, N. B. (2001). The effect of processing variables on the morphology of electrospun nanofibers and textiles. *Polymer, 42*, 261–272.
19. Yu, S.-X., et al. (2018). Morphology control of PLA microfibers and spheres via melt electrospinning. *Materials Research Express, 5*. http://doi.org/10.1088/2053-1591/aab9f4
20. Li, Y. M., et al. (2018). Bubble melt electrospinning for production of polymer microfibers. *Polymers (Basel), 10*. http://doi.org/10.3390/polym10111246
21. Dalton, P. D., Joergensen, N. T., Groll, J., & Moeller, M. (2008). Patterned melt electrospun substrates for tissue engineering. *Biomedical Materials, 3*, 034109.
22. Ramakrishna, S., Fujihara, K., Teo, W.-E., Lim, T.-C., & Ma, Z. (2005). *An introduction to electrospinning and nanofibers* (Vol. 90). World Scientific.
23. Brown, T. D., Dalton, P. D., & Hutmacher, D. W. (2011). Direct writing by way of melt electrospinning. *Advanced Materials, 23*, 5651–5657.
24. Lyons, J., & Ko, F. (2005). Melt electrospinning of polymers: A review. *Polymer News, 30*, 170–178.
25. Wahyudiono, Murakami, K., Machmudah, S., Sasaki, M., & Goto, M. (2012). Production of nanofibers by electrospinning under pressurized CO_2. *High Pressure Research, 32*, 54–59. http://doi.org/10.1080/08957959.2011.645474
26. Pourmortazavi, S. M., & Hajimirsadeghi, S. S. (2007). Supercritical fluid extraction in plant essential and volatile oil analysis. *Journal of Chromatography A, 1163*, 2–24. https://doi.org/10.1016/j.chroma.2007.06.021
27. Reverchon, E., & De Marco, I. (2006). Supercritical fluid extraction and fractionation of natural matter. *Journal of Supercritical Fluids, 38*, 146–166. https://doi.org/10.1016/j.supflu.2006.03.020
28. Reverchon, E. (1997). Supercritical fluid extraction and fractionation of essential oils and related products. *The Journal of Supercritical Fluids, 10*, 1–37. https://doi.org/10.1016/S0896-8446(97)00014-4
29. Campardelli, R., Baldino, L., & Reverchon, E. (2015). Supercritical fluids applications in nanomedicine. *The Journal of Supercritical Fluids, 101*, 193–214. https://doi.org/10.1016/j.supflu.2015.01.030
30. Agarwal, S., Wendorff, J. H., & Greiner, A. (2008). Use of electrospinning technique for biomedical applications. *Polymer, 49*, 5603–5621. https://doi.org/10.1016/j.polymer.2008.09.014
31. Liang, D., Hsiao, B. S., & Chu, B. (2007). Functional electrospun nanofibrous scaffolds for biomedical applications. *Advanced Drug Delivery Reviews, 59*, 1392–1412. https://doi.org/10.1016/j.addr.2007.04.021
32. Kim, K., et al. (2003). Control of degradation rate and hydrophilicity in electrospun non-woven poly(d, l-lactide) nanofiber scaffolds for biomedical applications. *Biomaterials, 24*, 4977–4985. https://doi.org/10.1016/S0142-9612(03)00407-1
33. Qin, C. C., et al. (2015). Melt electrospinning of poly(lactic acid) and polycaprolactone microfibers by using a hand-operated Wimshurst generator. *Nanoscale, 7*, 16611–16615. https://doi.org/10.1039/c5nr05367f

34. Xiao, P., et al. (2008). Synthesis and photopolymerization kinetics of benzophenone piperazine one-component initiator. *Polymers for Advanced Technologies, 19*, 409–413. https://doi.org/10.1002/pat.1024
35. Park, Y.-J., Lim, D.-H., Kim, H.-J., Park, D.-S., & Sung, I.-K. (2009). UV- and thermal-curing behaviors of dual-curable adhesives based on epoxy acrylate oligomers. *International Journal of Adhesion and Adhesives, 29*, 710–717. https://doi.org/10.1016/j.ijadhadh.2009.02.001
36. He, X.-X., et al. (2017). Electromagnetic functionalized micro-ribbons and ropes for strain sensors via UV-assisted solvent-free electrospinning. *Journal of Physics D: Applied Physics, 50*. http://doi.org/10.1088/1361-6463/aa8101
37. Kakisis, J. D., Liapis, C. D., Breuer, C., & Sumpio, B. E. (2005). Artificial blood vessel: The Holy Grail of peripheral vascular surgery. *Journal of Vascular Surgery, 41*, 349–354. https://doi.org/10.1016/j.jvs.2004.12.026
38. Tan, J. Y., et al. (2012). Esophageal tissue engineering: An in-depth review on scaffold design. *Biotechnology and Bioengineering, 109*, 1–15. https://doi.org/10.1002/bit.23323
39. Rinke, H. (1962). Elastomeric fibers based on polyurethanes. *Angewandte Chemie International Edition in English, 1*, 419–424. https://doi.org/10.1002/anie.196204191
40. Kang, Y. K., Park, C. H., Kim, J., & Kang, T. J. (2007). Application of electrospun polyurethane web to breathable water-proof fabrics. *Fibers and Polymers, 8*, 564–570.
41. Khil, M.-S., Cha, D.-I., Kim, H.-Y., Kim, I.-S., & Bhattarai, N. (2003). Electrospun nanofibrous polyurethane membrane as wound dressing. *Journal of Biomedical Materials Research Part B: Applied Biomaterials, 67B*, 675–679. https://doi.org/10.1002/jbm.b.10058
42. Guelcher, S. A. (2008). Biodegradable polyurethanes: Synthesis and applications in regenerative medicine. *Tissue Engineering Part B: Reviews, 14*, 3–17. https://doi.org/10.1089/teb.2007.0133
43. Liu, C., et al. (2015). Transparent air filter for high-efficiency PM2.5 capture. *Nature Communications, 6*. http://doi.org/10.1038/ncomms7205
44. Lv, F. Y., et al. (2016). In situ precise electrospinning of medical glue fibers as nonsuture dural repair with high sealing capability and flexibility. *International Journal of Nanomedicine, 11*, 4213–4220. https://doi.org/10.2147/IJN.S113560
45. Wang, L., et al. (2016). Ecofriendly fabrication of ultrathin colorful fibers via UV-assisted solventless electrospinning. *RSC Advances, 6*, 86597–86601. https://doi.org/10.1039/c6ra16268a
46. Dong, R. H., et al. (2015). In situ precision electrospinning as an effective delivery technique for cyanoacrylate medical glue with high efficiency and low toxicity. *Nanoscale, 7*, 19468–19475. https://doi.org/10.1039/c5nr05786h
47. Cao, L., Su, D., Su, Z., & Chen, X. (2014). Fabrication of multiwalled carbon nanotube/polypropylene conductive fibrous membranes by melt electrospinning. *Industrial & Engineering Chemistry Research, 53*, 2308–2317.
48. Bhardwaj, N., & Kundu, S. C. (2010). Electrospinning: A fascinating fiber fabrication technique. *Biotechnology Advances, 28*, 325–347.
49. Nagy, Z. K., et al. (2013). Solvent-free melt electrospinning for preparation of fast dissolving drug delivery system and comparison with solvent-based electrospun and melt extruded systems. *Journal of Pharmaceutical Sciences, 102*, 508–517. https://doi.org/10.1002/jps.23374
50. Reneker, D. H., & Chun, I. (1996). Nanometre diameter fibres of polymer, produced by electrospinning. *Nanotechnology, 7*, 216.
51. Lyons, J., Li, C., & Ko, F. (2004). Melt-electrospinning part I: Processing parameters and geometric properties. *Polymer, 45*, 7597–7603.
52. Hutmacher, D. W., & Dalton, P. D. (2011). Melt electrospinning. *Chemistry—An Asian Journal, 6*, 44–56.
53. Dalton, P. D., Grafahrend, D., Klinkhammer, K., Klee, D., & Möller, M. (2007). Electrospinning of polymer melts: Phenomenological observations. *Polymer, 48*, 6823–6833.
54. Sas, I., Gorga, R. E., Joines, J. A., & Thoney, K. A. (2012). Literature review on superhydrophobic self-cleaning surfaces produced by electrospinning. *Journal of Polymer Science Part B: Polymer Physics, 50*, 824–845.

55. Zhmayev, E., Zhou, H., & Joo, Y. L. (2008). Modeling of non-isothermal polymer jets in melt electrospinning. *Journal of Non-Newtonian Fluid Mechanics, 153*, 95–108.
56. Liu, Y., Wang, X., Yan, H., Guan, C., & Yang, W. (2011). Dissipative particle dynamics simulation on the fiber dropping process of melt electrospinning. *Journal of Materials Science, 46*, 7877–7882.
57. Zhmayev, E., Cho, D., & Joo, Y. L. (2011). Electrohydrodynamic quenching in polymer melt electrospinning. *Physics of Fluids (1994-present), 23*, 073102.
58. Yarin, A., Koombhongse, S., & Reneker, D. H. (2001). Bending instability in electrospinning of nanofibers. *Journal of Applied Physics, 89*, 3018–3026.
59. Hochleitner, G., et al. (2015). Additive manufacturing of scaffolds with sub-micron filaments via melt electrospinning writing. *Biofabrication, 7*, 035002.
60. Brown, T. D., et al. (2012). Design and fabrication of tubular scaffolds via direct writing in a melt electrospinning mode. *Biointerphases, 7*, 13.
61. Farrugia, B. L., et al. (2013). Dermal fibroblast infiltration of poly(ε-caprolactone) scaffolds fabricated by melt electrospinning in a direct writing mode. *Biofabrication, 5*, 025001.
62. Mota, C., Puppi, D., Gazzarri, M., Bártolo, P., & Chiellini, F. (2013). Melt electrospinning writing of three-dimensional star poly (ε-caprolactone) scaffolds. *Polymer International, 62*, 893–900.
63. Pham, Q. P., Sharma, U., & Mikos, A. G. (2006). Electrospinning of polymeric nanofibers for tissue engineering applications: A review. *Tissue Engineering, 12*, 1197–1211.
64. Sill, T. J., & von Recum, H. A. (2008). Electrospinning: Applications in drug delivery and tissue engineering. *Biomaterials, 29*, 1989–2006.
65. Agarwal, S., Wendorff, J. H., & Greiner, A. (2009). Progress in the field of electrospinning for tissue engineering applications. *Advanced Materials, 21*, 3343–3351.
66. Hu, X., et al. (2014). Electrospinning of polymeric nanofibers for drug delivery applications. *Journal of Controlled Release, 185*, 12–21.
67. Zhao, Y. T., et al. (2020). Self-powered portable melt electrospinning for in situ wound dressing. *Journal of Nanbiotechnology, 18*, 10. https://doi.org/10.1186/s12951-020-00671-w
68. Dvir, T., Timko, B. P., Kohane, D. S., & Langer, R. (2011). Nanotechnological strategies for engineering complex tissues. *Nature Nanotechnology, 6*, 13–22.
69. Brown, T. D., et al. (2014). Melt electrospinning of poly (ε-caprolactone) scaffolds: Phenomenological observations associated with collection and direct writing. *Materials Science and Engineering: C, 45*, 698–708.
70. Zaiss, S., Brown, T. D., Reichert, J. C., & Berner, A. (2016). Poly (ε-caprolactone) scaffolds fabricated by melt electrospinning for bone tissue engineering. *Materials, 9*, 232.
71. Farrugia, B. L., et al. (2013). Dermal fibroblast infiltration of poly(ε-caprolactone) scaffolds fabricated by melt electrospinning in a direct writing mode. *Biofabrication, 5*, 025001. https://doi.org/10.1088/1758-5082/5/2/025001
72. Langer, R. (1998). Drug delivery and targeting. *Nature, 392*, 5–10.
73. Allen, T. M., & Cullis, P. R. (2004). Drug delivery systems: Entering the mainstream. *Science, 303*, 1818–1822.
74. Yoo, H. S., Kim, T. G., & Park, T. G. (2009). Surface-functionalized electrospun nanofibers for tissue engineering and drug delivery. *Advanced Drug Delivery Reviews, 61*, 1033–1042.
75. Kenawy, E.-R., et al. (2002). Release of tetracycline hydrochloride from electrospun poly (ethylene-co-vinylacetate), poly (lactic acid), and a blend. *Journal of Controlled Release, 81*, 57–64.
76. Kataoka, K., Harada, A., & Nagasaki, Y. (2001). Block copolymer micelles for drug delivery: Design, characterization and biological significance. *Advanced Drug Delivery Reviews, 47*, 113–131.
77. Schneider, A., Wang, X. Y., Kaplan, D. L., Garlick, J. A., & Egles, C. (2009). Biofunctionalized electrospun silk mats as a topical bioactive dressing for accelerated wound healing. *Acta Biomaterialia, 5*, 2570–2578. https://doi.org/10.1016/j.actbio.2008.12.013
78. He, F.-L., et al. (2019). Controlled release of antibiotics from poly-ε-caprolactone/polyethylene glycol wound dressing fabricated by direct-writing melt electrospinning. *Polymers for Advanced Technologies, 30*, 425–434. https://doi.org/10.1002/pat.4481

79. Jiang, K., et al. (2014). Airflow-directed in situ electrospinning of a medical glue of cyanoacrylate for rapid hemostasis in liver resection. *Nanoscale, 6*, 7792–7798.



Yun-Ze Long received his B.S. degree in physics from the University of Science and Technology of China in 2000 and Ph.D. degree from the Institute of Physics, Chinese Academy of Sciences in 2005. He then worked in the Institut des Materiaux Jean Rouxel, CNRS, France, as a postdoctoral fellow. He has been with the Qingdao University since Dec. 2006, where he is currently a full Professor. From 2009 to 2011, he worked as a visiting researcher at the University of Sydney and the Hong Kong University of Science and Technology. His research interests focus on electrospinning, functional nanomaterials and their applications. He has published more than 360 papers and 12 book chapters and holds 88 Chinese patents and 6 Australian patents. He was awarded the Fellow of International Association of Advanced Materials, National Model Teacher, New Century Excellent Talent of Ministry of Education of China, Taishan Scholar and Young Expert with Outstanding Contributions of Shandong province of China.



Jun Zhang received the B.S. degree in physics from Qingdao University, China, in 2010 and the M.S. and Ph.D. degrees in physics from Nankai University, China, in 2016. From 2016 to 2019, he was a postdoctoral researcher with College of Materials Science and Engineering in Qingdao University, China. Since 2019, he has been an associate professor with the College of Physics, Qingdao University, China. He is the co-author of two books, and more than 80 articles, and holds 7 Chinese patents and 6 Australian patents. His research interests include electrospinning to prepare polymer, inorganic and composite nanofibers, antibiosis and medical dressing, fluorescence nanofiber processes and sensor applications.



Xiao-Fei Liu received the B.S. degree in electronic information from Qingdao University in 2017, and the M.S. degree in physics from Qingdao University in 2021. He is currently pursuing the Ph.D. degree in chemistry at Beihang University, Beijing, China. He is the author of 6 articles. His research interests include multifunctional micro/nano-materials, fundamental study of electrospinning, and the applications of oriented micro/nano-structures in tissue engineering.



Zhong Liu received his B.S. degree from Shandong University of Traditional Chinese Medicine, China, in 2008 and the M.S. and Ph.D. degrees from Zhejiang Chinese Medical University, China, in 2011 and 2019, respectively. From April 2012 to August 2016, he worked as an orthopedic doctor in the Shengli Hospital of Sinopec Shengli Petroleum Administration in Shandong province. He has been with the Qingdao University since May 2020, where he is currently a postdoctoral researcher. He is the co-author of 7 articles. He was awarded the Second Prize of Zhejiang Province Science and Technology Award. His research interests focus on electrospinning, functional nanofibers and their medical applications.



Miao Yu graduated from Nanjing University with a B.S. degree in Physics in 2010. He got his master's degree from Hong Kong University of Science and Technology, and Ph.D. degree in materials engineering from Columbia University. He co-authored one book chapter and more than 50 articles and holds 28 Chinese patents and 4 Australian patents. He was awarded the leader in Taishan industry in Shandong province (Taishan scholars from overseas experts in Shandong province) and the Second Prize of Shandong Province Science and Technology Award. His research interests focus on electrospinning, functional nanomaterials, their applications and industrialization.



Seeram Ramakrishna received the Ph.D. degree from the University of Cambridge (UK) in 1992, and the GMP training from Harvard University (USA) in 2001. From 1993 to 1996, he worked in the Kyoto Institute of Technology, Japan, as a visiting lecturer. He has been with the National University of Singapore since 1996, where he is currently a full Professor of materials engineering. From 1998 to 1999, he worked in MIT and Johns Hopkins University (USA) as a visiting scientist. He co-authored ten books, fifty book chapters, and more than 2000 articles with over 132,000 citations. His H-index is over 166. He is regarded as the guru of electrospinning and nanofibers. Google scholar ranked him among the top 36 salient authors out of three million materials researchers worldwide. He is named among the World's Most Influential Minds (Thomson Reuters), and the top 1% highly cited researchers in materials science and cross-field categories (Clarivate Analytics). He is a fellow of UK Royal Academy of Engineering, Academy of Engineering, Singapore, Indian National Academy of Engineering and ASEAN Academy of Engineering and Technology, and the Honorary Everest Chair of MBUST, Nepal.

Chapter 4
Melt Electrospinning Writing



Zeynep Aytac and Xinzhu Wang

Abstract Melt electrospinning is a technique using polymer melts to produce fibers in the micron range. The jet path of the polymer melts can be better controlled due to the low conductivity and this feature allows this technique to be used as an extrusion-based additive manufacturing technique named melt electrospinning writing (MEW). MEW can be used to manufacture complex structures with various pore sizes, pore geometries, and thicknesses. More importantly, the technique also enables the production of patient-specific materials at desired pore size, pore geometries, and thickness. In addition, the higher pore size of melt electrowritten fibers compared to the solution electrospun fibers leads to better cell infiltration in both in vitro and in vivo applications. As a result, MEW is widely used in various tissue engineering applications to support tissue regeneration in addition to reinforcing other types of materials employed in tissue engineering.

Keywords Additive manufacturing · Fibers · Electrospinning · Melt electrospinning writing (MEW) · PCL · Wound healing · Tissue regeneration

4.1 Introduction

Electrospinning is a technique to produce nanofibers mostly from polymers. In this technique, which is based on an electrohydrodynamic process, the polymer solution droplets are electrified thanks to the application of an electric field to the solution from the high voltage power supply. After the electrification, the jet is stretched and elongated. Finally, fibers are deposited on the collector by the evaporation of the

Z. Aytac (✉)
Department of Environmental Health, Harvard T. H. Chan School of Public Health, Center for Nanotechnology and Nanotoxicology, Harvard University, 665 Huntington Avenue, Boston, MA 02115, USA

X. Wang
Department of Chemical and Biomolecular Engineering, School of Chemical and Biomedical Engineering, Nanyang Technological University, 70 Nanyang Avenue, Singapore 637459, Singapore
e-mail: wang1294@e.ntu.edu.sg

© The Author(s), under exclusive license to Springer Nature Switzerland AG 2022

A. Vaseashta and N. Bölgen (eds.), *Electrospun Nanofibers*,
https://doi.org/10.1007/978-3-030-99958-2_4

solvent [1]. After the revival of the technique by Reneker et al. in the 1990s, its application areas expanded from filtration to tissue engineering since electrospun nanofibers have a highly porous nature and large surface-to-volume ratio [1]. Low cost, simple set-up, and capability of producing fibers from both natural and synthetic polymers [1, 2], as well as small molecules such as cyclodextrins [3, 4] are the main advantages of the method.

Solution electrospinning and melt electrospinning are the two main categories of electrospinning. However, until recently, most of the literature regarding electrospinning consists of studies about solution electrospinning, for which polymers are dissolved in a solvent [2]. The main reasons for the presence of only a few studies in the literature about melt electrospinning can be as follows. First, there is a limited number of polymers that can be melted due to their high melting point and associated cost of heating for melting those polymers. Second, melt electrospinning usually does not allow the production of fibers with a diameter at nano-size due to the low conductivity and high viscosity of the polymer melt. However, the optimization of various parameters can provide control to a certain extent on the diameter of melt electrospun fibers.

In tissue engineering, the fiber diameter and pore size of the scaffold are of utmost importance since the right choice of these might significantly promote cell invasion and vascularization [5]. Fiber diameters and pore sizes are known to be in micron levels for scaffolds to be ideal for cell attachment [6]. However, the diameters achieved in solution electrospinning are usually in the submicron-size and the pore size of solution electrospun fibers is much smaller than 20 μm even though the high surface area of the nanofibers triggers the attachment of cells to the scaffold to some extent [5]. Furthermore, the fibers are deposited in a random fashion on the collector while using a solution electrospinning set-up. In solution electrospinning, as the fibers are deposited on the collector, the fibers, which all carry the same charges, start to repel each other after a while. That is why it is not easy to maintain fiber placement in the same direction while performing additive manufacturing. Schematic representation of electrospinning and melt electrospinning writing (MEW) is given in Fig. 4.1. MEW enables the production of scaffolds having highly ordered structures with well-defined pore size, pore geometry, and thickness thanks to the less charged character of the jet compared to the solution-based system [5]. The main reason why melt electrospinning is preferred over solution electrospinning in additive manufacturing is the low conductivity of the polymer melt. This low conductivity is of vital importance for the continuous jet stability and fiber placement when hundreds of layers are deposited with close proximity on the collector during additive manufacturing [2]. Therefore, in contrast to solution electrospinning, MEW possesses better control on the fiber placement to develop scaffolds with suitable characteristics for cell infiltration [5]. Most importantly, MEW enables the production of patient-specific scaffolds thanks to the use of g-codes and computational methods that can be applied to precisely customize scaffolds with a patient's unique anatomy. As a conclusion, after the advancement in additive manufacturing technologies, it was seen that melt electrospinning can be used as an additive manufacturing method

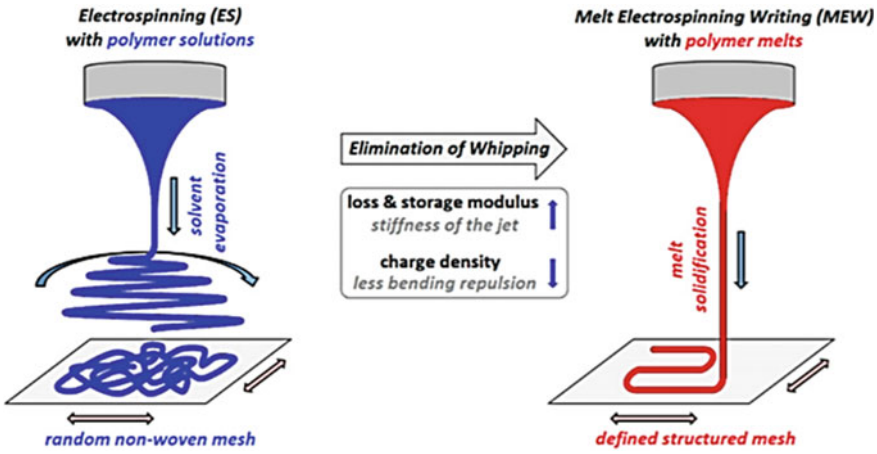


Fig. 4.1 Schematic representation of solution electrospinning and melt electrospinning writing (MEW) [9]

in the production of fibers [7]. Then, starting from 2016, the publications about melt electrospinning began to increase [7, 8].

Lastly, green-manufacturing with the elimination of the solvent in melt electrospinning during production, instead of an additional step for solvent removal after the production in solution electrospinning, provides another advantage for especially biomedical applications [2]. This is because harsh organic solvents are usually employed to dissolve the polymers and produce fibers using solution electrospinning. As a result, MEW becomes more popular than solution electrospinning when it comes to the additive manufacturing.

4.2 Melt Electrospinning Writing (MEW)

MEW is an additive manufacturing method that can produce fibers in micron size [10]. It is an extrusion-based additive manufacturing method and very similar to fused deposition modeling (FDM) [11]. The basic difference between MEW and FDM is the use of an electric field in MEW to obtain thinner filaments (fibers). The capability of MEW to produce thinner filaments extends the potential of melt electrowritten fibers in biomedical applications [11].

The set-up consists of a printing head, nozzle, heating system, delivery system (air/nitrogen pressure), high voltage power supply, moving collector, and computer [10]. The printing head is equipped with a heating system and used as a reservoir for the polymer melt until the melt is delivered to the nozzle, which is attached to the printing head [10]. The melt is sent through the nozzle with the help of a delivery system (i.e. air) and voltage is applied to either nozzle or collector [10]. As

a result of the applied electric field, charges accumulate at the tip of the nozzle or on the collector depending on where voltage is applied [10]. However, these charges cannot overcome the surface tension of the polymer solution in seconds as in solution electrospinning [10]. Therefore, jet initiation can take several minutes during MEW depending on many parameters such as the flow rate, voltage power supply, and nozzle-to-collector distance [10]. Finally, fibers are written on the moving collector over time according to the specific pattern designed on the software [10].

The viscosity of a polymer melt is much higher than a typical polymer solution, whereas the conductivity is not as high as a typical polymer solution since the solvents are not involved in MEW [12]. That's why, the diameters of melt electrowritten fibers, which is usually ranging from 1 to 50 μm, are larger than solution electrospun fibers [12]. However, the jet formed during the MEW process tends to maintain its straight path thanks to the lower conductivity of the polymer melt, and this allows MEW to be used as an additive manufacturing method in contrast to solution electrospinning.

4.2.1 Polymers Used for MEW

Poly(ε-caprolactone) (PCL) is still the most widely used polymer due to its low melting temperature and fast solidification rate, which enables it to be an easily processible polymer for MEW [12]. Abbasi et al. used PCL to fabricate scaffolds with precisely controlled patterns via MEW [13], while Pennings et al. produced a tubular bi-layered PCL scaffold, in which the outer layer was produced by MEW [14]. Moreover, PCL is a degradable polymer and it demonstrates good biocompatibility with a wide range of cell types, hence melt electrowritten PCL scaffolds are commonly used as substrates for cell culture [15–18]. However, PCL is a highly hydrophobic material, which may result in inefficient cell attachment, hence limits its application in tissue engineering [19]. That is why, many methods have been developed to increase the hydrophilicity of the PCL scaffolds, such as sodium hydroxide (NaOH) etching [18], collagen or fibronectin coating [14], incorporations of hydrophilic additives [20], and overnight cell seeding [21]. After the treatments, PCL scaffolds become less hydrophobic, serving as better substrates for cell adhesion and growth.

As MEW becomes more and more popular in additive manufacturing, an increasing number of polymers and copolymers are processed using this technique for various biomedical applications. Polylactic acid (PLA), another hydrophobic polymer, can be printed to form fibrous mats similar to PCL thanks to its rapid solidification rate [22]. Polyethylene glycol (PEG), a hydrophilic polymer, was also printed as 3D fibrous scaffolds that can rapidly swell in water to form a hydrogel [23]. However, hydrophilic polymers were rarely used for MEW because these polymers attract water in the air, leading to repulsion between fibers during the printing process, which makes the control of fiber morphology challenging. Therefore, to broaden the range of printing polymers for MEW, many amphiphilic copolymers were synthesized with improved hydrophilicity compared to pure PCL or PLA and

higher stability compared to PEG, while achieving specific functionalities or mechanical properties. Poly(oligo 3,4-ethylenedioxythiophene)-co-ε-caprolactone was used for MEW to produce electroactive fibrous mats that was able to guide neural growth under electrical stimulation thanks to high conductivity of the copolymer [24]. Poly(ε-caprolactone)-block-poly(ethylene glycol)-block-poly(ε-caprolactone) was synthesized to improve the hydrophilicity of the printing material by linking blocks of hydrophobic PCL and hydrophilic PEG, hence scaffolds fabricated by MEW showed great compatibility with cells while providing a mechanical support for cell growth and tissue regenerations [25]. Moreover, there are also blends of polymers, such as the blend of PCL and poly(hydroxymethylglycolide-co-ε-caprolactone) used to fabricate scaffolds that supported the growth of cells with an improved cell viability and alignment compared with the scaffolds fabricated by pure PCL thanks to the presence of biocompatible copolymer [26]. To conclude, various polymers can be applied in MEW based on the requirements for various biomedical applications. However, it is worth mentioning due to high temperature needed to melt some of the polymers, there are some limitations on polymer selection.

4.2.2 Parameters and Diameter of the Melt Electrowritten Fibers

In order to achieve homogenous, straight, and well-aligned fibers ultimately to manufacture scaffolds with highly ordered structure by MEW, the process parameters including flow rate, nozzle diameter, nozzle-to-collector distance, electrical voltage, temperature, collector speed, and pressure are required to be optimized in addition to the right choice of the molecular weight of the polymer [5, 7]. The diameter of fibers as well as the porosity of the scaffolds produced by MEW can be controlled by adjusting these parameters [12]. Studies showed that fibers having diameters around 275 nm can be even produced using a modified nozzle in MEW [27]. However, the diameters of melt electrowritten fibers usually range from sub-micron to hundreds of microns [12]. Figure 4.2 shows the SEM images of melt electrowritten fibers achieved [28].

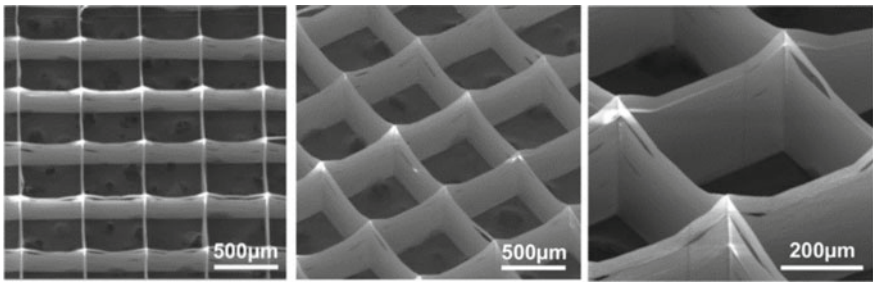


Fig. 4.2 SEM images of melt electrowritten fibers with 500 µm pore size [28]

Similar to electrospinning, as the flow rate, nozzle diameter, and nozzle-to-collector distance increase, the diameter of the fibers increases as well [12], whereas when the electrical voltage increases, the diameter of the fibers decreases.

Molecular weight: As in solution electrospinning, molecular weight of the polymer is of great importance for the spinnability of the fibers [5]. However, the concentration of the polymer cannot be changed because the solvent is not involved in the process of MEW [5]. That is why, temperature to melt the polymer is of vital importance for polymer melt to be extruded from the reservoir [5]. If the molecular weight is higher than required, the viscosity gets extremely high and extrusion of polymer melt cannot be done [5]. In addition, if the viscosity is too high, it is also very difficult for electrostatic forces to draw the polymer melt, and even though the filament can be achieved, diameter of the fibers can be large [5]. Therefore, the first step is choosing the right molecular weight for a certain polymer [5]. Then, the temperature is decided which can melt the polymer and make the extrusion of thin filaments possible [5].

Temperature: Temperature is decided depending on the melting temperature of the polymer chosen and it should be as low as possible since otherwise polymer melt might not solidify and deposit uniformly [12]. Fibers might even break into fractures due to the high temperature especially when the collector speeds are high [12]. It is also worth mentioning that, initially, as the temperature increases, the fiber diameter increases since delivery mass becomes more thanks to the reduced viscosity of the polymer melt. As the temperature continues to increase, the viscosity becomes very low, which causes the jet to be more readily elongated and hence thinner fibers are produced [12].

Collector speed: Collector speed is also a very important parameter in MEW. If a stationary collector is used as in most of the solution electrospinning set-ups, random coiled fibers will be formed on the collector because of the buckling effect [12]. On the contrary, when the collector moves laterally to the path of the jet, the wavelength of coiling reduces due to the tensile force acting against the buckling effect [5, 12]. The effect of increasing collector speed is displayed in Fig. 4.3a–d. If the collector speed is increased further to reach a speed that equals to the jet speed, coiling and tensile force will be balanced, and coiling will finally disappear completely [5, 12]. As a result, continuous fibers on a straight line can be achieved in the movement direction of the collector [5, 12]. If the collector speed is too high, jet lags behind the

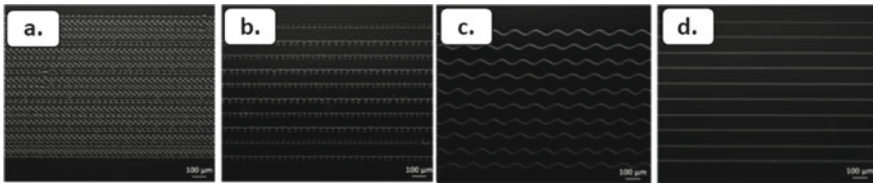


Fig. 4.3 Fiber collection performed at an increasing critical translational speed (CTS). **a**–**c** Below CTS, **d** above CTS [29]

impact point because of the domination of tensile force over buckling phenomena [5]. An increment in the collector speed might also decrease the diameter of the fibers but experiments show that this reduction is not as effective as the flow rate related parameters [5].

Collector type: Even though most of the MEW set-ups are designed with flat collectors, it was shown the possibility of using cylindrical collectors as well [30]. The use of these collectors enables the production of scaffolds with several patterns, and when the speed is applied to the collector, even more variant structures can be achieved [30].

Pressure: Pressure influences the mass delivery rate, thus, when the pressure is increased, more polymer melt will be sent through the nozzle, and diameter will be increased [29]. If the pressure is increased excessively, irregularity is observed in the edges of the fibers [29]. Therefore, if the pressure needs to be higher to increase the mass flow of the polymer melt, the electrical voltage can be increased to stabilize and balance the forces [29].

4.2.3 Challenges and Limitations

One of the most important limitations of solution electrospinning is the repelling of the jet because of the charge built up during the fiber deposition [5]. That is why, accurate placement of fibers is challenge leading to randomly deposited fibers with no control on the pattern, pore size, or geometry [5]. Even if the charge build-up is an issue that can be overcome by optimization of the parameters in MEW, some defects can be observed as shown in Fig. 4.4a, b.

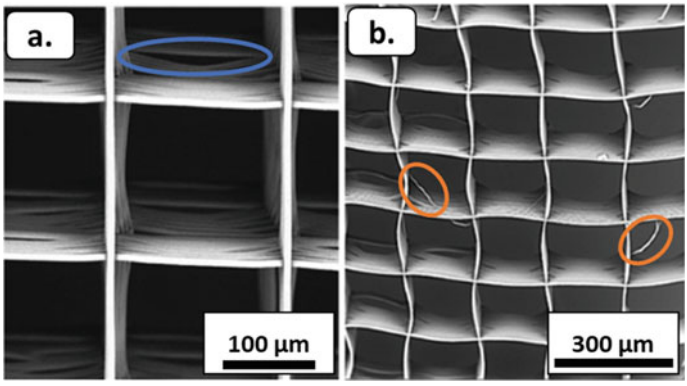


Fig. 4.4 Scanning electron microscopy (SEM) images showing fiber displacement: **a** defects like gaps (blue circle) [26], **b** fibers deposited in the pore areas (orange circles) [26]

Another disadvantage caused by the built-up charges is the limitation in the achievable thickness in the solution electrospun nanofibers [5]. In contrast, MEW allows the production of constructs with thickness up to cm height thanks to the less charged nature of polymer melts as long as the polymer is not conductive [5]. The charge build-up can be better controlled during MEW as there is no solvent that needs to be evaporated, which is the main reason for the charges in solution electrospinning [5]. Even though, it was suggested that there is a small amount of charge built up and trapped in the internal structure of the scaffold, the charge is not enough to repel the fibers [5]. Charge build up might be a problem for MEW after a certain number of layers are printed or when the pore size is smaller than 250 μm [5]. For example, if the number of layers is more than 50, some of the fibers start to deposit in the pore areas instead of the top of the previously aligned fibers and after a while the pores are also filled with fibers [5]. However, if the pore size is around 250 μm, even 450 layers of fibers can be printed [28].

4.3 Application of Melt Electrowritten Fibers

4.3.1 Tissue Regeneration

Tissue regeneration is a process to form or repair tissue that is damaged [31]. Recently, the most impactful research in this field is to construct complex scaffolds that support the stem cell growth and promote tissue formation. These scaffolds are also required to be biocompatible with cells [32]. MEW is widely used in tissue regeneration applications thanks to its capability of producing fibers with various pore sizes and geometries and the absence of solvents in the process. In addition, it is possible to design advanced structures with many layers each having different features in terms of pore size, pore geometry, and fiber diameter [33]. Figure 4.5 shows the photographs of fibrous membranes with decreasing pore size.

Fuchs et al. fabricated highly-ordered 3D PCL fibrous scaffolds via MEW for potential oral wound healing applications. The scaffolds were designed to be square-patterned 10-layered structures with varying pore sizes ranging from 225 to 500 μm and then seeded with osteoblasts (OBs). All PCL scaffolds showed good cytocompatibility indicated by high cell viability, and protein concentration. The scaffolds with 225 μm of pore size demonstrated the highest cell viability, which can be explained by its higher surface area leading to more cell attachment [33]. Bertlein et al. printed 3D PCL scaffolds by MEW to form capillary-like network structures for in vitro vascularization. The scaffolds were fabricated as a 0/90° crosshatch design with pore sizes ranging from 100 to 350 μm. Fibronectin, an extracellular matrix (ECM) component, was coated onto the scaffolds for the better attachment of human umbilical vein endothelial cells (HUVECs). As a next step, the normal human dermal fibroblasts (NHDFs), coated with fibronectin/gelatin nanofilms to improve cell interactions, were seeded into scaffolds to enable the formation of a vascular network.

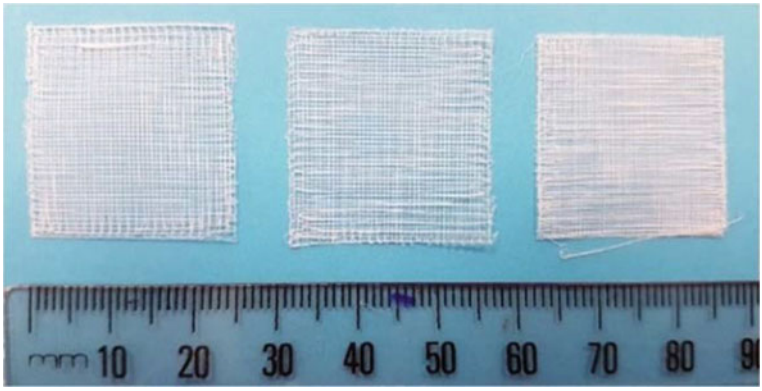


Fig. 4.5 Visual comparison of scaffolds with decreasing pose size from 500 to 300 μm [34]

The scaffolds with a larger pore size reduced hypoxic conditions for cells in the middle of the pore, thereof enhanced cell viability and promoted the formation of neovascular-like structures. Besides, increased consumption of vascular endothelial growth factors (VEGFs) by cells was observed in the scaffolds with an increasing pore size, which also indicated a positive correlation between pore size and vessel formation [35].

In order to ameliorate the regeneration in various tissues, bioactive agents were also incorporated into the scaffolds before printing [20, 34] or printed scaffolds were coated with bioactive agents as a post-modification method [15, 24, 36, 37]. In the study of Hewitt et al., PCL fibers embedded with milk proteins such as lactoferrin and whey protein were produced by MEW as a potential tissue-engineered scaffold for deep dermal regeneration. The melt electrowritten PCL scaffolds were designed as 5-layered 0/90° crosshatch with a pore size of 300 μm. The released milk proteins from the scaffold improved cell viability, proliferation, and migration of skin fibroblasts and epithelial keratinocytes in vitro and increased wound closure rate due to the anti-inflammatory and antioxidative effects of the milk proteins [34]. The study of Abdal-hay et al. introduced highly porous 3D fibrous scaffolds fabricated by MEW using the blend of PCL-hydroxyapatite (HA) nanoparticles for potential use in bone tissue engineering. The scaffolds were designed with a 0–90° crosshatch pattern and a pore size of ~190 μm. HA ameliorated thermal stability of the PCL scaffold while maintaining its good flexibility due to the formation of hydrogen bonding between PCL and HA nanoparticles. More importantly, the scaffolds displayed better infiltration and growth of OBs in vitro, evidenced by higher DNA content and cell activity than PCL scaffolds without HA. This can also be attributed to the higher surface roughness and wettability of the fiber thanks to HA that facilitated better cell growth and adhesion [20].

There are several studies in the literature using the post-modification methods to produce bioactive agent functionalized scaffolds [15, 24, 36, 37]. Ritzau-Reid

et al. synthesized a co-polymer named poly (oligo 3,4-ethylenedioxythiophene)-co-ε-caprolactone (oligoEDOT-PCL) and used this polymer to fabricate electroactive fibrous mats using MEW for the guidance of neural growth. The lattices with ~100 μm spacing were designed by using a blend of oligoEDOT-PCL and PCL at a 1:1 ratio. Melt electrowritten mats were able to be produced thanks to the processibility of PCL in MEW, whereas the electroactivity of the mats is attributed to the presence of oligoEDOT in the structure. The presence of conductive oligoEDOT-PCL in the structure enhanced neurite outgrowth and brunching of neural stem cells under electrical stimulation. Furthermore, melt electrowritten scaffolds, washed by Matrigel™, facilitated neural stem cells' adhesion on their heterogeneous macroarchitecture and further improved cell differentiation [24]. In the study of Hammerl et al., calcium phosphate (CaP) based apatite particles-coated PCL scaffolds were fabricated by MEW as a co-culture platform to assess the osteogenesis potential of the scaffolds for bone regeneration. PCL scaffolds were manufactured by MEW with an average pore size of 100 μm. CaP particles were then coated on the surface of the scaffolds by immersing them into simulated body fluid (SBF). The coated scaffolds were washed with NaOH to increase the hydrophilicity of the scaffolds prior to cell seeding. The CaP-coated PCL scaffolds enhanced cell proliferation and ECM mineralization due to the capability of CaP for osteogenesis. Moreover, the co-culture of OBs and peripheral blood mononuclear cells (PMBCs) in the scaffolds improved cell proliferation and mineralization compared to the monoculture of OB most likely because PMBC secreted cytokines that promoted OB differentiation in the early phase [37]. Muerza-Cascante et al. fabricated 3D PCL scaffolds using MEW to mimic the physiological microenvironment in vitro for the culture of OBs and mesenchymal stem cells (MSCs) that form endosteum-like tissue. The scaffolds were designed as a 0–90° crosshatch patterned structure consisting of 10 layers with a 100 μm pore size. To reduce hydrophobicity and facilitate the cell attachment, the surface of the scaffolds was etched with NaOH followed by CaP coating (Fig. 4.6). OB seeded NaOH etched scaffolds were also used for co-cultures with haematopoietic stem cells (HSCs) to investigate haematopoietic mechanisms in the derived endosteal bone-like tissue. The OB-seeded scaffolds showed a better ECM deposition and cell differentiation, indicated by significant deposition of endosteal proteins and expression of osteogenic markers compared to MSCs. The CaP coating further induced osteocalcin expression from OBs. The scaffolds also created a relevant endosteal environment to support the growth and migration of HSCs. This might be related to the expression of mixed endosteal proteins from OBs, especially heparin sulphate that potentially promoted the proliferation of HSCs [36]. Eichholz et al. modified the surface of the melt electrowritten PCL scaffolds, which has a square patterned structure and 50 μm pore size, with HA by three different methods for bone regeneration. The incorporation (iHA), plate coating (pHA), and nanoneedle coating (nnHA) methods were then used to decorate the scaffolds. For pHA and nnHA methods, melt electrowritten PCL scaffolds were immersed into either HA-containing SBF solution or calcium and phosphate solution, respectively. The incorporation of HA improved mechanical properties and hydrophilicity of the scaffolds. nnHA was the most powerful method

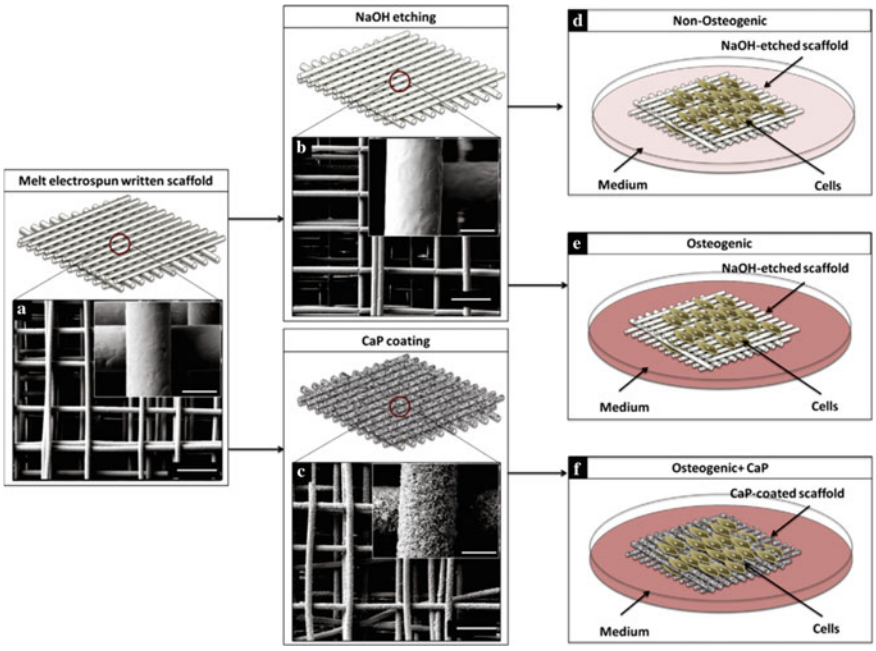


Fig. 4.6 SEM images of melt electrowritten scaffolds subjected to NaOH etching or CaP coating. **a** Before surface treatments, after **b** NaOH etching, and **c** CaP coating. Primary human OBs or placenta-derived MSCs were seeded onto surface-treated scaffolds and grown in **d** non-osteogenic and **e–f** osteogenic conditions. Scale bars: 100 μm, 20 μm (inserts) [36]

which significantly enhanced MSCs osteogenesis identified by the increased expression of alkaline phosphatase activity and production of collagen and calcium. This was associated with the extrafibrillar and nanoneedle-shaped coating morphology with an aggregate size of ~100 nm and the lowest crystallinity that best mimicked the native bone morphology. It was also demonstrated that nnHA facilitated the controlled release of bone morphogenetic protein 2 (BMP 2) to further enhance the osteogenesis [15].

To improve the effectiveness of the bioactive agent coated scaffold based therapies even further, various pore arrangement designs were created as well [13]. Abbasi et al. developed melt electrowritten PCL scaffolds with precisely controlled offset and gradient structures to increase cell entrapment in bone regeneration. The tri-layered offset structure was manufactured with a pore size of 500 μm in which each layer was printed with a horizontal shifting, whereas the tri-layered gradient structure was manufactured with 750 μm, 500 μm, and 250 μm pore size at the bottom, middle, and top layers, respectively. The subsequent CaP was coated by immersing the scaffolds into SBF to enhance hydrophilicity of the scaffolds for cell culture as well as to produce a rough surface facilitating the formation of a mineralized matrix and inducing cell osteogenesis. The results showed that both offset and gradient

scaffolds supported OBs' growth and differentiation by encouraging alkaline phosphatase activity, calcium deposition, and expression of osteocalcin and osteopontin [13].

In vivo studies were also conducted using bioactive agent coated melt electrowritten scaffolds [38]. In the study of Abbasi et al., bone regeneration capability of HA coated melt electrowritten PCL scaffolds with various designs was further investigated in vivo. The tri-layered offset structure was manufactured at the pore size of 500 μm with a horizontal shifting in each layer printed. The tri-layered gradient structure was manufactured to have 750 μm, 500 μm, and 250 μm pore size at the bottom, middle, and top layers, respectively. In addition, two more scaffolds having a uniform pore size (250 μm or 500 μm) were manufactured. HA coating on the scaffolds increased the hydrophilicity of the scaffolds to be implanted into the calvaria of the rats while improving the osteogenic ability of the material. The structure with a pore size of 500 μm and tri-layered gradient structure displayed a high expression of mineralization markers (collagen I, osteocalcin, and osteopontin) and an endothelial marker (VEGF) due to sufficient oxygen and nutrient supply for cell survival. Moreover, the gradient structure performed the best bone regeneration in calvaria defects after implantation compared to the other structures [38].

4.3.2 Improvement of Mechanical Properties of Materials

The melt electrospun fibers can also be used to reinforce various materials, including gelatin-methacrylamide (GelMA) [18, 39], alginate [18], GelMA/hyaluronic acid-methacrylamide (HAMA) [40], polyacrylamide (PAA), and poly(2-hydroxyethyl methacrylate) (pHEMA) hydrogels [41], or other types of materials such as polyvinyl alcohol (PVA) film [42].

In one of the first studies to reinforce hydrogels with melt electrowritten fibers, Visser et al. reinforced GelMA and alginate hydrogels with highly organized 3D printed fibrous PCL scaffolds printed to meet mechanical requirements for cartilage tissue repair. The scaffolds were designed with a well-aligned 0°–90° crosshatch structure. Hydrogel stiffness was significantly improved due to the resistance introduced from highly organized scaffolds against hydrogel's horizontal expansion under compression loading. Moreover, the reinforced GelMA hydrogels possessed good elasticity and recovery ability after repetitive compression because of the synergistic effect from fiber stretching and hydrogel confinement, which stimulated the fluid dynamics in the native articular cartilage as well [18]. In the study of Castilho et al., reinforcement mechanisms of melt electrowritten PCL fibrous scaffolds in GelMA hydrogel were investigated by using two finite element models. The models demonstrated a pulling effect of fibrous scaffolds against the lateral expansion of the hydrogels, by which the scaffolds confined the hydrogels, achieving a better mechanical strength. The models also presented a combinatory effect of load transfer at interconnections of the fibers and the hydrogel resistance against scaffolds' bulking, which led to uniform shear distribution through the scaffolds. The two reinforcement

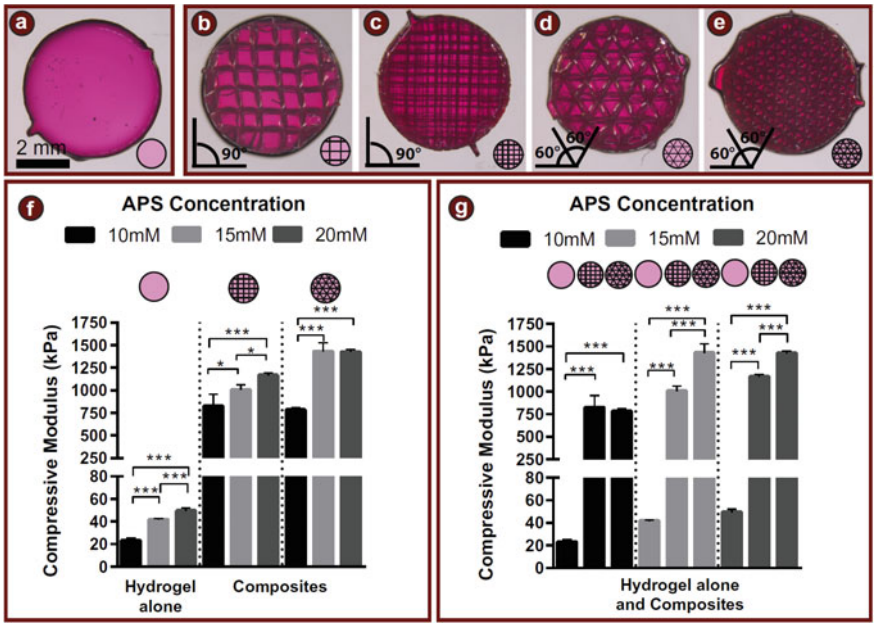


Fig. 4.7 Stereomicroscopy images of **a** hydrogel alone and **b–e** fiber-reinforced hydrogel with various designs, **f** effect of hydrogel matrix properties on the compressive Young's modulus of fiber-reinforced hydrogels in comparison to hydrogels alone group, **g** effect of the architecture of the reinforcement on the compressive Young's modulus of fiber-reinforced hydrogels in comparison to hydrogels alone group [40]

mechanisms provided novel insights on how melt electrowritten scaffolds improved mechanical properties of the hydrogels under uniaxial compression [39]. Bas et al. produced melt electrowritten fibrous PCL scaffolds to reinforce GelMA/HAMA composite hydrogel (Fig. 4.7a–g) [40]. Ruijter et al. fabricated melt electrowritten PCL fibers with a sinusoidal design to cross another melt electrowritten wall on top, forming a well-defined stabilizing scaffold to reinforce PAA and pHEMA hydrogels. The scaffolds improved shear modulus of the hydrogels, which simulated interactions between native tissues under mechanical compression better than hydrogels reinforced by scaffolds without sinusoidal design [41].

In addition to the hydrogels, the mechanical properties of other types of materials such as films were enhanced as well [42]. Agarwal et al. reinforced PVA film with melt electrowritten PCL scaffolds, forming thin films with improved tensile strength and stiffness. The improvement was explained by the presence of the scaffolds that were structurally resistant to deformation. Interactions between carboxyl and hydroxyl groups from the PCL and PVA also contributed to the improved mechanical properties of the hydrogels [42].

4.3.3 Combinatory Effect of Tissue Regeneration and Improvement of Mechanical Properties of Scaffolds

Melt Electrowritten Fibers

Melt electrowritten fibers are good candidates as scaffolds, where high mechanical properties are needed in addition to the contribution to tissue regeneration, thanks to their tunable pore size [21] as well as complex patterns [43, 44]. More importantly, MEW enables the production of personalized scaffolds matching perfectly with the patient's anatomy [17, 45].

Brennan et al. fabricated bone marrow stem cell-laden PCL fibrous scaffolds with varying pore sizes by MEW to better replicate the native environment of bone for tissue regeneration. The scaffolds were composed of 40-layers with square pores having 100 μm, 200 μm, or 300 μm size. The scaffolds with a pore size of 100 μm demonstrated the greatest stiffness and tensile strength due to the higher number of fibers in the load-bearing direction. In addition, small pore size and high surface area of the scaffolds led to the highest attachment and osteogenesis and ultimately to the highest collagen production and mineral deposition [21].

Various complex geometries were also shown to have great potential in many applications thanks to their improved mechanical properties [43, 44]. In the study of Saidy et al., highly-organized and biodegradable fibrous PCL scaffolds were fabricated in wave-like patterns with biomimetic mechanical properties of native tissues for heart valve tissue engineering. The scaffolds were designed with 20 layers and ~2 mm radial pore size. The scaffolds with precisely defined microstructure exhibited J-shaped strain stiffness, anisotropy, and viscoelastic properties similar to the native heart valves. The scaffolds also supported the growth of human umbilical cord vein smooth muscle cells and the regeneration of heart valve tissue owing to their special biomimetic structure designs. Moreover, the engineered tri-leaflet heart valves produced by MEW displayed good hydrodynamic performance in a mock circulation system at physiological aortic conditions [43]. In another study, Olvera et al. introduced an electroconductive cardiac patch, closely matching the mechanical properties of human myocardium for the treatment of myocardial infarction. Patches were made of melt electrowritten PCL fibers with an auxetic pattern and then coated with polypyrrole nanoparticles. Thanks to their pattern, the elasticity of the patches was improved, and it was much higher compared to the conventional square designs. The auxetic fibers were also shown to be consistent with the anisotropic ratio of the stiffness in the native human myocardium. Moreover, the polypyrrole coating provided electroconductivity to these patches in order to transmit electrical signals between cells, leading to synchronous cardiac contraction, which enabled more attachment of human mesenchymal stromal cells but similar cytocompatibility in vitro compared to non-coated patches [44].

One of the most important features of MEW as an additive manufacturing technique is its capability of producing personalized scaffolds [17, 45]. Somszor et al. developed melt electrowritten personalized stents made of PCL and reduced graphene oxide (rGO). In addition to the biodegradability, the mechanical properties of these

coronary artery stents were superior to traditional permanent stents. The composites were printed via MEW to fabricate stents with a thickness of 60–80 μm, which was below the thicknesses of the clinically used stents, and complex geometries including curved pattern, squared pattern, rectangular pattern, and the combination of curved and straight-angled pattern with varying pore sizes. They showed significant improvement in the mechanical properties including flexural stiffness compared to PCL fibers obtained without rGO, since rGO can act as a nucleation agent enhancing crystallinity of the material. The stents were also found to support endothelial cell adhesion, proliferation as well as platelet adhesion due to their high degree of geometrical complexity and the presence of rGO that absorbed proteins to regulate the interaction between cells/platelet and stents' surface. Most importantly, this study showed that the MEW technique allowed the production of personalized stents that fitted patient's anatomy [17]. In vivo studies were also performed using these personalized scaffolds [45]. Su et al. reported 3D coil compacted PCL scaffolds, with varying coil densities and highly-ordered patterns using MEW, for potential bone tissue engineering. The 10-layered coil-compacted melt electrowritten PCL scaffolds with rhombic patterns or lumbar vertebra-structure were printed by changing collector speed periodically. The coil density was tunable by changing collector speed and hence resulted in tunable mechanical properties of the scaffolds. Moreover, the scaffold with rhombic pattern-promoted cell growth and showed great biocompatibility indicated by normal level of inflammatory biomarkers in serum after implantation due to their highly ordered patterns and biocompatible material used. The scaffolds were also shown to be a suitable platform for the growth of MSCs thanks to the coil compacted scaffold patterning [45].

Hydrogels Reinforced with Melt Electrowritten Fibers

In addition to the printed scaffolds themselves, these scaffolds can also be used to reinforce hydrogels which are widely utilized materials supporting cell attachment thanks to their ability to mimic the ECM structure, to provide tunable mechanical support for the cells, and to maintain distinct 3D structure for homogenous cell loading [46, 47]. As mentioned above, in one of the first studies reported in the literature concerning the reinforcement of hydrogels by melt electrowritten scaffolds, Visser et al. reinforced soft GelMA hydrogels with highly organized microfibrous 3D networks printed via MEW to provide both biological and mechanical compatibility as an artificial cartilage tissue candidate [18]. In addition to the biopolymer-based hydrogels, the combination of biopolymer and synthetic hydrogels was also reinforced by melt electrowritten scaffolds [48]. Bas et al. developed PCL fibrous networks to reinforce highly-charged (PEG-peptide conjugate)/heparin hydrogel for regenerative cartilage tissue engineering. The scaffolds were designed with a 0°–90° crosshatch architecture and a fiber spacing between 200 and 600 μm. The hydrogel-based composites were prepared by crosslinking PEG-peptide conjugates and heparin after combining them with fibers in a mold. The composites were found to be mechanically more durable due to the presence of highly organized melt electrowritten fibrous scaffolds in the structure. In addition, the highly charged hydrogels led to charge-driven osmosis, which emulated mechanical-electrochemical properties of

proteoglycan matrix of the native cartilage tissue, to provide a suitable environment for cartilage regeneration in vitro [48].

Bioactive compounds such as growth factors and magnesium phosphate were also incorporated to enhance the cell attachment [25, 28]. In the study of Qiao et al., GelMA hydrogel reinforced with a tri-layered scaffold, made of melt electrowritten poly(ε-caprolactone)-block-poly(ethylene glycol)-block-poly(ε-caprolactone) (PCEC) fibers, was fabricated to enhance osteochondral regeneration. The tri-layered PCEC scaffold was composed of subchondral, mid-deep, and superficial layers which had different laydown patterns and fiber spacings ranging from 100 to 600 μm. GelMA hydrogel in each layer was loaded with various growth factors such as BMP 2 and transforming growth factor beta (TGF-β1), TGF-β1, and BMP 7 encapsulated in poly lactic-co-glycolic acid (PLGA) microspheres in subchondral, mid-deep, and superficial layer in addition to the MSCs. The integrated tri-layered scaffold was fabricated by stepwise addition of hydrogel and UV crosslinking. The introduction of the tri-layered PCEC scaffold in GelMA hydrogel significantly improved the mechanical strength of the scaffold. The reinforced hydrogel induced the differentiation of MSCs down to the chondrogenic and osteogenic lineages in vitro and showed cartilage and subchondral bone regeneration in vivo mainly due to the growth factors in each layer and the 3D matrix structure with various geometries (Fig. 4.8a–c) [25]. In the study of Dubey et al., bioactive amorphous magnesium phosphate (AMP)-laden GelMA hydrogels were reinforced with highly porous melt electrowritten PCL meshes as barrier membranes for the treatment of periodontitis. GelMA hydrogel was loaded with AMP to further improve the osteogenic ability of the material and then infiltrated into NaOH pretreated PCL meshes to form a fiber-reinforced hydrogel membrane. 450 layers of PCL fibers had a 0/90° crosshatch design with a pore size of 500 μm. Finally, the membrane was applied in calvaria defects created in rats for in vivo studies. The presence of melt electrowritten PCL fibers in the hydrogel delayed the degradation of hydrogel and prevented soft tissue invasion and allowed time for progenitor cells to migrate slowly and regenerate the bone. The hydrogel membranes also supported cell mineralization and osteogenic gene expression for bone regeneration in vivo. Fiber-reinforced hydrogels were shown to be quite useful for the treatment of periodontitis not only due to the reinforcement of hydrogels by PCL scaffolds but also due to the presence of bioactive AMP loaded in the hydrogels [28].

Hydrogels were known to show good biocompatibility with a wide range of cells, which supported cell growth and promoted ECM formation as well [47]. In addition, cells encapsulated in hydrogels are capable of remodeling their surrounding matrix and producing a new ECM for tissue regeneration [49]. Cell-laden hydrogels were also embedded with melt electrowritten scaffolds for better cell attachment and mechanical property improvement at the same time [26, 50–52]. Janzen et al. developed a Matrigel™ matrix, which was reinforced with melt electrowritten PCL scaffold, to culture cortical neurons for the study of the neuronal network in vitro. The melt electrowritten scaffold was designed to be a rectangular mesh with 10 layers and 200 μm of spacing. A cell suspension containing Matrigel™, a gelatinous protein mixture, was directly pipetted onto scaffolds. The PCL scaffolds

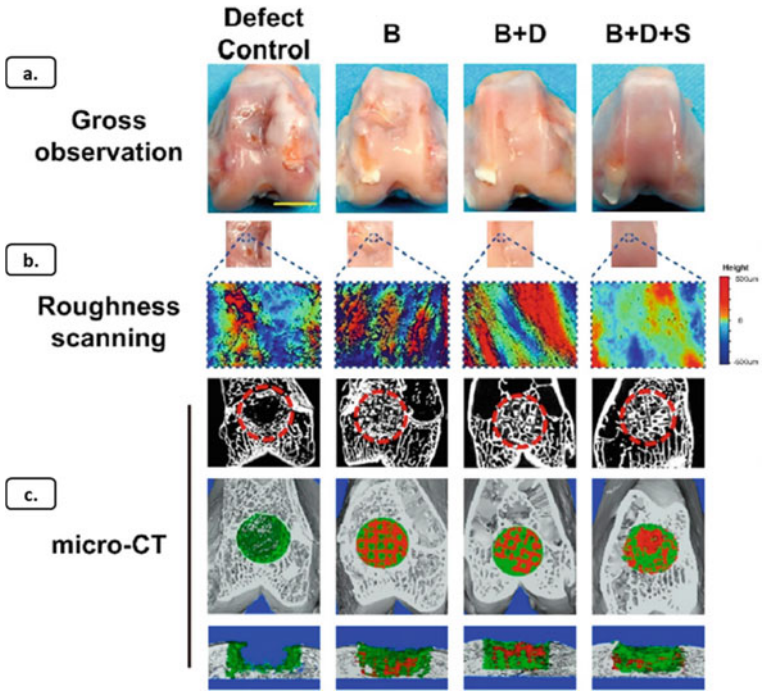


Fig. 4.8 The tri-layered constructs facilitated the tissue regeneration in a rabbit osteochondral defect model. **a** Gross observations of defect repair at 24 weeks post-surgery (scale bar 5 mm); **b** surface topography of the repaired cartilage; **c** micro-CT images (transverse view and sagittal view) of bone repair at 24 weeks post-surgery. The off-white color, green color and red color in CT images represent the primary bone, the regenerated bone and the implanted scaffold, respectively [25]

improved mechanical properties of the 3D matrix for easy handling of the formed neural networks for cell culture purposes. Moreover, the scaffolds also facilitated the growth of cortical neurons with higher viability and faster differentiation rate due to higher secretion of growth factors in a 3D matrix compared to a 2D matrix in which cells were seeded on poly-lysine coated glass coverslips [50]. Besides, Castilho et al. developed highly-organized ultrafine fibrous scaffolds by MEW using a blend of polymers, (poly(hydroxymethylglycolide-co-ε-caprolactone)/(poly-ε-caprolactone) (pHMGCL/PCL). This scaffold exhibited an improved mechanical tensile strength and biocompatibility for the development of cardiac engineered tissues. The scaffolds having rectangular and square patterns with pore sizes of $150 \times 300\ \mu m^2$ and $200 \times 200\ \mu m^2$ were printed using MEW, respectively. The cardiac progenitor cells (CPCs) were suspended in collagen solution and infused into the scaffolds, forming a fiber-reinforced CPCs-laden collagen hydrogel. The scaffolds with a rectangular pattern were shown to have similar mechanical properties as native cardiac tissue due to the better pore size matching than the scaffolds with a square pattern. Hence, the scaffolds with a rectangular pattern supported CPC growth and directed cell alignment

more efficiently. Furthermore, the presence of pHMGCL in the structure improved the biocompatibility of the material and promoted cellular alignment along the scaffolds [26]. In another study, Castilho et al. designed a bi-layered melt electrowritten PCL fiber-reinforced cell-laden cylindrical GelMA hydrogel that approximated the mechanical properties of the native cartilage. The MEW scaffolds were composed of two layers: a bottom layer with a uniform box structure and a thin superficial layer that was designed as an angle-plied PCL fibrous mat. The thin superficial layer significantly improved load-bearing properties of the composites under both uniform and non-uniform loading. The hydrogel-fiber composites also encouraged neo-cartilage formation upon mechanical stimulation owing to the presence of GelMA triggering the production of sulphated glycosaminoglycans and collagen II [51]. The study of Peiffer et al. presented the development of cell-laden GelMA hydrogel reinforced with melt electrowritten PCL fibrous scaffolds on curved substrates. These substrates, which were made from either conductive or non-conductive materials, were employed as collectors to replicate the native curvature of a biological joint for cartilage regeneration. The PCL scaffolds were designed with an interspacing of 400 μm by depositing 50 layers of fibers. Fibers were then filled with a cell-laden hydrogel. PCL fibers coated on the curved substrates with low conductivity provided a constant electrical field strength hence showed better compatibility with fibers and ensured accurate patterning compared to high conductivity. Besides, melt electrowritten scaffolds improved mechanical compression properties of the cell-laden hydrogel and supported neocartilage formation as an osteochondral implant in vitro [52].

Cell-laden hydrogels reinforced with melt electrowritten scaffolds were also applied in vivo [53]. The study of Baldwin et al. developed multi-layered tubular PCL scaffolds by MEW to reinforce cell-laden star-PEG/heparin hydrogels for periosteum regeneration in vivo. The tubular scaffolds were printed onto the surface of a rotating collector and washed with NaOH prior to cell seeding. MSCs and HUVECs were dispersed in VEGF-containing PEG/heparin hydrogels separately and then embedded into the inner and outer part of the scaffolds, respectively. The reinforced hydrogels were also placed over defect sites in mice femoral cortical for in vivo evaluations. Results showed that MSCs maintained undifferentiated phenotype in the reinforced hydrogels attributed to the encapsulation within positively charged hydrogels that slowed down the release of growth factors, while HUVECs differentiated into mature vessels to form endothelial network due to the presence of MSCs as perivascular cells to stabilize the angiogenic environment. Results also showed that HUVECs connected to native vasculature and matured to vessels, which improved overall vascularization in vivo [53].

The hydrogels reinforced with melt electrowritten scaffolds can be even injected into the body [54, 55]. In the study of Castilho et al., ultra stretchable PCL fibrous scaffolds was fabricated by MEW with a well-ordered hexagonal structure and pore size of 400 μm. This scaffold was used to reinforce collagen-based injectable hydrogel designed as heart patch enhancing pluripotent stem cell-derived cardiomyocyte (iPSC-CM) maturation for cardiac tissue repair. iPSC-CMs were suspended in the hydrogel solution and the solution was then embedded onto the fibrous scaffolds.

Finally, the reinforced hydrogels were rolled into tubular structures to be injected as heart patches onto a beating porcine heart. The hexagonal microstructure of melt electrowritten fibers not only exhibited a significant improvement of biaxial tensile strains but also enhanced iPSC-CM maturation compared to the rudimental structures. Moreover, the reinforced hydrogel heart patches showed injectability and shape recovery in vivo, allowing further IPSC-CM maturation when it was placed on a contracting heart [54]. The study of Wang et al. presented PCL-based melt electrowritten fibrous scaffolds coated with gold nanoparticles as an electroactive matrix for the nerve regeneration. The scaffolds were designed with a single-layered micro-grid pattern and then, sputter coated with gold nanoparticles. The gold coating improved conductivity of the scaffolds that enhanced transmissions of electric signals along the matrix, hence promoted neural differentiation and neurite outgrowth under electrical stimulation. An increase of gold coating from 10 to 80 nm thickness enhanced neurite length and neurite number per cell further. More importantly, PCL scaffolds were embedded in collagen solution to show their high flexibility and injectability that allowed reinforced hydrogels to serve as a potential nerve tissue-engineered implant [55].

4.3.4 Mathematical and Computational Modeling for Developing Melt Electrowritten Fibers

There are also studies in which various mathematical models [56], computational software [57, 58], and machine learning algorithms [59] were applied for MEW. Printing of PCL and strontium-substituted bioactive glass (PCL/SrBG) blend was difficult due to the rheological properties of the blend. In the study of Paxton et al., two predictive mathematical models were developed to optimize the formulation of the blend and the printing pressure during process. The first model quantified shear-viscosity profile of the blend using Power Law Regression to predict a suitable blend composition for easy melting. The second model predicted printing pressure required to extrude the blend. With an optimal blend compositions and printing pressure, PCL/SrBG blend was successfully melted, extruded, and finally printed via MEW. Therefore, the mathematical models were shown to facilitate MEW process [56].

Besides predictive mathematical models, computational software was also applied to assist the MEW process by generating suitable pattern designs for melt electrowritten scaffolds. Paxton et al. used a set of novel g-code generation software for the fabrication of complex, highly ordered and patient-specific PCL scaffolds via MEW. MATLAB, Mathematica, Autodesk NetFabb, and SolidWorks were used to design various patterns of the scaffolds. The software can interpret the patients' computed tomography scan data and then generate g-codes that precisely controlled the scaffolds' structure to be similar with the native tissues, which facilitated the

fabrication of anatomically matched scaffolds [57]. Bas et al. also proposed a computational model-based approach for the design of melt electrowritten fibrous PCL scaffolds to reinforce GelMA hydrogels. The computational approach was implemented with p-version of the finite element method to establish an in-silico design library, where the pore size and fiber diameter can be selected to target hydrogel compressive modulus similar to that of native articular cartilage. The mechanical testing results showed that the hydrogels with a selected pore size (200–800 μm) and fiber diameter (20–25 μm) successfully exhibited the target compressive modulus (500–2500 kPa). Hence, the library was shown to guide the design of the melt electrowrtitten fibrous scaffolds to reinforce hydrogels, achieving desired mechanical specifications of the hydrogels [58].

Machine learning can be a useful approach to analyze and control cell phenotypes when melt electrowritten scaffolds were used as substrates for cell culture. Tourlomousis et al. produced fibrous PCL meshes via MEW and trained a machine learning algorithm to classify the cell shape confinement within the meshes. The support vector machine was trained in MATLAB based on seven independent cell features transformed from cell immunofluorescent images. The algorithm was able to classify cells within melt electrowritten 3D meshes with a high accuracy mainly because the cell features in the 3D meshes possessed a highly separable distribution with narrow variance. This also indicated that melt electrowritten 3D meshes provided a tight control over cell morphology and focal adhesions level. The machine learning technology served as a useful approach to analysis and control cell phenotypes, demonstrating strong potential to be applied in a wide range of bioapplications [59].

4.4 Composites of Melt Electrowritten Fibers and Other Materials

In order to manufacture composite scaffolds, melt electrowritten fibers can be combined with the materials produced using various other techniques including casting [16], solution electrospinning [14, 60], and pneumatic extrusion printing [61]. This allows production of even more advanced composites suitable for specific applications since each of this technique has its own advantages. In the study of Fuchs et al., 3D scaffolds-reinforced membranes were developed by fusing melt electrowritten PCL scaffolds with casted PCL films as a mechanical barrier for the applications of bacterial infection-free bone and mucosal wound healing. Square-patterned PCL scaffolds were fabricated with pore sizes of 250 or 500 μm for osteoblast seeding, whereas triangular-patterned PCL scaffold was fabricated with a pore size of 250 μm for either keratinocytes or fibroblasts seeding. Finally, PCL films were fused in between the square-patterned scaffolds and triangular-patterned

scaffolds via heat sealing to form reinforced membranes. The membranes demonstrated good cytocompatibility indicated the high cell viability and good mechanical guidance of the cells along the highly-ordered scaffolds. Most importantly, the membranes displayed excellent bacterial tightness mainly due to the presence of casted PCL films that stopped bacteria to pass through the membranes [16].

In the studies combined with solution electrospinning [14, 60]. Pennings et al. designed a 3D tubular bi-layered scaffold produced for mimicking the vessel grafts regeneration. The tubular scaffolds were made from PCL while the inner and outer sides of the tubular scaffold was deposited by solution electrospinning and MEW, respectively. The scaffolds were then coated with collagen I and fibronectin to increase the hydrophilicity. Afterwards, the inner side was seeded with endothelial colony forming cells (ECFCs), whereas the outer side was seeded with multipotent mesenchymal stromal cells. Finally, the cell-laden scaffolds were mounted in a bioreactor chamber to mimic the blood flow in the vessels. The scaffolds maintained the growth of ECFCs and multipotent mesenchymal stromal cells and induced cell differentiation during flow perfusion of cell culture media. A cellular layer was formed between inner and outer compartments and stopped diffusion of culture media through the layers. This resulted in a bi-layered cell differentiation which mimicked the cellular organization of native vessel grafts. By using the bioreactor chamber, layer-specific cell differentiation was successfully induced which allowed the formation of a biomimetic bi-layered vascular graft to better mimic native vascular structures [14]. In another study, combining MEW and solution electrospinning, Zhang et al. reported the design of a bi-layered nerve guidance conduits composed of melt electrowritten PCL scaffolds and electrospun PNIPAM membrane. This bi-layered structure can be thermally self-crimpled at human body temperature for the purpose of repairing peripheral nerve injuries. The thermosensitive electrospun PNIPAM membrane was coated with gold by sputter coater to make surface conductive. The PCL scaffolds with a pore size ranging from 200 to 400 μm were then directly printed on top of the membrane to form the bi-layered structure. The anisotropic PCL scaffolds were manufactured with varying grid patterns or intersection angles. Lastly, functional graphene oxide (GO) and graphitic carbon nitride (g-C3N4) were coated as photocatalysts on the scaffolds. The whole structure was pre-coated by collagen type IV prior to PC12 cell seedings for improving the attachment of cells to the scaffolds. The PCL scaffolds with a smaller pore size supported a greater growth of cells potentially because of their higher surface area. The scaffolds also strengthened direction control of neurite extension along long arm of the rectangular pattern by reducing intersection degrees for the minimization of the obstructions at conjunctions. Moreover, GO and g-C3N4 coating initiated photocatalytic stimulation of neurons, which extended neurite further under a light irradiation [60].

Pneumatic extrusion printing was also used in convergence with MEW develop scaffolds with more advanced designs [61]. For this purpose, Diloksumpan et al. fabricated bone-mimetic CaP-based paste composed of α-tricalcium phosphate microparticles and HA coated PCL scaffolds by MEW. The MEW fiber meshes were organized in orthogonal square box patterns with a spacing of 300 μm and cut

into to cylinders. The paste that composed of α-tricalcium phosphate, HA, and Poloxamer (Pluronic® F-127) was directly printed over the melt electrowritten scaffolds via pneumatic extrusion printing. The scaffolds were then casted with cell laden GelMA hydrogel to mimic an osteochondral plug for bone and tissue regeneration. Melt electrowritten fibers improved compressive strength of the hydrogel and adhesion strength between hydrogel and CaP-based paste. This improvement provided better stability to the composite while handling. Furthermore, the composite was shown to support osteogenesis and cartilage matrix deposition vitro due to the presence of CaP-based paste. Hence, the developed composite offered a good idea to design a composite for regenerative tissue engineering in the bone-cartilage interface [61].

4.5 Conclusion

Melt electrospinning writing (MEW) is an extrusion-based advanced manufacturing technique. In contrast to nano-size of solution electrospun nanofibers, the diameter of the melt electrowritten fibers are in the micron range due to the low conductivity and high viscosity of polymer melts. In fact, the low conductivity of the polymer melts enables MEW to be used as an additive manufacturing technique due to the lack of charge build-up. The constructs with various pore size and geometry, thickness, as well as gradient structures with a variety of designs can be fabricated by MEW. Pore size along with the pore design flexibility result in better infiltration, attachment, and proliferation of the cells. Furthermore, melt electrowritten fibers can be designed to mimic the patient's anatomy to be used as patient-specific scaffolds for the repair of tissue defects. Therefore, melt electrowritten fibers possess great potential especially for tissue regeneration. In addition to that, thanks to the design flexibility of the technique enabling the production of patterns like auxetic, waves can be achieved by MEW and melt electrowritten fibers can be used in applications which require high mechanical properties. In addition, melt electrowritten scaffolds can also be used to reinforce hydrogels which are commonly used materials in biomedical applications. Last but not the least, melt electrowritten fibers can also be merged with other type of materials like films, electrospun nanofibers, 3D printed materials to design even more advanced structures for the specific needs in biomedical applications. The issues in scale-up production of melt electrowritten fibers and lack of clinical data limited the applications of melt electrowritten fibers in the clinics so far. Therefore, future perspectives of MEW will be focusing on the upscaling of the MEW process and conducting clinical trials to expand the applications of these fibers in the field of biomedical engineering.

References

1. Xue, J., Wu, T., Dai, Y., Xia, Y., & States, U. (2019). Electrospinning and electrospun nanofibers: Methods, materials, and applications. *Chemical Reviews, 119*(8), 5298–5415.
2. Dalton, P. D. (2017). Melt electrowriting with additive manufacturing principles. *Current Opinion in Biomedical Engineering, 2*, 49–57. https://doi.org/10.1016/j.cobme.2017.05.007
3. Celebioglu, A., & Uyar, T. (2010). Cyclodextrin nanofibers by electrospinning. *Chemical Communications, 46*(37), 6903. https://doi.org/10.1039/c0cc01484b
4. Aytac, Z., Yildiz, Z. I., Kayaci-Senirmak, F., et al. (2016). Fast-dissolving, prolonged release, and antibacterial cyclodextrin/limonene-inclusion complex nanofibrous webs via polymer-free electrospinning. *Journal of Agriculture and Food Chemistry, 64*(39), 7325–7334. https://doi.org/10.1021/acs.jafc.6b02632
5. Brown, T. D., Edin, F., Detta, N., Skelton, A. D., Hutmacher, D. W., & Dalton, P. D. (2015). Melt electrospinning of poly(ε-caprolactone) scaffolds: Phenomenological observations associated with collection and direct writing. *Materials Science and Engineering C, 45*, 698–708. https://doi.org/10.1016/j.msec.2014.07.034
6. Pham, Q. P., Sharma, U., & Mikos, A. G. (2006). Electrospun poly (ε-caprolactone) microfiber and multilayer nanofiber/microfiber scaffolds: Characterization of scaffolds and measurement of cellular infiltration. *Biomacromolecules, 7*(10), 2796–2805. https://doi.org/10.1021/bm060680j
7. Robinson, T. M., Hutmacher, D. W., & Dalton, P. D. (2019). The next frontier in melt electrospinning: Taming the jet. *Advanced Functional Materials, 29*(44), 1904664. https://doi.org/10.1002/adfm.201904664
8. Wunner, F. M., Florczak, S., Mieszczanek, P., Bas, O., De-juan-pardo, E. M., & Grove, K. (2017). Electrospinning with polymer melts—State of the art and future perspectives (Vol. 5). Elsevier Ltd. http://doi.org/10.1016/B978-0-12-803581-8.09318-8
9. Hochleitner, G., Jüngst, T., Brown, T. D., et al. (2015). Additive manufacturing of scaffolds with sub-micron filaments via melt electrospinning writing. *Biofabrication, 7*(3), 035002. http://doi.org/10.1088/1758-5090/7/3/035002
10. Kade, J. C., & Dalton, P. D. (2021). Polymers for melt electrowriting. *Advanced Healthcare Materials, 10*(1), 2001232. https://doi.org/10.1002/adhm.202001232
11. Youssef, A., Hollister, S. J., & Dalton, P. D. (2017). Additive manufacturing of polymer melts for implantable medical devices and scaffolds. *Biofabrication, 9*(1), 012002. http://doi.org/10.1088/1758-5090/aa5766
12. Brown, T. D., Dalton, P. D., & Hutmacher, D. W. (2011). Direct writing by way of melt electrospinning. *Advanced Materials, 23*(47), 5651–5657. https://doi.org/10.1002/adma.201103482
13. Abbasi, N., Ivanovski, S., Gulati, K., Love, R. M., & Hamlet, S. (2020). Role of offset and gradient architectures of 3-D melt electrowritten scaffold on differentiation and mineralization of osteoblasts. *Biomaterials Research, 24*(1), 1–16. https://doi.org/10.1186/s40824-019-0180-z
14. Pennings, I., Van Haaften, E. E., Jungst, T., et al. (2020). Layer-specific cell differentiation in bi-layered vascular grafts under flow perfusion. *Biofabrication, 12*(1), 15009. https://doi.org/10.1088/1758-5090/ab47f0
15. Eichholz, K. F., Von Euw, S., Burdis, R., Kelly, D. J., & Hoey, D. A. (2020). Development of a new bone-mimetic surface treatment platform: Nanoneedle hydroxyapatite (nnHA) coating. *Advanced Healthcare Materials, 9*(24), 1–18. https://doi.org/10.1002/adhm.202001102
16. Fuchs, A., Youssef, A., Seher, A., et al. (2019). A new multilayered membrane for tissue engineering of oral hard- and soft tissue by means of melt electrospinning writing and film casting—An in vitro study. *Journal of Cranio-Maxillofacial Surgery, 47*(4), 695–703. https://doi.org/10.1016/j.jcms.2019.01.043
17. Somszor, K., Bas, O., Karimi, F., et al. (2020). Personalized, mechanically strong, and biodegradable coronary artery stents via melt electrowriting. *ACS Macro Letters, 9*(12), 1732–1739. https://doi.org/10.1021/acsmacrolett.0c00644

18. Visser, J., Melchels, F. P. W., Jeon, J. E., et al. (2015). Reinforcement of hydrogels using three-dimensionally printed microfibres. *Nature Communications, 6*, 6933. https://doi.org/10.1038/ncomms7933
19. Bartnikowski, M., Dargaville, T. R., Ivanovski, S., & Hutmacher, D. W. (2019). Degradation mechanisms of polycaprolactone in the context of chemistry, geometry and environment. *Progress in Polymer Science, 96*, 1–20. https://doi.org/10.1016/j.progpolymsci.2019.05.004
20. Abdal-hay, A., Abbasi, N., Gwiazda, M., Hamlet, S., & Ivanovski, S. (2018). Novel polycaprolactone/hydroxyapatite nanocomposite fibrous scaffolds by direct melt-electrospinning writing. *European Polymer Journal, 105*(May), 257–264. https://doi.org/10.1016/j.eurpolymj.2018.05.034
21. Brennan, C. M., Eichholz, K. F., & Hoey, D. A. (2019). The effect of pore size within fibrous scaffolds fabricated using melt electrowriting on human bone marrow stem cell osteogenesis. *Biomedical Materials, 14*(6), 65016. https://doi.org/10.1088/1748-605X/ab49f2
22. Zhou, H., Green, T. B., & Joo, Y. L. (2006). The thermal effects on electrospinning of polylactic acid melts. *Polymer (Guildf), 47*(21), 7497–7505. https://doi.org/10.1016/j.polymer.2006.08.042
23. Jing, D., Vonk, N. H., Lamers, B. A. G., et al. (2020). Anisotropic hygro-expansion in hydrogel fibers owing to uniting 3D electrowriting and supramolecular polymer assembly. *European Polymer Journal, 141*, 110099. http://doi.org/10.1016/j.eurpolymj.2020.110099
24. Ritzau-Reid, K. I., Spicer, C. D., Gelmi, A., et al. (2020). An electroactive oligo-EDOT platform for neural tissue engineering. *Advanced Functional Materials, 30*(42), 2003710. https://doi.org/10.1002/adfm.202003710
25. Qiao, Z., Lian, M., Han, Y., et al. (2021). Bioinspired stratified electrowritten fiber-reinforced hydrogel constructs with layer-specific induction capacity for functional osteochondral regeneration. *Biomaterials, 266*, 120385. http://doi.org/10.1016/j.biomaterials.2020.120385
26. Castilho, M., Feyen, D., Flandes-Iparraguirre, M., et al. (2017). Melt electrospinning writing of poly-hydroxymethylglycolide-co-ε-caprolactone-based scaffolds for cardiac tissue engineering. *Advanced Healthcare Materials, 6*(18), 1700311. https://doi.org/10.1002/adhm.201700311
27. Großhaus, C., Bakirci, E., Berthel, M., et al. (2020). Melt electrospinning of nanofibers from medical-grade poly(ε-caprolactone) with a modified nozzle. *Small (Weinheim an der Bergstrasse, Germany), 16*(44), 2003471. https://doi.org/10.1002/smll.202003471
28. Dubey, N., Ferreira, J. A., Daghrery, A., et al. (2020). Highly tunable bioactive fiber-reinforced hydrogel for guided bone regeneration. *Acta Biomaterialia, 113*, 164–176. https://doi.org/10.1016/j.actbio.2020.06.011
29. Hochleitner, G., Youssef, A., Hrynevich, A., et al. (2016). Fibre pulsing during melt electrospinning writing. *BioNanoMaterials, 17*(3–4), 159–171. https://doi.org/10.1515/bnm-2015-0022
30. Jungst, T., Muerza-Cascante, M. L., Brown, T. D., et al. (2015). Melt electrospinning onto cylinders: Effects of rotational velocity and collector diameter on morphology of tubular structures. *Polymer International, 64*(9), 1086–1095. https://doi.org/10.1002/pi.4948
31. Boisseau, P., & Loubaton, B. (2011). Nanomedicine, nanotechnology in medicine. *Comptes Rendus Physique, 12*(7), 620–636. https://doi.org/10.1016/j.crhy.2011.06.001
32. Harrison, R. H., St-Pierre, J. P., & Stevens, M. M. (2014). Tissue engineering and regenerative medicine: A year in review. *Tissue Engineering Part B: Reviews, 20*(1), 1–16. https://doi.org/10.1089/ten.teb.2013.0668
33. Fuchs, A., Youssef, A., Seher, A., et al. (2019). Medical-grade polycaprolactone scaffolds made by melt electrospinning writing for oral bone regeneration—A pilot study in vitro. *BMC Oral Health, 19*(1), 1–11. https://doi.org/10.1186/s12903-019-0717-5
34. Hewitt, E., Mros, S., McConnell, M., Cabral, J. D., & Ali, A. (2019). Melt-electrowriting with novel milk protein/PCL biomaterials for skin regeneration. *Biomedical Materials, 14*(5), 055013. http://doi.org/10.1088/1748-605X/ab3344
35. Bertlein, S., Hikimoto, D., Hochleitner, G., et al. (2018). Development of endothelial cell networks in 3D Tissues by combination of melt electrospinning writing with cell-accumulation

technology. *Small (Weinheim an der Bergstrasse, Germany), 14*(2), 1–7. https://doi.org/10.1002/smll.201701521
36. Muerza-Cascante, M. L., Shokoohmand, A., Khosrotehrani, K., et al. (2017). Endosteal-like extracellular matrix expression on melt electrospun written scaffolds. *Acta Biomaterialia, 52*, 145–158. https://doi.org/10.1016/j.actbio.2016.12.040
37. Hammerl, A., Diaz Cano, C. E., De-Juan-Pardo, E. M., van Griensven, M., & Poh, P. S. P. (2019). A growth factor-free co-culture system of osteoblasts and peripheral blood mononuclear cells for the evaluation of the osteogenesis potential of melt-electrowritten polycaprolactone scaffolds. *International Journal of Molecular Sciences, 20*(5). http://doi.org/10.3390/ijms20051068
38. Abbasi, N., Lee, R. S. B., Ivanovski, S., Love, R. M., & Hamlet, S. (2020). In vivo bone regeneration assessment of offset and gradient melt electrowritten (MEW) PCL scaffolds. *Biomaterials Research, 24*(1), 1–24. https://doi.org/10.1186/s40824-020-00196-1
39. Castilho, M., Hochleitner, G., Wouter, W., Van Rietbergen, B., & Paul, D. (2018). Mechanical behavior of a soft hydrogel reinforced with three-dimensional printed microfibre scaffolds, 1–10. http://doi.org/10.1038/s41598-018-19502-y
40. Bas, O., De-Juan-Pardo, E. M., Chhaya, M. P., et al. (2015). Enhancing structural integrity of hydrogels by using highly organised melt electrospun fibre constructs. *European Polymer Journal, 72*, 451–463. https://doi.org/10.1016/j.eurpolymj.2015.07.034
41. de Ruijter, M., Hrynevich, A., Haigh, J. N., et al. (2018). Out-of-plane 3D-printed microfibers improve the shear properties of hydrogel composites. *Small (Weinheim an der Bergstrasse, Germany), 14*(8), 1–6. https://doi.org/10.1002/smll.201702773
42. Agarwal, K., Sahay, R., & Baji, A. (2020). Tensile properties of composite reinforced with three-dimensional printed fibers. *Polymers (Basel), 12*(5), 1–11. https://doi.org/10.3390/POLYM12051089
43. Saidy, N. T., Wolf, F., Bas, O., et al. (2019). Biologically inspired scaffolds for heart valve tissue engineering via melt electrowriting. *Small (Weinheim an der Bergstrasse, Germany), 15*(24), 1–36. https://doi.org/10.1002/smll.201900873
44. Olvera, D., Sohrabi Molina, M., Hendy, G., & Monaghan, M. G. (2020). Electroconductive melt electrowritten patches matching the mechanical anisotropy of human myocardium. *Advanced Functional Materials, 30*(44), 1–10. https://doi.org/10.1002/adfm.201909880
45. Su, Y., Zhang, Z., Wan, Y., et al. (2020). A hierarchically ordered compacted coil scaffold for tissue regeneration. *NPG Asia Materials, 12*(1), 4–13. https://doi.org/10.1038/s41427-020-0234-7
46. Chai, Q., Jiao, Y., & Yu, X. (2017). Hydrogels for biomedical applications: Their characteristics and the mechanisms behind them. *Gels, 3*(1), 6. https://doi.org/10.3390/gels3010006
47. Mantha, S., Pillai, S., Khayambashi, P., et al. (2019). Smart hydrogels in tissue engineering and regenerative medicine. *Materials (Basel), 12*(20), 3323. https://doi.org/10.3390/ma12203323
48. Bas, O., De-Juan-Pardo, E. M., Meinert, C., et al. (2017). Biofabricated soft network composites for cartilage tissue engineering. *Biofabrication, 9*(2), 025014. http://doi.org/10.1088/1758-5090/aa6b15
49. Ahearne, M., & Ahearne, M. (2014). Introduction to cell—hydrogel mechanosensing. *Interface Focus, 4*(2), 20130038. https://doi.org/10.1098/rsfs.2013.0038
50. Janzen, D., Bakirci, E., Wieland, A., Martin, C., Dalton, P. D., & Villmann, C. (2020). Cortical neurons form a functional neuronal network in a 3D printed reinforced matrix. *Advanced Healthcare Materials, 9*(9), 1901630. https://doi.org/10.1002/adhm.201901630
51. Castilho, M., Mouser, V., Chen, M., Malda, J., & Ito, K. (2019). Bi-layered micro-fibre reinforced hydrogels for articular cartilage regeneration. *Acta Biomaterialia, 95*, 297–306. https://doi.org/10.1016/j.actbio.2019.06.030
52. Peiffer, Q. C., de Ruijter, M., van Duijn, J., et al. (2020). Melt electrowriting onto anatomically relevant biodegradable substrates: Resurfacing a diarthrodial joint. *Materials and Design, 195*, 1–9. https://doi.org/10.1016/j.matdes.2020.109025
53. Baldwin, J. G., Wagner, F., Martine, L. C., et al. (2017). Periosteum tissue engineering in an orthotopic in vivo platform. *Biomaterials, 121*, 193–204. https://doi.org/10.1016/j.biomaterials.2016.11.016

54. Castilho, M., van Mil, A., Maher, M., et al. (2018). Melt electrowriting allows tailored microstructural and mechanical design of scaffolds to advance functional human myocardial tissue formation. *Advanced Functional Materials, 28*(40), 1–10. https://doi.org/10.1002/adfm.201803151
55. Wang, Y., Zhang, Y., Zhang, Z., et al. (2020). An injectable high-conductive bimaterial scaffold for neural stimulation. *Colloids Surfaces B Biointerfaces, 195*, 111210. http://doi.org/10.1016/j.colsurfb.2020.111210
56. Paxton, N. C., Ren, J., Ainsworth, M. J., et al. (2019). Rheological characterization of biomaterials directs additive manufacturing of strontium-substituted bioactive glass/polycaprolactone microfibers. *Macromolecular Rapid Communications, 40*(11), 1900019. https://doi.org/10.1002/marc.201900019
57. Paxton, N. C., Lanaro, M., Bo, A., et al. (2020). Design tools for patient specific and highly controlled melt electrowritten scaffolds. *Journal of the Mechanical Behavior of Biomedical Materials, 105*, 103695. http://doi.org/10.1016/j.jmbbm.2020.103695
58. Bas, O., Lucarotti, S., Angella, D. D., et al. (2018). Rational design and fabrication of multiphasic soft network composites for tissue engineering articular cartilage: A numerical model-based approach. *Chemical Engineering Journal, 340*, 15–23. https://doi.org/10.1016/j.cej.2018.01.020
59. Tourlomousis, F., Jia, C., Karydis, T., et al. (2019). Machine learning metrology of cell confinement in melt electrowritten three-dimensional biomaterial substrates. *Microsystems Nanoengineering, 5*(1), 1–9. https://doi.org/10.1038/s41378-019-0055-4
60. Zhang, Z., Lindh, M., Wang, Z., et al. (2020). Biomaterials 3D anisotropic photocatalytic architectures as bioactive nerve guidance conduits for peripheral neural regeneration. *Biomaterials, 253*, 120108. http://doi.org/10.1016/j.biomaterials.2020.120108
61. Diloksumpan, P., De Ruijter, M., Castilho, M., et al. (2020). Combining multi-scale 3D printing technologies to engineer reinforced hydrogel-ceramic interfaces. *Biofabrication, 12*(2). http://doi.org/10.1088/1758-5090/ab69d9



Zeynep Aytac received B.S. degree in Textile Engineering from Ege University in 2009. She obtained Ph.D. degree in Material Science and Nanotechnology from Bilkent University (2016), where she studied on the production of electrospun polymeric nanofibers incorporated with cyclodextrin-inclusion complexes (CD-ICs) of active ingredients (AIs), including drugs, antioxidant, and antibacterial agents, and flavor/fragrances, incorporated as well as non-polymeric nanofibers of CD-ICs. Next, she worked as a postdoctoral researcher at the University of Michigan to design melt electrospinning written nanofibrous materials for dental applications. Then, she moved to Harvard University to develop sustainable materials using nature-derived polymers and antimicrobials for food packaging applications.



Xinzhu Wang was born in Xi'an, Shaanxi, China in 1998. She received a B.E. degree in chemical and biomolecular engineering from Nanyang Technological University (NTU), Singapore, in 2021. She was a Research Assistant in the Center for Nanotechnology and Nanotoxicology at the Harvard School of Public Health in 2020. Her research interest includes the development of nanofibers using solution electrospinning or melt electrospinning writing technique. She is also focusing on the fundamental study of hydrogel-based drug delivery platforms in her undergraduate studies. Currently, she is pursuing a Ph.D. degree in biomedical engineering at NTU, designing novel non-invasive bioimaging probes for cancer diagnosis and treatment monitoring.

Chapter 5
Co-electrohydrodynamic Forming of Biomimetic Polymer Materials for Diffusion Magnetic Resonance Imaging



Feng-Lei Zhou and Geoff J. M. Parker

Abstract Magnetic resonance imaging (MRI) is routinely used as a medical imaging modality in the disease detection, monitoring, and therapy response assessment in neurology and cancer. An attractive feature of MRI is its ability to provide non-invasive quantitative measurements relating to the tissue microenvironment. In MRI, a technique known as diffusion MRI can provide non-invasive quantitative information that is reflective of the microstructure of tissues, ranging from measurements of axonal packing in the brain, through measurements of myocardial fiber orientation in the heart to measurements of tumor cell size. These measurements are powerful, but they are not commonly used clinically, in part due to a lack of validation. Synthetic tissues, with known microstructural properties, provide one approach to providing such validation. This chapter presents how co-electrohydrodynamic (co-EHD) forming of polymer materials can be used to create synthetic tissues (or phantoms) for diffusion MRI by mimicking the cellular structure of tissues in the brain, heart, and tumor. Two types of co-EHD polymeric structures, i.e. hollow microfibres and microspheres, will be discussed with the focus on the shell and core materials and the relevant processes used. Three types of tissue-mimicking phantoms and their performance in pre-clinical or clinical MRI measurements will be highlighted.

Keywords Diffusion MRI · Co-electrohydrodynamics forming · Phantoms · Tissue-mimicking

F.-L. Zhou (✉) · G. J. M. Parker
Department of Medical Physics and Biomedical Engineering, University College London, London, UK
e-mail: fenglei.zhou@ucl.ac.uk

G. J. M. Parker
e-mail: geoff.parker@ucl.ac.uk

F.-L. Zhou
School of Pharmacy, University College London, London, UK

G. J. M. Parker
Bioxydyn Limited, Manchester, UK

© The Author(s), under exclusive license to Springer Nature Switzerland AG 2022

A. Vaseashta and N. Bölgen (eds.), *Electrospun Nanofibers*,
https://doi.org/10.1007/978-3-030-99958-2_5

5.1 Introduction

Magnetic resonance imaging (MRI) is routinely used as a medical imaging modality in the diagnosis of a wide range of diseases. Part of the attraction of MRI is its ability to provide non-invasive quantitative measurements relating to the tissue microenvironment. In particular, a technique known as diffusion MRI is able to provide non-invasive quantitative information that is reflective of the microstructure of tissues, ranging from measurements of axonal packing in the brain to measurements of tumor cell size. These measurements are powerful, but they are not commonly used clinically, in part due to a lack of validation. Synthetic tissues, with known microstructural properties, provide one approach to providing such validation. Here we discuss how co-electrohydrodynamic forming of polymer materials can be used to create test objects (or phantoms) for diffusion MRI by mimicking the cellular structure of tissues.

5.2 Co-electrohydrodynamic Forming of Hollow Polymeric Materials

Hollow polymeric nano/microstructures with cylindrical or spherical geometries are of special interest for use in encapsulation, controlled release, filtration, and nanoreactors, which currently are mainly fabricated using hard-templating, soft-templating, and self-templating synthesis [1]. However, those templating strategies often require multiple steps due to extra procedures to remove the template/core materials. Co-electrohydrodynamic (co-EHD) forming was firstly demonstrated by Loscertales et al. in 2002 [2] to fabricate core–shell structured water–oil nanoparticles, and then in 2004 was extended by the same researchers to produce hollow polymeric nano/microfibres (later called co-electrospinning, Fig. 5.1a) [2] and nano/microspheres (later called co-electrospraying, Fig. 5.1b) [3]. The main advantage of co-electrospinning/spraying lies in the fact that they are one-step processes and allow flexibility of controlling the sizes (i.e. wall thickness, inner diameters) and patterning of hollow fibers and spheres.

5.2.1 Co-electrospinning of Hollow Polymeric Fibres

Co-electrospinning (or coaxial electrospinning) has greatly expanded the versatility of electrospinning by enabling core–shell structured or hollow fibre fabrication, providing multi-functional/structural properties from a single fibre. By forming a fibre that consists of two or more complementary materials in the core and the shell, one can design complex fibres with a combination of properties that are not achieved in homogeneous nanofibres from single-nozzle electrospinning.

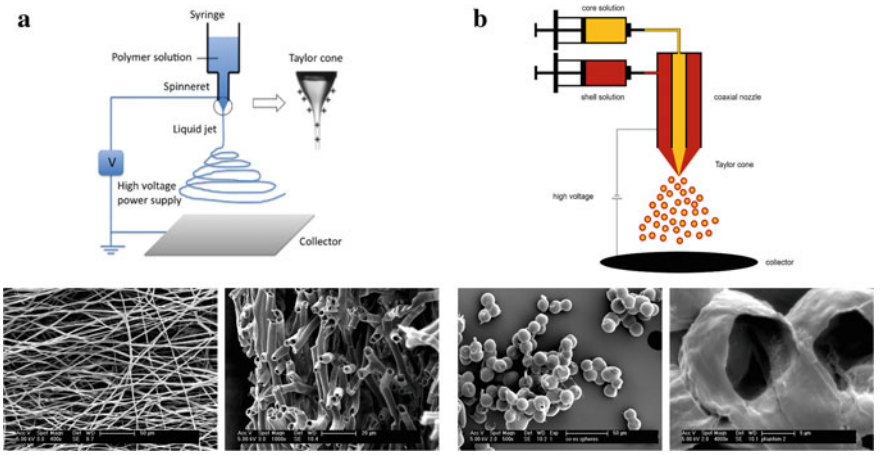


Fig. 5.1 Co-EHD forming of hollow polymeric materials. **a** Schematic of co-electrospinning (reproduced from [4], an open access journal published under a CC BY-NC-SA 3.0 license.) and SEM micrographs of morphology and cross-section of co-electrospun hollow microfibres; **b** schematic of co-electrospraying (reproduced from [5] with permission, copyright Elsevier) and SEM micrographs of morphology and cross-section of co-electrosprayed hollow microspheres

Co-electrospinning was firstly combined with sol–gel chemistry to produce tetraethylorthosilicate (TEOS) hollow nanofibres in one step from non-polymer core–shell combination [2]. In several following studies, Zussman et al. [6] extended this technique to different polymer solutions (e.g. poly (ε-caprolactone) (PCL) shell and poly(ethylene oxide) (PEO) core). The rapid solidification of shell solution and the evaporation of core solution through the shell was proposed to be responsible for one-step formation of hollow microfibres in coaxial electrospinning [6, 7]. The size and morphology of resultant co-electrospun fibres were closely affected by core/shell materials properties (e.g. solvent and concentration), process parameters (e.g. solution flow rate, electric field) [8]. Since then this field has been growing rapidly and extensively, as evidenced by two review articles published by Moghe et al. [9] in 2008 and Han et al. [10] in 2019, in which early history and current status, basic theories, process parameters of co-electrospinning and various applications of co-electrospun fibres were critically summarised.

Biomedical applications frequently using co-electrospun fibres, primary in tissue scaffolds, wound dressings and drug delivery, have been, and continue to be, vigorously investigated, resulting in promising advances and novel approaches. For instance, one of the most exciting developments in coaxial electrospinning is high-throughput production of hollow nanofibres by using a needleless coaxial slit spinneret [11].

Precise deposition of core–shell structured or hollow microfibres in coaxial electrospinning on a desired location or specific pattern is also an area of current progress. The concept of direct-writing co-electrospinning was firstly demonstrated by Zhou et al. [12]. Dramatically reducing the gap (often called working distance) between

the nozzle and the collector to a few millimetres suppressed the instability of the fluid jet. By using such a jet with a motor-controlled X–Y stage collector, position-controlled deposition of patterned fibres was realized, as shown in Fig. 5.2a. By utilizing a rotating collector (Fig. 5.2b) in direct writing co-electrospinning using

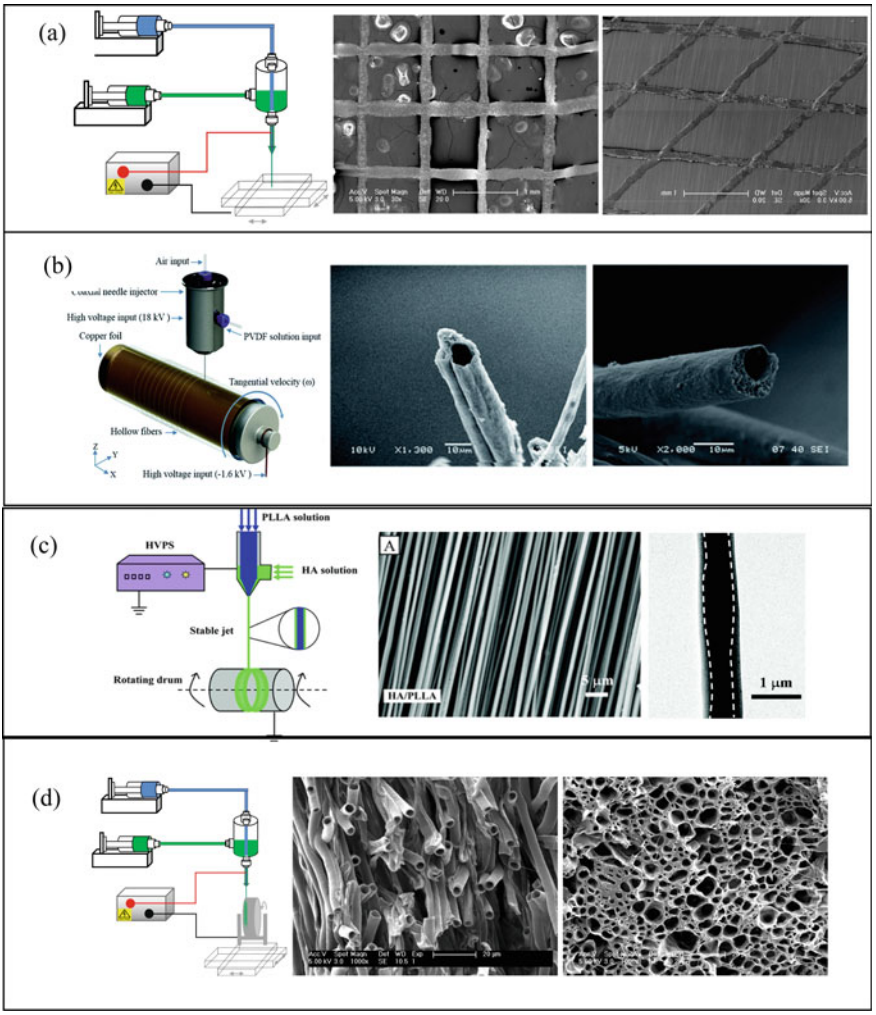


Fig. 5.2 Direct writing of core–shell structured or hollow polymeric fibres: **a** near-field coaxial electrospinning of patterned sugar-PCL core-sheath fibres (reproduced from [12] with permission, copyright Elsevier); **b** near-field coaxial electrospinning of hollow PVDF fibres (reproduced from [13] with the permission from the Royal Society of Chemistry); **c** far-field coaxial electrospinning of PLA-PEO shell and HA core (reproduced from [15] with the permission from the Royal Society of Chemistry); **d** far-field coaxial electrospinning of PCL shell and PEO core (reproduced from [16], an open access article published by Elsevier under a CC-BY license)

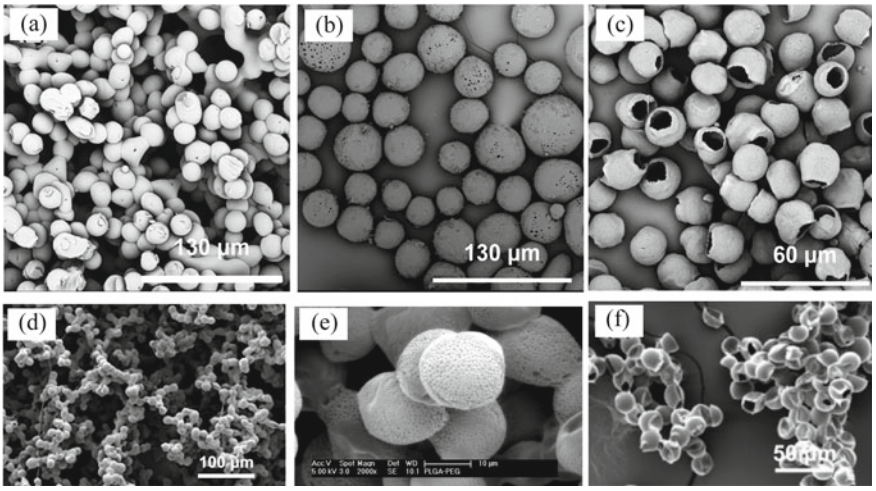


Fig. 5.3 Co-electrosprayed hollow polymeric microspheres with (**a**, **d**) solid surface, (**b**, **e**) porous surface, and (**e**, **f**) single surface opening, from PCL (**a**–**c**) (reproduced from [18], an open access article published by Elsevier under a CC-BY license) and PLGA (**d**–**f**) polymers [(**d**) and (**f**) were reproduced from [19], an open access article published by Elsevier under a CC-BY license]

an 1 mm working distance, well-defined hollow piezoelectric polyvinylidene fluoride (PVDF) fibres with tuneable inner diameters were fabricated [13]. At a working distance of 10 cm, a direct coaxial jet was still observed, which allowed the formation of well-defined and highly aligned hollow poly(d,l-lactic-co-glycolic acid) (PLGA) fibres from PLGA-PEO shell-core solution [14]. The addition of ultra-high molecular weight PEO (Mw > 5 M Da) into a poly(L-lactic acid) (PLA) shell solution helped maintain the state of the direct jet even when the working distance was further increased to 30 cm in the coaxial electrospinning using hyaluronic acid (HA) core solution (Fig. 5.2c) [15]. Zhou et al. further combined a rotating drum with an X–Y stage (Fig. 5.2d) to collect hollow PCL microfibres with variable fibre orientation/packing [16]. In particular, the gap between those hollow fibres could be tuned by varying the translation speed of the X–Y stage [16].

5.2.2 Coaxial Electrospraying of Hollow Polymer Particles

The studies of coaxial electrospraying can be divided into two categories. The first category is focused on developing biodegradable polymeric particles encapsulating biological agents for specific imaging and therapeutic applications. PCL and PLGA are two FDA-approved synthetic polymers having good biocompatibility and biodegradability, and are most commonly used materials in coaxial electrospraying of core–shell spherical particles for biomedical applications [17]. Co-electrospraying has been employed to fabricate hollow polymeric particles with various surface

microstructural characteristics, including solid surface, porous surface and with a single surface opening (Fig. 5.3). These are made from PCL and PLGA by varying factors including core/shell solution combinations, process parameters (e.g. flow rate) and/or collecting media [18, 19]. Furthermore, it has been shown that the ratio of shell thickness to radius of core–shell microspheres can also be adjusted by varying these factors [20].

The second coaxial electrospraying category includes theoretical studies focusing on computational and numerical simulations. The development of commercial software for computational fluid dynamics (CFD), including FLUENT 15.0 software (ANSYS), has encouraged the simulation of cone-jet behaviour and core–shell droplet formation from miscible shell/core solution combinations in single [21] and double-nozzle co-electrospraying [22]. More recently, a complete axisymmetric model of coaxial electrospraying under constant electrical permittivities and conductivities, and strict immiscibility of shell/core liquids was presented [23]. It can be envisaged that these computational and numerical simulations could greatly benefit the optimization of the co-electrospraying process.

5.3 Tissue Microstructure Mimicking Phantoms for Diffusion MRI

5.3.1 Brain, Heart and Tumour Microstructure

Axons in white matter create a highly anisotropic fibrous tissue. Myelinated axons are elliptic or circular in cross section, with diameters ranging from 0.16 and up to 9 μm [24] (Fig. 5.4a). Myocardial tissue (heart muscle) also consists of highly anisotropic fibrous tissues characterised by an array of interconnecting fibres with a radius of 21.4 ± 16.8 μm [25], as evidenced by longitudinal histology (Fig. 5.4b).

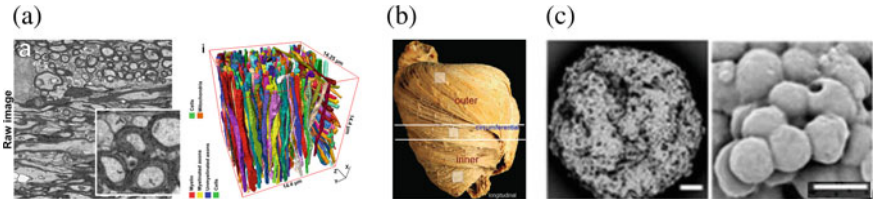


Fig. 5.4 Tissue microstructure in brain, heart and tumour: **a** 2D (left) SEM micrograph and simulation (right) showing axon size and axonal orientation in rat brain (reproduced from [24], an open access article published by Springer Nature under a CC-BY license); **b** a digital photograph showing a dissection (right) revealing the progression of the helical angle in porcine heart (reproduced from [26] with the permission from the BMJ Publishing Group Ltd.); **c** SEM micrographs of human pancreatic cancer cells (KP4) (reproduced from [27], an open access article published by Springer Nature under a CC-BY license). Scale bars in **c** are 50 μm (left) and 10 μm (right)

From the outer, through the middle to the outer layer in myocardium muscle there is a gradual and relatively even progression of helical angulation, from 'left-handed' through 'horizontal' to 'right-handed' orientation [26]. The microstructural properties (Fig. 5.4c) in solid tumour are often described in terms of cell size, which typically range from 10 to 20 μm [27], with intra- and extracellular packing density/volume fraction showing large variations. In each setting, the microstructural characteristics of tissue may vary with disease, and therefore represent an attractive target for diagnosis and monitoring of therapeutic interventions.

Diffusion MRI provides the ability to infer the microstructure of tissues by monitoring the diffusion of water molecules within and between cells; changes in cellularity affect water diffusion, and therefore macroscopically-recorded diffusion MRI signals. There have been an increasing number of studies on probing changes in tissue microstructure via diffusion MRI, not only as a diagnostic marker of diseases but also as a measure of treatment response to various therapies. There is increasing demand for diffusion MRI validation due to the exponential growth of the field of microstructural imaging [28].

5.3.2 Co-EHD Microstructural Phantoms for Diffusion MRI

The term "phantom" is used here for well-characterized test objects in terms of size and composition that can be used for evaluating the accuracy and precision of MRI methods to study tissue microstructure (for recent reviews of phantoms for quantitative MRI in general see [29, 30], respectively). The majority of microstructural phantoms currently in existence are used to provide a gold standard for the validation of MRI methods probing brain microstructure, although interest is growing in the development and application of such phantoms for validating microstructure measurements in tumours and in the heart.

Brain Tissue-Mimicking Phantom

As shown in Fig. 5.5a, co-electrospinning of uniaxially aligned hollow microfibres was achieved using a rotating drum fixed on an X–Y translation stage, resulting in fibres deposited in strip form; fibre strips were then characterised via SEM & μ-CT for ground truth, and finally packed as ~10–15 fibre layers into a MR visible liquid-filled test tube to form a phantom. Diffusion MRI measurement of these brain tissue mimicking phantoms has demonstrated that: (1) as shown in Fig. 5.5b, fractional anisotropy (FA—a composite diffusion MRI measurement of microscopic fibre orientation coherence and micro-geometric anisotropy) decreases linearly with an increase in the mean inner diameter of the fibres, whereas the radial diffusivity was shown to increase (indicating, as expected, that molecular diffusion across the section of the fibres is greater when the diameter of the section is larger) [31]; (2) fibre tractography results match the fibre orientations present in the white and grey matter phantoms (Fig. 5.5c) [32]; (3) diffusion MRI results for the phantoms show

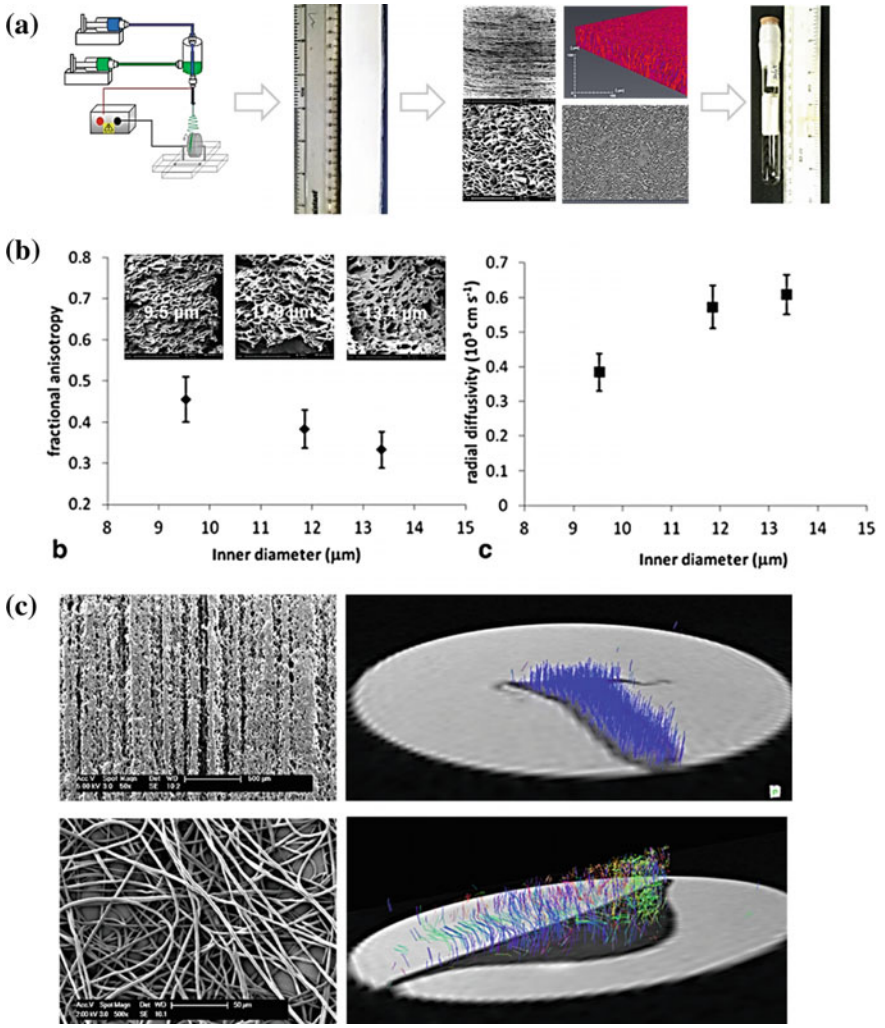


Fig. 5.5 Brain-mimicking fibre phantoms and their MRI performance: **a** flowchart of co-electrospinning of brain white matter phantom (reproduced from [34] with the permission from Springer, Cham); **b** effects of fibre size (reproduced from [31], an open access article published by John Wiley and Sons under a CC-BY license) and **c** fibre orientation (reproduced from [32] with permission form IEEE) in brain phantom on MR measurement (i.e., mean diffusivity and FA values); **d** repeatability over time of ADC and FA values on diffusion time of brain phantoms (reproduced from [33], an open access article published by John Wiley and Sons under a CC-BY license)

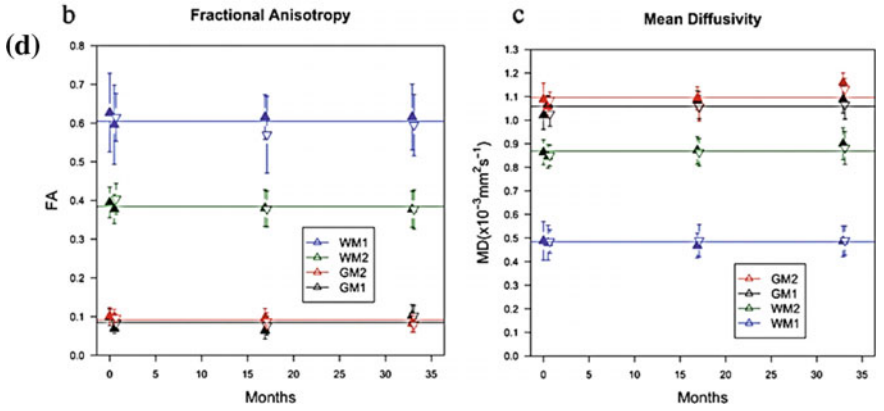


Fig. 5.5 (continued)

low variability for measured mean diffusivity and FA over a period of 33 months, indicating good material stability (Fig. 5.5d) [33].

Cardiac Tissue-Mimicking Phantom

Cardiac diffusion MRI can measure microstructural changes in the size and distribution of myocardial fibres, but despite recent developments, is not yet used for clinical management. The use of physiologically relevant phantoms helps the development of new imaging methods such as this by providing validation of the proposed measurements. However, the majority of current microstructure phantoms are for diffusion MRI in brain. They are also generally simplistic and lacking important features present in the myocardium, such as the helical arrangement of myocardial fibred. To address this, Teh et al. used three layers of co-electrospun hollow microfibres, wound at different helix angles, to design and construct the first-of-its-kind left-ventricular myocardium mimicking phantom (Fig. 5.6a) [35]. The values of apparent diffusion coefficient (ADC) and FA acquired from this phantom were found to be physiologically relevant and stable for a testing period of 4 months (a longer study was not conducted) (Fig. 5.6b). Importantly, the co-electrospun cardiac phantom had fibres orientations similar to those present in the left ventricle (Fig. 5.6c), suggesting that this phantom could act as a valuable tool for development and validation of new techniques for cardiac microstructure via diffusion MRI and for quality assurance in longitudinal and multicentre studies.

Tumor Cell-Mimicking Phantom

Diffusion MRI is considered as a useful tool to study solid tumours. However, the interpretation of the diffusion MRI signal and validation of quantitative measurements has to date proved challenging, due in part to the lack of a standard reference material that can mimic tumour cell microstructure. Zhou and McHugh et al. [19] showed that co-electrosprayed hollow PLGA microspheres can be used to mimic tumour cells mimicking materials and to construct a new generation of diffusion

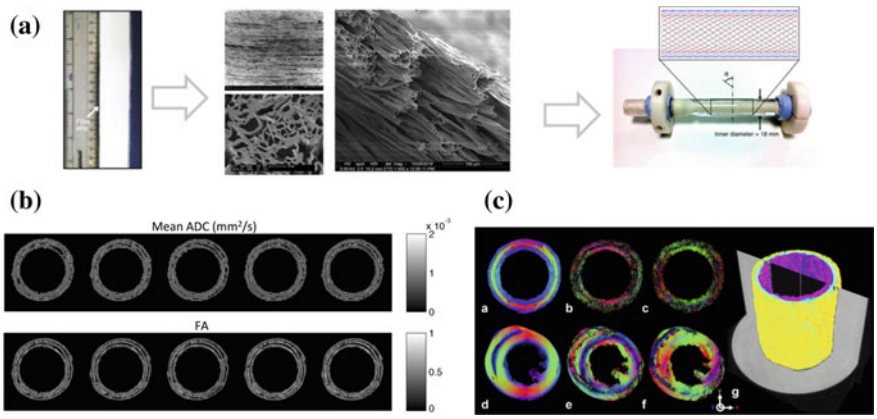


Fig. 5.6 Cardiac-mimicking fibre phantom and its MRI performance (reproduced from [35], an open access article published by John Wiley and Sons under a CC-BY license): **a** flowchart of co-electrospinning of cardiac phantom; **b** ADC and FA maps of cardiac phantom acquired over time; **c** fibre orientation transition in the phantom (top) and rat heart for comparison (bottom) and 3D fibre tractography (right) in the cardiac phantom

MRI phantom (Fig. 5.7a) [36]. The ADC values of the phantom were found to be dependent on the diffusion time, indicating that the phantom reflects the interaction of diffusing molecules with the cell-mimicking structure (Fig. 5.7b), and vary little over the test period of 42 weeks (Fig. 5.7c) [36]. These results provide evidence that co-electrosprayed hollow PLGA microspheres can restrict/hinder water diffusion as cells do in tumour tissue, implying that co-electrosprayed phantom may be suitable for use as a quantitative validation and calibration tool for diffusion MRI of cancer.

5.4 Summary

Diffusion MRI is a powerful non-invasive method for quantifying elements of tissue microstructure, with a range of diagnostic applications. Co-electrohydrodynamic forming of polymer materials has proven to be an effective approach to create tissue mimicking materials that allow this powerful medical imaging technique to be validated, allowing greater confidence in the technique and moving it a step closer to widespread clinical use.

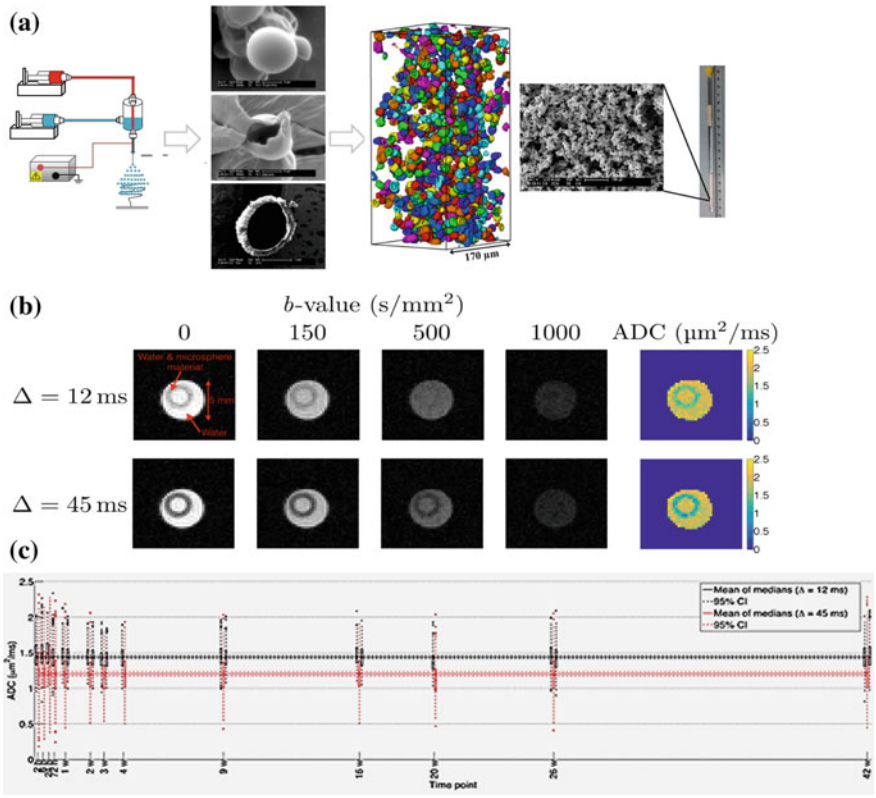


Fig. 5.7 Tumour cell-mimicking sphere phantom and its MRI performance: **a** flowchart of co-electrospraying of tumour cell phantom (reproduced from [19] with permission, copyright Elsevier)); **b** ADC maps acquired at two settings of diffusion time [36] and **c** the corresponding ADC values over 42 weeks reproduced from [36], an open access article published by John Wiley and Sons under a CC-BY license)

Acknowledgements This research was supported by NIHR UCLH Biomedical Research Centre (BRC) grant, and UK-MRC ImagingBioPro grant (MR/R025673/1), and UCL Department of Medical Physics and Biomedical Engineering and EPSRC (EP/M020533/1; CMIC Pump-Priming Award). GJM Parker has a shareholding and part time appointment and directorship at Bioxydyn Ltd. which provides MRI services. He is also a director and shareholder of Queen Square Analytics Ltd, which provides quantitative MRI services.

References

1. Wang, X., et al. (2016). Synthesis, properties, and applications of hollow micro-/nanostructures. *Chemical Reviews, 116*(18), 10983–11060.
2. Loscertales, I. G., et al. (2004). Electrically forced coaxial nanojets for one-step hollow nanofiber design. *Journal of the American Chemical Society, 126*(17), 5376–5377.
3. Loscertales, I. G., et al. (2002). Micro/nano encapsulation via electrified coaxial liquid jets. *Science, 295*(5560), 1695–1698.
4. Li, F., Song, Y., & Zhao, Y. (2010). Core-shell nanofibers: Nano channel and capsule by coaxial electrospinning. In A. Kumar (Ed.), *Nanofibres*. Intechopen.
5. Smeets, A., et al. (2020). Gastro-resistant encapsulation of amorphous solid dispersions containing darunavir by coaxial electrospraying. *International Journal of Pharmaceutics, 574*, 118885.
6. Dror, Y., et al. (2007). One-step production of polymeric microtubes by co-electrospinning. *Small (Weinheim an der Bergstrasse, Germany), 3*(6), 1064–1073.
7. Arinstein, A., & Zussman, E. (2007). Postprocesses in tubular electrospun nanofibers. *Physical Review E, 76*(5), 056303.
8. Halaui, R., et al. (2011). Development of micro-scale hollow fiber ultrafiltration membranes. *Journal of Membrane Science, 379*(1), 370–377.
9. Moghe, A. K., & Gupta, B. S. (2008). Co-axial electrospinning for nanofiber structures: Preparation and applications. *Polymer Reviews, 48*(2), 353–377.
10. Han, D., & Steckl, A. J. (2019). Coaxial electrospinning formation of complex polymer fibers and their applications. *ChemPlusChem, 84*(10), 1453–1497.
11. Yan, X., et al. (2015). Slit-surface electrospinning: A novel process developed for high-throughput fabrication of core-sheath fibers. *PLoS ONE, 10*(5), e0125407.
12. Zhou, F.-L., et al. (2011). Jet deposition in near-field electrospinning of patterned polycaprolactone and sugar-polycaprolactone core–shell fibres. *Polymer, 52*(16), 3603–3610.
13. Pan, C.-T., et al. (2015). Near-field electrospinning enhances the energy harvesting of hollow PVDF piezoelectric fibers. *RSC Advances, 5*(103), 85073–85081.
14. Sitt, A., et al. (2016). Microscale rockets and picoliter containers engineered from electrospun polymeric microtubes. *Small (Weinheim an der Bergstrasse, Germany), 12*(11), 1432–1439.
15. Yuan, H., et al. (2016). Highly aligned core–shell structured nanofibers for promoting phenotypic expression of vSMCs for vascular regeneration. *Nanoscale, 8*(36), 16307–16322.
16. Zhou, F.-L., et al. (2015). Production and cross-sectional characterization of aligned co-electrospun hollow microfibrous bulk assemblies. *Materials Characterization, 109*, 25–35.
17. Zhang, L., et al. (2012). Coaxial electrospray of microparticles and nanoparticles for biomedical applications. *Expert Review of Medical Devices, 9*(6), 595–612.
18. Zhou, F.-L., et al. (2017). Hollow polycaprolactone microspheres with/without a single surface hole by co-electrospraying. *Langmuir, 33*(46), 13262–13271.
19. Zhou, F.-L., et al. (2019). Co-electrospraying of tumour cell mimicking hollow polymeric microspheres for diffusion magnetic resonance imaging. *Materials Science and Engineering: C, 101*, 217–227.
20. Gao, Y., et al. (2016). Optimising the shell thickness-to-radius ratio for the fabrication of oil-encapsulated polymeric microspheres. *Chemical Engineering Journal, 284*, 963–971.
21. Yan, W.-C., et al. (2016). Computational study of core-shell droplet formation in coaxial electrohydrodynamic atomization process. *AIChE Journal, 62*(12), 4259–4276.
22. Yan, W.-C., Tong, Y. W., & Wang, C.-H. (2017). Coaxial electrohydrodynamic atomization toward large scale production of core-shell structured microparticles. *AIChE Journal, 63*(12), 5303–5319.
23. López-Herrera, J. M., et al. (2020). A numerical simulation of coaxial electrosprays. *Journal of Fluid Mechanics, 885*, A15.
24. Abdollahzadeh, A., et al. (2019). Automated 3D axonal morphometry of white matter. *Scientific Reports, 9*(1), 6084.

25. Wang, B., et al. (2012). Structural and biomechanical characterizations of porcine myocardial extracellular matrix. *Journal of Materials Science: Materials in Medicine*, *23*(8), 1835–1847.
26. Partridge, J. B., et al. (2014). Linking left ventricular function and mural architecture: What does the clinician need to know? *Heart, 100*(16), 1289.
27. Minami, F., et al. (2021). Morphofunctional analysis of human pancreatic cancer cell lines in 2- and 3-dimensional cultures. *Scientific Reports, 11*(1), 6775.
28. Novikov, D. S., et al. (2019). Quantifying brain microstructure with diffusion MRI: Theory and parameter estimation. *NMR in Biomedicine, 32*(4), e3998.
29. Keenan, K. E., et al. (2018). Quantitative magnetic resonance imaging phantoms: A review and the need for a system phantom. *Magnetic Resonance in Medicine, 79*(1), 48–61.
30. Fieremans, E., & Lee, H.-H. (2018). Physical and numerical phantoms for the validation of brain microstructural MRI: A cookbook. *NeuroImage, 182*, 39–61.
31. Hubbard, P. L., et al. (2015). Biomimetic phantom for the validation of diffusion magnetic resonance imaging. *Magnetic Resonance in Medicine, 73*(1), 299–305.
32. Ye, A. Q., et al. (2014). Diffusion tensor MRI phantom exhibits anomalous diffusion. In *2014 36th Annual International Conference of the IEEE Engineering in Medicine and Biology Society*.
33. Grech-Sollars, M., et al. (2018). Stability and reproducibility of co-electrospun brain-mimicking phantoms for quality assurance of diffusion MRI sequences. *NeuroImage, 181*, 395–402.
34. Zhou, F.-L., et al. (2015). Co-electrospun brain mimetic hollow microfibres for diffusion magnetic resonance imaging. In A. Macagnano, E. Zampetti, & E. Kny (Eds.), *Electrospinning for high performance sensors* (pp. 289–304). Springer International Publishing.
35. Teh, I., et al. (2016). Biomimetic phantom for cardiac diffusion MRI. *Journal of Magnetic Resonance Imaging, 43*(3), 594–600.
36. McHugh, D. J., et al. (2018). A biomimetic tumor tissue phantom for validating diffusion-weighted MRI measurements. *Magnetic Resonance in Medicine, 80*(1), 147–158.



Feng-Lei Zhou obtained the B.S. degree in textile engineering and the M.S. degree in textile materials from Qingdao University (China) and the Ph.D. degree in textiles from the University of Manchester (UK). He is a Senior Research Fellow at UCL, working in the Centre for Medical Image Computing and School of Pharmacy. From 2010 to 2019, he worked as a Research Associate and then a Research Fellow in the Manchester Centre for Imaging Sciences. He has general research interests in electrohydrodynamic (EHD) processing and polymer materials. In the past decade, he has participated in several cross-disciplinary research projects funded by the EU FP7, EPSRC and CRUK, in which he pioneered the development of tissue-mimicking phantoms for the validation of diffusion MRI in neurology, cancer, and heart. He has inspired and gathered together a circle of key collaborators with fruitful outputs from 10+ world-leading imaging centers in the UK, EU, USA and China. More recently his research has expanded to EHD 3D printing of dielectric elastomer actuators, MRI guided theranostic materials, and smart wearables. Dr. Zhou has published 46 articles in peer-reviewed journals and one edited book chapter in the book "Electrospinning for High-Performance Sensor", which is one of the most downloaded books of the last five years on the Springer website. He is a member of the Fiber Society (USA) and the Aerosol Society (UK).



Geoff J. M. Parker graduated with a B.Sc. degree in physics from the University of Manchester before completing his Ph.D. on dynamic contrast-enhanced MRI in cancer at the Institute of Cancer Research in London. He then moved to the NMR Research Unit at the Institute of Neurology, UCL, where he worked on a range of MRI techniques, including relaxation time measurement methods, brain atrophy measurements, and diffusion MRI tractography methods, which he applied to multiple sclerosis and epilepsy. In 2001 he moved to the Department of Imaging Science and Biomedical Engineering at the University of Manchester, where he continued to develop and apply quantitative MRI methods in a range of conditions, including cancer, neurology, and lung disease. Starting as a research fellow, he gained promotion to full professor in 2007. He moved to take up his current position—Professor of Healthcare Engineering, Imaging and Enterprise within UCL's Centre for Medical Image Computing (CMIC)—in 2019. His research group continues to work on quantitative MRI, including the development of tissue-mimicking phantom materials for diffusion MRI. In addition to his academic work, he founded Bioxydyn in 2009 to translate quantitative MRI methods into healthcare, and he continues to be the Chief Executive Officer of the company. In 2020 he co-founded Queen Square Analytics, which is pioneering the use of machine learning methods applied to MRI to help diagnose and treat neurological diseases. Prof. Parker is Deputy Editor for Magnetic Resonance in Medicine (MRM), Editorial Board member of BMC Medicine, Senior Fellow of the International Society for Magnetic Resonance in Medicine (ISMRM), Member of the ISMRM Board of Trustees, past Secretary and Treasurer of the British Chapter ISMRM, Deputy Director of the UCL Institute of Healthcare Engineering, and is a member of the EPSRC Peer Review College.

Chapter 6
Polysuccinimide and Polyaspartamide for Functional Fibers: Synthesis, Characterization, and Properties



Kristof Molnar, Eniko Krisch, and Judit E. Puskas

Abstract This chapter discusses the synthesis and characterization of polysuccinimide and polyaspartamide functional fibers made by electrospinning. Polysuccinimide is a biodegradable and tissue-friendly polymer made from L-aspartic acid. Under physiological conditions (pH = 7.4) it hydrolyzes to form water-soluble poly(aspartic acid). The poly(amino acid) structure provides biocompatibility and biodegradability to poly(aspartic acid)- based fibers and networks making them promising materials for biomedical applications such as soft tissue and drug delivery implants. However, the hydrolysis and the dissolution of the polysuccinimide fibers is fast, prohibiting their use as implants. To prevent dissolution, crosslinks between the polymer chains and thus a polymer network inside the electrospun fibers can be created. Then these fibers will swell, forming hydrogel fiber membranes. Polysuccinimide can easily be modified with *primary* amines, therefore a wide variety of polysuccinimides and poly(aspartic acids) with various properties can be synthesized. Three methods were successful for the synthesis of poly(aspartic acid) based hydrogel fiber networks: reactive electrospinning based on thiol–disulfide exchange, plasma-induced crosslinking of allyl-functionalized polysuccinimide followed by hydrolysis and submerging in 2,2,4(2,4,4)-trimethyl-1,6-hexanediamine/methanol solution to crosslink post-electrospinning. These synthetic strategies can be used with other polymers as well.

Keywords Polysuccinimide · Polyaspartamide · Functional fibers

K. Molnar · E. Krisch · J. E. Puskas (✉)
College of Food, Agricultural, and Environmental Sciences, Department of Food, Agricultural and Biological Engineering, The Ohio State University, 220 FABE, 1680 Madison Avenue, Wooster, OH 44691, USA
e-mail: puskas.19@osu.edu

K. Molnar
e-mail: molnar.182@osu.edu; molnarnekrisch.1@osu.edu

© The Author(s), under exclusive license to Springer Nature Switzerland AG 2022

A. Vaseashta and N. Bölgen (eds.), *Electrospun Nanofibers*,
https://doi.org/10.1007/978-3-030-99958-2_6

6.1 Introduction

Poly(amino acid)s are widely studied in biomedical fields, including regenerative medicine and drug delivery due to their excellent biological functionality, such as target specificity and biodegradability. On the other hand, a major drawback of poly(amino acid)s is that their functionalization is limited. Current synthesis techniques for the synthesis of polypeptides and poly(amino acid)s, such as solid-phase peptide synthesis and recombinant DNA techniques, still have limitations in their production capacity, atom economy and sequence regulation. In contrast, poly(aspartic acid) (PASP) is a pH-responsive, crosslinkable poly(amino acid), that can be synthesized easily and without the need of activating agent [in contrast to its analogue, poly(glutamic acid)] [1, 2].

PASP is usually synthesized from its anhydride, polysuccinimide (PSI), by hydrolysis. PSI can be prepared from aspartic acid, a natural amino acid by acid catalyzed thermal polycondensation (Fig. 6.1) [3]. In general, phosphoric acid is used as a catalyst and also for water distraction and the synthesis is carried out in a mixture of organic solvents with high boiling point (e.g. mesitylene and sulfolane) or without solvent, under reduced pressure [4]. Both methods are cost-effective compared to other technologies such as biotechnological production or polymerization of N-carboxyl acid anhydride of aspartic acids resulting directly in PASP. However, the solvent-free process should be favored if we take the environmental factors into consideration. Depending on the synthesis the molecular weight of PSI obtained in thermal polycondensation ranges from 10 to 180 kDa [3–7].

Furthermore, PASP is considered to be biocompatible and biodegradable because of its chemical structure [8, 9]. However, biodegradability of PASP has not been investigated extensively. First, Alford et al., then Nakato et al. studied the relationship between the chemical structure and the biodegradability of PASP and suggested that both the synthesis method and the existence of the branched structure in PASP should cause a difference in their biodegradability [4]. Juriga et al. studied the biodegradation

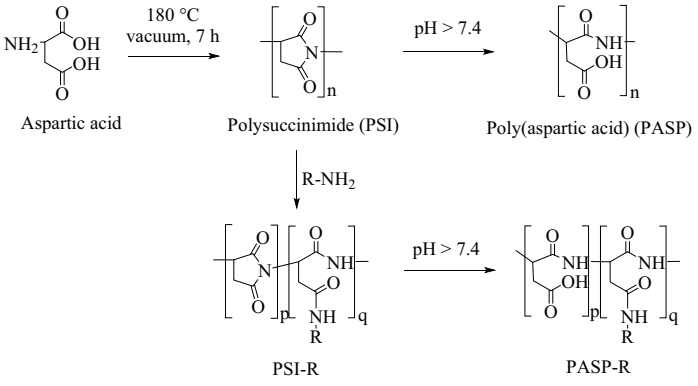


Fig. 6.1 Synthesis and modification of polysuccinimide and their hydrolysis to poly(aspartic acids)

of PASP hydrogels at physiological conditions in vitro and their biodegradability were proven in the presence of different enzymes and cell culture media by swelling and stress–strain measurements [10].

The succinimide rings in the repeating units of PSI can easily react with nucleophilic reagents (e.g., *primary* amines), thus PSI and PASP derivatives as well as crosslinked PSI and PASP can be synthesized in various ways (Fig. 6.1) [5, 6, 11–17]. In the reaction, the succinimide rings open on either side of the imide bond and the *primary* amine is added via an amide bond as a side group. If multifunctional amines such as diamines or triamines are reacted with PSI, crosslinks can be created between the PSI chains. Crosslinking of PSI with multifunctional *primary* amines thus leads to the formation of PSI networks or gels, which can easily be hydrolyzed into PASP hydrogels [18]. There is no need for activating agents, e.g., carbodiimides during synthesis, which simplifies the synthesis and purification.

First Gyenes et al. published the synthesis of PSI and PASP hydrogels using different diamines (e.g. 1,4-diaminobutan (DAB), lysine, cystamine) as crosslinker [11, 18]. PASP hydrogels show pH-dependent swelling character due to the polyelectrolyte nature of PASP, which is expressed in the volume change of the hydrogel [11, 19]. However, with the right choice of crosslinker, PASP hydrogels with additional properties can be synthesized as well. Using peptides for crosslinking results in enzymatically degradable hydrogels, while using a disulfide-containing crosslinker, PASP gels showing redox-sensitivity can be synthesized. Disulfide containing hydrogels undergo either gel-sol transition or volume change upon reduction, due to cleavage of the intermolecular disulfide bonds. Hydrogels, containing only disulfide bonds completely disintegrate in a reducing environment resulting in a polymer solution, while those containing other—non redox sensitive or permanent—chemical crosslinks beside the disulfides, swell upon reduction as the number of the crosslinks decreases in the polymer network [14].

Owing to the hereby mentioned advantageous properties of PASP, PSI and their derivatives, they have been extensively studied for biomedical application, in various shapes and sizes, such as drug delivery or tissue engineering [10, 20–22]. Nanogels (with diameter of a few hundred nanometers) gained a considerable attention in the field of drug delivery, as they possess all the advantages of the hydrogels and, due to their small size, they can be injected intravenously and thus reach the targeted tissues or cells from the blood stream. PASP nanogels showing pH and redox responsivity have been synthesized by Krisch et al. in inverse emulsion, for the intravenous delivery of anticancer drugs [23, 24]. For subcutaneous release of drugs, as well as for the preparation of artificial extracellular matrix, PSI and PASP nanofibers have been synthesized by an electrospinning method.

Electrospinning is a well-known technique for the synthesis of fibrous polymer meshes from a large variety of polymers. The most basic setup consists of a syringe filled with a polymer solution mounted into a syringe pump with a metal needle to which high DC voltage is applied and a flat metal sheet with the opposite electrode placed in front of it. If the electric field is strong enough to overcome the surface tension of the solution, a polymer jet emerges and ejects in the direction of the grounded target. During this flying period, this jet starts a whipping movement,

while it continuously elongates and its solvent evaporates, creating a web of randomly oriented dry fibers on the collector [25].

Based on our current knowledge, pure PASP cannot be electrospun. However, Nemeth et al. electrospun 3-(diethylamino)propyl and n-butyl side group modified PASP polymer loaded with vitamin B_{12} as model drug to synthesize rapidly dissolving fibrous membranes. PSI on the other hand is easier to electrospun. PSI based fibrous membranes were first synthesized by Molnar et al. using a 25 w% dimethylformamide (DMF) solution [5, 26, 27]. The resulting membrane consisted of fibers with average diameters ranging from 500 to 1000 nm in diameter, could be dry heat sterilized at 160 °C for 2 h without degradation and were strong enough to be folded without tearing and surgically sutured [5, 26, 27]. PSI based fibrous membranes undergo rapid hydrolysis in pH 7.4 and above resulting in water soluble PASP membranes. Although, this could be utilized in controlled drug release, it hinders its usage in implantation based applications. A possible solution is to establish chemical crosslinks between the PSI chains in the fibers and thus create a polymer network. These crosslinked PSI fibers can retain their integrity even in aqueous medium by absorbing the surrounding liquid and forming polymer hydrogel fibers.

Since PSI can be modified and/or crosslinked in many ways, synthesis of the PSI gel fibers can be achieved using various methods. Generally speaking, crosslinking methods of the polymer fibers can be divided into two groups: post-spinning methods, and reactive-electrospinning. In the case of post-spinning methods, first the polymer fibers are synthesized by electrospinning, and then the crosslinks are built inside the fibers afterwards. Crosslinks can be formed either by treatment with liquid or vapors containing the crosslinking agents [26], or using UV light [28], radiation [29] or—as we are going to show- plasma treatment [27]. Crosslinks can also be formed during the electrospinning process, which is called reactive electrospinning. In this case for example thiol containing polymers can be crosslinked by air oxidation during the flying time [5], or the polymer and the crosslinking solution can be electrospun at the same time, using a coaxial needle [30]. Other strategies and more details can be found in the recent review of Ghosh et al. [31]. In this Chapter we will describe four different methods for the preparation of PSI and PASP gel fibers, two post-electrospinning methods, and two examples for reactive electrospinning.

6.2 Synthesis of PSI Gel Fibers by Post-spinning Chemical Crosslinking

Zhang et al. showed that by immersing PSI fibers into the solution of 0.15 mol/l 1,2-diaminoethane in methanol solution, one can induce crosslinking of PSI inside the fibers [32]. First, they optimized PSI electrospinning by varying the PSI in DMF solution concentration: 26, 30 and 34 wt% (Electrospinning: 18 cm distance, 11 kV DC voltage) (Fig. 6.2a, b, c). Then, they immersed the 30 wt% sample in the crosslinker's solution for 2 h. Due to the crosslinking reaction fiber diameter rose from 822 to

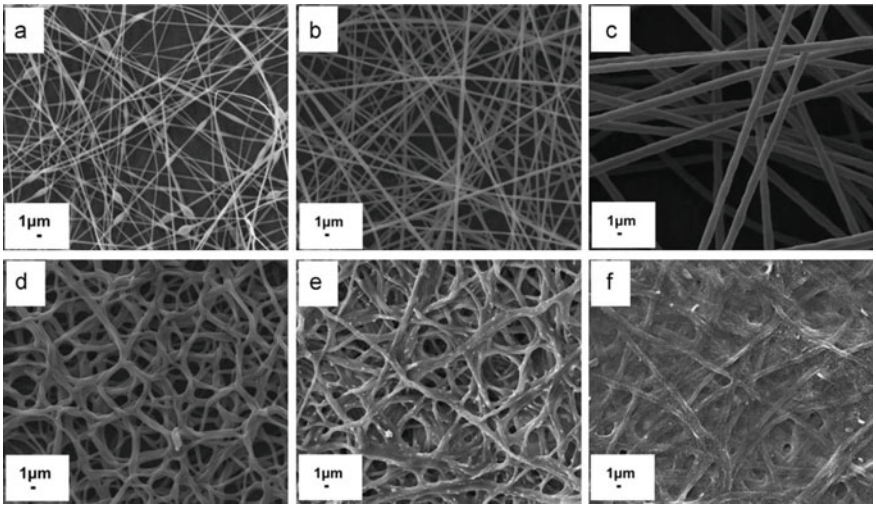


Fig. 6.2 SEM images of PSI nanofibers from different concentrations of **a** 26 wt%, **b** 30 wt%, **c** 34 wt%, **d** PASP nanofibers, **e** PASP nanofibers after immersing in PBS for 24 h, de-swelling in methanol, and then dried in vacuum, and **f** PASP nanofibers after immersing in PBS for 24 h and dried in vacuum. Reprinted with permission from [32]

1024 nm. After hydrolysis of the crosslinked fibrous membranes a flexible, semi-transparent hydrogel membrane was obtained consisting of fibers fused together, yet creating a porous/fibrous structure (Fig. 6.2d, e, f) [14].

Similarly, Molnar et al. used 0.5 mol/l 1,4-diaminobuthane (DAB) in ethanol solution to induce crosslinking in PSI fibers by immersing fibrous PSI membranes for an hour [26]. The reaction can be seen in Fig. 6.3. First, PSI fibers were synthesized by electrospinning 1 ml 25 w% PSI in DMF solution with 1 ml/h, at 15 cm collector distance with 10 kV [5]. The fiber membrane was then immersed into the crosslinker solution to induce crosslinking. DAB is a diamine that can create crosslinks between the succinimide repeating units in PSI after immersing the fibrous membrane into the ethanol solution of DAB. Ethanol was chosen as a solvent as PSI is insoluble in it and thus the fibrous membrane can retain its fibrous morphology. The DAB

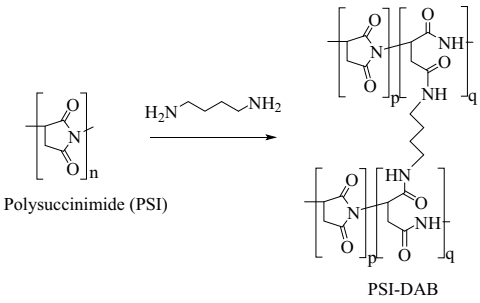


Fig. 6.3 Reaction of PSI and DAB and the formation of PSIDAB

crosslinked PSI fiber membrane is denoted as PSIDAB. SEM showed no observable difference between the morphology of PSI and PSIDAB fibers, both looked smooth and uniform without defects. The average fiber diameter of PSIDAB was slightly smaller [800 ± 30 nm, (n = 50, p = 0.05)] (Fig. 6.4a), compared to the PSI fibers used in the series [average fiber diameter of PSI fibers was 911 ± 41 nm, (n = 50, p = 0.05)]. To see how hydrolysis, thus the change from PSIDAB to the PASP based PASPDAB changes the morphology of fibers, disks of 16 mm in diameter were cut from PSIDAB and were hydrolyzed in pH 8 imidazole buffer solution. Due to hydrolysis the disks turned opaque and grew from 16 ± 0 mm to 21 ± 1 mm, which corresponds to 31 ± 7% (n = 3, p = 0.05) size change, marking the complete transformation into PASPDAB (Fig. 6.4c). SEM analysis on washed and freeze-dried PASPDAB fibers revealed that there was some fusion of the fibers (Fig. 6.4b), but less than presented by Zhang et al. This can be attributed to the longer crosslinking time as well as higher crosslinker concentration in the case of DAB.

Attenuated Total Reflectance Fourier Transform Infrared Spectroscopy (ATR-FTIR) was carried out to confirm the changes in the chemical structure of PSI due to crosslinking and hydrolysis. FTIR spectra of PSI, PSIDAB and PASPDAB can be seen in Fig. 6.5a, d, e [26]. The characteristic absorption bands of imide rings in PSI can be seen at 1710 cm^{-1} (asymmetric stretching vibration is attributed to the ν_{CO} of –(OC)2 N–), 1391 cm^{-1} (C–O bending vibration, δ) and 1355 cm^{-1} (stretching vibration, ν_{C-N} of –(OC)2 N–). After crosslinking the appearance of a shoulder of the peak at 1710 cm^{-1} marks the stretching vibration of the >N–C=O bond at

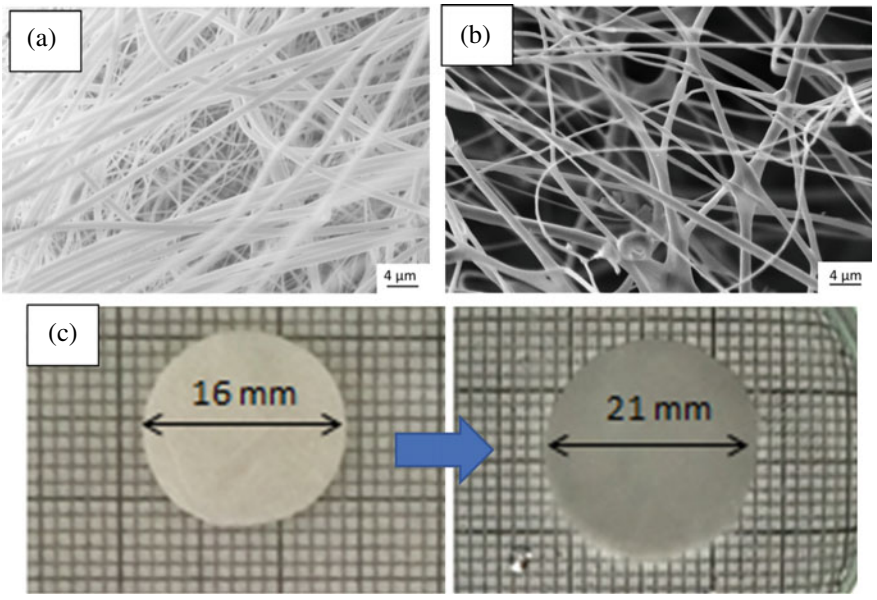


Fig. 6.4 SEM PSIDAB fibers (**a**) macroscopic picture (**b**) and SEM micrograph (**c**) of PASPDAB fibers. Reprinted with permission from [26]

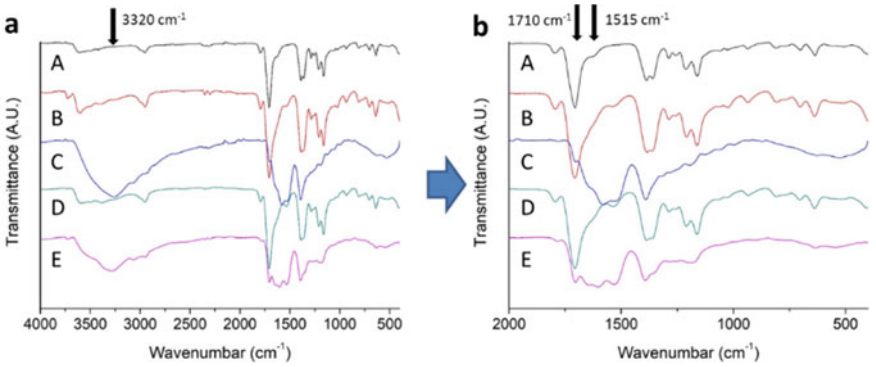


Fig. 6.5 ATR-FTIR spectra of the synthesized samples (**a**) and an enlarged part of the said spectra (**b**), where the samples are labeled with capital letters as follows: PSI (A), PSICYS (B), PASPCYS (C), PSIDAB (D), PASPDAB (E). Reprinted with permission from [26]

1636 cm^{-1}. Furthermore, there is another peak emerging at 1515 cm^{-1} related to the N–H bending in the amide bond. After hydrolysis, a new wide peak appeared at around 3320 cm^{-1}, assigned to –OH groups formed by hydrolysis of the imide rings in the polymer backbone (Fig. 6.1). Lastly, the decreased intensity of the imide peak at 1710 cm^{-1} and the increase of that of the stretching C =O in the amide peak at 1662 cm^{-1} confirm the opening of succinimide rings.

An in vivo study was carried out to see if hydrolysis of PSIDAB occurs and to investigate the implantability and short-term biological response to PSIDAB fiber membranes. Full description of the methodology of the study can be found in the paper of Molnar et al. [26]. Briefly, PSIDAB disks with the diameter of 16 mm, cut from the electrospun and crosslinked PSIDAB fibrous membrane, were sterilized by placing them into the solution of chlordioxide in PBS [33]. Disks were implanted under the skin at the nape (back-side of the neck) of 12 Wistar albino rats. Animals were monitored until days 3 and 7 when 6–6 were euthanized and dissected. Extracted samples were fixed in 4 V/V% formaldehyde solution then after water elimination, embedded in paraffin, sliced and stained using standard haematoxylin–eosin staining protocol.

PSIDAB fiber membranes were easy to manipulate, roll up and hold sutures that would enable laparoscopic surgery (Fig. 6.6). During the 3-day and 7-day observation no visible irritations, animal misbehavior or other macroscopically observable

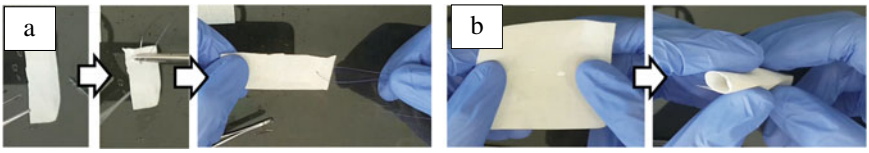


Fig. 6.6 Sutured PSIDAB sample (**a**), rolled up PSIDAB sample for e.g., laparoscopy (**b**)

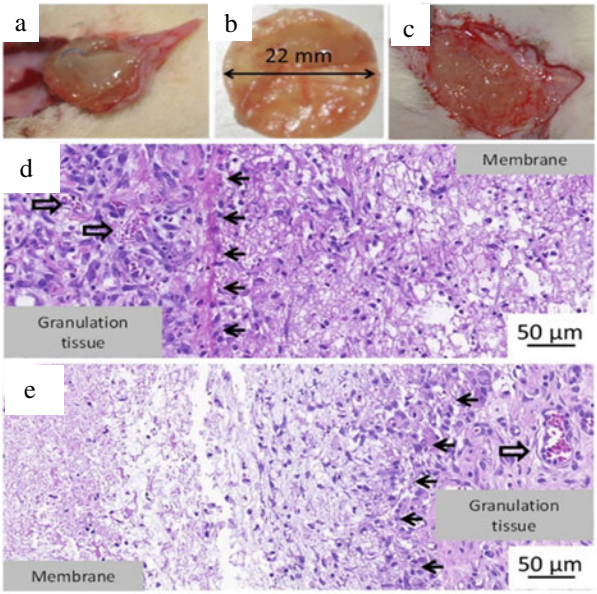


Fig. 6.7 PASPDAB sample 3 days after implantation (**a**), resected sample grew in size and changed consistency (**b**), 7 days after implantation (**c**); representation of histopathology of a sample at day 3 (**d**) and day 7 (**e**); Black arrows indicate the boundary between the sample and the tissue and empty black arrows indicate blood vessels. Reprinted with permission from [26]

complications were detected. The animals behaved just as they did before surgery: normal food intake and bowel movement, mobility, and behavior with the caretakers were observed. After 3 days, samples turned into soft, gel like membranes that grew by approximately 40% in diameter, similarly to the in vitro hydrolysis induced by pH 8 buffer solution (Fig. 6.7a, b). Therefore, one can assume that the hydrolysis of PSIDAB to PASPDAB occurs in vivo as well. There were no macroscopically visible complications in the implantation areas such as swollen or irritated tissue. Histopathology revealed moderate acute inflammation in the granulation tissue surrounding the implanted membrane with a mixture of neutrophil granulocytes, lymphocytes and histiocytes surrounding and invading the outer part of the membrane (Fig. 6.7d). After 7 days, PASPDAB samples were found in a swollen, softer and more fragile state than their 3-day counterparts (Fig. 6.7c). These samples were easily torn and dissected into separate layers or truncated by tweezers suggesting a high reduction in physical strength and consistency. There was no visible inflammation or irritation in the implantation area, and the surrounding tissue visibly invaded the membranes. Histopathology revealed that the moderate acute inflammation observed on the 3rd day reduced to a mild level. The incorporation of granulation tissue became more apparent making it almost impossible to find a clear border

between the granulation tissue and PASPDAB membrane (Fig. 6.7e). Vascularization clearly started in the new tissue invading the membranes. The living tissue being able to invade the membrane is an exceptional result as it suggests a proper tissue integration.

To conclude, PSIDAB fibers could be synthesized by immersing electrospun PSI fibers into the solution of a diamine crosslinker. PSIDAB membranes did not dissolve during hydrolysis as they turn into PASPDAB, but only swelled and took up the surrounding fluid, forming hydrogel fiber membranes. PSIDAB membranes were sutureable and easy to manipulate. 3 days after implanting them under the skin into rats revealed that the membranes swelled by about 40% and visibly changed their structure suggesting the hydrolysis to PASPDAB occurs in vivo. The initially observed moderate acute inflammation turned into mild inflammation for the 7th day with the surrounding granulation tissue invading the membranes.

6.3 Synthesis of PSI Gel Fibers by Post-spinning Plasma Crosslinking

The process of exposing materials to a purposefully generated plasma medium is called plasma treatment. The plasma state of the treating gas can be initiated and maintained by continuously conveying energy to it, which can be achieved by gaseous, metallic, and laser plasma sources among others [34]. The plasma itself consists of an unregulated mixture of ions, free radicals, electrons, photons and unstable molecule fragments making it a very aggressive and reactive medium. Capitalizing on these properties' plasma treatment is used to accomplish various tasks, such as sterilization, surface modification, surface etching, crosslinking and plasma implantation just to mention a few of the most common applications [35]. However, only a few attempts are published in the literature about using plasma treatment for the crosslinking of polymers. The available articles are based on gelatin, which are summarized in the recent review of Campiglio et al. [36]. Liguori et al. showed that plasma can effectively be used to induce crosslinking in fibrous gelatin membranes without the use of a crosslinking agent such as genipin [37]. In contrast to their work Sisson et al. showed that oxygen plasma could not adequately crosslink gelatin fibers as those dissolved after 12 h in cell culture medium regardless of plasma treatment optimization [38]. Dolci et al. also found that drug loaded gelatin films can be crosslinked using atmospheric air plasma [39]. Molnar et al. showed that electrospun allyl-modified PSI fibers can be crosslinked by plasma treatment to yield PSI fiber gels [27].

First, PSI was modified with allylamine (AA) in dimethyl sulfoxide (DMSO) to form allylamine modified PSI (PSI-AA) (Fig. 6.8). The grafting degree of PSI with allylamine was easily controlled with the stochiometric feed ratio of allylamine to the succinimide repeat units, and PSI-AAs with various grafting degrees (1; 2; 5; 10) were prepared. The structure of the polymers was confirmed by ^{1}H-NMR and Fourier Transform Infrared Spectroscopy (FTIR) [27].

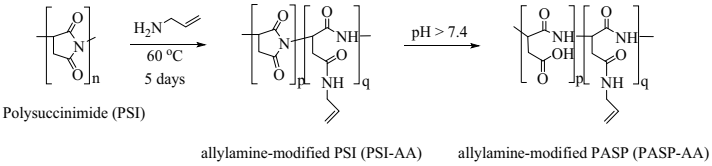


Fig. 6.8 Modification of PSI with allylamine

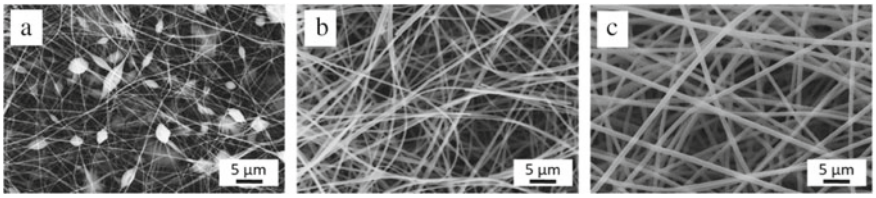


Fig. 6.9 SEM images of PSI-AA fiber mats electrospun from 35 wt% (**a**), 40 wt% (**b**) and 45 wt% (**c**) polymer solutions

PSI-AA was electrospun from dimethylformamide (DMF) using different concentrations (15 cm collector distance, 8–12 kV DC voltage, 1 ml/h feed rate). Fibers electrospun from a 35 wt% solution had larger globular or spindle-like structures. However, with higher concentrations entirely fibrous structure with no beads was yielded (Fig. 6.9). This observation is in agreement with the results of Fong et al. who examined the formation of beads as a function of the solution viscosity [40]. In the case of the 45 wt% solution the average fiber diameter was 955 ± 39 nm.

After fiber formation, crosslinking inside the fibers was induced by low pressure air plasma (~0.3 mbar), which was generated with a radio frequency plasma generator working at 40 kHz with 25 W in a tubular plasma chamber with 105 mm diameter and 300 mm length. Samples with diameters of 12 mm were placed into the center of the chamber on a borosilicate plate and exposed to plasma for 13 min. No visible macroscopic or microscopic changes occurred during the plasma treatment of the samples. To demonstrate the formation of chemical crosslinks, plasma-treated PSI-AA mats were immersed in dimethyl sulfoxide (DMSO), a good solvent of PSI. While non-treated mats immediately dissolved in DMSO, plasma-treated mats did not, because the gel structure protected the mats from dissolution. The exact chemistry of the crosslinking was not described, but the authors suggested it had occurred via recombination of the allyl radicals forming during plasma treatment.

As it was mentioned earlier, PSI undergoes hydrolysis in alkaline medium resulting in water-soluble poly(aspartic acid) (PASP). The plasma-treated PSI-AA mats' behavior in aqueous medium was tested as they were submerged into a phosphate buffer solution (PBS, pH = 7.4). After 24 h the samples were still visible and kept their integrity, but they became almost completely transparent as they hydrolyzed into PASP. The stability of the mats in aqueous medium showed that even after converting into PASP, the samples kept their gel-like structure due to the crosslinks

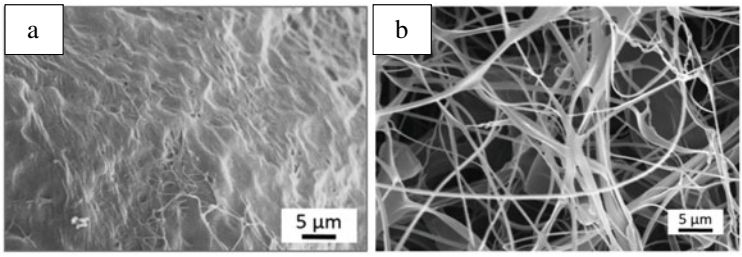


Fig. 6.10 SEM image of PASP-AA fiber mats plasma-treated for 13 min at 25 W (**a**) and for 17 min at 100 W (**b**)

established during plasma treatment. SEM images were taken of the PASP-AA mats in order to verify whether the mats retained their fibrous structure. As it was shown, the fibrous structure was almost entirely lost, the fibers merged to form an apparently continuous polymer layer. This is not unprecedented in the literature as it is often the case for fiber-based polymer networks [37, 41–43]. The loss of the fibrous structure upon hydrolysis was not a preferable outcome since it is this structure that grants special properties to the mats such as the large specific surface area and the structural resemblance to the extracellular matrix of the mammalian body, so the authors attempted to increase the stability of the PSI-AA fibrous structure. The conditions of the plasma treatment were optimized and with a 17 min low pressure plasma treatment at 100 W the fibers retained their fibrous structure after hydrolysis, and it was closely comparable to that of the PSI-AA mats before hydrolysis (Fig. 6.10).

The chemical structure of PSI-AA mat plasma-treated for 17 min at 100 W was first studied by FTIR. The spectrum of the plasma-treated samples was identical to the untreated samples. However, the solubility tests have clearly shown that the treatment is effective in producing crosslinks, so some chemical change had to occur. The authors theorized, that the crosslinking only occurred on the surface, and not in the core of the fibers [44]. However, the infrared light in attenuated total reflectance (ATR)-FTIR penetrates inside the fibers, and does not provide information on the surface area.

An important advantage of plasma treatment is its sterilizing effect. Thus, sterile, crosslinked mats can be produced without additional sterilization steps. As a sterility test, freshly plasma-treated PSI-AA mats were placed onto hard agar, then covered with soft agar in a sterile hood. The soft agar overlay provides easier counting of the colonies as microorganisms can't migrate into the hard agar and under sterile circumstances, only microorganisms from the surface or from the inside of the mats are able to grow. The addition of 1 ml M9 phosphate buffer allows the mats to slightly swell and therefore bacteria are able to grow in the surrounding soft agar. After 24 h, all membranes swelled visibly due to hydrolysis to PASP-AA. After 24 and 48 h, the Petri dishes were visually checked for colonies, and out of 6 samples, none had colonies growing on the fiber mats. Therefore, the plasma treatment proved to be an effective method not just for crosslinking but also for the sterilization of the samples.

To summarize, fiber mats from allylamine-modified polysuccinimide (PSI) and poly(aspartic acid) (PASP) were synthesized by electrospinning. Crosslinking of the polymer in the fibers was achieved via low pressure plasma treatment that also sterilized the fiber mats. Structural characterization has proven the fibrous structure of the mats and indicated their effective use in biomedical fields, such as tissue engineering.

6.4 Synthesis of PSI Gel Fibers by Coaxial Reactive Electrospinning

Reactive electrospinning is special as there is a chemical reaction, such as a crosslinking, during the electrospinning process. The easiest way to achieve reactive electrospinning is to directly mix the polymer and a crosslinker in one solution and use that mixture for electrospining. However, as the crosslinking reaction progresses, the viscosity of the solution constantly rises until it solidifies and blocks the nozzle. Therefore, in this case the spinning window (time frame where spinning is possible before gelation) is quite narrow, with the amount of fibers produced limited, and their diameter is changing in a wide range [42, 45]. Molnar et al. used coaxial electrospinning to synthesize crosslinked PSI fibers, where the solution of the crosslinker [2,2,4(2,4,4)-trimethyl-1,6-hexanediamine (THD)] was pumped in the core of the needle and the PSI solution was in the shell (Fig. 6.11a, b) [30]. When using a coaxial needle, the polymer and the crosslinker only meet at the end of the needle right before flying out, thus the aforementioned problems of early gelation can be avoided.

The gelation time, which is the time necessary for the mixture of the polymer and the crosslinker to not flow anymore, depends strongly on the concentration of both components. Also, the properties of the resulting gel depend strongly on the concentration of the components. In the experiments, the concentration of the components, thus the ratio between the polymer and the crosslinker was varied by varying the feed rate of the core (crosslinker) solution while the feed rate of the shell solution (polymer) was always fixed at 2 ml/h (target distance was 18 cm and 16–18 kV DC voltage was used). The success of gel crosslinking inside the fibers was tested by immersing the electrospun membranes into DMF. If crosslinking was successful and there were enough crosslinks in the membranes, they did not dissolve. This can be considered as an indirect proof for the presence of chemical crosslinks. At core feed rate of 0.12 ml/h, smooth fibers were obtained, but they dissolved in DMF suggesting an insufficient amount of crosslinks (PSI-THD1, Fig. 6.11c). 0.74 ml/h resulted in fibers with lots of beads that did not dissolve in DMF (PSI-THD3, Fig. 6.11d). However, electrospinning was difficult as the core and the shell solution separated at the tip of the needle, resulting in alternation between spinning of the polymer and spraying of the crosslinker. 0.5 ml/h resulted in smooth fibers with

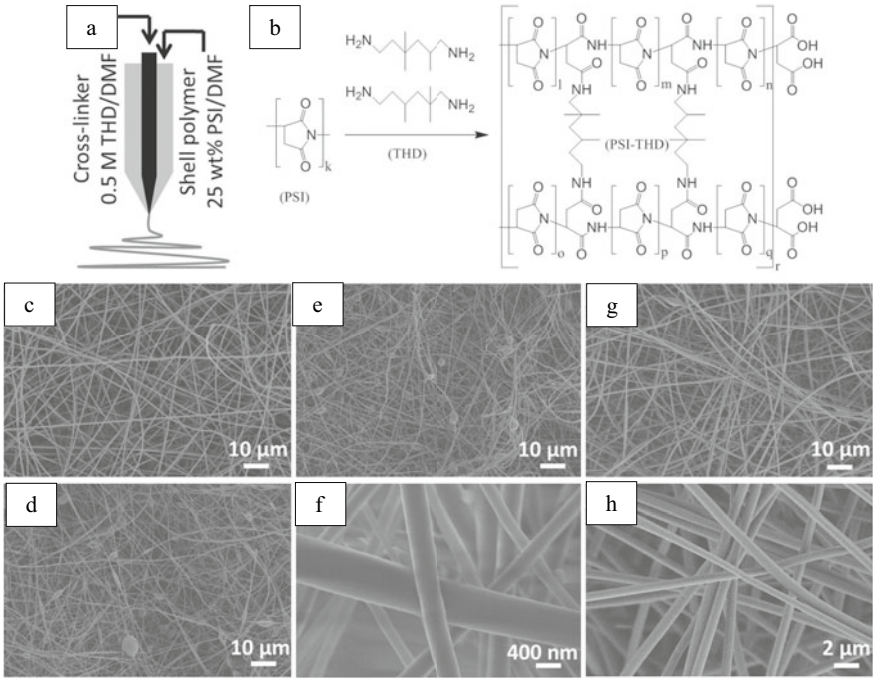


Fig. 6.11 Scheme of coaxial setup (**a**), reaction of PSI with THD (**b**). SEM images of electrospun fibers of PSI-THD1 (**c**), PSI-THD3 (**d**), PSI-THD2 (**e, f**) and PSI-THD-PEO (**g, h**)

beads without dissolving in DMF (PSI-THD1, Fig. 6.11e, f). Therefore, 0.5 ml/h was chosen as optimal feed rate.

The average fiber diameter reduced to 305 ± 41 nm compared to the pure PSI fibers' 595 ± 44 nm prepared with the coaxial setup. A large amount of smooth particles were incorporated into the fiber mats. This can be attributed to the instability during electrospinning caused by the difference between the viscosities of the shell PSI solution (1.8 Pas) and core THD solution (~1 mPas) and the chemical reaction. To raise jet stability and possibly eliminate or at least reduce the amount of beads in the final membranes, the viscosity of the core solution was raised by mixing poly(ethylene oxide) (PEO) into it. 2 wt% PEO (M_n 900 kDa) raised the viscosity of the core solution to 60 mPas and enabled smooth fiber preparation without beads in the resulting membranes. Additionally, it made the spinning process easier to control with less occasions of blockage of the nozzle due to gelation. The fibers (PSI-THD-PEO) had an average diameter of 320 ± 42 nm.

PSI-THD-PEO could be hydrolyzed into PASP-THD-PEO and could still maintain its integrity. Macroscopic pictures taken of PSI-THD-PEO before and after hydrolysis can be seen in Fig. 6.12a, b. The sample turned into a water-clear membrane with a slight opacity and also grew from 3.03 cm^2 area to 7.37 cm^2 similarly to bulk PSI hydrogels during hydrolysis [18]. SEM analysis on a washed and

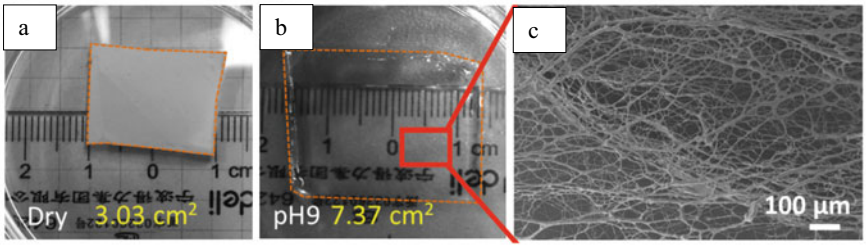


Fig. 6.12 Dry PSI-THD-PEO membrane (**a**), PASP-THD-PEO membrane in pH 9 buffer (**b**) and SEM micrograph of the PASP-THD-PEO membrane after washing and freeze-drying (**c**)

freeze-dried PASP-THD-PEO revealed that the fibrous structure was not completely maintained. Fibers fused together creating an interconnected membrane with pore sizes ranging from 5 to 20 µm (Fig. 6.12c).

In summary, coaxial electrospinning setup where a PSI in DMF solution was fed in the shell and the crosslinker THD solution was fed as the core of the needle enabled the synthesis of crosslinked fibers. Even after the optimization of the feeding rate of the crosslinker solution, beads and defects were found in the fibrous membranes, possibly due to the large difference in the viscosities of the two components. By adding PEO to the crosslinker solution and thus by raising its viscosity, better control of electrospinning and smooth fibers without particles were synthesized. If the appropriate chemistry enables it, the coaxial electrospinning setup can be used for the synthesis of crosslinked fibers of other polymers as well.

6.5 Synthesis of Redox-Sensitive PSI and PASP Gel Fibers by Reactive Electrospinning

The general idea was to add reactive thiol sidechains to PSI that can crosslink by forming disulfide bonds during electrospinning [5]. Disulfide bonds are well-known redox sensitive bonds that can be easily formed in mild oxidative conditions from thiols and vice versa, they can be cleaved in mild reductive conditions to form thiols again. For oxidation, hydrogen peroxide or even air and for cleavage D,L-dithiotreithol (DTT) or glutathione (GSH) can be used [24, 46, 47].

First, PSI was modified with cysteamine (CYSE) to have one thiol side group on every 10th succinimide repeating unit. For the modification of PSI with cysteamine, first 0.04 g of CYSE was dissolved in a mixture of 0.7 g DMF and 0.4 g DMSO in a glass reactor, then 2 g of PSI dissolved in DMF (25 w/w%) was added and mixed vigorously under Argon atmosphere at room temperature for 45 min [5]. The inert atmosphere ensured that the thiol groups did not form disulfide bonds before electrospinning. The reaction can be seen on Fig. 6.13. The resulting polymer solution was poured into a syringe and 1 ml of it was used for electrospinning. Electrospinning

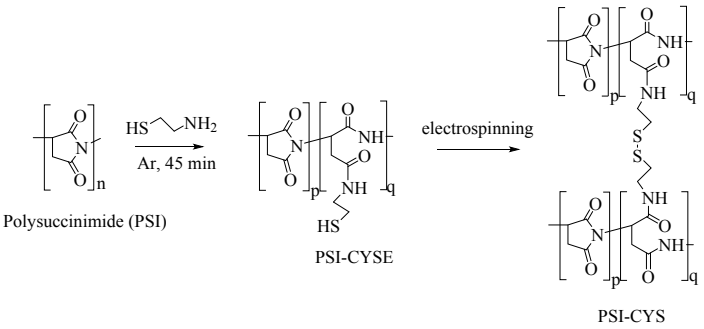


Fig. 6.13 Reaction of PSI and CYSE and the formation of PSICYS

parameters were 0.8 ml/h flow rate, 15 cm target distance (distance between the tip of the needle and collector) and 12 kV potential [26]. During the spinning process, thiol to disulfide oxidation could occur due to the presence of oxygen in the air.

The synthesized fibrous mat, as opposed to purely PSI fibers, did not dissolve after dipping it in DMF, but only swelled, hence proving the presence of crosslinked network inside the fibers. The crosslinked mat is denoted as PSICYS. Fiber diameter of PSICYS was 900 ± 70 nm (n = 50, p = 0.05) according to the SEM analysis (Fig. 6.14a).

PSICYS samples could be hydrolyzed in pH 8 imidazole buffer to form PASP based network fibers denoted as PASPCYS. During the hydrolysis the membrane took up the buffer and swelled to form a semi-transparent, soft hydrogel fibrous membrane (Fig. 6.14b). After thoroughly washing the gel membrane with distilled water and freeze-drying, SEM showed that the fibers in the PASPCYS are deformed and fused, thus they did not maintain their complete fibrous structure after hydrolysis (Fig. 6.14c). Therefore, fiber diameter analysis could not be carried out. However, the sample still had a porous structure with pore sizes in the several microns range that would enable movement of small organisms through the membrane.

As it was shown by Juriga et al. bulk PASPCYS hydrogels dissolve in the most commonly used MEM cell culturing medium, therefore in vitro studies on PASPCYS fibrous membranes were not carried out [10]. An in vivo study was carried out to see if hydrolysis of PSICYS occurs and to investigate the implantability and short-term



Fig. 6.14 SEM PSICYS fibers (**a**) macroscopic picture (**b**) and SEM micrograph (**c**) of PASPCYS fibers. Reprinted with permission from [5, 26]

biological response to PSICYS fibers. Full description of the methodology of the study can be found in the paper of Molnar et al. and summarized briefly in Sect. 7.2. [26].

During the 3-day and 7-day observation no visible irritations, animal misbehavior or other macroscopically observable complications were detected. The animals behaved just as they did before surgery: normal food intake and bowel movement, mobility, and behavior with the caretakers were observed. After 3 days, samples turned into soft, gel like membranes that were easily truncated with tweezers (Fig. 6.15a). Similarly to PSIDAB membranes PSICYS membranes also grew by approximately 40% in diameter. All this suggested that hydrolysis of PSICYS into PASPCYS occurs in vivo as well. There were no macroscopically visible complications in the implantation areas such as swollen or irritated tissue. Histopathology showed mild acute inflammation that is an acceptable and standard response of the body to implanted foreign objects. PASPCYS (PSICYS after hydrolysis) samples were easily found on the slides surrounded by a rim of inflammatory cells predominantly comprising neutrophil granulocytes yet cells did not enter the membranes (Fig. 6.15b). After 7 days a soft granulation tissue grew around the samples. Even after cutting the resected area in half, the PASPCYS samples were not distinguishable from the new tissue by the naked eye (Fig. 6.15c). However, the microscopic slides showed the fibrous PASPCYS membranes surrounded by a moderate band of granulation tissue (Fig. 6.15d). The previously moderate inflammation declined to mild inflammation whereas vascularization started in the granulation tissue, both indicating the progressive proliferative phase of physiological wound healing.

To conclude, PSICYS was easily synthesized by grafting cysteamine onto PSI. The thiol sidechains crosslinked PSI during electrospinning (reactive electrospinning), thus creating PSICYS network inside the fibers. 3 days after implantation under the skin of rats, PSICYS disks hydrolyzed into PASPCYS without causing

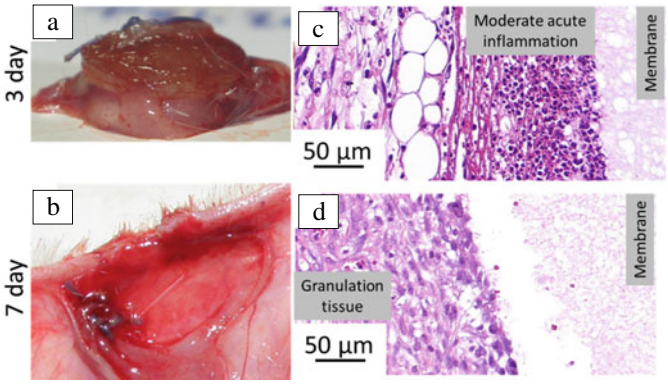


Fig. 6.15 PASPCYS sample resected 3 days after implantation (**a**) and a representative image from histopathology (**c**); implantation area without sample after 7 days after implantation (**b**), a representative image from histopathology (**d**). Reprinted with permission from [26]

severe complications and 7 days after, were completely covered with healthy granulation tissue. Hystopathology showed a moderate acute inflammation after 3 days that reduced to mild inflammation for the 7th day. This indicates the short-term biocompatibility and biodegradability of PSICYS fibrous membranes.

6.6 Summary

This Chapter has discussed different electrospinning methods for the preparation of crosslinked polysuccinimide (PSI) and poly(aspartic acid) (PASP) nanofibers. PSI and PASP are promising candidates for biomedical applications, such as tissue engineering, as they are biodegradable, biocompatible and easy to synthesize under mild conditions. PSI can react with primary amines, and thus its derivatives or crosslinked PSI can be prepared. With the hydrolysis of PSI or its derivatives, water-soluble PASP can be synthesized. However, water-solubility of PASP can set a barrier to its use in certain applications, such as implants or tissue engineering. A possible solution is crosslinking of the polymer that would prevent its dissolution in aqueous medium.

Crosslinking of the polymer fibers can be achieved either by post-spinning methods, or by reactive electrospinning. This Chapter discussed two post-spinning and two reactive electrospinning methods. In the first post-spinning method described in Sect. 7.2, PSI fibers were synthesized by electrospinning, and then immersed in the solution of the crosslinker to induce crosslinking. Crosslinked PSI fibers were hydrolyzed to PASP fibers, however, the fibers fused, and the mat has partly lost its fibrous structure. In the other method in Sect. 7.3, allylamine-modified PSI was electrospun, and then crosslinking was induced by plasma treatment. After optimization of the parameters of the electrospinning and the plasma treatment, PASP fiber mats without significant fusing of the fibers could be synthesized. Then in Sects. 7.4 and 7.5 reactive electrospinning methods were shown. In the first case coaxial needle was used for the electrospinning, where the solution of the crosslinker was in the core of the needle, while the PSI was in the shell. They got in contact at the top of the needle, and crosslinking reaction happened during the flying time, resulting in crosslinked PSI fibers on the collector. In the other case cysteamine-modified PSI was electrospun and the crosslinking occurred via air oxidation of the thiol groups to disulfide bonds during the flying time, which, again, resulted in crosslinked PSI fibers.

References

1. Yang, Z., Zhang, Y., Markland, P., & Yang, V. C. (2002). *Poly(glutamic acid) poly(ethylene glycol) hydrogels prepared by photoinduced polymerization: Synthesis, characterization, and preliminary release studies of protein drugs.*
2. Lin, W. C., Yu, D. G., & Yang, M. C. (2006). Blood compatibility of novel poly(γ-glutamic

acid)/polyvinyl alcohol hydrogels. *Colloids Surfaces B Biointerfaces, 47*, 43–49. https://doi.org/10.1016/j.colsurfb.2005.11.013
3. Tomida, M., Nakato, T., Matsunami, S., & Kakuchi, T. (1997). Convenient synthesis of high molecular weight poly(succinimide) by acid-catalysed polycondensation of l-aspartic acid. *Polymer (Guildf), 38*, 4733–4736. https://doi.org/10.1016/S0032-3861(96)01079-8
4. Nakato, T., Yoshitake, M., Matsubara, K., et al. (1998). Relationships between structure and properties of poly(aspartic acid)s. *Macromolecules, 31*, 2107–2113. https://doi.org/10.1021/ma971629y
5. Molnár, K., Juriga, D., Nagy, P. M. M., et al. (2014). Electrospun poly(aspartic acid) gel scaffolds for artificial extracellular matrix. *Polymer International, 63*, 1608–1615. https://doi.org/10.1002/pi.4720
6. Horvat, G., Gyarmati, B., Berko, S., et al. (2015). Thiolated poly(aspartic acid) as potential in situ gelling, ocular mucoadhesive drug delivery system. *European Journal of Pharmaceutical Sciences, 67*, 1–11. https://doi.org/10.1016/j.ejps.2014.10.013
7. Sikes, C. S. (2006). *Preparation of high molecular weight polysuccinimides*.
8. Roweton, S., Huang, S. J., & Swift, G. (1997). Poly(aspartic acid): Synthesis, biodegradation, and current applications. *Journal of Environmental Polymer Degradation, 5*, 175–181. https://doi.org/10.1007/BF02763661
9. Jalalvandi, E., & Shavandi, A. (2018). Polysuccinimide and its derivatives: Degradable and water soluble polymers (review). *European Polymer Journal, 109*, 43–54. https://doi.org/10.1016/j.eurpolymj.2018.08.056
10. Juriga, D., Nagy, K., Jedlovszky-Hajdú, A., et al. (2016). Biodegradation and osteosarcoma cell cultivation on poly(aspartic acid) based hydrogels. *ACS Applied Materials & Interfaces, 8*, 23463–23476. https://doi.org/10.1021/acsami.6b06489
11. Gyenes, T., Torma, V., Gyarmati, B., & Zrínyi, M. (2008). Synthesis and swelling properties of novel pH-sensitive poly(aspartic acid) gels. *Acta Biomaterialia, 4*, 733–744. https://doi.org/10.1016/j.actbio.2007.12.004
12. Némethy, Á., Solti, K., Kiss, L., et al. (2013). pH- and temperature-responsive poly(aspartic acid)-l-poly(N-isopropylacrylamide) conetwork hydrogel. *European Polymer Journal, 49*, 2392–2403. https://doi.org/10.1016/j.eurpolymj.2013.02.015
13. Gyarmati, B., Némethy, Á., & Szilágyi, A. (2014). Reversible response of poly(aspartic acid) hydrogels to external redox and pH stimuli. *RSC Advances, 4*, 8764. https://doi.org/10.1039/c3ra47530a
14. Zrinyi, M., Gyenes, T., Juriga, D., & Kim, J.-H. (2013). Volume change of double cross-linked poly(aspartic acid) hydrogels induced by cleavage of one of the crosslinks. *Acta Biomaterialia, 9*, 5122–5131. https://doi.org/10.1016/j.actbio.2012.08.046
15. Gyarmati, B., Meszar, E. Z., Kiss, L., et al. (2015). Supermacroporous chemically cross-linked poly(aspartic acid) hydrogels. *Acta Biomaterialia, 22*, 32–38. https://doi.org/10.1016/j.actbio.2015.04.033
16. Gyarmati, B., Krisch, E., & Szilágyi, A. (2014). In situ oxidation-induced gelation of poly(aspartic acid) thiomers. *Reactive & Functional Polymers, 84*, 29–36. https://doi.org/10.1016/j.reactfunctpolym.2014.08.007
17. Németh, C., Gyarmati, B., Abdullin, T., et al. (2017). Poly(aspartic acid) with adjustable pH-dependent solubility. *Acta Biomaterialia, 49*, 486–494. https://doi.org/10.1016/j.actbio.2016.11.065
18. Varga, Z., Molnár, K., Torma, V., & Zrínyi, M. (2010). Kinetics of volume change of poly(succinimide) gels during hydrolysis and swelling. *Physical Chemistry Chemical Physics: PCCP, 12*, 12670–12675. https://doi.org/10.1039/c0cp00527d
19. Brannon-Peppas, L., & Peppas, N. A. (1991). Equilibrium swelling behavior of dilute ionic hydrogels in electrolytic solutions. *Journal of Controlled Release, 16*, 319–329. https://doi.org/10.1016/0168-3659(91)90009-3
20. Juriga, D., Laszlo, I., Ludanyi, K., et al. (2018). Kinetics of dopamine release from poly(aspartamide)-based prodrugs. *Acta Biomaterialia, 76*, 225–238. https://doi.org/10.1016/j.actbio.2018.06.030

21. Juriga, D., Sipos, E., Hegedűs, O., et al. (2019). Fully amino acid-based hydrogel as potential scaffold for cell culturing and drug delivery. *Beilstein Journal of Nanotechnology, 10*, 2579–2593. https://doi.org/10.3762/bjnano.10.249
22. Hegedűs, O., Juriga, D., Sipos, E., et al. (2019). Free thiol groups on poly(aspartamide) based hydrogels facilitate tooth-derived progenitor cell proliferation and differentiation. *PLoS ONE, 14*, e0226363. https://doi.org/10.1371/journal.pone.0226363
23. Krisch, E., Messager, L., Gyarmati, B., et al. (2016). Redox- and pH-responsive nanogels based on thiolated poly(aspartic acid). *Macromolecular Materials and Engineering, 301*, 260–266. https://doi.org/10.1002/mame.201500119
24. Krisch, E., Gyarmati, B., & Szilágyi, A. (2016). Preparation of pH-responsive poly(aspartic acid) nanogels in inverse emulsion. *Periodica Polytechnica Chemical Engineering, 61*, 19. https://doi.org/10.3311/PPch.9788
25. Liu, L., Xu, W., Ding, Y., et al. (2020). A review of smart electrospun fibers toward textiles. *Composites Communications, 22*, 100506. https://doi.org/10.1016/j.coco.2020.100506
26. Molnar, K., Voniatis, C., Feher, D., et al. (2021). Poly(amino acid) based fibrous membranes with tuneable in vivo biodegradation. *PLoS ONE, 16*, e0254843. https://doi.org/10.1371/journal.pone.0254843
27. Molnar, K., Jozsa, B., Barczikai, D., et al. (2020). Plasma treatment as an effective tool for crosslinking of electrospun fibers. *Journal of Molecular Liquids, 303*, 112628. https://doi.org/10.1016/j.molliq.2020.112628
28. Zeng, J., Hou, H., Wendorff, J. H., & Greiner, A. (2005). Photo-induced solid-state crosslinking of electrospun poly(vinyl alcohol) fibers. *Macromolecular Rapid Communications, 26*, 1557–1562. https://doi.org/10.1002/marc.200500545
29. Dargaville, B. L., Vaquette, C., Rasoul, F., et al. (2013). Electrospinning and crosslinking of low-molecular-weight poly(trimethylene carbonate-co-l-lactide) as an elastomeric scaffold for vascular engineering. *Acta Biomaterialia, 9*, 6885–6897. https://doi.org/10.1016/j.actbio.2013.02.009
30. Molnar, K., Jedlovszky-Hajdu, A., Zrinyi, M., et al. (2017). Poly(amino acid)-based gel fibers with pH responsivity by coaxial reactive electrospinning. *Macromolecular Rapid Communications, 201700147*, 1700147–1700151. https://doi.org/10.1002/marc.201700147
31. Ghosh, T., Das, T., & Purwar, R. (2021). Review of electrospun hydrogel nanofiber system: Synthesis, properties and applications. *Polymer Engineering & Science, 61*, 1887–1911. https://doi.org/10.1002/pen.25709
32. Zhang, C., Wu, S., & Qin, X. (2014). Facile fabrication of novel pH-sensitive poly(aspartic acid) hydrogel by crosslinking nanofibers. *Materials Letters, 132*, 393–396. https://doi.org/10.1016/j.matlet.2014.06.031
33. Noszticzius, Z., Wittmann, M., Kály-Kullai, K., et al. (2013). Chlorine dioxide is a size-selective antimicrobial agent. *PLoS ONE, 8*, 1–10. https://doi.org/10.1371/journal.pone.0079157
34. Chu, P. K., Chen, J. Y., Wang, L. P., & Huang, N. (2002). Plasma-surface modification of biomaterials. *Materials Science and Engineering: R: Reports, 36*, 143–206.
35. Grace, J. M., & Gerenser, L. J. (2003). Plasma treatment of polymers. *Journal of Dispersion Science and Technology, 24*, 305–341. https://doi.org/10.1081/DIS-120021793
36. Campiglio, C. E., Contessi Negrini, N., Farè, S., & Draghi, L. (2019). Cross-linking strategies for electrospun gelatin scaffolds. *Materials (Basel), 12*, 2476. https://doi.org/10.3390/ma12152476
37. Liguori, A., Bigi, A., Colombo, V., et al. (2016). Atmospheric pressure non-equilibrium plasma as a green tool to crosslink gelatin nanofibers. *Science and Reports, 6*, 38542. https://doi.org/10.1038/srep38542
38. Sisson, K., Zhang, C., Farach-Carson, M. C., et al. (2009). Evaluation of cross-linking methods for electrospun gelatin on cell growth and viability. *Biomacromolecules, 10*, 1675–1680. https://doi.org/10.1021/bm900036s
39. Dolci, L. S., Liguori, A., Panzavolta, S., et al. (2018). Non-equilibrium atmospheric pressure plasma as innovative method to crosslink and enhance mucoadhesion of econazole-loaded gelatin films for buccal drug delivery. *Colloids Surfaces B Biointerfaces, 163*, 73–82. https://doi.org/10.1016/j.colsurfb.2017.12.030

40. Fong, H., Chun, I., & Reneker, D. (1999). Beaded nanofibers formed during electrospinning. *Polymer (Guildf), 40*, 4585–4592. https://doi.org/10.1016/S0032-3861(99)00068-3
41. Jeffries, E. M., Allen, R. A., Gao, J., et al. (2015). Highly elastic and suturable electrospun poly(glycerol sebacate) fibrous scaffolds. *Acta Biomaterialia, 18*, 30–39. https://doi.org/10.1016/j.actbio.2015.02.005
42. Tang, C., Saquing, C. D., Harding, J. R., & Khan, S. A. (2010). In situ cross-linking of electrospun poly(vinyl alcohol) nanofibers. *Macromolecules, 43*, 630–637. https://doi.org/10.1021/ma902269p
43. Xu, F., Sheardown, H., & Hoare, T. (2015). Reactive electrospinning of degradable poly(oligoethylene glycol methacrylate)-based nanofibrous hydrogel networks. *Chemical Communications, 52*, 1451–1454. https://doi.org/10.1039/C5CC08053C
44. Yalcinkaya, F. (2018). Effect of argon plasma treatment on hydrophilic stability of nanofiber webs. *Journal of Applied Polymer Science, 135*, 46751. https://doi.org/10.1002/app.46751
45. Jedlovszky-Hajdu, A., Molnar, K., Nagy, P. M., et al. (2016). Preparation and properties of a magnetic field responsive three-dimensional electrospun polymer scaffold. *Colloids and Surfaces A: Physicochemical and Engineering Aspects, 503*, 79–87. https://doi.org/10.1016/j.colsurfa.2016.05.036
46. Li, H., Gao, J., Shang, Y., et al. (2018). Folic acid derived hydrogel enhances the survival and promotes therapeutic efficacy of iPS cells for acute myocardial infarction. *ACS Applied Materials & Interfaces, 10*, 24459–24468. https://doi.org/10.1021/acsami.8b08659
47. Alcock, L. J., Perkins, M. V., & Chalker, J. M. (2018). Chemical methods for mapping cysteine oxidation. *Chemical Society Reviews, 47*, 231–268. https://doi.org/10.1039/c7cs00607a



Kristof Molnar was born in Budapest Hungary in 1987. He received B.Sc. (2011) and M.Sc. (2013) degrees in Chemical Engineering, Specialized in the Pharmaceutical Industry, from the Budapest University of Technology and Economics, Budapest, Hungary, followed by a Ph.D. degree in Theoretical Medicine from Semmelweis University, Budapest, Hungary in 2018.

Since 2019 he has been working as a research associate in the Department of Food, Agricultural and Biological Engineering of The Ohio State University, USA. He has authored and co-authored 2 book chapters and 13 journal articles. His research interests include nanofibers, hydrogels, polymer synthesis, polymer-based drug delivery systems, and soft medical implants. Dr. Molnar is a member of the ACS and the ACS Rubber Division, the Hungarian Colloidics Workgroup of the Hungarian Academy of Sciences and the Hungarian Chemical Society.



Eniko Krisch was born in Sopron, Hungary in 1988. She received B.Sc. (2010) and M.Sc. (2012) degrees in Chemical Engineering, Specialized in the Pharmaceutical Industry, followed by a Ph.D. degree in Chemistry from the Budapest University of Technology and Economics, Budapest, Hungary in 2019. Since 2019 she has been working as a volunteer researcher in the Department of Food, Agricultural and Biological Engineering of the Ohio State University, USA. Her interests are nanotechnology, intelligent hydrogels, nano-hydrogels, hydrogel and polymer-based drug delivery systems. She has authored and co-authored 1 book chapter and 12 journal articles.



Judit E. Puskas Ph. D., P. Eng, Distinguished Professor, AIMBE, IUPAC and NAI Fellow, External member, Hungarian Academy of Sciences, and co-inventor of the polymer coating on the Taxus drug-eluting coronary stent, implanted in over 10 million people. Her research is focusing on the integration of breast cancer diagnosis and treatment with breast reconstruction, in collaboration with the Cleveland Clinic and Semmelweis Medical University of Hungary. In 2012 was one of the five winners of the GE Healthymagination Breast Cancer Challenge Award, selected from 400 international applications. She is the winner of the 2017 Charles Goodyear Medal, the most prestigious award given by the Rubber Division of the American Chemical Society. She has over 400 publications and 33 US patents.

Part II
Applications of Electrospun Nanofibers

Chapter 7
Electrospun Fibers in Drug Delivery



V. Umayangana Godakanda, Karolina Dziemidowicz, Rohini M. de Silva, K. M. Nalin de Silva, and Gareth R. Williams

Abstract Electrospun fibers have been very widely explored in the context of drug delivery. The rapid drying nature of the electrospinning process tends to result in amorphous solid dispersions, and hence the use of a hydrophilic filament-forming polymer can give significant increases in dissolution rate, apparent solubility, and bioavailability. Electrospun formulations thus have great potential to overcome the solubility challenges faced by > 70% of emerging drug candidates. Beyond this, by careful choice of the polymer carrier and the nanoscale architecture of the fibers (monolithic, core/shell, Janus, etc.) it is possible to precisely control both the drug release rate and location, and in a number of cases much sought after zero-order (constant rate) release has been obtained with electrospun systems. Fibers from electrospinning have thus been widely explored for drug delivery via a range of routes, including oral, transdermal, ocular, and implantation. In this chapter, we will review the body of literature in the area, focusing on the various types of release modality that can be obtained and the most exciting recent findings in the field. We will further consider issues of translation from bench to bedside, covering the great progress made in the scale-up of the electrospinning process in recent years, the need for production under Good Manufacturing Practice conditions, and evaluating how close electrospun formulations are to becoming marketed products.

Keywords Drug delivery · Polymer carrier · Electrospun systems · Drug release modality

V. U. Godakanda · R. M. de Silva · K. M. N. de Silva (✉)
Centre for Advanced Materials and Devices, Department of Chemistry, University of Colombo, Colombo 03, Sri Lanka
e-mail: kmnd@chem.cmb.ac.lk

K. Dziemidowicz · G. R. Williams (✉)
UCL School of Pharmacy, University College London, 29—39 Brunswick Square, London WC1N 1AX, UK
e-mail: g.williams@ucl.ac.uk

K. Dziemidowicz
e-mail: k.dziemidowicz@ucl.ac.uk

© The Author(s), under exclusive license to Springer Nature Switzerland AG 2022

A. Vaseashta and N. Bölgen (eds.), *Electrospun Nanofibers*,
https://doi.org/10.1007/978-3-030-99958-2_7

7.1 Introduction

The ultimate goal of drug delivery systems is to deliver the drug locally, safely and in a controlled fashion in order to minimize side effects often associated with systemic administration of active pharmaceutical agents (APIs). To achieve the desired therapeutic effect, the correct API must be delivered to the required site of action, at the correct time, and in an appropriate amount. Inability to meet these criteria will render the medicine either ineffective or toxic to the patient. Although medicines can take a wide range of forms and be administered via numerous routes, for reasons of patient compliance and convenience the majority of APIs are given orally as solid dosage forms. This has a number of benefits: for instance, it is simple for a patient to take two tablets three times a day, and oral solid dosage forms can be administered by the patient themselves rather than requiring a healthcare professional (as is usually the case for injections).

There are also drawbacks to the use of oral solid dosage forms, however. In order to be active in the body, the API needs to be in solution. This requires a solid dosage form to *dissolve* into the fluids present in the gastrointestinal tract. In the process of dissolution, the large aggregates of molecules that make up a solid material are separated out, resulting in a solution in which each API molecule is surrounded by water molecules. Thus, API-API intermolecular interactions in the solid-state are replaced by API-water interactions. The dissolution rate and maximum concentration of the drug in solution (the *solubility*) are determined by the balance of these energies. Further, the majority of medicines given orally are intended to act systemically (throughout the body) rather than locally in the gastrointestinal tract. Thus, after it dissolves, the molecules from a solid dosage form need to pass through the lipid biomembranes which line the intestinal tract, so that they can reach the bloodstream. This process is termed *permeation.*

Some APIs have both high dissolution rates and solubilities and high permeability, but in most cases, there is a formulation challenge that needs to be overcome to improve at least one of these properties. The Biopharmaceutical Classification System (BCS) helps pharmaceutical scientists to classify APIs in terms of their properties: BCS class I drugs have high solubility and permeability; class II are poorly soluble but freely permeable; class III APIs are highly soluble but poorly permeable, and class IV materials are both poorly soluble and poorly permeable.

Beyond BCS considerations, pharmaceutical scientists need to consider carefully where in the body the drug will be released. For instance, many APIs cause irritation to the stomach lining, and thus it is desirable to avoid release there and instead target delivery to the latter stages of the gastrointestinal tract. The rate of release of a drug from a medicine also needs to be established, since this impacts both the therapeutic efficacy and the dosage frequency required. The stability of the API must additionally be established and understood. While small-molecule APIs such as paracetamol or ibuprofen are held together by covalent bonds and thus are generally stable in vivo, more complex biomolecules such as proteins rely heavily on weaker hydrogen and van der Waals interactions to sustain their 3D structure. A loss of 3D structure will

result in a loss of activity, and since the interactions holding the structure together are weak proteins degrade easily. Great care must thus be taken in formulating, to ensure that the API delivered is therapeutically active.

Electrospinning offers routes to improve solubility and dissolution rate by processing the API into an amorphous solid dispersion (ASD), where there is a molecular dispersion of drug in polymer and thus no API-API interactions to overcome during the process of dissolution. The addition of a permeation enhancer into the formulation can improve permeability. Further, the choice of the polymer used as the filament-forming carrier can allow the drug release location and rate to be tuned. The fact that electrospinning does not require heat to evaporate the solvent can aid in maintaining the stability of protein APIs, but the use of organic solvents can be problematic in this regard. These topics will be discussed in more detail below, with illustrative examples presented. We will first consider small molecule APIs and the types of release profiles that can be attained. Later in the chapter, we will also consider the use of electrospinning to process more complex biologic-based therapeutics and consider the next steps in moving electrospun medicines towards the market.

7.2 Fiber Architecture

A range of fiber architectures can be achieved by using spinnerets with different needle arrangements, as shown in Fig. 7.1. The simplest experiment is mono-axial

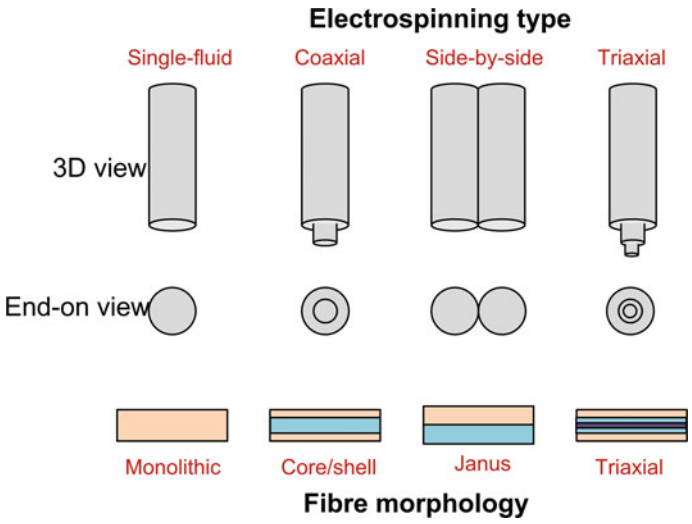


Fig. 7.1 Spinneret designs for different types of electrospinning, and the structures of the fibers produced. Reproduced from Williams G. R. et al. 2018. *Nanofibres* in Drug Delivery. London: UCL Press (https://doi.org/10.14324/111.9781787350182), under the terms of a CC BY 4.0 license

electrospinning, where a blunt-ended spinneret is used to generate monolithic fibers. These have a number of benefits, but their large surface area and the presence of drug at the fiber surface often results in an undesirable initial "burst" of release. To overcome this, co-axial spinning can be used to produce core/shell fiber architectures; if the drug is confined to the core then burst release can be reduced and/or release targeted to a particular part of the body. Tri-axial spinning allows the possibility of creating 3–layer fibers to provide further control over the drug release profile. Two-faced Janus fiber architectures can also be created using a side-by-side spinneret, resulting in two-compartment fibers where both sides can interact with their external environment.

7.3 Pharmaceutical Polymers

Several aspects need to be considered when choosing the polymer for the electrospinning solution. Probably the most important consideration is the intended application of the product. The polymer degradation half-life and by-products, biocompatibility, and solubility will heavily influence the potential applications of the product. For example, for fast-release applications, a polymer with a relatively rapid dissolution/degradation rate and high solubility in aqueous solvents (such as polyvinylpyrrolidone (PVP)) would be preferred [1]. In contrast, when designing a long-term surgical implant, a hydrophobic polymer with slow degradation rates would be more suitable. In some cases, polymers with special characteristics such as thermo- or pH-sensitivity are of interest, aiding targeted delivery to the action site [2].

One of the most commonly used pharmaceutical polymers in electrospinning is poly(lactic-co-glycolic) acid (PLGA) (Fig. 7.2a). PLGA is a synthetic copolymer formed of polylactic (PLA) and polyglycolic (PGA) acids. PLGA degrades by hydrolysis of its ester linkages via bulk erosion in aqueous environments. The rate of degradation can be controlled, for example by adjusting the molecular weight of the polymer or the molar ratio of the monomer components. As an example, PLGA copolymers with a higher content of lactic acid will degrade more slowly due to the presence of hydrophobic methyl groups [3].

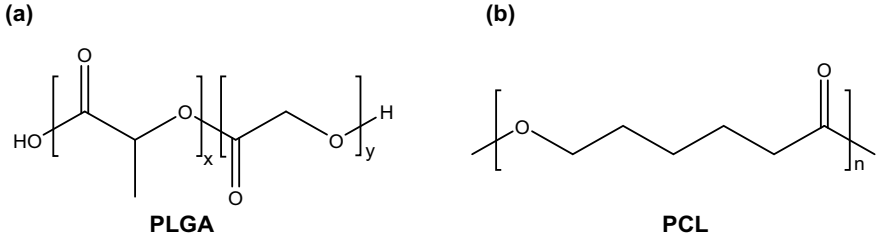


Fig. 7.2 Chemical structures of **a** PLGA and **b** PCL

Another medically important polymer is poly(ε-caprolactone) (PCL; Fig. 7.2b), which is an aliphatic polyester composed of hexanoate repeat units. It is a semi-crystalline polymer widely used in the manufacturing of surgical sutures, drug delivery systems and tissue engineering scaffolds, and biodegrades through hydrolysis over a time period ranging from several months to years, depending on the molecular weight [4, 5].

Biomaterials manufactured from PLGA and PCL follow a similar triphasic breakdown profile. In the hydration step, water penetrates into the amorphous region of the material, thus disrupting the van der Waals forces. Subsequently, the polymer chain starts to degrade either by end-chain or random-chain scission and the cleavage of covalent bonds. This leads to a decrease in the molecular weight [6]. The degradation process is then autocatalysed by carboxylic end groups and the particle structure is severely disrupted by the breakdown of backbone covalent bonds. The resulting metabolite monomers incorporate into the Krebs cycle and can be safely eliminated from the body [7, 8].

7.4 Small Molecule Drugs

There exist a range of drug release profiles which find utility in medicines development (Fig. 7.3). These range from very rapid release, aiming to deliver a drug cargo within a few minutes of administration, to formulations seeking to prolong release over days or weeks. Complex multi-stage profiles can also be desirable, for instance to provide an initial "loading" dose for rapid relief of pain followed by a maintenance dose to keep the concentration in the patient's bloodstream at a therapeutic level. Electrospun formulations have been explored for many of these modalities of small molecule API delivery, and we will discuss a series of examples below.

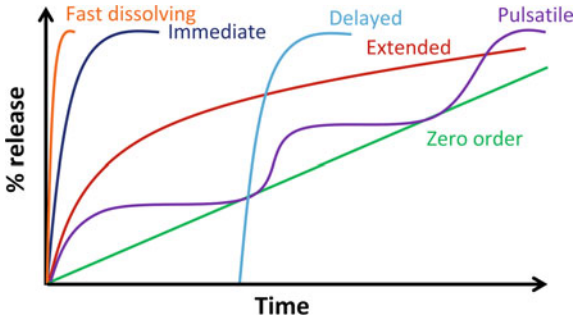


Fig. 7.3 Some common types of drug release profile. The plot depicts the percentage of drug loading freed from a formulation as a function of time

7.4.1 Fast Dissolving Drug Delivery Systems

Fast-dissolving drug delivery systems (FD-DDSs) offer a variety of advantages such as very rapid onset of action and enhanced bioavailability. This type of release is ideal for situations where instant drug dissolution is required to achieve rapid therapeutic effects. Electrospinning can be used to generate ASDs with very high surface area to volume ratios, and thus is ideal to achieve fast dissolution of otherwise poorly water-soluble drugs. Such electrospun FD-DDSs are commonly designed as solid films that undergo instant wetting by saliva to dissolve/disintegrate in the patient's mouth. These formulations are beneficial to administer drugs to children and patients with swallowing difficulties, as they can be used without consuming liquid or chewing [9].

Numerous electrospun FD-DDSs have been reported in the literature, often based on the hydrophilic and fast-dissolving PVP. For instance, fibers containing paracetamol and caffeine were generated by Illangakoon et al. The fiber mats disintegrated completely within a very short time (< 0.5 s) when added to simulated saliva solution and released the drug cargo within around 150 s in a dissolution test, giving notably faster dissolution compared to the pure drugs [10]. PVP fibers have also been used to enhance the dissolution rate of mebeverine hydrochloride [11], ketoprofen (KET) [12], indomethacin [13], ornidazole [14], borneol [15], emodin [16], sildenafil citrate [17], and loratadine [18]. Caution must be taken in designing the formulations, however: the drug loading in the system has been shown to be crucial in determining the release properties. In a very recent report, PVP was employed for the preparation of KET loaded fibers. ASDs were obtained, but while fibers with low KET loading (9% w/w) disintegrated quickly and hastened KET dissolution, fibers with 23% w/w drug did now show these benefits (Fig. 7.4) [12].

While PVP has attracted the most attention, other hydrophilic polymers can also be used to generate electrospun FD-DDSs. For instance, polyvinyl alcohol (PVA) fibers have been prepared loaded with caffeine and riboflavin [19]. Electrospun blends of polyethylene oxide are also reported to provide fast release of drugs such as lidocaine and diclofenac [20]. More recently, the natural polymers jelly fig polysaccharide and pullulan have been investigated for fast delivery of hydrophobic drugs such as ampicillin and dexamethasone [21].

7.4.2 Extended Release

Extended release systems (also termed sustained, controlled, prolonged, or slow-release) are designed to release their drug cargo over a prolonged period of time in the body, with the goal of maintaining a therapeutically potent dose over this period of time and reducing the required dosing frequency. For instance, electrospun (ES) mats capable of delivering analgesics or anti-inflammatory medications in a sustained manner could be very beneficial for patients suffering from long term

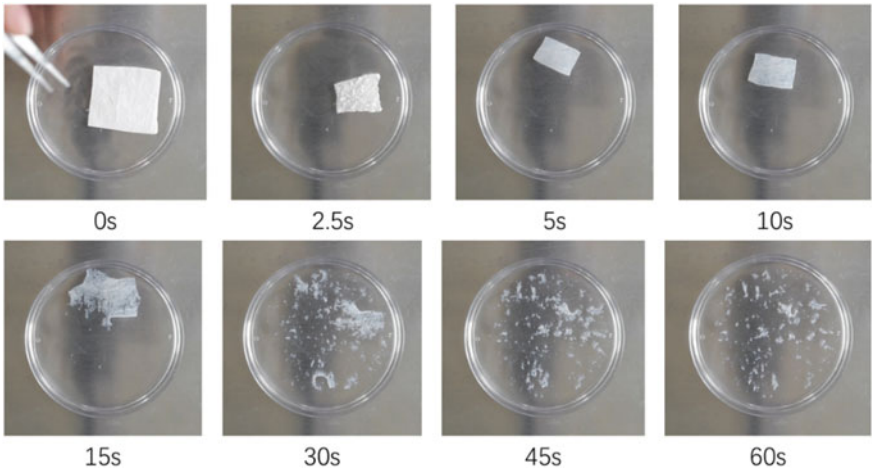


Fig. 7.4 Digital camera images of the disintegration of PVP fibers containing 9% w/w KET. Reprinted with permission from *Geng* et al. [12] Copyright 2020 Elsevier Ltd

diseases such as rheumatic arthritis. Thus, many publications report ES matrices for sustained release of analgesics over periods of hours (for oral delivery) or days (for wound care or cancer therapy), containing APIs such as diclofenac [22], naproxen [23], tramadol [24], ketoprofen [25], lidocaine [26], and steroidal drugs [27]. In addition to pain relief, ES fiber systems have been generated for sustained release of antibacterial agents (e.g. tetracyclines [28], gentamicin [29]), anti-viral drugs (e.g. acyclovir [30]), and anti-cancer APIs (e.g. niclosamide [31], hydroxycamptothecin [32], CPT-11 and SN-38 [33], oxaliplatin [34], 5-fluorouracil [35], paclitaxel [36], and doxorubicin [37, 38]). In the latter case, the formulations are often designed as implants to be placed for instance in a tumor resection site.

Suitable choice of polymer is key to develop an effective sustained-release ES formulation. Appropriate polymers are hydrophobic; they can be stable (in which case drug release occurs by diffusion out of the matrix) or degrade slowly into soluble monomers. Commonly explored biodegradable polymers include PLA [27], PGA, PLGA, and PCL [39, 40] while the non-degradable polyurethane [32], polycarbonate [32], and nylon-6 [41, 42] have also been investigated. Sustained release can additionally be achieved by using natural polymers like silk [43, 44], collagen [45, 46], gelatin [47, 48], alginate [49, 50], cellulose derivatives [23, 51], and chitosan [52, 53], either spinning them alone, or by blending with other components [54–59].

A widely observed phenomenon in fibers from mono-axial ES is an initial burst of API release due to the high surface area-to-volume ratio of the fibers and the presence of drug at or near the fiber surface. While this is not an issue with FD-DDSs (where release is intended to be rapid), it can be problematic when seeking to develop sustained release systems. Researchers worldwide have thus probed various strategies to overcome this effect. One strategy is to generate core/shell fibers, where drug loaded within the core has to diffuse through a drug-free polymer shell before

reaching the release media [60–63]. Designing composite ES fibers with drug-loaded nanoparticles can also be used to reduce the initial burst release. Silica nanoparticle (NP)-loaded PLGA fibers [64] and chitosan NPs in PCL fibers have both been explored to this end [65].

Core/shell systems can also be applied to deliver multiple APIs at different rates. Heydari et al. developed core/shell fibers composed of polyglycerol-sebacate as the shell and poly (hydroxybutyrate) elastomer as the core. Simvastatin, a drug known for accelerating diabetic wound healing by enhancing angiogenesis and lymphangiogenesis, was loaded into the fiber core, and the antibacterial drug ciprofloxacin included in the shell [66]. This resulted in a smart wound-healing system, since the fibers gave 60% ciprofloxacin release in 24 h, but simvastatin was released much more slowly [66].

7.4.3 Zero-Order Release

Therapeutic systems that can release an API at a constant rate are much sought after in order to minimize variations in plasma drug concentrations and help maintain the drug concentration within the therapeutic range [67]. Various strategies have been applied to achieve zero-order release using electrospun formulations. One of the earliest reports of this developed drug-loaded cellulose acetate (CA) nanofibers using a modified coaxial electrospinning process [61]. Core/shell fibers were produced with both compartments made of CA and the model drug KET confined to the core, and were able to provide zero-order release over 96 h [61]. Subsequent approaches using alternative core/shell fiber formulations have also been shown to yield zero-order release profiles [60, 61]. Three-layer fibers from triaxial spinning have additionally been investigated. By preparing a triaxial system with all three compartments made of ethyl cellulose (EC) and with an increasing w/w drug loading moving from the exterior to the core compartment, it was possible to achieve zero-order release of KET over 20 h (Fig. 7.5) [63].

7.4.4 Targeted Release

There exist a variety of different pH environments in the body, which can be used to target drug release. For instance, the stomach is acidic (*ca.* pH 1–2) whereas the small intestine is much closer to neutral. pH-responsive polymers can thus be used to target API release to the small intestine. Polymers such as Eudragit L-100 (EL100) or Eudragit L100-55 (EL100-55) have been exploited for such delayed-release delivery of many drugs. The Eudragits are methacrylate based copolymers; they contain myriad COOH groups which are unionized at low pH, rendering the polymer insoluble. As the pH increases the carboxylate groups ionize to COO^-, and the solubility of the polymer increases. Through careful control of the polymer

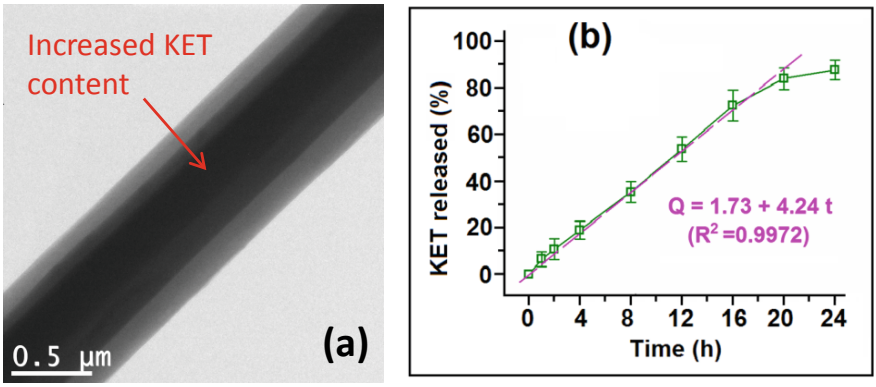


Fig. 7.5 Data on trilayer EC/KET fibers prepared by Yu et al. **a** Transmission electron micrograph showing the three-layer architecture of the fibers. **b** The KET release profile. Reprinted with permission from Yu et al. [63] Copyright 2015 American Chemical Society

chemical structure, systems can be developed with dissolve at certain distinct pHs: thus, EL100-55 is soluble at pH 5.5 or greater, while EL100 becomes soluble at pH 6.0. DDSs composed of Eudragit are insoluble in the stomach and release the drug only when it reaches the small intestine. Sustained release DDSs targeting delivery of mebeverine hydrochloride (MB-HCl) to the colon have been prepared by electrospinning EL100-55 [11]. Diclofenac sodium-loaded EL100 fibers have also been reported [68].

Beyond the Eudragit materials, a range of other polymers such as hydroxypropyl methyl cellulose phthalate and hydroxypropyl methylcellulose acetate succinate have been explored for targeted release, for instance of erythromycin [69] and theophylline [70]. Natural macromolecules can also be applied to give targeted release. Zein and shellac are both naturally occurring polymers with environment-responsive solubility. Shellac is insoluble under acid conditions but soluble in a neutral environment. Yang et al. observed that electrospun fibers with a shellac shell and diclofenac sodium/PVP core could resist acid erosion and thereby potentially deliver the API specifically to the colon [71].

Electrospun fibers have been extensively explored for applications in cancer therapy [72, 73]. Typically, the tumor microenvironment is at a slightly lower pH than the general physiological pH, and this difference can be used to target drug delivery. Electrospun fibers composed of PVA/PCL [74], and poly (N-isopropylacrylamide-co-methacrylic acid-co-vinylpyrrolidone) [P(NIPAAm-MAA-VP) [75] have been studied for delivery of doxorubicin (DOX) and keratin/PLA fibers for 5-fluorouracil [76]. Cellulose nanocrystal-poly[2-(dimethylamino)ethyl methacrylate] reinforced poly(3-hydroxybutyrate-co-3-hydroxy valerate) systems facilitating both pH and temperature sensitive drug release are additionally reported to have potential for cancer treatment [77, 78]. pH-sensitivity can also be imparted to fibers by the inclusion of additional components with polymers which are not themselves stimuli-responsive. For instance, incorporation of sodium bicarbonate has been employed

to generate electrospun systems giving accelerated release under acidic conditions, using polymers such as gelatin/PCL [79] and PLA [80].

7.4.5 Multi-stage Release

Multi-stage drug release can also be of great benefit, and there are a range of examples of ES formulations which have been developed to provide this. The core–shell nanofiber design can be used to obtain biphasic drug release, using a hydrophilic polymer shell to give an initial burst release of the drug and a hydrophobic core to give a sustained maintenance dose. Using this strategy, Qian et al. were able to develop core/shell EC/PVP fibers with biphasic drug release [81]. In other work, pulsatile release (with bursts of "on" and "off" release) has been reported using blend fibers composed of poly(ethylene oxide), sodium alginate and sodium ibuprofen [82]. These fibers give two stage pulsatile release at pH 3, with the extent of release in the "on" phases and the lag time between them tunable by dint of varying the w/w ratio of the ingredients in the formulation.

7.5 Electrospinning of Biologicals

Biological products, or 'biologics' are a potent group of APIs that include vaccines, cell and gene therapy, and recombinant therapeutic proteins [83]. With recent advancements in biotechnology, biological treatments are becoming key in therapeutic protocols for multiple conditions – most notably perhaps in cancer immunotherapy and tissue engineering. In tandem, interest in electrospun biologic formulations has accelerated in the past few years.

7.5.1 Proteins

The complex and fragile structures of many therapeutic proteins require advanced delivery methods and careful optimization of formulation and manufacturing conditions. Quite often the protein integrity is compromised by the route of administration, leading to denaturation, aggregation or misfolding. For example, the loss of fragile tertiary structures of proteins, defined by non-covalent interactions, may result in reduced biological activity. Currently, parenteral administration of proteins remains the gold standard as other delivery routes are limited or not yet clinically feasible [9, 84, 85].

The field of pharmaceutical technology has long sought possible solutions to protein formulation challenges, leading to the development of multiple inorganic, lipid or polymer-based formulations. Many biomaterial fabrication processes may

negatively impact the stability of the protein being formulated. Typical conventional encapsulation methods, such as spray-drying or hot melt extrusion, require harsh conditions (e.g. application of heat or prolonged contact with solvents) that can potentially cause protein misfolding or aggregation, and consequent loss of activity [9]. Electrospinning could offer a simple route to the fabrication of biocompatible protein-loaded scaffolds that can be easily implanted at the desired site of action. Multiple approaches have been proposed for the incorporation of therapeutic proteins within electrospun materials, including monoaxial and co-axial electrospinning [9]. While monoaxial spinning is attractive in its simplicity, and has been used to develop a number of protein-loaded formulations [86], prolonged exposure to the organic solvent typically required for electrospinning may cause misfolding or aggregation of labile biomolecules like proteins, leading to loss of activity. For this reason, the encapsulation of therapeutic proteins using blend electrospinning is used with caution.

Controlled and sustained protein delivery can be achieved using emulsion electrospinning, where a core–shell structure is formed by electrospinning of a water-in-oil emulsion formed from an aqueous phase (protein) and an organic phase (polymer). When subjected to electric charge, the organic phase (typically containing a volatile solvent) rapidly evaporates. This causes the migration of the aqueous phase (with protein) to the center of the jet, forming core–shell structures with favorable localization of proteins within the center of the fibers/particles, minimizing the risk of the initial burst release of therapeutic cargo. Although the relative simplicity of emulsion electrospinning is attractive from the manufacturability point of view, the protein-polymer blend composition must be carefully optimized to ensure there is no loss of bioactivity resulting from accidental exposure of the biomolecule to the organic solvent. A non-ionic surfactant is often incorporated in the formulation to decrease the contact between protein and organic solvents by forming reverse micelles (emulsions), therefore avoiding denaturation or aggregation [9]. In 2017, Frizzell et al. [2] developed enzyme-loaded electrospun fibers for peroral delivery using surfactant-assisted emulsion electrospinning. Horseradish peroxidase and alkaline phosphatase were blended with EL100 in the presence of the surfactant Tween 20. The nanofibers showed pH-dependent enzyme release patterns, with ~ 5% release at pH 2 and almost 100% at pH 7. Use of EL100 ensured dissolution of the fibers only occurred in neutral and basic pH conditions, leading to protected transit through the stomach and preventing acid- medicated protein degradation.

An alternative to emulsion electrospinning is the co-axial approach. As both solutions are physically separated until the formation of the fiber, protein exposure to organic solvents is limited and therefore accidental degradation can be minimized. The resulting fiber usually holds the protein in the core with a hydrophobic polymeric shell allowing for the gradual release of the cargo at the site of action. A notable example of protein encapsulation within electrospun fibers using this approach has been recently published by Angkawinitwong et al. [87], who explored coaxial electrospinning in the fabrication of bevacizumab-loaded PCL nanofibers for the treatment of age-related macular degeneration in the eye (Fig. 7.6). The study highlighted the importance of the pH of the protein solution. It was found that electrospinning protein

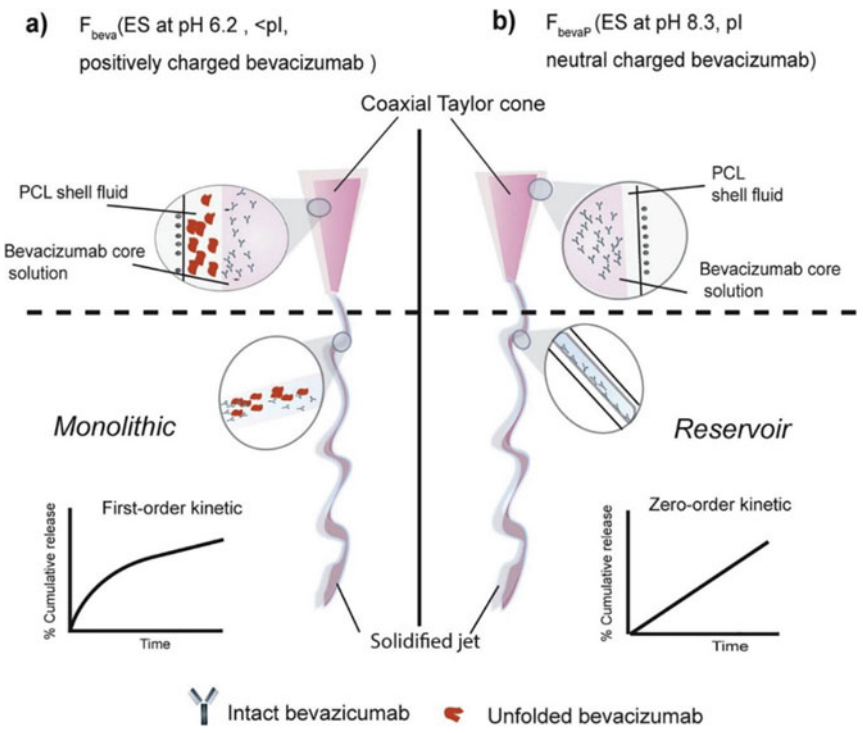


Fig. 7.6 A schematic diagram showing the effect of bevacizumab migration during electrospinning on the fiber properties. **a** When the protein solution is at pH 6.2, the protein carries a net positive charge; this causes it to migrate uncontrollably from the aqueous core to the polymer shell and become unfolded upon exposure to the shell solvent. The resultant distribution of both intact bevacizumab and unfolded bevacizumab within the core and shell leads to first-order release behavior. **b** In contrast, when working at pH 8.3, the pI of bevacizumab, the protein is neutral and does not interact with the electric field. This results in zero-order release of intact bevacizumab. Reprinted with permission from Angkawinitwong et al. [87] Copyright Elsevier 2017 Ltd

solutions at the isoelectric point (pI) of the antibody (where it is uncharged) significantly enhances its in-process stability. Bevacizumab released from the optimal core–shell fibers remained intact and biologically active, confirming the appropriateness of the approach for sustained and localized delivery of antibodies. However, the encapsulation efficiency was negatively affected by electrospinning at the pI of bevacizumab, which was attributed to the lack of electrostatic interactions driving the migration of protein towards the grounded electrode when the antibody is in its uncharged state.

7.5.2 Cells and Extracellular Vesicles

Cell therapies are gaining real momentum in the current landscape of medical innovations, but their clinical translation is often impeded by manufacturing constraints or poor cell survival post-transplantation. Biomaterials are often explored for example to aid stem cell differentiation or trafficking into the desired therapeutic location [88]. Delivering cells directly to the site of action within implantable and biocompatible scaffolds could be an attractive approach for a variety of conditions, such as cardiac repair [89]. Electrospinning has been shown to have significant potential in the generation of such scaffolds.

Cell electrospinning, first introduced by Jayasinghe in 2006 [90], refers to the incorporation of cell suspensions directly into electrospun fibers using a modified co-axial electrospinning apparatus. To ensure sterility, the experiments are often conducted in laminar flow hoods. Probably the most important modification in the setup arises from the fact that cell-containing fiber product cannot be allowed to dehydrate, as this would negatively influence cell viability. For this reason, traditional metal collecting substrates are unsuitable and instead fibers are collected directly into a dish containing cell culture media maintained at 37 °C. Cell electrospinning has now been tested on a variety of cell lines, and in all cases if the operating parameters are optimized it is possible to maintain cell integrity after fiber generation. It seems that exposure to a high voltage at low current (nanoamperes) during electrospinning does not affect the viability [90, 91] and functionality [89] of processed cells.

It is also important to note that the polymers traditionally used for standard electrospinning often require processing in solvents such as tetrahydrofuran, chloroform or acetone. Such solvents, however, are toxic to living organisms and therefore unsuitable for cell electrospinning. Natural polymers such as alginates, collagens and cellulose may appear more appropriate, but are rarely used due to their poor mechanical properties. Instead, water-soluble synthetic polymers such as PVA or poly(dimethylsiloxane) appear to be more effective for the development of cell-loaded mats [92].

Recently, Trindade et al. [93] tackled the unexplored concept of incorporating extracellular vesicles (EVs) into electrospun patches. EVs are cell-derived nanosized vesicles enclosed within a lipid bilayer [94, 95]. They are less immunogenic and easier to produce and process than stem cells and therefore hold great potential in tissue engineering applications [93]. High encapsulation efficiencies (> 70%) were obtained, and the EVs observed to retain their therapeutic potency after processing. This suggests that electrospinning could be an effective way of preserving EVs for long-term release formulations.

7.6 Translation

This chapter has presented a wide range of electrospun drug delivery systems and sought to highlight some of the key benefits of the approach. However, the vast majority of the work performed to date has been undertaken on the lab scale, and the throughput of such experiments is low: typical yields might be 100 mg per hour [96, 97]. This is clearly insufficient for industrial applications, and for electrospun formulations to make it to the market production on the ton scale is required. Recent years have seen rapid development of large-scale electrospinning, and are discussed elsewhere in this volume. Researchers in the pharmaceutical technology field have been quick to explore such high-throughput systems, and it is encouraging to see that, although increasing the production rate tends to result in more irregular fiber morphologies, the functional performance is unaffected [97, 98].

Most electrospun drug delivery systems have been developed using solution spinning. For translation, great attention must be paid to choosing the solvent system. First, there could be health and safety issues pertaining to the use of volatile solvents in large scale production [99]. Second, it is important to ensure that the final product is solvent free, as certain organic solvents (e.g. dimethylformamide or tetrahydrofuran) may result in harmful toxic effects if any residual solvent remains in the fibers [100–102]. Batch-to-batch consistency must additionally be assured, to ensure therapy is safe and effective.

Work has begun to implement the quality control procedures required for pharmaceutical applications (so called Good Manufacturing Practice, GMP), and industrial facilities now exist where it is possible to prepare large (ton) amounts of materials under GMP conditions. These recent developments auger well for the future translation of electrospun systems from the lab bench to the clinic [97, 103]. It should be noted however that while high-throughput monoaxial electrospinning is now possible, the scale-up of co-axial and other multi-fluid processes lags significantly behind. Thus, the first electrospun formulations to make it to market are likely to be those which exploit the ASD nature of the fibers to accelerate dissolution rates.

7.7 Conclusions

This chapter presents a brief overview of the applications of electrospun fibers in drug delivery. We have shown that it is possible to process both small molecule and biological active ingredients without any loss of functionality. A wide range of release profiles can be obtained. Many reports in the literature explore formulations designed to offer very rapid release of a drug cargo, using a hydrophilic and water soluble polymer to overcome problems of low API solubility and provide rapid relief of symptoms. Others use insoluble or slow-dissolving or degrading polymers to give extended release of an API, meaning there is the potential to reduce dosing frequency and improve patient compliance. Zero-order, targeted, and pulsatile release

can also be achieved through judicious choice of the polymer carrier. The high stability of small molecule drugs makes them relatively straightforward to incorporate into fibers, while there is significantly more challenge with biologics owing to their instability, particularly upon exposure to organic solvents. Nevertheless, a range of potent electrospun formulations containing proteins and even cells have been developed over recent years.

Elecrospinning thus has versatile applications in drug delivery. However, there are a number of challenges still to be addressed. More work is required to develop methods and provide quality control for high-throughput fiber production, particularly when it comes to multi-fluid processing. Maintaining batch-to-batch consistency and putting in place the quality control guidelines needed to comply with regulatory frameworks will be key for clinical applications. There are a number of researchers, both in academia and industry, who are working on these challenges, and at the time of writing several electrospun products have reached clinical trials (e.g. NCT02409628 or NCT03686800). In the authors' view therefore, the future for electrospun formulations is bright, and we confidently expect electrospun medicines to emerge in the market in the next few years.

References

1. Williams, G. R., Raimi-Abraham, B. T., & Luo, C. J. (2018). *Nanofibres in drug delivery*. UCL Press
2. Frizzell, H., Ohlsen, T. J., & Woodrow, K. A. (2017). Protein-loaded emulsion electrospun fibers optimized for bioactivity retention and PH-controlled release for peroral delivery of biologic therapeutics. *International Journal of Pharmaceutics, 533*(1), 99–110. https://doi.org/10.1016/j.ijpharm.2017.09.043
3. Anderson, J. M., & Shive, M. S. (2012). Biodegradation and biocompatibility of PLA and PLGA microspheres. *Advanced Drug Delivery Reviews, 64*, 72–82. https://doi.org/10.1016/j.addr.2012.09.004
4. Chiu, Y.-J., Zhang, Z., Dziemidowicz, K., Nikoletopoulos, C.-G., Angkawinitwong, U., Chen, J.-T., & Williams, R. G. (2020). The effect of solvent vapor annealing on drug-loaded electrospun polymer fibers. *Pharmaceutics*. https://doi.org/10.3390/pharmaceutics12020139
5. Labet, M., & Thielemans, W. (2009). Synthesis of polycaprolactone: A review. *Chemical Society Reviews, 38*(12), 3484–3504. https://doi.org/10.1039/B820162P
6. Fu, K., Pack, D. W., Klibanov, A. M., & Langer, R. (2000). Visual evidence of acidic environment within degrading poly(lactic-co-glycolic acid) (PLGA) microspheres. *Pharmaceutical Research, 17*(1), 100–106. https://doi.org/10.1023/A:1007582911958
7. Houchin, M. L., & Topp, E. M. (2008). Chemical degradation of peptides and proteins in PLGA: A review of reactions and mechanisms. *Journal of Pharmaceutical Science, 97* (7), 2395–2404. https://doi.org/10.1002/jps.21176
8. Castilla-Cortázar, I., Más-Estellés, J., Meseguer-Dueñas, J. M., Escobar Ivirico, J. L., Marí, B., & Vidaurre, A. (2012). Hydrolytic and enzymatic degradation of a poly(ε-caprolactone) network. *Polymer Degradation Stability, 97* (8), 1241–1248. https://doi.org/10.1016/j.polymdegradstab.2012.05.038
9. Dziemidowicz, K., Sang, Q., Wu, J., Zhang, Z., Zhou, F., Lagaron, J. M., Mo, X., Parker, G. J. M., Yu, D.-G., Zhu, L.-M., & Williams, G. R. (2021). Electrospinning for healthcare: Recent advancements. *Journal of Materials Chemistry B, 9*, 939–951. https://doi.org/10.1039/D0TB02124E

10. Illangakoon, U. E., Gill, H., Shearman, G. C., Parhizkar, M., Mahalingam, S., Chatterton, N. P., & Williams, G. R. (2014). Fast dissolving paracetamol/caffeine nanofibers prepared by electrospinning. *International Journal of Pharmaceutics, 477*(1–2), 369–379. https://doi.org/10.1016/j.ijpharm.2014.10.036
11. Illangakoon, U. E., Nazir, T., Williams, G. R., & Chatterton, N. P. (2014). Mebeverine-loaded electrospun nanofibers: Physicochemical characterization and dissolution studies. *Journal of Pharmaceutical Sciences, 103*, 283–292. https://doi.org/10.1002/jps.23759
12. Geng, Y., Zhou, F., Williams, G. R. (2021). Developing and Scaling up fast-dissolving electrospun formulations based on poly(Vinylpyrrolidone) and Ketoprofen. *Journal of Drug Delivery Science and Technology, 61,* 102138. https://doi.org/10.1016/j.jddst.2020.102138
13. Rasekh, M., Karavasili, C., Soong, Y. L., Bouropoulos, N., Morris, M., Armitage, D., Li, X., Fatouros, D. G., & Ahmad, Z. (2014). Electrospun PVP-indomethacin constituents for transdermal dressings and drug delivery devices. *International Journal of Pharmaceutics, 473*(1–2), 95–104. https://doi.org/10.1016/j.ijpharm.2014.06.059
14. Tort, S., Yıldız, A., Tuğcu-Demiröz, F., Akca, G., Kuzukıran, Ö., & Acartürk, F. (2019). Development and characterization of rapid dissolving ornidazole loaded PVP electrospun fibers. *Pharmaceutical Development and Technology, 24*(7), 864–873. https://doi.org/10.1080/10837450.2019.1615088
15. Li, X. Y., Wang, X., Yu, D. G., Ye, S., Kuang, Q. K., Yi, Q. W., & Yao, X. Z. (2012). Electrospun borneol-PVP nanocomposites. *Journal of Nanomaterials, 2012,* 731382. https://doi.org/10.1155/2012/731382
16. Dai, X. Y., Nie, W., Wang, Y. C., Shen, Y., Li, Y., & Gan, S. J. (2012). Electrospun emodin polyvinylpyrrolidone blended nanofibrous membrane: A novel medicated biomaterial for drug delivery and accelerated wound healing. *Journal of Materials Science. Materials in Medicine, 23*(11), 2709–2716. https://doi.org/10.1007/s10856-012-4728-x
17. Torres-Martínez, E. J., Vera-Graziano, R., Cervantes-Uc, J. M., Bogdanchikova, N., Olivas-Sarabia, A., Valdez-Castro, R., Serrano-Medina, A., Iglesias, A. L., Pérez-González, G. L., Cornejo-Bravo, J. M., & Villarreal-Gómez, L. J. (2020). Preparation and characterization of electrospun fibrous scaffolds of either PVA or PVP for fast release of sildenafil citrate. *E-Polymers, 20*(1), 746–758. https://doi.org/10.1515/epoly-2020-0070
18. Akhgari, A., Dezfuli, A. G., Rezaei, M., Kiarsi, M., & Abbaspour, M. (2016). The design and evaluation of a fast-dissolving drug delivery system for Loratadine using the electrospinning method. *Jundishapur Journal of Natural Pharmaceutical Products, 11*(2), e33613. https://doi.org/10.17795/jjnpp-33613
19. Li, X., Kanjwal, M. A., Lin, L., & Chronakis, I. S. (2013). Electrospun polyvinyl-alcohol nanofibers as oral fast-dissolving delivery system of caffeine and riboflavin. *Colloids Surfaces B Biointerfaces, 103*, 182–188. https://doi.org/10.1016/j.colsurfb.2012.10.016
20. Maver, T., Kurečič, M., Smrke, D. M., Kleinschek, K. S., & Maver, U. (2016). Electrospun nanofibrous CMC/PEO as a part of an effective pain-relieving wound dressing. *Journal of Sol-Gel Science and Technology, 79*(3), 475–486. https://doi.org/10.1007/s10971-015-3888-9
21. Ponrasu, T., Chen, B. H., Chou, T. H., Wu, J. J., & Cheng, Y. S. (2021). Fast dissolving electrospun nanofibers fabricated from jelly fig polysaccharide/pullulan for drug delivery applications. *Polymers (Basel), 13*(2), 1–17. https://doi.org/10.3390/polym13020241
22. El-newehy, M. H., El-naggar, M. E., Alotaiby, S., El-hamshary, H., Moydeen, M., & Al-deyab, S. (2016). Preparation of biocompatible system based on electrospun CMC/PVA nanofibers as controlled release carrier of diclofenac sodium. *Pure and Applied Chemistry, 53*(9), 566–573. https://doi.org/10.1080/10601325.2016.1201752
23. Godakanda, V. U., Li, H., Alquezar, L., Zhao, L., Zhu, L., De Silva, R., Nalin De Silva, K. M., & Williams, G. R. (2019). Tunable drug release from blend poly(vinyl pyrrolidone)—ethyl cellulose nanofibers. *International Journal of Pharmaceutics, 562*, 172–179. https://doi.org/10.1016/j.ijpharm.2019.03.035
24. Giannetti, R., Abraham, G. A., & Rivero, G. (2019). The role of emulsion parameters in tramadol sustained-release from electrospun mats. *Materials Science & Engineering C, 99*, 1493–1501. https://doi.org/10.1016/j.msec.2019.02.085

25. Hu, J., Li, H. Y., Williams, G. R., Yang, H. H., Tao, L., & Zhu, L. M. (2016). Electrospun poly(n-isopropylacrylamide)/ethyl cellulose nanofibers as thermoresponsive drug delivery systems. *Journal of Pharmaceutical Sciences, 105*(3), 1104–1112. https://doi.org/10.1016/S0022-3549(15)00191-4
26. Tseng, Y. Y., Liao, J. Y., Chen, W. A., Kao, Y. C., & Liu, S. J. (2014). Biodegradable poly([D, L]-lactide-co-glycolide) nanofibers for the sustainable delivery of lidocaine into the epidural space after laminectomy. *Nanomedicine, 9*(1), 77–87. https://doi.org/10.2217/nnm.13.42
27. Alves, P. E., Soares, B. G., Lins, L. C., Livi, S., & Santos, E. P. (2019). Controlled delivery of dexamethasone and betamethasone from PLA electrospun fibers: A comparative study. *European Polymer Journal, 117*, 1–9. https://doi.org/10.1016/j.eurpolymj.2019.05.001
28. Cheng, M., Qin, Z., Hu, S., Dong, S., Ren, Z., & Yu, H. (2017). Achieving long-term sustained drug delivery for electrospun biopolyester nanofibrous membranes by introducing cellulose nanocrystals. *ACS Biomaterials Science & Engineering*, *3*(8), 1666–1676. https://doi.org/10.1021/acsbiomaterials.7b00169
29. Pisani, S., Dorati, R., Chiesa, E., Genta, I., Modena, T., Bruni, G., Grisoli, P., & Conti, B. (2019). Release profile of gentamicin sulfate from polylactide-co-polycaprolactone electrospun nanofiber matrices. *Pharmaceutics*, *11*(4), 161. https://doi.org/10.3390/pharmaceutics11040161
30. Wang, M., Hou, J., Yu, D. G., Li, S., Zhu, J., & Chen, Z. (2020). Electrospun tri-layer nanodepots for sustained release of acyclovir. *Journal of Alloys and Compounds*, *846*, 156471. https://doi.org/10.1016/j.jallcom.2020.156471
31. Dubey, P., & Gopinath, P. (2016). Fabrication of electrospun poly(ethylene oxide)-poly(capro lactone) composite nanofibers for co-delivery of niclosamide and silver nanoparticles exhibits enhanced anti-cancer effects in vitro. *Journal of Materials Chemistry B, 4*(4), 726–742. https://doi.org/10.1039/c5tb02351c
32. Luo, X., Xie, C., Wang, H., Liu, C., Yan, S., & Li, X. (2012). Antitumor activities of emulsion electrospun fibers with core loading of hydroxycamptothecin via intratumoral implantation. *International Journal of Pharmaceutics, 425*(1–2), 19–28. https://doi.org/10.1016/j.ijpharm.2012.01.012
33. Yohe, S. T., Herrera, V. L. M., Colson, Y. L., & Grinstaff, M. W. (2012). 3D superhydrophobic electrospun meshes as reinforcement materials for sustained local drug delivery against colorectal cancer cells. *Journal of Controlled Release, 162*(1), 92–101. https://doi.org/10.1016/j.jconrel.2012.05.047
34. Zhang, J., Wang, X., Liu, T., Liu, S., & Jing, X. (2016). Antitumor activity of electrospun polylactide nanofibers loaded with 5-fluorouracil and oxaliplatin against colorectal cancer. *Drug Delivery, 23*(3), 794–800. https://doi.org/10.3109/10717544.2014.916768
35. Hadjianfar, M., Semnani, D., & Varshosaz, J. (2018). Polycaprolactone/chitosan blend nanofibers loaded by 5-fluorouracil: An approach to anticancer drug delivery system. *Polymers for Advanced Technologies, 29*(12), 2972–2981. https://doi.org/10.1002/pat.4417
36. Xie, J., & Wang, C. H. (2006). Electrospun micro- and nanofibers for sustained delivery of paclitaxel to treat c6 glioma in vitro. *Pharmaceutical Research, 23*(8), 1817–1826. https://doi.org/10.1007/s11095-006-9036-z
37. Habibi, M., Hosseini, S., & Mahboobnia, K. (2019). Simultaneous controlled release of 5-FU, DOX and PTX from chitosan/PLA/5-FU/g-C3N4-DOX/g-C3N4-PTX triaxial nano fibers for breast cancer treatment in vitro. *Colloids and surfaces B: Biointerfaces, 179* (November 2018), 495–504.
38. Anaraki, N. A., Rad, L. R., Irani, M., & Haririan, I. (2015). Fabrication of PLA/PEG/MWCNT electrospun nanofibrous scaffolds for anticancer drug delivery. *Journal of Applied Polymer Science, 132*(3), 1–9. https://doi.org/10.1002/app.41286
39. Zhang, A. Q., Li, Y., Yuan, Z., Lin, W., Wong, K. K. Y., Lin, M., Yildirimer, L., Zhao, X., & William, Z. Y. (2017). Electrospun polymeric micro/nanofibrous scaffolds for long-term drug release and their biomedical applications. *Drug Discovery Today, 22* (9), 1351–1366. https://doi.org/10.1016/j.drudis.2017.05.007

40. Budak, K., Sogut, O., & Sezer, U. A. (2020). A review on synthesis and biomedical applications of polyglycolic acid. *Journal of Polymer Research*, *27*, 208. https://link.springer.com/article/10.1007/s10965-020-02187-1
41. Sohrabi, A., Shaibani, P. M., Etayash, H., Kaur, K., & Thundat, T. (2013). Sustained drug release and antibacterial activity of ampicillin incorporated poly(methyl methacrylate)-nylon6 core/shell nanofibers. *Polymer, 54*(11), 2699–2705. https://doi.org/10.1016/j.polymer.2013.03.046
42. El-Newehy, M. H., Al-Deyab, S. S., Kenawy, E. R., & Abdel-Megeed, A. (2011). Nanospider technology for the production of nylon-6 nanofibers for biomedical applications. *Journal of Nanomaterials, 2011*, 626589. https://doi.org/10.1155/2011/626589
43. Farokhi, M., Mottaghitalab, F., Reis, R. L., Ramakrishna, S., & Kundu, S. C. (2020). Functionalized silk fibroin nanofibers as drug carriers: Advantages and challenges. *Journal of Controlled Release, 321*, 324–347. https://doi.org/10.1016/j.jconrel.2020.02.022
44. Dadras Chomachayi, M., Solouk, A., Akbari, S., Sadeghi, D., Mirahmadi, F., & Mirzadeh, H. (2018). Electrospun nanofibers comprising of silk fibroin/gelatin for drug delivery applications: Thyme essential oil and doxycycline monohydrate release study. *Journal of Biomedical Materials Research—Part A, 106* (4), 1092–1103. https://doi.org/10.1002/jbm.a.36303
45. Zhang, M., Li, Z., Liu, L., Sun, Z., Ma, W., Zhang, Z., Zhang, R., Sun, D. (2016). Preparation and characterization of vancomycin-loaded electrospun Rana Chensinensis skin collagen/poly(L-lactide) nanofibers for drug delivery. *Journal of Nanomaterials*, *2016,* 9159364. https://doi.org/10.1155/2016/9159364
46. Huo, P., Han, X., Zhang, W., Zhang, J., Kumar, P., Liu, B. (2021). Electrospun nanofibers of polycaprolactone/collagen as a sustained-release drug delivery system for artemisinin. *Pharmaceutics*, *13*(8), 1228. https://doi.org/10.3390/pharmaceutics13081228
47. Meng, Z. X., Xu, X. X., Zheng, W., Zhou, H. M., Li, L., Zheng, Y. F., & Lou, X. (2011). Preparation and characterization of electrospun PLGA/gelatin nanofibers as a potential drug delivery system. *Colloids Surfaces B Biointerfaces, 84*(1), 97–102. https://doi.org/10.1016/j.colsurfb.2010.12.022
48. Dongargaonkar, A. A., Bowlin, G. L., & Yang, H. (2013). Electrospun blends of gelatin and gelatin-dendrimer conjugates as a wound-dressing and drug-delivery platform. *Biomacromolecules, 14*(11), 4038–4045. https://doi.org/10.1021/bm401143p
49. De Silva, R. T., Dissanayake, R. K., Mantilaka, M. M. M. G. P. G., Wijesinghe, W. P. S. L., Kaleel, S. S., Premachandra, T. N., Weerasinghe, L., Amaratunga, G. A. J., & De Silva, K. M. N. (2018). Drug-loaded halloysite nanotube-reinforced electrospun alginate-based nanofibrous scaffolds with sustained antimicrobial protection. *ACS Applied Materials & Interfaces, 10*(40), 33913–33922. https://doi.org/10.1021/acsami.8b11013
50. Wongkanya, R., Chuysinuan, P., Pengsuk, C., Techasakul, S., Lirdprapamongkol, K., Svasti, J., & Nooeaid, P. (2017). Electrospinning of alginate/soy protein isolated nanofibers and their release characteristics for biomedical applications. *Journal of Science: Advanced Materials and Devices, 2*(3), 309–316. https://doi.org/10.1016/j.jsamd.2017.05.010
51. Khoshnevisan, K., Maleki, H., Samadian, H., Shahsavari, S., Sarrafzadeh, M. H., Larijani, B., Dorkoosh, F. A., Haghpanah, V., Khorramizadeh, M. R. (2018). Cellulose acetate electrospun nanofibers for drug delivery systems: Applications and recent advances. *Carbohydrate Polymers, 198,* 131–141. https://doi.org/10.1016/j.carbpol.2018.06.072
52. Jain, R., Shetty, S., Yadav, K. S. (2020). Unfolding the electrospinning potential of biopolymers for preparation of nanofibers. *Journal of Drug Delivery Science and Technology, 57,* 101604. https://doi.org/10.1016/j.jddst.2020.101604
53. Farshi Azhar, F., & Olad, A. (2014). A study on sustained release formulations for oral delivery of 5-fluorouracil based on alginate-chitosan/montmorillonite nanocomposite systems. *Applied Clay Science, 101*, 288–296. https://doi.org/10.1016/j.clay.2014.09.004
54. Reshmi C. R, Menon, T., Binoy, A., Mishra, N., Elyas K. K., & Sujith, A. (2017). Poly (L-lactide-co-caprolactone)/collagen electrospun mat: potential for wound dressing and controlled drug delivery. *International Journal of Polymeric Materials and Polymeric Biomaterials, 148* (13), 148–162. https://doi.org/10.1080/00914037.2016.1252357

55. López-Calderón, H. D., Avilés-Arnaut, H., Galán Wong, L. J., Almaguer-Cantú, V., Laguna-Camacho, J. R., Calderón-Ramón, C., Escalante-Martínez, J. E., & Arévalo-Niño, K. (2020). Cellulose acetate bi-layer scaffold loaded with gentamicin as possible wound dressing. *Polymers, 12*(2311), 1–12.
56. Tsekova, P. B., Spasova, M. G., Manolova, N. E., Markova, N. D., & Rashkov, I. B. (2017). Electrospun curcumin-loaded cellulose acetate/polyvinylpyrrolidone fibrous materials with complex architecture and antibacterial activity. *Materials Science and Engineering C, 73*, 206–214. https://doi.org/10.1016/j.msec.2016.12.086
57. Zandi, N., Lotfi, R., Tamjid, E., Shokrgozar, M. A., & Simchi, A. (2020). Core-sheath gelatin based electrospun nanofibers for dual delivery release of biomolecules and therapeutics. *Materials Science and Engineering C, 108*, 110432. https://doi.org/10.1016/j.msec.2019.110432
58. Bazhban, M., Nouri, M., Mokhtari, J. (2013). Electrospinning of cyclodextrin functionalized chitosan/PVA nanofibers as a drug delivery system. *Chinese Journal of Polymer Science* (*English Ed.*) *31* (10), 1343–1351. https://doi.org/10.1007/s10118-013-1309-5
59. Cui, Z., Zheng, Z., Lin, L., Si, J., Wang, Q., Peng, X., & Chen, W. (2018). Electrospinning and crosslinking of polyvinyl alcohol/chitosan composite nanofiber for transdermal drug delivery. *Advances in Polymer Technology, 37*(6), 1917–1928. https://doi.org/10.1002/adv.21850
60. Yang, G. Z., Li, J. J., Yu, D. G., He, M. F., Yang, J. H., & Williams, G. R. (2017). Nanosized sustained-release drug depots fabricated using modified tri-axial electrospinning. *Acta Biomaterialia, 53*, 233–241. https://doi.org/10.1016/j.actbio.2017.01.069
61. Yu, D. G., Li, X. Y., Wang, X., Chian, W., Liao, Y. Z., & Li, Y. (2013). Zero-order drug release cellulose acetate nanofibers prepared using coaxial electrospinning. *Cellulose, 20*(1), 379–389. https://doi.org/10.1007/s10570-012-9824-z
62. Liu, X., Yang, Y., Yu, D. G., Zhu, M. J., Zhao, M., & Williams, G. R. (2019). Tunable zero-order drug delivery systems created by modified triaxial electrospinning. *Chemical Engineering Journal, 356*, 886–894. https://doi.org/10.1016/j.cej.2018.09.096
63. Yu, D. G., Li, X. Y., Wang, X., Yang, J. H., Bligh, S. W. A., & Williams, G. R. (2015). Nanofibers fabricated using triaxial electrospinning as zero order drug delivery systems. *ACS Applied Materials & Interfaces, 7*(33), 18891–18897. https://doi.org/10.1021/acsami.5b06007
64. Song, B., Wu, C., Chang, J. (2012). Controllable delivery of hydrophilic and hydrophobic drugs from electrospun poly(lactic-co-glycolic acid)/mesoporous silica nanoparticles composite mats. *Journal of Biomedical Materials Research Part B: Applied Biomaterials, 100*(8), 2178–186. https://doi.org/10.1002/jbm.b.32785
65. Wang, Y., Wang, B., Qiao, W., Yin, T. (2010). A novel controlled release drug delivery system for multiple drugs based on electrospun nanofibers containing nanoparticles. *99* (12), 4805–4811. https://doi.org/10.1002/jps
66. Heydari, P., Varshosaz, J., Zargar Kharazi, A., & Karbasi, S. (2018). Preparation and evaluation of poly glycerol sebacate/poly hydroxy butyrate core-shell electrospun nanofibers with sequentially release of ciprofloxacin and simvastatin in wound dressings. *Polymers for Advanced Technologies, 29*(6), 1795–1803. https://doi.org/10.1002/pat.4286
67. Laracuente, M. L., Yu, M. H., & McHugh, K. J. (2020). Zero-order drug delivery: state of the art and future prospects. *Journal of Controlled Release, 327*, 834–856. https://doi.org/10.1016/j.jconrel.2020.09.020
68. Yu, D. G., Xu, Y., Li, Z., Du, L. P., Zhao, B. G., Wang, X. (2014). Coaxial electrospinning with mixed solvents: from flat to round Eudragit L100 nanofibers for better colon-targeted sustained drug release profiles. *Journal of Nanomaterials*, *2014*, 967295. https://doi.org/10.1155/2014/967295
69. Wang, M., Wang, L., Huang, Y. (2007). Electrospun hydroxypropyl methyl cellulose phthalate (HPMCP)/erythromycin fibers for targeted release in intestine. *Journal of Applied Polymer Science, 106* (4), 2177–2184. https://doi.org/10.1002/app.25666

70. Liu, M., Wang, X., Wang, Y., & Jiang, Z. (2020). Controlled stimulation-burst targeted release by PH-sensitive HPMCAS/theophylline composite nanofibers fabricated through electrospinning. *Journal of Applied Polymer Science, 137*(7), 1–7. https://doi.org/10.1002/app.48383
71. Yang, Y. Y., Liu, Z. P., Yu, D. G., Wang, K., Liu, P., & Chen, X. (2018). Colon-specific pulsatile drug release provided by electrospun shellac nanocoating on hydrophilic amorphous composites. *International Journal of Nanomedicine, 13*, 2395–2404. https://doi.org/10.2147/IJN.S154849
72. Khodadadi, M., Alijani, S., Montazeri, M., Esmaeilizadeh, N., Sadeghi-Soureh, S., & Pilehvar-Soltanahmadi, Y. (2020). Recent advances in electrospun nanofiber-mediated drug delivery strategies for localized cancer chemotherapy. *Journal of Biomedical Materials Research, Part A, 108*(7), 1444–1458. https://doi.org/10.1002/jbm.a.36912
73. Abid, S., Hussain, T., Raza, Z. A., Nazir, A. (2019). Current applications of electrospun polymeric nanofibers in cancer therapy. *Materials Science and Engineering C*, *97*, 966–977. https://doi.org/10.1016/j.msec.2018.12.105
74. Yan, E., Jiang, J., Yang, X., Fan, L., Wang, Y., An, Q., Zhang, Z., Lu, B., Wang, D., & Zhang, D. (2020). pH-sensitive core-shell electrospun nanofibers based on polyvinyl alcohol/polycaprolactone as a potential drug delivery system for the chemotherapy against cervical cancer. *Journal of Drug Delivery Science and Technology, 55*, 101455. https://doi.org/10.1016/j.jddst.2019.101455
75. Salehi, R., Irani, M., Eskandani, M., Nowruzi, K., Davaran, S., & Haririan, I. (2014). Interaction, controlled release, and antitumor activity of doxorubicin hydrochloride from PH-sensitive P(NIPAAm-MAA-VP) nanofibrous scaffolds prepared by green electrospinning. *International Journal of Polymeric Materials and Polymeric Biomaterials, 63*(12), 609–619. https://doi.org/10.1080/00914037.2013.854234
76. Zhang, J., Li, J., Xu, C., Xi, Z., Ren, Y., Song, Q., & Lu, S. (2020). Novel PH-sensitive drug-loaded electrospun nanofibers based on regenerated keratin for local tumor chemotherapy. *Textile Research Journal, 90*(19–20), 2336–2349. https://doi.org/10.1177/0040517520919920
77. Chen, Y., Abdalkarim, S. Y. H., Yu, H. Y., Li, Y., Xu, J., Marek, J., Yao, J., & Tam, K. C. (2020). Double stimuli-responsive cellulose nanocrystals reinforced electrospun PHBV composites membrane for intelligent drug release. *International Journal of Biological Macromolecules, 155*, 330–339. https://doi.org/10.1016/j.ijbiomac.2020.03.216
78. Zhao, X., Yuan, Z., Yildirimer, L., Zhao, J., Lin, Z. Y., Cao, Z., Pan, G., & Cui, W. (2015). Tumor-triggered controlled drug release from electrospun fibers using inorganic caps for inhibiting cancer relapse. *Small, 11*(34), 4284–4291. https://doi.org/10.1002/smll.201500985
79. Sang, Q., Li, H., Williams, G., Wu, H., & Zhu, L. M. (2018). Core-shell poly(lactide-Co-ε-caprolactone)-gelatin fiber scaffolds as PH-sensitive drug delivery systems. *Journal of Biomaterials Applications, 32*(8), 1105–1118. https://doi.org/10.1177/0885328217749962
80. Zhao, J., Liu, S., Li, B., Yang, H., Fan, C., & Cui, W. (2013). Stable acid-responsive electrospun biodegradable fibers as drug carriers and cell scaffolds. *Macromolecular Bioscience, 13*(7), 885–892. https://doi.org/10.1002/mabi.201200452
81. Qian, W., Yu, D. G., Li, Y., Liao, Y. Z., Wang, X., & Wang, L. (2014). Dual drug release electrospun core-shell nanofibers with tunable dose in the second phase. *International Journal of Molecular Sciences, 15*(1), 774–786. https://doi.org/10.3390/ijms15010774
82. Kaassis, A. Y. A., Young, N., Sano, N., Merchant, H. A., Yu, D. G., Chatterton, N. P., & Williams, G. R. (2014). Pulsatile drug release from electrospun poly(ethylene oxide)-sodium alginate blend nanofibres. *Journal of Materials Chemistry B, 2*(10), 1400–1407. https://doi.org/10.1039/c3tb21605e
83. What are biologics? FAQ. https://www.fda.gov/about-fda/center-biologics-evaluation-and-research-cber/what-are-biologics-questions-and-answers
84. Zhang, Y., Davis, D. A., AboulFotouh, K., Wang, J., Williams, D., Bhambhani, A., Zakrewsky, M., Maniruzzaman, M., Cui, Z., Williams, R. O. (2021). Novel formulations and drug delivery systems to administer biological solids. *Advanced Drug Delivery Reviews, 172*, 183–210. https://doi.org/10.1016/j.addr.2021.02.011

85. Durán-Lobato, M., López-Estévez, A. M., Cordeiro, A. S., Dacoba, T. G., Crecente-Campo, J., Torres, D., Alonso, M. J. (2021). Nanotechnologies for the delivery of biologicals: Historical perspective and current landscape. *Advanced Drug Delivery Reviews*, 176, 113899. https://doi.org/10.1016/j.addr.2021.113899
86. Moreira, A., Lawson, D., Onyekuru, L., Dziemidowicz, K., Angkawinitwong, U., Costa, P. F., Radacsi, N., Williams, G. R. (2021). Protein encapsulation by electrospinning and electrospraying. *Journal of Controlled Release, 329*, 1172–1197. https://doi.org/10.1016/j.jconrel.2020.10.046
87. Angkawinitwong, U., Awwad, S., Khaw, P. T., Brocchini, S., & Williams, G. R. (2017). Electrospun formulations of bevacizumab for sustained release in the eye. *Acta Biomaterialia, 64*, 126–136. https://doi.org/10.1016/j.actbio.2017.10.015
88. Hashemzadeh, M. R., Taghavizadeh Yazdi, M. E., Amiri, M. S., Mousavi, S. H. (2021). Stem cell therapy in the heart: Biomaterials as a key route. *Tissue and Cell*, *71*, 101504. https://doi.org/10.1016/j.tice.2021.101504
89. Ehler, E., & Jayasinghe, S. N. (2014). Cell electrospinning cardiac patches for tissue engineering the heart. *The Analyst, 139*(18), 4449–4452. https://doi.org/10.1039/C4AN00766B
90. Townsend-Nicholson, A., & Jayasinghe, S. N. (2006). Cell electrospinning: A unique biotechnique for encapsulating living organisms for generating active biological microthreads/scaffolds. *Biomacromolecules, 7*(12), 3364–3369. https://doi.org/10.1021/bm060649h
91. Jayasinghe, S. N., Irvine, S., & McEwan, J. R. (2007). Cell electrospinning highly concentrated cellular suspensions containing primary living organisms into cell-bearing threads and scaffolds. *Nanomedicine, 2*(4), 555–567. https://doi.org/10.2217/17435889.2.4.555
92. Jayasinghe, S. N. (2013). Cell electrospinning: A novel tool for functionalising fibres, scaffolds and membranes with living cells and other advanced materials for regenerative biology and medicine. *The Analyst, 138*(8), 2215–2223. https://doi.org/10.1039/C3AN36599A
93. Trindade, R. P., Renault, N., El Harane, N., Menasché, P., Williams, G. R. (2021). Extracellular vesicles can be processed by electrospinning without loss of structure or function. *Materials Letters, 282*, 128671. https://doi.org/10.1016/j.matlet.2020.128671
94. Vader, P., Mol, E. A., Pasterkamp, G., Schiffelers, R. M. (2016). Extracellular vesicles for drug delivery. *Advanced Drug Delivery Reviews, 106*, 148–156. https://doi.org/10.1016/j.addr.2016.02.006
95. Elsharkasy, O. M., Nordin, J. Z., Hagey, D. W., de Jong, O. G., Schiffelers, R. M., Andaloussi, S. E. L., Vader, P. (2020). Extracellular vesicles as drug delivery systems: Why and how? *Advanced Drug Delivery Reviews, 159*, 332–343. https://doi.org/10.1016/j.addr.2020.04.004
96. Radacsi, N., Giapis, K. P., Ovari, G., Szabó-Révész, P., & Ambrus, R. (2019). Electrospun nanofiber-based niflumic acid capsules with superior physicochemical properties. *Journal of Pharmaceutical and Biomedical Analysis, 166*, 371–378. https://doi.org/10.1016/j.jpba.2019.01.037
97. Vass, P., Szabó, E., Domokos, A., Hirsch, E., Galata, D., Farkas, B., Démuth, B., Andersen, S. K., Vigh, T., Verreck, G., Marosi, G., & Nagy, Z. K. (2020). Scale-up of electrospinning technology: Applications in the pharmaceutical industry. *Wiley Interdisciplinary Reviews: Nanomedicine and Nanobiotechnology, 12*(4), e1611. https://doi.org/10.1002/wnan.1611
98. Nagy, Z. K., Balogh, A., Démuth, B., Pataki, H., Vigh, T., Szabó, B., Molnár, K., Schmidt, B. T., Horák, P., Marosi, G., Verreck, G., Van Assche, I., & Brewster, M. E. (2015). High speed electrospinning for scaled-up production of amorphous solid dispersion of itraconazole. *International Journal of Pharmaceutics, 480*(1–2), 137–142. https://doi.org/10.1016/j.ijpharm.2015.01.025
99. Zhang, B., Yan, X., He, H. W., Yu, M., Ning, X., Long, Y. Z. (2017). Solvent-free electrospinning: Opportunities and challenges. *Polymer Chemistry, 8*, 333–352. https://doi.org/10.1039/c6py01898j
100. Li, H., Zhang, Z., Godakanda, V. U., Chiu, Y. J., Angkawinitwong, U., Patel, K., Stapleton, P. G., de Silva, R. M., de Silva, K. M. N., Zhu, L. M., & Williams, G. R. (2019). The Effect

of collection substrate on electrospun ciprofloxacin-loaded poly(vinylpyrrolidone) and ethyl cellulose nanofibers as potential wound dressing materials. *Materials Science and Engineering C, 104*, 1–27. https://doi.org/10.1016/j.msec.2019.109917

101. Russo, F., Ursino, C., Avruscio, E., Desiderio, G., Perrone, A., Santoro, S., Galiano, F., & Figoli, A. (2020). Innovative poly(vinylidene fluoride) (PVDF) electrospun nanofiber membrane preparation using DMSO as a low toxicity solvent. *Membranes, 10*(3), 36. https://doi.org/10.3390/membranes10030036
102. Shawon, J., & Sung, C. (2004). Electrospinning of polycarbonate nanofibers with solvent mixtures THF and DMF. *Journal of Materials Science, 9*(39), 4605–4613. https://doi.org/10.1023/B:JMSC.0000034155.93428.ea
103. Omer, S., Forgách, L., Zelkó, R., & Sebe, I. (2021). Scale-up of electrospinning: Market overview of products and devices for pharmaceutical and biomedical purposes. *Pharmaceutics, 13*(2), 286. https://doi.org/10.3390/pharmaceutics13020286



V. Umayangana Godakanda received her B.S. degree in Pharmacy from the University of Colombo and Graduateship in Chemistry from the Institute of Chemistry, Sri Lanka, both in 2017. She is currently pursuing a Ph.D. degree in Pharmaceutics at the University of Colombo and working as a Research Assistant with the Centre for Advanced Materials and Devices in the Department of Chemistry, University of Colombo. Her research interests include the development of smart fabrics for healthcare and specifically fabrication of drug-loaded electrospun formulations as advanced wound dressing materials. Umayangana was awarded a Research Scholarship in 2018 from the Sri Lankan National Science Foundation.



Karolina Dziemidowicz received her Master of Pharmacy degree from King's College London in 2015 and a PhD in Pharmaceutical Technology from University College London in 2021. During her undergraduate studies, Karolina undertook her MPharm dissertation at Utrecht University, working on drug-eluting bronchotracheal stents. She is a practicing pharmacist and completed her pre-registration training in 2016 at AstraZeneca, where she worked on parenteral protein formulations. During her PhD dissertation, Karolina developed antibody-functionalized biomaterials for cancer immunotherapy. She became a Postdoctoral Research Associate at the UCL Centre for Nerve Engineering in late 2020 and contributed to the development of now patented technology that uses drug-eluting electrospun fibers for the treatment of peripheral nerve injuries. She is currently an EPSRC Doctoral Prize Fellow at the UCL School of Pharmacy working on drug-loaded dual substitutes for use in traumatic spinal cord injuries.



Rohini M. de Silva was awarded a BSc (Hons) degree in Chemistry from the University of Colombo in 1993, and a Ph.D. from the University of Cambridge in 1998. She then returned to Sri Lanka as a Senior Lecturer in the Department of Chemistry at the University of Colombo and was promoted to Professor in 2016. She worked as a Postdoctoral Fellow at the Center for Advanced Microstructures and Devices at Louisiana State University from 2005 to 2007. Rohini's research interests revolve around the development of advanced functional materials for healthcare applications, water purification and nanobiotechnology. Her research team established the Center for Advanced Materials and Devices at the University of Colombo in 2018.



K. M. Nalin de Silva obtained a BSc (Hons) degree in Chemistry from the University of Colombo in 1992 and a Ph.D. from the University of Cambridge in 1998. He was appointed as a Senior Lecturer in the Department of Chemistry at the University of Colombo in 1998, and promoted to Professor in 2005, Senior Professor in 2013, and Chair Senior Professor in 2021. He worked as a Postdoctoral Fellow at the University of Cambridge and Louisiana State University in 1998 and 2005 respectively. From 2012 to 2019 he served as the Science Team Leader at the Sri Lankan Institute of Nanotechnology. In 2020 he was appointed as the Head of Chemistry at the University of Colombo. Nalin's research interests focus on the development of advanced functional materials for healthcare applications, water purification, and smart textiles. He is a co-founder of the Centre for Advanced Materials and Devices.



Gareth R. Williams received an MChem (Hons) degree from the University of Oxford in 2002. He remained in Oxford for a DPhil (Ph.D.), which was completed in 2005. He then worked as a post-doctoral researcher and in science programme management for the UK government. In September 2010 he joined London Metropolitan University as a Senior Lecturer in Pharmaceutical Science, and in November 2012 was appointed to the UCL School of Pharmacy as a Lecturer in Pharmaceutics. He was promoted to Associate Professor in 2016 and to full Professor in 2020, when he also became Head of Pharmaceutics. Gareth leads a group of around 20 researchers applying inorganic and polymer-based nanomaterials to overcome drug delivery challenges.

Chapter 8
Suitability of Electrospun Nanofibers for Specialized Biomedical Applications



Havva Başkan and Hale Karakaş

Abstract Nanofibers offer potential applications in the biomedical field and they have become popular as they have the possibility to be produced for various fields ranging from drug encapsulation, drug delivery, tissue regeneration, wound and burn care, vascular grafts, enzyme immobilization, etc. due to their high surface area to volume ratio, ability to be suitable for biomimicry, possibility to be designed according to the application by optimization of nanofiber production process parameters, ability to enhance cell adhesion and growth and their ease of functionalization. Electrospinning is the most preferred method for the fabrication of nanofibers since it is a simple, versatile, and efficient technique. The nanofibers produced by electrospinning have the potential to be used in various applications including biomedical applications due to the ability of electrospinning to result in targeted fiber morphologies and diameters. In this chapter, the electrospinning process, parameters, and single and co-axial electrospinning techniques were explained. Moreover, biomedical applications especially wound dressing, tissue engineering, drug delivery, vascular grafts, and enzyme immobilization of nanofibers, with a focus on electrospun nanofibers were considered, and examples were reviewed in detail.

Keywords Nanofibers · Electrospinning · Biopolymers · Biomedical applications

8.1 Introduction

As science and technology are being developed, the medical industry is experiencing the usage of new materials and technologies for the support of human health. In particular, nanotechnology is the most influential factor for the enhancements in the medical field since its significant contribution in terms of biomedical, and

H. Başkan (✉)
Integrated Manufacturing Research, and Application Center, Sabancı University, 34906 Pendik, Istanbul, Turkey
e-mail: havva.baskan@sabanciuniv.edu

H. Başkan · H. Karakaş
Textile Technologies and Design Faculty, Textile Engineering Department, Istanbul Technical University, 34437 Gumussuyu, Beyoglu, Istanbul, Turkey

© The Author(s), under exclusive license to Springer Nature Switzerland AG 2022

A. Vaseashta and N. Bölgen (eds.), *Electrospun Nanofibers*,
https://doi.org/10.1007/978-3-030-99958-2_8

pharmaceutical applications [1]. Nanotechnology allows obtaining of nanofibrous materials which have high porosity, high surface area to volume ratio, ultrafine thickness, continuity and potential to be used in various biomedical applications. Nanofibrous materials, nanofibers, can be obtained from several production techniques such as drawing, template synthesis, phase-separation, self-assembly, and electrospinning. Among these production routes, electrospinning is mentioned to be the most advantageous one because it is simple and efficient [2].

The electrospinning method is based on the fabrication of nanofibers by applying electrostatic forces to several solutions. The main equipment of it is a high voltage power supply, a syringe with a metal spinneret, and a collector [3]. The type of collector can be changed according to the desired nanofiber morphology [2]. In addition, the electrospinning process can be achieved by using a wide range of materials that can be natural, synthetic, ceramic, or inorganic. By the utilization of natural and synthetic biopolymeric electrospinning solutions, nanofibers with bio-features can be achieved and effectively used in biomedical applications such as drug encapsulation, drug delivery, tissue regeneration, wound and burn care, vascular grafts, enzyme immobilization. Those nanofibers have the ability to imitate extracellular matrix (ECM) due to their high-porous structure and to act as a carrier for drug delivery [4]. Moreover, these outstanding properties of nanofibers can be easily tuned by changing the applied electrospinning parameters [5]. In this chapter, the electrospinning process, usage of biopolymers in electrospinning, and suitable applications of electrospun nanofibers in the biomedical field, especially in wound dressing, tissue engineering, drug delivery, vascular grafts, and enzyme immobilization are examined and reported in detail. The development in the production of electrospun nanofibers for biomedical applications via different electrospinning set-ups is considered.

8.2 Wound Dressing

Importance of wound healing has been realized since ancient times with efforts on preparation of mixtures for treatment of wounds. However start of wide research in this area dates back to the World War I and World War II [6]. Skin and soft tissue infections are regarded as major concerns with respect to wound repair. Recently, anti-bacterial wound dressings have been emerging as promising candidates to reduce infection, thus accelerating the wound healing process. Wound dressings which can offer rapid healing and precent infection are being developed [7]. Among the alternatives such as membranes/sponges, hydrogels, films, nanogel/microgel, scaffolds/bandages and micro/nanofibers investigated for use as topological formulations, nano/micro fibers offer advantages for wound dressing. Their main advantages being remarkably large exposed surface area and nano-porosity. This allows easier interaction of the wounded cells with the extracellular matrix (ECM) structure. Additionally, they offer high specific surface area, antibacterial property, absorption of the exudate, water and oxygen permeability, increased inter-change of nutrients as well as exclusion of metabolic wastes [8]. Nanofibers can be manufactured using various

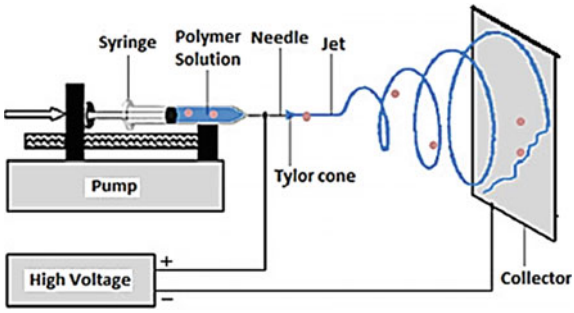


Fig. 8.1 Electrospinning set-up

methods including drawing, template synthesis, phase separation, self-assembly and electrospinning.

Electrospinning method is a simple, efficient, cost-effective and versatile technique, offering many advantages over the other techniques for nanofiber fabrication. It is regarded as the most practical method to produce ultrafine fibers having diameters in micrometer and nanometer range. It is also among the other nanofiber fabrication methods besides melt blowing, rotary jet spinning for manufacturing drug loaded nanofibrous scaffolds [3, 7–13]. A typical basic electrospinning equipment consists of a high voltage source, a solution feeding unit usually in the form of a capillary tube with pipette or needle of small diameter and a collector as seen in Fig. 8.1 [12].

Electrospinning uses high voltage to induce the formation of liquid jets and consequently it can be regarded as a variant of the electrospraying process. Small droplets or particles are formed as a result of the break-up of the electrified jet in electrospraying, whereas a solid fiber is formed as the electrified jet is stretched in electrospinning. The solution or melt is stretched during solidification by electrostatic forces and the fibers are collected as a distribution of continuous fibers. At first, high voltage is applied to the polymer solution to produce an electrical field between the tip and the collector to shape the droplet on the tip as Taylor Cone. When the electrostatic force is higher than the surface tension of the polymer solution, polymer jet is ejected from the tip to the collector. The jet undergoes stretching before reaching the collector, following a spiral way, getting longer and finer and it solidifies on the collector in the form of nanofibers by the evaporation of the solvent [4, 14–16].

Coaxial and triaxial configurations are present as advanced electrospinning techniques. These have been invented via modifications in conventional electrospinning set-up in order to attain enhanced nanofiber web performance. Core–shell nanofibers can be produced using co-electrospinning, using specially designed needle, to which core and shell solutions are fed independently using two syringe pumps. The same voltage source is used and type of the collector can vary according to the needs [17–19].

A wide range of biocompatible and biodegradable materials including poly (L-lactic acid) (PLLA), poly(ε-caprolactone) (PCL), poly(ethylene glycol) (PEG), poly lactic glycolic acid (PLGA), chitosan, chitin, cellulose, poly(vinyl alcohol) (PVA)

can be used as drug carriers, incorporating drugs such as captopril, curcumin, titanium dioxide, activated carbon nanoparticles, etc. [9].

Biopolymer based nanofibrous dressings offer the advantages of biocompatibility and biodegradability while biomimicking the extracellular matrix structure [7]. Use of biopolymers in dressings for wound healing also are also favorable in terms of their structure and surface characteristics similar to ECM [11]. Polysaccharides including cellulose, hyaluronic acid, chitin, chitosan, and alginates have been thoroughly investigated for their potential in wound healing. Collagen, silk fibroin, dextran and elastin have also been studied [7, 10, 20]. Incorporation of antibacterial nanoparticles, nature-derived compounds and bio-functional agents into this emerging class of wound dressings help to control the infection more efficiently. Hybridization of nanofibers with functional agents such as drugs, nanoparticles, essential oils is necessary [7].

Baykara and Taylan covered PVA nanofibers with Nigella seed oil via co-axial electrospinning for wound dressing applications. It was noted that co-axial electrospinning is an efficient process to produce the desired nanofiber morphology for targeted application area. Moreover, the nanofibers including bioactive agents which were obtained via co-axial electrospinning, could be used in wound dressing or tissue engineering successfully [21].

Komur et al. covered starch around PCL nanofibers by using co-axial electrospinning. It was observed that increased amount of starch led to stronger nanofibers. Moreover, the amount of starch increase could lead to enhanced cell viability of the resultant nanofibers, which allowed them to be used in wound dressing applications [22]. In order to encapsulate two different drugs into a nanofiber structure, Mao et al. prepared PLA/graphene-oxide (GO) core–shell nanofibers via electrospinning. It was seen that the presence of GO promoted the drug release performance [23].

In a study by Kalaoglu-Altan et al., a blend of poly(3-hydroxybutyrate)(P(3HB)) and poly(3-hydroxyoctanoate-co-3-hydroxy decanoate) (P(3HO-co-3HD)) was electrospun into P(3HB))/P(3HO-co-3HD) nanofibers, as shown in Fig. 8.2, which were then modified with silver nanoparticles (AgNPs) via the dip-coating method. The

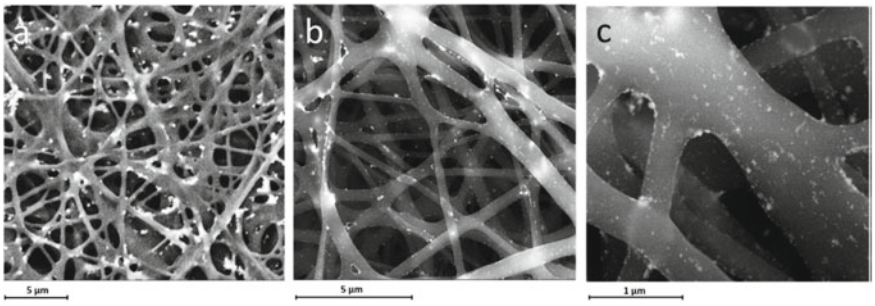


Fig. 8.2 SEM images of AgNP-containing P(3HB)/P(3HO-co-3HD) nanofibers with magnifications **a** ×12,000, **b** ×25,000, **c** ×100,000 exhibit the uniform and dense immobilization of AgNPs on the nanofibers [24]

silver-containing nanofiber meshes showed good cytocompatibility and interesting immunomodulatory properties in vitro and they displayed capability of stimulating the human beta defensin 2 and cytokeratin expression in human keratinocytes (HaCaT cells). They concluded that these nanofibers would be candidates for wound dressing applications [24].

Baskan produced poly(acrylonitrile-co itaconic acid)/silver P(AN-co-IA)/Ag nanofibers by coaxial electrospinning. In order to perform coaxial electrospinning, a special needle system (Raméhart Custom Needle, 100-10-COAXIAL-2016, outer needle diameter: 1.7 mm and inner needle diameter: 0.9 mm), two syringe pumps (KD Scientific Pump Series 100) and a power supply (Glassman High Voltage Series) were used. The coaxial needle is shown in Fig. 8.3. Core solution (PAN and P (AN-co-IA)-PAN in sequence) was directly connected to needle and shell solution (Al_2O_3/DMF) was fed to the coaxial needle via polytetrafluoroethylene (PTFE) tubings of which outer diameter was 1.6 mm. Feed-rate of the core solutions were kept as 1 ml/h and shell solution was fed to the coaxial needle via PTFE tubings with 0.2 ml/h feed-rate while the other electrospinning parameters were used as 20 kV applied voltage, 15 cm needle tip-to-collector distance. The coaxial electrospinning needle and set-up are given in Fig. 8.3 and Fig. 8.4, respectively. The resultant nanofibers showed satisfying antimicrobial results, being regarded as good candidates for potential use in the biomedical and pharmaceutical applications [18].

Bakhsheshi-Rad et al. developed (PVA/chitosan (CS)/silk sericin (SS)/tetracycline (TCN) porous nanofibers both invitro and in vivo to explore their applicability as wound dressings. The resultant nanofibers displayed very good water take up capability through swelling. Nanofibers loaded with high sericin and tetracycline content significantly inhibited the growth of *escherichia coli* and *staphylococcus aureus*. The results of this study demonstrate that the PVA/CS/SS-TCN nanofibers may be a potential alternative to traditional wound dressing materials as they allow enhanced wound healing, re-epithelialization, and collagen deposition in comparison to traditional gauze and nanofibers without sericin [25].



Fig. 8.3 The coaxial needle (Raméhart Custom Needle, 100-10-COAXIAL-2016) [18]

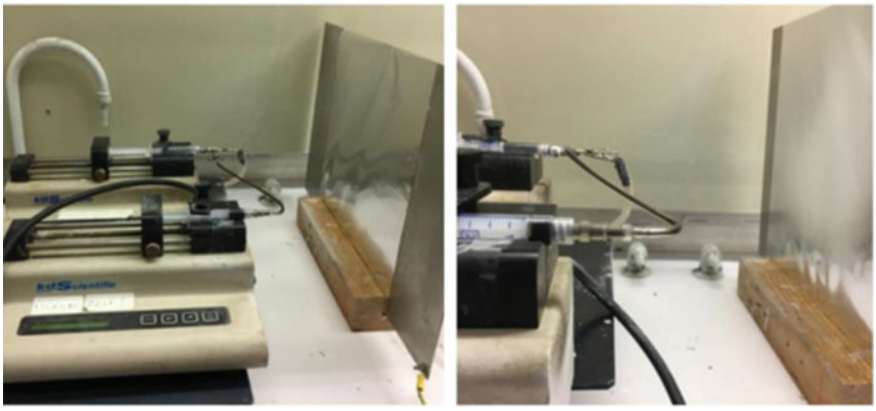


Fig. 8.4 The coaxial electrospinning set-up [18]

8.3 Drug Delivery

Topical drug delivery systems are composed of a formulation applied to the skin directly to heal disorders or disease of the skin which guide/target pharmacological effect of the drug to the skin surface. Gels, creams, ointment, liquid preparation, sprays and solid powders are among the various pharmaceutical dosage forms that can be used in topical drug delivery. Electrospun nanofibers are excellent materials for drug delivery systems due to high interconnected porosity, high surface area, ability to imitate the ECM, potential carrier for drug delivery. Utilization of nanofibers in drug delivery systems is based on the principle that the high surface area of the nanofibrous formulation increases the dissolution rate of the drug. Compared with other dosage forms such as; liposomes, micelles and hydrogels, major advantages of nanofibers are increment in drug loading efficiency and loading capacity, low systemic toxicity and excellent stability. Furthermore, several drugs can be carried within nanofibers with high local drug concentration due to their excellent targeting and drug transportation ability in a safe way [26–28].

Electrospinning offers the opportunity for direct loading of drugs or biological agents for instance antibacterial molecules, antibiotics, enzymes, growth factors, proteins, peptides, vitamins, DNA into the electrospun nanofibers. Electrospinning is one of the simplest among all methods to fabricate nano scaled fibers and it offers the opportunity for direct loading of drug into the electrospun nanofibers [29]. It is possible to load drugs and bioactive molecules such as rifampin, paclitaxel, tetracycline hydrochloride, doxorubicin hydrochloride, proteins, and DNA into nanofibers to improve bioavailability, bioactivity and to control delivery [30]. Different polymers have been electrospun into nanofiber such as gelatin, chitosan, silk fibroin, hyaluronic acid (HA), hydroxypropyl cellulose (HPC), polyurethane (PU), PVA, poly (lactic acid) (PLA), PCL, polyethylene oxide (PEO) and PLGA to fabricate patches for drug-delivery applications [31, 32].

Among the carrier polymers used for drug delivery, PCL, PLA and Poly (ethylene oxide) (PEO) are popular. The high aqueous solubility and ability of rapid interaction with the body fluids due to hydrophilicity of PEO renders it a widely used polymer in the polymer matrix, allowing bioavailability and solubility of drugs in drug delivery applications. PEO is a highly aqueous soluble polymer, that interacts with the body fluid quickly due to its hydrophilicity resulting in dissolution. PEO is widely used in the polymer matrix to enhance bioavailability and solubility of drugs because of its high aqueous solubility and unique properties in drug delivery applications [31, 33–36]. PCL and PLA are also favorable due to their compatibility with different types of drugs and slow degradation rates as they offer homogenous distribution of the drugs in the polymer matrix and prolonged drug delivery. Recently, studies have been conducted on drug delivery using electrospun nanofibers based on PCL, PEO, PLA and their blends, loading them with different drugs and biological agents such as, Niclosamide, Silver nanoparticles, Vitamin B12, Curcumin, Lysozyme, $AgNO_3$, Metronidazole (MNA).

The compatibility of PCL and PLA with different types of drugs enables uniform drug distribution in the polymer matrix and the slow degradation rate makes them favorable for prolonged drug delivery systems. In recent years, various studies were reported on the fabrication of drug delivery systems, generated by electrospinning of PCL, PEO, PLA and their blends. PCL, PEO, PLA nanofibers or their blends were loaded with different drugs and biological agents such as, Niclosamide, Silver nanoparticles, Vitamin B12, Curcumin, Lysozyme, $AgNO_3$, Metronidazole (MNA) [36–41].

Another approach is to prepare polymer blends, allowing control of physical, mechanical and biochemical properties of nanofibers. This has been used extensively by electrospinning hydrophilic/hydrophobic polymer blends for controlled drug delivery. The hydrophobic polymer forms the backbone and degrading slowly creates a long-term but steady-state drug release, whereas the hydrophilic polymer degrades more rapidly, accelerating the drug release. This mechanism has been very effective in drug delivery applications [26, 42].

Barbak produced a novel topical drug delivery system loaded with silver sulfadiazine (SSD), which is a non-ionized, water-insoluble, topical antibacterial agent that is used extensively in the topical treatment of infected burns. For this purpose, three different formulations were fabricated; namely, [PCL/(PEO + SSD)] nanofibers, PCL/(PEO + SSD) casting films and [PLA/(PEO + SSD)] nanofibers. It was observed that the fiber diameter decreased from 374 to 254 nm due to the inclusion of charged SSD particles [43].

Drug loading efficiency was achieved as 86% ± 4 for PCL/(PEO + SSD) nanofibers, 65% ± 2 for PCL/(PEO + SSD) casting film and 80% ± 4 for PLA/(PEO + SSD) nanofibers. The casting film formulation showed lower loading efficiency than the PCL/(PEO + SSD) and PLA/(PEO + SSD) nanofiber formulations. It was reported that the nanofiber formulations are better candidates than the PCL/(PEO + SSD) casting film formulation for topical drug delivery. In comparison with the other studies in the literature, the optimized PLA/(PEO + SSD) and PCL/(PEO + SSD) nanofibers formulations showed high loading efficiency. It was clearly pointed that

the nanofiber formulations were promising drug carriers for efficient drug loading thanks to the specific surface area and high porous structure of nanofibers [26, 43].

8.4 Vascular Grafts

The treatment of tissue damage and organ collapse caused by cardiovascular disease (CVD) is of great interest since cardiovascular disease is the leading cause of death both in Europe and USA [44–46]. It has been announced that the reason for 4.3 million deaths per year in Europe is CVD [46]. The most common cause of CVD is atherosclerosis which narrows the blood vessels by the formation of plaque and thus normal flow rate of blood is restricted. Since vascular tissue has a complex structure, it is very difficult to regenerate or restore the original tissue. When the application of angioplasty is not appropriate, autografts are used for the regeneration of the local tissue environment. However, the usage of autografts can result in disease transmission which may cause significant health problems to patients. In addition, the availability of autografts is a major challenge. The other treatment methods are mainly organ/tissue transplantation or replacement of the damaged tissue with synthetic vascular grafts or prosthetic heart valves [44, 47].

Synthetic vascular grafts which are made of are poly (ethylene terephthalate) (PET) and polytetrafluoroethylene (PFTE) are widely used for the replacement of large-diameter vessels (>6 mm). However, they cannot be used for the replacement of small-diameter vessels (<6 mm) due to intimal hyperplasia, atherosclerosis, infection, acute thrombogenicity, compliance mismatch, and aneurysm formation. Autologous arterial and venous grafts seem to be a solution for those dilemmas but their usage in patients is also limited because of their poor quality, and limited length. Therefore, vascular grafts with optimum functional properties as well as engineered structure are needed to be developed. Biocompatibility, nontoxicity, non-immunogenicity, non-thrombogenicity, mechanical strength are the main requirements for ideal vascular graft structure as in native artery structure [47–49].

The native artery structure is a multilayered tissue including different cell types and proteins. The wall of native artery is composed of three different layers named as *tunica intima*, *tunica media* and *tunica adventita*. The *intima* is mainly composed of continuous single layer endothelium cells (EC) which is in contact with the blood-stream and act as a barrier to platelet activation. The EC demonstrates antithrombotic features in their resting position. The ECs are connected to ECM where cell adhesion is supplied by interstitial fibrin and collagen I. The middle layer, *tunica media*, is composed of smooth muscle cells and responsible for the synthesis of collagen, elastin and amplification of cytokines. ECM governs the phenotype and activity of the smooth muscle cells. The outer layer, *tunica adventitia,* contains collagen fibers and fibroblast. When producing a vascular graft structure, it is compulsory to mimic the unique features of each layer as much as possible [49–51].

Electrospinning is an efficient technique used to produce nanofibers for the design of tissue engineered vascular grafts (TEVG) since the nanofibers have high surface

area to volume ratio, enabling adherence for cell attachment. The process is feasible by means of tubular scaffold design easily. It is possible to control the diameter and mechanical properties of the obtained electrospun TEVG via electrospinning, that is not the case for synthetic vascular grafts. Furthermore, it is crucial to select a proper polymer for vascular graft design because improper material can cause various problems such as thrombogenesis. Electrospinning process allows to use biodegradable synthetic polymers (PCL, PLA, polyester urethane urea, etc.) and biodegradable natural polymers (collagen, elastin, chitosan, gelatin, silk fibroin, collagen and elastin blends, etc.) either single or in combination. The resultant web properties and the alignment of the fibers affect the tissue integration significantly [46, 49, 50, 52].

Johnson studied on the biomechanical properties of small-diameter electrospun TEVGs obtained from various synthetic, fully resorbable polymers. Electrospinning solutions were prepared by dissolving each polymer in hexafluro-isopropanol (HFIP). The prepared polymer solutions, utilized solvent and polymer solution concentrations (wt. %) are given in Table 8.1. Electrospinning process was performed by the application of a high voltage ranging from 9–20 kV keeping the distance between the needle tip and the collector 20 cm with 5 ml/h feed-rate. The electrospun vascular graft was collected on a rotating cylindrical surface with a wall thickness of 650 μm ± 65 μm [45].

Mechanical characterization, suture retention strength and catheter balloon mechanical testing of the obtained electrospun vascular grafts were conducted and it was seen that all the samples meet the minimum mechanical requirements with a considerable improvement in burst pressure, compliance and suture retention strength [45]. Milleret et al. focused on the effect of fiber diameter and surface roughness of electrospun vascular grafts on blood activation in order to design a scaffold with minimal acute thrombogenicity. Appropriate amounts of polyester urethane (trade

Table 8.1 The prepared polymer solutions, utilized solvent and polymer solution concentrations (wt. %) [45]

Polymer	Solvent	Ratio of polymers	wt % of polymer in solution
Polycaprolactone	HFIP		5
Polycaprolactone and Chitosan blend	HFIP:Acetic Acid (9:1 wt %)	20:1	3.15
Polydioxanone	HFIP		7
Polyglycolic acid	HFIP		10
Poly (lactic-co-caprolactone)	HFIP	70:30	5
Poly (lactic-co-glycolic acid)	HFIP	82:18	6
Poly (lactic-co-glycolic acid)	HFIP	10:90	8
Poly-L-lactide	HFIP		8

Table 8.2 Electrospinning parameters used to produce electrospun vascular grafts from DegraPol and PLGA [46]

Polymer	Concentration (wt %)	Flow rate (ml/h)	Needle tip-to-collector distance (cm)	Applied Voltage (kV)
DegraPol	15	0.1	25	5
	25	0.4	20	10
	25	1	15	15
PLGA	15	0.4	25	10
	25	1	20	10
	25	1.5	15	10

name DegraPol) and PLGA were prepared in hexafluoro-propanol (HFP) and chloroform (CF), respectively prior to electrospinning. The prepared polymer solutions were electrospun and the process parameters are summarized in Table 8.2. The electrospun vascular grafts were collected on a hollow cylindrical rotating surface, which has 100 mm length: 100 mm, 80 mm diameter and 5 mm wall thickness [46].

Based on the characterization results it was observed that the diameter of DegraPol type electrospun fiber mats ranged between 1 and 3 μm whereas the results for PLGA type fibers were varied in the range of 5–6 μm. Moreover, based on the characterization results, it was mentioned that diameter increase resulted in better platelet adhesion and activation. It was informed that endothelial cell proliferation increases with increased fiber diameters [53–57].

A multi-layered vascular graft design was achieved by Yalcin et al. They dissolved PCL in CF: ethanol (9:1 v:v) binary solvent system at a concentration of 18 wt./v %. After a sufficient stirring time, the prepared solution was electrospun with the electrospinning parameters of 7.5 kV voltage, 2 ml/h feed-rate and 20 cm distance between the needle tip and the collector. The nanofibers were collected on a rotating mandrel whose rotational speed were changed as 250, 5000, 10,000, and 15,000 r/min during the process in order to supply radial fiber orientation. Pore size and porosity of the samples were analyzed to understand the suitability of the nanofibrous membrane for cell proliferation and diffusion through the tunica media. Moreover, biocompatibility of the fibers was assessed by mouse 3T3 fibroblasts. It was stated that continual increase of cell numbers during the experiment duration was observed however, it was also mentioned that fiber orientation was not much more significant for 3T3 mouse fibroblasts during static cultivation [49].

Besides neat electrospun PCL vascular grafts, Bertram et al. loaded various amounts of (5%, 25%, 50% and 75 wt. %) collagen type I into PCL and compare the efficiency of the prepared vascular graft samples for embryonic endothelial progenitor cell behavior with virgin electrospun PCL vascular grafts. In this regard, PCL and PCL/Collagen blends were dissolved in 1,1,1,3,3,3-hexafluoroisopropanol (HFIP) and then electrospun by the application of 20 kV voltage and 15 cm distance between the needle tip-to-collector while flow-rate was kept as 2 ml/h. Based on the characterization results, it was seen that PCL/collagen based vascular grafts were ideal

materials for vascular grafts due to their ability to promote the endothelial cell functionality. Moreover, it was pointed out that the best morphology and physiology of endothelial cell was supplied from the PCL vascular grafts that contain the lowest amount (25 wt. %) of collagen [58].

Kang et al. also studied on the production of collagen based vascular graft however they combined collagen with hyaluronic acid oligosaccharide to improve endothelial cell proliferation. For electrospinning, polymer solutions of neat collagen and collagen/ hyaluronic acid oligosaccharide were prepared in HFIP at a concentration of 8%. Then, the obtained electrospun nanofibers were assessed in vitro to observe the cell proliferation and vessel endothelialization. According to the characterization results, it was understood that cell proliferation was supported by hyaluronic acid oligosaccharide modified collagen nanofibers but loading higher amounts of hyaluronic acid oligosaccharide prevented the proliferation of endothelial cell. Furthermore, proliferated endothelial cells could regulate the cell cycle at mRNA level and perform normal function [59].

In addition to conventional electrospinning process, there are studies for the design of electrospun vascular grafts via co-axial electrospinning. For instance; Zhai et al. studied on the electrospinning of P(LLA-CL)/heparin for femoral artery substitution. In the study, heparin was utilized as the core while P(LLA-CL) was as the shell component. Prior to electrospinning, 6% w/v P(LLA-CL) was dissolved in 2, 2, 2-trifluoromethyl ethanol and 12% heparin was dissolved in ultra-pure water. During the coaxial electrospinning, flow rates of the core and shell solutions were kept as 0.1 and 1.0 mL/h, respectively. The electrospinning parameters were conducted as 16 kV applied voltage and 15 cm distance between the needle tip-to-collector whose rotational speed was 800 rpm/h [60]. The produced P(LLA-CL)/heparin vascular grafts were implanted into the femoral arteries of the dogs. Based on the characterization results, it was seen that the no stenosis of the anastomotic stoma occurred after implantation which meant that the obtained P(LLA-CL)/heparin vascular grafts can be used for the repairment of blood vessels [60].

Another coaxial electrospinning for vascular graft development was performed by Nagiah et al. They used three different types of polymers which were PU, PCL and PLA as core and gelatin as shell. Gelatin was selected due to its biocompatible and elastic feature. 1 wt. % PU, PCL or PLA and 5 wt. % gelatin polymer solutions were prepared in 1,1,1,3,3,3 hexafluoro-2-propanol (HFP). The feed rates of the solutions were 1 ml/h while the applied voltage was 10 kV and the distance between the needle tip-to-collector was 10 cm. It was declared that the presence of gelatin enhanced the elasticity, promoted the nutrient transport and allowed to obtain highly compliant tubular grafts. When the produced vascular grafts were compared based on the core material effect, it was understood that PCL-gelatin composition was the best to achieve strongest core-sheath interactions and the most compliant graft [61].

Mi et al. designed a triple-layered vascular graft whose inner layer, middle layer and outer layer are composed of a braided silk yarn, polyacrylamide (PAM) hydrogel and thermoplastic polyurethane (TPU), respectively. The aim of that design was to mimic the mechanical features of the native blood vessels. Silk fibers were used as an alternative model to collagen fibers whereas PAM hydrogel was utilized instead

of elastin component. Electrospinning was carried out with the parameters of 20 kV voltage, 0.5 ml/h flow-rate for the fabrication and deposition of TPU nanofibers on the surface of the middle layer. The speed of the rotating scaffold design was 500 rpm. TPU nanofibers were also aimed to mimic the elastin. In the study, it was claimed that specifically, PAM hydrogel layer contributed to enhance the burst pressure and the resultant multi-layered vascular graft structure could preserve normal blood flow [62].

As a conclusion, in order to prepare and use a vascular graft clinically, attention must be given for the production of biocompatible, cost-effective and available vascular graft designs. Most importantly, the challenge for small-diameter vascular graft production must be overcome. Using electrospinning for the vascular graft production enables to control the diameter of the resultant graft as well as conserving the required biological features. For the future perspectives, the subjects of 'facilitating cellular infiltration' and 'fast scaffold degradation' should be considered for the improvement of the efficiency of vascular grafts [50].

8.5 Tissue Engineering

Regenerative medicine and tissue regeneration have taken great attention in the past few decades. The repair or regeneration of the damaged soft tissues should result in demonstrating the features of replaced native tissue as much as possible [63, 64]. Autografts and allografts such as tendon, ligament and osteochondral are the most widely utilized materials for tissue repair. However, their limited availability and the possibility to cause disease transmission hinders their clinical usage [65, 66]. In order to solve these problems, tissue engineering has come into prominence. Tissue engineering uses cells, biomaterials and aims to improve and fasten the tissue regeneration effectively. In this regard, it is very crucial for biomaterials to mimic the structure and features of ECM [67].

Ideal tissue engineering scaffolds should be designed to trigger cell growth and formation while degrading in vivo as natural tissues [68]. The use of nanomaterials in tissue engineering field has a considerable effect on tissue regeneration since native tissues are composed of very fine ECM at the nanoscale approximately 50–300 nm. For example, a natural bone is a nanocomposite containing nano-crystallite collagen-rich matrix [68, 69]. Among the nanomaterials, nanofibers are the most widely preferred substrates for tissue regeneration due to their porous structure which significantly facilitates cell attachment [70]. Furthermore, nanofibrous webs have been shown to mimic in vivo-like organization [71].

Gomes et al. focused on the production of biomimetic scaffolds via electrospinning by utilizing chitosan, PCL and gelatin polymers. The obtained nanofibers were characterized by in-vitro and in-vivo with HFFF2 human fibroblasts and in Wistar rats, respectively in order to compare the biological performance of the samples. Based on the characterization results, it was observed that while chitosan nanofibers had the highest impact on healing it showed a very cell proliferation. In addition,

PCL also did not contribute to cell proliferation and adhesion significantly. However, gelatin nanofibers demonstrated the maximum performance on cell growth [72].

Examination of skin repair performance in terms of healing rate and the quality of regenerated skin of chitosan-PCL nanofibers was also conducted by Levengood et al. To this end, 7 wt. % of chitosan polymer solution was prepared in trifluoroacetic acid (TFA) and simultaneously 12 wt. % of PCL polymer solution was prepared in 2,2,2-trifluoroethanol (TFE). After a sufficient stirring of the polymer solutions, they were blended in the ratio of 4:6 wt. % chitosan: PCL as a resultant electrospinning solution. By the application of electrospinning parameters as 11 kV voltage and 18 cm working distance, chitosan: PCL electrospun nanofibers could be obtained. The comparison of the healing performance of the resultant nanofibrous web to the control sample (Tegaderm) was evaluated for 14 days. Biological investigation demonstrated that nanofiber diameter, surface area, porosity, and stiffness greatly affect the healing process [73].

Wang et al. also studied on the electrospinning of chitosan for wound healing but they were blended it with PVA instead of PCL. In the study, 3% (w/v) chitosan and 8% (w/v) PVA polymer solutions were prepared and mixed in ratios of 80/20, 50/50, and 20/80 (chitosan/PVA). Also, a widely used antibiotic, ampicillin, was dissolved n PVA polymer solution in the amount of 1wt %. Electrospinning was applied to chitosan/PVA polymer blends with the parameters of 17 kV voltage and 12 cm needle tip-to-collector distance. Moreover, the obtained nanofiber web was subjected to crosslinking with aqueous glutaraldehyde solution (50% v/v) for 4 days at room temperature. Related to the morphologic analysis of the nanofibers, it was understood that 50/50 blending ratio was the best to obtain beadless and continuous nanofiber structure which resembles the morphology of native tissue [74].

In addition to single electrospinning, Adeli-Sardou et al. prepared core shell nanofibers of gelatin-lawsone (core)/PCL (shell) via coaxial electrospinning and examined the antibacterial activity, wound healing capability and cell biocompatibility of the obtained nanofibers. Lawsone itself has a novel antibacterial, antifungal, anti-cancer and antioxidant features since it is a member of quinone group. According to the morphological characterization results, it was confirmed that beadless morphology could be obtained from electrospinning process. The most importantly, addition of addition of lawsone contributed to the cell proliferation even using it very small amounts (1%). In addition, two healing expressions, genes TGF-B1 and COL1, enhanced significantly when lawsone was used in the content of 0.5 and 1% [75].

Samadian et al. introduced a novel tissue engineering approach by combining the biological activities of electrospun gelatin nanofibers and taurine (an amino acid having a considerable effect on bone regeneration) with the structural properties of thermally-induced phase separated scaffolds. In this regard, 40% (w/v) gelation solution was prepared and gelatin nanofibers were obtained by the application of 20 kV voltage, 15 cm distance between the needle tip-to-collector and 0.4 ml/h flow-rate. Afterwards, the obtained gelatin nanofibers were crosslinked with glutaraldehyde. Simultaneously, PCL and PLA were dissolved in 1,4-dioxane in the ratio of 1:1 wt. % to obtain a 10% (w:v) polymer solution. The produced gelatin

nanofibers were incorporated into the prepared PCL/PLA solution as well as taurine. Then, PCL/PLA/taurine composite scaffolds were fabricated by thermally-induced phase separation [76]. The obtained scaffolds had interconnected pore microstructure (Fig. 8.5) which is crucial for cell nutrient and infiltration.

Biological evaluation of the scaffolds showed that the samples could be used in bone regeneration due to the interconnected structure and cytocompatibility [76]. Tissue regeneration not only comprises dermal wounds, skin or bone regeneration, but also includes repairment of tendons, ligaments, cartilage and muscle. Table 8.3 summarizes some of the polymeric nanofibers and their target usage area in tissue engineering.

To sum up, it can be said that various natural and synthetic polymers could be used in electrospinning to fabricate polymeric nanofibers and use them in tissue engineering applications such as skin, bone, ligament tendon and cartilage regeneration. It can be fairly mentioned that the most significant parameter for a nanofibrous web to be used in tissue engineering is to mimic the structure and features of ECM, allow cell growth and formation and at the same degrade in vivo as natural living tissues.

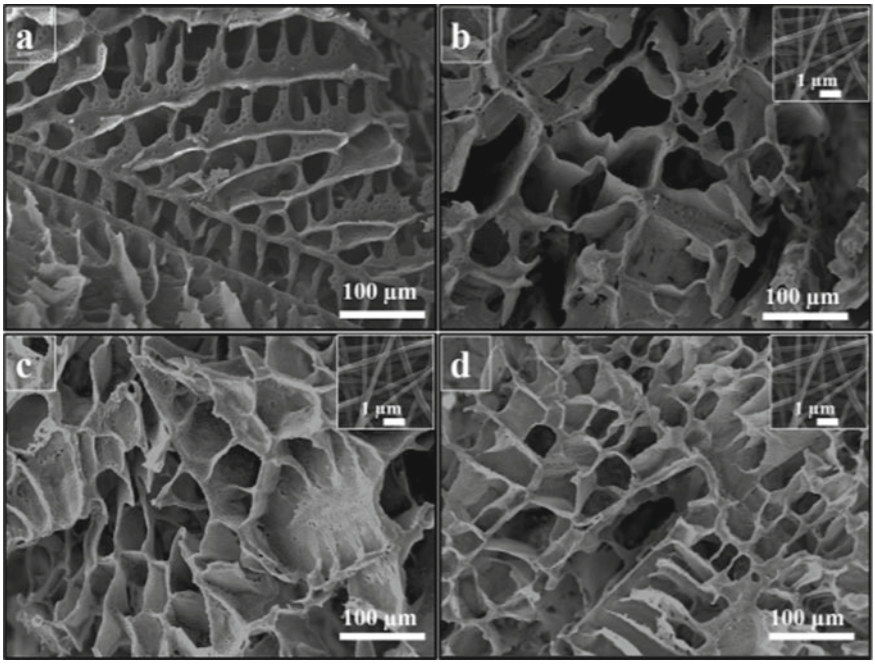


Fig. 8.5 SEM images of the scaffolds; **a** PCL/PLA/gelatin nanofibers, **b** PCL/PLA/ Gelatin nanofibers /Taurine 0.1%, **c** PCL/PLA/ Gelatin nanofibers / Taurine 1%, and (d) PCL/PLA/ Gelatin nanofibers /Taurine 10% [76]

Table 8.3 Polymeric nanofibers and their target usage area in tissue engineering

Polymeric Nanofibers	Target Usage Area
γ-PGA/PLA core-shell	Wound Healing [77]
Gelatin	Skin Regeneration [78]
Polyurethane (PU) /starch	Skin Regeneration [79]
Soy protein /silk fibroin	Skin Regeneration [80]
Gelatin/poly-3-hydroxybutyrate (P3HB)	Skin Regeneration [81]
PCL/ hydroxyapatite	Bone Regeneration [82]
Platelet rich plasma/PCL/PVA	Bone Regeneration [83]
PLGA	Bone Regeneration [84]
Poly (3, 4-ethylene dioxythiophene) (PEDOT)/Silk	Ligament Regeneration [85]
Polylactic acid (PLLA) /collagen	Ligament Regeneration [86]
PCL/chitosan	Ligament Regeneration [87]
Chitosan-collagen hydrogel/aligned PLLA	Tendon Regeneration [88]
PLLA	Tendon Regeneration [89]
Gelatin /PLA	Cartilage Regeneration [90]
PCL/Glucosamine sulfate	Cartilage Regeneration [91]

8.6 Enzyme Immobilization

Enzyme is a sort of protein which has a catalytic function and can be used in many application areas such as medicine, agriculture, food, industry, etc. However, they are very sensitive materials to the environmental conditional changes. Changes in the environmental conditions can cause activity loss in free enzymes. Enzyme immobilization has taken attention due to the difficulties on processing of free enzymes after a reaction. By the help of enzyme immobilization, reutilization, cost reduction and stability enhancement could be achieved. The features specifically catalytic activity of the immobilized enzymes are strongly affected by the immobilization method and the type of carrier materials. Among the carrier materials, the use of nanofibers is advantageous since they have large surface area to volume ratio, rich and novel structure, easy recycling, etc. [92, 93].

There are two major enzyme immobilization methods for electrospun nanofibers, which are encapsulation and surface immobilization. For the encapsulation process, enzymes could be added directly to the structure of nanofibers during electrospinning. Blend electrospinning, co-axial electrospinning and emulsion electrospinning are the widely used method for the encapsulation immobilization of enzymes into nanofibers [93]. Either virgin or modified nanofibers could be used for enzyme immobilization. The virgin nanofibers could be prepared by using both natural and synthetic polymers but since natural polymers are cheap, have high thermal, chemical and mechanical

stability, they are frequently utilized as carrier materials for enzyme immobilization [92, 93].

Lee et al. fabricated regenerated silk fibroin nanofibrous mat to be used as a carrier for alpha-chymotrypsin enzyme. The diameter of the produced silk fibroin nanofibers was in the range of 205–320 nm. It was mentioned that with a high capacity loading of enzyme, the effectiveness of the silk fibroin nanofibers as great. Moreover, the small diameter of the nat silk fibroin nanofibers had a significant impact on the function of the resultant enzyme immobilized nanofiber web [94]. Huang et al. also studied on the immobilization of chymotrypsin enzyme onto chitin nanofibers and assessed the stability, activity and reusability of the immobilized enzymes [95]. Bayazidi and coworkers immobilized lysozyme on bacterial cellulose nanofibers and characterized and compared the morphologic structure of the resultant nanofibers before and after enzyme immobilization [96]. On the other hand Ribeiro et al. reported on chitosan based nanofibers for enzyme immobilization in detail [97].

In addition to natural polymers, there are suggested studies on the enzyme immobilization onto synthetic polymer based electrospun nanofibers. Kamacı and Peksel combined the natural polymer, chitosan, and the synthetic polymer, PVA, to obtain electrospun nanofibers for phytase immobilization [98]. Canbolat et al. immobilized laccase into PCL nanofibers [99], Asfhari et al. focused on the glucose oxidase immobilization onto polyvinyl alcohol/malonic acid nanofibers [100], Li et al. prepared PAN/Fe_3O_4 electrospun nanofibers for the immobilization of horseradish peroxidase [101], Dai et al. produced laccase immobilized electrospun nanofiber web modified by multiwalled carbon nanotubes (MWCNTs) by using emulsion electrospinning [102], Alonso-González et al. fabricated PVA-based electrospun nanofibrous membranes and encapsulated glucose oxidase enzyme into the membrane structure [103]. To emphasize, it can be clearly said that enzyme immobilized electrospun nanofibers could be used in many applications mainly as biosensors, bioreactors, and in water treatment.

8.7 Conclusıons

Electrospinning technique is extensively used to obtain targeted fiber morphology and structure suitable for biomedical applications including wound healing, drug delivery, vascular grafts, tissue regeneration, and enzyme immobilization. In this chapter, biomedical applications of electrospun nanofibers were considered in detail. Electrospun nanofibers are good candidates for biomedical applications since they supply the requirements such as nontoxicity, resistance against microbial infections, resemblance to ECM, absorption of the exudate, water and oxygen permeability, and etc. Controlled release profiles can be obtained using electrospun nanofibers as drug carriers. Treatment of tissue damage and organ collapse can be achieved by electrospun vascular gfaft membranes. In addition, health problems can be eliminated by using electropsun autografts. Cell attachment and mimicking the in-vivo-like organization and the structure of ECM can be succeded by electrospun tissues. Furthermore,

electrospun nanofibers can be regarded as carrier materials in enzyme immobilization due to their large surface area to volume ratio and novel structure.

References

1. Sabra, S., Ragab, D. M., Agwa, M. M., & Rohani, S. (2020). Recent advances in electrospun nanofibers for some biomedical applications. *European Journal of Pharmaceutical Sciences*, *144*(September 2019), 105224. https://doi.org/10.1016/j.ejps.2020.105224
2. Karakaş, H. (2012). Electrospinning of nanofibers and their applications. *MDT 'Electrospinning'*, *3*, 1–35.
3. Hamzeh, S., Miraftab, M., & Yoosefinejad, A. (2014). Study of electrospun nanofibre formation process and their electrostatic analysis. *Journal of Industrial Textiles*, *44*(1), 147–158. https://doi.org/10.1177/1528083713480379
4. Reneker, D. H., Yarin, A. L., Zussman, E., & Xu, H. (2007). Electrospinning of Nanofibers from Polymer Solutions and Melts. *Advances in Applied Mechanics*, *41*, 43–195, 345–346. https://doi.org/10.1016/S0065-2156(07)41002-X
5. Ramakrishna, S., Fujihara, K., Teo, W. E., Lim, T. C., & Ma, Z. (2005). An introduction to electrospinning and nanofibers.
6. Attinger, C. E. (1912). A brief history of wound care. *Plastic and Reconstructive Surgery*, *117*(7S), 6–11. https://doi.org/10.1097/01.prs.0000225429.76355.dd
7. Homaeigohar, S., & Boccaccini, A. R. (2020). Antibacterial biohybrid nanofibers for wound dressings. *Acta Biomaterialia*, *107*, 25–49. https://doi.org/10.1016/j.actbio.2020.02.022
8. Andreu, V., Mendoza, G., Arruebo, M., & Irusta, S. (2015). Smart dressings based on nanostructured fibers containing natural origin antimicrobial, anti-inflammatory, and regenerative compounds. *Materials*, *8*(8), 5154–5193. https://doi.org/10.3390/ma8085154
9. Ambekar, R. S., & Kandasubramanian, B. (2019). Advancements in nanofibers for wound dressing: A review. *European Polymer Journal*, *117*, 334–336. https://doi.org/10.1016/j.eurpolymj.2019.05.020
10. Abrigo, M., McArthur, S. L., & Kingshott, P. (2014). Electrospun nanofibers as dressings for chronic wound care: Advances, challenges, and future prospects. *Macromolecular Bioscience*, *14*(6), 772–792. https://doi.org/10.1002/mabi.201300561
11. Huang, S., Fu, X. (2010). Naturally derived materials-based cell and drug delivery systems in skin regeneration. *Journal of Controlled Release*, *142*(2), 149–159. https://doi.org/10.1016/j.jconrel.2009.10.018
12. Huang, Z. M., Zhang, Y. Z., Kotaki, M., & Ramakrishna, S. (2003). A review on polymer nanofibers by electrospinning and their applications in nanocomposites. *Composites Science and Technology*, *63*(15), 2223–2253. https://doi.org/10.1016/S0266-3538(03)00178-7
13. Venugopal, J., Ramakrishna, S. (2005). Applications of polymer nanofibers in biomedicine and biotechnology. *Applied Biochemistry and Biotechnology—Part A Enzyme Engineering and Biotechnology*, *125*, 147–157. https://doi.org/10.1385/ABAB:125:3:147
14. Karakas, H. (2014). *Electrospinning of Nanofibers and Their Applications.*
15. Wang, H. -S., Fu, G. -D., & Li, X. -S. (2008). Functional polymeric nanofibers from electrospinning. *Recent Patents on Nanotechnology*, *3*(1), 21–31. https://doi.org/10.2174/187221009787003285
16. Deitzel, J. M., Kleinmeyer, J. D., Hirvonen, J. K., & Beck Tan, N. C. (2001). Controlled deposition of electrospun poly(ethylene oxide) fibers. *Polymer*, *42*(19), 8163–8170. https://doi.org/10.1016/S0032-3861(01)00336-6
17. Moghe, A. K., & Gupta, B. S. (2008). Co-axial electrospinning for nanofiber structures: Preparation and applications. *Polymer Reviews*, *48*, 353–377. https://doi.org/10.1080/15583720802022257
18. Başkan, H. (2021). *Electrospun Composite Nanofibers with Metal/Metaloxide Nanoparticles.*

19. Garg, K., Bowlin, G. L., Garg, K., & Bowlin, G. L. (2014). Electrospinning jets and nanofibrous structures *5*(2011), 013403. https://doi.org/10.1063/1.3567097
20. Mogoşanu, G. D., & Grumezescu, A. M. (2014). Natural and synthetic polymers for wounds and burns dressing. *International Journal of Pharmaceutics*, *463*(2), 127–136. https://doi.org/10.1016/j.ijpharm.2013.12.015
21. Baykara, T., Taylan, G. (2021). Coaxial electrospinning of PVA/Nigella seed oil nanofibers: Processing and morphological characterization. *Materials Science and Engineering B: Solid-State Materials for Advanced Technology*, *265*, 115012. https://doi.org/10.1016/j.mseb.2020.115012
22. Komur, B., Bayrak, F., Ekren, N., Eroglu, M. S., Oktar, F. N., Sinirlioglu, Z. A., Yucel, S., Guler, O., & Gunduz, O. (2017). Starch/PCL composite nanofibers by co-axial electrospinning technique for biomedical applications. *BioMedical Engineering Online*, *16*(1), 1–13. https://doi.org/10.1186/s12938-017-0334-y
23. Mao, Z., Li, J., Huang, W., Jiang, H., Zimba, B. L., Chen, L. Wan, J., Wu, Q. (2018). Preparation of poly(lactic acid)/graphene oxide nanofiber membranes with different structures by electrospinning for drug delivery. *RSC Advances*, *8*(30), 16619–16625. https://doi.org/10.1039/c8ra01565a
24. Kalaoglu-altan, O. I., Baskan, H., Meireman, T., Basnett, P., Azimi, B., & De Clerck, K. (2021). Silver nanoparticle-coated polyhydroxyalkanoate based electrospun fibers for wound dressing applications. *Materials*, *14*, 1–17
25. Bakhsheshi-Rad, H. R., Ismail, A. F., Aziz, M., Akbari, M., Hadisi, Z., Omidi, M., & Chen, X. (2020). Development of the PVA/CS nanofibers containing silk protein sericin as a wound dressing: In vitro and in vivo assessment. *International Journal of Biological Macromolecules*, *149*, 513–521. https://doi.org/10.1016/j.ijbiomac.2020.01.139
26. Barbak, Z. (2021). *Composite Nanofiber Patches for Topical Drug Delivery Systems.*
27. Hu, X., Liu, S., Zhou, G., Huang, Y., Xie, Z., & Jing, X. (2014). Electrospinning of polymeric nanofibers for drug delivery applications. *Journal of Controlled Release*, *185*, 12–21. https://doi.org/10.1016/j.jconrel.2014.04.018
28. Morie, A., Garg, T., Goyal, A. K., & Rath, G. (2016). Nanofibers as novel drug carrier - An overview. *Artificial Cells, Nanomedicine and Biotechnology*, *44*(1), 135–143. https://doi.org/10.3109/21691401.2014.927879
29. Sarac, A. S. (2016). Nanofibers of conjugated polymers.
30. Zamani, M., Prabhakaran, M. P., & Ramakrishna, S. (2013). Advances in drug delivery via electrospun and electrosprayed nanomaterials. *International Journal of Nanomedicine*, *8*, 2997. https://doi.org/10.2147/IJN.S43575
31. Gunn, J., & Zhang, M. (2010). Polyblend nanofibers for biomedical applications: Perspectives and challenges. *Trends in Biotechnology*, *28*(4), 189–197. https://doi.org/10.1016/j.tibtech.2009.12.006
32. Esentiirk, I., Erdal, M. S., & Giingtir, S. (2016). Electrospinning method to produce drug-loaded nanofibers for topical/ transdermal drug delivery applications. *Journal of Pharmacy of Istanbul University*, *46*(1), 49–69
33. Kohsari, I., Shariatinia, Z., & Pourmortazavi, S. M. (2016). Antibacterial electrospun chitosan-polyethylene oxide nanocomposite mats containing bioactive silver nanoparticles. *Carbohydrate Polymers*, *140*, 287–298. https://doi.org/10.1016/j.carbpol.2015.12.075
34. Wang, B., Li, H., Yao, Q., Zhang, Y., Zhu, X., Xia, T., Wang, J., Li, G., Li, X., & Ni, S. (2016). Local in vitro delivery of rapamycin from electrospun PEO/PDLLA nanofibers for glioblastoma treatment. *Biomedicine and Pharmacotherapy*, *83*, 1345–1352. https://doi.org/10.1016/j.biopha.2016.08.033
35. Cheng, F., Gao, J., Wang, L., & Hu, X. (2015). Composite chitosan/poly(ethylene oxide) electrospun nanofibrous mats as novel wound dressing matrixes for the controlled release of drugs. *Journal of Applied Polymer Science*, *13*(24). https://doi.org/10.1002/app.42060
36. Dubey, P., & Gopinath, P. (2016). Fabrication of electrospun poly(ethylene oxide)-poly(capro lactone) composite nanofibers for co-delivery of niclosamide and silver nanoparticles exhibits enhanced anti-cancer effects in vitro. *Journal of Materials Chemistry B*, *4*, 726–742. https://doi.org/10.1039/c5tb02351c

37. Dubey, P., Bhushan, B., Sachdev, A., Matai, I., Uday Kumar, S., & Gopinath, P. (2015). Silver-nanoparticle-Incorporated composite nanofibers for potential wound-dressing applications. *Journal of Applied Polymer Science*, *42473*, 2–12. https://doi.org/10.1002/app.42473
38. Xue, J., He, M., Liu, H., Niu, Y., Crawford, A., Coates, P. D., Chen, D., Shi, R., & Zhang, L. (2014). Drug loaded homogeneous electrospun PCL/gelatin hybrid nanofiber structures for anti-infective tissue regeneration membranes. *Biomaterials*, *35*(34), 9395–9405. https://doi.org/10.1016/j.biomaterials.2014.07.060
39. Merrell, J. G., Mclaughlin, S. W., Tie, L., Laurencin, C. T., Chen, A. F., Nair, L. S., Phil, M., Exp, C., & Author, P. P. (2009). Curcumin loaded poly(ε-caprolactone) nanofibers: Diabetic wound dressing with antioxidant and anti-inflammatory properties NIH public access author manuscript. *Clin Exp Pharmacol Physiol*, *36*(12), 1149
40. Li, Y., Jiang, H., & Zhu, K. (2008). Encapsulation and controlled release of lysozyme from electrospun poly(ε-caprolactone)/poly(ethylene glycol) non-woven membranes by formation of lysozyme-oleate complexes. *Journal of Materials Science: Materials in Medicine*, *19*(2), 827–832, https://doi.org/10.1007/s10856-007-3175-6
41. Kim, T. G., Lee, D. S., & Park, T. G. (2007). Controlled protein release from electrospun biodegradable fiber mesh composed of poly(ε-caprolactone) and poly(ethylene oxide). *International Journal of Pharmaceutics*, *338*(1–2), 276–283. https://doi.org/10.1016/j.ijpharm.2007.01.040
42. Dicks, L. M. T., & Heunis, T. D. J. (2010). Nanofibers offer alternative ways to the treatment of skin infections. *Journal of Biomedicine and Biotechnology*, *2010*, 510682. https://doi.org/10.1155/2010/510682
43. Barbak, Z., Karakas, H., Esenturk, I., Erdal, M. S., & Sarac, A. S. (2020). Silver sulfadiazine loaded poly (ϵ-Caprolactone)/poly (Ethylene Oxide) composite nanofibers for topical drug delivery. *Nano*, *15*(6), 2050073. https://doi.org/10.1142/S1793292020500733
44. Naito, Y., Shinoka, T., Duncan, D., Hibino, N., Solomon, D., Cleary, M., Rathore, A., Fein, C., Church, S., & Breuer, C. (2011). Vascular tissue engineering: Towards the next generation vascular grafts. *Advanced Drug Delivery Reviews*, *63*(4), 312–323. https://doi.org/10.1016/j.addr.2011.03.001
45. Devan Ohst, J. J. (2015). Development of novel, bioresorbable, small-diameter electrospun vascular grafts. *Journal of Tissue Science & Engineering*, *06*(02), 1000151. https://doi.org/10.4172/2157-7552.1000151
46. Milleret, V., Hefti, T., Hall, H., Vogel, V., & Eberli, D. (2012). Influence of the fiber diameter and surface roughness of electrospun vascular grafts on blood activation. *Acta Biomaterialia*, *8*(12), 4349–4356. https://doi.org/10.1016/j.actbio.2012.07.032
47. Sankaran, K. K., Subramanian, A., Krishnan, U. M., & Sethuraman, S. (2015). Nanoarchitecture of scaffolds and endothelial cells in engineering small diameter vascular grafts. *Biotechnology Journal*, *10*(1), 96–108. https://doi.org/10.1002/biot.201400415
48. Zhuang, Y., Zhang, C., Cheng, M., Huang, J., Liu, Q., Yuan, G., Lin, K., & Yu, H. (2021). Challenges and strategies for in situ endothelialization and long-term lumen patency of vascular grafts. *Bioactive Materials*, *6*(6), 1791–1809. https://doi.org/10.1016/j.bioactmat.2020.11.028
49. Yalcin, I., Horakova, J., Mikes, P., Sadikoglu, T. G., Domin, R., & Lukas, D. (2016). Design of polycaprolactone vascular grafts. *Journal of Industrial Textiles*, *45*(5), 813–833. https://doi.org/10.1177/1528083714540701
50. Fukunishi, T., Shoji, T., & Shinoka, T. (2017). *Nanofiber composites in vascular tissue engineering*. Elsevier Ltd.
51. Karkan, S. F., Davaran, S., Rahbarghazi, R., Salehi, R., & Akbarzadeh, A. (2019). Electrospun nanofibers for the fabrication of engineered vascular grafts. *Journal of Biological Engineering*, *13*(1), 1–13. https://doi.org/10.1186/s13036-019-0199-7
52. Malik, S., Sundarrajan, S., Hussain, T., Nazir, A., Berto, F., & Ramakrishna, S. (2020). Electrospun biomimetic polymer nanofibers as vascular grafts. *Material Design & Processing Communications*, (August), 1–21. https://doi.org/10.1002/mdp2.203

53. Ju, Y. M., Choi, J. S., Atala, A., Yoo, J. J., & Lee, S. J. (2010). Bilayered scaffold for engineering cellularized blood vessels. *Biomaterials*, *31*, 4313–4321. https://doi.org/10.1016/j.biomaterials.2010.02.002
54. Keun Kwon, I., Kidoaki, S., & Matsuda, T. (2005). Electrospun nano- to microfiber fabrics made of biodegradable copolyesters: Structural characteristics, mechanical properties and cell adhesion potential. *Biomaterials*, *26*, 3929–3939. https://doi.org/10.1016/j.biomaterials.2004.10.007
55. Xu, C., Yang, F., Wang, S., & Ramakrishna, S. (2004). In vitro study of human vascular endothelial cell function on materials with various surface roughness. *Journal of Biomedical Materials Research - Part A*, *71*, 154–161. https://doi.org/10.1002/jbm.a.30143
56. Zhong, S., Zhang, Y., & Lim, C. T. (2012). Fabrication of large pores in electrospun nanofibrous scaffolds for cellular infiltration: A review. *Tissue Engineering - Part B: Reviews*, *18*(2), 77–87. https://doi.org/10.1089/ten.teb.2011.0390
57. Tian, F., Hossinkhani, H., Yokoyama, Y., Gomes Estrada, G., & Kobayashi, H. (2007). The effect of diameter of electronspun pga scaffold for biological behaviour of human umbilical vein endothelial cells. *Key Engineering Materials*, *342–343*, 237–240. https://doi.org/10.4028/www.scientific.net/kem.342-343.237
58. Bertram, U., Steiner, D., Poppitz, B., Dippold, D., Köhn, K., Beier, J. P., Detsch, R., Boccaccini, A. R., Schubert, D. W., Horch, R. E., & Arkudas, A. (2017). Vascular tissue engineering: Effects of integrating collagen into a PCL based nanofiber material. *BioMed Research International*, *2017*, 1–11. https://doi.org/10.1155/2017/9616939
59. Kang, L., Jia, W., Li, M., Wang, Q., Wang, C., Liu, Y., Wang, X., Jin, L., Jiang, J., Gu, G., & Chen, Z. (2019). Hyaluronic acid oligosaccharide-modified collagen nanofibers as vascular tissue-engineered scaffold for promoting endothelial cell proliferation. *Carbohydrate Polymers*, *223* (July), 115106. https://doi.org/10.1016/j.carbpol.2019.115106
60. Zhai, W., Qiu, L. J, Mo, X. M., Wang, S., Xu, Y. F., Peng, B., Liu, M., Huang, J. H., Wang, G. C., & Zheng, J. H. (2019). Coaxial electrospinning of P(LLA-CL)/heparin biodegradable polymer nanofibers: potential vascular graft for substitution of femoral artery. *Journal of Biomedical Materials Research - Part B Applied Biomaterials*, *107*(3), 471–478. https://doi.org/10.1002/jbm.b.32972
61. Nagiah, N., Johnson, R., Anderson, R., Elliott, W., & Tan, W. (2015). Highly compliant vascular grafts with gelatin-sheathed coaxially structured nanofibers. *Langmuir*, *31*(47), 12993–13002. https://doi.org/10.1021/acs.langmuir.5b03177
62. Mi, H. Y., Jiang, Y., Jing, X., Enriquez, E., Li, H., Li, Q., & Turng, L. S., (2019). Fabrication of triple-layered vascular grafts composed of silk fibers, polyacrylamide hydrogel, and polyurethane nanofibers with biomimetic mechanical properties. *Materials Science and Engineering C*, *98*(December 2018), 241–249. https://doi.org/10.1016/j.msec.2018.12.126
63. Jiang, T., Carbone, E. J., Lo, K. W. H., & Laurencin, C. T. (2015). Electrospinning of polymer nanofibers for tissue regeneration. *Progress in Polymer Science*, *46*, 1–24. https://doi.org/10.1016/j.progpolymsci.2014.12.001
64. Cooper, J. A., Ferraro, B., & Christensen, A. (2013). Recent advancements in soft tissue regeneration. *Recent Patents on Biomedical Engineering*, *6*(1), 22–28. https://doi.org/10.2174/1874764711306010004
65. Laurencin, C. T., Ambrosio, A. M. A., Borden, M. D., & Cooper, J. A. (1999). Tissue engineering: Orthopedic applications. *Annual Review of Biomedical Engineering*, (1), 19–46. https://doi.org/10.1146/annurev.bioeng.1.1.19
66. Wang, W., & Yeung, K. W. K. (2017). Bone grafts and biomaterials substitutes for bone defect repair: A review. *Bioactive Materials*, *2*(4), 224–247. https://doi.org/10.1016/j.bioactmat.2017.05.007
67. Spector, M. (2006). Biomaterials-based tissue engineering and regenerative medicine solutions to musculoskeletal problems. *Swiss Medical Weekly*, *136*(19–20), 293–301, 2006/19/smw-11310
68. Xie, X., Chen, Y., Wang, X., Xu, X., Shen, Y., Khan, R., Aldalbahi, A., Fetz, A. E., Bowlin, G. L., El-newehy, M., & Mo, X. (2020). Electrospinning nanofiber scaffolds for soft and hard

tissue regeneration. *Journal of Materials Science & Technology*, *59*, 243–261. https://doi.org/10.1016/j.jmst.2020.04.037

69. Rho, J. Y., Kuhn-Spearing, L., & Zioupos, P. (1998). Mechanical properties and the hierarchical structure of bone. *Medical Engineering and Physics*, *20*, 92–102. https://doi.org/10.1016/S1350-4533(98)00007-1
70. Pham, Q. P., Sharma, U., & Mikos, A. G. (2006). Electrospinning of polymeric nanofibers for tissue engineering applications: A review. *Tissue Engineering*, *12*(5), 1197–1211. https://doi.org/10.1089/ten.2006.12.1197
71. Schindler, M., Ahmed, I., Kamal, J., Nur-E-Kamal, A., Grafe, T. H., Chung, H. Y., & Meiners, S. (2005). A synthetic nanofibrillar matrix promotes in vivo-like organization and morphogenesis for cells in culture. *Biomaterials*, *26*(28), 5624–5631. https://doi.org/10.1016/j.biomaterials.2005.02.014
72. Gomes, S. R., Rodrigues, G., Martins, G. G., Roberto, M. A., Mafra, M., Henriques, C. M. R., & Silva, J. C. (2015). In vitro and in vivo evaluation of electrospun nanofibers of PCL, chitosan and gelatin: A comparative study. *Materials Science and Engineering C*, *46*, 348–358. https://doi.org/10.1016/j.msec.2014.10.051
73. Levengood, S. L., Erickson, A. E., Chang, F., & Zhang, M. (2017). Chitosan-PCL nanofibers for skin repair. *Journal of Materials Chemistry B*, *5*, 1822–1833. https://doi.org/10.1039/c6tb03223k
74. Wang, M., Roy, A. K., Webster, T. J., & Webster, T. J. (2017). Development of chitosan/poly (Vinyl Alcohol) electrospun nanofibers for infection related wound healing. *7*(January), 2016–2018. https://doi.org/10.3389/fphys.2016.00683
75. Adeli-sardou, M., Mehdi, M., Torkzadeh-mahani, M., & Dodel, M. (2019). Controlled release of lawsone from polycaprolactone/gelatin electrospun nano fi bers for skin tissue regeneration. *International Journal of Biological Macromolecules*, *124*, 478–491. https://doi.org/10.1016/j.ijbiomac.2018.11.237
76. Samadian, H., Farzamfar, S., Vaez, A., Ehterami, A., Bit, A., Alam, M., Goodarzi, A., Darya, G., & Salehi, M. (2020). A tailored polylactic acid/polycaprolactone biodegradable and bioactive 3D porous scaffold containing gelatin nanofibers and Taurine for bone regeneration. *Scientific Reports*, *10*, 13366. https://doi.org/10.1038/s41598-020-70155-2
77. Fang, Y., Zhu, X., Wang, N., Zhang, X., Yang, D., Nie, J., & Ma, G. (2019). Biodegradable core-shell electrospun nanofibers based on PLA and γ-PGA for wound healing. *European Polymer Journal*, *116*, 30–37. https://doi.org/10.1016/j.eurpolymj.2019.03.050
78. Dias, J. R. Baptista-Silva, S., Oliveira, C. M. T., d. Sousa, A., Oliveira, A. L., Bártolo, P. J., & Granja, P. L. (2017). In situ crosslinked electrospun gelatin nanofibers for skin regeneration. *European Polymer Journal*, *95*, 161–173. https://doi.org/10.1016/j.eurpolymj.2017.08.015
79. Movahedi, M., Asefnejad, A., Rafienia, M., & Khorasani, M. T., (2020). Potential of novel electrospun core-shell structured polyurethane/starch (hyaluronic acid) nanofibers for skin tissue engineering: In vitro and in vivo evaluation. *International Journal of Biological Macromolecules*, *146*, 627–637. https://doi.org/10.1016/j.ijbiomac.2019.11.233
80. Varshney, N., Sahi, A. K., Poddar, S., & Mahto, S. K. (2020). Soy protein isolate supplemented silk fibroin nanofibers for skin tissue regeneration: Fabrication and characterization. *International Journal of Biological Macromolecules*, *160*, 112–127. https://doi.org/10.1016/j.ijbiomac.2020.05.090
81. Sanhueza, C., Hermosilla, J., Bugallo-Casal, A., Da Silva-Candal, A., Taboada, C., Millán, R., Concheiro, A., Alvarez-Lorenzo, C., & Acevedo, F. (2021). One-step electrospun scaffold of dual-sized gelatin/poly-3-hydroxybutyrate nano/microfibers for skin regeneration in diabetic wound. *Materials Science and Engineering C*, *119*, 111602. https://doi.org/10.1016/j.msec.2020.111602
82. Banimohamad-Shotorbani, B., Rahmani Del Bakhshayesh, A., Mehdipour, A., Jarolmasjed, S., & Shafaei, H. (2021). The efficiency of PCL/HAp electrospun nanofibers in bone regeneration: A review. *Journal of Medical Engineering & Technology*.
83. Cheng, G., Ma, X., Li, J., Cheng, Y., Cao, Y., Wang, Z., Shi, X., Du, Y., Deng, H., & Li, Z. (2018). Incorporating platelet-rich plasma into coaxial electrospun nanofibers for bone tissue

engineering. *International Journal of Pharmaceutics*, *547*(1–2), 656–666. https://doi.org/10.1016/j.ijpharm.2018.06.020
84. Stachewicz, U., Qiao, T., Rawlinson, S. C. F., Almeida, F. V., Li, W. Q., Cattell, M., & Barber, A. H. (2015). 3D imaging of cell interactions with electrospun PLGA nanofiber membranes for bone regeneration. *Acta Biomaterialia*, *27*, 88–100. https://doi.org/10.1016/j.actbio.2015.09.003
85. Dodel, M., Hemmati Nejad, N., Bahrami, S. H., Soleimani, M., Mohammadi Amirabad, L., Hanaee-Ahvaz, H., & Atashi, A. (2017). Electrical stimulation of somatic human stem cells mediated by composite containing conductive nanofibers for ligament regeneration. *Biologicals*, *46*, 99–107. https://doi.org/10.1016/j.biologicals.2017.01.007
86. Sensini, A., Cristofolini, L., Focarete, M. L., Belcari, J., Zucchelli, A., Kao, A., & Tozzi, G. (2018). High-resolution x-ray tomographic morphological characterisation of electrospun nanofibrous bundles for tendon and ligament regeneration and replacement. *Journal of Microscopy*, *272*(3), 196–206. https://doi.org/10.1111/jmi.12720
87. Wu, G., Deng, X., Song, J., & Chen, F. (2018). Enhanced biological properties of biomimetic apatite fabricated polycaprolactone/chitosan nanofibrous bio-composite for tendon and ligament regeneration. *Journal of Photochemistry and Photobiology B: Biology*, *178*, 27–32. https://doi.org/10.1016/j.jphotobiol.2017.10.011
88. Deepthi, S., Nivedhitha Sundaram, M., Deepti Kadavan, J., & Jayakumar, R. (2016). Layered chitosan-collagen hydrogel/aligned PLLA nanofiber construct for flexor tendon regeneration. *Carbohydrate Polymers*, *153*, 492–500. https://doi.org/10.1016/j.carbpol.2016.07.124
89. Yin, Z., Chen, X., Chen, J. L., Shen, W. L., Hieu Nguyen, T. M., Gao, L., & Ouyang, H. W. (2010). The regulation of tendon stem cell differentiation by the alignment of nanofibers. *Biomaterials*, *31*(8), 2163–2175. https://doi.org/10.1016/j.biomaterials.2009.11.083
90. Chen, W., Chen, S., Morsi, Y., El-Hamshary, H., El-Newhy, M., Fan, C., & Mo, X. (2016). Superabsorbent 3D Scaffold Based on Electrospun Nanofibers for Cartilage Tissue Engineering. *ACS Applied Materials and Interfaces*, *8*, 24415−24425. https://doi.org/10.1021/acsami.6b06825
91. Chen, W., Wang, C., Gao, Y., Wu, Y., Wu, G., Shi, X., Du, Y., & Deng, H. (2020). Incorporating chitin derived glucosamine sulfate into nanofibers via coaxial electrospinning for cartilage regeneration. *Carbohydrate Polymers*, *229*, 115544. https://doi.org/10.1016/j.carbpol.2019.115544
92. Sun, Y., Cheng, S., Lu, W., Wang, Y., Zhang, P., & Yao, Q. (2019). Electrospun fibers and their application in drug controlled release, biological dressings, tissue repair, and enzyme immobilization. *RSC Advances*, *9*(44), 25712–25729. https://doi.org/10.1039/c9ra05012d
93. Li, D., Wang, Q., Huang, F., & Wei, Q. (2018). *Electrospun nanofibers for enzyme immobilization*. Elsevier Inc.
94. Lee, K. H., Ki, C. S., Back, D. H., Kang, G. D., Ihm, D. W., & Park, Y. H. (2005). Application of electrospun silk fibroin nanofibers as an immobilization support of enzyme. *Fibers and Polymers*, *6*(3), 181–185. https://doi.org/10.1007/BF02875641
95. Huang, W. C., Wang, W., Xue, C., & Mao, X. (2018). Effective enzyme immobilization onto a magnetic chitin nanofiber composite. *ACS Sustainable Chemistry and Engineering*, *6*, 8118–8124. https://doi.org/10.1021/acssuschemeng.8b01150
96. Bayazidi, P., Almasi, H., & Asl, A. K. (2018). Immobilization of lysozyme on bacterial cellulose nanofibers: Characteristics, antimicrobial activity and morphological properties. *International Journal of Biological Macromolecules*, *107*, 2544–2551. https://doi.org/10.1016/j.ijbiomac.2017.10.137
97. Ribeiro, E. S., de Farias, B. S., Sant'Anna Cadaval Junior, T. R., de Almeida Pinto, L. A., & Diaz, P. S. (2021). Chitosan–based nanofibers for enzyme immobilization. *International Journal of Biological Macromolecules*, *183*, 1959–1970. https://doi.org/10.1016/j.ijbiomac.2021.05.214
98. Duru Kamaci, U., & Peksel, A. (2020). Fabrication of PVA-chitosan-based nanofibers for phytase immobilization to enhance enzymatic activity. *International Journal of Biological Macromolecules*, *164*, 3315–3322. https://doi.org/10.1016/j.ijbiomac.2020.08.226

99. Canbolat, M. F., Savas, H. B., & Gultekin, F. (2017). Enzymatic behavior of laccase following interaction with γ-CD and immobilization into PCL nanofibers. *Analytical Biochemistry*, *528*, 13–18. https://doi.org/10.1016/j.ab.2017.04.005
100. Afshari, E., Mazinani, S., Ranaei-Siadat, S. O., & Ghomi, H. (2016). Surface modification of polyvinyl alcohol/malonic acid nanofibers by gaseous dielectric barrier discharge plasma for glucose oxidase immobilization. *Applied Surface Science*, *385*, 349–355. https://doi.org/10.1016/j.apsusc.2016.05.119
101. Li, J., Chen, X., Xu, D., & Pan, K. (2019). Immobilization of horseradish peroxidase on electrospun magnetic nanofibers for phenol removal. *Ecotoxicology and Environmental Safety*, *170*, 716–721. https://doi.org/10.1016/j.ecoenv.2018.12.043
102. Dai, Y., Yao, J., Song, Y., Liu, X., Wang, S., & Yuan, Y. (2016). Enhanced performance of immobilized laccase in electrospun fibrous membranes by carbon nanotubes modification and its application for bisphenol a removal from water. *Journal of Hazardous Materials*, *317*, 485–493. https://doi.org/10.1016/j.jhazmat.2016.06.017
103. Alonso-González, M., Corral-González, A., Felix, M. Romero, A., & Martin-Alfonso, J. E., (2020). Developing active poly(vinyl alcohol)-based membranes with encapsulated antimicrobial enzymes via electrospinning for food packaging. *International Journal of Biological Macromolecules*, *162*, 913–921. https://doi.org/10.1016/j.ijbiomac.2020.06.217



Havva Başkan was born in Trabzon, Turkey in 1988. She received B.Sc, M.Sc and Ph.D. degrees in textile engineering from Istanbul Technical University, in 2012, 2015 and 2021, respectively. Between 2019 and 2020, she conducted her Ph.D. studies in Ghent University in the Centre of Textile Science and Engineering in Belgium. In addition, she has been in Manchester, United Kingdom as a researcher for the European Project 'E-TEXWELD (H2020-MSCA-RISE-2014)'. From 2013-2021, she was a Research Assistant in Textile Technologies and Design Faculty, Istanbul Technical University. Since July 2021, she has been studying as a post-doc researcher in Sabancı University, Istanbul. She is the author of more than 10 research articles, 1 US-patent, 18 conference papers. Dr. Baskan was a recipient of the 8th International R&D Project Market Second Prize Winner in the field of 'Medical Textiles and Medical Devices'. In addition, she has worked as a researcher in four projects during her M.Sc and Ph.D. term. Her research interest includes electrospinning of nanofibers, biomedical applications of nanofibers, in-situ polymerization of conducting monomers, emulsion polymerization of polyacrylonitrile, and itaconic acid, in-situ fabrication of silver nanoparticles, upcycling of waste plastics for graphene production and sustainability.



Hale Karakaş was born in Istanbul, Turkey in 1971. She received a Ph.D. degree in 1999. Between 1991 and 2001, she worked as a Research Assistant and in 2005 she got the Associate Professor degree. From 2011, she has been working in Textile Technologies and Design Faculty, Istanbul Technical University as a professor. In addition, she was the vice dean of the Textile Technologies and Design Faculty in 2009 and 2015. She is the lecturer of fiber science, textile testing, textile quality and related lectures in Textile Technologies and Design Faculty, Istanbul Technical University. Moreover, she is the director of Innovative Technical Textiles, an MSc program. Moreover, she worked as an editor Tekstil & Teknoloji, Nonwoven Technology& Technical Textiles. Prof. Dr. Karakas was also a recipient of the 8th International R&D Project Market Second Prize Winner in the field of 'Medical Textiles and Medical Devices'. She managed 11 M.Sc and 3 Ph.D. thesis. She is the author of more than 25 research articles, more than 25 conference papers, 1 US-patent, 1 book, and 1 book chapter. She has worked on many projects both as an advisor and researcher. Her research interest includes technical textiles, nanotechnology, electrospinning, recycling, and sustainability.

Chapter 9
Biopolymeric Electrospun Nanofibers for Wound Dressings in Diabetic Patients



Paola I. Campa-Siqueiros, Maria M. Castillo-Ortega, Jaime López-Cervantes, Jesús Fernando Ayala-Zavala, David Servin de la Mora-López, and Tomas J. Madera-Santana

Abstract Skin wounds are one of the most common afflictions worldwide, caused by laceration or as a consequence of different diseases, such as diabetes. This disease represents around 2.1 trillion dollars in expenses to the global health sector. Diabetic patients have a compromised wound healing process, coupled with a high possibility of infection upon a skin wound. A solution is developing wound dressings with new technologies to obtain new and more efficient materials to deal with this problem. With breakthroughs in nanotechnology, certain materials, such as nanofibers, have been proposed to function as active wound dressings. Morphologically similar to the extracellular matrix, nanofibers are among the most promising candidates to renovate the concept of wound dressings due to their unique property of high volume-surface area ratio. Electrospinning is a process that can use a broad spectrum of polymers to produce nanofibers. Nevertheless, to help the environment, many assayed proposals for these wound dressings are manufactured from polymers, either natural or synthetic. A collection of studies concerning the use of biopolymeric electrospun nanofibers for wound dressings is reviewed in the present contribution.

Keywords Wound dressing · Diabetes · Biopolymer · Chitosan · Electrospinning

P. I. Campa-Siqueiros (✉) · J. F. Ayala-Zavala · D. S. de la Mora-López · T. J. Madera-Santana (✉)
Centro de Investigación en Alimentación y Desarrollo A.C., Hermosillo, Sonora, Mexico
e-mail: paola.campa@estudiantes.ciad.mx

T. J. Madera-Santana
e-mail: madera@ciad.mx

M. M. Castillo-Ortega
Universidad de Sonora, Hermosillo, Sonora, Mexico
e-mail: monica.castillo@unison.mx

J. López-Cervantes
Instituto Tecnológico de Sonora, Ciudad Obregón, Sonora, Mexico
e-mail: jlopez@itson.edu.mx

© The Author(s), under exclusive license to Springer Nature Switzerland AG 2022

A. Vaseashta and N. Bölgen (eds.), *Electrospun Nanofibers*,
https://doi.org/10.1007/978-3-030-99958-2_9

9.1 Introduction

It is estimated that by 2040, over 642 million people worldwide will suffer from diabetes *mellitus* [19]. The economic impact of diabetes is wide. In 2020, the estimated global diabetes healthcare expenditure was approximately 760 billion USD [145]. A big part of the economic burden of diabetes is directed towards the treatment of skin wounds. Of the different complications presented to patients by diabetes, chronic skin wounds are common since they possess a compromised healing process. Typically, in the phase of inflammation, cytokines, chemokines, macrophage, growth factors, and platelets react upon diverse cellular receptors to start the signaling cascades to induce healing. However, in diabetic patients, these singling cascades are compromised, and therefore, cell proliferation, differentiation, and migration are also compromised. As such, different materials have been researched and assayed to help the wound healing process. One of those alternatives are nanofibers obtained by electrospinning [22].

Electrospinning is a versatile, efficient, and cheap process, which can produce nanofibers from a broad spectrum of polymers. Additionally, the intrinsic high surface area to volume ratio enables nanofibers to carry on applications in various branches from the biomedical field, such as tissue regeneration, drug delivery, and wound dressings [16, 21, 31, 65, 110]. Biopolymers are one of the most popular materials for wound dressings. Chitosan and gelatin are two of the most studied natural biopolymers for use in wound dressings, especially for those intended for diabetic patients, because they have antimicrobial and biocompatibility properties [10, 38, 55, 56]. On the other hand, some of the most commonly assayed synthetic biopolymers for wound dressings are polymers polyvinyl alcohol (PVA), polylactic acid (PLA), and polycaprolactone (PCL). A selection of studies of different natural and synthetic biopolymeric electrospun nanofibers for wound healing proposes in diabetic patients is summarized in this contribution.

9.2 Diabetes Mellitus and Impaired Wound Healing

Diabetes mellitus (DM) was first reported about 3000 years ago in an Egyptian manuscript. In simple terms, DM is a group of metabolic disorders, which by the secretion or action of insulin, causes a chronic elevated blood glucose condition, also known as hyperglycemia. An average blood glucose level is between 68.4 and 109.8 mg/dL. However, when hyperglycemia is present, blood glucose levels in plasma can reach up to 200–300 mg/dL [6]. The system to maintain normal blood glucose levels is complex, involving the liver, skeletal muscle, brain, adipose tissue, and the interaction between hormones, most notably insulin signaling, and glucose uptake and disposal [133].

Generally, DM is classified into two types, Type 1 and Type 2, depending on insulin behavior. Type 1, also known as insulin-dependent DM, is characterized by

absolute insulin deficiency consequence of pancreatic β-cell destruction, causing the patient to depend on exogenous insulin to survive [92]. Type 2 DM is the most common, with an occurrence in around 90% of diabetic patients. Type 2 is non-insulin-dependent DM, which may combine reduced insulin secretion levels and insulin resistance. There are two effects present in this scenario: an impairment of the ability of insulin to stimulate glucose uptake and suppress hepatic glucose output, causing chronically elevated insulin levels, and a failure of the pancreatic β-cell to maintain the hyperinsulinemia state [133]. One of the most common complications of DM is chronic non-healing wounds.

The skin wound repair process is a piece of dynamic and complex machinery that comprises a highly organized cascade between biochemical and cellular events (Fig. 9.1a). Overall, this process can be divided into four overlapping phases: hemostasis, inflammation, proliferation, and remodeling [113]. Different cell types are present in each of these phases, such as platelets, neutrophils, and macrophages, where their role is to control the pro- and anti-inflammatory balance in the wound [15]. Of the different cells as mentioned above, monocyte-derived macrophages are crucial for this process. On the inflammatory phase, macrophages undergo a classical activation (M1), which activates the expression of different pro-inflammatory cytokines, such as inducible nitrous oxide synthase (iNOS), tumor necrosis factor α (TNFα), and interleukins 1β (IL-1β). IL-12 and IL-6. These cytokines induce the apoptosis and remotion of neutrophil and microbial pathogens from the wound [20, 67, 68]. As time passes, the environment of the wound shift to an anti-inflammatory state, so that tissue repair and remodeling can occur. At this time, alternatively activated macrophages (M2) activates the expression of anti-inflammatory and pro-healing factors, such as IL-10 and transforming growth factor β (TGF-β) [119], therefore initiating the next phase.

During proliferation, the extracellular matrix (ECM) serves as a network for endothelial cells (EC) and fibroblasts migration (granulation tissue) [70, 92]. In the latter stages of proliferation, the primitive ECM is steadily replaced by new blood vessels by the action of different factors, such as vascular endothelial growth factor (VEGF) and fibroblast growth factor (FGF) [92]. Remodeling is considered the "last" phase for the wound healing process, characterized by the action of matrix metalloproteinase (MMP) and tissue inhibitor of matrix metalloproteinase (TIMP) upon the granulation tissue. MMP degrade provisional constitutes, being collagen I, III, IV, and VII some examples, whereas TIMP stops this degradation [125]. However, in diabetic patients, the wound healing processes could be impaired.

If untreated, DM could lead to several complications, such as chronic non-healing wounds (Fig. 9.1b). As mentioned before, in this type of wound, the tissue environment is constantly entrapped in a pro-inflammatory state by the presence of proteases and pro-inflammatory cytokines, preventing growth factor expression necessary to heal the wound [119]. Even though the drive for macrophages to activate by either classical or alternative form is not entirely clear, it is believed that their transition from M1 to M2 is vital for the wound environment to shift to an anti-inflammatory state. In diabetic patients, the macrophage's shift to anti-inflammatory phenotype is impaired, thus inducing the constant pro-inflammatory environment in the wound

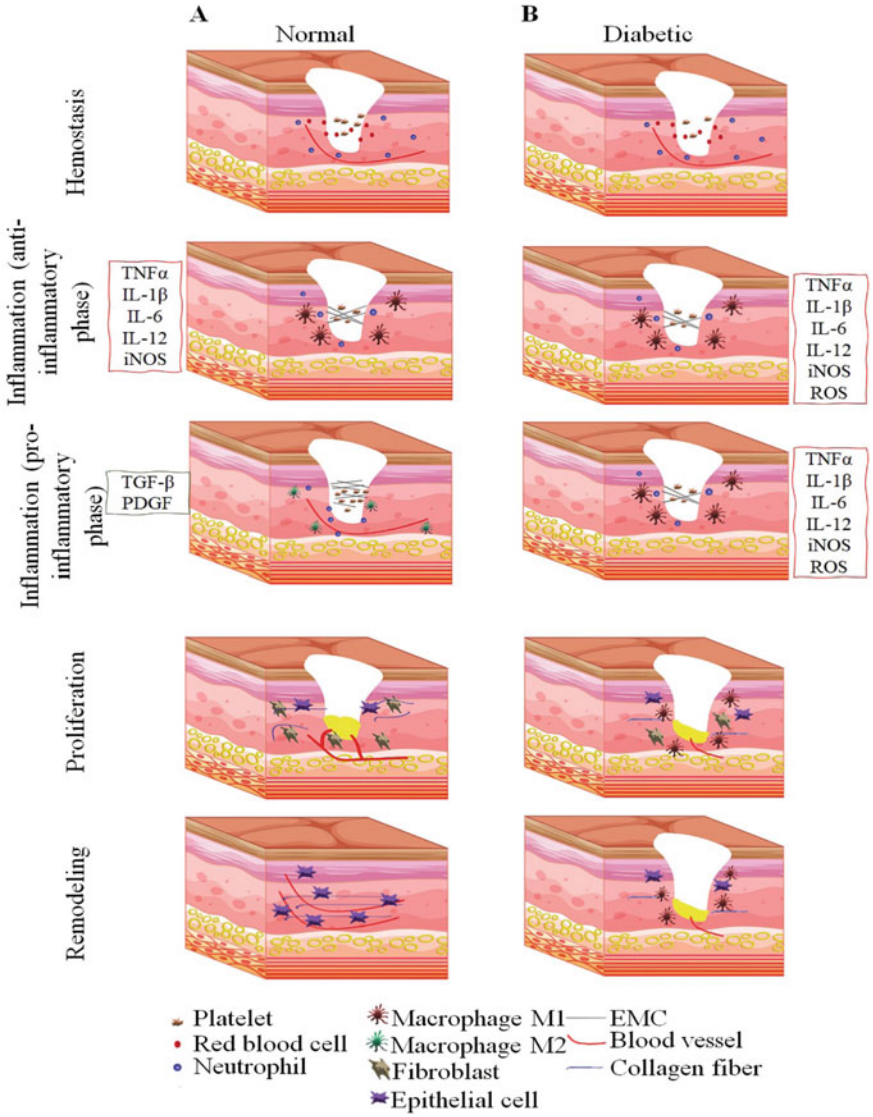


Fig. 9.1 The wound healing process in **a** healthy patient and **b** diabetic patient

and affects the proliferation phase [15]. Since macrophages are so critical for wound healing, they are a target for DM treatment studies. Al-Mulla et al. [8] studied the wound healing process upon Type II DM induced mice. These authors documented a change from the TGF-β singling pathway (anti-inflammatory) to the TNFα singling pathway (pro-inflammatory) in diabetic rats was in contrast with control. In this work

the treatment for skin wounds for diabetic patients using electrospun nanofibers for wound dressings are addressed.

9.3 Electrospun Nanofibers

Although the electrospinning technique was originated a century ago, it continues to be a simple, versatile, and viable alternative for the fabrication of continuous fibers ranging from micrometer to nanometer scales, with specifical diameters from 5 to 500 nm. Moreover, electrospinning has been widely employed to favor the processing of different polymers types and composite materials with controllable properties such as composition, diameters, porosities, and porous structures, in order to serve a wide variety of applications [27, 80, 147]. Some parameters can influence the fiber characteristics, such as solution properties like solvent type, concentration, viscosity, electrical conductivity, and surface tension; process parameters like the applied voltage, injection speed, needle-collector distance; and environmental factors, like humidity and temperature [32, 102].

Generally, the principle of this technique is based on an electrohydrodynamic process, where four critical systems are involved in carrying out the design and development of nanofibers (Fig. 9.2): A high-voltage power supply, a syringe pump to control the injection flow of the viscoelastic polymer solution, a spinneret consisting of a hypodermic needle with a blunt tip, and a collector system for the membranes [80, 150]. For a better understanding of the electrospinning technique, its operation has been divided into five steps: (i) the loading of the droplet from the viscoelastic solution; (ii) the formation of the cone-jet or also known as Taylor cone; (iii) the thinning of the jet as a consequence of the electrical charges provided by the power

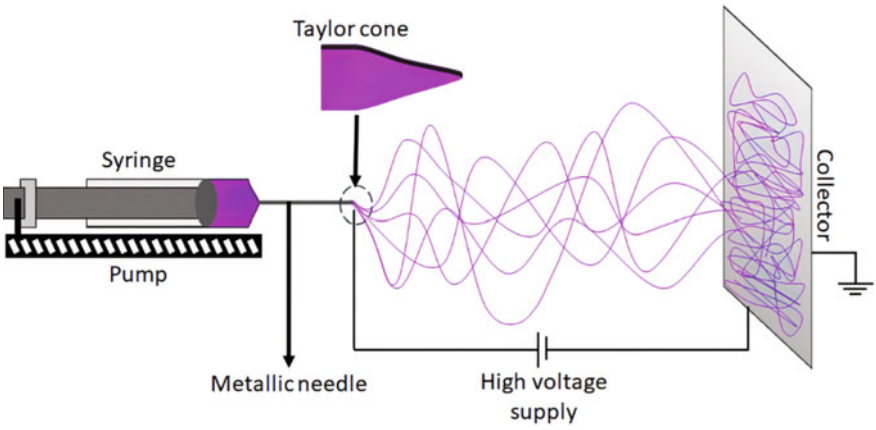


Fig. 9.2 Operation mode and components of the electrospinning system

source; (iv) elongation of the jet resulting in reductions of its diameter; and (v) collection of the solidified jet in a grounded collector [147].

The electrospinning principle could be explained as follows: The polymeric solution extruded from the spinneret begins to form a small spherical droplet due to surface tension. In conjunction, the high voltages supplied to the spinneret by the power supply build up charges of the same sign on the droplet surface to achieve electrostatic repulsion. If the repulsion is strong enough, it will surpass the surface tension, destabilizing the spherical shape of the droplet, giving way to a Taylor cone that will subsequently eject a jet of solution directed towards the collector system. Due to the high voltages supplied and the stretching given by the repulsions between the electrostatic charges, there is a continuous decrease in the jet size. As the jet stretches into finer sizes and diameters, evaporation of the solvent occurs, solidifying the jet and making its deposition in the collector system for the fibers generation with ultrafine diameters [80, 135, 149, 150].

As a result of this process, the fabrication of uniform and continuous polymeric nanofibers can be achieved in an electrospinning process when the solution concentration and processing parameters are appropriately chosen. Due to the high porosity and surface area/volume ratio, nanofibers have been applied in many areas, specifically in biomedicine, such as antimicrobial meshes, sponges for hemostasis, wound dressings, and drug delivery [79]. Furthermore, electrospun nanofibers have been found to exhibit good oxygen permeability properties, protection against infections, and healing promotion in moist environments [46]. The interest for using these materials in biomedicine arose thanks to electrospinning possessing the ability to create nanometric structures with mechanical and biological properties very similar to the extracellular matrix (ECM) of the skin [121]. The ECM is structured at the nanoscale and can function as a support element to sustain and bind cells in tissues. According to Chen et al. [30], the nanofibrous structure confers a better regenerative effect on tissues, since instead of interacting at cellular levels like most biomaterials, nanofibers can interact with the fibrillar structure of the ECM, leading to cells being able to bind better and organize around fibers with diameters smaller than them.

Several studies have shown that the morphology and cell growth of the ECM have a substantial impact depending on the material size [57]. Likewise, it has been shown that micro- and nanostructured materials, such as electrospun nanofibers, can contribute to the healing process, as they promote more efficient cell attachment, proliferation, and migration processes [57, 79]. Generally, skin ECM is constituted by fibrous structural proteins such as collagen, fibronectin, elastin, and laminin, as well as different kinds of polysaccharides, proteoglycans, and glycosaminoglycans, with fiber diameters ranging from 50 to 150 nm [28, 57]. Thanks to these characteristics, current research has opted to model and fabricate electrospun nanofibers based on the components, diameters, and dimensions possessed by natural ECM to mimic their structural and functional properties, helping these biomaterials to act as substitutes for the skin. Currently, a large number of polymers, both natural and synthetic, that can act as support materials and interact directly with the ECM of the skin during the wound healing process, have been used. However, in the present chapter, only those

polymers that have become more important in recent years and studied extensively will be considered.

9.3.1 Natural Biopolymers

9.3.1.1 Chitosan

Thanks to its antimicrobial, antifungal, biodegradable, biocompatible properties, and in addition to its adherent and non-toxic nature, chitosan has proved to be a polymer of great interest in biomedicine for the development of materials aimed at wound healing [82, 140]. Chitosan is a polymer derived from chitin by deacetylation processes, consisting of totally or partially removing the acetyl groups present in chitin using solid alkalis at high temperatures [72, 86]. Chitosan is naturally distributed in chitin and can be obtained from exoskeletons of crustaceans, insects, and fungi cell walls [5]. It is insoluble in water, but soluble in organic acids such as formic, tartaric, acetic, or citric acid [86]. The properties of chitosan are regularly associated with its degree of deacetylation, molecular weight, and the ionic forces it has molecularly [41].

Chitosan's importance in biomedicine lies in the fact that it is structurally composed of linear chains of β-(1–4)-D-glucosamine and N-acetyl-D-glucosamine units, as observed in Fig. 9.3 [140]. The amino groups present in the main chain are responsible for giving chitosan its functional properties [87]. One of the essential chitosan characteristics is its highly cationic nature, which confers its antimicrobial properties [50]. Several investigations have reported that chitosan can act against several genera of Gram (+) and Gram (−) bacteria, including those found in diabetic wounds, such as *Staphylococcus aureus*, present in 80–90% of mild skin lesions, and some genera of *Enterococcus* spp. and *Pseudomonas* spp. responsible for severe to moderate infections, such as the case of diabetic ulcers [41]. It has been hypothesized that chitosan's antibacterial mechanism is due to, when in acidic conditions, its positively charged NH_3^+ amino groups interact with the negative charges from the bacterial cell walls, producing electrostatic forces resulting in wall lysis, leading to the loss of intracellular compounds [50]. Thanks to this effect, chitosan has been widely studied to treat all types of wound infections.

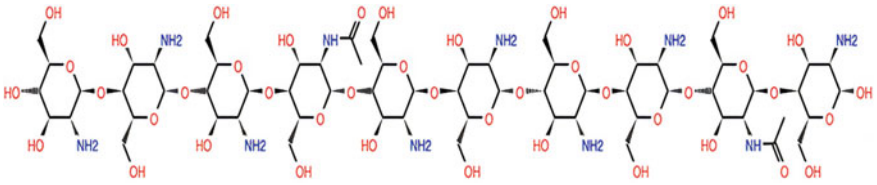


Fig. 9.3 Chitosan chemical structure

On the other hand, its biocompatibility and biodegradability properties have made chitosan show positive effects on wound healing [56]. Generally, there are some proteases and lysozymes in human lymphoid tissue that can degrade chitosan in vivo, to produce N-acetylglucosamine and N-glucosamine molecules, which result from very similar components–structurally–to glycosaminoglycans found naturally in native tissues [34, 59, 116]. In addition, according to Jayakumar et al. [56], the positive charges of the amino groups of chitosan help form electrostatic interactions with glycosaminoglycans to attract growth factors that promote cell development and proliferation. Likewise, Jiang et al. [59] mention that due to the biocompatibility of chitosan, it can promote adhesion and proliferation of different cell types, such as fibroblasts, osteoblasts, chondrocytes, endothelial cells, neuronal cells, and hepatocytes, without causing adverse effects. Kalantari et al. [61] mentioned chitosan could trigger macrophage activation and accelerate healing processes. They also point out that it can promote granulation tissue synthesis while inducing the early stage of healing through polymorphonuclear neutrophil migration (PNM) and collagen synthesis by fibroblasts. This has caused chitosan to show favorable effects upon re-epithelialization and restructuring the granular layer of the skin in several studies.

In order to take advantage of its properties, chitosan has recently been used as an object of study to treat various clinical pathologies associated with cutaneous wounds. Escárcega-Galaz et al. [41] applied chitosan to different diabetic patients presenting long-standing skin ulcers with second and third degree risks of the Wagner scale. The studies revealed that all patients presented a significant improvement, where granulation tissues and a healthy skin cover were developed without presenting infections or other adverse effects. Another study by López-Cervantes et al. [82] showed the effectiveness of using chitosan in diabetic patients with chronic infected skin ulcers that did not respond to traditional curative treatments. In vivo trials showed that at the end of treatment, chitosan was able to suppress all types of infections while promoting granulation tissues and complete healing in all patients, none of whom had adverse reactions.

Chitosan is well known for its wound-healing capabilities. It has been considered a suitable material for developing antimicrobial dressings, including its potential processing for electrospun nanofiber-based membranes. Because the structures of nanofibrous membranes are very similar to ECM, it is possible to improve further wound healing processes [61]. However, chitosan processing of electrospun nanofibers cannot be considered as easy. As explained before, chitosan possesses free positively charged amino groups, which causes an increased surface tension in the solution. When chitosan is subjected to electric fields, the strong hydrogen bonds it possesses favor the formation of three-dimensional network capable of restricting the movements caused by its polymeric chains. However, the aggregation of some water-soluble polymers, including ethylene oxide (EO), polyvinyl alcohol (PVA), methyl cellulose (MC), and polyvinylpyrrolidone (PVP), could be introduced into acetic acid solutions to help the processing of electrospun chitosan nanofibers [61, 126]. Recently, some studies for the development of electrospun nanofibers based on chitosan have been published. Chitosan presents a high capacity to treat various chronic conditions. One of the conditions is skin wounds caused by

diabetes. As presented before, chitosan presents antimicrobial and therapeutic properties, conferred to its ability to rapidly eliminate infections caused by various kinds of bacteria and considerably reducing the wound sizes until it heals completely. As a result, nanofibers based on this polymer for application as wound dressings have been developed, some of the most relevant research are summarized in Table 9.1.

Through a study, Majd et al. [85] elaborated electrospun chitosan and PVA nanofibers with average fiber diameters of 279.84 nm from voltage conditions of 18 kV, the injection rate of 0.35 ml/h, and a needle-collector distance of 15 cm. The processed biomaterials were treated in streptozotocin-induced diabetic rats with

Table 9.1 Development of chitosan-based electrospun nanofibers for potential applications as wound dressings

Nanofiber composition	Application	References
Chitosan/PVA	Wound dressing for streptozotocin-induced diabetic rats	[85]
Chitosan/PEO	Full-thickness wound dressings	[49]
Chitosan/PVA/Zinc oxide	Antibacterial dressings for diabetic wounds	[4]
Chitosan/PVA with tranexamic acid (TXA) incorporation	Hemostatic dressings	[123]
PVA/chitosan with carboxymethyl chitosan nanoparticles for antibacterial encapsulation of OH-CATH30	Antibacterial dressings for full-thickness wounds	[160]
Chitosan/PVA loaded with sulfanilamide and decorated with silver nanoparticles	Antibacterial dressings for full-thickness wounds	[45]
Chitosan/PCL	Antibacterial wound dressings	[143]
Quartenized chitosan / PLA	Antibacterial dressings for full-thickness wounds	[115]
Chitosan/PEO with the addition of green tea extract	Anti-inflammatory and antibacterial dressings for full-thickness wounds	[118]
ChitosanEDTA/PVA loaded with lysozyme	Full-thickness wound dressings	[26]
Chitosan/Silk fibroin	Antibacterial wound dressings	[23]
Chitosan/PEO with Henna leaves extract	Antibacterial dressings for full-thickness wounds	[152]
Chitosan/PVA loaded with tetracycline hydrochloride	Antibacterial wound dressings	[7]
Chitosan with bromelain incorporation	Second-degree burns dressings	[18]
Chitosan/PEO/human recombinant collagen peptide cross-linked with carbodiimide hydrochloride	Second-degree burns dressings	[36]
Chitosan/sericin	Antibacterial wound dressings	[157]
Chitosan/honey/PVA with *Allium sativum* and *Cleome droserifolia* extracts	Antibacterial wound dressings	[122]

wound dimensions of 1 * 1 cm^2. The study observations were evaluated within 4, 7, and 14 days of treatment. In vivo studies revealed that the average wound areas were 76 mm^2 at day seven and decreased to 0 mm^2 by day 14 of treatment. Microscopic observations indicated granulation tissue and angiogenesis on day 7, and by day 14, the epidermal layer was restored while no remaining scar formed and complete wound closure was achieved.

Ahmed et al. [4] developed and characterized mats based on electrospun nanofibers composed of chitosan, PVA, and Zinc oxide (ZnO). These authors used a needle-collector distance of 7 cm and an injection rate of 0.5 ml/h, obtaining fibers with average diameters of 891.72 nm. The materials were tested in vivo on diabetes-induced rabbits presenting skin wounds and wound healing evolution was registered at 4, 8, and 12 days of treatment. According to the results obtained, the chitosan/PVA/ZnO nanofibers showed a high antioxidant capacity and antibacterial effect against *E. coli*, *P. aeruginosa*, *B. subtilis,* and S. *aureus*. In vivo analysis showed a 90.5% decrease in wound contraction at day 12 of treatment. Histopathological studies indicated that by day 4, early granulation tissue formation with acute inflammatory exudate material had already occurred, and by day 8, this had been significantly reduced. By day 12, the epidermis and wound scar tissue had regenerated entirely with evidence of mature granulation tissue. These results demonstrated that chitosan/PVA/ZnO nanofibers possess high antibacterial efficacy and antioxidant capacity, which could be used as very promising wound dressings for diabetic wound applications due to their characteristic of promoting wound contraction in short times periods.

Through another study, Charernsriwilaiwat et al. [26] prepared nanofiber mats based on chitosan, EDTA, PVA with the incorporation of lysozyme. The operating conditions corresponding to the voltage used, injection rate, and needle-collector distance were 15 kV, 20 cm, and 0.25 ml/h, respectively. The material was evaluated in vivo as a dressing upon rats presenting full-thickness wounds of 0.8 cm^2. The evolution of the wounds was evaluated under observation at 1, 4, 7, and 10 days after surgery. The in vitro release study showed that 90% of the lysozyme present in the chitosan-EDTA/PVA membranes was effectively released during the first 4 h by polymer erosion and lysozyme diffusion mechanisms. In vivo test, chitosan-EDTA/PVA mats loaded with 30% lysozyme with average diameters of 143.65 nm were used. It was noted that by day 10 of treatment, the wound closure gradually increased until it reached 2% of the total wound area. This research demonstrated that chitosan-EDTA/PVA mats with lysozyme have better healing capabilities than traditional gauze and commercial antimicrobial gauze.

On the other hand, Ganesh et al. [45] achieved antibacterial chitosan/PVA nanofibers loaded with sulfanilamide and decorated with silver nanoparticles (NPsAg). Using voltages of 15 kV, a needle-collector distance of 15 cm, and an injection rate of 0.5 ml/min, they could generate fibers with average diameters of 150 nm, which were subsequently tested in vivo in rats with full-thickness wounds of 2 cm^2. The scheduled times for wound evolution observation were 7, 14, and 21 days after surgery. In vitro release profiles revealed that the cumulative release rates for both sulfanilamide and NpsAG on the nanofibers, were found to be 99%

after 24 h. Antimicrobial assays showed that the dressings had strong antibacterial activity against *S. aureus*, *E. coli,* and *P. aeruginosa* with inhibition zones of 11.58 mm, 15.21 mm, and 13.45 mm, respectively. In vivo studies, chitosan/PVA nanofibers loaded with sulfanilamide and NpsAG showed higher healing rates than control (chitosan/PVA). At 7 days of treatment, the wound closure rate had already reached 90.76%, and epithelialization had been completed, resulting in complete wound healing by day 21. The authors mention that the accelerated healing could be due to the nanofibrous matrices promoting cellular union and proliferation thanks to the prolonged drug release times. Both NPsAG and sulfanilamide formed complexes more easily across the cell membrane which leads to effective synergistic healing with antimicrobial functions.

9.3.1.2 Gelatin

Gelatin is known to be a natural biopolymer obtained from the partial hydrolysis of insoluble fibrous collagen from porcine or bovine tissues by acidic (Type A) or basic (Type B) treatments [64, 93]. Collagen is considered to be the structural protein of skin, bones, tendons, cartilage, and connective tissues from animals [96]. Gelatin consists of a triple helix protein structure with highly extended polypeptide chains [90]. Generally, it consists of three polypeptide chains where every third amino acid is glycine, while the other two must be proline and 4-hydroxyproline residues [103].

Gelatin and collagen share the same biocompatibility characteristics, with the only difference being the reduced production costs for gelatin. Because of this, gelatin has been used in various biomedical applications, mainly for its potential to be applied as a wound dressing or a drug delivery system [96]. Such applications are possible due to its hemostatic, adherent properties, high biocompatibility, low antigenicity and cytotoxicity, stable biodegradability, and its functions of promoting cell proliferation, adhesion and growth processes [46, 53]. Also, it has been shown that gelatin can trigger macrophage activation functions [42]. The wound healing effectiveness of gelatin may be due to its structure being arginine-glycine-aspartate sequences responsible for providing cell adhesion sites. In addition, it has a large number of glycine-proline-hydroxyproline sequences that are responsible for stimulating and accelerating soft tissue and wound healing [151]. These peptide sequences allow the integrin receptors in the cells to recognize them to carry out the process of adhesion and cell regeneration [158]. Besides, it has been proven that gelatin has been used to control bleeding in surgical procedures. It has also been used as a porous membrane to absorb many exudates and help moist environments during wound healing [46]. According to Wang et al. [144], gelatin has the functionality of absorbing excess exudate thanks to its ability to retain water 5–10 times its weight. However, it has been proven the main disadvantage of gelatin is that it does not have the antimicrobial capacity to prevent wound infections [64].

Gelatin has been widely used for film formation. On the other hand, it has proven to be very poor for processing electrospun nanofibers, as their handling practices by conventional wet/dry spinning are not very common nowadays [155]. Besides,

they result from fibrous structures that are highly soluble in aqueous environments and mechanically weak at 37 °C in the human body, so their applications may be limited in tissue engineering. These characteristics could be solved by modifying gelatin with functional groups and using common cross-linking agents such as glutaraldehyde, bis epoxies, or water-soluble carbodiimide, which could improve the water-resistance capacity as well as the thermomechanical properties of the resulting nanofibers [3, 155]. Likewise, the use of different types of synthetic hydrophobic polymers combined with gelatin for the formation of nanofibers with tissue-mimetic viscoelastic characteristics, with good mechanical strength, elastic and swelling properties has been reported. Some of the most commonly used include polyurethane (PU), polycaprolactone (PCL), and polylactic acid (PLA) [154]. Recently, gelatin-based electrospun matrices for application as wound dressings have been successfully developed. Some of their most relevant contributions are listed in Table 9.2.

Currently, the effectiveness of using gelatin-based nanofibers in different types of wounds, including diabetic wounds [120], deep burns [127], and full-thickness wounds [49], has been proven. [108] demonstrated, through in vitro study, that electrospun gelatin nanofibers promote high cell viability and organization and excellent barrier formation, which are favorable for use as skin substitutes. Through several in vivo investigations, it has been effectively proven that gelatin nanofibers possess a

Table 9.2 Development of gelatin-based electrospun nanofibers for potential applications as wound dressings

Nanofiber composition	Application	References
Cellulose acetate/gelatin with berberine incorporation	Antibacterial dressings for streptozotocin-induced full-thickness diabetic wounds	[120]
Gelatin/PVA with cephradine inclusion	Diabetic wound dressings	[112]
Gelatin/keratin/polyurethane	Full-thickness wound dressings	[151]
PCL/gelatin with lawsone incorporation	Wound dressings	[1, 2]
Gelatin cross-linked with glutaraldehyde	Full-thickness wound dressings	[49]
Gelatin cross-linked with 1,4-butanediol diglycidyl ether	Wound dressings	[37]
Gelatin/PCL with cerium oxide nanoparticles	Full-thickness wound dressings	[95]
Silk fibroin/gelatin with astragaloside IV	Partial-thickness burn dressings	[127]
Gelatin cross-linked with glutaraldehyde and the addition of vitamins A and E	Antibacterial dressings for full-thickness wounds	[75]
PCL/gelatin with taurine incorporation and cross-linked with carbodiimide	Full-thickness wound dressings	[44]
PCL/gelatin with trimethoxysilylpropyl octadecyl dimethyl ammonium chloride inclusion	Antibacterial wound dressings	[128]
Gelatin/PLC with silicate-based nanoparticles (Nagelschmidtite)	Full-thickness diabetic wounds dressings	[84]

regenerative effect on full-thickness wounds through the rapid synthesis of granulation and epithelialization tissue [49]. Similarly, very favorable results when treating wounds employing gelatin nanofibers with cross-linking agents such as glutaraldehyde [49], 1,4-butanediol diglycidyl ether [37], and carbodiimide [44] have been obtained.

In research conducted by Razzaq et al. [112], using voltages of 30 kV, needle-collector distance of 14 cm, and an injection rate of 1 ml/h, they were able to obtain average diameters of 350 nm in a nanofiber-based on gelatin, PVA with the incorporation of cephradine as an antibacterial agent. The nanofibers were evaluated in vitro and in vivo to demonstrate their efficiency as a dressing for healing chronic diabetic wounds infected by resistant *S. aureus* in mice. They made 7 mm deep wounds and subsequently subjected them to doses of resistant *S. aureus* strains. The nanofibers were then placed, and the observations were taken at 1, 7, and 11 days of treatment. The gelatin/PVA nanofibers with cephradine incorporation exhibited strong antibacterial activity against resistant *S. aureus* in both in vivo and in vitro studies due to the rapid release of the drug able to prevent and decrease infections caused by this pathogen. In conjunction with the above, in vivo studies revealed that by day 7, the nanofibers affected 15% of healing, and by day 11, healing had advanced by approximately 65%. The elimination of infections caused by resistant *S. aureus* was verified on day 11 of treatment. The authors noted that the dressings they developed could be used safely and efficiently in clinical practice to eliminate infections associated with resistant *S. aureus* in chronic diabetic wounds.

Through a similar study, Samadian et al. [120] evaluated the effectiveness of using functional gelatin/cellulose acetate nanofibers with berberine incorporation in streptozotocin-induced diabetic foot ulcers in rats. The membranes were prepared under conditions of voltage, needle-collector distance, and injection rate of 15 kV, 15 cm, and 0.2 ml/h, respectively. The average diameters of the fibers obtained were approximately 502 nm. In vitro assays exhibited potent antibacterial activity against *S. aureus* and *P. aeruginosa* in the developed nanofibers. In vivo tests were performed on full-thickness wounds with an area of 2 mm * 5 mm, and were kept under treatment for 16 days. Advanced epidermal proliferation and epidermal layer enlargement were observed due to the high rate of collagen production and angiogenesis promoted by the developed nanofibers, which helped significantly improve the healing process. [120] stated that berberine has stimulatory effects to enhance the proliferation of L929 fibroblast cells, which are mainly responsible for releasing collagen production to promote epithelialization in diabetic foot ulcers. The authors also noted that the anti-diabetic, anti-inflammatory, antimicrobial and wound-healing effects were closely related to the aggregation of berberine in gelatin/cellulose acetate composite nanofibers, making its use as a dressing highly suitable for the management of ulcers and wounds related to diabetes.

On the other hand, to treat deep open wounds, [75] fabricated gelatin-based nanofibers to incorporate vitamins A and E, using glutaraldehyde as a cross-linking agent. The membranes were characterized in vitro and in vivo. Optimal processing conditions included voltages of 16 kV, needle-collector distance of 15 cm, and an injection rate of 0.6 ml/h to generate structures with average diameters of 566 nm.

In vitro studies showed strong inhibition against *E. coli* and *S. aureus*. Adhesion and proliferation of L929 fibroblasts improved in the early stages of culture when subjected to the nanofibers, promoting increased collagen production. Moreover, the elaborated nanofibers were evaluated in vivo in mice with deep open wounds dimensions of 3 cm * 3 cm. Wound evaluation was performed at 5, 14, and 21 days after surgery. The studies revealed that wound closure was almost complete by day 21 of treatment, achieving a rate of 10.3%. The authors noted that gelatin nanofibers loaded with vitamin A and E can act as excellent antibacterial dressings to treat wounds more efficiently than the commercial gauze that has been used for this purpose.

9.3.2 Synthetic Polymers

Electrospinning may be a valuable method to produce polymeric nanofibers, to be utilized as scaffolds for tissue engineering applications at micro or nanoscale using natural or synthetic polymers [94]. Synthetic polymers have presented highly better mechanical properties than natural polymers, however, blending synthetic polymers with natural polymers can improve desirable properties in the electrospun fibers, such as biocompatibility, morphology, processability, mechanical strength, among other characteristics [138]. Over time, it can be noted that there is a general trend in developing polymers worldwide, as seen in Fig. 9.4. Currently, there is a focus on environmentally friendly polymers that are biodegradable at the end of their use, have a minimal carbon footprint, and are sustainable. At the end of the last century, the development of biodegradable polymers began, which comprise two major groups:

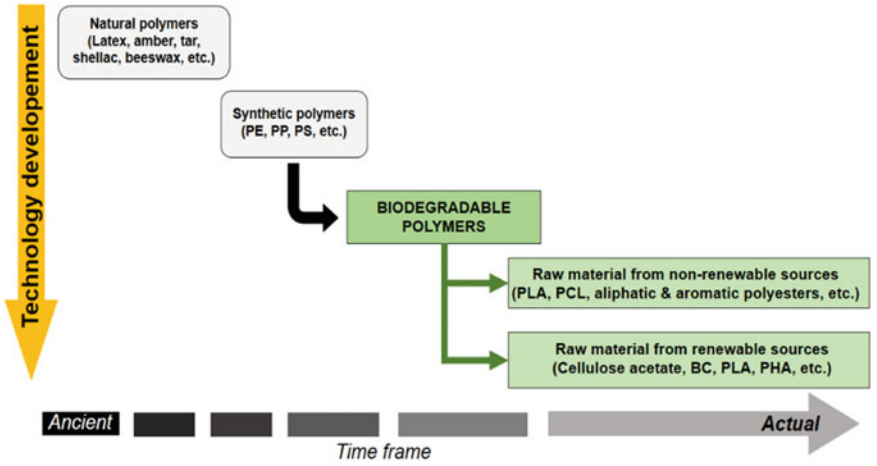


Fig. 9.4 Time frame in polymer development in the world. Abbreviations; PE—Polyethylene, PP—Polypropylene, PS—Polystyrene, PLA—Polylactiv acid, PCLPolycaprolactone, BC—Bacterial cellulose, Polyhydroxyalkanoates

Table 9.3 Commercial wound dressing products containing PVA, PLA, and PCL

Biodegradable polymer	Commercial product	Application	References
PVA	Cultinova gel and dressing, Biolex™ wound gel, Tegagel™, Tegaderm™, Nu-Gel™, Polyskin™, Silon-TSR®, Silon® dual–dress 50	Ulcers Chemotherapy peels Wound dressings Skin replacement Antimicrobial dressings	[62] [83] [12]
PLA	Dermlin (Yanssen, China), Rapidsorb® plates, Vicryl®, Dearmagraft®	Sutures anchors Skin substitutes Wound healing Tissue augmentation Scaffolds	[78] [54] [107]
PCL	MONOCRYLs®, SynBiosys®, DermaGraft™ (Organogenesis, Inc.), Proceed® (Ethicon Inc.), Capronor®, Urolon™ (Aqlane Medical Inc.)	Contraceptive pad Sutures (as a coating) Tissue repair Surgical mesh (dressing) Adhesion barriers Scaffolds for tissue engineering	[111] [78] [58] [139]

those from non-renewable resources and those from renewable resources. Some of these polymers have been shown to possess very particular characteristics and offer a significant performance when used to manufacture biomaterials by electrospinning.

The following is an overview of the uses of the biodegradable polymers polyvinyl alcohol (PVA), polylactic acid (PLA), and polycaprolactone (PCL); these biodegradable polymers are commercial and have been used for the development of biomaterials (wound dressings, sutures, contraceptive implants). These polymers have gathered particular attention since they do not require long-term biocompatibility, remain temporarily in the body and disappear upon biodegradation or by water dissolution. They also do not require a secondary surgery or medical procedure to remove from the patient [89, 153]. Table 9.3 describes some commercial dressings based on PVA, PLA, and PCL for wound dressings and other biomedical applications.

9.3.2.1 Polyvinyl Alcohol (PVA)

Polyvinyl alcohol (PVA or PVOH) is a semicrystalline linear synthetic polymer, with biodegradable, non-toxic, biocompatible, noncarcinogenic, bio-adhesive characteristic, low cost, and with remarkable optical properties [11]. PVA is synthetized from partial or complete hydrolysis of polyvinyl acetate (PVAc). During the synthesis reaction, the acetate groups are removed (Fig. 9.5a, b). The degree of hydroxylation determines the physical, chemical, and mechanical properties of PVA. PVA is a water-soluble polymer (WSP) and low or null solubility to organic solvents. Its electrical, optical, and mechanical properties have made PVA a polymer for biomedical use. Among its applications in this sector, are contact lenses, eye drops, surgical

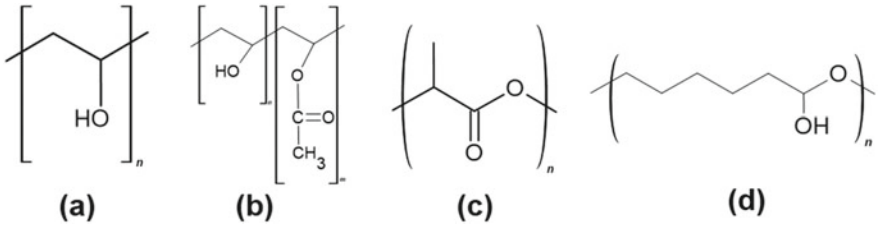


Fig. 9.5 Chemical structures of synthetic polymers used in electrospun process, **a** PVA monomer (completely hydrolyzed), **b** PVA partially hydrolyzed, **c** PLA, and **d** PCL

sponges, artificial cartilage, vascular embolic agents, tissue adhesion barrier [17]. Micro and nanofibers of PVA can be produced by electrospinning [25], however, the molecular weight of PVA has a significant effect on the nanofibers' diameter over viscosity, solution concentration, and conductivity. The high hydrophilicity of PVA shows a disadvantage when electrospun fibers are in contact with water; a solution to this is to modify PVA using other biopolymers and its modification by chemical or physical methods. Table 9.4 summarizes the development of wound dressing based on PVA.

9.3.2.2 Polylactic Acid (PLA)

PLA is a plastic produced from renewable sources, biodegradable and biocompatible, which is widely used in biomedical applications. Renewable sources used for PLA synthesis are corn, wheat, and sorghum [74]. The chemical synthesis of the lactic acid (LA) monomer at the industrial production level follows three routes: (1) the Acrylonitrile method, (2) the Lactonitrile method, and (3) Propionic acid method [13, 74]. To produce high molecular weight PLA (>10,000 Da), three synthesis methods can be followed: (1) ring-opening polymerization (ROP) after lactide formation, (2) solid-state or direct condensation, (3) azeotropic dehydration condensation [131].

Lactic acid, is a chiral molecule, where its two isomers, D-lactic acid and L-lactic acid, can synthesize three different polymer structures: poly-L-lactic acid (PLLA), poly-D-lactic acid, and poly-D, L-lactic acid (PDLLA) (Fig. 9.5c). The L-lactic acid is a stereoisomer of lactic acid, the polymerized polymer PLLA, which is more commonly used for medical applications than PDLA. PLA and its copolymers have been approved by U.S. Food and Drug Administration (FDA) as generally recognized as safe (GRAS) and European regulatory authorities for use in the food and drug-delivery systems [74, 97]. The first applications of PLA in biomaterials date back to 1966 when Kulkarni made the first medical application of poly(L-lactic acid) (PLLA) [69] in biomaterials. Subsequently, the use of PLA in other biomaterials such as sutures and orthopedic fixations was extended [35].

PLA has good biocompatibility, biodegradability, non-toxicity, antibacterial, and hydrophobic; for these reasons, the wide use of this polymer has extended to the

Table 9.4 Electrospun micro and nanofibers based on PVA, solvents, process parameters, and applications

Polymer system	Solvent	Process parameters	Average fiber diameter (nm)	Application	References
Sol PVA 6% w/v and sol. Carboxyethyl chitosan (CECS) 6% w/v. CECS/PVA ratios from 100/0 to 0/100	Dist. water	Voltage: 25 kV Flow rate: 0.1 mL/h Distance: 12 cm Needle diameter: 0.57 mm	131–456	CECS/PVA fiber mats with mouse fibroblasts (L929) showed no cytotoxicity and had good in vitro biocompatibility	[159]
Sol. PVA 6% w/v with 0.1% connective tissue growth factor (CTGF) (as core). Sol. PLLA 10% w/v	Hot water for PVA Dichloromethane: dimethyl-formamide (1:9)	Voltage: 15 kV Flow rate: 0.5 mL/h Distance: 10 cm Coaxial needle	2600	PVA-PLLA membranes with CTGF showed that fibroblasts, keratinocytes, and endothelial cells were able to grow. The results demonstrated that CTGF loaded PLA-PVA membranes can be used for diabetic wound healing applications	[14]
Sol. PVA 7.2% w/v and sodium alginate 0.8 w/v	Distilled water Honey (acasia) at 0, 5, 10, 15, and 20% v/v	Voltage: 15 kV Flow rate: 0.4 mL/h Distance: 10 cm Needle diameter: 0.50 mm	379–528	The addition of honey in the nanofibers inhibited the growth of both $Gram^+$ and $Gram^-$ bacterium	[134]
Sol. PVA 9% w/v, sol. Chitosan 2% w/v, at 90:10 and 50:50	Distilled water (90 °C) Acetic acid Sol. starch (0, 5, 10, and 15% wt.)	Voltage: 25 kV Flow rate: 0.5 mL/h Distance: 13 cm	305–429	PVA/chitosan/starch nanofibers dressings showed high porosity and water absorption. The dressings showed antimicrobial efficiency against the $Gram^-$ (*E. coli*) and $Gram^+$ (*S. aureus*)	[2]

fields of biomedicine biomaterials. Several authors have reported the biocompatibility of PLA, where it did not show inflammatory reactions in the tissue where this polymer is in contact with the human body [74, 99]. The degradation process of PLA has an intermediate LA, which can be metabolized and is non-toxic to the human body, this process is used for drug release when PLA is a carrier. PLA has shown excellent performance to electrospun micro and nanofibers for scaffolds in tissue engineering and other biomedical applications. PLA electrospun fibers are used as wound dressings and scaffolds for tissue regeneration (cardiac, neural, blood vessels, bone) and to carry bioactive agents (antibiotics, antibacterial, anticancer drugs, dental materials, enzymes immobilization scaffolds). PLA and its copolymers polylactide-co-glycolide acid (PLGA) are biocompatible materials in living tissues and used to produce sutures, screws, pins, and scaffolds. In-gel form, PLA and PLGA are used with goserelin acetate and paclitaxel to treat breast or prostate cancer [137]. Table 9.5 shows polymeric systems based on PLA, to produce wound dressings with bioactive compounds at different processing parameters and their applications.

9.3.2.3 Polycaprolactone (PCL)

As with other polyesters, polycaprolactone or poly-ε-caprolactone (PCL) is synthetized by the ring-opening polymerization of e-caprolactone using octanoate as catalyst [146]. The majority of commercial biodegradable polyester is derived from carbohydrate and petroleum-based sources; however, polypropylene carbonate (PPC), poly-3-hydroxybutyrate (PHB), and polylactic acid (PLA) originate from renewable sources. PCL is an aliphatic semicrystalline polyester (Fig. 9.5d), with a glass transition temperature of −60 °C and a melting temperature between 59 and 64 °C [39]. At human body temperature (36 °C), this polymer is flexible (soft) but tough, which imparts good mechanical properties (high strength and elasticity). Due to its non-toxicity, biocompatibility, and bioabsorbable characteristics, the FDA has approved this polymer to be processed in diverse forms and shapes, such as resorbable wound sutures, drug delivery vehicles, and scaffolds for regenerative tissue therapy (skin wounds) [60, 91]. This polyester has a degradation time between 2 and 3 years, which is considered long compared to other biodegradable polyesters, this is because the PCL chain has CH_2 molecules which are hydrophobic [9, 40, 106].

To produce PCL scaffolds, different techniques can be used for porous scaffolds, by saturation and release of carbon dioxide (CO_2), porogen leaching, and fused deposition modeling (FDM) (porous 3D scaffold) [39, 88]. For the fabrication of fibrous PCL scaffolds, electrospinning, melt spinning, gel spinning, dry spinning, and wet or solution spinning could be used [101]. The electrospinning process is ruled by parameters related to solution properties, processing, and ambient conditions. The solution properties are related to the molecular weight of the polymer, type of solvent, and concentration. Several authors in the literature have reported PCL use with a molecular weight of 80 kDa to produce micro and nanofibers of PCL by electrospinning. Common solvents of PCL for electrospinning are dimethyl formamide (DMF), tetrahydrofuran (THF), dichloromethane (DCM), chloroform,

Table 9.5 Electrospun micro and nanofibers based on PLA. Process parameters fiber diameter and applications

Polymer system	Solvent	Process parameters	Average fiber diameter (nm)	Applications	References
Neat PLA Sol. 20% w/v	Chloroform	Voltage: 25 kV Flow rate: 0.1 mL/h Distance: 15 cm	1000–2000		[66]
Neat PLA Sol. 14% w/v	Chloroform: dimethyl-formamide (15:3)	Voltage: 13 kV Flow rate: 1.5 mL/h Distance: 20 cm	800–3000		[141]
Neat PLLA Sol. 6% w/v	Chloroform	Voltage: 45–50 kV Flow rate: 3–4 mL/h Distance: 18 cm	300–1000		[148]
PLA Sol. 6% and 8% w/v and Biotin (0, 1, 2, 3% w)	Chloroform: acetone (3:1)	Voltage: 15 kV Flow rate: 5–10 mL/h Distance: 10–12 cm Needle diameter: 0.26–0.41 mm	200–5000	The nanofiber substrate showed a decrease in the fiber diameter as biotin loading increases functionalization of the PLA electrospun nanofibers for specific capture and detection of environmental pathogens	[73]
Sol. PLA 2.80 g in 20 mL of dichloromethane, Sol. γ-PGA 3.60 g in 20 mL acetic acid	Chloroform Coaxial spinneret Bioactive compounds: rhodamine and coumarin-6 (0.0005 g each)	Voltage: 25 kV Flow rate: 1 mL/h (shell), 0.2–0.6 mL/h (core) Distance: 18 cm Needle diameter: 0.56 mm (core) and 1.47 mm (shell)	120–330	Core–shell nanofibers with γ-PGA, PLA as the core and shell, respectively; were prepared using coaxial electrospinning technology In vitro cytotoxicity experiments showed that nanofibrous scaffolds had good biocompatibility and cell proliferation	[43]

(continued)

Table 9.5 (continued)

Polymer system	Solvent	Process parameters	Average fiber diameter (nm)	Applications	References
Sol. PLA 6% w/v in dichloromethane, Sol. 6% w/v cellulose acetate in dimethyl formamide	Dichloromethane N, N dimethyl formamide Bioactive compound: thymoquinone (TQ)	Voltage: 20–24 kV Flow rate: 1.5–3 mL/h Needle diameter: 27G	200–1000	The incorporation of cellulose acetate (CA) within the PLA matrix improved the physicochemical properties of the scaffolds PLA-CA with TQ-loaded showed significant antibacterial activity against *S. aureus* and *E.coli*	[48]
Sol. PLLA 0.6 g in 4.9 mL dichloromethane	Dichloromethane Active substance: Asiatic: acid (AA) (0–15 μM in methanol)	Voltage: 8 kV Flow rate: 0.02 mL/h Distance: 8 cm		PLLA electrospun fibrous scaffold with AA embedded was produced In vivo study demonstrated that 30 AA-PL had an excellent effect on accelerating re-epithelization, angiogenesis, and ECM formation	[52]
Sol. PLA-PCL (10–25%w/v)	Solvent mixture methylene chloride: N,N dimethyl formamide (100:0–50:50)	Voltage: 15–20 kV Flow rate: 0.2–1 mL/h Distance: 15 cm Needle diameter: 18G and 27G	750–900	The best formation of nanofibers was PLA-PCL 20% w/v in MC:DMF 70:30 PLA-PCL electrospun matrices are stable to 28 days in vitro degradation test	[105]
Sol. PLA 3% w/v) and Sol. PCL (12% w/v) (50:50)	Chloroform: dimethylformamide (7:3). Herbal drug thymol (1.2% v/v)	Voltage: 15 kV Flow rate: 0.7 mL/h Distance: 12 cm Needle diameter: 0.7 mm	288–373	Wound-dressing mats of PLA-PCL with thymol as an herbal drug showed anti-inflammatory and antibacterial properties	[63]

methanol, hexafluoroisopropanol (HFIP), 2,2,2-trifluoroethanol (TFE), hexafluoro-2-propanol (HFP), etc. Table 9.6 shows some PCL and PCL-blends used to produce wound dressings by electrospinning. PCL blends PCL-gelatin, PCL-chitosan, PCL-collagen, PCL-PLA-collagen, and PCL-PLA-gelatin-HA have been used as an electrospun scaffold [33, 51, 109, 124]. Roy et al. [117] reported PCL-natural silk fibroin (NSF) core–shell electrospun nanofibers, and they found that these showed better cytocompatibility and promoted cellular growth with the incorporation of NSF. PCL nanofibers, produced by electrospinning, show different morphologies and structures and incorporate different polymeric materials (biodegradable polymers) and active substances. PCL nanofibers for wound healing application have shown that the fiber scaffolds have a suitable stiffness, structural, and porosity; these characteristics facilitate cellular attachment, migration, proliferation, and differentiation [71]. Table 9.6 shows the solution properties, process parameters, and biological characteristics of PCL electrospun scaffolds.

9.4 Conclusion

Every year, the number of people diagnosed with diabetes rises worldwide, putting a strain on health-care spending. Patients have skin lesions that require therapy, which can develop to complications that necessitate surgery. In this sense, several authors have reported the development and use of dressings, which protect the wound and accelerate its healing. Dressings based on electrospun nanofibers are systems with diameters ranging from nanometers to micrometers, which allow the surface area to increase considerably and present different physicochemical properties. Electrospun nanofibers can contain within them chemical or biochemical active pharmaceutical ingredients (API), natural extracts, or stem cells; these can be dosed for the treatment of diabetic foot ulcers (DFU). In addition, they can perform crucial activities of exudate absorption, exchange of oxygen, water and other nutrients. Due to the similarity in diameter of nanofibers to the extracellular matrix (ECM), they allow oxygen exchange, promoting cell adhesion and proliferation and ECM reconstruction [81]. On the other hand, in the development of the dressings, particular attention has been focused to the materials used in their manufacture. These materials must be environmentally friendly, biodegradable, come from renewable sources and promote sustainability. One of the most important advantages of electrospun nanofibers made from biopolymers is that they meet the aforementioned characteristics. In addition, the use of these dressings for the treatment of skin wounds in patients with diabetes mellitus (DM) offers a practical and effective solution. This chapter has presented different studies that have reported the advantages of electrospun nanofibers for use as wound dressings for the treatment of cutaneous wounds in diabetic patients. The different alternatives for the manufacture of nanofibers shown in Table 9.1 indicate that electrospun nanofiber dressings owe their success largely to the type of biopolymer used in their manufacture. Therefore, we see that every day new dressing systems with bioactive compounds in electrospun nanofiber matrices with different

Table 9.6 Solution properties, process parameters, cell viability, and in vivo applications of PCL electrospun scaffolds

Polymer system	Solvent	Process parameters	Average fiber diameter (nm)	Membrane		Cell viability	In vivo application	References
				Area (mm^2)	Thickness (μm)			
PCL Sol. 10% w/v[a]	Chloroform: methanol (1:1)	Voltage: 12 kV Flow rate: 6 mL/h Distance: 30 cm Needle diameter: 1 mm	250		10	Begun beating after three days, cultured for 14 days	Implantation in rats	[129, 130]
PCL Sol. 14% w/v[a]	DMF:THF (1:1)	Voltage: 12 kV Flow rate: 0.4 mL/h Distance: 20 cm Needle diameter: 0.8 mm (18G)	500–900	100	~1000	Cultured for 21 days		[76, 77]

(continued)

Table 9.6 (continued)

Polymer system	Solvent	Process parameters	Average fiber diameter (nm)	Membrane		Cell viability	In vivo application	References
				Area (mm^2)	Thickness (μm)			
PCL Sol. 15% w/v[a]	Chloroform: ethanol (7:3)	Voltage: 12 kV Flow rate: 0.4 mL/h Distance: 20 cm Needle diameter: 0.8 mm (18G)	1900		200		In vivo articular cartilage repair of femoral condyles Implantation in the aorta of rats	[104]

(continued)

Table 9.6 (continued)

Polymer system	Solvent	Process parameters	Average fiber diameter (nm)	Membrane		Cell viability	In vivo application	References
				Area (mm^2)	Thickness (μm)			
PCL (a) Sol. 9.5% w/v[b] (b) Sol. 16% w/v[b]	(a) DCM: methanol (b) TFE: deionized H_2O	Voltage: (a) 13–15, (b) 16–18 kV Flow rate: (a) and (b) 1.51 mL/h Distance: (a) 9, (b) 14 cm Needle diameter: 0.4 mm (22G)	(a) 506 (b) 372			0, 3, 7, and 10 days	Biocompatibility test of subcutaneous implantation in rats. The monitoring of host response at weeks 1, 2, and 4	[24]

(continued)

Table 9.6 (continued)

Polymer system	Solvent	Process parameters	Average fiber diameter (nm)	Membrane		Cell viability	In vivo application	References
				Area (mm^2)	Thickness (μm)			
PCL Sol. 13 w/v	Chloroform: methanol (75:25)	Voltage: 15 kV Flow rate: 0.6 mL/h Distance: 12 cm Needle diameter: 0.8 mm (18G)	750		200	0–7 days	Implantation of electrospun PCL scaffolds into de brain of rats	[98]

(continued)

Table 9.6 (continued)

Polymer system	Solvent	Process parameters	Average fiber diameter (nm)	Membrane		Cell viability	In vivo application	References
				Area (mm^2)	Thickness (μm)			
PCL Sol. 15% w/v[a]	Chloroform:acetone (7:3), Chloroform: ethanol (3:1)	Voltage: 15–25 kV Flow rate: 12–24 mL/h Distance: 15–25 cm Needle diameter: 0.5 mm (21G)	From 200 to 1800	1–3 cm by side			A vascular graft was implanted as an abdominal aortic substitute in rats. After a 12-week implantation period, good patency, endothelization, and cell ingrowth were observed	[100]

(continued)

Table 9.6 (continued)

Polymer system	Solvent	Process parameters	Average fiber diameter (nm)	Membrane		Cell viability	In vivo application	References
				Area (mm^2)	Thickness (μm)			
PCL-gelatin Sol. PCL (10% w/v):gelatin (10% w/v). Mixture PCL:gelatin (5:5	TFE	Voltage: 20 kV Flow rate: 3 mL/h Distance: 18 cm	250–550		200	Nearly above 80%, non-toxic and cell proliferation during the 7 days of culture	PCL-gelatin nanofibrous membranes for potential application as GBR membranes. The gelatin improved wettability, cell viability and produced an enhancement in cell adhesion and proliferation	[114]
PCL-gelatin Sol. PCL (10% w/v)[a]: gelatin (type A) (10% w/v) (1:1)	TFE	Voltage: 10.5 kV Flow rate: 0.7 mL/h Distance: 15 cm Needle diameter: 0.4 mm	470	150 × 150 mm	28	Fibroblasts proliferate on both sides of the nanofiber scaffold. The optical density of the cells increased through the first 7 day span	This nanofibrous scaffold is a suitable dermal analog to assist in skin cover and regeneration	[31]

(continued)

Table 9.6 (continued)

Polymer system	Solvent	Process parameters	Average fiber diameter (nm)	Membrane		Cell viability	In vivo application	References
				Area (mm^2)	Thickness (μm)			
PCL-gelatin Sol. PCL (10% w/v)[a]: gelatin (type A) (10% w/v) (1:1)	TFE	Voltage: 0.5 kV/cm Flow rate: mL/h Distance: cm Needle diameter: 1 mm	~100	500		A relatively more significant number of cells on the gelatin/PCL scaffold than that of the PCL scaffold, 7 days	Gelatin component of PCL/gelatin scaffold is gradually dissolved during cell culture and produces empty space for cell migration	[156]
PCL-gelatin Sol. PCL (6% w/v)[a]: gelatin (type A) (10% w/v) (50:50 and 70:30)	HFP	Voltage: 12 kV Flow rate: 1 mL/h Needle diameter: 0.4 mm	431 (PCL) 113 (50:50) 189 (70:30)	500		The proliferation of cells on gelatin-containing scaffolds was higher than PCL scaffolds after 6 days of cell culture	PCL-gelatin (70:30) enhanced nerve differentiation and proliferation. Randomly oriented nanofibrous scaffolds are useful in tissue engineering	[47]

(continued)

Table 9.6 (continued)

Polymer system	Solvent	Process parameters	Average fiber diameter (nm)	Membrane		Cell viability	In vivo application	References
				Area (mm^2)	Thickness (μm)			
PCL-collagen Sol. PCL (10% w/v) and collagen (2.5% w/v)	HFP:chloroform (3:1)	Voltage: 10 kV Flow rate: 0.75 mL/h Distance: 15 cm Needle diameter: 0.5 mm (21G)	564 (PCL) 513 (PCL-collagen)	35 × 10		4–5 weeks in rabbit smooth muscle cells. The number of cells grown on the bottom face of the suspended nanofiber scaffolds increased after 2 weeks	In vitro data showed that the PCL/collagen better attachment, viability, and proliferative capacity than PCL	[29]

(continued)

Table 9.6 (continued)

Polymer system	Solvent	Process parameters	Average fiber diameter (nm)	Membrane		Cell viability	In vivo application	References
				Area (mm^2)	Thickness (μm)			
PCL-collagen Sol. PCL (10% w/v)[a] and collagen type I (10% w/v) (1:1)	DCM:DMF (75:25)	Voltage: 1 kV/cm Flow rate: 0.5 mL/h Needle diameter: 0.5 mm			100–120	Scaffold layers after 6 weeks of culture in the bioreactor disclosed dense cell arrangements accompanied by extracellular deposits	The multilayered scaffold was biocompatible and was fully integrated with the surrounding tissues with a cell density compared to the surrounding tissue	[132]
PCL-collagen Sol. PCL-collagen (1:1) crosslinked with 2.5% glutaraldehyde for 6 h	HFP	Voltage: 20 kV/cm Flow rate: 3 mL/h Distance: 10 cm Needle diameter: 0.8 mm (18G)		8 × 5	5	PCL-collagen electrospun scaffolds showed a high degree of patency and structural integrity in vivo without eliciting an abnormal inflammatory response (1 month)	The PCL-collagen scaffolds can support endothelial and muscle cell growth under pulsatile flow conditions	[136]

(continued)

Table 9.6 (continued)

Polymer system	Solvent	Process parameters	Average fiber diameter (nm)	Membrane		Cell viability	In vivo application	References
				Area (mm^2)	Thickness (μm)			
PCL-collagen Sol. 1: PCL (7.5% w/v), Sol. 2:PCL-collagen type I and III (40:20:10 mg/mL) Sol. 3: Collagen type I and III (80:40 mg/mL)	Sol 1: Chloroform: methanol (3:1) Sol. 2 and 3: HFP	Voltage: 12 kV Flow rate: 0.75 mL/h Distance: 13 cm Needle diameter: 0.21 mm (27G)	210–225		20	The proliferation of SMCs increased up to 63%, 73%, and 82% in modified PCL/collagen nanofiber scaffold compared to PCL nanofiber scaffold after 2, 4, and 6 days	PCL/collagen bio-composite nanofiber scaffolds influence cell adhesion, migration, and proliferation and support the formation of 3D blood vessels in vitro	[142]

GRB—guide bone regeneration
[a]PCL with a molecular weight of 80 kDa
[b]PCL with a molecular weight of 65 kDa

biopolymers are reported, which seek to have a positive impact on the health sector and on patients.

References

1. Adeli, H., Khorasani, M. T., & Parvazinia, M. (2019). Wound dressing based on electrospun PVA/chitosan/starch nanofibrous mats: Fabrication, antibacterial and cytocompatibility evaluation and *in vitro* healing assay. *International Journal of Biological Macromolecules, 122*, 238–254.
2. Adeli-Sardou, M., Yaghoobi, M. M., Torkzadeh-Mahani, M., & Dodel, M. (2019). Controlled release of lawsone from polycaprolactone/gelatin electrospun nano fibers for skin tissue regeneration. *International Journal of Biological Macromolecules, 124*, 478–491.
3. Agheb, M., Dinari, M., Rafienia, M., & Salehi, H. (2017). Novel electrospun nanofibers of modified gelatin-tyrosine in cartilage tissue engineering. *Materials Science and Engineering: C, 71*, 240–251.
4. Ahmed, R., Tariq, M., Ali, I., Asghar, R., Khanam, P. N., Augustine, R., & Hasan, A. (2018). Novel electrospun chitosan/polyvinyl alcohol/zinc oxide nanofibrous mats with antibacterial and antioxidant properties for diabetic wound healing. *International Journal of Biological Macromolecules, 120*, 385–393.
5. Ahsan, S. M., Thomas, M., Reddy, K. K., Sooraparaju, S. G., Asthana, A., & Bhatnagar, I. (2018). Chitosan as biomaterial in drug delivery and tissue engineering. *International Journal of Biological Macromolecules, 110*, 97–109.
6. Ajayi, E. I. O., Modo, E. U., Kiakubu, O. T., & Molehin, O. R. (2019). Diabetes care and wound healing using Nauclea latifolia, Manihot esculenta, and other natural products. In R. R Watson & V. R. Preedy (Eds.), *Bioactive food as dietary interventions for diabetes* (pp. 545–558). Elsevier Inc.
7. Alavarse, A. C., de Oliveira Silva, F. W., Colque, J. T., da Silva, V. M., Prieto, T., Venancio, E. C., & Bonvent, J. J. (2017). Tetracycline hydrochloride-loaded electrospun nanofibers mats based on PVA and chitosan for wound dressing. *Materials Science and Engineering: C, 77*, 271–281.
8. Al-Mulla, F., Leibovich, S. J., Francis, I. M., & Bitar, M. S. (2011). Impaired TGF-β signaling and a defect in resolution of inflammation contribute to delayed wound healing in a female rat model of type 2 diabetes. *Molecular BioSystems, 7*(11), 3006–3020.
9. Anderson, J. M., & Shive, M. S. (1997). Biodegradation and biocompatibility of PLA and PLGA microspheres. *Advanced Drug Delivery Reviews, 28*, 5–24.
10. Archana, D., Singh, B. K., Dutta, J., & Dutta, P. K. (2015). Chitosan-PVP-nano silver oxide wound dressing: In vitro and in vivo evaluation. *International Journal of Biological Macromolecules, 73*, 49–57.
11. Aslam, M., Kalyar, M. A., & Raza, Z. A. (2018). Polyvinyl alcohol: A review of research status and use of polyvinyl alcohol based nanocomposites. *Polymer Engineering & Science, 58*, 2119–2132.
12. Aswathy, S. H., Narendrakumar, U., & Manjubala, I. (2020). Commercial hydrogels for biomedical applications. *Heliyon*, *6*, e03719.
13. Athanasiou, K. A., Niederauer, G. G., & Agrawal, C. M. (1996). Sterilization, toxicity, biocompatibility and clinical applications of polylactic acid/polyglycolic acid copolymers. *Biomaterials, 17*, 93–102.
14. Augustine, R., Zahid, A. A., Hasan, A., Wang, M., & Webster, T. J. (2019). CTGF loaded electrospun dual porous core-shell membrane for diabetic wound healing. *International Journal of Nanomedicine, 14*, 8573–8588.
15. Bagchi, D., Roy, S., & Das, A. (2020). *Wound healing, tissue repair and regeneration in diabetes* (1st ed.). Elsevier.

16. Baker, B. M., Gee, A. O., Metter, R. B., Nathan, A. S., Marklein, R. A., Burdick, J. A., & Mauck, R. L. (2008). The potential to improve cell infiltration in composite fiber-aligned electrospun scaffolds by the selective removal of sacrificial fibers. *Biomaterials, 29*(15), 2348–2358.
17. Baker, M. I., Walsh, S. P., Schwartz, Z., & Boyan, B. D. (2012). A review of polyvinyl alcohol and its uses in cartilage and orthopedic applications. *Journal of Biomedical Materials Research Part B, 100B*, 1451–1457.
18. Bayat, S., Amiri, N., Pishavar, E., Kalalinia, F., Movaffagh, J., & Hashemi, M. (2019). Bromelain-loaded chitosan nanofibers prepared by electrospinning method for burn wound healing in animal models. *Life Sciences, 229*, 57–66.
19. Bommer, C., Sagalova, V., Heesemann, E., Manne-Goehler, J., Atun, R., Bärnighausen, T., Davies, J., & Vollmer, S. (2018). Global economic burden of diabetes in adults: Projections from 2015 to 2030. *Diabetes Care, 41*(5), 963–970.
20. Boniakowski, A. E., Kimball, A. S., Jacobs, B. N., Kunkel, S. L., & Gallagher, K. A. (2017). Macrophage-mediated inflammation in normal and diabetic wound healing. *The Journal of Immunology, 199*(1), 17–24.
21. Bonzani, I., George, J., & Stevens, M. (2006). Novel materials for bone and cartilage regeneration. *Current Opinion in Chemical Biology, 10*(6), 568–575.
22. Campa-Siqueiros, P. I., Madera-Santana, T. J., Castillo-Ortega, M. M., López-Cervantes, J. L., Ayala-Zavala, J. F., & Ortiz-Vázquez, E. L. (2021). Electrospun and co-electrospun biopolymer nanofibers for skin wounds on diabetic patients: An overview. *RSV Advances, 11*, 15340–15350.
23. Cai, Z. X., Mo, X. M., Zhang, K. H., Fan, L. P., Yin, A. L., He, C. L., & Wang, H. S. (2010). Fabrication of chitosan/silk fibroin composite nanofibers for wound-dressing applications. *International Journal of Molecular Sciences, 11*(9), 3529–3539.
24. Cao, H., McHugh, K., Chew, S. Y., & Anderson, J. M. (2010). The topographical effect of electrospun nanofibrous scaffolds on the *in vivo* and *in vitro* foreign body reaction. *Journal of Biomedical Materials Research Part A, 93*, 1151–1159.
25. Cengiz, F., Dao, T. A., & Jirsak, O. (2010). Influence of solution properties on the roller electrospinning of poly(vinyl alcohol). *Polymer Engineering & Science, 50*, 936–943.
26. Charernsriwilaiwat, N., Opanasopit, P., Rojanarata, T., & Ngawhirunpat, T. (2012). Lysozyme-loaded, electrospun chitosan-based nanofiber mats for wound healing. *International Journal of Pharmaceutics, 427*(2), 379–384.
27. Chen, J. P., Chang, G. Y., & Chen, J. K. (2008). Electrospun collagen/chitosan nanofibrous membrane as wound dressing. *Colloids and Surfaces A: Physicochemical and Engineering Aspects, 313–314*, 183–188.
28. Chen, S., Liu, B., Carlson, M. A., Gombart, A. F., Reilly, D. A., & Xie, J. (2017). Recent advances in electrospun nanofibers for wound healing. *Nanomedicine, 12*(11), 1335–1352.
29. Chen, Z. C. C., Ekaputra, A. K., Gauthaman, K., Adaikan, P. G., Yu, H., & Hutmacher, D. W. (2008). *In vitro* and *in vivo* analysis of co-electrospun scaffolds made of medical grade poly(ε-caprolactone) and porcine collagen. *Journal of Biomaterials Science, Polymer, 19*, 693–707.
30. Chen, Z., Mo, X., He, C., & Wang, H. (2008). Intermolecular interactions in electrospun collagen–chitosan complex nanofibers. *Carbohydrate Polymers, 72*(3), 410–418.
31. Chong, E., Phan, T., Lim, I., Zhang, Y., Bay, B., Ramakrishna, S., & Lim, C. (2007). Evaluation of electrospun PCL/gelatin nanofibrous scaffold for wound healing and layered dermal reconstitution. *Acta Biomaterialia, 3*(3), 321–330.
32. Chong, L. H., Lim, M. M., & Sultana, N. (2015). Fabrication and evaluation of polycaprolactone/gelatin-based electrospun nanofibers with antibacterial properties. *Journal of Nanomaterials, 2015*, 1–8.
33. Cipitria, A., Skelton, A., Dargaville, T. R., Dalton, P. D., & Hutmacher, D. W. (2011). Design, fabrication and characterization of PCL electrospun scaffolds—A review. *Journal of Materials Chemistry, 21*, 9419–9453.

34. Croisier, F., & Jérôme, C. (2013). Chitosan-based biomaterials for tissue engineering. *European Polymer Journal, 49*(4), 780–792.
35. Cutright, D. E., Hunsuck, E. E., & Beasley, J. D. (1971). Fracture reduction using a biodegradable material, polylactic acid. *Journal of Oral and Maxillofacial Surgery, 29*, 393–397.
36. Deng, A., Yang, Y., Du, S., & Yang, S. (2018). Electrospinning of *in situ* cross-linked recombinant human collagen peptide/chitosan nanofibers for wound healing. *Biomaterials Science, 6*(8), 2197–2208.
37. Dias, J. R., Baptista-Silva, S., De Oliveira, C. M. T., Sousa, A., Oliveira, A. L., Bártolo, P. J., & Granja, P. L. (2017). *In situ* cross-linked electrospun gelatin nanofibers for skin regeneration. *European Polymer Journal, 95*, 161–173.
38. Dubský, M., Kubinová, Š, Širc, J., Voska, L., Zajíček, R., Zajícová, A., Lesný, P., Jirkovská, A., Michálek, J., Munzarová, M., Holáň, V., & Syková, E. (2012). Nanofibers prepared by needleless electrospinning technology as scaffolds for wound healing. *Journal of Materials Science: Materials in Medicine, 23*(4), 931–941.
39. Dwivedi R., Kumar, S., Pandey, R., Mahajan, A., Nandana, D., Katti, D. S., & Mehrotra, D. (2020). Polycaprolactone as biomaterial for bone scaffolds: Review of literature. *Journal of Oral Biology and Craniofacial Research, 10*, 381–388.
40. Engelberg, I., & Kohn, J. (1991). Physico-mechanical properties of degradable polymers used in medical applications: A comparative study. *Biomaterials, 12*, 292–304.
41. Escárcega-Galaz, A. A., De La Cruz-Mercado, J. L., López-Cervantes, J., Sánchez-Machado, D. I., Brito-Zurita, O. R., & Ornelas-Aguirre, J. M. (2018). Chitosan treatment for skin ulcers associated with diabetes. *Saudi Journal of Biological Sciences, 25*(1), 130–135.
42. Fan, L., Du, Y., Huang, R., Wang, Q., Wang, X., & Zhang, L. (2005). Preparation and characterization of alginate/gelatin blend fibers. *Journal of Applied Polymer Science, 96*(5), 1625–1629.
43. Fang, Y., Zhu, X., Wang, N., Zhang, X., Yang, D., Nie, J., & Ma, G. (2019). Biodegradable core-shell electrospun nanofibers based on PLA and γ-PGA for wound healing. *European Polymer Journal, 116*, 30–37.
44. Farzamfar, S., Naseri-Nosar, M., Samadian, H., Mahakizadeh, S., Tajerian, R., Rahmati, M., Vaez, A., & Salehi, M. (2018). Taurine-loaded poly (ε-caprolactone)/gelatin electrospun mat as a potential wound dressing material: In vitro and in vivo evaluation. *Journal of Bioactive and Compatible Polymers, 33*(3), 282–294.
45. Ganesh, M., Aziz, A. S., Ubaidulla, U., Hemalatha, P., Saravanakumar, A., Ravikumar, R., Peng, M. M., Choi, E. Y., & Jang, H. T. (2016). Sulfanilamide and silver nanoparticles-loaded polyvinyl alcohol-chitosan composite electrospun nanofibers: Synthesis and evaluation on synergism in wound healing. *Journal of Industrial and Engineering Chemistry, 39*, 127–135.
46. Gaspar-Pintiliescu, A., Stanciuc, A. M., & Craciunescu, O. (2019). Natural composite dressings based on collagen, gelatin and plant bioactive compounds for wound healing: A review. *International Journal of Biological Macromolecules, 138*, 854–865.
47. Ghasemi-Mobarakeh, L., Prabhakaran, M. P., Morshed, M., Nasr-Esfahani, M. H., & Ramakrishna, S. (2008). Electrospun poly(ε-caprolactone)/gelatin nanofibrous scaffolds for nerve tissue engineering. *Biomaterials, 29*, 4532–4539.
48. Gomaa, S. F., Madkour, T. M., Moghannem, S., & El-Sherbiny, I. M. (2017). New polylactic acid/cellulose acetate-based antimicrobial interactive single dose nanofibrous wound dressing mats. *International Journal of Biological Macromolecules, 105*, 1148–1160.
49. Gomes, S. R., Rodrigues, G., Martins, G. G., Roberto, M. A., Mafra, M., Henriques, C. M. R., & Silva, J. C. (2015). *In vitro* and *in vivo* evaluation of electrospun nanofibers of PCL, chitosan and gelatin: A comparative study. *Materials Science and Engineering: C, 46*, 348–358.
50. Goy, R. C., de Britto, D., & Assis, O. B. G. (2009). A review of the antimicrobial activity of chitosan. *Polímeros: Ciência e Tecnologia, 19*(3), 241–247.
51. Gupta, D., Venugopal, J., Mitra, S., Giri Dev, V. R., & Ramakrishna, S. (2009). Nanostructured biocomposite substrates by electrospinning and electrospraying for the mineralization of osteoblasts. *Biomaterials, 30*, 2085–2094.

52. Han, Y., Jiang, Q., Li, Y., Wang, M., Fan, T., Liu, M., Ke, Q., Xu, H., & Yi, Z. (2019). An aligned porous electrospun fibrous scaffold embedded Asiatic acid for accelerating diabetic wound healing. *Journal of Materials Chemistry B, 40*, 1–36.
53. Huang, C. H., Chi, C. Y., Chen, Y. S., Chen, K. Y., Chen, P. L., & Yao, C. H. (2012). Evaluation of proanthocyanidin-crosslinked electrospun gelatin nanofibers for drug delivering system. *Materials Science and Engineering: C, 32*(8), 2476–2483.
54. Jamshidian, M., Tehrany, E. A., Imran, M., Jacquot, M., & Desobry, S. (2010). Poly-lactic acid: Production, applications, nanocomposites, and release studies. *Comprehensive Reviews in Food Science and Food Safety, 9*, 552–571.
55. Jana, S., Maiti, S., & Jana, S. (2017). *Biopolymer-based composites* (1st ed.). Elsevier.
56. Jayakumar, R., Prabaharan, M., Kumar, P. T. S., Nair, S. V., & Tamura, H. (2011). Biomaterials based on chitin and chitosan in wound dressing applications. *Biotechnology Advances, 29*, 322–337.
57. Jayakumar, R., Prabaharan, M., Nair, S. V., & Tamura, H. (2010). Novel chitin and chitosan nanofibers in biomedical applications. *Biotechnology Advances, 28*(1), 142–150.
58. Jiang, L., & Zhang, J. (2013). 6-Biodegradable polymers and polymer blends. In S. Ebnesajjad (Ed.), *Handbook of biopolymers and biodegradable plastics* (pp. 109–128). Boston.
59. Jiang, T., James, R., Kumbar, S. G., & Laurencin, C. T. (2014). Chitosan as a biomaterial: Structure, properties, and applications in tissue engineering and drug delivery. In S. G. Kumbar, C. T. Laurencin, & M. Deng (Eds.), *Natural and synthetic biomedical polymers* (pp. 91–113). Elsevier.
60. Jung, J. W., Lee, J. S., & Cho, D. W. (2016). Computer-aided multiple-head 3D printing system for printing of heterogeneous organ/tissue constructs. *Scientific Reports, 6*, 21685.
61. Kalantari, K., Afifi, A. M., Jahangirian, H., & Webster, T. J. (2019). Biomedical applications of chitosan electrospun nanofibers as a green polymer—Review. *Carbohydrate Polymers, 207*, 588–600.
62. Kamoun, E., Kenawy, E., & Chen, X. (2017). A review on polymeric hydrogel membranes for wound dressing applications: PVA-based hydrogel dressings. *Journal of Advanced Research, 8*, 217–233.
63. Karami, Z., Rezaeian, I., Zahedi, P., & Abdollahi, M. (2013). Preparation and performance evaluations of electrospun poly(ε-caprolactone), poly(lactic acid), and their hybrid (50/50) nanofibrous mats containing thymol as an herbal drug for effective wound healing. *Journal of Applied Polymer Science, 129*, 756–766.
64. Kavoosi, G., Dadfar, S. M. M., & Purfard, A. M. (2013). Mechanical, physical, antioxidant, and antimicrobial properties of gelatin films incorporated with thymol for potential use as nano wound dressing. *Journal of Food Science, 78*(2), E244–E250.
65. Khajavi, R., & Abbasipour, M. (2012). Electrospinning as a versatile method for fabricating coreshell, hollow and porous nanofibers. *Scientia Iranica, 19*(6), 2029–2034.
66. Kim, H. M., Lee, H. H., & Knowles, J. C. (2006). Electrospinning biomedical nanocomposite fibers of hydroxyapatite/poly(lactic acid) for bone regeneration. *Journal of Biomedical Materials Research, 79A*, 643–649.
67. Kimball, A. S., Joshi, A. D., Boniakowski, A. E., Schaller, M., Chung, J., Allen, R., Bermick, J., Carson, W. F., Henke, P. K., Maillard, I., Kunkel, S. L., & Gallagher, K. A. (2017). Notch regulates macrophage-mediated inflammation in diabetic wound healing. *Frontiers in Immunology, 8*, 635.
68. Kimball, A., Schaller, M., Joshi, A., Davis, F. M., denDekker, A., Boniakowski, A., Bermick, J., Obi, A., Moore, B., Henke, P. K., Kunkel, S. L., & Gallagher, K. A. (2018). Ly6C Hi blood monocyte/macrophage drive chronic inflammation and impair wound healing in diabetes mellitus. *Arteriosclerosis, Thrombosis, and Vascular Biology, 38*(5), 1102–1114.
69. Kulkarni, R. K., Pani, K. C., Neuman, C., & Leonard, F. (1966). Polylactic acid for surgical implants. *Archives of Surgery, 93*, 839–843.
70. Kunkemoeller, B., & Kyriakides, T. R. (2017). Redox signaling in diabetic wound healing regulates extracellular matrix deposition. *Antioxidants & Redox Signaling, 27*(12), 823–838.

71. Lanno, G.-H., Ramos, C., Preem, L., Putrinš, M., Laidmäe, I., Tenson, T., & Kogermann, K. (2020). Antibacterial porous electrospun fibers as skin scaffolds for wound healing applications. *ACS Omega, 5*, 30011–33002.
72. Lárez-Velázquez, C. (2006). Quitina y quitosano: Materiales del pasado para el presente y futuro. *Avances en química, 1*(2), 15–21.
73. Li, D., Frey, M. W., & Baeumner, A. J. (2006). Electrospun polylactic acid nanofiber membranes as substrates for biosensor assemblies. *Journal of Membrane Science, 279*, 354–363.
74. Li, G., Zhao, M., Xu, F., Yang, B., Li, X., Meng, X., Teng, L., Sun, F., & Li, Y. (2020). Synthetic and biological application of polylactic acid. *Molecules, 25*, 5023–5040.
75. Li, H., Wang, M., Williams, G. R., Wu, J., Sun, X., Lv, Y., & Zhu, L. M. (2016). Electrospun gelatin nanofibers loaded with vitamins A and E as antibacterial wound dressing materials. *RSC Advances, 6*(55), 50267–50277.
76. Li, W. J., Danielson, K. G., Alexander, P. G., & Tuan, R. S. (2003). Biological response of chondrocytes cultured in three dimensional nanofibrous poly(ε-caprolactone) scaffolds. *Journal of Biomedical Materials Research, 67*, 1105–1114.
77. Li, W. J., Mauck, R. L., Cooper, J. A., Yuan, X., & Tuan, R. S. (2007). Engineering controllable anisotropy in electrospun biodegradable nanofibrous scaffolds for musculoskeletal tissue engineering. *Journal of Biomechanics, 40*, 1686–1693.
78. Little, C. J., Bawolin, N. K., & Chen, X. (2011). Mechanical properties of natural cartilage and tissue-engineered constructs. *Tissue Engineering and Regenerative Medicine, 17*, 213–227.
79. Liu, M., Duan, X. P., Li, Y. M., Yang, D. P., & Long, Y. Z. (2017). Electrospun nanofibers for wound healing. *Materials Science and Engineering: C, 76*, 1413–1423.
80. Liu, W., Thomopoulos, S., & Xia, Y. (2012). Electrospun nanofibers for regenerative medicine. *Advanced Healthcare Materials, 1*(1), 10–25.
81. Liu, Y., Zhou, S., Gao, Y., & Zhai, Y. (2019). Electrospun nanofibers as a wound dressing for treating diabetic foot ulcer. *Asian Journal of Pharmaceutical Sciences, 14*, 130–143.
82. López-Cervantes, J., Escárcega-Galaz, A. A., Sánchez-Machado, D. I., De La Cruz-Mercado, J. L., Pérez-Gómez, L. E., & Ornelas-Aguirre, J. M. (2019). Characterization and efficacy of chitosan membranes in the treatment of skin ulcers. *Egyptian Journal of Basic and Applied Sciences, 6*(5), 1–11.
83. Lotfipour, F., Alami-Milani, M., Salatin, S., Hadavi, A., & Jelvehgari, M. (2019). Freeze-thaw-induced cross-linked PVA/chitosan for oxytetracycline-loaded wound dressing: The experimental design and optimization. *Research in Pharmaceutical Sciences, 14*, 175–189.
84. Lv, F., Wang, J., Xu, P., Han, Y., Ma, H., Xu, H., Chen, S., Chang, J., Ke, Q., Liu, M., Yi, Z., & Wu, C. (2017). A conducive bioceramic/polymer composite biomaterial for diabetic wound healing. *Acta Biomaterialia, 60*, 128–143.
85. Majd, S. A., Khorasgani, M. R., Moshtaghian, S. J., Talebi, A., & Khezri, M. (2016). Application of chitosan/PVA Nano fiber as a potential wound dressing for streptozotocin-induced diabetic rats. *International Journal of Biological Macromolecules, 92*, 1162–1168.
86. Mármol, Z., Páez, G., Rincón, M., Araujo, K., Aiello, C., Chandler, C., & Gutiérrez, E. (2011). Quitina y quitosano polímeros amigables. Una revisión de sus aplicaciones. *Revista Tecnocientífica URU, 1*, 53–58.
87. Martínez-Ibarra, D. M., Sánchez-Machado, D. I., López-Cervantes, J., Campas-Baypoli, O. N., Sanches-Silva, A., & Madera-Santana, T. J. (2019). Hydrogel wound dressings based on chitosan and xyloglucan: Development and characterization. *Journal of Applied Polymer Science, 136*(12), 47342.
88. Masood, S. H., Singh, J. P., & Morsi, Y. (2005). The design and manufacturing of porous scaffolds for tissue engineering using rapid prototyping. *International Journal of Advanced Manufacturing Technology, 27*, 415–420.
89. Mir, M., Najabat Ali, M., Barakullah, A., Gulzar, A., Arshad, M., Fatima, S., & Asad, M. (2018). Synthetic polymeric biomaterials for wound healing: A review. *Progress in Biomaterials, 7*, 1–21.

90. Mishra, R. K., Majeed, A. B. A., & Banthia, A. K. (2011). Development and characterization of pectin/gelatin hydrogel membranes for wound dressing. *International Journal of Plastics Technology, 15*(1), 82–95.
91. Mondal, D., Griffith, M., & Venkatraman, S. S. (2016). Polycaprolactone-based biomaterials for tissue engineering and drug delivery: Current scenario and challenges. *International Journal of Polymeric Materials and Polymeric Biomaterials, 65*, 255–265.
92. Moura, L. I. F., Dias, A. M. A., Carvalho, E., & de Sousa, H. C. (2013). Recent advances on the development of wound dressings for diabetic foot ulcer treatment—A review. *Acta Biomaterialia, 9*(7), 7093–7114.
93. Nagarajan, S., Belaid, H., Pochat-Bohatier, C., Teyssier, C., Iatsunskyi, I., Coy, E., Balme, S., Cornu, D., Miele, P., Kalkura, N. S., Cavallès, V., & Bechelany, M. (2017). Design of boron nitride/gelatin electrospun nanofibers for bone tissue engineering. *ACS Applied Materials & Interfaces, 9*(39), 33695–33706.
94. Nair, L. S., Bhattacharyya, S., & Laurencin, C. T. (2004). Development of novel tissue engineering scaffolds via electrospinning. *Expert Opinion on Biological Therapy, 4*, 659–668.
95. Naseri-Nosar, M., Farzamfar, S., Sahrapeyma, H., Ghorbani, S., Bastami, F., Vaez, A., & Salehi, M. (2017). Cerium oxide nanoparticle-containing poly (ε-caprolactone)/gelatin electrospun film as a potential wound dressing material: In vitro and in vivo evaluation. *Materials Science and Engineering: C, 81*, 366–372.
96. Nguyen, T. H., & Lee, B. T. (2010). Fabrication and characterization of cross-linked gelatin electrospun nano-fibers. *Journal of Biomedical Science and Engineering, 3*(12), 1117–1124.
97. Nicolas, J., Mura, S., Brambilla, D., Mackiewicz, N., & Couvreur, P. (2013). Design, functionalization strategies and biomedical applications of targeted biodegradable/biocompatible polymer-based nanocarriers for drug delivery. *Chemical Society Reviews, 42*, 1147–1235.
98. Nisbet, D. R., Rodda, A. E., Malcolm, K., Horne, M. K., Forsythe, J. S., & Finkelstein, D. I. (2009). Neurite infiltration and cellular response to electrospun polycaprolactone scaffolds implanted into the brain. *Biomaterials, 30*, 4573–4580.
99. Nottelet, B., Darcos, V., & Coudane, J. (2015). Aliphatic polyesters for medical imaging and theranostic applications. *European Journal of Pharmaceutics and Biopharmaceutics, 97*, 350–370.
100. Nottelet, B., Pektok, E., Mandracchia, D., Tille, J. C., Walpoth, B., Gurny, R., & Möller, M. (2009). Factorial design optimization and *in vivo* feasibility of poly(epsilon-caprolactone)-micro- and nanofiber-based small diameter vascular grafts. *Journal of Biomedical Materials Research Part A, 89*, 865–875.
101. Ojha, S. (2017). Structure-property relationship of electrospun fibers. In M. Afshari, (Ed.), *Electrospun fibers* (pp. 239–253). Woodhead Pub. Elsevier.
102. Okutan, N., Terzi, P., & Altay, F. (2014). Affecting parameters on electrospinning process and characterization of electrospun gelatin nanofibers. *Food Hydrocolloids, 39*, 19–26.
103. Pal, K., Banthia, A. K., & Majumdar, D. K. (2007). Biomedical evaluation of polyvinyl alcohol–gelatin esterified hydrogel for wound dressing. *Journal of Materials Science: Materials in Medicine, 18*(9), 1889–1894.
104. Pektok, E., Nottelet, B., Tille, J. C., Gurny, R., Kalangos, A., Moeller, M., & Walpoth, B. H. (2008). Degradation and healing characteristics of small diameter poly(ε-caprolactone) vascular grafts in the rat systemic arterial circulation. *Circulation, 118*, 2563–2570.
105. Pisani, S., Dorati, R., Conti, B., Modena, T., Bruni, G., & Genta, I. (2018). Design of copolymer PLA-PCL electrospun matrix for biomedical applications. *Reactive and Functional Polymers, 124*, 77–89.
106. Pitt, C. G., Chasalow, F. I., Hibionada, Y. M., Klimas, D. M., & Schindler, A. (1981). Aliphatic polyesters. I. The degradation of poly(ε-caprolactone) *in vivo. Journal of Applied Polymer Science, 26*, 3779–3787.
107. Pott, P. P., Schwarz, M. L. R., Gundling, R., Nowak, K., Hohenberger, P., & Roessner, E. D. (2012). Mechanical properties of mesh materials used for hernia repair and soft tissue augmentation. *PLoS ONE, 7*, e46978.

108. Powell, H. M., & Boyce, S. T. (2008). Fiber density of electrospun gelatin scaffolds regulates morphogenesis of dermal–epidermal skin substitutes. *Journal of Biomedical Materials Research Part A: An Official Journal of The Society for Biomaterials, 84*(4), 1078–1086.
109. Prabhakaran, M. P., Venugopal, J. R., Chyan, T. T., Hai, L. B., Chan, C. K., Lim, A. Y., & Ramakrishna, S. (2008). Electrospun biocomposite nanofibrous scaffolds for neural tissue engineering. *Tissue Engineering Part A, 14*, 1787–1797.
110. Raafat, D., von Bargen, K., Haas, A., & Sahl, H.-G. (2008). Insights into the mode of action of chitosan as an antibacterial compound. *Applied and Environmental Microbiology, 74*(12), 3764–3773.
111. Ratner, B. D., Hoffman, A. S., Schoen, F. J., & Lemons, J. E. (2013). Introduction-biomaterials science: An evolving, multidisciplinary endeavor. In B. D., Lemons, A. S., Ratner, F. J. Hoffman, & J. E., Shoen (Eds.), *Biomaterials science.* Academic Press.
112. Razzaq, A., Khan, Z. U., Saeed, A., Shah, K. A., Khan, N. U., Menaa, B., Iqbal, H., & Menaa, F. (2021). Development of cephradine-loaded Gelatin/Polyvinyl alcohol electrospun nanofibers for effective diabetic wound healing: In-vitro and in-vivo assessments. *Pharmaceutics, 13*(3), 349.
113. Reinke, J. M., & Sorg, H. (2012). Wound repair and regeneration. *European Surgical Research, 49*(1), 35–43.
114. Ren, K., Wang, Y., Sun, T., Yue, W., & Zhang, H. (2017). Electrospun PCL/gelatin composite nanofiber structures for effective guided bone regeneration membranes. *Materials Science and Engineering: C, 78*, 324–332.
115. Ren, Y., Huang, L., Wang, Y., Mei, L., Fan, R., He, M., Wang, C., Tong, A., Chen, H., & Guo, G. (2020). Stereocomplexed electrospun nanofibers containing poly(lactic acid) modified quaternized chitosan for wound healing. *Carbohydrate Polymers*, *247*, 116754.
116. Rodríguez-Vázquez, M., Vega-Ruíz, B., Ramos-Zúñiga, R., Saldaña-Koppel, D. A., & Quiñones-Olvera, L. F. (2015). Chitosan and its potential use as a scaffold for tissue engineering in regenerative medicine. *BioMed Research International*, *2015*.
117. Roy, T., Maity, P. P., Rameshbabu, A. P., Das, B., John, A., Dutta, A., Ghorai, S. K., Chattopadhyay, S. & Dhara, S. (2018). Core-shell nanofibrous scaffold based on polycaprolactone-silk fibroin emulsion electrospinning for tissue engineering applications. *Bioengineering*, *5*, 68–84.
118. Sadri, M., Arab-Sorkhi, S., Vatani, H., & Bagheri-Pebdeni, A. (2015). New wound dressing polymeric nanofiber containing green tea extract prepared by electrospinning method. *Fibers and Polymers, 16*(18), 1742–1750.
119. Salazar, J. J., Ennis, W. J., & Koh, T. J. (2016). Diabetes medications: Impact on inflammation and wound healing. *Journal of Diabetes and Its Complications, 30*(4), 746–752.
120. Samadian, H., Zamiri, S., Ehterami, A., Farzamfar, S., Vaez, A., Khastar, H., Alam, M., Ai, A., Derakhshankhah, H., Allahyari, Z., Goodarsi, A., & Salehi, M. (2020). Electrospun cellulose acetate/gelatin nanofibrous wound dressing containing berberine for diabetic foot ulcer healing: In vitro and in vivo studies. *Scientific Reports, 10*(1), 1–12.
121. Sánchez-Cepeda, A. A., Vera-Graziano, R., Muñoz-Prieto, E. J., Gómez-Pachón, E. Y., Bernad-Bernad, M. J., & Maciel-Cerda, A. (2016). Preparación y caracterización de membranas poliméricas electrohiladas de policaprolactona y quitosano para la liberación controlada de clorhidrato de tiamina. *Ciencia en Desarrollo, 7*(2), 133–151.
122. Sarhan, W. A., Azzazy, H. M. E., & El-Sherbiny, I. M. (2016). Honey/chitosan nanofiber wound dressing enriched with *Allium sativum* and *Cleome droserifolia*: Enhanced antimicrobial and wound healing activity. *ACS Applied Materials & Interfaces, 8*(10), 6379–6390.
123. Sasmal, P., & Datta, P. (2019). Tranexamic acid-loaded chitosan electrospun nanofibers as drug delivery system for hemorrhage control applications. *Journal of Drug Delivery Science and Technology, 52*, 559–567.
124. Schenke-Layland, K., Rofail, F., Heydarkhan, S., Gluck, J. M., Ingle, N. P., Angelis, E., Choi, C.-H., MacLellan, W. R., Beygui, R. E., Shemin, R. J., & Heydarkhan-Hagvall, S. (2009). The use of three-dimensional nanostructures to instruct cells to produce extracellular matrix for regenerative medicine strategies. *Biomaterials, 30*, 4665–4675.

125. Schreml, S., Szeimies, R.-M., Prantl, L., Landthaler, M., & Babilas, P. (2010). Wound healing in the 21st century. *Journal of the American Academy of Dermatology, 63*(5), 866–881.
126. Shabunin, A. S., Yudin, V. E., Dobrovolskaya, I. P., Zinovyev, E. V., Zubov, V., Ivan'kova, E. M., & Morganti, P. (2019). Composite wound dressing based on chitin/chitosan nanofibers: Processing and biomedical applications. *Cosmetics, 6*(1), 16.
127. Shan, Y. H., Peng, L. H., Liu, X., Chen, X., Xiong, J., & Gao, J. Q. (2015). Silk fibroin/gelatin electrospun nanofibrous dressing functionalized with astragaloside IV induces healing and anti-scar effects on burn wound. *International Journal of Pharmaceutics, 479*(2), 291–301.
128. Shi, R., Geng, H., Gong, M., Ye, J., Wu, C., Hu, X., & Zhang, L. (2018). Long-acting and broad-spectrum antimicrobial electrospun poly (ε-caprolactone)/gelatin micro/nanofibers for wound dressing. *Journal of Colloid and Interface Science, 509*, 275–284.
129. Shin, M., Ishii, O., Sueda, T., & Vacanti, J. P. (2004). Contractile cardiac grafts using a novel nanofibrous mesh. *Biomaterials, 25*, 3717–3723.
130. Shin, M., Yoshimoto, H., & Vacanti, J. P. (2004). *In vivo* bone tissue engineering using mesenchymal stem cells on a novel electrospun nanofibrous scaffold. *Tissue Engineering, 10*, 33–41.
131. Södergård, A., & Stolt, M. (2010). Industrial production of high molecular weight poly(lactic acid). In R. Auras, L. T. Lim, S. E. M. Selke, & H. Tsuji (Eds.), *Poly(lactic acid): Synthesis, structures, properties, processing, and applications* (pp. 27–41). Wiley.
132. Srouji, S., Kizhner, T., Suss-Tobi, E., Livne, E., & Zussman, E. (2008). 3-D Nanofibrous electrospun multilayered construct is an alternative ECM mimicking scaffold. *Journal of Materials Science: Materials in Medicine, 19*, 1249–1255.
133. Stocker, C. J. (2020). *Type 2 diabetes: Methods and protocols*. Springer.
134. Tang, Y., Lan, X., Liang, C., Zhong, Z., Xie, R., Zhou, Y., Miao, X., Wang, H., & Wang, W. (2019). Honey loaded alginate/PVA nanofibrous membrane as potential bioactive wound dressing. *Carbohydrate Polymers, 219*, 113–120.
135. Thenmozhi, S., Dharmaraj, N., Kadirvelu, K., & Kim, H. Y. (2017). Electrospun nanofibers: New generation materials for advanced applications. *Materials Science and Engineering: B, 217*, 36–48.
136. Tillman, B. W., Yazdani, S. K., Lee, S. J., Geary, R. L., Atala, A., & Yoo, J. J. (2009). The *in vivo* stability of electrospun polycaprolactone–collagen scaffolds in vascular reconstruction. *Biomaterials, 30*, 583–588.
137. Tin Sin, L., Razak Rahmat, A., & Wan Azian Wan Abdul Rahman, W. A. W. (2012). *Polylactic acid. PLA biopolymer technology and applications*. Elsevier Inc.
138. Tiwari, A. P., Joshi, M. K., Park, C. H., & Kim, C. S. (2018). Nano-nets covered composite nanofibers with enhanced biocompatibility and mechanical properties for bone tissue engineering. *Journal of Nanoscience and Nanotechnology, 18*, 529–537.
139. Ulery, B. D., Nair, L. S., & Laurencin, C. T. (2011). Biomedical applications of biodegradable polymers. *Journal of Polymer Science Part B: Polymer Physics, 49*, 832–864.
140. Valencia-Gómez, L. E., Martel-Estrada, S. A., Vargas-Requena, C. L., Rodríguez-González, C. A., & Olivas-Armendariz, I. (2016). Apósitos de polímeros naturales para regeneración de piel. *Revista Mexicana de Ingeniería Biomédica, 37*(3), 235–249.
141. Vaz, C. M., van Tuijl, C., Bouten, C. V. C., & Baaijens, F. P. T. (2005). Design of scaffolds for blood vessel tissue engineering using a multi-layering electrospinning technique. *Acta Biomaterialia, 1*, 575–582.
142. Venugopal, J., Zhang, Y. Z., & Ramakrishna, S. (2005). Fabrication of modified and functionalized polycaprolactone nanofibre scaffolds for vascular tissue engineering. *Nanotechnology, 16*, 2138–2142.
143. Wang, J., Planz, V., Vukosavljevic, B., & Windbergs, M. (2018). Multifunctional electrospun nanofibers for wound application—Novel insights into the control of drug release and antimicrobial activity. *European Journal of Pharmaceutics and Biopharmaceutics, 129*, 175–183.
144. Wang, T., Zhu, X. K., Xue, X. T., & Wu, D. Y. (2012). Hydrogel sheets of chitosan, honey and gelatin as burn wound dressings. *Carbohydrate Polymers, 88*, 75–83.

145. Williams, R., Karuranga, S., Malanda, B., Saeedi, P., Basit, A., Besançon, S., Bommer, C., Esteghamati, A., Ogurtsova, K., Zhang, P., & Colagiuri, S. (2020). Global and regional estimates and projections of diabetes-related health expenditure: Results from the International Diabetes Federation Diabetes Atlas, 9th edition. *Diabetes Research and Clinical Practice*, *162*, 108072–108077.
146. Woodruff, M. A., & Hutmacher, D. W. (2010). The return of a forgotten polymer—Polycaprolactone in the 21st century. *Progress in Polymer Science, 35*, 1217–1256.
147. Xie, J., Li, X., & Xia, Y. (2008). Putting electrospun nanofibers to work for biomedical research. *Macromolecular Rapid Communications, 29*(22), 1775–1792.
148. Xu, X., Yang, L., Xu, X., Wang, X., Chen, X., Liang, Q., Zeng, J., & Jing, X. (2005). Ultrafine medicated fibers electrospun from W/O emulsions. *Journal of Controlled Release, 108*, 33–42.
149. Xue, J., Wu, T., Dai, Y., & Xia, Y. (2019). Electrospinning and electrospun nanofibers: Methods, materials, and applications. *Chemical Reviews, 119*, 5298–5415.
150. Xue, J., Xie, J., Liu, W., & Xia, Y. (2017). Electrospun nanofibers: New concepts, materials, and applications. *Accounts of Chemical Research, 50*(8), 1976–1987.
151. Yao, C. H., Lee, C. Y., Huang, C. H., Chen, Y. S., & Chen, K. Y. (2017). Novel bilayer wound dressing based on electrospun gelatin/keratin nanofibrous mats for skin wound repair. *Materials Science and Engineering: C, 79*, 533–540.
152. Yousefi, I., Pakravan, M., Rahimi, H., Bahador, A., Farshadzadeh, Z., & Haririan, I. (2017). An investigation of electrospun Henna leaves extract-loaded chitosan based nanofibrous mats for skin tissue engineering. *Materials Science and Engineering: C, 75*, 433–444.
153. Zahedi, P., Rezaeian, I., Ranaei-Siadat, S.-O., Jafari, S.-H., & Supaphol, P. (2010). A review on wound dressings with an emphasis on electrospun nanofibrous polymeric bandages. *Polymers for Advanced Technologies, 21*, 77–95.
154. Zandi, N., Lotfi, R., Tamjid, E., Shokrgozar, M. A., & Simchi, A. (2020). Core-sheath gelatin based electrospun nanofibers for dual delivery release of biomolecules and therapeutics. *Materials Science and Engineering: C*, *108*, 110432.
155. Zhang, Y. Z., Venugopal, J., Huang, Z. M., Lim, C. T., & Ramakrishna, S. (2006). Crosslinking of the electrospun gelatin nanofibers. *Polymer, 47*(8), 2911–2917.
156. Zhang, Y., Ouyang, H., Lim, C. T., Ramakrishna, S., & Huang, Z. M. (2005). Electrospinning of gelatin fibers and gelatin/PCL composite fibrous scaffolds. *Journal of Biomedical Materials Research, 72*, 156–165.
157. Zhao, R., Li, X., Sun, B., Zhang, Y., Zhang, D., Tang, Z., Chen, X., & Wang, C. (2014). Electrospun chitosan/sericin composite nanofibers with antibacterial property as potential wound dressings. *International Journal of Biological Macromolecules, 68*, 92–97.
158. Zheng, Y., Liang, Y., Zhang, D., Sun, X., Liang, L., Li, J., & Liu, Y. N. (2018). Gelatin-based hydrogels blended with gellan as an injectable wound dressing. *ACS Omega, 3*, 4766–4775.
159. Zhou, Y., Yang, D., Chen, X., Xu, Q., Lu, F., & Nie, J. (2008). Electrospun water-soluble carboxyethyl chitosan/poly(vinyl alcohol) nanofibrous membrane as potential wound dressing for skin regeneration. *Biomacromolecules, 9*, 349–354.
160. Zou, P., Lee, W. H., Gao, Z., Qin, D., Wang, Y., Liu, J., Sun, T., & Gao, Y. (2020). Wound dressing from polyvinyl alcohol/chitosan electrospun fiber membrane loaded with OH-CATH30 nanoparticles. *Carbohydrate Polymers*, *232*, 115786.



Paola I. Campa-Siqueiros was born in Hermosillo, Sonora, México in 1990. She received her B.S. degree in Food Chemistry from the University of Sonora in 2014, the M.S. degree in Science from the Center for Research in Food and Development A.C. (CIAD) in 2016, and currently pursuing the Ph.D. degree in sciences, also in CIAD from Hermosillo, Sonora, México. Her B.S. and M.S. degrees were obtained through thesis modality. For her B.S. degree, she realized a physicochemical, mechanical, and transport characterization of biodegradable films based on agar impregnated with garlic extract. For her M.S. degree, she evaluated the effect of garlic sulfured compounds upon fungal glucanase enzyme and, therefore, gray mound incidence on grapes. From 2017 to 2022, she worked on her Ph.D. dissertation regarding the fabrication of electrospun nanofibers based on biopolymers for wound dressing applications. Her research interest includes utilizing natural or biopolymeric materials, for the fabrication, characterization, and biological testing of new technologies, particularly for medical applications.



María Mónica Castillo-Ortega was born in Pitiquito, Sonora, México in 1958. She received the title of Chemist-Biologist with honorable mention from the University of Sonora in 1982, the M.S. degree in Polymers and Materials from the University of Sonora in 1989, and the Ph.D. degree in Materials science from the University of Sonora, Hermosillo, Sonora, México, in 1997. From 1987 to 2021, she is a Research Professor Titular C in the Department of Research in Polymers and Materials, University of Sonora. She is the author of two book chapters, more than 70 articles, with more than 1,300 citations. Her research interests include synthesis, preparation, and characterization of materials with applications in health, especially in drug delivery and tissue engineering, and adsorption of metals in contaminated water. She holds one patent.

Dr. Castillo-Ortega was a recipient of the National Council of Science and Technology, CONACYT, received the distinction of National Researcher level 2 in the National System of Investigators since 2012. In 2016, a Distinguished Researcher Award of the University of Sonora.



Jaime López-Cervantes was born in Mocorito, Sinaloa, Mexico. He has a degree in Biochemical Engineering [1984], a Master in Business Administration [1989], Quality Control Specialty [1996], and a Diploma of Advanced Studies in Food Technology [2002]. In addition, he is a Doctor in Food Technology [2003, University of Santiago de Compostela, Spain]. He currently works as a Research Professor at the Technological Institute of Sonora, México. Professor Lopez-Cervantes has developed and optimized a clean technology for shrimp biowaste processing for chitin, protein, and astaxanthin recovery and separation. His research also includes native plants and active packaging technologies such as the preparation of chitosan-based films to improve food preservation and medical use. He has published more than 100 international papers and eight international patents. He participated as director of thesis guiding student of M.Sc. and Ph.D. Due to his academic and research trajectory to form research groups, he has been awarded the National Level III Researcher distinction and is a Member of the Mexican Academy of Sciences.



J. Fernando Ayala-Zavala received the B.S. degree in biochemical engineer from the Instituto Tecnologico de Los Mochis in Sinaloa, Mexico and the M.S. and Ph. D. in Food Science from the Centro de Investigacion en Alimentacion y Desarrollo (CIAD) in Hermosillo, Sonora, Mexico. He is currently working as a Titular Professor in CIAD, studying the bioactive properties of edible plants and fungi. He has also been working as an Editorial Board Member of the International Journal of Food Microbiology, Food Research International, LWT, data in Brief, and Chemical Biodiversity. He has 133 indexed publications with an h-index of 35, and these publications include 83 original research articles, 33 book chapters, 15 reviews, one book, and one editorial. He has been a visiting scientist in the U.S. Department of Agriculture, in the University of Lleida in Spain, and the Federal University of Ceara in Brazil. He has been honored by the U.S. State Department as part of the International Visitor Leadership Program Award. He is currently holding the level 3 distinction of the Mexican System of Researchers.



David Servín de la Mora López was born in Obregón city, Sonora, Mexico. He achieved his bachelor's degree in Biotechnology Engineering in 2017. Subsequently, his M.S. degree in natural resources at the end of 2019 both obtained at the Technological Institute of Sonora in Ciudad Obregón, Sonora, Mexico. David's studies have focused mainly on taking advantage of natural polymers from various sources to develop sustainable materials used in biomedicine as possible wound dressings. In 2017, he obtained his bachelor's degree through the modality by thesis. He managed to standardize and optimize a technique to extract hydrolyzed collagen from fish scales in his work. This polymer was employed in mixtures with chitosan to develop thin and transparent films. From 2017 to 2019, he developed his Master of Science thesis, optimizing a fast and straightforward technique to obtain pure starch from quinoa seed. This polymer was used to add to chitosan-collagen-based films for the formation of flexible thin films. From 2020 to date, David is working on his doctoral thesis at the Center for Research in Food and Development A.C., Sonora, Mexico. Its central theme is to use different biopolymers to develop new biodegradable and biocompatible dressings that can contribute to the healing process of wounds challenging to heal, such as severe burns and chronic ulcerations.



Tomás J. Madera-Santana was born in Merida, Yucatan, Mexico. He received a B.S. degree in Industrial Chemical Engineering from Merida Institute of Technology (Merida, Yuc.). M.S. and Ph.D. degrees in marine biology from the Center for Research and Advanced Studies of the National Polytechnic Institute Merida Unit, in 2006 and the Ph.D. degree in mechanical engineering from Drexel University, Philadelphia, PA, in 2009. From 1990 to 2000, he was a Research Assistant with the Materials Unit on Plasma Physics Laboratory. Since 2009, he has been a Senior Professor with the Packaging Laboratory at Food and Development Research center, Hermosillo, Mexico. The author has more than 50 articles, seven book chapters, and 30 oral invited presentations. His research interests include the development, formulation, and physicochemical characterization of biomaterials based on biopolymers. Development of active nano biomaterials by electrospinning and co-electrospinning process for potential application in biomedical dressings. He is a member of the National System of Researchers (SNI) from the Mexican government's National Council of Science and Technology (CONACyT). He is a reviewer of several international and indexed journals in polymers, material science, and biomaterials.

Chapter 10
Biomedical Applications of Fibers Produced by Electrospinning, Microfluidic Spinning and Combinations of Both



Filipa Vasconcelos, Rui L. Reis, Albino Martins, and Nuno M. Neves

Abstract Electrospinning and microfluidic spinning are two fascinating techniques used in the production of micro- and/or nano-fiber meshes with possible application in many scientific areas. Their ability to mimic the extracellular matrix of many tissues, high surface area, and porosity, and even their ability to create different fibrous structures according to their target application, justify their interest in the biomedical field. In this review, we present a detailed overview of two fiber processing methodologies—electrospinning and microfluidic spinning. The basic set-ups, the functional control of the process, the different types of fiber morphology and structures obtained, and their applications, most specifically in the biomedical field will address tissue-engineered scaffolds, wound healing, and drug delivery. Moreover, the production of fibrous systems combining electrospinning and microfluidics in innovative ways is also generating a growing interest in the scientific community. Hybrid technologies, usually engineered by the integration of electrospun fiber mats within a microfluidic chip, are also included in this review. The methods and the applications of those technologies such as hybrid tissue-engineered in vitro models, lab-on-a-chip

F. Vasconcelos · R. L. Reis · A. Martins · N. M. Neves (✉)
3B's Research Group, I3Bs—Research Institute on Biomaterials, Biodegradables and Biomimetics, University of Minho, Headquarters of the European Institute of Excellence on Tissue Engineering and Regenerative Medicine, AvePark, Parque de Ciência e Tecnologia, Zona Industrial da Gandra, 4805017 Barco, Guimarães, Portugal
e-mail: nuno@i3bs.uminho.pt

F. Vasconcelos
e-mail: filipav82.0@outlook.pt

R. L. Reis
e-mail: rgreis@i3bs.uminho.pt

A. Martins
e-mail: amartins@i3bs.uminho.pt

ICVS/3B's—PT Government Associate Laboratory, Braga/Guimarães, Portugal

R. L. Reis
The Discoveries Centre for Regenerative and Precision Medicine, Headquarters at University of Minho, Avepark, 4805017 Barco, Guimarães, Portugal

© The Author(s), under exclusive license to Springer Nature Switzerland AG 2022

A. Vaseashta and N. Bölgen (eds.), *Electrospun Nanofibers*,
https://doi.org/10.1007/978-3-030-99958-2_10

devices, and platforms for in vitro cancer research are described. Furthermore, their challenges and future perspectives will also be discussed.

Keywords Micro- and nano-fibers · Electrospinning · Microfluidic spinning · Tissue engineering · Drug delivery

10.1 Introduction

Inspired by spider webs and other natural fibrous systems, man-made fibers started to be produced using natural materials and their fabrication can be traced back to the pre-historical period [1–3]. Despite the discoveries and use of fibers in different aspects of everyday life such as fabrics and clothes, it was only in the 1930's that synthetic fibers were produced mainly because of the advances in chemistry and polymer science. In this way, the first commercially viable synthetic fiber (nylon) was introduced, broadening the scope of application of fibers [4]. After this breakthrough and until the present days, many methods have been developed to produce fibers with different diameters, shapes and morphologies being made of natural and/or synthetic polymers. The variety of properties raise the scientific interest in a wide range of areas, namely in the biomedical field to produce scaffolds for tissue engineering capable of mimicking the fibrous nature of the extracellular matrix (ECM) of connective tissues.

The ECM is a hierarchically organized structure composed of proteins (such as collagen, elastin and fibronectin), polysaccharides (such as glycosaminoglycans and hyaluronic acid), proteoglycans and water [5]. Those components interact with each other to create an interconnected micro- or nano-fibrous mesh bound to the cell membrane [6]. The distinct morphologies of the connective tissues are related to the different types and properties of proteins and their structural organization within the ECM. For instance, the ECM of skin tissues is a randomly aligned fibrous structure, while the ECM of the tendon is composed of parallel aligned collagen fibrils [5, 6]. The ECM of tissues can provide support to the cells and regulate their adhesion, differentiation, migration, proliferation, and also acts in the storage and controlled release of growth factors and other signaling molecules.

When creating a tissue engineered scaffold that aims at mimic the tissue ECM, some requirements must be taken into account, such as: the size and amount of pores, the degree of interconnectivity between the pores, the balance between the level of porosity and the mechanical properties, as well its degradation rate and biocompatibility of the scaffold [7]. To produce those scaffolds, numerous processing methods can be used. Amongst those technologies, electrospinning and microfluidic spinning have shown to be two promising approaches to produce fibers at micro- to nano-scale. They physically mimic the ECM structure of native tissues since the small diameter of the obtained fibers can match the one's from the ECM. Moreover, they have high surface area, enable control over the pore size and orientation according to the desired application by changing basic aspects in their set-ups and/or parameters.

Those resemblances are very important for the correct differentiation and to promote the adhesion, proliferation, and growth of the seeded cells [8, 9].

In this work, both techniques are explored regarding the different setups that can be used, and the processes involved in their correct operation and control. The different morphology and structures of the fibers that can be produced by both techniques are also discussed. Additionally, several applications of the fibers are introduced, mainly in the biomedical field and, particularly, in tissue engineering and drug delivery, but also in other areas of interest. Furthermore, there has been a growing research interest on hybrid systems combining electrospinning and microfluidics, that are based on the integration of electrospun nanofibrous meshes into microfluid systems [10, 11]. In this way, this review also describes the above-mentioned hybrid systems, namely their methods, applications, and challenges.

10.2 Electrospinning

Electrospinning is considered a versatile processing technique that enables the production of ultrathin fibers in a non-woven mesh-like structure [12]. Its fundamentals, however, are based in the early work of Lord Rayleigh on the stability of electrically charged water drops [13], calculating a theoretical charge that led to the burst of a droplet at a particular volume [14]. The electrospinning technique and its apparatus underwent many developments until its fundamental patent was filed by Anton Formhals [15] in 1934 regarding the electrospinning of plastics [14]. Unfortunately, only in the 90 s, this technique achieved substantial academic attention, grounded in the work of Reneker's group [16].

From that moment on, electrospinning became an adaptable technique for micro- and nano-fiber production in which, a wide range of polymers can be processed. Synthetic polymers such as Poly(ε-caprolactone) (PCL), Poly(Lactic Acid) (PLA), Poly(L-Lactic Acid) (PLLA), Poly(Glycolic Acid) (PGA), Poly(Lactic-co-Glycolic Acid) (PLGA), Poly(vinyl alcohol) (PVA), Poly(Ethylene Oxide) (PEO) and Poly(Ethylene Glycol) (PEG); natural (e.g. collagen, chitosan (CS), silk fibroin and gelatin), and even bio-functional polymers through the incorporation of nanoparticles and other bioactive agents (e.g. proteins, nucleic acids or drugs) [17, 18], can all be produced by these methods.

Many variations of the electrospinning technique were developed, being of special interest the so-called co-axial electrospinning, published in 2003 [19]. In this variant of the electrospinning process, two different and immiscible solutions flow through co-axial needles with the aim to produce uniform core–shell fibers, providing, in this way, multi-functional properties in a fiber mesh structure. Moreover, as derivates of the co-electrospinning process, with more modifications to the spinneret it is possible to create multi-axial electrospinning systems such as triaxial or quadriaxial electrospinning. This technique offers unmatched benefits such as a large variety of material combinations, a controllable stack of core-sheath fibers, and retained or even

enhanced properties [20]. Co-axial electrospinning is also the basis for the creation of nano- and microscopic hollow fibrous structures such as polymeric [21, 22].

Owing to the small diameter (ranging from several micrometers down to hundred nanometers or less) of electrospun nanofibers, the resulting meshes show distinctive properties such as high specific surface area, high level of porosity, porous with size in the micrometer range and high interconnectivity. In comparison with other nanostructures such as nanorods and nanotubes, nanofibers meshes are continuous, which gives them high axial strength combined with extreme flexibility [23]. Additionally, the nanofibers can connect to the macroscale world, since even if their diameters are in the nanometer range, the full length of the fibers can be in the order of kilometers (16). The electrospinning technique also provides many advantages such as the simplicity of the fabrication process, its cost-effectiveness, and the possibility for scaled-up fabrication [16, 23]. Although, it is an overly sensitive fabrication process since many parameters are involved, being also influenced by ambient conditions. Moreover, despite the electrospinning process has been known for a long time, the mechanism by which nanofibers are formed is still not totally understood [24].

10.2.1 Principles of Electrospinning

The basic set-up for this fabrication technique consists of four main components (Fig. 10.1): (i) a high voltage power supply (that can either be powered by direct current—DC, or alternate current—AC), (ii) a metallic needle (usually a hypodermic needle with blunt end) connected to a (iii) syringe or a glass capillary tube (also known

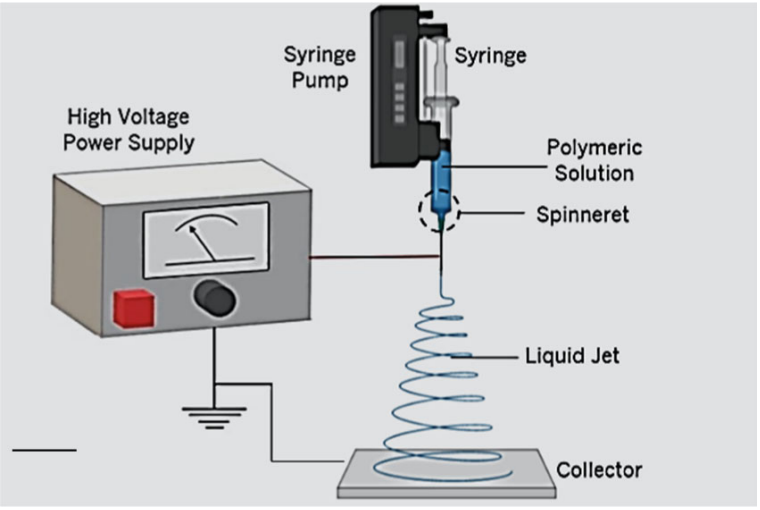


Fig. 10.1 Schematic representation of conventional electrospinning apparatus

as spinneret) where the polymeric solution is dispensed with controllable flow rate, and a (iv) grounded metal collector (usually a flat metal sheet, in the case of the use of a stationary collector; or a rotating cylinder) [25]. The apparatus is generally positioned inside of a chemical hood to allow safe exhaustion of the volatile solvents. Moreover, it is fundamental to work in a closed, non-conductive environment, with temperature and humidity control to avoid interference from environmental factors, as reviewed elsewhere [26]. The voltage supply introduces a high electrical potential (in the range of kilovolts—kV) between the needle (where an electrode is connected) and the grounded metal collector (typically in contact with the counter electrode). Both are electrically conductive and separated at an optimum distance. These high voltages are achieved due to currents in the range of few hundred nanoamperes (nA) to microamperes (mA) [27]. The syringe pump, where the syringe that contains the polymeric solution is mounted, is also a key component of the electrospinning set-up. It allows for the solution to flow from the tip of the needle at a constant and controllable rate that is optimized for each solution, as reviewed in detail elsewhere [28].

Electrospinning involves an electrohydrodynamic process used to fabricate micro- to nano-size polymeric fibers from a polymeric solution using the electrostatic force [25]. When the surface tension is overcome by the electrical force, the solution that flows from the tip of the spinneret creates a pendant droplet that deforms and elongates to form a conical structure—the Taylor cone. First, this jet extends in a straight line and then undergoes vigorous extensional spinning caused by the electrical field. With the increasing of the electrostatic stresses, a critical value is reached (distinct for each solution) when the electrostatic force surpasses the surface tension of the polymeric solution and the charged jet is being ejected continuously from the tip of the spinneret, becoming thinner by the extensional stresses experienced and caused by the electrostatic field, as it reaches the collector [29–32]. This jet gradually concentrates with the evaporation of the solvent from the polymeric solution, and precipitates in high velocities, forming solid fibers with a range of diameters. However, if the applied external electrostatic field is above the critical value, it can cause the jet to break into droplets instead of extending into fibers—phenomena called the Rayleigh instability [13]. Regarding co-axial electrospinning, its set-up is also very similar to the conventional one [19], despite requiring two different immiscible solutions, with independent control of the flow rates, being processed simultaneously (Fig. 10.2).

As reviewed elsewhere [33], the fundamental modification is made in the spinneret configuration by inserting a smaller (inner) capillary that fits concentrically inside the larger (outer) capillary. The outer needle is attached to the reservoir containing the sheath solution and the inner needle is connected to the one holding the core solution. It is also important to notice that these fibers, usually, have a larger diameter than the conventional ones [34]. The process behind co-axial electrospinning is very similar to the conventional method, where the polymeric solutions are pumped into the co-axial spinneret simultaneously and a high electrical voltage is applied. The generated stresses in the outer solution results to the shearing of the core solution via contact friction and viscous dragging, causing the formation of the co-axial Taylor cone from which a co-axial jet extends. The jet undergoes bending instability

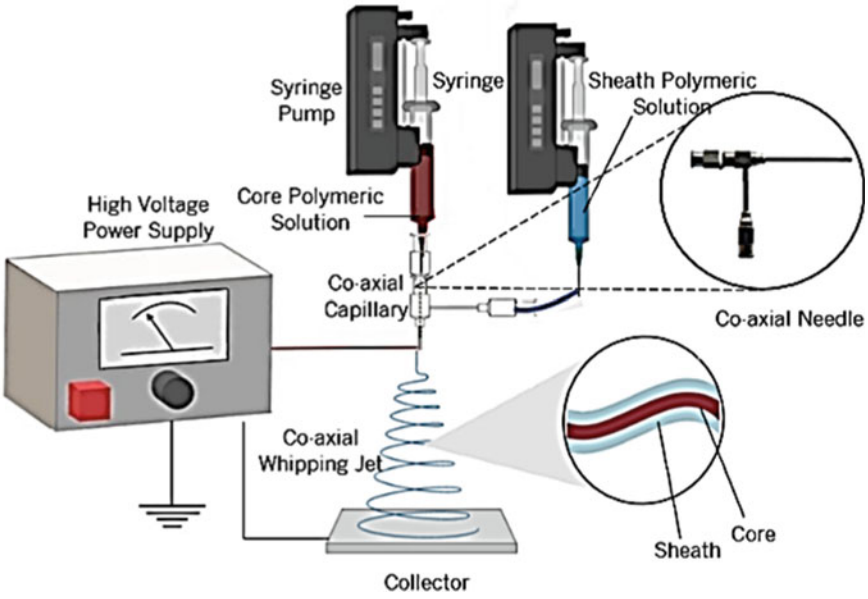


Fig. 10.2 Schematic representation of a co-axial electrospinning set-up

before reaching the grounded collector, as it happens for single electrospun fibers, which stretches the fiber and gives enough time to the solvent evaporates [33–36]. In addition, despite a polymeric solution being required to be used as shell, the core can be filled with a polymer solution, non-polymeric Newtonian liquid, or a powder are used to fill the inner core [37]. To eliminate the core and thus produce hollow fibers, the electrospinning process should be followed by selective removal of the core material (via solvents or heat treatment, or even by only use water in the core, for example) [22].

10.2.2 Control of the Electrospinning Process/Parameters

The electrospinning system is very sensitive to a large number of processing parameters that can be divided into three categories: process settings, polymer solution, and environmental parameters. These parameters are known to affect the formation, diameter, and the structure of the nanofibers, with consequences over the mesh properties, as reviewed elsewhere [38]. Due to this sensitivity, a major difficulty of electrospinning, similarly to other techniques lie on the lack of independent control over these parameters. Indeed since when one parameter or the surrounding environment is changed, the others are also influenced. For this reason, achieving reproducibility

in the production of microstructural features of a fibrous mesh remains a challenge [39].

The processing settings are largely used to control and define the diameter of the fibers in the mesh:

Applied voltage determines the amount of electrical charge applied in the jet, magnitude of electrostatic repulsion among the charges and the strength of the interactions between the jet and the external electric field [40]. An increase in the applied voltage is responsible for more intense stretching of the solution and the creation of a stronger electric field, also leading to faster solvent evaporation. Yet, if the applied voltage is too high, the jet might become discontinuous; if the voltage applied is low, there is a great probability of bead formation [41].

Flow rate of the liquid solution, it must be high enough to ensure a continuous supply of solution to the tip of the spinneret, but also low enough to allow solvent evaporation before the fibers reaching the collector. When the flow rate increases the diameter of the fibers also increases [41, 42].

Distance between the spinneret tip and the collector is essential to give the fibers an acceptable time to dry before reaching the collector. Thus, a minimum distance is required to ensure full extension of the jet, and thus forming meshes of solid fibers [42].

Collector: the type of collector used is also an important parameter since the collector serves as the conductive substrate where the fibers are deposited into a mesh-like structure. It is essential to notice that electrospun fibers are typically collected as a non-woven mat when using a stationary collector, meaning that the fiber meshes will have a random orientation [43] (Fig. 10.3a). However, some applications targeted with this technique, require highly ordered and well-aligned fibrous structures have emerged [44]. The most common, simple, and effective method of collecting aligned fibers (fibers are deposited in a parallel arrangement) is by using a dynamic rotating collector, such as a drum or mandrel [45] (Fig. 10.3b), or by using a parallel collector [46] (Fig. 10.3c). The degree of alignment, diameter and length in a fibrous mesh can be controlled based on the rotational speed of the collector [47]. It is known

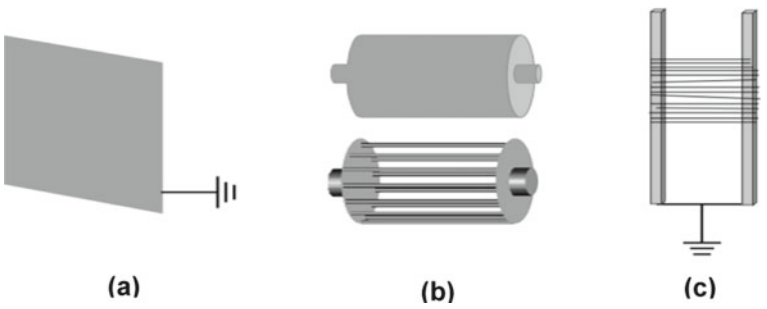


Fig. 10.3 Examples of stationary (**a**) and dynamic collectors (rotating drum collector (**b**) or parallel plate collector (**c**) used for electrospinning

that, when the velocity of the rotating collector is too excessive, necking and fiber breakage can happen because of the high extensional stresses applied. When the velocity is too low, a low-level of alignment is observed. Rotating collectors also have the benefit of assembling aligned fibers over a large area, and the higher the rotational speed (within acceptable values for each material) the thinner the fiber's diameter. This thinning phenomena happens due to the mechanical stretching of the fibers as they are deposited over the rotating collector [45, 48]. Parallel collectors may be used as alternatives collectors to create aligned fibers and consist of two strips or plates connected to the negative pole and the needle is connected to the positive pole of the power supply unit. The jet is drawn in between the two plates, ensuring the deposition of uniaxially aligned fibers perpendicular to the plates [49].

Intrinsic solution parameters are also of great importance in the electrospinning optimization process, namely:

Viscosity is crucial in the determination of the size and morphology of the fibers, and it is known that when the solution has a low viscosity is very hard to obtain a continuous fibers within a membrane. Conversely, a high viscosity leads to needle clogging [50];

Concentration of the solution: if it is high, it is difficult to maintain a homogenous flow of the jet, creating fibers with larger diameters; when the concentration is too low, a mixture of beads within the fibers is obtained rather than a continuous fiber [51, 52];

Molecular weight that affects electrical and rheological properties of the polymeric solution. High molecular weight polymers are widely used because they offer the desired viscosity for the fiber generation, whereas low molecular weight solutions tend to form beads rather than fibers [53];

Conductivity of the polymeric solution depends on the selected polymer, the solvent, and availability of ionizable salts. When the solution's conductivity is decreased, the elongation of the jet is not sufficient and leads to the formation of beaded fibers, while an increase in conductivity makes the solution extremely unstable [54];

Surface tension, that is correlated to the ability of the applied electrical potential to shear the polymer solution into electrospun fibers. Low surface tensions of the spinning solutions allow electrospinning to happen at a lower electric field [50];

Solvent vapor pressure, since the choice of an appropriate solvent for electrospinning affects mostly the morphology of the fibers, and it is necessary that the solvent volatilizes partially by the time the fibers reach the collector. Otherwise, wet fibers would deposit and fuse, resulting in the loss of their fibrous morphology. Therefore, to ensure that the fibers dry completely, the solvent must have high vapor pressure and volatility [50];

The environmental parameters also affect the formation of the solid fibers:

Humidity directly affects the morphology of the fibers, since high humidity decreases the evaporation rate of the solvent, leading to larger fiber diameters and to the appearance of small pores on the fiber's surface. On the other hand, low humidity increases the evaporation rate of the solvent, promoting a faster drying of the fibers, although with increased probability of clogging the needle [55].

Temperature: with its increase, the molecular mobility increases, there is a decreasing in the viscosity of the solution, leading to a decrease in the diameter of the fibers [56].

All the parameters can be combined in multiple ways, leading to the fabrication of meshes with a wide range of morphologies and diameters and to the optimization of the process.

10.2.3 Fibrous Meshes Morphologies and Structures

It is known that, when using a conventional electrospinning set-up, the fibers are randomly deposited into a stationary collector, forming a non-woven fiber mesh. However, as reviewed elsewhere [57] different fibrous morphologies in a mesh can be obtained by controlling the processing parameters, type of collector and spinneret, the distance between the needle tip and the collector, or even by introducing simple modifications into the electrospinning set-up to increase the capability and versatility of the processing technique. Electrospinning can produce smooth, as well as flat, beaded [58], helical, wavy or ribbon fibers [59]. This technique is also able to fabricate core–shell [60] or hollow fibers [61], multichannel tubular fibers, or fibers with controlled alignment with controlled alignment and/or porosity [28, 62]. The different shapes and morphologies of the electrospun fibers are shown below and can be divided into:

Solid fibrous meshes: in conventional/single-phase electrospinning, the fibers are composed of only one structure that can be composed of one biomaterial, a blend of biomaterials with a bioactive substance, where they usually show a cylindric shape with a smooth surface. As above mentioned, these fibers can also have random or highly aligned orientation depending on the type of collector used [45, 46] (Fig. 10.4a, b, and c).

Core–Shell fibrous meshes: the use of a co-axial needle enables to fabricate fibrous membranes with a co-axial structure. These fibers are composed by an outer fiber—shell; and an inner with smaller diameter fiber—core. Both parts must also have different compositions and be immiscible for the compound jet to phase separate in a concentric manner [20]. By increasing the number of inner needles it is possible to obtain multiple cores within the co-axial nanofibers [63] (Fig. 10.4d). Another approach to the creation of these fibers is via emulsion electrospinning. This technique consists in the electrospinning of a blend of two immiscible liquid phases [64]—emulsion, creating discontinuous co-axial nanofibers by the stretching and collapsing of that emulsion. Two types of emulsions can be used for the electrospinning process: (i) water in oil (W/O) or (ii) oil in water (O/W). Moreover, according to some authors [65] emulsion electrospinning does not require special spinnerets and can directly produce core–shell structures using a single nozzle.

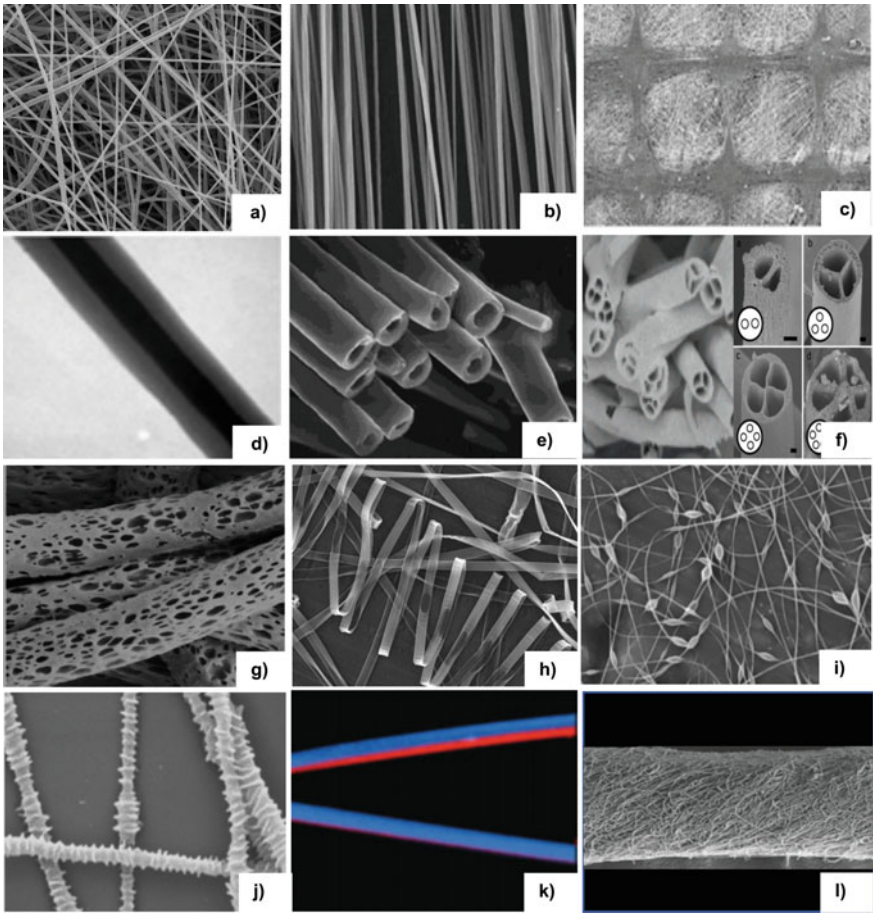


Fig. 10.4 Scanning electron microscopy (SEM) micrographs of different shapes and morphologies of fibers that compose an electrospun fibrous mesh: **a** Random Solid fibrous mesh, **b** Parallel aligned fibrous mesh. Reprinted from [79] (2016), with permission from Elsevier, **c** Pattern fibrous mesh. Reproduced from [80] (2011) with permission from Wiley©. TEM micrograph of the shape and morphology of **d** Co-axial fiber. Reprinted from [79] (2016), with permission from Elsevier. Scanning electron microscopy (SEM) micrographs of different shapes and morphologies of fibers that compose an electrospun fibrous mesh: **e** Hollow fibrous mesh. Reprinted with permission from [81] Copyright (2004), American Chemical Society, **f** Multichannel microtubes with different diameters and number of channels. Reprinted with permission from [68], Copyright (2007), American Chemical Society. **g** Porous fibrous mesh. Reproduced from [69] (2016) with permission from Wiley©, **h** Ribbon fibers. Reproduced from [59] (2001) with permission from Wiley©, Elsevier **i** Beaded fibrous mesh. Reprinted from [58] (1999), with permission from Elsevier, **j** Shish-kebab fibrous structures. Reprinted with permission from (82), Copyright (2008), American Chemical Society. **k** Confocal laser microscopy image of Janus fibers. Reproduced from [75] (2008) with permission from Wiley©. **l** Yarn fiber. Reprinted from [83]

Hollow and Multichannel fibrous meshes: co-axial electrospinning is the most versatile method for the fabrication of hollow fibers by selectively removing the core of core—shell fibers [62]. The outer diameters and wall thicknesses of the hollow nanofibers can be tuned by playing with the flow rates of the inner and outer fluids [66]. Hollow nanofibers can also be directly produced by inducing phase separation during emulsion electrospinning, as reported elsewhere [67]. Titanium dioxide (TiO_2) nanotubes in a water in oil emulsion system were created by electrospinning using a homogenous solution containing Polyvinylpyrrolidone (PVP) and a TiO_2 precursor (tetrabutyl titanate), in which the oil was dispersed and immediately evaporated. This led to the formation of PVP/tetrabutyl titanate hollow nanofibers. Based on a multifluidic co-axial electrospinning approach, hollow multi-channel and -polymer nanofibers were also fabricated (Fig. 10.4e). For example, tubes with two to five channels were already produced [68] (Fig. 10.4f).

Porous fibrous meshes: In general, fibrous meshes produced by electrospinning have a solid structure and, when pores are introduced in the fibers, the specific surface area of the resultant electrospun mesh is widely increased (Fig. 10.4g). The main strategy for generating pores in the fibers is by inducing phase separation during electrospinning and selectively removing a sacrificial phase from the spun membranes via leaching or calcination. The in-fiber porosity can be controlled by manipulating the density, size, shape, and distribution of the pores [62, 69].

Ribbon fibrous structures: in addition to the conventional cylindrical nanofibers, electrospinning can also produce fibers with a variety of cross-sectional shapes. The fabrication of electrospun ribbon fibers during electrospinning happens when a thin and mechanically distinct polymer creates a "skin" on the liquid jet. This tubelike skin collapses leading to the creation of ribbon like structures, since the regular circular cross section opens and flattens, forming a ribbon with a cross-sectional perimeter [59] (Fig. 10.4h). However, applications for these flat ribbon fibers are still to be developed.

Beaded fibrous meshes: these fibers can be formed by fine tuning of the surface tension and viscosity of the electrospinning solutions, as well as the density of charges carried by the jet. Usually, a lower viscosity and density of surface charges favor the formation of beaded nanofibers, whereas reduction of surface tension makes the beads to disappear gradually [70] (Fig. 10.4i). The composition of the beads and fibers is often of the same material. However, by combining with other approaches, beads can be made with a different material than the one used to create the fibers. Moreover, to create beaded fibers with different materials from the original one, the use of an outer liquid with a high surface energy is crucial, in order to prevent the sheath component from mixing to the core component [71, 72].

Shish-kebab fibrous structures: A hierarchical shish-kebab structure was produced by controlling the crystallization of a polymer during electrospinning. Studies have shown that solution electrospinning of polypropylene (PP) at a high temperature produced PP nanofibers consisting of nanofibrils with a shish-kebab structure [73].

The shish-kebab structure can also be produced by inducing oriented crystal growth on the as-spun nanofibers through a thermal post-treatment [74] (Fig. 10.4j).

Janus fibrous meshes: These fibers are formed by two distinct materials. This morphology has often been referred to as "Janus," in reference to the two-face god in Roman mythology. Although the creation of Janus nanofibers is usually made in a microfluidic system, one way to produce high-quality Janus nanofibers can be by using a two-fluid electrospinning process with a careful choice of spinneret design (two side-by-side needles or two acentric needles). The second mentioned configuration also ensures a relatively high contact area between the two polymer solutions, reduces repulsive forces between the two fluids and facilities the two fluids moving and drying simultaneously. Three-fluid electrospun Janus fibers were also obtained using a structured spinneret comprising two acentric needles into a third one, with an exterior solvent surrounding two core fluids arranged side-by-side, high quality Janus nanofibers were prepared [75, 76] (Fig. 10.4k).

Yarn fibrous structures: the collector can be modified in multiple ways by combining other techniques, such as lithography, aiming to organize the nanofibers into different patterns. A liquid bath was used as a collector, enabling the fabrication of fiber yarns and filaments [77, 78], rather than a non-woven mat of nanofibers (Fig. 10.4l).

10.3 Microfluidics

Microfluidics is a technology that involves the control and manipulation of fluids geometrically restricted at sub-millimeter dimensions using channels with dimensions in the micrometers range, also known as micro-channels [84]. This technique was object of a significative development since 1998, after the introduction of polydimethylsiloxane (PDMS) into the microfluidic field, once the use of this material led to the creation of more complex microfluidic devices such as microfluidic chips [85, 86].

The use of such miniaturized devices offer several significant advantages, such as: (i) the use of small quantities of samples and reagent volumes, allowing for the reduction of reactant consumption; (ii) enables well-defined and highly reproducible reaction times and mixing conditions within the micro-channels; (iii) can be made in wet conditions; (iv) reduces possible cross-contamination; (v) has a high surface area-to-volume ratios; (vi) improved control over mass and heat transfer; (vii) spatiotemporal control over the fabricated fibers; (viii) fast response and short analysis times; (ix) it is able to carry out separations and detections with high resolution; (x) has reduced sensitivity to operational parameters and thus a high degree of reproducibility. Moreover, the versatility of the microfluidic systems enables the integration of several fluidic units such as chips, mixers, valves, and pumps, achieving an even higher degree of flow control [87–89].

Microfluidics is an interdisciplinary field, merging distinct areas of microtechnology, engineering, biotechnology, chemistry, physics, and materials science.

Recently, microfluidic devices are the subject of great interest in the scientific community, due to their potential as tools for producing micro- and nano-scale structures with a wide variety of shapes, including fibers, tubes, or particles [90–92]. Therefore, this field has grown with the continuous development of micro-miniaturized analytical devices for biomedical analysis, chemical sensing, genetic analysis, and metabolic monitoring/detection. Microfluidics has shown the potential to solve problems that have not yet been solved by traditional macroscale methods, particularly in the diagnostics field [6].

10.3.1 Principles of Microfluidics and Microfluidic Spinning

When microfluidic systems are used, it involves the use of a microfluidic chip, that is a device decorated with micro-channel patterns engraved/molded into a surface and produced with [93]: (i) glass; (ii) silicon [94]; (iii) elastomers like PDMS [95], or thermoset polyesters (TPEs) [96]; (iv) thermoplastics [97] like polycarbonate (PC), polystyrene (PS) or poly-methyl methacrylate (PMMA); (v) paper [98]; or even with (vi) hydrogels [99]. Moreover, the use of these devices aims at confining and controlling the fluid flow at the micrometer-scale [93].

The network of micro-channels engraved on the surface of the microfluidic chip is connected to the outside by inlets and outlets pierced through the chip. This technology enables the production of an interface between the macro- and micro-world. It is through these holes that the fluids are injected and, posteriorly, removed from the microfluidic chip (with the help of adequate tubing and/or syringe adapters) with flow-control elements such as external active systems (i.e. pressure controller, syringe pump, or peristatic pump) or capillary flow [100].

PDMS is one of the most used materials for microfluidic chip fabrication due to its unique characteristics, namely transparency (allowing the micro-channels and their content to be imaged), elasticity (this property can be used for a better valve integration through the channel deformation), cost (less expensive than other materials used for microfluidic chip fabrication), and permeability (PDMS is gas permeable which can be used in cell culture, or gas sensors) [95]. A fluid software controller is also a key-component of microfluidic systems, being capable of adjusting the opening/closing time of the micro-channels, giving stability to the process [101].

Microfluidic spinning can be described as a typical wet spinning process. This can be applied to polymers that do not dissolve in non-volatile or thermal unstable solvents. More precisely, a non-volatile solvent is used to convert the raw material into a solution, which is later extruded through a spinneret (in the microfluidic case through one of the chip's micro-channels) into a bath. The solvent will be further washed out or removed by a chemical reaction with a reagent present in the spinning bath, being the final result a fibrous filament [102].

This recent technique involves micro-scale fluid dynamics. It is important to notice that the fluids that are flowing through the micro-channels are different from bulk fluids, mainly due to surface tension, energy dissipation, and fluid resistance factors.

Due to the size of the micro-channels, the fluid flows in a microfluidic system in the laminar regime, where two or more streams of the flow in contact with one another (co-axial flow) do not mix, except by diffusion at the interface. Mixing processes in microfluidics are a challenge due to the laminar flow within the micro-channels, which result from low Reynolds number (< 1) determined by the channel's hydraulic diameter, flow velocity and solution's kinetic viscosity [103]. Since laminar flows are highly predictable, the mathematical modelling of these systems is easier and the experiments are very reproducible [104].

When the goal is to produce solid fibers by using a microfluidic approach—microfluidic spinning—a polymerizable core fluid and non-polymerizable sheath fluid are introduced into separate input ports of the micro-channel and meet at a channel intersection. The 3D co-axial sheath flow stream surrounds the central sample flow [100, 105], functioning as a lubricant and preventing direct contact between the channel wall and the sample, preventing micro-channel clogging (Fig. 10.5a). Therefore, a process of phase separation in the microfluidic channels enables the production of a co-axial flow. To produce solid fibers, the central flowing fluid is, usually, solidified by using (Fig. 10.5b) [106].

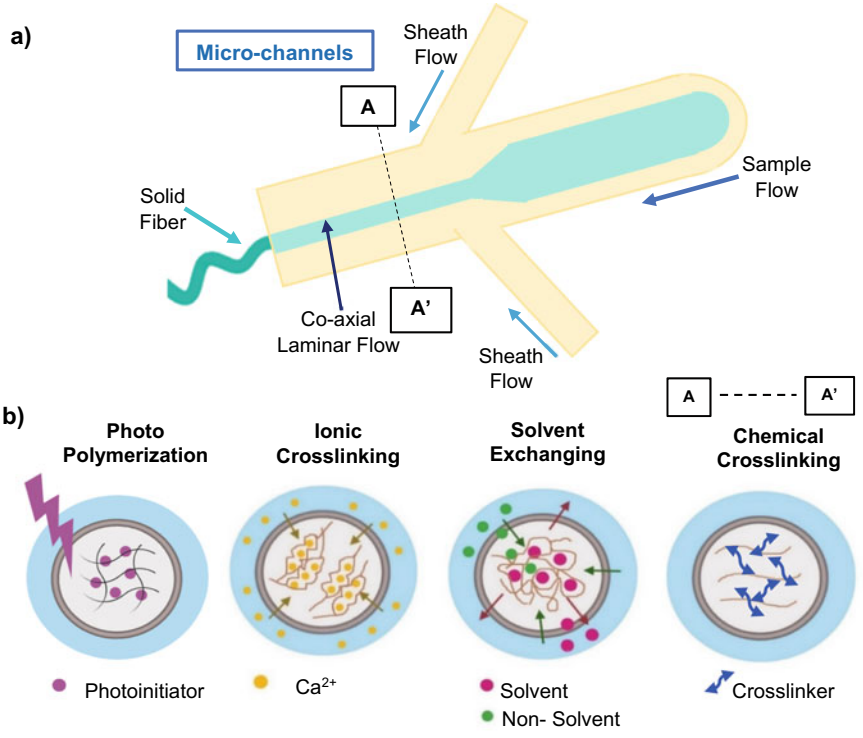


Fig. 10.5 **a** Behavior of a sample flow in a microfluidic system. **b** Different solidification methods in microfluidics. Adapted from [24] (2017) with permission from Elsevier

Photopolymerization using UV light (generally 365 nm) irradiated onto the flow stream. Photopolymerizable polymers such as Poly(ethylene glycol) diacrylate (PEG-D)A or 4-hydroxybutyl acrylate (4-HBA) are generally used as a backbone material, and photo-initiators are added to induce the photopolymerization of the system.

Solvent exchange involves mass diffusion between a polymer solution and a non-solvent, generating polymerized fibers.

Crosslinking processes (ionic or chemical) are used to prepare microfibers through the formation of covalent or noncovalent bonds between the polymer chains mediated by crosslinkers. It is important to highlight that the microfluidic spinning requires less parameters stabilization than electrospinning. Furthermore, size and configuration of the produced fibers are tuned by manipulating the solution's parameters such as concentration and viscosity, as well as the polymeric solution flow rate (processing parameter) [107].

10.3.2 Fibrous Structures

Despite the microfluidic technology being capable of producing a great variety of micro- and nano-scale structures, in this review only the fibrous structures will be addressed in detail. Depending on the materials used and the design of the microfluidic devices, a wide range of fibers with different shapes and geometries can be produced (Fig. 10.6), such as:

i. **Solid Fibers**: these fibers usually have a cylindrical shape and are the most popular in microfluidics because of easier spinning and safety for cell encapsulation (Fig. 10.6a). They can be solidified by photo or chemical reactions, and the fibers can have different diameters that can go until the range of hundreds of μ m [100]. These fibers can also have a porous morphology, since the appearance of porous fibrous structures is related to an increase in the surface area, enhancing cell migration and mass transfer and, consequently, cell adhesion (Fig. 10.6b) [108].
ii. **Tubular/Hollow Fibers**: the use of a double co-axial laminar flow microfluidic device allows the formation tubular/hollow fibers allied with the incorporation of glass micropipettes into a preformed hole in a PDMS chip containing a micro-channel network or even using a chip with a hierarchical, multilayer, microchannel structure [109, 110] (Fig. 10.6c).
iii. **Flat and Grooved Fibers**: Depending on the shape of the micro-channel cross-section, a variety of patterns may be engraved onto the surfaces of the fibers along the longitudinal direction. Thin and flat channels may be used as platforms for continuously spinning flat fibers (Fig. 10.6e), but several topographical information can be encoded using special designed microfluidic chips or computer-controlled switching [111–113]. For example, longitudinal grooves on the inner surfaces of cylindrical channels can enable the spinning

of microfibers bearing grooved surfaces (Fig. 10.6d). Moreover, the continuous fabrication of flat alginate microfibers (micro-ribbons) with size-tunable grooved microstructures using a microfluidic system was also studied [106].

iv. **Janus/ Hybrid or Pattern Coding Fibers**: These fibers are achievable by using co-axial micro-channels and side-by-side needles, producing a fiber with two different properties and chemical composition. Janus/Hybrid fibers can also be asymmetric or have a specific organizational pattern such as parallel (Fig. 10.6f

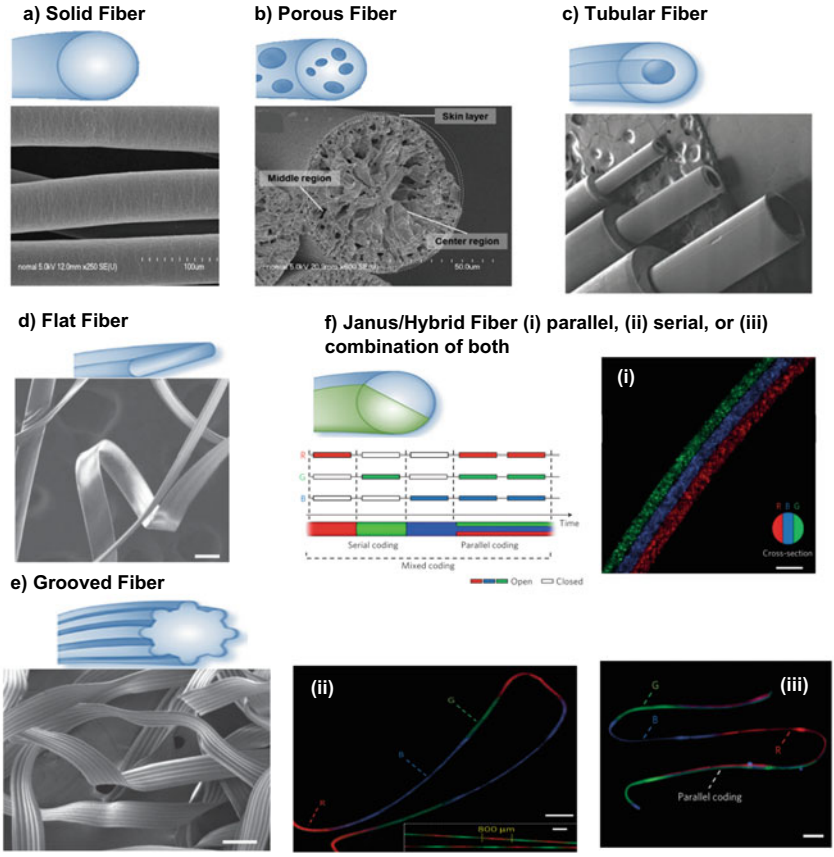


Fig. 10.6 Types of fibers fabricated with microfluidic spinning systems. Schematic and SEM micrograph of **a** Solid fiber. Reprinted (adapted) with permission from [117], Copyright (2008), American Chemical Society; **b** Porous fiber. Reprinted (adapted) with permission from [117], Copyright (2008), American Chemical Society; **c** Tubular fiber. Reproduced from [118] (2016) with permission from Wiley©; **d** Grooved fibers[106]; **e** Flat fibers. Reproduced from [106] (2012) with permission from Wiley©; Schematic and confocal microscopy images of **f** Janus/Hybrid fiber (i) parallel coding, (ii) mixed coding, (iii) serial coding. Reprinted/adapted by permission from Nature Publishing Group—Springer Nature [116] (2014); **g** Patterning fibers. Reproduced from [119] (2012) with permission from Wiley120 © and **h** Hierarchically coded fibers. Reproduced from [] (2014) with permission from Wiley©

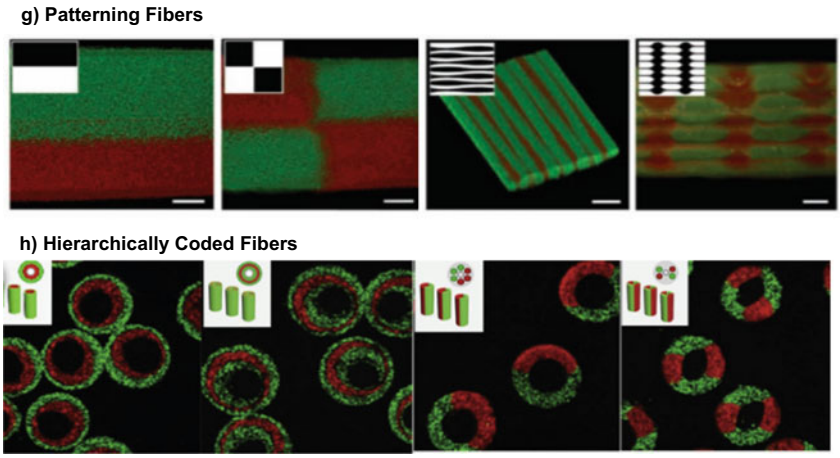


Fig. 10.6 (continued)

and i), serial (segmented) (Fig. 10.6f and ii) coding fibers, or a combination of both (Fig. 10.6f and iii) [114, 115]. Moreover, patterning multiple materials along the fiber direction has also been developed using digital valve control systems allowing us to achieve different fiber patterns (Fig. 10.6g) or even hierarchically coded fibers (Fig. 10.6h). As example, a novel microfluidic spinning method for producing tunable coded fibers, by testing diverse materials was proposed [116]. Such a capability of producing patterns can be used for the spatiotemporally programmed loading of cells or drugs with a controllable release profile.

10.4 Applications of Electrospinning and Microfluidic Spinning in the Biomedical Field

The versatility of both electrospinning and microfluidics techniques allows to adjust all the processing parameters aiming to achieve the desired fiber morphology and mechanical strength. The versatility coupled with other advantages of those techniques, justifies the great interest in the investigation of their applicability in many fields. Of particular interest is the biomedical field, where electrospun nanofibers are applied for tissue engineering approaches, mainly as scaffolds (applicable to tissues such as bone, cartilage, skin, skeletal muscle, blood vessels and neural tissues), as drug delivery systems, and wound dressings. On the other hand, the application of microfluidic systems in the biomedical field, can be divided into four main groups, as reviewed elsewhere [121]: (i) organ-on-a-chip devices, i.e. microfluidic chips to be used as predictive in vitro models, created via soft-lithography and replica molding that contains continuously perfused or actuated micro-channels arranged to simulate

tissue and organ (i.e. heart, brain, lung, kidney or even the eye) level physiology [122–124]; (ii) devices for the processing of biomaterials to be used as scaffolds or cell carriers for tissue engineering [114, 125]; (iii) devices for cell culture, sorting, migration [126, 127]; (iv) and, micro total analysis systems (μ-TAS) [128], which consist in devices designed to carry out specific analysis of biologically important molecules with applications in genomics, proteomics, clinical diagnosis, drug discovery and biosensors [129].

The use of microfluidics to create fibers allows obtaining a large variety of fiber morphologies and patterns, and high control over the flow of the fluids. Due to that, microfluidic spinning has become a great approach to cell encapsulation [125, 129], and also shares several biomedical applications with electrospinning such as scaffolds [100] for tissue engineering and drug delivery systems. Figure 10.7 summarizes the biomedical applications of fibers created with electrospinning and microfluidic spinning techniques.

10.4.1 Tissue Engineering

Generally, when a tissue or organ damage occurs, the body has the ability to self-repair. However, when this ability is not sufficient to regenerate large defects, the most common treatment options are surgical repair, namely using autografts, artificial prostheses, or transplantation (autologous or heterologous). Although they are all valid alternatives, in some circumstances, the body cannot achieve full regeneration of the damaged tissue and/or the outcomes are not satisfactory. The treatment can cause a chronic immune response leading to transplant rejection [130, 131] or negative outcomes either aesthetic or functional [132]. This is where tissue engineering comes in, as a valid alternative and against the shortage of donors/supplies. Tissue engineering is a multidisciplinary field that allows for the tissue regeneration, instead of replacement, by creating biological substitutes that can restore tissue function or even improve it [132, 133].

Scaffolds for Tissue Engineering: when compared to other fiber forming processing techniques, such as self-assembly and phase separation, electrospinning proved to be the simpler and most cost-effective way to produce fibrous scaffolds. The electrospun fiber mats must be non-toxic, biodegradable (the degradation rate should be compatible the rate of neo-tissue formation), easy processability into desired shapes, present mechanical strength and dimensional stability in order to prevent the scaffold to collapse [132, 133]. Furthermore, electrospun fibrous mats have the ability to enhance the adsorption of proteins and subsequent cell attachment [136]. It is important to note that the similar fibrous structure of electrospun scaffold with the natural ECM is very important for the behavior of the cultured cells on its surface [7].

Both synthetic such as Poly(ε-caprolactone) (PCL), Poly(Lactic Acid) (PLA), Poly(L-Lactic Acid) (PLLA), Poly(Glycolic Acid) (PGA), Poly(Lactic-co-Glycolic

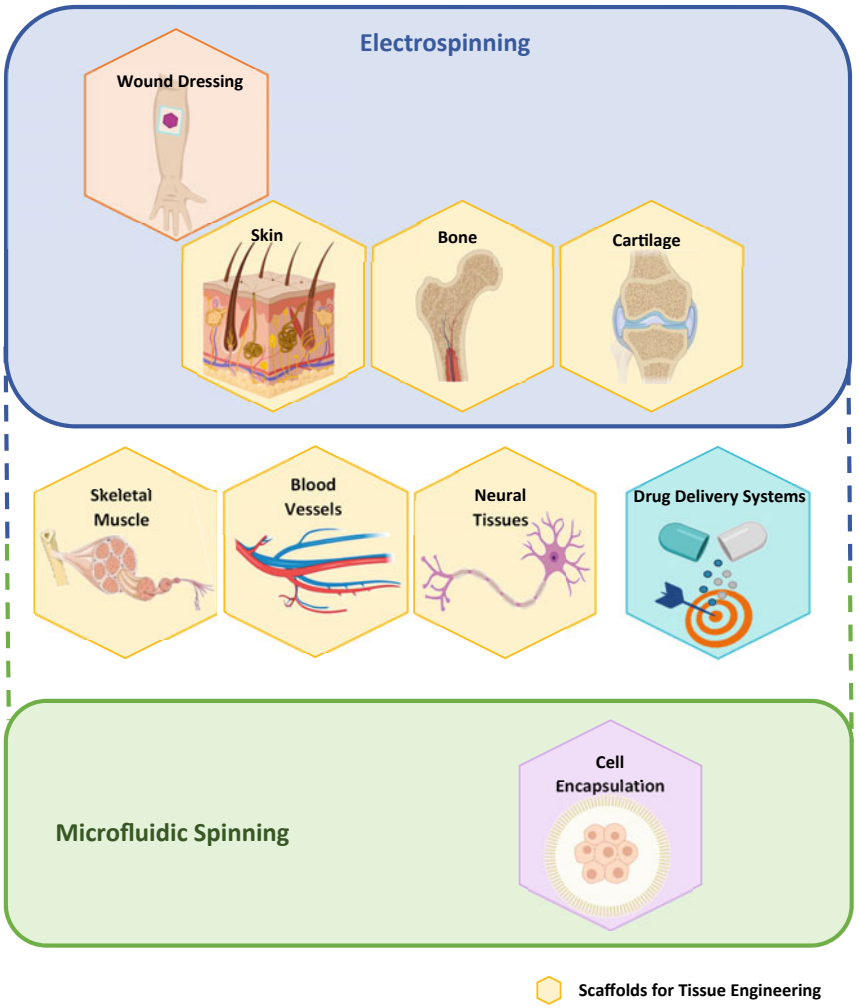


Fig. 10.7 Biomedical applications of fibers created with electrospinning and microfluidic spinning (summarized)

Acid) (PLGA), Poly(vinyl alcohol) (PVA), Poly(Ethylene Oxide) (PEO) and Poly(Ethylene Glycol) (PEG) and natural polymers (e.g. collagen, chitosan (CS), silk fibroin and gelatin), and even combinations of both were processed by electrospinning to produce tissue engineered scaffolds. Although natural polymers may exhibit biocompatibility, bio-functionality, and low immunogenicity, the synthetic ones can be modulated to have a wider range of properties such as tunable mechanical properties and kinetics of degradation, while having cytocompatibility of the scaffold [18].

Regarding co-axial electrospinning, this approach can be also used for scaffold production, offering some very important advantages such as the case when a core–shell structure is obtained by two polymers with different hydrophilicity. In most of the cases, a hydrophilic polymer is used as the core (in where active molecules are embedded) and a hydrophobic polymer is used as shell. Cases where a hydrophobic core is within a hydrophilic shell are less frequent. The coating of the core material, with poor cell binding properties, with a more biocompatible material has been accomplished to benefit cell-scaffold interaction and to increase cell adhesion. As an example, PCL was used as the core to take advantage of its mechanical strength, and gelatin as shell to have enhanced biocompatibility of the scaffold. It was confirmed that the contribution of the core can influence the mechanical properties of the fibers, while the shell material can enhance the interaction of the mesh with the environment, increasing the biocompatibility of the final solution [137].

The production of fibers by microfluidic spinning, and their integration in tissue engineering approaches is still in its early stages [100]. Nevertheless, microfluidic spinning has interesting properties that make it suitable for tissue engineering approaches [138], namely the easy encapsulation of cells or cell spheroids, and can provide spatiotemporal control of the composition, size, and morphology of the materials used [139–141]. These distinctive properties associated to the design of a microfluidic device amenable to fabricate complex or surface patterned fibers, make this technique more suitable for controlling cell alignment and guiding cell proliferation [106, 117]. As example, a 3D cell-laden fibrous scaffold was produced using a single microfluidic platform, in a one-step process. Moreover, rat hepatocytes encapsulated in this scaffold showed enhanced viability and albumin secretion than cells encapsulated in a bulk hydrogel, intending to generate a tissue structure capable of mimicking the liver [114]. Furthermore, it is known that most microfluidic fibers are obtained with hydrogels, and molecules can diffuse through the pores and migrate across the hydrogel structure [142]. Therefore, when cells are encapsulated within these fibers, the secreted molecules can easily diffuse out of the fibers into the surrounding tissue. As a result of these properties, cell-encapsulating microfluidic spinning fibers can be used for the regeneration of organs with complex functions [114, 116].

i. **Bone**: electrospun nanofibrous scaffolds that mimic the nanoscale morphological features of natural bone ECM have been studied and developed. Our group developed novel PCL electrospun nanofibrous membranes coated with a biomimetic calcium phosphate (BCP) layer to be used as an analogue for human bone extracellular matrix. The deposition of the BCP layer on fibrous mesh was achieved through surface modification, followed by treatment with solutions containing calcium and phosphate ions and a posterior immersion in a simulated body fluid (SBF) with nearly 1.5 $\times$ the inorganic concentration of the human blood plasma ions. Results demonstrated that the coating with bone-like BCP layer on PCL nanofiber meshes was more effective for supporting cell attachment and proliferation of osteoblasts when compared to

untreated meshes for long culture periods. Those structures, show that PCL-BCP coated nanofiber meshes are effective for bone-tissue engineering applications [143]. A bone ECM inspired structure by conjugating electrospun CS nanofibers with biodegradable polymeric microfibers of [poly(butylene succinate)] (PBS) assembled in a fibrous mat was also developed. The reinforced nanofibrous composite scaffolds were seeded with human bone marrow-derived MSCs and cultured under osteogenic differentiation conditions. The scaffolds demonstrated ECM deposition and mineralization, and the genotype of the cultured MSCs was validated by the expression of osteoblastic genes, involved in different stages of the osteogenesis [144]. It was also proposed the use of electrospun biodegradable non-woven PCL nanofiber scaffolds to culture and expand mesenchymal stem cells (MSCs) derived from the bone marrow of neonatal Lewis rats, aiming to study its potential for bone tissue engineering. The constructs were cultured with osteogenic supplements under dynamic culture conditions for 4 weeks in a rotating bioreactor, and subsequently implanted in the omenta of rats for 4 weeks. The scaffolds maintained their original size and shape. Cell penetration and abundant ECM like tissue were observed. Moreover, the surface of the constructs was covered with cell multilayers at 4 weeks, and osteoblast-like cells and globular agglomerations together with collagen bundles were present [9]. Other researchers produced PLLA electrospun nanofibers with random and aligned orientation immobilized with bone morphogenic protein-2 (BMP-2) to investigate how these signals could influence the in vitro osteogenic differentiation of human MSCs and in vivo bone regeneration in a mouse calvarial defect model. Cell adhesion and ECM assembly in vitro were directed by the underlying nanofiber morphology, while fiber alignment did not have a significant influence on in vitro osteogenic differentiation. In vivo bone regeneration was significantly higher in the nanofiber implanted groups (65–79%) as compared to the defect-only group (approximately 12%), while no significant difference in bone regeneration was observed between random and aligned groups [145].

ii. **Cartilage**: various studies, based on nanofibrous structures processed by the electrospinning technique, were conducted aiming to repair cartilage defects. Our research group also proposed the use of electrospun PCL nanofibrous meshes as a scaffold for cartilage tissue engineering [146]. hBM-MSC were seeded onto electrospun meshes and cultured in a multi-chamber flow perfusion bioreactor to determine their ability to produce cartilagineous extracellular matrix. Results show that the flow perfusion bioreactor increased the chondrogenic differentiation of hBM-MSCs. Cartilage-related genes such as AGC, Coll-II, and Sox9 were expressed, and histological tests detected ECM deposition. In an innovative approach, we immobilized key proteins involved in the regulation of chondrogenic differentiation (i.e. Transforming Growth Factor-β3 (TGF-β3) and Insulin-like Growth Factor-I (IGF-I) or fibronectin) at the surface of a single electrospun nanofibrous mesh [147]. The use of well-defined antibodies (anti-TGF-β3 and anti-IGF-I) for immobilization on the fibrous meshes allowed the selective retrieval of the abovementioned growth factor from

human platelet lysates. Biological assays demonstrated that the developed biofunctional nanofibrous can promote the chondrogenesis of human BM-MSC without the need of continuous supply of exogenous recombinant GFs. Another study investigate the potential of PVA/PCL nanofiber scaffolds seeded with rabbit bone marrow-MSCs (BM-MSC) for cartilage tissue engineering in vitro and in vivo [148]. Electrospun scaffolds revealed capacity to support proliferation chondrogenic differentiation of MSC in vitro. For the in vivo approach, PVA/PCL nanofiber scaffolds with or without seeded MSC were implanted into rabbit full-thickness cartilage defects. The rabbits treated with cell-seeded PVA/PCL scaffolds showed improved healing of defects compared with the untreated control and those which received cell-free scaffolds, suggesting that these PVA/PCL scaffolds incorporated with MSC can be used as a suitable graft for articular cartilage reconstruction. In another approach, a cell-seeded with allogeneic chondrocytes or xenogeneic hMSCs nanofibrous PCL scaffold works for cartilage repair in vivo was also created [149]. Both cell-seeded and acellular PCL scaffolds were implanted in 7 mm full-thickness cartilage defects in a swine model. Six months after implantation, MSC-seeded constructs showed the most complete repair in the defects compared to other groups: showed regenerated hyaline cartilage-like tissue and restored a smooth cartilage surface, while the chondrocyte-seeded constructs produced mostly fibrocartilage-like tissue with a discontinuous superficial cartilage contour. Incomplete repair containing fibrocartilage or fibrous tissue was found in the acellular constructs and the no-implant control group. It was proved that the cell-seeded nanofibrous scaffolds effectively deliver therapeutic cells to cartilage lesions and support chondrogenic activity during the cartilage regeneration in vivo. Aiming to reproduce the structural organization of cartilage's collagen fibrillar network, trilaminar scaffolds by sequential electrospinning with changeable fiber size and orientation were created [150]. Bovine chondrocytes cultured over those scaffolds proliferated and produced a type II collagen and a sulfated glycosaminoglycan-rich ECM, and even promoted significant upregulation of aggrecan and type II collagen genes expression, while downregulating type I collagen. Compressive testing at physiological strain levels also revealed that the mechanical properties of the trilaminar composite scaffolds approached those of native cartilage. Therefore, sequential electrospinning can be a promising way to produce a nanofibrous mat similar to the cartilage [150].

iii. **Skin**: electrospun fiber scaffolds have been widely investigated for skin TE applications since they can mimic the native ECM topography of skin, namely a certain degree of fibers orientation, and possess similar mechanical properties, have high porosity, and large surface area-to-volume ratio that allows cell proliferation [151]. Therefore, several alternative electrospinning set-ups were developed to achieve alignment such as collectors with configurations to match the desired orientation, or the use of near-field or melt electrospinning [152]. The use of chitosan-PVA (CS-PVA) blend nanofibers as dermal substitutes compared with 2D CS-PVA films was investigated both in vitro and in vivo. Mouse 3T3 fibroblast cells were shown to adhere and proliferate better at the

surface of CS-PVA nanofibers. In addition, CS-PVA blend nanofibers combined with topical administration of the growth factor R-Spondin 1 on full thickness rat wounds exhibited 98.6% wound closure after 2 weeks post-surgery. This study showed that the combination of those nanofibers with this growth factor is a promising strategy to accelerate wound healing [153]. Facing a translational perspective, a battery-operated electrospinning apparatus (BOEA), based on miniaturization and integration of the conventional electrospinning apparatus, was created for skin graft applications. Different polymers such as PCL, PLA, PS, PVP, and poly(vinylidene fluoride) (PVDF) were electrospun into fibers successfully, which confirms the stable performance and good real-time control capability of this apparatus [154].

iv. **Skeletal Muscle**: tissue-engineered electrospun scaffolds are were also proposed, since the fibers must present a certain degree of alignment to resemble the muscle surface [155]. Electrospun PLGA aligned fibers were seeded with myoblasts with a very similar topography to the one of the skeletal muscle (Fig. 10.8a, b and c), capable of providing contact guidance for myoblast elongation and alignment. In addition, the scaffold did not require further surface modifications or incorporation of biologic material for adhesion, elongation,

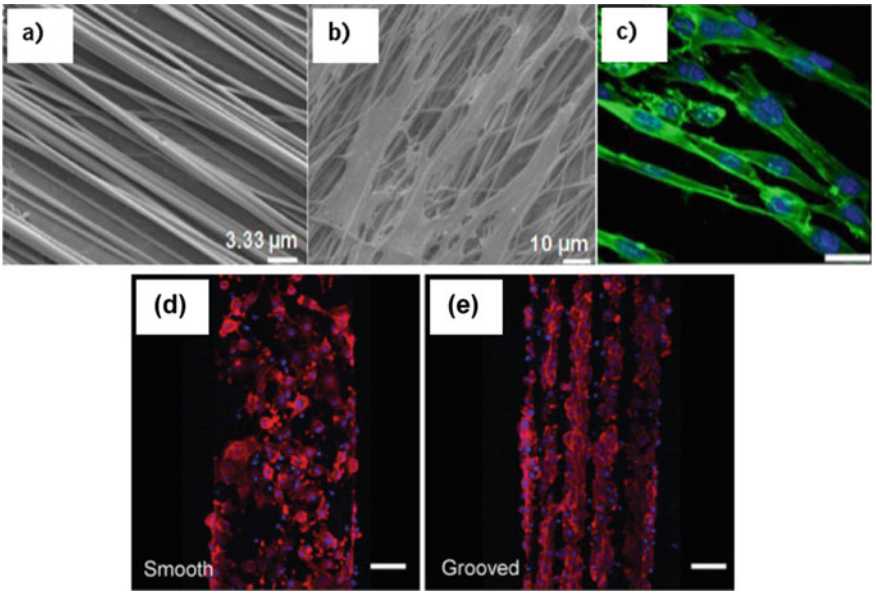


Fig. 10.8 **a** SEM micrograph of 1500 rpm electrospun aligned PLGA; **b** SEM micrographs of myoblasts seeded on electrospun 1500 rpm PLGA scaffolds (24 h of culture); **c** Confocal micrographs of myoblasts stained with FITC-phalloidin for the f-actin component of the cytoskeleton (green), and DAPI stained nuclei (blue)—24 h. Reproduced from [155] (2010) with signed permission from the authors. Fluorescence microscopy images microfluidic spinning of myoblasts on a (**d**) smooth flat fiber and **e** a grooved flat fiber. Reproduced from [106] (2012) with permission from Wiley©

and differentiation of C2C12 murine myoblasts [155]. Concerning the microfluidic spinning technique, a method to fabricate alginate flat microfibers with a grooved pattern with size control engraved in the channels of a microfluidic PDMS platform was proposed. Since grooved flat fibers are used to align cells in culture, myoblast (rat skeletal muscle cell line L6) cells were culture on smooth and grooved flat fibers. The myoblast cells appeared to be randomly oriented on the smooth fibers, whereas the cells aligned along the direction of the microgrooves on the grooved fiber, creating aggregates within the microgrooves and preventing the myoblasts from spreading over the edges, demonstrating that grooved flat fibers can be used to align other types of cells in culture (Fig. 10.8d and e) [106].

v. **Blood Vessels**: electrospinning can also fabricate polymeric fibrous scaffolds that easily satisfy the morphological requirements of native blood vessels [156]. For the creation of blood vessel-like structures, the result of electrospinning should be a tubular scaffold, as shown in Fig. 10.9a. It is known that tissue engineered small-diameter blood vessels are a challenge due to the risk of thrombosis and short-term patency. A novel strategy in vascular regeneration was the creation of a system composed of a bilayer vascular scaffold prepared via emulsion electrospinning of PEG-b-PCL and electrospinning of PCL and gelatin (Fig. 10.9a, b and c) in a hollow tubular shape. It served mainly as in a delivery system composed of electrospun fibrous membranes and target carriers for the intracellular delivery of miRNA-126 (miR-126) to endothelial cells (ECs) in the local specific vascular environment. Results shown that miR-126 released from the electrospun membrane could modulate ECs proliferation via down-regulation of SPRED-1 gene, while maintaining their tubular shape [157]. Other approach consisted in the creation of a 2 mm diameter PCL fibrous scaffold and compare it with the conventional expanded ePTFE grafts after implantation in vivo in a rat for 24 weeks. Blood vessel-like PCL scaffolds showed better patency rate when compared to ePTFE grafts. A faster growth of endothelial cells and fibroblast cells with extra cellular matrix (ECM), as

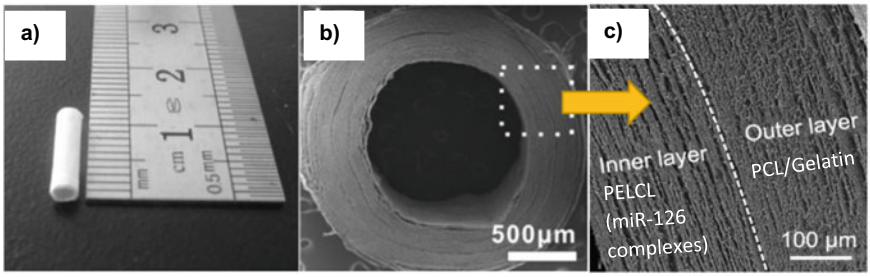


Fig. 10.9 Morphology of an electrospun vascular graft **a** Appearance; **b** SEM micrograph of the cross section; **c** SEM image showing the cross-section of a multilayered vascular conduit, with microRNA 126-incorporated PEG-b-PLCL fibers as the inner layer and a blend of PCL and gelatin fibers as the outer layer. Reproduced from [157] (2008) with permission from Elsevier

well as angiogenesis were also observed in the PCL grafts. Furthermore, the histological analysis of the blood vessel made of PCL electrospun fibrous scaffold showed no thrombosis or aneurysm after the implantation of blood vessels in an abdominal aortic of the rat after 12 weeks [158]. Our group created a PCL electrospun tubular fibrous (eTF) scaffold biofunctionalized with tropoelastin at the luminal surface as a small diameter vascular graft. This eTF scaffold demonstrated to be suitable for vascular applications since it had uniaxial tensile properties within the same range as those of native blood vessels. In addition, the functionalization of the luminal surface was confirmed by an increased zeta potential and by the insertion of NH2 groups. Tropoelastin was immobilized via its –NH2 or –COOH groups at the activated or aminolysed eTF scaffolds, respectively, to study the effect of exposed functional groups on human endothelial cells (ECs) behavior. Immobilized tropoelastin on activated eTF scaffolds endorsed an increase in ECs metabolic activity and proliferation, although when immobilized on aminolysed eTF scaffolds, significantly higher protein synthesis was observed [159].

By using a microfluidic spinning technique based on cell encapsulation approaches (immobilization of cells within a semi-permeable polymeric substrate, allowing the bidirectional diffusion of essential molecules from cell metabolism, as well of therapeutic proteins [160]), Core/shell hydrogel microfibers using a microfluidic device with a double co-axial laminar flow were created where the co-axial fibers were composed of an alginate shell, and natural ECM proteins and cells, in these case primary *human umbilical vein endothelial cells* HUVECS and collagen, in the core. Cells encapsulated into the core fibers proliferated and migrated along the longitudinal direction of the fibers, creating tubular cellular constructs resembling vascular structures [125].

vi. **Neural Tissues**: since electrospinning offers several advantages over the use of nerve grafts (autografts and allografts), namely a wider range of size selection, reduced axonal escape at the suture site, no extra surgery to harvest the donor nerve, and ability to stimulate and guide regenerating axons [161], this technique is being used to create nerve guidance conduits (NGCs). In addition, the possible anisotropic material properties shown to be an effective cue to direct and enhance neurite outgrowth [162]. A multichannel silk electrospun conduits bi-functionalized with Nerve Growth Factor (NGF) and Ciliary Neurotropic Factor (CNTF) to boost peripheral nerve regeneration was developed, where the bioactive guides involved longitudinally oriented channels and aligned nanofibers to reproduce the fascicular architecture and fibrous ECM found in the native nerve (Fig. 10.10a and b). The multichannel created nerve conduit demonstrated to have the correct diameter to create perineurium-like structures. Additionally, ELISA assays showed the absence of growth factors passively released from the functionalized fibers avoiding the topical accumulation of proteins [163].

Microfluidic spinning technique, a method to continuously fabricating alginate flat microfibers with a size-tunable grooved pattern engraved in the channels of a

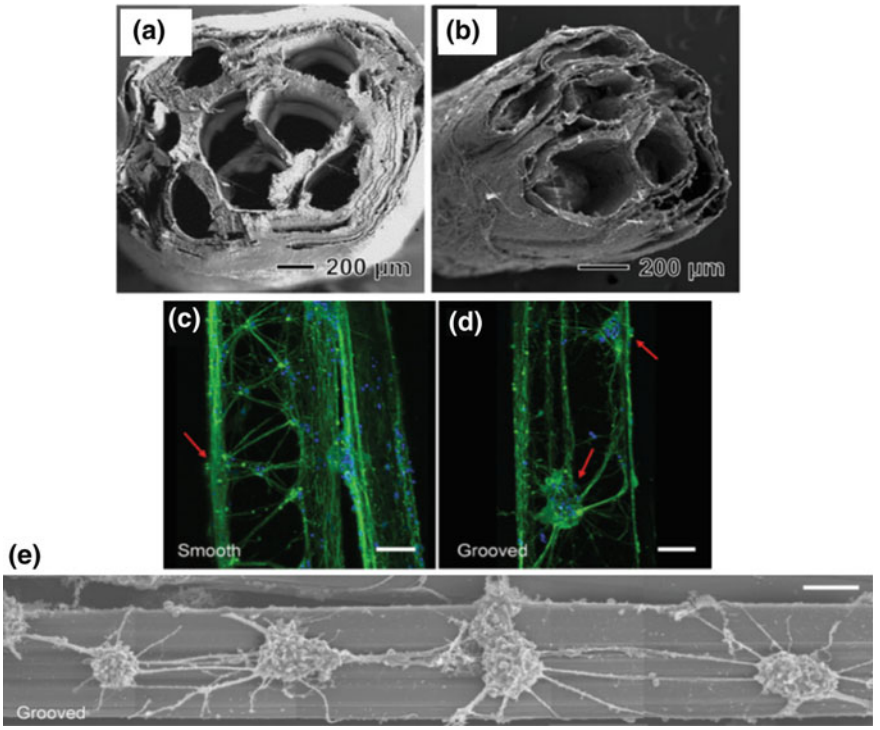


Fig. 10.10 SEM images of different Structures of electrospun NGCs: **a** Multichannel NGC made of silk fibroin fibers and **b** NGC of intraluminal microchannels with aligned nanofiber of RGD conjugated polyurea and PCL. Reproduced from [163] (2015) with permission from Elsevier. Fluorescence microscopy images of the microfluidic spinning of **c** neurons on a smooth flat fiber and **d** neuron on a grooved flat fiber. **e** SEM images of neurons on a grooved flat fiber by microfluidic electrospinning. Reproduced from [106] (2012) with permission from Wiley©

microfluidic PDMS platform was proposed. Since grooved flat fibers are used to align cells in culture, neuron (from the embryos of pregnant Sprague Dawley rats on the 16th day of gestation) cells were culture on smooth and grooved flat fibers. Most neuron cells on the smooth fibers migrated toward the sides and aggregated to form networks. In contrast, on the grooved fiber, many neuron cells adhered to the edges of the grooves and the neurites were projected along the edges of the grooved fiber (Fig. 10.10c, d and e) [106].

10.4.2 Wound Dressing

An ideal dressing for wound healing needs to have certain properties such as: hemostatic ability, appropriate water vapor transmission rate and gaseous exchange ability,

capacity to absorb excess exudates (wound fluid/pus), efficiency as bacterial barrier, adhesion to healthy tissue but non-adhesion to wound tissue, ability to conform to the contour of the wound area, painless to patient and ease of removal, and it must be low cost [164]. Electrospinning has proved to have most of the requirements for wound-healing polymeric devices [165, 166]. Cell behavior of normal human keratinocytes and fibroblasts onto electrospun silk fibroin nanofibrous membranes have been successfully investigated [167]. Furthermore, wound-healing properties of electrospun type I collagen fibrous mats were investigated [168]. The healing of the wounds in mice was superior to conventional wound care, especially in the early stages of the healing process. Apart from collagen, electrospun polyurethane fibrous meshes were also tested as wound dressings [169]. Furthermore, electrospun nanofibers (with or without additives) can be used as cosmetic skincare-masks for skin healing, cleansing, or other therapeutical applications, due to their small pore size and high surface area-to-volume ratio [17]. The high surface area of these electrospun skin masks allows a better utilization and speeds up the transfer rate between the additives and the skin. These masks can be used gently, painlessly and adapt directly to the 3D shape of the skin to provide healing or care treatment [170].

10.4.3 Drug Delivery Systems

Some therapeutic agents have severe side effects, mostly because of the interaction of the drug with healthy tissues that are not its target [171]. Trying to surpass this shortcoming, the use of drug delivery/release systems may be a suitable solution. In this way drug delivery systems are engineered technologies capable of controlling the rate and the location at which a certain therapeutic agent is released. Biocompatible and biodegradable polymers are, therefore, frequently used to develop drug delivery systems because they can be easily designed and tuned according to the needs.

Electrospun nanofibrous mats have been applied as drug carriers mainly due to the large surface area, and the fast and efficient solvent evaporation during processing, providing limited time to the incorporated drug recrystallize and favoring the formation of amorphous dispersions or solid solutions. A variety of solutions containing low molecular weight drugs have been electrospun, including lipophilic drugs such as *ibuprofen*, *cefazolin* and *paclitaxel*, and hydrophilic drugs such as *mefoxin* and *tetracycline*, as reviewed elsewhere [172]. Figure 10.11a shows the various strategies for the preparation of drug loaded nanofibers. The blending of the therapeutic agent with the appropriate polymeric solution remains the most predominant method for drug loading into fibrous meshes. This happens because the use of polymeric blends improves the equilibrium between mechanical and physicochemical properties of the drug-loaded nanofibers. In addition, the formulation design for drug release increases, and the release rate can be manipulated by altering the proportion of polymer in the blended solution. Drug encapsulation is achieved through electrospinning in a single step conventional way since the drugs are already dissolved or dispersed in the polymeric solution [173]. Furthermore, the electrospinning method

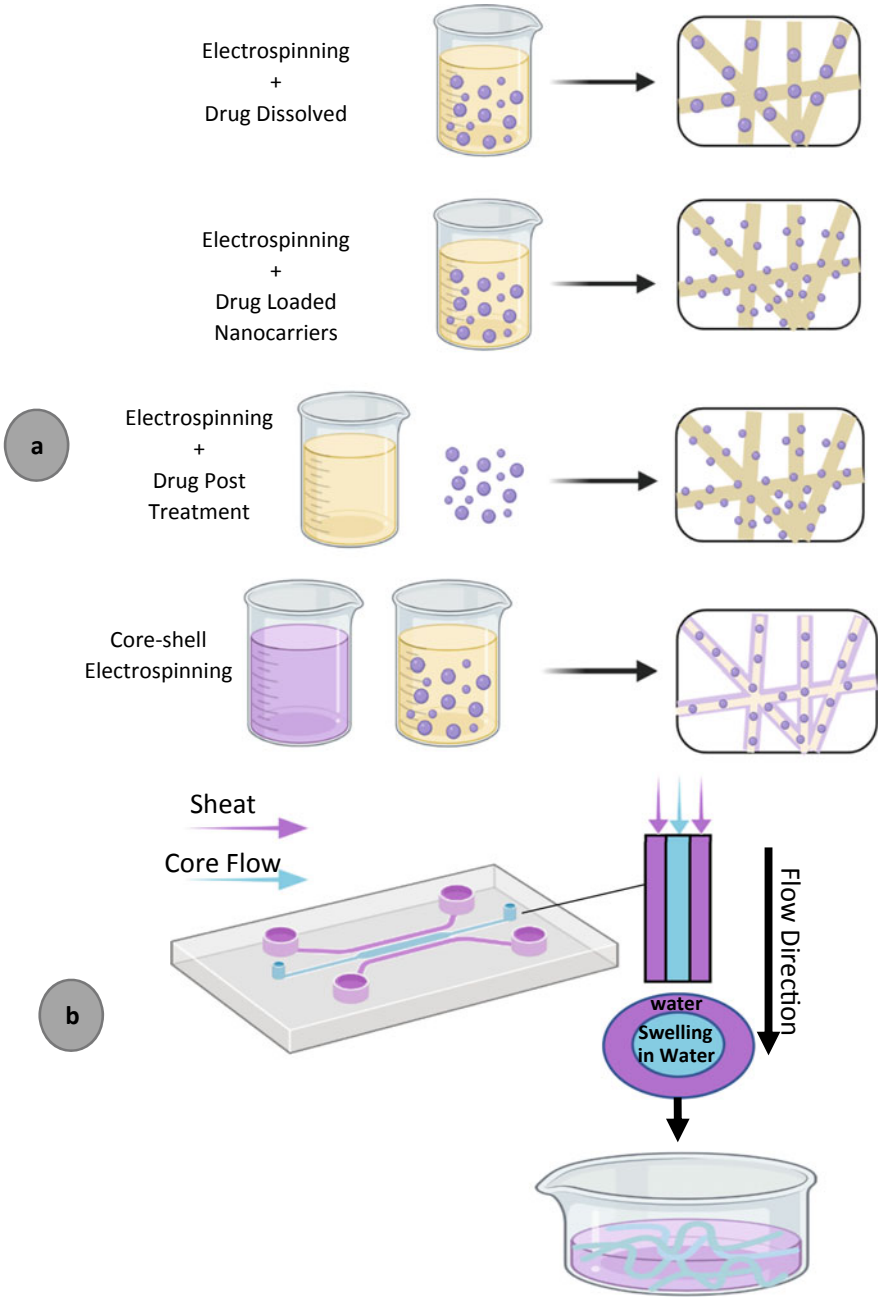


Fig. 10.11 Representation of the different strategies to produce drug-loaded nanofibers using **a** electrospinning or **b** microfluidic systems

can be also applied with drug loaded nanocarriers/particles, mostly for dual drug release approaches. First, a set of drug-loaded nanoparticles is prepared, and then electrospun into fibrous membranes in a one-step, single-nozzle way. This strategy avoids the fast initial burst release and slows down the rate of immobilization of the biological molecules on a particular surface [174].

Since the main goal of coaxial electrospinning is to obtain fibers with core–shell structures, it can be used to obtain fibers with specific drugs encapsulated, especially, in the core, leading to a sustained and controlled drug release. Coaxial meshes usually have a high surface area and three-dimensional network and because of that proteins, growth factor, antibiotics, and other biological agents have been successfully encapsulated into the coaxial fibrous mats. One of the main advantages of this technique is that the core–shell structure gives protection to the loaded drugs, as reviewed elsewhere [175]. In addition, in c-axial electrospinning, two kinds of medically pure drugs can be encapsulated. For example, the production of core–shell poly(L-lactide-co-caprolactone) (PLLACL)/collagen (3:1) nanofibers blended with dexamethasone (DEX) and BMP-2 for bone tissue engineering. BMP-2 and DEX were successfully incorporated into PLLACL/collagen nanofibers by means of blending or coaxial electrospinning, where DEX is loaded into the shell and bovine serum albumin (BSA)-BMP-2 was loaded into the core of the fiber. The viability and morphology of human MSC on the nanofibrous mats were used to explore the performance of the scaffolds. In vitro results showed that the release profiles of the growth factors on the core–shell nanofibers are more sustained than the ones with the blended electrospun fibers. Specifically, the shell loaded with DEX showed a sharp initial burst release, whereas the BSA-BMP-2 core results show a slow and steady long-term release for 22 days from coaxial electrospun fibers. Such release profiles, where the growth factors are released at sufficient amounts throughout the experiment can help induce hMSC differentiation into osteogenic cells [176].

Due to their hydrogel nature, microfluidic hydrogel fibers are considered to be a highly promising candidate for loading and delivering bio-sensitive macromolecules or drugs [177]. However, the large pores in the interior of the microfluidic hydrogel fiber and its fast degradation limit their applications for controlled delivery of small molecules [178, 179]. A pioneering exploration of microfluidic fibers as carriers for controlled drug delivery was carried out and, instead of an aqueous sheath flow, a Calcium-containing isopropyl alcohol solution was used as the sheath flow to crosslink an ampicillin-containing alginate fiber. As a result, alginate chains were well aligned along the longitudinal direction and densely compacted due to solvent exchange-induced phase separation and shear forces inside the micro-channel (Fig. 10.11b). These microfibers are highly promising for the synergistic encapsulation of multiple drugs and developing drug-loaded medical patches for wound healing [178].

10.5 Hybrid Systems

Both electrospinning and microfluidic techniques have certain properties that make them unique which generate a great interest among researchers. Of particular relevance to the biomedical field is the ability to create different structures, especially the production of fibers with distinct shapes and morphologies that can be achieved by controlling the process parameters and the type of materials (polymers). Moreover, there has been a growing increase in the number of publications on hybrid systems combining electrospinning and microfluidics, most of them based on the integration of electrospun nanofibrous meshes into microfluid systems [10].

10.5.1 Integration of Electrospun Nanofibrous Meshes into Microfluidic Systems

Electrospun nanofibrous mats have demonstrated to be a promising substrate for integration into different microfluidic devices due to versatile fabrication method, and high specific surface area [10]. In this way, these systems presented enhanced functionalities, namely the creation of new ways of generating complex tissue-engineered systems of considerable utility as in vitro models for toxicological studies [180, 181]. It enables the further development of portable devices (such as lab-on-a-chip devices) [182, 183] that require smaller reagent and sample volumes than traditional devices, making them accessible for use in point-of-care settings, such as for early cancer diagnosis [184].

Large electrospun membranes have been pressed and kept in place by the PDMS and the glass slide or sealed with adhesive tape [11]. The main issues with this approach were that despite the press fitting ability to generate tight seals, the hydraulic pressure applied in that system is lower as compared with the irreversible bonded PDMS microfluidic networks. Moreover, if the electrospun fibers were put inside the channel, at the PDMS glass interface, small amounts of liquid could easily leak out the channel boundaries [185]. More recently, a more innovative solution for the integration of spatially controlled electrospun meshes within microfluidics PDMS devices was designed. It consists in an electrolyte-assisted electrospinning process, engineered to fabricate a free-standing nanofibrous membrane on complex-shaped PDMS microcavities, using an electrolyte solution as a grounded collector instead of a conventional metal collector [186].

Engineered in vitro models: over the years, several researchers have shown that the incorporation of electrospun membranes into microfluidic chips could be beneficial for cell culture studies. Some authors developed a biomimetic system consisting of PU nanofibrous mesh integrated into a PDMS-based microfluidic chip, aiming to evaluate the viability of human bone marrow-derived mesenchymal stem cell culture under different perfusion conditions and surface characteristics [187]. Moreover, patterned electrospun fibers have been successfully integrated into microfluidic

devices with the aim to better mimic the topography of the natural ECM [191, 192]. These works demonstrated that cell microenvironments, created within spatially controlled fibrous structures, are fundamental for studying and/or controlling phenotype expression in tissue engineering and drug-delivery applications. Additionally, fibrous patterns have been integrated into microfluidic channels to study the combined effect of surface topography and chemical gradients over neural stem cells [188]. The combined effect of microfluidics and patterned-electrospun fibers on hepatocyte behavior was also studied. The hepatocytes cultured in such controlled system, under an optimized flow, exhibited restored hepatocyte polarity, biliary excretion, and maintained liver-specific functions [180].

Lab-on-a-chip-devices: miniaturized bioanalytical assays in microfluidics have several advantages in terms of reagent consumption, assay automation, and multiplexing capability [189]. Moreover, these devices benefited from the use of electrospun membranes due to their high specific surface area and porous structures that led to high levels of protein absorbance and immobilization efficiency [190]. In this way, electrospun membranes have been applied within bioanalytical microfluidic systems to enhance sample preparation and analyte detection. For some applications, water-soluble nanofibers have been used to facilitate on-chip reagent storage in microfluidic biosensors through the immobilization of biological molecules directly within fiber-spinning dopes. As example, a horseradish peroxidase-tagged antibody has been effectively encapsulated into water-soluble polyvinylpyrrolidone nanofibers, assuring stable and long-term storage of the antibody on-chip [182]. Non-water-soluble electrospun fibers have also been functionalized and used as a substrate for microfluidic HIV immunoassays and *Escherichia coli* detection [191, 192]. For example, the use of electrospun fibrous membrane as a protein-adsorption substrate in microfluidic immunoassays by the immobilization of the pathogenic antigen was studied [191]. This biofunctional substrate was incubated with the serum, and a second labeled detection antibody was introduced to determine the amount of the target antibody in the serum. These hybrid microfluidic immunoassays possess improved sensitivity that lead to a facilitation in the diagnosis of other diseases, for which the detection is based on antigen/antibody recognition (e.g. hepatitis, some venereal diseases, severe acute respiratory syndrome, and the avian flu virus) [10].

Platforms for Cancer Research: as reviewed elsewhere [193] there are four areas in cancer research in which microfluidics can be applied: cancer cell isolation, molecular diagnostics, tumor biology, and high-throughput screening for therapeutics. Regarding the cancer cellular isolation, the detection of circulating tumor cells (CTCs) is particularly valuable to cancer diagnosis in early stages, as well as treatment choice. A NanoVelcro cell-affinity substrate in which CTCs capture agent-coated (anti-EpCAM antibodies) nanostructured substrates capture CTCs with high efficiency was developed [194]. Based on the NanoVelcro mechanism, three generations of NanoVelcro chips capable of detecting, isolating, and purifying CTCs from blood samples have been already validated. In the most recent NanoVelcro chip, the non-transparent silicon substrate (used in the first generations of chips) was replaced by a transparent one, comprising electrospun PLGA nanofibers deposited onto a

commercial laser microdissection slide [184]. This hybrid system was capable not only of capturing CTCs but also enabling highly specific isolation of single CTCs, immobilized on the substrate without contamination by white blood cells. When different capture agents are used, these hybrid chips can be used to capture CTCs from several types of solid tumors, including prostate, breast, lung, and pancreatic cancer, as well as melanoma [194–196].

10.6 Conclusions

The production of fibers with diameters in the nano- to micro-range by electrospinning or microfluidic spinning have demonstrated to be valuable for multiple applications, particularly in the biomedical field. This interest is due to the unique properties of both techniques, such as their ability to create such different and complex fibrous structures with a wide range of available polymers (synthetic, natural, blends, or even their combination with cells and bioactive factors), along with the capability to mimic the physiological microenvironment. In this work, these two methods were compared concerning their own features, such as set-ups used, processing parameters, produced fiber morphologies, as well as their biomedical applications.

In electrospinning, many synthetic and natural polymers could be directly electrospun, using different set-ups and collectors. Electrospun nanofibers can be used as scaffolds for tissue engineered bone, cartilage, skin, skeletal muscle, blood vessels or neural tissues. Their high surface area, porosity, and good structural mechanical properties (tensile strength and stiffness) make electrospun fibers good drug delivery and can also be applied for wound dressings. Furthermore, the type of obtained fibrous structure (i.e. solid, core–shell, hollow or multichannel, porous fibers, among others) must be selected in agreement with their target application. Regardless of the concept and the apparatus simplicity, the electrospinning system is very sensitive to processing parameters, and one disadvantage of the technique is the absence of independent control over these parameters. Most of the polymers used in electrospinning are synthetic and hydrophobic, leading to a lack of cell-recognition signals, constraining their application in tissue engineering. Therefore, modifications to the polymer material or nanofibers surface, which favor the cell adhesion and proliferation, and the use of highly aligned nanofibrous scaffolds by using parallel or rotating collectors, are two of the solutions used to surpass this problem.

On the other hand, microfluidic spinning environment is milder than electrospinning, in which most natural proteins can be spun into hydrogel-based microfibers. The main advantage of microfluidic spinning systems is their ability to produce microfibers with spatiotemporal control with the use of specific designs of their microchannels. In this way, cell patterning can be created in a single microfiber, making this technique more suitable for cell encapsulation and in vivo immune-protection of implanted tissues for therapeutic purposes. Moreover, the reduced sensitivity to operational parameters and high degree of reproducibility, the good disposability, reduced cross-contamination, fast response and short analysis times

make microfluidics a technique to be used for other applications, such as miniaturized analytical devices for biomedical analysis and diagnostics. Notwithstanding their many advantages, microfluidic spinning still faces some challenges. The single fiber should be solidified within a relatively short time during the microfluidic spinning. Another big issue related to microfluidic systems is the slow pace of commercialization, due to the lack of standardization and the gap between the industrial needs and what is being studied.

Although the development of different hybrid systems, combining both techniques, is still in its early stages, a lot of progress needs to be made in this area. They allow to take advantage of some major characteristics of each technique (i.e. the reproducibility, and a high degree of control and tunability of the solutions of microfluidics, as the improved mechanical properties and surface area of the fibrous mesh produced by electrospinning) becoming a point of interest for biomedical applications such as tissue engineering and cancer research. For now, these hybrid systems consist in the integration of spatially controlled/tunable electrospun fibrous mats within a microfluidic chip. However, a sustained development of these hybrid spinning technologies, will allow, in time, a brand-new era for tissue engineering and organ regeneration.

References

1. Andersson, M., Jia, Q., Abella, A., Lee, X.-Y., Landreh, M., Purhonen, P. et al. (2017). Biomimetic spinning of artificial spider silk from a chimeric minispidroin. *Nature Chemical Biology,* [Internet] *13*(3), 262–264. Available from: https://doi.org/10.1038/nchembio.2269
2. Vollrath, F., & Knight, D. P. (2001). Liquid crystalline spinning of spider silk. *Nature, 410*(6828), 541–548.
3. Heim, M., Keerl, D., & Scheibel, T. (2009). Spider silk: From soluble protein to extraordinary fiber. *Angewandte Chemie International Edition, 48*(20), 3584–3596.
4. McIntyre, J. E. (2004). Synthetic fibres: Nylon, polyester, acrylic, polyolefin (1st ed.). In: J. E. McIntyre (Ed.), *Synthetic fibres: Nylon, polyester, acrylic, polyolefin* (1–300 p). Woodhead Publishing.
5. Bosman, F. T., & Stamenkovic, I. (2003). Functional structure and composition of the extracellular matrix. *The Journal of Pathology, 200*(4), 423–428.
6. Martins, A., Alves da Silva, M., Costa-Pinto, A., Reis, R. L., & Neves, N. M. (2014). Bio-inspired integration of natural materials. In: A. B. Brennan & C. M. Kirschner (Eds.), *Bio-inspired materials for biomedical engineering* (1st ed.) Wiley, pp. 101–130.
7. Karuppuswamy, P., & Reddy, J. (2014) Functionalized hybrid nanofibers to mimic native ECM for tissue engineering applications. *Applied Surface Science* [Internet] *322*, 162–168. Available from: https://doi.org/10.1016/j.apsusc.2014.10.074
8. Heydarkhan-Hagvall, S., Schenke-Layland, K., Dhanasopon, A. P., Rofail, F., Smith, H., Wu, B. M., et al. (2008). Three-dimensional electrospun ECM-based hybrid scaffolds for cardiovascular tissue engineering. *Biomaterials, 29*(19), 2907–2914.
9. Yoshimoto, H., Shin, Y. M., Terai, H., & Vacanti, J. P. (2003). A biodegradable nanofiber scaffold by electrospinning and its potential for bone tissue engineering. *Biomaterials, 24*(12), 2077–2082.
10. Giannitelli, S. M., Costantini, M., Basoli, F., Trombetta, M., & Rainer, A. (2018) Electrospinning and microfluidics: An integrated approach for tissue engineering and cancer. In: V. G. L. Ambrosio (Ed.), *Electrofluidodynamic technologies (EFDTs) for biomaterials and medical*

devices: Principles and advances [Internet], 1st ed. Elsevier Ltd. pp. 139–155. Available from: https://doi.org/10.1016/B978-0-08-101745-6.00008-6
11. Liu, Y., Yang, D., Yu, T., & Jiang, X. (2009). Incorporation of electrospun nanofibrous PVDF membranes into a microfluidic chip assembled by PDMS and scotch tape for immunoassays. *Electrophoresis, 30*(18), 3269–3275.
12. Chen, S., Li, R., Li, X., Xie, J. (2018). Electrospinning: An enabling nanotechnology platform for drug delivery and regenerative medicine. *Advanced Drug Delivery Reviews* [Internet] *132*, 188–213. Available from: https://doi.org/10.1016/j.addr.2018.05.001
13. Rayleigh, L. (2009, September 28). On the equilibrium of liquid conducting masses charged with electricity. *The London, Edinburgh, and Dublin Philosophical Magazine and Journal of Science* [Internet] *1882* [cited 2 November, 2018] *14*(87), 184–186. Available from: https://www.tandfonline.com/doi/full/10.1080/14786448208628425
14. Tucker, N., Stanger, J. J., Staiger, M. P., Razzaq, H., & Hofman, K. (2012). The history of the science and technology of electrospinning from 1600 to 1995. *Journal of Engineered Fibers and Fabrics, 7*(3), 63–73.
15. Formhals, A. (1934). *Process and apparatus for preparing artificial threads* [Internet] USA; US 1975504 [cited November 2, 2018]. Available from: https://patentimages.storage.googleapis.com/7c/80/a3/67e4165167ebc1/US1975504.pdf
16. Reneker, D. H. (1999). Nanometre diameter fibres of polymer, produced by electrospinning. *Nanotechnology, 7*(3), 216–223.
17. Huang, Z.-M., Zhang, Y.-Z., Kotaki, M., & Ramakrishna, S. (2003, November 1). A review on polymer nanofibers by electrospinning and their applications in nanocomposites. *Composites Science and Technology* [Internet] [cited March 25, 2019] *63*(15), 2223–2253. Available from: https://www.sciencedirect.com/science/article/pii/S0266353803001787
18. Bhattarai, D. P., Aguilar, L. E., Park, C. H., & Kim, C. S. (2018). A review on properties of natural and synthetic based electrospun fibrous materials for bone tissue engineering. *Membranes (Basel), 8*(62), 1–24.
19. Sun, Z., Zussman, E., Yarin, A. L., Wendorff, J. H., & Greiner, A. (2003, November 17). Compound core–shell polymer nanofibers by co-electrospinning. *Advanced Materials* [Internet] [cited November 9, 2018] *15*(22), 1929–1932. Available from: https://doi.org/10.1002/adma.200305136
20. Han, D., & Steckl, A. J. (2019). Coaxial electrospinning formation of complex polymer fibers and their applications. *ChemPlusChem, 84*, 1453–1497. Review.
21. Wen, X., & Tresco, P. A. (2006). Fabrication and characterization of permeable degradable poly(dl-lactide-co-glycolide) (PLGA) hollow fiber phase inversion membranes for use as nerve tract guidance channels. *Biomaterials, 27*(20), 3800–3809.
22. Dror, Y., Salalha, W., Avrahami, R., Zussman, E., Yarin, A. L., Dersch, R., et al. (2007). One-step production of polymeric microtubes by co-electrospinning. *Small (Weinheim an der Bergstrasse, Germany), 3*(6), 1064–1073.
23. Martins, A., Reis, R. L., & Neves, N. M. (2012). Critical aspects of electrospun meshes for biomedical applications. In: N. M. Neves (Ed.), Electrospinning for advanced biomedical applications and therapies, 1st ed. Smithers Rapra Technology (pp. 69–87).
24. Cheng, J., Jun, Y., Qin, J., & Lee, S.-H. (2017, January). Electrospinning versus microfluidic spinning of functional fibers for biomedical applications. *Biomaterial* (Review) [Internet] [cited January 17, 2019] *114*, 121–143. Available from: https://linkinghub.elsevier.com/retrieve/pii/S0142961216305890
25. Long, Y.-Z., Yan, X., Wang, X.-X., Zhang, J., Yu, M. (2019). Electrospinning: the setup and procedure. In: B. Ding, X. Wang, & J. Yu (Eds.), Electrospinning: nanofabrication and applications [Internet] (1st ed., pp. 21–52) Elsevier Inc. Available from: http://www.sciencedirect.com/science/article/pii/B9780323512701000029
26. Martins, A., Reis, R. L., & Neves, N. M. (2008). Electrospinning: Processing technique for tissue engineering scaffolding. *International Materials Reviews, 53*(5), 257–274.
27. Process, E., Doshi, J., & Reneker, D. H. (1995). Electrospinning process and applications of electrospun fibers. *Journal of Electrostatics, 35*, 151–160.

28. Greiner, A., & Wendorff, J. H. (2007). Electrospinning: A fascinating method for the preparation of ultrathin fibers. *Angewandte Chemie International Edition, 46*, 5670–5703. Review.
29. Reneker, D. H., & Chun, I. (1996). Nanometre diameter fibres of polymer, produced by electrospinning. *Nanotechnology, 7*(3), 216–223.
30. Morad, M. R., Rajabi, A., Razavi, M., & Pejman Sereshkeh, S. R. (2016). A very stable high throughput Taylor Cone-jet in electrohydrodynamics. *Scientific Reports* [Internet] *6*, 1–10. Available from: https://doi.org/10.1038/srep38509
31. Taylor, G. (1964). Disintegration of water drops in an electric field. *Proceedings of the Royal Society of London. Series A. Mathematical and Physical Sciences, 280*(1382), 383–397.
32. Taylor, G. (1969). A PRSL. Electrically driven jets. *Proceedings of the Royal Society of London. A. Mathematical and Physical Sciences, 313*(1515), 453–475
33. Moghe, A. K., & Gupta, B. S. (2008). Co-axial electrospinning for nanofiber structures: Preparation and applications. *Polymer Reviews, 48*(2), 353–377.
34. Hang, Y., Zhang, Y., Jin, Y., Shao, H., & Hu, X. (2012). Preparation of regenerated silk fibroin/silk sericin fibers by coaxial electrospinning. *International Journal of Biological Macromolecules* [Internet] *51*(5), 980–986. Available from: https://doi.org/10.1016/j.ijbiomac.2012.08.010
35. Huang, Z. M., He, C. L., Yang, A., Zhang, Y., Han, X. J., Yin, J., et al. (2006). Encapsulating drugs in biodegradable ultrafine fibers through co-axial electrospinning. *Journal of Biomedical Materials Research Part A: An Official Journal of The Society for Biomaterials, The Japanese Society for Biomaterials, and The Australian Society for Biomaterials and the Korean Society for Biomaterials, 77*(1), 169–179.
36. Qin, X. (2017). Coaxial electrospinning of nanofibers. In M. Afshari (Ed.), *Electrospun nanofibers* (1st ed., pp. 41–71). Elsevier Ltd.
37. Bazilevsky, A. V., Yarin, A. L., & Megaridis, C. M. (2007). Co-electrospinning of core-shell fibers using a single-nozzle technique. *Langmuir, 23*(5), 2311–2314.
38. Haider, A., Haider, S., & Kang, I. (2015). A comprehensive review summarizing the effect of electrospinning parameters and potential applications of nanofibers in biomedical and biotechnology. *Arabian Journal of Chemistry* [Internet] *11*, 1165–1188. Available from: https://doi.org/10.1016/j.arabjc.2015.11.015
39. Bogntizki, M., Frese, T., Steinhart, M., Greiner, A., Wendorff, J. H., Schaper, A., et al. (2001). Preparation of fibers with nanoscaled morphologies—ES of polymer blends. *Polymer Engineering & Science, 41*(6), 982–989.
40. Bakar, S. S. S., Fong, K. C., Eleyas, A., & Nazeri, M. F. M. (2018). Effect of voltage and flow rate electrospinning parameters on polyacrylonitrile electrospun fibers. *IOP Conference Series: Materials Science and Engineering, 318*(1), 2–8.
41. Theron, S. A., Zussman, E., & Yarin, A. L. (2004). Experimental investigation of the governing parameters in the electrospinning of polymer solutions. *Polymer* (Guildf) [Internet] [cited November 9, 2018] *45*, 2017–2030. Available from: http://www.bandj.com/Home.html.
42. Rafiei, S., Maghsoodloo, S., Noroozi, B., Mottaghitalab, V., & Haghi, A. K. (2013) Mathematical modeling in electrospinning process of nanofibers: A detailed review. *Cellulose Chemistry and Technology* [Internet] [cited November 9, 2018] *47*(6), 323–338. Available from: http://www.cellulosechemtechnol.ro/pdf/CCT5-6(2013)/p.323-338.pdf
43. Ulubayram, K., Calamak, S., Shahbazi, R., & Eroglu, I. (2015). Nanofibers based antibacterial drug design, delivery and applications. *Current Pharmaceutical Design, 21*(15), 1930–1943.
44. Cai, X., Zhu, P., Lu, X., Liu, Y., & Lei, T. (2017). Electrospinning of very long and highly aligned fibers. *Journal of Materials Science, 52*(24), 14004–14010.
45. Katta, P., Alessandro, M., Ramsier, R. D., & Chase, G. G. (2004). Continuous electrospinning of aligned polymer nanofibers onto a wire drum collector. *Nano Letters, 4*(11), 2215–2218.
46. Li, D., Wang, Y., Xia, Y., & Uni, V. (2003). Electrospinning of polymeric and ceramic nanofibers as uniaxially aligned arrays. *Nano Letters, 3*(8), 1167–1171.
47. Sundaray, B., Subramanian, V., Natarajan, T. S., Xiang, R. Z., Chang, C. C., & Fann, W. S. (2004). Electrospinning of continuous aligned polymer fibers. *Applied Physics Letters, 84*(7), 1222–1224.

48. Grigoryev, N. A., & Levon, K. (2018). Novel method of electrospinning; rotating dual electrode collector design. *Journal of Microelectromechanical Systems, 27*(2), 312–320.
49. Zander, N. E. (2013). Hierarchically structured electrospun fibers. *Polymers (Basel), 5*(1), 19–44.
50. Yarin, A. L., Koombhongse, S., & Reneker, D. H. (2001, March 23). Bending instability in electrospinning of nanofibers. *Journal of Applied Physics* [Internet] [cited November 9, 2018] *89*(5), 3018–3026. Available from: http://aip.scitation.org/doi/10.1063/1.1333035
51. Deitzel, J. M., Kleinmeyer, J., Harris, D., & Beck Tan, N. C. (2001). The effect of processing variables on the morphology of electrospun nanofibers and textiles. *Polymer (Guildf), 42*(1), 261–272.
52. Tarus, B., Fadel, N., Al-oufy, A., El-messiry, M. (2016). Effect of polymer concentration on the morphology and mechanical characteristics of electrospun cellulose acetate and poly(vinyl chloride) nanofiber mats. *Alexandria Engineering Journal* [Internet] *55*(3), 2975–2984. Available from: https://doi.org/10.1016/j.aej.2016.04.025
53. Koski, A., Yim, K., & Shivkumar, S. (2004). Effect of molecular weight on fibrous PVA produced by electrospinning. *Materials Letters, 58*, 493–497.
54. Kim, S. J., Lee, C. K., & Kim, S. I. (2005). Effect of ionic salts on the processing of poly(2-acrylamido-2-methyl-1-propane sulfonic acid) nanofibers. *Journal of Applied Polymer Science, 96*(4), 1388–1393.
55. Pelipenko, J., Kristl, J., Janković, B., Baumgartner, S., & Kocbek, P. (2013). The impact of relative humidity during electrospinning on the morphology and mechanical properties of nanofibers. *International Journal of Pharmaceutics, 456*(1), 125–134.
56. Huan, S., Liu, G., Han, G., Cheng, W., Fu, Z., Wu, Q., et al. (2015). Effect of experimental parameters on morphological, mechanical and hydrophobic properties of electrospun polystyrene fibers. *Materials (Basel), 8*(5), 2718–2734.
57. Wang, C., Wang, J., Zeng, L., Qiao, Z., Liu, X., & Liu, H. (2019). Fabrication of electrospun polymer nanofibers with diverse morphologies. *Molecules, 24*(834), 1–33. Review.
58. Fong, H., Chun, I., Reneker, D. H. (1999). Beaded nanofibers formed during electrospinning. *Polymer (Guildf)* [Internet] *40*(16), 4585–4592. Available from: http://www.sciencedirect.com/science/article/pii/S0032386199000683
59. Koombhongse, S., Liu, W., Reneker, D. H. (2001). Flat polymer ribbons and other shapes by electrospinning. *Journal of Polymer Science Part B: Polymer Physics* [Internet] *39*(1), 2363–2377. Available from: http://onlinelibrary.wiley.com/doi/10.1002/polb.10070/full
60. Zhang, J. F., Yang, D. Z., Xu, F., Zhang, Z. P., Yin, R. X., & Nie, J. (2009). Electrospun core-shell structure nanofibers from homogeneous solution of poly(ethylene oxide)/chitosan. *Macromolecules, 42*(14), 5278–5284.
61. Lee, G. H., Song, J. C., & Yoon, K. B. (2010). Controlled wall thickness and porosity of polymeric hollow nanofibers by coaxial electrospinning. *Macromolecular Research, 18*(6), 571–576.
62. McCann, J. T., Li, D., & Xia, Y. (2005). Electrospinning of nanofibers with core-sheath, hollow, or porous structures. *Journal of Materials Chemistry, 15*(7), 735–738.
63. Yu, D. G., Li, X. Y., Wang, X., Yang, J. H., Bligh, S. W. A., & Williams, G. R. (2015). Nanofibers fabricated using triaxial electrospinning as zero order drug delivery systems. *ACS Applied Materials & Interfaces, 7*(33), 18891–18897.
64. Samanta, A., Nandan, B., Srivastava, R. K. (2016). Morphology of electrospun fibers derived from high internal phase emulsions high internal fiber. *Journal of Colloid and Interface Science* [Internet] *471*, 29–36. Available from: https://doi.org/10.1016/j.jcis.2016.03.012
65. Yarin, A. L. (2011). Coaxial electrospinning and emulsion electrospinning of core—shell fibers. *Polymers for Advanced Technologies, 22*, 310–317.
66. Li, D., McCann, J. T., & Xia, Y. (2005). Use of electrospinning to directly fabricate hollow nanofibers with functionalized inner and outer surfaces. *Small (Weinheim an der Bergstrasse, Germany), 1*(1), 83–86.
67. Wang, T., Wei, J., Shi, H., Zhou, M., Zhang, Y., Chen, Q., et al. (2017). Preparation of electrospun Ag/TiO_2 nanotubes with enhanced photocatalytic activity based on water/oil

phase separation. *Physica E: Low-dimensional Systems and Nanostructures* [Internet] *86*, 103–110. Available from: https://doi.org/10.1016/j.physe.2016.10.016
68. Zhao, Y., Cao, X., & Jiang, L. (2007). Bio-mimic multichannel microtubes by a facile method. *Journal of the American Chemical Society, 129*(4), 764–765.
69. Katsogiannis, K. A. G., Vladisavljević, G. T., & Georgiadou, S. (2016). Porous electrospun polycaprolactone fibers: Effect of process parameters. *Journal of Polymer Science Part B: Polymer Physics, 54*(18), 1878–1888.
70. Tran, C., & Kalra, V. (2013). Fabrication of porous carbon nanofibers with adjustable pore sizes as electrodes for supercapacitors. *Journal of Power Sources* [Internet] *235*, 289–296. Available from: https://doi.org/10.1016/j.jpowsour.2013.01.080
71. Zuo, W., Zhu, M., Yang, W., Yu, H., Chen, Y., & Zhang, Y. (2005). Experimental study on relationship between jet instability and formation of beaded fibers during electrospinning. *Polymer Engineering & Science, 45*(5), 704–709.
72. Tian, X., Bai, H., Zheng, Y., & Jiang, L. (2011). Bio-inspired heterostructured bead-on-string fibers that respond to environmental wetting. *Advanced Functional Materials, 21*(8), 1398–1402.
73. Liu, S., Zhang, F., Zheng, G., Dai, K., Liu, C., Shen, C., et al. (2016). Direct microscopic observation of shish-kebab structure in high-temperature electrospun iPP fibers. *Materials Letters* [Internet] *172*, 149–52. Available from: https://doi.org/10.1016/j.matlet.2016.02.111
74. Murase, H., Jinnai, H., Toriyama, T., & Hashimoto, T. (2019). Cascade self-organization of Shish Kebabs in fibers spun from polymer solutions: crystalline fibrils bridging neighboring Kebabs discovered by transmission electron microtomography. *Macromolecules, 52*(2), 575–591.
75. Bhaskar, S., Roh, K. H., Jiang, X., Baker, G. L., & Lahann, J. (2008). Spatioselective modification of bicompartmental polymer particles and fibers via huisgen 1,3 -dipolar cycloaddition. *Macromolecular Rapid Communications, 29*(20), 1655–1660.
76. Yu, D. G., Li, J.-J., Zhang, M., & Williams, G. R. (2017). High-quality janus nanofibers prepared using three-fluid electrospinning. *ChemComm* [Internet] *53*(33), 10,715–10,722. Available from: http://xlink.rsc.org/?DOI=C5TC02043C
77. Wu, S., Duan, B., Liu, P., Zhang, C., Qin, X., Butcher, J. T., et al. (2016). Fabrication of aligned nanofiber polymer yarn networks for anisotropic soft tissue scaffolds. *ACS Applied Materials & Interfaces, 8*(26), 16950–16960.
78. Laranjeira, M., Domingues, R. M. A., Costa-almeida, R., & Reis, R. L. (2017). 3D mimicry of native-tissue-fiber architecture guides tendon-derived cells and adipose stem cells into artificial tendon constructs. *Small (Weinheim an der Bergstrasse, Germany), 13*(31), 1–13.
79. Rezvani, Z., Venugopal, J. R., Urbanska, A. M., Mills, D. K., Ramakrishna, S., & Mozafari, M. (2016). A bird's eye view on the use of electrospun nanofibrous scaffolds for bone tissue engineering: Current state-of-the-art, emerging directions and future trends. *Nanomedicine Nanotechnology, Biology and Medicine* [Internet] *12*(7), 2181–2200. Available from: https://doi.org/10.1016/j.nano.2016.05.014
80. Martins, A., Alves da Silva, M. L., Faria, S., Marques, A. P., Reis, R. L., & Neves, N. M. (2011). The influence of patterned nanofiber meshes on human mesenchymal stem cell osteogenesis. *Macromolecular Bioscience, 11*(7), 978–987.
81. Li, D., & Xia, Y. (2004). Direct fabrication of composite and ceramic hollow nanofibers by electrospinning. *Nano Letters, 4*(5), 933–938.
82. Bingbing, W., Bing, L., Jie, X., & Li, C. Y. (2008). Hierarchically ordered polymer nanofibers via electrospinning and controlled polymer crystallization. *Macromolecules, 41*(24), 9516–9521.
83. Aghaei-Ghareh-Bolagh, B., Mukherjee, S., Lockley, K. M., Mithieux, S. M., Wang, Z., Emmerson, S., et al. (2020). A novel tropoelastin-based resorbable surgical mesh for pelvic organ prolapse repair. *Materials Today Bio* [Internet] *8*(October), 100081. Available from: https://doi.org/10.1016/j.mtbio.2020.100081
84. Whitesides, G. M. (2006). The origins and the future of microfluidics. *Nature, 442*(7101), 368–373.

85. Xiong, B., Ren, K., Shu, Y., Chen, Y., Shen, B., & Wu, H. (2014). Recent developments in microfluidics for cell studies. *Advanced Materials, 26*(31), 5525–5532.
86. Chan, H. N., Chen, Y., Shu, Y., Chen, Y., Tian, Q., & Wu, H. (2015). Direct, one-step molding of 3D-printed structures for convenient fabrication of truly 3D PDMS microfluidic chips. *Microfluid Nanofluidics., 19*(1), 9–18.
87. Convery, N., & Gadegaard, N. (2019). 30 years of microfluidics. *Micro Nano Engineering, 2*, 76–91. Review.
88. Wang, X., Liu, J., Wang, P., DeMello, A., Feng, L., Zhu, X., et al. (2018). Synthesis of biomaterials utilizing microfluidic technology. *Genes (Basel), 9*(283), 1–28.
89. Amin, A. M., Thakur, R., Madren, S., Chuang, H. S., Thottethodi, M., Vijaykumar, T. N., et al. (2013). Software-programmable continuous-flow multi-purpose lab-on-a-chip. *Microfluid Nanofluidics, 15*(5), 647–659.
90. Gonidec, M., & Puigmartí-Luis, J. (2018). Continuous-versus segmented-flow microfluidic synthesis in materials science. *Crystals, 9*(1), 1–12.
91. Jiang, L., & Korivi, N. S. (2013). Microfluidics: Technologies and applications. In: M. Feldman (Ed.), *Nanolithography: The art of fabricating nanoelectronic and nanophotonic devices and systems* [Internet] (1st ed, pp. 424–443). Woodhead Publishing Limited. Available from: https://doi.org/10.1533/9780857098757.424
92. Andersson, H., & Van Den Berg, A. (2004). Microfabrication and microfluidics for tissue engineering: State of the art and future opportunities. *Lab on a Chip, 4*(2), 98–103.
93. Ren, K., Zhou, J., & Wu, H. (2013). Materials for microfluidic chip fabrication. *Accounts of Chemical Research, 46*(11), 2396–2406.
94. Iliescu, C., Taylor, H., Avram, M., Miao, J., & Franssila, S. (2012). A practical guide for the fabrication of microfluidic devices using glass and silicon. *Biomicrofluidics, 6*(1), 165051–1650516.
95. McDonald, J. C., & Whitesides, G. M. (2002). Poly(dimethylsiloxane) as a material for fabricating microfluidic devices. *Accounts of Chemical Research, 35*(7), 491–499.
96. Pan, T., Fiorini, G. S., Chiu, D. T., & Woolley, A. T. (2007). In-channel atom-transfer radical polymerization of thermoset polyester microfluidic devices for bioanalytical applications. *Electrophoresis, 28*(16), 2904–2911.
97. Tsao, C. W., & DeVoe, D. L. (2009). Bonding of thermoplastic polymer microfluidics. *Microfluid Nanofluidics., 6*(1), 1–16.
98. Martinez, A. W., Phillips, S. T., & Whitesides, G. M. (2010). Diagnostics for the developing world microfluidic. *Analytical Chemistry, 82*(1), 3–10.
99. Huang, G. Y., Zhou, L. H., Zhang, Q. C., Chen, Y. M., Sun, W., Xu. F., et al. (2011). Microfluidic hydrogels for tissue engineering. *Biofabrication, 3*(1).
100. Jun, Y., Kang, E., Chae, S., & Lee, S. H. (2014). Microfluidic spinning of micro- and nano-scale fibers for tissue engineering. *Lab on a Chip, 14*(13), 2145–2160.
101. Fidalgo, L. M., & Maerkl, S. J. (2011). A software-programmable microfluidic device for automated biology. *Lab on a Chip, 11*(9), 1612–1619.
102. Dam, H., Gyun, S., Min, G., Park, M., Ku, B., & Sang, H. (2021). Theoretical and experimental investigation of the wet-spinning process for mechanically strong carbon nanotube fibers. *Chemical Engineering Journal* [Internet] *412*(September 2020), 128650. Available from: https://doi.org/10.1016/j.cej.2021.128650
103. Beebe, D. J., Mensing, G. A., & Walker, G. M. (2002). Physics and applications of microfluidics in biology. *Annual Review of Biomedical Engineering, 4*(1), 261–286.
104. Cimrák, I., Gusenbauer, M., & Schrefl, T. (2012). Modelling and simulation of processes in microfluidic devices for biomedical applications. *Computers & Mathematics with Applications* [Internet] *64*(3), 278–288. Available from: https://doi.org/10.1016/j.camwa.2012.01.062
105. Zarrin, F., & Dovichi, N. J. (1985). Sub-Picoliter detection with the sheath flow cuvette. *Analytical Chemistry, 57*(13), 2690–2692.
106. Kang, E., Choi, Y. Y., Chae, S. K., Moon, J. H., Chang, J. Y., & Lee, S. H. (2012). Microfluidic spinning of flat alginate fibers with grooves for cell-aligning scaffolds. *Advanced Materials, 24*(31), 4271–4277.

107. Du, X., Li, Q., Wu, G., & Chen, S. (2019). Multifunctional micro/nanoscale fibers based on microfluidic spinning technology. *Advanced Materials, 1903733*, 1–38.
108. Marimuthu, M., Kim, S., & An, J. (2010). Amphiphilic triblock copolymer and a microfluidic device for porous microfiber fabrication. *Soft Matter, 6*(10), 2200–2207.
109. Yu, Y., Wei, W., Wang, Y., Xu, C., Guo, Y., & Qin, J. (2016). Simple spinning of heterogeneous hollow microfibers on chip. *Advanced Materials, 28*(31), 6649–6655.
110. Choi, C. H., Yi, H., Hwang, S., Weitz, D. A., & Lee, C. S. (2011). Microfluidic fabrication of complex-shaped microfibers by liquid template-aided multiphase microflow. *Lab on a Chip, 11*(8), 1477–1483.
111. Thangawng, A. L., Howell, P. B., Spillmann, C. M., Naciri, J., & Ligler, F. S. (2011). UV polymerization of hydrodynamically shaped fibers. *Lab on a Chip, 11*(6), 1157–1160.
112. Cho, S., Shim, T. S., & Yang, S. M. (2012). High-throughput optofluidic platforms for mosaicked microfibers toward multiplex analysis of biomolecules. *Lab on a Chip, 12*(19), 3676–3679.
113. Thangawng, A. L., Howell, P. B., Richards, J. J., Erickson, J. S., & Ligler, F. S. (2009). A simple sheath-flow microfluidic device for micro/nanomanufacturing: Fabrication of hydrodynamically shaped polymer fibers. *Lab on a Chip, 9*(21), 3126–3130.
114. Park, D. Y., Mun, C. H., Kang, E., No, D. Y., Ju, J., & Lee, S. H. (2014). One-stop microfiber spinning and fabrication of a fibrous cell-encapsulated scaffold on a single microfluidic platform. *Biofabrication, 6*(2).
115. Jung, J. H., Choi, C. H., Chung, S., Chung, Y. M., & Lee, C. S. (2009). Microfluidic synthesis of a cell adhesive Janus polyurethane microfiber. *Lab on a Chip, 9*(17), 2596–2602.
116. Kang, E., Jeong, G. S., Choi, Y. Y., Lee, K. H., Khademhosseini, A., Lee, S. H. (2011). Digitally tunable physicochemical coding of material composition and topography in continuous microfibres. *Nature Materials* [Internet] *10*(11), 877–883. Available from: https://doi.org/10.1038/nmat3108
117. Hwang, C. M., Khademhosseini, A., Park, Y., Sun, K., & Lee, S. H. (2008). Microfluidic chip-based fabrication of PLGA microfiber scaffolds for tissue engineering. *Langmuir, 24*(13), 6845–6851.
118. Kanik, M., Marcali, M., Yunusa, M., Elbuken, C., & Bayindir, M. (2016). Continuous triboelectric power harvesting and biochemical sensing inside poly(vinylidenefluoride) hollow fibers using microfluidic droplet generation. *Advanced Materials Technologies, 1*(9).
119. Leng, L., McAllister, A., Zhang, B., Ranu, A., Radisic, M., & Guenther, A. (2012). Osaic hydrogels: One-step formation of multiscale soft materials. *Advanced Materials, 24*, 3650–3658.
120. Cheng, Y., Zheng, F., Lu, J., Shang, L., Xie, Z., Zhao, Y., et al. (2014). Bioinspired multicompartmental microfibers from microfluidics. *Advanced Materials, 26*(30), 5184–5190.
121. Sackmann, E. K., Fulton, A. L., & Beebe, D. J. (2014). The present and future role of microfluidics in biomedical research. *Nature* [Internet] *507*(7491), 181–189. Available from: https://doi.org/10.1038/nature13118
122. Bhatia, S. N., & Ingber, D. E. (2014). Microfluidic organs-on-chips. *Nature Biotechnology* [Internet] *32*(8), 760–772. Available from: http://www.ncbi.nlm.nih.gov/pubmed/25093883
123. Yeon, J. H., Na, D., Choi, K., Ryu, S. W., Choi, C., & Park, J. K. (2012). Reliable permeability assay system in a microfluidic device mimicking cerebral vasculatures. *Biomedical Microdevices, 14*(6), 1141–1148.
124. Esch, M. B., Sung, J. H., Yang, J., Yu, C., Yu, J., March, J. C., et al. (2012). On chip porous polymer membranes for integration of gastrointestinal tract epithelium with microfluidic "body-on-a-chip" devices. *Biomedical Microdevices, 14*(5), 895–906.
125. Onoe, H., Okitsu, T., Itou, A., Kato-Negishi, M., Gojo, R., Kiriya, D., et al. (2013). Metre-long cell-laden microfibres exhibit tissue morphologies and functions. *Nature Materials* [Internet] *12*(6), 584–590. Available from: https://doi.org/10.1038/nmat3606
126. Shamloo, A., Ma, N., Poo, M. M., Sohn, L. L., & Heilshorn, S. C. (2008). Endothelial cell polarization and chemotaxis in a microfluidic device. *Lab on a Chip, 8*(8), 1292–1299.

127. Irimia, D., Geba, D. A., & Toner, M. (2006). Universal microfluidic gradient generator. *Analytical Chemistry, 78*(10), 3472–3477.
128. Lee, S. J., & Lee, S. Y. (2004). Micro total analysis system (μ-TAS) in biotechnology. *Applied Microbiology and Biotechnology, 64*(3), 289–299.
129. Lee, K. H., Shin, S. J., Park, Y., & Lee S.-H. (2009, June). Synthesis of cell-laden alginate hollow fibers using microfluidic chips and microvascularized tissue-engineering applications. *Small* [Internet] [cited 2019 Nov 1] *5*(11), 1264–1268. Available from: http://www.ncbi.nlm.nih.gov/pubmed/19296560
130. Francois, E., Dorcemus, D., & Nukavarapu, S. (2015). Biomaterials and scaffolds for musculoskeletal tissue engineering. *Regenerative Engineering of Musculoskeletal Tissues Interfaces, 14*(3), 3–23.
131. Anderson, J. M. (2012). Inflammation, wound healing, and the foreign-body response. In: B. D. Ratner, A. S. Hoffman, F. J. Schoen, & J. E. Lemons (Eds.), *Biomaterials science: An introduction to materials in medicine* [Internet] (3rd ed., pp. 503–512). Elsevier. Available from: https://doi.org/10.1016/B978-0-08-087780-8.00044-9
132. Furth, M. E., & Atala, A. (2014). Tissue engineering: Future perspectives. In: R. Lanza, R. S. Langer, & J. P. Vacanti (Eds.), *Principles of tissue engineering* [Internet] (4th ed., pp. 83–123). Elsevier. Available from: https://doi.org/10.1016/B978-0-12-398358-9.00006-9
133. Gomes, M. E., & Reis, R. L. (2004). Tissue engineering: Key elements and some trends. *Macromolecular Bioscience, 4*, 737–742.
134. Nemati, S. Kim, S., Shin, Y. M., & Shin, H. (2019). Current progress in application of polymeric nanofibers to tissue engineering. *Nano Convergence* [Internet] *6*(36), 1–16. Available from: https://doi.org/10.1186/s40580-019-0209-y
135. Jun, I., Han, H., Edwards, J. R., & Jeon, H. (2018). Electrospun fibrous scaffolds for tissue engineering: Viewpoints on architecture and fabrication. *International Journal of Molecular Sciences, 19*(745), 1–14. Review.
136. Chen, M., Patra, P. K., Lovett, M. L., Kaplan, D. L., & Bhowmick, S. (2009). Role of electrospun fibre diameter and corresponding specific surface area (SSA) on cell attachment. *Journal of Tissue Engineering and Regenerative Medicine, 3*, 269–279.
137. Han, D., Boyce, S. T., & Steckl, A. J. (2008). Versatile core-sheath biofibers using coaxial electrospinning. *Material research society* [Internet] (Boston) [cited November 11, 2018]. Available from: http://www.nanolab.uc.edu/Publications/PDFfiles/366.pdf
138. Wang, G., Jia, L., Han, F., Wang, J., Yu, L., Yu, Y., et al. (2019). Microfluidics-based fabrication of cell-laden hydrogel microfibers for potential applications in tissue engineering. *Molecules, 24*(8), 1–11.
139. Onoe, H., & Takeuchi, S. (2015). Cell-laden microfibers for bottom-up tissue engineering. *Drug Discovery Today, 20*(2), 236–246. Review.
140. Morimoto, Y., Hsiao, A. Y., & Takeuchi, S. (2015). Point-, line-, and plane-shaped cellular constructs for 3D tissue assembly. *Advanced Drug Delivery Reviews* [Internet] [cited November 1, 2019] *95*, 29–39. Available from: http://www.ncbi.nlm.nih.gov/pubmed/26387835
141. Lee, G. H., Lee, J. S., Wang, X., & Lee, S. H. (2016, January 7). Bottom-up engineering of well-defined 3d microtissues using microplatforms and biomedical applications. *Advanced Healthcare Materials* [Internet] [cited November 1, 2019] *5*(1), 56–74. Available from: http://www.ncbi.nlm.nih.gov/pubmed/25880830
142. Cheng, Y., Zheng, F., Lu, J., Shang, L., Xie, Z., Zhao, Y., et al. (2014, August 13). Bioinspired multicompartmental microfibers from microfluidics. *Advanced Materials, 26*(30), 5184–5190
143. Araujo, J. V., Martins, A., Leonor, I. B., Pinho, E. D., Reis, R. L., & Neves, N. M. (2008). Surface controlled biomimetic coating of polycaprolactone nanofiber meshes to be used as bone extracellular matrix analogues. *Journal of Biomaterials Science, Polymer Edition, 19*(10), 1261–1278.
144. Martins, A., Pinho, E. D., Correlo, V. M., Faria, S., Marques, A. P., Reis, R. L., et al. (2010). Biodegradable nanofibers-reinforced microfibrous composite scaffolds for bone tissue engineering. *Tissue Engineering Part A, 16*(12), 3599–3609.

145. Kim, D., Kim, K., & Shin, H. (2015). Effects of Immobilized BMP—2 and nano fiber morphology on in vitro osteogenic differentiation of hMSCs and in vivo collagen assembly of regenerated bone. *Applied Materials & Interfaces, 7*, 8798–8808.
146. Silva, M. L. A., Martins, A., Costa, P., Faria, S., Gomes, M., Reis, R. L., et al. (2010). Cartilage tissue engineering using electrospun PCL nanofiber meshes and MSCs. *Biomacromolecules, 11*, 3228–3236.
147. Casanova, M. R., Alves da Silva, M., Costa-Pinto, A. R., Reis, R. L., Martins, A., & Neves, N. M. (2019). Chondrogenesis-inductive nanofibrous substrate using both biological fluids and mesenchymal stem cells from an autologous source. *Materials Science and Engineering C* [Internet] *98*(January), 1169–1178. Available from: https://doi.org/10.1016/j.msec.2019.01.069
148. Shafiee, A., Soleimani, M., Chamheidari, G. A., Seyedjafari, E., Dodel M, Atashi A, et al. (2011). Electrospun nanofiber-based regeneration of cartilage enhanced by mesenchymal stem cells. *Journal of Biomedical Materials Research Part A* 467–478.
149. Li, W., Chiang, H., Kuo, T., Lee, H., Jiang, C., & Tuan, R. S. (2009). Evaluation of articular cartilage repair using biodegradable nanofibrous scaffolds in a swine model: A pilot study. *Journal of Tissue Engineering and Regenerative Medicine, 3*, 1–10.
150. McCullen, S. D., Autefage, H., Callanan, A., Gentleman, E., & Stevens, M. M. (2012). Anisotropic fibrous scaffolds for articular cartilage regeneration. *Tissue Engineering Part A, 18*(19–20), 2073–2083.
151. Groeber, F., Holeiter, M., Hampel, M., Hinderer, S., & Schenke-Layland, K. (2012). Skin tissue engineering-in vivo and in vitro applications. *Clinics in Plastic Surgery* [Internet] *39*(1), 33–58. Available from: https://doi.org/10.1016/j.addr.2011.01.005
152. Dias, J. R., Granja, P. L., & Bártolo, P. J. (2016). Advances in electrospun skin substitutes. *Progress in Materials Science* [Internet] *84*, 314–334. Available from: https://doi.org/10.1016/j.pmatsci.2016.09.006
153. Sundaramurthi, D., Vasanthan, K. S., Kuppan, P., Krishnan, U. M., & Sethuraman, S. (2012). Electrospun nanostructured chitosan-poly(vinyl alcohol) scaffolds: A biomimetic extracellular matrix as dermal substitute. *Biomedical Materials 7*(4).
154. Xu, S. C., Qin, C. C., Yu, M., Dong, R. H., Yan, X., Zhao, H., et al. (2015). A battery-operated portable handheld electrospinning apparatus. *Nanoscale, 7*(29), 12351–12355.
155. Aviss, K. J., Gough, J. E., & Downes, S. (2010). Aligned electrospun polymer fibres for skeletal muscle regeneration. *European Cells and Materials, 19*, 193–204.
156. Hasan, A., Memic, A., Annabi, N., Hossain, M., Paul, A., Dokmeci, M. R., et al. (2014). Electrospun scaffolds for tissue engineering of vascular grafts. *Acta Biomaterialia* [Internet] *10*(1), 11–25. Available from: https://doi.org/10.1016/j.actbio.2013.08.022
157. Zhou, F., Jia, X., Yang, Y., Yang, Q., Gao, C., Hu, S., et al. (2016). Nanofiber-mediated microRNA-126 delivery to vascular endothelial cells for blood vessel regeneration. *Acta Biomaterialia* [Internet] *43*, 303–313. Available from: https://doi.org/10.1016/j.actbio.2016.07.048
158. Pektok E, Nottelet B, Tille J, Gurny R, Kalangos A, Moeller M, et al. Poly (e-Caprolactone) Vascular Grafts in the Rat Systemic. J Am Heart Assoc. 2008;2563–70.
159. Felizardo, T., Amorim, S., Mithieux, S. M., Pires, R. A., Reis, R. L., Martins, A., et al. (2020) Tubular fibrous scaffolds functionalized with tropoelastin as a small-diameter vascular graft.
160. Lim, G. J., Lee, S. J., & Atala, A. (2005). Cell-based drug delivery. In: A. Atala, R. S. Langer, T. Mikos, & R. M. Nerem (Eds.), Principles of regenerative medicine [Internet] (3rd ed., pp. 954–966). Elsevier Inc. Available from: https://doi.org/10.1016/B978-0-12-369410-2.50057-7
161. Xie, J., MacEwan, M. R., Schwartz, A. G., & Xia, Y. (2010). Electrospun nanofibers for neural tissue engineering. *Nanoscale, 2*(1), 35–44.
162. Mo, X., Sun, B., Wu, T., & El-Hamshary, H. (2017). Nanofiber composites in neural tissue engineering. In M. Ramalingam & S. Ramakrishna (Eds.), *Nanofiber composites for biomedical applications* (1st ed., pp. 395–410). Elsevier Inc.

163. Dinis, T. M., Elia, R., Vidal, G., Dermigny, Q., Denoeud, C., Kaplan, D. L., et al. (2015). 3D multi-channel bi-functionalized silk electrospun conduits for peripheral nerve regeneration. *Journal of the Mechanical Behavior of Biomedical Materials* [Internet] *41*, 43–55. Available from: https://doi.org/10.1016/j.jmbbm.2014.09.029
164. Dhivya, S., Vijaya, V., & Santhini, E. (2015). Wound dressings—a review. *Biomedicine, 5*(4), 24–28.
165. Bhardwaj, N., & Kundu, S. C. (2010, May). Electrospinning: A fascinating fiber fabrication technique. *Biotechnology Advances* (Review) [Internet] [cited 2 November 2018] *28*(3), 325–347. Available from: http://www.ncbi.nlm.nih.gov/pubmed/20100560
166. Kenawy, E. R., Layman, J. M., Watkins, J. R., Bowlin, G. L., Matthews, J. A., Simpson, D. G., et al. (2003). Electrospinning of poly(ethylene-co-vinyl alcohol) fibers. *Biomaterials, 24*(6), 907–913.
167. Min, B.-M., Lee, G., Kim, S. H., Nam, Y. S., Lee, T. S., & Park, W. H. (2004). Electrospinning of silk fibroin nanofibers and its effect on the adhesion and spreading of normal human keratinocytes and fibroblasts in vitro. *Biomaterials, 25*(7–8), 1289–1297.
168. Rho, K. S., Jeong, L., Lee, G., Seo, B. M., Park, Y. J., Hong, S. D., et al. (2006). Electrospinning of collagen nanofibers: Effects on the behavior of normal human keratinocytes and early-stage wound healing. *Biomaterials, 27*(8), 1452–1461.
169. Khil, M. S., Cha, D. I., Kim, H. Y., Kim, I. S., & Bhattarai, N. (2003). Electrospun nanofibrous polyurethane membrane as wound dressing. *Journal of Biomedical Materials Research—Part B Applied Biomaterials, 67*(2), 675–679.
170. Ramakrishna, S., Fujihara, K., Teo, W E., Yong, T., Ma, Z., Ramaseshan, R. (2006). Electrospun nanofibers: Solving global issues. *Materials Today* (Review) [Internet] *9*(3), 40–50. Available from: https://doi.org/10.1016/S1369-7021(06)71389-X
171. Tiwari, G., Tiwari, R., Bannerjee, S., Bhati, L., Pandey, S., Pandey, P., et al. (2012). Drug delivery systems: An updated review. *International Journal of Pharmaceutical Investigation, 2*(1), 2.
172. Torres-Martinez, E. J., Cornejo Bravo, J. M., Serrano Medina, A., Pérez González, G. L., & Villarreal Gómez, L. J. (2018). A summary of electrospun nanofibers as drug delivery system: Drugs loaded and biopolymers used as matrices. *Current Drug Delivery, 15*(10), 1360–1374.
173. Tipduangta, P., Belton, P., Fábián, L., Wang, L. Y., Tang, H., Eddleston, M., et al. (2016). Electrospun polymer blend nanofibers for tunable drug delivery: The role of transformative phase separation on controlling the release rate. *Molecular Pharmaceutics, 13*(1), 25–39.
174. Wang, Y., Qiao, W., Wang, B., Zhang, Y., Shao, P., & Yin, T. (2011). Electrospun composite nanofibers containing nanoparticles for the programmable release of dual drugs. *Polymer Journal, 43*(5), 478–483.
175. Lu, Y., Huang, J., Yu, G., Cardenas, R., Wei, S., Wujcik, E. K., et al. (2016). Coaxial electrospun fibers: Applications in drug delivery and tissue engineering. *Wiley Interdisciplinary Reviews: Nanomedicine and Nanobiotechnology, 8*(5), 654–677.
176. Su, Y., Su, Q., Liu, W., Lim, M., Venugopal, J. R., Mo, X., et al. (2012). Controlled release of bone morphogenetic protein 2 and dexamethasone loaded in core-shell PLLACL-collagen fibers for use in bone tissue engineering. *Acta Biomaterialia* [Internet] *8*(2), 763–771. Available from: https://doi.org/10.1016/j.actbio.2011.11.002
177. Zhang, L., Chen, Q., Ma, Y., & Sun, J. (2020). Micro fluidic methods for fabrication and engineering of nanoparticle drug delivery systems. *ACS Applied Bio Materials, 3*(1), 107–120.
178. Ahn, S. Y., Mun, C. H., & Lee, S. H. (2015). Microfluidic spinning of fibrous alginate carrier having highly enhanced drug loading capability and delayed release profile. *RSC Advances, 5*(20), 15172–15181.
179. He, X. H., Wang, W., Deng, K., Xie, R., Ju, X. J., Liu, Z., et al. (2015). Microfluidic fabrication of chitosan microfibers with controllable internals from tubular to peapod-like structures. *RSC Advances, 5*(2), 928–936.
180. Liu, Y., Wang, S., & Wang, Y. (2016). Patterned fibers embedded microfluidic chips based on PLA and PDMS for Ag nanoparticle safety testing. *Polymers (Basel) 8*(11).

181. Hu, T., Li, Q., Dong, H., Xiao, W., Li, L., & Cao, X. (2017). Patterning electrospun nanofibers via agarose hydrogel stamps to spatially coordinate cell orientation in microfluidic device. *Small (Weinheim an der Bergstrasse, Germany), 13*(3), 1–7.
182. Jin, S., Dai, M., Ye, B. C., & Nugen, S. R. (2013). Development of a capillary flow microfluidic *Escherichia coli* biosensor with on-chip reagent delivery using water-soluble nanofibers. *Microsystem Technologies, 19*(12), 2011–2015.
183. Dai, M., Jin, S., & Nugen, S. R. (2012). Water-soluble electrospun nanofibers as a method for on-chip reagent storage. *Biosensors, 2*(4), 388–395.
184. Zhao, L., Lu, Y. T., Li, F., Wu, K., Hou, S., Yu, J., et al. (2013). High-purity prostate circulating tumor cell isolation by a polymer nanofiber-embedded microchip for whole exome sequencing. *Advanced Materials, 25*(21), 2897–2902.
185. Jo, E., Lim, M. C., Kim, H. N., Paik, H. J., Kim, Y. R., & Jeong, U. (2011). Microfluidic channels fabricated on mesoporous electrospun fiber mats: A facile route to microfluidic chips. *Journal of Polymer Science Part B: Polymer Physics, 49*(2), 89–95.
186. Park, S. M., & Kim, D. S. (2015). Electrolyte-assisted electrospinning for a self-assembled, free-standing nanofiber membrane on a curved surface. *Advanced Materials, 27*(10), 1682–1687.
187. Kwang, H. L., Gu, H. K., Su, J. S., Baek, J. Y., Dong, K. H., Park, Y., et al. (2009). Hydrophilic electrospun polyurethane nanofiber matrices for hMSC culture in a microfluidic cell chip. *Journal of Biomedical Materials Research Part A, 90*(2), 619–628.
188. Wallin, P., Zandén, C., Carlberg, B., Hellström Erkenstam, N., Liu, J., & Gold, J. (2012). A method to integrate patterned electrospun fibers with microfluidic systems to generate complex microenvironments for cell culture applications. *Biomicrofluidics, 6*(2).
189. Kim, D., & Herr, A. E. (2013). Protein immobilization techniques for microfluidic assays. *Biomicrofluidics, 7*(4), 1–47.
190. Matlock-Colangelo, L., & Baeumner, A. J. (2014). Biologically inspired nanofibers for use in translational bioanalytical systems. *Annual Review of Analytical Chemistry, 7*(1), 23–42.
191. Yang, D., Niu, X., Liu, Y., Wang, Y., Gu, X., Song, L., et al. (2008). Electrospun nanofibrous membranes: A novel solid substrate for microfluidic immunoassays for HIV. *Advanced Materials, 20*(24), 4770–4775.
192. Matlock-Colangelo, L., Coon, B., Pitner, C. L., Frey, M. W., & Baeumner, A. J. (2016). Functionalized electrospun poly(vinyl alcohol) nanofibers for on-chip concentration of *E. coli* cells. *Analytical and Bioanalytical Chemistry, 408*(5), 1327–1334.
193. Zhuo Zhang, J., & Nagrath, S. (2013). Microfluidics and cancer: Are we there yet? *Biomedical Microdevices, 15*(4), 595–609.
194. Lin, M., Chen, J. F., Lu, Y. T., Zhang, Y., Song, J., Hou, S., et al. (2014). Nanostructure embedded microchips for detection, isolation, and characterization of circulating tumor cells. *Accounts of Chemical Research, 47*(10), 2941–2950.
195. Hou, S., Zhao, L., Shen, Q., Yu, J., Ng, C., Kong, X., et al. (2013). Polymer nanofiber-embedded microchips for detection, isolation, and molecular analysis of single circulating melanoma cells. *Angewandte Chemie, 125*(12), 3463–3467.
196. Wang, S., Liu, K., Liu, J., Yu, Z. T.-F., Xu, X., & Zhao, L., et al. (2011). Highly efficient capture of circulating tumor cells by using nanostructured silicon substrates with integrated chaotic micromixers. *Angewandte Chemie, 123*(13):3140–3144.



Filipa Vasconcelos received the M.Sc. in Biomedical Engineering in 2021, from the University of Minho, Portugal. From 2019 to 2021 she developed her master thesis at 3B's Research Group, I3Bs—Research Institute on Biomaterials, Biodegradables and Biomimetics, University of Minho, in collaboration with the BIOtech Institute, University of Trento, Italy. Currently she is a Ph.D. student from Sapienza University of Rome. Her research interests include electrospinning, microfluidics, material characterization, tissue engineering, and drug delivery.



Rui L. Reis Ph.D., D.Sc., Hon. Causa M.D., Hon Causa Ph.D., FBSE, FTERM, member of NAE, FAIMBE, FEAMBES, is the Director of the 3B's Research Group—member of the I3Bs—Institute for Biomaterials, Biodegradables and Biomimetics, and the ICVS/3B's Associate Laboratory, both of the University of Minho. He is also the CEO of the European Institute of Excellence on Tissue Engineering and Regenerative Medicine (TERM), the Global Past-President of the TERM International Society (TERMIS), and the Editor-in-chief of the Journal of Tissue Engineering and Regenerative Medicine. His research is focused on the development of biomaterials from natural origin polymers (in some cases originally proposed by his group) for a wide range of biomedical applications, namely on tissue engineering (TE), regenerative and precision medicine, stem cells research, and drug delivery applications.



Albino Martins B.Sc., Ph.D., is an Assistant Researcher at the 3B's Research Group since 2013, a member of the Innovation & Services Subunit and of the Scientific Council of the I3B's. He has demonstrated expertise in mesenchymal stem cells biology, biomaterials' processing, biofunctionalization and characterization, and drug delivery systems. His research is focused on the development of advanced regenerative medicine strategies for cartilage, bone, and vascular tissues.



Nuno M. Neves CEng, M.Sc., Ph.D., is an Associate Professor with Habilitation and the vice-director of the 3B's Research Group of the University of Minho, Portugal. This is a research unit of Excellence that also integrates the Associate Laboratory ICVS/3B's, being a member of the Board of Directors. His main area of research is the development of biomaterials for a range of biomedical applications, including tissue engineering and regeneration with stem cells, advanced drug delivery systems and medical devices.

Chapter 11
Multifunctional Wound Dressings Based on Electrospun Nanofibers



Kelcilene B. R. Teodoro, Danilo M. Santos, Camilo A. S. Ballesteros, Paulo A. M. Chagas, Vittor P. V. Costa, Rodrigo Schneider, and Daniel S. Correa

Abstract The skin, the largest and most external organ of the human body, acts as the first line of protection against traumata. Therefore, skin wounds and injuries can expose the organism to many severe diseases. Some wounds show chronic aspects, usually taking a long time to heal and, therefore, being more susceptible to infections. Thus, for the sake of health, effective strategies to protect and coat the affected skin are highly demanded nowadays. In this context, applying wound dressings based on electrospun nanofibers at the local injury site can speed up the healing process by protecting the wound from external harm and enhancing tissue recovery, fluid draining, and moisture regulation. Besides, wound dressings can also present antibacterial activity and promote drug delivery, being easily integrated with regenerative therapies. In this context, we present recent developments in the design of multifunctional nanofiber-based systems produced by electrospinning for wound dressing applications. Besides basic fundamental aspects of skin wounds and the types of multifunctional nanofibers features suitable for wound dressing, we also discuss future trends and challenges related to the smart wound dressing.

Keywords Skin injuries · Wound healing · Wound dressing · Nonwovens · Polymer nanofibers

K. B. R. Teodoro · D. M. Santos · C. A. S. Ballesteros · P. A. M. Chagas · V. P. V. Costa · R. Schneider · D. S. Correa (✉)
Nanotechnology National Laboratory for Agriculture, Embrapa Instrumentação, São Carlos, SP, Brazil
e-mail: daniel.correa@embrapa.br

P. A. M. Chagas · V. P. V. Costa · D. S. Correa
PPGBiotec, Center for Exact Sciences and Technology, Federal University of São Carlos (UFSCar), São Carlos, SP, Brazil

R. Schneider · D. S. Correa
PPGQ, Department of Chemistry, Center for Exact Sciences and Technology, Federal University of São Carlos (UFSCar), São Carlos, SP, Brazil

C. A. S. Ballesteros
Bachelor of Natural Sciences and Environmental Education, Pedagogical and Technological, University of Colombia (UPTC), Tunja, Colombia

© The Author(s), under exclusive license to Springer Nature Switzerland AG 2022

A. Vaseashta and N. Bölgen (eds.), *Electrospun Nanofibers*,
https://doi.org/10.1007/978-3-030-99958-2_11

The skin is the largest and most external organ in the human body, being the first barrier against mechanical, chemical and biological shocks. Besides, it performs fundamental functions as thermoregulation, prevention of water and fluid loss, immune surveillance, hormone synthesis, and sensory detection [1]. Damages in skin's structure can make the organism susceptible to several diseases. The traditional technique to overcome this issue consists in cover the injured skin area with wound dressings, protecting it against external agents and waiting for the natural restoration of the tissue. Advanced interdisciplinary researches combining wound healing approaches and nanotechnology have resulted in novel strategies to assist the rapid wound healing, treatment of chronic wounds, and monitoring and combination of modern therapies. In this sense, wound dressings based on electrospun nanofibers structured as nonwoven layers can enable the protection of the injured area, absorption of exudates, and improve gas flow and exchange. Besides, their fibrous network offer a biomimetic environment that stimulates skin's cells proliferation, and can encapsulate active compounds for their controlled release. In the next sections we discuss the types of wound dressings fabricated by electro spinning, using both synthetic and natural polymers, as well as we discuss how their distinct properties can be used for designing distinct multifunctional wound dressings.

11.1 Introduction to Electrospun Nanofibers for Wound Dressing

11.1.1 Skin Wound and Wound Healing: Basic Aspects

The skin is the organ in the first line of defense of the body against environmental exposure, and also provides essential functions in thermoregulation, hydration, excretion and synthesis of vitamin D. Therefore, skin lesions could lead to the loss of essential functions of the human body [2–4]. When a skin injury occurs, it generates open and closed wounds, which are healed through four interconnecting phases to recover its functions, namely: hemostasis, inflammation, proliferation, and remodeling [5], as depicted in Fig. 11.1. The hemostasis and inflammation phases occur concurrently after injury and last from 1 to 5 days. In the hemostasis phase, neutrophils and later macrophages produce inflammatory mediators [interleukin (IL-4)], transforming growth factors β (TGF-β), which induce platelets to release coagulation factors, such as clots of fibrin that allow the migration of cells to the wound, and decrease the inflammation phase with the release of lipoxins and TGF-β [6, 7]. The proliferation phase lasts approximately 1 week, when the epidermal barrier is rebuilt from a matrix containing fibrin, fibronectin and keratinocytes, released from stem cells that proliferate and differentiate. Growth factors modulate this epithelialization process and promote tissue reconstruction through the action of biomolecules, such as fibroblasts, macrophages, blood vessels, and collagen [6, 7]. The tissue remodeling phase coincides with the proliferation phase, although this restoration process

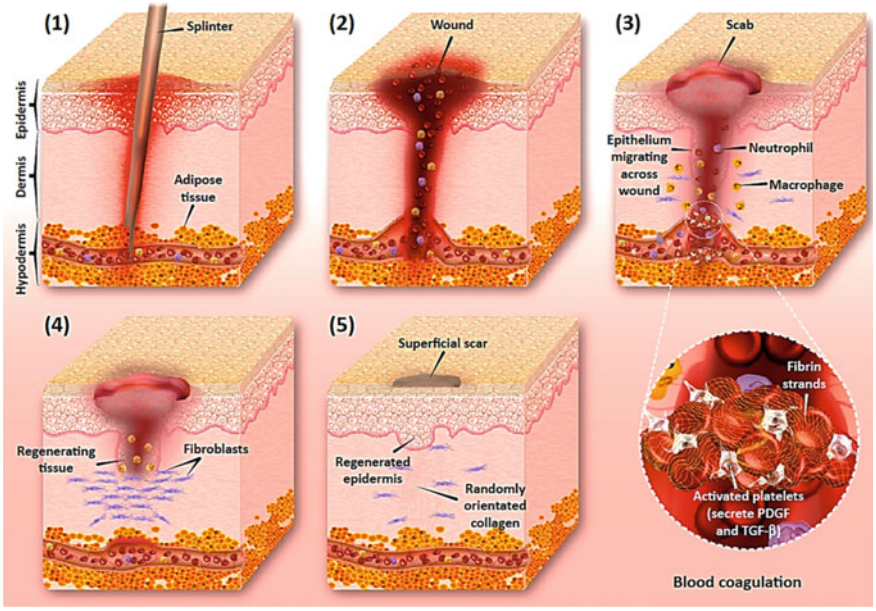


Fig. 11.1 The wound healing process involves four phases: hemostasis, inflammation, proliferation, and remodeling, in which a great diversity of biomolecules acts to reduce bacterial infection, and improving tissue remodeling. Adapted with permission from [5]. Copyright 2018 Elsevier

can take from 3 weeks to 2 years. It is the most clinically important phase where the assistance of growth factors such as TGF-β and platelet-derived growth factor (PDGF) contribute to the collagen deposition in the matrix to form an organized and healthy tissue [4, 8].

Skin wounds are classified into two types: acute and chronic. Acute wounds are wounds that heal in less than 3 months [4, 6]. Chronic wounds are the result of complications in tissue recovery, disease, pressure, and diabetic ulcers. Chronic wounds are the first focus of research for conventional and advanced treatment, since these wounds can stop healing in the inflammatory phase due to infections, hypoxia, biofilms, and poor delivery of biomolecules for tissue recovery [4, 9].

11.1.2 Types of Wound Dressing: Conventional and Novel Multifunctional Ones

Conventional treatments for wound healing usually employ dressings to protect the wound, creating a physical barrier against contamination and dangerous agents [10]. In addition, these dressings are designed to absorb exudate without causing dryness, allowing the production of a microclimate that promotes wound healing [11]. The

most suitable treatment is for chronic wounds, because of the economic costs and the impact on the life quality of patients. Conventional treatment methods are divided into two, namely: (i) passive dressings that coat the wound for protection after the healthcare specialist treatment, and (ii) multifunctional dressings that provide a humid environment that alters the wound atmosphere and interacts with the surface to promote healing [10, 12]. These types of wound dressing are designed with an optimal level of adhesion, thickness, contact area with the wound, absorption capacity, friction, and antibacterial properties. Such dressings are usually fabricated using three layers, in which the internal level prevents adherence to the wound dressing, the intermediate layer absorbs and retains the exudate excess, maintaining a humid environment, while the outer layer prevents bacterial invasion [10–12].

Nanostructured materials can be applied in wound dressings design, providing matrices for an organized cell growth and healthy regeneration of the skin, promoting scar formation, tissue integration, and avoiding bacterial infections [13, 14], as illustrated in Fig. 11.2. Among the most efficient nanomaterials for skin wound treatment are the electrospun nanofibers (here named as ESNF), which can yield a high surface/volume ratio platform displaying appealing properties such as biodegradability, high porosity, and the possibility of surface functionalization [15, 16]. Polymer nanofibers can mimic the biological extracellular matrix (ECM), contributing to the wound healing process, since the interaction of their large surface area improves drainage, nutrient exchange, antibacterial protection, and air permeability. In addition, nanofibers can be loaded with drugs [14, 17], antimicrobials, [18] and active biomolecules [19] to be released by diffusional process or triggered by external physicochemical stimuli, and thus promote cell regeneration, which makes this multifunctional treatment superior to conventional treatments [11, 12, 14, 15]. Multifunctional nanofibers for wound healing with externals agents activation and portable deposition in situ are called smart nanomaterials [20]. Besides the possibility to trigger the mechanism of interest, they can also be designed with advantageous properties such as biocompatibility and biodegradability, gas-permeability, surface hydrophilicity, antimicrobial properties, capability to absorb exudates and regulate nutrients and gases, and also to maintain local humid environment [12].

11.1.3 Electrospinning as a Suitable Alternative for Wound Dressing

11.1.3.1 Electrospun Nanofibers

Nonwovens based on ESNF have been employed in the last years for biomedical application, including as wound dressing, due to their advantageous features, including their unique physical and chemical properties, a morphology similar to the fibrous ECM, ability to encapsulate and release different bioactive compounds that improve the healing process (antimicrobial, micro and macromolecules, and

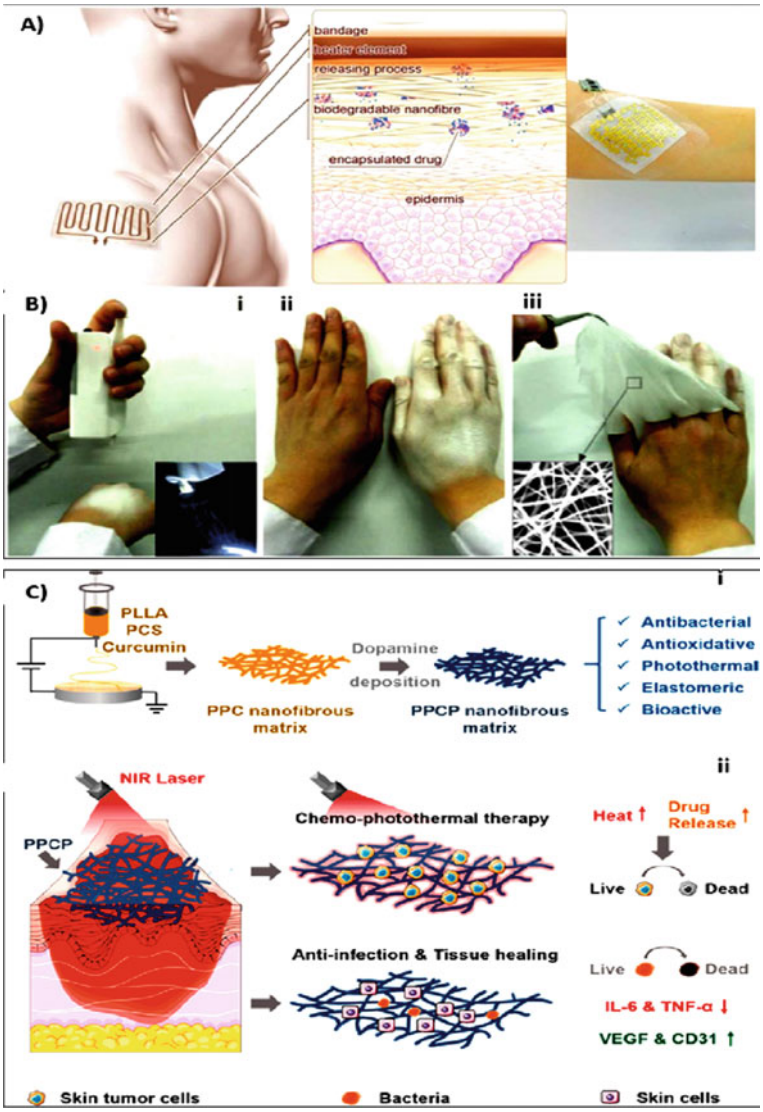


Fig. 11.2 **a** Thermosensitive drug nanocarriers are embedded within ESNF in a flexible system, in which the drugs are released as the temperature increases to enhance wound healing. Adapted with permission from Ref. [17]. Copyright 2017 Springer. **b** A battery-operated portable handheld electrospinning apparatus (BOEA) produce poly(lactic acid) (PLA) nanofibers to rapid hemostatic treatments. Adapted with permission from [21]. Copyright 2015 Willey. **c** (i) Multifunctional wound dressing composed of poly(l-lactic acid)–poly(citrate siloxane) nanofibers loaded with curcumin and polydopamine (PPCP), (ii) after NIR laser irradiation, the heat produced stimulates the release of curcumin, which exerts antibacterial and anti-inflammatory effects, improving skin healing. Adapted with permission from [22]. Copyright 2020 American Chemical Society

growth factors). Other properties of interest include release control modulated by different morphologies and compositions, exudate absorption capacity, and capability to prevent the penetration of bacteria and external microorganisms into the wound bed [23–26].

The electrospinning technique (ES) employs electrostatic forces to promote the elongation and stretching of a viscoelastic solution to form fibers at the nanometer scale [27]. Conventional components for ES setup are a high voltage source, a polymer solution with suitable viscosity, a syringe with a needle, and a grounded collector [28]. In the typical ES process, the polymer solution placed in the syringe flows through the needle at a constant rate, initially forming a polymer drop, as the electrical tension between the tip of the needle and the collector increases, leading to Taylor's cone formation. When the repulsive electrostatic forces on the surface of a droplet overcome surface tension forces, under a threshold value of high voltage, the Taylor's cone is stretched, starting the ES process, followed by evaporation of the solvent used in the solution and the formation of solid nanofibers, which are then collected in the grounded collector. Modifications in the ES process and apparatus have been reported including needleless ES [29], bubble ES [30], centrifugal ES [31], bubble melt ES [32], melt ES, [33] and portable ES [34].

The variables that influence the morphology, size, and homogeneity of the nanofibers are dependent on the properties of the chosen materials (e.g. types of synthetic and natural polymers, solvents, viscosity, conductivity, etc.), as well as processing parameters, such as the distance between the collector, and the ejection site of the polymeric solution, applied voltage, type of collector and diameter of the needle. Environmental parameters, such as temperature and humidity also play an essential role [35, 36].

The versatility of the ES process allows the use of more than 200 polymers, including synthetic and natural polymers [37, 38]. For applications in wound dressings, the most common materials include collagen [24], gelatin [39], chitosan [40], PLA [41], proteins [42], cellulose, [43] and poly(ε-caprolactone) (PCL) [44]. Composite materials have also been used to produce nanofibers applied to wound dressing [45].

11.1.3.2 Morphologies of Nanofibers

The ES process allows the incorporation of bioactive compounds and the modification of the nanofibers' morphology and properties by using (i) pre-modification or (ii) post-modification approaches. In (i), the modification is carried out before the ES step, that is, the bioactive agents are incorporated into the polymer solution [46]. For instance, Homaeigohar and coworkers [44] first developed a wound dressing using green ES to produce PCL nanofibers with bovine serum albumin (BSA). The protein was added to the polymeric solution before the ES process [44].

On the other hand, in ii) the modification is carried out after the ES process, where the compounds are added after the formation of nanofibers through different surface modification processes [47]. For example [48], quercetin-copper (Qu-Cu) chelates

and cuprorivaite (Cup), a highly bioactive bio-ceramic, have been incorporated into a PCL/gelatin solution for ESNF production. The nonwoven showed that the release of Qu, Cup and Cu acted in the regeneration of burned skin, hair follicle related cells, and antibacterial action against *S aureus* [48]. The layer-by-layer self-assembly technique coated the PCL/SF nanofibers with positively charged quaternized chitin and negatively charged SF. In another example, Hu and collaborators [49] used PCL and silk fibroin (SF) to design a multifunctional wound dressing and a hierarchical structure of electrospun nanofibers with antimicrobial activity against *E. coli* and *S. aureus*. The PLC/SF nanofibers were coated with positively charged quaternized chitin and negatively charged SF by layer-by-layer self-assembly technique. In vivo animal evaluation showed vascular reconstruction with hair follicle growth of 22 $\pm$ 4 mm^{-2}, comparable to normal tissue (27 $\pm$ 2 mm^{-2}) [49]. It is important to mention that in some cases, both pre-modification and post-modification approaches can be employed to render ESNF with optimized properties. In this direction, Ballesteros et al. [50] developed ESNF based on PCL ESNF containing silver nanoparticles (AgNP) in their bulk (by pre-modification approach) while their surface was further decorated (by post-modification approach) with photo-responsive nanogels containing AgNP.

The distinct morphologies presented by ESNF include core–shell [51], hollow [52], Janus [53], asymmetric dressings [1, 54], porous structure [55] and sponge [56] enable different performances as a wound dressing. For example, asymmetric dressings [1, 57] are composed of two or more layers and have great potential for wound healing by mimicking the dermis and epidermis layers and avoid the invasion of external microorganisms to the wound site. In another example, Khan and coworkers [58] reported core–shell multifunctional composite nanofibers with oregano essential oil and hyaluronic acid (HA) in the core and zinc oxide nanoparticles (ZnO) were blended with poly (*l*-lactide-co-caprolactone) in the shell layer. The ESNF produced showed strong antibacterial action, angiogenic potential, anti-inflammatory action, and complete healing of wounds with good vascularization and organized collagen fibers [58].

11.2 Characterization of ESNF for Wound Dressings

The performance of ESNF for wound dressings are highly dependent on diverse aspects including (i) morphological characteristics, (ii) porosity and surface area, (iii) fluid handling capacity, (iv) oxygen permeation, (v) mechanical properties, (vi) antimicrobial activity, as well as (vii) in vitro and in vivo cytotoxicity studies [59–61]. In the following subsections we present the main characteristics of ESNF for wound dressing applications.

11.2.1 Morphology, Porosity and Surface Area

ESNF morphology may influence the adhesion, spreading, and proliferation of cells related to the healing process [62, 63]. The surface morphology of these materials is usually characterized using scanning electron microscopy (SEM) and atomic force microscopy (AFM). At the same time, the internal structure of fibers can be assessed through transmission electron microscopy (TEM) and, in some cases, by fluorescence microscopy [51, 64, 65]. The inherent high porosity and surface area to volume ratio exhibited by ESNF matrices are beneficial for exuding fluid from the wound, transporting nutrients to cell and gas permeation [59]. Porosity measurements of electrospun nonwovens pose significant challenges and several methods such as water flux permeability [66] and liquid displacement [67] methods have been proposed to estimate the porosity. The surface area measurement and porosity of ESNF nonwovens can be performed by the Brunauer–Emmett–Teller (BET) gas adsorption method [68].

11.2.2 Fluid Handling Capacity and Oxygen Permeation

The fluid handling capacity allows estimating the ability of nonwoven on the control of moisture balance at the wound surface [60]. The fluid handling capacity is mainly assessed through three principal tests: (i) swelling capacity, (ii) surface hydrophilicity, and (ii) water vapor transmission rate. The swelling capacity is generally evaluated via gravimetric method and provides information about the ability of electrospun materials to absorb excessive exudates from the wound beds [67]. This property is highly related to other characteristics of the wound dressing material such as composition, pore size, and porosity [69]. The surface hydrophilicity character of ESNF is related to many interfacial processes such as absorption and wetting of aqueous fluids, and is intrinsically affected by nanofibers morphology, and composition, being evaluated through contact angle measurements [70, 71].

The ability of wound dressings to control the water loss from the wound to the atmosphere is evaluated by determining their water vapor transmission rate (WVTR) [72]. A wound dressing with a suitable WVTR is required to avoid excessive dehydration or exudate accumulation, where high WVTR values may result in dehydration and a low WVTR may lead to the accumulation of wound exudates [59]. The WVTR is mainly affected by the pore size, porosity, hydrophilicity, and thickness of ESNF, being commonly evaluated by the method E96/E96 M—16 proposed by the American Society for Testing and Materials (ASTM) [73].

The high porosity and surface area to volume ratio exhibited by ESNF nonwoven favor the oxygen permeation, which is beneficial for the wound healing process, since O_2 is an essential nutrient for cell metabolism [59]. To date, there is no standard test to measure the permeability of oxygen across the ESNF and a gas permeability analyzer is commonly used to evaluate this property [74].

11.2.3 Mechanical Properties

ESNF nonwoven should exhibit mechanical characteristics that facilitate handling during application at the wound site and also along the healing period [59]. Overall, the mechanical properties of ESNF are commonly assessed through uniaxial tensile tests, according to adaptations of the D882-18 standard test method proposed by ASTM (2002) [75]. The tensile properties of these materials are strongly influenced by the composition, diameter and degree of orientation of the fibers as well as by the wound dressing thickness [62, 76]. The mechanical properties are typically assessed in terms of Young modulus (or elasticity modulus), which expresses the tension applied to elastically deform a material by a set amount of elongation, relative to the original length. The calculation of the tension is based on the force applied by the measuring instrument, divided by the transversal section area of the material. Other important parameters are the tension at break or failure, the maximum amount of tension the material can receive before breaking or tearing apart, and the maximum elongation. Wound dressing materials typically present low Young modulus and tension at break, while the maximum elongation is high. These properties can be fine-tuned to better suit the needs with the usage of different polymers, different treatments, or the usage of additives or composite structures.

11.2.4 Chemical Composition

From the available techniques used to analyze the chemical composition of materials, the Fourier Transformed Infra-Red spectroscopy (FTIR) stands out. The technique allows a fast, cheap, and non-destructive analysis of the covalent chemical bonds the material, based on the different absorption of the infra-red spectrum wavelengths [77, 78]. Comparing the observed peaks in absorption with pre-established values, it is possible to infer what covalent bonds are present, and thus determine if the spinning process itself caused any alteration in the original material, or if the different molecules used are interacting with each other, creating or breaking bonds. Changes in the typical covalent bonds could mean a molecule of interest is strongly linked to the fiber material, or that a degradation process occurred, or even if there are impurities in the material [78].

11.2.5 Biological Characterizations

Micro- and nanofibrous materials are promising for wound dressing applications due to their physical similarity with ECM [79, 80]. In general, ESNF with a less compact structure [81], composed by fibers with rough surface, [82] and presenting moderate hydrophilicity (between 45 and 90° of water contact angle) [83] show better

cell adhesion. Hydrophobic materials would thus difficult the adhesion of microorganisms. Larger fiber diameters are also linked to fewer incidences of inflammatory responses [84]. Natural polymers or polymers derived from biomolecules are inherently biodegradable [79], which means that they are more readily degraded by biological entities, such as microorganisms present in the natural environment and more complex living beings. Natural polymers also present better biocompatibility [79]. They also less often trigger inflammatory responses and are also more prone to be bio-resorbed (or metabolized) by the host organism [85].

11.2.5.1 Biocompatibility Analyses

The biocompatibility of ESNF as wound dressings may be assessed through a great variety of experiments and analyses. ISO 10993-5 [86] lists in vitro tests to determine cytotoxic activity in mammalian cells, which must be chosen according to the desired application. All the tests must be conducted under aseptic conditions and with control of the material sterility.

Tests can be conducted using extract, direct contact, or indirect contact analyses [87]. For the usage of extracts, the conditions used, such as extracting vehicle composition, time of extraction, and temperature must match the desired application, avoiding significant alteration on the material, unless it is intended during the proper usage. The extract concentration may be varied through dilutions for better assessing the cytotoxic effects [87]. For the direct contact tests, it is advised that the solid test sample presents at least one flat surface, and samples that are adsorbent should be soaked with culture medium prior to testing [87]. Indirect contact tests are conducted with the usage of a diffusion medium, such as agar or other filtering medium, according to the leachate's ability to diffuse through the selected medium without altering itself or the chemical composition of the medium [87].

The determination of the impact on cell viability can be evaluated through the morphological analysis of cells with measurement of cell damage, measurement of cell growth, or measurements on specific aspects of the metabolism, in qualitative or quantitative terms. Cytotoxicity may be manifested as poor cellular adhesion (round shape), abnormal morphology, and metabolism and/or cellular lysis [87]. Cell lines of keratinocytes and fibroblasts are typically tested for wound dressings since they compose the cell population of skin layers [61]. Tests with immune system cells, such as leukocytes, could provide additional information on biocompatibility and inflammatory responses. ISO 10993-4 [88], which presents tests specifically for interaction with blood, could also be followed for assessing effects on blood cells lysis and blood clotting, which may be crucial for the usage of wound dressings.

It is relevant highlight that, although these in vitro tests provide preliminary data about the safety of the material, they do not provide definitive responses for the biological behavior. Simple cell cultures demonstrate whether the cells are affected or not by the exposure in an individual basis. The effect of fewer damages on cell function, although allowing it to thrive, might result in functional or structural losses when analyzed at tissue or organ levels of structural organization. It is fundamental

thus to assess the impact of the material on more complex structures. Organs-on-a-chip and bodies-on-a-chip templates may provide great models for toxicity analyses and bring less ethical concerns. However, the complexity and costs of producing these platforms render them unavailable for many research centers [89]. Then, the wound dressing must be tested in vivo for better assessment of therapeutic and toxic properties.

11.2.5.2 Antimicrobial Activity

The antimicrobial analysis is conducted similarly to the cytotoxicity tests, replacing the animal or human cells with microorganisms of interest, but with a small adjustment. Instead of analyzing the microbial cells growth and evaluating how the presence of the material stimulates or impairs the further development of the culture, the material is present since the beginning of the inoculation and the effects on growth inhibition, either by making the cells static, or effectively promoting their death, is investigated. For wound dressings, tested microorganisms are related to healthcare-associated infections (HAIs) [90]. Usually, *Staphylococcus aureus* and *Enterococcus* sp. are models for gram-positive bacteria; *Salmonella* sp., *Escherichia coli* and *Pseudomonas aeruginosa* are models for the gram-negative group; *Candida albicans* often represents fungal pathogens. Besides providing a physical barrier to microbial penetration [91], nanofibrous wound dressings do not possess intrinsic antimicrobial activity. Therefore, the usage of specific polymers or additives promotes the protective effect.

11.2.5.3 Degradation Analysis

Degradation can be defined as the loss of chemical or physical structure by any means, while biodegradation implies the participation of enzymes in a defined degradation route. There is proof of biological molecules being involved in the process [85]. Materials with adequate hydrophilicity not only enhance cell adhesion, but are also better suited for the action of enzymes [92]. Degradation rates could be determined by observing how the material loses weight or has its properties changed over time. Simulating the chemical environment of the wounded injuries is advised for a good estimation of the degradation behavior. However, the complexity of the whole metabolism is hardly represented by this simplified system. Therefore, in vivo tests are still crucial for the determination of the biological activity of the material. For the material itself, drugs loaded in it, or by the compounds resulted from the degradation of them, wound dressings desirably must not trigger inflammatory responses or in any other way negatively affect the healing process [93]. Significant losses on material integrity must be considered for determining removal and reapplication, although biopolymers could be used for absorbable wound dressings. For drug-loaded materials, the analysis of the release profile must be considered so the concentration is at the same time simultaneously antimicrobial and non-cytotoxic.

11.3 Applications of ESNF Wound Dressings

This section provides an organization of a wide range of ESNF formulations for application as wound dressings, essentially when combined with nanostructured materials in their polymer composition. They can be classified as natural polymers, synthetic polymers, polymer blends (synthetic/synthetic, synthetic/natural, natural/natural), or composite nanofibers, when combined with nanostructured materials. The following topics aim to help readers understand the types and properties of nanofibers formulations, exemplifying their uses and facilitating the search and reading.

11.3.1 Synthetic Polymers Applied to ESNF Wound Dressing Design

Synthetic polymers are fabricated through chemical reactions between monomers, yielding versatile macromolecules with outstanding properties for varied applications, including in modern medicine [94, 95]. The possibility of controlling physicochemical properties, including the absence or at least low level of impurities, good mechanical and chemical properties make them suitable to be processed by ES, and for wound dressing applications [95, 96], as depicted in the examples of Table 11.1. The current research strategies for wound dressings that employ synthetic polymers for wound dressings are developing with biocompatible synthetic polymers under the approval by government agencies, for example, Food and Drug Administration Agency (FDA).

Poly(lactic-co-glycolic acid) (PLGA) is a synthetic polymer that undergoes a thermal shrinkage near human body temperature (37 °C). This shrinkage behavior of PLGA allowed it to be explored as a tape to induce fibroblast growth in loose

Table 11.1 ESNF based on synthetic polymers and application as multifunctional wound dressing

Composition		Main finds	References
Pristine	PLA	Biodegradable, biocompatible and potential keratinocyte growth	[97]
	PS[a]	Non-biodegradableand potential keratinocyte growth	[97]
	PVP[b]	Non-biodegradable, water soluble and potential keratinocyte growth	[97]
	PLGA[c]	Biocompatible, poor hydrophilicity and potential fibroblast growth	[98]
	PVDF[d]	Poor hydrophilicity and comparison of aligned/random fibers for human-induced pluripotent stem cells growth	[99]
	PCL	Poor hydrophilicity, biocompatible, bioabsorbable and poor human skin foreskin fibroblast growth	[100]

[a] polystyrene, [b] poly(vinylpyrrolidone), [c] poly(lactic-co-glycolic acid), [d] poly vinilidene fluoride

soft tissue (LST) [101]. Firstly, the authors studied the contractability of a sample of PLGA fibrous tape—with a size of 4 cm × 4 cm—immersing in phosphate buffer and observed that PLGA tape shrank after five days to 2 cm × 2.1 cm approximately, changing their morphology from straight fibers to high crimped fiber. For comparison, poly(L-lactide)acid (PLLA) shrinkage was smaller than PLGA shrinkage and human vaginal fibroblasts (HVF) cultured over PLGA yielded a higher aspect ratio and propagation area than those cultured in PLLA, which was attributed to the dynamic shrinkage behavior of the PLGA polymer [101].

In another work, Castellano et al. reported the fabrication of two synthetic polymers nanofibers, PCL and PHB (Polyhydroxy butyrate-co-valerate). They compared them in terms of fibroblasts and keratinocytes growths. The PCL fibers presented lower fibroblast and keratinocyte proliferation than PHB fibers. The authors conclude that PHB nanofibers present promising vasculogenic behavior and cell adhesion [102]. In another work, the stratification of proteins from epidermal region growth over poly(ethylene terephthalate) (PET), poly(1,4-butylene terephthalate) (PBT) and poly(N,N′-hexametyleneadipinediamide) (N6/6) synthetic polymers ESNF was evaluated. The results from epidermal growth demonstrated that N6/6 ESNF prevented fibroblast growth, possible due to the small pore size of nonwovens associated with the fiber diameter (0.13 μm). On the other hand, the fiber diameters of PET (1.9 μm) and PBT (1.7 μm) nanofibers improved the fibroblast permeability, facilitating adhesion and proliferation. From this observation, the authors proposed that N6/6 ESNF with a small pore size mimicking human skin tissues can be used as a model for corrosion and irritation tests [103].

Antimicrobial synthetic polymers comprise another class of polymers suitable for wound dressings. They can be synthesized via functional group modifications during the polymer reaction synthesis, allowing the production of zwitterionic polymers. For example, the monomers of methyl methacrylate (MMA) (47 mmol) and carboxybetaine (4.7 mmol) reacted to produce a zwitterionic copolymer named poly(carboxybetaine-co-methyl methacrylate) (CBMA). After fabrication of CBMA ESNF, the authors demonstrated that cell proliferation assay was lower in CBMA than in pristine PMMA ESNF or the control sample. Moreover, this result indicates that zwitterionic nonwovens are less adherent to the wound than pristine neutral PMMA. The bacterial assays showed that the zwitterionic character confers to CBMA fiber antibacterial properties against *S. aureus*/*E. coli*, a property not observable in PMMA fibers [104].

Synthetic electrospun fibers can also improve wound healing performance by loading drugs or other medicinal compounds in their composition. Such strategy is suitable releasing medicinal compounds from wound dressings to accelerate wound injury recovery [105]. As the morphology of synthetic/natural nanofibers mimics ECM very well, novel functionalities and drugs to tailor their surface/bulk can be used to enhance the wound dressing final properties. As mentioned before, one pristine synthetic polymer that composes the ESNW can be modified by pre- or post-modifications to obtain a novel composite membranes, especially by encapsulating organic/inorganic substances, combining different polymers in blends, or combining membranes into unique devices.

Injuries in the wound of diabetic patients can result in sepsis, or in some extreme cases into foot ulcers. These are examples of the lack of appropriate therapies to treat this disease. In this context, Zehra and coworkers [106] synthesized PCL ESNF containing sodium percarbonate (SPC) salt at a loading capacity of 2% v/v^{-1} to be applied in chronic diabetic wounds induced in rats. The SPC-PCL ESNF improved local oxygen release accompanied by an increase in pH from 7.3 to ≈ 7.55, which can play a vital role in the recovery of chronic diabetic wounds. Additionally, SPC-PCL ESNF promoted the local angiogenic process and blood vessel formation better than PCL. The histological study and gene expression analysis confirmed that PCL-SPC ESNF enhanced the dermis and epidermis recovery, which were mainly associated with HIF-1α protein expression [106]. In the context of the dermatology viewpoint, the anti-scar property of wound dressings is another advantage presented by ESNF. For example, Guo and coworkers studied the wound recovery in a second-degree burn promoted by PCL/ALA (α-lactalbumin) nanofiber dressings, compared with commercial microfiber dressing Sorbalgon® and demonstrated that the anti-scar performance of PLA/ALA nanofibers is similar to commercial dressing [107].

Diverse nanofiber composites have been successfully prepared with the modification of sub-micrometer fibers with nanoparticles (NPs) including TiO_2 [108], CuNPs [109], AgNPs [110], ZnO [111], TeNPs [112], CQDs/SiNPs [113], sulfadiazine silver [114], CeO_2 [115], silver-MOF [116] conferring the ESNF antimicrobial activity properties. The adaptability of ES solution parameters allows the combination of NPs with antibacterial agents, enhancing electrospun antimicrobial performance [117–119]. In another strategy, Sun et al. proposed a novel approach to inorganic Upconvertion NPs (UCNPs), by preparing core–shell nanoparticles NaYF4:Er/Yb/Gd recovered by SiO_2 (S) and Methylene Blue (M) [120]. After the PVDF ESNF fabrication, they induced antibacterial properties in UCNPs/SM-PVDF upon excitation at 980 nm. Without NIR light, no S. aureus/E. coli mortality was perceived, while when NIR light was employed, remarkable antibacterial properties were observed [120].

Core–shell electrospun nano- and microfibers rely on spinning polymer solutions through coaxial configuration. The fiber morphology obtained by this approach opens a variety of opportunities to combine polymers into a single fiber and also prevent undesirable burst release in drug release systems [121–123]. Bi- and three-layered fibrous non-wovens compass another strategy for the developing of 3D wound dressing [124]. The design of these multilayered dressings allows the outer/top layer to protect the inner/bottom layer from environmental exposure, and contributes to enhancing mechanical performance [125–127].

Decellularized cells are cells in which the cellular and nuclear materials are removed from ECM without damage to the three-dimensional scaffold structure of ECM and to the vascular network, which provide a microenvironment for tissue regeneration, and minimize rejection risks [128]. Nanofibers from synthetic polymers loaded with these regenerative cells are another outstanding innovative possibility of ES for the fabrication of wound dressings [129, 130]. In this context, decellularized human amniotic membranes (HAM) were encapsulated in nanofibrous matrices [131]. The authors demonstrated that when HAM were embedded into

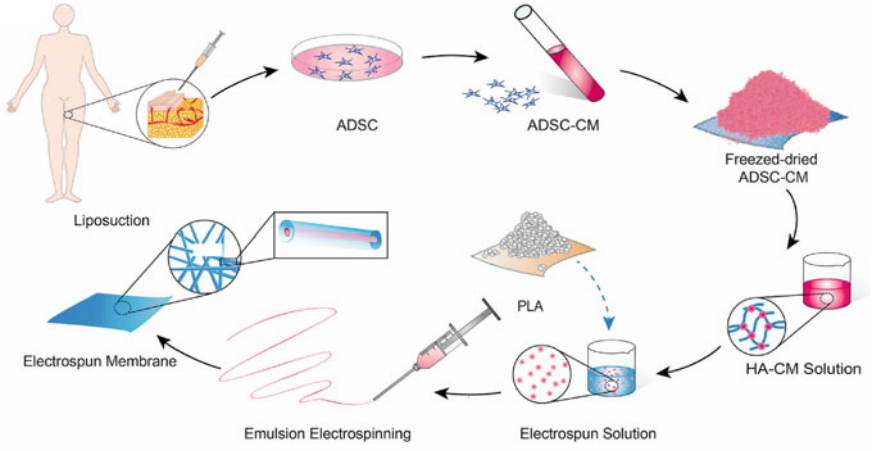


Fig. 11.3 Schematic representation of fabrication of micro-nano PLA fiber (MPF) with Adipose-derived stem cell (ADSC) Conditioned Medium (CM). Adapted with permission from [132]. Copyright 2020 Elsevier

PLGA aligned electrospun sub-micrometer fibers, skeletal muscle growth orientation was improved [131]. In another work, Adipose-derived stem cells conditioned medium (ADSC-CM) were successfully extracted from adipose tissue, freeze-dried and loaded into micro-nano PLA fibers (MPF) matrix to fabricate a regenerative wound therapy material, as outlined in Fig. 11.3 (B). In this case, electrospun emulsion fabrication leads to a core distribution of cells in the interior of the PLA fibers, which contributes to shielding the cell against external ambient conditions, affecting the kinetics release. In vitro studies indicated that MPF@CM decreased the expression of scar-related protein and the relative scar area after fifteen days [132].

11.3.2 Natural Polymers Applied to ESNF Wound Dressing Design

Natural polymers have been employed to design advanced wound dressings, offering a broad spectrum of groundbreaking solutions [133, 134]. The most advantageous properties is biocompatibility, since natural polymers' chemical structures are normally based on carbohydrates and proteins, which show great similarity to the native ECM [59]. Other advantageous properties include cell affinity, low antigenicity, and favorable bioactivity, which stimulate cell attachment, re-epithelialization, and healing effect, as well as antibacterial effect in some cases. Recent studies on the use of natural polymers for wound dressings are summarized in Table 11.2.

Table 11.2 ESNF based on natural polymers and application as multifunctional wound dressing

Composition		Main finds	References
Pristine	β-Chitin	The use of pristine β-chitin nanofibers allowed epithelial regenerating faster than control groups, higher percentage of collagen deposition at 3rd day	[135]
	Collagen	Electrospun of neat collagen extracted from tilapia skin allowed differentiation of human keratinocytes stimulated by collagen amino acids, and complete healing after 14 days, faster than the control group	[136]
	Zein	Bilayered dressing based on casting film layer and electrospun fiber layer. Synergistic effect of the different morphologies, in which the fiber layer ensured a high surface area for cell proliferation and the film layer protected the wound. Antibiotic effect given by sustained release of gentamicin	[137]
	Gelatin	Electrospun of neat gelatin enabled the release of vitamins A and E, proliferation of fibroblasts in presence of vitamin A, stimulated secretion of collagen in presence of both vitamins, and yield significant decrease of wound area after 14 days, with complete regeneration before control groups	[138]
	CA[a]	Controlled release of benzocaine at pH 9.0, which would correspond clinically to the pH of an infected wound. The loading of dye bromocresol green led to fast color changes according to the wound pH, as an easy-to-interpret indicator of the healing process	[139]
Multicomponent	Collagen/Elastin/PCL	Increased elasticity, while stiffness decreased due to presence of elastin. Keratinocyte and fibroblast proliferation, tissue integration and accelerated early-stage angiogenesis	[140]
	PU[b]/Keratin/AgNP	Significant level of fibroblasts differentiation, cell attachment and cytocompatibility in the presence of keratin. Antibacterial activity exerted by AgNP	[141]
	Chitosan/PVA[c]/ZnO	The presence of ZnO implied in antibacterial and antioxidant activity, which factors contributed to accelerate the healing of diabetic wounds	[142]

(continued)

Table 11.2 (continued)

Composition		Main finds	References
	SF/PCL e SF/HA	Mimetic asymmetric two-layered dressing, where the top one protects against bacteria and the bottom one releases antibacterial natural agent and enables fibroblasts growing and proliferation	[143]

[a] cellulose acetate; [b] polyurethane; [c] poly(vinyl alcohol)

Biomimetic ESNF constituted of collagen extracted from tilapia skin has enabled accelerated wound healing. Collagen comprises a protein of animal connective tissues found in bovine and porcine. Recently, fish collagen has been investigated for applications in skin wound healing, due to its immune-modulatory and anti-inflammatory activities. Besides, this material has also displayed antimicrobial effects, due the presence of collagencin, an antimicrobial peptide identified from fish collagen hydrolysate [144, 145]. For instance, Zhou and coworkers [136] employed collagen extracted from tilapia skin to produce ESNF and later crosslinked with glutaraldehyde vapor. Smooth surface nanofibers were obtained and due to the crosslinking, the ESNF presented good mechanical properties, hydrophilicity and swelling ratio of approximately fourfold than it dry weight owing to the presence of hydroxyl, carboxyl, and amino groups in collagen composition. The biomimicking of tilapia collagen nanofibers to the ECM was demonstrated by the firm attachment, and equal distribution of human keratinocytes along with the nanofiber network, as observable in Fig. 11.4 (A1), which was attributed to synergetic effects of collagen amino acids on stimulating the differentiation of human keratinocytes. The improved wound healing rate was verified comparing to the control groups, combined with a significantly lower inflammatory response. At the end of experiments, the epidermal cells were found fully differentiated, basal cells were closely arranged, the horny layer (the outermost layer of the epidermis) could be observed, and layers of keratinocytes were evident [Fig. 11.4 (A2)].

Polysaccharides represent a class of natural polymers that have received significant attention for the development of novel materials. Chitin and chitosan are structural carbohydrates obtained from the exoskeleton of various crustaceans and arthropods, such as crabs and shrimps [135, 146]. Jung et al. [135] developed a electrospun dressing constituted of β-chitin extracted from cuttlefish bone. Although the ES of the neat chitin only resulted in nanosized beads, as verified in Fig. 11.4 (B1), the blending with small concentrations of PEO allowed fiber formation (ratios of 2.0:0.1 to 2.0:1.0). PEO is commonly added to ES polymer solution to adjust its viscosity, and improve their electrospinnability. In this work, PEO was soaked in water and removed afterwards, which led to decreased nanofiber diameter and increased porosity, providing enhanced hydrophilicity and higher contact angle. The resultant β-chitin ESNF are shown in Fig. 11.4 (B2).The biocompatibility and wound

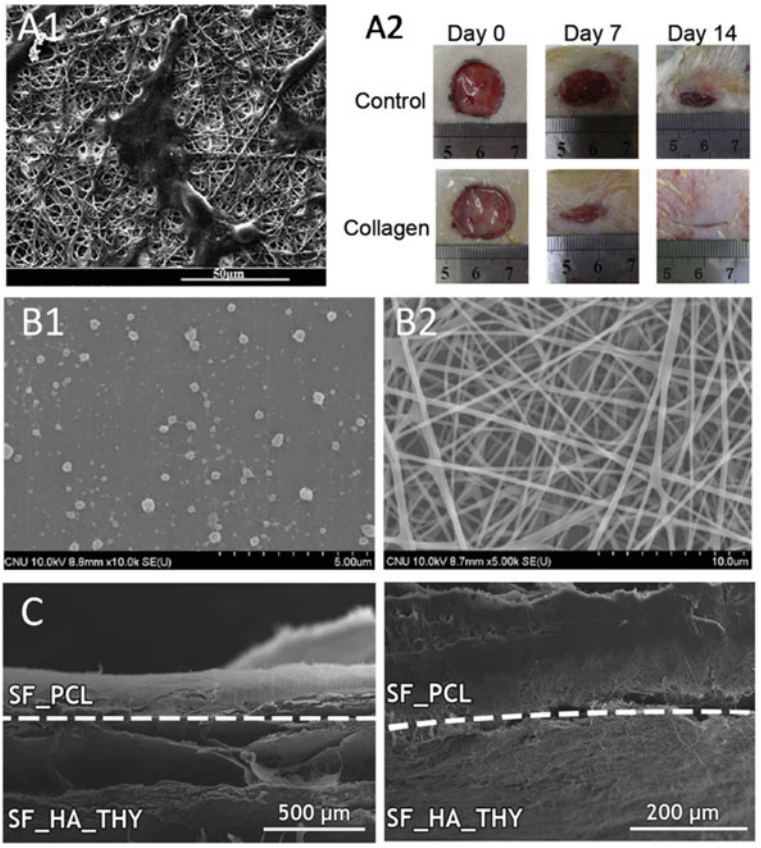


Fig. 11.4 (A1) human keratinocytes firmly attached and equally distributed along biomimetic ESNF constituted of collagen extracted from tilapia skin. (A2) Improved wound healing rate of biomimetic electrospun nanofibers in contrast to the control groups, combined with a significantly lower inflammatory response. Adapted with permission of [136. Copyright 2016 Elsevier. b ESNF constituted by β-chitin extracted from cuttlefish bone: (B1) neat chitin only resulted in nanosized beads, while in (B2) the blending with small concentrations of PEO followed by its removal, allowed the formation of porous and small diameter ESNF. Adapted with permission of [135]. Copyright 2018 Elsevier. **c** SEM image of zein asymmetric membrane designed as two layers aiming to mimic epidermis and dermis. Adapted with permission from [143]. Copyright 2018 Wiley

healing effects were evaluated by in vitro tests, showing enhanced collagen deposition and wound recovery when compared with control samples.

Cellulose acetate (CA), another polysaccharide widely applied in ES, was used as a dual nanocarrier system, namely (i) benzocaine, aiming the controlled delivery of anesthetic for local pain reduction, and (ii) dye bromocresol green, to detect different stages of wound healing by mean of wound pH variation [139]. The loading of dye bromocresol green led to fast color changes according to the wound pH, as an easy-to-interpret indicator of the healing process. The color change from green to yellow

indicates that the wound healing course follows as expected and the pH is decreases (since the pH of a healthy skin is slightly acidic). In contrast, while the color change to blue indicates the media alkalinization, suggesting bacterial infection and tissue inflammation, for example. Moreover, in vitro release test showed that the system behaved as pH-dependent benzocaine release and therefore controllable.

The number of recent research papers using ESNF based on neat natural polymers as a multifunctional wound dressing is lower when compared to ESNF based on blends and nanocomposites involving this class of polymers. An often challenge comprises the fabrication step, since in many cases, attaining flexible, smooth and uniform ESNF mat is limited by factors such as poor solubility in the solvents used in ES, degradation towards specific solvents, very high molecular weight, and therefore very high viscosity [59]. Innovative combinations of synthetic and biopolymers showed ability to overcome the issues related to both classes of polymers. For instance, the inclusion of collagen and elastin in PCL nanofiber formulation increases flexibility and elasticity [140], while the use of keratin extracted from human hair combined with PCL and AgNP enhances cell affinity and proliferation [141]. Some compounds can also add extra functions in dressings. The recent literature shows the practical application of antibacterial effect aside from of AgNP [141], ZnO [142], but also by incorporation of bacteriophages [147]. Controlled release of conventional therapeutical compounds can also be performed, such as tetracycline [148], erythromycin [149], nitrofurazone [150], gentamicin [137], *aloe vera* [151], grape seed extract [152], vitamins [138], among many others.

The combination of structures and materials has enabled the fabrication of asymmetric wound dressings, which are designed as two layers aiming to mimic both skin layers: epidermis and dermis. By exploring the silk fibroin (SF), Miguel and coworkers [143] produced an asymmetric wound dressing using ESNF of SF combined with other elements in both layers. As demonstrated by SEM image of Fig. 11.4c, a blend of PCL and SF was employed as top layer to reproduce the epidermis dense nature and waterproof ability. In contrast, the bottom layer was constituted of SF ESNF blended with hyaluronic acid. Moreover, the bottom layer was loaded with thymol (Thy), an herbal drug with antimicrobial effects.

The resultant ESNF presented excellent mechanical properties, whose data were similar to those displayed by the native skin [153], higher porosity in the bottom layer, superior swelling profile at alkaline pH, and cell adhesion, proliferation and spreading. SEM analysis demonstrated that bacteria were found only at upper side of the top layer, confirming that a denser structure protects the wound from bacteria colonization. Moreover, the thymol loaded in bottom layers increased inhibitory effect, demonstrating a 2–3 times larger inhibitory halo area and no biofim formation, unlike to ESNF without this compound.

Integrating (bio)sensor devices to wound dressings constitute an outstanding trend for smart wound dressings. As Kurecic et al. work [139], many recent investigations explores the possibility to monitor wounds and the healing process [154, 155]. Pakolpakçil et al. [155] described that ESNF based on sodium alginate and PVA containing anthocyanins extracted from black carrots undergo color changes under different pH environments. The selection of alginate and PVA nanofibers allowed

achieving a hydrophilic mat, which was fundamental for exudates absorption and for promoting the color change. Thereafter, they developed a similar halochromic system, just changing the anthocyanins extract, now from purple cabbage [154]. The color scheme for the ESNF containing cabbage anthocyanins ranged between purple and blue shades, clearly distinguishable by the naked eye and also measured by UV–Vis. The in vivo performance was tested, and in Fig. 11.4c is possible to observe the color changes of this system in contact with the wound in different stages.

11.4 Conclusions

Acute and chronic skin injuries affect many people worldwide and can be a serious source of diseases and infections. Therefore, novel treatments and innovative solutions concerning functional wound dressings are required to tackle this problem. This chapter presented some representative results related to advanced multifunctional electrospun nanofibers applied in wound dressings for skin healing. Such systems are highly suitable for this application because they can accelerate the healing process by protecting the wound, increasing fluid draining and tissue regeneration, besides helping in the moisture regulation. Additionally, appropriately modifying the bulk or the surface of wound dressings can render antibacterial properties and drug delivery capacity. It is important to say, though, that evaluating the safety and biocompatibility of such multifunctional dressings are also fundamental and considerable progress must be achieved in this direction to warrant biocompatibility and non-toxicity. Due to the similarity in composition with human tissue, natural polymers such as collagen, keratin, silk fibroin, chitosan and cellulose stand in performance regarding cell affinity, low antigenicity, cell attachment, and re-epithelialization. However, some synthetic polymer can also be tailored for this end. In summary, multifunctional advanced electrospun nanofibers applied in wound dressings have become a clear trend in the skin healing process, which products shall become more popularized and produced at a larger scale in following years.

Acknowledgements The authors thank the financial support from Fundação de Amparo à Pesquisa do Estado de São Paulo (FAPESP) (grant numbers: 2017/12174-4, 2017/20973-4 2018/22214-6, 2018/18468-2), Conselho Nacional de Desenvolvimento Científico e Tecnológico (CNPq), MCTI-SisNano (CNPq/402.287/2013-4), Coordenação de Aperfeiçoamento de Pessoal de Nível Superior—Brasil (CAPES) (Financing Code 001) and Rede Agronano-EMBRAPA from Brazil.

References

1. Graça, M. F. P., de Melo-Diogo, D., Correia, I. J., & Moreira, A. F. (2021). Electrospun asymmetric membranes as promising wound dressings: A review. *Pharmaceutics, 13*(2), 1–25. https://doi.org/10.3390/pharmaceutics13020183
2. Genchi, G. G., Marino, A., Grillone, A., Pezzini, I., & Ciofani, G. (2017). Remote control of cellular functions: The role of smart nanomaterials in the medicine of the future. *Advanced Healthcare Materials, 6*(9), 1700002. https://doi.org/10.1002/adhm.201700002
3. Silva, W. N., Leonel, C., Prazeres, P. H. D. M., Sena, I. F. G., Guerra, D. A. P., Heller, D., Diniz, I. M. A., Fortuna, V., & Mintz, A. (2018). Role of Schwann cells in cutaneous wound healing. *Wound Repair and Regeneration, 26*, 392–397. https://doi.org/10.1111/wrr.12647
4. Zeng, R., Lin, C., Lin, Z., Chen, H., Lu, W., Lin, C., & Li, H. (2018). Approaches to cutaneous wound healing: Basics and future directions. *Cell and Tissue Research, 374*, 217–232. https://doi.org/10.1007/s00441-018-2830-1
5. Farokhi, M., Mottaghitalab, F., Fatahi, Y., Khademhosseini, A., & Kaplan, D. L. (2018). Overview of silk fibroin use in wound dressings. *Trends in Biotechnology, 36*(9), 907–922. https://doi.org/10.1016/j.tibtech.2018.04.004
6. Sorg, H., Tilkorn, D. J., Hager, S., Hauser, J., & Mirastschijski, U. (2017). Skin wound healing: An update on the current knowledge and concepts. *European Surgical Research, 58*(1–2), 81–94. https://doi.org/10.1159/000454919
7. Witte, M. B., & Barbul, A. (1997). General principles of wound healing. *Surgical Clinics of North America, 77*(3), 509–528. https://doi.org/10.1016/S0039-6109(05)70566-1
8. Chicharro-Alcantara, D., Rubio-zaragoza, M., Damiá-Giménez, E., Carrillo-Poveda, J. M., Cuervo-Serrato, B., Peláez-Gorrea, P., & Sopena-Juncosa, J. J. (2018). Platelet rich plasma: New insights for cutaneous wound healing management. *Journal of Functional Biomaterials, 9*(1), 10. https://doi.org/10.3390/jfb9010010
9. Tocco, I., Zavan, B., Bassetto, F., & Vindigni, V. (2012). Nanotechnology-based therapies for skin wound regeneration. *Journal of Nanomaterials, 2012*(Article ID 714134), 11. https://doi.org/10.1155/2012/714134
10. Bredow, J., Hoffmann, K., Oppermann, J., Hellmich, M., Eysel, P., & Zarghooni, K. (2018). Evaluation of absorbent versus conventional wound dressing—A randomized controlled study in orthopedic surgery. *Deutsches Ärzteblatt International, 115*(13), 213–219. https://doi.org/10.3238/arztebl.2018.0213
11. Pilehvar-Soltanahmadi, Y., Dadashpour, M., Mohajeri, A., Fattahi, A., Sheervalilou, R., & Zarghami, N. (2017). An overview on application of natural substances incorporated with electrospun nanofibrous scaffolds to development of innovative wound dressings. *Mini Reviews in Medicinal Chemistry, 18*(5), 414–427. https://doi.org/10.2174/1389557517666170308112147
12. Ambekar, R. S., & Kandasubramanian, B. (2019). Advancements in nanofibers for wound dressing: a review. *European Polymer Journal, 117*(May), 304–336. https://doi.org/10.1016/j.eurpolymj.2019.05.020
13. Avossa, J., Pota, G., Vitiello, G., Macagnano, A., Zanfardino, A., Di Napoli, M., Pezzella, A., D'Errico, G., Varcamonti, M., & Luciani, G. (2021). Multifunctional mats by antimicrobial nanoparticles decoration for bioinspired smart wound dressing solutions. *Materials Science and Engineering C, 123*, 111954. https://doi.org/10.1016/j.msec.2021.111954
14. Huang, H. Y., Skripka, A., Zaroubi, L., Findlay, B. L., Vetrone, F., Skinner, C., Oh, J. K., & Cuccia, L. A. (2020). Electrospun upconverting nanofibrous hybrids with smart NIR-light-controlled drug release for wound dressing. *ACS Applied Bio Materials, 3*(10), 7219–7227. https://doi.org/10.1021/acsabm.0c01019
15. Li, H., Zhang, Z., Godakanda, V. U., Chiu, Y. J., Angkawinitwong, U., Patel, K., Stapleton, P. G., de Silva, R. M., de Silva, K. M. N., Zhu, L. M., & Williams, G. R. (2019). The effect of collection substrate on electrospun ciprofloxacin-loaded poly(vinylpyrrolidone) and ethyl cellulose nanofibers as potential wound dressing materials. *Materials Science and Engineering C, 104*, 109917. https://doi.org/10.1016/j.msec.2019.109917

16. Ochoa, M., Rahimi, R., Zhou, J., Jiang, H., Yoon, C. K., Maddipatla, D., Narakathu, B. B., Jain, V., Oscai, M. M., Morken, T. J., Oliveira, R. H., Campana, G. L., Cummings, O. W., Zieger, M. A., Sood, R., Atashbar, M. Z., & Ziaie, B. (2020). Integrated sensing and delivery of oxygen for next-generation smart wound dressings. *Microsystems & Nanoengineering, 6*(1), 46. https://doi.org/10.1038/s41378-020-0141-7
17. Tamayol, A., Hassani Najafabadi, A., Mostafalu, P., Yetisen, A. K., Commotto, M., Aldhahri, M., Abdel-Wahab, M. S., Najafabadi, Z. I., Latifi, S., Akbari, M., Annabi, N., Yun, S. H., Memic, A., Dokmeci, M. R., & Khademhosseini, A. (2017). Biodegradable elastic nanofibrous platforms with integrated flexible heaters for on-demand drug delivery. *Science and Reports, 7*(1), 1–10. https://doi.org/10.1038/s41598-017-04749-8
18. Schneider, R., Mercante, L. A., Andre, R. S., Brandão, H. D. M., Mattoso, L. H., & Correa, D. S. (2018). Biocompatible electrospun nanofibers containing cloxacillin: Antibacterial activity and effect of pH on the release profile. *Reactive & Functional Polymers, 132*(September), 26–35. https://doi.org/10.1016/j.reactfunctpolym.2018.09.001
19. Fahimirad, S., & Ajalloueian, F. (2019). Naturally-derived electrospun wound dressings for target delivery of bio-active agents. *International Journal of Pharmaceutics, 566*, 307–328. https://doi.org/10.1016/j.ijpharm.2019.05.053
20. dos Santos, D. M., Correa, D. S., Medeiros, E. S., Oliveira, J. E., & Mattoso, L. H. C. (2020). Advances in functional polymer nanofibers: From spinning fabrication techniques to recent biomedical applications. *ACS Applied Materials & Interfaces, 12*(41), 45673–45701. https://doi.org/10.1021/acsami.0c12410
21. Xu, S.-C., Qin, C.-C., Yu, M., Dong, R.-H., Yan, X., Zhao, H., Han, W.-P., Zhang, H.-D., & Long, Y.-Z. (2015). A battery-operated portable handheld electrospinning apparatus. *Nanoscale, 7*(29), 12351–12355. https://doi.org/10.1039/C5NR02922H
22. Sharifi, S., Hajipour, M. J., Gould, L., & Mahmoudi, M. (2021). Nanomedicine in healing chronic wounds: Opportunities and challenges. *Molecular Pharmaceutics, 18*(2), 550–575. https://doi.org/10.1021/acs.molpharmaceut.0c00346
23. Croitoru, A. -M., Ficai, D., Ficai, A., Mihailescu, N., Andronescu, E., & Turculet, C. F. (2020). Nanostructured fibers containing natural or synthetic bioactive compounds in wound dressing applications. *Materials (Basel), 13*(10), 2407. https://doi.org/10.3390/ma13102407
24. Hernández-Rangel, A., Martin-Martinez, E. S. (2021). Collagen based electrospun materials for skin wounds treatment. *Journal of Biomedical Materials Research Part A* 1–14. https://doi.org/10.1002/jbm.a.37154
25. Wang, J., & Windbergs, M. (2017). Functional electrospun fibers for the treatment of human skin wounds. *European Journal of Pharmaceutics and Biopharmaceutics, 119*, 283–299. https://doi.org/10.1016/j.ejpb.2017.07.001
26. Yan, X., Yu, M., Ramakrishna, S., Russell, S. J., & Long, Y. -Z. (2019). Advances in portable electrospinning devices for in situ delivery of personalized wound care. *Nanoscale, 11*(41), 19166–19178. https://doi.org/10.1039/C9NR02802A
27. Lee, J. K. Y., Chen, N., Peng, S., Li, L., Tian, L., Thakor, N., & Ramakrishna, S. (2018). Polymer-based composites by electrospinning: Preparation & functionalization with nanocarbons. *Progress in Polymer Science, 86*, 40–84. https://doi.org/10.1016/j.progpolymsci.2018.07.002
28. Khan, A. R., Morsi, Y., Zhu, T., Ahmad, A., Xie, X., Yu, F., & Mo, X. (2021). Electrospinning: An emerging technology to construct polymer-based nanofibrous scaffolds for diabetic wound healing. *Frontiers of Materials Science, 15*(1), 10–35. https://doi.org/10.1007/s11706-021-0540-1
29. Karim, M., Fathi, M., & Soleimanian-Zad, S. (2021). Nanoencapsulation of cinnamic aldehyde using zein nanofibers by novel needle-less electrospinning: Production, characterization and their application to reduce nitrite in sausages. *Journal of Food Engineering, 288*, 110140. https://doi.org/10.1016/j.jfoodeng.2020.110140
30. Li, Y., Dong, A., & He, J. (2020). Innovation of critical bubble electrospinning and its mechanism. *Polymers (Basel), 12*(2), 304. https://doi.org/10.3390/polym12020304

31. Norzain, N. A., & Lin, W. C. (2021). Orientated and diameter-controlled fibrous scaffolds fabricated using the centrifugal electrospinning technique for stimulating the behaviours of fibroblast cells. *Journal of Industrial Textiles* https://doi.org/10.1177/1528083720988127
32. Li, Y. -M., Wang, X. -X., Yu, S. -X., Zhao, Y. -T., Yan, X., Zheng, J., Yu, M., Yan, S. -Y., & Long, Y. -Z. (2018). Bubble melt electrospinning for production of polymer microfibers. *Polymers (Basel), 10*(11), 1246. https://doi.org/10.3390/polym10111246
33. Bachs-Herrera, A., Yousefzade, O., del Valle, L. J., & Puiggali, J. (2021). Melt electrospinning of polymers: blends, nanocomposites, additives and applications. *Applied Sciences, 11*(4), 1808. https://doi.org/10.3390/app11041808
34. Yue, Y., Gong, X., Jiao, W., Li, Y., Yin, X., Si, Y., Yu, J., & Ding, B. (2021). In-situ electrospinning of thymol-loaded polyurethane fibrous membranes for waterproof, breathable, and antibacterial wound dressing application. *Journal of Colloid and Interface Science, 592*, 310–318. https://doi.org/10.1016/j.jcis.2021.02.048
35. Ghaderpour, A., Hoseinkhani, Z., Yarani, R., Mohammadiani, S., Amiri, F., & Mansouri, K. (2021). Altering the characterization of nanofibers by changing the electrospinning parameters and their application in tissue engineering, drug delivery, and gene delivery systems. *Polymers for Advanced Technologies, 32*(5), 1924–1950. https://doi.org/10.1002/pat.5242
36. Jahan, I., & Wang, X. (2021). Evolvement of spinneret in electrospinning toward large-scale production of nanofibers. In: Dong, Y., Baji, A., & Ramakrishna SBT-EP and C (Eds.), *Electrospun polymers and composites*. Elsevier, pp. 765–788. https://doi.org/10.1016/B978-0-12-819611-3.00023-6
37. Juncos Bombin, A. D., Dunne, N. J., & McCarthy, H. O. (2020). Electrospinning of natural polymers for the production of nanofibres for wound healing applications. *Materials Science and Engineering: C, 114*, 110994. https://doi.org/10.1016/j.msec.2020.110994
38. Khalid, A., Bai, D., Abraham, A. N., Jadhav, A., Linklater, D., Matusica, A., Nguyen, D., Murdoch, B. J., Zakhartchouk, N., & Dekiwadia, C. (2020). Electrospun nanodiamond-silk fibroin membranes: a multifunctional platform for biosensing and wound-healing applications. *ACS Applied Materials & Interfaces, 12*(43), 48408–48419. https://doi.org/10.1021/acsami.0c15612
39. Başaran, D. D. A., Gündüz, U., Tezcaner, A., & Keskin, D. (2021). Topical delivery of heparin from PLGA nanoparticles entrapped in nanofibers of sericin/gelatin scaffolds for wound healing. *International Journal of Pharmaceutics, 597*, 120207. https://doi.org/10.1016/j.ijpharm.2021.120207
40. Augustine, R., Rehman, S. R. U., Ahmed, R., Zahid, A. A., Sharifi, M., Falahati, M., & Hasan, A. (2020). Electrospun chitosan membranes containing bioactive and therapeutic agents for enhanced wound healing. *International Journal of Biological Macromolecules, 156*, 153–170. https://doi.org/10.1016/j.ijbiomac.2020.03.207
41. Cui, S., Sun, X., Li, K., Gou, D., Zhou, Y., Hu, J., & Liu, Y. (2019). Polylactide nanofibers delivering doxycycline for chronic wound treatment. *Materials Science and Engineering: C, 104*, 109745. https://doi.org/10.1016/j.msec.2019.109745
42. Akhmetova, A., & Heinz, A. (2020). Electrospinning proteins for wound healing purposes: opportunities and challenges. *Pharmaceutics, 13*(1), 4. https://doi.org/10.3390/pharmaceutics13010004
43. Teixeira, M. A., Paiva, M. C., Amorim, M. T. P., & Felgueiras, H. P. (2020). Electrospun nanocomposites containing cellulose and its derivatives modified with specialized biomolecules for an enhanced wound healing. *Nanomaterials, 10*(3), 557. https://doi.org/10.1016/j.msec.2019.109745
44. Homaeigohar, S., Monavari, M., Koenen, B., & Boccaccini, A. R. (2021). Biomimetic biohybrid nanofibers containing bovine serum albumin as a bioactive moiety for wound dressing. *Materials Science and Engineering C, 123*, 111965. https://doi.org/10.1016/j.msec.2021.111965
45. Al-Dhahebi, A. M., Gopinath, S. C. B., & Saheed, M. S. M. (2020). Graphene impregnated electrospun nanofiber sensing materials: A comprehensive overview on bridging laboratory set-up to industry. *Nano Convergence, 7*(1), 27. https://doi.org/10.1186/s40580-020-00237-4

46. Contardi, M., Kossyvaki, D., Picone, P., Summa, M., Guo, X., Heredia-Guerrero, J. A., Giacomazza, D., Carzino, R., Goldoni, L., Scoponi, G., Rancan, F., Bertorelli, R., Di Carlo, M., Athanassiou, A., & Bayer, I. S. (2021). Electrospun polyvinylpyrrolidone (PVP) hydrogels containing hydroxycinnamic acid derivatives as potential wound dressings. *Chemical Engineering Journal, 409*, 128144. https://doi.org/10.1016/j.cej.2020.128144
47. Song, Y., Li, L., Zhao, W., Qian, Y., Dong, L., Fang, Y., Yang, L., & Fan, Y. (2021). Surface modification of electrospun fibers with mechano-growth factor for mitigating the foreign-body reaction. *Bioactive materials, 6*(9), 2983–2998. https://doi.org/10.1016/j.bioactmat.2021.02.020
48. Zhang, Z., Dai, Q., Zhang, Y., Zhuang, H., Wang, E., Xu, Q., Ma, L., Wu, C., Huan, Z., & Guo, F. (2020). Design of a multifunctional biomaterial inspired by ancient Chinese medicine for hair regeneration in burned skin. *ACS Applied Materials & Interfaces, 12*(11), 12489–12499. https://doi.org/10.1021/acsami.9b22769
49. Hu, W., Wang, Z., Zha, Y., Gu, X., You, W., Xiao, Y., Wang, X., Zhang, S., & Wang, J. (2020). High flexible and broad antibacterial nanodressing induces complete skin repair with angiogenic and follicle regeneration. *Advanced Healthcare Materials, 9*(23), 2000035. https://doi.org/10.1002/adhm.202000035
50. Ballesteros, C. A. S., Correa, D. S., & Zucolotto, V. (2020). Polycaprolactone nanofiber mats decorated with photoresponsive nanogels and silver nanoparticles: slow release for antibacterial control. *Materials Science and Engineering: C, 107* (October 2019), 110334. https://doi.org/10.1016/j.msec.2019.110334
51. dos Santos, D. M., Chagas, P. A. M., Leite, I. S., Inada, N. M., de Annunzio, S. R., Fontana, C. R., Campana-Filho, S. P., & Correa, D. S. (2020). Core-sheath nanostructured chitosan-based nonwovens as a potential drug delivery system for periodontitis treatment. *International Journal of Biological Macromolecules, 142*, 521–534. https://doi.org/10.1016/j.ijbiomac.2019.09.124
52. Wang, B., Zheng, H., Chang, M.-W., Ahmad, Z., & Li, J.-S. (2016a). Hollow polycaprolactone composite fibers for controlled magnetic responsive antifungal drug release. *Colloids Surfaces B Biointerfaces, 145*, 757–767. https://doi.org/10.1016/j.colsurfb.2016.05.092
53. Yang, J., Wang, K., Yu, D.-G., Yang, Y., Bligh, S. W. A., & Williams, G. R. (2020). Electrospun Janus nanofibers loaded with a drug and inorganic nanoparticles as an effective antibacterial wound dressing. *Materials Science and Engineering C, 111*, 110805. https://doi.org/10.1016/j.msec.2020.110805
54. Miguel, S. P., Moreira, A. F., & Correia, I. J. (2019). Chitosan based-asymmetric membranes for wound healing: A review. *International Journal of Biological Macromolecules, 127*, 460–475. https://doi.org/10.1016/j.ijbiomac.2019.01.072
55. Li, Y., Lim, C. T., & Kotaki, M. (2015). Study on structural and mechanical properties of porous PLA nanofibers electrospun by channel-based electrospinning system. *Polymer (Guildf) 56*, 572–580. https://doi.org/10.1016/j.polymer.2014.10.073
56. Zhang, K., Bai, X., Yuan, Z., Cao, X., Jiao, X., Li, Y., Qin, Y., Wen, Y., & Zhang, X. (2019). Layered nanofiber sponge with an improved capacity for promoting blood coagulation and wound healing. *Biomaterials, 204*, 70–79. https://doi.org/10.1016/j.biomaterials.2019.03.008
57. Chagas, P. A. M., Schneider, R., dos Santos, D. M., Otuka, A. J. G., Mendonça, C. R., Correa, D. S. (2021). Bilayered electrospun membranes composed of poly(lactic-acid)/natural rubber: A strategy against curcumin photodegradation for wound dressing application. *Reactive and Functional Polymers, 163*, 104889. https://doi.org/10.1016/j.reactfunctpolym.2021.104889
58. Khan, A. R., Huang, K., Khalaji, M. S., Yu, F., Xie, X., Zhu, T., Morsi, Y., Jinzhong, Z., & Mo, X. (2021a). Multifunctional bioactive core-shell electrospun membrane capable to terminate inflammatory cycle and promote angiogenesis in diabetic wound. *Bioactive Materials, 6*(9), 2783–2800. https://doi.org/10.1016/j.bioactmat.2021.01.040
59. Memic, A., Abudula, T., Mohammed, H. S., Joshi Navare, K., Colombani, T., & Bencherif, S. A. (2019). Latest progress in electrospun nanofibers for wound healing applications. *ACS Applied Bio Materials, 2*(3), 952–969. https://doi.org/10.1021/acsabm.8b00637

60. Mennini, N., Greco, A., Bellingeri, A., De Vita, F., & Petrella, F. (2016). Quality of wound dressings: A first step in establishing shared criteria and objective procedures to evaluate their performance. *Journal of Wound Care, 25*(8), 428–437. https://doi.org/10.12968/jowc.2016.25.8.428
61. Morgado, P. I., Aguiar-Ricardo, A., & Correia, I. J. (2015). Asymmetric membranes as ideal wound dressings: an overview on production methods, structure, properties and performance relationship. *Journal of Membrane Science, 490*, 139–151. https://doi.org/10.1016/j.memsci.2015.04.064
62. Dos Santos, D. M., Leite, I. S., de Lacerda Bukzem, A., de Oliveira Santos, R. P., Frollini, E., Inada, N. M., & Campana-Filho, S. P. (2018). Nanostructured electrospun nonwovens of poly(ε-caprolactone)/quaternized chitosan for potential biomedical applications. *Carbohydrate Polymers, 186*, 110–121. https://doi.org/10.1016/j.carbpol.2018.01.045
63. Liu, C., Zhu, C., Li, J., Zhou, P., Chen, M., Yang, H., & Li, B. (2015). The effect of the fibre orientation of electrospun scaffolds on the matrix production of rabbit annulus fibrosus-derived stem cells. *Bone Res, 3*(1), 1–9. https://doi.org/10.1038/boneres.2015.12
64. Migliorini, F. L., Teodoro, K. B. R., dos Santos, D. M., Fonseca, F. J., Mattoso, L. H. C., & Correa, D. S. (2020). Electrospun nanofibers versus drop casting films for designing an electronic tongue: Comparison of performance for monitoring geosmin and 2-methylisoborneol in water samples. *Polymers for Advanced Technologies, 31*(9), 2075–2082. https://doi.org/10.1002/pat.4930
65. Tawfik, E. A., Craig, D. Q. M., & Barker, S. A. (2020). Dual drug-loaded coaxial nanofibers for the treatment of corneal abrasion. *International Journal of Pharmaceutics, 581*, 119296. https://doi.org/10.1016/j.ijpharm.2020.119296
66. Ghasemi-Mobarakeh, L., Semnani, D., & Morshed, M. (2007). A novel method for porosity measurement of various surface layers of nanofibers mat using image analysis for tissue engineering applications. *Journal of Applied Polymer Science, 106*(4), 2536–2542. https://doi.org/10.1002/app.26949
67. Liang, D., Lu, Z., Yang, H., Gao, J., & Chen, R. (2016). Novel asymmetric wettable AgNPs/chitosan wound dressing: in vitro and in vivo evaluation. *ACS Applied Materials & Interfaces, 8*(6), 3958–3968. https://doi.org/10.1021/acsami.5b11160
68. Pakravan, M., Heuzey, M.-C., & Ajji, A. (2012). Core-shell structured PEO-Chitosan nanofibers by coaxial electrospinning. *Biomacromolecules, 13*(2), 412–421. https://doi.org/10.1021/bm201444v
69. de Lacerda, B. A., dos Santos, D. M., Leite, I. S., Inada, N. M., & Campana-Filho, S. P. (2021). Tuning the properties of carboxymethylchitosan-based porous membranes for potential application as wound dressing. *International Journal of Biological Macromolecules, 166*, 459–470. https://doi.org/10.1016/j.ijbiomac.2020.10.204
70. Schoolaert, E., Cossu, L., Becelaere, J., Van Guyse, J. F. R., Tigrine, A., Vergaelen, M., Hoogenboom, R., & De Clerck, K. (2020). Nanofibers with a tunable wettability by electrospinning and physical crosslinking of poly(2-n-propyl-2-oxazoline). *Materials and Design, 192*, 108747. https://doi.org/10.1016/j.matdes.2020.108747
71. Szewczyk, P. K., Ura, D. P., Metwally, S., Knapczyk-Korczak, J., Gajek, M., Marzec, M. M., Bernasik, A., & Stachewicz, U. (2018). Roughness and fiber fraction dominated wetting of electrospun fiber-based porous meshes. *Polymers (Basel), 11*(1). https://doi.org/10.3390/polym11010034
72. Xu, R., Xia, H., He, W., Li, Z., Zhao, J., Liu, B., Wang, Y., Lei, Q., Kong, Y., Bai, Y., Yao, Z., Yan, R., Li, H., Zhan, R., Yang, S., Luo, G., & Wu, J. (2016). Controlled water vapor transmission rate promotes wound-healing via wound re-epithelialization and contraction enhancement. *Science and Reports, 6*, 24596. https://doi.org/10.1038/srep24596
73. ASTME96/E96M-16. (2016). Standard test methods for water vapor transmission of materials. *ASTM International*.
74. Xu, H., Chang, J., Chen, Y., Fan, H., & Shi, B. (2013). Asymmetric polyurethane membrane with inflammation-responsive antibacterial activity for potential wound dressing application. *Journal of Materials Science, 48*(19), 6625–6639. https://doi.org/10.1007/s10853-013-7461-z

75. Standard Test Method for Tensile Properties of Thin Plastic Sheeting 1. https://doi.org/10.1520/D0882-18
76. Zhou, X., Ding, C., Cheng, C., Liu, S., Duan, G., Xu, W., Liu, K., & Hou, H. (2020). Mechanical and thermal properties of electrospun polyimide/rGO composite nanofibers via in-situ polymerization and in-situ thermal conversion. *European Polymer Journal, 141*, 110083. https://doi.org/10.1016/j.eurpolymj.2020.110083
77. Haack, M. D. S. (2010). Análise de materiais por espectroscopia no infravermelho dentro do sistema de gestão de qualidade conforme ABNT NBR ISO/IEC 17025. Universidade Federal do Rio Grande do Sul.
78. Kassouf, A., Ruellan, A., Jouan-Rimbaud Bouveresse, D., Rutledge, D. N., Domenek, S., Maalouly, J., Chebib, H., Ducruet, V. (2016). Attenuated total reflectance-mid infrared spectroscopy (ATR-MIR) coupled with independent components analysis (ICA): A fast method to determine plasticizers in polylactide (PLA). *Talanta*, *147*, 569–580. https://doi.org/10.1016/j.talanta.2015.10.021
79. Homaeigohar, S., & Boccaccini, A. R. (2020). Antibacterial biohybrid nanofibers for wound dressings. *Acta Biomaterialiaa, 107*, 25–49. https://doi.org/10.1016/j.actbio.2020.02.022
80. Kalantari, K., Mostafavi, E., Afifi, A. M., Izadiyan, Z., Jahangirian, H., Rafiee-Moghaddam, R., & Webster, T. J. (2020). Wound dressings functionalized with silver nanoparticles: Promises and pitfalls. *Nanoscale, 12*(4), 2268–2291. https://doi.org/10.1039/c9nr08234d
81. Blakeney, B. A., Tambralli, A., Anderson, J. M., Andukuri, A., Lim, D. J., Dean, D. R., & Jun, H. W. (2011). Cell infiltration and growth in a low density, uncompressed three-dimensional electrospun nanofibrous scaffold. *Biomaterials, 32*(6), 1583–1590. https://doi.org/10.1016/j.biomaterials.2010.10.056
82. Afanasiev, S. A., Muslimova, E. F., Nashchekina, Y. A., Nikonov, P. O., Rogovskaya, Y. V., Bolbasov, E. N., & Tverdokhlebov, S. I. (2017). Peculiarities of cell seeding on polylactic acid-based scaffolds fabricated using electrospinning and solution blow spinning technologies. *Bulletin of Experimental Biology and Medicine, 164*(2), 281–284. https://doi.org/10.1007/s10517-017-3973-x
83. Khang, G., Rhee, J. M., Lee, J. H., Lee, I., & Lee, H. B. (2000). Interaction of different types of cells on poly(L-lactide-co-glycolide) surface with wettability chemogradient. *Korea Polymer Journal, 8*(6), 276–284. https://doi.org/10.1002/app.10680.
84. Wade, R. J., & Burdick, J. A. (2014). Advances in nanofibrous scaffolds for biomedical applications: From electrospinning to self-assembly. *Nano Today, 9*(6), 722–742. https://doi.org/10.1016/j.nantod.2014.10.002
85. Liu, Y., Zheng, Y., & Hayes, B. (2017). Degradable, absorbable or resorbable—What is the best grammatical modifier for an implant that is eventually absorbed by the body? *Science China Materials, 60*(5), 377–391. https://doi.org/10.1007/s40843-017-9023-9
86. International Organization for Standardization. (2009a). 10993-5:2009 Biological evaluation of medical devices—Part 5: tests for in vitro cytotoxicity. *International Organization for Standardization, 34*
87. International Organization for Standardization. (2009b). Tests for in vitro cytotoxicity. ISO 10993—*Biological Evaluation of Medical Devices, 34*
88. International Organization for Standardization. (2002). Selection of tests for interactions with blood. *ISO 10993—Biological Evaluation of Medical Devices, 34*
89. Azizipour, N., Avazpour, R., Rosenzweig, D. H., Sawan, M., & Ajji, A. (2020). Evolution of biochip technology: A review from lab-on-a-chip to organ-on-a-chip. *Micromachines, 11*(6), 1–15. https://doi.org/10.3390/mi11060599
90. Lobdell, K. W., Stamou, S., & Sanchez, J. A. (2012). Hospital-acquired infections. *Surgical Clinics of North America, 92*(1), 65–77. https://doi.org/10.1016/j.suc.2011.11.003
91. Devi, N., & Dutta, J. (2019). Development and in vitro characterization of chitosan/starch/halloysite nanotubes ternary nanocomposite films. *International Journal of Biological Macromolecules, 127*, 222–231. https://doi.org/10.1016/j.ijbiomac.2019.01.047
92. Jayakumar, R., Prabaharan, M., Sudheesh Kumar, P. T., Nair, S. V., & Tamura, H. (2011). Biomaterials based on chitin and chitosan in wound dressing applications. *Biotechnology Advances, 29*(3), 322–337. https://doi.org/10.1016/j.biotechadv.2011.01.005

93. Vowden, K., & Vowden, P. (2017). Wound dressings: Principles and practice. *Surgery (United Kingdom), 35*, 489–494. https://doi.org/10.1016/j.mpsur.2017.06.005
94. Englert, C., Brendel, J. C., Majdanski, T. C., Yildirim, T., Schubert, S., Gottschaldt, M., Windhab, N., & Schubert, U. S. (2018). Pharmapolymers in the 21st century: synthetic polymers in drug delivery applications. *Progress in Polymer Science, 87*, 107–164. https://doi.org/10.1016/j.progpolymsci.2018.07.005
95. Maitz, M. F. (2015). Applications of synthetic polymers in clinical medicine. *Biosurface and Biotribology, 1*(3), 161–176. https://doi.org/10.1016/j.bsbt.2015.08.002
96. Keshvardoostchokami, M., Majidi, S. S., Huo, P., Ramachandran, R., Chen, M., & Liu, B. (2020). Electrospun nanofibers of natural and synthetic polymers as artificial extracellular matrix for tissue engineering. *Nanomaterials, 11*(1), 21. https://doi.org/10.3390/nano11010021
97. Wongkaew, N., Simsek, M., Heider, J., Wegener, J., Baeumner, A. J., Schreml, S., & Stolwijk, J. A. (2020). Cytocompatibility of mats prepared from different electrospun polymer nanofibers. *ACS Applied Bio Materials, 3*(8), 4912–4921. https://doi.org/10.1021/acsabm.0c00426
98. Park, H., Lee, J. W., Park, K. E., Park, W. H., & Lee, K. Y. (2010). Stress response of fibroblasts adherent to the surface of plasma-treated poly(lactic-co-glycolic acid) nanofiber matrices. *Colloids Surfaces B Biointerfaces, 77*(1), 90–95. https://doi.org/10.1016/j.colsurfb.2010.01.011
99. Adadi, N., Yadid, M., Gal, I., Asulin, M., Feiner, R., Edri, R., & Dvir, T. (2020). Electrospun fibrous PVDF-TrFe scaffolds for cardiac tissue engineering, differentiation, and maturation. *Advanced Materials Technologies, 5*(3), 1900820. https://doi.org/10.1002/admt.201900820
100. Asadian, M., Grande, S., Onyshchenko, I., Morent, R., Declercq, H., & De Geyter, N. (2019). A comparative study on pre- and post-production plasma treatments of PCL films and nanofibers for improved cell-material interactions. *Applied Surface Science, 481*(January), 1554–1565. https://doi.org/10.1016/j.apsusc.2019.03.224
101. Saiding, Q., Jin, J., Qin, M., Cai, Z., Lu, M., Wang, F., Cui, W., & Chen, X. (2021). Heat-shrinkable electrospun fibrous tape for restoring structure and function of loose soft tissue. *Advanced Functional Materials, 31*(8), 2007440. https://doi.org/10.1002/adfm.202007440
102. Castellano, D., Sanchis, A., Blanes, M., Pérez del Caz, M. D., Ruiz-Saurí, A., Piquer-Gil, M., Pelacho, B., Marco, B., Garcia, N., Ontoria-Oviedo, I., Cambra, V., Prosper, F., & Sepúlveda, P. (2018). Electrospun poly(hydroxybutyrate) scaffolds promote engraftment of human skin equivalents via macrophage M2 polarization and angiogenesis. *Journal of Tissue Engineering and Regenerative Medicine, 12*(2), e983–e994. https://doi.org/10.1002/term.2420
103. Camarena, D. E. M., Matsuyama, L. S. A. S., Maria-Engler, S. S., & Catalani, L. H. (2020). Development of epidermal equivalent from electrospun synthetic polymers for in vitro irritation/corrosion testing. *Nanomaterials, 10*(12), 2528. https://doi.org/10.3390/nano10122528
104. Unnithan, A. R., Ghavami Nejad, A., Sasikala, A. R. K., Thomas, R. G., Jeong, Y. Y., Murugesan, P., Nasseri, S., Wu, D., Park, C. H., & Kim, C. S. (2016). Electrospun zwitterionic nanofibers with in situ decelerated epithelialization property for non-adherent and easy removable wound dressing application. *Chemical Engineering Journal, 287*, 640–648. https://doi.org/10.1016/j.cej.2015.11.086
105. Massella, A., Ferri, G., Giraud, C., & Barresi, S. (2019). Bio-functional textiles: Combining pharmaceutical nanocarriers with fibrous materials for innovative dermatological therapies. *Pharmaceutics, 11*(8), 403. https://doi.org/10.3390/pharmaceutics11080403
106. Zehra, M., Zubairi, W., Hasan, A., Butt, H., Ramzan, A., Azam, M., Mehmood, A., Falahati, M., Chaudhry, A. A., Rehman, I. U., & Yar, M. (2020). Oxygen generating polymeric nano fibers that stimulate angiogenesis and show efficient wound healing in a diabetic wound model. *International Journal of Nanomedicine, 15*, 3511–3522. https://doi.org/10.2147/IJN.S248911
107. Guo, X., Liu, Y., Bera, H., Zhang, H., Chen, Y., Cun, D., Foderà, V., & Yang, M. (2020). α-Lactalbumin-based nanofiber dressings improve burn wound healing and reduce scarring.

ACS Applied Materials & Interfaces, 12(41), 45702–45713. https://doi.org/10.1021/acsami.0c05175

108. Ashraf, R., Sofi, H. S., Akram, T., Rather, H. A., Abdal-hay, A., Shabir, N., Vasita, R., Alrokayan, S. H., Khan, H. A., & Sheikh, F. A. (2020). Fabrication of multifunctional cellulose/TiO_2/Ag composite nanofibers scaffold with antibacterial and bioactivity properties for future tissue engineering applications. *Journal of Biomedical Materials Research Part A, 108*(4), 947–962. https://doi.org/10.1002/jbm.a.36872
109. Lemraski, E. G., Jahangirian, H., Dashti, M., Khajehali, E., Sharafinia, S., Moghaddam, R. R., & Webster, T. J. (2021). Antimicrobial double-layer wound dressing based on chitosan/polyvinyl alcohol/copper: In vitro and in vivo assessment. *International Journal of Nanomedicine, 16*, 223–235. https://doi.org/10.2147/IJN.S266692
110. Pagnotta, G., Graziani, G., Baldini, N., Maso, A., Focarete, M. L., Berni, M., Biscarini, F., Bianchi, M., & Gualandi, C. (2020). Nanodecoration of electrospun polymeric fibers with nanostructured silver coatings by ionized jet deposition for antibacterial tissues. *Materials Science and Engineering C, 113*(April), 110998. https://doi.org/10.1016/j.msec.2020.110998
111. Tiplea, R. E., Lemnaru, G. M., Trușcă, R. D., Holban, A., Kaya, M. G. A., Dragu, L. D., Ficai, D., Ficai, A., & Bleotu, C. (2020). Antimicrobial films based on Chitosan, Collagen, and ZnO for skin tissue regeneration. *Biointerface Research Applied Chemistry, 11*(4), 11985–11995. https://doi.org/10.33263/BRIAC114.1198511995
112. Doostmohammadi, M., Forootanfar, H., Shakibaie, M., Torkzadeh-Mahani, M., Rahimi, H., Jafari, E., Ameri, A., & Ameri, A. (2021). Polycaprolactone/gelatin electrospun nanofibres containing biologically produced tellurium nanoparticles as a potential wound dressing scaffold: Physicochemical, mechanical, and biological characterisation. *IET Nanobiotechnology, 15*(3), 277–290. https://doi.org/10.1049/nbt2.12020
113. Abolghasemzade, S., Pourmadadi, M., Rashedi, H., Yazdian, F., Kianbakht, S., & Navaei-Nigjeh, M. (2021). PVA based nanofiber containing CQDs modified with silica NPs and silk fibroin accelerates wound healing in a rat model. *Journal of Materials Chemistry B, 9*(3), 658–676. https://doi.org/10.1039/d0tb01747g
114. Ahmadian, S., Ghorbani, M., & Mahmoodzadeh, F. (2020). Silver sulfadiazine-loaded electrospun ethyl cellulose/polylactic acid/collagen nano fibrous mats with antibacterial properties for wound healing. *International Journal of Biological Macromolecules, 162*, 1555–1565. https://doi.org/10.1016/j.ijbiomac.2020.08.059
115. Fei, Y., Huang, Q., Hu, Z., Yang, X., Yang, B., & Liu, S. (2020). Biomimetic cerium oxide loaded gelatin PCL nanosystems for wound dressing on cutaneous care management of multidrug-resistant bacterial wound healing. *Journal of Cluster Science, 9*(37). https://doi.org/10.1007/s10876-020-01866-9
116. Zhang, S., Ye, J., Sun, Y., Kang, J., Liu, J., Wang, Y., Li, Y., Zhang, L., & Ning, G. (2020). Electrospun fibrous mat based on silver (I) metal-organic frameworks-polylactic acid for bacterial killing and antibiotic-free wound dressing. *Chemical Engineering Journal, 390*(January), 124523. https://doi.org/10.1016/j.cej.2020.124523
117. Al-Musawi, S., Albukhaty, S., Al-Karagoly, H., Sulaiman, G. M., Alwahibi, M. S., Dewir, Y. H., Soliman, D. A., & Rizwana, H. (2020). Antibacterial activity of honey/chitosan nanofibers loaded with capsaicin and gold nanoparticles for wound dressing. *Molecules, 25*(20), 4770. https://doi.org/10.3390/molecules25204770
118. El-Aassar, M. R., El-Beheri, N. G., Agwa, M. M., Eltaher, H. M., Alseqely, M., Sadik, W. S., & El-Khordagui, L. (2021). Antibiotic-free combinational hyaluronic acid blend nanofibers for wound healing enhancement. *International Journal of Biological Macromolecules, 167*, 1552–1563. https://doi.org/10.1016/j.ijbiomac.2020.11.109
119. Wang, L., Yang, J., Yang, X., Hou, Q., Liu, S., Zheng, W., Long, Y., & Jiang, X. (2020). Mercaptophenylboronic acid-activated gold nanoparticles as nanoantibiotics against multidrug-resistant bacteria. *ACS Applied Materials & Interfaces, 12*(46), 51148–51159. https://doi.org/10.1021/acsami.0c12597

120. Sun, J., Zhang, P., Fan, Y., Zhao, J., Niu, S., Song, L., Ma, L., Ren, L., & Ming, W. (2019). Near-infrared triggered antibacterial nanocomposite membrane containing upconversion nanoparticles. *Materials Science and Engineering: C, 103*(August 2018):109797. https://doi.org/10.1016/j.msec.2019.109797
121. Mahdieh, Z., Mitra, S., & Holian, A. (2020). Core-shell electrospun fibers with an improved open pore structure for size-controlled delivery of nanoparticles. *ACS Applied Polymer Materials, 2*(9), 4004–4015. https://doi.org/10.1021/acsapm.0c00643
122. Shiny, P. J., Vimala Devi, M., Felciya, S. J. G., Ramanathan, G., Fardim, P., & Sivagnanam, U. T. (2021). In vitro and in vivo evaluation of poly-3-hydroxybutyric acid-sodium alginate as a core-shell nanofibrous matrix with arginine and bacitracin-nanoclay complex for dermal reconstruction of excision wound. *International Journal of Biological Macromolecules, 168*, 46–58. https://doi.org/10.1016/j.ijbiomac.2020.12.025
123. Zhang, P., Jiang, Y., Liu, D., Liu, Y., Ke, Q., & Xu, H. (2020). A bioglass sustained-release scaffold with ECM-like structure for enhanced diabetic wound healing. *Nanomedicine, 15*(23), 2241–2253. https://doi.org/10.2217/nnm-2020-0053
124. Li, J., Hu, Y., He, T., Huang, M., Zhang, X., Yuan, J., Wei, Y., Dong, X., Liu, W., Ko, F., & Zhou, W. (2018). Electrospun sandwich-structure composite membranes for wound dressing scaffolds with high antioxidant and antibacterial activity. *Macromolecular Materials and Engineering, 303*(2), 1700270. https://doi.org/10.1002/mame.201700270
125. Nada, A. A., Ali, E. A., Soliman, A. A. F., Shen, J., Abou-Zeid, N. Y., & Hudson, S. M. (2020). Multi-layer dressing made of laminated electrospun nanowebs and cellulose-based adhesive for comprehensive wound care. *International Journal of Biological Macromolecules, 162*, 629–644. https://doi.org/10.1016/j.ijbiomac.2020.06.184
126. Nejaddehbashi, F., Hashemitabar, M., Bayati, V., Abbaspour, M., Moghimipour, E., & Orazizadeh, M. (2019). Application of polycaprolactone, chitosan, and collagen composite as a nanofibrous mat loaded with silver sulfadiazine and growth factors for wound dressing. *Artificial Organs, 43*(4), 413–423. https://doi.org/10.1111/aor.13369
127. Rezk, A. I., Lee, J. Y., Son, B. C., Park, C. H., & Kim, C. S. (2019). Bi-layered nanofibers membrane loaded with titanium oxide and tetracycline as controlled drug delivery system for wound dressing applications. *Polymers (Basel), 11*(10), 1602. https://doi.org/10.3390/polym11101602
128. Arenas-Herrera, J. E., Ko, I. K., Atala, A., & Yoo, J. J. (2013). Decellularization for whole organ bioengineering. *Biomedical Materials, 8*(1), 014106. https://doi.org/10.1088/1748-6041/8/1/014106
129. Afsharian, Y. P., & Rahimnejad, M. (2021). Bioactive electrospun scaffolds for wound healing applications: a comprehensive review. *Polymer Testing, 93*, 106952. https://doi.org/10.1016/j.polymertesting.2020.106952
130. Kim, T. H., Jung, Y., & Kim, S. H. (2018). Nanofibrous electrospun heart decellularized extracellular matrix-based hybrid scaffold as wound dressing for reducing scarring in wound healing. *Tissue Engineering Part A, 24*(9–10), 830–848. https://doi.org/10.1089/ten.tea.2017.0318
131. Hasmad, H., Yusof, M. R., Mohd Razi, Z. R., Hj Idrus, R. B., & Chowdhury, S. R. (2018). Human amniotic membrane with aligned electrospun fiber as scaffold for aligned tissue regeneration. *Tissue Engineering. Part C, Methods, 24*(6), 368–378. https://doi.org/10.1089/ten.tec.2017.0447
132. Chen, L., Cheng, L., Wang, Z., Zhang, J., Mao, X., Liu, Z., Zhang, Y., Cui, W., & Sun, X. (2021). Conditioned medium-electrospun fiber biomaterials for skin regeneration. *Bioact Mater, 6*(2), 361–374. https://doi.org/10.1016/j.bioactmat.2020.08.022
133. Maciel, J. V., Durigon, A. M. M., Souza, M. M., Quadrado, R. F. N., Fajardo, A. R., & Dias, D. (2019). Polysaccharides derived from natural sources applied to the development of chemically modified electrodes for environmental applications: A review. *Trends in Environmental Analytical Chemistry, 22*, e00062. https://doi.org/10.1016/j.teac.2019.e00062
134. Ummartyotin, S., & Manuspiya, H. (2015). A critical review on cellulose: From fundamental to an approach on sensor technology. *Renewable and Sustainable Energy Reviews, 41*, 402–412. https://doi.org/10.1016/j.rser.2014.08.050

135. Jung, H. S., Kim, M. H., Shin, J. Y., Park, S. R., Jung, J. Y., & Park, W. H. (2018). Electrospinning and wound healing activity of β-chitin extracted from cuttlefish bone. *Carbohydrate Polymers, 193*(April), 205–211. https://doi.org/10.1016/j.carbpol.2018.03.100
136. Zhou, T., Wang, N., Xue, Y., Ding, T., Liu, X., Mo, X., & Sun, J. (2016). Electrospun tilapia collagen nanofibers accelerating wound healing via inducing keratinocytes proliferation and differentiation. *Colloids Surfaces B Biointerfaces, 143*, 415–422. https://doi.org/10.1016/j.colsurfb.2016.03.052
137. Kimna, C., Tamburaci, S., & Tihminlioglu, F. (2019). Novel zein-based multilayer wound dressing membranes with controlled release of gentamicin. *Journal of Biomedical Materials Research Part B: Applied Biomaterials, 107*(6), 2057–2070. https://doi.org/10.1002/jbm.b.34298
138. Li, H., Wang, M., Williams, G. R., Wu, J., Sun, X., Lv, Y., & Zhu, L. M. (2016). Electrospun gelatin nanofibers loaded with vitamins A and e as antibacterial wound dressing materials. *RSC Advances, 6*(55), 50267–50277. https://doi.org/10.1039/c6ra05092a
139. Kurečič, M., Maver, T., Virant, N., Ojstršek, A., Gradišnik, L., Hribernik, S., Kolar, M., Maver, U., & Kleinschek, K. S. (2018). A multifunctional electrospun and dual nano-carrier biobased system for simultaneous detection of pH in the wound bed and controlled release of benzocaine. *Cellulose, 25*(12), 7277–7297. https://doi.org/10.1007/s10570-018-2057-z
140. Chong, C., Wang, Y., Fathi, A., Parungao, R., Maitz, P. K., & Li, Z. (2019). Skin wound repair: Results of a pre-clinical study to evaluate electropsun collagen–elastin–PCL scaffolds as dermal substitutes. *Burns, 45*(7), 1639–1648. https://doi.org/10.1016/j.burns.2019.04.014
141. Wang, Y., Li, P., Xiang, P., Lu, J., Yuan, J., & Shen, J. (2016). Electrospun polyurethane/keratin/AgNP biocomposite mats for biocompatible and antibacterial wound dressings. *Journal of Materials Chemistry B, 4*, 635–648. https://doi.org/10.1039/c5tb02358k
142. Ahmed, R., Tariq, M., Ali, I., Asghar, R., Noorunnisa Khanam, P., Augustine, R., & Hasan, A. (2018). Novel electrospun chitosan/polyvinyl alcohol/zinc oxide nanofibrous mats with antibacterial and antioxidant properties for diabetic wound healing. *International Journal of Biological Macromolecules, 120*, 385–393. https://doi.org/10.1016/j.ijbiomac.2018.08.057
143. Miguel, S. P., Simões, D., Moreira, A. F., Sequeira, R. S., & Correia, I. J. (2019). Production and characterization of electrospun silk fibroin based asymmetric membranes for wound dressing applications. *International Journal of Biological Macromolecules, 121*, 524–535. https://doi.org/10.1016/j.ijbiomac.2018.10.041
144. Elbialy, Z. I., Atiba, A., Abdelnaby, A., Al-Hawary, I. I., Elsheshtawy, A., El-Serehy, H. A., Abdel-Daim, M. M., Fadl, S. E., & Assar, D. H. (2020). Collagen extract obtained from Nile tilapia (*Oreochromis niloticus* L.) skin accelerates wound healing in rat model via up regulating VEGF, bFGF, and α-SMA genes expression. *BMC Veterinary Research, 16*(1), 352. https://doi.org/10.1186/s12917-020-02566-2
145. Ennaas, N., Hammami, R., Gomaa, A., Bédard, F., Biron, É., Subirade, M., Beaulieu, L., & Fliss, I. (2016). Collagencin, an antibacterial peptide from fish collagen: activity, structure and interaction dynamics with membrane. *Biochemical and Biophysical Research Communications, 473*(2), 642–647. https://doi.org/10.1016/j.bbrc.2016.03.121
146. Khattak, S., Wahid, F., Liu, L. P., Jia, S. R., Chu, L. Q., Xie, Y. Y., Li, Z. X., & Zhong, C. (2019). Applications of cellulose and chitin/chitosan derivatives and composites as antibacterial materials: Current state and perspectives. *Applied Microbiology and Biotechnology, 103*(5), 1989–2006. https://doi.org/10.1007/s00253-018-09602-0
147. Cheng, W., Zhang, Z., Xu, R., Cai, P., Kristensen, P., Chen, M., & Huang, Y. (2018). Incorporation of bacteriophages in polycaprolactone/collagen fibers for antibacterial hemostatic dual-function. *Journal of Biomedical Materials Research Part B: Applied Biomaterials, 106*(7), 2588–2595. https://doi.org/10.1002/jbm.b.34075
148. Alhusein, N., Blagbrough, I. S., Beeton, M. L., Bolhuis, A., & De Bank, P. A. (2016). Electrospun zein/PCL fibrous matrices release tetracycline in a controlled manner, killing staphylococcus aureus both in biofilms and ex vivo on pig skin, and are compatible with human skin cells. *Pharmaceutical Research, 33*(1), 237–246. https://doi.org/10.1007/s11095-015-1782-3

149. Doostan, M., Maleki, H., Doostan, M., Khoshnevisan, K., Faridi-Majidi, R., & Arkan, E. (2021). Effective antibacterial electrospun cellulose acetate nanofibrous patches containing chitosan/erythromycin nanoparticles. *International Journal of Biological Macromolecules, 168*, 464–473. https://doi.org/10.1016/j.ijbiomac.2020.11.174
150. Rivero, G., Meuter, M., Pepe, A., Guevara, M. G., Boccaccini, A. R., & Abraham, G A. (2020). Nanofibrous membranes as smart wound dressings that release antibiotics when an injury is infected. *Colloids Surfaces A: Physicochemical and Engineering Aspects, 587*(October 2019), 124313. https://doi.org/10.1016/j.colsurfa.2019.124313
151. Salehi, M., Farzamfar, S., Bastami, F., & Tajerian, R. (2016). Fabrication and characterization of electrospun plla/collagen nanofibrous scaffold coated with chitosan to sustain release of aloe vera gel for skin tissue engineering. *Biomedical Engineering: Applications, Basis and Communications, 28*(5), 1–8. https://doi.org/10.4015/S1016237216500356
152. Locilento, D. A., Mercante, L. A., Andre, R. S., Mattoso, L. H. C., Luna, G. L. F., Brassolatti, P., Anibal, F. F., Correa, & D. S. (2019). Biocompatible and biodegradable electrospun nanofibrous membranes loaded with grape seed extract for wound dressing application. *Journal of Nanomaterials, 2019*, 1–12. https://doi.org/10.1155/2019/2472964
153. Miguel, S. P., Ribeiro, M. P., Coutinho, P., & Correia, I. J. (2017). Electrospun polycaprolactone/Aloe Vera_chitosan nanofibrous asymmetric membranes aimed for wound healing applications. *Polymers (Basel), 9*(5), 183. https://doi.org/10.3390/polym9050183
154. Pakolpakçıl, A., Osman, B., Göktalay, G., Özer, E. T., Şahan, Y., Becerir, B., & Karaca, E. (2021). Design and in vivo evaluation of alginate-based pH-sensing electrospun wound dressing containing anthocyanins. *Journal of Polymer Research, 28*(2), 50. https://doi.org/10.1007/s10965-020-02400-1
155. Pakolpakçıl, A., Osman, B., & Özer, E. T., Şahan, Y., Becerir, B., Göktalay, G., & Karaca, E. (2020). Halochromic composite nanofibrous mat for wound healing monitoring. *Materials Research Express, 6*(12), 1250c3. https://doi.org/10.1088/2053-1591/ab5dc1



Kelcilene B. R. Teodoro is graduated in chemistry from Federal University of Sao Carlos (Brazil) and received her M. S. degree in physical chemistry (2014) and Ph.D. in chemistry (2019) from Federal University of Sao Carlos (Brazil). She is currently developing her postdoctoral research in the Nanotechnology National Laboratory for Agriculture (LNNA) at the Embrapa Instrumentation, Brazil. Dr. Teodoro is author of 18 scientific papers, including articles, book chapters and reviews and her research interests include the development of novel materials based on natural polymers for advanced applications.



Danilo M. Santos received his Ph.D. in Chemistry in 2018 from the São Carlos Institute of Chemistry, University of São Paulo (USP). Since June 2018 he is a postdoctoral fellow at Nanotechnology National Laboratory for Agriculture (LNNA), Embrapa Instrumentação, Brazil. His research interests include the synthesis, characterization, and applications of novel functional nanomaterials for biomedical and sensing applications.



Camilo A. S. Ballesteros holds a B.Sc. in Physics from Pedagogical and Technological University of Colombia (2010), a Master in Biomolecular Physics (2012) from São Paulo University (USP) and Ph.D. in Biomolecular Physics (2017) from São Paulo University (USP) and Embrapa Instrumentation, Brazil. He is currently an assistant professor at Pedagogical and Technological University of Colombia and a collaborator at the Nanotechnology National Laboratory for Agriculture (LNNA) - Embrapa Instrumentation, Brazil. Currently, his research is focused on the didactics of experimental nanoscience and the development of functional nanomaterials for agricultural, environmental, and biomedical areas.



Paulo A. M. Chagas received his doctoral degree in biotechnology from the Federal University of São Carlos (UFSCar), São Carlos (Brazil) in 2021. He graduated in biotechnology engineering from São Paulo State University (Unesp), School of Sciences, Humanities and Languages, Assis (Brazil) in 2016. Then he joined Prof. Dr. Daniel Correa's group at the Nanotechnology National Laboratory for Agriculture (LNNA) in Embrapa Instrumentação, São Carlos (Brazil). His scientific interests are smart materials, nanomaterials, the design and preparation of nanofibers, and their application as wound dressings.



Víttor P. V. Costa is graduated in biotechnology engineering (2017) from São Paulo State University (UNESP), campus Assis, Brazil. He is currently a Ph.D. student at the Federal University of São Carlos (UFSCar) and develops his doctoral project at the Nanotechnology National Laboratory for Agriculture (LNNA)—Embrapa Instrumentation, Brazil. His research interests include the development of biomaterials based on natural polymers.



Rodrigo Schneider received his bachelor's degree in Chemistry in 2016 from the Universidade Estadual do Oeste do Paraná (UNIOESTE), Brazil and his M. S. degree in Chemistry in 2018, at the Federal University of São Carlos (UFSCar), Brazil. He is currently a Ph.D. student at the UFSCar and develops his doctoral project at the Nanotechnology National Laboratory for Agriculture (LNNA)—Embrapa Instrumentação under the supervision of Dr. Daniel S. Correa. Rodrigo is the author of 13 scientific publication including articles, books, and reviews. His research interests include the synthesis and characterization of two-dimensional nanosheets/nanoflakes and spinning of nanofibrous composites for environmental applications.



Daniel S. Correa holds a B.Sc. in Materials Engineering (2004) from Federal University of São Carlos (UFSCar) and a PhD in Materials Science and Engineering (2009) from São Paulo University (USP), in Brazil. He was a visiting scholar at Friedrich-Schiller-University (Germany) (2003) and at Harvard University (USA) (2007). During 2009–2010 he worked as a post-doctoral fellow at the IFSC-USP. He is currently a full researcher at the Nanotechnology National Laboratory for Agriculture (LNNA) in Embrapa Instrumentation and also holds appointments as collaborating professor in post-graduation programs at UFSCar and USP. His current editorial activities include: Associate Editor—Journal of Cluster Science (Springer), Associate Editor—Frontiers in Sensors—Section: Chemical Sensors (Frontiers), Guest editor—Sensors and Actuators Reports (Elsevier), Editorial Board Member - Scientific Reports (Nature). His research group is focused on the development and application of functional and composite nanomaterials for agricultural, environmental, and biomedical areas.

Chapter 12
Incorporating Poorly Soluble Drugs into Electrospun Nanofibers for Improved Solubility and Dissolution Profile

Taha Umair Wani, Taseen Aamir Wani, Anjum Hamid Rather, Rumysa Saleem Khan, Mushtaq A. Beigh, and Faheem A. Sheikh

Abstract Every year many newly discovered drugs are added to the existing drug library. However, not all drugs make it to the following stages of development and approval for clinical use. One of the most prominent reasons for this is their low aqueous solubility. This results in inferior dissolution properties, low absorption and bioavailability, and overall poor in vivo performance. To overcome these limitations, formulation development scientists always seek to enhance drug solubility and dissolution properties. Thus, many strategies have been adopted to achieve this goal, including the salt formation of drugs, prodrug formation, particle size reduction, solid dispersions, inclusion complexes, polymorphic conversion, etc. Nanotechnology-based formulations are a novel strategy to improve drug solubility and dissolution profile, including nanoparticles, liposomes, micelles, etc., for the improved solubilization of poorly soluble drugs. Electrospun nanofibers are another nanotechnology-based approach used by many researchers to increase the solubility of drugs. This increase in the solubility using nanofibers is owed to the nanonization of drugs, the increased surface-to-volume ratio of nanofibers, polymorphic conversion of drugs, overcoming the hydrophobicity barrier of drugs, etc. This chapter discusses the use of electrospun nanofibers in the delivery of poorly water-soluble drugs, some drug incorporation methods, and various mechanisms of solubility enhancement using nanofibers.

Keywords Drug delivery · Poorly soluble drugs · Surface modification · Immobilization · Aqueous solubility

T. U. Wani · A. H. Rather · R. S. Khan · M. A. Beigh · F. A. Sheikh (✉)
Department of Nanotechnology, University of Kashmir, Hazratbal, Srinagar, Jammu and Kashmir 190006, India
e-mail: faheemnt@uok.edu.in

T. A. Wani
Department of Analytical Chemistry, School of Chemical Sciences, Guindy Campus, University of Madras, Chennai, Tamil Nadu 600085, India

© The Author(s), under exclusive license to Springer Nature Switzerland AG 2022

A. Vaseashta and N. Bölgen (eds.), *Electrospun Nanofibers*,
https://doi.org/10.1007/978-3-030-99958-2_12

12.1 Introduction

The efficacy of a drug depends upon the amount of free drug available for action in blood. Therefore, the overall amount of the drug reaching the blood, which is a function of several physicochemical and physiological factors, is very important [1, 2]. Among the numerous factors, aqueous solubility is a critical physicochemical factor that governs the fate of a drug inside the body. Solubility and thus dissolution rate of drugs determine their absorption, biodistribution, bioavailability, metabolism, and overall efficacy [3]. With the introduction of combinatorial chemistry, many drugs are produced every year; however, the major drawback that halts the progress of these drugs during the formulation development is their poor aqueous solubility [4, 5]. This is because until a drug is present in solution form, it cannot be absorbed through the gastrointestinal tract, which results in the poor bioavailability of the drug and the inability to show its desired pharmacological action. Thus, a drug must possess adequate solubility before being considered for formulation development.

Some general principles regarding the solubility of drugs are listed below and depicted in Fig. 12.1.

1. The amorphous form of the drugs has more excellent solubility than the crystalline form [6].
2. The metastable form of a drug possesses greater solubility than the stable forms [7].
3. Anhydrous drugs are more soluble than the hydrate forms [8, 9].

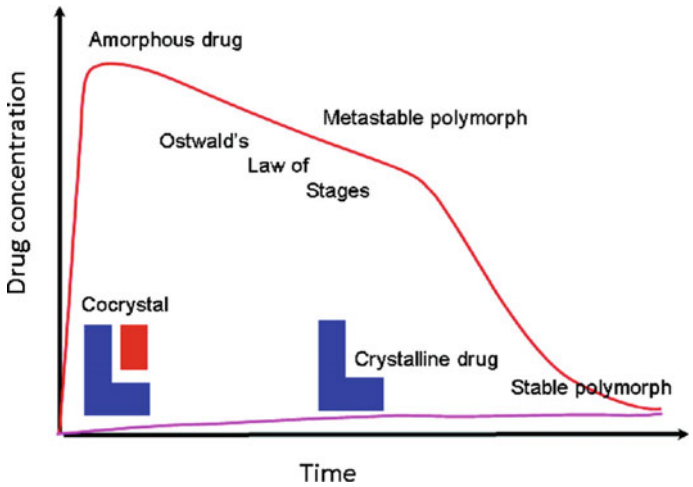


Fig. 12.1 Graphical illustration comparing the solubilities of the various polymorphic forms of drugs depicting Ostwald's rule, which states that a drug's less stable polymorphic form undergoes the crystallization first. Reprinted with permission from [6]. Copyright (2011), American Chemical Society

4. Organic drug solvates are more soluble than the non-solvated drug forms [10, 11].
5. Salt forms of drugs possess higher aqueous solubility compared to the non-salt forms [12].

To enhance the aqueous solubility of drugs, formulation development scientists have devised several strategies. These include prodrug or salt formation [12], polymorph conversion [13], inclusion complexation [14, 15], micellization [16, 17], solid dispersions [18, 19], size reduction or nanonization [20–22]. A novel approach to enhancing drug solubility and dissolution rate is through incorporation into electrospun nanofibers [23]. Before the actual electrospinning process begins, the drug may be dispersed into the polymer solution, which forms a uniform solution where the drug and the polymer molecules are in continuous random motion and molecularly distributed. During electrospinning, which is a speedy process, the polymer droplets containing the uniformly distributed drug are rapidly molded into the fibers, thus maintaining the state of the molecular drug distribution in the nanofiber polymer matrix. This renders the drug distribution in the final nanofibers uniform and thus transforms the drug into an amorphous state. This molecular distribution is also facilitated by other molecular interactions between the drug and the polymer-like hydrogen bonding, electrostatic and hydrophobic forces [24]. This chapter will discuss the application of electrospun nanofibers in increasing the solubility and dissolution profile of poor solubility drugs. Hence we discuss the mechanisms of solubility enhancement by nanofibers, e.g., nanonization, high fiber porosity, polymorphic conversion and overcoming drug hydrophobicity. Further, the use of electrospun nanofiber complexes in solubility enhancement is also discussed. Finally, the enhancement in the bioavailability of the drugs due to enhanced solubility and dissolution using electrospun nanofibers is reflected.

12.2 Methods of Drug Incorporation into Electrospun Nanofibers

Drug incorporated in the electrospun nanofibers can be carried out by loading the drugs into the polymeric solution before the electrospinning process or surface functionalization of as-spun nanofibers through immobilization. The choice of a particular method depends upon the physicochemical properties of the drug. For example, certain drugs that cannot form uniform dispersion with a specific polymeric solution cannot be loaded into nanofibers by simple blending and thus require to be immobilized onto the nanofibers. Moreover, certain drugs can lose their chemical nature and functionality during electrospinning due to the solvent interaction and exposure to high voltage [25]. In this course, the drug loading into the electrospun nanofibers can be carried out by various methods, such as blending, surface immobilization, co-axial electrospinning, etc. These are discussed in separate sections below.

12.2.1 Blending

In this method, the drug incorporation into nanofibers is carried out by blending the drug with the polymeric solution used in the electrospinning process (Fig. 12.2). The drug in the polymeric solution is dispersed/dissolved uniformly by proper stirring and the blend is loaded into syringes for electrospinning. The advantage of this method is that the drug release from the nanofiber can be modulated by varying the concentration of the drug or polymer used during electrospinning. Depending upon the lipophilicity or the hydrophobicity of the drugs, proper polymers and solvents are chosen for the purpose, e.g., lipophilic drugs can be blended efficiently with hydrophobic polymers. Examples of drugs compatible with hydrophobic polymers (like polyethylene glycol, gelatin, poly(vinyl alcohol) are paclitaxel, rifampin, etc. [26, 27]. Other process variables determine the efficiency of drug loading into nanofibers, e.g., solution viscosity, the solubility of polymer, etc. However, the solubility of polymer and solution viscosity are the functions of the solvent used for dissolution. Typically the solvent used should be chemically inert to not react with the drug and change its chemical nature. The most common solvents used in the electrospinning process include ethanol, acetone, acetic acid, dimethylformamide, tetrahydrofuran, dichloromethane, etc. [28]. Water is also used as a solvent for nanofiber fabrication [29]; however, due to the poor solubility of most of the polymers in water, its use is restricted to only hydrophilic polymers. Moreover, with water, the polymeric solutions obtained exhibit high viscosity, which makes it difficult for the solution to form nanofibers during the electrospinning process. Also, since water is less volatile than the other organic solvents, its evaporation during electrospinning is improper, resulting in inefficient nanofiber formation. This drug loading technique is not suitable for proteins, peptides, enzymes, etc., since these may denature while the high voltage is applied during electrospinning.

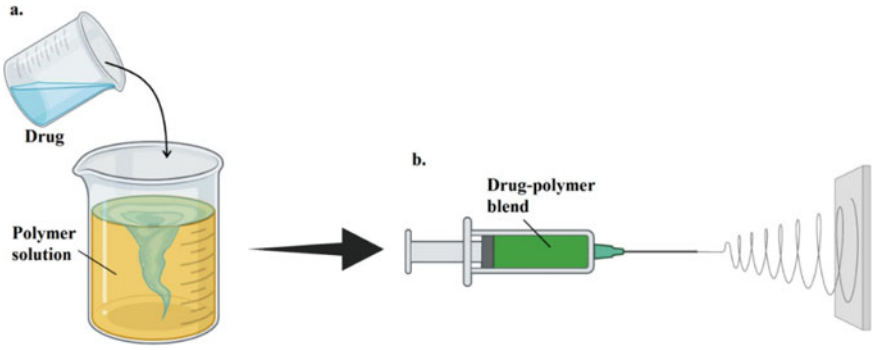


Fig. 12.2 Drug incorporation into electrospun nanofibers by blending technique; **a** drug is dispersed into the polymer solution, and a homogenous dispersion is prepared by thorough blending, **b** drug-polymer dispersion fabricated into nanofibers using electrospinning technique

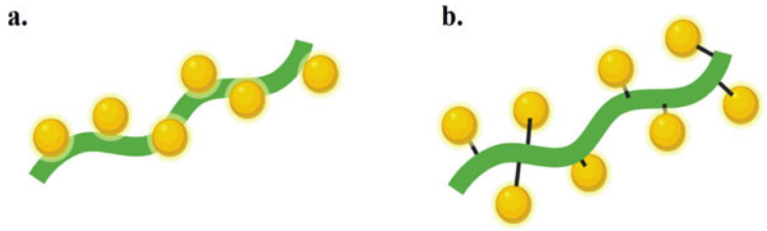


Fig. 12.3 Drug loading into nanofibers through surface functionalization. **a** Physical adsorption of drugs onto nanofibers mediated by physical forces like hydrophobic and electrostatic interaction or Van der Waal's forces; **b** chemical adsorption of drugs onto nanofibers mediated through the chemical bond formation

12.2.2 Surface Modification/Immobilization

While in the case of the blending method of drug loading, the polymer and the drug solutions are blended before electrospinning. In the surface modification, the polymer solution is initially electrospun into nanofibers followed by loading with the drug on the surface of the nanofibers. This method is suitable for the loading of biological agents like proteins, peptides, enzymes, etc., since these are liable to denaturation in the presence of high voltage and the presence of organic solvents [30, 31]. Moreover, the drug loading can be precisely controlled by regulating the amount of the drug fed onto the nanofibers. The drugs onto the nanofibers are loaded either by physical or chemical interaction between the drug and the nanofiber surface [32]. Physical immobilization is mediated by forces like hydrogen bond formation, electrostatic, van der Waals, or hydrophobic interactions.

On the other hand, the chemical surface modification is led by interaction with functional groups of the drugs and the formation of chemical bonds. This is illustrated in Fig. 12.3. During surface modification, the nanofibers are often coated with a suitable ligand, e.g., heparin, that has a high affinity with the therapeutic agent (e.g., biological proteins or growth factors) indented to be immobilized onto the nanofibers. The coated ligand forms a strong bond with the drug and binds it firmly with the nanofiber.

12.2.3 Co-axial Electrospinning

In this type of electrospinning also, the drug is not dispersed into the polymer solution before the electrospinning process. However, the drug and the polymer solutions run co-axially from the separate compartments and simultaneously directed onto the collector drum, as represented in Fig. 12.4 [33]. Multiple drug-loaded core layers are deposited on the collector surrounded by drug-free nanofiber layers during the nanofiber deposition process. The type of nanofibers formed by this electrospinning

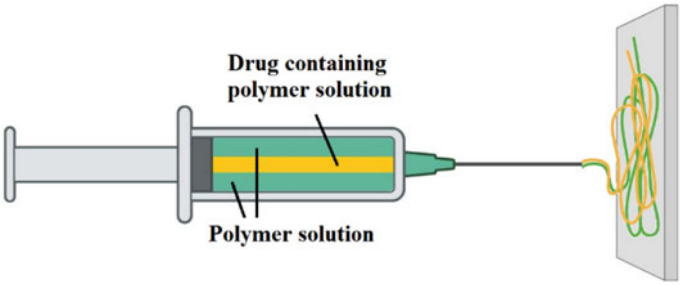


Fig. 12.4 Schematic depicting co-axial electrospinning for drug incorporation into nanofibers. The polymer and the drug-containing solution are run parallel to each other

technique exhibit some advantages like protection of the drug from the outside environment both during and after the process and provides better-sustained drug release properties [34]. Generally, a hydrophobic, e.g., poly-ε-caprolactone, the swelling polymer, is used for sheath layer formation, which swells on coming in contact with water and allows the slow release of drug from the nanofiber [35].

12.2.4 Emulsion Electrospinning

In this type of electrospinning technique, an oil/water or water/oil emulsion is first prepared, which is subsequently subjected to electrospinning [36]. The advantage of this electrospinning method is that it forms a drug-loaded core layer surrounded by polymer layer instantly and does not require the drug and the polymer solutions to be ejected from separate compartments. Moreover, it does not require the drug and the polymer to be soluble in the same solvent, unlike in the case of the blending technique [37]. As the emulsion is ejected from the nozzle, both the polymer and the emulsion droplets are subjected to extension under the influence of high voltage, which ultimately results in the spindle formation and deposition of drug-loaded nanofiber onto the collector. A schematic of emulsion electrospinning is shown in Fig. 12.5.

12.2.5 Layer by Layer Electrospinning

Layer by layer electrospinning is a technique where the polymer and the drug solutions are collected onto the collector by depositing a drug-free nanofiber layer followed by the drug-loaded layer alternately [38]. In this way, multiple nanofiber layers are stacked, and a multilayered nanofiber containing alternate drug-loaded layers is fabricated. This type of electrospinning technique is suitable for loading two or more drugs into the same nanofiber. Figure 12.6 shows an illus-

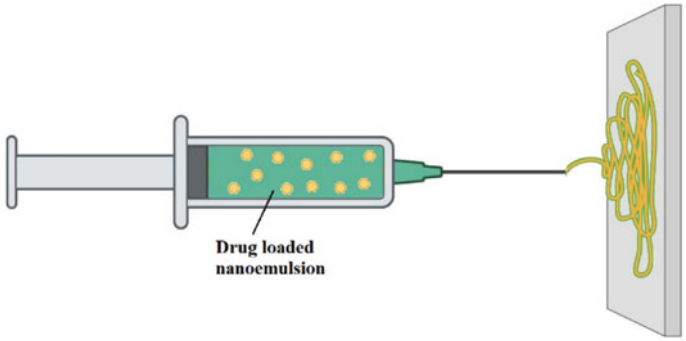


Fig. 12.5 Emulsion electrospinning for drug incorporation into nanofibers. A nano-emulsion of the drug in a hydrophilic polymer is electrospun under high voltage to form drug-loaded nanofibers

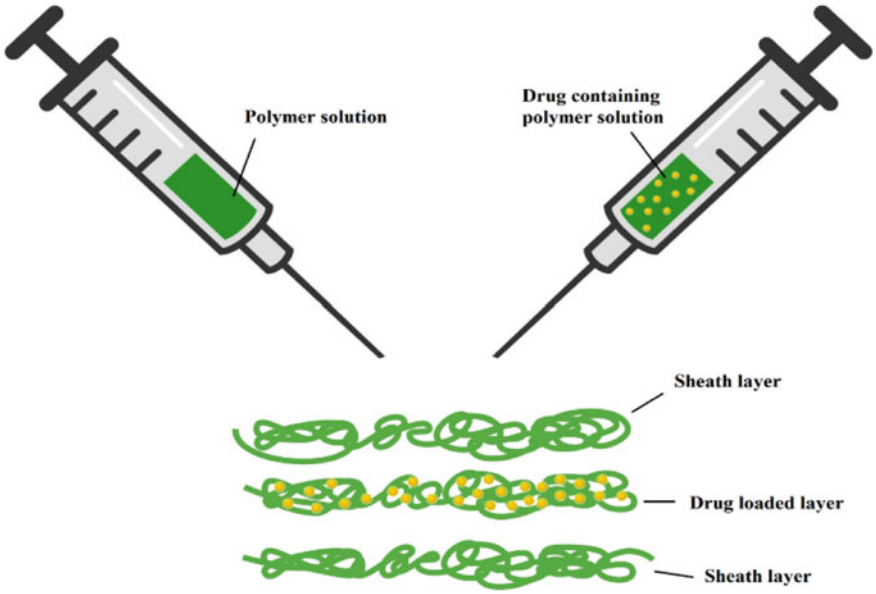


Fig. 12.6 Layer-by-layer electrospinning. Drug-free and drug-containing polymer solutions are run alternately under high voltage to deposit alternate layers of drug-free (sheath layer) and drug-containing nanofibers

tration demonstrating the strategy used for creating nanofibers by layer-by-layer electrospinning.

12.3 Mechanism of Solubility Enhancement Using Electrospun Nanofibers

12.3.1 Nanonization

Nanonization refers to the process of rendering bigger size drug particles to nanometer size. It is well established that the solubility of drugs increases with decreasing particle size. This is because the surface area of solids in contact with the medium increases, which increases the solvation process resulting in rapid dissolution [39]. The use of nanofibers for solubility enhancement works on the same basis. The incorporation of drugs into nanofibers reduces the size of the drug particles and leads to drug particles with nanometric size with greater overall surface area. The drug particle size reduction increases the general surface area of the drug, increasing the dissolution rate and solubility of the drug [40]. However, this proportionality is not so simple, and several theoretical treatments have been put forward. Several equations have been derived from achieving a coherent relationship between particle size and solubility. Such derivations involve implementing the general laws of thermodynamics considering the equilibrium state between the drug in solid and the solution form. During an equilibrium state between the drug particles in the solid and solution phase, the partial Gibbs energy of the two is equal. The relation between solubility and particle size was first anticipated by Wollaston in 1813 and was further elaborated by many theories [41]. The basis of these equations is the Thomson and Helmholtz equation explaining the relation between the vapor pressure of a liquid and the size of its vapors given by Eq. 12.1.

$$\frac{\mathrm{RT}}{M} \ln \frac{p_2}{p_1} = \frac{2\gamma}{\rho}\left(\frac{1}{r_2} - \frac{1}{r_1}\right) \tag{12.1}$$

It is this analogy that was used by Ostwald to determine the relationship between the solubility and the particle size of the drugs, which has already been mentioned in the previous paragraph [42]. One of the most suitable theories that explain the improved solubility profile of low solubility drugs through nanonization is Ostwald–Freundlich equation which is the corrected form of the Ostwald equation as given by Eq. 12.2 [41].

$$\rho v \frac{\mathrm{RT}}{M} \ln \frac{S_r}{S_\infty} = \frac{2\lambda_{sl}}{r}. \tag{12.2}$$

where "ρ" and "M" are the density and the molar mass of the solid drug respectively; "R" and "T" are the gas constant and temperature respectively; "v" denotes the number of moles of ions generated from one mole of electrolyte, its value for non-electrolytes is "1"; "S_r" and "S_∞" are the solubilities of particles of radius and "r" and large particles respectively, "λ_{sl}" = solid–liquid interfacial tension.

$$S_r = S_\infty \exp\left(\frac{2\gamma V_m}{r\mathrm{RT}}\right) \tag{12.3}$$

Equation 12.3 is derived from the Kelvin equation [41, 43], which explains the relation between solubility (S_r) and the particle size (i.e., radius "r") as indicated by their inverse proportionality. "γ" denotes the interfacial tension between the solid particle and the liquid. As the particle size decreases, the term on the left-hand side of the equation increases.

Nanonization affects some parameters that increase the solubility of a drug (or a solid in general). Particle size affects parameters like interfacial energy [44], surface tension, wettability/contact angle, which explain the solubility enhancement of the drug with the size reduction. For this purpose, several equations have been introduced in the literature. Further, the Noyes-Whitney equation [45, 46] gives the relation between the surface area, diffusion layer thickness, and the solubility of drugs. It shows that the surface area directly affects the solubility of the drug, as evident from Eq. 12.4.

$$\frac{\mathrm{d}X}{\mathrm{d}t} = \left(A \times \frac{D}{\delta}\right) \times \left(S_0 - \frac{X}{V}\right). \tag{12.4}$$

where "$\mathrm{d}X/\mathrm{d}t$" depicts the rate of drug dissolution, "A" as the surface area of the solid drug particle, "δ" as the thickness of the diffusion layer, "D" as diffusion coefficient, "S_0" as drug solubility and "V" as a volume of the medium. From this equation, it is evident that as the surface area of the drug increases, the dissolution rate of the drug also increases, which means that the incorporation of the drug into nanofibers increases the surface area of the drug and can improve the dissolution profile of the drug.

12.3.2 Porosity

The high porosity and the large surface area of the nanofibers is another mechanism through which nanofibers improve the solubility and the dissolution profile of drugs. Due to their 3-D nanoweb-like architecture nanofibers are regarded as highly porous structures [47]. Considering that the drug inside the nanofibers is homogenously dispersed, the high porosity of the nanofiber plays a significant role in increasing the dissolution rate and the solubility of the drug. This is because the high nanofiber porosity permits uniform solvent diffusion into the nanofibers, allowing more contact with the drug and subsequent increase in the solvation. This leads to high drug-solvent interactions and the subsequent diffusion of the drug in the solution phase from the nanofiber [48]. Another important reason for the improved solubility of drugs using nanofibers is the reduced thickness of the diffusion layer around the periphery of the nanofiber. Since the nanofibers possess nanoscale diameters, the thickness of the

diffusion layer formed around the nanofiber is small, leading to improved wettability and, hence, more significant dissolution and solubility. From the Noyes-Whitney equation, it can be inferred that as diffusion layer thickness (δ) decreases, the rate of the dissolution of the drug (dX/dt) increases, which again explains the above phenomenon.

Yu et al. formulated solid dispersions based on electrospun nanofibers to increase the solubility of acetaminophen using the polymer polyvinylpyrrolidone [49]. This approach combined the conventional solid dispersions and the nanofibers to impart nanonization to the solid dispersions while possessing the appropriate microstructure. The nanofibers were highly porous and provided a higher dissolution rate than the pure drug particles and solid dispersion. Besides, vacuum dried and freeze-dried membranes also demonstrated slower dissolution rates than the electrospun nanofibers, which also shows that high porosity increases the dissolution rate of the drug.

12.3.3 Crystalline to Amorphous Conversion

Polymorphism is a well-known phenomenon in drugs that governs their efficacy and overall performance in vitro and in vivo [50]. A drug may exist in many polymorphic forms like crystalline, amorphous, hydrate, anhydrous, metastable, etc. All the polymorphic forms of a drug possess different physicochemical properties, such as solubility and dissolution, and thus, their pharmacokinetic profiles also differ in absorption, bioavailability, etc. With respect to the above phenomenon, it indicates that the crystalline form of a drug is more stable than the amorphous form. This is because a crystalline solid is composed of evenly arranged particles and crystal units, due to which these possess lower Gibbs free energy [51, 52]. Therefore, these drugs are more stable and require higher energy for disintegration and dissolution in a medium. On the other hand, amorphous drugs possess a highly disordered molecular structure, and the intermolecular interactions are not stronger, thus requiring less energy for dissolution. Some examples of drugs whose amorphous forms include higher solubility profiles than their crystalline counterparts, that are given in Table 12.1.

12.3.4 Overcome Hydrophobicity

One of the main reasons for the low aqueous solubility of drugs is their hydrophobic character. Several techniques have been put forward to decrease or hide the hydrophobicity and increase the solubilization of such drugs. These include incorporation of drugs into lipid-based nanoparticles [58], micelle formation [59], encapsulation into liposomes [60], etc. Electrospun nanofibers used to enhance the solubility of some low solubility drugs impart this effect by camouflaging the hydrophobic nature of

Table 12.1 Examples of some drugs comparing the solubilities of their amorphous and crystalline forms

S. no.	Drug	Solubility of the amorphous form higher than crystalline	References
1	Macrolide antibiotic	10 fold	[53]
2	Cefalexin	2 fold	[54]
3	Novobiocin acid	10 fold	[55]
4	Indomethacin	1.4 fold	[56]
5	Tetracycline	2.5 fold	[57]

the drug. Such nanofibers are fabricated using hydrophilic polymers that offer fast dissolution and enhance the solubility of the drugs. Many workers have used electrospinning employing hydrophilic polymers to enhance the solubility of hydrophobic drugs.

A very good example of this is the work done by Soukasene et al. to incorporate the antitumor hydrophobic drug camptothecin into peptide amphiphile nanofibers [61]. The solubility of the drug was enhanced by more than 50 times. The novel camptothecin-loaded nanofiber formulation possessed enhanced antitumor activity as evaluated in human breast cancer cells and mouse breast cancer. Dubey et al. fabricated electrospun nanofibers using hydrophilic polymer, i.e., polyvinylpyrrolidone for solubility enhancement of hydrophobic drug and undecapeptide cyclosporine A, in addition to micelle formation [62]. Gordon et al. used electrospun nanofibers fabricated from a hydrophilic polymer, poly(vinyl alcohol), to increase the solubility of celecoxib [63]. Celecoxib is a lipophilic drug possessing very low solubility in aqueous media. The non-volatile oil/water drug encapsulating nano-emulsion (prepared from retinyl palmitate) was incorporated into the electrospun nanofibers during the electrospinning process. During the solidification of the polymer jet, the nano-emulsion droplets present on the surface detach while the other droplets are entrapped within the polymeric fibers [54].

12.4 Nanofiber Complexes for Solubility Enhancement

Many researchers have developed nanofiber complexes to increase the solubility of drugs. Such complexes include the functionalization of nanofibers with moieties like cyclodextrin and solid dispersions. Aytac et al. developed ciprofloxacin-loaded electrospun nanofibers of gelatin to improve the drug solubility [64]. The nanofibers also encapsulated the cyclodextrin inclusion complex, which underwent complexation with the drug through Van der Waals and hydrophobic forces as demonstrated by the computational modeling studies. The nanofibers formed were fast dissolving and dissolved within 3 s in water. This was attributed to the high wettability of the cyclodextrin-loaded nanofibers. Celebioglu et al. fabricated electrospun

nanofibers for the solubility enhancement of acyclovir by complex formation with hydroxypropyl-beta-cyclodextrin before incorporating them into nanofibers manufactured using the same cyclodextrin [65]. The fabricated nanofibers significantly increased the solubility of the drug when compared to the solubility of polyvinyl pyrrolidine nanofiber-loaded drugs. This was due to the presence of the drug in the cyclodextrin complexed drug-loaded nanofibers in less crystalline form than the highly crystalline drug in the polyvinyl pyrrolidine nanofibers. Another reason for the improved solubility of the drug using the cyclodextrin nanofibers was the fast-dissolving property of the nanofibers.

Another example of fast dissolving nanofibers is pullulan nanofibers developed by Lee et al. for solubility enhancement of rutin [66]. Rutin is a polyphenolic flavonoid with antioxidant action, which has been used to perform scavenging actions and prevent certain blood vessel diseases. However, being poorly water-soluble, its oral use is largely hampered owing to its low bioavailability resulting from its low solubility. Thus Lee et al. employed a solubility enhancing strategy by developing pullulan nanofibers containing drug-loaded pluronic solid dispersions. Using the electrospun nanofibers, it was shown that the drug release from the nanofibers into the medium was increased, which was attributed to the enhanced solubility of the drug.

Masoumia et al. used nanofiber/cyclodextrin complexation for enhancing the solubility of ciprofloxacin [67]. Ciprofloxacin is a broad-spectrum antibiotic that has applications against various infectious conditions caused by either gram-negative or gram-positive bacteria. Inclusion complexes of ciprofloxacin with cyclodextrin were first prepared before incorporating them into electrospun poly(ε-caprolactone) nanofibers. The solubility of the drug as evaluated by phase solubility analysis using UV–vis spectroscopy was found to be significantly increased using the drug-containing cyclodextrin-loaded nanofiber.

12.5 Bioavailability Enhancement

Solubility is regarded as the most critical parameter that affects the concentration of a drug in the blood. The prime goal of formulation development scientists is to improve the amount of the drug reaching the blood since the overall drug concentration in blood determines the efficacy of drugs. High efficacy of drugs ensures the use of low drug doses and decreases the incidences of toxicities. With an improved solubility profile, the bioavailability of the drug drastically improves. This is because the dissolution of the high solubility drugs in the gastrointestinal fluid increases and thus, a more tremendous amount of the drug is available for absorption into the blood. The improved bioavailability of drugs after incorporation into nanofibers has been demonstrated by many workers.

Wang et al. developed electrospun polyvinylpyrrolidone nanofibers for improved bioavailability and anticancer activity of curcumin [68]. The nanofibers improved the dissolution profile of the drug and increased the release rate of the drug as well. The nanofibers resulted in a drastic increase in the dissolution and solubility of

curcumin. The pharmacokinetic evaluation showed that the C_{max} detected in the mouse plasma using nanofibers was 11 times higher than that of pure curcumin, while the AUC increased 10 folds. This improvement was attributed to the increase in the dissolution and solubility of the drug, which was in turn due to the conversion of curcumin from crystalline to the amorphous form, as revealed by XRD. The drug-containing nanofiber also exhibited in vitro anticancer activity, as shown by the cytotoxicity studies using B16 cells. The cytotoxic effect of pure curcumin and curcumin-loaded nanofibers was similar up to 72 h beyond which a decrease in the action of pure curcumin was observed. This was attributed to the inability of large drug particles to dissolve in the medium.

Vigh et al. also demonstrated the application of electrospun nanofibers in increasing the bioavailability of the drug flubendazole [69]. These workers used hydroxypropyl-β-cyclodextrin and polyvinyl pyrrolidone for the fabrication of nanofibers by electrospinning technique. The nanofibers remarkably increased the dissolution profile of the drug, providing faster drug release where 40 mg drug would release only in 15 min. This led to the drastic increase in the AUC and C_{max} and hence bioavailability of the drug as evaluated in Sprague–Dawley rats. Irbesartan, a low solubility antihypertensive agent, was incorporated into nanofibers by Adeli et al. for solubility and dissolution rate enhancement using polyvinyl pyrrolidine [70]. The nanofiber-based solid dispersion was fabricated by electrospinning using a specific drug/polymer weight ratio. The FTIR, DSC, XRD, and SEM confirmed the formation of nanofibers. These workers found that the solubility of the drug increased significantly in the case of electrospun nanofiber-based solid dispersions compared to the pure drug and the physical mixture of the drug and the polymer. The C_{max} and T_{max} significantly increased and decreased respectively after using the electrospun nanofiber-based solid dispersions. The AUC also showed a significant increase. Finally, the bioavailability of the drug using the novel electrospun nanofiber-based solid dispersions was calculated, and it was found that the relative bioavailability of the drug increased almost 3 fold.

12.6 Conclusion

Solubility is a critical physicochemical factor governing the fate of a drug inside the body. Solubility enhancement of poorly water-soluble drugs has been a prime focus of formulation development scientists. Among the existing methods of solubility enhancement, the electrospun nanofibers certainly offer an excellent choice for improving the solubility of poorly soluble drugs. Nanofibers can show versatile improvement in the solubility of drugs through a combination of multiple mechanisms like particle size reduction through nanonization, increasing the surface to volume ratio, conversion from crystalline to amorphous state and overcoming hydrophobicity. Besides, inclusion complexes and solid dispersions complexation with nanofibers have also offered an advanced drug delivery approach for better drug release and efficacy.

Acknowledgements Dr. Taha would like to thank the Indian Council of Medical Research (ICMR), New Delhi, File No: 45/13/2020-Nan/BMS, for providing the fellowship. The authors would also like to acknowledge the Science and Engineering Research Board (SERB) (CRG/2020/000113) and Council of Scientific & Industrial Research (CSIR), File No: 22(0846)/20/EMR-II, research.

References

1. Song, N.-N., Zhang, S.-Y., & Liu, C.-X. (2004). Overview of factors affecting oral drug absorption. *Asian Journal of Drug Metabolism Pharmacokinetics, 4*(3), 167–176.
2. Jambhekar, S. S., & Breen, P. J. (2013). Drug dissolution: Significance of physicochemical properties and physiological conditions. *Drug Discovery Today, 18*(23–24), 1173–1184.
3. Ashford, M. (2013). Bioavailability—Physicochemical and dosage form factors. *Aulton's pharmaceutics: The design and manufacture of medicines* (p. 314). Elsevier Health Sciences.
4. Wilson, S. R., & Czarnik, A. W. (1997). *Combinatorial chemistry: Synthesis and application.* Wiley.
5. Jung, G. (2008). *Combinatorial chemistry: Synthesis, analysis, screening*. Wiley.
6. Babu, N. J., & Nangia, A. (2011). Solubility advantage of amorphous drugs and pharmaceutical cocrystals. *Crystal Growth & Design, 11*(7), 2662–2679.
7. Nicoud, L. C., Licordari, F., & Myerson, A. S. (2018). Estimation of the solubility of metastable polymorphs: A critical review. *Crystal Growth & Design, 18*(11), 7228–7237.
8. Poole, J. W., & Bahal, C. K. (1968). Dissolution behavior and solubility of anhydrous and trihydrate forms of ampicillin. *Journal of Pharmaceutical Sciences, 57*(11), 1945–1948.
9. Lu, J., et al. (2012). Solubility of L-phenylalanine anhydrous and monohydrate forms: Experimental measurements and predictions. *Journal of Chemical & Engineering Data, 57*(5), 1492–1498.
10. Griesser, U. J. (2006). The importance of solvates. *Polymorphism in the pharmaceutical industry* (pp. 211–233).
11. Shefter, E., & Higuchi, T. (1963). Dissolution behavior of crystalline solvated and nonsolvated forms of some pharmaceuticals. *Journal of Pharmaceutical Sciences, 52*(8), 781–791.
12. Serajuddin, A. T. (2007). Salt formation to improve drug solubility. *Advanced Drug Delivery Reviews, 59*(7), 603–616.
13. Censi, R., & Di Martino, P. (2015). Polymorph impact on the bioavailability and stability of poorly soluble drugs. *Molecules, 20*(10), 18759–18776.
14. Rawat, S., & Jain, S. K. (2004). Solubility enhancement of celecoxib using β-cyclodextrin inclusion complexes. *European Journal of Pharmaceutics and Biopharmaceutics, 57*(2), 263–267.
15. Gandhi, S. R., et al. (2020). The use of cyclodextrin inclusion complexes to improve anticancer drug profiles: A systematic review. *Expert Opinion on Drug Delivery, 17*(8), 1069–1080.
16. Esmaili, M., et al. (2011). Beta casein-micelle as a nano vehicle for solubility enhancement of curcumin; food industry application. *LWT-Food Science and Technology, 44*(10), 2166–2172.
17. Liu, R. R., Dannenfelser, R.-M., & Li, S. (2008). Micellization and drug solubility enhancement. *Water-insoluble drug formulation* (pp. 269–320). CRC Press.
18. Patel, B. B., Patel, J. K., & Chakraborty, S. (2015). Solubility enhancement using poly (meth) acrylate based solid dispersions. *Powder Technology, 270*, 27–38.
19. Jermain, S. V., Brough, C., & Williams, R. O., III. (2018). Amorphous solid dispersions and nanocrystal technologies for poorly water-soluble drug delivery—An update. *International Journal of Pharmaceutics, 535*(1–2), 379–392.
20. Hammond, R. B., et al. (2007). Quantifying solubility enhancement due to particle size reduction and crystal habit modification: Case study of acetyl salicylic acid. *Journal of Pharmaceutical Sciences, 96*(8), 1967–1973.

21. Da Silva, F. L. O., et al. (2020). Nanonization techniques to overcome poor water-solubility with drugs. *Expert Opinion on Drug Discovery, 15*(7), 853–864.
22. Mitrović, J. R., et al. (2021). Overcoming the low oral bioavailability of deuterated pyrazoloquinolinone Ligand DK-I-60-3 by nanonization: A knowledge-based approach. *Pharmaceutics, 13*(8), 1188.
23. Kamble, R. N., et al. (2016). Fabrication of electrospun nanofibres of BCS II drug for enhanced dissolution and permeation across skin. *Journal of Advanced Research, 7*(3), 483–489.
24. Williams, G. R., et al. (2012). Electrospun nanofibers in drug delivery: Recent developments and perspectives. *Therapeutic Delivery, 3*(4), 515–533.
25. Yang, Y., et al. (2008). Release pattern and structural integrity of lysozyme encapsulated in core–sheath structured poly (DL-lactide) ultrafine fibers prepared by emulsion electrospinning. *European Journal of Pharmaceutics and Biopharmaceutics, 69*(1), 106–116.
26. Zeng, J., et al. (2003). Biodegradable electrospun fibers for drug delivery. *Journal of Controlled Release, 92*(3), 227–231.
27. Xie, J., & Wang, C.-H. (2006). Electrospun micro-and nanofibers for sustained delivery of paclitaxel to treat C6 glioma in vitro. *Pharmaceutical Research, 23*(8), 1817–1826.
28. Morie, A., et al. (2016). Nanofibers as novel drug carrier—An overview. *Artificial Cells, Nanomedicine, and Biotechnology, 44*(1), 135–143.
29. Yang, R., et al. (2009). Bubble-electrospinning for fabricating nanofibers. *Polymer, 50*(24), 5846–5850.
30. Smith, S., et al. (2020). A comprehensive review of the covalent immobilization of biomolecules onto electrospun nanofibers. *Nanomaterials, 10*(11), 2142.
31. Son, Y. J., Kim, W. J., & Yoo, H. S. (2014). Therapeutic applications of electrospun nanofibers for drug delivery systems. *Archives of Pharmacal Research, 37*(1), 69–78.
32. Yoo, H. S., Kim, T. G., & Park, T. G. (2009). Surface-functionalized electrospun nanofibers for tissue engineering and drug delivery. *Advanced Drug Delivery Reviews, 61*(12), 1033–1042.
33. Moghe, A., & Gupta, B. (2008). Co-axial electrospinning for nanofiber structures: Preparation and applications. *Polymer Reviews, 48*(2), 353–377.
34. Huang, Z. M., et al. (2006). Encapsulating drugs in biodegradable ultrafine fibers through co-axial electrospinning. *Journal of Biomedical Materials Research Part A: An Official Journal of The Society for Biomaterials, The Japanese Society for Biomaterials, and The Australian Society for Biomaterials and the Korean Society for Biomaterials, 77*(1), 169–179.
35. Coimbra, P., et al. (2017). Coaxial electrospun PCL/Gelatin-MA fibers as scaffolds for vascular tissue engineering. *Colloids and Surfaces B: Biointerfaces, 159*, 7–15.
36. Hu, J., et al. (2013). Preparation and characterization of electrospun PLGA/gelatin nanofibers as a drug delivery system by emulsion electrospinning. *Journal of Biomaterials Science, Polymer Edition, 24*(8), 972–985.
37. Mohammadian, F., & Eatemadi, A. (2017). Drug loading and delivery using nanofibers scaffolds. *Artificial Cells, Nanomedicine, and Biotechnology, 45*(5), 881–888.
38. Jeckson, T. A., et al. (2020). Delivery of therapeutics from layer-by-layer electrospun nanofiber matrix for wound healing: An update. *Journal of Pharmaceutical Sciences*.
39. Kumar, D., Chirravuri, S. S., & Shastri, N. R. (2014). Impact of surface area of silica particles on dissolution rate and oral bioavailability of poorly water soluble drugs: A case study with aceclofenac. *International Journal of Pharmaceutics, 461*(1–2), 459–468.
40. Möschwitzer, J. (2010). Particle size reduction technologies in the pharmaceutical development process. *American Pharmaceutical Review, 2010*, 54–59.
41. Wu, W., & Nancollas, G. H. (1998). A new understanding of the relationship between solubility and particle size. *Journal of Solution Chemistry, 27*(6), 521–531.
42. Kaptay, G. (2012). On the size and shape dependence of the solubility of nano-particles in solutions. *International Journal of Pharmaceutics, 430*(1–2), 253–257.
43. *Particle size-solubility relation.* In T. Tadros (Ed.), *Encyclopedia of colloid and interface science* (pp. 910–910). Springer Berlin Heidelberg.
44. Kuna, J. J., et al. (2009). The effect of nanometre-scale structure on interfacial energy. *Nature Materials, 8*(10), 837–842.

45. Dokoumetzidis, A., & Macheras, P. (2006). A century of dissolution research: From Noyes and Whitney to the biopharmaceutics classification system. *International Journal of Pharmaceutics, 321*(1–2), 1–11.
46. Dokoumetzidis, A., Papadopoulou, V., & Macheras, P. (2006). Analysis of dissolution data using modified versions of Noyes-Whitney equation and the Weibull function. *Pharmaceutical Research, 23*(2), 256–261.
47. Venugopal, J., & Ramakrishna, S. (2005). Applications of polymer nanofibers in biomedicine and biotechnology. *Applied Biochemistry and Biotechnology, 125*(3), 147–157.
48. Park, J.-Y., & Lee, I.-H. (2011). Controlled release of ketoprofen from electrospun porous polylactic acid (PLA) nanofibers. *Journal of Polymer Research, 18*(6), 1287–1291.
49. Yu, D.-G., et al. (2010). Dissolution improvement of electrospun nanofiber-based solid dispersions for acetaminophen. *An Official Journal of the American Association of Pharmaceutical Scientists, 11*(2), 809–817.
50. Ayala, A. P. (2007). Polymorphism in drugs investigated by low wavenumber Raman scattering. *Vibrational Spectroscopy, 45*(2), 112–116.
51. Vranic, E. (2004). Amorphous pharmaceutical solids. *Bosnian Journal of Basic Medical Sciences, 4*(3), 35.
52. Hao, X., et al. (2019). Crystal structure optimization and Gibbs free energy comparison of five sulfathiazole polymorphs by the embedded fragment QM method at the DFT level. *Crystals, 9*(5), 256.
53. Sato, T., et al. (1981). Difference in physico-pharmaceutical properties between crystalline and noncrystalline 9, 3"-diacetylmidecamycin. *Chemical and Pharmaceutical Bulletin, 29*(9), 2675–2682.
54. Egawa, H., et al. (1992). Solubility parameter and dissolution behavior of cefalexin powders with different crystallinity. *Chemical and Pharmaceutical Bulletin, 40*(3), 819–820.
55. Mullins, J. D., & Macek, T. J. (1960). Some pharmaceutical properties of novobiocin. *Journal of the American Pharmaceutical Association, 49*(4), 245–248.
56. Imaizumi, H., Nambu, N., & Nagai, T. (1980). Stability and several physical properties of amorphous and crystalline forms of indomethacin. *Chemical and Pharmaceutical Bulletin, 28*(9), 2565–2569.
57. Miyazaki, S., Hori, R., & Arita, T. (1975). Physico-chemical property and gastrointestinal absorption of some solid phases to tetracycline (author's transl). *Yakugaku zasshi: Journal of the Pharmaceutical Society of Japan, 95*(6), 629–633.
58. Wang, G., et al. (2015). Advances in lipid-based drug delivery: Enhancing efficiency for hydrophobic drugs. *Expert Opinion on Drug Delivery, 12*(9), 1475–1499.
59. Zhang, N., Wardwell, P. R., & Bader, R. A. (2013). Polysaccharide-based micelles for drug delivery. *Pharmaceutics, 5*(2), 329–352.
60. Allen, T. M. (1997). Liposomes. *Drugs, 54*(4), 8–14.
61. Soukasene, S., et al. (2011). Antitumor activity of peptide amphiphile nanofiber-encapsulated camptothecin. *ACS Nano, 5*(11), 9113–9121.
62. Dubey, P., Barker, S. A., & Craig, D. Q. (2020). Design and characterization of cyclosporine A-loaded nanofibers for enhanced drug dissolution. *ACS Omega, 5*(2), 1003–1013.
63. Gordon, V., Marom, G., & Magdassi, S. (2015). Formation of hydrophilic nanofibers from nanoemulsions through electrospinning. *International Journal of Pharmaceutics, 478*(1), 172–179.
64. Aytac, Z., et al. (2019). Fast-dissolving electrospun gelatin nanofibers encapsulating ciprofloxacin/cyclodextrin inclusion complex. *Colloids and Surfaces B: Biointerfaces, 178*, 129–136.
65. Celebioglu, A., & Uyar, T. (2021). Electrospun formulation of acyclovir/cyclodextrin nanofibers for fast-dissolving antiviral drug delivery. *Materials Science and Engineering: C, 118*, 111514.
66. Lee, I. W., et al. (2017). Fabrication of electrospun antioxidant nanofibers by rutin-pluronic solid dispersions for enhanced solubility. *Journal of Applied Polymer Science, 134*(21).

67. Masoumi, S., Amiri, S., & Bahrami, S. H. (2018). PCL-based nanofibers loaded with ciprofloxacin/cyclodextrin containers. *The Journal of The Textile Institute, 109*(8), 1044–1053.
68. Wang, Chuan, et al. (2015). Enhanced bioavailability and anticancer effect of curcumin-loaded electrospun nanofiber: in vitro and in vivo study. Nanoscale research letters 10(1):1–10.
69. Vigh, T., et al. (2017). Oral bioavailability enhancement of flubendazole by developing nanofibrous solid dosage forms. *Drug Development and Industrial Pharmacy, 43*(7), 1126–1133.
70. Adeli, E. (2015). Irbesartan-loaded electrospun nanofibers-based PVP K90 for the drug dissolution improvement: Fabrication, in vitro performance assessment, and in vivo evaluation. *Journal of Applied Polymer Science*, *132*(27).



Taha Umair Wani received his bachelor's degree in pharmacy from the University of Kashmir, J&K, India, in 2012 and a master's degree in pharmaceutics from Punjab Technical University, Punjab, India, in 2014. He completed his Ph.D. degree in pharmaceutics from the University of Kashmir, India in 2020.

He is currently working as a Research Associate under the supervision of Dr. Faheem A. Sheikh, Department of Nanotechnology, University of Kashmir. He is the author of more than 25 publications. His research interest includes drug formulation development, nanomedicine, biopharmaceutical and pharmacokinetic evaluation of new drug formulations, bioanalytical method development, and fabrication of nanotechnology-based materials for tissue engineering applications.



Taseen Aamir Wani was born in 1989 in J&K India. He received his bachelor's degree in science from the University of Kashmir, Srinagar, J&K, India, in 2010 and the master's degree in chemistry from Lovely professional University, Punjab, India, in 2013. He completed his M.Phil. in 2021 in analytical chemistry from the Department of Chemistry, University of Madras, Tamil Nadu, India. He is the author of 2 publications. His research interests include natural product chemistry, essential oil extraction, characterization drug delivery systems, and photocatalytic reactions.



Anjum Hamid Rather was born in Bandipora, India, and studied for her M.Sc. in the Department of Bioresources, University of Kashmir, Hazratbal Srinagar. In 2020, she became the recipient of a Maulana Azad National Fellowship by University Grants Commission (UGC) for pursuing her Ph.D. research for five years. From the last year, she has been a Ph.D. scholar in the Department of Nanotechnology, University of Kashmir, Srinagar, under the supervision of Dr. Faheem A. Sheikh. She is working on nano-regenerative medicine that develops polymeric nanofibers for advanced tissue engineering and wound healing applications. She has contributed to 2 manuscripts published in the International Journal of Molecular Sciences and Catalysts.



Rumysa Saleem Khan was born in Srinagar, J&K, India in 1995. She received a B.S. degree in Biochemistry in 2016 and an M.S. degree in Biotechnology from the University of Kashmir, Srinagar, in 2018 and was receiving DBT Fellowship. From 2019 to 2020, she was a JRF with Biochemical engineering lab in NIT, Srinagar, where she received MHRD Junior Research Fellowship.

She is currently pursuing a Ph.D. degree under the supervision of Dr. Faheem A. Sheikh at the University of Kashmir, Srinagar, J&K, India and is receiving the Science and Engineering Research Board (SERB) Junior Research Fellowship. She is the author of two articles published in the International Journal of Molecular Sciences and Catalysts journals. Ms. Khan's research interests include biomimicking of biological molecules in the lab, fabrication of biocompatible scaffolds for tissue engineering, nanofiber formation for wound healing and bone regeneration, and exploiting the roles of different nanoparticles in tissue engineering.



Mushtaq A. Beigh is working as an Assistant Professor at the Department of Nanotechnology, University of Kashmir, India. Dr. Beigh has postdoctoral research experience in cellular signaling and disease modeling (2013–2016). He had completed his Ph.D. from the University of Kashmir, India (2008–2012). He heads a laboratory at the University of Kashmir, where they work on a bio-nano interface to understand the molecular basis of nanoconjugate internalization. They also try to understand the growth factor signaling inputs directed at multiple cellular receptors like NRP1 and Integrins in order to work out the mechanistic details of receptor-based internalization.



Faheem A. Sheikh is an Assistant Professor at the Department of Nanotechnology, University of Kashmir, India (2015). He served as an Assistant Professor at the Department of Biotechnology at the Central University of Kashmir, India (2015–2016); Research Assistant Professor, Myongji University, South Korea (2014–2015); Research Professor at Hallym University, South Korea (2012–2014); Post-Doc/Research fellow at the University of Texas Rio Grande Valley, Texas, United States of America (2010–2012) and Research Professor at Myongji University, South Korea (2010). Currently, he is heading a lab, which works on creating different nanomaterials that can be used in various biological applications; this includes cell culturing and microbial assays. He has considerable expertise in the fabrication of polymeric, ceramic, and metal oxide nanofibers using electrospinning, as well as the production of porous scaffolds by solvent casting, salt-leaching, 3D printing, gas forming, sol–gel synthesis, phase separation, freeze-drying, and particulate leaching and self-assembly for hard and soft tissue engineering. He believes that we will always need new and intelligent materials to address the different challenges faced in tissue engineering science. He has more than 15 years of research experience in nanotechnology, focusing on tissue engineering and drug delivery. He has published more than 100 peer-reviewed articles and several book chapters.

Chapter 13
Electrospun Nanofibers based Electrodes and Electrolytes for Supercapacitors



Dheeraj Kumar Maurya and Subramania Angaiah

Abstract In the past decades, over depletion of non-renewable energy sources, ecological concern and abruptly increasing energy demands prompted us to look towards clean energy conversion and storage systems. Electrospinning technology amends its versatility in producing nanofibers from a few to hundred nanometers. The unique properties of 1-D nanofibers (NFs) with high surface to volume ratio and high porosity with low density prevailed them for potential energy application. NFs based materials have received significant attention in electrochemical supercapacitors in the pursuit of modern energy conversion and storage technologies. The present chapter intends to introduce an encompassing overview of electrospun nanofibers' progress in supercapacitor application. The entire chapter comprises four major parts. First part briefs about the introduction of supercapacitors for energy conversion devices. The second part encapsulates the types of supercapacitors, emphasizing their basic mechanisms for energy storage. Present supercapacitors-based technologies have redeemed electrospun NFs as cathodes, anodes, and electrolytes. Principle components of these devices like electrodes and electrolytes have extensively harvested the electrospun NFs in the form of nanowires and nanofibrous mats with different functionalities. The third part summarizes the NFs based on ongoing research on electrode materials for supercapacitors comprising carbon-based materials and nanocomposites, simple metal-oxides, perovskites, spinel-type oxides, etc. The fourth part deals with the electrospun membrane-based electrolytes for supercapacitors. Finally, the chapter concludes with a summary and future outlook of electrospun nanofibrous for advanced energy storage.

Keywords Electrospun nanofibers · Supercapacitors · Electrospun membrane electrolyte · Carbon nanofibers

D. K. Maurya · S. Angaiah (✉)
Electro-Materials Research Laboratory, Centre for Nanoscience and Technology, Pondicherry University, Puducherry 605 014, India
e-mail: a.subramania@gmail.com

© The Author(s), under exclusive license to Springer Nature Switzerland AG 2022

A. Vaseashta and N. Bölgen (eds.), *Electrospun Nanofibers*,
https://doi.org/10.1007/978-3-030-99958-2_13

13.1 Introduction

Electrochemical supercapacitors, preferably termed as ultracapacitors or supercapacitors are electrochemical energy storage devices in which charge storage is achieved by the charging and discharging process at the electrode–electrolyte interface. Such devices have superior advantages like high power densities, ultra-long calendar life and fast charge–discharge capability as compared to batteries [1, 2]. The supercapacitors are generally categorized into two types depending upon their charge accommodation mechanism i.e., electrical double-layer supercapacitors and pseudocapacitors. The third type of supercapacitor so-called hybrid supercapacitor is the combination of EDLCs and pseudocapacitive supercapacitors [3, 4].

Primarily, electrical energy can be stored in two distinct ways i.e. through the Faradic and non-Faradic processes. Faradic process, where the charge accumulation is achieved under electrochemical reaction in the form of oxidation and reduction at electrode–electrolyte interface causing a change in an oxidation state of electroactive materials governing Faraday's law [5–8]. This process follows irreversibility in chemical inter-conversion of electrode materials that impose a constraint of limited cycle life of charging-discharging. Electrochemical energy storage in batteries involves the Faradic process. Battery is the energy storage device in which electrical energy is stored and released through electrochemical conversion via redox processes occurs at anode and cathode [9]. High energy density and cyclic stability serves batteries as a reliable candidate for energy storage. In contrast, the charge storage is achieved by charging and discharging of double layer without any change in phase of electroactive material in non-Faradic process [10]. This process is independent of physical and chemical change during charge–discharge cycles which leads to an unlimited cyclic ability. Supercapacitors relies on the non-faradic processes. The comparison of performance characteristics among capacitor, electrochemical capacitor and battery is tabulated in Table 13.1.

Table 13.1 Comparison of performance characteristics among capacitor, electrochemical capacitor and battery

Characteristics	Capacitor	Electrochemical capacitors	Battery
Storage mechanism	Physical	Chemical	Chemical
Specific power	>10,000	500–10,000	<1000
Specific energy	<0.1	1–10	10–100
Energy limitation	Electrode surface area		Electrode mass
Charge time	10^{-6} to 10^{-3}	Few sec	1–5 h
Columbic efficiency	100	85–98	70–85
Cycle life	Infinite	>500,000	About 1000

13.2 Electric Double-Layer Capacitors (EDLC)

Electric double-layer capacitors (EDLCs) are one in which the capacitance arises due to interfacial charge separation or due to absorption of positive (cation) and negative (anion) ions at the electrode–electrolyte interface [11, 12]. Highly porous carbonaceous materials are extensively used electrode materials because such capacitance profoundly relies on the surface morphology i.e., porosity and chacracteristic surface area of electrode material. Helmholtz firstly introduced the model to formulate specific capacitance obtained by charge separation using the conventional equation for capacitance in a parallel plate capacitor [13–16].

$$\mathbf{C} = \frac{\varepsilon_0 \varepsilon_r A}{d}$$

where ε_0 and ε_r the electrolyte dielectric constant in a vacuum and medium, respectively, d refers to the adequate thickness of the double layer or distance between electrode and electrolyte ions and A refers to the electrode's characteristic surface area. The schematic model for the proposed mechanism for the formation of the electrical double layer model is depicted in Fig. 13.1.

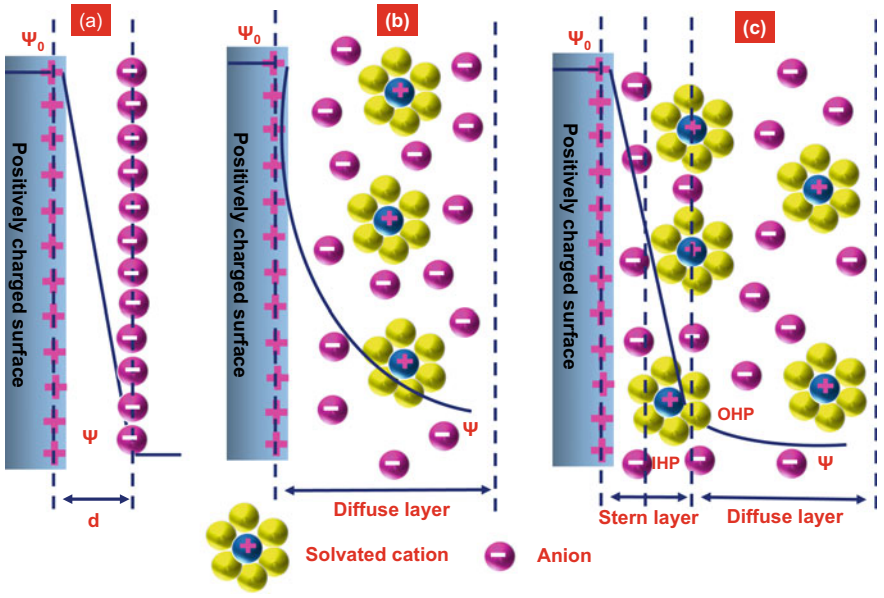


Fig. 13.1 Schematic diagram of **a** Helmholtz model. **b** Guoy-Chapman model. **c** Stern model of the mechanism for formation of electrical double layer model

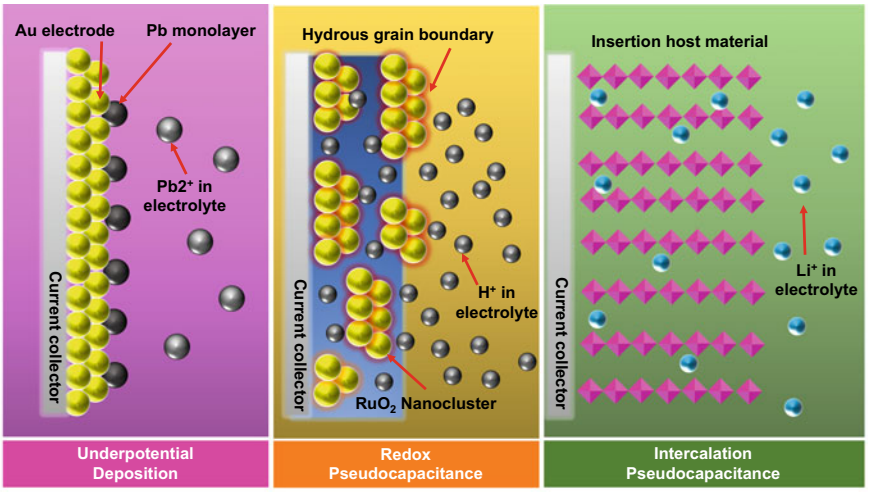


Fig. 13.2 Schematic diagram for types of reversible redox mechanism occurs in pseudocapacitive material

13.2.1 Pseudocapacitors

The term 'pseudo capacitance' was coined by Conway, which mainly refers to the material that exhibits superactive characteristics similar to EDLCs [1]. In contrast with the EDLCs, pseudocapacitors rely on faradic intercalation of charges, i.e., transfer charges between electrode and electrolyte [17–19]. The charge transfer process is thrived via surface adsorption of ions, redox reactions and intercalation occurs at electrodes. The charge storage mechanisms in pseudocapacitive materials can be interpreted based on the following charge accumulation process involved; (i) whether charge accumulates at or near surface-redox reactions; (ii) charge intercalation-type reactions (reversible oxidation and reduction process) [20, 21]. The schematic for a different type of redox mechanism that occurs in pseudocapacitive materials is shown in Fig. 13.2.

13.2.2 Hybrid Supercapacitors

Hybrid supercapacitors have emerged from the coupling of Faradic and Non-Faradic processes. It involves the pseudocapacitive as well as EDLC type electrode material. The high pseudocapacitance produces a higher specific capacitance, whereas a EDLC electrode enables high power density with ultra-long cyclic stability [22–25]. The hybrid supercapacitors are dominant over the pseudocapacitive and EDLC based capacitors in terms of electrochemical performance. These capacitors employ both EDLC and faradic charge mechanisms to store [6, 26]. Despite decades of research,

electrochemical capacitors are suffering from the lack of high energy density equivalent to batteries and fuel cells. These devices are incapable of proving their viability for the applications demanding excellent energy density to run. Generally, the energy density of an electrochemical capacitor can be formulated by using the following formula [27],

$$E = \frac{1}{2}CV^2$$

where C refers to the specific capacitance offered by electrochemical capacitor and V refers to the working voltage. It is noteworthy from the above expression that energy density could be enthusiastically enhanced by empowering either the capacitance (C) or voltage (V) of electrochemical capacitors or both involving parameters to be increased simultaneously [6, 11, 28, 29]. It is evident that higher effort to be laid to the new electrolyte materials for widening working potential window rather than improving capacitance of electrochemical capacitors via development of advanced nanostructured material for high energy density supercapacitors. Electrolyte research has gained exceptional attention for advanced electrolyte systems with new and optimized structures.

Owing to the controllable architecture, high surface area, and facile synthesis, the electrospinning technique is highly preferred over other processes such as template-directed synthesis, solution-phase preparation, melt-blown synthesis, self-assembly preparation and electrodeposition etc. [30–32] Electrospun polymer membranes (ESPMs) have a wide application in efficient air and liquid filtration, electrolyte cum separator, electrode material in the battery, fuel cells and supercapacitors, electrolyte for dye-sensitized solar cells, wound healing, tissue engineering, sensors and drug delivery, etc. [33–36] In the context of the electrochemical supercapacitor, enormous work has been reported for the development of electrospun materials as an electrode and several excellent studies are published in recent years [31, 33, 37, 38]. The presently investigated nanofiber-based materials for electrochemical supercapacitors are shown in Fig. 13.3.

13.3 Electrospun NFs Based Electrodes

A large emphasis has been devoted to the research on advanced materials for electrodes due to their exceptional characteristics like active surface, high characteristic surface area, small diffusion path, facile stress relaxation processes, etc. [33, 34, 36, 39] A wide range of nanostructured materials like carbonaceous materials and pseudocapacitive materials have been scrutinized to improve the supercapacitor characteristics. Despite these advantages, the materials suffer from critical challenges such as tedious synthesis process, extended time interval, insubstantial utilization of active sites and intriguing composition miscibility. Unlike traditional nanostructured materials, one-dimensional (1D) NFs extensively addresses the limitations of

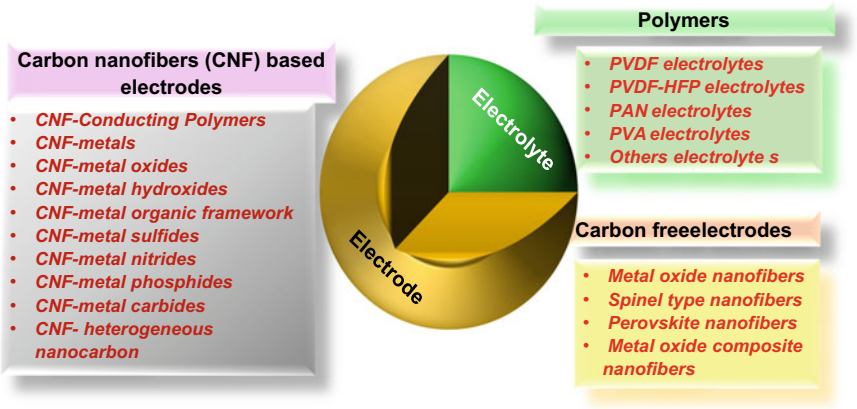


Fig. 13.3 Various types of nanofiber-based materials used for electrochemical supercapacitors

existing electrode materials owing to high mechanical strength, reasonable diffusion length and active electron transport. The advantage of the nanofibrous electrodes is the tuneable surface morphologies, high aspect ratio, wide surface area, excellent wettability and ability to act as a freestanding electrode free of binders conductive agents [30, 31]. Therefore, the electrospun one dimensional NFs have shown an extreme potential as an electrode for supercapacitors.

13.3.1 Carbon Nanofibers (CNFs)

CNFs are the excellent electrode material dominant over other nanostructured materials due to their exceptional chemical and physical characteristics like abundant in nature, high conductivity, admirable corrosion resistance, high thermal stability, chemical inertness, and easy processability at the industrial scale [40–42]. Different carbon functionalities CNFs can be prepared due to their existence in other allotropic forms. This feature of carbon serves them as potential electrode material with required physical and chemical characteristics for the electrochemical energy storage applications. The optimal condition to obtain CNF relies on the polymer precursors employed for electrospinning. A wide variety of polymers and natural materials such as polyacrylonitrile (PAN) [43], polymethacrylate (PMMA) [44], sucrose [45], polyethylene oxide (PEO) [46], poly(vinylidene fluoride) (PVDF) [47], lignin [48], poly(vinyl alcohol) (PVA) [49], polyvinylchloride (PVC) [50], polystyrene (PS) [51], polybenzimidazole [52], polyimide (PI) [53], phenolic resin [54], biochar [55], poly(vinyl pyrrolidone) (PVP) [56] and cellulose [57] acts as an host polymer to produce CNFs after subjecting to carbonization process at an elevated temperature and inert atmosphere [37, 58]. Among all the precursor materials, polyacrylonitrile

(PAN) is an extensively used polymer due to its high melting point, high yield (50–55%), low monomer content, flexibility, eco-friendliness and high strength. Preparation of CNFs proceeds into two steps i.e. stabilization followed by a carbonization process. As obtained carbonized carbon are generally used in two ways i.e. either directly or grounded in powder form with a binder, solvent, active materials and current collector for electrode preparation. These hierarchical CNFs facilitate a better diffusion and electro-sorption of electrolyte ions. Moreover, the different architectural form of CNFs (i.e. micropores, mesopores and macropores) have been extensively harvested for current electrochemical capacitor applications.

Further improvement in electrochemical characteristics of electrospun CNFs is done by adopting approaches such as activation treatment with chemicals and gases, polymer blending, the addition of metal salts, insertion of heteroatoms and employing templates in polymer-based solutions [40, 41]. For example, CNFs with varying porosity were produced using PAN polymer-based electrospun NFs with different gases (N_2, H_2O and CO_2) as an activation media at temperature of 800 and 900 °C, respectively. The CNFs produced via activation in H_2O media exhibited a maximum reduction in diameter of synthesized CNFs. The pore structure of CNFs is also engineered via carbonization of electrospun polymer blends. In another report, CNFs were prepared using nanocasting and electrospinning technique with adjustable microporosity. Phenolic resol and partial-hydrolyzed tetraethyl orthosilicate were used as a carbon precursor and template, respectively for CNF formations shown in Fig. 13.4a. As prepared CNFs, based symmetric supercapacitor device with (PVA)-H_2SO_4 gel-electrolyte delievered a specific capacitance of 220 F g^{-1}@0.5 A g^{-1} with a 92% of its initial capacitance over 3000 charge-dishcarge cycles shown in Fig. 13.4b–f [59].

In reported work, CNFs were derived from the PAN/PMMA (5 wt%) polymer blend dissolved in N, N′-dimethyl formamide (DMF) with subsequent carbonization and activation using CO_2 at a temperature of 1000 °C in a helium atmosphere. As synthesized CNFs, demonstrated a high characteristic surface area of 2419 m^2 g^{-1} [44]. The fabricated EDLC device employing an ionic liquid electrolyte (ethylmethyl imidazolium bis (trifluoromethylsulfonyl) imide (EMITFSI)) delivers a capacitance of 140 F g^{-1}@1 A g^{-1} with an energy density of 67 and 101 W h kg^{-1} in the operating potential of 3.5 and 4 V, respectively. Interestingly, the addition of inorganic metal salts induces porous structure in electrospun CNFs. Previous studies stated that the adding NaCl to polymer solution felicitates more oxygen moieties on CNF's surface whereas $NaNO_3$ addition in lignin solution promotes the higher energy density of CNFs. Highly porous CNFs were also prepared using mesoporous silica template into polymer solution (PAN/PVDF) and finally, etching out the silica. As prepared CNFs, shows a high surface area of 593 m^2 g^{-1} and also delivered a high capacitance of 287 F g^{-1}@0.4 A g^{-1} [60]. Similarly, PAN-based CNFs with macroporous, mesoporous and microporous morphology have been synthesised to employ SiO_2 (50 wt%) as a template followed by KOH activation. As synthesized CNF, displays a high characteristic surface area and micro, meso, and macro-volume of 1632 m^2 g^{-1}, 0.60 cm^3 g^{-1}, 0.93 cm^3 g^{-1}, and 12.09 cm^3 g^{-1}, respectively. Heteroatom doping (N, P, S, B, F, etc.) in CNFs also lead to the superior electrochemical performance of

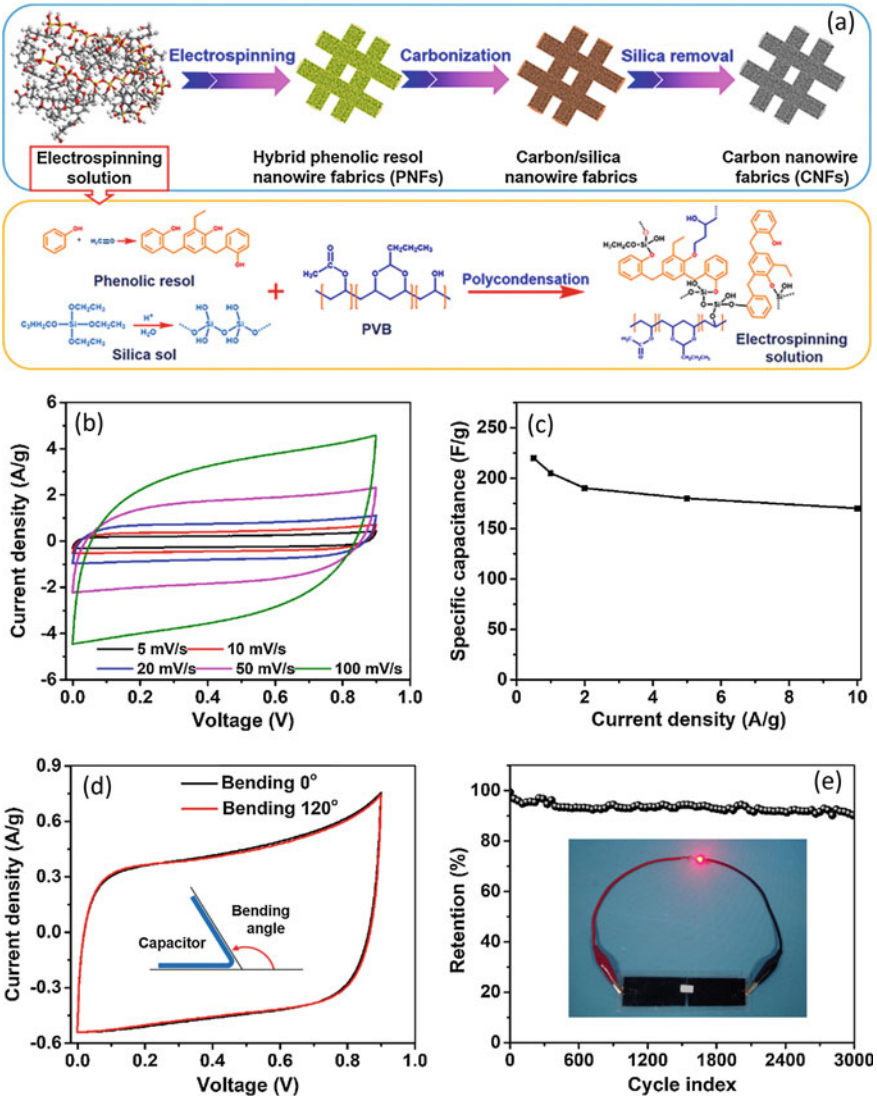


Fig. 13.4 **a** Schematic diagram for the preparation of CNFs. **d–e** Device performance of assembled solid-state supercapacitors using optimized CNF-20-10. Reused from Ref. [59] Copyright © 2018 Published by Elsevier

supercapacitors due to the synergistic effect. Among all doped heteroatoms, N-doped CNFs are extensively explored as electrode material.

13.3.2 Carbon-Composite NFs

Recently, one-dimensional CNFs with high aspect ratio, chemical inertness, extended length, presence of defects serves them as an excellent host material to develop advanced carbon composite electrode materials for electrochemical supercapacitors. Recently reported metal and metal oxides are widely investigated due to their high theoretical specific capacity. Burning issues like low electronic conductivity, instability and poor ion-diffusion limited their practical ability. Coupling of carbon nanofiber with the metal or metal oxide provides several advantages like inhibition of Aggregation of active material, improved electroactive surface area, widen electrochemical stability window and efficient electron transport in electrochemical supercapacitor applications. Carbon nanofiber-based composites are widely investigated in the form of CNF/Metals, CNF/Metal oxide, CNF/Conducting Polymer, CNF/Metal–organic framework, CNF/Metal hydroxide, CNF/Metal Phosphides, CNF/Metal Carbide, CNF/Metal Nitride and CNF/Metal Sulfide have been explored for supercapacitors.

The inclusion of metals (Ni, Co, Cu, Sn) [61–64] in CNFs serves as redox centers for improving the electrochemical performance of supercapacitors. Very recently, CNF/Ni (22.4 wt%) NFs were synthesised from solution of nickel acetate with PAN polymer via electrospinning. As obtained NFs were further subjected to the heat treatment in an air atmosphere at 280 °C for stabilization and further calcined at 1000 °C. CNF/Ni NFs shows a high capacitance of 164 F g^{-1}@0.25 F g^{-1} in 6 M KOH solution. The obtained value of capacitance was found three times higher as compared to the pristine CNFs [61]. Tremendous research work has been done on CNF/metal composite (CNF/Ru, CNF/Pt, CNF/A g, CNF/Ru–A g and CNF/Fe–Co) [65–69] for supercapacitors.

Metal oxides are the reliable pseudocapacitive electrode materials due to their excellent redox chemistry. These pseudocapacitive materials along with EDLC type CNFs have been emerged as a promising candidates. Presently, a large number of CNF-metal oxide composites such as CNF/MnO_2 [70], CNF/V_2O_5 [71], CNF/Co_3O_4 [72], CNF/Bi_2O_3 [73], CNF/FeO_x [74], CNF/TiO_2 [75], CNF/SnO_2 [76], CNF/Nb_2O_5 [77], CNF/ZnO [78], CNF/NiO [79], CNF/RuO_2 [80] have been reported for supercapacitor applications. Since, manganese oxide is the most pronounced pseuocapacitive transition metal oxide electrode material as an electrode. Coupling of MnO with CNFs is reported by large number of research groups. For instance, CNF/MnO_2 were synthesized via in-situ redox reaction between $KMnO_4$ and CNFs. As prepared CNF/MnO_2 electrodes demonstrated a capacitance of 557 F g^{-1}@1 A g^{-1} 0.1 M of Na_2SO_4 with an capacity retention of 94% over 1500 cycles [81]. Similarly, MnO_2 nanoparticles embedded PAN/DMF solution were used for preparing CNF/MnO_2 nanocomposite via electrospinning followed by carbonization. As fabricated CNF/MnO_2 delivered a high capacitance of 211 F g^{-1}@0.25 A g^{-1} in 0.1 M of Na_2SO_4 electrolyte solution with an affordable capacity retention of 78.3% over 2000 charge–discharge cycles. In another reported work, a flexible composite

membrane was fabricated using electrosprayed MnO_2 nanoparticle anchored on electropinning derived Fe_3O_4 doped CNFs Fe_3O_4@CNF_{Mn} shown in Fig. 13.5a [82]. As fabricated electrode exhibited a high capacitance of 306 F g^{-1} with 85% capacity retention over 2000 charge–discharge cycles. As prepared nanofibers exhibited a flexible nature which can able to withstand, when subjected to bending force demonstrated in Fig. 13.5b. This is anticipiated due to presence of Fe_3O_4 and MnO_2 beads in interconnected mesh architecture of CNFs shown in Fig. 13.5c–f, which are capable to absorb forces and further serves as a buffer to resist the enlargement of tiny cracks forms during bending. Subsequently, Fe_3O_4 and MnO_2 beads fragment the applied stress in the fiber axis resulting to the decrease in acting force per unit area.

Transition metal sulfides also inherit the advantage of mechanical stability, versatile structural features and attracting electrochemical response have the potential to form CNF/metal sulfides composites but they are suffering from sluggish diffusion reaction and low surface area. Recently a wide variety of electrospun CNF/metal sulfides composites like CNF/CoS_x [83], CNF/NiS [84], CNF/MoS_2 [85], CNF/FeS_2 [86], CNF/VS_2 [87], CNF/WS_2 [88], CNF/NiCoS [89], CNF/$FeCo_2S_4$ [90], CNF/$NiCo_2S_4$ [91] and CNF/$MoSe_2$ [92] etc. have been served as an electrodes for spercapacitors. Recently, CNF/CoS_xNFs were prepared using $Co(NO_3)_2$. $6H_2O$/PAN followed by carbonization and calcination of CNF/Co_3O_4 NFs. As prepared CNF/Co_3O_4 nanofbers were further sulfurized by Na_2S–$9H_2O$ via hydrothermal reaction to obtain CNF/CoS_x. Similar to the metal oxides and metal inclusion, CNF/transition metal nitrides also induce superiorities like enhanced

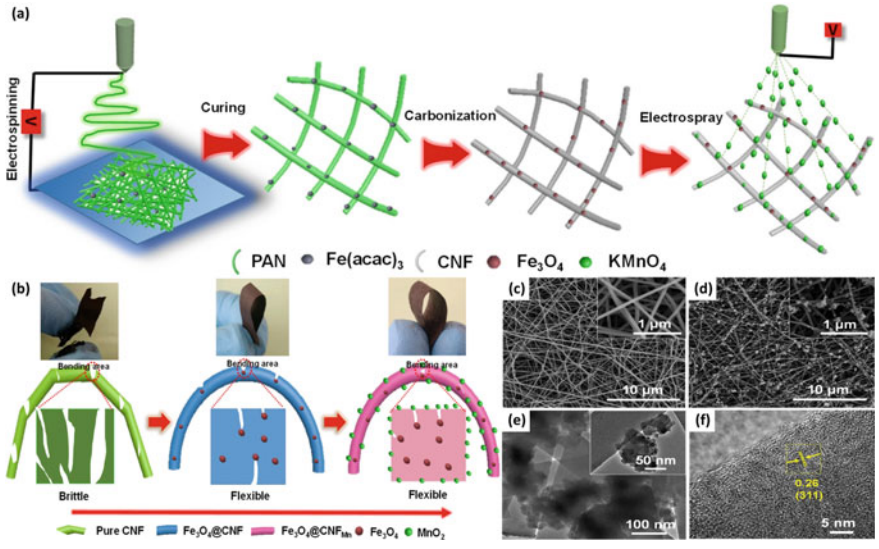


Fig. 13.5 **a** Schematic diagram for the fabrication of Fe_3O_4@CNF_{Mn}. **b** Schematic diagram for the structure and mechanism for the flexibile Fe_3O_4@CNF_{Mn}. **c–d** FESEM images of Fe_3O_4@CNF and Fe_3O_4@CNF_{Mn}. **e–f** TEM and HRTEM image of Fe_3O_4@CNF_{Mn}. Reused from Ref. [82] Copyright © 2017 Springer Nature

capacitance and improved energy densities. Some of the systems like C/VN [93], C/Mo_xN [94], C/FeN_x [95], etc. are recently studied for the supercapacitors applications. Likewise, CNF/transition metal phosphides like CNF/NiCoP, CNF/Ni_1Co_9P, etc. with the feature of multi-electron orbitals, endow outstanding electrochemical performance have been stabilized as a potential electrode material for supercapacitors. Combination of metal carbides with CNF offers a promising alternative for electrode in supercapacitors. Different types of CNF-metal carbide composites (CNF/TiC [96], CNF/$Ti_3C_2T_x$ [97], CNF/W_2C [98], and CNF/Fe_2MoC [99], etc.) have been reported for supercapacitors. Very recently, a $Ti_3C_2T_x$ MXene flakes/PAN/DMF-based precursor solution produced $Ti_3C_2T_x$ MXene flakes-PAN NFs with high loading of MXENE. As obtained NFs further subjected to the carbonization at a temperature of 800 °C in the Ar atmosphere to get CNF/MXene composites. As synthesized CNF/$Ti_3C_2T_x$ MXene based electrode demonstrated an areal capacitance of 239 mF cm^{-2}@10 mV s^{-1}, three times larger than the pristine CNFs [100]. Presently, electrospun CNF/metal hydroxide hybrids have also gained immense attention as an electrode materials. A variety of CNF/metal hydroxide hybrids like CNF/$Ni(OH)_2$ [101], CNF/$Co(OH)_2$ [102] and CNF/NiCoLDH [103] etc. have been reported. Electrospun CNF/metal organic frameworks hybrids also exhibited a potential to use as a supercapacitor electrode. The ability of MOF to turn into versatile architectures same as CNFs, combination of CNFs and MOFs in the form of CNF/MOFs (CNF/ZIF-8 [104], CNF/Ni-CAT [105]) composites may have extensive role in supercapacitors.

Conducting polymers are the extensively explored pseudocapacitive electrode materials. Synergistic coupling of these pseudocapacitive materials with highly EDLC type CNFs is of much interest to improve the electrochemical performance. From previous studies, CNF/PANI [106], CNF-PPy [107], CNF/PPy-rGO [108], CNF/CNT-PANI [109] and CNF/CB-PANI [110], etc. are the reported CNF/conducing polymer composites based electrode materials for supercapacitors. For instance, N-doped C was synthesized via carbonising electrospun PAN/PANI composite NFs. In-situ polymerization method was adopted in conversion of core–shell type N-doped C into PANI-modified N-doped CNFs. Synergistically combined CNF/PANI nanocomposite NFs revealed a remarkable capacitance of 260 F g^{-1} @0.5 A g^{-1} with a 60% of its initial capacitance at 12 A g^{-1}. As fabricated device retains 80.1% of its initial capacitance value over 10,000 charge–discharge cycles at 2 A g^{-1} [111]. Designing a new composites relies on the hybridization of carbon-based nanostructures to achieve improved electrochemical performance. Graphene is a highly exploited additive material for improving the electrochemical performance of pristine CNFs. Carbon nanotubes (CNTs) with a one-dimensional tube-like morphology and appreciable electrical conductivity have also a scope to intervene into electrospun CNFs to further improve the electrochemical characteristics of CNFs. Recently, a wide variety of CNFsbased composites (CNF/MWCNT [112], CNF/graphene [113], CNF/rGO [114], CNF/GNWs [115] and CNF/AC [116], etc.) have been studied for supercapacitor applications.

13.3.3 Metal-Oxide NFs

Metal oxide-based electroactive materials have been deemed as a potential candidates for electrodes due to their large earth abundance, facile processability to transform into diverse morphologies, high characteristic surface area and excellent theoretical specific capacitance values. Availability of controllable defect chemistry and diverse surface morphology allows them to improve their practical capacitance values in supercapacitors. A wide variety of metal oxide NFs such as RuO [117], Mn_3O_4 [118], MnO_2, NiO [119], Co_3O_4 [120], TiO_2 [121], Fe_2O_3 [122] and V_2O_5 [122] etc. are reported as an electrode material for supercapacitors. Among all NFs, Ruthenium oxide (RuO_2) NFs exhibits the highest electrochemical characteristics such as high electronic conductivity and unique redox chemistry. Manganese oxide (MnO_2) NFs are also a highly exploited transitional metal oxide materials as an electrode material due to their superior characteristics like excellent redox activity, high occurrence and economical cheaper cost. Cobalt oxide NFs (Co_3O_4) are also a promising candidate as an active electrodes materials due to its high value of theoretical capacitance. In addition to the above-explored metal oxide NFs, Fe_2O_3, CuO, and TiO_2 are marginally used active materials due to the lower theoretical capacities. A huge volume of research articles on 1D-nanofibers has been reported so far, for supercapacitor application.

RuO_2 based nanofiber mats primarily composed of RuO_2 nanoparticles (10 nm) were reported in which these NFs exhibited a high capacitance of 886.9 F g^{-1}@10 mV s^{-1}. For further improving the charge accommodation capacity and proton transport, RuO_2 NFs were coated with RuO_2 thin hydrous layer using the electro-deposition technique. As modified RuO_2 NFs demonstrated a capacitance of 104 F g^{-1} with a capacity retention of 87.2% over 30,000 charge–discharge cycles [123]. In other work, a symmetric supercapacitor based on MnO_2 NFs was reported which delivered a capacitance of 289 F g^{-1} in 0.5 M Na_2SO_4. NiO-based hollow NFs decorated by NiO nanosheets were also produced by electrospinning. As synthesized NiO NFs delivered a higher pseudocapacitance of 336 F g^{-1}@5 mA cm^{-2} as compared to the solid NiO NFs exhibiting an affordable pseudocapacitance of 136 F g^{-1} [124]. Similarly, NiO-based hollow NFs (diameter 10–30 nm) comprising of NiO nanoparticles were derived by electrospinning using PAA as a sacrificial template. As prepared hollow NiO NFs are accomodates large volume variations, thus exhibiting a capacitance of 700 F g^{-1}@2 A g^{-1}, with 80% of its initial value [125]. In another work, tubes like V_2O_5 NFs derived by electrospinning delivered a capacitance of 210 F g^{-1}@1 mA cm^{-2} in an electrolyte solution (2 M KCl) [126]. A remarkable improvement in specific capacitance is also observed for electrospun Co_3O_4 NFs delivering an appreciable electrochemical performance of 340 F g^{-1}@1.0 A g^{-1} in 6 m KOH [120]. In other reported work, Co_3O_4 mesoporous nanotubes were synthesized by optimizing the gradient distribution of PVA molecular weights of $Co(CH_3COO)_2 \cdot 4H_2O$/PVA during electrospinning [127]. This tobular architecture contains PVA low molecular weight at the centre and high molecular PVA at the

outer layer. As synthesized electroactive Co_3O_4 mesoporous were further used for supercapacitor, showing a specific capacitance of 25 F cm^{-3} at 0.01 V s^{-1}.

13.3.4 Spinel Oxides NFs

Spinel oxides have been recently drawn an immense attention asadvanced electrodes for supercapacitors due to their fascinating characteristics like mixed spinel geometry, which involves transition metal with variable oxidation states. Synergistic coupling of two metal oxide systems provides structural robustness, enhanced electronic conductivity, and availability of a 3D migration network with desirable morphology facilitating high charge storage. Recently, a wide range of complex architectures in the form of spinel-type metal oxide NFs such as $CuCo_2O_4$ [128], $ZnCo_2O_4$ [129], $NiCo_2O_4$ [130], $NiMoO_4$ [131], $ZnMn_2O_4$ [132], $CuCo_2O_4$ [133], $TiNb_2O_7$ [134], $LiMn_2O_4$ [135], $LiNi_{0.4}Co_{0.6}O_2$ [136] and $LiNd_{0.01}Mn_{1.99}O_4$ [137] have been employed as an electrode material for supercapacitor application. Core–shell tube-in tube-like hierarchical architectures are more productive in terms of supercapacitor performance as compared to nanotubular and nanofibrous architectures. Recently, reported $NiCo_2O_4$ based tube in-tube architecture delivered a capacitance of 1756 F g^{-1}@1 A g^{-1} in 2 M KOH solution, as compared to the individual $NiCo_2O_4$ based NFs and hollow nanotubes [138]. In other work, $CuCo_2O_4$ webs derived by electrospinning delievered a capacitance of 443.9 mF cm^{-2} [133]. Asymmetric supercapacitor cell with configuration $CuCo_2O_4$/AC demonstrating a high energy and power density of 0.806 mWh cm^{-3} and 7.8 mW cm^{-3}, respectively. The versatile nanoweb-like architecture not only provides an OH^- pathway for ionic transport but also minimizes the electrode–electrolyte interfacial resistance. Similarly, $ZnCo_2O_4$ based NFs and nanowires also serve as a reliable alternative as an electrode for supercapacitor [139]. $ZnCo_2O_4$ NFs based electrodes delivered a capacitance of 770 F g^{-1}@10 A g^{-1} in 6 M KOH while in another work, assemble 10 electrospun $ZnCo_2O_4$ NWs based microelectrodes delivered an excellent energy and power density of 0.065 μWh cm^{-2} and 0.092 mW cm^{-2}, respectively. $TiNb_2O_7$ NFs has also been used for anode for supercapacitor comprising of AC as a cathode and a non-aqueous electrolyte [140]. Electrospun $LiNd_{0.01}Mn_{1.99}O_4$ NFs are also a promising insertion cathode material, when combined with black pearl carbon (BPC) anode in standard 1 M $LiNO_3$ displayed an appreciable energy and power density of 17 Wh kg^{-1} and 397 W kg^{-1}, respectively. The fabricated supercapacitor also retained 86% capacity retention up to 2500 cycles. Same research group further reported $LiNd_{0.01}Mn_{1.99}O_4$ NFs and black pearl carbon based anode material for supercapacitor. Asymmetric supercapacitor cell with configuration $LiNd_{0.01}Mn_{1.99}O_4$ NFs||BPC in 1 M $LiNO_3$ delivers a high capacitance of 48 F g^{-1} @ 0.5 A g^{-1} with 86% of initial capacitance upto 2500 cycles [137].

13.3.5 Perovskites NFs

Perovskites type metal oxide serves as a reliable electrode material exhibiting appreciable capacitive performance toward supercapacitors. The excellent electrochemical characteristics are due to the rich concentration of oxygen vacancies in these perovskites. A supercapacitor based on $La_xSr_{1-x}NiO_{3-d}$ ($0.3 \leq x \leq 1$) NFs was reported which exhibited excellent electrochemical properties (719 F g^{-1}@2 A g^{-1}) [141]. Similarly, $La_xSr_{1-x}Co_{0.1}Mn_{0.9}O_{3-\delta}$ ($0.3 \leq x \leq 1$) NFs demonstrated a capacitance of 485 F g^{-1} @1 A g^{-1} in 1 M KOH. The influence of doping Ba, Ca on Sr site and Co, Fe, Ni on Mn site were studied, respectively in terms of their supercapacitive performance of $SrMnO_3$NFs [142]. This work witnessed that the addition of 20 mol% Ba into $SrMnO_3$ matrix led to improved capacitance from 321.7 F g^{-1} to 446.8 F g^{-1}@0.5 A g^{-1}. As fabricated asymmetric type supercapacitor with configuration $Sr_{0.8}Ba_{0.2}MnO_3$/0.5 M Na_2SO_4/AC exhibited demonstrated a capacitance of 423 F g^{-1}.

13.3.6 Metal-Oxide Metal-Oxide Composites NFs

Recently, the strategy of combining metal-oxide with hierarchical architecture with the other metal-oxide-based heterostructure is gaining interest. Efforts have been laid toward enhancing the supercapacitor performance of binary or multiple metal oxides with complementary characteristics. These composite NFs offer more affluent redox chemical capability causing an enhancement in specific capacitance and energy density. Tin doped indium oxide@Manganese oxide (ITO@Mn_3O_4) based nanocomposite electrode aiming to overcome shortcomings of Mn_3O_4. ITO@Mn_3O_4 nanocomposite electrodes demonstrated a capacitance up to 823 F g^{-1} at 1 mA cm^2 in Na_2SO_4 electrolyte [143]. As fabricated symmetrical supercapacitors device demonstrated an appreciable energy and power density of 88 Wh kg^{-1} and 550 W kg^{-1}, respectively in the potential window of 2.2 V. Similarly, shortcomings of low ionic conductivity of MnO_2 and TiO_2 are successfully overcome by synthesizing three-dimensional core cell structure TiO_2 NFs wrapped by homogeneously grown MnO_2 nanosheets [144]. The developed hierarchical structure demonstrated an improved capacitance of 525 F g^{-1}@0.25 A g^{-1} superior to pristine MnO_2 nanosheets exhibiting a capacitance of 220 F g^{-1}. As fabricated supercapacitor cell exhibited excellent stability with 81% capacity retention over 2000 charge–discharge cycles. In other work, CuO@Co_3O_4 nanowires comprised of densely packed nanoparticles with a size regime of 5–10 nm were reported for supercapacitor application. Synergistically twinned highly conducting metal oxides demonstrated a capacitance of 1273 F g^{-1}@1 A g^{-1} than the pristine Co_3O_4 nanowires (1105 F g^{-1}) and CuO NWs (657 F g^{-1}), respectively. As fabricated cell exhibited excellent cyclic stability up to 2000 cycles [145]. Full cell with configuration (CuO/Co_3O_4 NWs//AC) demonstrated a high energy and power density of 44 Wh kg^{-1} and 14 kW kg^{-1},

respectively. Similarly, other metal oxides ZnO@MnO_2 [146], ITO@Mn_3O_4 [143], Co_3O_4@NiO [147], Co_3O_4@RuO_2 [148], Co_3O_4@CuO [145], $NiFe_2O_4$@$CoFe_2O_4$ [149], $La_{0.7}Sr_{0.3}CoO_{3-\delta}$@$MnO_2$ [150], SnO_2@TiO_2 [151], Mn_2O_3@$ZnMn_2O_4$ [152], MnO_2@TiO_2 [144] and Co_3O_4@$NiMoO_4$ [147] based electrodes are reported for supercapacitors. The advantage of different electrode materials is summarized in Table 13.2.

Table 13.2 Reported 1D-nanofibrous materials as the electrode in supercapacitors and their advantages

Electrode materials	Advantage	Examples
Metal-oxide	Large earth-abundance, ability to transform into diverse morphologies, high characteristic surface area, high theoretical specific capacitance	RuO, Mn_3O_4, MnO_2, NiO, Co_3O_4, TiO_2, Fe_2O_3, V_2O_5, CuO
Perovskites	High power and energy densities, high oxygen vacancies	$CeMnO_3$, $La_xSr_{1-x}NiO_{3-\delta}$, $Sr_{0.8}Ba_{0.2}MnO_3$, $La_{0.85}Sr_{0.15}Mn_{0.9}Ni_{0.1}O_3$, $La_{0.7}Sr_{0.3}FeO_3$, $Gd_{0.7}Sr_{0.3}NiO_3$
Spinel type	Mixed spinel geometry, high structural stability, improved electronic conductivity, 3D migration network	$CuCo_2O_4$, $ZnCo_2O_4$, $NiCo_2O_4$, $NiMoO_4$, $ZnMnO_4$, $CuMn_2O_4$, $TiNb_2O_7$, $LiMn_2O_4$, $LiNi_{0.5}Mn_{0.4}O_4$, $LiNd_{0.01}Mn_{1.99}O_4$
Metal oxide-metal oxide composite	High concentration of active sites, high characteristic surface area, variable oxidation state, Diverse morphologies	Co_3O_4/$NiMoO_4$, Co_3O_4/NiO, Co_3O_4/RuO_2, Co_3O_4/CuO, $NiFe_2O_4$/$CoFe_2O_4$, $La_{0.7}Sr_{0.3}CoO_{3-\delta}$/$MnO_2$, SnO_2/TiO_2, Mn_2O_3/$ZnMn_2O_4$, MnO_2/TiO_2, TiO_2/MnO
Carbon	Earth-abundant, High characteristics surface area, chemical inertness, easy processability, diverse morphological functionalities	–
Carbon composite	High characteristics surface area, high stiffness, chemical resistance, high temperature tolerance	CNF/Metals, CNF/Metal oxide, CNF/Conducting Polymer, CNF/Metal organic framework, CNF/Metal hydroxide, CNF/Metal Phosphides, CNF/Metal Carbide, CNF/Metal Nitride, CNF/Metal Sulfide

13.4 Electrospun Polymer Membrane Electrolytes (ESPMEs)

Recently, there has been a large wave of publications in the past decade reporting a variety of polymer-based electrolytes for electrochemical supercapacitor applications. Non-woven polymer membranes electrolytes via electrospinning also gaining an exceptional interest exhibiting a reliable performance.

13.4.1 PVDF Based ESPMEs

Polyvinylidene fluoride (PVDF) polymer-based electrolytes are promising candidates suitable for batteries [153–156]. Notable growth in the supercapacitor applications is also observed for PVDF-based electrolytes. PVDF is a semi-crystalline polymer composed of a $–CH_2CF_2$ monomer units. The presence of a highly electronegative fluorine atom and hydrogen atom causes a vital dipole moment in PVDF [157]. Orientation of dipoles is implicitly dominated by the molecular conformation and arrangement of their molecules during crystallization. Based on the crystallization conditions of PVDF, it occurs in four major crystal phases, classified as α, β, γ, and δ crystals. Due to attractive semi-crystalline properties and having a high dielectric constant, PVDF-based electrospun polymer electrolytes are gaining immense attention in Li-ion supercapacitors (LICs).

Recently, one group investigated the supercapacitive performance of commercial cellulose (TF4425), polypropylene (CelAgard 2400) and lab synthesized TUX10 (25% PVDF dissolved in N–N-dimethylacetamide), TUX5 (22.5% PVDF dissolved in DMF/acetone (8:2,w:w)) based electrospun PVDF separators at various temperatures (+24 °C, +10 °C, −10 °C and −30 °C) [158]. They have tested the role of temperatures and separator material characteristics on their supercapacitive performance. It was concluded from the study that supercapacitor characteristics like specific power, specific energy density, time constant, parallel capacitance, and ideal polarizability ($\Delta E \geq 3.2$ V) noticeably depend on the working temperature, morphology, thickness and porosity of an electrolyte separator. Impedance analysis studies revealed that the relaxation time constant increases with a decrease in molar conductivity of the electrolyte in the separator matrix. For temperature ≥ -10 °C, specific energy is independent of separator characteristics. The maximum power density was observed for nanofibrous separator TUX10. Thus, the generation of high power pulses at low temperatures ($T \leq -30$ °C) needs thorough monitoring of separator characteristics. Similarly, the influence of different concentrations of black carbon nanoparticles (0, 0.25, 0.5, 1, 2, and 4 wt%) on the electrochemical behaviour of composite PVDF/PVP nanofibrous membranes were investigated [159]. PVP was blended with PVDF to overcome conductivity limitation due to the high crystallinity of PVDF and also to improve electrospinnability of polymeric solution. 4 wt% of carbon embedded PVDF/PVP nanocomposite separator exhibited the highest value

of the dielectric constant of 6.28 at 150 °C. Minor improvement in thermal stability was observed upon addition of carbon lack nanoparticles PVDF/PVP nanocomposite. PVDF/PVP electrospun membranes containing 4 wt% of carbon black nanoparticles demonstrated an affordable specific capacitance of 2.544 F g^{-1}. Improvement of the specific capacitance is attributed to the high conductivity. In another work, the development of a flexible supercapacitor consists of polypyrrole nanoparticles-coated bacterial cellulose core–shell composite network (PPy-TOBC) electrodes and electrospun PVDF membrane as an electrolyte was reported [160]. LIC delivered a capacitance of 153 F g^{-1} at a current density of 0.2 A g^{-1} with cyclic stability of ~93% over 100 cycles. The specific capacitance of the flat supercapacitor is retained even after bending with an angle of 150 °C. Excellent electrochemical characteristics are credited to the highly meso-macroporous morphology that improved the ion transfer efficiency and charges accomodation capacity and the short ion diffusion path. Similarly, the role of PVDF-based electrospun separator-cum-electrolyte for supercapacitor was investigated [161]. Blending PVP with PVDF causes phase separation to form microdomains of PVP in PVDF/PVP nanofibrous membrane. Accompanying this behavior, PVP micro domains were leached using ultrasound, which led to a highly meso/macroporous electrospun membrane formation. Sample PUPF with PVDF:PVP mass ratio (10:5) shows the highest electrolyte uptake (360%) and ionic conductivity (1.8 mS cm^{-1}). Characteristic surface area is also increased optimum mass ratio (10:5) due to abundant meso/micropores on the surface. As developed electrolyte exhibited a wide electrochemical stability window of 0–3.3.V. Supercapacitor was developed using activated carbon-based electrodes and liquid electrolyte soaked PVDF electrospun membrane as an electrolyte [162]. This device shows appreciable electrochemical performance of 39.5 F g^{-1} at 100 mA g^{-1}. The flexible polyvinylidene fluoride/tetrabutyl ammonium hexafluorophosphate nanofiber membrane (PVDF/$TBAPF_6$ HNM) was also reported as a separator for LIC to achieve impressive ionic conductivity of 4.28×10^{-3} S cm^{-1} and minimized interfacial resistance im comparison from the commercial celgard 2340 separator well depicted in Fig. 13.6a–f.

13.4.2 PVDF-HFP Based ESPMEs

Recently, PVDF-based copolymers such as polyvinylidene-hexafluorophosphate (PVDF-HFP) drew immense attention in the development of electrolyte materials in modern energy storage devices. The incorporation of hexafluoropropylene functional group enhanced the physicochemical properties like lower crystalline nature, higher solubility, improved mechanical strength and better hydrophobicity compare to PVDF [163–166]. This copolymer is widely investigated for the lithium-ion battery application, but its applicability as an electrolyte material for supercapacitors is still in its infancy stage. Exceptional properties of PVDF-HFP and stability with battery type and EDLC type electrodes make this copolymer suitable for LICs application. For instance, the influence of different concentrations of ZrO_2 (0, 3, 5, 7 and 10 wt%)

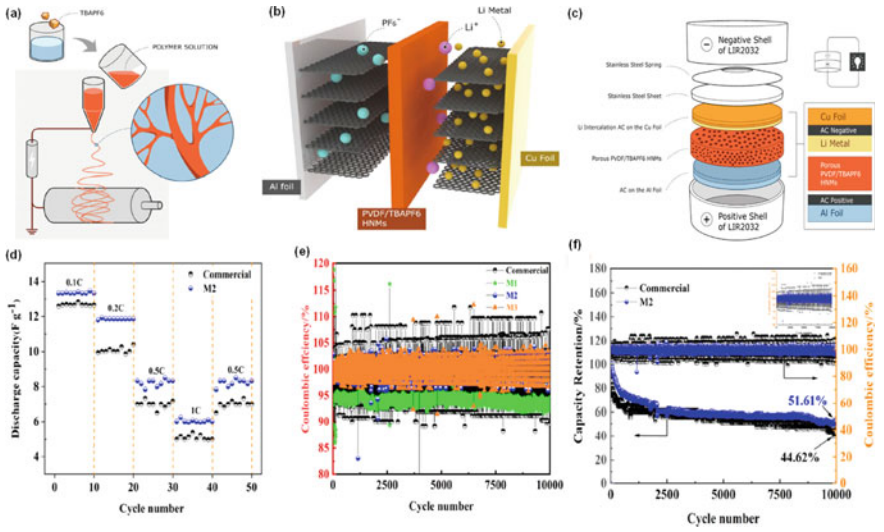


Fig. 13.6 Schematic diagram of **a** synthesis using electrospinning, **b** LIC device, **c** fabrication LIC, **d** rate capabilities, **e** coulombic efficiency, **f** capacity retention and coulombic efficiency of commercial separator and M2. Reused from Ref. [162] Copyright © 2019 Published by Elsevier

on the physical charcateristics and electrochemical performance of PVDF-HFP was carefully studied. The research group in 2017, developed SiO_2 [167] and montmorillonite [168] incorporated electrospun nanocomposite membrane-based electrolytes for LICs shown in Fig. 13.7a. Different weight percentages (3, 5, 7 and 10 wt%) of metal oxide fillers were added to the PVDF-HFP polymer matrix to achieve improved physical and electrochemical properties. $LiCo_{0.2}Mn_{1.8}O_4$/Carbon based LIC was fabricated using these electrolytes membranes soaked in liquid electrolyte. LIC based on PVDF–HFP/MMT (5 wt%) found electrolyte delievered a specific capacitance of 149.2 F g^{-1}@ 1 A g^{-1} with cyclic stability of 90% after 2000 cycles. LIC device fabricated using PVDF–HFP/SiO_2 (7 wt%) based electrolyte delievered a capacitance of 128 F g^{-1}@ 1 A g^{-1} with cyclic stability of 86% after 1000 cycles. Improved characteristics of developed electrolytes are credited to the synergistic interaction between inorganic oxide fillers and organic PVDF-HFP polymer. The impact of different concentrations of ZrO_2 (3, 5, 7 and 10 wt%) on physical and electrochemical properties of PVDF-HFP was systematically investigated. $LiCo_{0.2}Mn_{1.8}O_4$/Carbon-based LIC was assembled using electrospun PVDF-HFP/ZrO_2 nanofibrous composite membrane soaked in 1 M $LiPF_6$ in EC and DMC (1:1 v/v). 7 wt% of ZrO_2 embedded PVDF-HFP electrospun composite polymer membrane demonstrated an excellent electrochemical performance (182.5 F g^{-1}@ 1 A g^{-1}, 92% capacitance retention after 2000 charge–discharge cycles) [169] shown in Fig. 13.7b–d. Similarly, LIC was reported using an electrolyte comprising $Li_{7.1}La_3Sr_{0.05}Zr_{1.95}O_{12}$ incorporated PVDF-HFP nanohybrid membrane [170]. As fabricated LIC with $LiCoO_2$/15 wt%LLSZO/PVDF-HFP/AC exhibited an affordable

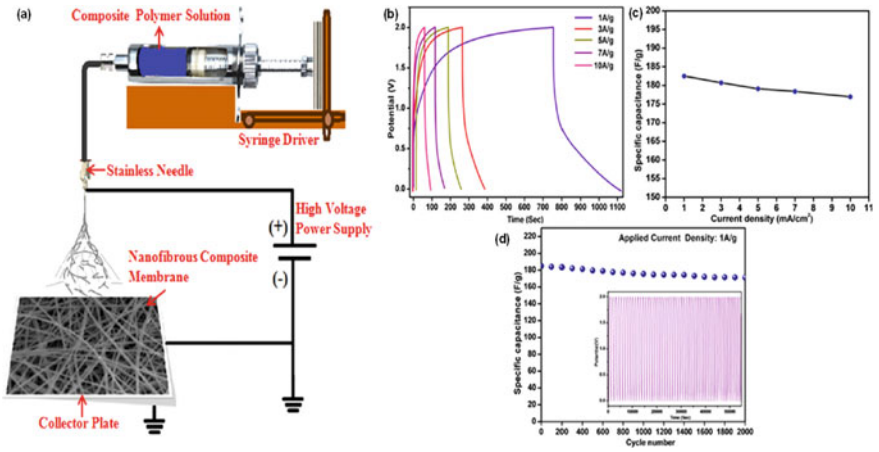


Fig. 13.7 Schematic diagram for preparation of esPM and esCPM (PVDF–HFP/MMT) using electrospinning. **a** is reused from from Ref. [168] Copyright © 2016 Elsevier. **b** GCD plot of LIC. **c** Specific capacitance versus current density. **d** Cyclic stability of LIC assembled using esCPME (7 wt% ZrO_2). **b–d** are reused from Ref. [169] Copyright © 2017 Springer

electrochemical performance (68.75 F g^{-1} @ 1 A g^{-1}, 80% of its initial capacitance after 1000 cycles).

13.4.3 PAN-Based ESPMEs

PAN-based polymer electrolytes are highly desired in batteries due to their superior characteristics like appreciable ion-solvating capability, high thermal stability, flame retarding behaviour, resistance towards oxidative degradation and electrochemical stability [171]. For LIC application, electrospun PAN membrane-based electrolyte has been reported by several research groups. An electrospun PAN NFs as an electrolyte combining the electrospinning and vapor phase evaporation method was reported [172]. The fabricated supercapacitor stack assembly was immersed in a liquid electrolyte containing PVDF-co-HFP and $EMIBF_4$ (1:2). The cell demonstrate an appreciable capacitance of 20 F g^{-1} of active materials, whereas the positive and negative electrode-based half cells have capacitance 75 F g^{-1} and 85 F g^{-1}, respectively. In another work, a supercapacitor based on electrospun PAN polymer fiber-electrolyte membrane with different thicknesses via electrospinning was studied [173]. Electrospun membrane gets extensively swollen when exposed to the DMF vapor. Compressing these solvent-absorbed NFs interlocked them physically. Hence substantial improvement was observed in mechanical properties. As fabricated, solid polymer membrane electrolyte was found superior to the liquid electrolyte. It exhibited a capacitance of 44.2 F g^{-1} along with ohmic resistance of 4.26 Ω. Solid polymer electrolytes with a thickness of 90 μm exhibit better capacitive performance than the

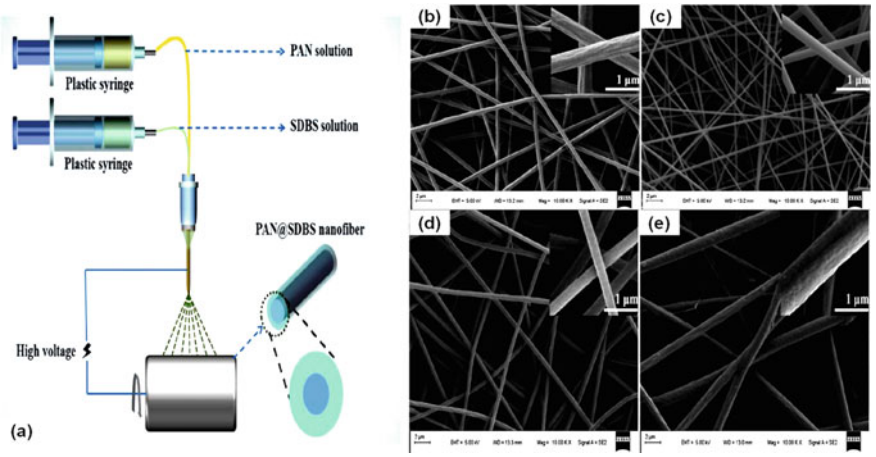


Fig. 13.8 **a** Schematic diagram of preparation of coaxial NFs using electrospinning. SEM images **b** PS-0, **c** PS-5, **d** PS-10 and **e** PS-15 samples. Reused from Ref. [175] Copyright © 2019 Elsevier

solid polymer electrolyte with thickness 30 and 150 μm. In other work, all fiber-based solid-state electrospun supercapacitor was reported in which both the electrodes and electrolytes are in the form of NFs [174]. PAN-nanofiber soaked in 0.25 M aqueous bis(trifluoromethane)sulfonamide lithium (LiTFSI) was used as the electrolyte cum separator. High loading of 40 wt% Manganese acetylonate (MnACAC) was incorporated in PAN polymer solution, causing improved electroactive property through the pseudocapacitive mechanism, ultimately proven better electrochemical performance undoped carbon nanofiber electrodes. PAN separator witnessed remarkable electrochemical performance of 200 F g^{-1} than the pristine PAN nanofiber-based separator and celgard separator. A sodium dodecyl benzene sulfonate coated PAN-based electrospun separator by coaxial electrospinning process was employed to improve the separator's self-discharge behavior on adding different concentrations of sodium dodecyl benzene sulfonate shown in Fig. 13.8a with corresponding SEM images of different samples are also depicted in Fig. 13.8b–e. As prepared, the PAN@SDBS NFs membrane exhibited an excellent inhibition of self-discharge behavior without any sacrificial capacitance.

13.4.4 PVA Based ESPMEs

PVA based polymer have drawn an immense attention for developing electrospun polymer membrane electrolyte (ESPMEs) for supercapacitors. A LIC comprising poly(vinyl alcohol) (PVA)/poly(acrylic acid) (PAA) nanofiber membrane/PVA/H_3PO_4 based gel electrolyte material was reported [32]. As fabricated, LIC delievered a capacitance of 379 F g^{-1}@0.5 A g^{-1}. The architecture

efficiently increases the characteristic surface area of PANI nanoparticles, thus led to the enthusiastic diffusion of electrolyte ions and successive electron transfer in the electrode materials. In another work, an electrospun mat containing graphene oxide (GO) reinforced polyvinyl alcohol (PVA) was reported to get better performance retention [176] shown in Fig. 13.9a and the corresponding SEM image shown

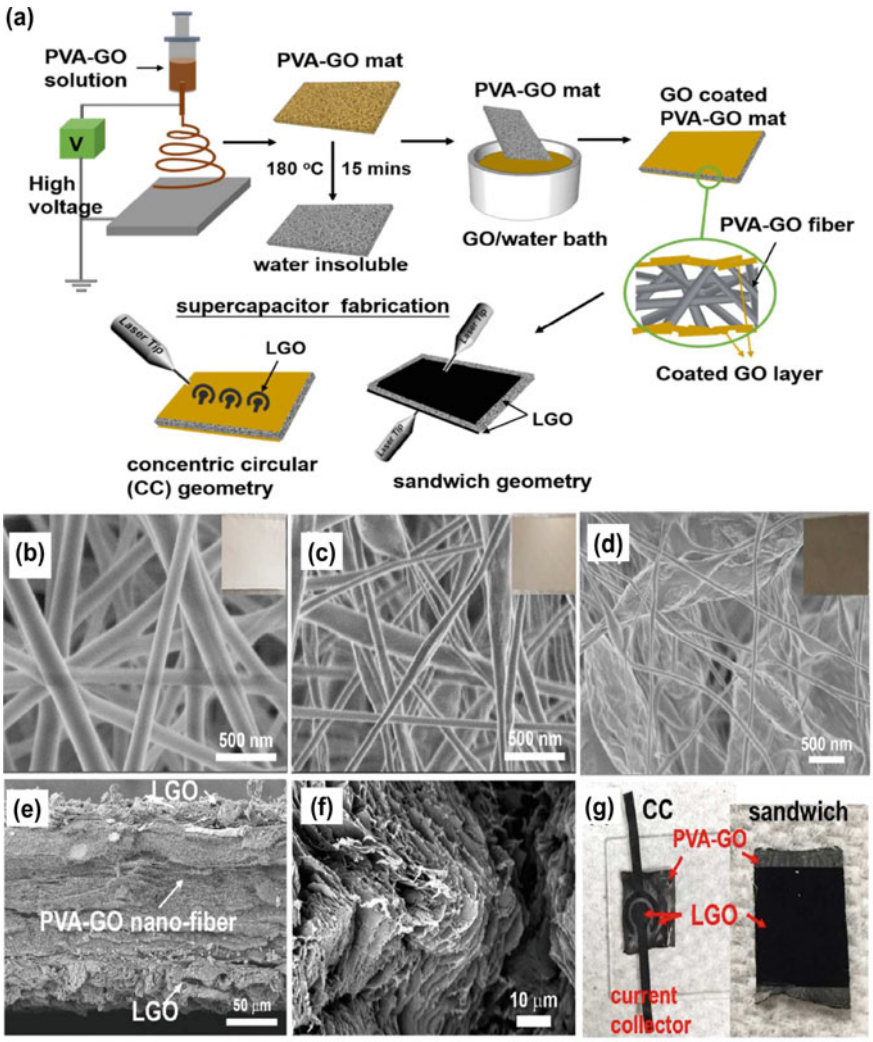


Fig. 13.9 **a** Schematic diagram of preparation of PVA-GO mat and supercapacitor fabrication by using laser patterning processes. SEM images of **b** pure PVA, **c** PVA-GO (25:1, w/w), **d** PVA-GO (10:1, w/w) with insets of their photographic images; **e** cross-sectional SEM of monolithic supercapacitor **f** laser reduced GO (LGO) region; **g** Image of PVA-GO supercapacitor. Images are reused from Ref. [176] Copyright © 2018 American Chemical Society

in Fig. 13.9b–f. PVA-GO mats overcome the low ionic conductivity issue among new PVA mats upon drying, mainly due to graphene oxide's hygroscopic nature and three-dimensional interconnected network. Hygroscopic graphene can retain moisture content over polymer gel electrolytes when subjected to a dry atmosphere, thus improving the long-term stability in energy storage. The developed supercapacitor on the PVA-GO mat shown in Fig. 13.9g, exhibits a capacitance density of 9.9 mF cm^{-2} at 40 mV s^{-1} after one month. LIC shows an appreciable energy density and power density of 0.13 mWh $cm^{-3}$and 2.48 W cm^{-3}, respectively. As developed, LIC was found superior in terms of electrochemical performance compared to its analogs prepared by the solution casting technique.

13.4.5 Other Polymers Based ESPMEs

In addition to the aforementioned electrolyte materials, other polymers like sulfonated poly (ether ether ketone) (SPEEK) and gelatin have been also reported for electrolyte application. An EDLC based capacitor was reported using sulfonated poly (ether ether ketone)/polysulfone (PSF) composite films impregnated with polyvinyl alcohol (PVA)/H_2SO_4 gel and activated carbon as EDLC electrodes. The electrolyte containing SPEEK (SP) and PSF (PS) with 10 g of solution in different characteristic mass ratios (0:1, 1:9, 3:7, 1:1, 7:3 and 1:0) was derived using electrospinning. Among all samples, SP:PS = 3:7 soaked PVA/H_2SO_4 gel demonstrated better electrochemical performance [177]. As fabricated EDLC device demonstrated a high capacitance of 117.1 F g^{-1}. LIC exhibited a 97% capacity retention after 1500 cycles. Gelatine is a polypeptide-based amphoteric polyelectrolyte comprising proline, hydroxyproline and glycine. It is mainly derived from denatured collagen and soluble in boiling water to with pale-yellow colored appearance, semi-transparent and viscous solution. The presence of the hydrophilic group, high salt conductivity, high flexibility and eco-friendly nature prevails gelatine as a potential candidate for polymer electrolytes. Gelatin NFs based gel polymer electrolyte impregnated with 1-ethyl-3-methylimidazolium tetrafluoroborate ($EMImBF_4$) and composite carbon as an electrode was investigated for LIC [178]. An inorganic (Al_2O_3)-organic polyimide (PI) composite membrane was also assessed for LICs [179]. Highly alumina NFs with high thermal stability (Fig. 13.10a), flame retardancy (Fig. 13.10b–e), excellent wettability, coupled with organic PI NFs, are endowed with high flexibility and high ionic conductivity. 50 wt% Al_2O_3-PI nanofibrous composite membrane exhibits an ionic conductivity of 3.85×10^{-3} S cm^{-1}. As developed LIC, this separator showed an appreciable energy density of 57.3 Wh kg^{-1} at 0.5 A g^{-1}.

In other work, buckled single-walled carbon nanotube-based electrodes with electrospun polyurethane (PU) soaked in 1 M organic electrolyte (tetraethylammoniumtetrafluoroborate in propylene carbonate) were employed to fabricate a stretchable supercapacitors [180]. The three-dimensional conduction network of the nanofibrous membrane provides appropriate porosity acts as a channel for ionic conduction of electrolyte ions to drift through the elastomeric separator when subjected to

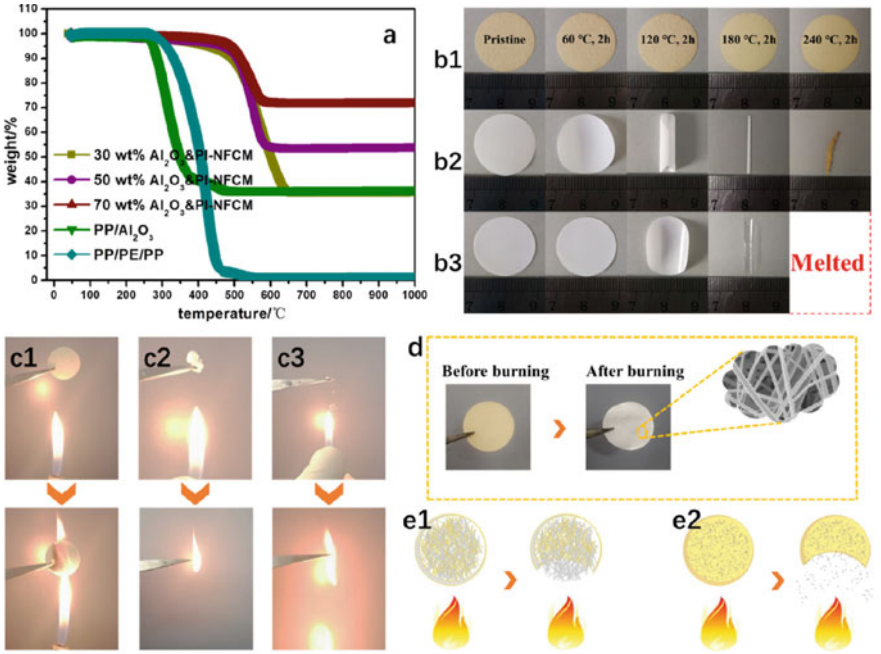


Fig. 13.10 **a** TGA plots for PI NFs membranes, **b** dimensional stability test for (1) 50 wt% Al_2O_3 and PI-NFCMs, (2) PP/Al_2O_3 and (3) PP/PE/PP membranes at different temperatures, **c** Ignition test for (1) 50 wt% Al_2O_3 and PI-NFCMs, (2) PP/Al_2O_3 membranes and (3) PP/PE/PP membranes; **d** Images of 50 wt% Al_2O_3 and PI-NFCMs of pre and post-ignition and **e** the schematic diagram of combustion performance of (1) Al_2O_3 and PI-NFCMs and (2) PP/Al_2O_3 membranes. Images are reused from Ref. [179] Copyright © 2020 Elsevier

dynamic stretching/releasing shown in Fig. 13.11a, b. As fabricated device demonstrated a specific capacitance and total capacitance of ~44 F g^{-1} and 13.2 mF, respectively. Areal capacitance lies from 2.64 mF cm^{-2} at 0% strain applied condition to 3.47 mF cm^{-2}, when 31.5% strain is applied as shown in Fig. 13.11c–f. The performance of ESPMEs for supercapacitors applications is tabulated in Table 13.3.

13.5 Conclusion and Future Outlook

The present chapter discusses the overview of nanofibrous materials harvested for electrochemical capacitors, particularly for Li-ion capacitors. Nanofibrous materials can be designed in different architectural structures like nanofibres, nanorods, nanowires, nanowebs and membranes act as electrode and electrolyte materials for such devices. The versatile morphology of electrospun NFs can be easily tuned by altering electrospinning precursor solution, process parameters, surface modification and post-electrospinning treatments (annealing, stabilization and calcination). It can

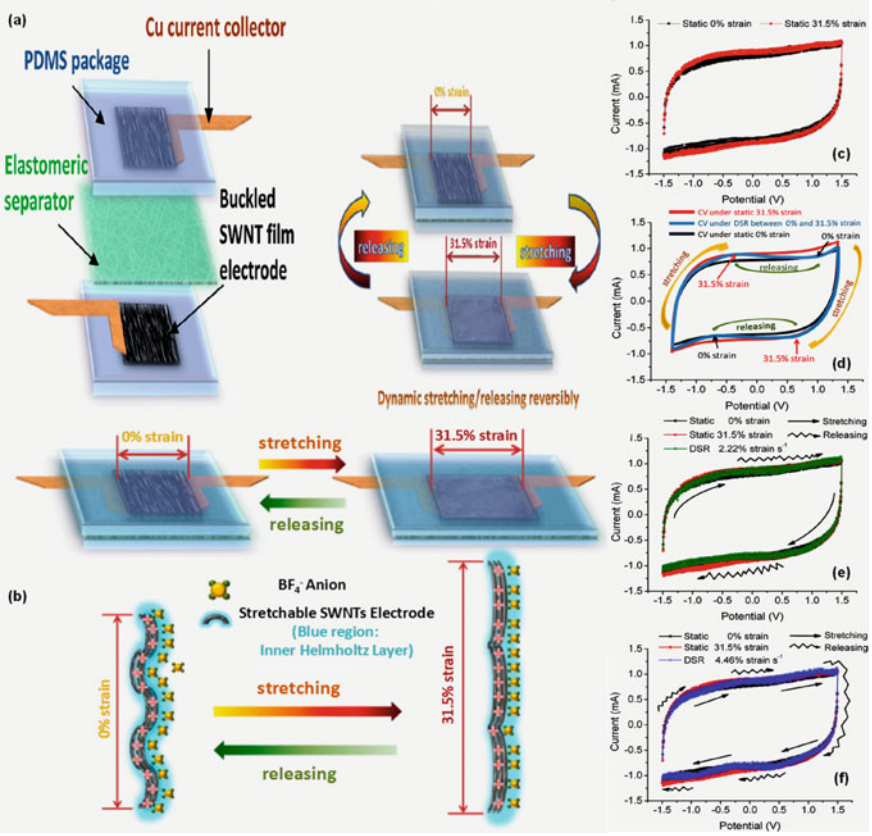


Fig. 13.11 **a** Schematic illustration of stretchable supercapacitor **b** under dynamical conditions between 0 and and 31.5% applied strain. CV curves for **c** CV curves under static modes, **d** DSR modes, **e** DSR modes at strain rate of 2.22% strain s^{-1} and **e** DSR mode at strain rate of 4.46% strain s^{-1}. Images are reused from Ref. [180] Copyright © 2012 American Chemical Society

be concluded from the chapter that the usage of electrospun nanofibers in hybridization of battery and supercapacitor could be a promising approach for current electrochemical energy storage technologies. Meanwhile, realistic applications highly urged for high energy and power density. It is anticipated that explored electrospun nanofiber-based electrode and electrolyte materials are capable to deliver high performance for supercapacitor applications. Nevertheless, technical, experimental and theoretical paradigms should be addressed for the implementation of electrospun nanofibrous materials in electrochemical supercapacitors. Electrospinning parameters should be optimized in a way that there will be the formation of bead-free, uniform and interpenetrating network nanofiber for electrode application. Formation of nanocomposite and nanohybrids using inactive and passive fillers is highly desired for electrolyte development. These practices will certainly scale up the laboratory scale synthesis to the commercial-scale assembly of supercapacitors. Despite

Table 13.3 Performance of ESPMEs for supercapacitors application

Host polymer	Electrodes	Specific capacitance	Energy density	Power density	Cyclic stability	ESW (V)	References
PVDF	Microporous titanium carbide–derived carbon electrodes	–	–	–	–	3.2	[162]
PVDF	Manganese dioxide and lithium	35 at 0.1 C	–	–	10,000 cycles	3.9	[181]
PVDF	PPy-TEMPO-oxidized bacterial cellulose (TOBC)	153 F g^{-1} @0.2 A g^{-1}	6.59	–	93% after 1000 cycles	−0.5 to + 0.5	[160]
PVDF	AC//AC	39.5 F g^{-1}	–	–	–	0–3.3	[161]
PVDF-HFP	AC/$LiCoO_2$	123@1 A g^{-1}	43.77	7.973	83% after 1000	0–1.6	[182]
PVDF-HFP	AC/$LiCo_{0.2}Mn_{1.8}O_4$	182.5@1 A g^{-1}	–	–	92% after 2000	0–2.0	[169]
PVDF-HFP	AC/$LiCoO_2$	68.75@1 A g^{-1}			80% after 1000	0–1.6	[170]
PVDF-HFP	AC/$LiCo_{0.2}Mn_{1.8}O_4$	128@1 A g^{-1}	71.1	9.89	86% after 2000	0–2.87	[167]
PVDF-HFP	AC/$LiCo_{0.2}Mn_{1.8}O_4$	149.2@1 A g^{-1}	–	–	90% after 2000	0–3.1	[168]
PAN	AC//AC	44.2	39.1	12.6		0–2.5	[173]
Manganese acetylacetonate (MnACAC) @ PAN	Carbonised nanofiber electrodes	200@ 2.5 mV s^{-1}	–	–	10,000 cycles	0–1.6	[174]
(PAN@SDBS) NFs	Activated carbon (AC) spread on Ni foam	42.8@0.5 A g^{-1}			84.6% after 10,000	0–1.0	[175]

(continued)

Table 13.3 (continued)

Host polymer	Electrodes	Specific capacitance	Energy density	Power density	Cyclic stability	ESW (V)	References
PVA-GO	Polyaniline (PANI)/carbonized polyimide (CPI)	379 F g^{-1} @0.5 A g^{-1}	–	–	94% after 1000	−0.2 to 0.8	[176]
PVA/PAA	Prelithiated-AC//AC		57.3	750	10,000	3	[32]
PI @ Al_2O_3	AC//AC	117@1 A g^{-1}	12.5	15	10,000	5.3	[179]
SPEEK/polysulfone	–	117@1 A g^{-1}	–	–	97% after 1500 cycles	0–1.0	[177]
PVB @ Al_2O_3 nanowires	AC//AC	181@5 A g^{-1}	–	–	98% after 1500 cycles	0–1.0	[183]

extensive efforts, better insight chemistry of electrospun fiber-based electrode and electrolyte materials need to be understood deeply and more facile protocols for electrospinning technique will be adopted for supercapacitor development.

Acknowledgements Dr. A. S. is thankful to the Council of Scientific and Industrial Research (CSIR), New Delhi (Ref. No. 01(2810)14/EMR-II, dt. 26/04/2017) and the UGC-BSR-Mid Career Award (No. F.19-214/2018(BSR)) for their financial support.

References

1. Simon, P., & Gogotsi, Y. (2008). Materials for electrochemical capacitors. *Nature Materials, 7*(11), 845–854. https://doi.org/10.1038/nmat2297
2. Lang, X., Hirata, A., Fujita, T., & Chen, M. (2011). Nanoporous metal/oxide hybrid electrodes for electrochemical supercapacitors. *Nature Nanotechnology, 6*(4), 232–236. https://doi.org/10.1038/nnano.2011.13
3. Winter, M., & Brodd, R. J. (2004). What are batteries, fuel cells, and supercapacitors? *Chemical Reviews, 104*(10), 4245–4270. https://doi.org/10.1021/cr020730k
4. Conway, B. E. (1999) Similarities and differences between supercapacitors and batteries for storing electrical energy. In B. E. Conway (Ed.), *Electrochemical supercapacitors: Scientific fundamentals and technological applications* (pp. 11–31). Springer US. https://doi.org/10.1007/978-1-4757-3058-6_2
5. Dubal, D. P., Ayyad, O., Ruiz, V., & Gómez-Romero, P. (2015). Hybrid energy storage: The merging of battery and supercapacitor chemistries. *Chemical Society Reviews, 44*(7), 1777–1790. https://doi.org/10.1039/C4CS00266K
6. Chodankar, N. R., Pham, H. D., Nanjundan, A. K., Fernando, J. F. S., Jayaramulu, K., Golberg, D., Han, Y.-K., & Dubal, D. P. (2020). True meaning of pseudocapacitors and their performance metrics: Asymmetric versus hybrid supercapacitors. *Nano-Micro Small, 16*(37), 2002806. https://doi.org/10.1002/smll.202002806
7. Conway, B. E., Birss, V., & Wojtowicz, J. (1997). The role and utilization of pseudocapacitance for energy storage by supercapacitors. *Journal of Power Sources, 66*(1), 1–14. https://doi.org/10.1016/S0378-7753(96)02474-3
8. Bruce, P. G., Scrosati, B., & Tarascon, J.-M. (2008) Nanomaterials for rechargeable lithium batteries. *Angewandte Chemie International Edition, 47*(16), 2930–2946. https://doi.org/10.1002/anie.200702505
9. Tarascon, J. M., & Armand, M. (2001). Issues and challenges facing rechargeable lithium batteries. *Nature, 414*(6861), 359–367. https://doi.org/10.1038/35104644
10. Dubal, D. P., Wu, Y. P., & Holze, R. (2016). Supercapacitors: From the Leyden jar to electric busses. *ChemTexts, 2*(3), 13. https://doi.org/10.1007/s40828-016-0032-6
11. Zhao, J., & Burke, A. F. (2021). Review on supercapacitors: Technologies and performance evaluation. *Journal of Energy Chemistry, 59*, 276–291. https://doi.org/10.1016/j.jechem.2020.11.013
12. Electrochemical Double-Layer Capacitors (EDLC). (2017). *Supercapacitors based on carbon or pseudocapacitive materials* (pp. 1–25). https://doi.org/10.1002/9781119007333.ch1
13. Simon, P., & Gogotsi, Y. (2020). Perspectives for electrochemical capacitors and related devices. *Nature Materials, 19*(11), 1151–1163. https://doi.org/10.1038/s41563-020-0747-z
14. González, A., Goikolea, E., Barrena, J. A., & Mysyk, R. (2016). Review on supercapacitors: Technologies and materials. *Renewable and Sustainable Energy Reviews, 58*, 1189–1206. https://doi.org/10.1016/j.rser.2015.12.249

15. Muzaffar, A., Ahamed, M. B., Deshmukh, K., & Thirumalai, J. (2019). A review on recent advances in hybrid supercapacitors: Design, fabrication and applications. *Renewable and Sustainable Energy Reviews, 101*, 123–145. https://doi.org/10.1016/j.rser.2018.10.026
16. Simon, P., Gogotsi, Y., & Dunn, B. (2014). Where do batteries end and supercapacitors begin? *Science, 343*(6176), 1210–1211. https://doi.org/10.1126/science.1249625%JScience
17. Augustyn, V., Simon, P., & Dunn, B. (2014). Pseudocapacitive oxide materials for high-rate electrochemical energy storage. *Energy and Environmental Science, 7*(5), 1597–1614. https://doi.org/10.1039/C3EE44164D
18. Jiang, Y., & Liu, J. (2019). Definitions of pseudocapacitive materials: A brief review. *Energy and Environmental Materials, 2*(1), 30–37. https://doi.org/10.1002/eem2.12028
19. Wang, J., Dong, S., Ding, B., Wang, Y., Hao, X., Dou, H., Xia, Y., & Zhang, X. (2017). Pseudocapacitive materials for electrochemical capacitors: From rational synthesis to capacitance optimization. *National Science Review, 4*(1), 71–90. https://doi.org/10.1093/nsr/nww072
20. Fleischmann, S., Mitchell, J. B., Wang, R., Zhan, C., Jiang, D.-e, Presser, V., & Augustyn, V. (2020). Pseudocapacitance: From fundamental understanding to high power energy storage materials. *Chemical Reviews, 120*(14), 6738–6782. https://doi.org/10.1021/acs.chemrev.0c00170
21. Choi, C., Ashby, D. S., Butts, D. M., DeBlock, R. H., Wei, Q., Lau, J., & Dunn, B. (2020). Achieving high energy density and high power density with pseudocapacitive materials. *Nature Reviews Materials, 5*(1), 5–19. https://doi.org/10.1038/s41578-019-0142-z
22. Zuo, W., Li, R., Zhou, C., Li, Y., Xia, J., & Liu, J. (2017). Battery-supercapacitor hybrid devices: Recent progress and future prospects. *Advanced Science, 4*(7), 1600539. https://doi.org/10.1002/advs.201600539
23. Dong, S., Lv, N., Wu, Y., Zhu, G., & Dong, X. (2021). lithium-ion and sodium-ion hybrid capacitors: From insertion-type materials design to devices construction. *Advanced Functional Materials, 31*(21), 2100455. https://doi.org/10.1002/adfm.202100455
24. Wang, H., Zhu, C., Chao, D., Yan, Q., & Fan, H. J. (2017). Nonaqueous hybrid lithium-ion and sodium-ion capacitors. *Advanced Materials, 29*(46), 1702093. https://doi.org/10.1002/adma.201702093
25. Feng, W., Zhang, J., Yusuf, A., Ao, X., Shi, D., Etacheri, V., & Wang, D.-Y. (2022). Quasi-solid-state sodium-ion hybrid capacitors enabled by UiO-66@PVDF-HFP multifunctional separators: Selective charge transfer and high fire safety. *Chemical Engineering Journal, 427*, 130919. https://doi.org/10.1016/j.cej.2021.130919
26. Amatucci, G. G., Badway, F., Du Pasquier, A., & Zheng, T. (2001). An asymmetric hybrid nonaqueous energy storage cell. *Journal of The Electrochemical Society, 148*(8), A930. https://doi.org/10.1149/1.1383553
27. Pal, B., Yang, S., Ramesh, S., Thangadurai, V., & Jose, R. (2019). Electrolyte selection for supercapacitive devices: A critical review. *Nanoscale Advances, 1*(10), 3807–3835. https://doi.org/10.1039/C9NA00374F
28. Arunachalam, S., Kirubasankar, B., Pan, D., Liu, H., Yan, C., Guo, Z., & Angaiah, S. (2020). Research progress in rare earths and their composites based electrode materials for supercapacitors. *Green Energy and Environment*. https://doi.org/10.1016/j.gee.2020.07.021
29. Eftekhari, A. (2018). The mechanism of ultrafast supercapacitors. *Journal of Materials Chemistry A, 6*(7), 2866–2876. https://doi.org/10.1039/C7TA10013B
30. Wei, K., Kim, I.-S. (2014). *Application of nanofibers in supercapacitors* (pp. 163–181). https://doi.org/10.1007/978-3-642-54160-5_7
31. Liang, J., Zhao, H., Yue, L., Fan, G., Li, T., Lu, S., Chen, G., Gao, S., Asiri Abdullah, M., & Sun, X. (2020). Recent advances in electrospun nanofibers for supercapacitors. *Journal of Materials Chemistry A, 8*(33), 16747–16789. https://doi.org/10.1039/D0TA05100D
32. Miao, Y.-E., Yan, J., Huang, Y., Fan, W., & Liu, T. (2015). Electrospun polymer nanofiber membrane electrodes and an electrolyte for highly flexible and foldable all-solid-state supercapacitors. *RSC Advances, 5*(33), 26189–26196. https://doi.org/10.1039/C5RA00138B
33. Xue, J., Wu, T., Dai, Y., & Xia, Y. (2019). electrospinning and electrospun nanofibers: Methods, materials, and applications. *Chemical Reviews, 119*(8), 5298–5415. https://doi.org/10.1021/acs.chemrev.8b00593

34. Islam, M. S., Ang, B. C., Andriyana, A., & Afifi, A. M. (2019). A review on fabrication of nanofibers via electrospinning and their applications. *SN Applied Sciences, 1*(10), 1248. https://doi.org/10.1007/s42452-019-1288-4
35. Ibrahim, H. M., & Klingner, A. (2020). A review on electrospun polymeric nanofibers: Production parameters and potential applications. *Polymer Testing, 90*, 106647. https://doi.org/10.1016/j.polymertesting.2020.106647
36. Zhang, C., Li, Y., Wang, P., & Zhang, H. (2020) Electrospinning of nanofibers: Potentials and perspectives for active food packaging. *Comprehensive Reviews in Food Science and Food Safety, 19*(2), 479–502. https://doi.org/10.1111/1541-4337.12536
37. Lu, X., Wang, C., Favier, F., & Pinna, N. (2017). electrospun nanomaterials for supercapacitor electrodes: Designed architectures and electrochemical performance. *Advanced Energy Materials, 7*(2), 1601301. https://doi.org/10.1002/aenm.201601301
38. Miao, Y.-E., & Liu, T. (2019). Electrospun nanofiber electrodes: A promising platform for supercapacitor applications. In B. Ding, X. Wang, J. Yu (Eds.), *Electrospinning: Nanofabrication and applications* (William Andrew Publishing) (pp. 641–669) (Chapter 21). https://doi.org/10.1016/B978-0-323-51270-1.00021-2
39. Niu, H., Zhou, H., & Lin, T. (2021). Electrospun carbon nanofibers as electrode materials for supercapacitor applications. In Y. Dong, A. Baji, & S. Ramakrishna (Eds.), *Electrospun polymers and composites* (pp. 641–688). Woodhead Publishing (Chapter 21). https://doi.org/10.1016/B978-0-12-819611-3.00021-2
40. Veerakumar, P., Sangili, A., Manavalan, S., Thanasekaran, P., & Lin, K.-C. (2020). Research progress on porous carbon supported metal/metal oxide nanomaterials for supercapacitor electrode applications. *Industrial and Engineering Chemistry Research, 59*(14), 6347–6374. https://doi.org/10.1021/acs.iecr.9b06010
41. De, B., Banerjee, S., Verma, K. D., Pal, T., Manna, P. K., & Kar, K. K. (2020). Carbon nanofiber as electrode materials for supercapacitors. In K. K. Kar (Ed.), *Handbook of nanocomposite supercapacitor materials II: Performance* (pp. 179–200). Springer International Publishing. https://doi.org/10.1007/978-3-030-52359-6_7
42. Pan, H., Li, J., & Feng, Y. (2010). Carbon nanotubes for supercapacitor. *Nanoscale Research Letters, 5*(3), 654. https://doi.org/10.1007/s11671-009-9508-2
43. Mataram, A., Ismail, A. F., Abdullah, M. S., Ng, B. C., & Matsuura, T. (2011) A review of assembled polyacrylonitrile-based carbon nanofiber prepared electrospinning process. *International Journal of Nanoscience, 10*(03), 455–469. https://doi.org/10.1142/s0219581x11008228
44. Abeykoon, N. C., Bonso, J. S., & Ferraris, J. P. (2015). Supercapacitor performance of carbon nanofiber electrodes derived from immiscible PAN/PMMA polymer blends. *RSC Advances, 5*(26), 19865–19873. https://doi.org/10.1039/C4RA16594B
45. Chakravarty, A., Maiti, S., Mahanty, S., & De, G. (2017). Green synthesis of electrospun porous carbon nanofibers from sucrose and doping of Ag nanoparticle with improved electrical and electrochemical properties. *ChemistrySelect, 2*(7), 2265–2276. https://doi.org/10.1002/slct.201601920
46. Hérou, S., Bailey, J.J., Kok, M., Schlee, P., Jervis, R., Brett, D. J. L., Shearing, P. R., Ribadeneyra. M/C., & Titirici. M. (2021). High-density lignin-derived carbon nanofiber supercapacitors with enhanced volumetric energy density. *Carbon, 8*(17), 2100016. https://doi.org/10.1002/advs.202100016
47. Yang, Y., Centrone, A., Chen, L., Simeon, F., Alan Hatton, T., & Rutledge, G. C. (2011). Highly porous electrospun polyvinylidene fluoride (PVDF)-based carbon fiber. *Carbon, 49*(11), 3395–3403. https://doi.org/10.1016/j.carbon.2011.04.015
48. Kumar, M., Hietala, M., & Oksman, K. (2019). Lignin-based electrospun carbon nanofibers. *Frontiers in Materials, 6*(62). https://doi.org/10.3389/fmats.2019.00062
49. Fatema, U.K., Uddin, A.J., Uemura, K., & Gotoh, Y. (2011). Fabrication of carbon fibers from electrospun poly(vinyl alcohol) nanofibers. *Textile Research Journal, 81*(7), 659–672. https://doi.org/10.1177/0040517510385175

50. Qiao, W. M., Yoon, S. H., Korai, Y., Mochida, I., Inoue, S., Sakurai, T., & Shimohara, T. (2004). Preparation of activated carbon fibers from polyvinyl chloride. *Carbon, 42*(7), 1327–1331. https://doi.org/10.1016/j.carbon.2004.01.035
51. Bhoyate, S., Kahol, P. K., Sapkota, B., Mishra, S. R., Perez, F., & Gupta, R. K. (2018). Polystyrene activated linear tube carbon nanofiber for durable and high-performance supercapacitors. *Surface and Coatings Technology, 345*, 113–122. https://doi.org/10.1016/j.surfcoat.2018.04.026
52. Kim, C., Kim, Y.-J., & Kim, Y.-A. (2004). Fabrication and structural characterization of electro-spun polybenzimidazol-derived carbon nanofiber by graphitization. *Solid State Communications, 132*(8), 567–571. https://doi.org/10.1016/j.ssc.2004.08.035
53. Xuyen, N. T., Ra, E. J., Geng, H.-Z., Kim, K. K., An, K. H., & Lee, Y. H. (2007). Enhancement of conductivity by diameter control of polyimide-based electrospun carbon nanofibers. *The Journal of Physical Chemistry B, 111*(39), 11350–11353. https://doi.org/10.1021/jp075541q
54. Chen, Y., Yue, M., Huang, Z.-H., & Kang, F. (2014). Electrospun carbon nanofiber networks from phenolic resin for capacitive deionization. *Chemical Engineering Journal, 252*, 30–37. https://doi.org/10.1016/j.cej.2014.04.099
55. Nan, W., Zhao, Y., Ding, Y., Shende, A. R., Fong, H., & Shende, R. V. (2017). Mechanically flexible electrospun carbon nanofiber mats derived from biochar and polyacrylonitrile. *Materials Letters, 205*, 206–210. https://doi.org/10.1016/j.matlet.2017.06.092
56. He, T.-S., Yu, X.-D., Bai, T.-J., Li, X.-Y., Fu, Y.-R., & Cai, K.-D. (2020). Porous carbon nanofibers derived from PAA-PVP electrospun fibers for supercapacitor. *Ionics, 26*(8), 4103–4111. https://doi.org/10.1007/s11581-020-03529-1
57. Xu, J., Liu, Z., Zhang, F., Tao, J., Shen, L., & Zhang, X. (2020). Bacterial cellulose-derived carbon nanofibers as both anode and cathode for hybrid sodium ion capacitor. *RSC Advances, 10*(13), 7780–7790. https://doi.org/10.1039/C9RA10225F
58. Zhi, M., Liu, S., Hong, Z., & Wu, N. (2014). Electrospun activated carbon nanofibers for supercapacitor electrodes. *RSC Advances, 4*(82), 43619–43623. https://doi.org/10.1039/C4RA05512H
59. Ma, C., Ruan, S., Wang, J., Long, D., Qiao, W., & Ling, L. (2018). Free-standing carbon nanofiber fabrics for high performance flexible supercapacitor. *Journal of Colloid and Interface Science, 531*, 513–522. https://doi.org/10.1016/j.jcis.2018.06.093
60. Gopalakrishnan, A., Sahatiya, P., & Badhulika, S. (2018). Template-assisted electrospinning of bubbled carbon nanofibers as binder-free electrodes for high-performance supercapacitors. *ChemElectroChem, 5*(3), 531–539. https://doi.org/10.1002/celc.201700962.
61. Li, J., Liu, E.-H, Li, W., Meng, X.-Y., & Tan, S.-T.. (2009). Nickel/carbon nanofibers composite electrodes as supercapacitors prepared by electrospinning. *Journal of Alloys and Compounds, 478*(1), 371–374. https://doi.org/10.1016/j.jallcom.2008.11.024
62. Tiwari, A. P., Chae, S.-H., Ojha, G. P., Dahal, B., Mukhiya, T., Lee, M., Chhetri, K., Kim, T., & Kim, H.-Y. (2019). Three-dimensional porous carbonaceous network with in-situ entrapped metallic cobalt for supercapacitor application. *Journal of Colloid and Interface Science, 553*, 622–630. https://doi.org/10.1016/j.jcis.2019.06.070
63. Lavanya, T., & Ramaprabhu, S. (2019). Copper nanoparticles incorporated porous carbon nanofibers as a freestanding binder-free electrode for symmetric supercapacitor with enhanced electrochemical performance. *Materials Research Express, 6*(10), 105005. https://doi.org/10.1088/2053-1591/ab3569
64. Liu, J., Sun, X., Li, C., & Bai, J. (2019). Tin-embedded carbon nanofibers as flexible and freestanding electrode materials for high-performance supercapacitors. *Ionics, 25*(10), 4875–4890. https://doi.org/10.1007/s11581-019-03019-z
65. Aboagye, A., Liu, Y., Ryan, J. G., Wei, J., & Zhang, L. (2018). Hierarchical carbon composite nanofibrous electrode material for high-performance aqueous supercapacitors. *Materials Chemistry and Physics, 214*, 557–563. https://doi.org/10.1016/j.matchemphys.2018.05.009
66. Ju, Y.-W., Choi, G.-R., Jung, H.-R., Kim, C., Yang, K.-S., & Lee, W.-J. (2007). A hydrous ruthenium oxide-carbon nanofibers composite electrodes prepared by electrospinning. *Journal of The Electrochemical Society, 154*(3), A192. https://doi.org/10.1149/1.2426898

67. Kim, Y. I., Samuel, E., Joshi, B., Kim, M.-W., Kim, T. G., Swihart, M. T., & Yoon, S. S. (2018). Highly efficient electrodes for supercapacitors using silver-plated carbon nanofibers with enhanced mechanical flexibility and long-term stability. *Chemical Engineering Journal, 353*, 189–196. https://doi.org/10.1016/j.cej.2018.07.066
68. An, G. H., & Ahn, H. J. (2013). Carbon nanofibre composites decorated with Ru–Ag nanophases for high-efficiency electrochemical capacitors. *ECS Solid State Letters, 2*(5), M33–M36. https://doi.org/10.1149/2.005305ssl
69. Kurtan, U., Sahinturk, U., Aydın, H., Dursun, D., & Baykal, A. (2020). CoFe nanoparticles in carbon nanofibers as an electrode for ultra-stable supercapacitor. *Journal of Inorganic and Organometallic Polymers and Materials, 30*(9), 3608–3616. https://doi.org/10.1007/s10904-020-01524-7
70. Jun, J., Lee, J. S., Shin, D. H., Kim, S. G., & Jang, J. (2015). Multidimensional MnO_2 nanohair-decorated hybrid multichannel carbon nanofiber as an electrode material for high-performance supercapacitors. *Nanoscale, 7*(38), 16026–16033. https://doi.org/10.1039/C5NR03616J
71. Huang, G., Li, C., Sun, X., & Bai, J. (2017). Fabrication of vanadium oxide, with different valences of vanadium, -embedded carbon fibers and their electrochemical performance for supercapacitor. *New Journal of Chemistry, 41*(17), 8977–8984. https://doi.org/10.1039/C7NJ01482A
72. Huang, J., Xu, Y., Xiao, Y., Zhu, H., Wei, J., & Chen, Y. (2017). Mussel-inspired, biomimetics-assisted self-assembly of Co_3O_4 on carbon fibers for flexible supercapacitors. *ChemElectroChem, 4*(9), 2269–2277. https://doi.org/10.1002/celc.201700369
73. Li, L., Zhang, X., Zhang, Z., Zhang, M., Cong, L., Pan, Y., & Lin, S. (2016). A bismuth oxide nanosheet-coated electrospun carbon nanofiber film: A free-standing negative electrode for flexible asymmetric supercapacitors. *Journal of Materials Chemistry A, 4*(42), 16635–16644. https://doi.org/10.1039/C6TA06755G
74. Pai, R., Singh, A., Simotwo, S., & Kalra, V. (2018). In situ grown iron oxides on carbon nanofibers as freestanding anodes in aqueous supercapacitors. *Advanced Engineering Materials, 20*(6), 1701116. https://doi.org/10.1002/adem.201701116
75. Pant, B., Park, M., & Park, S.-J. (2019). TiO_2 NPs assembled into a carbon nanofiber composite electrode by a one-step electrospinning process for supercapacitor applications. *Polymers, 11*(5), 899.
76. Luan, Y., Nie, G., Zhao, X., Qiao, N., Liu, X., Wang, H., Zhang, X., Chen, Y., & Long, Y.-Z. (2019). The integration of SnO_2 dots and porous carbon nanofibers for flexible supercapacitors. *Electrochimica Acta, 308*, 121–130. https://doi.org/10.1016/j.electacta.2019.03.204
77. Zhang, W., Shen, P., Qian, L., Mao, P., Ahmad, M., Chu, H., Zheng, R., Wang, Z., Bai, L., Sun, H., Yu, Y., & Liu, Y. (2021). Tuning the phase composition in polymorphic Nb_2O_5 nanoplates for rapid and stable lithium ion storage. *Electrochimica Acta, 399*, 139368. https://doi.org/10.1016/j.electacta.2021.139368
78. Lee, G., Seo, Y. D., & Jang, J. (2017). ZnO quantum dot-decorated carbon nanofibers derived from electrospun ZIF-8/PVA nanofibers for high-performance energy storage electrodes. *Chemical Communications, 53*(83), 11441–11444. https://doi.org/10.1039/C7CC05206E
79. Li, Q., Guo, J., Xu, D., Guo, J., Ou, X., Hu, Y., Qi, H., & Yan, F. (2018). Electrospun N-doped porous carbon nanofibers incorporated with NiO nanoparticles as free-standing film electrodes for high-performance supercapacitors and CO_2 capture. *Small, 14*(15), 1704203. https://doi.org/10.1002/smll.201704203
80. Yang, K. S., Kim, C. H., & Kim, B.-H. (2015). Preparation and electrochemical properties of RuO_2-containing activated carbon nanofiber composites with hollow cores. *Electrochimica Acta, 174*, 290–296. https://doi.org/10.1016/j.electacta.2015.05.176
81. Wang, J.-G., Yang, Y., Huang, Z.-H., & Kang, F. (2011). Coaxial carbon nanofibers/MnO_2 nanocomposites as freestanding electrodes for high-performance electrochemical capacitors. *Electrochimica Acta, 56*(25), 9240–9247. https://doi.org/10.1016/j.electacta.2011.07.140

82. Iqbal, N., Wang, X., Babar, A. A., Zainab, G., Yu, J., & Ding, B. (2017). Flexible Fe_3O_4@carbon nanofibers hierarchically assembled with MnO_2 particles for high-performance supercapacitor electrodes. *Scientific Reports, 7*(1), 15153. https://doi.org/10.1038/s41598-017-15535-x
83. Liu, Y., Zhou, J., Fu, W., Zhang, P., Pan, X., & Xie, E. (2017). In situ synthesis of CoS_x@carbon core–shell nanospheres decorated in carbon nanofibers for capacitor electrodes with superior rate and cycling performances. *Carbon, 114*, 187–197. https://doi.org/10.1016/j.carbon.2016.12.018
84. Tong, F., Wu, X., Jia, W., Guo, J., Pan, Y., Lv, Y., Jia, D., & Zhao, X. (2020). NiS nanosheets with novel structure anchored on coal-based carbon fibers prepared by electrospinning for flexible supercapacitors. *CrystEngComm, 22*(9), 1625–1632. https://doi.org/10.1039/C9CE01560D
85. Kumuthini, R., Ramachandran, R., Therese, H. A., & Wang, F. (2017). Electrochemical properties of electrospun MoS_2@C nanofiber as electrode material for high-performance supercapacitor application. *Journal of Alloys and Compounds, 705*, 624–630. https://doi.org/10.1016/j.jallcom.2017.02.163
86. Wang, Z., Liu, C., Shi, G., Wang, G., Zhang, H., Zhang, Q., Jiang, X., Li, X., Luo, F., Hu, Y., & Yi, K. (2020). Preparation and electrochemical properties of electrospun FeS/carbon nanofiber composites. *Ionics, 26*(6), 3051–3060. https://doi.org/10.1007/s11581-020-03455-2
87. Xu, D., Wang, H., Qiu, R., Wang, Q., Mao, Z., Jiang, Y., Wang, R., He, B., Gong, Y., Li, D., & Hu, X. (2020). Coupling of bowl-like VS2 nanosheet arrays and carbon nanofiber enables ultrafast Na^+-storage and robust flexibility for sodium-ion hybrid capacitors. *Energy Storage Materials, 28*, 91–100. https://doi.org/10.1016/j.ensm.2020.03.002
88. Qiu, X., Wang, L., & Fan, L.-Z. (2018). Immobilization of tungsten disulfide nanosheets on active carbon fibers as electrode materials for high performance quasi-solid-state asymmetric supercapacitors. *Journal of Materials Chemistry A, 6*(17), 7835–7841. https://doi.org/10.1039/C8TA01047A
89. Sami, S. K., Siddiqui, S., Feroze, M. T., & Chung, C.-H. (2017). Electrodeposited nickel–cobalt sulfide nanosheet on polyacrylonitrile nanofibers: A binder-free electrode for flexible supercapacitors. *Materials Research Express, 4*(11), 116309. https://doi.org/10.1088/2053-1591/aa985b
90. Huang, Y., Zhao, Y., Bao, J., Lian, J., Cheng, M., & Li, H. (2019). Lawn-like $FeCo_2S_4$ hollow nanoneedle arrays on flexible carbon nanofiber film as binder-free electrodes for high-performance asymmetric pseudocapacitors. *Journal of Alloys and Compounds, 772*, 337–347. https://doi.org/10.1016/j.jallcom.2018.08.212
91. Liu, Y., Jiang, G., Sun, S., Xu, B., Zhou, J., Zhang, Y., & Yao, J. (2018). Decoration of carbon nanofibers with $NiCo_2S_4$ nanoparticles for flexible asymmetric supercapacitors. *Journal of Alloys and Compounds, 731*, 560–568. https://doi.org/10.1016/j.jallcom.2017.10.078
92. Shen, Q., Jiang, P., He, H., Chen, C., Liu, Y., & Zhang, M. (2019). Encapsulation of $MoSe_2$ in carbon fibers as anodes for potassium ion batteries and nonaqueous battery–supercapacitor hybrid devices. *Nanoscale, 11*(28), 13511–13520. https://doi.org/10.1039/C9NR03480C
93. Ran, F., Wu, Y., Jiang, M., Tan, Y., Liu, Y., Kong, L., Kang, L., & Chen, S. (2018). Nanocomposites based on hierarchical porous carbon fiber@vanadium nitride nanoparticles as supercapacitor electrodes. *Dalton Transactions, 47*(12), 4128–4138. https://doi.org/10.1039/C7DT04432A
94. Tan, Y., Meng, L., Wang, Y., Dong, W., Kong, L., Kang, L., & Ran, F. (2018). Negative electrode materials of molybdenum nitride/N-doped carbon nano-fiber via electrospinning method for high-performance supercapacitors. *Electrochimica Acta, 277*, 41–49. https://doi.org/10.1016/j.electacta.2018.04.214
95. Wang, G., Sun, X., Bai, J., & Han, L. (2019). Preparation of Fe–C nanofiber composites by metal organic complex and potential application in supercapacitors. *Journal of Materials Science: Materials in Electronics, 30*(5), 4665–4675. https://doi.org/10.1007/s10854-019-00760-z

96. Ren, Y., Dai, J., Pang, B., Liu, X., & Yu, J. (2015). Synergistic enhancement of electrochemical performance of electrospun TiC/C hybrid nanofibers for supercapacitor application. *Electrochimica Acta, 176*, 402–409. https://doi.org/10.1016/j.electacta.2015.07.025
97. Levitt, A. S., Alhabeb, M., Hatter, C. B., Sarycheva, A., Dion, G., & Gogotsi, Y. (2019). Electrospun MXene/carbon nanofibers as supercapacitor electrodes. *Journal of Materials Chemistry A, 7*(1), 269–277. https://doi.org/10.1039/C8TA09810G
98. Tian, J., Shi, Y., Fan, W., & Liu, T. (2019). Ditungsten carbide nanoparticles embedded in electrospun carbon nanofiber membranes as flexible and high-performance supercapacitor electrodes. *Composites Communications, 12*, 21–25. https://doi.org/10.1016/j.coco.2018.12.003
99. Hao, X., Bi, J., Wang, W., Yan, W., Gao, X., Sun, X., & Liu, R. (2020). Electrospun Fe_2MoC/C nanofibers as an efficient electrode material for high-performance supercapacitors. *Journal of Power Sources, 451*, 227802. https://doi.org/10.1016/j.jpowsour.2020.227802
100. Tolosa, A., Krüner, B., Fleischmann, S., Jäckel, N., Zeiger, M., Aslan, M., Grobelsek, I., & Presser, V. (2016). Niobium carbide nanofibers as a versatile precursor for high power supercapacitor and high energy battery electrodes. *Journal of Materials Chemistry A, 4*(41), 16003–16016. https://doi.org/10.1039/C6TA06224E
101. Cai, J., Niu, H., Li, Z., Du, Y., Cizek, P., Xie, Z., Xiong, H., & Lin, T. (2015). High-performance supercapacitor electrode materials from cellulose-derived carbon nanofibers. *ACS Applied Materials and Interfaces, 7*(27), 14946–14953. https://doi.org/10.1021/acsami.5b03757
102. Tai, Z., Lang, J., Yan, X., & Xue, Q. (2012). Mutually enhanced capacitances in carbon nanofiber/cobalt hydroxide composite paper for supercapacitor. *Journal of The Electrochemical Society, 159*(4), A485–A491. https://doi.org/10.1149/2.110204jes
103. Lai, F., Huang, Y., Miao, Y.-E., & Liu, T. (2015). Controllable preparation of multidimensional hybrid materials of nickel-cobalt layered double hydroxide nanorods/nanosheets on electrospun carbon nanofibers for high-performance supercapacitors. *Electrochimica Acta, 174*, 456–463. https://doi.org/10.1016/j.electacta.2015.06.031
104. Mi, K., Song, L., Nie, H., Liu, T., & Li, X. (2020). Layer-by-layer growth of ZIF-8 on electrospun carbon nanofiber membranes for high-performance supercapacistor electrode. *Journal of Energy Chemistry, 47*, 221–224. https://doi.org/10.1016/j.jechem.2019.10.028
105. Zhao, S., Wu, H., Li, Y., Li, Q., Zhou, J., Yu, X., Chen, H., Tao, K., & Han, L. (2019). Core–shell assembly of carbon nanofibers and a 2D conductive metal–organic framework as a flexible free-standing membrane for high-performance supercapacitors. *Inorganic Chemistry Frontiers, 6*(7), 1824–1830. https://doi.org/10.1039/C9QI00390H
106. Wang, X., Wu, D., Song, X., Du, W., Zhao, X., & Zhang, D. (2019). Review on carbon/polyaniline hybrids: Design and synthesis for supercapacitor. *Molecules, 24*(12), 2263. https://doi.org/10.3390/molecules24122263
107. Fu, Q., Wang, Y., Liang, S., Liu, Q., & Yao, C. (2020). High-performance flexible freestanding polypyrrole-coated CNF film electrodes for all-solid-state supercapacitors. *Journal of Solid State Electrochemistry, 24*(3), 533–544. https://doi.org/10.1007/s10008-019-04491-3
108. Chen, L., Li, D., Chen, L., Si, P., Feng, J., Zhang, L., Li, Y., Lou, J., & Ci, L. (2018). Core–shell structured carbon nanofibers yarn@polypyrrole@graphene for high performance all-solid-state fiber supercapacitors. *Carbon, 138*, 264–270. https://doi.org/10.1016/j.carbon.2018.06.022
109. Miao, F., Shao, C., Li, X., Wang, K., Lu, N., & Liu, Y. (2016). Electrospun carbon nanofibers/carbon nanotubes/polyaniline ternary composites with enhanced electrochemical performance for flexible solid-state supercapacitors. *ACS Sustainable Chemistry and Engineering, 4*(3), 1689–1696. https://doi.org/10.1021/acssuschemeng.5b01631
110. Iqbal, N., Wang, X., Babar, A. A., Yan, J., Yu, J., Park, S.-J., & Ding, B. (2017). Polyaniline enriched flexible carbon nanofibers with core–shell structure for high-performance wearable supercapacitors. *Advanced Materials Interfaces, 4*(24), 1700855. https://doi.org/10.1002/admi.201700855

111. Sun, H., Li, S., Shen, Y., Miao, F., Zhang, P., & Shao, G. (2020). Integrated structural design of polyaniline-modified nitrogen-doped hierarchical porous carbon nanofibers as binder-free electrodes toward all-solid-state flexible supercapacitors. *Applied Surface Science, 501*, 144001. https://doi.org/10.1016/j.apsusc.2019.144001
112. Kshetri, T., Thanh, T. D., Singh, S. B., Kim, N. H., & Lee, J. H. (2018). Hierarchical material of carbon nanotubes grown on carbon nanofibers for high performance electrochemical capacitor. *Chemical Engineering Journal, 345*, 39–47. https://doi.org/10.1016/j.cej.2018.03.143
113. Zhou, Z., & Wu, X.-F. (2013). Graphene-beaded carbon nanofibers for use in supercapacitor electrodes: Synthesis and electrochemical characterization. *Journal of Power Sources, 222*, 410–416. https://doi.org/10.1016/j.jpowsour.2012.09.004
114. Kuzmenko, V., Wang, N., Haque, M., Naboka, O., Flygare, M., Svensson, K., Gatenholm, P., Liu, J., & Enoksson, P. (2017). Cellulose-derived carbon nanofibers/graphene composite electrodes for powerful compact supercapacitors. *RSC Advances, 7*(73), 45968–45977. https://doi.org/10.1039/C7RA07533B
115. Hsu, H.-C., Wang, C.-H., Nataraj, S. K., Huang, H.-C., Du, H.-Y., Chang, S.-T., Chen, L.-C., & Chen, K.-H. (2012). Stand-up structure of graphene-like carbon nanowalls on CNT directly grown on polyacrylonitrile-based carbon fiber paper as supercapacitor. *Diamond and Related Materials, 25*, 176–179. https://doi.org/10.1016/j.diamond.2012.02.020
116. He, S., Chen, L., Xie, C., Hu, H., Chen, S., Hanif, M., & Hou, H. (2013). Supercapacitors based on 3D network of activated carbon nanowhiskers wrapped-on graphitized electrospun nanofibers. *Journal of Power Sources, 243*, 880–886. https://doi.org/10.1016/j.jpowsour.2013.06.104
117. Majumdar, D., Maiyalagan, T., & Jiang, Z. (2019). Recent progress in ruthenium oxide-based composites for supercapacitor applications. *ChemElectroChem, 6*(17), 4343–4372. https://doi.org/10.1002/celc.201900668
118. Wei, W., Cui, X., Chen, W., & Ivey, D. G. (2011). Manganese oxide-based materials as electrochemical supercapacitor electrodes. *Chemical Society Reviews, 40*(3), 1697–1721. https://doi.org/10.1039/C0CS00127A
119. Chime, U. K., Nkele, A. C., Ezugwu, S., Nwanya, A. C., Shinde, N. M., Kebede, M., Ejikeme, P. M., Maaza, M., & Ezema, F. I. (2020). Recent progress in nickel oxide-based electrodes for high-performance supercapacitors. *Current Opinion in Electrochemistry, 21*, 175–181. https://doi.org/10.1016/j.coelec.2020.02.004
120. Kumar, M., Subramania, A., & Balakrishnan, K. (2014). Preparation of electrospun Co_3O_4 nanofibers as electrode material for high performance asymmetric supercapacitors. *Electrochimica Acta, 149*, 152–158. https://doi.org/10.1016/j.electacta.2014.10.021
121. He, X., Yang, C. P., Zhang, G. L., Shi, D. W., Huang, Q. A., Xiao, H. B., Liu, Y., & Xiong, R. (2016). Supercapacitor of TiO_2 nanofibers by electrospinning and KOH treatment. *Materials and Design, 106*, 74–80. https://doi.org/10.1016/j.matdes.2016.05.025
122. Jiang, H., Niu, H., Yang, X., Sun, Z., Li, F., Wang, Q., & Qu, F. (2018). Flexible Fe_2O_3 and V_2O_5 nanofibers as binder-free electrodes for high-performance all-solid-state asymmetric supercapacitors. *Chemistry—A European Journal, 24*(42), 10683–10688. https://doi.org/10.1002/chem.201800461
123. Chou, J.-C., Chen, Y.-L., Yang, M.-H., Chen, Y.-Z., Lai, C.-C., Chiu, H.-T., Lee, C.-Y., Chueh, Y.-L., & Gan, J.-Y. (2013). $RuO2/MnO_2$ core–shell nanorods for supercapacitors. *Journal of Materials Chemistry A, 1*(31), 8753–8758. https://doi.org/10.1039/C3TA11027C
124. Ren, B., Fan, M., Liu, Q., Wang, J., Song, D., & Bai, X. (2013). Hollow NiO nanofibers modified by citric acid and the performances as supercapacitor electrode. *Electrochimica Acta, 92*, 197–204. https://doi.org/10.1016/j.electacta.2013.01.009
125. Zhang, M., Li, Q., Fang, D., Ayhan, I. A., Zhou, Y., Dong, L., Xiong, C., & Wang, Q. (2015). NiO hierarchical hollow nanofibers as high-performance supercapacitor electrodes. *RSC Advances, 5*(116), 96205–96212. https://doi.org/10.1039/C5RA17011G
126. Lala, N. L., Jose, R., Yusoff, M. M., & Ramakrishna, S. (2012). Continuous tubular nanofibers of vanadium pentoxide by electrospinning for energy storage devices. *Journal of Nanoparticle Research, 14*(11), 1201. https://doi.org/10.1007/s11051-012-1201-1

127. Niu, C., Meng, J., Wang, X., Han, C., Yan, M., Zhao, K., Xu, X., Ren, W., Zhao, Y., Xu, L., Zhang, Q., Zhao, D., & Mai, L. (2015). General synthesis of complex nanotubes by gradient electrospinning and controlled pyrolysis. *Nature Communications, 6*(1), 7402. https://doi.org/10.1038/ncomms8402
128. Sun, J., Xu, C., & Chen, H. (2021). A review on the synthesis of $CuCo_2O_4$-based electrode materials and their applications in supercapacitors. *Journal of Materiomics, 7*(1), 98–126. https://doi.org/10.1016/j.jmat.2020.07.013
129. Niu, H., Yang, X., Jiang, H., Zhou, D., Li, X., Zhang, T., Liu, J., Wang, Q., & Qu, F. (2015). Hierarchical core–shell heterostructure of porous carbon nanofiber@$ZnCo_2O_4$ nanoneedle arrays: Advanced binder-free electrodes for all-solid-state supercapacitors. *Journal of Materials Chemistry A, 3*(47), 24082–24094. https://doi.org/10.1039/C5TA07439H
130. Wu, Z., Zhu, Y., & Ji, X. (2014). $NiCo_2O_4$-based materials for electrochemical supercapacitors. *Journal of Materials Chemistry A, 2*(36), 14759–14772. https://doi.org/10.1039/C4TA02390K
131. Sudheendra Budhiraju, V., Sharma, A., & Sivakumar, S. (2017). Structurally stable mesoporous hierarchical $NiMoO_4$ hollow nanofibers for asymmetric supercapacitors with enhanced capacity and improved cycling stability. *ChemElectroChem, 4*(12), 3331–3339. https://doi.org/10.1002/celc.201700503
132. Bhagwan, J., Kumar, N., Yadav, K. L., & Sharma, Y. (2018). Probing the electrical properties and energy storage performance of electrospun $ZnMn_2O_4$ nanofibers. *Solid State Ionics, 321*, 75–82. https://doi.org/10.1016/j.ssi.2018.04.007
133. Wang, Q., Chen, D., & Zhang, D. (2015). Electrospun porous $CuCo_2O_4$ nanowire network electrode for asymmetric supercapacitors. *RSC Advances, 5*(117), 96448–96454. https://doi.org/10.1039/C5RA21170K
134. Aravindan, V., Sundaramurthy, J., Jain, A., Kumar, P. S., Ling, W. C., Ramakrishna, S., Srinivasan, M. P., & Madhavi, S. (2014). Unveiling $TiNb_2O_7$ as an insertion anode for lithium ion capacitors with high energy and power density. *ChemSusChem, 7*(7), 1858–1863. https://doi.org/10.1002/cssc.201400157
135. Jayaraman, S., Aravindan, V., Suresh Kumar, P., Ling, W. C., Ramakrishna, S., & Madhavi, S. (2013). Synthesis of porous $LiMn_2O_4$ hollow nanofibers by electrospinning with extraordinary lithium storage properties. *Chemical Communications, 49*(59), 6677–6679. https://doi.org/10.1039/C3CC43874K
136. Bhuvanalogini, G., Muruganantham, N., Shobana, V., & Subramania, A. (2014). Preparation, characterization, and evaluation of $LiNi_{0.4}Co_{0.6}O_2$ nanofibers for supercapacitor applications. *Journal of Solid State Electrochemistry, 18*(9), 2387–2392. https://doi.org/10.1007/s10008-014-2460-9
137. Vijayan, S., Kirubasankar, B., Pazhamalai, P., Solarajan, A. K., & Angaiah, S. (2017). Electrospun Nd^{3+}-doped $LiMn_2O_4$ nanofibers as high-performance cathode material for li-ion capacitors. *ChemElectroChem, 4*(8), 2059–2067. https://doi.org/10.1002/celc.201700161
138. Peng, S., Li, L., Hu, Y., Srinivasan, M., Cheng, F., Chen, J., & Ramakrishna, S. (2015). Fabrication of spinel one-dimensional architectures by single-spinneret electrospinning for energy storage applications. *ACS Nano, 9*(2), 1945–1954. https://doi.org/10.1021/nn506851x
139. Zhou, G., Zhu, J., Chen, Y., Mei, L., Duan, X., Zhang, G., Chen, L., Wang, T., & Lu, B. (2014). Simple method for the preparation of highly porous $ZnCo_2O_4$ nanotubes with enhanced electrochemical property for supercapacitor. *Electrochimica Acta, 123*, 450–455. https://doi.org/10.1016/j.electacta.2014.01.018
140. Wang, X., & Shen, G. (2015). Intercalation pseudo-capacitive $TiNb_2O_7$@carbon electrode for high-performance lithium Ion hybrid electrochemical supercapacitors with ultrahigh energy density. *Nano Energy 15*, 104–115. https://doi.org/10.1016/j.nanoen.2015.04.011
141. Cao, Y., Lin, B., Sun, Y., Yang, H., & Zhang, X. (2015). Sr-doped lanthanum nickelate nanofibers for high energy density supercapacitors. *Electrochimica Acta, 174*, 41–50. https://doi.org/10.1016/j.electacta.2015.05.131

142. George, G., Jackson, S. L., Luo, C. Q., Fang, D., Luo, D., Hu, D., Wen, J., & Luo, Z. (2018). Effect of doping on the performance of high-crystalline $SrMnO_3$ perovskite nanofibers as a supercapacitor electrode. *Ceramics International, 44*(17), 21982–21992. https://doi.org/10.1016/j.ceramint.2018.08.313
143. Beknalkar, S. A., Teli, A. M., Harale, N. S., Pawar, K. K., Patil, D. S., Shin, J. C., & Patil, P. S. (2021). Hierarchical ITO nanofibers coated Mn_3O_4 nanoplates core–shell nanocomposites for high performance all-solid-state symmetric supercapacitor device. *Ceramics International, 47*(21), 29771–29785. https://doi.org/10.1016/j.ceramint.2021.07.149
144. Da Silva, E. P., Rubira, A. F., Ferreira, O. P., Silva, R., & Muniz, E. C. (2019). In situ growth of manganese oxide nanosheets over titanium dioxide nanofibers and their performance as active material for supercapacitor. *Journal of Colloid and Interface Science, 555*, 373–382. https://doi.org/10.1016/j.jcis.2019.07.064
145. Harilal, M., Vidyadharan, B., Misnon, I. I., Anilkumar, G. M., Lowe, A., Ismail, J., Yusoff, M. M., & Jose, R. (2017). One-dimensional assembly of conductive and capacitive metal oxide electrodes for high-performance asymmetric supercapacitors. *ACS Applied Materials and Interfaces, 9*(12), 10730–10742. https://doi.org/10.1021/acsami.7b00676
146. Radhamani, A. V., Shareef, K. M., & Rao, M. S. R. (2016). $ZnO@MnO_2$ core–shell nanofiber cathodes for high performance asymmetric supercapacitors. *ACS Applied Materials and Interfaces, 8*(44), 30531–30542. https://doi.org/10.1021/acsami.6b08082
147. Ren, B., Fan, M., Zhang, B., & Wang, J. (2018). Novel hollow $NiO@Co_3O_4$ nanofibers for high-performance supercapacitors. *Journal of Nanoscience and Nanotechnology, 18*(10), 7004–7010. https://doi.org/10.1166/jnn.2018.15451
148. Gong, D., Zhu, J., & Lu, B. (2016). $RuO_2@Co_3O_4$ heterogeneous nanofibers: A high-performance electrode material for supercapacitors. *RSC Advances, 6*(54), 49173–49178. https://doi.org/10.1039/C6RA04884F
149. Wang, Q. N., Gao, H., Qin, X., Dai, J., & Li, W. (2020). *Fabrication of $NiFe_2O_4@CoFe_2O_4$ core–shell nanofibers for high-performance supercapacitors.*
150. He, L., Shu, Y., Li, W., Liu, M. (2019). Preparation of $La_{0.7}Sr_{0.3}CoO_{3-\delta}$ (LSC)@MnO_2 core/shell nanorods as high-performance electrode materials for supercapacitors. *Journal of Materials Science: Materials in Electronics, 30*(1), 17–25. https://doi.org/10.1007/s10854-018-0331-3
151. Pal, B., Bakr, Z. H., Krishnan, S. G., Yusoff, M. M., & Jose, R. (2018). Large scale synthesis of 3D nanoflowers of SnO_2/TiO_2 composite via electrospinning with synergistic properties. *Materials Letters, 225*, 117–121. https://doi.org/10.1016/j.matlet.2018.04.120
152. Radhamani, A. V., Krishna Surendra, M., & Ramachandra Rao, M. S. (2018). Tailoring the supercapacitance of Mn_2O_3 nanofibers by nanocompositing with spinel-$ZnMn_2O_4$. *Materials and Design, 139*, 162–171. https://doi.org/10.1016/j.matdes.2017.11.005
153. Long, L., Wang, S., Xiao, M., & Meng, Y. (2016). Polymer electrolytes for lithium polymer batteries. *Journal of Materials Chemistry A, 4*(26), 10038–10069. https://doi.org/10.1039/C6TA02621D
154. Rajeevan, S., John, S., & George, S. C. (2021). Polyvinylidene fluoride: A multifunctional polymer in supercapacitor applications. *Journal of Power Sources, 504*, 230037. https://doi.org/10.1016/j.jpowsour.2021.230037
155. Boaretto, N., Meabe, L., Martinez-Ibañez, M., Armand, M., & Zhang, H. (2020). Review—Polymer electrolytes for rechargeable batteries: From nanocomposite to nanohybrid. *Journal of The Electrochemical Society, 167*(7), 070524. https://doi.org/10.1149/1945-7111/ab7221
156. Qiao, L., Judez, X., Rojo, T., Armand, M., & Zhang, H. (2020). Review—Polymer electrolytes for sodium batteries. *Journal of The Electrochemical Society, 167*(7), 070534. https://doi.org/10.1149/1945-7111/ab7aa0
157. Wu, Y., Li, Y., Wang, Y., Liu, Q., Chen, Q., & Chen, M. (2022). Advances and prospects of PVDF based polymer electrolytes. *Journal of Energy Chemistry, 64*, 62–84. https://doi.org/10.1016/j.jechem.2021.04.007
158. Tõnurist, K., Thomberg, T., Jänes, A., & Lust, E. (2013). Specific performance of supercapacitors at lower temperatures based on different separator materials. *Journal of The Electrochemical Society, 160*(3), A449–A457. https://doi.org/10.1149/2.044303jes

159. Jabbarnia, A., Khan, W. S., Ghazinezami, A., & Asmatulu, R. (2016). Investigating the thermal, mechanical, and electrochemical properties of PVdF/PVP nanofibrous membranes for supercapacitor applications. *Journal of Applied Polymer Science, 133*(30). https://doi.org/10.1002/app.43707
160. Wang, F., Kim, H.-J., Park, S., Kee, C.-D., Kim, S.-J., & Oh, I.-K. (2016). Bendable and flexible supercapacitor based on polypyrrole-coated bacterial cellulose core–shell composite network. *Composites Science and Technology, 128*, 33–40. https://doi.org/10.1016/j.compscitech.2016.03.012
161. He, T., Jia, R., Lang, X., Wu, X., & Wang, Y. (2017). Preparation and electrochemical performance of PVdF ultrafine porous fiber separator-cum-electrolyte for supercapacitor. *Journal of The Electrochemical Society, 164*, E379–E384. https://doi.org/10.1149/2.0631713jes
162. Shen, X., Li, Z., Deng, N., Kang, W., Fan, J., & Liu, Y. (2019). PVDF/TBAPF6 hierarchical nanofiber gel membrane for lithium ion capacitor with ultrahigh ion conductivity and excellent interfacial compatibility. *Electrochimica Acta, 318*, 801–808. https://doi.org/10.1016/j.electacta.2019.06.095
163. Subramania A, Sundaram NTK, Priya AR, Gangadharan R, Vasudevan T (2005) Preparation of a microporous gel polymer electrolyte with a novel preferential polymer dissolution process for Li-ion batteries. *Journal of Applied Polymer Science, 98*(5), 1891–1896. https://doi.org/10.1002/app.22114
164. Maurya, D. K., Murugadoss, V., Guo, Z., & Angaiah, S. (2021). Designing $Na_2Zn_2TeO_6$-embedded 3D-nanofibrous poly(vinylidenefluoride)-co-hexafluoropropylene-based nanohybrid electrolyte via electrospinning for durable sodium-ion capacitors. *ACS Applied Energy Materials*. https://doi.org/10.1021/acsaem.1c01682
165. Kalyana Sundaram, N. T., & Subramania, A. (2007). Nano-size $LiAlO_2$ ceramic filler incorporated porous PVDF-co-HFP electrolyte for lithium-ion battery applications. *Electrochimica Acta, 52*(15), 4987–4993. https://doi.org/10.1016/j.electacta.2007.01.066
166. Subramania, A., Kalyana Sundaram, N. T., Sathiya Priya, A. R., & Vijaya Kumar, G. (2007). Preparation of a novel composite micro-porous polymer electrolyte membrane for high performance Li-ion battery. *Journal of Membrane Science, 294*(1), 8–15. https://doi.org/10.1016/j.memsci.2007.01.025
167. Solarajan, A. K., Murugadoss, V., & Angaiah, S. (2017). High performance electrospun PVdF-HFP/SiO_2 nanocomposite membrane electrolyte for Li-ion capacitors. *Journal of Applied Polymer Science, 134*(32), 45177. https://doi.org/10.1002/app.45177
168. Solarajan, A. K., Murugadoss, V., & Angaiah, S. (2016). Montmorillonite embedded electrospun PVdF–HFP nanocomposite membrane electrolyte for Li-ion capacitors. *Applied Materials Today, 5*, 33–40. https://doi.org/10.1016/j.apmt.2016.09.002
169. Solarajan, A. K., Murugadoss, V., & Angaiah, S. (2017). Dimensional stability and electrochemical behaviour of ZrO_2 incorporated electrospun PVdF-HFP based nanocomposite spolymer membrane electrolyte for Li-ion capacitors. *Scientific Reports, 7*(1), 45390. https://doi.org/10.1038/srep45390
170. Maurya, D. K., Balan, B., Murugadoss, V., Yan, C., & Angaiah, S. (2020) A fast Li-ion conducting $Li_{7.1}La_3Sr_{0.05}Zr_{1.95}O_{12}$ embedded electrospun PVDF-HFP nanohybrid membrane electrolyte for all-solid-state Li-ion capacitors. *Materials Today Communications, 25*, 101497. https://doi.org/10.1016/j.mtcomm.2020.101497
171. Wang, Z., Zhu, M., Pei, Z., Xue, Q., Li, H., Huang, Y., & Zhi, C. (2020). Polymers for supercapacitors: Boosting the development of the flexible and wearable energy storage. *Materials Science and Engineering: R: Reports, 139*, 100520. https://doi.org/10.1016/j.mser.2019.100520
172. Laforgue, A. (2011). All-textile flexible supercapacitors using electrospun poly(3,4-ethylenedioxythiophene) nanofibers. *Journal of Power Sources, 196*(1), 559–564. https://doi.org/10.1016/j.jpowsour.2010.07.007
173. Lee, P.-C., Han, T.-H., Hwang, T., Oh, J.-S., Kim, S.-J., Kim, B.-W., Lee, Y., Choi, H. R., Jeoung, S. K., Yoo, S. E., & Nam, J.-D. (2012). Electrochemical double layer capacitor performance of electrospun polymer fiber-electrolyte membrane fabricated by solvent-assisted and

thermally induced compression molding processes. *Journal of Membrane Science, 409–410*, 365–370. https://doi.org/10.1016/j.memsci.2012.04.007
174. Liu, X., Naylor Marlow, M., Cooper, S. J., Song, B., Chen, X., Brandon, N. P., & Wu, B. (2018). Flexible all-fiber electrospun supercapacitor. *Journal of Power Sources, 384*, 264–269. https://doi.org/10.1016/j.jpowsour.2018.02.081
175. Peng, H., Xiao, L., Sun, K., Ma, G., Wei, G., & Lei, Z. (2019). Preparation of a cheap and environmentally friendly separator by coaxial electrospinning toward suppressing self-discharge of supercapacitors. *Journal of Power Sources, 435*, 226800. https://doi.org/10.1016/j.jpowsour.2019.226800
176. Pan, Q., Tong, N., He, N., Liu, Y., Shim, E., Pourdeyhimi, B., & Gao, W. (2018). Electrospun mat of poly(vinyl alcohol)/graphene oxide for superior electrolyte performance. *ACS Applied Materials and Interfaces, 10*(9), 7927–7934. https://doi.org/10.1021/acsami.7b14498
177. Ji, Y., Li, S., Li, G., Xu, J., Zuo, D., & Zhang, H. (2019). Preparation and electrochemical properties of SPEEK/PSF based membrane for supercapacitors. *Materials Research Express, 6*(10), 105538. https://doi.org/10.1088/2053-1591/ab406c
178. Kotatha, D., Hirata, M., Ogino, M., Uchida, S., Ishikawa, M., Furuike, T., & Tamura, H. (2019). Preparation and characterization of electrospun gelatin nanofibers for use as nonaqueous electrolyte in electric double-layer capacitor. *Journal of Nanotechnology, 2019*, 2501039. https://doi.org/10.1155/2019/2501039
179. Liu, W., Ju, J., Deng, N., Wang, L., Wang, G., Li, L., Kang, W., & Cheng, B. (2020). Designing inorganic-organic nanofibrous composite membrane for advanced safe Li-ion capacitors. *Electrochimica Acta, 337*, 135821. https://doi.org/10.1016/j.electacta.2020.135821
180. Li, X., Gu, T., & Wei, B. (2012). Dynamic and galvanic stability of stretchable supercapacitors. *Nano Letters, 12*(12), 6366–6371. https://doi.org/10.1021/nl303631e
181. Shen, X.-I., Li, Z.-J., Deng, N.-P., Fan, J., Wang, L., Xia, Z.-P., Kang, W.-M., & Liu, Y. (2020). A leaf-vein-like MnO_2@PVDF nanofiber gel polymer electrolyte matrix for Li-ion capacitor with excellent thermal stability and improved cyclability. *Chemical Engineering Journal, 387*, 124058. https://doi.org/10.1016/j.cej.2020.124058
182. Maurya, D. K., Murugadoss, V., & Angaiah, S. (2019) All-solid-state electrospun poly(vinylidene fluoride-co-hexafluoropropylene)/$Li_{7.1}La_3Ba_{0.05}Zr_{1.95}O_{12}$ nanohybrid membrane electrolyte for high-energy li-ion capacitors. *The Journal of Physical Chemistry C, 123*(50), 30145–30154. https://doi.org/10.1021/acs.jpcc.9b09264
183. Liu, M., Turcheniuk, K., Fu, W., Yang, Y., Liu, M., & Yushin, G. (2020). Scalable, safe, high-rate supercapacitor separators based on the Al_2O_3 nanowire Polyvinyl butyral nonwoven membranes. *Nano Energy, 71*, 104627. https://doi.org/10.1016/j.nanoen.2020.104627



Dheeraj Kumar Maurya received M.Sc. (Applied Physics) and M.Phil. (Physics) degrees in 2014 and 2016, respectively from the Babasaheb Bhimrao Ambedkar University, Lucknow. Currently, he is working with Prof. Subramania as a Research scholar at Electro-Materials Research Laboratory, Centre for Nanoscience and Technology, Pondicherry University, Puducherry, India. His research interests include the development of electrospun nanofibrous hybrid materials for energy storage devices and polymer-based nanocomposites for humidity sensing.



Subramania Angaiah is working as a Professor at the Centre for Nanoscience and Technology, Pondicherry University, India. He obtained his Ph.D. degree from Alagappa University and CSIR-CECRI (2001) and Postdoctoral training from the Korean Institute of Science and Technology (KIST), Seoul, South Korea (2007–2008). His current research interests include the development of Nanostructured materials for M-ion Batteries, Supercapacitors, IT-SOFC, DSSC, QDSSC, PSC, and Gas sensors. Besides that he is also working on the development of Metal matrix nanocomposites, Functional Nanocoating, Electrospun membranes for wound healing, Water purification, and Shelf-Life improvement of fruits and vegetables, Anti-Corrosive packaging materials for metals etc. He has published more than 150 scientific publications (h-index: 46, citations: >6500) and filed 11 patents in INDIA, US and EU. He is also the recipient of several awards and honors like Fellow of Royal Society of Chemistry (FRSC), Fellow of Indian Chemical Society, Fellow of the Academy of Science, Chennai, UGC Mid-Career Award, AICTE-Career Award, etc.

Chapter 14
Energy Harvesting Solutions Based on Piezoelectric Textiles Structures from Macro Nano Approach



Zhongchen He, Elham Mohsenzadeh, François Rault, Maryline Lewandowski, and Fabien Salaün

Abstract Reports on the global market for smart textiles show regularly interesting growth levels in the coming years. These textiles, capable of reacting to a stimulus with an appropriate response, are the subject of much research to remove the barriers that still slow down their penetration in markets as diverse as sports, health, transport, and fashion. One of the brakes facing these textile structures is directly related to the energy supply necessary for the proper functioning of the various sensors, actuators, etc., of these e-textiles. The current solution consists of using batteries which, beyond the problems of integration, comfort, use, etc., represent a real environmental challenge. However, alternatives exist in the design of energy harvesting systems. This chapter deals briefly with different sources of available energy and the associated phenomena for designing energy harvesting textile structures. A synthesis of studies focused on the realization of textiles that convert mechanical energy into electrical energy through the phenomenon of piezoelectricity is finally presented by addressing at different scales (micro and/or nano) the issues resulting from the choice of materials, their processes, and the properties obtained with the final textile structures.

Keywords Smart textile · Energy harvesting · Piezoelectricity · Micro/nano textile structure

Z. He (✉) · E. Mohsenzadeh (✉) · F. Rault · M. Lewandowski · F. Salaün
Univ. Lille, ENSAIT, ULR 2461, GEMTEX - Génie et Matériaux Textiles, 59000 Lille, France
e-mail: zhongchen.he@ensait.fr

E. Mohsenzadeh
e-mail: elham.mohsenzadeh@junia.com

F. Rault
e-mail: francois.rault@ensait.fr

M. Lewandowski
e-mail: maryline.lewandowski@ensait.fr

F. Salaün
e-mail: fabien.salaun@ensait.fr

E. Mohsenzadeh
Junia, 59000 Lille, France

© The Author(s), under exclusive license to Springer Nature Switzerland AG 2022

A. Vaseashta and N. Bölgen (eds.), *Electrospun Nanofibers*,
https://doi.org/10.1007/978-3-030-99958-2_14

14.1 Introduction

In recent years of research, smart textiles have received more and more attention. In addition to the advantages of traditional textiles (flexibility, comfortability, etc.), smart textiles also have other high added values, such as providing energy, which helps solve the world's growing energy shortage. One of the main challenges to be solved in the development of such structures is to ensure the power supply of the various electronic components (sensors, actuators, etc.) integrated into the textiles. Currently, electrical energy is provided by using batteries, and the batteries are integrated into the textile structure. However, the addition of batteries decreased the flexibility of the textile, and the batteries were less well-integrated into the textile structure, which limits the acceptability of the product consumer. One of the alternatives is to develop textile-based energy harvesting systems.

There are several effects or phenomena that ensure energy production independently or jointly. Textile-based energy harvesting systems are classified into three types based on recent research: electromagnetic waves (development of solar cells based on the use of photovoltaic effect, development of textile antennas for radiofrequency energy harvesting operating on various bands [1–3]), heat (development of textiles based on the pyroelectric effect or thermoelectric textiles exploiting the Seebeck effect [4–6]) and movements (development of triboelectric textiles or piezoelectric textiles [7–9]).

The energy from ambient light is a kind of energy that can provide more recovered energy than mechanical or thermal energy. However, the ambient light is not available continuously. The photovoltaic cells are less efficient when the application is used indoors because of the lower light power density. The application used by thermal energy is based on the phenomena named the Seebeck effect [10]: a temperature gradient between two dissimilar electrical conductors causes charge carriers from the hot zone to the cooler one. However, the temperature variation for standard applications is relatively insignificant, limiting the use of energy harvesters based on the Seebeck effect.

The daily power associated with human body movements (especially limb movements) can represent up to a few tens of watts. Harvesting a tiny part of the energy dissipated during the various movements would be enough to power some electronic elements associated with the e-textile function. Energy harvesting systems based on the piezoelectric effect can convert mechanical energy into electrical energy. In 1880, Jacques Curie and Pierre Curie have discovered the piezoelectric effect. It is a phenomenon that electricity can be generated when external pressure is applied to a piezoelectric material that has a non-centrosymmetric crystal structure [11]. For decades, the piezoelectric performance of many materials has been researched, including inorganic piezoelectric materials [12–15], as well as organic materials [16–18].

In this chapter, the materials used for piezoelectric application are introduced firstly. Then, the effects of micro and nanostructures on the structure and performance of energy harvesters are systematically explained. Throughout this chapter,

the importance of materials and structures at various scales (micro/nano) is discussed. In addition, the application of smart textiles in the field of energy harvesting has also been further elaborated and prospected.

14.2 Materials Used for Piezo Applications

Piezoelectric materials can convert mechanical energy into electrical energy and store it. Therefore, piezoelectric materials are usually used in piezoelectric applications (sensors, energy harvesting devices, etc.). Piezoelectric materials are mainly divided into two categories: ceramic materials, and polymer materials. The important parameters of piezoelectric materials are piezoelectric strain coefficient (d), piezoelectric voltage coefficient (g), electromechanical coupling (k_{33}, k_{31}, k_t), dielectric constant (K), dielectric loss tangent (tan δ), mechanical quality factor (Q), acoustic impedance (ρc). The piezoelectric coefficient of different piezoelectric materials is shown in Table 14.1.

As shown in Table 14.1, compared to polymer materials, ceramic piezoelectric materials have a higher piezoelectric coefficient, greater electromechanical coupling. This shows that ceramic piezoelectric materials have better dielectric and piezoelectric properties. Therefore, ceramic materials are widely used in piezoelectric applications. However, they have some disadvantages, such as lack of flexibility, and high density. Due to these disadvantages, ceramic materials cannot be used in some piezoelectric applications. It is difficult, for example, to prepare wearable piezoelectric devices. However, even if piezoelectric devices are prepared, they lack a comfortable fit. In contrast, although the piezoelectric properties of piezoelectric polymer materials are not as good as some ceramic materials, the advantages of polymer materials, such as easy process, flexibility, low density, and high break strength, allow polymer materials to be more widely used in piezoelectric applications, especially in the field of wearable piezoelectric applications. In addition, some polymer

Table 14.1 The piezoelectric coefficient of different piezoelectric materials

Material	Piezoelectric coefficient (d)	Ref.
$PbZr_xTi_{1-x}O_3$(PZT)	300–1000 pC/N	[19, 20]
$Na_xK_{1-x}NbO_3$(NKN)	100–400 pC/N	[21, 22]
AlN	3–5 pm/V	[23]
ZnO	14–26 pm/V	[23]
$BaTiO_3$	191 pC/N	[24]
PVDF	20–28 pC/N	[25]
P(VDF-TrFE)	6–12 pC/N	[26]
PS	3 pC/N	[27]
PAN	2–3 pC/N	[28]

materials also have piezoelectric properties (such as PVDF) that are not inferior to ceramic materials. Compared with other bulk or thin-film, unique features such as extremely long length and small diameters make nanofibers have higher piezoelectricity because of the alignment of dipoles responsible for polarization inside the confined fiber dimensions at small scales [29]. Therefore, polymer fibers are widely researched in piezoelectric applications.

14.3 Microscale Fibers Used in Piezo Applications

As mentioned in the previous section, the materials used in applications based on piezoelectric phenomena are mainly ceramics or polymeric materials and are often in the form of bulk or thin films. In the case of the development of textile structures, the basic element is fiber. The fineness, as well as the material, is a parameter of the fiber that has a direct impact on the specificities of the textiles produced. In the case of the development of piezoelectric fiber, a distinction will be made between fibers with a diameter on the nanoscale and those with a diameter of up to several tens of microns ("microscale"). Although other processes for producing nanofibers (centrifugal spinning, etc.) can be used, most piezoelectric nanofibers are produced by electrospinning (Sect. 14.4). Studies on the development of piezoelectric polymer fibers used in traditional textile structures (woven or knitted fabrics) have mainly been conducted using a process called melt spinning. This process consists of melting polymer pellets and then passing them through spinnerets to obtain filaments ("continuous fibers") of a few tens of microns. A drawing stage is associated with this process in order to control the diameter of the fibers. In the case of polymorphic polymers, such as those that can be used to produce piezoelectric filaments, this drawing influences the crystal structure obtained. Although the literature mentions some research on the development of piezoelectric mono- or multi-filaments based on PP [30, 31], PA11 [31, 32], or PLA [33], the research teams working on the development of piezoelectric filaments have focused on PVDF due to its interesting compromise in terms of piezoelectric properties, cost, and availability on an industrial scale for mass applications of this polymer. In Europe PVDF piezoelectric filaments were produced at the Institute for Materials Research and Innovation (IMRI) laboratory of the University of Bolton (UK), at the Department of Materials and Manufacturing Technology of Chalmers University of Technology (Sweden) [34, 35], at ITA from RWTH Aachen University (Germany) [34, 36], at Minho University (Portugal) [37] and at GEMTEX laboratory (France) [38, 39]. These research teams investigated the influence of the spinning parameters, especially the influence of the drawing ratio, on the crystalline structure of PVDF. The main objective was to optimize the content of the polar phase (mainly the β-phase). Except for the modification of the process parameters, researchers tried to optimize the piezoelectric character of PVDF by adding fillers such as nanoparticles. From all these studies it can be concluded that the drawing ratio is a predominant parameter to optimize the β-phase content. Some of these researchers have conducted studies on the development of multicomponent fibers in order to integer directly in

the filaments the electrodes necessary to harvest the charges generated during the mechanical stress of the PVDF layer. This "all-in-one" strategy, although attractive, has certain disadvantages, including limiting the possible drawing of filaments and consequently impacting on the formation of the β-phase. Obtaining the β-phase is a prerequisite for the production of piezoelectric textile structures based on PVDF. However, to optimize the piezoelectric response, a poling step is necessary. Studies were carried out for its realization during the spinning step [40]. Another way is to perform the poling after the development of the textile fabrics. However, the porosity of such textile structures limits the electric fields used. The development of PVDF fibers by electrospinning can overcome this because a high electrical field is applied during the process.

14.4 Nanofibers

Nanofibers are beneficial to increase the piezoelectric properties of smart textiles. The deformation is limited by the axial direction if the size of the structure in the orthogonal direction is reduced [30]. As a result, the dipoles in piezoelectric materials are better aligned, increasing their piezoelectric potential [31]. Table 14.2 shows the electrical performance of polymer nanofibers in recent research. According to the results, the material plays an important role in electrical performance. In the field of piezoelectric nanofibers, PVDF and its copolymers are extensively studied. PLA, PAN, and nanocomposite are also being researched because of their own advantages (For example, the biocompatibility and biodegradable characteristics of PLA [41]; the thermal stability and solvent resistance of PAN [42]). In this section, the piezoelectric properties of nanofibers prepared from different materials are described in detail, as well as their advantages, disadvantages, and applications.

14.4.1 PVDF

PVDF ($(–CH_2–CF_2–)_n$) is a thermoplastic semi-crystalline polymer with high purity, lightweight and flexible, solvent resistance, and electrical field stability [65]. Researchers have studied the piezoelectric properties of PVDF since Kawai discovered the piezoelectric effect of PVDF films in 1969 [66]. The PVDF crystalline structure exhibits five different polymorphs, α-, β-, γ-, δ-, and ε-phases [67]. The polar β- and γ-phases of PVDF show good piezoelectric responses because of the high dipolar moment per unit cell. Thus, the piezoelectric performance of PVDF is mostly related to the presence of polar crystalline phases [68, 69]. Compared with other methods (spin-coating, coprecipitation, etc.), electrospinning technology can significantly improve the polar phase in PVDF [70, 71]. During the electrospinning process, the flow of the polymer under the electric field causes the orientation of the polymer chain and polarizes the fibers. This can effectively improve the crystallinity

Table 14.2 The electrical performance of different polymer nanofibers

Material	Fiber diameter	Electrical performance	Test condition	Ref.
PVDF	–	15–20 mV, 0.2–0.3 nA	–	[43]
PVDF	500 nm to 6.5 μm	5–30 mV, 0.5–3 nA	2 Hz	[44]
PVDF	1.46 ± 0.61 μm	0.91 μW, 0.60 μW/cm^2,	20 N, 1 Hz	[45]
PVDF	–	210 V, 45 μA, 2.1 mW	1.8 Hz	[46]
PVDF	100–120 nm	48 V, 6 μA	8.3 kPa	[47]
PVDF	875 ± 150 nm	3.5 V, 241 nA	1 Hz	[48]
PVDF	100–300 nm	14 V, 180 nA	5 N, 1 Hz	[49]
P(VDF-TrFE)	1062 nm	139.5 V, 22.8 μW, 10.13 μW/cm^2	0.67 Hz	[29]
P(VDF-TrFE)	622 nm	8.75 μW/cm^2 (70 MΩ)	2 kPa, 1.5 Hz	[50]
P(VDF-TrFE)	509 ± 87 nm	0.517 mV/V, 35.5 ± 3.4 pm/V	–	[51]
P(VDF-HFP)	300–700 nm	2.6 V	–	[52]
P(VDF-HFP)-TiO_2/ZnO	196 ± 76 nm	14 V	2.5 N, 45 Hz	[53]
PLA	–	500 V, 5 W/m^2	50 N, 5 Hz	[54]
PLA	904 ± 105 nm	186 ± 28 pm	PFM, 0.2 Hz, ±25 V	[55]
PLA	–	0.9 nC, 19 pC/N	30 N	[56]
PAN	610 ± 50 nm	6.2 V, 5.0 μA	15 N, 2 Hz	[57]
PAN/PVDF	–	1.2 V (PAN/PVDF = 8:2)	–	[58]
PAN/$BaTiO_3$	–	1.5 V, 150 nA	2 N	[59]
PAN	650 ± 50 nm	2.4 V, 1.0 μA, 3.2 mW/m^2 (800 kΩ)	8 N, 2 Hz	[42]
PAN/ZnO	–	6.5 V, 2.3 μA, 10.8 mW/m^2 (700 kΩ)	8 N, 2 Hz	[42]
PVDF/PZT	109 nm	6.35 μW	15 Hz	[60]
P(VDF-$BaTiO_3$)	–	6 V, 1.5 μA	700 N, 3 Hz	[61]
PVDF/CNT	261 nm	161.66 V, 2.22 W/m^2	3.3 Hz	[62]
PVDF-graphene	150–350 nm	1511 V, 130 W/m^2	50 N, 5 Hz	[63]
PVDF-GO	0.1–0.25 um	16 V, 700 nA	2 Hz	[64]

and polar phase of PVDF [72]. Therefore, electrospinning is usually used to prepare PVDF nanofibers for the design of energy harvesting systems.

In the early research on the preparation of energy harvesting systems with PVDF nanofibers, the prepared PVDF nanofibers were generally directly connected to metal electrodes to measure the output and other properties of the energy harvesting system. For example, in 2010, in the researches of Hansen et al. [43] and Chang et al. [44], the nanogenerators were prepared by connecting the PVDF nanofibers with two metal

electrodes, the output voltage was 15–20 mV and 5–30 mV, respectively. This is a simple way to prepare an energy harvesting system, which can effectively detect the piezoelectric properties of the samples. Therefore, this assembly method is still widely used in the research of the piezoelectric properties of PVDF nanofibers. In 2020, Szewczyk et al. [45] compared the different power output of different PVDF-based energy harvesting with different F(β) by controlling the ambient humidity. The nanofibers were placed between Al electrodes and connected to copper wires. However, this method of directly connecting with the metal electrode also has some disadvantages. For example, the addition of the metal electrode reduces the flexibility of the textile. It is difficult to significantly improve piezoelectric performance. In recent years, the preparation of 3D nanofibrous structure (all-organic, etc.) energy harvesting systems has attracted more and more attention.

In 2014, Huang et al. [46] reported an all-fiber triboelectric nanogenerator based on electrospun PVDF nanofibers. The nanogenerators were composed of PVDF nanofibers and a pair of conducting fabric electrodes and can effectively harvest energy during human walking. The maximum output voltage, power, and current of the nanogenerator were 210 V, 2.1 mW, and 45 μA at a frequency of 1.8 Hz under the external load of 8 MΩ.

In 2018, Maity et al. [47] reported an all-organic piezoelectric nanogenerator based on multilayer assembled electrospun PVDF nanofiber mats. In this nanogenerator, the polymerized PEDOT-coated PVDF nanofibers are assembled as electrodes and electrospun PVDF nanofibers are used as an active component (middle layer). In the characterization results of electrospun PVDF nanofibers, the diameter of the fibers ranges from 100 to 120 nm, and the relative proportion of the β phase [F(β)] is greater than 90%. Furthermore, the F(β) does not change significantly with the PEDOT coating, which indicates PVDF nanofibers are responsible for most of the electrical performance. According to the energy-harvesting performance of the nanogenerator, the output voltage was increased with the increase of the imparting pressure. When the pressure was increased to 8.3 kPa, the output voltage and short-circuit current of the nanogenerator were 48 V and 6 μA, respectively.

In addition to the 3D nanofibrous structure energy harvesting, some PVDF nanofiber-based energy harvesting systems with other properties have been researched. In the research of Ju et al. [48], a superhydrophobic electrospun PVDF web for energy harvesting applications was developed. PVDF webs were electrospun and etched in CF_4 plasma, then immersed in water to create a superhydrophobic membrane. Although the content of the β-phase was slightly decreased after CF_4 plasma etching and water immersion, this reduction was so small that the content of the β-phase still shows good piezoelectric properties for energy harvesting. In the case of bend motion at 1 Hz, the superhydrophobic electrospun PVDF web showed an output voltage and current of 3.5 V and 241 nA, respectively. Besides the traditional solution electrospinning to prepare PVDF nanofibers for energy harvesting, there are many novel preparation methods for energy harvesting. For example, Shaikh et al. [49] used a highly scalable multi-nozzle far-field centrifugal electrospinning to prepare PVDF nanofiber for energy harvesting. A woven triboelectric nanogenerator was prepared by using PVDF nanofibers and commercial nylon cloth. In addition, the

precipitation-printed [73], near-field electrospinning [74] fast-centrifugal spinning [64], and other novel methods are used in the field of recent PVDF energy harvesting research.

14.4.2 Copolymers

The piezoelectric copolymers are widely used to prepare piezoelectric devices. For example, Ellingford et al. [75] demonstrated that SBS has electrical properties for energy harvesting applications. The main piezoelectric copolymer is PVDF copolymers. PVDF copolymers, such as P(VDF-TrFE) and P(VDF-HFP) [53], have been widely studied in energy harvesting applications due to their similar properties to PVDF (such as mechanical flexibility, ferroelectricity, etc.).

In 2017, Najjar et al. [52] reported a biocompatible P(VDF-HFP) based energy harvesting. The energy harvesting was assembled by PDMS and P(VDF-HFP). By stretching P(VDF-HFP) nanofibers by 200%, the diameter of PVDF-HFP nanofiber decreased from 600–1600 nm to 300–700 nm, and the fiber alignment was enhanced. The F(β) was increased by stretching. The results of the energy harvesting measurement showed that the output voltage increased from 0.21 to 2.6 V through stretching. A decrease in fiber diameter and an increase in F(β) cause an increase in piezoelectricity of P(VDF-HFP). Alternatively, the same orientation facilitates the output signal because the longitudinal piezoelectric effect along the force-acting vector contributes to the output signal.

Compared with PVDF, P(VDF-TrFE) has a higher ferroelectric β phase because the introduction of TrFE into PVDF favors the formation of the ferroelectric phase [76]. P(VDF-TrFE) nanofiber energy harvesting has been investigated in recent years. In 2016, Baniasadi et al. [51] prepared P(VDF-TrFE) energy harvesting by annealing the electrospinning P(VDF-TrFE) nanofiber at 135 °C. The annealing is aimed to increase the piezoelectricity of P(VDF-TrFE). Although the diameter of the nanofiber did not change after annealing (before: 490 ± 78 nm, after: 509 ± 87 nm), the annealing increased the β-phase content, and the degree of crystallinity was significantly increased from 25 to 52%. According to the results of PFM, the slope of PFM response of annealed samples was 0.517 mV/V whereas the slope of PFM response of as-made fiber is 0.32 mV/V. The piezoelectric constant of 35.5 ± 3.4 and 22 ± 1.6 pm/V were obtained for annealed nanofibers and as-made nanofibers, respectively. These results indicate that the degree of crystallinity and β phase plays an important role in the piezoelectricity of P(VDF-TrFE). In 2019, Zhang et al. [50] reported a piezoelectric nanogenerator based on aligned P(VDF-TrFE) nanofiber and 3D interdigital electrodes. The nanogenerator was assembled by PMMA, P(VDF-TrFE), and PDMS. The maximum power density is 8.75 $\mu W/cm^2$ at a load resistance of 70 MΩ. In 2020, Kim et al. [29] enhanced the piezoelectric energy harvesting of electrospinning P(VDF-TrFE) nanofibers by controlling the solvent. The maximum degree of crystallinity and content of β phase of electrospun P(VDF-TrFE) nanofibers were obtained by controlling the solvent. When DMF was used as the solvent, the

highest output voltage (117.9 V) was obtained at a frequency of 0.67 Hz. Similar to the experiment of Baniasadi [51], Kim increased the degree of crystallinity and content of β phase of P(VDF-TrFE) nanofiber by annealing the nanofibers at 125 °C, and the highest output voltage at 0.67 Hz was increased to 139.5 V.

14.4.3 PLA

PLA is a bioactive thermoplastic polymer material. Compared with traditional piezoelectric materials, such as PZT, ZnO, PVDF, etc. the piezoelectric properties of PLA are not excellent (d_{33} of PLA film: 5–12 pC/N [77]). However, PLA is a non-toxic and biodegradable piezoelectric material. The biocompatibility and biodegradable characteristics allow PLA to be widely studied in the field of green chemistry and medical fields like implanted medical devices [78–80]. In 2018, Pan et al. [54] reported fully biodegradable nanogenerators based on electrospun PLA nanofibers. The gelatin and PLA nanofibers were collected on Mg foil electrodes. Then PLA and gelatin were supported by 2 PET plates. The output voltage and maximum power density of the nanogenerator were 500 V and 5 W/m^2 under 50 N contact force and 5 Hz frequency. A PLA-based nanogenerator can degrade completely into the water in about 40 days, compared with another polymer-based energy harvesting. This is beneficial to environmental protection and sustainable development. However, the frequency (5 Hz) used in the experiment is much greater than the frequency that the human body can provide in daily exercise (usually the frequency of 1 Hz used in the experiment simulates human movement), which shows that PLA may have difficulty preparing wearable energy harvesting devices. PLA has advantages over other piezoelectric materials in the field of medical devices. It may be necessary to implant some devices into organisms, and if the materials used are toxic, they will cause harm to the health of the organism. Furthermore, if the materials cannot be degraded, the equipment needs to be surgically removed again. Piezoelectric devices made of PLA are less hazardous to organisms and are directly degradable in the organisms. Currently, the main challenges in PLA medical applications research are how to improve its biodegradation rate and its piezoelectric properties. According to the results of Zheng et al. [55], PLA/PLGA composites degrade at a faster rate than PLA material alone. In contrast to pure PLA nanofibers, PLA/PLGA composites have reduced piezoelectric properties. When the content of PLGA is increased from 0 to 25 wt%, the results of PFM decrease from 186 ± 28 pm to 89 ± 12 pm. This is because PLGA is a faster degrading polymer without piezoelectric responses. This research result allows people to choose between the piezoelectric properties of PLA and its biodegradability.

Curry et al. [56] used electrospinning to prepare PLA nanofibers with stable piezoelectric performance. The results show that the increase of nanofibers alignment by using a rotating drum collector can increase the piezoelectric properties of PLA. When the rotating speed is 4000 rpm, the d_{14} of the obtained sample is 19 pC/N, while the d_{14} of the conventional PLA sample is 12 pC/N. These PLA nanofibers can

be used to prepare a highly sensitive biodegradable pressure sensor, with a stable charge output for over 10,000 cycles when the impact force is 10 N. It can also be used to prepare a biodegradable ultra-sonic transducer. The authors implanted the devices into the back and intracranial cavities of rats. Histological images at 2 and 4 weeks after implantation showed that biodegradable PLA transducers can be safely implanted into the brain and open the blood–brain barrier effectively. These applications show that PLA has very broad prospects in drug delivery, implanted medical devices, and other fields.

14.4.4 PAN

PAN is a semicrystalline polymer with cyano (–CN) groups in each repeat unit. PAN has been widely used in the field of filtration because of its hydrophobic properties, thermal stability, and solvent resistance [81, 82]. Compared with PVDF, the piezoelectricity of commercially PAN is not as good as PVDF. For example, the piezoelectric effect charge constant (d_{13}) of PAN films is 2–3 pC/N, the d_{13} of PVDF films is 6–28 pC/N [26]. However, PAN has the potential to have excellent piezoelectric properties. PAN macromolecular chains have two conformations when PAN is in the solid state, 3^1-helical and planar zigzag (or "saw-tooth") [83–85]. The zigzag conformation has an all-transform (TTTT) structure which is like the β-phase PVDF. Meanwhile, the dipole moment of zigzag conformation is larger than β-phase PVDF (zigzag of PAN: 3.5 Debye [86] β-phase PVDF: 2.1 Debye [87]). In the research of PAN fibers piezoelectric applications, the main problem that needs to be solved is how to improve the content of zigzag conformation in PAN. There are mainly two ways to improve the content of zigzag conformation, namely electric field polarization and material recombination.

Electrospinning can effectively improve the zigzag conformation in PAN nanofibers through electric field polarization. Therefore, electrospinning is widely used in the research of preparing PAN nanofibers with piezoelectric properties [88, 89]. Wang et al. [57] prepared PAN nanofiber membranes with unexpectedly high piezoelectricity by using the electrospinning method. The PAN nanofiber membrane generated an electric output of 2.0 V and 1.2 μA, which was higher than the PVDF nanofiber membrane (1.2 V and 0.8 μA) when the frequency was 2 Hz. This is due to the fact that electrospinning can effectively improve the zigzag conformation of PAN. The content of zigzag conformation of PAN cast film is 73.6%, and its content in electrospun PAN nanofibrous membranes can increase to 79.7%. The article also proved that the use of a rotating drum collector to orient and stretch PAN nanofibers can improve the formation of the zigzag conformation. The results showed that when the rotating speed was increased to 1200 mm/s, electrospun PAN membranes generated the electric output increased from 2.0 V and 1.2 μA to 6.2 V and 5.0 μA.

The material recombination is usually to add materials with piezoelectric properties into PAN. On the one hand, this method can improve the zigzag conformation

in PAN. On the other hand, the selected material has excellent piezoelectric properties. These two advantages of material recombination are conducive to improving the piezoelectric properties of the PAN. For example, Cai et al. [59] prepared a PAN nanogenerator by adding $BaTiO_3$ to electrospinning PAN nanofibers, the nanogenerator has high flexibility and piezoelectric performance, which can generate 1.5 V and 150 nA when the applied force was 2 N. The research of Cai et al. [90] and others have shown that the increase in the piezoelectric properties of PAN nanofibers is because the addition of $BaTiO_3$ can promote the conversion of the 3^1-helical conformation in PAN to the zigzag conformation. Other piezoelectric materials such as ZnO also have similar effects to $BaTiO_3$. Sun et al. [42] add ZnO to PAN nanofibers to prepare PAN piezoelectric nanogenerator. For PAN electrospinning nanofibers without ZnO, the content of zigzag conformation is 45.59%, and the piezoelectric performance of PAN is not excellent (2.4 V, 1.0 μA). After adding ZnO, the content of zigzag conformation in PAN nanofibers increases to 51.55%, and the piezoelectric performance of PAN is also significantly improved (6.5 V, 2.3 μA).

14.4.5 Nanocomposite

Nanoparticles and polymers are used in electrospinning to produce nanocomposites with enhanced piezoelectric properties. Nanocomposite-based energy harvesting has therefore gained increasing attention in recent years. As was mentioned in this chapter PVDF is an attractive polymer due to its low cost, flexibility, and biocompatibility to be used in energy harvesting applications. Researchers have been working on the influence of adding some additives on the polymer's solutions prior to the electrospinning process. Up to now different organic and inorganic fillers such as ZnO, GO, PZT, $BaTiO_3$, and inorganic salts (NaCl, KBr, LiCl, KCl) [91], clay [92], ionic liquid [93], CNT [94], nanowire [95], or nanofiller such as palladium [96] and silver [97] have been added to the PVDF matrix. The results demonstrated that combining these fillers in the polymer matrix plays a distinct role in influencing the crystallization kinetics, crystallite size, crystalline morphology, degree of crystallinity, and the β phase content of the matrix by enhancing α to β transformation. We recap some of the scientific findings on the topic in this section of the chapter.

In the application of nanogenerators, ceramic composites materials such as lead zirconate titanate (PZT) and barium titanate ($BaTiO_3$) [61] are widely used. The lead zirconate titanate ($PbZr1\text{-}xTixO_3$), also known as PZT, occupies a prominent position among piezoelectric ceramics due to its high dielectric (~3000), electromechanical coupling factor (~0.71), piezoelectric, and pyroelectric properties. The piezoelectric constant (d_{33}) of PZT is about 289 m/v, significantly higher than that of ceramic piezoelectric [98–101]. In 2020, Koç et al. [60] fabricated a piezoelectric nanogenerator based on electrospun PVDF/PZT nanofibers. According to the output signal of electrospun PVDF/PZT-based nanogenerator, the addition of PZT significantly increased the output power from 3.44 μW (without PZT) to 6.35 μW (10

vol% PZT) under the frequency of 16 Hz. Their results showed that the addition of PZT could reduce the biocompatibility of nanocomposites.

Although other types of nanoparticles such as graphene [63], GO [102], and CNTs [103] do not have the high piezoelectric properties as ceramic materials, their addition can improve the electroactive phase of polymer materials. CNTs and GO are widely used due to their high aspect ratios and their electron-rich large surface areas as embedding electromechanical and electrochemical sensing particles inside composite film structures.

The nanofibrous structured membrane combined with well dispersed conductive particles will behave as smart materials due to the combination of the electrical properties of conductive particles, and the piezoelectricity of PVDF, and the improve of the β phase content. For instance, the results of Abolhasani et al. [104] who worked on the application of graphene-PVDF composite nanofibers for portable self-powering electronic devices showed that the addition of graphene (0.1 wt%) increased F(β) from 77 to 83%.

Because of the strong interaction between CNT and PVDF molecular chains, PVDF molecular chains and CNT are aligned along the fiber axis and are not destroyed, allowing highly oriented β-type crystals to form at the interface [105]. In 2018, Song et al. [62] reported mechanical energy harvesting based on electrospinning PVDF-CNT-$BaTiO_3$ nanofiber. The energy harvesting has an output voltage of 161.66 V and an electric power density of 2.22 W/m^2, which can drive 150 LEDs.

The research studies reported that the ferroelectric, pyroelectric, and piezoelectric properties of PVDF nanofibers were improved with large amounts of well-dispersed CNT. The piezoelectricity of PVDF combined with the conductivity of CNT and high levels of β phase formation during electrospinning may enable nanocomposites prepared from them to function as smart materials.

Many researchers worked on the influence of coaxial electrospinning in generating energy. In a study, Pan et al. [106] produced hollow PVDF nanofibers by coaxial electrospinning, showing output voltages 2.46 times greater than those produced by simple PVDF nanofibers. By combining PVDF and its copolymer PVDF-HFP with two semiconducting metal oxides of TiO_2 and ZnO, Deepalekshmi et al. [53] developed a flexible piezoelectric nanogenerator. They concluded that PVDF-HFP/PVDF (core/shell) containing ZnO and TiO_2 nanoparticles displays a maximum voltage of 14 V. According to their results, polymer fibers become thinner and more crystalline by the presence of nanoparticles in their inner cores and outer shells, and their breakdown strength is reduced.

14.5 Applications

According to the description in the above sections, the piezoelectric performance of smart textile-based energy harvesting is rapidly improving and has to get more

applications on a laboratory scale. In this section, the application of smart textile-based energy harvesting has been explained, and the research results have been presented.

14.5.1 Nanogenerators

Nanogenerators based on the smart textiles are a promising means of generating energy by directly using the mechanical energy produced by human movement. Different body movements produce different levels of energy. The amount of power varies from 0.007 to 67 W for finger motions and footfalls, respectively [107]. It is therefore essential to develop flexible nanogenerators based on smart textiles with high piezoelectric sensitivity. Nanogenerators can be divided based on the difference of mechanical energy into piezoelectric strain nanogenerators [108], piezoelectric kinetic nanogenerators [109], and triboelectric nanogenerators [110].

Liu et al. [111] prepared wearable piezoelectric nanogenerators based on PVDF using solution blow spinning. Their nanogenerators is a three-layer structure device: an aluminum foil is used as the lower electrode, then a PVDF nanofibrous membrane, PVA and PEDOT:PSS that covered the nanofibrous membrane is used as the upper electrode. The nanogenerators are fixed to an elbow and the results show that the nanogenerators can store the energy in commercial capacitors by swinging arm. One 47 μF commercial capacitor can be charged with the energy produced by the nanogenerator. By stimulating people's daily walking and jogging (swing arm frequency is about 0.3 and 1 Hz), the current output ranges are −4 nA to 6 nA and −10 nA to 15 nA, respectively.

Over the past few years, nanogenerators based on different types of energy have been widely studied and developed. By combining different kinds of smart materials to create hybrid nanogenerators, a more interesting area has been discovered that requires further investigation. Piezo-triboelectric hybrid nanogenerators, for example, can be constructed by combining piezo-triboelectric properties. In the work of Singh et al. [112], they prepared ZnO-PVDF film and synthesized piezo-tribo nanogenerators by coupling them to PTFE. The piezoelectric and triboelectric properties of PVDF are enhanced by adding ZnO. The maximum output power of piezo-tribo based hybrid nanogenerators is 24.5 $\mu W/cm^2$. Another kind of hybrid nanogenerator can combine two kinds of energy conversion, such as thermal to mechanical to electrical. For example, Gusarov et al. [113] developed a novel flexible composite thermal nanogenerators energy harvester based on the coupled pyro/piezoelectric effect of PVDF with shape memory effects of NiTiCu alloy.

14.5.2 Sensors

Since the smart textile converts mechanical deformation into electrical signals, it is widely used in sensors. The most widely used sensor application is the force sensor, such as pressure sensor, tactile sensors, etc. In the research of Zhao et al. [114], they prepared a force sensor made from carbonized electrospun PAN/barium titanate nanofibers that can detect pressure (0.15–25 N within a gauge factor of 1.44 V/N) and curvature (58.9°–120.2° within a sensitivity of 1.12 deg^{-1}). Meanwhile, the sensor demonstrated long-life stability that can work over 60,000 cycles. Reza et al. [115] fabricated a hybrid force sensor based on electrospun Spandex-PVDF nanofibers capable of detecting both dynamic force change and static force.

In recent years, many researchers have developed sensors with more complex functions based on force sensors. Hu et al. [116] developed highly sensitive pressure sensors based on P(VDF-TrFE)/BTO nanofiber film and high-density micropyramid array in their research. The results showed that the sensor can detect sound pressure as low as 0.6 Pa. The sensor can recognize the melody of "Twinkle Twinkle Little Star" produced by the speaker. Syu et al. [117] proposed designing biomimetic and flexible hybrid self-powered sensors based on Near-field electrospinning PVDF nanofibers. This force sensor can recognize five human gestures by using the learning algorithm of Long Short-Term Memory in the context of gesture recognition. The overall classification rate is 82.3%.

In addition to the force sensor, based on the nature of the material itself, the smart textile is also used in some other sensors such as humidity sensors. For example, the resistance of $Ti_3C_2T_x$ (MXene) film is increased when the humidity is increased. Therefore, the sensor developed based on MXene film have different electrical response under different humidity when other factors remain unchanged. In 2021, Wang et al. [118] fabricated a humidity sensor based on PVA/ MXene nanofibers membrane. The humidity sensor can detect the humidity in the range of 11–97% RH. Meanwhile, the discussed humidity sensor can respond and recover fast (0.9 and 6.3 s).

14.5.3 Energy Storage

In recent years, energy harvesting and energy storage based on smart textiles have attracted more and more attention. Smart textiles are usually integrated into energy harvesting devices with self-charging supercapacitors for energy storage. In the research of He et al. [119], they developed a piezoelectric driven self-powered patterned electrochromic supercapacitor. The supercapacitor device is prepared by using patterned PANI according to couple of methods. Piezoelectric nanogenerators are prepared by using electrospun PVDF nanofibers. The results showed that this device can charge and discharge a supercapacitor by harvesting energy generated by human motion.

The current research on energy storage devices is moving towards higher stability and higher energy density. Stojanovska et al. [120] prepared freestanding polymer/carbon electrodes based on PVDF nanofibers and carbon nanoparticles, then the electrodes were used in an aqueous supercapacitor and organic supercapacitors. Based on the results, it was found that the energy storage application has high areal capacitance (1120 mF/cm^2) and stability (retains 96.4% of capacitance after 10,000 cycles). In addition, Subramani et al. [121] also developed an energy storage device with high stability. The PTA/PVA/GO composite nanofibers worked as electrodes, and the energy storage capacity was 90% after 5000 cycles. The asymmetric supercapacitor fabricated by Tian et al. [122] has a capacity of 702.8 F/g and a maximum energy density of 51.4 Wh/kg, which is higher than many other reports (For example, in the research of Liu et al. [123], the capacitance was 141 F/g and energy density was 12.5 Wh/kg).

14.6 Conclusion

The application of piezoelectric textiles in energy harvesting is extremely broad. Piezoelectric textiles made from polymer fibers have several advantages over traditional ceramic piezoelectric materials, including flexibility and comfort, and can be more effectively used in wearable piezoelectric devices. In piezoelectric materials, micro and nanofibers improve the alignment of the dipoles, which results in a higher piezoelectric potential. A high piezoelectric coefficient is responsible for the wide study of the piezoelectric properties of PVDF and copolymers. In the field of medical devices, PLA with biodegradable and biocompatible properties has great potential. PAN nanofibers prepared by electrospinning have piezoelectric properties that are comparable to PVDF. In addition, adding nanoparticles can significantly enhance the piezoelectric properties of nanofibers. Currently, smart textiles with micro and nanostructures are widely used in nanogenerators, sensors, and energy storage.

References

1. Pan, S., Yang, Z., Chen, P., Deng, J., Li, H., & Peng, H. (2014). Wearable solar cells by stacking textile electrodes. *Angewandte Chemie—International Edition, 53*, 6110–6114. https://doi.org/10.1002/anie.201402561
2. Lin, C. H., Chiu, C. W., & Gong, J. Y. (2018). A wearable rectenna to harvest low-power RF Energy for wireless healthcare applications. In *2018 11th International Congress on Image and Signal Processing, BioMedical Engineering and Informatics (CISP-BMEI)* (pp. 1–5). https://doi.org/10.1109/CISP-BMEI.2018.8633222
3. Zhang, Z., Yang, Z., Wu, Z., Guan, G., Pan, S., Zhang, Y., Li, H., Deng, J., Sun, B., & Peng, H. (2014). Weaving efficient polymer solar cell wires into flexible power textiles. *Advanced Energy Materials, 4*, 1–6. https://doi.org/10.1002/aenm.201301750

4. Du, Y., Cai, K., Chen, S., Wang, H., Shen, S. Z., Donelson, R., & Lin, T. (2015). Thermoelectric fabrics: Toward power generating clothing. *Science and Reports, 5*, 1–6. https://doi.org/10.1038/srep06411
5. Wu, Q., & Hu, J. (2017). A novel design for a wearable thermoelectric generator based on 3D fabric structure. *Smart Materials and Structures*, *26*, 045037. https://doi.org/10.1088/1361-665X/aa5694
6. You, M. H., Wang, X. X., Yan, X., Zhang, J., Song, W. Z., Yu, M., Fan, Z. Y., Ramakrishna, S., & Long, Y. Z. (2018). A self-powered flexible hybrid piezoelectric-pyroelectric nanogenerator based on non-woven nanofiber membranes. *Journal of Materials Chemistry A, 6*, 3500–3509. https://doi.org/10.1039/c7ta10175a
7. Kwak, S. S., Kim, H., Seung, W., Kim, J., Hinchet, R., & Kim, S. W. (2017). Fully stretchable textile triboelectric nanogenerator with knitted fabric structures. *ACS Nano, 11*, 10733–10741. https://doi.org/10.1021/acsnano.7b05203
8. Choi, A. Y., Lee, C. J., Park, J., Kim, D., & Kim, Y. T. (2017). Corrugated textile based triboelectric generator for wearable energy harvesting. *Science and Reports, 7*, 7–12. https://doi.org/10.1038/srep45583
9. Anand, S., Soin, N., Shah, T. H., & Siores, E. (2016). Energy harvesting "3-D knitted spacer" based piezoelectric textiles. *IOP Conference Series Materials Science and Engineering, 141*, 6–11. https://doi.org/10.1088/1757-899X/141/1/012001
10. Zhou, W., Yamamoto, K., Miura, A., Iguchi, R., Miura, Y., Uchida, K. I., & Sakuraba, Y. (2021). Seebeck-driven transverse thermoelectric generation. *Nature Materials*, *20*, 463–467. https://doi.org/10.1038/s41563-020-00884-2
11. Lee, C., Park, H., & Lee, J. H. (2020). Recent structure development of poly(vinylidene fluoride)-based piezoelectric nanogenerator for self-powered sensor. *Actuators*, *9*. https://doi.org/10.3390/ACT9030057
12. Lee, K. Y., Bae, J., Kim, S. M., Lee, J. H., Yoon, G. C., Gupta, M. K., Kim, S., Kim, H., Park, J., & Kim, S. W. (2014). Depletion width engineering via surface modification for high performance semiconducting piezoelectric nanogenerators. *Nano Energy, 8*, 165–173. https://doi.org/10.1016/j.nanoen.2014.06.008
13. Kim, D., Lee, K. Y., Gupta, M. K., Majumder, S., & Kim, S. W. (2014). Self-compensated insulating ZnO-based piezoelectric nanogenerators. *Advanced Functional Materials, 24*, 6949–6955. https://doi.org/10.1002/adfm.201401998
14. Niu, X., Jia, W., Qian, S., Zhu, J., Zhang, J., Hou, X., Mu, J., Geng, W., Cho, J., He, J., et al. (2019). High-performance PZT-based stretchable piezoelectric nanogenerator. *ACS Sustainable Chemistry & Engineering, 7*, 979–985. https://doi.org/10.1021/acssuschemeng.8b04627
15. Lee, Y., Kim, S., Kim, D., Lee, C., Park, H., & Lee, J. H. (2020). Direct-current flexible piezoelectric nanogenerators based on two-dimensional ZnO nanosheet. *Applied Surface Science*, *509*, 145328. https://doi.org/10.1016/j.apsusc.2020.145328
16. Kim, D., Han, S. A., Kim, J. H., Lee, J. H., Kim, S. W., & Lee, S. W. (2020). Biomolecular piezoelectric materials: from amino acids to living tissues. *Advanced Materials, 32*, 1–16. https://doi.org/10.1002/adma.201906989
17. Liao, W. Q., Tang, Y. Y., Li, P. F., You, Y. M., & Xiong, R. G. (2018). Competitive halogen bond in the molecular ferroelectric with large piezoelectric response. *Journal of the American Chemical Society, 140*, 3975–3980. https://doi.org/10.1021/jacs.7b12524
18. Kim, J., Lee, J. H., Ryu, H., Lee, J. H., Khan, U., Kim, H., Kwak, S. S., & Kim, S. W. (2017). High-performance piezoelectric, pyroelectric, and triboelectric nanogenerators based on P(VDF-TrFE) with controlled crystallinity and dipole alignment. *Advanced Functional Materials, 27*, 1–8. https://doi.org/10.1002/adfm.201700702
19. Shrout, T. R., & Zhang, S. J. (2007). Lead-free piezoelectric ceramics: Alternatives for PZT? *Journal of Electroceramics, 19*, 111–124. https://doi.org/10.1007/s10832-007-9047-0
20. Kang, M. G., Jung, W. S., Kang, C. Y., & Yoon, S. J. (2016). Recent progress on PZT based piezoelectric energy harvesting technologies. *Actuators*, *5*. https://doi.org/10.3390/act5010005

21. Tao, H., Wu, J., Xiao, D., Zhu, J., Wang, X., & Lou, X. (2014). High strain in (K, Na)NbO_3-based lead-free piezoceramics. *ACS Applied Materials & Interfaces, 6*, 20358–20364. https://doi.org/10.1021/am505887y
22. Rubio-Marcos, F., Ochoa, P., & Fernandez, J. F. (2007). Sintering and properties of lead-free (K, Na, Li)(Nb, Ta, Sb)O_3 ceramics. *Journal of the European Ceramic Society, 27*, 4125–4129. https://doi.org/10.1016/j.jeurceramsoc.2007.02.110
23. Zhang, M., Yang, J., Si, C., Han, G., Zhao, Y., & Ning, J. (2015). Research on the piezoelectric properties of AlN thin films for MEMS applications. *Micromachines, 6*, 1236–1248. https://doi.org/10.3390/mi6091236
24. Banerjee, S., Bairagi, S., & Wazed Ali, S. (2021). A critical review on lead-free hybrid materials for next generation piezoelectric energy harvesting and conversion. *Ceramics International, 47*, 16402–16421. https://doi.org/10.1016/j.ceramint.2021.03.054
25. Usher, T. D., Cousins, K. R., Zhang, R., & Ducharme, S. (2018). The promise of piezoelectric polymers. *Polymer International, 67*, 790–798. https://doi.org/10.1002/pi.5584
26. Ramadan, K. S., Sameoto, D., & Evoy, S. (2014). A review of piezoelectric polymers as functional materials for electromechanical transducers. *Smart Materials and Structures*, *23*. https://doi.org/10.1088/0964-1726/23/3/033001
27. Hundal, J. S., & Nath, R. (1997). Correlation of piezoelectric effect and TSC in stretched polystyrene-acrylonitrile films. *IEEE Transactions on Dielectrics and Electrical Insulation, 4*, 742–747. https://doi.org/10.1109/94.654690
28. Street, R. M., Minagawa, M., Vengrenyuk, A., & Schauer, C. L. (2019). Piezoelectric electrospun polyacrylonitrile with various tacticities. *Journal of Applied Polymer Science, 136*, 2–10. https://doi.org/10.1002/app.47530
29. Kim, M., Lee, S., & Kim, Y. I. (2020). Solvent-controlled crystalline beta-phase formation in electrospun P(VDF-TrFE) fibers for enhanced piezoelectric energy harvesting. *APL Materials*, *8*. https://doi.org/10.1063/5.0011686
30. Bayramol, D. V. (2016). Investigation on the effect of draw ratio on voltage outputs of polarised isotactic polypropylene monofilaments. *Tekstil ve Muhendis, 23*, 166–171. https://doi.org/10.7216/1300759920162310301
31. Matsouka, D., Vassiliadis, S., Prekas, K., Bayramol, D. V., Soin, N., & Siores, E. (2016). On the measurement of the electrical power produced by melt spun piezoelectric textile fibres. *Journal of Electronic Materials, 45*, 5112–5126. https://doi.org/10.1007/s11664-016-4710-3
32. Vatansever, D., Hadimani, R. L., Shah, T., & Siores, E. (2012). Piezoelectric mono-filament extrusion for green energy applications from textiles. *Tekstil ve Muhendis, 19*, 1–5. https://doi.org/10.7216/130075992012198501
33. Oh, H. J., Kim, D. K., Choi, Y. C., Lim, S. J., Jeong, J. B., Ko, J. H., Hahm, W. G., Kim, S. W., Lee, Y., Kim, H., et al. (2020). Fabrication of piezoelectric poly(l-lactic acid)/$BaTiO_3$ fibre by the melt-spinning process. *Science and Reports, 10*, 1–12. https://doi.org/10.1038/s41598-020-73261-3
34. Yang, Z., Peng, H., Wang, W., & Liu, T. (2010). Crystallization behavior of poly(ε-caprolactone)/layered double hydroxide nanocomposites. *Journal of Applied Polymer Science, 116*, 2658–2667. https://doi.org/10.1002/app
35. Lund, A., Gustafsson, C., Bertilsson, H., & Rychwalski, R. W. (2011). Enhancement of β phase crystals formation with the use of nanofillers in PVDF films and fibres. *Composites Science and Technology, 71*, 222–229. https://doi.org/10.1016/j.compscitech.2010.11.014
36. Walter, S., Steinmann, W., Schütte, J., Seide, G., Gries, T., Roth, G., Wierach, P., & Sinapius, M. (2011). Characterisation of piezoelectric PVDF monofilaments. *Materials Technology, 26*, 140–145. https://doi.org/10.1179/175355511X13007211258962
37. Ferreira, A., Costa, P., Carvalho, H., Nobrega, J. M., Sencadas, V., & Lanceros-Mendez, S. (2011). Extrusion of poly(vinylidene fluoride) filaments: Effect of the processing conditions and conductive inner core on the electroactive phase content and mechanical properties. *Journal of Polymer Research, 18*, 1653–1658. https://doi.org/10.1007/s10965-011-9570-1
38. Boudriaux, M., Rault, F., Cochrane, C., Lemort, G., Campagne, C., Devaux, E., & Courtois, C. (2016). Crystalline forms of PVDF fiber filled with clay components along processing steps. *Journal of Applied Polymer Science, 133*, 1–9. https://doi.org/10.1002/app.43244

39. Talbourdet, A., Rault, F., Lemort, G., Cochrane, C., Devaux, E., & Campagne, C. (2018). 3D interlock design 100% PVDF piezoelectric to improve energy harvesting. *Smart Materials and Structures*, *27*. https://doi.org/10.1088/1361-665X/aab865
40. Hadimani, R. L., Bayramol, D. V., Sion, N., Shah, T., Qian, L., Shi, S., & Siores, E. (2013). Continuous production of piezoelectric PVDF fibre for e-textile applications. *Smart Materials and Structures*, *22*. https://doi.org/10.1088/0964-1726/22/7/075017
41. Min, T., Sun, X., Yuan, Z., Zhou, L., Jiao, X., Zha, J., Zhu, Z., & Wen, Y. (2021). Novel antimicrobial packaging film based on porous poly(lactic acid) nanofiber and polymeric coating for humidity-controlled release of thyme essential oil. *LWT*, *135*, 110034. https://doi.org/10.1016/j.lwt.2020.110034
42. Sun, Y., Liu, Y., Zheng, Y., Li, Z., Fan, J., Wang, L., Liu, X., Liu, J., & Shou, W. (2020). Enhanced energy harvesting ability of ZnO/PAN hybrid piezoelectric nanogenerators. *ACS Applied Materials & Interfaces, 12*, 54936–54945. https://doi.org/10.1021/acsami.0c14490
43. Hansen, B. J., Liu, Y., Yang, R., & Wang, Z. L. (2010). hybrid nanogenerator for concurrently harvesting biomechanical and biochemical energy. *ACS Nano, 4*, 3647–3652. https://doi.org/10.1021/nn100845b
44. Chang, C., Tran, V. H., Wang, J., Fuh, Y. K., & Lin, L. (2010). Direct-write piezoelectric polymeric nanogenerator with high energy conversion efficiency. *Nano Letters, 10*, 726–731. https://doi.org/10.1021/nl9040719
45. Szewczyk, P. K., Gradys, A., Kim, S. K., Persano, L., Marzec, M., Kryshtal, A., Busolo, T., Toncelli, A., Pisignano, D., Bernasik, A., et al. (2020). Enhanced piezoelectricity of electrospun polyvinylidene fluoride fibers for energy harvesting. *ACS Applied Materials & Interfaces, 12*, 13575–13583. https://doi.org/10.1021/acsami.0c02578
46. Huang, T., Wang, C., Yu, H., Wang, H., Zhang, Q., & Zhu, M. (2014). Human walking-driven wearable all-fiber triboelectric nanogenerator containing electrospun polyvinylidene fluoride piezoelectric nanofibers. *Nano Energy, 14*, 226–235. https://doi.org/10.1016/j.nanoen.2015.01.038
47. Maity, K., & Mandal, D. (2018). All-organic high-performance piezoelectric nanogenerator with multilayer assembled electrospun nanofiber mats for self-powered multifunctional sensors. *ACS Applied Materials & Interfaces, 10*, 18257–18269. https://doi.org/10.1021/acsami.8b01862
48. Ju, B. J., Oh, J. H., Yun, C., & Park, C. H. (2018). Development of a superhydrophobic electrospun poly(vinylidene fluoride) web via plasma etching and water immersion for energy harvesting applications. *RSC Advances, 8*, 28825–28835. https://doi.org/10.1039/c8ra04652b
49. Shaikh, M. O., Huang, Y. B., Wang, C. C., & Chuang, C. H. (2019). Wearable woven triboelectric nanogenerator utilizing electrospun PVDF nanofibers for mechanical energy harvesting. *Micromachines*, *10*. https://doi.org/10.3390/mi10070438
50. Zhang, L., Gui, J., Wu, Z., Li, R., Wang, Y., Gong, Z., Zhao, X., Sun, C., & Guo, S. (2019). Enhanced performance of piezoelectric nanogenerator based on aligned nanofibers and three-dimensional interdigital electrodes. *Nano Energy*, *65*, 103924. https://doi.org/10.1016/j.nanoen.2019.103924
51. Baniasadi, M., Xu, Z., Hong, S., Naraghi, M., & Minary-Jolandan, M. (2016). Thermo-electromechanical behavior of piezoelectric nanofibers. *ACS Applied Materials & Interfaces, 8*, 2540–2551. https://doi.org/10.1021/acsami.5b10073
52. Najjar, R., Luo, Y., Jao, D., Brennan, D., Xue, Y., Beachley, V., Hu, X., & Xue, W. (2017). Biocompatible silk/polymer energy harvesters using stretched poly (vinylidene fluoride-cohexafluoropropylene) (PVDF-HFP) Nanofibers. *Polymers (Basel). 9*. https://doi.org/10.3390/polym9100479
53. Ponnamma, D., Chamakh, M. M., Alahzm, A. M., Salim, N., Hameed, N., & Almaadeed, M. A. A. (2020). Core-shell nanofibers of polyvinylidene fluoride-based nanocomposites as piezoelectric nanogenerators. *Polymers (Basel)., 12*, 1–16. https://doi.org/10.3390/polym12102344

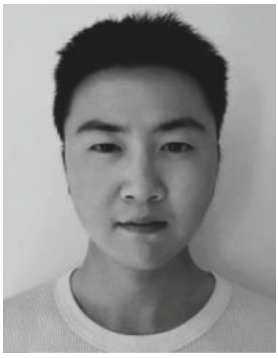
54. Pan, R., Xuan, W., Chen, J., Dong, S., Jin, H., Wang, X., Li, H., & Luo, J. (2018). Fully biodegradable triboelectric nanogenerators based on electrospun polylactic acid and nanostructured gelatin films. *Nano Energy, 45*, 193–202. https://doi.org/10.1016/j.nanoen.2017.12.048
55. Zheng, T., Yue, Z., Wallace, G. G., Du, Y., & Higgins, M. J. (2020). Nanoscale piezoelectric effect of biodegradable PLA-based composite fibers by piezoresponse force microscopy. *Nanotechnology*, *31*. https://doi.org/10.1088/1361-6528/ab96e3
56. Curry, E. J., Le, T. T., Das, R., Ke, K., Santorella, E. M., Paul, D., Chorsi, M. T., Tran, K. T. M., Baroody, J., Borges, E. R., et al. (2020). Biodegradable nanofiber-based piezoelectric transducer. *Proceedings of the National Academy of Sciences of the United States of America, 117*, 214–220. https://doi.org/10.1073/pnas.1910343117
57. Wang, W., Zheng, Y., Jin, X., Sun, Y., Lu, B., Wang, H., Fang, J., Shao, H., & Lin, T. (2019). Unexpectedly high piezoelectricity of electrospun polyacrylonitrile nanofiber membranes. *Nano Energy, 56*, 588–594. https://doi.org/10.1016/j.nanoen.2018.11.082
58. Ke, G., Jin, X., & Hu, H. (2020). Electrospun polyvinylidene fluoride/polyacrylonitrile composite fibers: Fabrication and characterization. *Iranian Polymer Journal*, *29*, 37–46. https://doi.org/10.1007/s13726-019-00773-9
59. Cai, T., Yang, Y., Bi, T., Bi, E., & Li, Y. (2020). $BaTiO_3$ assisted PAN fiber preparation of high performance flexible nanogenerator. *Nanotechnology*, *31*. https://doi.org/10.1088/1361-6528/ab7b87
60. Koç, M., Paralı, L., & Şan, O. (2020). Fabrication and vibrational energy harvesting characterization of flexible piezoelectric nanogenerator (PEN) based on PVDF/PZT. *Polymer Testing*, *90*. https://doi.org/10.1016/j.polymertesting.2020.106695
61. Guan, X., Xu, B., & Gong, J. (2020). Hierarchically architected polydopamine modified $BaTiO_3$@P(VDF-TrFE) nanocomposite fiber mats for flexible piezoelectric nanogenerators and self-powered sensors. *Nano Energy*, *70*, 104516. https://doi.org/10.1016/j.nanoen.2020.104516
62. Song, J., Yang, B., Zeng, W., Peng, Z., Lin, S., Li, J., & Tao, X. (2018). Highly flexible, large-area, and facile textile-based hybrid nanogenerator with cascaded piezoelectric and triboelectric units for mechanical energy harvesting. *Advanced Materials Technologies, 3*, 1–15. https://doi.org/10.1002/admt.201800016
63. Shi, L., Jin, H., Dong, S., Huang, S., Kuang, H., Xu, H., Chen, J., Xuan, W., Zhang, S., Li, S., et al. (2021). High-performance triboelectric nanogenerator based on electrospun PVDF-graphene nanosheet composite nanofibers for energy harvesting. *Nano Energy*, *80*, 105599. https://doi.org/10.1016/j.nanoen.2020.105599
64. Yang, J., Zhang, Y., Li, Y., Wang, Z., Wang, W., An, Q., & Tong, W. (2021). Piezoelectric nanogenerators based on graphene oxide/PVDF electrospun nanofiber with enhanced performances by in-situ reduction. *Materials Today Communications*, *26*. https://doi.org/10.1016/j.mtcomm.2020.101629
65. Alhasssan, Z. A., Burezq, Y. S., Nair, R., & Shehata, N. (2018). Polyvinylidene difluoride piezoelectric electrospun nanofibers: Review in synthesis, fabrication, characterizations, and applications. *Journal of Nanomaterials*. https://doi.org/10.1155/2018/8164185
66. Bae, J.-H., & Chang, S.-H. (2019). PVDF-based ferroelectric polymers and dielectric elastomers for sensor and actuator applications: A review. *Functional Composites and Structures*, *1*, 012003. https://doi.org/10.1088/2631-6331/ab0f48
67. Samadi, A., Hosseini, S. M., & Mohseni, M. (2018). Investigation of the electromagnetic microwaves absorption and piezoelectric properties of electrospun Fe3O4-GO/PVDF hybrid nanocomposites. *Organic Electronics, 59*, 149–155. https://doi.org/10.1016/j.orgel.2018.04.037
68. Martins, P. M., Ribeiro, S., Ribeiro, C., Sencadas, V., Gomesd, A. C., Gamae, F. M., & Méndeza, S. L. (2013). Effect of poling state and morphology of piezoelectric poly(vinylidene fluoride) membranes for skeletal muscle tissue engineering. *RSC Advances, 3*, 17938–17944. https://doi.org/10.1039/C3RA43499K

69. Ruan, L., Yao, X., Chang, Y., Zhou, L., Qin, G., & Zhang, X. (2018). Properties and applications of the β phase poly(vinylidene fluoride). *Polymers (Basel). 10*.
70. Reneker, D. H., Yarin, A. L., Fong, H., & Koombhongse, S. (2000). Bending instability of electrically charged liquid jets of polymer solutions in electrospinning. *Journal of Applied Physics, 87*, 4531–4547. https://doi.org/10.1063/1.373532
71. Yee, W. A., Kotaki, M., Liu, Y., & Lu, X. (2007). Morphology, polymorphism behavior and molecular orientation of electrospun poly(vinylidene fluoride) fibers. *Polymer (Guildf)., 48*, 512–521. https://doi.org/10.1016/j.polymer.2006.11.036
72. Liu, Y. L., Li, Y., Xu, J. T., & Fan, Z. Q. (2010). Cooperative effect of electrospinning and nanoclay on formation of polar crystalline phases in poly(vinylidene fluoride). *ACS Applied Materials & Interfaces, 2*, 1759–1768. https://doi.org/10.1021/am1002525
73. Tu, R., Sprague, E., & Sodano, H. A. (2020). Precipitation-printed high-β phase poly(vinylidene fluoride) for energy harvesting. *ACS Applied Materials & Interfaces*, *12*. https://doi.org/10.1021/acsami.0c16207
74. Fuh, Y. K., Li, S. C., Chen, C. Y., & Tsai, C. Y. (2018). A fully packaged self-powered sensor based on near-field electrospun arrays of poly(Vinylidene fluoride) nano/micro fibers. *Express Polymer Letters, 12*, 136–145. https://doi.org/10.3144/expresspolymlett.2018.12
75. Ellingford, C., Pengchaicharoen, A., Wemyss, A. M., & Wan, C. (2020). Structure and dielectric properties of electroactive tetraaniline grafted non-polar elastomers. *Journal of Composites Science, 4*, 25.
76. Yang, J., Chen, Q., Xu, F., Jiang, H., Liu, W., Zhang, X., Jiang, Z., & Zhu, G. (2020). Epitaxy enhancement of piezoelectric properties in P(VDF-TrFE) copolymer films and applications in sensing and energy harvesting. *Advanced Electronics Materials, 6*, 1–13. https://doi.org/10.1002/aelm.202000578
77. Ando, M., Kawamura, H., Kitada, H., Sekimoto, Y., Inoue, T., & Tajitsu, Y. (2013). Pressure-sensitive touch panel based on piezoelectric poly(L-lactic acid) film. *Japanese Journal of Applied Physics*, *52*. https://doi.org/10.7567/JJAP.52.09KD17
78. Zhao, Y., Xiong, J., Shi, X., & Ko, F. (2019) Capturing cancer cells using hyaluronic acid-immobilized electrospun random or aligned PLA nanofibers. *Colloids and Surfaces A: Physicochemical and Engineering Aspects*, *583*, 123978. https://doi.org/10.1016/j.colsurfa.2019.123978
79. Drumright, R. E., Gruber, P. R., & Henton, D. E. (2000). Polylactic acid technology. *Advanced Materials, 12*, 1841–1846. https://doi.org/10.1002/1521-4095(200012)12:23%3c1841::AID-ADMA1841%3e3.0.CO;2-E
80. Bose, S., Vahabzadeh, S., & Bandyopadhyay, A. (2013). Bone tissue engineering using 3D printing. *Materials Today, 16*, 496–504. https://doi.org/10.1016/j.mattod.2013.11.017
81. Selvam, A. K., & Nallathambi, G. (2015). Polyacrylonitrile/silver nanoparticle electrospun nanocomposite matrix for bacterial filtration. *Fibers and Polymers, 16*, 1327–1335. https://doi.org/10.1007/s12221-015-1327-8
82. Wu, Y. B., Bi, J., Lou, T., Song, T. B., & Yu, H. Q. (2015). Preparation of a novel PAN/cellulose acetate-Ag based activated carbon nanofiber and its adsorption performance for low-concentration SO2. *International Journal of Minerals Metallurgy and Materials*, *22*, 437–445. https://doi.org/10.1007/s12613-015-1091-1
83. Rizzo, P. (1996). Conformational disorder in the pseudohexagonal form of atactic polyacrylonitrile. *Macromolecules, 29*, 8852–8861. https://doi.org/10.1021/ma960699m
84. Hobson, R. J., & Windle, A. H. (1993). Crystalline structure of atactic poly(acrylonitrile). *Macromolecules, 26*, 6903–6907. https://doi.org/10.1021/ma00077a030
85. Grobelny, J., Sokól, M., & Turska, E. (1984). A study of conformation, configuration and phase structure of polyacrylonitrile and their mutual dependence by means of WAXS and 1H BL-n.m.r. *Polymer (Guildf). 25*, 1415–1418. https://doi.org/10.1016/0032-3861(84)90102-2
86. Minagawa, M., Miyano, K., Takahashi, M., & Yoshii, F. (1988). Infrared characteristic absorption bands of highly isotactic poly(acrylonitrile). *Macromolecules, 21*, 2387–2391. https://doi.org/10.1021/ma00186a015

87. Shao, H., Fang, J., Wang, H., & Lin, T. (2015). Effect of electrospinning parameters and polymer concentrations on mechanical-to-electrical energy conversion of randomly-oriented electrospun poly(vinylidene fluoride) nanofiber mats. *RSC Advances, 5*, 14345–14350. https://doi.org/10.1039/c4ra16360e
88. Shamsabadi, A. S., Ranjbar, M., Tavanai, H., & Farnood, A. (2019). Electrospinning of gold nanoparticles incorporated PAN nanofibers via in-situ laser ablation of gold in electrospinning solution. *Materials Research Express*, *6*, 0–12. https://doi.org/10.1088/2053-1591/ab0709
89. Ahmadi, Z., Ravandi, S. A. H., Haghighat, F., & Dabirian, F. (2020). Enhancement of the mechanical properties of PAN nanofiber/carbon nanotube composite mats produced via needleless electrospinning system. *Fibers and Polymers, 21*, 1200–1211. https://doi.org/10.1007/s12221-020-9726-x
90. Ueda, H., & Carr, S. H. (1984). Piezoelectricity in polyacrylonitrile. *Polymer Journal, 16*, 661–667.
91. Mokhtari, F., Shamshirsaz, M., Latifi, M., & Asadi, S. (2017). Comparative evaluation of piezoelectric response of electrospun PVDF (polyvinilydine fluoride) nanofiber with various additives for energy scavenging application. *Journal of the Textile Institute, 108*, 906–914. https://doi.org/10.1080/00405000.2016.1202091
92. Shah, A. A., Cho, Y. H., Nam, S. E., Park, A., Park, Y. I., & Park, H. (2020). High performance thin-film nanocomposite forward osmosis membrane based on PVDF/bentonite nanofiber support. *Journal of Industrial and Engineering Chemistry, 86*, 90–99. https://doi.org/10.1016/j.jiec.2020.02.016
93. Mahdavi Varposhti, A., Yousefzadeh, M., Kowsari, E., & Latifi, M. (2020). Enhancement of β-phase crystalline structure and piezoelectric properties of flexible PVDF/ionic liquid surfactant composite nanofibers for potential application in sensing and self-powering. *Macromolecular Materials and Engineering, 305*, 1–8. https://doi.org/10.1002/mame.201900796
94. Wang, S. H., Wan, Y., Sun, B., Liu, L. Z., & Xu, W. (2014). Mechanical and electrical properties of electrospun PVDF/MWCNT ultrafine fibers using rotating collector. *Nanoscale Research Letters, 9*, 1–7. https://doi.org/10.1186/1556-276X-9-522
95. Hansen, B. J., Liu, Y., Yang, R., & Wang, Z. L. (2010). Hybrid nanogenerator for concurrently harvesting biomechanical and biochemical energy. *ACS Nano, 4*, 3647–3652. https://doi.org/10.1021/nn100845b
96. Samanta, S., Layek, R. K., & Nandi, A. K. (2011). Active immobilized palladium catalyst based on multiporous amphiphilic graft copolymer. *Reactive & Functional Polymers, 71*, 1045–1054. https://doi.org/10.1016/j.reactfunctpolym.2011.07.006
97. Sharma, M., Srinivas, V., Madras, G., & Bose, S. (2016). Outstanding dielectric constant and piezoelectric coefficient in electrospun nanofiber mats of PVDF containing silver decorated multiwall carbon nanotubes: Assessing through piezoresponse force microscopy. *RSC Advances, 6*, 6251–6258. https://doi.org/10.1039/c5ra25671b
98. Feng, S., Zhang, H., He, D., Xu, Y., Zhang, A., Liu, Y., & Bai, J. (2019). Synergistic effects of $BaTiO_3$/multiwall carbon nanotube as fillers on the electrical performance of triboelectric nanogenerator based on polydimethylsiloxane composite films. *Energy Technology*, *7*. https://doi.org/10.1002/ente.201900101
99. Sriphan, S., Charoonsuk, T., Maluangnont, T., & Vittayakorn, N. (2019). High-performance hybridized composited-based piezoelectric and triboelectric nanogenerators based on $BaTiO_3$/PDMS composite film modified with $Ti_0.8O_2$ nanosheets and silver nanopowders cofillers. *ACS Applied Energy Materials*, *2*, 3840–3850. https://doi.org/10.1021/acsaem.9b00513
100. Sriphan, S., Nawanil, C., & Vittayakorn, N. (2018). Influence of dispersed phase morphology on electrical and fatigue properties of $BaTiO_3$/PDMS nanogenerator. *Ceramics International, 44*, S38–S42. https://doi.org/10.1016/j.ceramint.2018.08.264
101. Beeby, S. P., Tudor, M. J., & White, N. M. (2006). Energy harvesting vibration sources for microsystems applications. *Measurement Science and Technology*, *17*. https://doi.org/10.1088/0957-0233/17/12/R01

102. Yang, J., Zhang, Y., Li, Y., Wang, Z., Wang, W., An, Q., & Tong, W. (2020). Piezoelectric nanogenerators based on graphene oxide/PVDF electrospun nanofiber with enhanced performances by in-situ reduction. *Materials Today Communication*. https://doi.org/10.1016/j.mtcomm.2020.101629
103. Huang, X., Jiang, P., Kim, C., Liu, F., & Yin, Y. (2009). Influence of aspect ratio of carbon nanotubes on crystalline phases and dielectric properties of poly(vinylidene fluoride). *European Polymer Journal, 45*, 377–386. https://doi.org/10.1016/j.eurpolymj.2008.11.018
104. Abolhasani, M. M., Shirvanimoghaddam, K., & Naebe, M. (2017). PVDF/graphene composite nanofibers with enhanced piezoelectric performance for development of robust nanogenerators. *Composites Science and Technology, 138*, 49–56. https://doi.org/10.1016/j.compscitech.2016.11.017
105. Huang, S., Yee, W. A., Tjiu, W. C., Liu, Y., Kotaki, M., Boey, Y. C. F., Ma, J., Liu, T., & Lu, X. (2008). Electrospinning of polyvinylidene difluoride with carbon nanotubes: Synergistic effects of extensional force and interfacial interaction on crystalline structures. *Langmuir, 24*, 13621–13626.
106. Pan, C. T., Yen, C. K., Wang, S. Y., Lai, Y. C., Lin, L., Huang, J. C., & Kuo, S. W. (2015). Near-field electrospinning enhances the energy harvesting of hollow PVDF piezoelectric fibers. *RSC Advances, 5*, 85073–85081. https://doi.org/10.1039/c5ra16604g
107. Roundy, S., & Trolier-Mckinstry, S. (2018). Materials and approaches for on-body energy harvesting. *MRS Bulletin, 43*, 206–213. https://doi.org/10.1557/mrs.2018.33
108. Chung, J., Song, M., Chung, S.-H., Choi, W., Lee, S., Lin, Z.-H., Hong, J., & Lee, S. (2021). Triangulated cylinder origami-based piezoelectric/triboelectric hybrid generator to harvest coupled axial and rotational motion. *Research, 2021*, 1–9. https://doi.org/10.34133/2021/7248579
109. Jian, G., Jiao, Y., Meng, Q., Shao, H., Wang, F., & Wei, Z. (2020). 3D $BaTiO_3$ flower based polymer composites exhibiting excellent piezoelectric energy harvesting properties. *Advanced Materials Interfaces, 7*, 1–10. https://doi.org/10.1002/admi.202000484
110. Patnam, H., Dudem, B., Graham, S. A., & Yu, J. S. (2021). High-performance and robust triboelectric nanogenerators based on optimal microstructured poly(vinyl alcohol) and poly(vinylidene fluoride) polymers for self-powered electronic applications. *Energy*, *223*, 120031. https://doi.org/10.1016/j.energy.2021.120031
111. Liu, R. Q., Wang, X. X., Fu, J., Zhang, Q. Q., Song, W. Z., Xu, Y., Chen, Y. Q., Ramakrishna, S., & Long, Y. Z. (2019). Preparation of nanofibrous PVDF membrane by solution blow spinning for mechanical energy harvesting. *Nanomaterials*, *9*. https://doi.org/10.3390/nano9081090
112. Singh, H. H., & Khare, N. (2018). Flexible ZnO-PVDF/PTFE based piezo-tribo hybrid nanogenerator. *Nano Energy, 51*, 216–222. https://doi.org/10.1016/j.nanoen.2018.06.055
113. Gusarov, B., Gusarova, E., Viala, B., Gimeno, L., Boisseau, S., Cugat, O., Vandelle, E., & Louison, B. (2016). Thermal energy harvesting by piezoelectric PVDF polymer coupled with shape memory alloy. *Sensors Actuators, A Physical, 243*, 175–181. https://doi.org/10.1016/j.sna.2016.03.026
114. Zhao, G., Zhang, X., Cui, X., Wang, S., Liu, Z., Deng, L., Qi, A., Qiao, X., Li, L., Pan, C., et al. (2018). Piezoelectric polyacrylonitrile nanofiber film-based dual-function self-powered flexible sensor. *ACS Applied Materials & Interfaces, 10*, 15855–15863. https://doi.org/10.1021/acsami.8b02564
115. Reza, M. S., Kim, K. J., & Kim, H. (2020). Novel hybrid pressure sensor based on electrospun spandex-polyvinylidene fluoride composite nanofiber webs. *Fibers and Polymers, 21*, 2962–2975. https://doi.org/10.1007/s12221-020-0247-4
116. Hu, X., Jiang, Y., Ma, Z., He, Q., He, Y., Zhou, T., & Zhang, D. (2020). Highly sensitive P(VDF-TrFE)/BTO nanofiber-based pressure sensor with dense stress concentration microstructures. *ACS Applied Polymer Materials, 2*, 4399–4404. https://doi.org/10.1021/acsapm.0c00411
117. Syu, M. H., Guan, Y. J., Lo, W. C., & Fuh, Y. K. (2020). Biomimetic and porous nanofiber-based hybrid sensor for multifunctional pressure sensing and human gesture identification

via deep learning method. *Nano Energy*, *76*, 105029. https://doi.org/10.1016/j.nanoen.2020.105029
118. Wang, D., Zhang, D., Li, P., Yang, Z., Mi, Q., & Yu, L. (2021). Electrospinning of flexible poly(vinyl alcohol)/MXene nanofiber-based humidity sensor self-powered by monolayer molybdenum diselenide piezoelectric nanogenerator. *Nano-Micro Letters, 13*, 1–13. https://doi.org/10.1007/s40820-020-00580-5
119. He, Z., Gao, B., Li, T., Liao, J., Liu, B., Liu, X., Wang, C., Feng, Z., & Gu, Z. (2019). Piezoelectric-driven self-powered patterned electrochromic supercapacitor for human motion energy harvesting. *ACS Sustainable Chemistry & Engineering, 7*, 1745–1752. https://doi.org/10.1021/acssuschemeng.8b05606
120. Stojanovska, E., Ozturk, N. D., Polat, Y., Akbulut, H., & Kilic, A. (2019). Solution blown polymer/biowaste derived carbon particles nanofibers: An optimization study and energy storage applications. *Journal of Energy Storage*, *26*, 100962. https://doi.org/10.1016/j.est.2019.100962
121. Subramani, S., & Rajiv, S. (2021). Electrospun based polythioaniline/polyvinylalcohol/graphene oxide composite nanofibers for supercapacitor application. *Ionics (Kiel).* 2203–2218. https://doi.org/10.1007/s11581-021-03993-3
122. Tian, D., Lu, X., Zhu, Y., Li, M., & Wang, C. (2019). Fabrication of two-dimensional metal-organic frameworks on electrospun nanofibers and their derived metal doped carbon nanofibers for an advanced asymmetric supercapacitor with a high energy density. *Journal of Power Sources, 413*, 50–58. https://doi.org/10.1016/j.jpowsour.2018.12.014
123. Liu, Y., Zeng, Z., Sharma, R. K., Gbewonyo, S., Allado, K., Zhang, L., & Wei, J. (2019). A bi-functional configuration for a metal-oxide film supercapacitor. *Journal of Power Sources, 409*, 1–5. https://doi.org/10.1016/j.jpowsour.2018.10.084



Zhongchen He was born in Anhui, China in 1994. He received the B.S degree in polymer materials and engineering from Sichuan University, Chengdu, China, in 2016 and the M.S degree in polymer science and engineering from Sichuan University, Chengdu, China, in 2019. He is currently pursuing a Ph.D. degree at Centrale Lille University, Lille, France.

From 2019 to 2021, he was a Ph.D. student and worked at Ecole Nationale Supérieure des Arts et Industries Textiles (ENSAIT) in GEMTEX Laboratory. His research interest includes 3D nanofibrous macrostructures for piezoelectric energy harvesting via electrospinning/electrospray of polyvinylidene fluoride (PVDF) based material. Mr. He's awards and honors include the Sichuan University Scholarship, National Scholarship for Postgraduates and State Scholarship Fund.



Elham Mohsenzadeh was born in Yazd, Iran, in 1988. She received her bachelor's degree in textile engineering in 2007 from Yazd State University. She obtained her master's degree in Mechanic and Science of Fibers at Haute Alsace University in Mulhouse France. Her Ph.D. thesis focused on 'Study and Development of Electrospun Fibrous Multilayers Material for Medical Applications: Substitutive Membranes' and she received her degree in 2018. She is now an Associate Professor in the Innovative Textile Materials Group in JUNIA-HEI Graduate School of Engineering in Lille, France, since 2018. Her research interests include electrospinning and nanofibers for composites, tissue engineering, wound dressing, filtration, and sensors. She works on several national and European projects focused on textile functionalization, photonic textile, textile gas sensors, and facial mask filters by using electrospinning technic.



François Rault was born in Dunkerque, France in 1980. He received the M.S. degree in textile engineering from the Ecole Nationale Supérieure des Arts et Industries Textiles (ENSAIT), French Textile Engineering Institute, Roubaix, in 2004 and the Ph.D. degree in sciences and technology from the Université de Valenciennes et du Hainaut Cambrésis, in 2008.

Multifunctional Textiles and Processes group of GEMTEX, ENSAIT, Roubaix, France. He is the author of three book chapters and more than 25 articles. He develops functional fibers by melt spinning and innovative structures by various textile processes. He possesses strong experience in research and innovation in the field of smart (especially for energy harvesting, wireless communication, and data transfer) and multifunctional textiles (Fire Retardant textiles, etc.). He worked and managed research activities in European and French project.



Fabien Salaün got his master's degree in Organic and Macromolecular Chemistry at Lille 1 University (France) in 2001. In 2004, he got the Ph.D. Organic and Macromolecular Chemistry. In 2007, he obtained the position of Assistant Professor at ENSAIT (France) and from September 2017 he is full time Professor in Polymers Science and Textile Technologies. He has co-authored more than 65 peer-reviewed papers (1250 total citations; h Index: 20), 16 book chapters and several Communications to National and International Congresses. His main research activities include the formulation of microencapsulation processes, the synthesis of nano and microcapsules, the surface functionalization of textiles, the modification of polymers, their physico-chemical and thermo-mechanical characterization, and

the investigation of the structure-property relationships. Furthermore, the last years he has developed several microencapsulation processes based on sol-gel chemistry, and has an expertise in textile comfort, smart coating, and fiber science.

Chapter 15
Morphological and Mechanical Properties of Electrospun Polyurethane Nanofibers—Air-Filtering Application



Parian Mohamadi, Elham Mohsenzadeh, Cedric Cochrane, and Vladan Koncar

Abstract Currently, nanofibers have received attention due to their properties, such as high porosity, high aspect ratio, and lightweight. The most inexpensive and high-efficiency method to produce nanofibers is electrospinning, which includes single, or multi-jet and core/shell approaches. The structures and diameter of nanofibers depend on electrospinning parameters comprising a solution, environmental, and process parameters. Among different materials used in this system, such as natural polymers, conductive materials, drugs, and nanoparticles, adding synthetic polymers could improve mechanical properties. Polyurethane is one of the synthetic polymers, which is becoming popular in various applications such as composite, food packaging, wound dressing, and electrical sensors due to its flexibility and elasticity. Besides, polyurethane demonstrates diverse behaviors according to polymer basics obtained by several polymerization methods. In this chapter, the electrospinning of polyurethane, its applications relative to the air-filters clogging detection sensors, and more importantly its morphology and mechanical properties as nanofibers are described.

Keywords Polyurethane nanofibers · Electrospinning · Characterization · Air filtering

P. Mohamadi · E. Mohsenzadeh (✉) · C. Cochrane · V. Koncar
ENSAIT, GEMTEX–Laboratoire de Génie et Matériaux Textiles, University of Lille, 59000 Lille, France
e-mail: elham.mohsenzadeh@junia.com

P. Mohamadi
e-mail: parian-sadat.mohamm@ensait.fr

C. Cochrane
e-mail: cedric.cochrane@ensait.fr

V. Koncar
e-mail: Vladan.koncar@ensait.fr

E. Mohsenzadeh
Junia, 59000 Lille, France

© The Author(s), under exclusive license to Springer Nature Switzerland AG 2022

A. Vaseashta and N. Bölgen (eds.), *Electrospun Nanofibers*,
https://doi.org/10.1007/978-3-030-99958-2_15

15.1 Introduction

These days, many people are suffering from respiratory diseases so the Global Burden of Diseases reported that air pollution is the fourth greatest risk after high blood pressure, dietary risks, and smoking [1]. Besides, ANSES (**French Agency for Food, Environmental and Occupational Health & Safety**) announced the Indoor Air Quality Guidelines (IAQGs) for molecules concentrations in indoor air, and in the particular case of formaldehyde and chloramine, it is set at 10 $\mu g.m^{-3}$ (8 ppb) and 300 $\mu g.m^{-3}$ (60 ppb), respectively. That is why air filters play an important role nowadays in purifying the air especially in closed areas such as swimming pools or shopping centers [1]. An appropriate filter is a filter with high efficiency for removing the dust and low-pressure drop to let the air pass through it while these properties should preserve during use. For the production of air filters, the structures like nonwoven, nanofibers, paper, and foam and materials like polyacrylonitrile, polyphenylene sulfide, polyimide, Polyester, nomex, polyetherimide, glass fiber, and ceramic are applied. In addition, these structures should have air permeability, thermal, chemical, and dimensional stability [2]. Currently, large varieties of air filter technologies are available according to particle size (PM10, PM2.5, and PM1.0) and filtration efficiency. High-efficiency particulate air (HEPA) is a commercial filter that takes in the particles with 0.3 μm of diameter, volatile organic components, and bacteria with 99.97% efficiency, and this property will increase for particle diameters less and greater than 0.3 μm [3]. Figure 15.1 shows the structure of the air filter system.

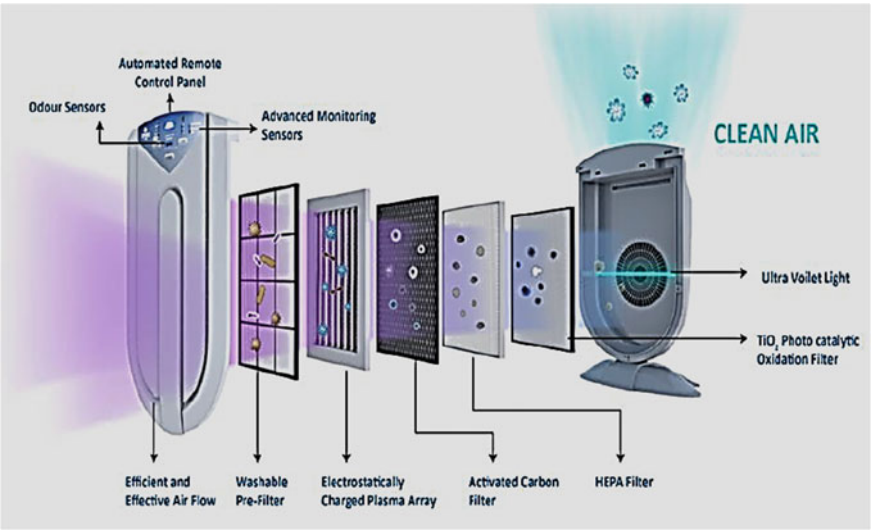


Fig. 15.1 The air filtration machine

In addition, the nonwoven filter is increasingly noticed because of proper performance, low cost, porosity, and flexibility [2]. Cai and Sorial (2009) [4] and Hassan and Sorial (2011) [5] worked on the absorption of volatile organic compounds (VOCs) including formaldehyde, trichloramine, toluene, and benzene by filters [1]. Presently, one of the most remarkable problems in air filtering is the detection of clogging of them by particles for changing or cleaning. The clogging occurs when the particles deposit thusly become a part of the filter [6]. Following this event the pressure drop increases and the efficiency also augments dramatically until cake formation and then falls [7]. In this case, the flexible textile sensors such as pressure, strain, humidity, and temperature sensors have attracted much attention in personalized health monitoring, human motion detection, structural health monitoring, smart garments, and robots. The important factors for evaluating these sensors are classified by sensitivity, stretchability, and repeatability. According to considerable academic results, the materials, structure, and method involve the performance of textile sensors. The textile sensors can be made from natural or synthetic fibers like cellulose acetate, cotton and wool or polyamide, polyester and polyurethane, and fabricated through several methods some of which are melt spinning, weaving, knitting, electrospinning, printing, and screening. Besides, by using flexible polymers like polyurethane and embedding conductive materials like carbon nanotube, the flexible textile sensors could be fabricated with the capability of integration in electronic devices or to be attached to human skin [8].

By some chemical modifications, polymerization, synthesis, or adding some conductive materials such as metallic particles, they will become conductive and be able to react to several stimuli comprising mechanical, chemical, electrical, and thermal. Moreover, the electronic devices could be interconnected in textile structures using weaving, embroidering, and printing due to their flexibility and deformability. The structure of the component, the fabrication approach, and the used materials influence the sensing mechanism that is determined by three principal factors: behaviors of the sensing integrant, formation of a crack in the sensing layer creating the conduction network, and geometrical transformation [9].

In 1996, Volatile Organic Compound (VOC) electronic sensors embedded in textile structures have been demonstrated for the first time [10]. However, the technology was not mature enough at that time to integrate multiple sensors and sensitive materials were not intelligent to detect very low VOC concentration. Lately, enhanced sensitivity has been achieved for VOC detection thanks to graphene composites (5 ppb for H2S), assuming that molecularly imprinted conjugated polymer materials could improve selectivity even if they are not as sensitive yet (1 ppm) [11]. Today state the art of commercial chloramine detection applies consumable optical components as a sensor and requires 20 min for a one-time analysis.

Knowing the air filtration condition such as low airflow that passes through the filter as shown in Fig. 15.2, the nanofibers are chosen as a textile sensor thanks to their special properties of being equally light-weighted, permeability, and high surface area [12]. The morphological structure of nanofibers provides a larger

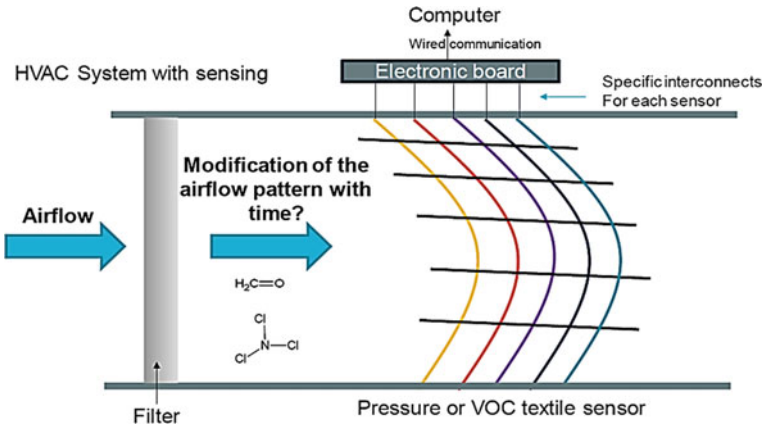


Fig. 15.2 The air filtration system

measurement surface, which permits lower detection thresholds for the same materials. The nanofibers should be adapted to functionalization to detect VOC, especially formaldehyde and trichloramine that exist in swimming pools locally with high attention and sensitivity, and permeable enough to allow airflow without any disturbing actions decreasing filtering efficiency [13]. Electrospinning is a cost-effective, simple, and versatile procedure to fabricate nanofibers in the diameter range of Nano to Micrometers [14].

The goal of this study is the fabrication of polyurethane nanofibers by electrospinning technique as a permeable to airflow and flexible sensor. This multi-sensory flexible structure should ameliorate the sensitivity and selectivity of VOC detection, providing a low-cost method facile to take part in air filtration systems. As a result, during the clogging where the air cannot pass and the pressure drop increases, the pressure drop measurement notifies apparatus operators about the level of filter clogging and its position, to anticipate its modification and provide efficient energy saving, a key mark for economic and environmental aspects. Besides, this system could be sensitive to a specific molecule by adsorption inducing an electrical impedance variation using functionalized materials, such as conjugated polymers with molecular imprints, or nano-structured carbonaceous materials. In this study, we propose monitoring of the indoor environment with an exceptional technology capable of evaluating the aging of filtration systems and controlling the quality of filtrated indoor air in buildings.

15.2 Materials and Methods

15.2.1 Electrospinning

Electrospinning was first developed by Formhals in 1930 [12]. The principle of this technique consists of repulsive electrostatic force created from different voltages between needle and collector. The Coulomb interactions in the fluid jet make polymer jet form Taylor cone at the tip of the needle. Following drawing the polymeric solution because of force on it, the solvent evaporates and the filaments deposit on the collector [15]. Figure 15.3 shows the electrospinning device and mechanism. The collector may be a film, nonwoven, mesh, or electrode depending on the final application. Besides, various setups such as rotating drums, disc collectors, multiple spinnerets, needleless and coaxial devices are applied to obtain different fibrous assemblies [16].

There are three different categories of parameters, which should be controlled during electrospinning: (i) solution parameters such as polymer molecular weight, the molecular weight distribution of the polymer, concentration, viscosity, conductivity and surface tension of the solution, and type of solvent; (ii) ambient parameters including temperature and humidity and (iii) process parameters such as feed rate, voltage, needle size, and distance between the capillary and collector. The following parameters affect the electrospinning process and final sample properties [17]. In electrospinning techniques, natural polymers like gelatin, sericin, and chitosan are employed because of their biodegradability and hydrophilicity. Synthetic polymers such as polycaprolactone, polyurethane, and polyacrylamide can be used due to their good mechanical properties [14].

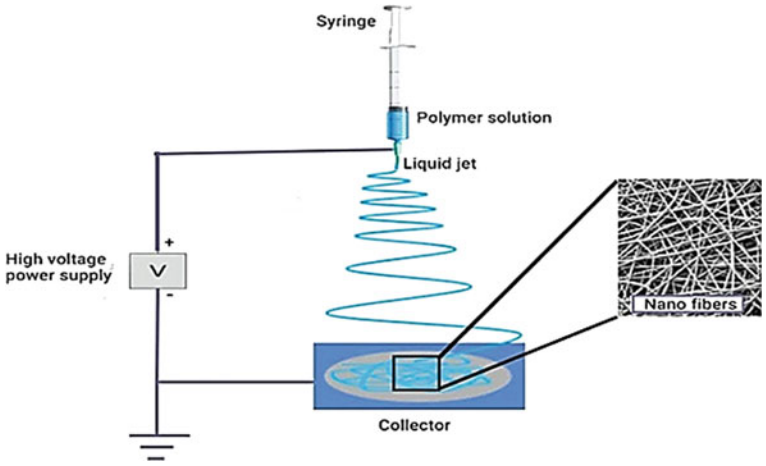


Fig. 15.3 The electrospinning system

15.2.2 Polymers

Among different synthetic polymers used in electrospinning, polyurethane is the most interesting because of its properties and facility to be electrospun. Moreover, this polymer dissolves in many ecologies and non-ecologies solvents. The nanofibers produced from polyurethane could be in the range of 100 nm–2 μm performing homogeneity, uniformity, and appropriate mechanical properties. Polyurethanes (PU) are a significant class of polymers composing hard (isocyanate) and soft (polyols) segments with a basic repetitive unit of urethane bond (NHCOO). This polymer was synthesized for the first time by Otto Bayer in 1937 and has been used in vast scopes on account of its unique properties such as good mechanical properties, corrosion and abrasion resistance, and processability. The structure of polyurethane is represented in Fig. 15.4.

Polyurethanes are synthesized through the addition reaction of a diisocyanate (or polyisocyanate) and an oligomeric polyol, followed by the addition of a diol or diamine chain extender to form a polymer of high molecular weight, linear, branched, or cross-linked as shown in Fig. 15.5.

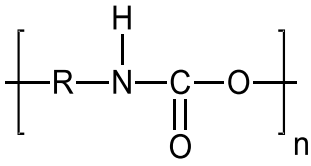


Fig. 15.4 The structure of polyurethane

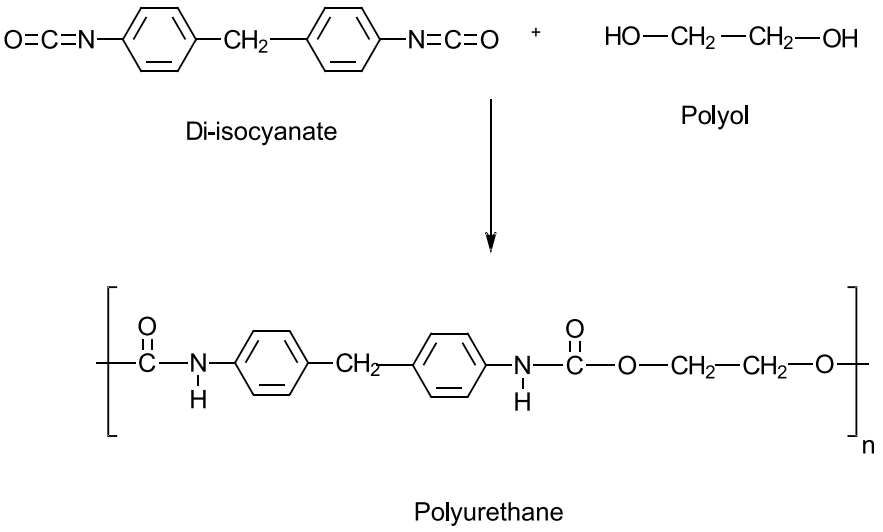


Fig. 15.5 The polymerization of polyurethane

Depending on the types of monomers, methods of production, and final application, distinct polyurethane such as waterborne polyurethane (WPU), poly (hydroxyl) urethane (PHU), ionic polyurethane, and biodegradable polyurethane could be synthesized [18].

Polyurethane Applications

Today, polyurethane has gained much interest in various fields comprising electronic, medical, food packaging, filtration, and automobile in the form of film, composite, foam, fabric, and nanofiber structures [19]. On the other hand, its properties such as flexibility, elasticity, and good tenacity, make it an ideal candidate for liquid coatings and paints, printing inks, adhesives, composite wood, and printed circuit boards [20]. The shape memory properties of polyurethane make it convenient to be used in aerospace, energy, and optical devices. Shape memory polymers can recover their original shape after reacting to some external stimuli such as heat, light, pH, and electric or magnetic fields [21]. One of the significant advantages of polyurethane is its capability to adjust its properties by optimizing its synthesis protocol, composition, the relative content of the soft and hard block, and molecular weight. Moreover, the intervention of this diverse filler makes it possible to be responsive to external stimulations [22].

Zareanshahrak et al., produced Non-isocyanate polyurethanes by different chemical routes and UV curing for exterior aerospace applications [23]. Also, a non-isocyanate polyurethane was prepared and functionalized with azetidine groups by Gholami et al. for wound dressing application. This physical strength membrane could maintain its dimensional stability under a wet state and moisture in the lesion environment during healing. According to their results, this membrane demonstrated excellent antibacterial and biological properties because of the presence of ionic groups in its polymeric structure [24].

Ahmadi et al., worked on the phase change materials (PCMs) using polyethylene glycol (PEG) and their derivatives as phase change diols using graft copolymerization, step-growth polymerization, physical blending, and structural modification methods. They announced that PU-PCMs could be appropriate for thermal energy storage applications due to their high durability, mechanical, thermal, and morphological properties [25].

Polyurethanes are useful in sound absorption and seat cushioning because of their cost-effectiveness and ease of use. Choe et al. added $CaCO_3$ fillers to polyurethane foam and compared the filler before and after chemical treatment by oleic acid. When chemically treated fillers were used, high interfacial contact and compatibility between the filler and foam were observed and the sound absorption coefficient increased [26].

Conductive and thermoresponsive thin film from dialdehyde water-born polyurethane, N-carboxyethyl chitosan, and double-bonded chitosan grafted polypyrrole was synthesized by Xu et al. They confirmed that this film might be a good solution for polymer coating with proper hydrophilicity, biocompatibility, and conductivity. Further, the mechanical properties of the heat-responsive films improve when the temperature increases [27].

Table 15.1 The properties of polymers used

Type	Nature	Viscosity BF (25 °C in DMF 25%) (mPa.s)	Melting point (°C)	Elongation (%)
LP 075/88	Polycarbonate copolymer	4000–12,000	210	379
LP SH 1020	Ether-Esther	4000–20,000	205	510
LP S860	Polyester	5000–20,000	170–180	450

Villani et al. incorporated different antibacterial agents to thermoplastic polyurethane composite by melt mixing. They studied and compared the effects of particles on the properties of the system. Finally, silver and chitosan were suggested in comparison with TiO_2 to use in medical devices due to their limited influence on morphological, thermal, and mechanical properties of composites [28].

In this study, we chose polyurethane as a flexible and strong polymer because of the demand for flexibility to be interconnected into an electronic circuit structure. As the polymer's nature and molecular weight affect the electrospinning system and final properties, we used four different types of aromatic polyurethane from the Coim group with different nature and properties, which is demonstrated in Table 15.1. The molecular weight of all polymers is estimated around 100,000–200,000 Dalton.

15.2.3 Solvents

Solvents and their constant dielectric have a key role in the electrospinning process. The charges often have a greater effect on polar solvents than non-polar solvents. As the load carried by the jet increases, more bonding forces are applied to the jet under the electric field and consequently fewer beads and nanofibers will be fabricated with smaller diameters. On that account, one of the more significant parameters of electrospinning is the choice of solvent for the polymer. Mondal et al. worked on this topic by comparing the effects of different solvents of polyurethane on the final structure of nanofibers. The most popular solvents for electrospinning of polyurethane are DMF (Dimethylformamide), THF (Tetrahydrofuran), DMSO (Dimethyl sulfoxide), and DMAc (Dimethylacetamide). Although it is preferred to use eco-friendly solvents such as DMSO and DMAc according to Table 15.2, their high boiling point and low vapor pressure could be a significant problem during electrospinning [29].

In this research, first DMSO was used as a green solvent to protect the environment, and then the results were compared with DMF: THF, which are common solvents for polyurethane.

Table 15.2 The different solvents of PU with their properties

Solvents	Molar mass (g/mol)	Density (g/cc)	Boiling point (°C)	Solvent vapor pressure (mmHg at 21 °C)	Dielectric constant (20 °C)	Surface tension (dyne/cm at 20 °C)
THF	72	0.888	66	133	7.6	28
DMF	73	0.945	153	3.8	36.7	35
DMAc	87	0.945	166	1	37.8	34
DMSO	78	1.101	189	0.7	46.6	43.7

15.2.4 Polymeric Concentration

To find proper polymeric concentration for electrospinning, there are three different methods:

(i) overlapping concentration formula:

$$C^* = \frac{M/N_A}{4/3 \times \pi \times R_g^3}$$
$$r^2 = C_\infty n L^2$$
$$R_g^2 = 1/6 \times r^2 \tag{15.1}$$

where C^* is overlapping concentration, M molecular weight of the polymer, N_A Avogadro constant, R_g radius of gyration, n number of c–c bonding in the original chain, L length of the bond, and C_∞ characteristic ratio of polymer [30].

(ii) The formula for finding the good shear rate by feed rate and needle radius of device:

$$\gamma = \frac{4Q}{\pi R^3} \tag{15.2}$$

whereas Q is the feed rate (mL/h), R the needle radius (mm) and, Υ the shear rate (1/s).

(iii) Preparation of polymeric solution in different concentrations and measuring the viscosity in shear rate obtained from formula (15.2).

The state of polymer in solvent categories is in four forms: (1) dilute (2) semi dilute unentangled which titles overlap concentration where the polymeric chain start to entangle (3) semi dilute entangled which names entanglement concentration where there is an entanglement between polymeric chain and the concentration equal or above this state is proper for electrospinning and, (4) concentrated [31]. Also,

the curve achieved from formula (15.2) shows the overlapping and entanglement concentration according to the change of viscosity.

15.2.5 Conductive Materials

To improve the conductivity and mechanical properties of polyurethane nanofibers, conductive materials such as nanoparticles, nanowires, and Nanosheets are employed. In this project, we used multi-wall carbon nanotube (MWCNTs) and carbon black bought from Nanocyl and Ketjenblack, respectively. The properties of MWCNTs mentioned 9.5 nm in diameter and 1.5 μm in length. Besides, the 1-butyl-3-methylimidazolium hexafluorophosphate (BMIM) (PF6) ionic liquid provided from Sigma was used to ameliorate the conductivity. Ionic liquids (ILs) are molten salts with a melting point below 100 °C, which have fascinated much importance due to their high chemical and thermal stability, low vapor pressure, and electrochemical potential. They are also suitable to improve the interface between polymer and particles by their ionic structure [32].

15.2.6 Preparation of Polymeric Solutions

PU granules were dissolved in DMSO: Acetone (50:50 v/v) and DMF: THF (50:50 w/w) for 3–5 and 5–10 h depending on polymer type, respectively. To disperse the particles, different percentages of MWCNTs (0.5, 1, 1.5, and 2 wt%) and carbon black were mixed in ultra-turrax at 2000 rpm for 15 min and then 60 min in ultrasonic (37 kHz frequency and 70% power). To avoid the decrease of particle length, UV–Vis was applied to find the appropriate time for ultra-sonication. After each 15 min of ultra-sonication, the UV spectra of solutions were recorded and the absorbance curve shift by augmenting the dispersion until when the increase of absorbance is stabilized. At that point, the particles are well dispersed and there is no agglomeration [33]. Finally, the PU granules were added and the solutions stirred for some hours. For solving IL, first IL in different concentrations (5, 10, and 15 wt%) was dissolved in solvents for 1 h and the PU granules were added. It is mentioned that DMF is a good solvent for dissolving and dispersion of IL and MWCNTs, respectively.

15.3 Characterization

To characterize the properties of samples, different tests may be applied. These assays are about the polymeric solution before processes such as viscosity, conductivity, and surface tension, and the morphology, diameters, physical and mechanical

properties of nanofibers after fabrication. In this research, the viscosity and concutivity of polymeric solutions before electrospinning were studied and to characterize the morphology of nanofibers SEM and TEM were applied.

15.3.1 Solution Characterization

In electrospinning, the polymeric entanglement following the molecular weight and viscosity of the solution must be sufficient to have the spinning capability and not so high to prevent stretching the jet under the electrical field. On the other hand, the viscosity of the electrified solution has a significant effect on the formation of beads, which is one of the most important defects occurring during the electrospinning of polymeric solutions. The researches have shown that in low viscosities, these defects happen more severely. The concentration of solutions influences viscosity and surface tension. Increasing the concentration raises the mass of the polymer in the jet spins and in this condition, the viscosity goes up and a stronger bond is created between the polymer chains, which makes extension more difficult and causes an increase in the diameters.

15.3.2 Morphology Characterization

SEM (Scanning electron microscope), FESEM (Field Emission Scanning Electron Microscope), and TEM (Transmission electron microscope) are utilized to characterize the morphology and structure of the obtained nanofibrous membrane. In this study, SEM and TEM were applied to see the morphology of PU nanofibers and core/shell nanofibers of PU/ionic liquid, respectively.

SEM and FESEM

To prepare the samples for investigating the structure using SEM, first, the cut specimens are placed in the metalizing machine to deposit a thin layer of gold or carbon on their surface before being placed under the microscope. Then, the samples are photographed with a digital camera connected to the microscope [34]. To determine the diameter of nanofibers, ImageJ and Digimizer softwares are applied [14]. The mean value of diameters is calculated by measuring around 100 fibers diameters as shown in Fig. 15.6.

FESEM is a device like the SEM and supplies broad information from the sample surface, but with much greater resolution and energy range. One of the advantages of FESEM is that there is no need to make conductive the surface of the sample, which decreases the sample damage. Its other benefits are high quality, low voltage, and the possibility of higher magnification to analyze the cell culture on the surface of nanofibers [35]. Baghersad et al. applied FESEM to see the fibroblast cell on the surface of PCL/gelatin nanofibers [17].

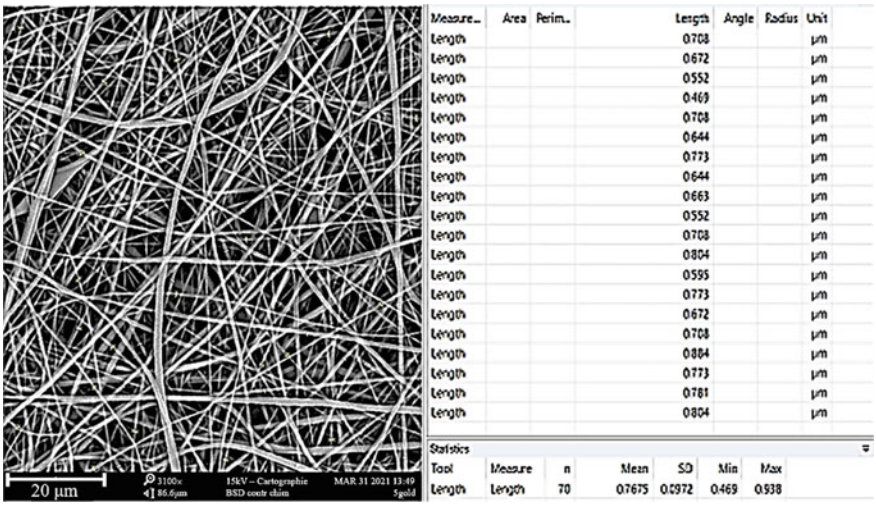


Fig. 15.6 Measurement of diameters of PU nanofibers using Digimizer

TEM

For sample preparation, the first nanofibers must be cut in thin slides, be dehydrated, and be placed on the plastic support. The samples are stained on the grids by lead solution and the microscope takes a picture from the surface of nanofibers. This method could be practical for nanofibers containing the particles or core/shell structure as indicated in Fig. 15.7 [36].

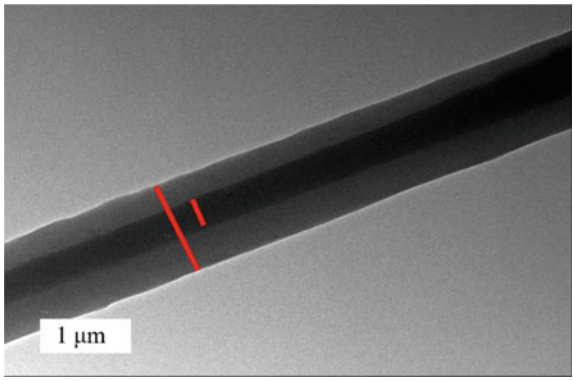


Fig. 15.7 TEM image of PU/ionic liquid core shell nanofibers

15.3.3 Physical Characterization

To evaluate the physical properties of nanofibers surface such as atomic elements combination, roughness, amorphous and crystalline phase and calculation of surface area, EDS (Energy Dispersive Spectroscopy), AFM (Atomic Force Microscopy), and BET (Brunauer, Emmett and Teller) are employed, respectively.

EDX

After taking an image from SEM, the elemental composition of materials on the surface of nanofibers could be detected by the Energy Dispersive Spectroscopy. Following the collection and sorting of the X-ray by EDS, the plot of elements labeled and their energy distribution appear on the screen. This method of characterization is operated to identify the drugs or particles in nanofibers structure [37]. Nirmala et al. used EDX to prove the presence of copper oxide in PU nanofibers structure [38].

AFM

Atomic Force Microscopy is a type of scanning probe microscopy, which include sensing, detecting, and positioning system. AFM provides the image of nanofibers in two and three-dimension and shows the roughness, defects, amorphous and crystalline phases of nanofibers [39]. Chen et al. used AFM to investigate the surface roughness of core/shell nanofibers of PU/collagen and according to results, the roughness increased by incorporating collagen in the shell in comparison with neat PU nanofibers, which improve cell attachment [40].

BET

To investigate the surface area of nanofibers, BET surface area measurements are employed which are based on the physical adsorption of a gas on the surface of the nanofibers. This amount of gas could be calculated from the Langmuir isotherm model. Another system to determine the specific surface area of nanofibers is the adsorption of chemical composition from an organic solvent or adsorption of the isotopically labeled compound. Normally, the obtained values from this method are lower than BET because of the large chemical compounds that cannot pass across the small pores of nanofibers [41]. The N_2 adsorption–desorption isotherms of PU/PSA nanofibers including different concentrations of $BaTiO_3$ produced by Yang et al. showed that the surface area increased by adding particles until 5 wt% and then reduced slightly, which depends on diameters and roughness of nanofibers and agglomeration of particles [42].

15.3.4 Mechanical Properties

The mechanical properties of nanofibers play a critical role in many applications such as composites, sensors, and tissue engineering. Among mechanical tests such as bend,

compression, cyclic, and tensile tests, tensile tests are more common for nanofibers. While there are two difficulties to control. First, avoiding slipping or breaking of samples from the grips because of the small size of the samples. Secondly, preventing misalignment between sample axis and loading direction that cause sample failure. The most favorable preparation method of nanofibers without manipulation is binding them in a paper frame so that they can be fixed between the grips. Moreover, the thickness measurement of nanofibers is troublesome, however; it is realizable by cross-section images obtained by SEM.

On the other hand, the bend test is largely useful to perform for the mechanical properties of nanofibers. One of the methods of bend tests is the three-point bend where the nanofibers are deposited on a substrate with holes and grooves. Young's modulus and fracture strength could be obtained for conductive polymer nanofibers and biodegradable polymer nanofibers from this technique. Moreover, AFM is capable to apply force and measure deformation in nanoscale. That is why it is a very suitable device for the mechanical test of nanomaterials [43].

Mechanical properties depend on polymers, solvents, and even types of collectors. It is reported that using a solvent with low-pressure vapor like Tetrahydrofuran leads to crystal growth over fiber formation and improves crystallinity and mechanical properties. Additionally, the polymeric solution containing these solvents has more chain mobility that allows relaxing of polymer chains from an anisotropic state at the time of process to an isotropic state at the collector [44].

In the goal of enhancing the mechanical properties of nanofibers, heat treatment drawing or twisting nanofibers are applied [44, 45]. Besides, to improve mechanical properties of nanofibers, synthesis, adding and electrospray of nanoparticles or post-treatments such as immersion of samples in nanoparticles solution might be a good solution. The nanoparticles such as MWCNTs and SWCNTs make nanofibers tough, strong, and stiff [46].

Eivazi Zadeh et al. announced that CNTs augment Young's modulus of polyurethane nanofibers. However, the percentage of CNTs is an important point because the agglomeration of particles could have the opposite effect and diminish strength [47].

Despite the high stiffness, elasticity, and recoverability of polyurethane nanofibers, their hydrophobicity could be a limit for many sectors. For this reason, the surface of polyurethane nanofibers is modified by different materials. One of the versatile and facile methods of surface modification is in situ polymerization of biocompatible polydopamine polymer. Polydopamine could be coated on any type of substrate with a strong interface between PDA and surface due to owing to catechol and amine groups and also, rise hydrophilicity. Lin et al. studied the polyurethane nanofibers coated by in situ polymerization of polydopamine in various coating times. The results indicated that the presence of PDA on the surface of samples and the hydrogen bonding between PDA particles, furthermore between PDA and nanofibers surface improves mechanical properties. According to cycle tests, all of the samples demonstrated low energy loss and excellent fatigue resistance in ten loading/unloading cycles [48]. Table 15.3 Indicates the mechanical test parameters used in publications.

Table 15.3 The parameters used for the tensile test

The thickness of samples (mm)	Size of samples (length × width mm)	Speed of tests (mm/min)	Standard	References
–	30 × 10	5	–	[49]
0.15–0.3	10 × 2	1	ASTM Standard D638-14, ASTM E2714-13, E606/E606M19e1	[50]
–	20 × 10	100	–	[51]
0.03	60 × 8	5	–	[52]
–	10 × 30	10	–	[53]
–	15 × 5	10	–	[47]

In this study, the mechanical properties of polyurethane nanofibers produced by different electrospinning parameters and having different diameters were investigated by the MTS criterion machine. Generally, the ISO 527-3, 1, and ASTM D882 are applied for the mechanical test of nanofibers.

15.4 Results and Discussion

15.4.1 Viscosity and Conductivity of Solutions

As mentioned in the characterization part, the viscosity and conductivity of solutions play an important role in the diameter and final properties of nanofibers. In our study, we prepared the PU/DMSO: Acetone and PU/DMF: THF solution with different concentrations of polymer, and then the viscosity was measured in different shear rates as shown in Figs. 15.8 and 15.9 by Viscometer (Rheomat RM 100).

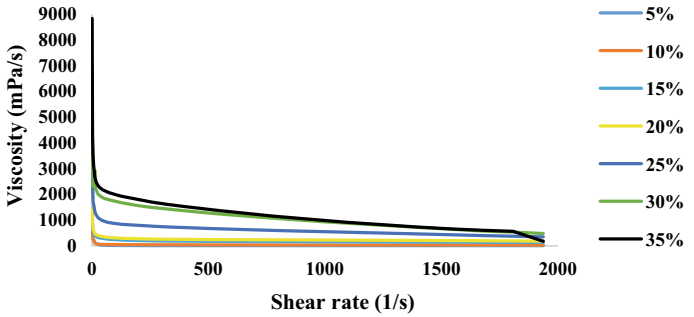


Fig. 15.8 The viscosity of PU/DMSO: Acetone with different concentrations of the polymer by different shear rates

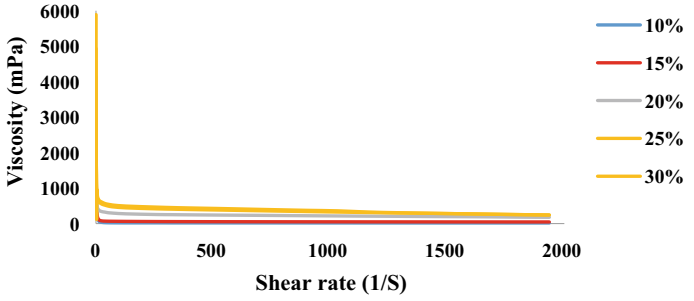


Fig. 15.9 The viscosity of PU/DMF: THF with different concentrations of the polymer according to different shear rates

The trend of viscosity change was the same for DMSO: Acetone and DMF: THF, which could be because of the same power solubility of these solvents for polyurethane (Fig. 15.10).

As reported in earlier studies, adding CNTs increases the viscosity and conductivity of solutions as shown in Tables 15.4 and 15.5. That is why it is recommended to reduce the polymeric concentration to equilibrium the viscosity and decrease its effect on diameters. Eivazi Zadeh et al., decreased the PU concentration from 11 to 10 wt% for 0.5 and 1 wt% of CNTs to gain similar diameters [47].

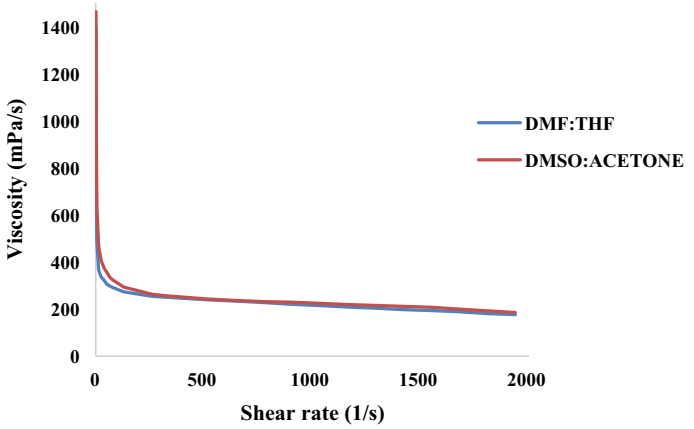


Fig. 15.10 The viscosity of PU 20 wt% dissolved in DMSO: Acetone and DMF: THF by different shear rates

Table 15.4 The viscosity of solutions including different CNT percentages in the shear rate of 25 (1/s)

Viscosity (mPa/s)	Solutions (wt%)
405	PU 20%
765	PU/0.5%CNT
531	PU/1%CNT
724	PU/1.5%CNT
835	PU/2%CNT

Table 15.5 The conductivity of solutions containing different MWCNTs contents

Conductivity (mS)	Solutions (wt%)
0.004	PU 20%
0.01	PU/0.5%CNT
0.016	PU/1%CNT
0.025	PU/1.5%CNT
0.033	PU/2%CNT

Table 15.6 The viscosity and conductivity of solutions comprising different percentages of IL

Polymeric solutions (wt%)	Viscosity (mPa/s)	Conductivity (mS)
PU 20%	405	0.004
PU/IL 5%	361	1.2
PU/IL 10%	301	1.8
PU/IL 15%	368	2.25

Almuhamed et al. [54] reported that adding CNT to PAN solution increases the conductivity of the solution and reduced the diameters of nanofibers. Incorporating IL in solutions increased the conductivity and decreased the viscosity as demonstrated in Table 15.6. Xing et al. produced the PU/IL nanofibers and according to the results, the augmentation of conductivity by adding IL improved the morphology and disappeared the beads. In addition, this phenomenon and diminishing viscosity lead to a decrease in the diameters [32].

15.4.2 Morphology of Nanofibers

As our study is industrial, the preference was to use a green solvent such as DMSO to dissolve PU. 25% of each type of polymers were dissolved in DMSO and the viscosity was measured (Table 15.7). The parameters of electrospinning were performed at (12–30 kV) voltage, (0.2–1.5 ml/h) feed rate, and (15–30 cm) distance according to articles.

To investigate the structure of nanofibers, SEM images were used (Fig. 15.11). The diameters of nanofibers were calculated 1.7 ± 0.17 μm, 1.6 ± 0.16 μm, and 1.18 ± 0.08 μm, respectively.

The SEM images demonstrated that the high boiling point, viscosity, surface tension, and low-pressure vapor of DMSO cause thicker nanofibers, adhesion between the fibers, beads, and the residue of solvent on the surface. On the other hand, the PU SH 1020 and 075/88 were not suitable for electrospinning according to the viscosity and SEM images because of their molecular weight and chain entanglement. In some studies, adding acetone is recommended for increasing the evaporation ratio of solvents. That is why DMSO: acetone with a 50:50 v/v ratio was chosen as solvents in this project. However, despite that, there is no trace of solvent and the numbers of beads decreased; an attachment among the filaments was observed as

Table 15.7 The viscosity of solutions in 25 (1/s) shear rate

Polymers	Viscosity (mPa/s)
S 680	309
SH 1020	204
075/88	286

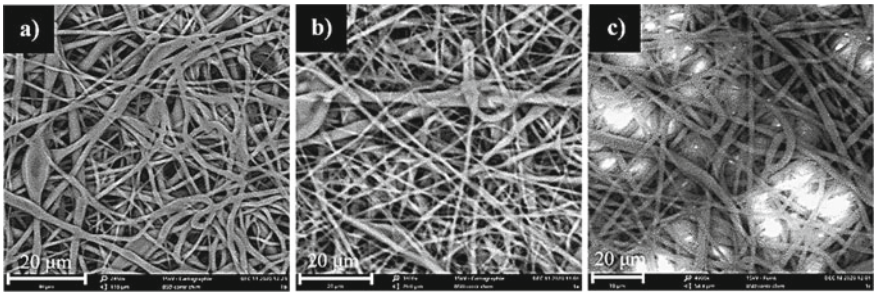


Fig. 15.11 SEM images of **a** S860 **b** SH 1020, and **c** 075/88 with 15 kV, 15 cm, and 0.5 ml/h of parameters (20 µm magnification)

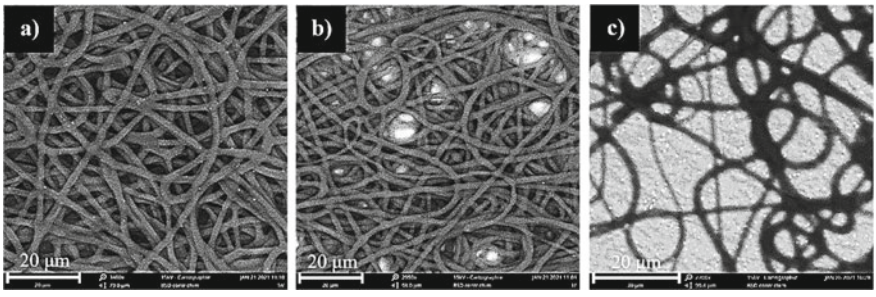


Fig. 15.12 SEM images of **a** S860 25 wt% **b** 20 wt%, and **c** 17 wt% with 15 kV, 30 cm, and 0.5 ml/h of parameters (20 µm magnification)

illustrated in Fig. 15.12. In addition, high viscosity makes the extension of polymer jet difficult and leads to fabrication of thicker nanofibers. For that reason, we tried to reduce the polymeric concentration to 20 and 17 wt% with a viscosity of 132 and 116 mPa.s for decreasing the diameters. As shown in Fig. 15.12 and the results obtained from formula (15.2), 20 wt% of PU was reported as an optimal polymeric concentration. The diameters were measured 1.83 ± 0.09 µm, 1.72 ± 0.12 µm, and 2.4 ± 0.29 µm, respectively.

After finding the optimal polymeric concentration and electrospinning parameters, the MWCNTs with 0.5, 1, 1.5, and 2 wt% were added to the solution and electrospun. Figure 15.13, indicates the SEM image of samples including MWCNTs with diameters of 940 ± 110 nm, 949 ± 80 nm, 835 ± 110 nm, and 693 ± 120 nm, respectively. As imagined the diameters decreased due to the conductivity of solutions, however, the structures were not satisfactory, especially for samples with 2 wt% of particles which became a film. Consequently, the parameters should be optimized because of the change of viscosity and conductivity of polymeric solutions. Darbandi et al. and Tondnevis et al. reported that an increase in viscosity hinders the solution droplet and creates bead defects [55, 56]. Besides, to achieve a good conductive pathway following the contact between the particles, the structure of nanofibers should be

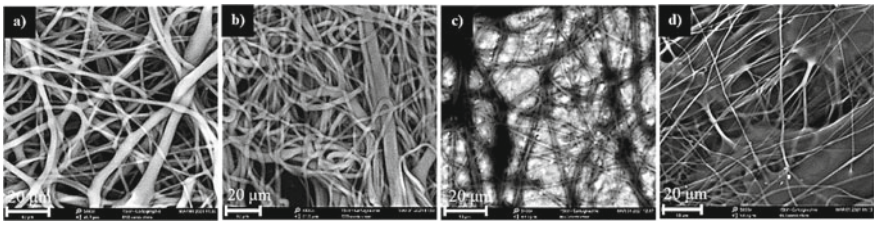


Fig. 15.13 SEM images of PU nanofibers containing **a** 0.5 wt%, **b** 1 wt%, **c** 1.5 wt%, and **d** 2 wt% MWCNTs with 15 kV, 30 cm, and 0.5 ml/hr of parameters (10 μm magnification)

uniform and with thinner fibers to have the particles on the surface of samples. Almuhamed et al. [54] informed the volume resistance of PU/CNTs nanofibers but not surface resistance because of the absence of particle contacts on the surface of samples. Although it is desirable to use ecologic solvents especially in industrial projects, the blend of DMF: THF could be the best solvent for polyurethane while increasing the concentration of DMF in THF allows producing smoother and thinner nanofibers [29]. As a result, to produce uniform nanofibers, decrease the numbers of beads and avoid adhesion between fibers, DMSO: acetone was replaced by DMF: THF with a 50:50 w/w ratio. According to Fig. 15.14, the nanofibers are uniform, bead-free, homogenous, and smooth.

The electrospinning parameters were fixed at 12 kV, 15 cm, 1.5 ml/h for sample a, 12 kV, 19 cm, 1 ml/h sample b, 15 kV, 15 cm, 0.5 ml/h sample c, and 20 kV, 15 cm, 0.5 ml/h sample d. In this study, we attempted to reduce the diameters by increasing the distance and decreasing the feed rate as shown in Fig. 15.14. The electrospinning parameters were accomplished at 15 kV, 17 cm, 0.5 ml/h for sample a, 15 kV, 23 cm, 0.5 ml/h sample b, 15 kV, 23 cm, 0.2 ml/h sample c, and 20 kV, 26 cm, 0.5 ml/h sample d.

The IL with 5, 10, and 15 wt% concentrations were added to PU solutions and electrospun. Figure 15.16, demonstrates the morphology of samples. the electrospinning parameters were 15 cm, 20 kV, 0.5 ml/h for sample a, 15 cm, 12 kV, 1.5 ml/h sample b, and 23 cm, 15 kV, 0.2 ml/h sample c. The diameters were calculated 1.08 ± 0.08 μm, 1.04 ± 0.13 μm, and 538 ± 80 nm, respectively. No trend was observed for diameters that could be owing to different electrospinning parameters. But the comparison between the 5 and 10 wt% of IL with Fig. 14a, c, confirmed that the diameters increased by adding IL, and the comparison between 15 wt% and Fig. 15c showed a decrease of diameter that could be related to increasing the conductivity of the solution. In any case, the parameters of the machine must be adjusted again because the viscosity and conductivity of solutions have changed. Xing et al. proclaimed that adding IL changes the forms of beads from spherical to spindle-like, and the numbers of beads reduced by 10 wt% of IL because of the conductivity of the solution. In addition, the diameters decreased following a diminution in viscosity and augmentation in conductivity [32].

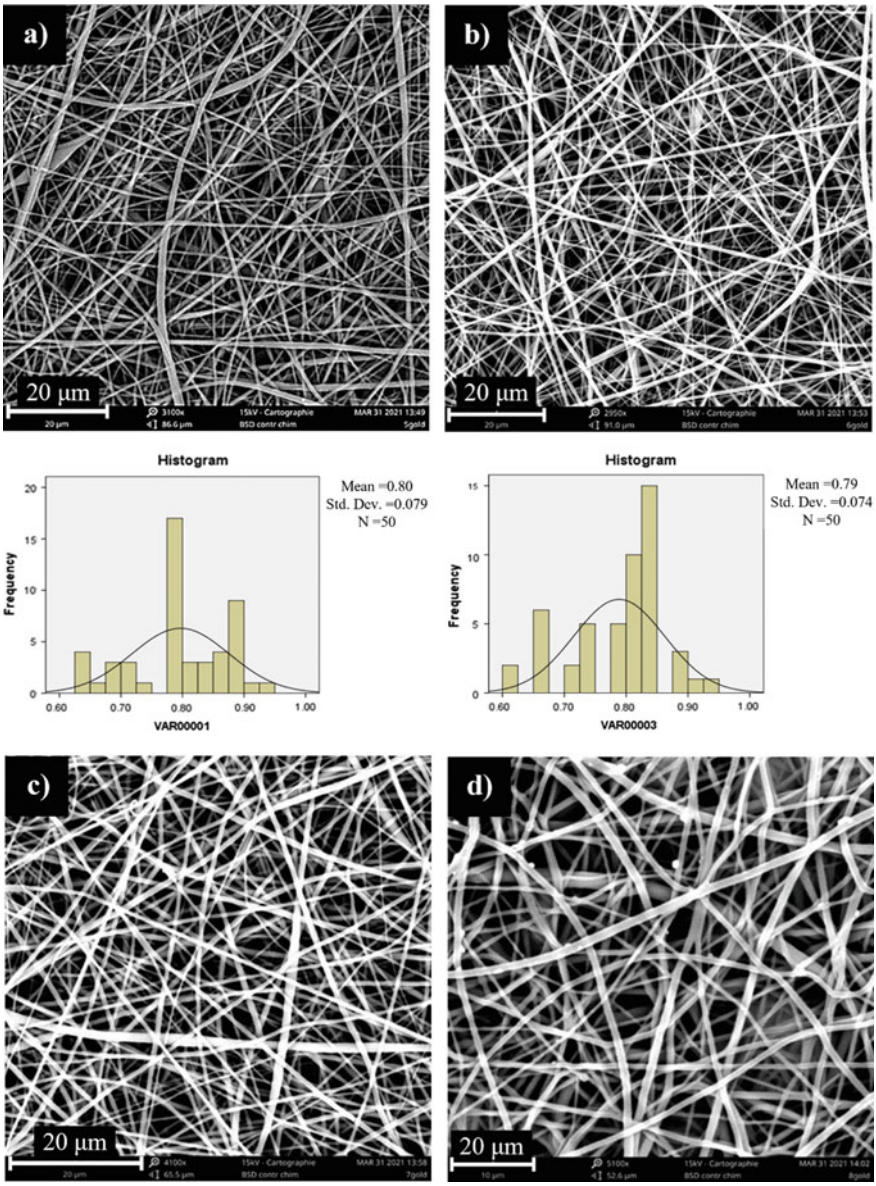


Fig. 15.14 SEM images of PU nanofibers with diameters of **a** 796 ± 79 nm **b** 788 ± 73 nm, **c** 731 ± 84 nm, and **d** 835 ± 87 nm (20 µm magnification)

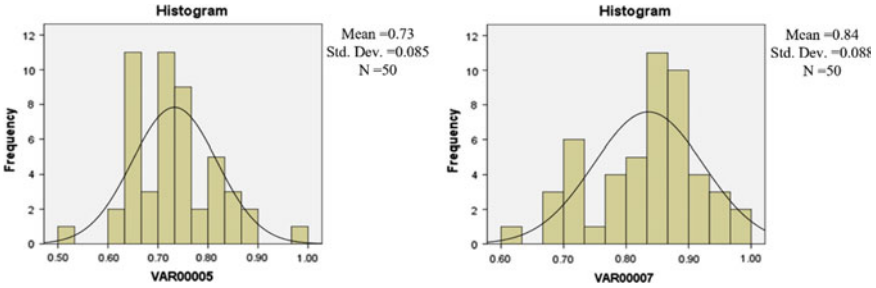


Fig. 15.14 (continued)

15.4.3 Mechanical Properties

As mentioned in the characterization part, the mechanical properties of nanofibers play a key role in the final application especially in air filtration and the sensors, which are under the effects of air, temperature, humidity, and tension. Mechanical elements such as Young's modulus, elongation at break, and tensile strength are influenced by the components, structure, morphology, and diameters of nanofibers. Although, the poor mechanical properties of nanofibers restrict their use. That is why the strength of synthetic polymers as polyacrylonitrile (PAN), polyamide (PA), and polyurethane are recommended. Besides, to enhance mechanical properties, chemical resistance, and antifouling properties, two polymers or nanoparticles could be combined, and reducing the diameters of nanofibers ameliorates filtration performance agreeing to boost mechanical properties. Therefore, producing the webs on a nonwoven substrate makes them facile to use due to their low mechanical properties [57–59]. Polyurethane is known as a flexible and elastic polymer, which is useful in many sectors of science and industry.

Movahedi et al. worked on core–shell electrospinning of polyurethane/starch nanofibers and confirmed that adding polyurethane increased elastic modulus, tensile strength, and strain at break value. Given that the tensile strength should be from 0.8 to 18 MPa in wound dressing application, this scaffold could be advantageous with 7.93 ± 0.17 MPa tensile strength for cell culture [49].

The nanofibers of shape memory polyurethane were fabricated by Guan et al. in two forms of random and aligned with 20 mm/min and 3 m/min speed of spinneret and collector, respectively. Then, the aligned samples were cut with different degrees of 0°, 45°, and 90°. To investigate the creep and relaxation behavior of samples, the cyclic test was performed in the condition of 50% strain and speed of 3 mm/min for 60 cycles. The elongation at break above 200% showed that all samples are flexible. As the volume fraction of nanofibers across the tensile direction, surface area, and density have a significant role in mechanical properties, aligned nanofibers with higher density resist a tensile test. On the other hand, aligned nanofibers indicated a storage modulus five times higher than random samples due to stretching of their molecular chains in the longitude direction by high-speed rotation of the

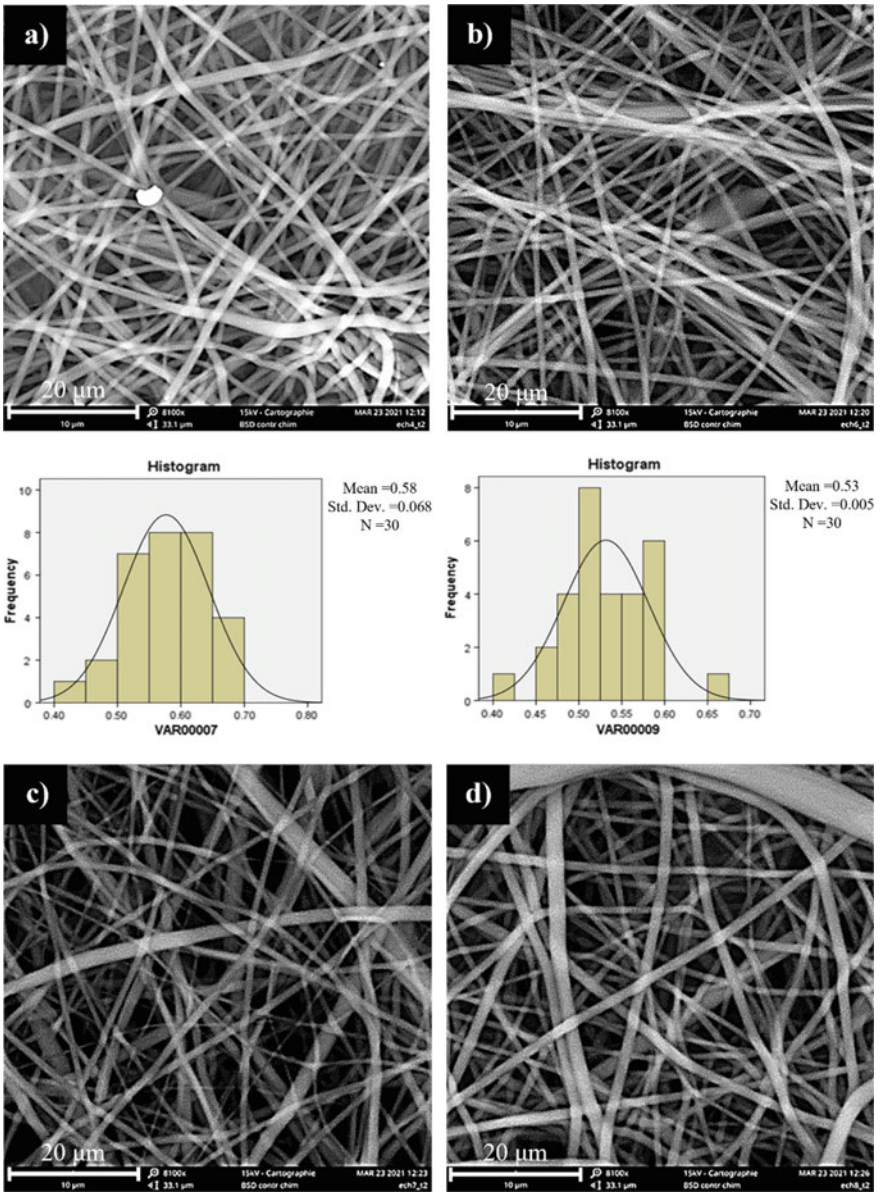


Fig. 15.15 SEM images of PU nanofibers with diameters of **a** 576 ± 67 nm, **b** 531 ± 49 nm, **c** 509 ± 53 nm, and **d** 509 ± 58 nm (10 µm magnification)

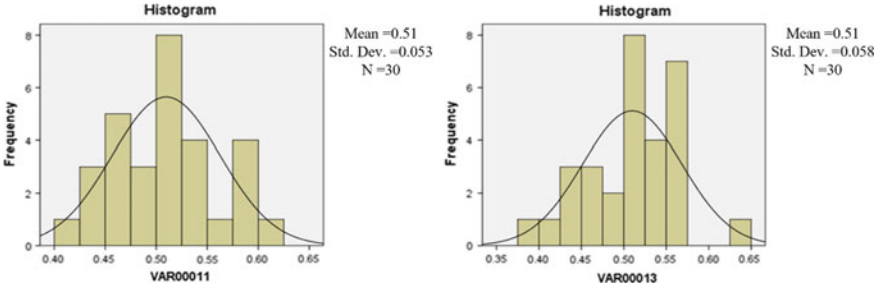


Fig. 15.15 (continued)

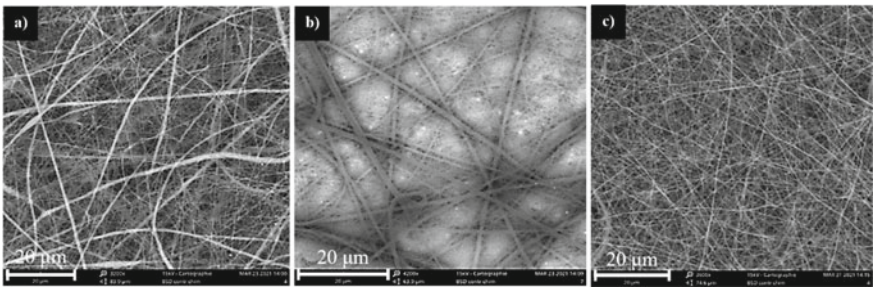


Fig. 15.16 SEM images of PU nanofibers containing **a** 5 wt%, **b** 10 wt%, and **c** 15 wt% IL (20 µm magnification)

collector. The tensile test was repeated at 40 and 65 °C and according to the results, by increasing the temperature to *Tg*, the tensile strength of samples decreases following by augmentation of soft segment mobility of polymers and the start of rubbery state. The aligned nanofibers demonstrated higher dimensional stability and elastic recovery capability than random nanofibers under 60 cycles of loading and unloading. As well, higher stress relaxation and lower reduction rate were observed for aligned samples and these results were similar at 40 and 65 °C. In conclusion, the aligned nanofibers exhibited better mechanical properties and durability during cyclic tests than random nanofibers [50].

Wang et al., polymerized polydopamine on the surface of polyurethane nanofibers coated by CNTs for strain sensors application. To do tensile tests, they stretched the nanofibers in two different directions: parallel and vertical. By increasing the speed of the collector, elastic modulus and tensile strength increased for P-PU (parallel) thanks to more stretching force and molecular chain alignment in nanofibers. While the vertical samples showed the opposite results. The tensile strength and elongation at break of P-PU samples reduced after CNTs coating that could be related to damage of ultra-sonication. Although, the trend was different for V-PU (vertical) samples and the reason might be the interaction between particles and nanofibers, which improve

mechanical properties. Finally, this system indicated the good potential for wearable strain sensors after 5000 cycles of stretching and releasing [60].

Yang et al. worked on the production of polyurethane/polysulfonamide nanofibers containing barium titanate nanoparticles. Combining the polyurethane and PSA (1:1) enhanced the morphology of samples because of the proper viscosity. Adding $BaTiO_3$ increases the contact area between dust particles and filaments resulting in more roughness of samples. The diameters of nanofibers were about 160–180 nm depending on nanoparticle concentration. Incorporating the PU as a flexible polymer and $BaTiO_3$ to PSA increased the elongation at break and tensile strength, respectively. The presence of nanoparticles raised surface roughness, area, and charge storage capacity, which helps improve filtration efficiency. To conclude, the $BaTiO_3$@PU/PSA membrane showed excellent thermal stability and chemical resistance against acid and alkali with a capture efficiency of 99.99% and a low-pressure drop of 39.4 ± 0.2 Pa that could be a good candidate for purification of PM2.5 [42].

Liu et al. confirmed that polyurethane (12 wt%) nanofibers with a diameter of 500 nm could filter the particles of different diameters and under low air resistance. To enhance mechanical properties and filtration performance through electrostatic adhesion, inorganic particles such as TiO_2, SiO_2, Si_3N_4 and, Boehmite were added. Among the nanoparticles, Si_3N_4 indicated proper distribution on the surface of nanofibers with decreasing the diameter to 300 nm and increased the contact area between samples and target particles by increasing the surface roughness. Moreover, this structure had sufficient mechanical properties with 18.05 MPa of stress and 170% of strain. The filtration efficiency and quality factor value of the PU-Si3N4 membranes were noticed as high as 79.36% and 0.065 Pa^{-1}, respectively [53].

In a study, polysulphone and polyurethane were electrospun on the collector with hexagonal grids for air filtration application. An air pump was considered in the chamber with a speed of 0.25 m/s to increase the fluffiness of nanofibers. As the polymer jets tend to deposit on conductive grids, fibers density is higher in that part than in empty parts and the diameter of nanofibers on empty areas was calculated 520 nm while it was 780 nm for fibers collected on grids. The reason could be attributed to the residual charge of fibers that accumulated on the surface of fibers at empty areas and this helps more stretch of the jets. To improve the mechanical properties of thin and fragile nanofibers and avoid using another protective layer, the honeycomb collector was used and the results showed using this structure and incorporating the polyurethane boosted the bursting pressure and bending stiffness of samples. The thick fiber on the grids and the thin fiber at the empty regions could manage strength and flexibility, respectively. Moreover, in the large empty zones, the thinner fibers with bigger pores were observed that influence air permeability. Although the PSU has a greater surface potential for absorbing PMs, PU enhanced the mechanical properties under pressure. The nonwoven honeycomb structure has a similar filtration efficiency to plain membranes but pressure drop was improved. Besides, the QF for this system was higher (0.0344 Pa^{-1}) than commercial products such as nonwoven mask (0.0288 Pa^{-1}) and melt-blown polypropylene (0.0320 Pa^{-1}).

Brief, the honeycomb nanofibers structure could capture both inorganic particles and organic beads during the filtration process [61].

Zhu et al. coated the surface of polyurethane nanofibers with CNT/CNC (cellulose nanocrystals) by vacuum filter method. They noted that the porous structure of nanofibers leads to absorb the coating layer. In this system, the presence of CNC help to good dispersion and interaction between CNT and PU, and according to the SEM image CNT/CNC coated the surface of samples like a film. The location of CNC between CNT could separate the conductive network by creating cracks on the surface under stretch and improve the sensitivity of the sensor. The strain sensor showed high stretchability ($\geq$500%) because of using flexible polyurethane polymer and high sensitivity with 321 GF and it could be useful for human body motion measurements [62].

In another study, the polyurethane nanofibers were cut vertical and parallel according to drum collector and then they were placed in CNTs solutions and treated with ultrasonic for 50 min. The distribution of CNTs was observed on the surface and the pores of nanofibers by SEM. The tensile test demonstrated that P-PU had higher tensile strength but lower elongation at break than V-PU. The existence of CNT enhanced the mechanical properties while there was the same trend for P-PU and V-PU including CNT. The hysteresis of V-PU increased by increasing the strain range but this value was lower for P-PU due to the aligned structure of mats and flexibility of polyurethane. For the electromechanical test, the samples were stretched in two vertical and parallel directions, and as give a result the V-PU sample was selected as a strain sensor because of its high elasticity. Finally, this system could be practiced in wearable applications with a large sensing range (0–900%), a fast response time (70 ms), a low detection limit (0.5%), and good stability and repeatability (10,000 at a strain of 200%) [63].

The PU Nanofibrous prepared by two 100 (PU-100) and 200 (PU-200) rpm speeds of collector were immersed in carbon black/deionized water under ultrasonication for 3 h. No significant orientation was observed for both samples and the diameters for PU-100 and PU-200 was 2.28 $\pm$ 0.04 μm and 1.77 $\pm$ 0.05 μm, respectively that presented more stretch of fibers reduce their diameters. Although, the thicker sample creates a larger matrix for connection of CB and PU resulting in providing a more conductive pathway. Contrarily, the dense structure of PU-100 makes it less sensitive. In the strain-sensing test, the Gf (the ratio of the relative change in resistance to mechanical strain) value increased by increasing the strain for both samples. The reason could be the separations between CB according to the tunneling mechanism, which causes an increase in the resistance. The tensile test revealed no significant change in mechanical properties of PU with and without CB that confirmed that the nanofibers did not damage during ultrasonication. The tensile strength of PU-100 was lower than PU-200 while the elongation at break was higher due to more stretching force over electrospinning in the PU-200 sample. In addition, CB with good dispersion on the surface of nanofibers boosted the mechanical properties of the system. In summary, this system could be used for finger bending, muscle tremor, and vocal cord vibrations owing to ultra-high sensitivity, fast response time, desired stability, and reproducibility [64].

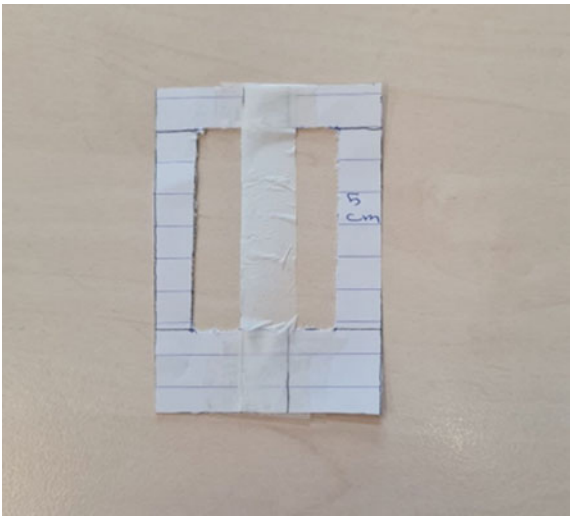


Fig. 15.17 The nanofibers between paper frames for tensile test

In this research, the mechanical properties of PU nanofibers were measured using an MTS criterion machine and according to ISO 527-3, 1. The samples were cut into 50 × 10 mm (length × width) and the speed of the test was fixed at 10 mm/min (Fig. 15.17). The electrospinning parameters were performed at 17 cm, 15 kV, 0.5 ml/h with 576 ± 67 nm diameter, and 19 cm, 12 kV, 1 ml/h with 788 ± 73 nm diameter for samples 1 and 2, respectively. This test was repeated 3 times for each sample.

Conforming to Fig. 15.18, the PU nanofibers showed proper mechanical properties and about 200% of strain proved that polyurethane could be a good choice for strain sensors thanks to its flexibility and elasticity. In comparison between the two samples, there is no significant difference in force but the elongation at break was more for the sample with a lesser diameter (Table 15.8). As reported, the elongation force during the electrospinning process aligns the polymer chain in parallel to the nanofibers axis and decreases the diameters of nanofibers and this phenomenon boosts mechanical properties due to having more fibers in cross-section, which help to resist more force [14]. However, fewer differences between the mechanical properties of samples could be related to fewer differences between diameters.

15.5 Conclusion

Nowadays, industries focus on air filtration systems to reduce respiratory diseases because of the existence of various types of particles and volatile organic compounds in public areas. One of the most important problems to solve in this system is the clogging's detection of filters for improving their quality factor. In this matter, the

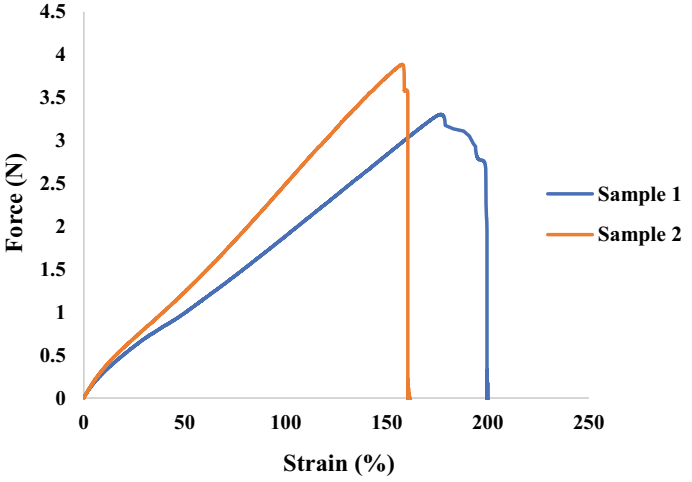


Fig. 15.18 The force/strain curve of PU nanofibers

Table 15.8 The mechanical properties of PU nanofibers

Max strain (%)	Force (N)	Samples
174.99	3.29	Sample 1
157.26	3.88	Sample 2

textile sensors could be the best solution due to their piezo resistivity and flexibility. According to air filtering conditions such as low airflow that passes over the filter, the nanofibers were chosen as sensor in this study because of their lightweight and high surface area properties. On the other hand, the porosity of nanofibers avoids blocking the passage of air in front of the filter. The most common methods to produce the nanofibers are electrospinning and, in this technique, machine parameters: voltage, feed rate, and distance between nozzle and collector, ambient parameters: temperature, humidity, and polymeric solution parameters: concentration, viscosity, and type of solvents should be optimized to obtain the beads-free, uniform, and smooth nanofibers. Among different synthetic and natural polymers used in electrospinning, polyurethane was chosen for its elasticity, flexibility, and great mechanical properties. Today, polyurethane has attracted much attention in electronic, medical, food packaging, filtration, and automobile applications. There are various types of polyurethane with different molecular weights according to monomer and polymerization method applied, which could show different properties. In this work, for preparing the polymeric solutions first the eco-friendly solvents like DMSO and acetone were used to help the ecology but then DMF, and THF were replaced as best solvents of polyurethane.

In the publications, it is noted that the high viscosity, surface tension, and boiling point of DMS and DMAC cause the adhesion between fibers, an increase in diameters, and the problem of evaporation during electrospinning. Overlap concentration theory

was employed to find the optimal concentration of the polymeric solution. Moreover, the optimal shear rate for the electrospinning device was calculated using a formula and then the viscosity of solutions was measured in obtained shear rate. In order to make the piezo resistive samples, conductive materials such as multiwall carbon nanotube and ionic liquid were used and the optimal ultra-sonication time was calculated by UV–Vis to achieve the good dispersion of particles in solutions. According to the results, the viscosity and conductivity of solutions increased by incorporating IL and MWCNTs that influence on the electrospinning mechanism. To investigate the morphology of nanofibers, SEM and TEM are applied. SEM images showed the beads-free and homogenous morphology of nanofibers, while, the IL and MWCNTs changed the morphology. As a result, the electrospinning parameters should be again optimized. Finally, the mechanical test indicated the high mechanical properties and flexibility of PU nanofibers until 200% of strain as reported in earlier researches.

References

1. Liu, G., Xiao, M., Zhang, X., Gal, C., Chen, X., Liu, L., et al. (2017). A review of air filtration technologies for sustainable and healthy building ventilation. *Sustainable Cities and Society, 32*, 375–396.
2. Maduna, L., & Patnaik, A. (2017). Textiles in air filtration. *Textile Progress, 49*(4), 173–247.
3. Tamana, S. K., Gombojav, E., Kanlic, A., Banzrai, C., Batsukh, S., Enkhtuya, E., et al. (2021). Portable HEPA filter air cleaner use during pregnancy and children's body mass index at two years of age: The UGAAR randomized controlled trial. *Environment International*, *156*, 106728.
4. Cai, Z., & Sorial, G. A. (2009). Treatment of dynamic VOC mixture in a trickling-bed air biofilter integrated with cyclic adsorption/desorption beds. *Chemical Engineering Journal, 151*(1–3), 105–112.
5. Hassan, A. A., & Sorial, G. A. (2011). Treatment of dynamic mixture of hexane and benzene vapors in a trickle bed air biofilter integrated with cyclic adsorption/desorption beds. *Chemosphere, 82*(4), 521–528.
6. Brown, R. (1989). Modern concepts of air filtration applied to dust respirators. *The Annals of Occupational Hygiene, 33*(4), 615–644.
7. Song, C.-B., Park, H.-S., & Lee, K. (2006). Experimental study of filter clogging with monodisperse PSL particles. *Powder Technology, 163*(3), 152–159.
8. Castano, L. M., & Flatau, A. B. (2014). Smart fabric sensors and e-textile technologies: A review. *Smart Materials and Structures*, *23*(5), 053001.
9. Seyedin, S., Zhang, P., Naebe, M., Qin, S., Chen, J., Wang, X., et al. (2019). Textile strain sensors: A review of the fabrication technologies, performance evaluation and applications. *Materials Horizons, 6*(2), 219–249.
10. Collins, G. E., & Buckley, L. (1996). Conductive polymer-coated fabrics for chemical sensing. *Synthetic Metals, 78*(2), 93–101.
11. Zhang, J., Liu, X., Neri, G., & Pinna, N. (2016). Nanostructured materials for room-temperature gas sensors. *Advanced Materials, 28*(5), 795–831.
12. Thandavamoorthy, S., Gopinath, N., & Ramkumar, S. (2006). Self-assembled honeycomb polyurethane nanofibers. *Journal of Applied Polymer Science, 101*(5), 3121–3124.
13. Chinnappan, A., Baskar, C., Baskar, S., Ratheesh, G., & Ramakrishna, S. (2017). An overview of electrospun nanofibers and their application in energy storage, sensors and wearable/flexible electronics. *Journal of Materials Chemistry C, 5*(48), 12657–12673.

14. Mohamadi, P. S., Hivechi, A., Bahrami, H., Hemmatinegad, N., & Milan, P. B. (2021). Antibacterial and biological properties of coconut oil loaded poly (ε-caprolactone)/gelatin electrospun membranes. *Journal of Industrial Textiles*, 1528083721991595.
15. Ahmed, F. E., Lalia, B. S., & Hashaikeh, R. (2015). A review on electrospinning for membrane fabrication: Challenges and applications. *Desalination, 356*, 15–30.
16. Teo, W. E., & Ramakrishna, S. (2006). A review on electrospinning design and nanofibre assemblies. *Nanotechnology, 17*(14), R89.
17. Baghersad, S., Bahrami, S. H., Mohammadi, M. R., Mojtahedi, M. R. M., & Milan, P. B. (2018). Development of biodegradable electrospun gelatin/aloe-vera/poly (ε-caprolactone) hybrid nanofibrous scaffold for application as skin substitutes. *Materials Science and Engineering: C, 93*, 367–379.
18. Honarkar, H. (2018). Waterborne polyurethanes: A review. *Journal of Dispersion Science and Technology, 39*(4), 507–516.
19. Naldzhiev, D., Mumovic, D., & Strlic, M. (2020). Polyurethane insulation and household products—A systematic review of their impact on indoor environmental quality. *Building and Environment*, *169*, 106559.
20. Sawpan, M. A. (2018). Polyurethanes from vegetable oils and applications: A review. *Journal of Polymer Research, 25*(8), 1–15.
21. Kausar, A. (2020). Shape memory polyurethane/graphene nanocomposites: Structures, properties, and applications. *Journal of Plastic Film & Sheeting, 36*(2), 151–166.
22. Gorbunova, M., Anokhin, D., & Badamshina, E. (2020). Recent advances in the synthesis and application of thermoplastic semicrystalline shape memory polyurethanes. *Polymer Science, Series B, 62*(5), 427–450.
23. Zareanshahraki, F., Asemani, H., Skuza, J., & Mannari, V. (2020). Synthesis of non-isocyanate polyurethanes and their application in radiation-curable aerospace coatings. *Progress in Organic Coatings*, *138*, 105394.
24. Gholami, H., & Yeganeh, H. (2021). Soybean oil-derived non-isocyanate polyurethanes containing azetidinium groups as antibacterial wound dressing membranes. *European Polymer Journal*, *142*, 110142.
25. Ahmadi, Y., Kim, K.-H., Kim, S., & Tabatabaei, M. (2020). Recent advances in polyurethanes as efficient media for thermal energy storage. *Energy Storage Materials*.
26. Choe, H., Lee, J. H., & Kim, J. H. (2020). Polyurethane composite foams including $CaCO_3$ fillers for enhanced sound absorption and compression properties. *Composites Science and Technology*, *194*, 108153.
27. Xu, J., Fu, C.-Y., Tsai, Y.-L., Wong, C.-W., & Hsu, S.-h. (2021). Thermoresponsive and conductive chitosan-polyurethane biocompatible thin films with potential coating application. *Polymers, 13*(3), 326.
28. Villani, M., Consonni, R., Canetti, M., Bertoglio, F., Iervese, S., Bruni, G., et al. (2020). Polyurethane-based composites: Effects of antibacterial fillers on the physical-mechanical behavior of thermoplastic polyurethanes. *Polymers, 12*(2), 362.
29. Mondal, S. (2014). Influence of solvents properties on morphology of electrospun polyurethane nanofiber mats. *Polymers for Advanced Technologies, 25*(2), 179–183.
30. Graessley, W. W. (1980). Polymer chain dimensions and the dependence of viscoelastic properties on concentration, molecular weight and solvent power. *Polymer, 21*(3), 258–262.
31. He, H., Kara, Y., & Molnar, K. (2019). Effect of needle characteristic on fibrous PEO produced by electrospinning. *Resolution and Discovery, 4*(1), 7–11.
32. Xing, C., Guan, J., Chen, Z., Zhu, Y., Zhang, B., Li, Y., et al. (2015). Novel multifunctional nanofibers based on thermoplastic polyurethane and ionic liquid: Towards antibacterial, antielectrostatic and hydrophilic nonwovens by electrospinning. *Nanotechnology*, *26*(10), 105704.
33. Grossiord, N., Regev, O., Loos, J., Meuldijk, J., & Koning, C. E. (2005). Time-dependent study of the exfoliation process of carbon nanotubes in aqueous dispersions by using UV−Visible spectroscopy. *Analytical Chemistry, 77*(16), 5135–5139.
34. Mazumder, M., Ahmed, R., Ali, A. W., & Lee, S.-J. (2018). SEM and ESEM techniques used for analysis of asphalt binder and mixture: A state of the art review. *Construction and Building Materials, 186*, 313–329.

35. Nallusamy, S., & Manoj Babu, A. (Eds). (2016). X-ray differaction and FESEM analysis for mixture of hybrid nanoparticles in heat transfer applications. *Journal of Nano Research*. Trans Tech Publ.
36. Deepak, F. L., Mayoral, A., & Arenal, R. (2015). *Advanced transmission electron microscopy: Applications to nanomaterials*. Springer.
37. Verma, N., Sharma, V., Kumar, R., Sharma, R., Joshi, M., Umapathy, G., et al. (2019). On the spectroscopic examination of printed documents by using a field emission scanning electron microscope with energy-dispersive X-ray spectroscopy (FE-SEM-EDS) and chemometric methods: Application in forensic science. *Analytical and Bioanalytical Chemistry, 411*(16), 3477–3495.
38. Nirmala, R., Jeon, K. S., Lim, B. H., Navamathavan, R., & Kim, H. Y. (2013). Preparation and characterization of copper oxide particles incorporated polyurethane composite nanofibers by electrospinning. *Ceramics International, 39*(8), 9651–9658.
39. Butt, H.-J., Cappella, B., & Kappl, M. (2005). Force measurements with the atomic force microscope: Technique, interpretation and applications. *Surface Science Reports, 59*(1–6), 1–152.
40. Chen, R., Huang, C., Ke, Q., He, C., Wang, H., & Mo, X. (2010). Preparation and characterization of coaxial electrospun thermoplastic polyurethane/collagen compound nanofibers for tissue engineering applications. *Colloids and Surfaces B: Biointerfaces, 79*(2), 315–325.
41. Širc, J., Hobzova, R., Kostina, N., Munzarová, M., Juklíčková, M., Lhotka, M., et al. (2012). Morphological characterization of nanofibers: Methods and application in practice. *Journal of Nanomaterials*, *2012*.
42. Yang, X., Pu, Y., Zhang, Y., Liu, X., Li, J., & Yuan, D., et al. (2020). Multifunctional composite membrane based on $BaTiO_3$@ PU/PSA nanofibers for high-efficiency PM2. 5 removal. *Journal of Hazardous Materials*, *391*, 122254.
43. Tan, E., & Lim, C. (2006). Mechanical characterization of nanofibers—A review. *Composites Science and Technology, 66*(9), 1102–1111.
44. Mitchell, G. R. (2015). Electrospinning: Principles, practice and possibilities. *Royal Society of Chemistry*.
45. Wei, L., & Qin, X. (2016). Nanofiber bundles and nanofiber yarn device and their mechanical properties: A review. *Textile Research Journal, 86*(17), 1885–1898.
46. Shakil, U. A., Hassan, S. B., Yahya, M. Y., & Nauman, S. (2020). Mechanical properties of electrospun nanofiber reinforced/interleaved epoxy matrix composites—A review. *Polymer Composites, 41*(6), 2288–2315.
47. Zadeh, Z. E., Solouk, A., Shafieian, M., & Nazarpak, M. H. (2021). Electrospun polyurethane/carbon nanotube composites with different amounts of carbon nanotubes and almost the same fiber diameter for biomedical applications. *Materials Science and Engineering: C*, *118*, 111403.
48. Lin, J., Wang, W., Cheng, J., Cui, Z., Si, J., Wang, Q., et al. (2020). Modification of thermoplastic polyurethane nanofiber membranes by in situ polydopamine coating for tissue engineering. *Journal of Applied Polymer Science, 137*(41), 49252.
49. Movahedi, M., Asefnejad, A., Rafienia, M., & Khorasani, M. T. (2020). Potential of novel electrospun core-shell structured polyurethane/starch (hyaluronic acid) nanofibers for skin tissue engineering: In vitro and in vivo evaluation. *International Journal of Biological Macromolecules, 146*, 627–637.
50. Guan, X., Dong, Y., Xia, H., Yao, J., & Ni, Q.-Q. (2020). Mechanical and shape memory performance of shape memory polyurethane-based aligned nanofibers. *Polymer Testing*, *91*, 106778.
51. Wang, D., Yue, Y., Wang, Q., Cheng, W., & Han, G. (2020). Preparation of cellulose acetate-polyacrylonitrile composite nanofibers by multi-fluid mixing electrospinning method: Morphology, wettability, and mechanical properties. *Applied Surface Science*, *510*, 145462.
52. Yang, S., Zhang, X., & Zhang, D. (2019). Electrospun chitosan/poly (vinyl alcohol)/graphene oxide nanofibrous membrane with ciprofloxacin antibiotic drug for potential wound dressing application. *International Journal of Molecular Sciences, 20*(18), 4395.

53. Liu, F., Li, M., Shao, W., Yue, W., Hu, B., Weng, K., et al. (2019). Preparation of a polyurethane electret nanofiber membrane and its air-filtration performance. *Journal of Colloid and Interface Science, 557*, 318–327.
54. Almuhamed, S., Khenoussi, N., Schacher, L., Adolphe, D., & Balard, H. (2012). Measuring of electrical properties of MWNT-reinforced PAN nanocomposites. *Journal of Nanomaterials, 2012*.
55. Darbandi, S. M. A., Nouri, M., & Mokhtari, J. (2012). Electrospun nanostructures based on polyurethane/MWCNTs for strain sensing applications. *Fibers and Polymers, 13*(9), 1126–1131.
56. Tondnevis, F., Keshvari, H., & Mohandesi, J. A. (2019). Physico-mechanical and in vitro characterization of electrically conductive electrospun nanofibers of poly urethane/single walled carbon nano tube by great endothelial cells adhesion for vascular tissue engineering. *Journal of Polymer Research, 26*(11), 1–16.
57. Zhang, S., Rind, N. A., Tang, N., Liu, H., Yin, X., Yu, J., et al. (2019). Electrospun nanofibers for air filtration. *Electrospinning: Nanofabrication and Applications* (pp. 365–389). Elsevier.
58. Zhu, M., Han, J., Wang, F., Shao, W., Xiong, R., Zhang, Q., et al. (2017). Electrospun nanofibers membranes for effective air filtration. *Macromolecular Materials and Engineering, 302*(1), 1600353.
59. Li, Y., Yin, X., Yu, J., & Ding, B. (2019). Electrospun nanofibers for high-performance air filtration. *Composites Communications, 15*, 6–19.
60. Wang, Y., Li, W., Zhou, Y., Jiang, L., Ma, J., Chen, S., et al. (2020). Fabrication of high-performance wearable strain sensors by using CNTs-coated electrospun polyurethane nanofibers. *Journal of Materials Science, 55*, 12592–12606.
61. Chen, X., Xu, Y., Liang, M., Ke, Q., Fang, Y., Xu, H., et al. (2018). Honeycomb-like polysulphone/polyurethane nanofiber filter for the removal of organic/inorganic species from air streams. *Journal of Hazardous Materials, 347*, 325–333.
62. Zhu, L., Zhou, X., Liu, Y., & Fu, Q. (2019). Highly sensitive, ultrastretchable strain sensors prepared by pumping hybrid fillers of carbon nanotubes/cellulose nanocrystal into electrospun polyurethane membranes. *ACS Applied Materials & Interfaces, 11*(13), 12968–12977.
63. Ren, M., Zhou, Y., Wang, Y., Zheng, G., Dai, K., Liu, C., et al. (2019). Highly stretchable and durable strain sensor based on carbon nanotubes decorated thermoplastic polyurethane fibrous network with aligned wave-like structure. *Chemical Engineering Journal, 360*, 762–777.
64. Wang, X., Liu, X., & Schubert, D. W. (2021). Highly sensitive ultrathin flexible thermoplastic polyurethane/carbon black fibrous film strain sensor with adjustable scaffold networks. *Nano-Micro Letters, 13*(1), 1–19.



Parian Mohamadi received the B.Sc. degree in textile engineering—chemistry science from Azad University-South Tehran branch, Tehran, Iran in 2017 and the M.Sc. degree in textile engineering—fiber science from Amirkabir University of Technology, Tehran, Iran in 2019. She is currently a Ph.D. student in textile engineering from the National School of Arts and Textile Industries (ENSAIT), University of Lille, Lille, France. For her bachelor's degree she conducted a study on sleeping bags and their constituent materials. Later, in 2016, she applied for an Internship in Derakhshan factory of spinning, weaving, dyeing, Research and Development. During her master's degree she worked about applying electrospinning technique on nanofibers for wound dressing applications and published an article entitled: Antibacterial and biological properties of coconut oil loaded poly (ε-caprolactone)/gelatin electrospun membranes in the Journal of Industrial Textiles, 2021. Currently, she is focused

on her thesis, which is electrospinning of nanofibers to develop strain sensors for detection of clogged air filters.



Elham Mohsenzadeh was born in Yazd, Iran, in 1988. She received her bachelor's degree in textile engineering in 2007 from Yazd State University. She obtained her master's degree in Mechanic and Science of Fibers at Haute Alsace University in Mulhouse France. Her Ph.D. thesis focused on 'Study and Development of Electrospun Fibrous Multilayers Material for Medical Applications: Substitutive Membranes' and she received her degree in 2018. She is now an Associate Professor in the Innovative Textile Materials Group in JUNIA-HEI Graduate School of Engineering in Lille, France, since 2018. Her research interests include electrospinning and nanofibers for composites, tissue engineering, wound dressing, filtration, and sensors. She works on several national and European projects focused on textile functionalization, photonic textile, textile gas sensors, and facial mask filters by using electrospinning technic.



Cedric Cochrane received the Ph.D. degree and the Habilitation à diriger des Recherches (HDR) degree in automatic (Highest University Diploma in France) from the University of Lille, in 2007 and 2018, respectively. He is currently an Associate Professor with the Ecole Nationale Supérieure des Arts et Industries Textile, Roubaix, France, where he conducts research with the GEMTEX Laboratory. He possesses strong experience in research and innovation in the field of smart and multifunctional textiles. He has participated in many national and European projects focused on the design of mechanical sensors and electrodes, design of actuators (color change or light-emitting textile structure), and energy harvesting textile. He has authored or coauthored over 60 scientific publications or book chapters in international peer-reviewed journals. His research interests include reliability of the systems (washability for instance) and especially interconnection, networks, wireless communication, and data transfer are also investigated.



Vladan Koncar is Distinguished Professor (Classe exceptionelle) at ENSAIT (Ecole Nationale Supérieure des Arts et Industries Textiles) textile engineering institute in Roubaix, France—at University of Lille. He obtained his Ph.D. in 1991 at the University of Lille 1 in Villeneuve d'Ascq. From November 2009 to November 2015, he was Head of Research at ENSAIT and Director of GEMTEX research laboratory. Professor Koncar was AUTEX (Association of Universities for Textiles, www.autex.org) President from June 2007 to June 2010. Professor Koncar has also been Deputy Director of ENSAIT from 2005 to 2007 and Director of International Relations from 2007 to 2009. He still serves as an elected member of the ENSAIT Governing Board. He has been promoted to Doctor Honoris Causa of the University of Iasi, Romania in January 2010. Professor Koncar was the Scientific coordinator and Coordinator of Large-Scale

EU Integrated Projects in FP7 and Horizon 2020 and Coordinator of National (French) research projects. His research interests cover the area of flexible textile sensors and actuators, smart textile structures, and modeling and control of complex systems. He teaches in the area of Automation, Computer Networks, Virtual Reality, and Smart textiles.

Chapter 16
Electrospun Polymeric Nanofibers: An Innovative Application for Preservation of Fruits and Vegetables



Juliana Botelho Moreira, Jorge Alberto Vieira Costa, Michele Greque de Morais, and Eliezer Avila Gandra

Abstract Fruits and vegetables are susceptible to microbial contamination caused mainly during harvesting operations. In this context, nanotechnology appears with the production of nanomaterials capable of encapsulating active components to provide thermal stability, controlled release, and antioxidant and antimicrobial properties. The nanometric diameter and the high surface area per unit volume make nanofibers promising materials for use in food packaging. Nanofibers can be applied in active packaging to preserve and extend the shelf life of food. Besides, these nanostructures can be incorporated in intelligent packaging to indicate the quality of foods to consumers. In this way, this chapter will address the advancement of nanotechnology, specifically materials such as nanofibers, for the preservation of fruits and vegetables, reporting recent studies on applications and future perspectives in the field.

Keywords Active packaging · Electrospinning · Food security · Intelligent packaging · Nanotechnology

J. B. Moreira (✉) · M. G. de Morais
Laboratory of Microbiology and Biochemistry, College of Chemistry and Food Engineering, Federal University of Rio Grande, Rio Grande, RS 96203-900, Brazil
e-mail: julianamoreira@furg.br

M. G. de Morais
e-mail: michele.morais@pq.cnpq.br

J. A. V. Costa
Laboratory of Biochemical Engineering, College of Chemistry and Food Engineering, Federal University of Rio Grande, Rio Grande, RS 96203-900, Brazil

E. A. Gandra
Laboratory of Food Science and Molecular Biology, Center for Chemical, Pharmaceutical and Food Sciences, Federal University of Pelotas, Pelotas, RS 96010-900, Brazil

© The Author(s), under exclusive license to Springer Nature Switzerland AG 2022

A. Vaseashta and N. Bölgen (eds.), *Electrospun Nanofibers*,
https://doi.org/10.1007/978-3-030-99958-2_16

16.1 Introduction

Fruits and vegetables, including plant components such as leaves, roots, bulbs, and tubers, have different morphological and metabolic functions [3]. Intrinsic characteristics, such as pH close to neutrality and high-water activity, make these foods more susceptible to microbial growth. Besides, harvesting, transporting, processing, and handling products in inadequate conditions may result in microbial contamination [81].

There are several methods used to reduce the microbial population in fresh food. However, the urgency to prevent foodborne diseases has accelerated the search for the development of antimicrobial packaging. These packaging systems release active substances to prevent or delay the deterioration of food. Active packaging also extends the product's shelf life by ensuring food safety [10]. Another system, called intelligent packaging, can be used in fruits and vegetables to detect and indicate physical–chemical and biochemical changes in these foods due to microbial contamination [51].

For the production of active and intelligent packaging, innovative materials have been developed based on nanotechnology. Nanofibers obtained by the electrospinning technique have advantages over other materials. The large surface area of these structures, with high pore volume and different sizes, facilitates the loading of active molecules and the transport of nutrients. In addition to these characteristics, thermal stability and controlled release of active compounds make nanofibers promising materials for packaging applications [49]. Nanofibers developed with the addition of antimicrobial compounds have been studied to preserve various foods, such as strawberries, lemons, mushrooms, and apples [74]. However, there is little knowledge about the long-term interaction of these nanomaterials with products and human metabolism, which compromises the acceptance of these packaging materials by producers and consumers [50]. Thus, this review addresses the advancement of nanotechnology, specifically materials such as nanofibers, for the preservation of fruits and vegetables, reporting recent studies on applications, as well as future perspectives in the field.

16.2 Quality Attributes of Fruits and Vegetables

Fruits and vegetables have a comprehensive nutritional profile, rich in macro and micronutrients, with attractive freshness and flavor. It has led to a global trend of increasing consumption and investment in research on these foods in recent years [55]. Even if they are subjected to minimal processing, they more easily deteriorate when compared to other unprocessed raw materials. Deterioration occurs mainly due to damage caused during peeling, cutting, slicing, and shredding [41]. These

processing operations can contribute to the softening of the tissues, decreased nutritional value, and unpleasant taste during storage. In addition, the exposed surface after processing can benefit the growth of pathogenic microorganisms [19, 41].

The quality of fresh produce can be affected by intrinsic factors, including morphological, physiological and biochemical defense mechanisms, fruit type, genotype, stress-induced senescence programs, and extrinsic factors that represent environmental situations, such as storage temperature and humidity [81]. Extending the shelf life of fruits, for example, is more complicated than that of other vegetables, due to its more complex physiology concerning ethylene production and maturation stages [84]. The estimation of the sensory quality of fruits and vegetables, including appearance, color, flavor, shape, and texture, is usually carried out by consumers subjectively. The change in these attributes influences the acceptance of the product, as well as its shelf life [41].

The main component of fruits and vegetables is water. The loss of water interferes with the quality of these foods and can result in withered, wrinkled, and excessively soft texture, also, loss of nutritional value [81]. Fruits and vegetables, with a firm appearance and crunchy texture, are desired by consumers. The lack of these attributes is associated with tissue deterioration. Loss of firmness is mainly associated with the enzymatic degradation of pectins [7].

Enzymatic browning is one of the limiting factors of the shelf life, commercialization, and acceptance of fresh products. The action of polyphenol oxidase in polyphenols is the main cause of browning reactions [43, 85]. Moreover, peroxidase is also involved in the enzymatic browning that appears along the cut surface of products [2].

In addition to appearance, color, and firmness, the taste is another important attribute associated with fruits and vegetables. The taste of a fresh product depends on the product's composition (sugar, organic acids, phenolic compounds, and volatile compounds), genetic factors, maturity, and post-harvest treatments [22]. Flavor involves taste and aroma, and it can act as an indicator of food shelf life [6]. The destruction of cells in freshly cut products and the consequent stress of the underlying tissues cause reactions that compromise sensory aspects, including unpleasant taste [84].

The composition of the storage gas can affect post-harvest metabolism and post-processing deterioration of fresh-cut products [8]. In addition to the physical–chemical, organoleptic, and nutritional properties, fruits and vegetables are particularly susceptible to microbial attack due to the natural protection removal in the processes used for their preparations (peeling, cutting, and slicing). Microbial contamination can occur in one or more procedures during harvesting, processing, packaging, preservation, transportation, and distribution [41]. Also, cross-contamination during cutting and shredding operations and fermentation of juices and sugars by yeasts released from damaged tissues can occur [84].

16.3 Methods to Prolong the Shelf Life of Fruits and Vegetables

There are a variety of methods used to reduce the microorganism concentration in whole and minimally processed products [9, 14, 42, 83]. In general, traditional methods of preserving fresh fruits and vegetables are classified into physical processes, chemical processes, and bio-preservation technologies. Physical preservation refers to techniques that control extrinsic factors such as ambient temperature, humidity, pressure, and gas composition to prolong the shelf life of food [41]. Cold storage is one of the most widely used physical methods because it is highly efficient. However, the process demands high energy and can cause damage to the tissues of different varieties of fresh fruits and vegetables when stored in the same condition [45].

Vacuum packaging is another technique used to conserve fruits and vegetables. Food is packed in a film with low oxygen permeability (O_2), the air is evacuated, and thus the packaging is sealed [5]. Among other physical methods employed, we can highlight the modified atmosphere packaging (MAP) [17], which involves changing the composition of the internal atmosphere of the packaging, reducing the level of O_2, replacing it with carbon dioxide (CO_2) and/or nitrogen (N_2). Active packaging [13] and intelligent packaging [5] act in the preservation [25] and monitoring [12] of food quality, respectively. Gamma irradiation [86], ultraviolet light [38, 87], pulsed light [11, 64], ultrasound [20, 30], could plasma [70] and high-pressure processing [15] are other techniques used to extend the shelf life of fruits and vegetables. Each method has its advantages and limitations according to the desired application.

In terms of chemical-based preservation technology, natural or synthetic agents can be used to extend the shelf life of fresh fruits and vegetables [45]. However, consumers have become more critical of synthetic additives as they have become more aware of food safety. Thus, this required the insertion of preservation techniques based on natural additives [41]. Moreover, several sanitizing agents, such as hypochlorite, chlorine dioxide, organic acids, iodine, bromine, ozone, and hydrogen peroxide, are used to wash fruits and vegetables to reduce the risk of microbial contamination. In this way, sanitization helps to prevent post-harvest and food-borne diseases [45, 61].

Biopreservation uses microorganisms and their antibacterial products to extend the shelf life of foods and improve food safety [36]. Bacteriophages, bioprotective microorganisms [45], and bacteriocins [31, 78] have received attention. However, this preservation method is still little explored and needs further investigation to be applied commercially [84].

16.4 Nanotechnology Applied to Food

Nanotechnology involves the development, characterization, and manipulation of materials on a nanoscale. Nanotechnology has great potential for generating new products in the food field with numerous benefits, especially in the packaging area (Fig. 16.1). However, the application of nanotechnology in food is inceptive compared to the biomedical area and the information technology industries [59]. Most nanotechnology applications are used to increase the bioavailability of nutrients, improve the characteristics and stability of products during processing and storage [50].

Nanomaterials can be classified into two main classes, such as nanoparticles and nanofibers. Due to their nanometric dimensions, these materials have a high surface area per unit of volume, which allows applications in several fields [49]. When added to compatible polymers, nanomaterials can improve the mechanical and barrier properties of food packaging. Moreover, these materials can be used in active and intelligent structures [69].

The addition of active compounds in nanomaterials for packaging development is a promising application for food science. With nanotechnology, these components are incorporated into the packaging material to generate a carrier able to interact with internal and external factors of the packaging. Thus, an intended action that improves shelf life, food quality, and product safety is activated [47]. In this way, nanomaterials can be applied to prolong the storage period, keeping the products fresh [68]. Nanomaterials of zinc oxide [1, 18] and silver [44, 71] showed to be effective in protecting products from foodborne pathogens. Nanostructured titanium dioxide can be used for the elimination of pathogens microorganisms on food contact surfaces due to its strong photocatalytic activity under ultraviolet irradiation [62, 79].

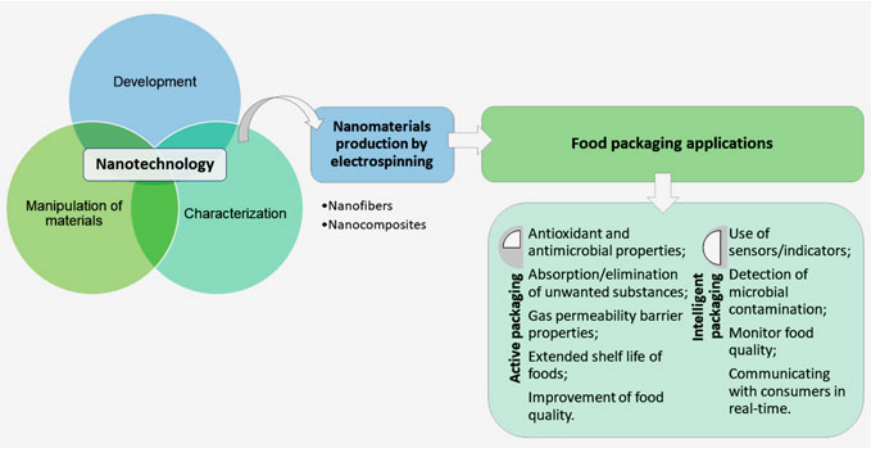


Fig. 16.1 Schematic illustration of the application of nanotechnology in food packaging systems

On the other hand, intelligent packaging systems, based on nanotechnology, interact with internal factors (food components and headspace), and/or external environmental factors, generating a response that can be an electrical or visual signal, which correlates with the state of the food product [72]. Nanosensors can be used in food packaging to monitor microbial contamination, toxins, and chemicals. With this, it will provide a quality status of food products in real-time [73]. The information generated by the indicators/sensors is useful for communicating with consumers, informing them about the safety and quality of products. In addition, the use of intelligent systems can assist producers in determining when and what actions should be taken throughout the production and distribution processes [35].

Moreover, nanostructures reduce the permeability of food packaging materials to atmospheric oxygen, moisture, or CO_2 [68, 69]. Modified nanoclays like montmorillonite can be incorporated into food packaging to increase mechanical resistance, forming a barrier against gases (oxygen), volatile components (flavors), or moisture [29]. Nanoscale membranes can be used to remove unwanted compounds in foods. Gialleli et al. [23] developed a nanoporous cellulose filter to replace industrial pasteurization techniques. The filter in the nanoscale eliminated the microbial contamination of apple juice.

Therefore, most nanotechnological applications in food are focused on the development of new products, materials, and technologies for the preservation and maintenance of food quality. Besides, the nutritional value of food products can be improved with nanotechnology. The encapsulation of active compounds (such as antioxidants, vitamins, polyphenols, and fatty acids), from nanometric structures, contributes to the bioavailability of these biocompounds [50].

16.5 Development of Nanofibers

Nanofibers are materials composed of synthetic polymers, natural polymers, or biopolymers. These nanomaterials can be produced by techniques such as drawing, template synthesis, phase separation, self-assembly, and electrospinning. Drawing is a process similar to electrospinning, where long nanofibers are made one by one [26]. The template synthesis consists of applying nanoporous membranes as a template for the production of nanofibers. The method is performed by oxidative polymerization, which can be performed electrochemically or chemically [50, 53]. In the phase separation process, nanofibers are formed due to the instability of the polymer inside the solvent, which creates two distinct phases due to physical incompatibility [50]. In self-assembly, small molecules are used as building blocks that aggregate to form nanofibers [53].

Electrospinning is the most widely adopted technique for forming polymeric nanofibers. This process has advantages such as repeatability, ease of scaling the process and producing long and continuous nanofibers. Electrospinning produces nanofibers with a diameter ranging from 10 to 1000 nm. Depending on the characteristics of the polymer used, the nanofibers can present high elasticity, strength,

and surface area concerning the volume. In addition, the large surface area of these structures provides nanofibers with high pore volume and different sizes. These pores facilitate the loading of bioactive molecules, nutrients transport, allowing those polymeric nanofibers to become an important class of nanomaterials [49, 65].

The principle of electrospinning is the application of high voltage to a polymer solution that results in the formation of nanofibers through repulsion of electrostatic charges and elongation of the solution. The polymeric solution is fed through a constant flow capillary loaded with a high voltage potential (10–30 kV). When the electric field produces enough force to overcome the surface tension at the capillary tip, the formation of the "Taylor cone" occurs. The solvent gradually evaporates, and thus the nanofibers are produced and deposited in the collector, which can be stationary or rotary [48, 50].

16.5.1 Antimicrobial Nanofibers Applied to Food

The advancement in research and development of new packaging materials has grown dramatically to meet the demands of protecting food against oxidation and microbial contamination [52]. Nanofibers can be used in food preservation due to their ability to immobilize and encapsulating compounds. Thus, these nanomaterials can be applied in active packaging to improve stability and preserve antimicrobial properties [33]. The use of antimicrobial agents capable of spreading in food and inhibiting the proliferation of microorganisms during storage is a type of active packaging system [54]. Active packaging systems can be divided into active scavenging systems (absorbers) and active-releasing systems (emitters). Active scavenging systems are used to remove or control environmental parameters, such as humidity and odor, as well as concentrations of oxygen, CO_2, and ethylene. Active-releasing systems add and release compounds in the free space within the packaging or packaged food [80].

In this context, nanofibers produced by electrospinning can encapsulate antimicrobial and antioxidant substances to preserve the freshness of various products (Table 16.1). Nanofibers allow the controlled release of antimicrobial agents with high transport capacity, mainly due to their porosity [34, 50]. Moreover, the high surface area of the nanofibers increases the material's reactivity. Absorption or release mechanisms are accelerated, increasing the number of sites for interaction of reactive materials for packaging development [46].

16.5.2 Potential of Nanofibers in the Preservation of Fruits and Vegetables

Perishable food products increase the risk of foodborne diseases, in addition to being easily deteriorated, causing waste and economic loss [63]. Different methods

Table 16.1 Recent studies on antimicrobial polymeric nanofibers with potential application in foods

Polymers	Active compound	Properties	Diameter (nm)	Potential applications/observations	References
Poly (vinyl alcohol) (PVA)	Pleurocidin	Antibacterial	890–960	Material with the potential to inhibit foodborne pathogens (*Escherichia coli* and *Staphylococcus aureus*) and prolong the shelf life of food	Wang et al. [76]
Polyhydroxybutyrate	Phenolic compounds	Antibacterial	810	Nanofibers showed inhibition of the growth of *Staphylococcus aureus* ATCC 25,923 with thermal and mechanical properties that confer potential for application in food packaging	Kuntzler et al. [34]
Chitin	N-halamine	Antibacterial and antifungal	–	The chlorinated chitin nanofibers film proved to be efficient against *Escherichia coli* and *Staphylococcus aureus*. The nanostructures also showed 100 and 80% inhibition of the germination of the spores of fungi *Alternaria alternata* and *Penicillium digitatum*, respectively	Dutta et al. [16]

(continued)

Table 16.1 (continued)

Polymers	Active compound	Properties	Diameter (nm)	Potential applications/observations	References
Chitosan	Chitosan	Antibacterial	78	Nanofibers showed potential for the application of meat preservation. The order of bacterial susceptibility was: *Escherichia coli* > *Listeria innocua* > *Staphylococcus aureus* > *Salmonella Typhimurium*	Arkoun et al. [4]
Polycaprolactone	Biopeptides	Antioxidant	438	Nanofibers provided greater stability and control of oxidative processes of chicken cuts during 12 days of storage	Gonçalves et al. [24]
Polyethylene oxide and polysaccharide Dendrobium	Adipic acid	Antibacterial	143–575	Nanofibers exhibited antibacterial activity against *Escherichia coli* in pork, without affecting the quality of the product	Zhu et al. [88]

(continued)

Table 16.1 (continued)

Polymers	Active compound	Properties	Diameter (nm)	Potential applications/observations	References
Gelatine	Chitosan nanoparticle and Moringa oil	Antibacterial	142.5	The nanomaterials showed high antibacterial activity against *Listeria monocytogenes* and *Staphylococcus aureus* at 4 and 25 °C for 10 days, without affecting the sensory quality of cheese. The encapsulation by nanofibers contributed to control the rate of release of moringa oil	Lin et al. [39]
Soluble potato starch	Carvacrol	Antioxidant and antibacterial	73–95	The application of nanofibers resulted in a reduction of 89% for Listeria monocytogenes, 68% for *Salmonella Typhimurium*, 62% for *Escherichia coli* and 49% for *Staphylococcus aureus*, maintaining antimicrobial activity for at least 30 days against *Staphylococcus aureus*	Fonseca et al. [21]

(continued)

Table 16.1 (continued)

Polymers	Active compound	Properties	Diameter (nm)	Potential applications/observations	References
Isolated soy protein and polyethylene oxide	Essential oil of ginger	Antibacterial	102–625	The essential oil encapsulated in nanofibers reduced the proliferation of *Listeria monocytogenes* in fresh Minas cheese, by the action of volatiles, during the cold storage of 12 days	Silva et al. [67]

have been applied to slow the metabolic processes of fresh fruits and vegetables. Controlled atmosphere storage [8], edible film coating [28], and irradiation [75] have been tested to improve the physiological quality and prolong the shelf life of these foods. The application of edible film coatings has been indicated to preserve fruits and vegetables as they prevent the evolution of factors that accelerate the deterioration of these foods. Nanotechnology-based films/coatings contribute to further reducing weight loss. In addition, nanotechnology materials applied to edible films can improve product appearance and extend shelf life by creating barriers to gases and moisture [27]. Nanofibers emerge in this context as an innovative reinforcement alternative to upgrade the properties of edible films. Moreover, delaying fruit ripening by controlling the level of ethylene in the fruit is made possible by coating with a semi-permeable material such as nanofibers. Due to the high porosity of nanofibers, the use of these nanostructures to develop edible films applied to fruits and vegetables also contributes to improving the intermediate permeability to gases to enable gas exchange.

Besides, nanotechnology has generated many perspectives in products development and innovative applications in food packaging from nanofibers. Yilmaz et al. [82] tested the use of zein nanofibers added with curcumin to maintain postharvest quality in apples infected with *Penicillium expansum* and *Botrytis cinerea.* Antimicrobial tests were performed on fruits with and without nanomaterials coating, for 6 days at 23 °C and 75% humidity. The diameter of the lesion decreased by 50% in coated apples that were infected with *Penicillium expansum*, demonstrating the potential of nanofibers as antifungal materials for food packaging.

Silver nanoparticles have been studied for application in active food packaging, due to their antimicrobial efficiency against microorganisms such as bacteria, yeasts, fungi, and viruses [60]. In a study performed by Kowsalya et al. [32], the in vitro analysis revealed that the poly (vinyl alcohol) (PVA) nanofibers loaded with the silver nanoparticles showed antimicrobial potential against *Bacillus cereus*, *Staphylococcus aureus*, *Escherichia coli,* and *Pseudomonas aeruginosa*, extending the shelf life of lemons and strawberries. The active nanofibers allowed the inhibition of microorganisms in the fruits for 10 days (3 × longer than the control condition − without nanofiber coating) of storage at room temperature, and without the use of a modified atmosphere.

Essential oils encapsulated in nanofibers can be used in antimicrobial packaging for the controlled release of active compounds, mainly in the form of volatiles [77]. Pan et al. [57] produced PVA nanofibers loaded with cinnamon essential oil to analyze in vitro antibacterial activity in mushrooms. The authors observed that nanomaterials inhibited the growth of *Staphylococcus aureus* and *Escherichia coli.* Furthermore, by increasing the concentration of essential oil, the nanofibers reduced the decomposition of the mushroom during 5 days of storage.

Liu et al. [40] developed polylactic acid/carbon nanotubes/chitosan composite fibers that contributed to the antimicrobial activity of fibers against microorganisms, such as *Staphylococcus aureus*, *Escherichia coli*, *Botrytis cinerea*, and *Rhizopus.* Besides, the antimicrobial activity of nanomaterials was more effective against

bacteria than against fungi. The preservation experiments showed that nanofibers developed with 7% chitosan showed potential for application in strawberries.

Other studies have evaluated the application of nanofibers for the preservation of strawberries [37, 66]. Shao et al. [66] produced and applied nanofibers from sodium pullulan-carboxymethylcellulose in strawberries, which significantly reduced the weight loss of fruits. Therefore, the nanomaterials contributed to maintaining firmness, improving the food quality during the storage. Li et al. [37] produced gelatin nanofibers loaded with butylated hydroxyanisole. According to the authors, the nanomaterials showed antioxidant, antibacterial, antifungal properties, providing preservation of strawberries. Moreover, the nanofibers exhibited antibacterial activity against *Staphylococcus aureus* and antifungal activity against four genera of fungi (*Mucor* sp., *Rhizopus* sp., *Penicillium* sp., and *Aspergillus* sp.).

Intelligent packaging provides consumers with information regarding food quality, dynamically and stably. Indicators/sensors can be developed from nanofibers to detect physical–chemical and biochemical changes in food that may compromise the quality of the product. Intelligent systems respond from variations in parameters such as pH, temperature, humidity, and gas composition [49]. Phycocyanin, for example, is a natural pigment that changes color depending on the pH of the medium in which it is exposed [72]. Moreira et al. [51] developed a colorimetric indicator consisting of polylactic acid nanofibers with this pigment. The authors observed that the color change was more noticeable at pH 3 and 4, suggesting application in citrus juice packaging. Terra et al. [73] develop nanofibers with polycaprolactone (PCL) and polyethylene oxide (PEO) with the phycocyanin addition. When tested in pH buffers ranging from 3–4 to 5–6, PCL/PEO nanofibers developed with 2% (w/v) phycocyanin showed color change values $\geq$8.5. Moreover, the study evaluated the color irreversibility of the system, where no membrane returned to the initial stain color. Therefore, these results confirmed that the indicators are entrusted and cannot be tampered with, showing the promising potential to monitor the viability of foods.

Therefore, it is clear that nanotechnology is advancing, since it allows to develop new studies that expand the potential of application of nanofibers, including their use in fruits and vegetables. The use of bioactive compounds and nanoparticles has been extensively studied to provide antioxidant and antimicrobial properties to active packaging materials. However, more studies about intelligent packaging systems should be carried for detecting oxidation and microbial contamination in food.

16.6 Future Perspectives

The introduction of nanotechnology in the food sector is affected by several factors, including technological feasibility, cost-effectiveness, regulatory requirements, and consumer acceptance [59]. Nanotechnology is better accepted in the development of new packaging than by direct application in food. Thus, proof that there is no migration of the packaging nanomaterial to the food matrix will

contribute to the acceptance of the products by the consumer. Labeling and regulations for marketing nanotechnology-enriched foods can also increase government and consumer acceptability.

Nanotechnology will transform many areas of food science, as there is an increasing demand for a longer shelf life of fresh food, as well as the need to protect against foodborne diseases [32]. In this way, nanotechnology is expected to be an impetus to develop advanced packaging systems that meet consumer needs through materials such as nanofibers. Besides, for nanotechnology to be disseminated and applied in the food industry, the safety of these new products must be evaluated and reported, demonstrating the potential long-term risks for the consumer and the environment.

Nanotechnology also has the prospect of making agriculture more efficient by using nanoparticles to improve the accuracy of nutrient supply. This new approach, which uses nano-principles, has immense possibilities to deal with the global challenges of safety and environmental sustainability, food production, food security, and climate change [58]. Technological validation, the success of science, and the immense potential of nanotechnology applications will be the precursors to the true emancipation of food science and technology [56].

16.7 Conclusions

Nanotechnology offers a series of benefits to fruit and vegetable preservation and ensures food safety and product quality. The potential applications are in the research and development and acceptance phase of nanotechnology by consumers and producers. To improve the acceptance of the use of this technology in food, the effects and potential risks of nanomaterials in the body and environmental issues throughout the production process should be clarified.

Compounds with antioxidant and antimicrobial properties have been incorporated into polymeric matrices to develop nanofibers that allow the controlled release of active components in packaging systems to extend the life of the products. Besides, indicators/sensors can be produced by these nanomaterials to detect microbial changes in food, providing feedback to consumers and producers. Thus, nanofibers are innovative materials with the potential to be applied in the preservation of fruits and vegetables through active and intelligent packaging systems. The large-scale application of nanotechnology to preserve and extend the shelf life of fresh food is promising and deserves further investigation.

Acknowledgements This research was developed within the scope of the Capes-PrInt Program (Process # 88887.310848/2018-00). The authors also are grateful to the Coordenaç˜ao de Aperfeiçoamento de Pessoal de Nível Superior—Brasil (CAPES)—Finance Code 001.

References

1. Akbar, A., Sadiq, M. B., Ali, I., Muhammad, N., Rehman, Z., Khan, M. N., Muhammad, J., Khan, S. A., Rehman, F. U., & Anal, A. K. (2019). *Biocatalysis and Agricultural Biotechnology, 17*, 36–42.
2. Alvarez, M. V., Moreira, M. R., & Ponce, A. (2015). Peroxidase activity and sensory quality of ready to cook mixed vegetables for soup: Combined effect of biopreservatives and refrigerated storage. *Food Science and Technology, 35*, 86–94.
3. Annegowda, H., & Majumder, P. (2021). Valuable bioactives from vegetable wastes. In R. Bhat (Ed.), *Valorization of agri-food wastes and by-products* (pp. 83–109). Academic Press.
4. Arkoun, M., Daigle, F., Heuzey, M.-C., & Ajji, A. (2017). Antibacterial electrospun chitosan-based nanofibers: A bacterial membrane perforator. *Food Science & Nutrition, 5*, 865–874.
5. Arvanitoyannis, I. (2012). *Modified atmosphere and active packaging technologies*. CRC Press INC.
6. Ayhan, Z., Chism, G. W., & Richter, E. R. (1998). The shelf-life of minimally processed fresh-cut melons. *Journal of Food Quality, 21*, 29–40.
7. Barbagallo, R. N., Chisari, M., & Caputa, G. (2012). Effects of calcium citrate and ascorbate as inhibitors of browning and softening in minimally processed 'Birgah' eggplants. *Postharvest Biology and Technology, 73*, 107–114.
8. Belay, Z. A., Caleb, O. J., & Opara, U. L. (2019). Influence of initial gas modification on physicochemical quality attributes and molecular changes in fresh and fresh-cut fruit during modified atmosphere packaging. *Food Packaging and Shelf Life*, *21*, 100359.
9. Bisht, B., Bhatnagar, P., Gururani, P., Kumar, V., Tomar, M. S., Sinhmar, R., Rathi, N., & Kumar, S. (2021). Food irradiation: Effect of ionizing and non-ionizing radiations on preservation of fruits and vegetables—A review. *Trends in Food Science & Technology*, *114*, 372–385.
10. Carbone, M., Donia, D. T., Sabbatella, G., & Antiochia, R. (2016). Silver nanoparticles in polymeric matrices for fresh food packaging. *Journal of King Saud University—Science, 28*, 273–279.
11. Charles, F., Vidal, V., Olive, F., Filgueiras, H., & Sallanon, H. (2013). Pulsed light treatment as new method to maintain physical and nutritional quality of freshcut mangoes. *Innovative Food Science & Emerging Technologies, 18*, 190–195.
12. Chen, H., Zhang, M., Bhandari, B., & Guo, Z. (2018). Applicability of a colorimetric indicator label for monitoring freshness of fresh-cut green bell pepper. *Postharvest Biology and Technology*, *140*, 85–92.
13. Cruz-Romero, M. C., Murphy, T., Morris, M., Cummins, E., & Kerry, J. P. (2013). Antimicrobial activity of chitosan, organic acids and nano-sized solubilisates for potential use in smart antimicrobially-active packaging for potential food applications. *Food Control, 34*, 393–397.
14. Denoya, G. I., Colletti, A. C., Vaudagna, S. R., & Polenta, G. A. (2021). Application of non-thermal technologies as a stress factor to increase the content of health-promoting compounds of minimally processed fruits and vegetables. *Current Opinion in Food Science, 42*, 224–236.
15. Denoya, G. I., Vaudagna, S. R., & Polenta, G. (2015). Effect of high pressure processing and vacuum packaging on the preservation of fresh-cut peaches. *LWT—Food Science and Technology, 62*, 801–806.
16. Dutta, A. K., Egusa, M., Kaminaka, H., Izawa, H., Morimoto, M., Saimoto, H., & Ifuku, S. (2015). Facile preparation of surface N-halamine chitin nanofiber to endow antibacterial and antifungal activities. *Carbohydrate Polymers, 115*, 342–347.
17. Dziedzic, E., Błaszczyk, J., Bieniasz, M., Dziadek, K., & Kopeć, A. (2020). Effect of modified (MAP) and controlled atmosphere (CA) storage on the quality and bioactive compounds of blue honeysuckle fruits (*Lonicera caerulea* L.). *Scientia Horticulturae*, *265*, 109226.
18. Espitia, P. J. P., Soares, N. D. F., Coimbra, J. S. D., de Andrade, N. J., Cruz, R. S., & Medeiros, E. A. A. (2012). Zinc oxide Nanoparticles: Synthesis, antimicrobial activity and food packaging applications. *Food and Bioprocess Technology, 5*, 1447–1464.

19. Finnegan, E., & O'Beirne, D. (2015). Characterising deterioration patterns in freshcut fruit using principal component analysis. II: Effects of ripeness stage, seasonality, processing and packaging. *Postharvest Biology and Technology, 100*, 91–98.
20. Firouz, M. S., Farahmandi, A., & Hosseinpour, S. (2019). Recent advances in ultrasound application as a novel technique in analysis, processing and quality control of fruits, juices and dairy products industries: A review. *Ultrasonics—Sonochemistry*, *57*, 73–88.
21. Fonseca, L. M., Cruxen, C. E. S., Bruni, G. P., Fiorentini, A. M., Zavareze, E. R., Lim, L.-T., & Dias, A. R. G. (2019). Development of antimicrobial and antioxidant electrospun soluble potato starch nanofibers loaded with carvacrol. *International Journal of Biological Macromolecules, 139*, 1182–1190.
22. Francis, G. A., Gallone, A., Nychas, G. J., Sofos, J. N., Colelli, G., Amodio, M. L., & Spano, G. (2012). Factors affecting quality and safety of fresh-cut produce. *Critical Reviews in Food Science and Nutrition, 52*, 595–610.
23. Gialleli, A. I., Bekatorou, A., Kanellaki, M., Nigam, P., & Koutinas, A. A. (2015). Apple juice preservation through microbial adsorption by nano/micro-tubular cellulose. *Innovative Food Science and Emerging Technologies, 33*, 416–421.
24. Gonçalves, C. F., Schmatz, D. A., Uebel, L. S., Kuntzler, S. G., Costa, J. A. V., Zimmer, K. R., & Morais, M. G. (2017). Microalgae biopeptides applied in nanofibers for the development of active packaging. *Polímeros, 27*, 290–297.
25. Hanif, J., Khalid, N., Khan, R. S., Bhatti, M. F., Hayat, M. Q., Ismail, M., Andleeb, S., Mandoor, Q., Khan, F., Amin, F., Hanif, R., Hashmi, M. U., & Janjua, H. A. (2019). Formulation of active packaging system using Artemisia scoparia for enhancing shelf life of fresh fruits. *Materials Science & Engineering C, 100*, 82–93.
26. Huang, Z.-M., Zhang, Y.-Z., Kotaki, M., & Ramakrishna, S. (2003). A review on polymer nanofibers by electrospinning and their applications in nanocomposites. *Composites Science and Technology, 63*, 2223–2253.
27. Jafarzadeh, S., Nafchi, A. M., Salehabadi, A., Oladzad-abbasabadi, N., Jafari, S. M. (2021). Application of bio-nanocomposite films and edible coatings for extending the shelf life of fresh fruits and vegetables. *Advances in Colloid and Interface Science*, *291*, 102405.
28. Jiao, W., Shu, C., Li, X., Cao, J., Fan, X., & Jiang, W. (2019). Preparation of a chitosan-chlorogenic acid conjugate and its application as edible coating in postharvest preservation of peach fruit. *Postharvest Biology and Technology, 154*, 129–136.
29. Jorda-Beneyto, M., Ortuno, N., Devis, A., Aucejo, S., Puerto, M., Gutierrez-Praena, D., Houtman, J., Pichardo, S., Maisanaba, S., & Jos, A. (2014). Use of nanoclay platelets in food packaging materials: Technical and cytotoxicity approach. *Food Additives and Contaminants Part A-Chemistry Analysis Control Exposure & Risk Assessment, 31*, 354–363.
30. Khademi, O., Ashtari, M., & Razavi, F. (2019). Effects of salicylic acid and ultrasound treatments on chilling injury control and quality preservation in banana fruit during cold storage. *Scientia Horticulturae, 249*, 334–339.
31. Kirtonia, K., Salauddin, M., Bharadwaj, K. K., Pati, S., Dey, A., Shariati, M. A., Tilak, V. K., & Kuznetsova, E. (2021). Bacteriocin: A new strategic antibiofilm agent in food industries. *Biocatalysis and Agricultural Biotechnology, 36*, 102141.
32. Kowsalya, E., MosaChristas, K., Balashnmugam, P., Tamil Selvi, A., Jaquline Chinna Rani, I. (2019). Biocompatible silver nanoparticles/poly(vinyl alcohol) electrospun nanofibers for potential antimicrobial food packaging applications. *Food Packaging and Shelf Life*, *21*, 100379.
33. Kumar, T. S. M., Kumar, K. S., Rajini, N., Siengchin, S., Ayrilmis, N., & Rajulu, A. V. (2019). A comprehensive review of electrospun nanofibers: Food and packaging perspective. *Composites Part B: Engineering, 175*, 1–11.
34. Kuntzler, S. G., Almeida, A. C. A., Costa, J. A. V., & Morais, M. G. (2018). Polyhydroxybutyrate and phenolic compounds microalgae electrospun nanofibers: A novel nanomaterial with antibacterial activity. *International Journal of Biological Macromolecules, 113*, 1008–1014.
35. Kuntzler, S. G., Costa, J. A. V., Brizio, A. P. D. R., & Morais, M. G. (2020). Development of a colorimetric pH indicator using nanofibers containing *Spirulina* sp. LEB 18. F*ood Chemistry*, *328*, 126768.

36. Leneveu-Jenvrin, K., Charles, F., Barba, F. J., & Remize, F. (2020). Role of biological control agents and physical treatments in maintaining the quality of fresh and minimally processed fruit and vegetables. *Critical Reviews in Food Science and Nutrition, 60*, 2837–2855.
37. Li, L., Wang, H., Chen, M., Jiang, S., Jiang, S., Li, X., & Wang, Q. (2018). Butylated hydroxyanisole encapsulated in gelatin fiber mats: Volatile release kinetics, functional effectiveness and application to strawberry preservation. *Food Chemistry, 269*, 142–149.
38. Liao, C., Liu, X., Gao, A., Zhao, A., Hu, J., & Li, B. (2016). Maintaining postharvest qualities of three leaf vegetables to enhance their shelf lives by multiple ultraviolet-C treatment. *LWT—Food Science and Technology, 73*, 1–5.
39. Lin, L., Gu, Y., & Cui, H. (2019). Moringa oil/chitosan nanoparticles embedded gelatin nanofibers for food packaging against *Listeria monocytogenes* and *Staphylococcus aureus* on cheese. *Food Packaging and Shelf Life, 19*, 86–93.
40. Liu, Y., Wang, S., Lan, W., & Qin, W. (2019). Fabrication of polylactic acid/carbon nanotubes/chitosan composite fibers by electrospinning for strawberry preservation. *International Journal of Biological Macromolecules, 121*, 1329–1336.
41. Ma, L., Zhang, M., Bhandari, B., & Gao, Z. (2017). Recent developments in novel shelf life extension technologies of fresh-cut fruits and vegetables. *Trends in Food Science & Technology, 64*, 23–38.
42. Mao, L., Mhaske, P., Zing, X., Kasapis, S., Majzoobi, M., & Farahnaky, A. (2021). Cold plasma: Microbial inactivation and effects on quality attributes of fresh and minimally processed fruits and Ready-to-Eat vegetables. *Trends in Food Science & Technology, 116*, 146–175.
43. Martinez, M. V., & Whitaker, J. R. (1995). The biochemistry and control of enzymatic browning. *Trends in Food Science & Technology, 6*, 195–200.
44. Martinez-Abad, A., Lagaron, J. M., & Ocio, M. J. (2012). Development and characterization of silver-based antimicrobial ethylene-vinyl alcohol copolymer (EVOH) films for food-packaging applications. *Journal of Agricultural and Food Chemistry, 60*, 5350–5359.
45. Meireles, A., Giaouris, E., & Simoes, M. (2016). Alternative disinfection methods to chlorine for use in the fresh-cut industry. *Food Research International, 82*, 71–85.
46. Mercante, L. A., Scagion, V. P., Migliorini, F. L., Mattoso, L. H. C., & Correa, D. S. (2017). Electrospinning-based (bio)sensors for food and agricultural applications: A review. *Trends in Analytical Chemistry, 91*, 91–103.
47. Mihindukulasuriya, S. D. F., & Lim, L.-T. (2014). Nanotechnology development in food packaging: A review. *Trends in Food Science & Technology, 40*, 149–167.
48. Morais, M. G., Vaz, B. S., Morais, E. G., & Costa, J. A. V. (2014). Biological effects of *Spirulina* (*Arthrospira*) biopolymers and biomass in the development of nanostructured scaffolds. *BioMed Research International, 2014*, 1–9.
49. Moreira, J. B., Kuntzler, S. G., Terra, A. L. M., Costa, J. A. V., & Morais, M. G. (2020). Electrospun nanofibers: Fundamentals, food packaging technology, and safety. In S. M. Rangappa, J. Parameswaranpillai, S. M. K. Thiagamani, S. Krishnasamy, & S. Siengchin (Eds.), *Food packaging advanced materials, technologies, and innovations* (pp. 223–254). Taylor and Francis.
50. Moreira, J. B., Morais, M. G., Morais, E. G., Vaz, B. S., & Costa, J. A. V. (2018). Electrospun polymeric nanofibers in food packaging. In A. M. Grumezescu & A. M. Holban (Eds.), *Impact of Nanoscience in the Food Industry* (pp. 387–418). Academic Press.
51. Moreira, J. B., Terra, A. L. M., Costa, J. A. V., & Morais, M. G. (2018). Development of pH indicator from PLA/PEO ultrafine fibers containing pigment of microalgae origin. *International Journal of Biological Macromolecules, 118*, 1855–1862.
52. Müller, P., & Schmid, M. (2019). Intelligent packaging in the food sector: A brief overview. *Foods (Basel, Switzerland), 8*(1), 16.
53. Nayak, R., Padhye, R., Kyratzis, I. L., Truong, Y. B., & Arnold, L. (2011). Recent advances in nanofibre fabrication techniques. *Textile Research Journal, 82*, 129–147.
54. Neo, Y. P., Ray, S., Jin, J., Gizdavic-Nikolaidis, M., Nieuwoudt, M. K., Liu, D., & Quek, S. Y. (2013). Encapsulation of food grade antioxidant in natural biopolymer by electrospinning technique: A physicochemical study based on zein–gallic acid system. *Food Chemistry, 136*, 1013–1021.

55. Oliveira, M., Abadias, M., Usall, J., Torres, R., Teixido, N., & Viñas, I. (2015). Application of modified atmosphere packaging as a safety approach to fresh-cut fruits and vegetables—A review. *Trends in Food Science & Technology, 46*, 13–26.
56. Palit, S. (2020). Recent advances in the application of nanotechnology in food industry and the vast vision for the future. In A. M. Grumezescu, & A. M. Holban (Eds.), *Nanoengineering in the beverage industry* (pp. 1–34). Academic Press.
57. Pan, J., Ai, F., Shao, P., Chen, H., & Gao, H. (2019). Development of polyvinyl alcohol/βcyclodextrin antimicrobial nanofibers for fresh mushroom packaging. *Food Chemistry*, *300*, 125249.
58. Pandey, G. (2018). Challenges and future prospects of agri-nanotechnology for sustainable agriculture in India. *Environmental Technology & Innovation, 11*, 299–307.
59. Peters, R. J. B., Bouwmeester, H., Gottardo, S., Amenta, V., Arena, M., Brandhoff, P., Marvin, H. J. P., Mech, A., Moniz, F. B., Pseudo, L. Q., Rauscher, H., Schoonjan, R., Undas, A. K., Vettori, M. V., Weigel, S., & Aschberger, K. (2016). Nanomaterials for products and application in agriculture, feed and food. *Trends in Food Science & Technology, 54*, 155–164.
60. Rai, M., Yadav, A., & Gade, A. (2009). Silver nanoparticles as a new generation of antimicrobials. *Biotechnology Advances, 27*, 76–83.
61. Ramos, B., Miller, F. A., Brandão, T. R. S., Teixeira, P., & Silva, C. L. M. (2013). Fresh fruits and vegetables—An overview on applied methodologies to improve its quality and safety. *Innovative Food Science and Emerging Technologies, 20*, 1–15.
62. Ravishankar Rai, V., & Jamuna Bai, A. (2011). Nanoparticles and their potential application as antimicrobials. In A. Mendez-Villas (Ed.), *Science against microbial: Communicating current research and technological advances* (pp. 197–209). Formatex Research Center.
63. Saeed, B. Q., Osaili, T. M., & Taha, S. (2021). Foodborne diseases risk factors associated with food safety knowledge and practices of women in Sharjah-United Arab Emirate. *Food Control*, *125*, 108024.
64. Salinas-Roca, B., Soliva-Fortuny, R., Welti-Chanes, J., & Martín-Belloso, O. (2016). Combined effect of pulsed light, edible coating and malic acid dipping to improve fresh-cut mango safety and quality. *Food Control, 66*, 190–197.
65. Schmatz, D. A., Uebel, L. S., Kuntzler, S. G., Dora, C. L., Costa, J. A. V., & Morais, M. G. (2016). Scaffolds containing *Spirulina* sp. LEB 18 biomass: Development, characterization and evaluation of in vitro biodegradation. *Journal of Nanoscience and Nanotechnology, 16*, 1050–1059.
66. Shao, P., Niu, B., Chen, H., & Sun, P. (2018). Fabrication and characterization of tea polyphenols loaded pullulan-CMC electrospun nanofiber for fruit preservation. *International Journal of Biological Macromolecules, 107*, 1908–1914.
67. Silva, F. T., Cunha, K. F., Fonseca, L. M., Antunes, M. D., El Halal, S. L. M., Fiorentini, A. M., Zavareze, E. R., & Dias, A. R. G. (2018). Action of ginger essential oil (*Zingiber officinale*) encapsulated in proteins ultrafine fibers on the antimicrobial control in situ. *International Journal of Biological Macromolecules, 118*, 107–115.
68. Silvestre, C., & Ciminno, S. (2013). *Ecosustainable polymer nanomaterials for food packaging: Innovative solutions, characterization needs*. CRC Press.
69. Primožič, M., Knez, Ž, & Leitgeb, M. (2021). (Bio)nanotechnology in food science—Food packaging. *Nanomaterials, 11*, 292.
70. Sudheesh, C., & Sunooj, K. V. (2020). Cold plasma processing of fresh-cut fruits and vegetables. In M. W. Siddiqui (Ed.), *Fresh-cut fruits and vegetables* (pp. 339–356). Academic Press.
71. Terra, A. M., Kosinski, R. C., Moreira, J. B., Costa, J. A. V., & Morais, M. G. (2019). Microalgae biosynthesis of silver nanoparticles for application in the control of agricultural pathogens. *Journal of Environmental Science and Health Part B-Pesticides Food Contaminants and Agricultural, 55*, 1–8.
72. Terra, A. M., Moreira, J. B., Costa, J. A. V., & Morais, M. G. (2021a). Development of pH indicators from nanofibers containing microalgal pigment for monitoring of food quality. *Food Bioscience*, *44*, 101387.

73. Terra, A. M., Moreira, J. B., Costa, J. A. V., & Morais, M. G. (2021b). Development of time-pH indicator nanofibers from natural pigments: An emerging processing technology to monitor the quality of foods. *Lebensmittel-Wissenschaft & Technologie*, *142*, 111020.
74. Topuz, F., & Uyar, T. (2020). Antioxidant, antibacterial and antifungal electrospun nanofibers for food packaging applications. *Food Research International*, *130*, 108927.
75. Wang, C., & Meng, X. (2016). Effect of 60Co γ-irradiation on storage quality and cell wall ultra-structure of blueberry fruit during cold storage. *Innovative Food Science & Emerging Technologies, 38*, 91–97.
76. Wang, X., Yue, T., & Lee, T. (2015). Development of Pleurocidin-poly(vinyl alcohol) electrospun antimicrobial nanofibers to retain antimicrobial activity in food system application. *Food Control, 54*, 150–157.
77. Wen, P., Zhu, D.-H., Wu, H., Zong, M.-H., Jing, Y. R., & Han, S.-Y. (2016). Encapsulation of cinnamon essential oil in electrospun nanofibrous film for active food packaging. *Food Control, 59*, 366–376.
78. Xiang, Y. Z., Li, X. Y., Zheng, H. L., Chen, J. Y., Lin, L. B., & Zhang, Q. L. (2021). Purification and antibacterial properties of a novel bacteriocin against *Escherichia coli* from *Bacillus subtilis* isolated from blueberry ferments. *Lebensmittel-Wissenschaft & Technologie*, *146*, 111456.
79. Yemmireddy, V. K., Farrell, G. D., & Hung, Y. C. (2015). Development of titanium dioxide TiO_2 nanocoatings on food contact surfaces and method to evaluate their durability and photocatalytic bactericidal property. *Journal of Food Science, 80*, N1903–N1911.
80. Yildirim, S., Röcker, B., Pettersen, M. K., Nilsen-Nygaard, J., Ayhan, Z., Rutkaite, R., Radusin, T., Suminska, P., Marcos, B., & Coma, V. (2018). Active packaging applications for food. *Comprehensive Reviews in Food Science and Food Safety, 17*, 165–199.
81. Yahia, E. M., Gardea-Béjar, A., Ornelas-Paz, J. J., Maya-Meraz, O., Rodríguez-Roque, M. J., Rios-Velasco, C., Ornelas-Paz, J., & Salas-Marina, M. A. (2019). Preharvest factors affecting postharvest quality. In E. M. Yahia (Ed.), *Postharvest technology of perishable horticultural commodities* (pp. 99–128). Elsevier.
82. Yilmaz, A., Bozkurt, F., Cicek, P. K., Dertli, E., Durak, M. Z., & Yilmaz, M. T. (2016). A novel antifungal surface-coating application to limit postharvest decay on coated apples: Molecular, thermal and morphological properties of electrospun zein–nanofiber mats loaded with curcumin. *Innovative Food Science & Emerging Technologies, 37*, 74–83.
83. Yousuf, B., & Qadri, O. S. (2020). Preservation of fresh-cut fruits and vegetables by edible coatings. In S. M. Wasim (Ed.), *Fresh-cut fruits and vegetables* (pp. 225–242). Academic Press.
84. Yousuf, B., Qadri, O. S., & Srivastava, A. K. (2018). Recent developments in shelf-life extension of fresh-cut fruits and vegetables by application of different edible coatings: A review. *LWT—Food Science and Technology, 89*, 198–209.
85. Zambrano-Zaragoza, M. L., Gutierrez-Cortez, E., Del Real, A., González-Reza, R. M., Galindo-Perez, M. J., & Quintanar-Guerrero, D. (2014). Fresh-cut red delicious apples coating using tocopherol/mucilage nanoemulsion: Effect of coating on polyphenol oxidase and pectin methylesterase activities. *Food Research International*, *62*, 974–983.
86. Zarbakhsh, S., & Rastegar, S. (2019). Influence of postharvest gamma irradiation on the antioxidant system, microbial and shelf life quality of three cultivars of date fruits (*Phoenix dactylifera* L.). *Scientia Horticulturae, 247*, 275–286.
87. Zhang, W., & Jiang, W. (2019). UV treatment improved the quality of postharvest fruits and vegetables by inducing resistance. *Trends in Food Science & Technology, 92*, 71–80.
88. Zhu, Y., Cui, H., Li, C., & Lin, L. (2019). A novel polyethylene oxide/Dendrobium officinale nanofiber: Preparation, characterization and application in pork packaging. *Food Packaging and Shelf Life*, *21*, 100329.



Juliana Botelho Moreira is graduated in Food Engineering, Master and Ph.D. in Food Science and Engineering from the Federal University of Rio Grande. She developed part of his Thesis at the University of Guelph, in Canada, addressing the development of nanofibers for potential application in food packaging. She did post-doctoral studies at Federal University of Rio Grande. Currently, she is a Visiting Professor in the Graduate Program in Food Engineering and Science at the Federal University of Rio Grande. She has published articles in specialized journals, and book chapters in the topics of biopolymers, nanobiotechnology, microalgae biomass, nanomaterials. She works in the area of nanobiotechnology with an emphasis on the use of compound extracted from microalgae for the production of bionanocomposites. She also develops projects in polymers and packaging field.



Jorge Alberto Vieira Costa is a Food Engineer from the Federal University of Rio Grande and a Ph.D. in Food Engineering from the State University of Campinas. He did post-doctoral studies at the Scripps Institution of Oceanography at the University of California—San Diego. He is currently Full Professor at the Federal University of Rio Grande, in the Biochemical Engineering course and in the Graduate Program in Food Engineering and Science. He is also an advisor in the graduate program in Bioprocess Engineering and Biotechnology at the Federal University of Paraná. He has published articles in specialized journals, patented processes and products, book chapters and articles in the annals of events on the topics of microalgal biotechnology, food and bioproduct development from microalgae biomass and açaí fruit. He works in the area of Food Science with an emphasis on Food Engineering/Biotechnology.



Michele Greque de Morais is a Food Engineer, Master's, and Ph.D. in Food Science and Engineering at the Federal University of Rio Grande. She developed part of her thesis on the development of nanofibers at Philipps-Universität Marburg, Germany. She did post-doctoral studies at Scripps Institution of Oceanography at the University of California—San Diego. Currently, she is a professor at the Federal University of Rio Grande teaching the disciplines of microbiology and nanobiotechnology in the course of Biochemical Engineering. She has published articles in specialized journals, patented processes and products, book chapters, and papers in annals of events in the topics nanobiotechnology, microalgae, and bioproducts extracted from microalgae biomass. She works in Food Science with emphasis on Food Engineering/Biotechnology.



Eliezer Avila Gandra is graduated in food engineering from the Federal University of Rio Grande with, Masters, and Ph.D. in Agroindustrial Science and Technology from the Federal University of Pelotas. He is currently an associate professor at the Center for Chemical, Pharmaceutical and Food Sciences and permanent professor of the Food Science Graduate Course (specialization), Professional Master's degree in Food Science and Technology, and the Graduate Program in Food and Nutrition, acting on research mainly on the following subjects: antimicrobials, bioactive coverings, pathogenic microorganisms, and molecular methods applied.

Chapter 17
Encapsulation of Bioactive Compounds in Electrospun Nanofibers for Food Packaging



Michele Greque de Morais, Suelen Goettems Kuntzler, Ana Claudia Araujo de Almeida, Ana Gabrielle Pires Alvarenga, and Jorge Alberto Vieira Costa

Abstract The food industry has been seeking the use of bioactive compounds in packaging. These compounds increase the shelf life of foods and provide higher quality and safety to products. Thus, nanofiber encapsulation is considered a promising approach for food packaging. The electrospinning technique is an alternative for nanofibers production, which acts as a support for bioactive compounds. Nanofibers improve stability and control the release of the compounds into the food. Nanoencapsulation of bioactive compounds allows the development of active, functional bioactive, intelligent, and edible packaging. Therefore, the chapter discusses the polymeric nanofibers as an encapsulation material for bioactive compounds by the electrospinning method. Also, the main characteristics of bioactive compounds and nanostructures' applications in food packaging are addressed.

Keywords Active packaging · Intelligent packaging · Nanoencapsulation · Food safety

17.1 Introduction

Nanotechnology is a promising technique for developing innovative products, including enhancements in the food sector [13, 21]. The use of nanotechnology can improve food safety, increase food packaging efficiency, shelf life, and nutritional value through additives that do not alter the taste and physical characteristics of food products [32]. In this sense, food industries have been seeking innovations in packaging materials due to consumer demand for safe and quality products [52].

M. G. de Morais (✉) · S. G. Kuntzler · A. C. A. de Almeida · A. G. P. Alvarenga
Laboratory of Microbiology and Biochemistry, College of Chemistry and Food Engineering, Federal University of Rio Grande, Rio Grande, RS, Brazil
e-mail: michele.morais@pq.cnpq.br

J. A. V. Costa
Laboratory of Biochemical Engineering, College of Chemistry and Food Engineering, Federal University of Rio Grande, Rio Grande, RS, Brazil

© The Author(s), under exclusive license to Springer Nature Switzerland AG 2022

A. Vaseashta and N. Bölgen (eds.), *Electrospun Nanofibers*,
https://doi.org/10.1007/978-3-030-99958-2_17

Nanofibers are an alternative in packaging development because they have a nanoscale diameter, which provides a higher surface area relative to volume and high porosity [58]. The electrospinning technique that produces nanofibers is efficient for encapsulating bioactive compounds. This process is characterized using room temperature that prevents the early degradation or volatilization of bioactive [33, 54]. In addition, the main advantages are the possibility of scale-up and the excellent repeatability of the process [47, 88].

Nanoencapsulation of bioactive compounds by nanofibers for application in food packaging can enhance the industrial sector and generate new functions and benefits for products and consumers [33]. However, the stability and degradation of these compounds are affected by external factors such as temperature, light exposure, and oxygen. Direct application of the bioactive in food can alter sensory properties [71, 81, 94]. Nanoencapsulation is effective for protecting biological activities, increasing stability, and assigning new functions to food packaging [4].

In this sense, the chapter discusses the polymeric nanofibers as an encapsulation material for bioactive compounds by the electrospinning method. Also, the main characteristics of bioactive compounds and nanostructures' applications in food packaging are addressed.

17.2 Polymeric Nanofibers as Material for Encapsulation by the Electrospinning Process

Electrospinning produces nanofibers based on applicating electrostatic forces on the drop of polymer solution, which is then elongated to produce fibers with nanoscale diameters [1]. The equipment consists of a positive displacement pump into which the polymer solution is inserted, two electrodes, and a high electric potential source. The polymer in a liquid phase is expelled from the capillary at a constant rate by the positive displacement pump. When the small volume of the solution exposing to the electric field, the droplet extends toward the grounded metal collector forming the Taylor cone [100].

Several synthetic and natural polymers individually or blends are explored for producing nanofibers by electrospinning (Table 17.1). These polymers must exhibit characteristics such as biodegradability, low toxicity, and mechanical properties, which are essential for food packaging production [88]. The morphology of nanofibers is an important aspect to direct their application in various technological fields. To improve or obtain different morphologies, several experimental parameters related to the polymer solution (polymer molecular weight, concentration, viscosity, and conductivity), the production process (electric potential, distance from capillary to collector, solution feed rate), and the environment (temperature and humidity) need to be optimized [99].

The molecular mass and polymer concentration are parameters that influence the viscosimetric properties of solutions. High molecular weight polymers have a larger

Table 17.1 Polymers and process parameters to produce nanofibers for food packaging

Polymer	Process parameters (EP; FR; DCC)	Food packagin applications	References
Poly(hydroxybutyrate)	15 kV; 150 μL h^{-1}; 150 mm	Antibacterial packaging	[42]
Zein	10–13 kV; 0.005 mL min^{-1}; 130 mm	Packaging to extend the shelf life of mushrooms (*Agaricus bisporus*)	[63]
Gelatin	23 kV, 0.2 mL h^{-1}; 150 mm	Antibacterial packaging for cheese preservation	[48]
Microalgal protein	50 kV; 100 mm s^{-1}; 300 mm	Antioxidant packaging	[61]
Starch	+25 kV e–3 kV; 0.60 mL h^{-1}; 200 mm	Antioxidant and antibacterial packaging	[27]
Hydroxypropylmethyl cellulose	12 kV; 0.6 mL h^{-1}; 300 mm	Antioxidant packaging for the preservation of nuts	[5]
Chitosan	20 kV; 0.5 mL h^{-1}; 150 mm	Antibacterial packaging for the preservation of beef	[83]
Polyvinyl alcohol	10 kV; 1 mL h^{-1}; 120 mm	Antibacterial packaging	[101]
Chitosanand polyethylene oxide	20 kV; 300 μL h^{-1}; 100 mm	Antibacterial packaging	[44]

EP—electric potential; FR—flow rate; DCC—distance from capillary to collector

surface area, which facilitates entanglement of the polymer chain, resulting in higher solution viscosity. This increased viscosity has been associated with the production of larger diameter nanofibers [9]. The highly concentrated solutions can produce flat ribbon nanofibers or provide capillary clogging during the electrospinning process. Determining the optimum concentration is necessary to obtain continuous and homogeneous nanofibers, which depend on the polymer properties and process parameters [18].

The electrical conductivity of the solution is another parameter that influences the morphology of the nanofibers, facilitating the elongation of the drop and the formation of one or more jets. The addition of salts, ions, or conductive polymers to the solution can increase the conductivity, resulting in nanofibers with fewer defects and smaller diameters [60]. Schmatz et al. [75] added sodium chloride to solutions containing polycaprolactone and bioactive compounds. The authors found that addicting the salt in the solutions reduced the diameter of the nanofibers, improved the homogeneity in morphology, and there was an absence of defects or droplets.

During electrospinning, nanofibers are forming due to the stretching of the polymer droplet by electrostatic forces. The stretching occurs under the action of the electric potential, in which the electrostatic force present in the droplet is higher

than those originated by surface tension [1, 45]. Therefore, the proper electric potential and distance between the capillary and the collector are essential parameter for developing continuous nanofibers because it influences the solution droplet deformation and jet behavior. Also, the proper distance is critical for evaporation of the solvent, as volatile solvents require smaller working distances, which vary around 10 cm, compared to non-volatile solvents [45, 53]. The flow rate of the solution influences the size of the droplets and the morphology of the nanofibers. A high flow rate can form large droplets, nanofibers with larger diameters. At low flow rates tend to form nanofibers with smaller diameters [60].

17.3 Bioactive Compounds for Encapsulation by Electrospinning

17.3.1 Phycocyanin

Phycocyanin is a commercially relevant photosynthetic pigment present in microalgae biomass. This compound has an intense blue coloration which is extracted mainly from *Spirulina platensis* [25, 56]. Phycocyanin accounts for approximately 20% of the total proteins that constitute microalgal biomass [92]. However, changes in the modes or media of cultivation can favor the accumulation of this compound [59].

Obtaining phycocyanin can be under heterotrophic conditions from *Spirulina* cultivation. The composition of the culture medium may contain freshwater, sodium bicarbonate, nitrates, sulfates, and microelements that inhibit the growth of microorganisms contaminating the culture, providing large-scale production [22]. In addition, light intensity, nutrient sources such as carbon and nitrogen, room temperature (30 °C), and alkaline pH (9,0) can enhance phycocyanin productivity [64, 98].

The commercial interest in phycocyanin can be attributed to its properties as natural dyes and fluorescent markers [56]. In addition, it has therapeutic applications such as antioxidant activity [28], anti-inflammatory [70], and anticancer [97]. However, phycocyanin is sensitive to light, moisture, oxygen, and heat, which restricts the application and bioavailability [56]. Thus, nanoencapsulation of phycocyanin is an alternative to protecting its biological activities, increasing the stability and shelf life [12].

Studies address the use of phycocyanin as a substitute for artificial dyes in the food industry, being added in products such as ice cream, milk, and gum [55, 57]. Phycocyanin is also used as a fluorescent label due to its characteristics, such as wavelength absorption and emission, high fluorescence quantum yield, and photostability [40, 41]. In addition, phycocyanin has other applications as a marker for gel electrophoresis, isoelectric focusing and gel exclusion chromatography, fluorescence microscopy, fluorescence in situ hybridization, and marker for proteins, antibodies, and nucleic acids [59].

17.3.2 Phenolic Compounds and Essential Oils

Phenolic compounds are found in vascular plants as secondary metabolites. These compounds can be water-soluble (phenolic acids, phenylpropanoids, flavonoids, and quinones) or insoluble (condensed tannins, lignins, and hydroxycinnamic acids bound to the cell wall) [34]. Studies with phenolic compounds are interesting for the food industry, as they exhibit antioxidant [65], anti-inflammatory [102], and antimicrobial [44] properties.

The efficiency of phenolic compounds depends on their stability, bioavailability, and bioactivity during the processing, storage, and consumption steps [24]. However, external factors such as light and high temperature and gastrointestinal tract conditions such as enzymes, pH, and interactions with other nutrients, inhibit the biological properties of these compounds [10, 23]. Therefore, micro/nanoencapsulation methods of phenolics have been used to maintain and protect from early degradation [17].

Essential oils are natural compounds certified as Generally Recognized As Safe (GRAS) by the Food and Drug Administration (FDA). Obtaining these compounds can be from plant raw materials such as flowers (bergamot orange, *Citrus bergamia*), leaves (lemon grass, *Cymbopogon citratus*), wood (sandalwood, *Santalum acuminatum*), rhizomes (*Zingiber officinale*), ginger, turmeric, fruits (anise, *Pimpinella anisum*), and roots (vetiver grass, *Chrysopogon zizanioides*) [69]. Essential oils have potential antiviral, antibacterial, antioxidant, and antiparasitic applications [7]. In addition, the interest in using essential oils is attributed to the development of natural products and the need to obtain safe and low toxicity compounds [86]. However, the direct addition of essential oils in foods is limited because of the alteration of the sensory characteristics of the product [95]. Therefore, essential oils are used for producing packaging films for food preservation [91]. Javaherzadeh et al. [36] developed poly (lactic acid)/nanochitosan films incorporated with essential oil for potential application as active packaging in chicken. The results showed that films containing 1.5% of essential oil were desirable in the sensorial properties of the food with a storage time of more than 10 days.

17.3.3 Anthocyanins

Anthocyanins belong to the group of flavonoids which are water-soluble pigments. The color diversity of anthocyanins varies depending on the environmental pH, from salmon pink to red and violet to dark blue. Anthocyanins are synthesized via secondary metabolites in natural sources such as red and black fruits, radish, eggplant, sweet potato, and purple onion [31].

Protection against neurological diseases, control of cognitive functions, reduced risk of heart disease, and enhancement of vision and brain functions are being associated with the use of anthocyanins [82]. In addition, studies have shown that anthocyanins exert beneficial health properties such as anticancer [80], antimicrobial [49], and antioxidant [93].

The stability and degradation of anthocyanins are affected by the temperature, light exposure, oxygen, and enzymes [15, 16, 90]. Thus, micro/nanoencapsulation methods increase the stability of anthocyanins and extend the applications of anthocyanin-based films in food packaging [67, 76, 84]. Anthocyanins have been applied as colorants in intelligent packaging films [72]. Qin et al. [67] studied the nanoencapsulation of anthocyanins to produce food packaging films. The nanoencapsulation allowed for increased stability of anthocyanins in the films and product shelf life. In another study, the development of antioxidant packaging films loaded with anthocyanins demonstrated potential application to protect olive oil from oxidation [93].

17.4 Nanotechnology and Food Safety

Nanotechnology spans several areas of science and refers to the use of nanoscale materials ranging from 1 to 999 nm. The materials exhibit physical and chemical properties that undergo modifications in molecular dimensions [79]. Therefore, this technology has enhanced the areas of food science that involve processing, packaging, storage, transportation, and food safety aspects [6]. In this regard, nanostructures exhibit enhanced properties that enable the encapsulation of bioactive compounds and application in controlled release [8], development of intelligent food packaging [20]. Nanotechnology applied in the food industry has advantages such as increased product shelf life, development of innovative packaging materials, and reduction of environmental impacts [11, 35]. Although the material is considered GRAS, studies to examine the risk are of utmost importance because the physicochemical properties of nanomaterials are different on the macroscale. In addition, the size of these nanomaterials favors an increased risk of bioaccumulation in body organs and tissues [74].

Therefore, regulatory bodies have created laws and guidance documents related to the potential risks of nanostructure production. European Union regulations have established that any food product with nanotechnology applications must be evaluated for safety before approval for consumption. European Food Safety is the body that aims to monitor the application of nanotechnology for human use [68]. Another regulator is National Industrial Chemicals Notification and Assessment Scheme that belongs to Australia and operates in the United States [78].

17.5 Electrospun Nanofibers Containing Bioactive Compounds for Application in Food Packaging

Nanofibers produced by electrospinning with natural and synthetic polymers can be used for the nanoencapsulation of bioactive compounds. The use of nanofibers in the food sector is growing as it provides stability and preservation of biological activities of compounds. Uebel et al. [89] encapsulated quercetin and curcumin on nanofibers to protect these compounds from anticipated degradation and maintain antioxidant activity. Nanofibers also exhibit high surface area by volume, which results in increased sensitivity of the encapsulated compounds with the aqueous medium. Thus, this property allows for the development of intelligent packaging, such as the study by Kuntzler et al. [43]. The authors incorporated *Spirulina* biomass into nanofibers for application as a colorimetric pH indicator. This section presents recent studies on nanofibers embedded with natural compounds and the potential application of these materials in active, intelligent, bioactive, and edible packaging (Fig. 17.1).

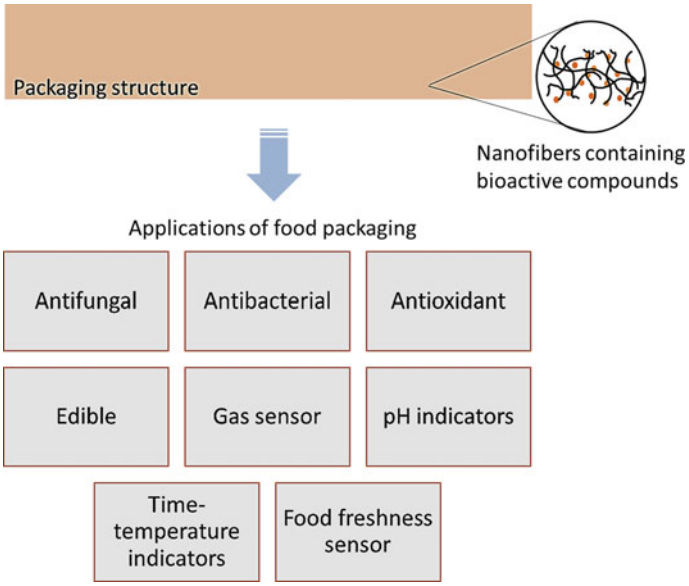


Fig. 17.1 Applications of electrospun nanofibers with bioactive compounds in food packaging

17.5.1 Active Packaging

Active packaging has been used in the food area to preserve food quality by releasing active compounds (organic acids, enzymes, bacteriocins, fungicides, natural extracts, and ions) without the direct addition of any substances to the products [3]. The principal active packaging systems involve oxygen scavenging agents, ethylene absorbers, carbon dioxide emitters, flavor release/absorption systems, antioxidants, antimicrobials, and moisture controllers [26]. Polymeric nanofibers have been applied to developing active food packaging [19]. These nanostructures exhibit high encapsulation capacity, stability, and controlled release of bioactive compounds besides being produced with polymers that can be applied in food [87].

Duan et al. [19] developed pullulan/chitin nanofibers containing curcumin and anthocyanins for application in active food packaging. The authors evaluated the antioxidant and antimicrobial capacity of the nanofibers with the pigments, as well as the color variation upon pH change. The nanofibers containing the pigments presented higher antioxidant (61.72%) and antimicrobial (inhibition zone of 22.67 mm to *Staphylococcus aureus* and 22.83 mm to *Escherichia coli*) capacity in comparison to the control (without the compounds) (5.2%, 14.5 mm, and 16.17 mm, respectively).

Color analysis as a function of pH showed that nanofibers containing anthocyanins showed significantly higher color variation to nanofibers with curcumin. Kuntzler et al. [42] evaluated the antimicrobial capacity of polyhydroxybutyrate (PHB) nanofibers containing phenolic compounds from microalgae *Spirulina* sp. LEB 18. The nanofibers produced with 35% PHB and 1% phenolic compounds showed an inhibition zone of 7.5 ± 0.4 mm for the microorganism *Staphylococcus aureus*.

17.5.2 Functional Bioactive Packaging

Bioactive systems have been developed to improve the impact of food on consumer health so that the packaging contributes to the food providing more than the traditional nutrients [3, 51, 52]. To this end, bioactive or functional compounds are added to the packaging material, which can interact with the food through their controlled release or capture of substances generated or present in the food. Thus, bioactive packaging is an innovative strategy to produce healthier packaged foods [73].

Active compounds with antioxidant properties have been applied in food. However, these compounds are characterized by instability and oxidation when exposed to the combination of oxygen, light, and heat. Thus, the characteristics of the food can be affected, as well as the biological activity of the bioactive compound [62, 96]. Another aspect is the bioavailability of active compounds applied to food packaging since some polyphenols, carotenoids, fatty acids, and omega-3s are insoluble in water and have low intestinal permeability [62]. Thus, encapsulation and

delivery systems are needed to achieve controlled release of actives and improve availability in the consumer body [29]. The electrospinning technique has a high ability to encapsulate bioactive compounds in nanofibers [96].

Bruni et al. [14] developed active inner packaging using nanofibers produced by electrospinning through the emulsion. In this way, the antioxidant molecule β-carotene was encapsulated in a mixture of soy protein isolate and polyvinyl alcohol that was electro-spun directly onto polyhydroxybutyrate-co-valerate film. The authors obtained encapsulation efficiency of β-carotene of 65.0 ± 2.6% and slow and sustained release of the bioactive compound applying a post-electrospinning annealing process.

17.5.3 Intelligent Packaging

The intelligent system monitors changes from food such as freshness, ripeness, and spoilage [39]. Intelligent packaging informs the consumer of the quality of the food and changes that may have occurred during transportation to storage. The application of this technology can prevent food poisoning and reduce food waste, as well as act against product tampering [46].

Real-time monitoring of the product can be accomplished using indicators, data carriers, and sensors applied to food packaging. Most indicators are intended to report changes in temperature, freshness, gases, and pH. Data carriers include bar codes and Radio Frequency Identification tags. Gas sensors (CO_2 and O_2), volatile amines, and biosensors are the most studied categories for food quality monitoring [39].

Terra et al. [85] developed time–pH indicator nanofibers with natural pigments for application in food packaging. Nanofibers of the poly (lactic acid) and polyethylene oxide with curcumin, quercetin, and phycocyanin were produced. The authors evaluated the color change of the pigments with the variation of time and pH. The nanofibers with phycocyanin did not lose their colorimetric profile during the experiment and presented the greatest spectrum of color variation in the pH 2–7 ranges, which is perceptible to the naked eye. Silva et al. [77] developed ultrafine fibers with anthocyanins extracted from açaí for application as pH sensors in food packaging. According to the authors, the composite assay with 3% w v^{-1} of anthocyanins showed color-changing ability when subjected to pH differences, resulting in ΔE detectable by the human eye ($\Delta E > 5$).

17.5.4 Edible Packaging

Active, biodegradable, and edible systems have been attracting interest from the food industry. The food industry considers materials that are renewable, recyclable, biodegradable, and require minimal or no disposal to be a priority [37]. Edible packaging is based on food-grade materials, applied to food like a coating or film, and

can be ingested by the consumer. This packaging system is characterized by versatility, production from various materials, and the possibility to carry different active substances with antioxidant and antimicrobial activities. For this reason, research has been directed with the goal of adequate and safe industrial expansion of this type of packaging [2, 66].

Edible packaging is considered suitable for human consumption, as it is composed of ingredients that can be ingested by consumers, such as polysaccharides, proteins, and lipids. As packaging materials are safe for human consumption, the transmission of packaging molecules to food does not pose a health risk to the consumer [38]. Liu et al. [50] developed edible nanofiber films of gelatin, chitosan, and phenyl 3-acid for application in food packaging. The addition of 2% phenyl 3-acid obtained higher thermal stability, water stability, and water vapor permeability to the control experiment (without phenyl 3-acid). In addition, this film showed antibacterial activity, with a reduction of approximately 4 log UFC/mL of *Salmonella enteritidis* and *Staphylococcus aureus* in 30 min. According to the results, the edible film can be applied in active food packaging.

Ghosh et al. [30] developed an edible coating based on cellulose nanofibers functionalized with iron from curcumin and chitosan to maintain the quality of kiwifruit during storage. The edible coating materials provided reduced mass loss, higher firmness, and respiration rate in addition to lower microbial counts of kiwifruit for 10 days storage at 10 °C. Thus, the development of edible materials is an alternative to produce packaging with low potential risk to consumer health, which contributes to the quality of the food product and does not harm the environment.

17.6 Conclusion and Future Trends

Bioactive compounds are promising for the food industry because they have antioxidant, anti-inflammatory, antimicrobial, and nutraceutical properties. However, the efficiency of the compounds is affected by external factors such as light, temperature, oxygen, conditions in the gastrointestinal tract such as enzymes, and pH. Direct addition of the compounds into foods is limited because it can alter the sensory product characteristics. Therefore, nanoencapsulation methods increase the stability, bioavailability, and bioactivity of bioactive compounds during food packaging. Nanofibers produced by electrospinning have a relevant role in food packaging and the encapsulation function of the compounds. The incorporation of bioactive compounds into nanofibers allows to increase the nutritional value of products, ensure consumer safety and avoid microbiological contamination. These nanostructures also can protect bioactive from early degradation and promote the controlled release of the compounds from the package into the food. Thus, the improvement of food packaging through nanofibers with bioactive compounds is a promising alternative to maintain the quality and freshness of products.

Acknowledgements The authors would like to thank the Coordenação de Aperfeiçoamento de Pessoal de Nível Superior – Brazil – (CAPES) Finance Code 001, CNPq (National Council of Technological and Scientific Development), MCTIC (Ministry of Science Technology, Innovation and Communication), FAPERGS (Fundação de Amparo à Pesquisa do Estado do Rio Grande do Sul), and Project CAPES-PRint FURG for their support of this study.

References

1. Agarwal, S., Greiner, A., & Wendorff, J. H. (2013). Functional materials by electrospinning of polymers. *Progress in Polymer Science, 38*, 963–991.
2. Aguirre-Joya, J. A., Zapata, M. A. L., Alvarez-Perez, O. B., Torres-Leon, C., Nieto Oropeza, D. E., Ventura-Sobrevilla, J. M., Aguillar, M. A., Ruelas-Chacón, X., Rojas, R., Ramoa-Aguiaga, M. E. R, & Aguillar, C. N. (2018). Basic and applied concepts of edible packaging for foods. In A. M. Grumezescu, & A. M. Holban (Eds.), *Food packaging and preservation handbook of food bioengineering* (Vol. 9, pp. 1–61). Academic Press.
3. Ahmed, I., Lin, H., Zou, L., Brody, A. L., Qase, I., Payase, T. R., & Liangtao, L. V. (2017). A comprehensive review on the application of active packaging technologies to muscle foods. *Food Control, 82*, 163–178.
4. Akbari-Alavijeh, S., Shaddel, R., & Jafari, M. S. (2020). Encapsulation of food bioactives and nutraceuticals by various chitosan-based nanocarriers. *Food Hydrocolloids*, *105*, 105774.
5. Aydogdu, A., Sumnu, G., & Sahin, S. (2019). Fabrication of gallic acid loaded hydroxypropyl methylcellulose nanofibers by electrospinning technique as active packaging material. *Carbohydrate Polymers, 208*, 241–250.
6. Bajpai, V. K., Kamle, M., Shukla, S., Mahato, D. K., Chandra, P., Hwang, S. K., Kurnar, P., Huh, Y. S., & Han, Y. K. (2018). Prospects of using nanotechnology for food preservation, safety, and security. *Journal of Food and Drug Analysis, 26*, 1201–1214.
7. Baptista-Silva, S., Borges, S., Ramos, O. L., Pintado, M., & Sarmento, B. (2020). The progress of essential oils as potential therapeutic agents: A review. *Journal of Essential Oil Research, 32*, 279–295.
8. Bazana, M. T., Codevilla, C. F., & Menezes, C. R. (2019). Nanoencapsulation of bioactive compounds, challenges and perspectives. *Current Opinion In Food Science, 26*, 2214–7993.
9. Bhardwaj, N., & Kundu, S. C. (2010). Electrospinning, a fascinating fiber fabrication technique. *Biotechnology Advances, 28*, 325–347.
10. Bhushani, J. A., & Anandharamakrishnan, C. (2014). Electrospinning and electrospraying techniques, potential food based applications. *Trends in Food Science and Technology, 38*, 21–33.
11. Bradley, E. L., Castle, L., & Chaudhry, Q. (2011). Applications of nanomaterials in food packaging with a consideration of opportunities for developing countries. *Trends in Food Science and Technology, 22*, 604–610.
12. Braga, A. R. C., Figueira, F. D. S., Silveira, J. T. D., Morais, M. G., Costa, J. A. V., & Kalil, S. J. (2016). Improvement of thermal stability of C-phycocyanin by nanofiber and preservative agents. *Journal of Food Processing and Preservation, 40*, 1264–1269.
13. Brody, A. (2006). Nano and food packaging technologies converge. *Food Technology, 60*, 92–94.
14. Bruni, G. P., Oliveira, J. P., Gómez-Mascaraque, L. G., Fabra, M. J., Martins, V. G., Zavareze, E. R., & López-Rúbio, A. (2020). Electrospun β-carotene–loaded SPI: PVA fiber mats produced by emulsion electrospinning as bioactive coatings for food packaging. *Food Packaging and Shelf Life*, *23*, 100426.
15. Bueno, J. M., Sáez-Plaza, P., Ramos-Escudero, F., Jiménez, A. M., Fett, R., & Asuero, A. G. (2012). Analysis and antioxidant capacity of anthocyanin pigments. Part II: Chemical

structure, color, and intake of anthocyanins. *Critical Reviews in Analytical Chemistry, 42*, 126–215.
16. Castañeda-Ovando, A., Pacheco-Hernández, M. L., Páez-Hernández, M. E., Rodríguez, J. A., & Galán-Vidal, C. A. (2009). Chemical studies of anthocyanins: A review. *Food Chemistry, 113*, 859–871.
17. Chen, L., Gnanaraj, C., Arulselvan, P., El-Seedi, H., & Teng, H. (2019). A review on advanced microencapsulation technology to enhance bioavailability of phenolic compounds, based on its activity in the treatment of Type 2 Diabetes. *Trends in Food Science and Technology, 85*, 149–162.
18. Deitzel, J., Kleinmeyer, J., Harris, D., & Tan, N. B. (2001). The effect of processing variables on the morphology of electrospun nanofibers and textiles. *Polymer, 42*, 261–272.
19. Duan, M., Yu, S., Sun, J., Jiang, H., Zhao, J., Tong, C., Pang, J., & Wu, C. (2021). Development and characterization of electrospun nanofibers based on pullulan/chitin nanofibers containing curcumin and anthocyanins for active-intelligent food packaging. *International Journal of Biological Macromolecules, 187*, 240–332.
20. Duran, N., & Marcato, P. D. (2013). Nanobiotechnology perspectives. Role of nanotechnology in the food industry: A review. *International Journal of Food Science & Technology, 48*, 1127–1134.
21. Enescu, D., Cerqueira, M. A., Fucinos, P., & Pastrana, L. M. (2019). Recent advances and challenges on applications of nanotechnology in food packaging. A literature review. *Food and Chemical Toxicology*, *134*, 110814.
22. Eriksen, N. T. (2008). Production of phycocyanin—A pigment with applications in biology, biotechnology, foods and medicine. *Applied Microbiology and Biotechnology, 80*, 1–14.
23. Esfanjani, A. F., & Jafari, S. M. (2016). Biopolymer nano-particles and natural nano-carriers for nano-encapsulation of phenolic compounds. *Colloids and Surfaces B, 146*, 532–543.
24. Fang, Z., & Bhandari, B. (2010). Encapsulation of polyphenols—A review. *Trends in Food Science and Technology, 21*, 510–523.
25. Fernández-Rojas, B., Hernández-Juárez, J., & Pedraza-Chaverri, J. (2014). Nutraceutical properties of phycocyanin. *Journal of Functional Foods, 11*, 375–392.
26. Firouz, M. S., Mohi-Alden, K., & Omid, M. (2019). A critical review on intelligent and active packaging in the food industry: Research and development. *Food Research International, 141*, 110113.
27. Fonseca, L. M., Cruxen, C. E. S., Bruni, G. P., Fiorentini, A. M., Zavareze, E. R., Lim, L. T., & Dias, A. R. G. (2019). Development of antimicrobial and antioxidant electrospun soluble potato starch nanofibers loaded with carvacrol. *International Journal of Biological Macromolecules, 139*, 1182–1190.
28. Fratelli, C., Burck, M., Amarante, M. C. A., & Braga, A. R. C. (2021). Antioxidant potential of nature's "something blue", Something new in the marriage of biological activity and extraction methods applied to C-phycocyanin. *Trends in Food Science and Technology, 107*, 309–323.
29. Ghorani, B., & Tucker, N. (2015). Fundamentals of electrospinning as a novel delivery vehicle for bioactive compounds in food nanotechnology. *Food Hydrocolloids, 51*, 227–240.
30. Ghosh, T., Nakano, K., & Katiyar, V. (2021). Curcumin doped functionalized cellulose nanofibers based edible chitosan coating on kiwi fruits. *International Journal of Biological Macromolecules, 184*, 936–945.
31. He, J., & Giusti, M. M. (2010). Anthocyanins, natural colorants with health-promoting properties. *Annual Review of Food Science and Technology, 1*, 163–187.
32. He, X., & Hwang, H. M. (2016). Nanotechnology in food science, functionality, applicability, and safety assessment. *Journal of Food and Drug Analysis, 24*, 671–681.
33. Hemmati, F., Bahrami, A., Esfanjani, A. F., Hosseini, H., McClements, D. J., & Williams, L. (2021). Electrospun antimicrobial materials, advanced packaging materials for food applications. *Trends in Food Science and Technology, 111*, 520–533.
34. Jafari, S. M., Jabari, S. S., Dehnad, D., & Shahidi, S. A. (2017). Effects of thermal processing by nanofluids on vitamin C, total phenolics and total soluble solids of tomato juice. *Journal of Food Science and Technology, 54*, 679–686.

35. Jain, A., Ranjan, S., Dasgupta, N., & Ramalingam, C. (2018). Nanomaterials in food and agriculture, an overview on their safety concerns and regulatory issues. *Critical Reviews in Food Science and Nutrition, 58*, 297–317.
36. Javaherzadeh, R., Bafroee, A. T., & Kanjari, A. (2020). Preservation effect of Polylophium involucratum essential oil incorporated poly lactic acid/nanochitosan composite film on shelf life and sensory properties of chicken fillets at refrigeration temperature. *LWT*, *118*, 108783.
37. Jeevahan, J., & Chandrasekaran, M. (2019). Nanoedible films for food packaging: A review. *Journal of Materials Science, 54*, 12290–12318.
38. Jeevahan, J. J., Chandrasekaran, M., Venkatesan, S. P., Sriram, V., Joseph, G. B., Magessharan, G., & Durairaj, R. B. (2020). Scaling up difficulties and commercial aspects of edible films for food packaging: A review. *Trends in Food Science & Technology, 100*, 210–222.
39. Kalpana, S., Priyadarshini, S. R., Leena, M. M., Moses, J. A., & Anandharamakrishnan, C. (2019). Intelligent packaging: Trends and applications in food systems. *Trends in Food Science and Technology, 93*, 145–157.
40. Kathiravan, A., Chandramohan, M., Renganathan, R., & Sekar, S. (2009). Spectroscopic studies on the interaction between phycocyanin and bovine serum albumin. *Journal of Molecular Structure, 919*, 210–214.
41. Kuddus, M., Singh, P., Thomas, G., & Al-Hazimi, A. (2013). Recent developments in production and biotechnological applications of C-phycocyanin. *BioMed Research International, 2013*, 1–9.
42. Kuntzler, S. G., Almeida, A. C. A., Costa, J. A. V., & Morais, M. G. (2018). Polyhydroxybutyrate and phenolic compounds microalgae electrospun nanofibers: A novel nanomaterial with antibacterial activity. *International Journal of Biological Macromolecules, 113*, 1008–1014.
43. Kuntzler, S. G., Costa, J. A. V., Brizio, A. P. D. R., & Morais, M. G. (2020). Development of a colorimetric pH indicator using nanofibers containing *Spirulina* sp. LEB 18. *Food Chemistry*, *328*, 126768.
44. Kuntzler, S. G., Costa, J. A. V., & Morais, M. G. (2018). Development of electrospun nanofibers containing chitosan/PEO blend and phenolic compounds with antibacterial activity. *International Journal of Biological Macromolecules, 117*, 800–806.
45. Kuntzler, S. G., Uebel, L. S., Schmatz, D. A., Barcia, M. T., Costa, J. A. V., & Morais, M. G. (2018). Nanofibers and their applications. In H. S. Nalwa (Ed.), *Encyclopedia of nanoscience and nanotechnology* (pp. 387–414). American Scientifc Publishers.
46. Kuswandi, B., & Jumina. (2020). Active and intelligent packaging, safety, and quality controls. In: M. W. Siddiqui (Ed.), *Fresh-cut fruits and vegetables technologies and mechanisms for safety control* (1st ed., pp. 243–294). Academic Press.
47. Leidy, R., & Ximena, Q. C. M. (2019). Use of electrospinning technique to produce nanofibres for food industries, a perspective from regulations to characterisations. *Trends in Food Science and Technology, 85*, 92–106.
48. Lin, L., Gu, Y., & Cui, H. (2019). Moringa oil/chitosan nanoparticles embedded gelatin nanofibers for food packaging against Listeria monocytogenes and Staphylococcus aureus on cheese. *Food Packaging and Shelf Life, 19*, 86–93.
49. Liu, B., Xu, H., Zhao, H., Liu, W., Zhao, L., & Li, Y. (2017). Preparation and characterization of intelligent starch/PVA films for simultaneous colorimetric indication and antimicrobial activity for food packaging applications. *Carbohydrate Polymers, 157*, 842–849.
50. Liu, Y., Wang, D., Sun, Z., Liu, F., Du, L., & Wang, D. (2021). Preparation and characterization of gelatin/chitosan/3-phenylacetic acid food-packaging nanofiber antibacterial films by electrospinning. *International Journal of Biological Macromolecules, 169*, 161–170.
51. López-Rúbio, A. (2011). Bioactive food packaging strategies. In J. M. Lagarón (Ed.), *Multifunctional and nanoreinforced polymers for food packaging* (pp. 460–482). Woodhead.
52. López-Rúbio, A., Gavara, R., & Lagaron, J. M. (2006). Bioactive packaging, turning foods into healthier foods through biomaterials. *Trends in Food Science and Technology, 17*, 567–575.
53. Luo, C. J., Stoyanov, S. D., Stride, E., Pelan, E., & Edirisinghe, M. (2012). Electrospinning versus fibre production methods, from specifics to technological convergence. *Chemical Society Reviews, 41*, 4708–4735.

54. Macagnano, A., Zampetti, E., & Kny, E. (Eds.). (2015). *Electrospinning for high performance sensors.* Springer Nature.
55. Manirafasha, E., Ndikubwimana, T., Zeng, X., Lu, Y., & Jing, K. (2016). Phycobiliprotein, potential microalgae derived pharmaceutical and biological reagent. *Biochemical Engineering Journal, 109*, 282–296.
56. Martelli, G., Folli, C., Visai, L., Daglia, M., & Ferrari, D. (2014). Thermal stability improvement of blue colorant C-Phycocyanin from Spirulina platensis for food industry applications. *Process Biochemistry, 49*, 154–159.
57. Mishra, S. K., Shrivastav, A., Pancha, I., Jain, D., & Mishra, S. (2010). Effect of preservatives for food grade C-Phycoerythrin, isolated from marine cyanobacteria *Pseudanabaena* sp. *International Journal of Biological Macromolecules, 47*, 597–602.
58. Mohammadi, M. A., Hosseini, S. M., & Yousefi, M. (2020). Application of electrospinning technique in development of intelligent food packaging, a short review of recent trends. *Food Science & Nutrition, 8*, 4656–4665.
59. Morais, M. G., Fontoura, P. D., Moreira, J. B., Duarte, J. H., & Costa, J. A. V. (2018). Phycocyanin from microalgae, properties, extraction and purification, with some recent applications. *Industrial Biotechnology, 14*, 30–37.
60. Moreira, J. B., Kuntzler, S. G., Terra, A. L. M., & Costa, J. A. V. (2020). Electrospun nanofibers. In S. M. Rangappa, P. Jyotishkumar, S. M. K. Thiagamani, S. Krishnasamy, & S. Siengchin (Eds.), *Food packaging* (pp. 223–254). CRC Press.
61. Moreira, J. B., Lim, L. T., Zavareze, E. R., Dias, A. R. G., Costa, J. A. V., & Morais, M. G. (2019). Antioxidant ultrafine fibers developed with microalga compounds using a free surface electrospinning. *Food Hydrocolloids, 93*, 131–136.
62. Niu, B., Shao, P., Luo, Y., & Sun, P. (2020). Recent advances of electrosprayed particles as encapsulation systems of bioactives for food application. *Food Hydrocolloids*, *99*, 105376.
63. Niu, B., Zhan, L., Shao, P., Xiang, N., Sun, P., Chen, H., & Gao, H. (2020). Electrospinning of zein-ethyl cellulose hybrid nanofibers with improved water resistance for food preservation. *International Journal of Biological Macromolecules, 142*, 592–599.
64. Ogbonda, K. H., Aminigo, R. E., & Abu, G. O. (2007). Influence of temperature and pH on biomass production and protein biosynthesis in a putative *Spirulina* sp. *Bioresource Technology, 98*, 2207–2211.
65. Paini, M., Aliakbarian, B., Casazza, A. A., Lagazzo, A., Botter, R., & Perego, P. (2015). Microencapsulation of phenolic compounds from olive pomace using spray drying: A study of operative parameters. *LWT, 62*, 177–186.
66. Petkoska, A. T., Daniloski, D., D'Cunha, N., Naumoyski, N., & Broach, A. T. (2021). Edible packaging, sustainable solutions and novel trends in food packaging. *Food Research International*, *140*, 109981.
67. Qin, Y., Yun, D., Xu, F., Chen, D., Kan, J., & Liu, J. (2021). Smart packaging films based on starch/polyvinyl alcohol and *Lycium ruthenicum* anthocyanins-loaded nano-complexes, Functionality, stability and application. *Food Hydrocolloids*, *119*, 106850.
68. Rauscher, H., Rasmussen, K., & Sokull-Klüttgen, B. (2017). Regulatory aspects of nanomaterials in the EU. *Chemie Ingenieur Technik, 89*, 224–231.
69. Regnault-Roger, C., Vincent, C., & Arnason, J. T. (2012). Essential oils in insect control, low-risk products in a high-stakes world. *Annual Review of Entomology, 57*, 405–424.
70. Romay, C. H., Gonzalez, R., Ledon, N., Remirez, D., & Rimbau, V. (2003). C-phycocyanin, a biliprotein with antioxidant, anti-inflammatory and neuroprotective effects. *Current Protein & Peptide Science, 4*, 207–216.
71. Rostamabadi, H., Falsafi, S. R., Boostani, S., Katouzian, I., Rezaei, A., Assadpour, E., & Jafari, S. M. (2020). Design and formulation of nano/micro-encapsulated natural bioactive compounds for food applications. In S. M. Jafari (Ed.), *Application of nano/microencapsulated ingredients in food products* (Vol. 6, pp. 1–41). Academic Press.
72. Roy, S., & Rhim, J. W. (2021). Anthocyanin food colorant and its application in pH-responsive color change indicator films. *Critical Reviews in Food Science and Nutrition, 61*, 2297–2325.

73. Salgado, P. R., Di Giorgio, L., Musso, Y. M., & Mauri, A. N. (2019). Bioactive packaging, combining nanotechnologies with packaging for improved food functionality. In A. López-Rúbio, J. M. F. Rovira, M. M. Sanz, & L. G. Gómez-Mascaraque (Eds.), *Nanomaterials for food applications* (1st ed., pp. 233–270). Elsevier.
74. Savolainen, K., Pylkkänen, L., Norppa, H., Falck, G., Lindberg, H., Tuomi, T., Vippola, M., Alenius, H., Hameri, K., Koivisto, J., Brouwer, D., Mark, D., Bard, D., Berges, M., Jankowska, E., Posniak, M., Farmer, P., Singh, R., & Seipenbusch, M. (2010). Nanotechnologies, engineered nanomaterials and occupational health and safety—A review. *Safety Science, 48*, 957–963.
75. Schmatz, D. A., Uebel, L. S., Kuntzler, S. G., Dora, C. L., Costa, J. A. V., & Morais, M. G. (2016). Scaffolds containing *Spirulina* sp. LEB 18 biomass, development, characterization and cvaluation of in vitro biodegradation. *Journal of Nanoscience and Nanotechnology, 15*, 4708–4735.
76. Sharif, N., Khoshnoudi-Nia, S., & Mahdi, S. (2020). Nano/microencapsulation of anthocyanins; A systematic review and meta-analysis. *International Food Research Journal*, *132*, 109077.
77. Silva, C. K., Mastrantonio, D. J. S., Costa, J. A. V., & Morais, M. G. (2019). Innovative pH sensors developed from ultrafine fibers containing acai (*Euterpe oleracea*) extract. *Food Chemistry, 294*, 397–404.
78. Silvestre, C., & Cimmino, S. (2013). *Ecosustainable polymer nanomaterials for food packaging, innovative solutions, characterization needs, safety and environmental issues*. CRC Press.
79. Singh, T., Shukla, S., Kumar, P., Wahla, V., Bajpai, V. K., & Rather, I. A. (2017). Application of nanotechnology in food science, perception and overview. *Frontiers in Microbiology, 8*, 1501.
80. Sinopoli, A., Calogero, G., & Bartolotta, A. (2019). Computational aspects of anthocyanidins and anthocyanins: A review. *Food Chemistry*, *297*, 124898.
81. Smaoui, S., Hlima, H. B., Braiek, O. B., Ennouri, K., Mellouli, L., & Khaneghah, A. M. (2021). Recent advancements in encapsulation of bioactive compounds as a promising technique for meat preservation. *Meat Science*, *181*, 108585.
82. Subash, S., Essa, M. M., Al-Adawi, S., Memon, M. A., Manivasagam, T., & Akbar, M. (2014). Neuroprotective effects of berry fruits on neurodegenerative diseases. *Neural Regeneration Research, 9*, 1557–1566.
83. Surendhiran, D., Li, C., Cui, H., & Lin, L. (2020). Fabrication of high stability active nanofibers encapsulated with pomegranate peel extract using chitosan/PEO for meat preservation. *Food Packaging and Shelf Life*, *23*, 100439.
84. Tarone, A. G., Cazarin, C. B. B., & Junior, M. R. M. (2020). Anthocyanins: New techniques and challenges in microencapsulation. *Food Research International*, *133*, 109092.
85. Terra, A. L. M., Moreira, J. B., Costa, J. A. V., & Morais, M. G. (2021). Development of time-pH indicator nanofibers from natural pigments: An emerging processing technology to monitor the quality of foods. *LWT*, *142*, 111020.
86. Thormar, H. (2011). *Lipids and essential oils as antimicrobial agents*. Wileys.
87. Tian, J., Deng, H., Liu, R., Yi, Y., & Dong, X. (2019). Nanofibers for food and food packaging technology. In B. Ding, X. Wang, & J. Yu (Eds.), *Electrospinning, nanofabrication and applications* (1st ed., pp. 455–516). Elsevier.
88. Topuz, F., & Uyar, T. (2020). Antioxidant, antibacterial and antifungal electrospun nanofibers for food packaging applications. *Food Research International*, *130*, 108927.
89. Uebel, L. S., Schmatz, D. A., Kuntzler, S. G., Dora, C. L., Muccillo-Baisch, A. L., Costa, J. A. V., & Morais, M. G. (2016). Quercetin and curcumin in nanofibers of polycaprolactone and poly(hydroxybutyrate-co-hydroxyvalerate): Assessment of in vitro antioxidant activity. *Journal of Applied Polymer Science, 133*, 1–7.
90. Valls, J., Millán, S., Martí, M. P., Borràs, E., & Arola, L. (2009). Advanced separation methods of food anthocyanins, isoflavones and flavanols. *Journal of Chromatography A, 1216*, 7143–7172.

91. Vergis, J., Gokulakrishnan, P., Agarwal, R. K., & Kumar, A. (2013). Essential oils as natural food antimicrobial agents: A review. *Critical Reviews in Food Science and Nutrition, 55*, 1320–1323.
92. Vonshak, A. (1997). Spirulina platensis *(Arthrospira): Physiology, cell-biology and biotechnology*. Taylor & Francis Group, CRC Press.
93. Wang, S., Xia, P., Wang, S., Liang, J., Sun, Y., Yue, P., & Gao, X. (2019). Packaging films formulated with gelatin and anthocyanins nanocomplexes: Physical properties, antioxidant activity and its application for olive oil protection. *Food Hydrocolloids, 96*, 617–624.
94. Wang, W., Sun, C., Mao, L., Ma, P., Liu, F., & Yang, Y. (2016). The biological activities, chemical stability, metabolism and delivery systems of quercetin: A review. *Trends in Food Science and Technology, 56*, 21–38.
95. Wen, P., Zhu, D. H., Wu, H., Zong, M. H., Jing, Y. R., & Han, S. Y. (2016). Encapsulation of cinnamon essential oil in electrospun nanofibrous film for active food packaging. *Food Control, 59*, 366–376.
96. Wen, P., Zong, M. H., Linhardt, R. J., Feng, K., & Wu, H. (2017). Electrospinning, A novel nano-encapsulation approach for bioactive compounds. *Trends in Food Science and Technology, 70*, 56–58.
97. Wen, Y., Wen, P., Hu, T. G., Linhardt, R. J., Zong, M. H., Wu, H., & Chen, Z. Y. (2020). Encapsulation of phycocyanin by prebiotics and polysaccharides-based electrospun fibers and improved colon cancer prevention effects. *International Journal of Biological Macromolecules, 149*, 672–681.
98. Xie, Y., Jin, Y., Zeng, X., Chen, J., Lu, Y., & Jing, K. (2015). Fed-batch strategy for enhancing cell growth and C-phycocyanin production of *Arthrospira (Spirulina) platensis* under phototrophic cultivation. *Bioresource Technology, 180*, 281–287.
99. Xue, J., Wu, T., Dai, Y., & Xia, Y. (2019). Electrospinning and electrospun nanofibers, methods, materials, and applications. *Chemical Reviews, 119*, 5298–5415.
100. Yarin, A., Koombhongse, S., & Reneker, D. (2001). Bending instability in electrospinning of nanofibers. *Journal of Applied Physics, 89*, 3018–3026.
101. Zhang, T., Gu, J., Liu, X., Wei, D., Zhou, H., Xiao, H., Zhang, Z., Yu, H., & Chen, S. (2020). Bactericidal and antifouling electrospun PVA nanofibers modified with a quaternary ammonium salt and zwitterionic sulfopropylbetaine. *Materials Science and Engineering C*, *111*, 110855.
102. Zhang, T., Qiu, F., Chen, L., Liu, R., Chang, M., & Wang, X. (2021). Identification and in vitro anti-inflammatory activity of different forms of phenolic compounds in *Camellia oleifera* oil. *Food Chemistry*, *344*, 128660.



Michele Greque de Morais is a Food Engineer, Master, and Ph.D. in Food Science and Engineering from the Federal University of Rio Grande. She developed part of her thesis on the development of nanofibers at Philipps-Universität Marburg, Germany. She did post-doctoral studies at Scripps Institution of Oceanography (SIO) at the University of California—San Diego (UCSD). Currently, she is a professor at the Federal University of Rio Grande teaching the disciplines of microbiology and nanobiotechnology in the course of Biochemical Engineering. She is the Coordinator of the Graduate Program in Food Science and Engineering (2021–2022) and a permanent faculty member, where she teaches Food Microbiology and Nanofiber Engineering. She has published articles in specialized journals, patented processes and products, book chapters, and papers in annals of events in the topics nanobiotechnology, microalgae,

and bioproducts extracted from biomass. She works in Food Science with an emphasis on Food Engineering/Biotechnology.



Suelen Goettems Kuntzler is a Biochemical Engineer, Master, and Ph.D. in Food Science and Engineering from the Federal University of Rio Grande. She works on the use of bio compounds from microalgae biomass and nanobiotechnology applied in the development of active and intelligent packaging. She also works in the field of biotechnology through studies on the biofixation of CO_2 by microalgae. Currently, she is post-doctor in Politech at the Université Clermont Auvergne.



Ana Claudia Araujo de Almeida is a Biochemical Engineer who graduated from the Federal University of Rio Grande. She is currently a Master's student in the Graduate Program in Food Science and Engineering at the same university. She works in the areas of nanotechnology and microalgal biotechnology.



Ana Gabrielle Pires Alvarenga is a Food Engineer at the Federal University of São João del Rei. She is currently a Master's student in Food Science and Engineering at the Federal University of Rio Grande. She has experience in new product development, nanobiotechnology, microalgae, and biopolymers.



Jorge Alberto Vieira Costa is a Food Engineer from the Federal University of Rio Grande and a Ph.D. in Food Engineering from the State University of Campinas. He did postdoctoral studies at the Scripps Institution of Oceanography (SIO) at the University of California—San Diego (UCSD). He is currently a Full Professor at the Federal University of Rio Grande, in the Biochemical Engineering course and in the Graduate Program in Food Science and Engineering. He is also an advisor in the Graduate Program in Bioprocess Engineering and Biotechnology at the Federal University of Paraná. He is a 1B research productivity fellow. He has published articles in specialized journals, patented processes and products, book chapters and articles in the annals of events on the topics of microalgal biotechnology, food and bioproduct development from microalgae biomass and açaí fruit. He works in the area of Food Science with an emphasis on Food Engineering/Biotechnology.

Chapter 18
Application of Electrospun Polyaniline (PANI) Based Composites Nanofibers for Sensing and Detection

Nayana D. Sonwane, Sanchit S. Kondawar, Pitambar V. Gayakwad, and Subhash B. Kondawar

Abstract In recent times there is continuous increasing demand for highly sensitive sensors in various fields such as food quality inspection, medical treatment, environmental cleanliness, domestic purposes, etc. Overall to make our life safer and more effortless highly efficient sensors in terms of cost and time are needed. Therefore, it is necessary to develop a gas sensor that can detect gas quickly in real-time. Electrospun nanofibers are found to be potential candidates for nanosensors to improve the sensing phenomenon. The high surface area to volume ratio of electrospun nanofibers leads to an increase in chances of interaction between analyte and sensor. In this chapter, the application of electrospun nanofibers comprising semiconductor metal oxides, conducting polymer (polyaniline, PANI), and their composites for the detection of various toxic and harmful gases will be described. Reliability of composites towards chemiresistive gas sensors using sensing parameters and their mechanism of sensing are also discussed.

Keywords Electrospinning · Nanofibers · Polyaniline · Composites · Metal oxides · Sensor

18.1 Introduction

In the last few decades, gas sensors play a very important role for the safety of human beings. The need for gas sensors has been successively increased in different areas like air quality control [1, 2], agriculture [3], and medical diagnostics [4, 5].

N. D. Sonwane
Department of Physics, Rashtrasant Tukadoji Maharaj Nagpur University, Nagpur, India

S. S. Kondawar
Government College of Engineering, Jalgaon, India

P. V. Gayakwad
Department of Mathematics, Arvindbabu Deshmukh Mahavidyalaya, Bharsingi, Nagpur, India

S. B. Kondawar (✉)
Department of Physics, Rashtrasant Tukadoji Maharaj Nagpur University, Nagpur, India
e-mail: sbkondawar@yahoo.co.in

© The Author(s), under exclusive license to Springer Nature Switzerland AG 2022

A. Vaseashta and N. Bölgen (eds.), *Electrospun Nanofibers*,
https://doi.org/10.1007/978-3-030-99958-2_18

According to the World Health Organisation report (WHO) in 2019, around 90% of the population lives in an environment where the air is unhealthy to breathe [6]. Now it is widely accepted that exposure to harmful air pollutants leads to severe health effects such as respiratory and cardiovascular diseases which can cause physiological impacts or death [7, 8]. Furthermore, the study of the Global Burden of Diseases, Injuries, and Risk Factors (GBD) 2015 recognizes air pollution as a leading cause of global disease burden mostly in low-income and middle-income countries [9]. Therefore, the sensing and detection of toxic and hazardous gases is a major need for human and environmental protection, which creates the field of interest for making a variety of sensing materials [10, 11].

To develop a high-performance gas sensor lots of research has been done on the fabrication of sensing materials [12, 13]. Out of which metal oxide semiconductor-based sensing materials are widely used for the detection of more than 150 hazardous gases due to their suitable electrochemical properties and powerful interface [14–18]. Nowadays, chemiresistors and field-effect transistors (FET) are the two commonly used configurations of metal oxide semiconductor-based sensor devices [19]. These sensors can also be integrated in other sensor types such as optical sensors, quartz crystal microbalance sensors (QCM), surface acoustic sensors [20–23]. Among all types of sensors, chemiresistor type sensor is widely used for sensing and detection purposes due to their efficient properties like simple fabrication and direct measurement. Sensing phenomenon in chemiresistor sensor detected by the change in resistance due to physical and chemical adsorption/desorption process on the sample surface after exposing the gas [21, 23].

In metal oxide semiconductor-based sensors, sensing performance is totally influenced by the morphology and operating temperature of the sample [3, 24]. Hence different morphologies of the semiconductive metal oxides have been reported for making sensing materials [1, 25–27]. The sensitivity of the sample towards any target gas directly link to the number of available active sites and the interaction between sample and gas species thereby increasing adsorption/desorption rates [26]. The above-stated properties are achieved by nanomaterials for improved gas sensing characteristics due to its large surface to volume ratio and enough number of reaction sites on the surface which promotes the increase in adsorption rates of gas species. Hence different nanostructure materials are appearing as the promising candidate to enhance gas sensing properties [28].

Several nanostructure materials such as nanoparticles (0D) nanotubes (1D), nanofilms (2D), nanocrystals (0D), nanorods (1D), nanoflakes (2D), nanofibers (1D), etc. have been reported for gas sensing applications. In recent years, one-dimensional (1D) metal oxide nanostructures have growing attention due to their high aspect ratio (length to diameter ratio), unique physical and chemical characteristics that enable them to conduct the electric signal in one dimension [29–31]. Among one dimensional nanostructure, nanofibers are long polymeric filaments, which exhibit the ideal advantages in high porosity, high surface area, high encapsulation efficiency, controllable morphology, high chemical, and thermal stability. The properties of nanofibers could significantly influence the polymeric raw material resulting in efficient adsorption and better reaction kinetics of gas-sensitive materials. There are

many techniques available for the fabrication of nanofibers such as drawing, electrospinning, self-assembly, polymerization, plasma-induced, sonochemical, electrohydrodynamic, and template-based synthesis. Among different techniques of making one-dimensional nanofibers, the electrospinning technique is widely used because of low cost and the ability to produce porous nanofibers of different kinds of nanocrystalline metal oxides [32, 33]. Such porous nanofibers through electrospinning technique are produced with very small diameters (D ≤ Debye length) [34] which enhance the adsorption/desorption process and hence greater chance of increasing sensitivity. Electrospun nanofibers with a remarkable specific surface area which is approximately twice that of the thin films and porosity around 70–90% due to large and small pores on the surface make them an attractive candidate for designing ultrasensitive sensors [21, 22, 35]. Moreover, metal oxide semiconductor-based nanofibers can be fabricated in various assemblies such as mixed nanocomposites, core–shell/hollow, and double layers by electrospinning technique [21, 36, 37].

Along with the wide application and numerous advantages of the metal oxide semiconductor nanofiber-based sensor for the detection of toxic gases, it has certain limitations such as lack of flexibility, selectivity in addition to the operation at high temperature (≥200 °C) [38–42]. Lack of selectivity is considered as a major drawback of metal oxide semiconductor nanofiber-based gas sensor which typically denotes the ability of the gas sensor to detect the existence of a specific analyte in the environment where other gases coexist. On the other hand, such types of sensors that operate at high temperatures have high power consumption, safety issues, and restricted lifetimes [43]. Furthermore, the fundamental strategy to fabricate the sensitive, selective, and cost-effective gas sensor which can operate at room temperature is the addition of different new functionalities to them. The different methods include doping or surface decoration with noble metals, forming a composite of distinct nanomaterials, and the addition of conducting polymers to form heterojunction structures [29]. Among them, the strategy to combine conducting polymer with metal oxides can help to overcome the limitations of metal oxide semiconductor-based gas sensors and to enhance the sensor performance in the resulting metal oxide/conducting polymer composites [43]. Conducting polymers possess great potential for building next-generation sensing devices. The organic conducting polymers, for example, polypyrrole (PPy), poly (3, 4-ethylenedioxythiophene) (PEDOT), polyaniline (PANI), polyacetylene (PA), and their derivatives have been widely used for the gas sensing purpose. These polymers could detect gas species with high sensitivity, fast response, and complete recovery at room temperature. Furthermore, mechanical flexibility, lightweight, and tunable chemical/electrical properties are the key feature of the conducting polymers [43, 44]. Recently nanostructured conducting polymers have paid great attention in the field of gas sensing due to their multidimensional architectures, high surface areas, and the property of easy functionalization with different functional groups which leads to excellent sensing of trace amount of target gases [45]. However, the conducting polymer-based sensor faces certain problems along with problems regarding long-term stability which needs improvement. Hence in the field of gas sensing the synergistic effect of metal oxide and conducting polymers have been extensively studied [46].

In this chapter, an overview of the use of electrospinning technique for fabrication of metal oxide semiconductor-based nanofibers and conducting polymer polyaniline (PANI) based composite nanofibers are reported. The chapter aims to show the advantages of porous morphology of metal oxide nanofibers and how it can enhance the sensing properties for the detection of a variety of gas species. Furthermore, how the innovative composite materials by using conducting polymers can enhance the sensing mechanism is explored. Composite-based structures and synergistic property enhancement are also highlighted to understand the sensing mechanism.

18.2 Electrospun Nanofibers Fabrication

Different methods are available for the fabrication of nanofibers such as self-assembly, hydrothermal, and template synthesis. There are several spinning methods available including solution blow spinning, draw spinning, centrifugal spinning, and electrospinning [47]. Among all techniques, electrospinning is a simple, low-cost, and robust technique for generating nanofibers [48, 49]. William Gilbert in 1600 described the electrostatic effect which laid the foundation for the electrospinning technique. From the series of experiments, he noticed that for a strong charge, water droplets attain a conical shape and small droplets would evolve from it [29]. In 1887 electrospinning was given as a synthesis method for one-dimensional fibers by Boys [50] and later various theories have been reported. Nowadays electrospinning is considered as a convenient method for the synthesis of nanofibers of single and composite materials. It has been applied to ceramics, metal oxides, natural and synthetic polymers, and carbon-based materials. A typical electrospinning setup consists of the metallic needle, plastic syringe with electrospinning solution, a syringe pump to control the feeding rate, high voltage power supply, and grounded conducting collector.

Figure 18.1 represents a schematic diagram of electrospinning set up and shows the physical (distance, voltage, flow rate, and collector), chemical (concentration, conductivity, molecular weight, viscosity, solvent volatility, and molecular structure), and environmental (humidity and temperature) parameters on which the diameter of the fibers depends. The electrospinning method can produce different types of nanofiber structures such as core–shell, ribbon-shaped, and hollow types [51]. However, electrospinning gained attention for 1-D nanofiber synthesis due to its capability of mass production, and ability to produce nanofibers having controlled diameters [29]. By continuous research, various electrospinning setups have been reported to meet the requirement of specific areas by allowing the customization of assemblies and other modifications in the electrospinning setup [52].

When a metallic needle is attached to a syringe it acts as an electrode whereas the collector connected with applied voltage acts as the counter electrode. In the typical electrospinning setup, the distance between the collector (counter electrode) and syringe tip (primary electrode) is usually 10–25 cm. The voltage applied usually ranges from 10 to 50 kV which provides the electrostatic field between them [53].

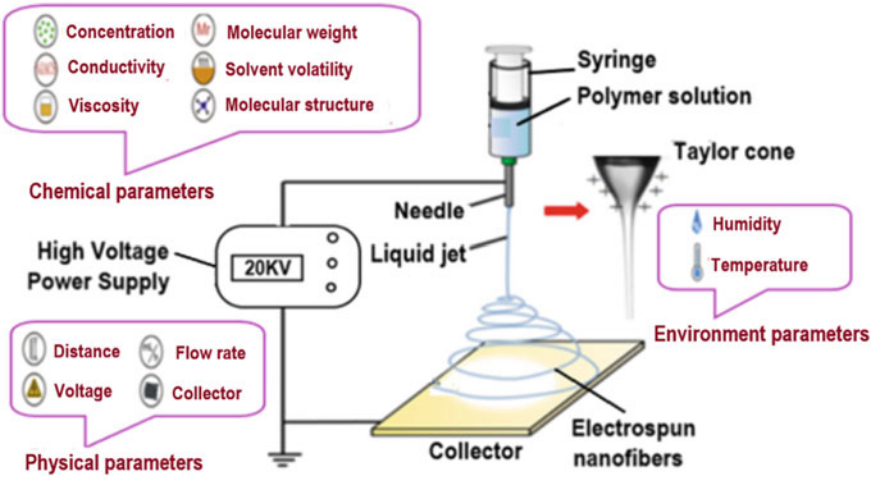


Fig. 18.1 Schematic diagram of electrospinning with chemical, physical, and environment parameters

During the process of electrospinning, droplet through the syringe elongates into the conical shape (Taylor cone) at the needle tip in response to the application of high voltage. When enough value of electrostatic force overcomes the surface tension of solution droplets, a finely charged jet is emitted from the Taylor cone which results in the formation of thin fibers by fast evaporation of solvent from the needle tip [54]. The morphology of the electrospun nanofibers depends on various factors such as physical, chemical, and environmental parameters [55].

The morphology of the electrospun nanofibers depends on various factors such as physical, chemical, and environmental parameters [55]. By considering these parameters, the preparation of the homogeneous solution of metallic precursor and polymer matrix is necessary for efficient nanofiber production. Following this approach, the process of calcination is needed to remove the organic matrix and to obtain the crystalline metal oxide nanofibers [29]. The preservation of nanofibers after calcination depends on different parameters which are considered during heat treatment. Low heating rates during calcination cause removal of polymer matrix without disturbing the fiber morphology and uniformity. The low calcination temperature was applied to form a smooth surface whereas high temperature leads to the porous structure by the degradation of organic compound [56]. In this context, Chu et al. reported the sensing properties of $NiGa_2O_4$ nanofibers synthesized by electrospinning technique, and samples obtained at calcination temperature 500 and 700 °C are observed to be very smooth whereas at 600 °C the fiber surface was rough [57]. While pores can eliminate due to the phenomenon of grain coarsening by a further increase in temperature [58]. Senthamizhan et al. studied that different annealing temperature growth of nanograins affects the morphology of ZnO nanofibers [59].

Multiphasic nanofibers are composed by the mixing of two or more inorganic materials such as mixed metal oxides and metal oxides combined with metallic nanoparticles. Mixed metal oxide nanofibers can be prepared by direct addition of required metallic precursors into the polymeric solution before the electrospinning procedure while doped nanofibers can be obtained by adding metallic nanoparticles into metallic cation solution before carrying the electrospinning step. In the later case, after calcination metallic nanoparticles are incorporated into the nanofiber core such as SnO_2–TiO_2, $ZnOSnO_2$, Fe_2O_3–SnO_2, In_2O_3–WO_3, NiO–SnO_2 [60–65]. However, hybrid nanofibers include metal oxide nanofibers combined with organic compounds such as a combination of carbon nanomaterials and conjugated polymers. Also, the hybrid nanofibers can either be synthesized by incorporating the required material into the electrospinning solution or by functionalization of crystalline nanofibers after electrospinning [3]. The post electrospinning process is a powerful way to incorporate materials that cannot resist at high temperatures, for example, a combination of metal oxide nanofibers with conjugated polymers [66] such as polyaniline (PANI) combined with TiO_2 nanofibers [67].

Along with the variety of composition, the nanofiber morphology is a specific characteristic that is responsible for the enhancement of the sensor performance [68]. With conventional nanofibers of solid microstructure, porous, and hierarchical structures can also be obtained by varying annealing temperature as demonstrated by Wang et al. [69]. Hollow metal oxide nanofibers have the remarkable property of the open structure. Hollow metal oxide nanofibers can be obtained by distinct approaches. In the first approach, sacrificial templates can be removed from the core of nanofiber after the fiber formation through the electrospinning technique [70, 71]. In the second approach, the coaxial electrospinning is carried out with two immiscible solutions, and the core is removed after the electrospinning process. On the other hand, the non-removal of nanofiber core leads to the multiphasic coaxial nanofibers having a core–shell-like structure [72]. The fabrication of core–shell structure through the coaxial electrospinning technique depends on the viscosity of each solution, feeding rate, and alignment of the outer and inner needle tip [73]. Different polymers are used for the core–shell nanofiber solutions hence heating rate will be adjusted for simultaneous removal of both the polymers and simultaneous crystallization of different inorganic phases by maintaining the core–shell structure [72, 74]. Coaxial electrospinning with modified nozzle configuration is shown in Fig. 18.2. Two syringes are used to prepare core–shell nanofibers by this technique. The core solution is filled in one syringe and the shell solution is filled in another syringe. Additionally, hierarchical nanofibers can be elaborated as one-dimensional nanostructures with some secondary structure attached to it which can be produced either by post electrospinning treatment or through an in-situ route [75, 76]. Cao et al. reported the fabrication of hierarchical structured Co_3O_4 nanofibers by electrospinning technique followed by hydrothermal and annealing process for enhanced acetone gas sensing [77]. In the same context, Hwang et al. synthesized the TiO_2 nanofibers with hierarchical structure showing increased surface area and pore volume higher than the nanoparticle. However, multiphase nanofibers with hierarchical structures can be produced by adding more than one metallic element. Mostly the hierarchical nanofibers are

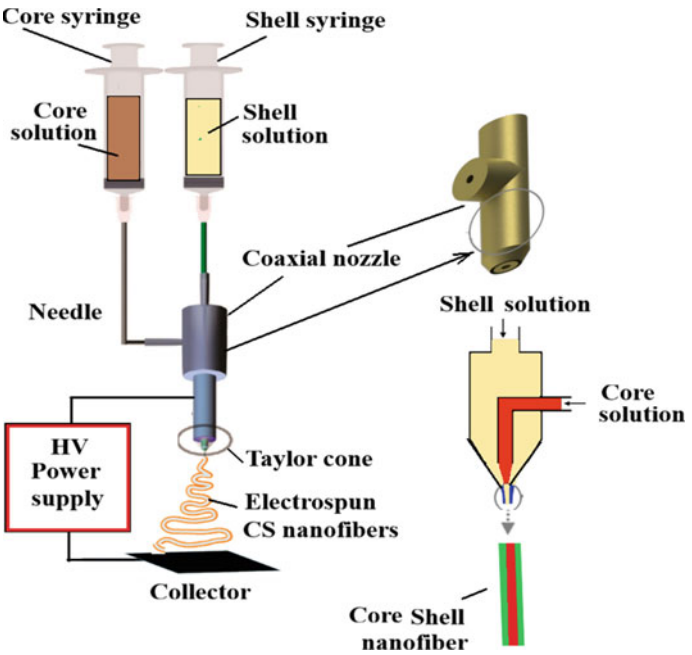


Fig. 18.2 Coaxial electrospinning with modified nozzle configuration

obtained from composite and hybrid type nanofiber structures by processing them after nanofibers production. For instance, hierarchical nanofibers can yield by metal oxide nanofibers decorated with metallic nanoparticles and nanofibers combine with conjugated polymers [76, 78, 79].

18.3 Electrospun Metal Oxide Nanofibers-Based Sensor

Semiconductor metal oxides are most used for the fabrication of chemiresistive type gas sensors [15]. In this type, sensing material is deposited on substrate attached with integrated electrodes. Electrodes measure change in electrical resistance/conductance in the sample after interacting with target gas which depends on nature of target gas (reducing/oxidising), working temperature, and type of material (p-type/n-type) [80, 81]. Also, several aspects have been considered in gas sensing mechanism such as, oxygen adsorption on semiconductor surface, catalysis-based sensing, Schottky barrier contact, heterojunction based sensing, and band gap [26, 72, 80]. The widely accepted gas sensing mechanism depends on change in resistance after exposure/removal of target gas by adsorption/desorption process [82–84]. Typically, upon exposure to target gases, the volatile material adsorbed on the sensing layer by charge transfer process and surface interaction which leads to change in

resistance of sample. When the sample is again exposed to air, desorption of gas molecules occurs and hence sample retain its original resistance [85]. However, the physisorption and chemisorption are two processes which decides the ability of metal oxide surface to adsorb and to react with the target gas. The physisorption is the adsorption of target gas molecules on metal oxide surface which dominates at low temperatures. Whereas chemisorption is due to the charge transfer between the adsorbed gas molecules and surface atoms [82]. On the other hand, different types of metal oxide sensing materials (p-type/n-type) will be exhibited different sensing behaviours for same target gas. For instance, on exposure of oxidising gases (NO_2, Cl_2, O_3, etc.) which acts like electron acceptor, resistance will increase for n-type semiconductor and decreases for p-type semiconductor. On the other hand, for exposure of reducing gases (CO, NH_3, H_2, HCHO, etc.) the results are vice versa [27]. Among all metal oxides SnO_2, TiO_2, ZnO, and In_2O_3 are the mostly used metal oxides in the field of gas sensing due to their low cost, wide band gap, and capability of detection of wide range of gases [15, 25]. Other key advantage includes chemical and thermal stability [86], high intrinsic dopability [18], and large exciting binding energy [87].

One-dimensional nanofibers as gas sensors based on pure semiconducting metal oxides are produced by electrospinning [71–79]. For instance, Leonardi et al. compared the sensing performance of α-Fe_2O_3 nanofibers and nanoparticles for ethanol sensing at operating temperatures varying from 200 to 400 °C. The investigation reveals that sensing properties depends on sample morphology and operating temperature. α-Fe_2O_3 nanofibers show better performance due to the effective gas diffusion on the porous network structure of nanofibers comparative to α-Fe_2O_3 nanoparticles [88].

Spinel type metal oxide nanofibers are also a promising group of gas sensing materials. Chen et al. investigated the sensing properties of MGa_2O_4 (M =Ni, Cu, Co) nanofibers prepared by electrospinning. Out of which best sensing performance was shown by $NiGa_2O_4$ nanofibers at 260 °C and states the influence of transition metal ion on sensing. The order of sensitivity was found to be $NiGa_2O_4 > CuGa_2O_4 > CoGa_2O_4$. The experiment states the importance of material composition by considering the type of target gas [89]. Overall pure metal oxide-based sensors are operated at high temperatures. To overcome this issue and for more enhanced performance of gas sensors, various types of composite, doped, and hybrid materials came into the limelight.

Composite nanofibers or multiphase nanofibers can be formed by deciding the stoichiometry ratio of material to form a charge depletion layer with a shared interface which leads to a change in resistance of the material. Kim et al. investigated NO_2 sensing response of electrospun SnO_2–NiO composite nanowebs varies according to Sn:Ni stoichiometry ratio [90]. To obtain a more selective and high response sensor for a particular gas, the junction interface can be modulated by adjusting the stoichiometry. The gas-sensing performance can be increased by synergistic effect between interface junctions of two different metal oxides. The porous structure of multiphase nanofibers leads to an increase in the intrinsic surface area along with the presence of a synergistic effect between the junction interfaces [91, 92].

Hollow nanofibers show increased surface area and charge transport with a one-dimensional confinement effect [93]. Choi et al. reported the ZnO–SnO_2 hollow composite nanofibers for NO_2 gas sensing with different zinc percentages [94]. Similarly, multichannel hollow nanofibers can be more capable of adsorbing and entrapping the target gas molecules [95]. In this way, Jeong et al. reported nanoscale PtO_2 loaded multichannel SnO_2 porous nanofibers showing higher relative response for acetone gas detection [96]. Another promising alternative for setting up the junction interface between different materials is dense coaxial nanofibers. Core–shell nanofibers are one-dimensional nanostructures with each shell having a different composition. Besides, core–shell nanofibers with a shared interface having a high length-to-width ratio provide the advantage to expose just one material towards the target gas. Shared interface and synergistic effects due to distinct composition are the key features for the high sensing abilities of core–shell nanofibers. Huang et al. reported the ZnO@In_2O_3 Core–shell nanofibers synthesized through coaxial electrospinning technique as shown in Fig. 18.3a, b. Here In_2O_3 shell in ZnO@In_2O_3 Core–shell nanofibers plays an important role in modulating the response by forming shell depletion [97]. Response of ZnO@In_2O_3 CSNFs, ZnO, and In_2O_3 nanofiber gas sensors to 100 ppm ethanol as a function of operating temperature and sensor response with respect to ethanol concentration (5–5000 ppm) at 225 °C are shown in Fig. 18.3c, d. The gas sensing mechanism was explained by using the depletion-controlled carrier transport model by considering the In_2O_3 layer as shell depletion [97].

Li et al. compare the sensing performance of pure, composite and core–shell nanofibers. They reported the better sensing performance of SnO_2@WO_3 composite with 25% SnO_2 and 75% WO_3, compared to pristine SnO_2 and WO_3. They also showed the superior response of SnO_2@WO_3 core–shell nanofiber structure towards ethanol detection. Due to dissimilar work functions between SnO_2 and WO_3, electrons are supposed to flow from SnO_2 to WO_3 in the case of SnO_2@WO_3 core–shell nanofiber. This triggering of electrons and contact at the interface due to radial modulation of depleted shell layers enhances the response of the sensor [98]. In addition to the above-mentioned techniques, nanofibers can also be formed by doping or incorporation of suitable dopants into nanofiber's structure. It is an effective strategy that contributes in the formation of enhanced gas sensing nanofibrous material. Many dopants like noble metal and metallic cations have been reported for better sensing performance [71, 78, 99]. Feng et al. fabricated the In-doped NiO nanofiber based sensor for methanol. The SEM and HRTEM images stated the doping of In into NiO lattice (Fig. 18.4a(i)). The best sensing response was obtained with 3% In_3^+ at 300 °C (Fig. 18.4a(ii)). On comparing with the pure NiO nanofibers, doped nanofibers showed enhanced sensing for methanol (reducing gas) by increasing the resistance. The sensing phenomenon proposed the modulation in the depletion layers and lowering the hole concentration after In_3^+ addition which in turn leads to higher variations in resistance. In short, modulation of charge carrier through doping causes metal oxide nanofiber to serve as a high-performance gas sensor [100]. For instance, Jaroenapibal et al. demonstrated the fabrication and sensing of Ag-doped WO_3 nanofibers. The sensor was tested for undoped WO_3 and Ag dopant WO_3

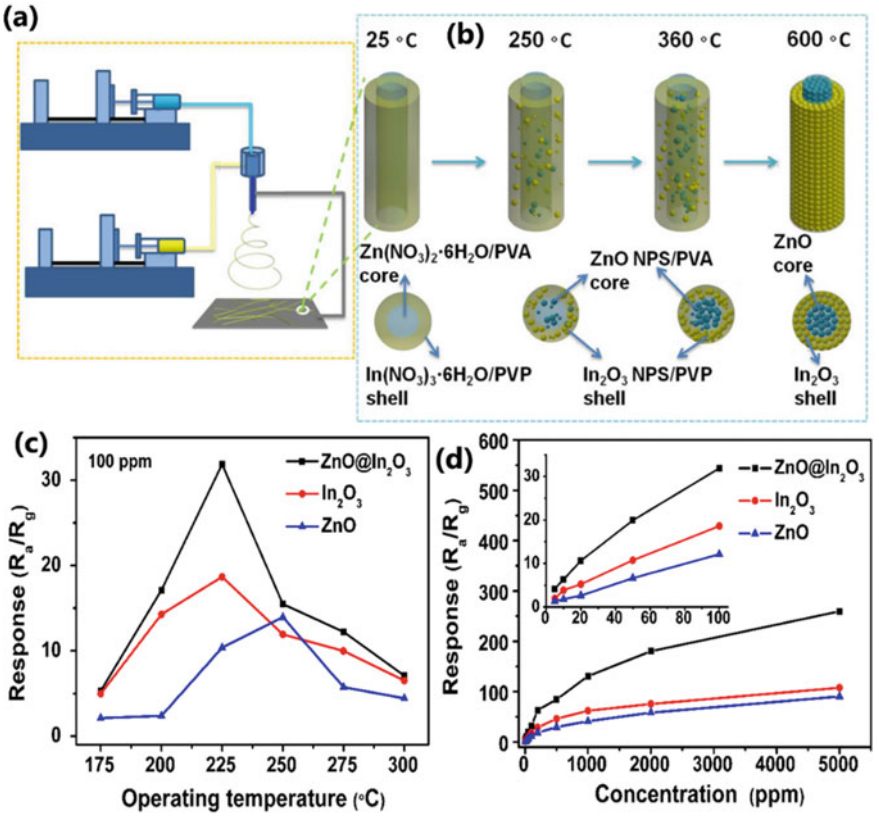


Fig. 18.3 Schematic diagram of the coaxial electrospinning set-up used (**a**), Formation of $ZnO@In_2O_3$ core–shell nanofibers (NPS-Nanoparticles) (**b**), Response of $ZnO@In_2O_3$ CSNFs, ZnO and In_2O_3 nanofiber gas sensors to 100 ppm ethanol as a function of operating temperature (**c**), and Sensor response versus ethanol concentration (5–5000 ppm) at 225 °C (**d**). Reproduced with permission from Ref. [97], Copyright 2018 Elsevier

with different Ag concentrations (1–10 mol%) for different operating temperatures and various gas concentrations. The XPS spectra revealed the formation of WO_3 nanofibers by WO_3 nanoparticles and also the formation of a thin Ag_2O layer onto its surface. The sensing properties of Ag-doped WO_3 nanofibers have been improved compared to pristine WO_3 and it was found to be more sensitive for NO_2 gas. The mechanism of gas sensing suggested the flow of electrons from a layer of Ag nanoparticles to WO_3 due to dissimilar work functions hence thereby widening of depletion layer as compared to pristine WO_3. The presence of Ag_2O layer supports the effect of chemical sensitization in presence of NO_2 gas. Besides modulation of the depletion layer can be improved by exposing the NO_2 gas (oxidizing gas) to Ag-doped WO_3 nanofibers (Fig. 18.4b) [101]. Thus doping with noble metals is attributed to both

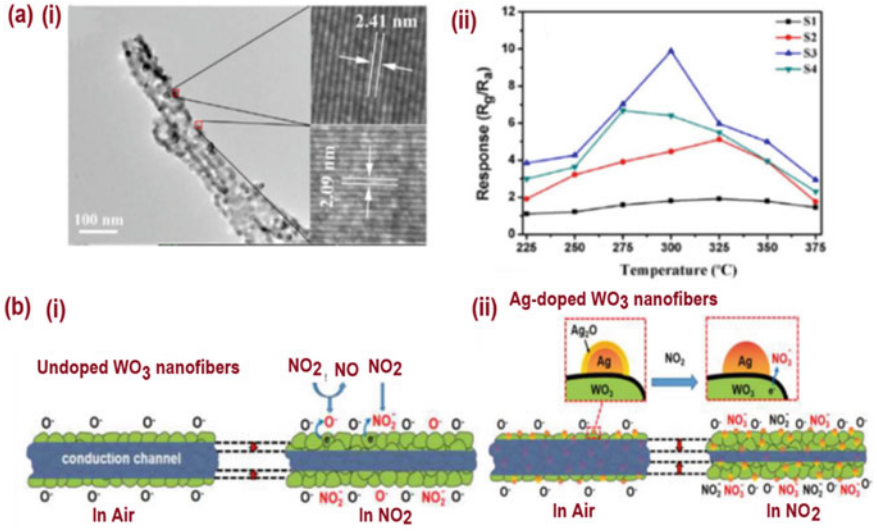


Fig. 18.4 **a** (i) TEM images pattern of the In-doped NiO nanofiber (S4). The insets are the HRTEM images of selected areas. (ii) Response of sensors based on S1, S2, S3 and S4 nanofibers to 200 ppm methanol as function of the operating temperature. Reproduced with permission from Ref. [100]. Copyright 2017 Elsevier. **b** Schematic representation of the NO_2-sensing mechanism for (i) undoped WO_3 nanofibers and (ii) Ag-doped WO_3 nanofibers. Reproduced with permission from Ref. [101]. Copyright 2017 Elsevier

chemical and electronic modulation of the sample which directly leads to greater response.

18.4 Electrospun Polyaniline (PANI) Based Composites Nanofibers Sensor

Conducting polymers (CPs) are very special class in the polymers having sp^2 hybridize structure showing alternate π-bonds which allows the delocalized charge transport [101, 102]. CPs have many advantages such as environmental stability, tunable properties and easy of synthesis. The most important conducting polymers include polyaniline (PANI), polythiophene (PTh), polypyrole (PPy), etc. CPs possess the property of electrical insulators or semiconductors in an undoped state. As low conductivity is one of the shortcomings of CPs that can be eliminated by doping process in which extraction of electrons is done from the backbone of CPs thereby increasing the electrical conductivity [102–104]. The unique properties of CPs make them promising candidates for room temperature chemical sensors. One-dimensional nanostructured conducting polymers are advantageous for gas sensing due to their large surface area compared to their bulk counterparts [103, 105]. Among different

CPs, polyaniline was found to be most investigated in the field of gas sensing due to its high environmental stability, room temperature operation, ease of synthesis, and reversible doping/de-doping properties [104, 106]. Polyaniline can be synthesized through the oxidizing polymerization of aniline monomer with two structural units called reduced unit (B-NH-B-NH) and oxidized unit (B−N = Q = N−), where B and Q represent benzenoid and quinoid ring respectively. PANI can be reversibly doped under acidic (proton doping) and basic environment. In acidic conditions, the imine nitrogen on PANI backbone is protonated which induces the charge carriers leading to an increase in PANI conductivity. The undoped form of PANI is called an emeraldine base whereas the doped form is known as emeraldine salt or emeraldine oxidation state. The introduction of a new component into PANI nanostructure can further enhance the sensing abilities by the synergistic effect that arises due to the combination of two distinct phases. For tuning the sensing properties of PANI, different materials such as polymers, nanoparticles, metal-oxides, and carbon contained materials (Graphene, CNTs) can be combined with it. Further, we discuss the gas sensing of PANI nanofibers and their composite form [105, 107]. PANI sensors can be fabricated in two different ways (1) Synthesis of PANI nanofibers and their composites by electrospinning technique and (2) Growth of PANI through non-electrospinning technique on electrospun materials. Both methods are reported for sensing of various gas among them ammonia gas sensing is most common.

18.4.1 Electrospun PANI/Polymer Composites Nanofibers

The conducting polymer PANI has delocalized π-electrons on its backbone which leads to the special electrical properties. Due to its ability to conduct electricity through charge delocalization, it comes into the class of intrinsic conducting polymers. Conducting polymer PANI has been enormously investigated for their reversible doping/de-doping character, good environmental stability, and modifiable electrical conductivity. The unique ability to get doped by protonic acids make the PANI suitable for gas sensing purpose [103, 104]. While PANI has a relatively low molecular weight, poor solubility and rigid backbone comparative to other polymers which causes the modest elasticity of the solution. As we know elasticity and viscosity are the crucial parameters for uniform fiber production in electrospinning technique [105, 106, 108, 109]. Hence to prepare PANI nanofibers by electrospinning, PANI requires the blending with other spinnable polymers such as polyvinyl alcohol (PVA), polyethylene oxide (PEO), polyvinylpyrrolidone (PVP), polysterene (PS) due to its poor solubility in organic solvents [107–112]. The thermal and mechanical stability of the sample increases through the incorporation of these polymers. Macagnano et al. investigated that PANI-PVP, PANI-PS, and PANI-PEO nanofibers can be obtained through electrospinning technique by mixing sulfonic acid (CSA) doped PANI with PVP, PS, and PEO respectively. The obtained nanofibers were tested for 20–1000 ppm ammonia gas at ambient temperature. The sensing mechanism of these structures has supposed to base on the doping/de-doping process which is reversible in nature. On

the exposure of ammonia, PANI becomes de-doped to form NH_4^+ ions whereas in no ammonia condition PANI comes to its initial form through decomposition of NH_4^+ to NH_3 [108, 111]. The type of polymer blend with PANI also plays an important role in sensing. For instance, nanofibers based on PANI-PEO and PANI-PS showed greater response for NH_3 in comparison to PANI-PVP nanofibers. The quality of the polymeric layer and distribution of PANI in the blended polymer is the proposed responsible factors for the differences in responses of composite nanofibers. On the other hand for constructing only PANI-based nanofibers, other polymers should be removed from the composite after electrospinning. For instance, Zhang et al. reported successful production of HCSA doped pure PANI nanofibers through coaxial electrospinning by removal of shell polymer PMMA (polymethyl methacrylate). Typically, for core fluid, PANI was blended with HCSA followed by the addition of chloroform and DMF whereas, PMMA was mixed with DMF for shell fluid. The PANI-PMMA core–shell nanofibers were produced through electrospinning and finally, PMMA shell was removed by one-hour isopropyl alcohol treatment. The PANI nanofiber sensor exhibited a noticeable response for ammonia and nitrogen [106, 109]. In the same way, Li et al. prepared HCSA doped PANI-PEO nanofibers by electrospinning for ammonia sensing at room temperature. This PANI-PEO based ammonia sensor-generated sensing signals in terms of increased resistance due to de-protonation of PANI (forming NH_4^+ ions) and swelling the polymer matrix after ammonia exposure. They have tested the ammonia for different compositions of PANI, out of which fiber mats with 26 wt% PANI content showed the greater sensing performance [110, 113]. In the case of PANI-PVA nanofibers investigated by Bitencourt and coworkers, PANI was initially de-doped with ammonium hydroxide and then mixed in PVA solution with 1, 2, 3, 4 and 5% composition of PANI. The authors only check the presence of ammonia at room temperature [107, 110].

Another polymer, Poly-3-hydroxybutyrate (PHB) which is insoluble in water and biodegradable in nature studied by Macagnano et al. for sensing purposes in combination with PANI. The PANI/PHB composite was fabricated by electrospinning technique and tested for ammonia sensing at room temperature. The composite of PANI/PHB leads to improved mechanical strength, biodegradability and sensing capabilities based on doping-de-doping chemistry [111, 114]. Reddy et al. studied the Polyaniline/poly(styrene-co-acrylonitrile) (SAN) blend nanofibers for enhanced nitrogen and ammonia gas sensing. The PANI/SAN blend was electrospun and directly deposited on inter-digited electrodes (IDE) which were placed on a rotating collector. SAN helps for electrospinning as well as to improve the chemical resistance, mechanical strength, and transparency of the final product. The sensor shows excellent sensitivity and response at ppm levels as low as 10. The results shown by Transmission electron microscopy (TEM) and Fourier Transform Infrared spectroscopy (FTIR) revealed the molecular-level interaction between PANI and SAN which states the reason behind the excellent gas sensitivity of PANI/SAN nanofibers [112, 115].

Electrospun PANI-based composites are found to be good chemiresistor gas sensors. In addition to that PANI can also be used to improve the gas sensing performance of electrospun nanofibers synthesized from some other materials such as other

polymers and metal/metal oxides [113–118]. In the same context, Zhang et al. synthesized the PMMA nanofibers by electrospinning process followed by growth of PANI on their surface for enhanced ammonia gas sensing at room temperature. The coating of PANI on PMMA nanofibers was done by in-situ polymerization. The thin coating of PANI nanoclusters was formed on the PMMA nanofibers which clearly states the compatibility between PANI and PMMA nanofibers. The sensor even responds to 1, 2, 3, 4, 5, and 7 ppm of ammonia. This type of parallel assembly of fibers leads to an increase in sensing properties due to the easy transfer of electrons [116, 119]. Anwane et al., Jia et al., and Tang et al. reported that PANI can coat on PMMA nanofibers through in-situ polymerization as well as dip coating [117–122].

Wu and co-worker synthesized the single yarn from core-sheath PANI/polyacrylonitrile (PAN) nanofibers by electrospinning and in-situ polymerization method as shown in Fig. 18.5a–d. The PANI/polyacrylonitrile (PAN) uniaxially aligned coaxial nanofiber yarn (UACNY) offered a high surface area and unidirectional transmission of charge carriers which give rise the excellent sensitivity and fast response/recovery time for ammonia gas sensing at room temperature as shown in Fig. 18.5e, f. According to the proposed theory, ammonia reaction with PANI/PAN UCANY leads to protonation and de-protonation of PANI [120, 123]. Kondawar et al. reported the fabrication of electrospun PVDF/PANI to blend nanofibers through electrospinning and dip-coating polymerization for sensing ammonia gas at room temperature. The change in the conductivity of the sample on exposure to ammonia gas due to coating of conducting PANI on PVDF

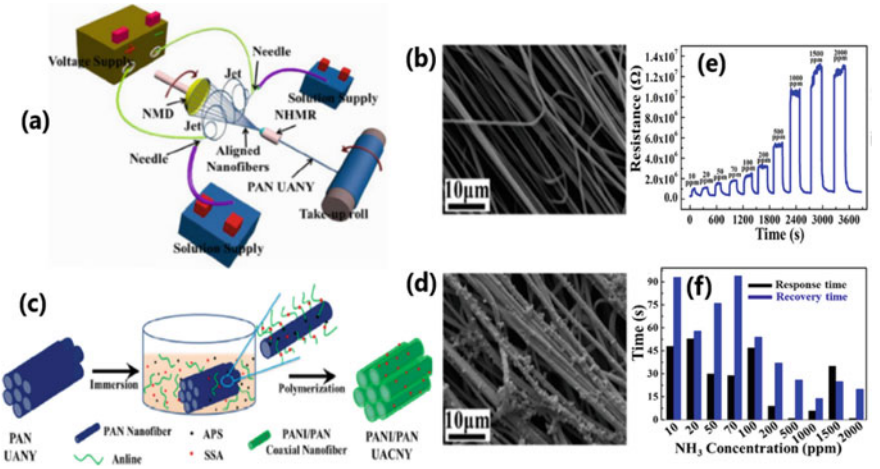


Fig. 18.5 **a** Schematic illustration of modified electrospinning setup, **b** SEM image of PAN UANY, **c** Schematic of the Fabrication of UACNY composed with core-sheath PANI/PAN nanofibers, **d** SEM image of PANI/PAN UACNY, **e** Sensing of PANI/PAN UACNY sensor exposed to 10–2000 ppm NH_3 at room temperature, and **f** Response-Recovery time of PANI/PAN UACNY sensor exposed to different NH_3 concentrations at room temperature. Reproduced with permission from Ref. [120, 123]. Copyright 2017 Elsevier

nanofibers ensured as a potential chemical gas sensor [121, 124]. In the same way, many reports have been found which proposed the modification of polymer nanofibers through polyaniline for excellent sensing characteristics [122–127].

Viscoelasticity is one of the well-known intrinsic properties of polymers whereas conductivity is the main characteristic of the conducting polymer or polymer composites. Moreover, special characteristics of PANI leads to the effective adsorption of the analyte. Lin et al. fabricated the SAW (Surface Acoustic Wave) humidity sensor (Fig. 18.6a) based on electrospun PANI/PVB nanofiber. They have studied the different polymers such as PMMA (polymethyl methacrylate), PVP (polyvinyl pyrrolidone), PEO (polyethylene oxide), PVDF (polyvinylidene fluoride), and PVB (polyvinyl butyral) and the humidity response of corresponding SAW humidity sensors were investigated. Among all five polymers, PANI/PVB nanofiber sensor was found to be sensitive and showed an almost linear response over a wide range

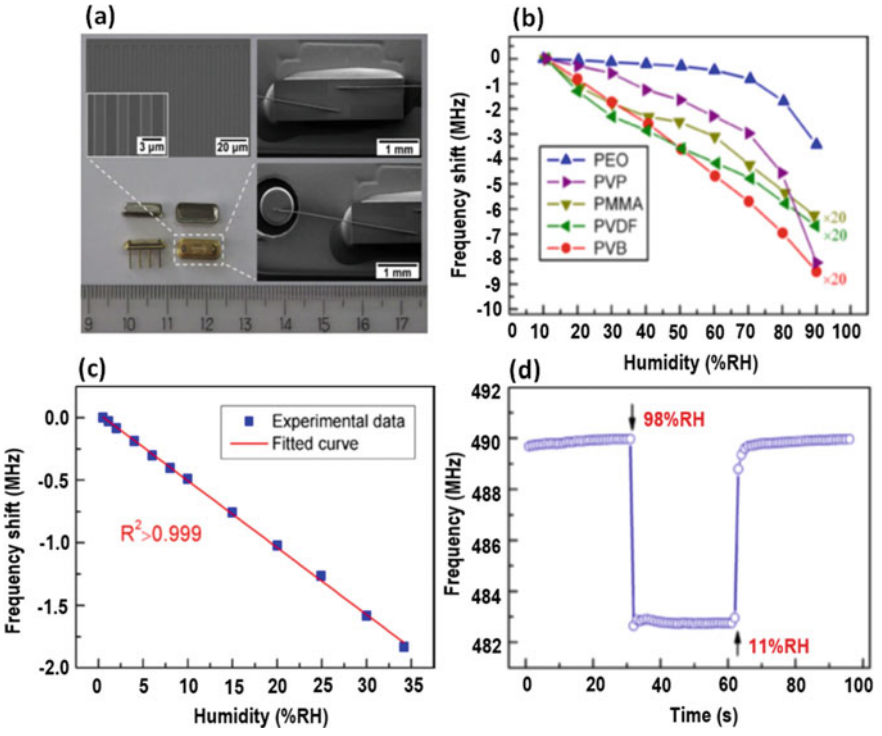


Fig. 18.6 **a** Photo and SEM images of the (Surface Acoustic Wave) humidity sensor, **b** Frequency response of different SAW sensors for humidity (temperature: 30 °C), **c** Frequency response to low humidity of the SAW sensor based on electrospun PANI/PVB nanofibers, **d** Humidity response curve of the SAW sensor based on electrospun PANI/PVB nanofibers. Reproduced with permission from Ref. [128]. Copyright 2012 Elsevier

of humidity (Fig. 18.6b). The frequency response at the low humidity range (0.5–35%RH) was also examined (Fig. 18.6c) which concluded the efficient low humidity measurement by the sensor.

The response time of the PANI/PVB nanofiber sensor was also tested which was found to be useful for the real-time sensor (1 s). The cyclic test indicates the good repeatability of the PANI/PVB nanofiber sensor by exhibiting the same response curves (Fig. 18.6d). The results revealed that PVB was suitable as a matrix to form nanofibers with PANI by electrospinning. The PANI/PVB composite nanofiber sensor showed very high sensitivity, ultrafast response, good sensing linearity, quick response time with good repeatability [125, 128]. Materials with high conductivity and mechanical compliance are promising stretchable conductors. However, the development of conductive elastic materials with maintaining high conductivity under significant strain is still a challenge. In this context, Huang et al. developed the strain sensor using well-organised coaxial PANI/PVDF (polyaniline/polyvinylidene fluoride) microfibers which combines the benefits of conducting polymer and elastic material. The results concluded that the resistance of the fibers was changed with the curvature variation which makes the PANI/PVDF microfibers suitable strain sensor showing high flexibility, high sensitivity, and stable repeatability [126, 129].

18.4.2 Electrospun PANI/Metal Oxide Composites Nanofibers

To fabricate gas sensors with high sensitivity, response, and excellent reproducibility, composite of conducting polymer and metal oxide nanofibers has attracted particular interest due to hybridization and synergistic effect between organic and inorganic materials [127–132]. As stated, earlier PANI is the most investigated p-type conducting polymer due to its environmental stability and tunable conducting property. Many reports stated that PANI composite can improve the sensing performance of pure PANI sensors and pure metal oxide-based sensors [130–136]. TiO_2 nanofibers are most extensively used for gas sensing in combination with PANI [118, 134, 135, 137]. The p-type PANI and n-type TiO_2 forming p-n heterojunction at the interface enhances the gas sensing mechanism. On the exposure of target gas, PANI alters the level of charge carriers on the PANI backbone which causes the changes in the depletion region thereby variations in the sensing signals. Gong et al. fabricated a gas sensor based on polyaniline nano-grain encapsulated on the electrospun TiO_2 fibers. With this structure, the sensor was able to detect 50 ppm of ammonia [118, 134]. In another report, Gong et al. also prepared PANI/TiO_2 composite nanofibers where the TiO_2 and PANI nanoparticles are randomly spread on entire area of nanofibers. For the preparation of PANI/TiO_2 composite nanofibers, first Mn_3O_4/TiO_2 nanofibers were prepared via the electrospinning technique. Mn_3O_4 has an oxidizing property which would help in the polymerization of aniline. In the sensing properties, PANI/TiO_2

composite nanofibers showed enhanced sensing properties than that of pure PANI at room temperature up to 25–200 ppb of ammonia [135–138].

Another type includes composite of PANI and electrospun TiO_2/organic/inorganic materials (TiO_2/Polyamide 6, TiO_2/Cellulose, TiO_2/CuO, and TiO_2/SiO_2) which can be used for gas sensing [118 , 121, 137–142]. Pang et al. developed the gas sensor based on electrospun PA6/TiO_2/PANI composite nanofiber for ammonia gas sensing. PA6/TiO_2 nanofibers were prepared by electrospinning-electrospraying technique in which TiO_2 nanoparticles were inserted into PA6 nanofiber's mat using two syringes separately and finally, PA6/TiO_2 combine with PANI through polymerization technique (Fig. 18.7a). The response of the PA6/TiO_2/PANI and PA6/ PANI composite nanofibers-based sensors towards ammonia and the response values obtained are depicted in Fig. 18.7b, c respectively. In comparison, the response of PA6/TiO_2/PANI composite nanofibers sensor was found to be much higher than that of PA6/PANI nanofibers sensor. The p–n junction formed at the interface between PANI and TiO_2 due to which the interaction of ammonia with PANI leads to an increase in the width of depletion region and hence PA6/TiO_2/PANI composite nanofibers exhibited good improvement in response than that of PA6/PANI composite nanofibers [118, 121].

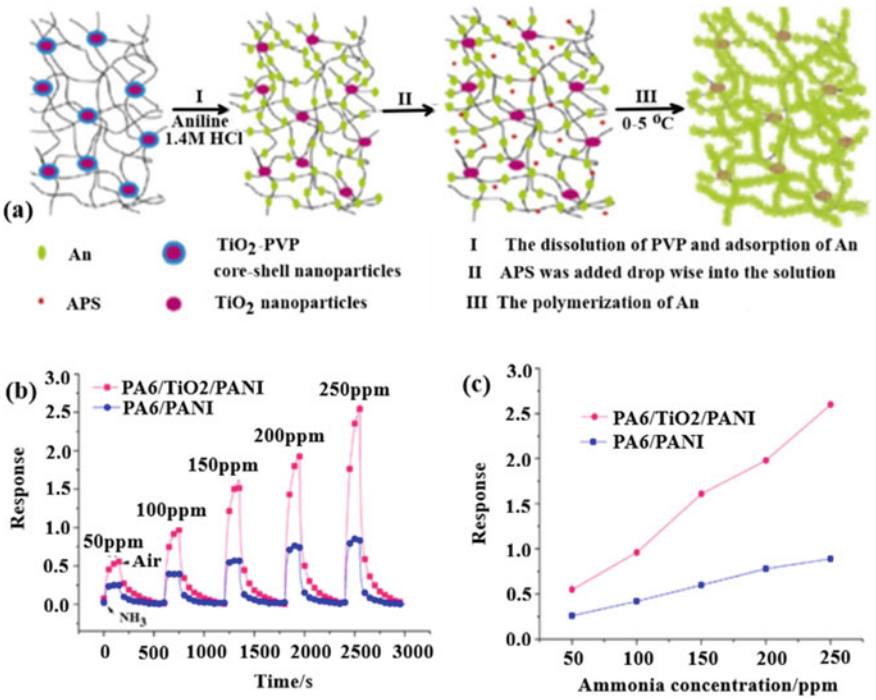


Fig. 18.7 **a** Fabrication of PA6/TiO_2/PANI composite nanofibers by chemical oxidative polymerization of aniline, **b** Dynamic response of PA6/TiO_2/PANI and PA6/PANI composite nanofibers, **c** Response values of PA6/TiO_2/PANI and PA6/PANI composite nanofibers at room temperature. Reproduced with permission from Ref. [118, 121]. Copyright 2014 Elsevier

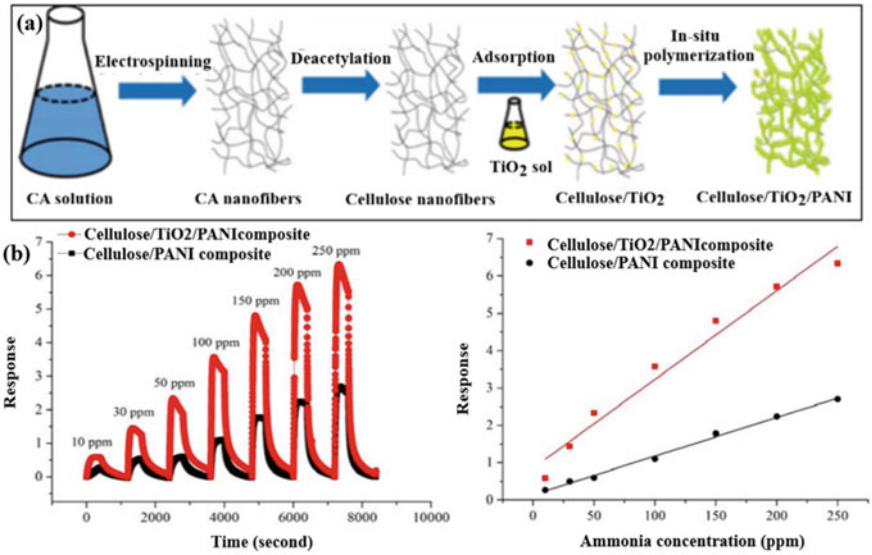


Fig. 18.8 **a** Fabrication of Cellulose/TiO_2/PANI composite nanofibers, **b** Dynamic response of cellulose/PANI and cellulose/TiO_2/PANI composite nanofibers to 10–250 ppm ammonia and the response values. Reproduced with permission from Ref. [137, 139]. Copyright 2016 Elsevier

In other work, Pang et al. also proposed the method for PANI/TiO_2 nanocomposite with cellulose acetate nanofiber structure for ammonia gas sensing at ambient conditions. The first cellulose acetate nanofiber structure was prepared by electrospinning technique followed by a de-acetylation process. Obtained cellulose nanofibers were immersed into TiO_2 solution to get cellulose/TiO_2 composite nanofiber templates followed by in-situ polymerization for PANI/TiO_2 composite nanofibers (Fig. 18.8a). Due to the synergistic effect of PANI and cellulose/TiO_2 nanofibers, resulting cellulose/TiO_2/PANI composite nanofibers showed a higher response almost two times those of those cellulose/PANI (Fig. 18.8b). The interaction of PANI with ammonia led to the reduction in hole concentration hence increasing the width of the depletion layer thereby increasing the sample resistance and this PANI-based composite nanofiber could be the potential candidate as a chemical sensor [137, 139].

Pang and co-workers reported the combination of CuO–SiO_2–TiO_2/PANI composite nanofiber prepared by electrospinning followed by calcination and in-situ polymerization. The sensor was found to be sensitive for ammonia at room temperature. It is proposed that the enhanced sensing properties are due to p–p, p–n heterojunction, and similar structure as Field-effect transistors formed due to interaction of PANI (p-type), TiO_2 (n-type), and CuO (p-type). The prepared sample was easy to handle and freestanding with appropriate flexibility which can be used in wearable sensor [138, 140]. Nie et al. also reported the fabrication of freestanding SiO_2/PANI nanofibers for room temperature ammonia gas sensing. The

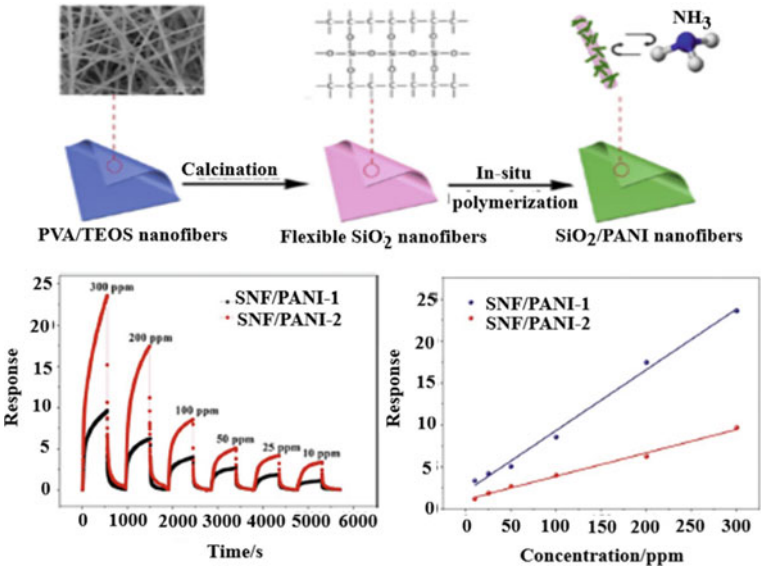


Fig. 18.9 Schematic of the preparation of flexible SiO_2/PANI nanofibers and dynamic response of SNF/PANI-1 and SNF/PANI-2 sensors to NH_3, and their corresponding response values. Reproduced with permission from Ref. [139, 141]. Copyright 2018 Elsevier

PANI coated SiO_2 nanofiber (SNF) membranes were prepared by the sol–gel, electrospinning, calcination, and in-situ polymerization methods (Fig. 18.9). Depending on the calcination temperature, SNF1 and SNF2 at 600 °C and 800 °C had been used for the preparation of SNF/PANI-1 and SNF/PANI-2 sensors. These sensors had been compared for their response towards ammonia and found that the response values of SNF/PANI-2 were significantly higher than those of SNF/PANI-1 gas sensor [139, 141].

Sonwane et al. reported the preparation of nickel cobaltite/polyaniline ($NiCo_2O_4$/PANI) composite nanofibers by electrospinning and in-situ polymerization for room temperature ammonia sensing [140, 142]. The unique features of both PANI and $NiCo_2O_4$ spinel nanostructure exhibited p-type heterojunction behavior leads to ultrahigh sensing response for a wide range from 500 to 1 ppm of ammonia with good selectivity at room temperature. Figure 18.10a shows dynamic response/recovery curves of $NiCo_2O_4$/PANI composite nanofiber-based sensor towards different gases including ethanol, methanol, ammonia, hydrogen, formaldehyde, and acetone for 100 ppm concentration. Figure 18.10b shows the response/recovery curves to high (500–10 ppm) and low (8–1 ppm) concentrations of ammonia. Response of $NiCo_2O_4$/PANI composite nanofiber-based sensor for ammonia was found to be much higher than that of pristine PANI. The composite nanofibers based on PANI contributed an increased number of sites for ammonia diffusion, and hence such composite nanofibers are potential candidates for ammonia sensing at room temperature.

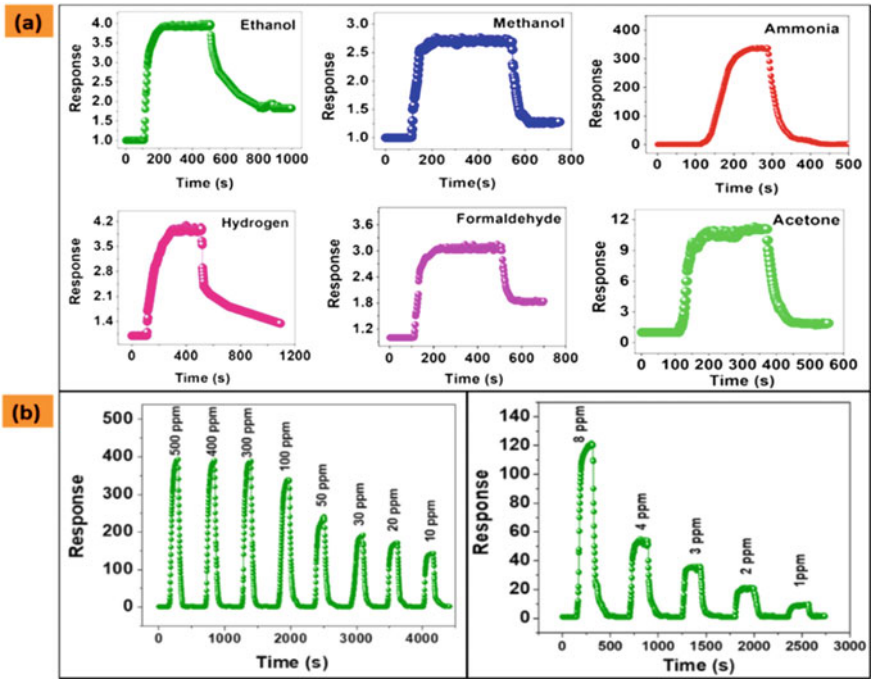


Fig. 18.10 **a** Response of $NiCo_2O_4$/PANI composite nanofibers sensor for various gases for 100 ppm concentration at room temperature, **b** Response of $NiCo_2O_4$/PANI composite nanofibers sensor for ammonia gas for different concentrations at room temperature. Reproduced with permission from Ref. [140, 142]. Copyright 2021 Elsevier

18.5 Conclusions

In this chapter, we have effectively studied the recent results on metal oxide nanofibers and PANI-based composite nanofibers synthesized by electrospinning technique and in-situ polymerization for gas sensing applications. For such an application, the sample needs to have good sensitivity, response, and quick response/recovery rate. Hence highly reactive sensors made up of composites and hybrid materials are demonstrated in various fields such as industries, medical use, agriculture, and domestic use. The development in the one-dimensional nanofibers, such as metal oxide/PANI-based nanofibers, is gaining more attention in the past decade. The electrospinning technique allows the mass production of one-dimensional nanofibers with controlled morphology. On the other hand, the calcination step has been required for removing the organic solvents and provides mechanical strength. From the study, the operating temperature of metal oxide nanofibers is usually too high and selectivity for particular gas is very low. To eradicate this type of limitations conducting polymers especially PANI is extensively used due to their special electrochemical properties which leads to low energy consumption and lesser chances of explosions. Finally,

these types of sensors can be used for the internet of things and mobile systems to continuously monitor the harmful gases in the environment.

References

1. Woellner, M., Hausdorf, S., Klein, N., Mueller, P., Smith, W., & Kaskel, S. (2018). *Advanced Materials, 30*, 1704679.
2. Fang, X., Zong, B., & Mao, S. (2018). *Nano-Micro Letters, 10*, 64.
3. Mercante, L. A., Scagion, V. P., Migliorini, F. L., Mattoso, L. H. C., & Correa, D. S. (2017). *TrAC, Trends in Analytical Chemistry, 91*, 91–103.
4. Broza, Y. Y., Vishinkin, R., Barash, O., Nakhleh, M. K., & Haick, H. (2018). *Chemical Society Reviews, 47*, 4781–4859.
5. Jalal, A. H., Alam, F., Roychoudhury, S., Umasankar, Y., Pala, N., & Bhansali, S. (2018). *ACS Sensors, 3*, 1246–1263.
6. Rai, A. C., Kumar, P., Pilla, F., Skouloudis, A. N., Di Sabatino, S., Ratti, C., Yasar, A., & Rickerby, D. (2017). *Science of the Total Environment, 2017*(607–608), 691–705.
7. West, J. J., Cohen, A., Dentener, F., Brunekreef, B., Zhu, T., Armstrong, B., Bell, M. L., Brauer, M., Carmichael, G., Costa, D. L., Dockery, D. W., Kleeman, M., Krzyzanowski, M., Künzli, N., Liousse, C., Lung, S.-C. C., Martin, R. V., Pöschl, U., Pope, C. A., Roberts, J. M., Russell, A. G., Wiedinmyer, C. (2016). *Environmental Science & Technology, 50*, 4895−4904.
8. Kampa, M., & Castanas, E. (2008). *Environmental Pollution, 151*, 362–367.
9. Cohen, A. J., Brauer, M., Burnett, R., Anderson, H. R., Frostad, J., Estep, K., Balakrishnan, K., Brunekreef, B., Dandona, L., Dandona, R., Feigin, V., Freedman, G., Hubbell, B., Jobling, A., Kan, H., Knibbs, L., Liu, Y., Martin, R., Morawska, L., … Forouzanfar, M. H. (2017). *Lancet, 389*, 1907–1918.
10. Xu, K., Fu, C., Gao, Z., Wei, F., Ying, Y., Xu, C., & Fu, G. (2018). *Instrumentation Science and Technology, 46*, 115–145.
11. Ge, L., Mu, X., Tian, G., Huang, Q., Ahmed, J., & Hu, Z. (2019). *Frontiers in Chemistry, 7*, 839.
12. Andre, R. S., Sanfelice, R. C., Pavinatto, A., Mattoso, L. H. C., & Correa, D. S. (2018). *Materials and Design, 156*, 154–166.
13. Vikrant, K., Kumar, V., Ok, Y. S., Kim, K. H., & Deep, A. (2018). *TrAC, Trends in Analytical Chemistry, 105*, 263–281.
14. Sun, Y. F., Liu, S. B., Meng, F. L., Liu, J. Y., Jin, Z., Kong, L. T., & Liu, J. H. (2012). *Sensors, 12*, 2610–2631.
15. Dey, A. (2018). *Materials Science and Engineering B, 229*, 206–217.
16. Choi, P. G., Izu, N., Shirahata, N., & Masuda, Y. (2019). *ACS Applied Nano Materials, 2*, 1820–1827.
17. Liu, X., Zhao, K., Sun, X., Zhang, C., Duan, X., Hou, P., Zhao, G., Zhang, S., Yang, H., Cao, R., & Xu, X. (2019). *Sensors and Actuators, B: Chemical Sensors and Materials, 285*, 1–10.
18. Zhang, Z. G., Wang, X. X., Zhang, J., Yu, M., Zhang, J. C., Zhang, H. D., & Long, Y. Z. (2018). *Journal of Alloys and Compounds, 752*, 359–375.
19. Liu, X., Ma, T., Pinna, N., & Zhang, J. (2017). *Advanced Functional Materials, 27*, 1702168.
20. Jiang, T., Du, B., Zhang, H., Yu, D., Sun, L., Zhao, G., Yang, C., Sun, Y., Yu, M., & Ashfold, M. N. R. (2019). *Applied Surface Science, 483*, 922–928.
21. Imran, M., Motta, N., & Shafiei, M. (2018). *Beilstein Journal of Nanotechnology, 9*, 2128–2170.
22. Ding, B., Wang, M., Yu, J., & Sun, G. (2009). *Sensors, 9*, 1609–1624.
23. Ma, Y., Qu, Y., & Zhou, W. (2013). *Microchimica Acta, 180*, 1181–1200.
24. Tang, X., Du, A., & Kou, L. (2018). *Wiley Interdisciplinary Reviews: Computtational Molecular Science, 8*, 1361.

25. Dral, A. P., & Ten Elshof, J. E. (2018). *Sensors and Actuators, B: Chemical Sensors and Materials, 272*, 369–392.
26. Lin, T., Lv, X., Li, S., & Wang, Q. (2017). *Sensors, 17*, 2779.
27. Zhang, J., Qin, Z., Zeng, D., & Xie, C. (2017). *Physical Chemistry Chemical Physics: PCCP, 19*, 6313–6329.
28. Varghese, S. S., Lonkar, S., Singh, K. K., Swaminathan, S., & Abdala, A. (2015). *Sensors and Actuators B: Chemical, 218*, 160−183.
29. Mercante, L. A., Andre, R. S., Mattoso, L. H. C., & Correa, D. S. (2019). *ACS Applied Nano Materials, 2*, 4026–4042.
30. Niu, H., Zhou, H., & Wang, H. (2020). Electrospinning: an advanced nanofiber production technology. *Energy Harvesting Properties of Electrospun Nanofibers; IOP Publishing: Bristol*, 1–44.
31. Shi, X., Zhou, W., Ma, D., Ma, Q., Bridges, D., Ma, Y., & Hu, A. (2015). *Journal of Nanomaterial, 2015*, 140716.
32. Lu, X., Wang, C., & Wei, Y. (2009). *Small (Weinheim an der Bergstrasse, Germany), 5*, 2349–2370.
33. Xue, J., Wu, T., Dai, Y., & Xia, Y. (2019). *Chemical Reviews, 119*, 5298–5415.
34. Korotcenkov, G., & Cho, B. K. (2017). *Sensors and Actuators, B: Chemical Sensors and Materials, 244*, 182–210.
35. Li, Y., Abedalwafa, M. A., Tang, L., Li, D., & Wang, L. (2019). *Electrospinning Nanofabrication and Applications*, 571−601.
36. Patil, J. V., Mali, S. S., Kamble, A. S., Hong, C. K., Kim, J. H., & Patil, P. S. (2017). *Applied Surface Science, 423*, 641–674.
37. Kim, I. D., & Rothschild, A. (2011). *Polymers for Advanced Technologies, 22*, 318–325.
38. Ramgir, N., Datta, N., Kaur, M., Kailasaganapathi, S., Debnath, A. K., Aswal, D. K., & Gupta, S. K. (2013). *Colloids and Surfaces A, 439*, 101–116.
39. Choi, K. J., & Jang, H. W. (2010). *Sensors, 10*, 4083–4099.
40. Wang, Y., Wu, T., Zhou, Y., Meng, C., Zhu, W., & Liu, L. (2017). *Sensors, 17*, 1971.
41. Guo, L., Kou, X., Ding, M., Wang, C., Dong, L., Zhang, H., Feng, C., Sun, Y., Gao, Y., Sun, P., & Lu, G. (2017). *Sensors and Actuators, B: Chemical Sensors and Materials, 244*, 233–242.
42. Abideen, Z. U., Kim, J. H., Lee, J. H., Kim, J. Y., Mirzaei, A., Kim, H. W., & Kim, S. S. (2017). *Han'guk Seramik Hakhoechi, 54*, 366–379.
43. Thomas, S., Joshi, N., & Tomer, V. K. (2020). *Functional nanomaterials advances in gas sensing technologies* (pp. 19–70).
44. Bai, H., & Shi, H. (2007). *Sensors, 7*, 267–307.
45. Kwon, O. S., Song, H. S., Park, T. H., & Jang, J. (2019). *Chemical Reviews, 119*, 36–93.
46. Zhang, J., Liu, X., Neri, G., & Pinna, N. (2016). *Advanced Materials, 28*, 795–831.
47. Huang, Y., Song, J., Yang, C., Long, Y., & Wu, H. (2019). *Materials Today, 28*, 98–113.
48. Kanaparthi, S., & Singh, S. G. (2019). *ACS Applied Nano Materials, 2*, 700–706.
49. Toda, K., Furue, R., & Hayami, S. (2015). *Analytica Chimica Acta, 878*, 43–53.
50. Boys, C. V. (1887). *Proceedings of the Physical Society of London: IOP Publishing Ltd., 9*, 1874–1925.
51. Esfahani, H., Jose, R., & Ramakrishna, S. (2017). *Materials, 10*, 1238.
52. Teo, W. E., & Ramakrishna, S. (2006). *Nanotechnology, 17*, 89–106.
53. Zhang, W., He, Z., Han, Y., Jiang, Q., Zhan, C., Zhang, K., Li, Z., & Zhang, R. (2020). *Composites Part A: Applied Science and Manufacturing, 137*, 106009.
54. Jiang, S., Chen, Y., Duan, G., Mei, C., Greiner, A., & Agarwal, S. *Polymer Chemistry*, *9*, 2685–2720.
55. Fong, H., Chun, H., & Reneker, D. H. (1999). *Polymer, 40*, 4585–4592.
56. Liu, Z., Lu, Q., Wei, M., & Guo, E. (2017). *Journal of Sol-Gel Science and Technology, 82*, 67–77.
57. Chu, X., Wang, J., Bai, L., Dong, Y., & Sun, W. (2018). *Materials Science and Engineering B, 228*, 45–51.

58. Katoch, A., Choi, S. W., & Kim, S. S. (2015). *Metals and Materials International, 21*, 213–221.
59. Senthamizhan, A., Balusamy, B., Aytac, Z., & Uyar, T. (2016). *CrystEngComm, 18*, 6341–6351.
60. Feng, C., Li, X., Ma, J., Sun, Y., Wang, C., Sun, P., Zheng, J., & Lu, G. (2015). *Sensors and Actuators, B: Chemical Sensors and Materials, 209*, 622–629.
61. Li, W., Ma, S., Li, Y., Yang, G., Mao, Y., Luo, J., Gengzang, D., Xu, X., & Yan, S. (2015). *Sensors and Actuators, B: Chemical Sensors and Materials, 211*, 392–402.
62. Pascariu, P., Airinei, A., Olaru, N., Petrila, I., Nica, V., Sacarescu, L., & Tudorache, F. (2016). *Sensors and Actuators, B: Chemical Sensors and Materials, 222*, 1024–1031.
63. Liu, Y., & Lei, Y. (2013). *Sensors and Actuators, B: Chemical Sensors and Materials, 188*, 1141–1147.
64. Fan, X. X., Xu, Y. J., He, W. M., Huang, X., He, X. L. (2019). *Material Science and Engineering, 479*, 012121.
65. Chen, K., Chen, S., Pi, M., & Zhang, D. (2019). *Solid-State Electronics, 157*, 42–47.
66. Wang, D., Liu, X., Fang, Z., Li, J., & Sun, M. (2015). *Chemical Research in Chinese Universities, 31*, 581–584.
67. Seif, A., Nikfarjam, A., Ghassem, H. H. (2019). *Sensors and Actuators, B: Chemical Sensors and Materials, 298*, 126906.
68. Khalil, A., Kim, J. J., Tuller, H. L., Rutledge, G. C., & Hashaikeh, R. (2016). *Sensors and Actuators, B: Chemical Sensors and Materials, 227*, 54–64.
69. Wang, H., Ma, D., Huang, Y., & Zhang, X. (2012). *Chemistry—A European Journal, 18*, 8987–8993.
70. Pascariua, P., & Homocianua, M. (2019). *Ceramics International, 45*, 11158–11173.
71. Ma, L., Ma, S. Y., Kang, H., Shen, X. F., Wang, T. T., Jiang, X. H., & Chen, Q. (2017). *Materials Letters, 209*, 188–192.
72. Li, F., Gao, X., Wang, R., Zhang, T., & Lu, G. (2017). *Sensors and Actuators, B: Chemical, 248*, 812–819.
73. Yoon, J., Yang, H. S., Lee, B. S., & Yu, W. R. (2018). *Advanced Materials, 30*, 1704765.
74. Li, F., Zhang, T., Gao, X., Wang, R., & Li, B. (2017). *Sensors and Actuators, B: Chemical, 252*, 822–830.
75. Chen, K., Lu, H., Li, G., Zhang, J., Tian, Y., Gao, Y., Guo, Q., Lu, H., & Gao, J. (2020). *Sensors and Actuators, B: Chemical, 308*, 127716.
76. Fu, W., Dai, Y., Tian, J., Huang, C., Liu, Z., Liu, K., Yin, L., Huang, F., Lu, Y., & Sun, Y. (2018). *Nanotechnology, 29*, 34.
77. Cao, J., Wang, S., Zhang, H., & Zhang, T. (2019). *Journal of Alloys and Compounds, 799*, 513–520.
78. Kim, J. H. H., Zheng, Y., Mirzaei, A., & Kim, S. S. (2016). *Han'guk Chaelyo Hakhoechi, 26*, 741–750.
79. Nie, Q., Pang, Z., Li, D., Zhou, H., Huang, F., Cai, Y., & Wei, Q. (2018). *Colloids and Surfaces A, 537*, 532–539.
80. Zappa, D., Galstyan, V., Kaur, N., Munasinghe Arachchige, H. M. M., Sisman, O., & Comini, E. (2018). *Analytica Chimica Acta, 1039*, 1–23.
81. Yuliarto, B., Gumilar, G., & Septiani, N. L. W. (2015). *Advances in Material Science and Engineering, 201*.
82. Karnati, P., Akbar, S., & Morris, P. A. (2019). *Sensors and Actuators, B: Chemical Sensors and Materials, 295*, 127–143.
83. Xu, X., Chen, Y., Zhang, G., Ma, S., Lu, Y., Bian, H., & Chen, Q. (2017). *Journal of Alloys and Compounds, 703*, 572–579.
84. Guo, L., Chen, F., Xie, N., Kou, X., Wang, C., Sun, Y., Liu, F., Liang, X., Gao, Y., Yan, X., Zhang, T., & Lu, G. (2018). *Sensors and Actuators, B: Chemical Sensors and Materials, 272*, 185–194.
85. Kannan, P. K., Late, D. J., Morgan, H., & Rout, C. S. (2015). *Nanoscale, 7*, 13293–13312.
86. Xiang, J., Chen, X., Zhang, X., Gong, L., Zhang, Y., & Zhang, K. (2018). *Materials Chemistry and Physics, 213*, 122–129.

87. Zhu, L., & Zeng, W. (2017). *Sensors and Actuators, A: Physical, 267*, 242–261.
88. Leonardi, S. G., Mirzaei, A., Bonavita, A., Santangelo, S., Frontera, P., Panto, F., Antonucci, P. L., & Neri, G. (2016). *Nanotechnology*, *27*, 075502.
89. Chen, H., Li, G. D., Fan, M., Gao, Q., Hu, J., Ao, S., Wei, C., & Zou, X. (2017). *Sensors and Actuators, B: Chemical Sensors and Materials, 240*, 689–696.
90. Kim, J. H., Lee, J. H., Mirzaei, A., Kim, H. W., & Kim, S. S. (2018). *Actuators B, 258*, 204–214.
91. Zhang, J., Lu, H., Liu, C., Chen, C., & Xin, X. (2017). *RSC Advances, 7*, 40499–40509.
92. Yan, C., Lu, H., Gao, J., Zhu, G., Yin, F., Yang, Z., Liu, Q., & Li, G. (2017). *Journal of Alloys and Compounds, 699*, 567–574.
93. Choi, S. H., Ankonina, G., Youn, D. Y., Oh, S. G., Hong, J. M., Rothschild, A., & Kim, I. D. (2009). *ACS Nano, 3*, 2623–2631.
94. Bai, S., Fu, H., Zhao, Y., Tian, K., Luo, R., Li, D., & Chen, A. (2018). *Sensors and Actuators, B: Chemical Sensors and Materials, 266*, 692–702.
95. Zhao, T., Liu, Z., Nakata, K., Nishimoto, S., Murakami, T., Zhao, Y., Jiang, L., & Fujishima, A. (2010). *Journal of Materials Chemistry, 20*, 5095.
96. Jeong, Y. J., Koo, W. T., Jang, J. S., Kim, D. H., Kim, M. H., & Kim, I. D. (2018). *ACS Applied Materials & Interfaces, 10*, 2016–2025.
97. Huang, B., Zhang, Z., Zhao, C., Cairang, L., Bai, J., Zhang, Y., Mu, X., Du, J., Wang, H., Pan, X., Zhou, J., & Xie, E. (2018). *Sensors and Actuators, B: Chemical Sensors and Materials, 255*, 2248–2257.
98. Li, F., Gao, X., Wang, R., & Zhang, T. (2018). *Applied Surface Science, 442*, 30–37.
99. Jiang, Z., Yin, M., & Wang, C. (2017). *Materials Letters, 194*, 209–212.
100. Feng, C., Kou, X., Chen, B., Qian, G., Sun, Y., & Lu, G. (2017). *Sensors and Actuators, B: Chemical Sensors and Materials*, *253*, 584−591.
101. Jaroenapibal, P., Boonma, P., Saksilaporn, N., Horprathum, M., Amornkitbamrung, V., & Triroj, N. (2018). *Sensors and Actuators, B: Chemical Sensors and Materials*, *255*, 1831−1840.
102. Heeger, A. J. (2001). *Angewandte Chemie International Edition, 40*, 2591–2611.
103. Le, T. H., Kim, Y., & Yoon, H. (2017). *Polymers, 9*, 150.
104. Hangarter, C. M., Chartuprayoon, N., Hernández, S. C., Choa, Y., & Myung, N. V. (2013). *Nano Today, 8*, 39–55.
105. Zhang, J., Xianghong, L., Neri, G., & Pinna, N. (2016). *Advanced Materials, 28*, 795–831.
106. Sen, T., Mishra, S., & Shimpi, N. G. (2016). *RSC Advances, 6*, 42196–42222.
107. Mirzaei, A., Kumar, V., Bonyani, M., Majhi, S. M., Bang, J. H., Kim, J. Y., Kim, H. W., Kim, S. S., & Kim, K. H. (2020). *Asian Journal of Atmospheric Environment, 14*, 85–104.
108. Kumar, V., Mirzaei, A., Bonyani, M., Kim, K. H., Kim, H. W., & Kim, S. S. (2020). *TrAC Trends in Analytical Chemistry*, *129*, 115938.
109. Zhang, Y., Kim, J. J., Chen, D., Tuller, H. L., & Rutledge, G. C. (2014). *Advanced Functional Materials, 24*, 4005–4014.
110. Bittencourt, J. C., de Santana Gois, B. H., Rodrigues, V. J., de Oliveira da Silva Agostini, D. L., & Olivati, C. A. (2019). *Journal of Applied Polymer Science*, *136*, 47288.
111. Macagnano, A., Zampetti, E., Pantalei, S., De Cesare, F., Bearzotti, A., & Persaud, K. (2011). *Thin Solid Films, 520*, 978–985.
112. Meng, N., Wang, X., Xin, B., Chen, Z., & Liu, Y. (2019). *Textile Research Journal, 89*, 2490–2499.
113. Li, C., Chartuprayoon, N., Bosze, W., Low, K., Lee, K. H., Nam, J., & Myung, N. V. (2014). *Electroanalysis, 26*, 691–711.
114. Macagnano, A., Perri, V., Zampetti, E., Bearzotti, A., & De Cesare, F. (2016). *Sensors and Actuators, B: Chemical Sensors and Materials, 232*, 16–27.
115. Reddy, N. R., & Anandhan, S. (2016). *Journal of Materials Science: Materials in Electronics, 27*, 13329–13337.
116. Anwane, R. S., Kondawar, S. B., & Late, D. J. (2018). *Materials Letters, 221*, 70–73.
117. Pang, Z., Zhu, Y., Li, X., Chen, M., & Ge, M. (2019). *IEEE Sensors Journal, 19*, 11021–11026.

118. Gong, J., Li, Y., Hu, Z., Zhou, Z., & Deng, Y. (2010). *Journal of Physical Chemistry C, 114*, 9970–9974.
119. Zhang, H. D., Tang, C. C., Long, Y. Z., Zhang, J. C., Huang, R., Li, J. J., & Gu, C. Z. (2014). *Sensors and Actuators, A: Physical, 219*, 123–127.
120. Anwane, R. S., & Kondawar, S. B. (2018). *Journal of Physical Science, 29*, 101–119.
121. Jia, X. S., Tang, C. C., Yan, X., Yu, G. F., Li, J. T., Zhang, H. D., Li, J. J., Gu, C. Z., & Long, Y. Z. (2016). *Journal of Nanomaterial, 2016*.
122. Tang, C. C., Huang, R., Long, Y. Z., Sun, B., Zhang, H. D., Gu, C. Z., Wang, W. X., & Li, J. J. (2012). *Trans Tech Publications*, 308–311.
123. Wu, S., Liu, P., Zhang, Y., Zhang, H., & Qin, X. (2017). *Sensors and Actuators, B: Chemical Sensors and Materials, 252*, 697–705.
124. Kondawar, S., Late, D. J., Anwane, R. S., Kondawar, S. B., Koinkar, P., & Parinov, I. A. (2019). *Advanced Materials, 224*, 3–15.
125. Wu, D. Q., Wu, L. L., Cui, H. C., Zhang, H. N., & Yu, J. Y. (2016). *Journal of Materials Chemistry B, 4*, 1520–1527.
126. Pan, Y. J., Dong, X. J., Wei, Q. F., Hung, W. M., Lin, C. Y., Ho, Y. H., & Hsieh, C. T. (2012). *Trans Tech Publications*, 23–26.
127. Xue, B., Qi, S., Gong, J., Gao, Y., Yao, S., Yin, R., & Qu, L. (2007). *Journal of Nanoscience and Nanotechnology, 7*, 4515–4521.
128. Lin, Q., Li, Y., & Yang, M. (2012). *Analytica Chimica Acta, 748*, 73–80.
129. Huang, R., Long, Y., Tang, C., & Zhang, H. (2014). *Advances in Materials Research, 853*, 79–82.
130. Qi, Y., Shen, L., Zhang, J., Yao, J., Lu, R., & Miyakoshi, T. (2019). *Environmental Pollution, 245*, 810–819.
131. Garcia-Gonzales, D. A., Shonkoff, S. B., Hays, J., & Jerrett, M. (2019). *Annual Review of Public Health, 40*, 283–304.
132. Yarragunta, Y., Srivastava, S., Mitra, D., & Chandola, H. C. (2020). *GIscience & Remote Sensing, 57*, 1–17.
133. Korotcenkov, G. (2007). *Materials Science and Engineering B, 139*, 1–23.
134. Mirzaei, A., Leonardi, S., & Neri, G. (2016). *Ceramics International, 42*, 15119–15141.
135. Yamazoe, N. (2005). *Sensors and Actuators, B: Chemical Sensors and Materials, 108*, 2–14.
136. Azad, A., Akbar, S., Mhaisalkar, S., Birkefeld, L., & Goto, K. (1992). *Journal of the Electrochemical Society, 139*, 3690–3704.
137. Li, Y., Gong, J., He, G., & Deng, Y. (2011). *Materials Chemistry and Physics, 129*, 477–482.
138. Li, Y., Gong, J., He, G., & Deng, Y. (2011). *Synthetic Metals, 161*, 56–61.
139. Pang, Z., Fu, J., Luo, L., Huang, F., & Wei, Q. (2014). *Colloids and Surfaces A, 461*, 113–118.
140. Pang, Z., Yang, Z., Chen, Y., Zhang, J., Wang, Q., Huang, F., & Wei, Q. (2016). *Colloids and Surfaces A, 494*, 248–255.
141. Pang, Z., Nie, Q., Lv, P., Yu, J., Huang, F., & Wei, Q. (2017). *Nanotechnology, 28*, 225501.
142. Sonwane, N. D., & Kondawar, S. B. (2021). *Materials Letters, 303*, 130566.



Nayana D. Sonwane obtained M.Sc. (Physics) from Rashtrasant Tukadoji Maharaj Nagpur University, Nagpur, India in 2015. She is currently pursuing for doctoral degree in the field of one-dimensional nanostructure composites for gas sensing at Department of Physics, Rashtrasant Tukadoji Maharaj Nagpur University, India under the supervision of Dr. Subhash B. Kondawar. Her research interest includes the fabrication of electrospun mixed transition metal oxide nanofibers/PANI composites for gas sensing application.



Sanchit S. Kondawar obtained B.Tech. (Electronics and Telecommunication) from Government College of Engineering, Jalgaon, India in 2018. He is pursuing a doctoral degree in the field of integrated terahertz quantum cascade laser for space research in the University of Leeds, United Kingdom. He has been awarded Best Oral Paper Presentation Award in International Conference on "*Physics and Mechanics of New Materials and Their Applications*" *(PHENMA 2018)* held at Korea Maritime and Ocean University, Busan, *South Korea* on 9–11 August 2018.



Pitambar V. Gayakwad is currently working as an Assistant Professor and Head at Department of Mathematics, Arvindbabu Deshmukh Mahavidyalaya, Bharsingi, Dist. Nagpur, Maharashtra, India. He obtained his doctoral degree on the topic bimetric theory, alternative theory of gravitation from Rashtrasant Tukadoji Maharaj Nagpur University, India. He is a life member of IAGRG, office at IUCAA, Pune. He has total of 7 years of teaching experience including of science and engineering stream.



Subhash B. Kondawar is currently working as Professor in the Department of Physics, Rashtrasant Tukadoji Maharaj Nagpur University, Nagpur, India. He obtained Ph.D. (Physics) in the field of Conducting Polymers from Rashtrasant Tukadoji Maharaj Nagpur University, Nagpur, India. His main research is focused on conducting polymers and nanocomposites for gas sensors, biosensors, supercapacitors, Li-ion batteries, and light-emitting properties. He has authored more than 100 scientific articles of international reputes, 2 books, and 16 book chapters on conducting polymer nanocomposites. He has guided 23 Ph.D. students. He has completed four research projects funded by University Grants Commission, New Delhi (India). He also worked as Coordinator for the Department of Science and Technology—Fund for Improvement in Science and Technology (DST-FIST) Program of Government of India from 2013 to 2018 at the Department of Physics, Rashtrasant Tukadoji Maharaj Nagpur University, Nagpur, India. He has been awarded by Advanced Materials Letters Scientist Award-2013 by International Association of Advanced Materials at Cesme-Izmir, Turkey and Best Researcher Award-2020 by Rashtrasant Tukadoji Maharaj Nagpur University, Nagpur, India.

Chapter 19
Protective Facemask Made of Electrospun Fibers



Sonia Javed, Misbah Hameed, Ahsan Nazir, Tanveer Hussain, Nabyl Khenoussi, and Sharjeel Abid

Abstract Personal protective equipments (PPEs) are the tools to protect from various physical, chemical, radiological, electrical, mechanical, and biological workplace hazards, related injuries and illnesses. Among various PPEs, facemasks are used to protect from environmental pathogens and pollution. The COVID-19 pandemic has well highlighted the importance of facemasks. Globally, the demand for facemasks has increased considerably. There are various kinds of facemasks available in the market with different attributes and protection levels. Apart from high filtration efficiency, there are numerous other essential attributes for consideration while choosing an appropriate facemask. These properties include breathability, fit, filtration efficiency, pressure drop, and comfort to the wearer. The first part of this chapter summarized the types of protective facemasks, their fabrication techniques, commercially available products, their efficiency, and the international testing standards for protective facemasks. In the second part, the role of electrospun fibers in protective facemasks has been highlighted. Various nanofibers' attributes that influence protective facemasks' performance have been described, like size and morphology of nanofibers, number of layers, structure, and others. Furthermore, recent advancements in the fabrication of antiviral facemasks have been discussed, which could benefit researchers and industrialists.

Keywords Electrospinning · Facemasks · Nanofibers · Filtration

S. Javed
Government College Women University (GCWUF), Faisalabad, Pakistan

M. Hameed
Institute of Pharmacy, Lahore College for Women University (LCWU), Lahore, Pakistan

A. Nazir · T. Hussain · S. Abid (✉)
Electrospun Materials and Polymeric Membranes Research Group (EMPMRG), National Textile University (NTU), Faisalabad, Pakistan
e-mail: sharjeel.abid@ntu.edu.pk

N. Khenoussi
Mulhouse, France

© The Author(s), under exclusive license to Springer Nature Switzerland AG 2022

A. Vaseashta and N. Bölgen (eds.), *Electrospun Nanofibers*,
https://doi.org/10.1007/978-3-030-99958-2_19

19.1 Introduction

There are various physical, chemical, radiological, electrical, mechanical, and biological workplace hazards in different fields to which the related workers may be exposed at different levels. Apart from taking environmental and engineering measures, personal protective equipments (PPEs) provide health and safety protections for the workers. PPEs are essential devices designed to prevent and avoid workers' exposure to workplace hazards, related illnesses and injuries. PPEs protect both healthcare workers and patients with high risks of transmitting pathogens. Thus, it protects the direct exposure of health care workers to infectious agents by creating a physical barrier to the infectious environment and helps in infection control [22]. PPEs are now considered an essential component of healthcare workers' kits, having the risks of frequent exposures to the pathogenic biological environment. The evolution of the current pandemic has, even more, emphasized the need and regular use of different PPEs. An example of commonly used PPEs is given in Fig. 19.1.

The use of PPE was observed back in the fourteenth century during the outbreak of the Black Death. A hat, shawl, gloves, robe, trousers, shoes, and a walking stick were part of the "beak suit" used by the doctors to treat the plague patients. The use of PPEs has been discussed in various infectious outbreaks like acute respiratory syndrome (SARS), Middle Eastern respiratory syndrome (MERS), Ebola viral disease (EVD), Acquired immune deficiency syndrome (AIDS), and influenza. Plague doctors used protective gowns to prevent contamination while dealing with the plague victims. The Occupational Safety and Health Act of 1970 increased PPEs use in the united states in 1970–80 [23]. It was followed by recommendations published by United States Centers for Disease Control and Prevention (CDC) for the clinical and laboratory workers dealing with AIDS patients [3]. Another CDC recommendation was published in 1985, encouraging the use of PPEs like gowns, masks, and protective goggles to avoid the transmission of blood-borne pathogens [2]. Rules and regulations concerning handling blood-borne pathogens were published in 1991 by Occupational Safety and Health Administration [1].

Protective personal equipment can be categorized on different bases, such as the area of the body on which they are to be used, the type of hazard against



Fig. 19.1 Commonly used PPEs

which protection is needed, or the material or garment used for the synthesis of PPEs. Choice of PPEs depends upon the task to be performed, the level of safety required, and durability. The level of protection provided depends upon the physical and chemical characteristics of the material or fabric used, the shape, size, and movement of microorganisms, and certain other external factors. Examples of commonly used PPEs include bodysuits, coveralls, vests, gowns, helmets, masks, gloves, safety glasses, earplugs, and shoes.

In the current pandemic situation, as the spread of the disease is airborne thus the protection of mouth, nose, eyes, and hands is critical for which masks, face shields, and gloves are commonly used by medical professionals, hospital cleaners, patient and patient visitors or caretakers. As the COVID-19 is a high-risk situation, the use of fluid-resistant or impermeable masks, gowns, or overalls is advised. In addition to that, hand hygiene is highly effective [26]. As was observed in previous coronavirus outbreaks that the virus could survive on PPEs; thus, adherence to standard precautions and removal and disposal of PPEs is also critical [10]. In PPEs, facemasks have more prominent role as these directly block the transmission from a carrier to the healthy person.

19.2 Facemasks

Among PPEs, facemasks are the most commonly used items. Health care professionals use facemasks, clinical and laboratory staff working in healthcare facilities, individuals working in businesses where fumes or dust is produced like pharmaceutical, fabric, chemical industry, and general people also use these facemasks to avoid inhaling dust and smoke. Facemasks are one of the most common and effective non-pharmaceutical interventions (NPIs). Masks provide a simple barrier to help prevent the inhalation and spread of the respiratory or airborne droplets from one individual to another. Facemasks are recommended to be used in the diseases that are transmitted through air droplets. The appropriate use, storage, and cleaning or disposal of masks are essential to make them as effective as possible. Facemasks serve as a physical barrier to particles and respiratory droplets of various sizes. Particles filtered through masks vary in size and shape. This may include pollens in the air (10^{-4} m), airborne dust particles (10^{-6} m), bacteria, and viruses (up to 10 nm). In addition to the filtration capacity, other factors like user ease, comfort, pressure drop, and breathability helps in selecting and using the masks.

The use of facemasks dates back to the bubonic plague of the Middle Ages, where the doctors used beak-like masks filled with herbs like clove or cinnamon to prevent them from the smell of infectious agents, which was then considered to be the cause of the spread of plague [52]. American Lewis Hassley made the first mask in 1848 for the miners. The mask was similar to gas masks.

The history of modern masks starts with the introduction of germ theory and antiseptics. Johann Mikulicz, head of the University of Breslau, Poland, and Paul Berge, a French surgeon in 1897, started covering their mouth and nose with the

gauze mask during the surgical procedure [39]. Until 1910, the use of facemasks was still not every day by surgeons; however, in 1910–11, the era of the Manchurian plague, facemasks were used as a means of protection by health care workers. Later on, the same practice was observed in the influenza pandemic of 1918–19, during which the use of masks became compulsory for medical workers, police forces. Even for the general public in some US cities and cities like San Francisco, the decline in the death rate due to influenza was observed partly due to masks' use [56].

Till 1935, facemasks were used by the majority of the surgeons working in Europe and the US. Then, the search shifted to determine the most efficient type of mask. Initially, masks made up of several layers of gauze with another layer of impervious material held by a metal frame were most popular. They can be easily washed and sterilized hence can be reused. At the same time, the filtering efficacy of the reused masks was also tested and compared with the new masks. It was observed that the reused masks varied in their filtering capacity but still provided protection against infectious diseases. Disposable masks then replaced gauze masks; in the 1960s, cup-shaped disposable masks made of non-woven synthetic fibers were introduced. These masks were better fitted on the face and filter both inhaling and exhaling air, unlike the traditional masks, which only filter the exhaled air. Thus, with this evolution, the reuse of the mask was discouraged, and disposable masks were further developed [56].

Facemasks utilization behaviors are observed in the general population in Asian countries, such as China, Singapore, South Korea, and Japan. This practice of wearing masks has been adopted since the SARS epidemic of 2003. In the current COVID-19 pandemic, many regulatory authorities have stressed to use of facemasks throughout the world. COVID-19 spreads mainly through respiratory droplets. Respiratory droplets spread and travel into the air when an individual cough, sneeze, talk or sing. These droplets can settle on the mouths or noses of surrounding people, or they may breathe these droplets in. The Centers for Disease Control and Prevention (CDC) and the World Health Organization recommend using face masks for the general public to avoid spreading the infection. Facemasks are now mandatory to be used in public places or gatherings where specifically appropriate social distancing cannot be practiced. Thus, the pandemic has increased the utilization of facemasks, as highlighted in Fig. 19.2. Previous studies using population transmission models suggested that the population-wide use of face masks could delay an influenza pandemic [9]. Furthermore, the effects studied in closed settings also suggested that masks can prevent infection spread [34, 67]. Also, facemasks were used in EBOLA, SARS, and MERS outbreaks stressing its effectiveness in the COVID-19 pandemic.

19.3 The Global Market of Facemask

WHO has recommended using facemasks as a strategy to limit the spread of various respiratory infections, including COVID-19. Thus, the demand for facemasks has shown a robust increase in the recent past. The general public's awareness of rising

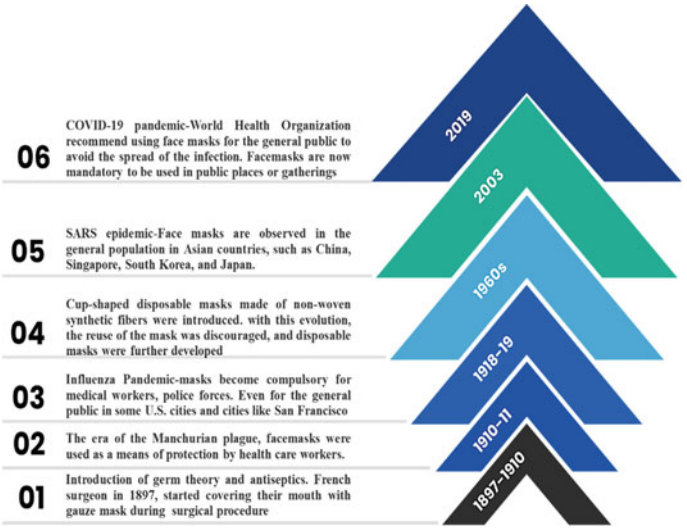


Fig. 19.2 Evolution in the usage of facemask throughout the years

air pollution and airborne diseases has anticipated a boost in the use of facemasks. The increasing infection rate and the strict authorities' guidelines worldwide propelled the increased market demand for face masks. According to WHO, a 40% increase in the production of facemasks is needed to fulfill the global demand for masks. With the spread of the disease, governments worldwide have restricted exports of the masks to compete with their demand, resulting in a shortage of masks in many countries depending on their imports. This resulted in the shortage of masks with hiked prices in many countries [43].

A tremendous increase in the global facemask market has been reported recently. The global market of facemasks was USD 737 million in 2019, which increased to USD 22,143 million in 2021, showing a 448% increase. Among different types, disposable facemasks production leads the market. There is enormous demand ranging from cloth masks to N95. This type includes surgical respirators and dust masks comprising the largest segment of the facemask market, followed by N95 respirators and face shields.

The North American region holds the most significant market of facemasks as the highest COVID cases reported in this region. America was the top importer of COVID-19 critical products in 2020, and 41% of these imports were sourced from China. The European facemask market was more than USD 1.3 billion in 2020 as the pandemic significantly hit Europe, and 140 million cases were reported until April 2021. Consequently, it propelled the demand for the increased production of masks. China is the largest manufacturing country, meeting 50% of the world's demand. China had increased production by 110% to reduce the gap between supply and demand. In China, imports increased by 692.16%, and exports decreased by 22.08% in the first quarter of 2020 due to the COVID pandemic. 56% of the total world's

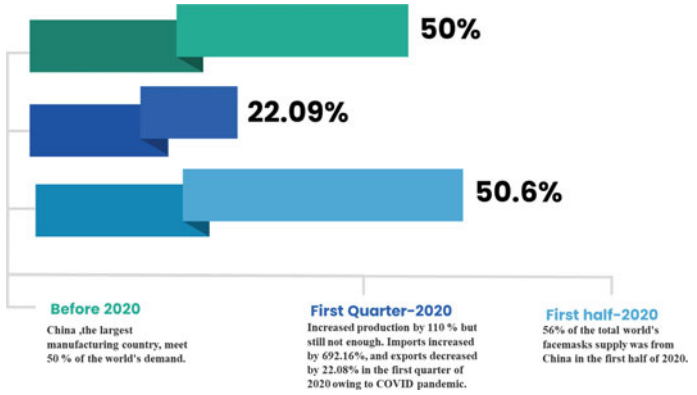


Fig. 19.3 Effect of COVID-19 on the export rate of a facemask in China

facemasks supply was from China in the first half of 2020. Chins immediately sourced raw materials required to ramp up the production of masks, which was almost double that imported during 2019, as demonstrated in Fig. 19.3.

Different organizations are working and helping nations in need to cope up with the shortage of masks. UNICEF and UNO have collaborated with governments and industry to ensure the availability and distribution of masks at acceptable prices and in the required quality, particularly to low-income countries. Since of the pandemic outbreak, UNICEF has provided over 200 million medical masks to more than 100 countries. The major market shareholders in the face masks market in 2020 were the 3M Company, Honeywell International Inc., Louis M, Reckitt Benckiser Group, Shanghai Dasheng Health Products Manufacturer Company Ltd. MSA, Gerson Company, Inc., Kimberly Clark Corporation.

The global facemask market is predicted to maintain its growth even after the COVID pandemic is over because of the rising concern of the general public related to health and safety and increased demand for facemasks from health care institutions and professionals. Besides conventional surgical and fabric masks, research is diverted to prepare more innovative antibacterial facemasks to combat infectious agents.

Surgical facemasks and N95 respirators are disposable thus have a recurrent demand. They are ineffective after a certain period as the external surface gets covered with germs, and the moisture by exhaling decreases filtration efficacy. Surgical masks can be used for a maximum of 4 h, and N95 can be used for up to 24 h. An increase in the use of masks has also called in some environmental issues. Most of these masks are made of synthetic polymers, which are also non-biodegradable. These masks contain 90% plastic material; thus, their disposable has become an environmental hazard. Thus, the best approach may still be reusable masks to overcome the shortage and address environmental hazards.

19.4 Types of Facemasks

Different types of facemasks are in use ranging from cloth, cotton masks, medical or surgical and N95, N99, N100, P2, and P3 respirators. The evolution in the types of facemasks continued with outbreaks of several infectious diseases, with the rise of industrialization, smoke, and smog. Masks are differentiated into various types depending upon their design and intended use. The products or materials used in facemasks keep improving for better filtration of pollutants, bacteria, and viruses.

Factors affecting filtration capacity of facemasks,

- Size of filtrate: The choice and selection of masks depend upon the size of the particles needed to be filtered. As already discussed, the size of particles presents in the air that needs to be filtered varies from 100 μm to 10 nm in size. Larger particles drop on the ground while smaller particles remain suspended for some time before settlement [24, 25]; thus, the material and pore size of the mask are important factors that affect the selection of one type of facemask over the other.
- Material of the mask: There are different types of materials that are used in facemasks. The combination of materials used, several layers used, the use of filters, and the strength of weaving determines the filtration capacity of masks.
- Mask fitting around the face: face masks should create a seal around the mouth and the nose to prevent the entry of unfiltered air and should not be uncomfortable to the wearer.

Furthermore, facemasks are broadly divided into two major categories,

- Medical (professional respirators (N95), surgical and non-surgical face masks)
- Non-medical (homemade masks and filtered masks)

19.4.1 Non-medical Masks

Non-medical masks are homemade cloth or fabric masks, as shown in Fig. 19.4. These masks are made from various woven and non-woven materials such as Cotton, Polypropylene, Cellulose, Polyester Gauze, and Silk. Fabric masks made of tightly woven cotton with high thread count sheets, a mixture of fabric like cotton and flannel, or cotton and chiffon arranged in multilayers can provide filtration against novel coronavirus. These masks are made from everyday materials of low cost and can be used as an additional voluntary measure. Although non-medical cloth or fabric facemasks are neither a medical device nor personal protective equipment, they help to limit the spread of infectious agents by controlling the droplets while sneezing, coughing, or talking [20].

These masks are commonly used but not recommended to be used in health care settings. These facemasks are good enough to protect against the inhalation of common airborne particles (dust, pollens, bacteria). However, they may not be that efficient in controlling the spread of viral contaminants like coronavirus. The



Fig. 19.4 Non-medicated fabric facemask

efficacy of non-medical face masks has always been questioned as not much evidence is available on their filtration efficacy compared to medicated masks. A study stated that non-medicated masks have a percentage efficacy ranging between 49–86% for exhaled particles of 0.02 μm size, while medicated masks are 89% efficient to filter identical particles [24, 25]. When compared to surgical masks and N95, they have less filtration efficiency. However, even then, the CDC recommends using cloth masks by the general public. It reduces the risk of community spread of disease, especially by those who are asymptomatic or pre-symptomatic.

Konda et al. reported that the filtration efficacy of these masks depends on the combination of different materials used in multiple layers [31]. The filtration efficiency of multiple hybrid layers is much more than single-layer due to the combined electrostatic and mechanical filtration. Several factors affect the efficacy of non-medical masks, like poor fluid resistance, inadequate sealing around the mouth and nose, and frequent readjustments. Even then, WHO has suggested that non-medicated masks are made up of tightly-woven multiple layers of cotton or linen that can be used.

In the current COVID-19 pandemic, WHO recommends using non-medical face-masks by the general public under the age of 60 and with no underlying health risks. These masks can be cleaned by washing with a detergent or soap, preferably with hot water (at least 60 °C). If not possible to use hot water after washing with soap, it should be boiled for at least 1 min. If the mask is dirty, wet, or torn, it should be discarded. Non-medical face masks are locally manufactured worldwide and are readily available; thus, they are not adequately regulated. These fabric masks vary broadly in type and quality thus are not subject to regulation.

19.4.2 Medical Face Masks

Medical masks include surgical masks and N95 respirators. Non-woven fibrous mats of wool felt fiberglass or polypropylene are used in these masks, as shown

in Fig. 19.5. The material forms a tortuous pathway resulting in the adhesion of particles to the fibers without blocking the open spaces, thus allowing air to cross the filter easily. Surgical masks are single-use disposable masks commonly used by health care workers. These masks vary in design but are often flat, rectangular with folds or pleats on their surface. On the top side, there is a metal strip that helps in good fitting around the nose. These masks completely cover the mouth and nose, but they are usually loose fitting and do not prevent leakage, especially around the nose, thus providing complete protection against germs.

It is made up of non-woven fabric with better filtration, air permeability and is less slippery when compared to woven fabric facemasks. These surgical masks are commonly made up of polypropylene, polystyrene, polycarbonate, polyethylene, or polyester, having 20 or 25 g per square meter (gsm) in density. Generally, they are composed of three or four layers with filtration layers sandwiched in the Middle. Typically, a layer of textile with non-woven bonded fabric on both sides and available in different thicknesses with various levels of fluid resistance and filtration efficacy. The filtration capacity of these masks depends on the fiber type, the way it is manufactured, the structure of the web, and the cross-sectional shape of fibers. It may or may not contain electret-filtering media. Surgical masks provide reasonable protection against large airborne particulates like bacteria, splashes, or splatter containing germs.

N95 are respirators recommended to be used by health practitioners. The N95 masks are made up of wonderful fibers of melt-blown non-woven fabric. The most commonly used respirators are N95, where N is a Respirator Rating Letter Class. It stands for "Non-Oil," meaning that it can be used in an environment if no oil-based particulates are present. Other masks ratings are R (resistant to oil for 8 h) and P (oil proof). The number 95 means 95% efficiency. Masks ending in number 99 mean 99% efficiency. Masks ending in 100 are 99.97% efficient same as that of the HEPA filter. According to the Centers for Disease Control and Prevention (CDC.), these respirators filter out dust, fumes, and airborne pathogens of size up to 0.3 μm or larger droplets. These masks are composed of electrostatic non-woven polypropylene



Fig. 19.5 Surgical facemask



Fig. 19.6 N95 facemask

fiber. Some N95 masks have an optional exhalation valve to reduce the exhalation resistance for the wearer's comfortable breathing, as shown in Fig. 19.6.

It fits tightly to the face without providing any gaps, thus preventing the entrance of unfiltered air. The edges of these masks are made to seal the nose and mouth of the wearer completely. The N95s are typically composed of electret filter media. These respirators are defined and regulated based on their filtration capacity.

All masks should be cleaned or replaced when damaged, wet, dirty, contaminated (e.g., blood, respiratory fluids), or when breathing through it becomes problematic. Ensure to clean the mask between the uses if reusing is permitted or discard it properly if reuse is not recommended.

19.5 Properties of Facemasks

19.5.1 Filtration Efficiency

The first and foremost feature of the facemasks is their filtration efficiency. Whether using a fabric mask, surgical mask, or N95, it must provide an extra level of protection against airborne particulates and germs. The filters must be dense enough to stop the passage of small particles, also must be comfortable and breathable without causing discomfort to the user. As the size of the airborne particles varies largely, so does the filtration efficacy of various masks.

19.5.2 Face Fitting

The masks must provide a snug fit around the nose, nose to chin, mouth, and backward towards the ears. The fitting must be comfortable enough not to need to be removed

when working and allow easy breathing. Masks having gap lines between the face and the mask's edges will ultimately allow some unfiltered air to pass through. Properly sealed masks allow all the inhaled air to pass through the filters without leaving any slippage or leakage of inhaled or exhaled air.

19.5.3 Breathable

Facemasks must allow comfortable breathing without causing excessive sweat to the wearer. As masks are to be worn for hours during work, they must not cause gasping to the wearer. At the same time, it must keep in the exhaled air and particulates during talking, coughing, or sneezing. In the current pandemic, masks are required to be used continuously by the health care workers and people working in public places, so they must be breathable without causing any discomfort or hurdle in breathing, which may lead to the lack of compliance by the user and hence increases the chances of contamination.

19.5.4 Fluid Resistance

The masks should have good resistance to fluids, especially when at risk of blood, bodily fluids, or splatter. During coughing or sneezing, there are increased chances that masks become wet with the saliva. Health care workers are more commonly exposed to this kind of risk; thus, it is recommended to use fluid-resistant masks. The fabric mask is wetted easily thus needs to be washed for reuse, while surgical and N95 masks are made up of material that is resistant to fluids.

19.5.5 Reusable

As in the current pandemic, masks are the "new normal" and are recommended to be used by all, especially when in gatherings; thus, masks have a recurrent use, for which reusable masks are preferable. The colossal waste of used masks is being produced daily, dumping of these facemasks is causing new environmental hazards, especially for marine life. Thus, reusable masks are encouraged to be used where ever possible by the general public.

19.5.6 Audible

The masks should not hinder the voice quality of the wearer, and the individual using them must be audible clearly and does not need to lift it during verbal communication.

19.5.7 Durable

Masks must be used for hours during routine work, so they must be strong enough to withstand wear and washing daily rigors. They must not shed any particles that can cause breathing discomfort to the wearer. The ear loops must be strong enough to remain intact throughout the use period. Features of non-medical and medical types of face masks are summarized in Table 19.1.

19.6 Characterization Techniques for Facemasks

ASTM International, formerly known as the American Society for Testing and Materials, is an international standards organization. It formulates and publishes technical standards for different materials, products, systems, and services. PPEs are under the scope of ASTM International's committee on personal protective clothing and equipment (F23) and its subcommittee on biological (F23.40). Medical face masks are tested according to the standards of ASTM. The basic tests include filtration efficiency (F2101), differential pressure (EN 14,683), sub-micron particulate filtration efficiency (F2299), resistance to penetration by synthetic blood (F1862), and flammability (16 CFR Part 1610). Fabric face masks are being produced worldwide. Even household fabric masks are in use these days. However, these masks are not subjected to any testing. Few studies have been published to access and compare specific characteristics of fabric masks to medical masks.

19.6.1 Bacteria Filtration Efficiency In Vitro (BFE)

The primary function of all kinds of masks is to protect against airborne droplets (germs), which are checked by invitro bacteria filtration test. For this, an aerosol-containing bacterial suspension (*Staphylococcus aureus*) is sprayed on a mask at 28.3 l per minute which ensures the mask can be exposed to the percentage of bacteria during use. ASTM specifies testing with a droplet size of 3.0 μm for which *Staphylococcus aureus* has an average size ranging between 0.6–0.8 μm is used. For surgical masks, 95% of bacterial filtration efficiency is required. Then the capacity of the mask to filter out bacteria is measured by drawing aerosol droplets through a

Table 19.1 Features of medical and non-medical facemasks

Features	Non-medical (cloth masks)	Medical (surgical masks)	Medical (N95 respirator)
Filtration efficiency	Do not provide a consistent shield against airborne small size particulates	Do not provide a consistent shield against airborne small size particulates	Provide a 95% protection against airborne large and small size particulates
Material	Made up of a variety of materials ranging from cotton, chiffon, Polypropylene, Cellulose, Polyester Gauze, and Silk, Woven	Made up of polypropylene, polystyrene, polycarbonate, polyethylene, or polyester, Non-woven	Made up of polypropylene, cellulose, polyester, non-woven
Face fit	Depending upon the design, and material may fit tightly across the mouth and nose but do not provide a complete seal. No face fit testing required	Do not fit completely as gaps are left between mask edges and face, do not provide a seal, no face fit testing is required	The edges of the mask make a complete seal on the face, tested for face fit
Authorization and approval	Not authorized or has any approval body. WHO and CDC encourages the use of adequately designed cloth masks	Cleared by FDA, not authorized by NIOSH	Approved by NIOSH after evaluation and testing
Fluid resistance	Not resistant to fluids	Resistant to fluids	Resistant to fluids and tested against standards
Leakage	As do not provide a complete seal thus leakage occurs across the edges when the wearer exhales	As do not provide a complete seal thus leakage occurs across the edges when the wearer exhales	Provide a complete seal; thus, no leakage occurs across the edges when the wearer exhales

six-stage Andersen sampler for collection. The number of bacterial aerosol droplets that contact the mask is determined by conducting challenge controls without filter medium in the test system. Challenge controls are carried out at 1700–3000 colony-forming units (CFU) with a mean particle size (MPS) of 3.0 ± 0.3 μm. This allows filtration efficiencies to be reported up to >99.9%. The ratio of the number of bacterial aerosols challenging the mask versus the amount that could penetrate the mask is calculated.

19.6.2 Differential Pressure Test

BFE testing is usually performed along with the Differential Pressure (Delta P) test. This test is the measure of breathability in which the airflow resistance of the mask is calculated. It is the measure of differential air pressure on both sides of the test mask with the help of a manometer, at a constant flow rate of 8 L/min Delta P is measured in H_2O/cm^2. According to ASTM, low values mean more breathable masks; thus, Delta P-value of 4.0 or less means low barrier masks, while values less than 5.0 means high or moderate barrier masks.

19.6.3 Particle Filtration Efficiency

Also known as the latex particle challenge, which is the measure of filtration efficiency of the mask filter media to nonviable particulates. The test is performed by spraying an aerosol of polystyrene microspheres with monodispersed particle size with a mean diameter of 0.1–5 μm. The aerosol produced is passed through a charge neutralizer and mixed with preconditioned air resulting in a stable, neutral, and dried aerosol of microspheres. Particles are then counted with a particle counter. Particles tend to clump together in the air. Charge neutralization prevents the particles from clumping in air and behaving erratically due to electrostatic charge and electrostatic cling.

19.6.4 Breathing Resistance

This test is conducted to ensure that the mask will hold its shape and will provide proper ventilation while the wearer breathes. Breathing resistance is observed by airflow at the mask, then calculating the difference in air pressure on both sides of the mask.

19.6.5 Splash Resistance

Splash resistance tests measure the mask's ability to resist the fluid concentration that could transfer across the layers of the mask as a result of splash or spray. All medical face masks should resist liquid penetration, which depends on the surface tension and viscosity of the fluids themselves, the structure and relative hydrophilicity or hydrophobicity of the material used, and the mask's design. Medical masks are splashed with simulated blood with specific forces similar to human blood pressure to ensure that liquid cannot pass through the mask. For this, 2 ml of simulated blood

is splashed with the help of a cannula at the center of the test mask. The other side of the mask is then observed for the simulated blood penetration. According to ASTM specifications, simulated blood at different velocities corresponding to human blood pressure 80 mm Hg (venous pressure), 120 mm Hg (arterial pressure), and 160 mm Hg (high pressure irrigation) is used. If the mask show resistance to the highest pressure, there is no need to perform the test with lower pressures. The surface tension of blood and other body fluids ranges between 42–60 dynes/cm; however, to increase the wetting characteristics of synthetic blood, surface tension is adjusted to the lower limit(40 ± 5 dynes/cm).

19.6.6 Flammability

Several elements of an operating room can easily cause fire as it contains oxygen, heat, and fuel sources. Thus, surgical masks are tested for flame resistance or time of flame spread. For this, the test masks are being set on fire, and the time it catches fire and how long it takes to burn is noted. According to standards, all the masks used in a hospital setting must withstand exposure to fire (within a specified distance) for three seconds.

19.6.7 Biocompatibility and Toxicological Risk Assessments

All medical face masks are required to be tested to an international standard (ISO 10993-5, 10) for cytotoxicity and skin sensitivity to ensure that no materials that come in direct contact with the user's skin are harmful. Among these test cytotoxicity, sensitization, and irritation tests are most common to measure the presence of any toxic, leachable material.

19.6.8 Additional Test for Respirators (N95)

19.6.8.1 Sodium Chloride Aerosol Challenge

The Sodium Chloride Aerosol Challenge test is down to ensure the filtration efficiency measurements up to 99.999%. For this test, an automated Filter Tester reservoir is used and is filled with a 2% NaCl solution. The test samples are sealed on a cylinder filter holder, and aerosolized NaCl is sprayed on the sample. The concentration of NaCl that passes through the sample is measured and is used to calculate the filtration efficiency of the sample. The respirators are kept at $85 \pm 5\%$ RH and 38 ± 2.5 °C for 25 h before the filtration efficiency test. As there are three categories for NIOSH-certified, nonpowered, air-purifying, particulate-filter respirators: N (Not resistant to

oil), R (resistant to oil), and P (oil proof), this test using NaCl aerosol is done for the N series. For evaluation of the R or P series, oil-based aerosols are required to be used.

19.6.8.2 Dioctyl Phthalate (DOP) Challenge Test

The DOP aerosol test is used to evaluate air flow resistance and particle penetration properties of respirators. The test is performed using an Automated Filter Tester in which aerosol of DOP is employed. Samples are tested at flow rates up to 90 l per minute and can measure filter efficiency up to 99.999% for particle size in the range of 0.3 μm.

19.7 The Effect of COVID-19 on Demand for Facemasks

The usage of personal protective equipments (PPEs) has become essential for healthcare workers to prevent infection and continue the proper functioning of healthcare systems. The monthly need for PPEs for medical workers alone estimated by World Health Organization was 76 million gloves, 89 million masks, and 1.6 million goggles. Consequently, the global demand for facemasks surged, as demonstrated in Fig. 19.7. However, with the growing spread of COVID-19, the public need for PPEs to prevent the transmission of the virus cannot be quantified in number at such a wide scale. In an estimation for the monthly need for PPEs, a country with 60.4 million people requires about 0.5 billion gloves and 1 billion face masks [50]. The scientists suggested that using facemasks can potentially reduce the risk of virus transmission, and it has become mandatory to wear facemasks in public spaces. From a cost perspective, it has been estimated that marginal benefit from a single cloth mask ranges between 3000 and 6000 US$ [25].

In 2020, the market value of facemask rose from 0.79 billion US$ in 2019 to 166 billion US$. To fulfill the critical need for a facemask, the global production of the facemask has increased many folds. As the leading producer of facemasks, China's production increased 12 times higher than usual, 116 million per day [13]. However, the disposal of such a large quantity of facemask has become a concern. It has become additional plastic disposal and environmental litter in aquatic and terrestrial environments [44]. The highly recommended N95 masks are polyethylene terephthalate (PET) and polypropylene (PP). The surgical masks and gloves are also made of non-woven materials incorporated polymers like PET, PP, and polyethylene. Such material causes severe damage to the environment by blocking sewerage systems, adverse effects on water percolation, and detrimental effects on agricultural soil. The size, type, and shape of polymer used are important factors to keep in mind for producing plastic material [48].

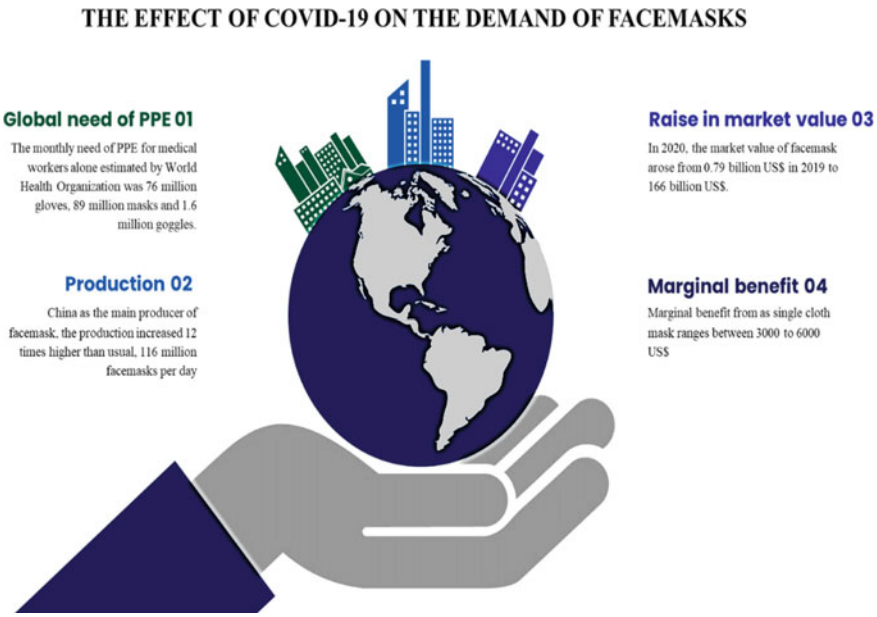


Fig. 19.7 Effect of COVID-19 on the global demand for a facemask

19.8 Electrospun Nanofibers

Electrospinning is an effective and advanced technique with several advantages over other methods, and polymeric nanofibers can be prepared. Such as;

- A cost-effective and straightforward technique
- Can easily incorporate bioactive compounds in nanofibers
- Beneficial for sensitive compounds as heating does not require during the process [28].

The electrospinning process (Fig. 19.8) has five main components to produce nanofiber materials: power supply-high voltage, a system to take polymeric solution, a reservoir, a needle or needless dispensing unit, and a collector. The high voltage is applied between the collector and needle, which aids the polymeric solution to travel towards the collector. Due to unstable motion, the solvent evaporates and polymer stretching followed by deposition on the collector. Characteristics of polymeric solution and process parameters like the viscosity of the solution, conductivity, concentration, humidity, temperature, and atmospheric pressure affect the structure and morphology of nanofibers [45].

The concentration and viscosity of polymer solution affect the size, diameter, and production efficiency of nanofibers. To run an electrospinning machine, only a small amount of solution is required. The concentration of polymer solution needs to be optimized to achieve a uniform and smooth nanofiber. If the concentration of the

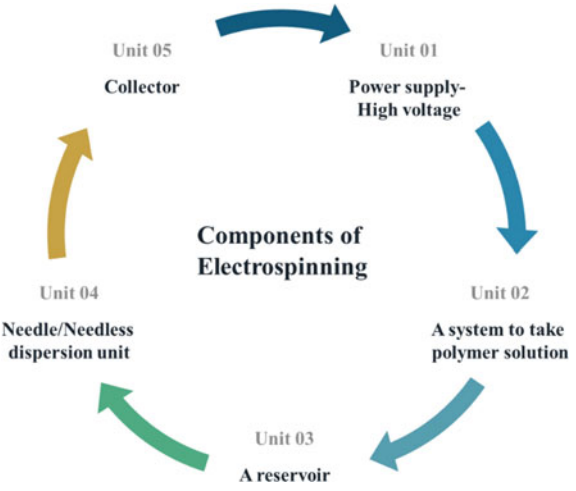


Fig. 19.8 Basics of an electrospinning set-up

solution is too low, it results in the formation of beads, whereas the diameter of fiber increases at a very high concentration [40]. The viscosity of the solution is another factor that influences the morphology of nanofibers. Highly viscous solutions are challenging to be pumped via capillary, dried up on the tip of the needle. If the viscosity is low, it results in the dropping of polymer solution on the collector. The molecular weight of the polymer is a crucial factor that influences the viscosity of the solution [51].

In a study on chitosan, nanofiber mats were prepared via electrospinning to evaluate the effect of polymer solution viscosity. Acetic acid (5% v/v) was used as solvent and polyethylene oxide as a copolymer. Morphological analysis of nanofibers indicated that smooth and homogenous fibers were formed as the polymer solution concentration increased from 2.5 to 3.5% [17]. Some polymers are difficult to handle while electrospinning, like alginate. Therefore, they are blended with a carrier polymer which changes the solution properties (viscosity and surface tension). Alginate is blended with polyethylene oxide (PEO) or polyvinyl alcohol (PVA) to prepare a stable solution by hydrogen bonding between ether and hydroxyl group. Thus,the addition of co-polymer changes the solution properties and makes electrospinning desirable [57].

19.8.1 Properties and Application of Nanofibers

Electrospun nanofibers have unique characteristics like large surface area, small pore size, high porosity, which make them useful in various applications, including air filtration membrane, drug delivery, tissue engineering, and wound dressings. Due to the unique properties of nanofibers, they have been used in extensive applications such as biomedical, drug delivery, air filtration, photoelectric cells, and textile

materials [28]. Nanofibers loaded with antitumor drug (cisplatin) were prepared using polycaprolactone (PCL) and chitosan blend. In vivo antitumor analysis indicated that prepared nanofibers could be used as a promising drug carrier. It reduced the tumor from 4.65 to 2.79 mm^3 within 14–21 days, compared with control (free cisplatin) 5.16 and 4.75 mm^3 [4]. Heparin, a drug that controls blood clotting, was loaded in electrospun nanofibers of PCL. After 14 days, a controlled release of the drug was observed. Heparin was observed to be homogeneously distributed throughout the nanowebs, and about half of the drug was released within 14 days [21].

Multilayer nanofibers have also been prepared to form delayed-release nanofibrous structures. Five layered poly(L-lactide) containing cisplatin was formed and evaluated for drug release. A delay in drug release was observed compared to single-layered nanofibers, which are beneficial in preventing liver carcinoma relapse (a state where few cancer cells survive initial treatment) [49]. Electrospun nanofibers are also used in optical sensory applications like toxic gas sensors, biosensors, pH sensors, heavy metal sensors, and temperature sensors [61]. Food and packaging material made of natural polymers provided longer shelf life to the food material. The addition of antioxidant materials to the packaging can prevent the deterioration of food quality. Nanofiber packaging material infused with deoxidizing agents prevents the rotting of food, oxidation cause spoilage of food [32]. Nanofibers blended with herbal extracts are gaining progress due to their application in wound healing. Herbal extracts are said to be a suitable replacement for antibiotics to prevent side effects. Herbal extracts contain compounds that help in accelerating the wound healing process. Moreover, they are suitable for cell adhesion, hydroxyproline formation, and skin regeneration [47]. Similarly, these nanofibers are being used for filtration applications with a high efficiency compared to the conventional filtration assemblies.

Applications of electrospun nanofibers incorporated with active substances are presented in Table 19.2.

Table 19.2 Applications of electrospun nanofibers incorporated with active substances

Electrospun material	Active substance	Application	References
Hydroxypropyl β-cyclodextrin (polymer-free)	Vitamin E	Healthcare and food pharmaceuticals	[11]
Polyvinyl alcohol	Aloe vera	Protective clothing-Antimicrobial material	[30]
Polyacrylonitrile	silver	Air filtration membrane	[8]
Polyvinyl alcohol/polyvinyl alcohol, soluplus	Natural extract of *Angelica gigas*	Oral Drug Delivery (Cancer therapy)	[42]
Polyacrylonitrile	graphene oxide	Water treatment	[35]
Chitosan, polyethylene oxide	Insulin	Drug delivery	[33]
Polycaprolactone/collagen	Gehlenite Nano-powder	Bone tissue engineering	[18]

19.8.2 Use of Nanofibers in Filtration Applications

Filtration membranes are effective in controlling and preventing air pollution. Nanofiber-based filtration membranes are used in different filtration applications, mainly in combination with other filtration materials. In comparison to a typical surgical mask, nanofibers have high filtration efficiency against nanoscale air particles. Nanofibers' properties, such as fine porous structure, high surface to volume ratio, high strength, and high surface energy, added to the higher filtration efficiency and pressure drop in nanofiber filtration membranes. A non-woven bifunctional facial mask was prepared using polyetherimide via electrospinning [65]. This kind of mask has the property of removing particulate matter by generating electricity.

Apart from outdoor pollution, indoor air quality is also a concern, especially in hospitals where a dust-free and antiseptic environment is needed. Electrospun nanofibers incorporated with antibacterial and antiviral bioactive substances are a good choice for indoor air filtration membranes that keep the air circulation system clean from bacteria, viruses, and other air contaminants. Moreover, these nanofiber membranes are helpful as an alternative to air filters at industrial units. Electrospun membranes are capable of adsorbing more air pollutants than conventional air filters. Nanofiber filter membranes are cost-effective, can easily be cleaned by backflushing and reused [36].

19.8.3 Use of Nanofibers for Facemasks

The typical facemasks are prepared by using electrostatic filter media. However, nanofiber masks have superior properties like higher filtration efficiency, smaller pore size, and more significant pressure drop; thus do not lose efficiency over time. Different types of nanofibers-based facemask are under research [19].

19.9 Nanofibers as Sole Facemasks

Nanofibers are an excellent replacement for typical facemask due to their higher filtration efficiency. Normal microfilters are not efficient against viruses, mainly in the range of 20–200 nm, but such viruses can easily be filtered with an efficiency of 99% by nanofibers [41]. Nanofiber filters can adsorb nanosized and submicron particles, and aerosol particles fall in this range. However, utilization of pure nanofibers without any backing material has rarely been reported. Thus, they are either deposited on another susbstrate (mask) or its layer is incorporated (sandwiched) in other layers to increase the protection levels.

19.9.1 Nanofibers Coatings on Facemasks

With the increasing demand for a facemask, disinfecting and reuse of N95 filtration is a primary concern. For this purpose, several coatings were applied to the filters, which helped in disinfection and provided additional properties to the filter. A reusable graphene and silver nanoparticles coated facemask has been developed by the dual-mode laser-induced forward transfer method. Graphene provides hydrophobic property to the mask, which enables it to bounce off the aqueous droplets. After photothermal sterilization at 80 °C under sunlight, the mask is sterilized and can be reused. Silver nanoparticles coating provided silver ions that stopped microbes in respiration droplets and provided better protection against viruses. This technology has been applied to N95, which enhanced its properties. However, from a cost perspective, these masks limit their use for the public [69]. Even though nanocoating provided additional properties to the facemask, there have been several reports on discomfort and thermophysical responses of nano-treated surgical and N95 masks. It has been reported that wearing nano-treated masks lowers the heart rate of the subject. It is due to an increase in temperature of the outer surface of the nano-treated mask compared to N95. However, in the nano-treated surgical masks skin temperature was lower compared to N95 mask. Humidity inside the mask surface was also lower in nano-treated surgical masks compared to N95 [60]. Facemasks coated with superabsorbent nanofibers were prepared using polyvinyl alcohol and superabsorbent polymer (PVA/SAP). To evaluate the air permeability and virus protection, prepared nanofibers were coated onto commercially available typical facemasks via electrospinning. Results indicated that nanofiber coating decreases the air permeability, which is helpful to prevent virus transmission and high hydrophobicity, can absorb sweat in vaporous form, and added comfort to the wearer [55].

19.9.2 Nanofibers from the Synthetic Origin for Facemasks

Natural polymers are normally hydrophilic which increase their chances of virus adherence due to humidity. As facemask is used to stop the transmission of the virus can become a virus collector through repeated breathing, specifically when contaminated droplets come in contact with the outer surface. Thus, the viruses can survive in a humid and warm environment for a more extended period and penetrate the fabric [58]. Thus, the additional synthetic polymeric nanofiber-based layer could enhance the protection (being hydrophobic). When combined with facemask, Nanofibers enhanced the filtration property and affect the capability of the viruses that interact with them. Polymers that are commonly used for facemasks include polyester, polyethylene, polycarbonates, and polyamides. Polypropylene does not absorb moisture thus considered very useful in facemask application. Similarly, polyester woven fabrics are hygroscopic and can maintain a static charge longer than natural fibers [31].

Furthermore, the addition of polymer coatings like polyethyleneimine can damage the structure of the virus due to polycationic hydrophobic coatings. Electrostatic and hydrophobic interactions destroy the viral structure by causing leakage in viral RNA [46]. Polyacrylonitrile has been used to produce three different nanofiber membranes for air filtration embedded with zinc oxide, silver, and titanium oxide. Their filtration efficiency was observed for NaCl aerosol particles of size ranging from 9–300 nm. Minor fiber diameter was attained by titanium oxide-containing nanofibers resulted in 99.9% filtration efficiency. However, a higher-quality factor was observed in silver-containing nanofibers, greater than commercially available facemasks [8].

19.9.3 Nanofibers from the Natural Origin for Facemasks

Environmental concerns regarding the disposal of synthetic polymer-based materials lead to bio-based media to produce nanofibers for medical applications. Biodegradable materials decompose into carbonaceous soil, water, and non-toxic gases over time via natural biological procedures [5]. Gelatin is a biopolymer produced from partial hydrolysis of collagen that is present in numerous biomaterials. Gelatin has been used in various medical applications like wound healing, drug delivery, and tissue engineering. Nanofibers made from gelatin were studied to be used as air filtration media. The cross-linked gelatin nanofibers showed better mechanical properties, equivalent filtration performance, and excellent environmental stability [14]. Gelatin and β-cyclodextrin containing nanofibrous mats were made to be used as air filtration media for various applications, including filtration of nanosized viruses. Gelatin/β–cyclodextrin nanofibers were found to capture 0.3–5 μm aerosols having <95% air filtration efficiency at 0.029/Pa quality factor. They absorb a significant amount of benzene (242 mg/g), formaldehyde (0.75 mg/g), and xylene (287 mg/g), volatile organic compounds (VOCs). The VOCs adsorption property was higher than the commercial facemask [27].

Nanofibers produced from biodegradable material, Cellulose acetate (CA), and cationic surfactant cetyl pyridinium bromide (CPB) were used to retain aerosol particles. Some of the extensively used biodegradable polymeric materials for filtration application are shown in Fig. 19.9. The average diameter of CA/CPB nanofibers was 239 nm with 100% filtration efficiency of aerosol nanoparticles and permeability of about 10^{-9} cm^2, which may include black carbon and coronavirus. The retention efficiency for black carbon particles was 60–90%, depending upon particle size [16]. Poly (L-lactic acid), a biopolymer, was electrospun to prepare an air filtration membrane having high filtration efficiency against (particulate matter) PM2.5 (95%). PLLA electrospun fibers generate electrostatic forces that aid in the adsorption of submicron particles [66].

Electrospun nanofibers prepared from poly (vinyl alcohol)/cellulose were considered biocompatible, reusable, and used as a filter for PM removal [68]. A by-product of cereal industries, wheat gluten, is a biopolymer used to produce nanofiber filter media for facemasks. Gluten degrades into nitrogen-based components and acts as



Fig. 19.9 Biodegradable natural polymers for air filtration

a soil conditioner. Thus, prevent the environment from microplastic contamination [15]. Nanofibrous filter was prepared from poly(lactic acid), a bio-based polymer, to be used as facemask filter. It exhibited greater filtration efficiency of PM0.3—99.996%, which is greater than commercial filter N95 [62]. Poly(butylene succinate) is a well-known biodegradable polymer used to produce nanofiber to capture the particulate matter and microfiber mats to reduce pressure drop. Chitosan was coated on these fibers as a nanowhisker. Chitosan contains polar amide groups and cationic sites which attract the ultrafine PM like NO_3^- and SO_4^{2-} [12].

19.9.4 Composite Nanofibers for Facemasks

In recent years, nanotechnology's most highly developed research area has been composite-based nanofibers due to their enhanced properties like thermal stability, electrical conductivity, and dimensional stability. Nanocomposites are consisted of two or more different chemical structures, having one of the two a nanometric constituent. Due to nanocomposites' improved chemical and physical properties, they have been used in various applications, i.e., sensors, intelligent materials, biomedical, filtration, and biotechnology [53]. Production of composite nanofiber air filter membranes for facemask is a new approach. Polyurethane polymer and polyvinyl chloride mixture were used to develop composite air filter membrane having good air permeability 706.84 mm s^{-1}, excellent tensile strength (9.9 MPa), slight pressure drop (144 Pa), and greater filtration efficiency (99.5%). However, higher filtration efficiency of 99.99% was achieved by fabricating composite membranes with

PAN and Nylon 6. Properties like superoleophobicity and superhydrophobicity of composite nanofiber membranes are tunable as per requirement [63].

19.10 Properties of Nanofibers that Influence the Facemasks

The physical properties of nanofibers like ultrathin diameter and high porosity, fiber structure, and morphology greatly influence the filtration efficiency of nanofiber filters. Characteristics of nanofiber mats like small fiber diameter and large surface area impart other advantages as well. The pore size and mechanical stability of nanofibers are tunable, which helps in the selective production of nanofibers according to the application [38].

19.10.1 Influence of Fiber Diameter on Filtration Efficiency

The diameter of nanofibers greatly influences the filtration efficiency of nanofiber filters. The main parameter that influences the fiber diameter is the concentration of the solution. As the concentration of a solution is directly related to the viscosity, the lower the concentration of polymer solution, the lower the viscosity, resulting in resistance to fiber deformation when high voltage is applied. However, with a high polymer solution concentration, high viscoelastic forces can be attained, resisting elongation during the formation process. Polyethylene terephthalate (PET) is a resin of polyester used in nanofiber air filtration membrane formation. Two different concentrations of PET were used to verify the average diameter of nanofibers (20 and 10%), keeping other parameters constant. A decrease in diameter from 3.25 to 0.65 μm was observed with the decrease in PET solution concentration. On the other hand, increase in mechanical strength and formation of denser fibers was observed. A denser network of nanofibers has a small pore size which prevents the air particles and microbes from passing through it [6].

19.10.2 Influence of Fiber Morphology on Filtration Efficiency

Structure and morphology are other vital factors that influence filtration efficiency and performance of electrospun nanofiber filters. On modification in experimental parameters like applied voltage, solution concentration, humidity, and distance between needle and collector, nanofibers with desired morphology are prepared to be used in various filtration applications [8]. In a study on the morphology of nanofiber

filter membrane made by poly(silsesquioxane) (PSQ)-immobilizing poly (lactic acid) (PLA-PSQ), results indicated that beads distributed evenly between the fibers and increased the inter-fiber distance that reduced the pressure drop [37]. The bead on string structure nanofiber membranes showed relatively lower pressure drop and higher filtration performance. It is due to the increase in inter-fiber distance that decreases the volume fraction of fibers which allows the airflow through the filter.

19.10.3 Influence of Porosity on Filtration Efficiency

Filterability and breathability of facemask depend on porosity and surface area of fibers. These two properties can easily be controlled during the formation of nanofibers. By changing polymer solution, collector geometry, and spinning nozzles, the porosity of the nanofibrous mat can be tuned. The collection method of nanofibers also influences the breathability and porosity of nanofibers which can be adjusted by controlling the time and geometry of fiber collection during spinning [59]. Nanofiber filter membrane prepared from polycaprolactone (PCL) showed a decrease in pore size from 5.72 ± 0.62 to 1.42 ± 0.34 μm as compared to a commercial mask (Henry Schein Earloop Procedure Mask). The diameter of the commercial mask was 48 times greater than an average microorganism (~120 nm). Thus, the PCL containing a nanofiber membrane was said to be more effective against viruses [29]. The addition of different concentrations of nano-clay to the Polyvinylpyrrolidone (PVP) significantly influences the fiber pore size. As the concentration of nano-clay increases, an apparent reduction in pore size and a combination of thin and thick fibers was observed. A combination of pore size enables the filter membrane to capture more particles and prevent the heavily compact membrane filter structure. Moreover, nano-clay provided certain roughness to the fibers, improving air filtration efficiency [7].

19.10.4 Influence of Structure on Filtration Efficiency

Multilayered nanofibers can be formed by stacking layers of nanofibers having each layer made of different material and structure. The layering of nanofibers provided additional characteristics to the membrane filters. In a study on combining beaded and non-beaded bilayer electrospun fibers, two kinds of membrane filters were formed with a beaded layer on top of bead-free electrospun nanofibers and vice versa. The results showed that for the membrane with a beaded layer on top and a bead-free layer on the bottom, the pressure drop was 202 Pa and filtration efficiency of 95%. In reverse order, the filtration efficiency was 95.7%, and the reduction in pressure was found to be 137 Pa. It was concluded that structural layering does not cause any promising effect on the filtration performance of membrane filters. The prepared membrane filters were equally capable of filtering PM particles, making them suitable

for protective clothing and respirator masks. Moreover, the incorporation of beads imparts many additional characteristics by increasing thickness, pore characteristics, and packing density [6].

Multilayered polyacrylonitrile (PAN) nanofibrous membrane filters were prepared via the needless electrospinning method. Stacked layers of nanofibers were of different sizes (172 ± 21 and 772 ± 118 nm). The resulting sandwiched structure showed lower filtration resistance (151.9 Pa) and high filtration efficiency (99.89%) than the nanofiber structured filter (99.92%, 2207.76 Pa) for sodium chloride aerosol particles of 260 nm. The composite membrane filters maintain the pore size and reduce the package density as compared to single-layered nanofibers. Moreover, sandwiched structure membranes have high productivity of about 20 gh^{-1}, multiple times greater than conventional electrospinning, suitable for commercial and industrial application [64].

19.11 Bioactive/Antiviral Nanofibers for Facemasks

The spread of the COVID-19 pandemic has played a profound role in making antiviral PPEs that can reduce or stop virus transmission. Different bioactive agents have been used to impart bioactivity in facemasks. Among these bioactive materials, various plant species have been studied for their antiviral characteristics, such as *Acacia nilotica, Allium sativum, Alhagi maurorum, Camellia japonica, Echinacea angustifolia, Glycyrrhiza glabra, Litchi chinensis, and Ocimum kilimandscharicum* (Sytar et al. 2021). Electrospun nanofiber facemask incorporated with licorice root extract was prepared for the first time. The licorice root contains glycyrrhizin (GL) and glycyrrhetinic acid (GA), which have an antiviral property that disables the virus and terminates the replication. GA and GL destroy the structure of biomolecules such as lipids, DNA, and protein. The pore size of nanofibers was 75 nm which is lesser than the COVID-19 virus, thus proper as an antiviral filter membrane [13]. Polyacrylonitrile (PAN)/zinc oxide (ZnO) hybrid nanocomposite loaded with Viroblock (VB) was prepared to be used as an antiviral filter membrane for PPE. The prepared samples showed good antibacterial activity 88.64% (*Pseudomonas aeruginosa*), 92.59% (*Staphylococcus aureus*), and 37%, respectively and killed the virus. It was concluded that these membranes are helpful against common influenza and coronavirus and valuable for developing PPE [54]. A simple illustration of antiviral activity using nanofibers-based facemask has been given in Fig. 19.10.

19.12 Conclusions and Future Perspective

The COVID-19 pandemic has well highlighted the importance of facemasks. Globally, the demand for facemasks has increased considerably. There are various kinds of facemasks available in the market with different attributes and protection levels.

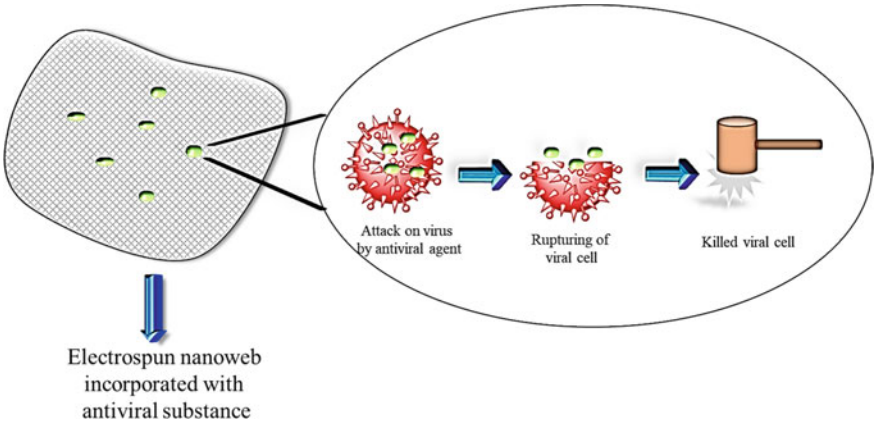


Fig. 19.10 Antiviral activity of substance incorporated in electrospun nanofibers

The first and foremost feature of the facemasks is their filtration efficiency. Whether using a fabric mask, surgical mask, or N95, it must provide an extra level of protection against airborne particulates and germs.

In comparison to a typical surgical mask, nanofibers have high filtration efficiency against nanoscale air particles. Nanofibers' properties, such as fine porous structure, high surface to volume ratio, high strength, and high surface energy, added to the higher filtration efficiency and pressure drop in nanofiber filtration membranes. The physical properties of nanofibers like ultrathin diameter and high porosity, fiber structure, and morphology greatly influence the filtration efficiency of nanofiber filters. The pore size and mechanical stability of nanofibers are tunable, which helps in the selective production of nanofibers according to the application. The spread of the COVID-19 pandemic has played a profound role in making antiviral PPEs that can reduce or stop virus transmission. These nanofibers-based facemasks have shown promising results regarding infection prevention.

Though, there are many studies availalble in the literature which focused on the addition of various nanoparticles and active pharmacuetical agents to make them bioactive. Less consideration has been given to natural plant extracts which are excellent source of bioactive compunds. However, the plant extracts-loaded nanofibrous facemask has not been explored for such a purpose. Plant extracts and nanoparticles can be incorporated into electrospun nanowebs for application in personal protective equipment. It can be done at an industrial scale with low cost and high production rate to fulfill time needs. The extracts are also eco-friendly and biocompatible. Thus, there is a solid need to utilize natural ingredients for the sake of a green environment. Furthermore, due to the complex nature of natural extracts, it is hard for pathogens to show resistance against these which is also a plus point and could offer guaranteed protection. So, in the future, a lot of work is required to identify and apply the potential natural extracts having antiviral, antibacterial and antioxidant acitivity for the said purpose using nanofiber as a carrier in facemasks and other applications.

References

1. (OSHA), OS and HA. (1991). Final rule on occupational exposure to blood-borne pathogens.
2. (US), C. for DC, Committee, C. for DC (US). IPA. (1985). Recommendations for protection against viral hepatitis. US Department of Health and Human Services, *Public Health Service.* Centers ….
3. Acquired immune deficiency syndrome (AIDS). (1982). Precautions for clinical and laboratory staffs. *Morbidity and Mortality Weekly Report (MMWR), 31*, 577–580.
4. Aggarwal, U., Goyal, A. K., & Rath, G. (2017). Development and characterization of the cisplatin loaded nanofibers for the treatment of cervical cancer. *Materials Science and Engineering C, 75*, 125–132. https://doi.org/10.1016/j.msec.2017.02.013
5. Babaahmadi, V., Amid, H., Naeimirad, M., & Ramakrishna, S. (2021). Biodegradable and multifunctional surgical face masks: A brief review on demands during COVID-19 pandemic, recent developments, and future perspectives. *Science of the Total Environment, 798*, 149233. https://doi.org/10.1016/j.scitotenv.2021.149233
6. Bonfim, D. P. F., Cruz, F. G. S., Guerra, V. G., & Aguiar, M. L. (2021). Development of filter media by electrospinning for air filtration of nanoparticles from pet bottles. *Membranes (Basel), 11*, 293. https://doi.org/10.3390/membranes11040293
7. Borojeni, I. A., Jenab, A., Sanjari, M., Boudreault, C., Klinck, M., Strong, S., & Riahi, A. R. (2021). Effect of nanoclay addition on the morphology, fiber size distribution and pore size of electrospun polyvinylpyrrolidone (PVP) composite fibers for air filter applications. *Fibers*, *9*. https://doi.org/10.3390/fib9080048
8. Bortolassi, A. C. C., Guerra, V. G., Aguiar, M. L., Soussan, L., Cornu, D., Miele, P., & Bechelany, M. (2019). Composites based on nanoparticle and pan electrospun nanofiber membranes for air filtration and bacterial removal. *Nanomaterials, 9*, 1740. https://doi.org/10.3390/nano9121740
9. Brienen, N. C. J., Timen, A., Wallinga, J., Van Steenbergen, J. E., & Teunis, P. F. M. (2010). The effect of mask use on the spread of influenza during a pandemic. *Risk Analysis: An International Journal, 30*, 1210–1218.
10. Casanova, L., Rutala, W. A., Weber, D. J., & Sobsey, M. D. (2010). Coronavirus survival on healthcare personal protective equipment. *Infection Control and Hospital Epidemiology, 31*, 560–561.
11. Celebioglu, A., & Uyar, T. (2017). Antioxidant vitamin E / cyclodextrin inclusion complex electrospun nanofibers : Enhanced water-solubility, prolonged shelf-life and photostability of Vitamin E. *Journal of Agricultural and Food Chemistry, 65*, 5404–5412. https://doi.org/10.1021/acs.jafc.7b01562
12. Choi, S., Jeon, H., Jang, M., Kim, H., Shin, G., Koo, J. M., Lee, M., Sung, H. K., Eom, Y., Yang, H. S., Jegal, J., Park, J., Oh, D. X., & Hwang, S. Y. (2021). Biodegradable, efficient, and breathable multi-use face mask filter. *Advancement of Science, 8*, 1–8. https://doi.org/10.1002/advs.202003155
13. Chowdhury, H., Chowdhury, T., & Sait, S. M. (2021). Estimating marine plastic pollution from COVID-19 face masks in coastal regions. *Marine Pollution Bulletin, 168*, 112419. https://doi.org/10.1016/j.marpolbul.2021.112419
14. Dadras Chomachayi, M., Solouk, A., Akbari, S., Sadeghi, D., Mirahmadi, F., & Mirzadeh, H. (2018). Electrospun nanofibers comprising of silk fibroin/gelatin for drug delivery applications: Thyme essential oil and doxycycline monohydrate release study. *Journal of Biomedical Materials Research Part A, 106*, 1092–1103. https://doi.org/10.1002/jbm.a.36303
15. Das, O., Neisiany, R. E., Capezza, A. J., Hedenqvist, M. S., Försth, M., Xu, Q., Jiang, L., Ji, D., & Ramakrishna, S. (2020). The need for fully bio-based facemasks to counter coronavirus outbreaks: A perspective. *Science of the Total Environment, 736*, 139611. https://doi.org/10.1016/j.scitotenv.2020.139611

16. de Almeida, D. S., Martins, L. D., Muniz, E. C., Rudke, A. P., Squizzato, R., Beal, A., de Souza, P. R., Bonfim, D. P. F., Aguiar, M. L., & Gimenes, M. L. (2020). Biodegradable CA/CPB electrospun nanofibers for efficient retention of airborne nanoparticles. *Process Safety and Environment Protection, 144*, 177–185. https://doi.org/10.1016/j.psep.2020.07.024
17. Dodero, A., Brunengo, E., Alloisio, M., Sionkowska, A., Vicini, S., & Castellano, M. (2020). Chitosan-based electrospun membranes: Effects of solution viscosity, coagulant and crosslinker. *Carbohydrate Polymers, 235*, 115976. https://doi.org/10.1016/j.carbpol.2020.115976
18. Doostmohammadi, M., Mehrasa, M., Amini, S., Komeily-Nia, Z., Heidarian, P., & Nasri-Nasrabadi, B. (2021). Fabrication of gehlenite nanopowder containing electrospun nanofibers for bone tissue engineering. *Fibers and Polymers*, 1–8. https://doi.org/10.1007/s12221-021-0168-x
19. Essa, W., Yasin, S., Saeed, I., & Ali, G. (2021). Nanofiber-based face masks and respirators as COVID-19 protection: A review. *Membranes (Basel), 11*, 250. https://doi.org/10.3390/membranes11040250
20. Fisher, E. M., Noti, J. D., Lindsley, W. G., Blachere, F. M., & Shaffer, R. E. (2014). Validation and application of models to predict facemask influenza contamination in healthcare settings. *Risk Analysis, 34*, 1423–1434.
21. Ghafoor, B., Aleem, A., Najabat Ali, M., & Mir, M. (2018). Review of the fabrication techniques and applications of polymeric electrospun nanofibers for drug delivery systems. *Journal of Drug Delivery Science and Technology, 48*, 82–87. https://doi.org/10.1016/j.jddst.2018.09.005
22. Gurung, P., Dahal, M., Baral, K., Pathak, A., & Khanal, S. (2021). Knowledge and understanding of personal protective equipment use among laborer population of the nepalese workforce. *Journal of Environmental and Public Health, 2021*, 7679185. https://doi.org/10.1155/2021/7679185
23. Honda, H., & Iwata, K. (2016). Personal protective equipment and improving compliance among healthcare workers in high-risk settings. *Current Opinion in Infectious Diseases, 29*, 400–406. https://doi.org/10.1097/QCO.0000000000000280
24. Howard, J., Huang, A., Li, Z., Tufekci, Z., Zdimal, V., van der Westhuizen, H.-M., von Delft, A., Price, A., Fridman, L., & Tang, L.-H. (2021). An evidence review of face masks against COVID-19. *Proceedings of the National Academy of Sciences, 118*.
25. Howard, J., Huang, A., Li, Z., Tufekci, Z., Zdimal, V., van der Westhuizen, H. M., von Delft, A., Price, A., Fridman, L., Tang, L. H., Tang, V., Watson, G. L., Bax, C. E., Shaikh, R., Questier, F., Hernandez, D., Chu, L. F., Ramirez, C. M., & Rimoin, A. W. (2021). An evidence review of face masks against COVID-19. *Proceedings of the National Academy of Sciences USA, 118*, 1–12. https://doi.org/10.1073/pnas.2014564118
26. Jefferson, T., Del Mar, C., Dooley, L., Ferroni, E., Al-Ansary, L. A., Bawazeer, G. A., van Driel, M. L., Foxlee, R., & Rivetti, A. (2009). Physical interventions to interrupt or reduce the spread of respiratory viruses: Systematic review. *BMJ, 339*, b3675. https://doi.org/10.1136/bmj.b3675
27. Kadam, V., Truong, Y. B., Schutz, J., Kyratzis, I. L., Padhye, R., & Wang, L. (2021). Gelatin/β–cyclodextrin bio-nanofibers as respiratory filter media for filtration of aerosols and volatile organic compounds at low air resistance. *Journal of Hazardous Materials, 403*, 123841. https://doi.org/10.1016/j.jhazmat.2020.123841
28. Kalantari, K., Afifi, A. M., Jahangirian, H., & Webster, T. J. (2019). Biomedical applications of chitosan electrospun nanofibers as a green polymer—Review. *Carbohydrate Polymers, 207*, 588–600. https://doi.org/10.1016/j.carbpol.2018.12.011
29. Khandaker, M., Progri, H., Arasu, D. T., Nikfarjam, S., & Shamim, N. (2021). Use of polycaprolactone electrospun nanofiber mesh in a face mask. *Materials (Basel), 14*, 4272. https://doi.org/10.3390/ma14154272
30. Khanzada, H., Salam, A., Hassan, T., Munir, M. U., Pasha, K., & Hassan, N. (2020). *Fabrication of Promising Antimicrobial Aloe, 13*, 3884.
31. Konda, A., Prakash, A., Moss, G. A., Schmoldt, M., Grant, G. D., & Guha, S. (2020). Aerosol filtration efficiency of common fabrics used in respiratory cloth masks. *ACS Nano, 14*, 6339–6347. https://doi.org/10.1021/acsnano.0c03252

32. Kumar, T., Senthil Kumar, K., Rajini, N., Siengchin, S., Ayrilmis, N., & Varada Rajulu, A. (2019). A comprehensive review of electrospun nanofibers: Food and packaging perspective. *Composites. Part B, Engineering, 175*, 107074. https://doi.org/10.1016/j.compositesb.2019.107074
33. Lancina, M. G., Shankar, R. K., & Yang, H. (2017). Chitosan nanofibers for transbuccal insulin delivery. *Journal of Biomedical Materials Research Part A, 105*, 1252–1259. https://doi.org/10.1002/jbm.a.35984
34. Larson, E. L., Ferng, Y.-H., Wong-McLoughlin, J., Wang, S., Haber, M., & Morse, S. S. (2010). Impact of non-pharmaceutical interventions on URIs and influenza in crowded, urban households. *Public Health Reports, 125*, 178–191.
35. Lee, J., Yoon, J., Kim, J. H., Lee, T., & Byun, H. (2018). Electrospun PAN–GO composite nanofibers as water purification membranes. *Journal of Applied Polymer Science, 135*, 1–9. https://doi.org/10.1002/app.45858
36. Lv, D., Zhu, M., Jiang, Z., Jiang, S., Zhang, Q., Xiong, R., & Huang, C. (2018). Green electrospun nanofibers and their application in air filtration. *Macromolecular Materials and Engineering, 303*, 1–18. https://doi.org/10.1002/mame.201800336
37. Lyu, C., Zhao, P., Xie, J., Dong, S., Liu, J., Rao, C., & Fu, J. (2021). Electrospinning of nanofibrous membrane and its applications in air filtration: A review. *Nanomaterials, 11*, 1501. https://doi.org/10.3390/nano11061501
38. Mamun, A., Blachowicz, T., & Sabantina, L. (2021). Electrospun nanofiber mats for filtering applications technology, structure and materials. *Polymers (Basel), 13*, 1–14. https://doi.org/10.3390/polym13091368
39. Mikulicz, J. (1897). Das operieren in sterilisierten zwirnhandschuhen und mit mundbinde. *Centralblatt für Chirurgie, 26*, 714–717.
40. Mishra, R. K., Mishra, P., Verma, K., Mondal, A., Chaudhary, R. G., Abolhasani, M. M., & Loganathan, S. (2019). Electrospinning production of nanofibrous membranes. In *Environmental Chemistry Letters,* Springer International Publishing. https://doi.org/10.1007/s10311-018-00838-w
41. Molnár, K., & Mészáros, L. (2020). Editorial corner—a personal view the role of electrospun nanofibers in the fight against the COVID-19. *Express Polymer Letters, 14*, 605. https://doi.org/10.3144/expresspolymlett.2020.49
42. Nam, S., Lee, J. J., Lee, S. Y., Jeong, J. Y., Kang, W. S., & Cho, H. J. (2017). Angelica gigas nakai extract-loaded fast-dissolving nanofiber based on poly(vinyl alcohol) and soluplus for oral cancer therapy. *International Journal of Pharmaceutics, 526*, 225–234. https://doi.org/10.1016/j.ijpharm.2017.05.004
43. World Health Organization. (2020). Shortage of personal protective equipment endangering health workers worldwide.
44. Ormaza-Gonzaìlez, F. I., Castro-Rodas, D., & Statham, P. J. (2021). COVID-19 impacts on beaches and coastal water pollution at selected sites in ecuador, and management proposals post-pandemic. *Frontiers in Marine Science, 8*, 1–16. https://doi.org/10.3389/fmars.2021.669374
45. Palazzetti, R., & Zucchelli, A. (2017). Electrospun nanofibers as reinforcement for composite laminates materials—A review. *Composite Structures, 182*, 711–727. https://doi.org/10.1016/j.compstruct.2017.09.021
46. Palmieri, V., De Maio, F., De Spirito, M., & Papi, M. (2021). Face masks and nanotechnology: Keep the blue side up. *Nano Today, 37*, 101077. https://doi.org/10.1016/j.nantod.2021.101077
47. Parham, S., Kharazi, A. Z., Bakhsheshi-Rad, H. R., Ghayour, H., Ismail, A. F., Nur, H., & Berto, F. (2020). Electrospun nano-fibers for biomedical and tissue engineering applications: A comprehensive review. *Materials (Basel), 13*, 1–25. https://doi.org/10.3390/ma13092153
48. Patrício Silva, A. L., Prata, J. C., Walker, T. R., Duarte, A. C., Ouyang, W., Barcelò, D., & Rocha-Santos, T. (2021). Increased plastic pollution due to COVID-19 pandemic: Challenges and recommendations. *Chemical Engineering Journal, 405*, 126683. https://doi.org/10.1016/j.cej.2020.126683
49. Poláková, L., Širc, J., Hobzová, R., Cocârță, A. I., & Heřmánková, E. (2019). Electrospun nanofibers for local anticancer therapy: Review of in vivo activity. *International Journal of Pharmaceutics, 558*, 268–283. https://doi.org/10.1016/j.ijpharm.2018.12.059

50. Prata, J. C., Silva, A. L. P., Walker, T. R., Duarte, A. C., & Rocha-Santos, T. (2020). COVID-19 pandemic repercussions on the use and management of plastics. *Environmental Science and Technology, 54*, 7760–7765. https://doi.org/10.1021/acs.est.0c02178
51. Rahmati, M., Mills, D. K., Urbanska, A. M., Saeb, M. R., Venugopal, J. R., Ramakrishna, S., & Mozafari, M. (2021). Electrospinning for tissue engineering applications. *Progress in Materials Science, 117*, 100721. https://doi.org/10.1016/j.pmatsci.2020.100721
52. Ruisinger, M. M. (2020). Die pestarztmaske im deutschen medizinhistorischen museum IngolstadtThe "Plague Doctor's Mask" in the german museum for the history of medicine, Ingolstadt.
53. Sahay, R., Kumar, P. S., Sridhar, R., Sundaramurthy, J., Venugopal, J., Mhaisalkar, S. G., & Ramakrishna, S. (2012). Electrospun composite nanofibers and their multifaceted applications. *Journal of Materials Chemistry, 22*, 12953–12971. https://doi.org/10.1039/c2jm30966a
54. Salam, A., Hassan, T., Jabri, T., Riaz, S., Khan, A., Iqbal, K. M., Khan, S., Wasim, M., Shah, M. R., Khan, M. Q., & Kim, I. (2021). Electrospun nanofiber-based viroblock/ZnO/PAN hybrid antiviral nanocomposite for personal protective applications. *11*, 2208. https://doi.org/10.3390/nano11092208
55. Sivri, Ç. (2018). Improvement of protective and comfort properties of face masks using superabsorbent polymer containing nanofibers. *International Journal of Clothing Science and Technology, 30*, 668–686. https://doi.org/10.1108/IJCST-10-2017-0169
56. Strasser, B. J., & Schlich, T. (2020). A history of the medical mask and the rise of throwaway culture. *The Lancet, 396*, 19–20. https://doi.org/10.1016/S0140-6736(20)31207-1
70. Sytar, O., Brestic, M., Hajihashemi, S., Skalicky, M., Kubeš, J., Lamilla-Tamayo, L., Ibrahimova, U., Ibadullayeva, S., & Landi, M. (2021). COVID-19 prophylaxis efforts based on natural antiviral plant extracts and their compounds. Mol. 2021,*26*, 727. https://doi.org/10.3390/MOLECULES26030727
57. Taemeh, M. A., Shiravandi, A., Korayem, M. A., & Daemi, H. (2020). Fabrication challenges and trends in biomedical applications of alginate electrospun nanofibers. *Carbohydrate Polymers, 228*, 115419. https://doi.org/10.1016/j.carbpol.2019.115419
58. Tcharkhtchi, A., Abbasnezhad, N., Zarbini Seydani, M., Zirak, N., Farzaneh, S., & Shirinbayan, M. (2021). An overview of filtration efficiency through the masks: Mechanisms of the aerosols penetration. *Bioactive Materials, 6*, 106–122. https://doi.org/10.1016/j.bioactmat.2020.08.002
59. Tebyetekerwa, M., Xu, Z., Yang, S., & Ramakrishna, S. (2020). Electrospun nanofibers-based face masks. *Advanced Fiber Materials, 2*, 161–166. https://doi.org/10.1007/s42765-020-00049-5
60. Ullah, S., Ullah, A., Lee, J., Jeong, Y., Hashmi, M., Zhu, C., Joo, K. I., Cha, H. J., & Kim, I. S. (2020). Reusability comparison of melt-blown vs nanofiber face mask filters for use in the coronavirus pandemic. *ACS Applied Nano Materials, 3*, 7231–7241. https://doi.org/10.1021/acsanm.0c01562
61. Venkatesan, M., Veeramuthu, L., Liang, F. C., Chen, W. C., Cho, C. J., Chen, C. W., Chen, J. Y., Yan, Y., Chang, S. H., & Kuo, C. C. (2020). Evolution of electrospun nanofibers fluorescent and colorimetric sensors for environmental toxicants, pH, temperature, and cancer cells—A review with insights on applications. *Chemical Engineering Journal*. https://doi.org/10.1016/j.cej.2020.125431
62. Wang, L., Gao, Y., Xiong, J., Shao, W., Cui, C., Sun, N., Zhang, Y., Chang, S., Han, P., Liu, F., & He, J. (2021). Biodegradable and high-performance multiscale structured nanofiber membrane as mask filter media via poly(lactic acid) electrospinning. *Journal of Colloid and Interface Science, 606*, 961–970. https://doi.org/10.1016/j.jcis.2021.08.079
63. Wibisono, Y., Fadila, C. R., Saiful, S., & Bilad, M. R. (2020). Facile approaches of polymeric face masks reuse and reinforcements for micro-aerosol droplets and viruses filtration: A review. *Polymers (Basel), 12*, 1–18. https://doi.org/10.3390/polym12112516

64. Xiong, J., Zhou, M., Zhang, H., Quan, Z., Wang, R., & Qin, X. (2019). Sandwich-structured fibrous membranes with low filtration resistance for effective PM2.5 capture via one-step needleless electrospinning. *Materials Research Express, 6*, 035027. https://doi.org/10.1088/2053-1591/aaf760
65. Yang, A., Cai, L., Zhang, R., Wang, J., Hsu, P.-C., Wang, H., Zhou, G., Xu, J., & Cui, Y. (2017). Thermal management in nanofiber-based face mask. *Nano Letters, 17*, 3506–3510. https://doi.org/10.1021/acs.nanolett.7b00579
66. Zhang, J., Gong, S., Wang, C., Jeong, D. Y., Wang, Z. L., & Ren, K. (2019). Biodegradable electrospun poly(lactic acid) nanofibers for effective PM 2.5 removal. *Macromolecular Materials and Engineering, 304*, 1–8. https://doi.org/10.1002/mame.201900259
67. Zhang, L., Peng, Z., Ou, J., Zeng, G., Fontaine, R. E., Liu, M., Cui, F., Hong, R., Zhou, H., & Huai, Y. (2013). Protection by face masks against influenza A (H1N1) pdm09 virus on Trans-Pacific Passenger Aircraft, 2009. *Emerging Infectious Diseases, 19*, 1403.
68. Zhang, Z., Ji, D., He, H., & Ramakrishna, S. (2021). Electrospun ultrafine fibers for advanced face masks. *Materials Science & Engineering R Reports, 143*, 100594. https://doi.org/10.1016/j.mser.2020.100594
69. Zhong, H., Zhu, Z., You, P., Lin, J., Cheung, C. F., Lu, V. L., Yan, F., Chan, C. Y., & Li, G. (2020). Plasmonic and superhydrophobic self-decontaminating N95 respirators. *ACS Nano, 14*, 8846–8854. https://doi.org/10.1021/acsnano.0c03504



Sonia Javed was born in Faisalabad, Punjab, Pakistan, in 1995. She received the B.S. and M.S. degrees in chemistry from Government College Women University, Faisalabad, in 2018 and 2021, respectively. From 2019 to 2021, she was a Research Assistant for Higher Education Commission, a Pakistan-funded project titled "Development of Green Electrospun Nano Composites for Wound Dressing" at GCWUF. She is the author of a Book Chapter titled "Natural plant extract treated bio-active textiles for wound healing," Journal-Elsevier, 2021. Her research interests include the development of eco-friendly sustainable extraction media and the production of nanostructured materials incorporated with natural extracts and applications in drug delivery systems.



Misbah Hameed received a Pharm D degree from Lahore College for Women University (LCWU), Lahore, Pakistan, in 2008. She did M. Phil in Pharmaceutics from the same Institute in 2012. She received a Ph.D. degree in Pharmaceutics from Government College University Faisalabad, Pakistan. In her Ph.D. research project, she worked on nanofibers topical dressing for complicated and uncomplicated wound healing. She is serving as an Assistant Professor at the Institute of Pharmacy, LCWU. Her research interest includes nanomaterials, nanoformulations, specifically nanofibers, and drug development. She authored several international and national research articles and book chapters. She has presented papers at various conferences of international significance. She has expertise in pharmaceutical and industrial microbiology. Currently, she is actively engaged in teaching and advanced research activities at the Institute of Pharmacy, LCWU.



Ahsan Nazir is working as Director ORIC at National Textile University (NTU) Faisalabad, Pakistan. He is a Textile Engineer and graduated from National Textile University with a specialization in Textile Processing. He worked in Textile Industry for almost five years and has been working in NTU for almost Nine years. He did his Doctoral Studies from Universite de Haute Alsace, France, on developing nanofibrous membranes for air filtration. After his Ph.D., he mainly focused on filtration of pollutants in air/water, biomedical and protective applications of textile materials, and process improvement and optimization. He has supervised several Ph.D. and M.S. students. He has been associated with Pakistan National Accreditation Council as Technical Assessor and has assessed several laboratories. Other than this work, he has carried out valuable work in textile and provided consultancy services to several national organizations.



Tanveer Hussain is Professor of Textile Engineering and Rector at National Textile University Faisalabad Pakistan. He got his PhD in 2004 from Heriot-Watt University, United Kingdom. He has published more than 100 research papers in peer-reviewed journals. He has been awarded several research grants from the Higher Education Commission of Pakistan and has won various awards, including Gold Medal in B.Sc. Textile Engineering, Bronze Medal from the Society of Dyers and Colourists U.K., and Best University Teacher Award from the Higher Education Commission Pakistan. Previously, he has served at various positions at National Textile University, including Head of Textile Processing Department and Dean Faculty of Engineering & Technology.



Nabyl Khenoussi was born in Mulhouse Alsace, France. He was awarded a Technical degree in 2004 in Polymer processing from Université de Haute Alsace. He continued with a license and master's degree in Polymers engineering, respectively, obtained in 2005 and 2007. He received his doctoral degree in 2010 on electrospun fibers for biomedical application. He started as an Assistant professor in 2011 and spent 10 years researching structural, mechanical approaches to develop targeted applications. He organized conferences and workshops on innovative textiles, managed European projects in the form of cost, and was dedicated to such advanced medicals.



Sharjeel Abid is currently working as an Assistant Professor at National Textile University, Pakistan. He has over 30 international research publications with a cumulative impact factor of 80+. He did his Ph.D. in Textile Engineering from the same institution in 2020, and during his Ph.D. work, he went to the National University of Singapore and South Korea for research activities. He has served at various key positions in the textile processing industry for four years. Currently, his focus areas are biomedical textiles, nanofibers, and sustainable textiles.

Part III
Advanced Manufacturing

Chapter 20
Electrospinning and Three-Dimensional (3D) Printing for Biofabrication



Nureddin Ashammakhi, Maryam Tavafoghi, Arman Jafari, Sumama Nuthana Kalva, Robin Augustine, Anwarul Hasan, Houman Savoji, Yavuz Nuri Ertas, and Song Li

Abstract Biofabrication of engineered cell-laden constructs and scaffolds is essential for tissue engineering and tissue modeling. Electrospinning is a highly scalable technology to fabricate porous scaffolds with micro or nano-fibrous structure. Three-dimensional (3D) bioprinting has been recently developed for tissue engineering by providing control over cell location and multicellular structure. With the availability of electrospinning techniques, it is possible to combine nano- and microfiber-based

N. Ashammakhi (✉) · M. Tavafoghi · S. Li
Department of Bioengineering, Henry Samueli School of Engineering, University of California, Los Angeles, CA, USA
e-mail: n.ashammakhi@ucla.edu; ashammak@msu.edu

S. Li
e-mail: songli@ucla.edu

N. Ashammakhi
Department of Biomedical Engineering and Institute for Quantitative Health Science and Engineering (IQ), Michigan State University, East Lansing, MI 48824, USA

A. Jafari · H. Savoji
Department of Pharmacology and Physiology, Faculty of Medicine, Institute of Biomedical Engineering, University of Montreal, Montreal, QC, Canada
e-mail: arman.jafari@umontreal.ca

H. Savoji
e-mail: houman.savoji@umontreal.ca

Research Center, The Centre Hospitalier Universitaire Sainte-Justine, Montreal, QC, Canada

Montreal TransMedTech Institute, Montreal, QC, Canada

S. N. Kalva · R. Augustine · A. Hasan
Department of Mechanical and Industrial Engineering, College of Engineering, Qatar University, 2713, Doha, Qatar

Biomedical Research Center (BRC), Qatar University, 2713, Doha, Qatar

Y. N. Ertas
Department of Biomedical Engineering, Erciyes University, Kayseri, Turkey
e-mail: yavuzertas@erciyes.edu.tr

ERNAM-Nanotechnology Research and Application Center, Erciyes University, Kayseri, Turkey

© The Author(s), under exclusive license to Springer Nature Switzerland AG 2022

A. Vaseashta and N. Bölgen (eds.), *Electrospun Nanofibers*,
https://doi.org/10.1007/978-3-030-99958-2_20

structures with 3D bioprinted constructs, to obtain composite structures that have biomimetic or functional features and improved mechanical stability. In addition, electrospun fibers can add various functions such as drug release properties to the developed 3D bioprinted constructs. In this chapter, we will discuss the techniques for electrospinning, 3D bioprinting, and the approach of combining electrospinning and 3D bioprinting for biofabrication. We also highlight current challenges and future research directions.

Keywords 3D bioprinting · Electrospinning · Regeneration · Tissue engineering · Tissue models

20.1 Introduction

Tissue loss results in the loss of function and integrity of tissues and organs and therefore, it requires treatment [1]. The gold standard of treatment is the use of autografts [2]. However, because of limited supply and donor site morbidity, their use is not widely spread [3]. Allografts or even xenografts can also be used for the treatment of tissue defects [4]. Although these are available without limitations, their use is associated with the risk of infective agent transmission [5] and other concerns [6]. Therefore, the use of biomaterials for tissue repair has been explored [7–11]. For the purpose of tissue replacement, reconstruction and repair, various biostable or biodegradable biomaterials were developed [7, 12]. Unfortunately, these are not living and can lead to unwanted inflammatory response [13, 14], fibrous tissue encapsulation [15, 16], infection [17] and failure [18]. The use of bioabsorbable membranes for in situ tissue formation by guiding tissue regeneration has been explored [19–22]. However, this is limited to the treatment of small tissue defects. The advent of tissue engineering led to the development of tissue-like constructs produced by seeding cells into biodegradable scaffolds that have been usually made from polymers [23] with or without ceramics [24, 25] and additives such as growth factors [26–28]. Inability to ensure homogenous cell distribution in these scaffolds often led to failure of engineered tissues in vivo [29, 30]. The development of three-dimensional (3D) printing [31] and its adoption to 3D bioprinting led to development of a more advanced generation of engineered tissue constructs [32–35]. In 3D bioprinting, cells are combined with biomaterial and together printed into constructs. This way, more homogeneous and controlled deposition of cells, pore size or the spatial distribution of pores in the constructs can be achieved [36]. Furthermore, different types of materials or cells and additives as well as gradients can be built into these constructs [37, 38] to develop more complex structures and interface tissues such as muscle/tendon, tendon/bone or bone/cartilage interface tissues [39–43].

Today, 3D bioprinting represents a powerful approach for the fabrication of potentially successful engineered tissue constructs that can be used for the repair or regeneration of human tissues and organs [44–46]. Despite major advances that have been made in 3D bioprinting [3, 47–49], this method is still associated with many

limitations that hinder its translation to the clinic [50, 51]. Among the important challenges is the relatively low mechanical properties of 3D bioprinted constructs [52], which limits their use in mechanically demanding applications such as hard tissue engineering [33, 53, 54]. To tackle this problem, various approaches have been investigated, and they included so far the use of ceramic particles [55–57] or fibers [58–60] in the bioinks and external support frames [61, 62] or sacrificial materials that provide temporary support [63, 64]. The latter helps to build larger sized of constructs but does not provide permanent support to printed constructs and thus, it does not contribute to the improvement of their mechanical properties. In addition, pore size in constructs created by 3D bioprinting promote the deposition of cells in the bottom of scaffolds [65]. Constructs made using 3D bioprinting also lack the nano-/microfibrous structure the native extracellular matrix (ECM) has [66], which beside other functions is suggested to enhance initial cell attachment and proliferation [67]. Native ECM can also store and release biomolecules [68], which can similarly be mimicked by using drug releasing nanofibers to develop novel biomimetic 3D bioprinted constructs.

Therefore, the development of methods to enhance mechanical properties of the 3D bioprinted scaffolds and improve their biomimetic properties are necessary to overcome the current limitations of 3D bioprinted tissue constructs and enhance their applications in the clinic [69, 70]. Among important strategies to achieve this is the combination of the 3D bioprinting technique with other fabrication methods to create the 3D constructs that have controlled pore structures and nano-scale features [65] as well as improved mechanical properties [71, 72]. In this respect, the use of nanofibers is an attractive and useful technique in many aspects, that include providing mechanical reinforcement to the constructs and improving their ECM biomimetic properties. There are different methods that can be used for the production of nanofibers, among which electrospinning [73] is an attractive technique because it is characterized by its simplicity, versatility and scalability [73–75]. Recently, methods to combine electrospinning and 3D bioprinting have been developed [76–79], and are expected to have an impact on the development of new generation of engineered tissue constructs, that can have enhanced cell attachment and function. Therefore, in this chapter, we go over electrospinning and 3D bioprinting methods and their combination towards developing better engineered constructs and look at challenges and future directions to provide important information for readers and stimulate the development of new ideas to advance the field of tissue engineering.

20.2 Electrofabrication

Electrofabrication techniques are electrohydrodynamic methods that use electrostatic forces to generate polymeric nano-microstructures. Electrospinning is the most widely investigated electrofabrication technique for fabricating nano-microfiber based membranes for tissue engineering and wound healing applications [80, 81]. Other related approaches such as electro-spraying and melt electrospinning are also

explored in biomedical applications. In electrospinning, an electric field is applied to polymer solution so that polymer droplets can move towards an oppositely charged collector as fibers. Unlike electrospinning, electrospraying uses less viscous polymer solutions and generates nano-microparticles that can be used in drug delivery applications. Melt electrospinning uses molten polymer which is taken in a heated syringe or comes from an extruder, followed by charging the polymer melt with an electric field to produce fibers. Electrospun nanofibrous materials have a high surface-to-volume porosity ratio and can be produced in a broad range of sizes and forms [82]. These specific characteristics of nanofibrous materials provide flexibility to use them in a wide variety of biomedical and tissue engineering applications [83, 84].

Electrospinning is one of the well-established methods for generating nano/submicron fibrous materials having a soldering-like attachment at intersections formed by entanglement of polymer fibers [85]. Nanofibrous membranes are well accepted in bioengineering applications due to their high processing flexibility that helps to optimize their physical parameters like fiber diameter, thickness, porosity and pattern formation. One of the most significant advantages of electrospinning technique is that the fibers produced by it can mimic the fiber-like architecture of extracellular matrix (ECM). Electrospun fibers can be used in various tissue engineering applications, including vascular grafts [86], skin tissue engineering, and bone regeneration [87, 88]. Electrospun membranes are also being used as wound dressings and wound healing patches [89, 90]. The advantage of electrospinning in the context of biomedical applications is that fibers based made of a wide range of polymers, and their blends with other polymers, their composites with non-polymeric fillers can be produced with varying physicochemical as well as biological performance. Moreover, electrospun polymeric meshes can be loaded with suitable bioactive molecules or drugs [91–95] to provide tissue regeneration capacity as well as to prevent problems at the implantation site [96].

20.2.1 Electrofabrication Methods: Principles, Techniques and Conditions

20.2.1.1 Electrospinning

Electrospinning employs a direct current (DC) electric voltage in the range of 5–30 kV to generate highly porous mesh like structures composed of nano-micron fibers with high surface area to volume ratio [97]. Both synthetic polymers such as poly(vinyl alcohol) (PVA) [98], poly-L/D-lactide (PLDLA) [99, 100], poly(lactide-*co*-glycolide) (PLGA) [92], polycaprolactone (PCL) [100, 101] and poly(3-hydroxybutyrate-co-3-hydroxyvalerate) (PHBV)] and natural polymers such as chitosan, elastin, collagen, gelatin, fibrinogen and fibrin [102, 103] hyaluronic acid (HA) [104], and silk fibroin) or the combination of both classes can be used to make electrospun scaffolds. Generally, polymers which are dissolved in an appropriate

solvent or molten polymer are constantly expelled from a syringe at slow flow rate (Usually, 0.5–3 mL/h). When a high DC voltage in the range of 5–30 kV is applied on the polymer droplet coming out, the polymer solution in the syringe gets charged, and the droplet tends to move towards the grounded collector as submicron fibers. The solvent evaporates and relatively dried polymer fibers will be deposited on the collecting platform as a membrane or a mesh. Typical electrospun scaffolds used for biomedical applications show 70–90% porosity and pores with 5–150 μm of average diameters [105]. The scaffolds have the potential to produce functional tissues with nano-size fibrous structures that replicate native ECMs and have connected pores [106–108].

Synthetic polymer-based scaffolds show excellent mechanical properties, stability, and controlled degradability. However, they generally lack bioactivity. Other natural materials, such as different collagen types, laminin and glycosaminoglycans may be used as coating on fibers to promote cell differentiation, growth, and adhesion [109, 110]. Electrospun scaffolds can be used for a wide range of purposes, including bone, cartilage, vascular and neural tissue engineering [111, 112]. Natural polymers generally show good biocompatibility and cell proliferation properties [113]. However, their strength and stability in the human body are not very high. Thus, blending of natural polymers with synthetic biopolymers is promising approach in biomedical research. For example, vascular scaffolds developed by blending of natural polymers like collagen or elastin and synthetic polymers like PLGA or PCL are highly promising for vascular reconstruction due to their suitable mechanical properties, degradability, cell proliferation and biocompatibility [114].

Electrospinning process is influenced by several equipment related, polymer solution related and ambient parameters (Table 20.1). These factors influence fiber morphology. Through proper control of these parameters, fibers with desirable morphologies and diameters can be produced [115]. A stable process requires a suitable range of viscosity and polymer solution concentration [116, 117]. Conductivity and polarity of the solvent is another important property of the polymer solution that influence the process of electrospinning. The increased conductivity or charge density of polymer solutions usually results in enhanced ion mobility and polymer jet whipping instability during electrospinning [118, 119]. Solvent properties, such as the boiling point, can influence solvent evaporation in electrospinning, causing either smooth surfaced fibers or those with nano-porosity on the surface. It can also affect the morphology of electrospun fibers [120]. The Taylor cone, a cone like structure formed by the deformation of polymer droplet at the tip of spinneret, shrinks and stretches towards collector as the applied voltage is increased during electrospinning, resulting in the formation of fibers with smaller diameters. A low feeding rate usually generates small droplets at the tip of needle, smaller Taylor cone and facilitates the rapid evaporation of solvents, which produces electrospun fibers with smaller diameters.

The consequences of environmental factors such as temperature and moisture on electrospinning must not be neglected. A slight temperature rise can reduce polymer solution viscosity and can result fibers with smaller diameters. Electrospinning at sufficiently low temperatures can considerably delay solvent evaporation and lead

Table 20.1 Summary of the effect of various electrospinning parameters on fiber morphology, fiber diameter, porosity and fiber spacing

Parameter	Effect on fiber morphology	Effect on fiber diameter	Effect on porosity
Solution parameters			
Polymer concentration	Low-bead generation, disappearance of beads with increase in concentration [125, 126]	Increase in fiber diameter with increased polymer-concentration [127–129]	Decrease in porosity with increased polymer concentration [130]
Viscosity	Low-bead formation, disappearance of beads with increase in viscosity [131]	Increase in fiber diameter with increase in viscosity [132]	–
Molecular weight of the polymer	Reduction in the number of beads and droplets with increase in molecular weight [133–135]	Increase in fiber diameter with increase in molecular weight [136]	Increase in molecular weight decreases porosity [137]
Solution conductivity	Higher conductivity leads to defect-free fibers [138–140]	Decrease in fiber diameter with an increase in conductivity [126, 128]	Increasing conductivity leads to increased porosity [141, 142]
Processing parameters			
Flow rate	Generation of beads with too high flow rate [143, 144]	Decrease in fiber diameter with decrease in flow rate [145]	Increase in flow rate results in increased porosity [146]
Distance between tip and collector	Generation of beads with too small and too large distance, minimum distance required for uniform fibers [147]	Decrease in fiber diameter with increase in distance [148, 149]	Increase in distance leads to decrease in porosity [150]
Applied voltage	Increase in voltage results in bead formation [139, 151]	Increase in voltage may decrease fiber diameter [115, 152, 153]	Increase in applied voltage increases porosity [154]
Collector type	Influence structural morphology of electrospun fibers. A non-conductive collector creates a porous structure with circular pores on fiber surfaces. Using patterned collectors influences fiber alignment and uniformity [155]	Fiber diameter can be tailored by modifying the collector according to requirements [156, 157]	Porosity can be tuned by using appropriate collectors [158]

(continued)

Table 20.1 (continued)

Parameter	Effect on fiber morphology	Effect on fiber diameter	Effect on porosity
Ambient parameters			
Humidity	High humidity results in circular pores on the fibers [122, 159]	Increasing humidity results in uniform fibers upto a certain limit [160]	Porosity increases with increasing humidity followed by flat beads
Temperature	Increasing temperature leads to decrease in viscosity and increase in solvent evaporation resulting in low bead formation [161]	Increase in temperature results in decrease in fiber diameter [162]	–

to solid–liquid phase separation and consequently lead to the generation of tunable porous surface morphology on the fibers [121]. The effects of increasing humidity on the fiber surface are similar for solvent evaporation and pore formation [122]. The combination of breath figures and supercritical fluids ($SCCO_2$) techniques allows the preparation of porous scaffolds with interconnected outer and inner porosity. These scaffolds with secondary pore formation and fiber interconnectivity exhibit good cell adhesion as well as cell proliferation indicating their huge potential in tissue engineering and wound healing applications [123, 124].

20.2.1.2 Melt Electrospinning

Melt electrospinning, an advanced technique in electrospinning, can produce precisely deposited fibrous scaffolds having a porous architecture and has been inspired by additive manufacturing techniques. A molten polymer jet is ejected or extruded from a reservoir and driven towards the collector with the help of a high-voltage as in solution electrospinning. In recent years, this technique has become increasingly popular because it permits the direct production of scaffolds with defined structures as in 3D printing [163]. Melt electrospinning creates 3D fibers by programmed stacking and addresses issues such as difficulty in the formation of thick and interconnected pores with a defined pattern of fibers. The range of suitable materials that can be used for melt electrospinning is however limited as most of the bioactive agents are susceptible to damage at high-temperature required in melt electrospinning [164].

Melt spinning is the most cost-effective spinning method because no solvent is recovered or evaporated, as in solution spinning, and the spinning rate is relatively high. Sutures are the most common biomaterials that can be produced with the help of melt-electrospinning. However, the use of melt electrospun matrices as tissue

engineering scaffolds is increasingly being investigated [163]. Melt electrospun scaffolds with multifilament yarns are also being investigated as vascular grafts. Melt electro writing (MEW), which incorporates 3D printing technology to melt electrospinning, makes it possible to print porous scaffolds with well-defined geometrical features of ultrafine fibers for tissue engineering applications [165, 166]. No solvent is needed in the spinning process, so spun polymers are highly pure. In another study, double-layered tubular scaffolds containing both melt-spun macrofibers (<200 μm in diameter) and electrospun submicron fibers (>400 nm in diameter) were developed [167]. Thus, melt electrospinning can be considered as a promising electrofabrication method in tissue engineering and wound healing applications due to the advantages such as solvent free fabrication process and the ability to control the fiber architecture using recent approaches like MEW [69].

20.2.1.3 Electrospraying

Electrospraying is a process that uses the same processes as in electrospinning, but which produces nano or microcapsules. Fluid from a capillary nozzle is exposed to electrical forces, and due to this, droplets move towards the oppositely charged collecting platform as nano or microparticles. First, electric forces deform the natural spherical meniscus and result in the formation of Taylor cones, just as in electrospinning process. Electrically charged jet is accelerated through an electric field by electric repulsion of charges on the surface and breaks into droplets at the free-end. Droplet production process can be pulsating or continuous, depending on the physical properties of the solution, fluid flow rate, magnitude and the polarity of the potential imposed on the nozzle [168, 169]. No mechanical energy other than the electric field supplied is used for electrohydrodynamic atomization. Droplets formed by electrohydrodynamic atomization have an electric charge that is typically half that of the Rayleigh limit, which is the maximum amount of power on a drop that produces a repulsive force equal to the strength of the surface tension. Electrospraying has several advantages over traditional mechanical induction-based droplet spraying systems such as the ability to develop equally sized droplets, droplet sizes can be less than 1 μm in diameter, less agglomeration and coagulation of droplets, and the ability to control spatial deposition of charged droplets. Electrospraying has been extensively used to develop drug delivery systems for diverse medical applications [170–172].

20.2.2 Developments and Generations of Electrofabrication Methods

Early in the twentieth century, the first patent on electrospinning was granted. Zeleny published a paper in 1914, in which he tried to mathematically model the behavior of

fluids in an electrostatically charged field [173]. In the early 1960s, Taylor was a trailblazer in the field of jet-forming mechanisms [174]. In subsequent literature, the conical shape of the jet was referred to as "Taylor cone" by scholars. To offset the surface with electrostatic forces, Taylor discovered that a 49.3° angle is required. In the following years, researchers concentrated on researching the structural morphology of nanofibers and gaining a better understanding of how nanofiber properties are affected by fiber morphology and process parameters. In 1987, Hayati et al. investigated the effects of an electrical field, laboratory circumstances, and all other factors that influence fiber stability, morphology, and atomization [175]. They found that coupling a high-conducting fluid with a high electrostatic field resulted in an extremely unstable current that looped and whipped around in different directions. Their findings also showed that this unstable jet generated fibers with much wider diameter distributions. Due to expanded awareness of the possible applications of electrospun nanofibers in different industries, electrospinning activity has increased significantly after a two-decade hiatus [176].

Researchers are also trying to improve the productivity of electrospinning as it is very important for commercialization. By replacing the needle with a wide-open bath of polymer solution and a copper spiral coil (electrode) inside the polymer solution, needleless electrospinning solves the issue of low efficiency and nonuniform fiber orientation [177, 178]. The copper coil acts as a fiber generator when an electrostatic force is applied. When the copper coil and polymer solution are charged, several jets are launched from the copper coil. More and more jets are launched from the coil and deposited on the spinning drum's surface as the voltage is increased. This method has the benefit of increased production as well as improved fiber orientation and alignment. Electrospinning with rotating electrodes is another approach for dealing with problems like poor efficiency and fiber orientation uniformity [179]. A collector screen is suspended over strings of electrodes rotating in a bath of polymer solution. The electrodes are usually attached to the positive terminal of the power supply, while the collector screen is either grounded or connected to the negative terminal of the power supply. Electrode strings, rather than using several spinnerets, execute the same operation with more control and ease of fabrication [180]. Compared to conventional electrospinning, this process is less costly and quicker. In addition to these, several other experiments were carried out to develop electrospinning method with large scale production potential.

Stable (non-porous) nanofibers with a smooth or nano-porous surface are generated by conventional electrospinning with a polymer solution (due to gradual evaporation of solvent from the polymer solution) (Fig. 20.1a). Electrospinning using an emulsion is known as emulsion electrospinning, where fibers with core–shell structure can be obtained. Cores of nanofibers made by emulsion electrospinning is ideal reservoirs for the encapsulation and protection of bioactive molecules [181]. As a result, emulsion electrospinning has been thoroughly investigated for the development of nanofibrous delivery vehicles for the controlled release of medications, growth factors, genes, and other biomolecules. During emulsion electrospinning, two immiscible solutions are spun out through two spinnerets and extended by electrostatic force. The driving liquid is a solution with a high conductivity that passes the

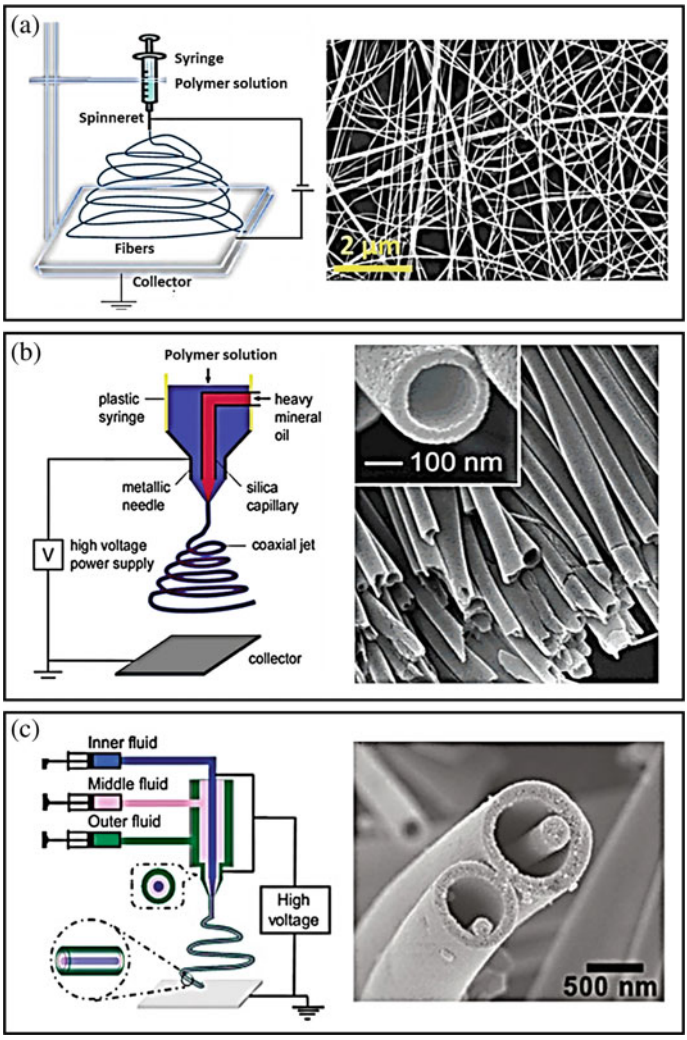


Fig. 20.1 Major types of electrospinning based on spinnerets. **a** Single needle approach. **b** Coaxial electrospinning. **c** Triaxial electrospinning. Figure a is reproduced from [209], with permission from Elsevier. Figure b is reproduced from [210], with the permission of American Chemical Society. Figure c is reproduced from [211], with permission from the American Chemical Society

tangential electrostatic force by viscosity on the liquid interface and deforms fused droplets to form small jets with an aqueous interior, gradually resulting in core–shell shaped nanofibers when stretched enough [182, 183]. If bioactive factors can be directly dissolved or evenly blended in the polymer solution before electrospinning, this can facilitate high loading and uniform distribution of the active agents in the resulting fibers [184, 185]. When this method is used alone, a large burst release of

active agents is observed [186]. It has been shown that altering the polymer structure of the fibers changes the release profile and, in some cases, greatly increases release time. It has been shown that coating fibers with a polymer slows burst release and decreases the severity of burst release [187]. Sometimes, phase separation can occur between protein and polymer solution, decreasing protein encapsulation efficiency and resulting in the formation of thin, brittle fibers. In such situations, surfactant or compatibilizer may be used to resist phase separation.

When initial burst release of drugs must be stopped or their functioning is harmed by the solvents used for dissolving the polymer, the use of coaxial electrospinning is highly recommended. In this procedure, two or three solutions are applied to the concentric needle independently from various tubes, resulting in the production of core shell layered fibers. Typically, drug-containing solution is loaded in the middle core component (Fig. 20.1b). Drug release profile can be fully or partially regulated by controlling the thickness, presence of pores and biodegradation rate of the shell polymer. Cell adhesion and proliferation profiles on scaffolds and their nanofibrous surfaces can also be fine-tuned using this approach. Coaxial electrospinning has been used in several reports to build scaffolds with better cell and skin-friendly surface properties, such as optimal hydrophobicity and cell affinity [188, 189]. Chen et al. suggested a new nanowire-in-microtube structure for fabricating core/shell ultrathin fibers (Fig. 20.1c).

Fiber orientation in scaffolds influence cell morphology and differentiation. For instance, the ECM of certain human tissues, such as cardiac tissue and ligament/tendon, provides topographical cues for guiding cell elongation and cytoskeleton growth on electrospun scaffolds with aligned nanofibers [190, 191]. By modifying the type of collector used for electrospinning, it is possible to control the morphology of the collected fibers. Spinning discs, drums, and mandrels are examples of specialized collectors in which the rate of fiber deposition is influenced by the rotation speed. A basic collector plate can generate fiber mat or mesh composed of randomly oriented fibers, while a drum or a rod collector can generate meshes with oriented fibers at fast rotation (more than 1000 rpm). At lower rotation speeds, drum-based collectors generate non-aligned cylinder like scaffolds. These hollow tubes could be used in a number of tissue engineering applications, including vascular scaffolds and nerve lead conduits [192]. Scaffolds with well aligned nanofibers can be generated by electrospinning with a point electrode and a ring electrode as collector, which can be useful for wound closure because these scaffolds can facilitate skin cell migration towards the center of the scaffold [193]. It is possible to control both the alignment and architecture of electrospun nanofibers by varying collector design. Micropatterned collectors have been used to make scaffolds that can better support cell adhesion, cell proliferation, and differentiation [194, 195]. Microtopography features of the collector such as shape and depth of patterns affect fiber conformity and alignment. In comparison to fibers collected on a flat surface, those collected on patterned surfaces show an increase in pore size and pore size distribution [156, 196]. Patterned fibrous scaffolds with defined ridges and grooves can be obtained by electrospinning on the top of metallic strips [195]. Interestingly, cell spreading was much higher in ridges than in the grooves. In another study, micropatterned

polydimethylsiloxane (PDMS) templates were used as collectors to obtain patterned scaffolds [157]. Cell morphology, cellular organization and cell migration were influenced by the 3D scaffold structure formed by the patterns on collector. Zhu et al. created a bilayer nanofibrous nerve conduit with longitudinally aligned nanofibers in the luminal layer to facilitate nerve regeneration and randomly arranged nanofibers in the outer layer for mechanical support [197].

Unlike electrospun microfibrous scaffolds, small pores are common in electrospun nanofibrous scaffolds, limiting cell penetration and vascularization. Increased fiber diameter, on the other hand, often leads to poor cell adhesion and migration due to the lack of ECM-like nanofibrous architecture [198]. Particulate-leaching electrospinning, wet electrospinning and selective removal of sacrificial electrospun fibers or electrosprayed microparticles have been investigated to increase fiber spacing in electrospun scaffolds [199, 200]. For instance, as water-soluble gelatin fibers are removed from gelatin and PLGA bicomponent scaffolds generated through dual-electrospinning, it was found that micropores were greatly expanded and the nanofibrous features were well maintained [201]. Another method is salt leaching, which involves mixing salt crystals with polymer solution and then leaching them in water after spinning [202]. While these methods are effective in increasing scaffold pore sizes and overall porosity, they had unintended consequence such as decreased structural integrity and poor mechanical properties of resulting scaffolds. Because maintain the bioactivity or functionality of drugs that can be damaged by strong electrical field or solvent(s) used during electrospinning, more complex scaffold surface functionalization chemistries may be employed [121, 203, 204]. To boost physical adsorption, controlling electrostatic or van der Waals interactions between the drug and the scaffolds may be needed (For example, by introducing surface functional groups on the surface of fibers) [205].

Near-field electrospinning (NFES) has been proposed and developed in recent years to improve controllable deposition of electrospun fibers [206]. NFES greatly extends the spectrum of fiber-fabrication uses, including electronic parts, energy harvesting, lightweight sensors, and tissue engineering, thanks to its position-controlled deposition characteristics. Overall, NFES technique demonstrated that it has the ability to be used in tissue engineering and bioprinting [207]. Melt electro writing (MEW) is a layer-by-layer additive manufacturing technique for fabricating highly ordered 3D tissue engineering scaffolds from micron-diameter fibers [208]. A voltage is applied to create a steady fluid jet with a predictable direction that is continuously deposited on a collector. The diameter of the fibers varies in the process, and it works with polymers that have been previously used in clinical settings.

20.2.3 Advantages and Limitations

Advantages: Electrospinning has gained a lot of attention in the past several years due to it potential use for producing highly porous tissue engineering scaffolds. Loosely connected 3D mats having high porosity and high surface area, which

can easily mimic native ECM, can be generated through this method [212–214]. Nano-submicron fibrous wound coverage matrices show more promising ability to support wound healing as compared to traditional bandages, due to their ability to partially recapitulate native ECM structure (Fig. 20.2). This encourages fibroblast/keratinocyte attachment and migration, which facilitates skin tissue regeneration in the wound. Electrospun membranes can act as barrier to invading microbes and prevent [215]. Electrospinning can be used to generate fibrous scaffolds consisting of a wide variety of materials with tunable properties, composition, shape, and fiber dimension, as compared to other nanofiber generating techniques. These benefits allow researchers to use electrospinning to produce wound dressing and tissue engineering scaffolds that recapitulate the native tissue microenvironment and use them to treat wounds more effectively. Moreover, electrospun meshes possess strongly intertwined porous structure that allows oxygen permeation, absorbs wound exudate, exchanges fluids, and prevents the wound dehydration [216]. Long et al. recently created a battery-operated, compact electrospinning system with a total circuit length of just 10 cm to directly electrospin fibers over the wound [217]. This advance could make electrospinning more widely accessible in hospitals and surgical centers, allowing for more personalized individualized wound treatment. Advanced bioactive wound dressings also require regulated, on-demand release of therapeutic agents to

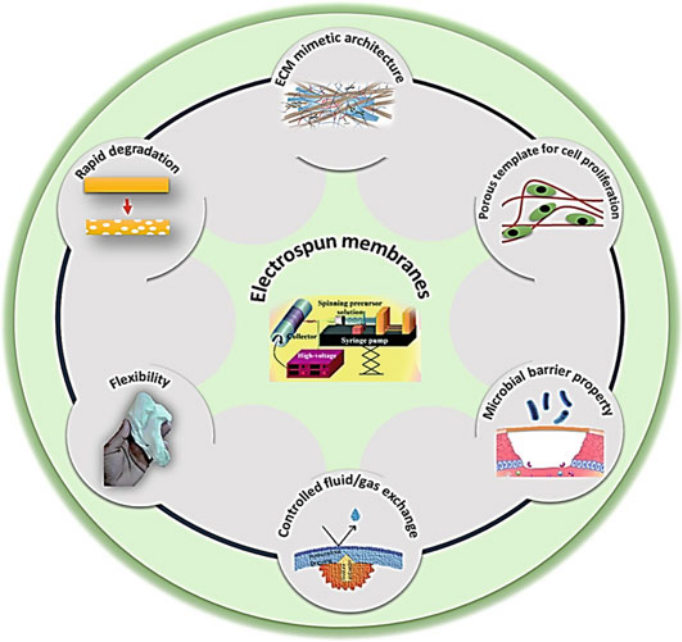


Fig. 20.2 Schematic showing the major advantages of using electrospun membranes for in tissue engineering and wound healing applications

facilitate wound healing without producing unwanted side effects [218]. Electrospinning holds great promise in this respect, as it allows loading of therapeutic agents and other active agents/biomolecules that can support tissue regeneration. Unlike bulk form, electrospun scaffolds may also have customized physiochemical properties, such as tunable degradation and drug release profiles. Bioactive agents such as growth factors, peptides and chemokines may be added after electrospinning or integrated into the scaffolds during the fabrication process.

Nano-fibrous membranes have been shown to adsorb more serum proteins than macro-fibrous membranes that are less porous [219]. In addition, compared to macroporous scaffolds, nano-fibrous scaffolds adsorbed more fibronectin from serum, according to other absorption study reports [220]. These findings suggest that nanofibrous scaffolds have a greater chance of mimicking natural ECM with improved tissue regeneration, as well as avoiding potentially negative immune response and pathogen transmission risks associated with naturally derived ECM-based constructs. Owing to the ECM mimicking features, electrospun nanofibers-based structures have shown excellent cell proliferation and differentiation capabilities both in vitro and in vivo [221, 222].

Limitations: Many of the parameters that influence electrospinning process are highly related and thus it is difficult to individually study the effects of such parameters. For instance, changing the concentration of a polymer solution, may also change its viscosity. Due to the high speed of the ejected liquid and the dynamic bending motion, it is difficult to control the deposition of fibers. It is also difficult to fabricate scaffolds in the shape of specific organs. Controlling fiber spacing is another challenge yet to be tackled. The complex process of fiber formation is still not fully understood. While electrospinning is ideal for producing thin membranes with large surface area and small pore size, it is not ideal for producing thicker sheets as this requires long production times. Melt electrospinning can only be used with polymers that have high decomposition temperatures and low melt viscosities. As a result of denaturation or decomposition of sensitive materials, the range of biopolymers that can be used in melt electrospinning is also limited.

Challenges: Even though electrospinning is a commonly used method for fabricating nanofibers, there are still many challenges to tackle. The use of toxic solvents in the polymeric solution, for example, causes health and safety concerns, and it limits industrial scalability. Electrospun scaffolds have several intrinsic limitations, one of which being their slow production rate. A typical laboratory experimental setup spins at a rate of a few mL/h (usually about 0.25–2 mL/h), which implies that if a solution containing 10% w/v polymer is spun for 10 h, the maximum amount of nanofibers formed is 1 g. To address this issue, multi-needle spinnerets have been proposed for industrial applications as a modification to the existing lab scale electrospinning setup. Multi-needle spinnerets, on the other hand, pose certain difficulties including polymer clogging on the spinneret, difficulty to clean the spinneret etc. Because of the effect of the electric field of adjacent needles, interference between the jets will affect the homogeneity of generated membrane/scaffold [223].

Another major challenge in electrospinning is the selection of appropriate solvent and ensuring that the solvent is fully removed from the finished product [224]. Electrospinning a polymer in its liquid state without the use of a solvent is better for polymers that are not soluble in common solvents. However, due to the high viscosity of polymers in the liquid state and the high melting temperature of most polymers, this process can only be used with a small number of natural and synthetic polymers. Because of the low solubility and high viscosity of high molecular weight natural polymers, the high density of intramolecular and intermolecular hydrogen bonding, the polyelectrolyte nature of aqueous solution, and the lack of appropriate organic solvent, electrospinning of natural polymers such as alginate and pectin is difficult [225]. While recent attempts to fabricate chitosan-based nanofibers are promising, crosslinking them under non-toxic conditions remains a challenge [90]. While it is highly desirable to combine natural and synthetic polymers to create natural synthetic hybrid scaffolds with superior physio-chemical properties of synthetic polymers while retaining favorable biological properties of natural polymers, finding a common solvent for both material types poses a challenge.

Total cell penetration through the pores is another problem for electrospun fibrous mats. Therefore, a combination of nano- and microfibers was introduced for cartilage tissue engineering [226]. Ideally, a scaffold should have a hierarchical geometry, adequate compressive power, and densely interconnected pores. While incorporating salt particles into electrospun scaffolds and their removal to generate pores has shown promising cell infiltration effects, uniform particle distribution within the structure remains a challenge [227, 228]. Using electrospun scaffolds to have most of the topographic and biochemical properties of native tissues is currently a difficult to achieve task and has not been realized yet. Another challenge when performing electrospinning is maintaining the bioactivity of drugs during and after spinning [229]. To summarize, the use of electrospun scaffolds for tissue engineering poses several challenges that must be carefully addressed and tackled by coupling with other recent approaches such as 3D printing/bioprinting so that electrospun scaffolds can be used for clinical applications.

20.3 3D Bioprinting

The main 3D bioprinting techniques include microextrusion, inkjet, and laser-assisted bioprinting (LAB). Also, the use of stereolithography (SLA) has recently been extended into bioprinting applications [230]. The efficacy of bioprinting techniques for fabricating biomimetic tissue constructs can be evaluated based on critical printing parameters, such as printing resolution, cell viability, and printing speed (Table 20.2). The deposition of bioinks in bioprinters is controlled by a digital system, which results in the fabrication of customized and complex constructs (Fig. 20.3) [231].

Table 20.2 Comparison of different types of three-dimensional (3D) bioprinting techniques and their characteristics

Property	3D Bioprinting type				
	Inkjet	Microextrusion	Laser-assisted	Stereolithography	Electrospinning
Material viscosity	3.5–12 mPa/s	30 mPa/s to >6 × 10^7 mPa/s	1–300 mPa/s	Not required	High, usually >300 mPa/s
Gelation methods	Chemical, photo-crosslinking	Chemical, photo-crosslinking, sheer-thinning, temperature	Chemical, photo-crosslinking	Light	Chemical, photocrosslinking
Preparation time	Short	Short to medium	Medium to long	Short	Short to medium
Printing speed	Fast (1–10,000 droplets per second)	Slow (10–50 μm/s)	Medium-fast (200–1600 mm/s)	Fast	Slow
Resolution or droplet size	<1 pL to >300 pL droplets, 50 μm wide	5 μm to millimeters wide	Microscale resolution	Micrometers	Nanometers to micrometers
Cell viability	>85%	40–80%	>95%	>85%	N/A
Cell density	Low, <10^6 cells/mL	High, cell spheroids	Medium, 10^8 cells/mL	Medium, 10^8 cells/mL	N/A
Printer cost	Low	Medium	High	High	Low

Adapted from Murphy and Atala [232], with permission from Nature Publishing Group and from Ashammakhi et al. [233], with permission from Wiley

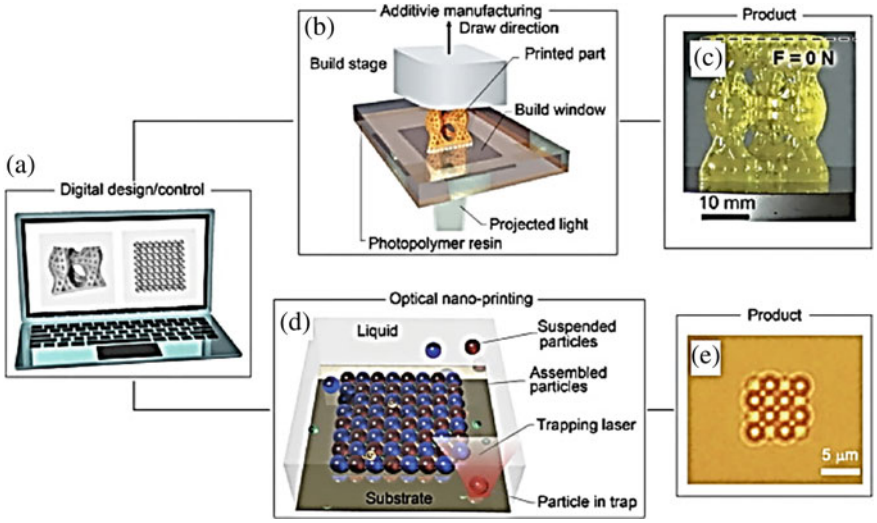


Fig. 20.3 Schematic illustration of digital manufacturing technique. **a** Computer-aided design for three-dimensional (3D) printing and the digital control of the printing process. **b** and **c** Printing of Kagome tower using the stereolithography (SLA) technique. **d** and **e** Nano-printing of a hybrid structure composed of particles at different sizes. Reproduced from Lin et al. [231], with permission from Elsevier

20.3.1 Microextrusion 3D Bioprinting

Microextrusion 3D bioprinting technique involves extruding printing bioinks into continuous filaments, which can be patterned based using a CAD program. Microextrusion technique enables simultaneous deposition of cells and matrix materials through multiple printheads to generate geometrically complex and hybrid biological structures. This technique can provide higher structural integrity due to its ability to deposit continuous filaments of printed material [234].

20.3.1.1 Principle

In microextrusion, printing material is pushed through printer nozzles by using a pressure-assisted system, which can either be pneumatic or mechanical (Fig. 20.4a, b). The extrusion of the ink can also be driven by a solenoid-based system, as shown in Fig. 20.4c [235]. Microextrusion printing would generate continuous streams of materials, which can be patterned to desired 3D structures by using a printing software connected to the 3D printer. Most of the extrusion-based 3D printers provide single nozzle dispensing systems. However, recent advances in multi-head deposition systems enable simultaneous deposition of multiple materials.

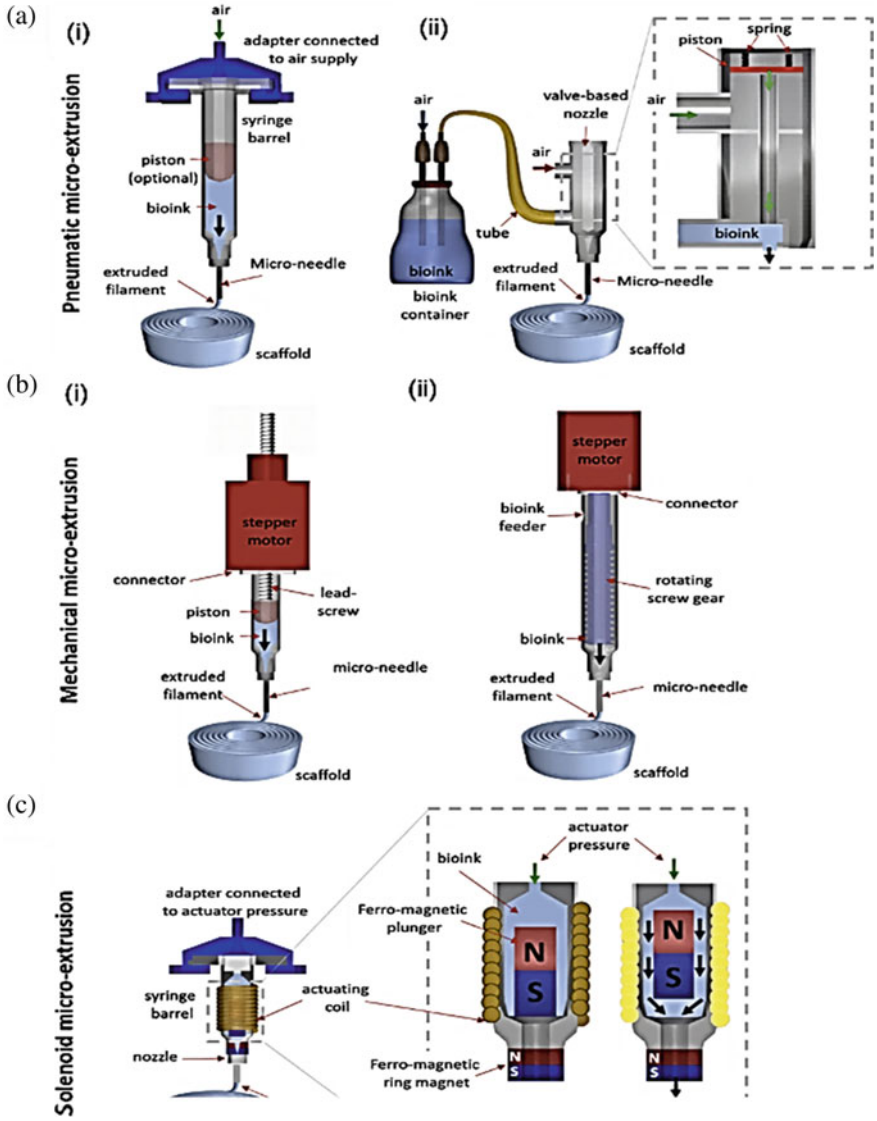


Fig. 20.4 Schematic illustration of different types of microextrusion three-dimensional (3D) printing techniques. **a** Pneumatic microextrusion can be either (i) valve-free or (ii) valve-based system. **b** Mechanical microextrusion that includes (i) piston- or (ii) screw-based system. **c** Solenoid microextrusion technique. Reproduced from Ozbolat et al. [235], with permission from Elsevier

Pneumatic Systems

Pneumatic 3D microextrusion systems are based on the use of a simple extrusion mechanism, where force needed to dispense ink is generated by using compressed air and a valve-free or valve-based configuration. Valve-free systems have been used more commonly due to their simple structure; however, valve-based systems have the advantage of better control over the printing pressure for high-resolution printing applications [235]. Overall, pneumatic systems are generally characterized by slow material deposition process due to the use of compressed gas.

Mechanical Systems

Mechanical extrusion systems usually have a more complex structure, resulting in a more precise deposition of materials or cells compared to the pneumatic-based microextrusion systems. However, this would reduce the maximum force that the instrument can apply to dispense the printing ink [236]. Piston-based microextrusion systems have demonstrated a high capability to control the flow of ink [235] while the screw-based systems can dispense highly viscous inks [237]. However, the high pressure needed for the screw-based systems to dispense viscous materials can adversely affect cell viability and function. To mitigate this problem, the use of shelf screws should be avoided. For example, Visser et al. employed a screw-driven system to melt and deposit polycaprolactone (PCL) while a piston-driven syringe was used to print a hydrogel [238].

Solenoid-Based Systems

Solenoid-based microextrusion systems utilize electrical pulses to control ferromagnetically or piezoelectrically actuated valve systems [239] (Fig. 20.4c). For instance, upon applying voltage, solenoid coil on the top of the printhead becomes magnetic and applies a magnetic force that can pull up the plunger to open the orifice and extrude the ink [240].

20.3.1.2 Development and Generations

Microextrusion-based 3D printing method has long been used for some time for applications that include the shape forming of metals and plastics [235]. However, this technique was first used in tissue engineering back in 2002, when fused deposition modeling (FDM) technique was employed to print melted biomaterials into porous scaffolds to support cell proliferation and growth [241]. Until about a decade ago (2005), 3D printers were generally expensive, and their high cost limited their use. Later, low-cost multimaterial extrusion-based 3D printers became accessible to the public [242]. Since then, various types of extrusion-based 3D printers have

been developed and commercialized by different laboratories and companies worldwide. These products range from large-size printers to small desktop printers that can easily fit within bio-hoods for cell-involving printing applications. Most of these printers are based on a syringe extrusion technique that allows controlling the extruded ink diameter by adjusting the needle size and properties of printing material [243]. Some new microextrusion printers have also demonstrated the capability to deposit and assemble tissue spheroids into 3D structures, which are on their way to commercialization [244].

20.3.1.3 Advantages and Limitations

Microextrusion 3D printing enables the printing of high-viscosity materials [230, 233]. Also, it allows printing of high-density bioinks to achieve physiological cell densities in the printed constructs [245, 246]. Microextrusion can easily be equipped with multiple printheads to print multimaterial constructs, mimicking the heterogeneous composition of native tissues [243].

20.3.2 Inkjet 3D Bioprinting

Inkjet bioprinting has been the first 3D bioprinting technology developed based on conventional 2D ink printers, where the ink was replaced with a biomaterial and paper with a moving stage that enabled the printing of 3D constructs by its controlled move along the x-y-z axis [243].

20.3.2.1 Principle

In inkjet 3D bioprinting, small bioink droplets are generated using thermal or piezoelectric actuation and subsequently deposited onto predefined locations in a layer-by-layer fashion to build a 3D structure. Thermal inkjet printers include electrical elements that are heated to create air bubbles that push the bioink down to the nozzle and dispense it. Alternatively, many inkjet printers are based on piezoelectric waves that can break the bioink into droplets of different sizes, thus resulting in a higher printing resolution. This technique reduces the risk of cells being exposed to excessive heat or pressure. Moreover, the nozzle-free configuration of inkjet printers can help to mitigate nozzle clogging issues [247].

20.3.2.2 Development and Generations

Inkjet 3D printing technique was invented by Thomas Boland in 2003 [243]. Later in 2015, an inkjet 3D printer, with a capability to simultaneously deposit multiple materials, was developed [248]. More recently, inkjet 3D bioprinting has been combined with a spray crosslinking, which enabled the fabrication of multimaterial large constructs [249]. Also, a high-resolution inkjet bioprinter was commercialized, with the capability to deposit low- and high-viscosity materials and even cell culture media [250].

20.3.2.3 Advantages and Limitations

Inkjet is a desirable 3D printing technique due to its low-cost and ability to print different types of biomaterials. Moreover, using this technique, it is possible to achieve printing resolutions as low as 50 μm with the capability for the precise deposition of biomaterials and cells [251]. Inkjet bioprinting is also characterized by high speed, with a deposition rate ranging from 1 to 10,000 droplet/s [252]. Inkjet printers can include multiple printheads enabling the deposition of multiple materials at the same time [248]. Another advantage is their ability to induce gradients in terms of cells or materials concentrations throughout the 3D bioprinted constructs by changing droplet size or density [237]. However, heat and mechanical stresses generated during this process may damage the cells [253]. However, no significant impact on cell activity was observed as the cooling of the printed constructs occurs within a few seconds. One major drawback of inkjet 3D bioprinting is the limitation related to the viscosity of inks. Excessive force is required to break and eject solutions of high viscosities. Bioink must be in liquid form to be inkjet-printed, and subsequently, it should have the ability to form a rigid structure after printing by using one of the crosslinking mechanisms [254]. Such processes may drastically alter the properties of the bioink or induce serious cytotoxicity effects. Difficulty with printing bioinks having high cell density (>10^6 cells/mL) is another limitation associated with the use of inkjet 3D bioprinting [232, 233].

20.3.3 Laser-Assisted 3D Bioprinting

Laser-assisted 3D bioprinting (LAB) is a less commonly used printing technique compared to inkjet and extrusion-based 3D bioprinting. However, there has been an increasing demand for the use of LAB for biomedical applications due to its high printing resolutions.

20.3.3.1 Principle

In LAB, laser is used to volatilize a donor layer (usually made of a glass coated with an energy-absorbing metallic layer) under which a cell-laden liquid bioink is suspended. This would generate a high-energy bubble that throw droplets of bioink onto the receiving plate placed below the bioink. This process continues until the 3D construct fabrication is completed (nozzle-free 3D printing) [230, 255].

20.3.3.2 Development and Generations

Laser 3D printing was initially used for high-resolution printing of metallic compounds, such as computer chips. In 2007, the use of laser 3D printing was extended to biological applications by patterning an array of micro-sized droplets [256]. LAB technique has been commercialized for 3D printing and was used for printing cosmetic tissue products, such as artificial human skin. However, widespread use of LAB for tissue engineering applications is not anticipated in near future [244].

20.3.3.3 Advantages and Limitations

LAB has a high printing resolution, and it can be used for printing bioinks at high cell densities (up to 10^8 cells/mL). This nozzle-free technique has enabled printing materials of diverse properties with viscosities ranging from 1 to 300 mPa/s. The nozzle-free system also reduces shear stresses exerted on cells during printing, thus increasing cell viability up to >95% [257, 258]. However, LAB is limited by its high production and maintenance costs, which are related mainly to the high-resolution laser diodes used in this technique [257, 258].

20.3.4 Stereolithography 3D Bioprinting

SLA 3D printing technique is based on the photocrosslinking process, where UV or visible light is used to solidify liquid ink into a desired 3D pattern. This technique is particularly interesting for printing photocurable materials, such as acrylics and epoxies [237].

20.3.4.1 Principle

In SLA, cell-laden photopolymers are deposited layer by layer, and selectively photo-crosslinked on each layer based on 2D digital models (Fig. 20.2d) [243]. After the 2D pattern is printed onto the printing bed, the printing stage is moved up along the z-axis and the photo-crosslinking process continues until 3D structure is fabricated.

20.3.4.2 Development and Generations

SLA 3D printing was first patented in 1986 [259]. This technique was subsequently introduced into the field of bioengineering in 1993 by fabricating detailed models for reconstructive head surgery [260]. More recent studies have shown the ability of SLA techniques to incorporate cells into the printed structures [261]. In this regard, high-speed and high-resolution SLA 3D bioprinters have been developed for fabricating ultra-fine structures, such as human capillaries and fine ECMs [262]. The printing process was shown to be non-toxic, and it could be used for printing cell-laden bioinks [262]. Also, recent reports have demonstrated the development of a digital micromirror device (DMD)-based SLA bioprinting. This technique includes millions of micron-sized mirrors that can be controlled individually for precise projection of light onto the polymerization stage to create high-resolution 3D structures [263].

20.3.4.3 Advantages and Limitations

SLA is a high-speed and high-resolution technique that can be used for printing complex structures at resolutions as high as <5 μm [264]. Similar to the LAB technique, SLA is a nozzle-free technique; therefore, no shear stress will be generated during printing, and high cell viability (>85%) will be achieved using this technique [243, 265]. However, in SLA, there is a need to use transparent bioinks to achieve uniform bioink photo-crosslinking, and this has limited the cell density of bioinks to $<10^8$ cells/mL [243]. Also, the use of UV light in this technique can induce cell toxicity, which has been partially resolved using visible light-assisted SLA [266].

20.3.5 Electrospinning-Based 3D Printing

Electrospinning is a high-resolution fabrication technique that can generate a small diameter of randomly oriented fibers for constructing mechanically strong structures.

20.3.5.1 Principle

Electrospinning-based printing includes charged filaments of solutions or melts, which are pulled out and deposited by electrical forces and subsequently dried to form a fibrous mat [80, 243]. This technique can produce fibers with diameters as small as 2 nm, resulting in the formation of high-resolution constructs that can be used for a variety of tissue engineering applications [73, 209, 267]. In this method, a digitally controllable stage with the capability to move spatially is combined with the conventional electrospinning machine, where a solution is extruded by a syringe or pneumatic force, making it possible to pattern a 3D construct in a customized manner. The main characteristic of electrospinning-based printers is their shorter

collecting distance (0.5–3 mm) as compared to tens of centimeters for conventional electrospinning technique. This enables the deposition of electrospun fibers in a more controllable manner. Also, the working voltage in electrospinning-based printers is usually lower than classical electrospinning, but this depends on the conductivity of biomaterial to be 3D printed [243].

20.3.5.2 Development and Generations

In recent years, electrospinning-based printing has captured special attention due to the increasing interest in nanotechnology and the fabrication of ultra-fine 3D structures in a controlled manner. In 2011, Brown et al. combined melt electrospinning with a digitally controlled collector and developed a new class of 3D printers called melt electrospinning writing (MEW), which enabled the deposition of well-defined filaments [268]. Since then, several laboratories across the world have developed custom-built devices to combine electrospinning with inkjet or extrusion-based 3D printing techniques [269–278]. Also, companies such as Spraybase® (Ireland) [279], NovaSpider (Spain) [280], and RegenHU Inc. (Switzerland) [281] have attempted to commercialize some MEW-based printers for various tissue engineering applications.

20.3.5.3 Advantages and Limitations

Melt electrospinning-based printing is an emerging printing technique that can print fibers with diameter in the range of a few nanometers to micron (0.650–1 μm), providing a high degree of resolution, porosity, and pore interconnectivity [271, 282, 283]. Also, a high surface area of the electrospun fibers relative to their diameters can provide highly bioactive structures. However, one major limitation is the rapid whipping of the charged fibers which results in a spatially unstable 3D structure [243]. Also, the encapsulation of cells in the electrospun biomaterials is still a significant challenge due to the high temperatures and voltages involved in the electrospinning process [243]. Melt electrospinning-based printing; however, allows for the fabrication of well-defined and highly porous structures with the possibility to seed the cells in the scaffolds after the printing process to provide a high degree of cell activity and morphogenesis in the printed structure [284–287].

20.4 Combining Electrospinning and 3D Bioprinting

20.4.1 Need, Approaches and Conditions

Advances in the field of biomaterials in the last few decades have contributed to significant improvements in tissue engineering and regenerative medicine [69, 288–291]. Specifically, biomaterials are used in 3D bioprinting to formulate bioinks to encapsulate the cells and produce highly organized structures [292]. In most cases, these bioinks are developed as hydrogels useful for bioprinting. They can provide a hydrated environment, like native tissue, due to their high water absorption and retention capability [293]. Moreover, hydrogels have favorable biocompatibility, and biodegradation profiles, as well as porous structure important for the transportation of nutrients, oxygen, and cell metabolic waste [294, 295]. Moreover, hydrogels can ensure cell viability over time. However, there are some drawbacks related to hydrogels. Most importantly, the lack of sufficient mechanical properties, which is considered a significant disadvantage. Hydrogels cannot keep their 3D structure and they deform due to gravitational forces, which reduces 3D bioprinted structure resolution and fidelity [296]. Moreover, after bioprinting, the construct is usually fragile, which makes its handling very difficult. This drawback is problematic for in vivo application of such scaffolds and it significantly hinders load-bearing applications [293, 297, 298].

To tackle this problem, most researchers try to increase the crosslinking density by increasing the crosslinking time and/or use of a second crosslinker [299–301]. Consequently, binding sites increase, and scaffold mechanical integrity improves. Other options include combining several biomaterials in the bioink or increasing the concentration of the biomaterial in the bioink. However, these solutions can reduce cell viability due to decreased diffusion rate of nutrients and oxygen. In other words, there is a trade-off between the mechanical properties of bioprinted scaffolds and the bioactivity of the scaffolds [293, 296]. As an alternative, it is possible to combine 3D bioprinting with other advanced manufacturing techniques to obtain a hybrid construct. This combination is advantageous since it can combine the benefits of two or several different fabrication techniques to compensate for each other's shortcomings.

Electrospinning is considered a simple and powerful tool that can be used to produce nanofibrous mats prepared for regenerative medicine purposes due to high porosity, high surface-to-volume ratio, and, more importantly, structural resemblance to the native extracellular matrix (ECM) [302, 303]. These structures can also enhance cell attachment and accelerate cell proliferation [304–306]. Besides, this technique can produce thin sheets from synthetic and natural polymers with great mechanical flexibility [293, 307]. Consequently, the combination of electrospinning and 3D bioprinting could be considered a promising approach to fabricate scaffolds suitable for cell survival and proliferation and mechanically stable for handling and in vivo applications. Ideally, these hybrid structures can have more complex hierarchical structures ranging from nanometer-size up to micrometer scale.

20.4.2 Application in Tissue Engineering

Xu et al. combined electrospun PCL/Pluronic F-127 nanofibers with inkjet bioprinting of fibrinogen/collagen/chondrocytes bioink for cartilage tissue engineering [297]. The two fabrication techniques were combined in one device. The addition of Pluronic F-127 into the electrospinning solution resulted in enhanced hydrophilicity of the nanofibers. In a layer-by-layer assembly, the scaffold was prepared as a five-layer structure with two layers of bioprinted hydrogels embedded within three layers of nanofibers (thickness of 1 mm). This was beneficial since extremely thin layers of nanofibers (average diameter of 422 ± 62 nm) were electrospun which is challenging to handle if they were electrospun separately. The hybrid scaffold showed better mechanical integrity with higher ultimate tensile strength than pure alginate hydrogels, pure PCL, and collagen/fibrin gels. Moreover, live/dead assay showed high cell viability (~82%) of chondrocytes within these hybrid structures, which confirmed structures' biocompatibility. Besides, after four weeks of in vitro culture, the encapsulated cells produced native ECM components, including collagen and glycosaminoglycans. The in vivo evaluations showed that hybrid scaffolds were capable of producing collagen and glycosaminoglycans after eight weeks. Deposited ECM compounds were observed to be well-organized and to resemble the native ECM. Encapsulated chondrocytes also retained normal phenotype as observed in native cartilage, demonstrating this approach's high potential for cartilage tissue engineering.

Paul et al. used this approach for vaginal wall repair [304]. PCL nanofibers were fabricated using melt electro-writing technique (a combination of melt electrospinning and 3D printing). The structure possessed suitable biocompatibility and appropriate surface topography for cell attachment, migration, and proliferation. Alginate/aloe vera hydrogels containing endometrial mesenchymal stem/stromal cells (EMSCs) were printed on top of the nanofibers using an extrusion bioprinting method. It was observed that alginate/aloe vera bioink with a 1:1 mass ratio performs the best biocompatibility and cell viability. Besides, the results revealed a homogenous cell distribution after bioprinting over PCL mesh (Fig. 20.5a). In vivo mice experiments showed that cell encapsulated hybrid scaffolds recruited lower inflammatory cells as compared to cell-free hybrid scaffolds and PCL nanofibers. More interestingly, histological analysis showed that after implantation, EMSC-loaded hybrid scaffolds resulted in infiltration of more M2 macrophages. This was attributed to the anti-inflammatory properties of EMSCs (Fig. 20.5a). Besides, cell-encapsulated hybrid structures showed better integration with host tissue.

As an alternative to the layer-by-layer stacking of nanofibers and bioprinted hydrogels perspective, Ko et al. combined the electrospinning and 3D bioprinting by dispersing nanofibers within the formulated bioink [296]. To this aim, fragmented poly(lactic-*co*-glycolic acid) (PLGA) nanofibers were dispersed in the bioink (gelatin methacryloyl, GelMA solution) through a mechanical homogenizer (Fig. 20.5b, c). Nanofibers were homogeneously distributed in the bioink and addition of PLGA nanofiber fragments (PLGA-NF) resulted in a significant increase in the compressive

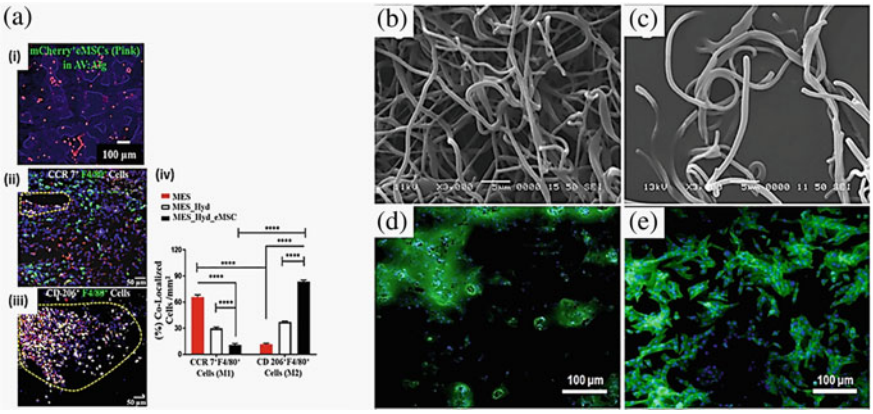


Fig. 20.5 Combination of electrospinning and three-dimensional (3D) bioprinting. **a** Combination of melt electro writing and 3D bioprinting. (i) distribution of mCherry^{+} endometrial mesenchymal stem cells (EMSCs) over the 3D printed structures, (ii, iii) M1 and M2 macrophages in tissue explant after one week, and (iv) quantification of obtained results. Reproduced from Paul et al. [304], with permission from Elsevier. **b** Scanning electron microscopy (SEM) images of poly(lactide-*co*-glycolide) (PLGA) nanofibers and grinded PLGA nanofibers (**c**). Fluorescence microscopy of fibroblast cells encapsulated in pure gelatin methacryloyl (GelMA) hydrogel (**d**), and poly(lactic-*co*-glycolic acid) nanofiber fragments (PLGA-NF) loaded (GelMA) hydrogel (**e**) after 3 days. **d–g** Reproduced from Ko et al. [296], with permission from Elsevier

strength. However, at high concentrations of PLGA-NF (10%), clogging occurred, and non-uniform strands were printed. Biocompatibility assessment revealed that nanofibers did not adversely affect cell viability. Moreover, since nanofibers could provide cells with binding sites, cells start to retain their phenotype faster than pure GelMA bioinks (Fig. 20.5d, e). A summary of the previous works that combined 3D bioprinting and electrospinning is presented in Table 20.3.

20.4.3 Advantages and Limitations

The idea of combining 3D bioprinting with other manufacturing methods is a fascinating phenomenon that can result in the formulation of hybrid structures with exclusive capabilities and features [296]. This combination can help to develop more complex structures that resemble native ECM more effectively [298]. Using 3D bioprinting, it is possible to construct exceptionally well-defined 3D structures with several cells encapsulated within the structure [310]. On the other hand, electrospinning can produce highly porous fibrous structures similar to native ECM [311]. This hybrid approach provides excellent opportunities to use and combine synthetic and natural polymers in the structure. For example, collagen, fibrin, and gelatin can be utilized in hybrid structures with significantly higher mechanical and biological

Table 20.3 Summary of works combining electrospinning and three-dimensional (3D) bioprinting

Application	Material for electrospinning	Material for 3D bioprinting	Cell types	Results	Refs.
Soft tissue engineering	PLGA	GelMA	NIH3T3 fibroblast	• Enhanced viscosity and compressive modulus of the bioink by incorporation of nanofibers • Increased cell proliferation rate in bioprinted structures by the addition of nanofibers • Cells retained their stretched phenotype faster in fiber-loaded structures	[308]
Cell/surface interaction analysis	Polyurethane	Cell spheroids	Primary human fibroblast	• Visualization of cell-fiber interfaces and cell membrane protrusions • Quantification of several important morphological and cell-scaffold interfaces	[309]
Vaginal wall repair	PCL	Alginate/aloe vera	Endometrial mesenchymal stem/stromal cells (EMSCs)	• Stimulated tissue integration in NSG mice • Improved EMSCs retention • Improved collagen deposition in EMSCs bioprinted scaffolds	[304]
Soft tissue engineering	PCL	Alginate	NIH3T3 fibroblast	• Improved mechanical properties • Decreased shrinkage and enhanced fidelity and resolution • Enhanced cell proliferation	[293]

(continued)

Table 20.3 (continued)

Application	Material for electrospinning	Material for 3D bioprinting	Cell types	Results	Refs.
NA	PLLA	GelMA	Pre-osteoblast MC3T3 cells	• Enhanced printability • Enhanced viscosity • Enhanced printing fidelity • Slightly higher cell viability compared to pure GelMA	[295]
Neural tissue engineering	PCL	Alginate	PC12 neural cells	• Improved mechanical properties • High cell viability and cell proliferation	[298]
Cartilage tissue engineering	PCL/Pluronic F-127	Collagen/fibrinogen	Rabbit chondrocytes	• Control of construct organization • Production of thin layers for layer-by-layer assembly • Improved mechanical properties • High (>80%) cell viability • Maintaining the phenotype and ECM production of cells in vivo	[297]

properties than the scaffolds made using a single soft hydrogel. These hybrid structures showed promising properties in mimicking the ECM of native tissues that might ultimately lead to clinical evaluations.

However, despite numerous advantages, there are some shortcomings with this approach. Generally, electrospinning is a time-consuming technique to fabricate thick structures. Hence, when both techniques are used simultaneously, it could take a considerable amount of time to fabricate scaffolds. Besides, any residual solvent within the electrospun fibers can negatively affect the viability of cells in the construct cell viability and final functionality. Moreover, nanofiber layers between each layer of the 3D bioprinted construct can alter nutrients and oxygen diffusion rate with some potential adverse effects on cellular behavior [297]. Besides these disadvantages, this combination is still promising and can create several new opportunities to solve critical issues in tissue engineering, regenerative medicine, and healthcare.

20.5 Challenges and Future Directions

Sterility of the fabricated constructs is a critical consideration for 3D bioprinting. Since cells are directly incorporated into the scaffold upon fabrication, any contamination could cause severe problems for further use. This phenomenon could become even more important when different fabrication techniques are combined. Especially, if electrospinning and 3D bioprinting are conducted separately, careful consideration should be held to make sure that both scaffolds (i.e., fibers and hydrogels) are prepared in a sterile environment and are kept sterile upon combination. Direct integration of electrospinning and bioprinting may pose additional challenges due to the presence of organic solvents used in electrospinning. Sufficient time should be provided between electrospinning and bioprinting processes to facilitate the evaporation of hazardous solvents from electrospun fibers before coming in contact with the bioink. Providing a higher temperature in the spinning hood may help in rapid solvent removal. A washing step can also be introduced between electrospinning and bioprinting processes to minimize the presence of residual solvent. Material level incompatibility of electrospun fibers, particularly in the case of hydrophobic electrospun fibers, in bioprinted hydrogel construct can also be a challenge. Surface modification of electrospun fibers can be a prerequisite before incorporating electrospun fibers in bioprinted constructs.

One specific consideration for future examinations could be the modulation of degradation behavior. Generally, nanofibers are added to 3D bioprinted hydrogels to enhance the mechanical properties [312–314]. For this purpose, synthetic polymers were used which are known to have a much slower degradation profile than the investigated hydrogels [315, 316]. This degradation variation could alter the remodeling of the structures and subsequently the integration of the scaffold. Hence, in future works, attempts should be made to balance the degradation rates of both hydrogels and fibers to match the specific requirements of the targeted tissue.

Vascularization is known to be a bottleneck limiting the engineering of large-scale tissues [317–319]. Consequently, in future studies, it is possible to exploit smart materials and encapsulate angiogenesis factors and biomolecules into engineered constructs to formulate stimuli-responsive scaffolds that can release the molecules upon need and accelerate vascularization. Incorporating growth factors in electrospun fibers and into 3D bioprinted constructs can be a useful approach to improve vascularization. Electrospun tubular constructs [320, 321] can be integrated in bioprinted constructs to act as vascular channels for media transport during in vitro construct maturation and as vascular network after in vivo implantation.

The widespread use of the natural polymer-based hydrogels is limited because of their low mechanical strength. Combining mechanically less stable natural polymers with electrospun synthetic polymers may solve such challenges to some extent. However, precisely mimicking the mechanical properties of ECM of various native tissues in engineered constructs is still challenging. Future research may focus on this aspect, where tissue specific ECM mimetic scaffolds with matching tensile strength, modulus and elasticity will be developed by combining electrospun fibers within 3D bioprinted constructs. Furthermore, structures with high degree of resemblance to native ECM and native tissues could be developed by using a mixture of specifically cell-laden hydrogel along with organized distribution of nanofibers. In addition, biofouling is another main challenge that limits wider clinical use of both nanofibrous membranes and 3D bioprinted constructs. To tackle infection problems, loading of antibiotics or antimicrobial nanoparticles in electrospun nanofibers has been reported [322–326]. Incorporating chopped electrospun membranes loaded with antibiotics or nanoparticles in bioprinted constructs is an interesting area for further investigation.

In addition to the integration of electrospinning and 3D bioprinting methods, combination of multiple techniques such as the use of microfluidic techniques [37], may be a promising approach for developing smart multifunctional and stimuli responsive constructs for regenerative medicine, drug delivery and personalized therapy [327–329]. In addition, other beneficial techniques and different methods could be used to promote cell movement through non-woven structures, such as the application of electrical fields, the production of gradient properties (i.e., stiffness, pore diameter, chemical gradient, directional porosity, etc.) within scaffolds.

To develop a robust construct by combining electrospinning and 3D bioprinting, it is important to completely understand all the factors related to electrospinning and 3D bioprinting processes, and to find an effective way to quantify the interaction between factors/parameters affecting these techniques and their combination. To achieve this, morphological and chemical effects need to be studied and influence of these parameters on the relationships between each variable of electrospinning and 3D bioprinting should be addressed. After this has been determined for several similar materials, a mathematical models can be drawn up to estimate conditions needed to perform electrospinning and 3D bioprinting simultaneously or one after the other in compliance with the requirements for desired application.

20.6 Conclusions

Although there has been increasing developments in 3D bioprinting toward the development of functional tissue constructs, the production of mechanically robust and durable constructs using 3D bioprinting has been a challenging task. Various strategies have been explored to overcome this limitation that recently included the integration of nanofibers that have been produced by using electrospinning to 3D bioprinted constructs. This resulted in the production of reinforced constructs with better properties. The use of nanofiber-based structures adds native ECM-mimicking properties to engineered tissue constructs. In addition, this approach enables the integration of drug release properties and building gradients into the engineered tissue constructs and widening the applications of 3D bioprinting for interface tissues. It is expected that such a combinatorial approach will be further explored in future and its applications increased.

Acknowledgements Authors acknowledge funding from the National Institutes of Health (1UG3TR003148-01, N.A.), the American Heart Association (COVID-19 Rapid Response Award 20203858, N.A.) and Qatar National Research Fund (a part of Qatar Foundation, NPRP12S-0310-190276, A.H.). Y. N. E. acknowledges funding support from 2232 International Fellowship for Outstanding Researchers Program of TÜBİTAK (Project No: 118C346). M.T. acknowledges financial support from Fonds de la recherche en sant du Quebec.

References

1. Ashammakhi, N., et al. (2019). Minimally invasive and regenerative therapeutics. *Advanced Materials, 31*(1).
2. Gobbi, A., et al. (2006). Osteochondral lesions of the talus: Randomized controlled trial comparing chondroplasty, microfracture, and osteochondral autograft transplantation. *Arthroscopy—The Journal of Arthroscopic and Related Surgery, 22*(10), 1085–1092.
3. Potyondy, T., et al. (2021). Recent advances in 3D bioprinting of musculoskeletal tissues. *Biofabrication, 13*(2).
4. Amini, Z., & Lari, R. (2021). A systematic review of decellularized allograft and xenograft-derived scaffolds in bone tissue regeneration. *Tissue & Cell, 69*.
5. Nellore, A., & Fishman, J. A. (2018). Donor-derived infections and infectious risk in xenotransplantation and allotransplantation. *Xenotransplantation, 25*(4).
6. Oryan, A., et al. (2014). Bone regenerative medicine: Classic options, novel strategies, and future directions. *Journal of Orthopaedic Surgery and Research, 9*.
7. Ashammakhi, N., et al. (2019). Bioinks and bioprinting technologies to make heterogeneous and biomimetic tissue constructs. *Materials Today Bio, 1*.
8. Khan, F., & Tanaka, M. (2018). Designing smart biomaterials for tissue engineering. *International Journal of Molecular Sciences, 19*(1).
9. Sharma, K., Mujawar, M. A., & Kaushik, A. (2019). State-of-art functional biomaterials for tissue engineering. *Frontiers in Materials, 6*.
10. Abdulghani, S., & Mitchell, G. R. (2019). Biomaterials for in situ tissue regeneration: a review. *Biomolecules, 9*(11).
11. Al-Sukhun, J., Penttilä, H., & Ashammakhi, N. (2011). Orbital stress analysis: Part III: Biomechanics of orbital blowout fracture repair using bioresorbable poly-L/DL-lactide (P[L/DL]LA 70:30) implant. *The Journal of Craniofacial Surgery, 22*(4), 1299–1303.

12. Ashammakhi, N., et al. (2019). Spine intervention—An update on injectable biomaterials. *Canadian Association of Radiologists Journal, 70*(1), 37–43.
13. Reich, K. M., et al. (2020). The effect of diclofenac sodium-loaded PLGA rods on bone healing and inflammation: A histological and histomorphometric study in the femur of rats. *Micromachines (Basel), 11*(12).
14. Franz, S., et al. (2011). Immune responses to implants—A review of the implications for the design of immunomodulatory biomaterials. *Biomaterials, 32*(28), 6692–6709.
15. Zhang, D. H., et al. (2021). Dealing with the foreign-body response to implanted biomaterials: Strategies and applications of new materials. *Advanced Functional Materials, 31*(6).
16. Ashammakhi, N. (2005). Reactions to biomaterials: The good, the bad, and ideas for developing new therapeutic approaches. *The Journal of Craniofacial Surgery, 16*(2), 195–196.
17. Arciola, C. R., Campoccia, D., & Montanaro, L. (2018). Implant infections: Adhesion, biofilm formation and immune evasion. *Nature Reviews Microbiology, 16*(7), 397–409.
18. Saini, M., et al. (2015). Implant biomaterials: A comprehensive review. *World Journal of Clinical Cases, 3*(1), 52–57.
19. Ashammakhi, N., et al. (1995). Strength retention of self-reinforced polyglycolide membrane: An experimental study. *Biomaterials, 16*(2), 135–138.
20. Ashammakhi, N., et al. (1995). Repair of bone defects with absorbable membranes. A study on rabbits. *Annales Chirurgiae et Gynaecologiae*, *84*(3), 309–315.
21. Elgali, I., et al. (2017). Guided bone regeneration: Materials and biological mechanisms revisited. *European Journal of Oral Sciences, 125*(5), 315–337.
22. Puumanen, K., et al. (2005). A novel bioabsorbable composite membrane of polyactive 70/30 and bioactive glass number 13–93 in repair of experimental maxillary alveolar cleft defects. *Journal of Biomedical Materials Research. Part B, Applied Biomaterials, 75*(1), 25–33.
23. Langer, R., & Vacanti, J. P. (1993). Tissue engineering. *Science, 260*(5110), 920–926.
24. Dziadek, M., Stodolak-Zych, E., & Cholewa-Kowalska, K. (2017). Biodegradable ceramic-polymer composites for biomedical applications: A review. *Materials Science & Engineering C—Materials for Biological Applications, 71*, 1175–1191.
25. Alizadeh-Osgouei, M., Li, Y. C., & Wen, C. E. (2019). A comprehensive review of biodegradable synthetic polymer-ceramic composites and their manufacture for biomedical applications. *Bioactive Materials, 4*, 22–36.
26. Xue, C., et al. (2020). Synthesis of injectable shear-thinning biomaterials of various compositions of gelatin and synthetic silicate nanoplatelet. *Biotechnology Journal, 15*(8), 1900456.
27. Liu, C. Y., et al. (2018). Incorporation and release of dual growth factors for nerve tissue engineering using nanofibrous bicomponent scaffolds. *Biomedical Materials, 13*(4).
28. Gómez, G., et al. (2006). Effect of FGF and polylactide scaffolds on calvarial bone healing with growth factor on biodegradable polymer scaffolds. *The Journal of Craniofacial Surgery, 17*(5), 935–942.
29. Kolesky, D. B., et al. (2014). 3D bioprinting of vascularized, heterogeneous cell-laden tissue constructs. *Advanced Materials, 26*(19), 3124–3130.
30. Fedorovich, N. E., et al. (2011). Distinct tissue formation by heterogeneous printing of osteo- and endothelial progenitor cells. *Tissue Engineering Part A, 17*(15–16), 2113–2121.
31. Hull, C. W. (1986). In U.P. Office (Ed.), *Apparatus for production of three-dimensional objects by stereolithography*. UVP, Inc.
32. Zhang, Y. S., et al. (2017). 3D bioprinting for tissue and organ fabrication. *Annals of Biomedical Engineering, 45*(1), 148–163.
33. Ashammakhi, N., et al. (2019). Advancing frontiers in bone bioprinting. *Advanced Healthcare Materials, 8*(7), e1801048.
34. Ashammakhi, N., & Kaarela, O. (2018). Three-dimensional bioprinting can help bone. *The Journal of Craniofacial Surgery, 29*(1), 9–11.
35. Pountos, I., et al. (2021). 3D bioprinting. In S. Atallah (Ed.), *Digital surgery* (pp. 215–232). Springer International Publishing.

36. Vijayavenkataraman, S., et al. (2018). 3D bioprinting of tissues and organs for regenerative medicine. *Advanced Drug Delivery Reviews, 132*, 296–332.
37. Davoodi, E., et al. (2020). Extrusion and microfluidic-based bioprinting to fabricate biomimetic tissues and organs. *Advanced Materials Technologies, 5*(8), 1901044.
38. Ashammakhi, N., et al. (2019). Bioinks and bioprinting technologies to make heterogeneous and biomimetic tissue constructs. *Materials Today Bio, 1*, 100008.
39. Laternser, S., et al. (2018). A novel microplate 3D bioprinting platform for the engineering of muscle and tendon tissues. *SLAS Technology, 23*(6), 599–613.
40. Merceron, T. K., et al. (2015). A 3D bioprinted complex structure for engineering the muscle-tendon unit. *Biofabrication, 7*(3).
41. Park, S. H., et al. (2018). Three-dimensional bio-printed scaffold sleeves with mesenchymal stem cells for enhancement of tendon-to-bone healing in anterior cruciate ligament reconstruction using soft-tissue tendon graft. *Arthroscopy—The Journal of Arthroscopic and Related Surgery, 34*(1), 166–179.
42. Shie, M. Y., et al. (2017). 3D printing of cytocompatible water-based light-cured polyurethane with hyaluronic acid for cartilage tissue engineering applications. *Materials, 10*(2).
43. Daly, A. C., et al. (2017). 3D bioprinting for cartilage and osteochondral tissue engineering. *Advanced Healthcare Materials, 6*(22).
44. Xie, Z. L., et al. (2020). 3D bioprinting in tissue engineering for medical applications: The classic and the hybrid. *Polymers, 12*(8).
45. Erdem, A., et al. (2020). 3D bioprinting of oxygenated cell-laden gelatin methacryloyl constructs. *Advanced Healthcare Materials, 9*(15), 1901794.
46. Seyedmahmoud, R., et al. (2019). Three-dimensional bioprinting of functional skeletal muscle tissue using gelatinmethacryloyl-alginate bioinks. *Micromachines (Basel), 10*(10).
47. Liu, N. B., et al. (2021). Advances in 3D bioprinting technology for cardiac tissue engineering and regeneration. *Bioactive Materials, 6*(5), 1388–1401.
48. Zhang, Y., et al. (2021). Recent advances in 3D bioprinting of vascularized tissues. *Materials & Design, 199*.
49. Lee, S. J., et al. (2018). Advances in 3D bioprinting for neural tissue engineering. *Advanced Biosystems, 2*(4).
50. Zhang, B., et al. (2018). 3D bioprinting: An emerging technology full of opportunities and challenges. *Bio-Design and Manufacturing, 1*(1), 2–13.
51. Zhang, J. H., et al. (2021). 3D bioprinting of human tissues: Biofabrication, bioinks, and bioreactors. *International Journal of Molecular Sciences, 22*(8).
52. Theus, A. S., et al. (2020). Bioprintability: Physiomechanical and biological requirements of materials for 3D bioprinting processes. *Polymers, 12*(10) (2020)
53. Potyondy, T., Uquillas, J. A., Tebon, P. J., Byambaa, B., Hasan, A., Tavafoghi, M., Mary, H., Aninwene, G. E., Pountos, I., Khademhosseini, A., & Ashammakhi, N. (2021). Recent advances in 3D bioprinting of musculoskeletal tissues.*Biofabrication, 13*(2), 022001.
54. Wang, X. H., et al. (2016). 3D bioprinting technologies for hard tissue and organ engineering. *Materials, 9*(10).
55. Turnbull, G., et al. (2018). 3D bioactive composite scaffolds for bone tissue engineering. *Bioactive Materials, 3*(3), 278–314.
56. Lin, K., et al. (2019). 3D printing of bioceramic scaffolds-barriers to the clinical translation: From promise to reality, and future perspectives. *Materials, 12*(17).
57. Kosik-Koziol, A., et al. (2019). 3D bioprinted hydrogel model incorporating beta-tricalcium phosphate for calcified cartilage tissue engineering. *Biofabrication, 11*(3).
58. Pi, Q. M., et al. (2018). Digitally tunable microfluidic bioprinting of multilayered cannular tissues. *Advanced Materials, 30*(43).
59. Liu, W. J., et al. (2017). Extrusion bioprinting of shear-thinning gelatin methacryloyl bioinks. *Advanced Healthcare Materials, 6*(12).
60. Narayanan, L. K., et al. (2016). 3D-bioprinting of polylactic acid (PLA) nanofiber-alginate hydrogel bioink containing human adipose-derived stem cells. *ACS Biomaterials Science & Engineering, 2*(10), 1732–1742.

61. Zhang, G. L., et al. (2020). ECM concentration and cell-mediated traction forces play a role in vascular network assembly in 3D bioprinted tissue. *Biotechnology and Bioengineering, 117*(4), 1148–1158.
62. Wang, Z., et al. (2018). 3D bioprinted functional and contractile cardiac tissue constructs. *Acta Biomaterialia, 70*, 48–56.
63. Compaan, A. M., Christensen, K., & Huang, Y. (2017). Inkjet bioprinting of 3D silk fibroin cellular constructs using sacrificial alginate. *ACS Biomaterials Science & Engineering, 3*(8), 1519–1526.
64. Aydin, L., Kucuk, S., & Kenar, H. (2020). A universal self-eroding sacrificial bioink that enables bioprinting at room temperature. *Polymers for Advanced Technologies, 31*(7), 1634–1647.
65. Yu, Y. Z., et al. (2014). Fabrication of hierarchical polycaprolactone/gel scaffolds via combined 3D bioprinting and electrospinning for tissue engineering. *Advances in Manufacturing, 2*(3), 231–238.
66. Askari, M., et al. (2021). Recent progress in extrusion 3D bioprinting of hydrogel biomaterials for tissue regeneration: A comprehensive review with focus on advanced fabrication techniques. *Biomaterials Science, 9*(3), 535–573.
67. Stocco, T. D., et al. (2018). Nanofibrous scaffolds for biomedical applications. *Nanoscale, 10*(26), 12228–12255.
68. Lienemann, P. S., et al. (2013). A versatile approach to engineering biomolecule-presenting cellular microenvironments. *Advanced Healthcare Materials, 2*(2), 292–296.
69. Ashammakhi, N., et al. (2021). Highlights on advancing frontiers in tissue engineering. *Tissue Engineering Part B: Reviews*.
70. Jeong, H. J., et al. (2020). 3D bioprinting strategies for the regeneration of functional tubular tissues and organs. *Bioengineering (Basel), 7*(2).
71. De Mori, A., et al. (2018). 3D printing and electrospinning of composite hydrogels for cartilage and bone tissue engineering. *Polymers (Basel), 10*(3).
72. Pensa, N. W., et al. (2019). 3D printed mesh reinforcements enhance the mechanical properties of electrospun scaffolds. *Biomaterials Research, 23*, 22.
73. Ashammakhi, N., et al. (2009). Electrospinning: Methods and development of biodegradable nanofibres for drug release. *Journal of Biomedical Nanotechnology, 5*(1), 1–19.
74. Yang, X. L., et al. (2020). Structural design toward functional materials by electrospinning: A review. *E-Polymers, 20*(1), 682–712.
75. Ashammakhi, N., et al. (2007). Tissue engineering: A new take-off using nanofiber-based scaffolds. *The Journal of Craniofacial Surgery, 18*(1), 3–17.
76. Chen, T. T., et al. (2018). Combining 3D printing with electrospinning for rapid response and enhanced designability of hydrogel actuators. *Advanced Functional Materials, 28*(19).
77. Lee, S. J., et al. (2015). Characterization and preparation of bio-tubular scaffolds for fabricating artificial vascular grafts by combining electrospinning and a 3D printing system. *Physical Chemistry Chemical Physics, 17*(5), 2996–2999.
78. Maver, T., et al. (2018). Combining 3D printing and electrospinning for preparation of pain-relieving wound-dressing materials. *Journal of Sol-Gel Science and Technology, 88*(1), 33–48.
79. Yan, F. F., et al. (2014). A multi-scale controlled tissue engineering scaffold prepared by 3D printing and NFES technology. *AIP Advances, 4*(3).
80. Ashammakhi, N., et al. (2008). Advancing tissue engineering by using electrospun nanofibers. *Regenerative Medicine, 3*(4), 547–574.
81. Ndreu, A., et al. (2008). Electrospun biodegradable nanofibrous mats for tissue engineering. *Nanomedicine (London, England), 3*(1), 45–60.
82. Nayak, R., et al. (2012). Recent advances in nanofibre fabrication techniques. *Textile Research Journal, 82*(2), 129–147.
83. Liu, X., et al. (2010). In vivo wound healing and antibacterial performances of electrospun nanofibre membranes. *Journal of Biomedical Materials Research—Part A, 94*(2), 499–508.
84. Bagheri, B., et al. (2020). Tissue engineering with electrospun electro-responsive chitosan-aniline oligomer/polyvinyl alcohol. *International Journal of Biological Macromolecules, 147*, 160–169.

85. Luo, C. J., et al. (2012). Electrospinning versus fibre production methods: From specifics to technological convergence. *Chemical Society Reviews, 41*(13), 4708–4735.
86. Rickel, A. P., Deng, X., Engebretson, D., & Hong, Z. (2021). Electrospun nanofiber scaffold for vascular tissue engineering. *Materials Science and Engineering: C, 129*, 112373.
87. Stachewicz, U., et al. (2015). 3D imaging of cell interactions with electrospun PLGA nanofiber membranes for bone regeneration. *Acta Biomaterialia, 27*, 88–100.
88. Bhattarai, D. P., et al. (2018). A review on properties of natural and synthetic based electrospun fibrous materials for bone tissue engineering. *Membranes, 8*(3), 62.
89. Augustine, R., et al. (2021). Growth factor loaded in situ photocrosslinkable poly(3-hydroxybutyrate-co-3-hydroxyvalerate)/gelatin methacryloyl hybrid patch for diabetic wound healing. *Materials Science & Engineering, C: Materials for Biological Applications, 118*, 111519.
90. Augustine, R., et al. (2020). Electrospun chitosan membranes containing bioactive and therapeutic agents for enhanced wound healing. *International Journal of Biological Macromolecules*, 153–170.
91. Will, O. M., et al. (2016). Increased survival rate by local release of diclofenac in a murine model of recurrent oral carcinoma. *International Journal of Nanomedicine, 11*, 5311–5321.
92. Nikkola, L., et al. (2015). Fabrication of electrospun poly(D, L lactide-co-glycolide)80/20 scaffolds loaded with diclofenac sodium for tissue engineering. *European Journal of Medical Research, 20*(1), 54.
93. Nikkola, L., et al. (2006). Electrospun multifunctional diclofenac sodium releasing nanoscaffold. *Journal of Nanoscience and Nanotechnology, 6*(9–10), 3290–3295.
94. Piras, A. M., et al. (2006). Development of diclofenac sodium releasing bio-erodible polymeric nanomats. *Journal of Nanoscience and Nanotechnology, 6*(9–10), 3310–3320.
95. Nikkola, L., et al. (2008). Multilayer implant with triple drug releasing properties. *Journal of Biomedical Nanotechnology, 4*(3), 331–338.
96. Ye, K., et al. (2019). Electrospun nanofibers for tissue engineering with drug loading and release. *Pharmaceutics, 11*(4), 182.
97. Feltz, K. P., et al. (2017). A review of electrospinning manipulation techniques to direct fiber deposition and maximize pore size. *Electrospinning, 1*(1), 46–61.
98. Puppi, D., et al. (2010). Poly(vinyl alcohol)-based electrospun meshes as potential candidate scaffolds in regenerative medicine. *Journal of Bioactive and Compatible Polymers, 26*(1), 20–34.
99. Wimpenny, I., et al. (2012). Improvement and characterization of the adhesion of electrospun PLDLA nanofibers on PLDLA-based 3D object substrates for orthopedic application. *Journal of Biomaterials Science, Polymer Edition, 23*(14), 1863–1877.
100. Wimpenny, I., Hampson, K., Yang, Y., Ashammakhi, N., & Forsyth, N. R. (2010). One-step recovery of marrow stromal cells on nanofibers.*Tissue Engineering Part C: Methods, 16*(3), 503–509.
101. Araujo, J. V., Cunha-Reis, C., Rada, T., da Silva, M. A., Gomes, M. E., Yang, Y., et al. (2010). Dynamic culture of osteogenic cells in biomimetically coated poly(Caprolactone) nanofibre mesh constructs. *Tissue Engineering Part A, 16*(2), 557–563.
102. Morton, T., et al. (2007). Electrospun fibrinogen and fibrin nanofibers for angiogenesis in vitro: 126. *Wound Repair and Regeneration, 15*(2).
103. Tatjana Sindelar, L. N., Ashammakhi, N., van Griensven, M., & Redl, H. (2006). Electrospinning of fibrinogen nanofibers. In *2nd International Conference Strategies in Tissue Engineering*, Würzburg, Germany.
104. Yang, Y., Nikkola, L., Ylikauppila, H., & Ashammakhi, N. (2006). Investigation of cell attachment on the scaffolds manufactured by electrospun PCL-hyaluronan blend. In *TNT2006 "Trends in Nanotechnology" Conference*, Grenoble, France.
105. Augustine, R., et al. (2020). Cerium oxide nanoparticle incorporated electrospun poly(3-hydroxybutyrate-co-3-hydroxyvalerate) membranes for diabetic wound healing applications. *ACS Biomaterials Science & Engineering, 6*(1), 58–70.

106. Zhang, Y. Z., et al. (2007). Biomimetic and bioactive nanofibrous scaffolds from electrospun composite nanofibers. *International Journal of Nanomedicine, 2*(4), 623.
107. Burger, C., & Chu, B. (2007). Functional nanofibrous scaffolds for bone reconstruction. *Colloids and Surfaces B: Biointerfaces, 56*(1–2), 134–141.
108. Grande, D., et al. (2017). Design of functionalized biodegradable PHA-based electrospun scaffolds meant for tissue engineering applications. *New Biotechnology, 37*, 129–137.
109. Koh, H. S., et al. (2008). Enhancement of neurite outgrowth using nano-structured scaffolds coupled with laminin. *Biomaterials, 29*, 3574–3582.
110. Maghdouri-White, Y., et al. (2014). Mammary epithelial cell adhesion, viability, and infiltration on blended or coated silk fibroin-collagen type i electrospun scaffolds. *Materials Science and Engineering C, 43*, 37–44.
111. Babaie, A., et al. (2020). Synergistic effects of conductive PVA/PEDOT electrospun scaffolds and electrical stimulation for more effective neural tissue engineering. *European Polymer Journal, 140*.
112. Ashammakhi, N., et al. (2012). Nanofiber-based scaffolds for tissue engineering. *European Journal of Plastic Surgery, 35*(2), 135–149.
113. Augustine, R., et al. (2019). Chitosan ascorbate hydrogel improves water uptake capacity and cell adhesion of electrospun poly(epsilon-caprolactone) membranes. *International Journal of Pharmaceutics, 559*, 420–426.
114. Liu, H., et al. (2011). Electrospun sulfated silk fibroin nanofibrous scaffolds for vascular tissue engineering. *Biomaterials, 32*(15), 3784–3793.
115. Augustine, R., Kalarikkal, N., & Thomas, S. (2016). Clogging-free electrospinning of polycaprolactone using acetic acid/acetone mixture. *Polymer-Plastics Technology and Engineering, 55*(5), 518–529.
116. Gupta, P., et al. (2005). Electrospinning of linear homopolymers of poly(methyl methacrylate): Exploring relationships between fiber formation, viscosity, molecular weight and concentration in a good solvent. *Polymer, 46*, 4799–4810.
117. Tiwari, S. K., & Venkatraman, S. S. (2012). Importance of viscosity parameters in electrospinning: Of monolithic and core-shell fibers. *Materials Science and Engineering C, 32*, 1037–1042.
118. Uyar, T., & Besenbacher, F. (2008). Electrospinning of uniform polystyrene fibers: The effect of solvent conductivity. *Polymer, 49*, 5336–5343.
119. Wang, Y., & Wang, C. (2021). Extension rate and bending behavior of electrospinning jet: The role of solution conductivity. *Polymer*, 123672.
120. Augustine, R., et al. (2014). Electrospun polycaprolactone/ZnO nanocomposite membranes as biomaterials with antibacterial and cell adhesion properties. *Journal of Polymer Research, 21*(3), 347.
121. Thamer, B. M., et al. (2019). Fabrication of functionalized electrospun carbon nanofibers for enhancing lead-ion adsorption from aqueous solutions. *Scientific Reports, 9*, 1–15.
122. Augustine, R., et al. (2019). CTGF loaded electrospun dual porous core-shell membrane for diabetic wound healing. *International Journal of Nanomedicine, 14*, 8573–8588.
123. Duarte, A. R. C., et al. (2017). From honeycomb- to microsphere-patterned surfaces of poly(lactic acid) and a starch-poly(lactic acid) blend via the breath figure method. *Journal of Applied Biomaterials & Functional Materials, 15*, 31–42.
124. Castano, M., et al. (2018). Combining breath figures and supercritical fluids to obtain porous polymer scaffolds. *ACS Omega, 3*, 12593–12599.
125. Kim, H. S., et al. (2005). Morphological characterization of electrospun nano-fibrous membranes of biodegradable poly (l-lactide) and poly (lactide-co-glycolide). In *Macromolecular Symposia.* Wiley Online Library.
126. Zhao, Z., et al. (2005). Preparation and properties of electrospun poly (vinylidene fluoride) membranes. *Journal of Applied Polymer Science, 97*(2), 466–474.
127. Gupta, P., et al. (2005). Electrospinning of linear homopolymers of poly (methyl methacrylate): Exploring relationships between fiber formation, viscosity, molecular weight and concentration in a good solvent. *Polymer, 46*(13), 4799–4810.

128. Mit-uppatham, C., et al. (2004). Ultrafine electrospun polyamide-6 fibers: Effect of solution conditions on morphology and average fiber diameter. *Macromolecular Chemistry and Physics, 205*(17), 2327–2338.
129. Megelski, S., et al. (2002). Micro-and nanostructured surface morphology on electrospun polymer fibers. *Macromolecules, 35*(22), 8456–8466.
130. Ding, J., et al. (2019). Electrospun polymer biomaterials. *Progress in Polymer Science, 90*, 1–34.
131. Ramakrishna, S., et al. (2006). Electrospun nanofibers: Solving global issues. *Materials Today, 9*(3), 40–50.
132. Drew, C., et al. (2003). The effect of viscosity and filler on electrospun fiber morphology. *Journal of Macromolecular Science, Part A, 40*(12), 1415–1422.
133. Koski, A., Yim, K., & Shivkumar, S. J. M. L. (2004). Effect of molecular weight on fibrous PVA produced by electrospinning. *Materials Letters, 58*(3–4), 493–497.
134. Tao, J., & Shivkumar, S. J. M. l. (2007). Molecular weight dependent structural regimes during the electrospinning of PVA. *Materials Letters, 61*(11–12), 2325–2328.
135. Malik, R., et al. (2015). Polymeric nanofibers: Targeted gastro-retentive drug delivery systems. *Journal of Drug Targeting, 23*(2), 109–124.
136. Lee, J. S., et al. (2004). Role of molecular weight of atactic poly (vinyl alcohol)(PVA) in the structure and properties of PVA nanofabric prepared by electrospinning. *Journal of Applied Polymer Science, 93*(4), 1638–1646.
137. Jabur, A. R., Najim, M. A., & Al-Rahman, S. A. A. (2018). Study the effect of flow rate on some physical properties of different polymeric solutions. *Journal of Physics: Conference Series, 1003*, 012069.
138. Fong, H., Chun, I., & Reneker, D. H. J. P. (1999). Beaded nanofibers formed during electrospinning. *Polymer, 40*(16), 4585–4592.
139. Jarusuwannapoom, T., et al. (2005). Effect of solvents on electro-spinnability of polystyrene solutions and morphological appearance of resulting electrospun polystyrene fibers. *European Polymer Journal, 41*(3), 409–421.
140. Lee, J., et al. (2015). Conductive fiber-based ultrasensitive textile pressure sensor for wearable electronics. *Advanced Materials, 27*(15), 2433–2439.
141. Xu, Y., et al. (2017). Effect of different solvent systems on PHBV/PEO electrospun fibers. *RSC Advances, 7*(7), 4000–4010.
142. Zong, X., et al. (2002). Structure and process relationship of electrospun bioabsorbable nanofiber membranes. *Polymer, 43*(16), 4403–4412.
143. Jeun, J. P., et al. (2005). Study on morphology of electrospun poly (caprolactone) nanofiber. *Journal of Industrial and Engineering Chemistry, 11*(4), 573–578.
144. Nadri, S., Nasehi, F., & Barati, G. (2017). Effect of parameters on the quality of core-shell fibrous scaffold for retinal differentiation of conjunctiva mesenchymal stem cells. *Journal of Biomedical Materials Research Part A, 105*(1), 189–197.
145. Zuo, W., et al. (2005). Experimental study on relationship between jet instability and formation of beaded fibers during electrospinning. *Polymer Engineering & Science, 45*(5), 704–709.
146. Ameer, J. M., Pr, A. K., & Kasoju, N. (2019). Strategies to tune electrospun scaffold porosity for effective cell response in tissue engineering. *Journal of Functional Biomaterials, 10*(3).
147. Yuan, X., et al. (2004). Morphology of ultrafine polysulfone fibers prepared by electrospinning. *Polymer International, 53*(11), 1704–1710.
148. Lee, K. H., et al. (2002). Influence of a mixing solvent with tetrahydrofuran and N, N-dimethylformamide on electrospun poly (vinyl chloride) nonwoven mats.*Journal of Polymer Science Part B: Polymer Physics, 40*(19), 2259–2268.
149. Ki, C. S., et al. (2005). Characterization of gelatin nanofiber prepared from gelatin–formic acid solution. *Polymer, 46*(14), 5094–5102.
150. Dehghan, S. F., et al. (2016). Optimization of electrospinning parameters for polyacrylonitrile-MgO nanofibers applied in air filtration. *Journal of the Air & Waste Management Association, 66*(9), 912–921.

151. Deitzel, J. M., et al. (2001). The effect of processing variables on the morphology of electrospun nanofibers and textiles. *Polymer, 42*(1), 261–272.
152. Topuz, F., & Uyar, T. (2017). Electrospinning of gelatin with tunable fiber morphology from round to flat/ribbon. *Materials Science and Engineering: C, 80*, 371–378.
153. Geng, X., Kwon, O.-H., & Jang, J. J. B. (2005). Electrospinning of chitosan dissolved in concentrated acetic acid solution. *Biomaterials, 26*(27), 5427–5432.
154. Can-Herrera, L. A., et al. (2021). Morphological and mechanical properties of electrospun polycaprolactone scaffolds: Effect of applied voltage. *Polymers (Basel), 13*(4).
155. Sill, T. J., & Von Recum, H. A. J. B. (2008). Electrospinning: Applications in drug delivery and tissue engineering. *Biomaterials, 29*(13), 1989–2006.
156. Li, D., et al. (2005). Collecting electrospun nanofibers with patterned electrodes. *Nano Letters, 5*(5), 913–916.
157. Cheng, Q., et al. (2013). Engineering the microstructure of electrospun fibrous scaffolds by microtopography. *Biomacromolecules, 14*(5), 1349–1360.
158. Vaquette, C., & Cooper-White, J. J. (2011). Increasing electrospun scaffold pore size with tailored collectors for improved cell penetration. *Acta Biomaterialia, 7*(6), 2544–2557.
159. Bedane, A. H., et al. (2016). Theoretical modeling of water vapor transport in cellulose-based materials. *Cellulose, 23*(3), 1537–1552.
160. Nezarati, R. M., Eifert, M. B., & Cosgriff-Hernandez, E. (2013). Effects of humidity and solution viscosity on electrospun fiber morphology. *Tissue Engineering. Part C, Methods, 19*(10), 810–819.
161. Liu, Q., et al. (2016). Scalable fabrication of nanoporous carbon fiber films as bifunctional catalytic electrodes for flexible Zn-air batteries. *Advanced Materials, 28*(15), 3000–3006.
162. Ramazani, S., & Karimi, M. (2014). Investigating the influence of temperature on electrospinning of polycaprolactone solutions. *e-Polymers, 14*(5), 323–333.
163. Jin, Y., et al. (2020). Fabrication of heterogeneous scaffolds using melt electrospinning writing: Design and optimization. *Materials and Design, 185*.
164. Brown, T. D., Dalton, P. D., & Hutmacher, D. W. (2016). Melt electrospinning today: An opportune time for an emerging polymer process. In *Progress in polymer science* (pp. 116–166). Elsevier Ltd.
165. Ristovski, N., et al. (2015). Improved fabrication of melt electrospun tissue engineering scaffolds using direct writing and advanced electric field control. *Biointerphases, 10*, 011006.
166. Jin, Y., et al. (2021). Fabrication of multi-scale and tunable auxetic scaffolds for tissue engineering. *Materials and Design, 197*, 109277.
167. Chung, S., et al. (2010). Bioresorbable elastomeric vascular tissue engineering scaffolds via melt spinning and electrospinning. *Acta Biomaterialia, 6*, 1958–1967.
168. Kurakula, M., & Raghavendra Naveen, N. (2021). Electrospraying: A facile technology unfolding the chitosan based drug delivery and biomedical applications. *European Polymer Journal*, 110326.
169. Rostamabadi, H., et al. (2021). Electrospraying as a novel process for the synthesis of particles/nanoparticles loaded with poorly water-soluble bioactive molecules. In *Advances in colloid and interface science*. Elsevier B.V.
170. Wang, K., et al. (2018). Electrosprayed hydrophilic nanocomposites coated with shellac for colon-specific delayed drug delivery. *Materials and Design, 143*, 248–255.
171. Tsiapla, A. R., et al. (2019). Biodegradable electrosprayed NPS as drug carriers for optimal treatment of orthopaedic infections. In *Materials Today: Proceedings* (pp. 110–116). Elsevier Ltd.
172. Kang, S., et al. (2021). Drug–zein@lipid hybrid nanoparticles: Electrospraying preparation and drug extended release application. *Colloids and Surfaces B: Biointerfaces, 201*.
173. Tucker, N., et al. (2012). The history of the science and technology of electrospinning from 1600 to 1995. *Journal of Engineered Fibers and Fabrics, 7*(2_suppl), 155892501200702S10.
174. Taylor, G. I. (1964). Disintegration of water drops in an electric field. *Proceedings of the Royal Society of London. Series A. Mathematical and Physical Sciences, 280*, 383–397.

175. Hayati, I., Bailey, A. I., & Tadros, T. F. (1987). Investigations into the mechanisms of electrohydrodynamic spraying of liquids: I. Effect of electric field and the environment on pendant drops and factors affecting the formation of stable jets and atomization. *Journal of Colloid and Interface Science, 117*(1), 205–221.
176. Abdul Hameed, M. M., et al. (2020). Core-shell nanofibers from poly(vinyl alcohol) based biopolymers using emulsion electrospinning as drug delivery system for cephalexin drug. *Journal of Macromolecular Science, Part A: Pure and Applied Chemistry, 58*(2), 130–144.
177. Karim, M., Fathi, M., & Soleimanian-Zad, S. (2020). Incorporation of zein nanofibers produced by needle-less electrospinning within the casted gelatin film for improvement of its physical properties. *Food and Bioproducts Processing, 122*, 193–204.
178. Zahran, S. M. E., et al. (2020). Fabrication of nanofiltration membrane based on non-biofouling PVP/lecithin nanofibers reinforced with microcrystalline cellulose via needle and needle-less electrospinning techniques. *International Journal of Biological Macromolecules, 157*, 530–543.
179. Grigoryev, N. A., & Levon, K. (2018). Novel method of electrospinning; rotating dual electrode collector design. *Journal of Microelectromechanical Systems, 27*, 312–320.
180. Chen, X., et al. (2021). String electrospinning based on the standing wave vibration. *Journal of Materials Science, 56*, 9518–9531.
181. Ghosal, K., et al. (2021). Novel drug delivery systems based on triaxial electrospinning based nanofibers. *Reactive and Functional Polymers, 163*, 104895.
182. Coimbra, P., et al. (2019). Preparation of gentamicin sulfate eluting fiber mats by emulsion and by suspension electrospinning. *Materials Science and Engineering C, 94*, 86–93.
183. Zhang, C., et al. (2019). Electrospinning of bilayer emulsions: The role of gum Arabic as a coating layer in the gelatin-stabilized emulsions. *Food Hydrocolloids, 94*, 38–47.
184. Li, H., et al. (2017). A thermosensitive drug delivery system prepared by blend electrospinning. *Colloids and Surfaces B: Biointerfaces, 159*, 277–283.
185. Li, H., et al. (2018). Dual-responsive drug delivery systems prepared by blend electrospinning. *International Journal of Pharmaceutics, 543*, 1–7.
186. Wang, J., & Windbergs, M. (2018). Influence of polymer composition and drug loading procedure on dual drug release from PLGA:PEG electrospun fibers. *European Journal of Pharmaceutical Sciences, 124*, 71–79.
187. Fathi, M., Akbari, B., & Taheriazam, A. (2019). Antibiotics drug release controlling and osteoblast adhesion from Titania nanotubes arrays using silk fibroin coating. *Materials Science and Engineering C, 103.*
188. Han, D., & Steckl, A. J. (2009). Superhydrophobic and oleophobic fibers by coaxial electrospinning. *Langmuir, 25*, 9454–9462.
189. Khalf, A., & Madihally, S. V. (2017). Recent advances in multiaxial electrospinning for drug delivery. *European Journal of Pharmaceutics and Biopharmaceutics, 112*, 1–17.
190. Yeo, M., & Kim, G. H. (2020). Micro/nano-hierarchical scaffold fabricated using a cell electrospinning/3D printing process for co-culturing myoblasts and HUVECs to induce myoblast alignment and differentiation. *Acta Biomaterialia, 107*, 102–114.
191. Hacking, S. A., Ashammakhi, N., & Khademhosseini, A. (2020). Cells and surfaces in vitro. In W. R. Wagner, et al. (Eds.), *Biomaterials science* (4th ed., pp. 661–681). Academic Press.
192. Clinical nerve repair and reconstruction. In *Nerve injury and repair* (p. 168-cp1) Elsevier.
193. Sahay, R., Thavasi, V., & Ramakrishna, S. (2011). Design modifications in electrospinning setup for advanced applications. *Journal of Nanomaterials, 2011.*
194. Xu, H., Cui, W., & Chang, J. (2013). Fabrication of patterned PDLLA/PCL composite scaffold by electrospinning. *Journal of Applied Polymer Science, 127*(3), 1550–1554.
195. Liu, Y., et al. (2012). Electrospun fibrous mats on lithographically micropatterned collectors to control cellular behaviors. *Langmuir, 28*(49), 17134–17142.
196. Zhang, D., & Chang, J. (2007). Patterning of electrospun fibers using electroconductive templates. *Advanced Materials, 19*(21), 3664–3667.
197. Zhu, Y., et al. (2011). Engineering bi-layer nanofibrous conduits for peripheral nerve regeneration. *Tissue Engineering. Part C, Methods, 17*(7), 705–715.

198. Chen, P., et al. (2017). Electrospun scaffolds for neural tissue engineering. In T. Uyar & E. Kny (Eds.), *Electrospun materials for tissue engineering and biomedical applications* (pp. 299–320). Woodhead Publishing.
199. Wulkersdorfer, B., et al. (2010). Bimodal porous scaffolds by sequential electrospinning of poly(glycolic acid) with sucrose particles. *International Journal of Polymer Science, 2010*.
200. Ko, J., Kan, D., & Jun, M. B. G. (2015). Combining melt electrospinning and particulate leaching for fabrication of porous microfibers. *Manufacturing Letters, 3*, 5–8.
201. Meng, Z. X., et al. (2010). Electrospinning of PLGA/gelatin randomly-oriented and aligned nanofibers as potential scaffold in tissue engineering. *Materials Science and Engineering: C, 30*(8), 1204–1210.
202. Kim, T. G., Chung, H. J., & Park, T. G. (2008). Macroporous and nanofibrous hyaluronic acid/collagen hybrid scaffold fabricated by concurrent electrospinning and deposition/leaching of salt particles. *Acta Biomaterialia, 4*, 1611–1619.
203. Nielsen, S. R., Besenbacher, F., & Chen, M. (2013). Mussel inspired surface functionalization of electrospun nanofibers for bio-applications. *Physical Chemistry Chemical Physics, 15*, 17029–17037.
204. Nagarajan, S., et al. (2019). Various techniques to functionalize nanofibers. In *Handbook of nanofibers* (pp. 347–372). Springer International Publishing.
205. Isfahani, V. B., et al. (2021). Functionalized magnetic composite nano/microfibres with highly oriented van der Waals CrI3 inclusions by electrospinning. *Nanotechnology, 32*, 145703.
206. He, X. X., et al. (2017). Near-field electrospinning: Progress and applications. *Journal of Physical Chemistry C, 121*, 8663–8678.
207. Kolan, K. C. R., et al. (2019). Near-field electrospinning of a polymer/bioactive glass composite to fabricate 3D biomimetic structures. *International Journal of Bioprinting, 5*.
208. Dalton, P. D. (2017). Melt electrowriting with additive manufacturing principles. In *Current opinion in biomedical engineering* (pp. 49–57). Elsevier B.V.
209. Bhardwaj, N., & Kundu, S. C. (2010). Electrospinning: A fascinating fiber fabrication technique. *Biotechnology Advances, 28*(3), 325–347.
210. Li, D., & Xia, Y. (2004). Direct fabrication of composite and ceramic hollow nanofibers by electrospinning. *Nano Letters, 4*, 933–938.
211. Chen, H., et al. (2010). Nanowire-in-microtube structured core/shell fibers via multifluidic coaxial electrospinning. *Langmuir, 26*, 11291–11296.
212. Han, D., & Gouma, P. I. (2006). Electrospun bioscaffolds that mimic the topology of extracellular matrix. *Nanomedicine: Nanotechnology, Biology, and Medicine, 2*(1), 37–41.
213. Chen, H., et al. (2013). Fabrication of nanofibrous scaffolds for tissue engineering applications. In *Nanomaterials in tissue engineering: Fabrication and applications.*
214. Chanda, A., et al. (2018). Electrospun chitosan/polycaprolactone-hyaluronic acid bilayered scaffold for potential wound healing applications. *International Journal of Biological Macromolecules, 116*, 774–785.
215. Augustine, R., Kalarikkal, N., & Thomas, S. (2015). An in vitro method for the determination of microbial barrier property (MBP) of porous polymeric membranes for skin substitute and wound dressing applications. *Tissue Engineering and Regenerative Medicine, 12*(1), 12–19.
216. Augustine, R., et al. (2018). Electrospun polyvinyl alcohol membranes incorporated with green synthesized silver nanoparticles for wound dressing applications. *Journal of Materials Science: Materials in Medicine, 29*(11), 163.
217. Xu, S.-C., et al. (2015). A battery-operated portable handheld electrospinning apparatus. *Nanoscale, 7*(29), 12351–12355.
218. Augustine, R., Kalarikkal, N., & Thomas, S. (2014). Advancement of wound care from grafts to bioengineered smart skin substitutes. *Progress in Biomaterials, 3*(2–4), 103–113.
219. Woo, K. M., Chen, V. J., & Ma, P. X. (2003). Nano-fibrous scaffolding architecture selectively enhances protein adsorption contributing to cell attachment. *Journal of Biomedical Materials Research—Part A, 67*, 531–537.
220. Formentín, P., et al. (2018). Collagen and fibronectin surface modification of nanoporous anodic alumina and macroporous silicon for endothelial cell cultures. *Journal of Biological Engineering, 12*(1), 21.

221. Wang, Z., et al. (2017). Graphene oxide incorporated PLGA nanofibrous scaffold for solid phase gene delivery into mesenchymal stem cells. *Journal of Nanoscience and Nanotechnology, 18*(4), 2286–2293.
222. Feng, B., et al. (2019). Bioresorbable electrospun gelatin/polycaprolactone nanofibrous membrane as a barrier to prevent cardiac postoperative adhesion. *Acta Biomaterialia, 83*, 211–220.
223. Zheng, G., et al. (2020). Nanofiber membranes by multi-jet electrospinning arranged as arc-array with sheath gas for electrodialysis applications. *Materials and Design, 189*, 108504.
224. Deshawar, D., Gupta, K., & Chokshi, P. (2020). Electrospinning of polymer solutions: An analysis of instability in a thinning jet with solvent evaporation. *Polymer, 202*.
225. Taemeh, M. A., et al. (2020). Fabrication challenges and trends in biomedical applications of alginate electrospun nanofibers. In *Carbohydrate polymers* (p. 115419). Elsevier Ltd.
226. Wimpenny, I., Ashammakhi, N., & Yang, Y. (2012). Chondrogenic potential of electrospun nanofibres for cartilage tissue engineering. *Journal of Tissue Engineering and Regenerative Medicine, 6*(7), 536–549.
227. Lee, C. K., Kim, S. I., & Kim, S. J. (2005). The influence of added ionic salt on nanofiber uniformity for electrospinning of electrolyte polymer. In *Synthetic metals* (pp. 209–212).
228. Topuz, F., et al. (2021). Nanofiber engineering of microporous polyimides through electrospinning: Influence of electrospinning parameters and salt addition. *Materials and Design, 198*.
229. Luraghi, A., Peri, F., & Moroni, L. (2021). Electrospinning for drug delivery applications: A review. *Journal of Controlled Release*, *334*, 463–484.
230. Bishop, E. S., et al. (2017). 3-D bioprinting technologies in tissue engineering and regenerative medicine: Current and future trends. *Genes and Diseases, 4*(4), 185–195.
231. Lin, L., Kollipara, P. S., & Zheng, Y. (2019). Digital manufacturing of advanced materials: Challenges and perspective. *Materials Today, 28*, 49–62.
232. Murphy, S. V., & Atala, A. (2014). 3D bioprinting of tissues and organs. *Nature Biotechnology, 32*(8), 773–785.
233. Ashammakhi, N., et al. (2019). Advancing frontiers in bone bioprinting. *Advanced Healthcare Materials, 8*(7), 1801048.
234. Pati, F., et al. (2015). Chapter 7—Extrusion bioprinting. In A. Atala & J. J. Yoo (Eds.), *Essentials of 3D biofabrication and translation* (pp. 123–152). Academic Press.
235. Ozbolat, I. T., & Hospodiuk, M. (2016). Current advances and future perspectives in extrusion-based bioprinting. *Biomaterials, 76*, 321–343.
236. Angelo, S. M., et al. (2017). Deterministic encapsulation of single cells in thin tunable microgels for niche modelling and therapeutic delivery. *Nature Materials, 16*(2), 236–243.
237. Murphy, S. V., & Atala, A. (2014). 3D bioprinting of tissues and organs. *Nature Biotechnology, 32*, 773.
238. Visser, J., et al. (2013). Biofabrication of multi-material anatomically shaped tissue constructs. *Biofabrication, 5*(3), 035007.
239. Khalil, S., Nam, J., & Sun, W. (2005). Multi-nozzle deposition for construction of 3D biopolymer tissue scaffolds. *Rapid Prototyping Journal, 11*(1), 9–17.
240. Donderwinkel, I., van Hest, J. C. M., & Cameron, N. R. (2017). Bio-inks for 3D bioprinting: Recent advances and future prospects. *Polymer Chemistry, 8*(31), 4451–4471.
241. Zein, I., et al. (2002). Fused deposition modeling of novel scaffold architectures for tissue engineering applications. *Biomaterials, 23*(4), 1169–1185.
242. Malone, E., & Lipson, H. (2007). Fab@Home: The personal desktop fabricator kit. *Rapid Prototyping Journal, 13*(4), 245–255.
243. Heinrich, M. A., et al. (2019). 3D bioprinting: From benches to translational applications. *Small*, 1805510.
244. Pereira, F. D. A. S., et al. (2018). Commercial 3D bioprinters. In A. Ovsianikov, J. Yoo, & V. Mironov (Eds.), *3D printing and biofabrication* (pp. 1–16). Springer International Publishing.
245. Mironov, V., Kasyanov, V., & Markwald, R. R. (2011). Organ printing: From bioprinter to organ biofabrication line. *Current Opinion in Biotechnology, 22*(5), 667–673.

246. Marga, F., et al. (2012). Toward engineering functional organ modules by additive manufacturing. *Biofabrication, 4*(2), 022001.
247. Demirci, U., & Montesano, G. (2007). Single cell epitaxy by acoustic picolitre droplets. *Lab on a Chip, 7*(9), 1139–1145.
248. Gao, G., et al. (2015). Improved properties of bone and cartilage tissue from 3D inkjet-bioprinted human mesenchymal stem cells by simultaneous deposition and photocrosslinking in PEG-GelMA. *Biotechnology Letters, 37*(11), 2349–2355.
249. Yoon, S., et al. (2018). Inkjet-spray hybrid printing for 3d freeform fabrication of multilayered hydrogel structures. *Advanced Healthcare Materials, 7*(14), e1800050.
250. CELLINK. (2018). *CELLINK releases game changer inkjet printhead*, October 8. Available from: https://www.cellink.com/cellink-releases-game-changer-inkjet-printhead/
251. Sears, N. A., et al. (2016). A review of three-dimensional printing in tissue engineering. *Tissue Engineering Part B: Reviews, 22*(4), 298–310.
252. Colosi, C., et al. (2014). Rapid prototyping of chitosan-coated alginate scaffolds through the use of a 3D fiber deposition technique. *Journal of Materials Chemistry B, 2*(39), 6779–6791.
253. Gao, G., & Cui, X. (2016). Three-dimensional bioprinting in tissue engineering and regenerative medicine. *Biotechnology Letters, 38*(2), 203–211.
254. GhavamiNejad, A., et al. (2020). 3D Bioprinting: Crosslinking strategies for 3D bioprinting of polymeric hydrogels. *Small (Weinheim an der Bergstrasse, Germany), 16*(35), 2070195.
255. Dababneh, A. B., & Ozbolat, I. T. (2014). Bioprinting technology: A current state-of-the-art review. *Journal of Manufacturing Science and Engineering, 136*(6), 61016.
256. Duocastella, M., et al. (2007). Study of the laser-induced forward transfer of liquids for laser bioprinting. *Applied Surface Science, 253*, 7855–7859.
257. Chang, C. C., et al. (2011). Direct-write bioprinting three-dimensional biohybrid systems for future regenerative therapies. *Journal of Biomedical Materials Research. Part B, Applied Biomaterials, 98*(1), 160–170.
258. Murphy, S. V., Skardal, A., & Atala, A. (2013). Evaluation of hydrogels for bio-printing applications. *Journal of Biomedical Materials Research. Part A, 101*(1), 272–284.
259. Hull Charles, W. (1986). *Apparatus for production of three-dimensional objects by stereolithography*. UVP INC.
260. Klimek, L., et al. (1993). Stereolithographic modelling for reconstructive head surgery. *Acta Oto-Rhino-Laryngologica Belgica, 47*(3), 329–334.
261. Miri, A. K., et al. (2018). Microfluidics-enabled multimaterial maskless stereolithographic bioprinting. *Advanced Materials, 30*(27), e1800242.
262. CELLINK. (2020). *Holograph X*. Available from: https://www.cellink.com/product/holograph-x/
263. Raman, R., et al. (2016). High-resolution projection microstereolithography for patterning of neovasculature. *Advanced Healthcare Materials, 5*(5), 610–619.
264. Castro, N. J., O'Brien, J., & Zhang, L. G. (2015). Integrating biologically inspired nanomaterials and table-top stereolithography for 3D printed biomimetic osteochondral scaffolds. *Nanoscale, 7*(33), 141–1422.
265. Gauvin, R., et al. (2012). Microfabrication of complex porous tissue engineering scaffolds using 3D projection stereolithography. *Biomaterials, 33*(15), 3824–3834.
266. Wang, Z., et al. (2017). Visible light-based stereolithography bioprinting of cell-adhesive gelatin hydrogels. IEEE.
267. Ashammakhi, N., et al. (2006). Biodegradable nanomats produced by electrospinning: Expanding multifunctionality and potential for tissue engineering. *Journal of Nanoscience and Nanotechnology, 6*(9–10), 2693–2711.
268. Brown, T. D., Dalton, P. D., & Hutmacher, D. W. (2011). Direct writing by way of melt electrospinning. *Advanced Materials, 23*(47), 5651–5657.
269. Bertlein, S., et al. (2018). Development of endothelial cell networks in 3D tissues by combination of melt electrospinning writing with cell-accumulation technology. *Small (Weinheim an der Bergstrasse, Germany), 14*(2), 1701521.

270. Jordahl, J. H., et al. (2018). 3D jet writing: Functional microtissues based on tessellated scaffold architectures. *Advanced Materials, 30*(14), 1707196.
271. Bisht, G. S., et al. (2011). Controlled continuous patterning of polymeric nanofibers on three-dimensional substrates using low-voltage near-field electrospinning. *Nano Letters, 11*(4), 1831–1837.
272. Park, Y.-S., et al. (2020). Near-field electrospinning for three-dimensional stacked nanoarchitectures with high aspect ratios. *Nano Letters, 20*(1), 441–448.
273. Lee, M., & Kim, H.-Y. (2014). Toward nanoscale three-dimensional printing: Nanowalls built of electrospun nanofibers. *Langmuir, 30*(5), 1210–1214.
274. Tourlomousis, F., et al. (2019). Machine learning metrology of cell confinement in melt electrowritten three-dimensional biomaterial substrates. *Microsystems & Nanoengineering, 5*, 15.
275. Tourlomousis, F., et al. (2019). Machine learning metrology of cell confinement in melt electrowritten three-dimensional biomaterial substrates. *Microsystems & Nanoengineering, 5*(1), 15.
276. Malgarim Cordenonsi, L., et al. (2019). Platelet lysate loaded electrospun scaffolds: Effect of nanofiber types on wound healing. *European Journal of Pharmaceutics and Biopharmaceutics, 142*, 247–257.
277. Wunner, F. M., Eggert, S., Maartens, J., Bas, O., Dalton, P. D., De-Juan-Pardo, E. M., & Hutmacher, D. W. (2019). Design and development of a three-dimensional printing high-throughput melt electrowriting technology platform.*3D Printing and Additive Manufacturing, 6*(2), 82–90.
278. Mota, C., et al. (2013). Melt electrospinning writing of three-dimensional star poly(ε-caprolactone) scaffolds. *Polymer International, 62*(6), 893–900.
279. Spraybase. (2018). *Melt electrospinning by Spraybase®*. Available from: https://www.spraybase.com/meltelectrospin
280. SPIDER, N. *Fabricate multi-phase nanocomposites with 3D ultra-thin fiber structures.* Available from: http://www.novaspider.com/
281. regenHU. (2020). *3DDiscover™ evolution.* Available from: https://www.regenhu.com/3d-bioprinters#3ddiscovery-evolution.
282. Park, J.-S. (2011). Electrospinning and its applications. *Advances in Natural Sciences: Nanoscience and Nanotechnology, 1*(4), 043002.
283. Hochleitner, G., et al. (2015). Additive manufacturing of scaffolds with sub-micron filaments via melt electrospinning writing. *Biofabrication, 7*(3), 035002.
284. Visser, J., et al. (2015). Reinforcement of hydrogels using three-dimensionally printed microfibres. *Nature Communications, 6*, 6933.
285. Farrugia, B. L., et al. (2013). Dermal fibroblast infiltration of poly(epsilon-caprolactone) scaffolds fabricated by melt electrospinning in a direct writing mode. *Biofabrication, 5*(2), 025001.
286. Wunner, F. M., et al. (2018). Melt electrospinning writing of highly ordered large volume scaffold architectures. *Advanced Materials, 30*(20), 1706570.
287. Chen, W., et al. (2019). Three-dimensional printed electrospun fiber-based scaffold for cartilage regeneration. *Materials & Design, 179*, 107886.
288. Khademhosseini, A., & Langer, R. (2016). A decade of progress in tissue engineering. *Nature protocols, 11*(10), 1775–1781.
289. Ashammakhi, N., Hoque Apu, E., & Caterson, E. J. (2020). Self-healing biomaterials to heal tissues. *Journal of Craniofacial Surgery, 32*(3), 819–820.
290. Rammal, H., et al. (2021). Advances in biomedical applications of self-healing hydrogels. *Materials Chemistry Frontiers, 5*(12), 4368–4400.
291. Alizadeh, P., Soltani, M., Tutar, R., Hoque Apu, E., Maduka, C. V., Unluturk, B. D., et al. (2021). Use of electroconductive biomaterials for engineering tissues by 3D printing and 3D bioprinting. *Essays in Biochemistry, 65*(3), 441–466.
292. Gungor-Ozkerim, P. S., et al. (2018). Bioinks for 3D bioprinting: An overview. *Biomaterials Science, 6*(5), 915–946.

293. Yoon, Y., et al. (2019). 3D bioprinted complex constructs reinforced by hybrid multilayers of electrospun nanofiber sheets. *Biofabrication, 11*(2), 025015.
294. Youngblood, R. L., et al. (2018). It's all in the delivery: Designing hydrogels for cell and non-viral gene therapies. *Molecular Therapy, 26*(9), 2087–2106.
295. Lee, J., Park, C. H., & Kim, C. S. (2018). Microcylinder-laden gelatin-based bioink engineered for 3D bioprinting. *Materials Letters, 233*, 24–27.
296. Ko, Y.-G., & Kwon, O. H. (2020). Reinforced gelatin-methacrylate hydrogels containing poly (lactic-co-glycolic acid) nanofiber fragments for 3D bioprinting. *Journal of Industrial and Engineering Chemistry, 89*, 147–155.
297. Xu, T., et al. (2012). Hybrid printing of mechanically and biologically improved constructs for cartilage tissue engineering applications. *Biofabrication, 5*(1), 015001.
298. Dreher, R., & Starly, B. (2015). Biofabrication of multimaterial three-dimensional constructs embedded with patterned alginate strands encapsulating PC12 neural cell lines. *Journal of Nanotechnology in Engineering and Medicine, 6*(2).
299. Shin, J. Y., et al. (2020). Dual-crosslinked methylcellulose hydrogels for 3D bioprinting applications. *Carbohydrate Polymers, 238*, 116192.
300. Zhou, M., Lee, B. H., & Tan, L. P. (2017). A dual crosslinking strategy to tailor rheological properties of gelatin methacryloyl. *International Journal of Bioprinting, 3*(2), 003–003.
301. Mansouri, N., et al. (2019). Advancing fabrication and properties of three-dimensional graphene–alginate scaffolds for application in neural tissue engineering. *RSC Advances, 9*(63), 36838–36848.
302. Jafari, A., et al. (2020). Bioactive antibacterial bilayer PCL/gelatin nanofibrous scaffold promotes full-thickness wound healing. *International Journal of Pharmaceutics, 583*, 119413.
303. Koudan, E., et al. (2016). Spreading of tissue spheroids on an electrospun polyurethane matrix. *Biomedical Engineering, 50*(1), 1–4.
304. Paul, K., et al. (2019). 3D bioprinted endometrial stem cells on melt electrospun poly ε-caprolactone mesh for pelvic floor application promote anti-inflammatory responses in mice. *Acta Biomaterialia, 97*, 162–176.
305. Pelipenko, J., et al. (2013). The topography of electrospun nanofibers and its impact on the growth and mobility of keratinocytes. *European Journal of Pharmaceutics and Biopharmaceutics, 84*(2), 401–411.
306. Zheng, J., et al. (2015). Enhanced Schwann cell attachment and alignment using one-pot "dual click" GRGDS and YIGSR derivatized nanofibers. *Biomacromolecules, 16*(1), 357–363.
307. Martins, A., Reis, R., & Neves, N. (2008). Electrospinning: Processing technique for tissue engineering scaffolding. *International Materials Reviews, 53*(5), 257–274.
308. Dalton, P. D., et al. (2020). Advances in hybrid fabrication toward hierarchical tissue constructs. *Advanced Science, 7*(11), 1902953.
309. Efimov, A., et al. (2019). 3D scanning probe nanotomography of tissue spheroid fibroblasts interacting with electrospun polyurethane scaffold. *Express Polymer Letters, 13*(7), 632–641.
310. Mao, H., et al. (2020). Recent advances and challenges in materials for 3D bioprinting. *Progress in Natural Science: Materials International, 30*(5), 618–634.
311. Jun, I., et al. (2018). Electrospun fibrous scaffolds for tissue engineering: Viewpoints on architecture and fabrication. *International Journal of Molecular Sciences, 19*(3), 745.
312. De Mori, A., et al. (2018). 3D printing and electrospinning of composite hydrogels for cartilage and bone tissue engineering. *Polymers, 10*(3).
313. Liu, X. Y., et al. (2020). HBC-nanofiber hydrogel scaffolds with 3D printed internal microchannels for enhanced cartilage differentiation. *Journal of Materials Chemistry B, 8*(28), 6115–6127.
314. Huang, L., et al. (2021). 3D printed hydrogels with oxidized cellulose nanofibers and silk fibroin for the proliferation of lung epithelial stem cells. *Cellulose, 28*(1), 241–257.
315. Liu, F., & Wang, X. H. (2020). Synthetic polymers for organ 3D printing. *Polymers, 12*(8).
316. Ozdil, D., & Aydin, H. M. (2014). Polymers for medical and tissue engineering applications. *Journal of Chemical Technology and Biotechnology, 89*(12), 1793–1810.

317. Shahabipour, F., et al. (2020). Key components of engineering vascularized 3-dimensional bioprinted bone constructs. *Translational Research, 216*, 57–76.
318. Markowicz, M., Koellensperger, E., Neuss, S., Steffens, G. C. M., & Pallua, N. (2005). Enhancing the vascularization of three-dimensional scaffolds: New strategies in tissue regeneration and tissue engineering. In R.R. N Ashammakhi (Ed.), *Topics in tissue engineering*. Oulu University.
319. Goonoo, N., et al. (2013). An assessment of biopolymer- and synthetic polymer-based scaffolds for bone and vascular tissue engineering. *Polymer International, 62*(4), 523–533.
320. Hasan, A., et al. (2014). Electrospun scaffolds for tissue engineering of vascular grafts. *Acta Biomaterialia, 10*(1), 11–25.
321. Joy, J., et al. (2019). Electrospun microporous gelatin-polycaprolactone blend tubular scaffold as a potential vascular biomaterial. *Polymer International, 68*(7), 1367–1377.
322. Yang, J. K., et al. (2020). Electrospun Janus nanofibers loaded with a drug and inorganic nanoparticles as an effective antibacterial wound dressing. *Materials Science & Engineering C—Materials for Biological Applications, 111*.
323. Gounani, Z., et al. (2020). Polycaprolactone-gelatin nanofibers incorporated with dual antibiotic-loaded carboxyl-modified silica nanoparticles. *Journal of Materials Science, 55*(36), 17134–17150.
324. Annur, D., et al. (2015). Plasma-synthesized silver nanoparticles on electrospun chitosan nanofiber surfaces for antibacterial applications. *Biomacromolecules, 16*(10), 3248–3255.
325. Taheri, P., & Khajeh-Amiri, A. (2020). Antibacterial cotton fabrics via immobilizing silver phosphate nanoparticles onto the chitosan nanofiber coating. *International Journal of Biological Macromolecules, 158*, 282–289.
326. de Faria, A. F., et al. (2015). Antimicrobial electrospun biopolymer nanofiber mats functionalized with graphene oxide-silver nanocomposites. *ACS Applied Materials & Interfaces, 7*(23), 12751–12759.
327. Ashammakhi, N., & Kaarela, O. (2017). Stimuli-responsive biomaterials: Next wave. *The Journal of Craniofacial Surgery, 28*(7), 1647–1648.
328. Lu, Y., et al. (2016). Bioresponsive materials. *Nature Reviews Materials, 2*(1), 16075.
329. Elmusrati, M., & Ashammakhi, N. (2018). Cancer-on-a-chip and artificial intelligence: Tomorrow's cancer management. *Journal of Craniofacial Surgery, 29*(7), 1682–1683.



Nureddin Ashammakhi is leading translational research in biomaterials and regenerative therapeutics. He has extensive experience with biodegradable implants, drug release, and nanofiber-based scaffolds. Currently, he is leading research on 3D bioprinting and organ-on-a-chip technology for personalized medicine and regenerative therapy. He was previously a Professor of Biomaterials Technology in Tampere University of Technology, Finland, Chair of Regenerative Medicine in Keele University, UK, Adjunct Professor in Oulu University, Finland, and Visiting Scholar and Adjunct Professor at the University of California, Los Angeles before he joined Michigan State University.



Maryam Tavafoghi received her Ph.D. degree in Materials Engineering from McGill University, Canada. For her Ph.D. project, she worked on developing osteogenic biomaterials for hard tissue engineering applications. In 2018, Maryam joined Dr. Khademhosseini laboratory at the University of California-Los Angeles as a Fonds de recherche du Québec - santé (FRQS) Postdoctoral Fellow. For her postdoctoral research, she developed mechanically strong and bioadhesive hydrogels for engineering and minimally invasive sealing of soft tissues. Maryam's research interests lie primarily in the area of tissue engineering and 3D bioprinting. Maryam has been the recipient of multiple international awards and fellowships, and she is the first author of more than 10 peer-reviewed articles published in reputable journals, such as Advanced Healthcare Materials and Biofabrication.



Arman Jafari received his B.Sc. in Chemical Engineering from Shiraz University, Shiraz, Iran in 2016 and his M.Sc. degree in Chemical Engineering from the same university in 2019. He is currently a Ph.D. student in Biomedical Engineering at the University of Montreal, Canada. His research interests include biomaterials, tissue engineering, and advanced manufacturing. He has conducted research in the development of hydrogels/scaffolds for wound healing and tissue engineering purposes. He also has worked on stem cells differentiation and fate regulation using physical/mechanical stimulus. Currently, he is working on the development of biomaterials and biomaterials' application in the formulation of novel inks for 3D printing and 3D bioprinting of tissues.



Sumama Nuthana Kalva received the B. Tech. degree in Mechanical engineering from National Institute of Technology Srinagar, J&K, India, in 2018 and the M.S. degree in Mechanical engineering from Qatar University, Doha, Qatar, in 2021. He works as a Research Assistant at the College of Engineering as well as the Biomedical Research Center in Qatar University. His research interest includes the development of extracellular matrix mimetic fibrous scaffolds for wound healing applications through various fabrication techniques. He also has a great interest in bridging the advances in computational fluid dynamics and computational modeling techniques to solve various problems faced in real-world applications. He published several research articles in leading international journals and conference proceedings.



Robin Augustine is a Postdoctoral Research Assistant at College of Engineering and Biomedical Research Center of Qatar University, Doha, Qatar. Dr. Augustine received his Master's degree in Bioengineering from Madurai Kamaraj University, India (2010) and a Ph.D. degree in Nanoscience and Nanotechnology from Mahatma Gandhi University, India (2015). Soon after the submission of his Ph.D. thesis (2015), Augustine received a postdoctoral fellowship from Israel Higher Education Council (VATAT) and joined in Technion Israel Institute of Technology, Israel. In 2016, Augustine received National Postdoctoral Fellowship from the government of India (SERB) and joined at National Institute of Technology (NIT Calicut, India). After a year, Augustine joined Qatar University as a postdoctoral researcher (2017). In Qatar University, Dr. Augustine is working on multiple projects such as bioprinting, diabetic wound healing, development of in vitro cancer models, microfluidic lab on a chip, and blood-brain barrier models. He has published more than 60 research articles in reputed international journals and dozens of book chapters in the books of leading publishers.



Anwarul Hasan is an Associate Professor of Mechanical and Industrial Engineering at Qatar University as of Feb 2020. His current research interests include Advanced Biomaterials and Tissue Engineering for cardiovascular diseases, diabetic wound healing, and Cancer. Earlier he served as an Assistant Professor in the same department and University as well as in the Biomedical Engineering and the Department of Mechanical Engineering at the American University of Beirut in Lebanon. He also served as a visiting Professor at the Harvard-MIT Division of Health Sciences and Technology at the Harvard Medical School and Massachusetts Institute of Technology in Boston, USA. Dr. Hasan obtained his Ph.D. from the University of Alberta, Canada in 2010 and worked in Alberta Innovates Technology Futures in Edmonton, Canada, and Champion Technologies LTD in Calgary, Alberta, Canada during 2010–2011. Dr. Anwarul Hasan has more than 150 peer-reviewed papers including more than 115 journal articles and more than 25 conference proceeding papers. Dr. Hasan is a winner of more than sixteen national and international awards.



Houman Savoji is an Assistant Research Professor in the Institute of Biomedical Engineering and Department of Pharmacology and Physiology of the University of Montreal and a full-time researcher at the Sainte-Justine Hospital Research Centre. He is also a Montreal TransMedTech Chair in 3D Bioprinting and Regenerative Medicine. His primary research focus lies in the general area of Advanced Biofabrication Strategies, with particular emphasis on Micro- and Nano-fabrication of Functional Biomaterials for Tissue Engineering, Regenerative Medicine and Organ-on-a-Chip Applications.



Yavuz Nuri Ertas received the B.S. degree in biomedical engineering from Baskent University, Turkey in 2007 and the M.S. degree in materials science and nanotechnology from Bilkent University, Turkey in 2010. He later moved to USA for the doctoral studies and received the Ph.D. degree in biomedical engineering from University of California, Los Angeles (UCLA), in 2017. From 2018 to 2020, he was a Postdoctoral Researcher in the department of chemistry at the UCLA. Since 2020, he has been an Assistant Professor with the Biomedical Engineering Department, Erciyes University, Turkey, and he has been directing an interdisciplinary laboratory (ertaslab.com) at Erciyes University Nanotechnology Research and Application Center (ERNAM). During the doctoral studies, he worked towards producing bare gadolinium nanoparticles. Until then, it was not possible to produce such particles using standard chemical methods. He developed a synthetic nanofabrication method to produce highly magnetic and oxide-free gadolinium nanocrystals which are used as magnetic resonance imaging (MRI) contrast agents. His current research interests include nanoparticle synthesis and applications, micro-nano fabrication, biomaterials and 3D-bioprinting. Dr. Ertas was a recipient of the International Fellowship for Outstanding Researchers Program (TUBITAK 2232) in 2020.



Song Li Ph.D., earned his B.S. and M.S. in Peking University and had his Ph.D. and postdoctoral training in Bioengineering at UC San Diego. He was a professor of bioengineering at UC Berkeley between 2001 and 2015, where he served as a Co-Chair of UC Berkeley-UCSF Graduate Program and Co-Director of the Master in Translational Medicine program. In 2016, Dr. Li joined the Bioengineering faculty at UC Los Angeles. He is currently a Chancellor Professor and the Chair of the Bioengineering Department with a joint appointment in the Department of Medicine. Dr. Li's research is focused on cell engineering, biomaterials, drug delivery, mechanobiology, and regenerative engineering. He takes an interdisciplinary approach to developing therapeutics by engineering stem cells and micro/nanomaterials. His research also advances the understanding of how biophysical factors regulate cell reprogramming and tissue remodeling. Dr. Li has been elected as a Fellow of the American Institute of Medical and Biological Engineering, a Fellow of Biomedical Engineering Society, and a Fellow of the International Academy of Medical and Biological Engineering.

Chapter 21
Application of Hand-Held Electrospinning Devices in Medicine



Yun-Ze Long, Jun Zhang, Zhong Liu, Bing-Chang Wang, Miao Yu, and Seeram Ramakrishna

Abstract The current situation of traditional nanofiber preparation devices appears in difficult transportation, the requirement of external power supply, and poor flexibility. With the aim of solving the problem of limited usage in medical wound dressings, this paper summarizes the composition and medical applications of small portable electrospinning devices independent of an external power supply. The concept of in-situ electrospinning has become increasingly refined by discussing the morphological structure, antibacterial properties, hemostatic effect, and promoting tissue repair ability of electrospun nanofibers. In other words, the nanofiber dressing film can be directly and quickly prepared on the wound according to the patient's situation, especially in hemostasis of liver, burn and scald treatment, meningeal sealing. This paper also contains a general overview of the functional nanofibers, which facilitate further selection of effective dressings. Finally, the challenges and development trends of portable electrospinning devices in individual cosmetic and wound dressings still require more investigation. This review provides a reference for the application of portable in-situ electrospinning devices in medicine.

Y.-Z. Long (✉) · J. Zhang · Z. Liu · B.-C. Wang · M. Yu
Collaborative Innovation Center for Nanomaterials and Devices, College of Physics, Qingdao University, Qingdao, China
e-mail: yunze.long@qdu.edu.cn

Y.-Z. Long
State Key Laboratory of Bio-Fibers and Eco-Textiles, Collaborative Innovation Center for Eco-Textiles of Shandong Province, Qingdao 266071, China

B.-C. Wang
Transformation et Qualité des Matériaux, Universite de Technologie de Troyes, 12 rue Marie Curie-CS 42060, 10004 Troyes Cedex, France

M. Yu
Junada (Qingdao) Technology Co. Ltd., Qingdao International Academician Park, Qingdao 266199, China

S. Ramakrishna
Department of Mechanical Engineering, Center for Nanofibers and Nanotechnology, National University of Singapore, Singapore 117574, Singapore

© The Author(s), under exclusive license to Springer Nature Switzerland AG 2022

A. Vaseashta and N. Bölgen (eds.), *Electrospun Nanofibers*,
https://doi.org/10.1007/978-3-030-99958-2_21

Keywords In-situ electrospinning · Handheld electrospinning device · Wound dressing

21.1 Introduction

Electrospinning represents a rising process for manufacturing nanofibers. Under the influence of high-voltage electricity, polymer solutions or melts are sprayed and stretched. Through this method, we can acquire nanofiber materials, which are widely used in the energy environment [1, 2], medical care [3, 4], nanodevice development [5, 6], and other areas. Recently in the emerging biomedicine with a focus on wound care, the barrier formed by nanofiber dressings protects the wound from infection, provides better air permeability, and accelerates hemostasis [7, 8]. Medical-grade electrospinning three-dimensional (3D) materials can align nanofibers and guide cells' directional growth and migration [9]. These nanofibers also ensure compatibility and degradability with living organisms by adapting processing and materials [10]. Due to the high specific surface area and porosity, it is suitable for drug delivery and cell proliferation [11]. Several scaffolds have been prepared that highly mimic the extracellular matrix (ECM) structure in vivo, offering suitable conditions for soft tissue regeneration [7, 8, 12–14].

The traditional wound dressings process includes producing electrospun mesh materials, packing in advance, and applying at an opportune moment. The preparation and utilization restrict conventional dressing, and these two parts are independent and separate from each other. In an effort to prepare ideal dressings for wounds, Long et al. developed a series of portable devices for hand-held operation. The degradable liquid medicine was sprayed into nanofibers directly on the wound. They have designed these new devices based on their in-depth understanding of the principles and effects of fibers deposition. In that case, the process of preparation and usage are integrated from two to one. This direct method, named in-situ depositing nanofibers on the wound, is simple to operate, reduces pain and bleeding and can customize dressings according to patients' individual needs [8–19]. With the continuous development of technology and demands for highly portable, hand-held electrospinning devices that can satisfy personalized wound care demands have become increasingly urgent. The application prospects are promising.

Electrospinning technology started in 1934. Since the 1990s, the rapid development of nanotechnology has introduced a convenient and accessible method for preparing micro/nanofibers. As shown in Fig. 21.1a, the traditional electrospinning device consists of three parts: a high-voltage power supply, a spinning nozzle, and a grounding metal collector. The fiber diameter varies from the nanoscale to the microscale level. In more detail, the diameter distribution is affected by solution viscosity, conductivity, extrusion rate, electrostatic field, syringe diameter, selected distance, temperature, and humidity [15]. The polymer solution (or melt) overcomes the surface tension to form a jet through high-voltage electrostatic action. As the solvent evaporates or solidifies, they are finally deposited on different collectors to

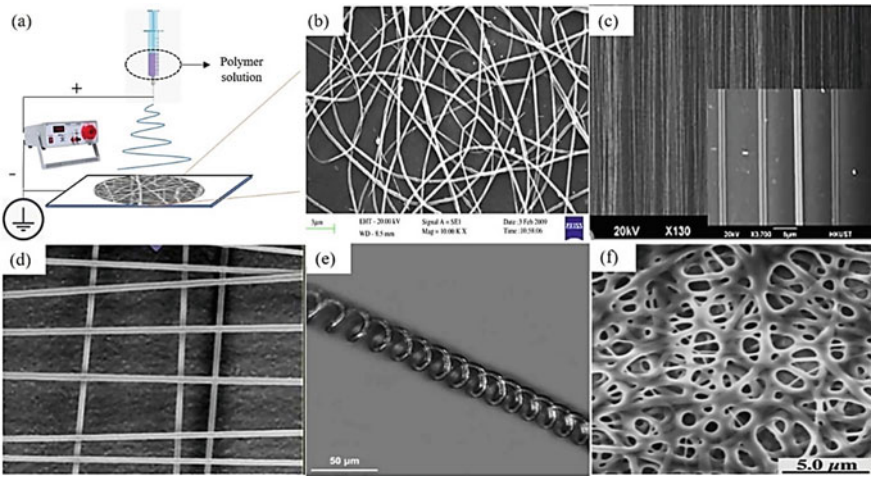


Fig. 21.1 Electrospinning and nanofibers. **a** Traditional electrospinning device; **b** electrospun fibers of silk fibroin [21]; **c** parallel nanofibers [22]; **d** crossed nanofibers [22]; **e** helical nanofibers [24]; **f** short pitch interconnected nanofibers [26]

build up non-woven fibers' nets of different shapes (Fig. 21.1b–f), e. g. yarns [16–20]. Alternatively, the nanofibers are directly assembled in different orientations [21–26].

During the electrospinning process, the polymer solution passes through the nozzle. The droplets stretch as it draws support from the high voltage field. There will be an interaction between charges. When the electrostatic repulsion between the charged solutions is stronger than the surface tension, a jet stream is ejected from the top of the cone, causing the Taylor cone [27, 28]. The movement of the electrospinning polymer jet is very complicated. At the tip of the spinneret, the path can be divided into three parts (e. g. straight-line area, conversion area, and unstable area), as explained in Fig. 21.2a–c [27–29]. In particular, Fig. 21.2c shows the principle of path instability. First, a coil with a slender enveloping cone was formed. Then, the slender coil forms a larger curved coil, which increases in diameter more rapidly. The gray line inside the coil illustrates the centerline of the larger loop that forms the anadem surrounding.

21.2 Characteristics and Advantages of Portable Electrospinning Devices

Improving the conventional preparation process is essential to realize the controllability of the orientation and morphology in the fibrous mesh [30, 31]. A case in point is the self-assembly and modification of the nozzle and collector. Traditional electrospinning devices, include an electrostatic high-voltage power supply, a spinneret, a microfluidic pump, and a collection plate. Yang et al. [27] reviewed

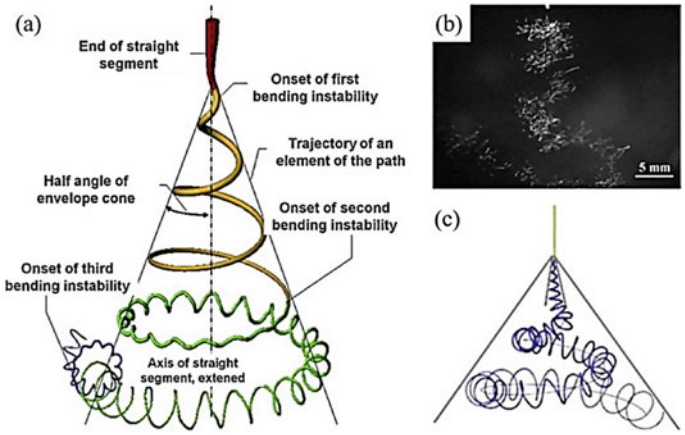


Fig. 21.2 Electrospinning jet path diagram. **a** Ordinary path [28]; **b–c** "Flower ring" path [29]

some representative strategies: for example, using different nozzles (coaxial spinneret [32], triaxial spinneret [33], and multichannel spinneret [34]), needleless (electrode nanospider [35], bubble interference [36], disk [37], and helix [38]), current collectors [39], parallel electrode [40], double collector rings and collected oriented nanofibers [41], rotating drum with parallel wires [42], turntable collector [43], parallel track [44], water bath [45], dynamic support system [46], near-field electrospinning [47], microfluidics assisted electrospinning [48], and combination of 3D printing and electrospinning [49]. In addition, patterned collectors are also possible to generate complex fiber geometries [50–52]. Fixed tips and centrifugal spinnerets are also favorable for the formation of oriented nanofibers [53–55]. These simple improvements enumerated above can optimize the structure and performance of the electrospinning mesh, especially in biomedical fields such as drug delivery, tissue engineering, and diagnosis [27]. However, tissue repair is a specific biological process covering a broad spectrum of collagen metabolism, wound contraction, epithelialization and inflammation. Overall, if the collector of a portable electrospinning device needs to be compatible with a physical wound, it is necessary to unilaterally rely on developing some part of the device (sprinkler or collector).

To accommodate biological collections' characteristics and enhance portability and operability, the components of the original large-scale desktop devices require more modifications. The following are some practical measures: To simulate the working of wounds emergency treatment under the field conditions, the built-in lithium battery and high-voltage converter can supply power without an external source, enhancing portability [56]. Zhao et al. assembled ultra-high heat conduction and high insulation unit into the head to solve the electrostatic interference between the high-voltage and the heating unit [57]; For accurate dressing placement, a directional-assisted cover can be used to protect the wound [58, 59]. Other efficient improvements are available, including hand-held spinnerets [60–64], miniature high-voltage power supplies with converters [64–68], and alternative power sources

Table 21.1 The advantages and disadvantages between desktop and portable devices

Type of devices	Advantages	Disadvantages
Desktop	Controllable environmental parameters High pressure adjustable Accurate voltage and flow values Reliable safety management	Transportation difficulties Requires external power supply Poor flexibility Expensive
Portable	Portability (small, light, hand-held) Flexible direction, wide application target In-situ spinning Manually control spinning/spraying Battery-powered Safe to use Fair price Suitable for medical applications	Current limit, high-pressure instability Battery capacity limitation Fixed-size

(batteries or generators) [69–74]. Table 21.1 lists the advantages and disadvantages of the two common types of electrospinning devices.

The advantages of portable electrospinning devices are combining biodegradable polymers, repair adjuvants, and tissue substitutes in dressings. This pairing expands the functional applications of electrospinning in wound dressings (e.g., antibacterial, immunomodulation, cell proliferation, and blood vessel formation). The critical point to note is that electrospun dressings are restrained by complex and diverse wounds, such as serious injury [75], surface area defect [75], burns and scalds [66, 76], visceral resection [77, 78], and meningeal repair [79]. Consequently, personalized wound treatment seems to be significant. In-situ electrospinning, precise deposition of conductive polymers, presents opportunities for rapid treatment and healing of the wound site [80]. During operation, their safety mainly depends on the low current (about 0.1 mA to a few mA) and the adjustable distance between the nozzle and the wound site (about 2–12 cm) [81].

21.3 Portable Electrospinning Devices and Its In-situ Application

The portable electrospinning devices do not require an external power supply. Their built-in battery allows the equipment to perform for more than 3 h [57]. Hence, it has the benefit of being small in size and lightweight. The one-handed active operation is appropriate both indoor and outdoor, particularly in emergency or remote areas. The lower cost and higher safety (to avoid an electric shock) have attracted much attention. Throughout the rest of this chapter, we will discuss the applications of several portable electrospinning devices.

21.3.1 Hand-Held Electrospinning Devices and Its Applications

Long et al. [62] designed an airflow-oriented in-situ electrospinning device for rapid liver hemostasis in the pig. As indicated in Fig. 21.3a, the device was mainly composed of four parts: a high-voltage power supply, injection pump, air pump, and self-assembled spinneret handle. In Fig. 21.3b–d, the high-velocity airflow (applicable rate is 12 L min^{-1}) allowed precise deposition range and location control. Figure 21.3e also showed that the device could function as a pen for writing "electrospinning" and other characters. For further adequate verification of in-situ electrospinning, Long et al. performed porcine hemostasis experiments in vivo. Firstly, the porcine abdominal cavity was opened under anesthesia, and a pair of hemostatic forceps fixed the liver. Secondly, part of the liver tissue was incised to create a visible wound. Next, long et al. thoroughly cleaned the bleeding area with sterile gauze and airflow, and then the wound was swiftly covered by a layer of medical glue (*N*-octyl-2-cyanoacrylate, NOCA) fiber membrane using airflow oriented in-situ electrospinning device within 20 s. After 1 min, they removed the hemostatic forceps, and there was no bleeding within 3 h. Figure 21.4 shows the experimental process.

Subsequently, Dong et al. [82] used fresh animal livers to establish a bleeding model caused by hepatectomy. They found that the device accurately deposited NOCA fibers on the wound, improving operational performance and safety. There was a significant 80% reduction in the amount of NOCA as well as alleviating side effects and inflammatory reactions. As seen in Fig. 21.5, this in-situ electrospinning device enabled precise deposition, efficient stopping of bleeding, minor damage to liver cells, and promoted tissue regeneration compared with traditional spraying and electrospinning.

Afterward, the team explored in-situ electrospinning NOCA for endocranium repair in goat brain. Experiments had proven that a flexible and dense membrane was electrospun by this method, which rapidly contribute to suture the endocranium defect and repairing it with the avoidance of tissue adhesion [79], presented in Fig. 21.6.

Depositing in-situ nanofibers on living organs can increase the adhesion of nanofiber membranes to the organs, leading to an accelerated hemostatic effect. Zhang et al. [83] combined in-situ electrospinning with minimally invasive surgery. With the help of a laparoscope, they observed the living organs and deposited nanofibers directly on them. In a minimally invasive surgery in porcine, the long laparoscopic tube (37 cm) (Fig. 21.7a) minimized the impact of handshaking on the wound site. In terms of hemostasis time, the in-situ electrospinning group (Fig. 21.7g) was 5 s, which was shorter than the traditional suture hemostasis group (3 min, Fig. 21.7e) and the coated NOCA group (14 s, Fig. 21.7f). The deposition area of the nanofiber membranes could be fine-tuned through the tapered convergence structure without affecting the diameters of the fibers. It indicated a potentiality to accelerate hemostasis, reduce postoperative inflammation, and promote recovery.

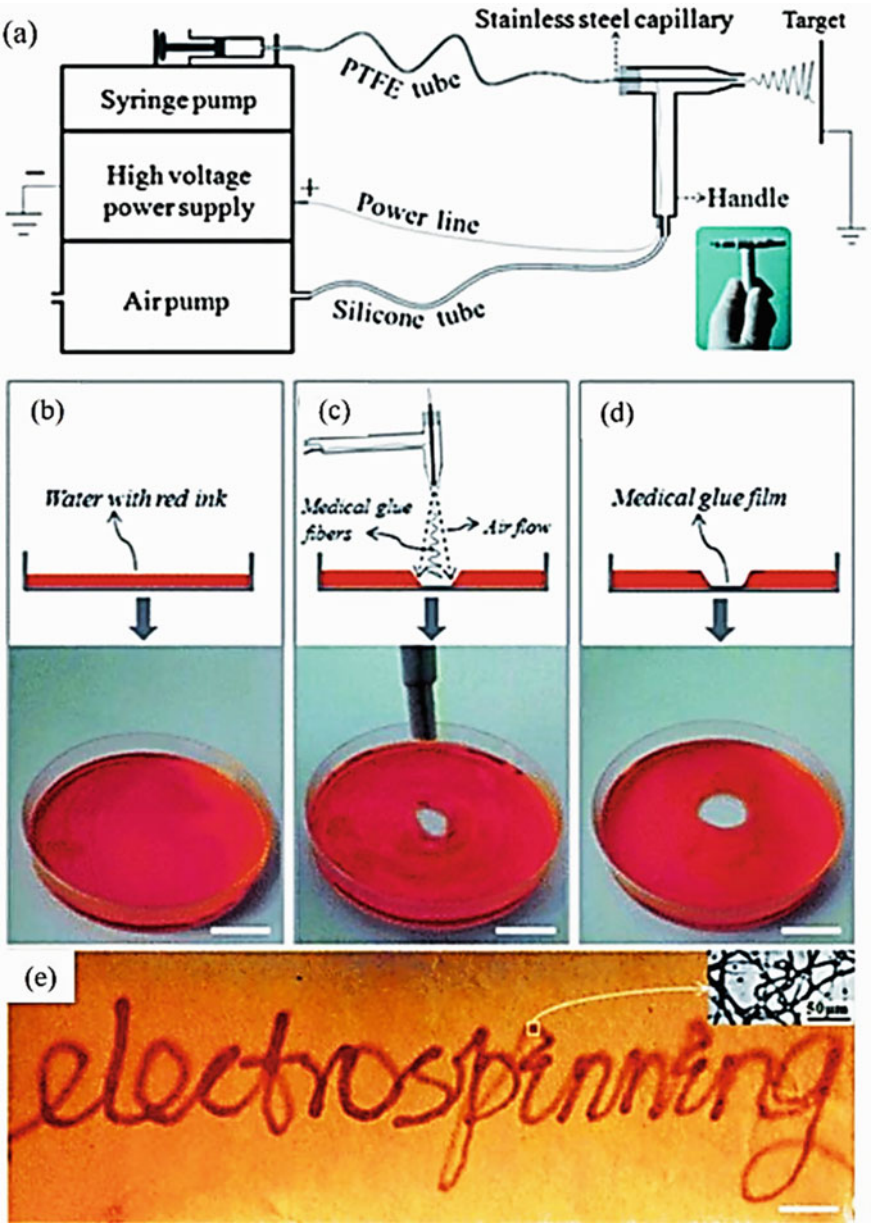


Fig. 21.3 Air flow oriented in-situ electrospinning [62]. **a** Schematic diagram of air flow oriented in-situ electrospinning device (including self-assembled head and handle); **b–d** precise deposition of NOCA fibers; **e** the device was used as a pen to write an optical fiber image

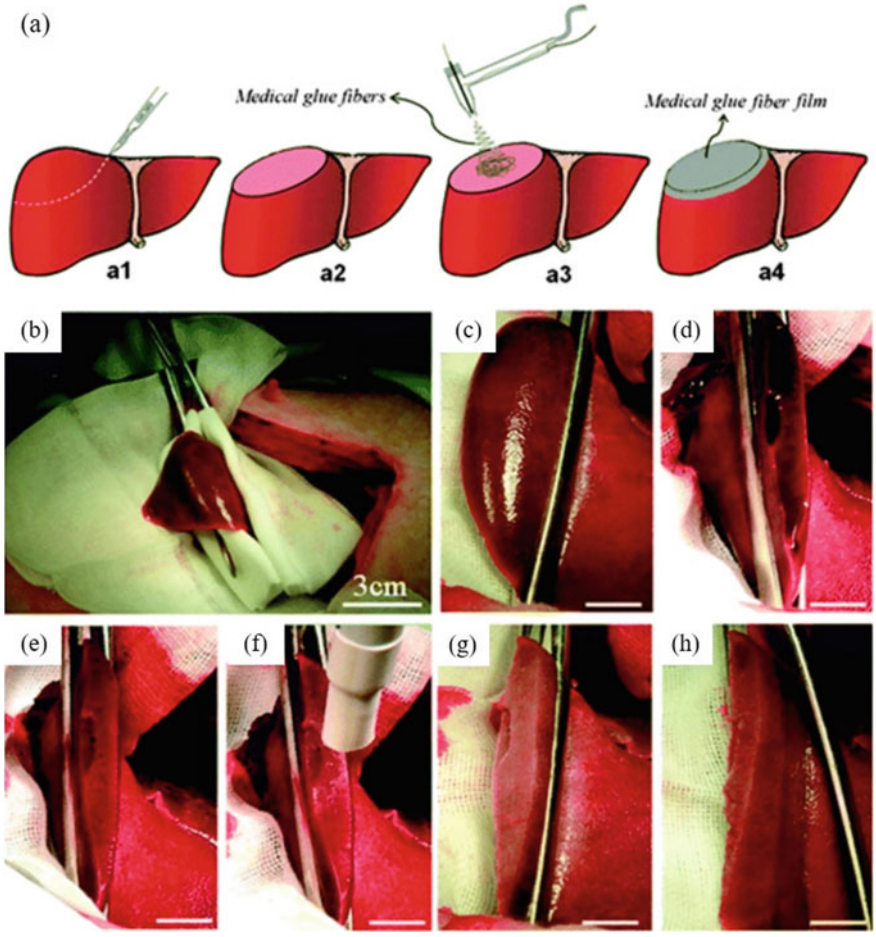


Fig. 21.4 Porcine liver hemostasis in vivo [62]. **a** Experimental flow diagram; **b**–**h** the photographs were shot by camera during each stage of pig liver wound section of hemostasis experiment; **f** wound was deposited in-situ; **g** covering the wound quickly within 20 s; **h** no bleeding or bile exudation were found after removing the hemostatic forceps

In 2018, Wang et al. [84] reported a single-electrode piezoelectric nanogenerator sensor based on polyvinylidene fluoride (PVDF) nanofibers (Fig. 21.8b) which were prepared by in-situ electrospinning (Fig. 21.8a). The steady-state sensing of cold/heat integrated pressure could be realized in a single unit. The square wave signals expressed piezoelectric voltage, and the pulse signal indicated the heat. The electronic skin composed of such nanofibers permitted highly sensitive temperature and pressure detection (Fig. 21.8c–e).

Recently, because of the complex intestinal contents and higher wound sealing requirements, Zhou et al. [85] applied in-situ electrospinning for hemostasis of

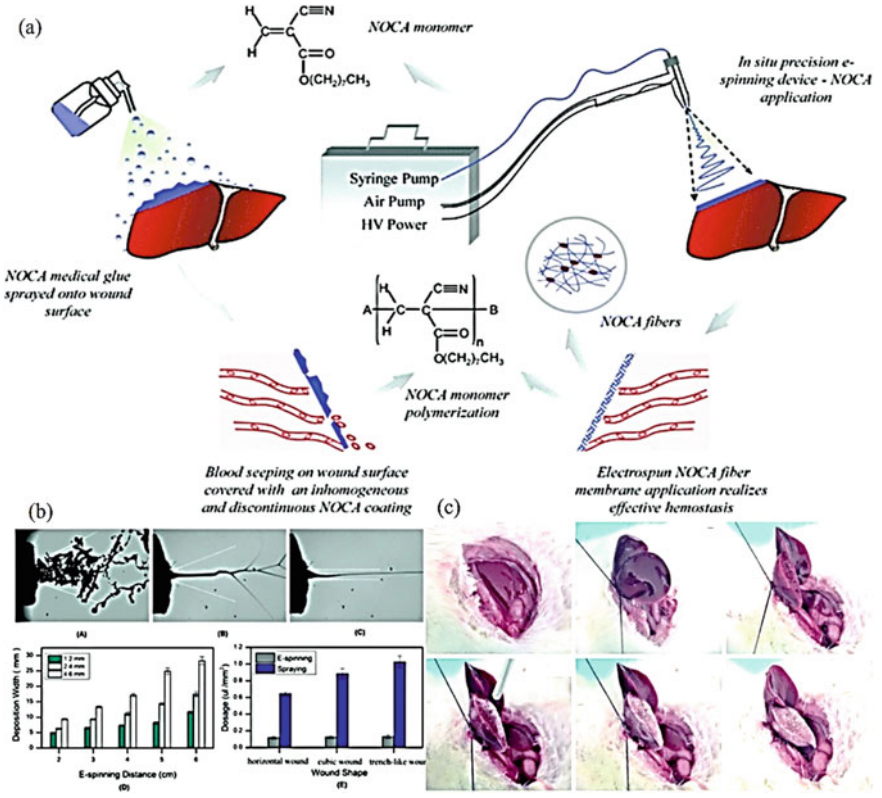


Fig. 21.5 Air flow-oriented in-situ electrospinning device for hemostasis in vitro [82]. **a** Principle of spraying method and in situ electrospinning method; **b** comparison of deposition width and unit area of NOCA prepared by different methods; **c** in-situ electrospinning hemostasis of rat liver, process included exposing the liver, fixing the liver lobe, removing the liver, and depositing NOCA

intestinal wounds in vitro experiments. They have found that nanofiber membranes effectively prevented intestinal effusions. The average diameter of nanofibers was about 0.5 μm, which could be extended by 90% without fracture. The portability and controlled deposition of the device increased the potential application of in-situ electrospinning in wound healing.

21.3.2 Battery-Driven Portable Electrospinning Devices and Its Applications

The high-voltage and heating components of the early traditional spinning devices required 220 V working voltage. Heavy size and external power supply limited its application in terms of portability and flexible extensibility. In order to overcome the

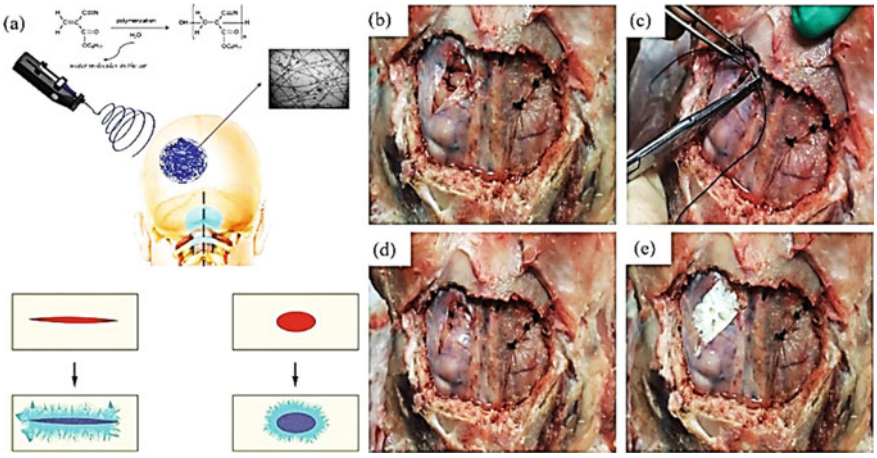


Fig. 21.6 Experimental study on endocranium repair in goat brain with in-situ electrospinning NOCA fibers [79]. **a** Experimental design; **b** a 7-cm-length defect was produced; **c** suturing to avoid rupture; **d** NOCA fibers were accurately electrospun onto the defect; **e** the defect was obviously repaired by NOCA fibrous membranes

shortcomings, the team led by Long has developed several battery-driven portable spinning devices. A brief description are as follows.

The handheld melt electrospinning device [86] was presented in Fig. 21.9a, with 450 g weight, 24 cm length, 6 cm thickness, and 13 cm height. The high voltage and the heating units, integrated into the device, were fully powered by rechargeable lithium batteries. The built-in power supply functions continuously for more than 2 h (Fig. 21.9b). Furthermore, the device was equipped with a high-efficiency thermoelectric insulation unit to solve the electrostatic interference between the heating unit and the high-voltage unit. It was convenient to carry and operate with one hand, allowing the fibers to be deposited directly on the other hand (Fig. 21.9c). The PCL/Fe_3O_4 magnetic nanocomposite fibers prepared by this device had a diameter of 4–17 μm. These nanofibers converted electromagnetic energy into heat energy for magnetic hyperthermia.

The hand-held battery-driven electrospinning device [87] (Chinese patent number: ZL201210229010.3), as illustrated in Fig. 21.10b, included a syringe that was pressed by a finger. It used two alkaline AAA batteries and a high-voltage inverter to generate a 3 V DC voltage. By the inverter, the voltage was amplified from 3 V to 10 kV. The positive pole of the inverter was connected to the needle on the syringe, while the negative electrode was attached to the conductive metal foil, presented in Fig. 21.10a. The device could work continuously for more than 15 h. The distance between the needle and the collector was 2–10 cm. Due to its good portability, Fig. 21.10c showed an example of using the hand-held device to stop bleeding in vitro. Multiple polymers, including polyvinyl pyrrolidone (PVP), polyvinylidene fluoride (PVDF), and polycaprolactone (PCL), were successfully electrospun [81]. The diameter was distributed between hundreds of nanometers.

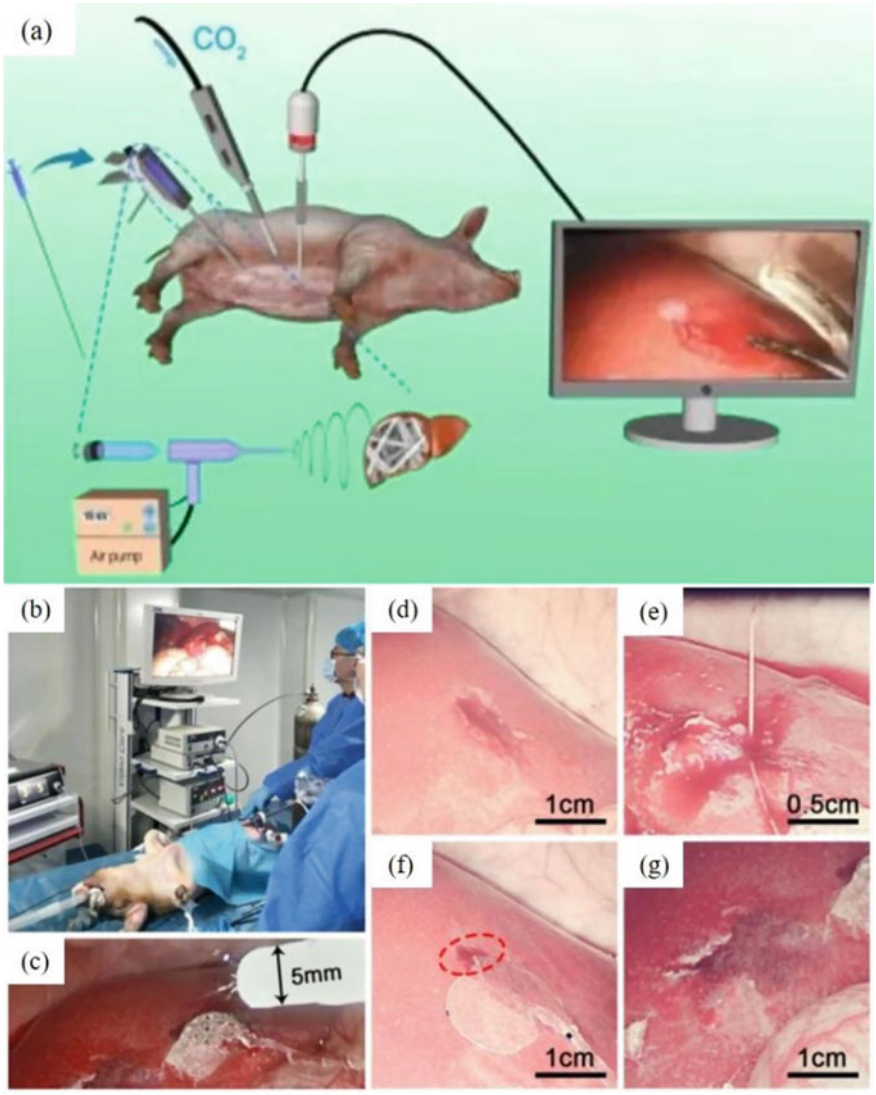


Fig. 21.7 In-situ electrospinning and animal minimally invasive hemostasis surgery [83]. **a** Schematic diagram of hemostasis in minimally invasive surgery with long needle electrospinning device combined with laparoscopy; **b** hemostasis experiment of laparoscopic minimally invasive surgery with long needle electrospinning device; **c** seen under the microscope; **d** incision on the surface of the liver; **e** suturing hemostasis; **f** applying NOCA to stop bleeding; **g** in-situ electrospinning

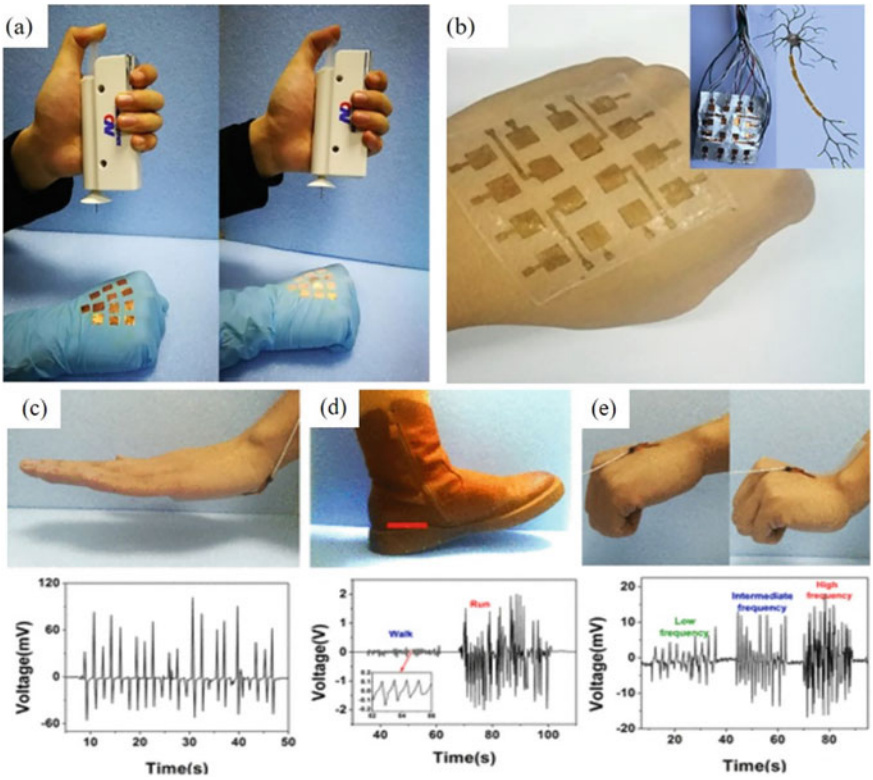


Fig. 21.8 In-situ electrospinning skin process [84]. **a** Schematic diagram; **b** electrospinning skin with gold electrode, the illustration showed its similarity with neuronal cells; **c–e** electronic skin imitated the posture of hand patting the table, foot walking and joint running, bending at different frequencies and corresponding out-put voltage

Some antibacterial and therapeutic agents could be effortlessly combined to obtain multifunctional nanofiber membranes. Dong et al. [67] electrospun modified mesoporous silica particles containing silver with PCL into nanofiber membranes (Fig. 21.11a). The results demonstrated that as the silver content increased from 3 to 8%, the diameter of the average fibers increased from 389 to 986 nm, but the fibers became much rougher. As an ideal example of 5 wt% nanofiber membrane (average fiber diameter of 658 nm), it had good antibacterial activity against *Staphylococcus aureus* and *E. coli* (Fig. 21.11d). This antibacterial nanofiber membrane reduced inflammation in Wistar rats and encouraged wound healing (Fig. 21.11b, c).

In order to achieve rapid hemostasis in internal organs, such as the liver, lung, kidney, and other organs, a metal cone was installed on the spinning nozzle to form a directional cover (Fig. 21.12a). By changing the distribution of the electrostatic field and reducing the jet emission angle, the electrospun fibers' deposition range was adjusted for better controllable and precise deposition [58, 59]. In Fig. 21.12b, c,

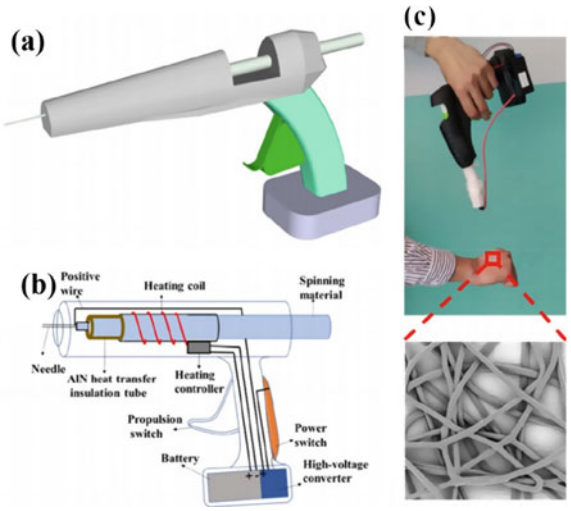


Fig. 21.9 Hand-held melt electrospinning device [86]. **a** Three-dimensional model diagram; **b** internal structure; **c** melt electrospinning

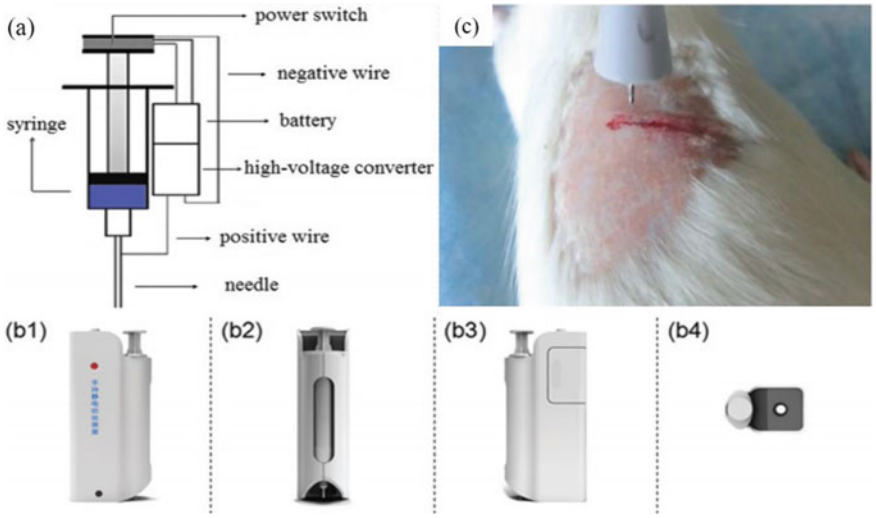


Fig. 21.10 Hand-held battery-driven electrospinning device [87]. **a** Schematic diagram of internal structure; **b1**–**b4** appearance in different directions; **c** wound hemostasis experiment

the electric field could be gathered by adjusting the electrospinning distance and the side length of the metal cone. In addition, the traditional air-assisted electrospinning required an additional air pump power supply. However, the metal cone got rid of this problem, which improved portability. The voltage in this device was fully qualified.

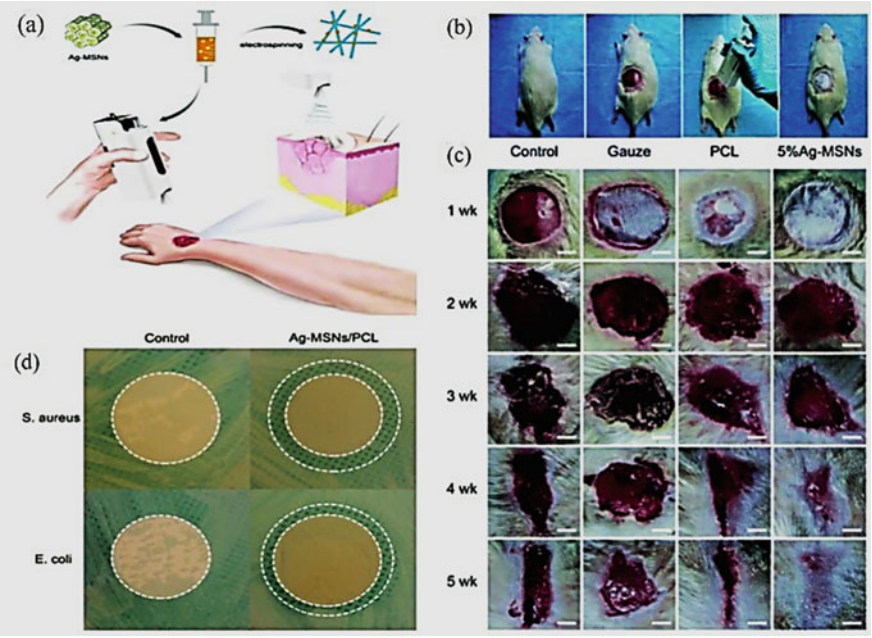


Fig. 21.11 Preparation of antibacterial dressing by portable device [67]. **a** Diagram; **b** display of skin injury models and treatment process in Wistar rats; **c** at 1, 2, 3, 4 and 5 weeks after injury, the skin wounds were treated with gauze, PCL and Ag/PCL respectively, and the untreated wounds were as the control group; **d** antibacterial activity, in which the top is *Staphylococcus aureus* and the bottom is *Escherichia coli*

Therefore, the primary constraints were the physical properties and dimensions of the in-situ dressing. The transportation of the spinning solution depended on the pressure exerted by the finger on the trigger, which would produce inconsistent fiber deposition during usage.

21.3.3 Generator-Driven Portable Electrospinning Device and Its Application

The traditional electrospinning devices could not operate without a power source, and the battery life of the hand-held electrospinning devices remained to be upgraded. For this purpose, Han et al. [69] designed a self-powered electrospinning device based on a manual Wimshurst generator. As showed in Fig. 21.13a, the high-voltage unit was replaced by the Wimshurst generator. The two discs rotated in the opposite direction by turning the handle. The positive and negative charges generated by electrostatic induction were stored respectively in two Leyden jars. As the handle

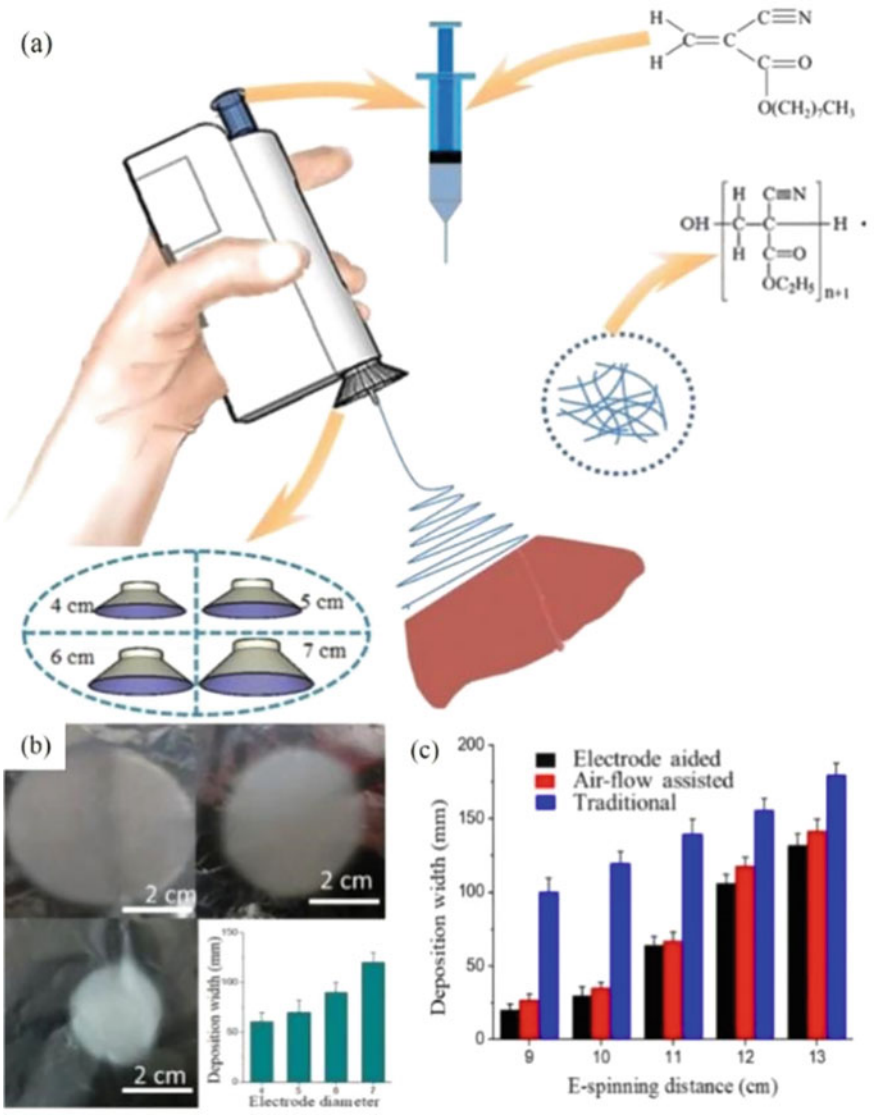


Fig. 21.12 Directional metal cone assisted electrospinning deposition [58, 59]. **a** Directional of different sizes; **b** numerical relationship between deposition area and orientation cone diameter; **c** numerical relationship between deposition area and electrospinning distance

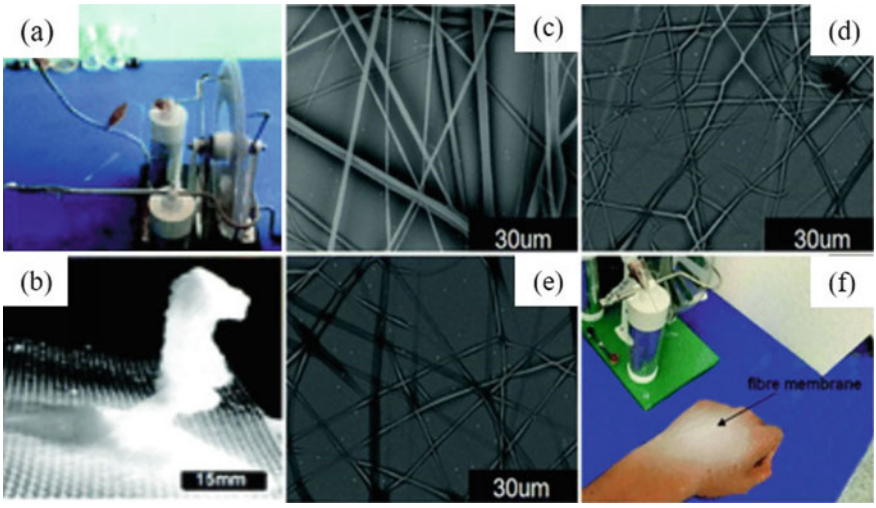


Fig. 21.13 Self-powered device based on manual Wimshurst generator [69]. **a** Device; **b** three-dimensional structure of PS fibers; **c** SEM image of PVDF fibers; **d** SEM image of PCL fibers; **e** SEM image of PLA fibers; **f** PLA fibers were electrospun onto the skin

rotated continuously, an electrical charge accumulated. The high voltage was then induced between the needle and the collector.

Furthermore, polymers such as polystyrene (PS), polyvinylidene fluoride (PVDF), polycaprolactone (PCL), and polylactic acid (PLA) were successfully made into ultra-thin fibers by the device (Fig. 21.13c–e). The electrospinning distance was controllable at 10–30 cm. Within 2 min, a three-dimensional stacking structure of PS fibers with several centimeters height began to come into shape (Fig. 21.13b). Moreover, PLA fibers could be rapidly in-situ electrospun onto the skin in the form of a thin film (Fig. 21.13f), which preliminarily suggested that this device had potential in the area of medical cosmetology.

Qin et al. [88] designed a self-powered melt electrospinning device based on a Wimshurst generator (Fig. 21.14a, b), replacing the conical nozzle and adding a heating gun with a temperature controller. The device successfully produced PLA and PCL ultrafine fibers, with 15–45 μm diameter. These ultrafine fibers were directly melted and electrospun onto a pig liver (Fig. 21.14c, d). The effects of speed (1.5 rpm) and distance (8–10 cm) on the fibers were studied and optimized. The temperature of the deposited fibers (24–44 °C) was more similar to the body temperature. The adhesion of PCL fibers reached 1.2 N, suggesting that the device and the melted electrospun ultrafine polymer fibers were better suited for wound healing dressings.

Along with battery power and manual power generation, Yan et al. [71] introduced a portable electrospinning device driven by a solar battery and hand-cranked generators, available for outdoor use without a power plug (Fig. 21.15a). The power system included a solar battery (5 V/140 mA), a hand-held generator (5 V/200 mA), a set of rechargeable batteries, and a high-voltage converter (Fig. 21.15b). This device

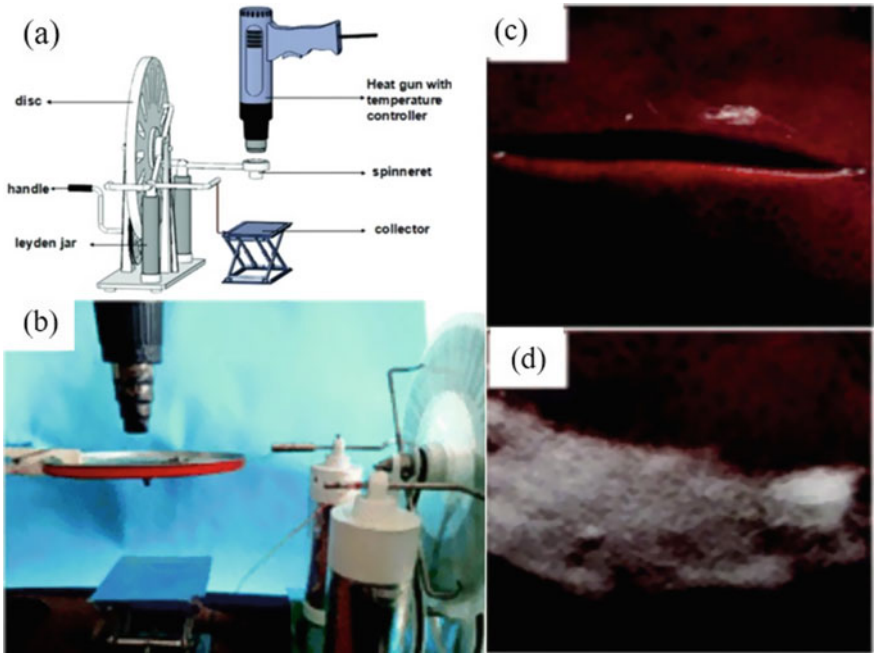


Fig. 21.14 Self-powered melt electrospinning device based on manual Wimshurst generator [88]. **a** Principle; **b** device; **c** experiment of liver wound in vitro; **d** PCL fibers were deposited on the liver and covered the wound

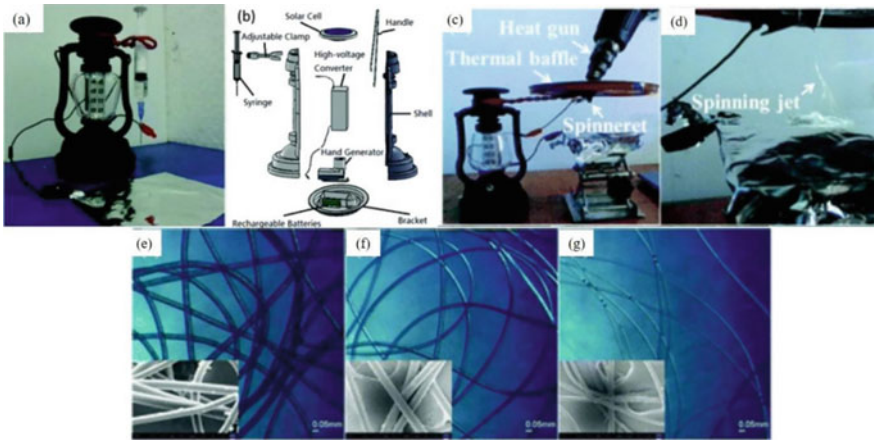


Fig. 21.15 Portable device driven by solar and hand generator [71]. **a** Device; **b** internal structure; **c** melt electrospinning experiment; **d** melt electrospinning process; **e**–**g** PCL, PLA and PLGA microfibers

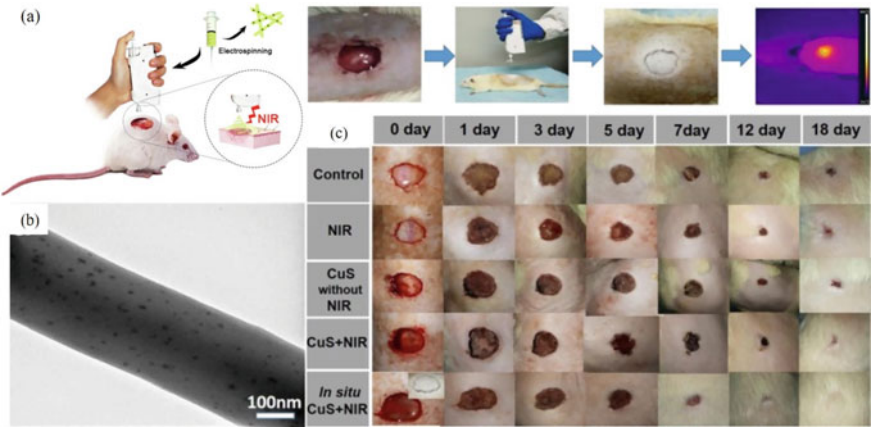


Fig. 21.16 Multifunctional nanofiber dressing [90]. **a** Simultaneous hemostasis and anti-pseudomonas aeruginosa; **b** TEM image of CuS composite nanofibers; **c** the order of experimental charts was: the bacterial infection model of Pseudomonas aeruginosa, in-situ electrospinning, rapid hemostasis, infrared thermal imaging, and the recovery of bacterial infection wounds treated by different methods

could be placed under the sun to generate electricity through solar cells and charged the battery by turning the handle of the generator. Both of these methods could supply continuous power for the solution or molten electrospinning. Figure 21.15c, d showed that the spinneret and syringe were changed into a conical metal nozzle. A heat gun could melt polymer particles. Different materials, including PCL, PLA, and poly lactic-co-glycolic acid (PLGA), were melted and electrospun into ultrafine fibers by this device, seen in Fig. 21.16e–g.

21.4 Functional Materials of Nanofibers

Many portable electrospinning devices have been used for in-vitro hemostasis experiments, providing opportunities to apply antibacterial dressings on the wound. Functional materials of nanofibers prepared by portable electrospinning equipment are essential to the development of wound dressings. The ideal functional dressings should have rapid hemostasis, good antibacterial and biocompatibility, strong adhesion, and air permeability. Meanwhile, nanofibers also contain some antibacterial agents, for example, traditional Chinese medicine preparations, metals, non-metals, and medical glues. Table 21.2 briefly summarizes the spinning materials mentioned above for wound dressings.

At present, functional dressings are moving towards simple, easy-to-use, and multi-functional rapid hemostasis. Liu et al. [90] used a portable electrospinning device (Fig. 21.16a, b) to synthesize CuS composite nanofibers, and they achieved rapid hemostasis and sterilization outdoors. The hemostasis time of nanofibers was

Table 21.2 Functional materials of electrospun nanofibers in medicine (wound dressings)

Polymer	Solvent	Antibacterial material	Diameter	References
PVP	Ethanol	Isatis root	0.72–1.71 μm	[56]
PMMA	–	NOCA	–	[58, 59, 62, 79, 82]
PCL	Acetone	Ag	389–986 nm	[67]
PS	Tetrahydrofuran	–	1.589–1.317 μm	[69]
PVDF	*N*,*N*-dimethylformamide	–	–	[69]
PCL PLA	Acetone	–	–	[69]
PVP	Ethanol	–	379 ± 120 nm	[71]
PCL	Acetone	–	1130 ± 295 nm	[71]
PS	Tetrahydrofuran	–	2266 ± 517 nm	[71]
PLA	Trichloromethane	–	845 ± 188 nm	[71]
PLGA	Trichloromethane	–	437 ± 100 nm	[71]
PVDF	*N*,*N*-dimethylformamide: ethanol (1:1)	–	2153 ± 172 nm	[71]
PVP PVB PCL	–	NOCA	5–34 μm	[83]
PCL	Acetone	–	200–400 nm	[85]
PCL	Acetone	Fe_3O_4	4–17 μm	[86]
PVDF	*N*,*N*-dimethylformamide: acetone (1:1)	–	170 nm	[87]
PCL PLA	–	–	PCL: 15.71–47.42 μm PLA: 21.36–44.97 μm	[88]
PVP PVB	Ethanol	Iodine	849–1485 nm	[89]
PVP	Acetic acid	CuS	400 nm	[90]
PCL PVP	Acetone	Lanthanide doped upconversion nanoparticles	400 nm	[91]

less than 6 s, and Pseudomonas aeruginosa infection also decreased during wound healing (Fig. 21.16c). Additionally, photodynamic nanofibers with core–shell structure were obtained by in-situ deposition [91], which effectively killed Methicillin-resistant *Staphylococcus aureus*, delivered reactive oxygen species to the wound, and enhanced the photodynamic effect. It could meanwhile integrate with hemostatic agents for application as an antibacterial dressing.

21.5 Conclusions and Prospects

From the perspective of biomedicine, electrospun nano dressings are the most promising materials. Their morphology and dimensions are similar to the extracellular matrix structure. With high porosity, they promote cellular respiration. Flexibility stimulated three-dimensional reorganization and regeneration of the skin. They could also be served as an effective carrier of antibiotics, growth factors, and vitamins. In particular, the dressings do not need to be changed frequently. Therefore, they avoid causing pain and fear, making them more prevalent among patients. In the past few years, portable electrospinning devices powered by batteries or generators have made significant progress, in which their performance and portability have been systematically improved. In the future, research can be considered from the following aspects: (1) Developing electrospinning devices that require uncomplicated using conditions under external environment, inexpensive, and enable accurate deposition of hemostatic drugs on the wound surface. (2) To assess the suitability of various functional materials for handheld electrospinning devices that are deposited directly at the wound site, both on the body surface and in the body cavity. They can avoid tissue adhesion and allow long-term, cyclical use as delivery carriers of antibiotics and growth factors. (3) The preclinical evaluation in vivo/vitro experiments of multi-center and large samples will provide a factual basis for the extensive application of individual cosmetic and wound dressings.

Acknowledgements This work was supported by the National Natural Science Foundation of China (51973100 and 11904193), the National Key Research Development Project (2019YFC0121402), and State Key Laboratory of Bio-Fibers and Eco-Textiles, Qingdao University (RZ2000003334 and ZDKT202108).

References

1. Cui, J. X., Li, F. H., Wang, Y. L., et al. (2020). Electrospun nanofiber membranes for wastewater treatment applications. *Separation and Purification Technology, 250*, 16.
2. Wang, M. L., Wang, K., Yang, Y. Y., et al. (2020). Electrospun environment remediation nanofibers using unspinnable liquids as the sheath fluids: a review. *Polymers, 12*(1), 13.
3. Ghosal, K., Agatemor, C., Spitalsky, Z., et al. (2019). Electrospinning tissue engineering and wound dressing scaffolds from polymer-titanium dioxide nanocomposites. *Chemical Engineering Journal, 358*, 1262–1278.
4. Abrigo, M., McArthur, S. L., & Kingshott, P. (2014). Electrospun nanofibers as dressings for chronic wound care: Advances, challenges, and future prospects. *Macromolecular Bioscience, 14*(6), 772–792.
5. Kim, F. S., Ren, G. Q., & Jenekhe, S. A. (2011). One-dimensional nanostructures of pi-conjugated molecular systems: Assembly, properties, and applications from photovoltaics, sensors, and nanophotonics to nanoelectronics. *Chemistry of Materials, 23*(3), 682–732.
6. Xue, J. J., Wu, T., Dai, Y. Q., et al. (2019). Electrospinning and electrospun nanofibers: Methods, materials, and applications. *Chemical Reviews, 119*(8), 5298–5415.

7. Zahedi, P., Rezaeian, I., Ranaei-Siadat, S. O., et al. (2010). A review on wound dressings with an emphasis on electrospun nanofibrous polymeric bandages. *Polymers for Advanced Technologies, 21*(2), 77–95.
8. Pereira, R. F., Barrias, C. C., Granja, P. L., et al. (2013). Advanced biofabrication strategies for skin regeneration and repair. *Nanomedicine, 8*(4), 603–621.
9. Liu, Y., Gao, X., Wang, Z. P., et al. (2021). Controlled synthesis of bismuth oxychloride-carbon nanofiber hybrid materials as highly efficient electrodes for rocking-chair capacitive deionization. *Chemical Engineering Journal, 403*, 11.
10. Graca, M. F. P., Miguel, S. P., Cabral, C. S. D., et al. (2020). Hyaluronic acid-based wound dressings: A review. *Carbohydrate Polymers, 241*, 17.
11. Topuz, F., & Uyar, T. (2019). Electrospinning of cyclodextrin functional nanofibers for drug delivery applications. *Pharmaceutics, 11*(1), 35.
12. Dias, J. R., Granja, P. L., & Bartolo, P. J. (2016). Advances in electrospun skin substitutes. *Progress in Materials Science, 84*, 314–334.
13. Mele, E. (2016). Electrospinning of natural polymers for advanced wound care: Towards responsive and adaptive dressings. *Journal of Materials Chemistry B, 4*(28), 4801–4812.
14. Chen, S. X., Liu, B., Carlson, M. A., et al. (2017). Recent advances in electrospun nanofibers for wound healing. *Nanomedicine, 12*(11), 1335–1352.
15. Gao, F. F., Jiang, M. L., Liang, W. C., et al. (2020). Co-electrospun cellulose diacetate-graft-poly(ethylene terephthalate) and collagen composite nanofibrous mats for cells culture. *Journal of Applied Polymer Science, 137*(44), 11.
16. Levitt, A., Seyedin, S., Zhang, J. Z., et al. (2020). Bath electrospinning of continuous and scalable multifunctional MXene-infiltrated nanoyarns. *Small (Weinheim an der Bergstrasse, Germany), 16*(26), 12.
17. Yalcinkaya, F., & Komarek, M. (2019). Polyvinyl butyral (pvb) nanofiber/nanoparticle-covered yarns for antibacterial textile surfaces. *International Journal of Molecular Sciences, 20*(17), 11.
18. Levitt, A. S., Vallett, R., Dion, G., et al. (2018). Effect of electrospinning processing variables on polyacrylonitrile nanoyarns. *Journal of Applied Polymer Science, 135*(25), 9.
19. O'Connor, R. A., & McGuinness, G. B. (2016). Electrospun nanofibre bundles and yarns for tissue engineering applications: A review. *Proceedings of the Institution of Mechanical Engineers Part H-Journal of Engineering in Medicine, 230*(11), 987–998.
20. Wu, J. L., Huang, C., Liu, W., et al. (2014). Cell infiltration and vascularization in porous nanoyarn scaffolds prepared by dynamic liquid electrospinning. *Journal of Biomedical Nanotechnology, 10*(4), 603–614.
21. Bhardwaj, N., & Kundu, S. C. (2010). Electrospinning: A fascinating fiber fabrication technique. *Biotechnology Advances, 28*(3), 325–347.
22. Sun, B., Long, Y. Z., Zhang, H. D., et al. (2014). Advances in three-dimensional nanofibrous macrostructures via electrospinning. *Progress in Polymer Science, 39*(5), 862–890.
23. Yu, M., Dong, R. H., Yan, X., et al. (2017). Recent advances in needleless electrospinning of ultrathin fibers: From academia to industrial production. *Macromolecular Materials and Engineering, 302*(7), 19.
24. Han, T., Reneker, D. H., & Yarin, A. L. (2007). Buckling of jets in electrospinning. *Polymer, 48*(20), 6064–6076.
25. Angammana, C. J., & Jayaram, S. H. (2016). Fundamentals of electrospinning and processing technologies. *Particulate Science and Technology, 34*(1), 72–82.
26. Buchko, C. J., Chen, L. C., Shen, Y., et al. (1999). Processing and microstructural characterization of porous biocompatible protein polymer thin films. *Polymer, 40*(26), 7397–7407.
27. Yang, G., Li, X. L., He, Y., et al. (2018). From nano to micro to macro: Electrospun hierarchically structured polymeric fibers for biomedical applications. *Progress in Polymer Science, 81*, 80–113.
28. Reneker, D. H., & Yarin, A. L. (2008). Electrospinning jets and polymer nanofibers. *Polymer, 49*(10), 2387–2425.

29. Xin, Y., & Reneker, D. H. (2012). Garland formation process in electrospinning. *Polymer, 53*(16), 3629–3635.
30. Sun, B., Long, Y. Z., Chen, Z. J., et al. (2014). Recent advances in flexible and stretchable electronic devices via electrospinning. *Journal of Materials Chemistry C, 2*(7), 1209–1219.
31. Huang, Z. M., Zhang, Y. Z., Kotaki, M., et al. (2003). A review on polymer nanofibers by electrospinning and their applications in nanocomposites. *Composites Science and Technology, 63*(15), 2223–2253.
32. Li, D., McCann, J. T., & Xia, Y. N. (2005). Use of electrospinning to directly fabricate hollow nanofibers with functionalized inner and outer surfaces. *Small (Weinheim an der Bergstrasse, Germany), 1*(1), 83–86.
33. Han, D., & Steckl, A. J. (2013). Triaxial electrospun nanofiber membranes for controlled dual release of functional molecules. *ACS Applied Materials & Interfaces, 5*(16), 8241–8245.
34. Wang, N., Chen, H. Y., Lin, L., et al. (2010). Multicomponent phase change microfibers prepared by temperature control multifluidic electrospinning. *Macromolecular Rapid Communications, 31*(18), 1622–1627.
35. Alamein, M. A., Liu, Q., Stephens, S., et al. (2013). Nanospiderwebs: Artificial 3d extracellular matrix from nanofibers by novel clinical grade electrospinning for stem cell delivery. *Advanced Healthcare Materials, 2*(5), 702–717.
36. Yang, R. R., He, J. H., Xu, L., et al. (2009). Bubble-electrospinning for fabricating nanofibers. *Polymer, 50*(24), 5846–5850.
37. Niu, H. T., Lin, T., & Wang, X. G. (2009). Needleless electrospinning. I. A comparison of cylinder and disk nozzles. *Journal of Applied Polymer Science, 114*(6), 3524–3530.
38. Wang, X., Niu, H. T., Wang, X. G., et al. (2012). Needleless electrospinning of uniform nanofibers using spiral coil spinnerets. *Journal of Nanomaterials, 2012*, 9.
39. Hejazi, F., Mirzadeh, H., Contessi, N., et al. (2017). Novel class of collector in electrospinning device for the fabrication of 3d nanofibrous structure for large defect load-bearing tissue engineering application. *Journal of Biomedical Materials Research Part A, 105*(5), 1535–1548.
40. Li, D., Wang, Y. L., & Xia, Y. N. (2004). Electrospinning nanofibers as uniaxially aligned arrays and layer-by-layer stacked films. *Advanced Materials, 16*(4), 361–366.
41. Dalton, P. D., Klee, D., & Moller, M. (2005). Electrospinning with dual collection rings. *Polymer, 46*(3), 611–614.
42. Katta, P., Alessandro, M., Ramsier, R. D., et al. (2004). Continuous electrospinning of aligned polymer nanofibers onto a wire drum collector. *Nano Letters, 4*(11), 2215–2218.
43. Zussman, E., Theron, A., & Yarin, A. L. (2003). Formation of nanofiber crossbars in electrospinning. *Applied Physics Letters, 82*(6), 973–975.
44. Beachley, V., Katsanevakis, E., Zhang, N., et al. (2013). A novel method to precisely assemble loose nanofiber structures for regenerative medicine applications. *Advanced Healthcare Materials, 2*(2), 343–351.
45. Smit, E., Buttner, U., & Sanderson, R. D. (2005). Continuous yarns from electrospun fibers. *Polymer, 46*(8), 2419–2423.
46. Teo, W. E., Gopal, R., Ramaseshan, R., et al. (2007). A dynamic liquid support system for continuous electrospun yarn fabrication. *Polymer, 48*(12), 3400–3405.
47. Bisht, G. S., Canton, G., Mirsepassi, A., et al. (2011). Controlled continuous patterning of polymeric nanofibers on three-dimensional substrates using low-voltage near-field electrospinning. *Nano Letters, 11*(4), 1831–1837.
48. Zhang, X., Gao, X. H., Jiang, L., et al. (2012). Flexible generation of gradient electrospinning nanofibers using a microfluidic assisted approach. *Langmuir, 28*(26), 10026–10032.
49. Park, S. H., Kim, T. G., Kim, H. C., et al. (2008). Development of dual scale scaffolds via direct polymer melt deposition and electrospinning for applications in tissue regeneration. *Acta Biomaterialia, 4*(5), 1198–1207.
50. Zhang, D. M., & Chang, J. (2007). Patterning of electrospun fibers using electroconductive templates. *Advanced Materials, 19*(21), 3664.
51. Xu, H., Li, H. Y., & Chang, J. (2013). Controlled drug release from a polymer matrix by patterned electrospun nanofibers with controllable hydrophobicity. *Journal of Materials Chemistry B, 1*(33), 4182–4188.

52. Yu, G. F., Yan, X., Yu, M., et al. (2016). Patterned, highly stretchable and conductive nanofibrous PANI/PVDF strain sensors based on electrospinning and in situ polymerization. *Nanoscale, 8*(5), 2944–2950.
53. Kameoka, J., Orth, R., Yang, Y. N., et al. (2003). A scanning tip electrospinning source for deposition of oriented nanofibres. *Nanotechnology, 14*(10), 1124–1129.
54. King, W. E., & Bowlin, G. L. (2021). Near-field electrospinning and melt electrowriting of biomedical polymers-progress and limitations. *Polymers, 13*(7), 23.
55. Liu, S. L., Long, Y. Z., Zhang, Z. H., et al. (2013). Assembly of oriented ultrafine polymer fibers by centrifugal electrospinning. *Journal of Nanomaterials, 2013*, 9.
56. Dong, W. H., Liu, J. X., Mou, X. J., et al. (2020). Performance of polyvinyl pyrrolidone-isatis root antibacterial wound dressings produced in situ by handheld electrospinner. *Colloids and Surfaces B-Biointerfaces, 188*, 6.
57. Zhao, Y. T., Zhang, J., Gao, Y., et al. (2020). Self-powered portable melt electrospinning for in situ wound dressing. *Journal of Nanobiotechnology, 18*(1), 10.
58. Luo, W. L., Qiu, X., Zhang, J., et al. (2019). In situ accurate deposition of electrospun medical glue fibers on kidney with auxiliary electrode method for fast hemostasis. *Materials Science & Engineering C-Materials for Biological Applications, 101*, 380–386.
59. Luo, W. L., Zhang, J., Qiu, X., et al. (2018). Electric- field-modified in situ precise deposition of electrospun medical glue fibers on the liver for rapid hemostasis. *Nanoscale Research Letters, 13*, 8.
60. Sofokleous, P., Stride, E., Bonfield, W., et al. (2013). Design, construction and performance of a portable handheld electrohydrodynamic multi-needle spray gun for biomedical applications. *Materials Science & Engineering C-Materials for Biological Applications, 33*(1), 213–223.
61. Lau, W. K., Sofokleous, P., Day, R., et al. (2014). A portable device for in situ deposition of bioproducts. *Bioinspired Biomimetic and Nanobiomaterials, 3*(2), 94–105.
62. Jiang, K., Long, Y. Z., Chen, Z. J., et al. (2014). Airflow-directed in situ electrospinning of a medical glue of cyanoacrylate for rapid hemostasis in liver resection. *Nanoscale, 6*(14), 7792–7798.
63. Song, C., Wang, X. X., Zhang, J., et al. (2018). Electric field-assisted in situ precise deposition of electrospun gamma-Fe_2O_3/polyurethane nanofibers for magnetic hyperthermia. *Nanoscale Research Letters, 13*, 11.
64. Brako, F., Luo, C. J., Craig, D. Q. M., et al. (2018). An inexpensive, portable device for point-of-need generation of silver-nanoparticle doped cellulose acetate nanofibers for advanced wound dressing. *Macromolecular Materials and Engineering, 303*(5), 6.
65. Yue, Y. P., Gong, X. B., Jiao, W. L., et al. (2021). In-situ electrospinning of thymol-loaded polyurethane fibrous membranes for waterproof, breathable, and antibacterial wound dressing application. *Journal of Colloid and Interface Science, 592*, 310–318.
66. Haik, J., Kornhaber, R., Blal, B., et al. (2017). The feasibility of a handheld electrospinning device for the application of nanofibrous wound dressings. *Advances in Wound Care, 6*(5), 166–174.
67. Dong, R. H., Jia, Y. X., Qin, C. C., et al. (2016). In situ deposition of a personalized nanofibrous dressing via a handy electrospinning device for skin wound care. *Nanoscale, 8*(6), 3482–3488.
68. Chui, C. Y., Mouthuy, P. A., & Ye, H. (2018). Direct electrospinning of poly(vinyl butyral) onto human dermal fibroblasts using a portable device. *Biotechnology Letters, 40*(4), 737–744.
69. Han, W. P., Huang, Y. Y., Yu, M., et al. (2015). Self-powered electrospinning apparatus based on a hand-operated Wimshurst generator. *Nanoscale, 7*(13), 5603–5606.
70. Li, C. J., Yin, Y. Y., Wang, B., et al. (2017). Self-powered electrospinning system driven by a triboelectric nanogenerator. *ACS Nano, 11*(10), 10439–10445.
71. Yan, X., Yu, M., Zhang, L. H., et al. (2016). A portable electrospinning apparatus based on a small solar cell and a hand generator: Design, performance and application. *Nanoscale, 8*(1), 209–213.
72. Yan, X., Duan, X. P., Yu, S. X., et al. (2017). Portable melt electrospinning apparatus without an extra electricity supply. *RSC Advances, 7*(53), 33132–33136.

73. Duan, X. P., Yan, X., Zhang, B., et al. (2016). Simple piezoelectric ceramic generator-based electrospinning apparatus. *RSC Advances, 6*(70), 66252–66255.
74. Mouthuy, P. A., Groszkowski, L., & Ye, H. (2015). Performances of a portable electrospinning apparatus. *Biotechnology Letters, 37*(5), 1107–1116.
75. Azimi, B., Maleki, H., Zavagna, L., et al. (2020). Bio-based electrospun fibers for wound healing. *Journal of Functional Biomaterials, 11*(3), 36.
76. Mogosanu, G. D., & Grumezescu, A. M. (2014). Natural and synthetic polymers for wounds and burns dressing. *International Journal of Pharmaceutics, 463*(2), 127–136.
77. Gao, Y., Xiang, H. F., Wang, X. X., et al. (2020). A portable solution blow spinning device for minimally invasive surgery hemostasis. *Chemical Engineering Journal, 387*, 7.
78. Li, D. J., Nie, W., Chen, L., et al. (2017). Fabrication of curcumin-loaded mesoporous silica incorporated polyvinyl pyrrolidone nanofibers for rapid hemostasis and antibacterial treatment. *RSC Advances, 7*(13), 7973–7982.
79. Lv, F. Y., Dong, R. H., Li, Z. J., et al. (2016). In situ precise electrospinning of medical glue fibers as nonsuture dural repair with high sealing capability and flexibility. *International Journal of Nanomedicine, 11*, 4213–4220.
80. Guo, B. L., & Ma, P. X. (2018). Conducting polymers for tissue engineering. *Biomacromolecules, 19*(6), 1764–1782.
81. Yan, X., Yu, M., Ramakrishna, S., et al. (2019). Advances in portable electrospinning devices for in situ delivery of personalized wound care. *Nanoscale, 11*(41), 19166–19178.
82. Dong, R. H., Qin, C. C., Qiu, X., et al. (2015). In situ precision electrospinning as an effective delivery technique for cyanoacrylate medical glue with high efficiency and low toxicity. *Nanoscale, 7*(46), 19468–19475.
83. Zhang, J., Zhao, Y. T., Hu, P. Y., et al. (2020). Laparoscopic electrospinning for in situ hemostasis in minimally invasive operation. *Chemical Engineering Journal, 395*, 7.
84. Wang, X. X., Song, W. Z., You, M. H., et al. (2018). Bionic single-electrode electronic skin unit based on piezoelectric nanogenerator. *ACS Nano, 12*(8), 8588–8596.
85. Zhou, T. T., Wang, Y. Z., Lei, F. C., et al. (2020). In-situ electrospinning for intestinal hemostasis. *International Journal of Nanomedicine, 15*, 3869–3875.
86. Hu, P. Y., Zhao, Y. T., Zhang, J., et al. (2020). In situ melt electrospun polycaprolactone/Fe_3O_4 nanofibers for magnetic hyperthermia. *Materials Science & Engineering C-Materials for Biological Applications, 110*, 8.
87. Xu, S. C., Qin, C. C., Yu, M., et al. (2015). A battery-operated portable handheld electrospinning apparatus. *Nanoscale, 7*(29), 12351–12355.
88. Qin, C. C., Duan, X. P., Wang, L., et al. (2015). Melt electrospinning of poly(lactic acid) and polycaprolactone microfibers by using a hand-operated Wimshurst generator. *Nanoscale, 7*(40), 16611–16615.
89. Liu, G. S., Yan, X., Yan, F. F., et al. (2018). In situ electrospinning iodine-based fibrous meshes for antibacterial wound dressing. *Nanoscale Research Letters, 13*, 7.
90. Liu, X. F., Zhang, J., Liu, J. J., et al. (2020). Bifunctional CuS composite nanofibers via in situ electrospinning for outdoor rapid hemostasis and simultaneous ablating superbug. *Chemical Engineering Journal, 401*, 12.
91. Liu, C. L., Yang, J., Bai, X. H., et al. (2021). Dual antibacterial effect of in situ electrospun curcumin composite nanofibers to sterilize drug-resistant bacteria. *Nanoscale Research Letters, 16*(1), 8.



Yun-Ze Long received his B.S. degree in physics from the University of Science and Technology of China in 2000 and Ph.D. degree from the Institute of Physics, Chinese Academy of Sciences in 2005. He then worked in the Institut des Materiaux Jean Rouxel, CNRS, France, as a postdoctoral fellow. He has been with the Qingdao University since Dec. 2006, where he is currently a full Professor. From 2009 to 2011, he worked as a visiting researcher at the University of Sydney and the Hong Kong University of Science and Technology. His research interests focus on electrospinning, functional nanomaterials and their applications. He has published more than 360 papers and 12 book chapters and holds 88 Chinese patents and 6 Australian patents. He was awarded the Fellow of International Association of Advanced Materials, National Model Teacher, New Century Excellent Talent of Ministry of Education of China, Taishan Scholar and Young Expert with Outstanding Contributions of Shandong province of China.



Jun Zhang received the B.S. degree in physics from Qingdao University, China, in 2010 and the M.S. and Ph.D. degrees in physics from Nankai University, China, in 2016. From 2016 to 2019, he was a postdoctoral researcher with College of Materials Science and Engineering in Qingdao University, China. Since 2019, he has been an associate professor with the College of Physics, Qingdao University, China. He is the co-author of two books, and more than 80 articles, and holds 7 Chinese patents and 6 Australian patents. His research interests include electrospinning to prepare polymer, inorganic and composite nanofibers, antibiosis and medical dressing, fluorescence nanofiber processes and sensor applications.



Zhong Liu received his B.S. degree from Shandong University of Traditional Chinese Medicine, China, in 2008 and the M.S. and Ph.D. degrees from Zhejiang Chinese Medical University, China, in 2011 and 2019, respectively. From April 2012 to August 2016, he worked as an orthopedic doctor in the Shengli Hospital of Sinopec Shengli Petroleum Administration in Shandong province. He has been with the Qingdao University since May 2020, where he is currently a postdoctoral researcher. He is the co-author of 7 articles. He was awarded the Second Prize of Zhejiang Province Science and Technology Award. His research interests focus on electrospinning, functional nanofibers and their medical applications.



Bing-Chang Wang received a B.S. degree in materials engineering and an M.S. degree in the transformation of materials from the University of Technology of Troyes, Aube, France in 2022. From 2020 to 2021, he was a Research Assistant with the Marine Chemical Researche Institute. Since 2021, he has been a Researcher with the Collaborative Innovation Center for Nanomaterials and Devices, Qingdao University. His research interests include the development of medical dressings using electrospinning technology, fundamental study of nanoelectrocatalyst and fabrication of peelable coating.



Miao Yu graduated from Nanjing University with a B.S. degree in Physics in 2010. He got his master's degree from Hong Kong University of Science and Technology, and Ph.D. degree in materials engineering from Columbia University. He co-authored one book chapter and more than 50 articles and holds 28 Chinese patents and 4 Australian patents. He was awarded the leader in Taishan industry in Shandong province (Taishan scholars from overseas experts in Shandong province) and the Second Prize of Shandong Province Science and Technology Award. His research interests focus on electrospinning, functional nanomaterials, their applications and industrialization.



Seeram Ramakrishna received the Ph.D. degree from the University of Cambridge (UK) in 1992, and the GMP training from Harvard University (USA) in 2001. From 1993 to 1996, he worked in the Kyoto Institute of Technology, Japan, as a visiting lecturer. He has been with the National University of Singapore since 1996, where he is currently a full Professor of materials engineering. From 1998 to 1999, he worked in MIT and Johns Hopkins University (USA) as a visiting scientist. He co-authored ten books, fifty book chapters, and more than 2000 articles with over 132,000 citations. His H-index is over 166. He is regarded as the guru of electrospinning and nanofibers. Google scholar ranked him among the top 36 salient authors out of three million materials researchers worldwide. He is named among the World's Most Influential Minds (Thomson Reuters), and the top 1% highly cited researchers in materials science and cross-field categories (Clarivate Analytics). He is a fellow of UK Royal Academy of Engineering, Academy of Engineering, Singapore, Indian National Academy of Engineering and ASEAN Academy of Engineering and Technology, and the Honorary Everest Chair of MBUST, Nepal.

Chapter 22
Hierarchical Integration of 3D Printing and Electrospinning of Nanofibers for Rapid Prototyping



Ashok Vaseashta, Didem Demir, Burcu Sakım, Müge Aşık, and Nimet Bölgen

Abstract Electrospinning is an effective and versatile technique used to produce porous structures ranging from submicron to nanometer diameters. Using a variety of high-performance polymers and blends, several porous structure configurations have become possible for applications in tactile sensing, energy harvesting, filtration, and biomedical applications, however, the structures lack mechanical complexity, conformity, and desired three-dimensional single/multi-material constructs necessary to mimic desired structures. A simple, yet versatile, strategy is through employing digitally-controlled fabrication of shape-morphing by combining two promising technologies, viz., electrospinning and 3D printing/additive manufacturing. Using hierarchical integration of configurations, elaborate shapes and patterns are printed on mesostructured stimuli-responsive electrospun membranes, modulating in-plane and interlayer internal stresses induced by swelling/shrinkage mismatch, and thus guiding morphing behaviors of electrospun membranes to adapt to changes of the environment. Recent progress in 3D/4D printing/additive manufacturing processes includes materials and scaffold constructs for tactile and wearable sensors, filtration

A. Vaseashta (✉)
International Clean Water Institute, Manassas, VA, USA
e-mail: prof.vaseashta@ieee.org

Faculty of Civil Engineering, Transylvania University of Brasov, Brasov, Romania

D. Demir · B. Sakım · M. Aşık · N. Bölgen
Department of Chemical Engineering, Faculty of Engineering, Mersin University, TR-33343 Mersin, Turkey
e-mail: didemdemir@tarsus.edu.tr

B. Sakım
e-mail: 1902120171002@mersin.edu.tr

M. Aşık
e-mail: 1702120171002@mersin.edu.tr

N. Bölgen
e-mail: nimet@mersin.edu.tr

D. Demir
Department of Chemistry and Chemical Process Technologies, Vocational School of Technical Sciences at Mersin Tarsus Organized Industrial Zone, Tarsus University, 33100 Mersin, Turkey

© The Author(s), under exclusive license to Springer Nature Switzerland AG 2022

A. Vaseashta and N. Bölgen (eds.), *Electrospun Nanofibers*,
https://doi.org/10.1007/978-3-030-99958-2_22

structures, sensors for structural health monitoring, biomedical scaffolds, tissue engineering, and optical patterning, among many other applications to support the vision of synthetically prepared material systems that mimic many of the structural aspects with digital precision. A novel technology called 3D jet writing was recently reported that catapults electrospinning to adaptive technologies for the manufacturing of scaffolds according to user-defined specifications of the shape and size of both the pores and the overall geometric footprint. This chapter reviews the hierarchical synergy between electrospinning and 3D printing as part of precision micromanufacturing for rapid prototyping of structures that are likely to evolve next-generation structures into reality.

Keywords Electrospinning · 3D printing · 4D printing · Prototyping · Jet printing

22.1 Introduction

Three-dimensional (3D) printing and nanotechnology are two relatively new fields of study that have been recently been conjoined to create a highly functional and diverse nature of materials to generate complex shapes of desired structures and sizes with digital precision. 3D printing, also referred to as additive processing, is to generate three-dimensional solid objects from a digital file by laying down successive layers of material until the desired object is created. Each of these layers can be seen as a thinly sliced horizontal cross-section of the eventual object. By adjusting processing parameters, variations of lightweight, adaptable, resilient, biodegradable, and highly multifunctional materials are produced as smart structures. However, one of the bottlenecks to smart-structure promulgation is the manufacturing methods which have become increasingly complex, outpacing traditional manufacturing methods. In addition, the traditional manufacturing methods present challenges in the integrated processing of heterogeneous materials, hence, the complete structure needs to be divided into multiple components and processed individually and separately. 3D printing has emerged as a versatile method and an alternative to traditional manufacturing methods. During the 3D printing process, objects are virtually sliced into multiple layers, blocks, or sections using computer-assisted design software. The restrictions imposed by traditional manufacturing on what can be made are generally not relevant for additive manufacturing. While there are certain restrictions on the minimum size features that can be accurately printed, most of the limitations of additive processing center around how to optimally position a print to reduce support dependency and the likelihood of print failure. Additive processing methods, generally, only use the material needed to build a certain part. Most processes use raw materials that can be recycled and reused in more than one builds, thus adding to overall sustainability. This allows a large amount of design freedom and enables the creation of very complex geometries with relative ease.

To give a context of nanomaterials, such solids in nanoscale dimensions have reduced coordination number, hence, electrons have less opportunity to hop from

site to site; thus have less kinetic energy of electrons. A higher Coulomb interaction/bandwidth ratio at a site enhances electron correlation and Mott-transition leading to the appearance of magnetism. Furthermore, the system symmetries are lowered and the appearance of new boundary conditions leads to surface and interface states. A change of the quantization conditions alters the Eigenvalue spectrum and transport properties of the solid. Below a certain critical size-comparable with the double space-charge layer thickness of the semiconductors, there is a marked change in physical characteristics along with a high surface area/volume ratio. Thus, systems in reduced dimensions possess novel characteristics due to their dimensionality. Furthermore, nanomaterials have geometrical dimensions that are comparable to the smallest engineered unit, among the largest living organism molecules, and fundamental physical quantities, hence they offer unique characteristics due to enhanced surface activity, more so with target-specific functionalization. This, coupled with the recent developments in synthesis and characterization methods has offered the means to study, understand, control, or even alter the transitional characteristics between isolated atoms, molecules, and bulk materials, thus rendering additional capabilities. Reduced dimensional systems are normally characterized in either one or more smaller dimensions, such that the material begins to display quantifiable novel characteristics. The onset of deviation from bulk to reduced dimensions has resulted in many exceptional characteristics. Studies to calculate surface elastic constants using molecular dynamics (MD) simulations, the curvature effect by the Cauchy-Born rule, and electronic effects by effective nuclei-nuclei interaction density function theory (DFT) calculations provide a superior understanding of surface and interface effects. Size and surface collectively control interactions of nanoscale materials due to the existence of large boundaries and interplay of Physico-chemical interactions. The surface free energy is size-dependent and hence increases almost inversely with the decreasing feature sizes of the material. The collective response of a nanomaterial-medium system is attributable to reduced dimensions and is vital to its response model.

Electrospinning is a versatile, efficient, inexpensive, and reproducible technique that can be used to produce 1D fibrous materials or composites with a wide range of diameters (from nm to mm), simply by applying an electrostatic field to a solution. With the recent advances in nanotechnology, new multifunctional materials are produced by combining nanomaterials with electrospun nanofibers. There are several investigations that show that such nanofibers demonstrate sensitivity to chemical and biological agents and hence nanofibrous structures fabricated using electrospinning are excellent candidates for the fabrication of e-textiles, tactile membranes, and protective clothing due to their adsorptive, lightweight, and functionalization properties [1]. By choosing certain combinations of high-performance polymers and nanomaterials, the newly developed composite materials have functional properties, such as flame resistance [2], gas sensing [3], self-detoxifying [4], UV protection [5], self-cleaning [6], and antimicrobial ability [7]. We describe later in this chapter, how recent developments in electrospinning in hierarchical conjunction with additive processing is used to enhance defense and security by providing force protection [2],

hazardous environment sensing/detection [8], tactile interface [9] for improved functionality, comfortable outwear for soldiers and emergency responders, biomedical support in the battlefield, energy harvesting patches and devices with communication capabilities [10].

Complex, functionalized and hierarchically integrated scaffolds composed of micro-and nanoscale structures are a key objective of conjoining 3D printing with electrospun nanofibers, especially when combined with nanomaterials [1]. In this framework, devices and constructs fabricated using 3D printing and electrospinning have great potential in the production of complex structures required for several unique and specialized applications, such as in intervertebral disc tissue engineering [12], smart scaffolds for abdominal walls [13], and bi-layer scaffold for guided bone regeneration [14]. Complex and hierarchically functionalized structures consisting of micro and nano-scale structures can now be produced by the convergence of the two methods and several commercial instruments are currently designing instruments by the combination of 3D printing and electrospinning. One such instrument is 3D jet writing which allows the creation of customizable structures that enable the production of 3D structures with unmatched precision and resolution [15, 16]. The method involves a device called a 3D jet writer, which can create high-resolution structures, with appropriate pore sizes. This chapter focusses on some of the potential applications utilizing strategic convergence of the two processing techniques in biomedical technology, sensors/detectors in wearable textiles, devices for force protection, filtration mechanisms, and specialized devices for structural health monitoring.

22.2 Overview of Processes

The objective of this study to strategically integrate 3D printing or advanced additive technologies with micro/nanofibers that are produced using electrospinning processes, to engineer unique applications for applications such as biomedical technologies, e-textile for forced protection, tactile membranes, sensors for structural health monitoring and energy harvesting. It is, therefore, instructive to provide an overview of the two processes, while use of nanomaterials in any one or both processes is part of materials selection to engineer the end-product or prototype for certain specific applications. The aim is to evaluate a combined 3D printed/electrospun architecture, in comparison to solely 3D printed micro fibrous or solely electrospun nanofibrous scaffolds, for their ability to support a specific application.

22.2.1 3D Printing—Overview of the Basic Process

3D printing, commonly known as additive technology (or advanced additive manufacturing technology), has been developed rapidly in last few years [17, 18]. The

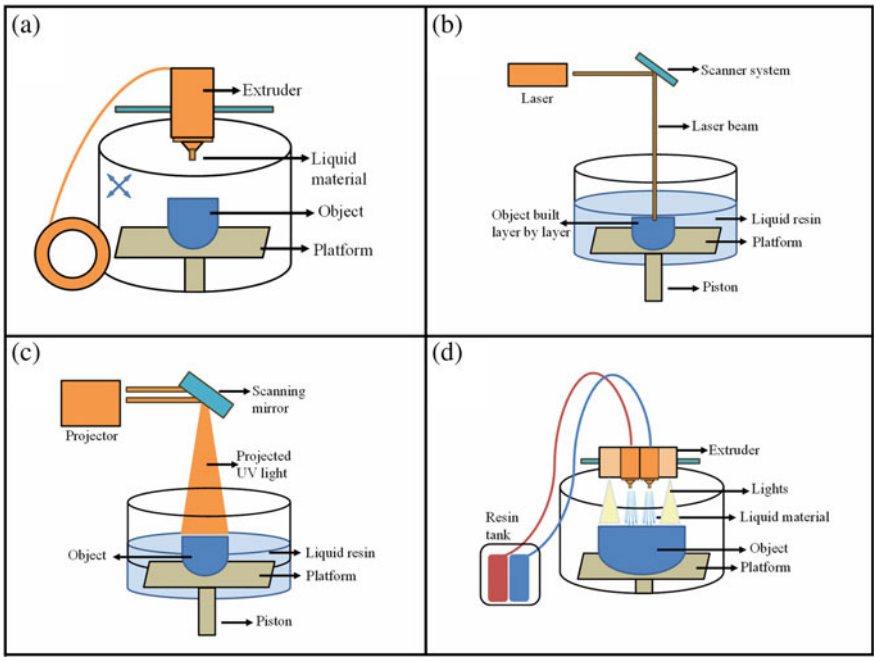


Fig. 22.1 Commonly used 3D printing techniques. **a** Fused deposition modeling, **b** Stereolithography, **c** Digital light processing and **d** PolyJet photopolymer 3D printing

technology is based on the layer-by-layer production of 3D structures directly from computer-aided design (CAD) drawings. In this context, fused deposition modeling, stereolithography, digital light processing and PolyJet photopolymer are commonly used 3D printing techniques, and are illustrated in Fig. 22.1 [19]. The method of depositing the polymers by fusion (Fig. 22.1a) is a widely preferred process due to its advantages of being inexpensive and ease of use with which polymer composites containing both thermoplastic polymers and solid particles, can be used for printing. However, poor mechanical properties, layer-by-layer appearance, poor surface quality and the limited number of thermoplastic materials are among the disadvantages of this method [20]. As another option, stereolithography (SLA) is a low cost, short cycle time, and high precision process to manufacture complex-shaped structures (SiO_2, Al_2O_3, ZrO_2, bio ceramics). SLA is based on solidification of liquid photopolymer resins layer by layer by a UV laser or electron beam (Fig. 22.1b). When this method is applied in the presence of a light projector, it simultaneously exposes the entire layer to UV light, and the process is called digital light processing (DLP) (Fig. 22.1c). It is used in both methods, especially in the manufacturing of dental implants and patient-specific tissue engineered scaffolds [19, 21]. In PolyJet printing (short for 'photopolymer jetting'), similar to inkjet technology, the process is based on the principle of spraying small droplets of liquid resin from nozzles and then solidifying these droplets by exposing them to UV light in each layer (Fig. 22.1d)

[22]. One of the most important advantages of this type of printer is that it can work in normal room conditions without requiring a special laboratory environment and can produce a wide range of high resolution materials [22].

Unlike traditional methods, 3D printing offers unusual possibilities, such as ease of operation and relative flexibility, along with controllable and precise design production. Complex materials, the production process of which is time-consuming and expensive, can be produced quickly and accurately without wastage, in a shorter period of time and at a lower cost. The method has started to attract attention for special uses in desired areas, primarily due to its wide material capacity, such as conductive, non-conductive polymers, metals, inks, bio-inks and ferromagnetic elastomers. Besides, graphene-based materials, thermoplastics, ceramics, and metals can now be printed using this digital fabrication technology [23].

Along with developing technology, 3D printing approaches have opened up wide research avenues for applications such as electromagnetic structures, 3D-printed quantum dot-based light-emitting diodes, wearable sensors, food products, biomedical implants, tissue engineered scaffolds and wound patches [24–26]. Due to rapid population growth worldwide, there is an enhanced demand for the treatment of organs due to diseases or deficiencies. An ability to fabricate artificial tissues of certain sizes and shapes with high self-renewal potential with 3D printing technology has attracted the attention of many researchers. As a result, in the last 10 years, 3D printing has made remarkable progress in the field of tissue engineering, due to its ability to create tissue with a porous and robust mechanical structure required for cell growth and substance transport. As part of our ongoing investigation in tissue engineering using electrospun nanofibers, we have expanded research into integration of the 3D printing capabilities with its controllable production and its use in patient-specific organ/tissue production, which appears extremely promising [27].

In tissue engineering, scaffolds are conventionally produced by freeze drying, salt leaching, gelation, wet spinning and electrospinning methods. However, it is difficult to obtain well-defined architectures of predetermined sizes and shapes in a controlled manner using these techniques. In addition, cells are seeded on such scaffolds after production and may not penetrate deep into the structure; therefore, cells may not be homogeneously distributed within the scaffold. To overcome this drawback, 3D printing is an attractive alternative method to produce patient-specific scaffolds. With bio-printing technology, production of 3D and porous biomaterials, simply involves creating the specific model with appropriate software and using a 3D printer to print the model, layer by layer. Furthermore, in recent years, in addition to the production of scaffolds with well-defined internal organization, 4D printing technology has also taken its place among the production methods in order to mimic the dynamic structure of tissues and the responses to natural stimuli using smart ("shape memory" or "self-actuation") materials [28, 29].

Another area where the extraordinary features of 3D printing can be used is in tactile and wearable structures. Tactile sensors have been developed to provide information about human health status and analysis using onboard artificial intelligence systems by collecting mechanical data of the human body and local environment. Adding a high level of wearability (flexibility and stretchability) to tactile sensors has

the potential to significantly improve their interface capability with contact objects by providing chronically reliable functionality [15]. 3D printed structures can be produced by optimizing the rheology of polymer solutions or melts. However, by adjusting the rheological properties of the solution, the size of the polymer threads can only be reduced to around 50 μm. When it needs to be reduced further below that dimension, natural limitations such as swelling or incompatible surface tensions are encountered [30]. Multifunctional and dynamic printable inks are needed to fully exploit the great potential of 3D printing. Despite the extensive advances made to date in tissue engineering and wearable sensors, there are still major challenges encountered in producing robust, flexible and sensitive sensors.

Yet another application of 3D printing is in structural health monitoring. Modern design codes are now requiring a much longer service life. However, worldwide, many critical infrastructures are aging and require renovation and constant monitoring before either renovation are done or replacement—either entirely or in parts. Owners and maintenance managers of capital-intensive assets are looking for cost-effective and reliable inspection and monitoring solutions to ensure safety and reliability of these structures using real-time monitoring systems, in additional to conventional periodic non-destructive evaluation. Structural health monitoring (SHM) refers to an array of connected sensors to collect and analyze data, at every moment during the service life of the structure. The goal of such system is to identify and quantify any damage or deterioration state that might occur over the service life. Recently, use of polyvinylidene fluoride (PVDF) based sensors were investigated as inexpensive solution to monitor vibrations and stress/strain in such structures [30]. However, such sensors must be inserted in appropriate scaffolds to be strategically placed at several locations. 3D printed scaffolds provide an inexpensive, yet reliable alternative for SHM, which is a step forward towards proactive maintenance indication systems for structures. Hence, the nexus of 3D printing technology together with electrospinning has become an attractive alternative for proactive measures and predictive intelligence for structural health monitoring.

22.2.2 Electrospinning—Overview of the Basic Process

With the advent of nanotechnology, researchers have become more interested in studying and exploiting the unique properties of nanoscale materials. Electrospinning technique, which is a versatile approach to produce nanofibers, is based on electrostatic field applied on a polymeric solution to yield fibers at nanoscale, has attracted a lot of attention due to its ease of use, with widely ranging applications potential in various fields. In general, the electrospinning technique involves the fabrication of nanoscale membranes with very large surface-to-volume ratio employing polymers and their composites with other functional agents (plant extracts, drugs, nanoparticles, nanotubes, quantum dots, etc.) in the form of melt or solution in the presence of high electrical fields. The method involves an electrohydrodynamic process in which a polymeric droplet is electrified to form a jet called a “Taylor cone” [31], followed

by stretching and elongation to form fibers on a grounded collector [32]. The classical electrospinning setup as shown in Fig. 22.2a, which basically consists of a syringe pump, spinneret, high voltage power supply and a grounded collector, has been modified with the addition of different collectors and needle tips, with the evolving technology over time in order to enhance the features and the functionalities of the resulting nanofiber structures [33]. One of the methods of electrospinning, termed as coaxial electrospinning (Fiber 2B), effectively enables the production of core–shell structure fibers by combining different system materials in the same fiber. The materials produced by this method are particularly suitable for use as an extended drug release system [34]. Important application areas include tissue engineering, biosensors, filtration, wound dressings, drug delivery, enzyme immobilization, defense and security materials, solar cells and food packaging [35–37].

Electrospun structures can be applied easily and effectively for many different fields, but they have limitations for some special applications. The 2D fibrous structure produced by conventional electrospinning has poor cellular infiltration and ingrowth, not applicable for 3D defects, poor absorption capacity, limited thickness, small pore size, poor mechanical properties, inadequate control of geometric features, etc. causing several limitations [38, 39]. In order to eliminate or minimize these restrictions that limit the application potential, multifunctional 3D fiber assemblies with micro/nano topographic properties can be created by integrating other production technologies into the electrospinning method [40]. One of these technologies is the combination of 3D printing and electrospinning methods as mentioned in the above section. The mechanics and strategic details of the integration, properties of the materials produced, specific application areas are presented in the following sections.

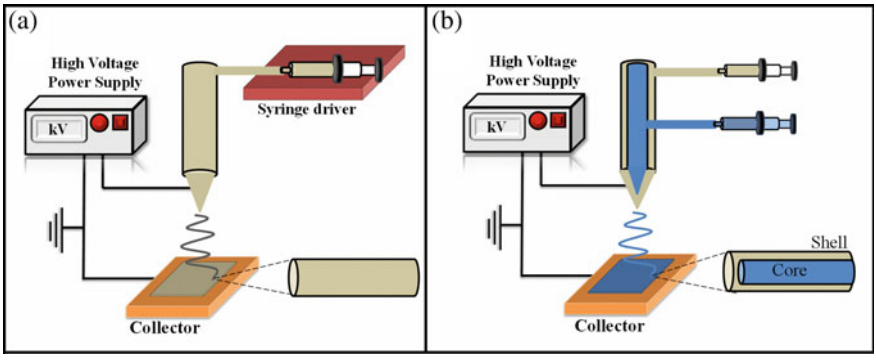


Fig. 22.2 Electrospinning techniques. **a** Conventional method with basic fiber structure, **b** Coaxial method with core–shell structure

22.3 Configurations of Hierarchal Integration

The combination of 3D printing and electrospinning technologies is a relatively new and developing methodology to create customized shapes and patterns for several unique and specific application, as described in the following section. Although, preliminary investigations have been in works, a strategic collaboration of 3D printing methodology by the biotech companies, has pushed 3D bioprinting capabilities into the future. An aging population with high chronic respiratory rates, a global severe acute respiratory syndrome novel coronavirus 2 (SARS-nCOV2) pandemic and minimal organ donors have all paved the way for 3D bioprinting to become a potential replacement organ solution—all using new generation materials with 3D configuration in micro/nano structures. Bio fabrication, in general, can be defined as the production of complex living and non-living biological products from raw materials, such as living cells, molecules, extracellular matrices, and biomaterials using 3D printing, and now with recently termed as 4D printing [29] due to time, as one of the dimensions. Bioprinting works in almost the exact same way as 3D printers, however, instead of delivering materials such as plastic, ceramic, metal or food, they deposit layers of biomaterial, that may include living, or have potential to grow, cells to build complex structures, such as blood vessels or skin tissue following detailed computer designs and models that are based on scans taken directly from patients. The precision printer heads deposit cells and organic objects using a large number of very thin layers, typically over the course of several hours. Some of the classical examples of bioprinting clinical markets include cardiovascular, craniofacial repair, orthopedics, and wound care, which include acute wounds, chronic wounds, and hernia repair. As we describe below, a complex, strategic and hierarchical integration of electrospun nanofibers with 3D printing provides desired functionality of several critical structure, which otherwise, would not be readily available.

In the literature, this combined technology is also referred to as "3D jet writing", "electro-jetting" and "electrospinning writing". The method can, in principle, be described as a modified electrospinning process, which produces 3D structures with unprecedented precision and resolution, thereby offering customizable pore geometries and scalability down to several millimeters [11]. Considering the installation of the combined technologies, a combination system consists of a classical electrospinning apparatus and computer-controlled x–y motion stage (Fig. 22.3). Similar to the electrospinning method, the polymeric liquid droplets at the needle tip are deformed and are accelerated towards the collector electrode in the presence of a high applied electric field in a conical (Taylor cone) fashion. Charged polymer fiber jets accelerate towards the grounded collector, resulting in finer patterned filaments compared to extrusion-based printing. With the application of a second ring electrode, the direction of the electrical potential is diverted towards the center of the circular electrode and suppresses the flagellum instabilities. Combining this methodology with a computer-controlled x–y stage ensures accurate modeling of the jet ink [41]. Apart from the new experimental setup created by using the 3D writing and electrospinning methods introduced above, it is possible to produce 3D structures

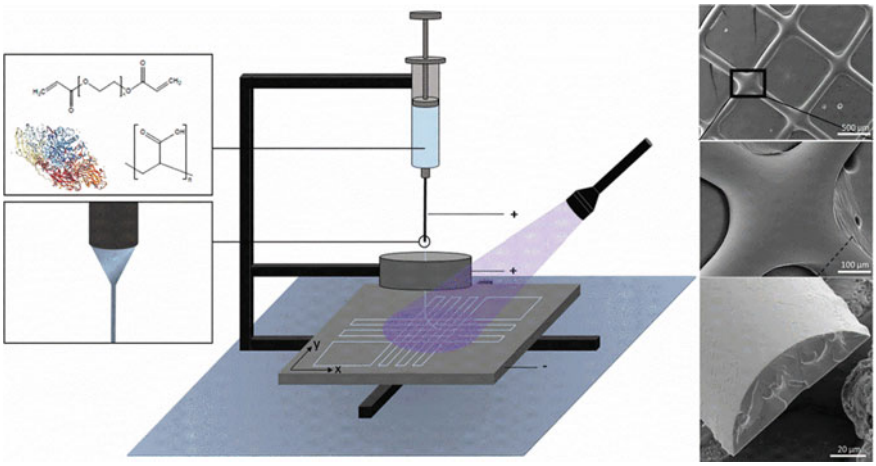


Fig. 22.3 Schematic representation of 3D jet writing technique. Reproduced with permission from John Wiley and Sons [41]

integrated with nanofiber by combining the materials produced by keeping these methods separately. Here, composite materials are produced in multiple stages. In the first step, the nanofibers produced by electrospinning are cut into very small pieces and dispersed homogeneously without allowing them to dissolve in a suitable solvent environment. In step 2, the pre-designed material is produced by 3D printing. Finally, in step 3, dispersed nanofibers are grafted into the 3D printed material and the final composite is dried. As necessary, the crosslinking step is also included in the process [42].

The production of nanofibers directly on 3D printed microfiber collectors is yet another method used for the preparation of dual scale materials (Fig. 22.4). Using this configuration, aligned fibrous structures can be produced, with the printed fibers acting as a space collector to orient the electrospun fibers [43]. As an example, Vyas et al. [43] used a screw-assisted extrusion 3D printer and electrospinning system to create poly-caprolactone double-scale scaffolds with multiple mesh layers and fiber densities. Dual-scale scaffolds with different meshes evenly spaced throughout the scaffold were produced by electrospinning directly onto the 3D scaffold at the appropriate layer during printing. The software was preprogrammed to pause at a specific layer to allow electrospinning before further printing can be resumed [43].

In addition, direct 3D printing on electrospun nanofiber mats have also been used for preparation of double-sided materials. Kozior et al. [44] showed that PLA polymer printing on raw polyacrylonitrile nanofiber mats is possible by choosing the appropriate height of the printing nozzle. In another example, use of polyvinylidene fluoride (PVDF), also known as poly(1,1-difluoroethylene), in electrospun nanofibers is described [30]. PVDF is a high-performance polymer and has useful electroactive features, such as piezoelectricity, pyroelectricity, ferroelectricity, and optoelectronics. When used with other fluoropolymers, such as polytetrafluoroethylene, and

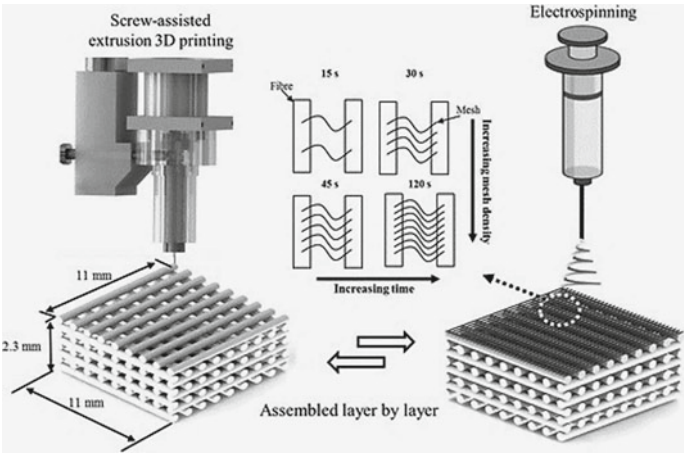


Fig. 22.4 Schematic representation of the 3D printing and electrospinning to create of a dual-scale scaffold. Reproduced with permission from Mary Ann Liebert, Inc. [43]

its copolymers, several attractive features, such as electro-optic transducers, waveguides, sensors, actuators, energy harvesting, and electro-optic transducers memory, and biomimetic robotics are possible [45–50]. Most of these applications requires that PVDF membranes are integrated with scaffolds printed using 3D printing and using hierarchical integration, configurations, hereto unachievable, are possible. In the following section, we describe several applications of methods described here.

22.4 Spectrum of Potential Applications

So far, the applications of 3D printed parts have been for specialized parts, fixtures, models and proof-of-concept prototypes. Using bioprinting, several groups have demonstrated their use in tissue engineered scaffolds [51], abdominal walls [52], wound dressings [53], and wearable textile [54] materials. There are many investigations on the use of materials and devices produced separately, using 3D printing and electrospinning. However, both methods have their own limitations. For example, cells are difficult to infiltrate into the nanoporous structure of conventional electrospun scaffolds obtained by electrospinning, while the 3D printing technique has the disadvantage of low printing resolution [42]. In a conjoined methodology, electrospun fibers in 3D structure format have a high potential for use as tissue engineering scaffolds, given their fibrous and porous structure that closely mimics the morphological properties of the natural extracellular matrix [51]. With this approach, researchers have focused on the production of complex and multidimensional biomaterials by using electrospinning and 3D printer integrated together in a strategic and hierarchical way. Furthermore, PVDF due to its excellent characteristics, as described

above, and in conjunction with nanomaterials, presents the potential of the nexus of both technologies that offer tremendous capacity for smart structures, Internet-of-things (IoT) devices and biomedical scaffolds, which otherwise would not have been possible. While a full spectrum of applications is beyond the scope of this chapter, we describe below selected applications on the topics of tissue regeneration, wound dressing material, enzyme immobilization, piezoelectric devices for e-textile and structural health monitoring [51, 53–55].

22.4.1 Tissue Engineering

The electrospun nanofibrous structures have been used in biomedical applications including targeted drug delivery [56], and scaffolds [51] for tissue engineering and regeneration. As mentioned earlier that electrospun nanofibers are excellent candidates for mimicking the extracellular matrix due to their loosely connected 3D network with high porosity and high surface area, Wang et al. [57] fabricated multilayer composite scaffolds in a 3D controllable structure, using the combination of melt electrospinning writing and conventional electrospinning techniques to imitate the microstructure and nanostructure of bone for micro/nano hybrid bone regeneration. They used a micro/nano hierarchical scaffold consisting of a polycaprolactone (PCL) microfiber rectangular grid structure frame fabricated with melt electrospinning writing and interlayer gelatin nanofiber matrices fabricated with solution electrospinning. A schematic representation of the methods used in alternating stacking of random gelatin solution electrospinning nanofibers and ordered PCL melt electrospinning writing microfibers and a representative microscopic image of the produced material are shown in Fig. 22.5. They concluded that while PCL microfibers, as the backbone, provide the mechanical strength of the scaffold and can guide cell orientation, the addition of gelatin nanofibers increases the overall hydrophilicity of the scaffold, promoting cell adhesion and proliferation [57].

In another study by Zhu et al. [58] introduced electrospinning fibers into the 3D printed scaffold to construct a biomimetic artificial intervertebral disc for therapeutic implantation. The scaffold is mainly composed of three parts, including the 3D printed polylactide frame, the annulus fibrosus structure simulated by the oriented polylactide electrospun fiber bundles and the nucleus pulposus structure simulated by hydrogel encapsulating living rat bone marrow mesenchymal stem cells. They demonstrate that the 3D-printed framework provides reliable mechanical support, while the electrospinning fiber bundles can simulate the tissue structure, and the double mesh hydrogel also provides a physiological environment for the loading cells.

3D printed tissue engineering constructs have been widely developed based on the fundamental characteristics of biodegradability, biocompatibility, and rapid-prototyping. However, further research is done towards the tissue integration using modification of polymer-cell adhesion and scaffold biodegradability coupled with

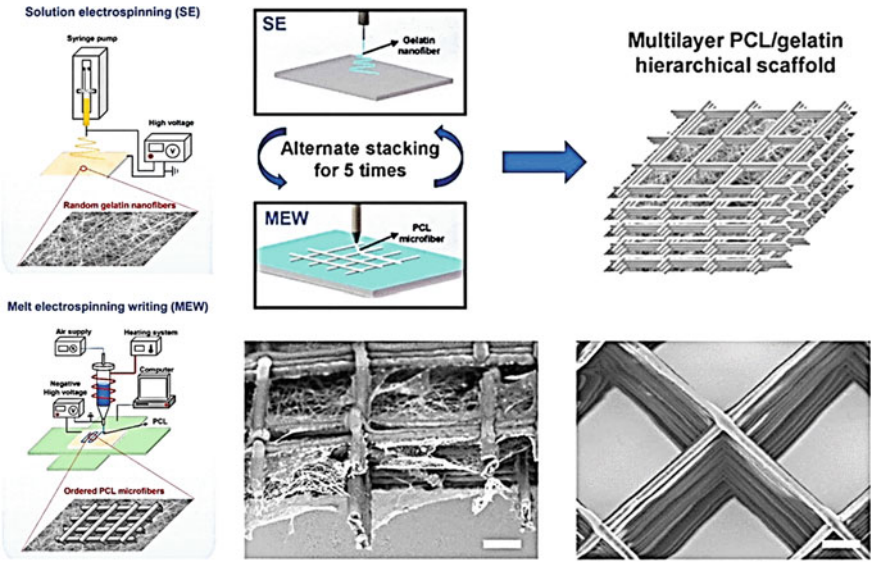


Fig. 22.5 Schematic illustration of the fabrication micro/nano scale 3D scaffolds by combing melt electrospinning writing and conventional electrospinning techniques and, microscopy image of the cross section of multi-layer composite scaffold. Scale bar = 40 μm. Reproduced with permission from Elsevier [57]

cellular maturation. Various 3D printed scaffolds of polymeric, hydrogel and inorganic materials in conjunction with electrospinning based nanofibrous offer viable options for the bone regenerative and osteogenesis engineering with various properties, especially for drug and bioactive factors delivery. Since the challenge of vascularization has been to form a network of channels, such configurations are feasible with 3D printed vascular channels for tissue engineering construct to repair cardiovascular functions.

22.4.2 Wound Dressing, Physical Augmentation and Personal Protective Equipment

In our earlier investigations, we have demonstrated that the electrospun nanofibrous structures are used in several biomedical applications, including wound dressing, due to their excellent characteristics for mimicking the extracellular matrix. Advances in drug encapsulation, regenerative medicine and tissue engineering have paved the way for several healing processes and overcome several existing complications. In an earlier investigation concerning artificial shape-morphing membrane materials, as conducted by Chen et al. [59] to enhance the limited mass transport of actuators by reducing bulk and increasing specific area, the research

produced meso-structured electrospun thermo-responsive poly (N-isopropyl acrylamide) membranes, as the morphogenetic substrates with porous structure ensuring fast absorption and desorption of water with changes in temperature, below and above its lower critical solution temperature. To achieve this, the electrospinning was first used to obtain membranes, followed by obtaining poly(N-isopropylacrylamide)-4-acryloylbenzophenone comonomer P(NIPAm-ABP) membranes, which were then fixed on non-adhesive tapes and different patterns were printed on these electrospun membranes and cured for 10 min under the illustration of UV light. It was concluded that electrospun mesostructured substrates offer a fast response due to the porous structure-induced rapid mass transport, while well-designed rigid patterns on the substrate generated by 3D printing provide guidance in the formations of 3D structures in water and the subsequent stimuli-responsiveness. A nexus of such wound dressings held in place with 3D scaffolds to stabilize the location of wound, is an ideal platform for wound dressing. In addition, certain locations of wounds are rather tricky to stabilize and hence a custom designed scaffold to hold wound dressings in place, is extremely suitable for such applications.

In addition, with aging population, increased traffic worldwide has increased the probability of traffic accidents, sports injuries and other similar procedures, physical augmentation using prosthetics, Osseointegration, bionic and robotic prosthetic limbs are gaining much attention in giving amputees full restoration of their lost limbs. A strategic integration of 3D printing coupled with electrospun nanofibers provide a range of applications in various stages of recovery and integration for human performance augmentation efforts. The effort has special application for wounded warriors returning from battlefield, where injuries are severe and different for different patients. A strategic integration of would dressing, coupled with 3D printed limb or a replacement bone plays a key role in giving amputees full restoration of their physical range of motions. With the advances in artificial intelligence, sensors and energy harvesting mechanisms, the prosthetic limbs now have the capability to interact at the neuron level, understand thoughts and using advanced sensors, the movements are closer to human-like range-of-motions. This is likely to provide additional capabilities, hitherto unrealistic. Figure 22.6 shows certain options that are being considered.

During COVID-19 crisis, acquisition of personal protective equipment (PPE) has become ever more critical. While face masks, face shields, hand-held sanitization mounts etc. have become essential commodities, several designs have appeared in market and some creative, home-made PPEs have also been observed. In addition, COVID-19 pandemic also has cast a spotlight on ventilators to support breathing during surgery or during condition of hyperinflated lungs, ventilator pumps air—usually with extra oxygen—into patients' airways when they are unable to breathe adequately on their own. Due to immense shortage, 3D printed design were widely prototyped and used by several people. Other PPEs are also feasible using 3D printing while electrospun nanofiber based membranes provide filtration from airborne contaminants, germs and viruses. In a recent interesting study, He [60] and her colleagues have developed remarkable study by making biodegradable mask filters using a method based on electrospinning and 3D printing (Fig. 22.7), as masks have

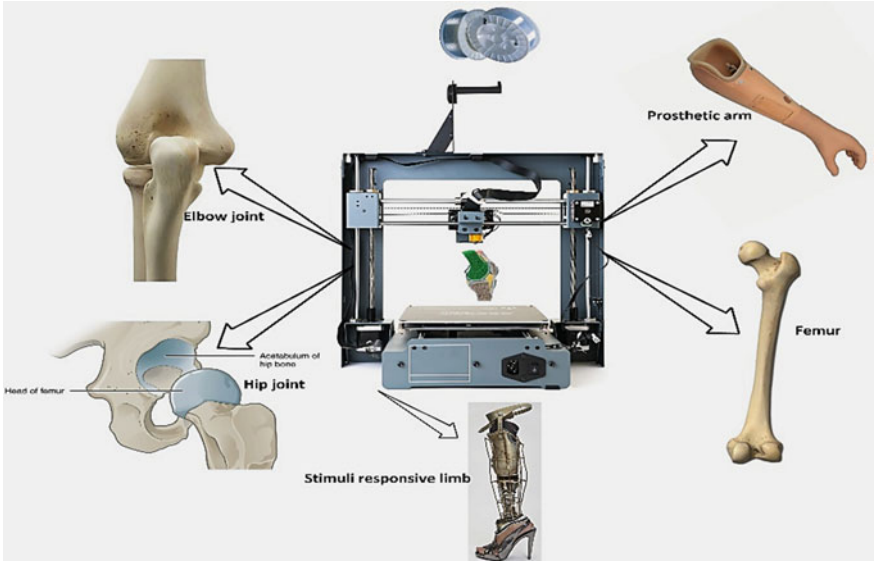


Fig. 22.6 3D printed human physical augmentation mechanisms

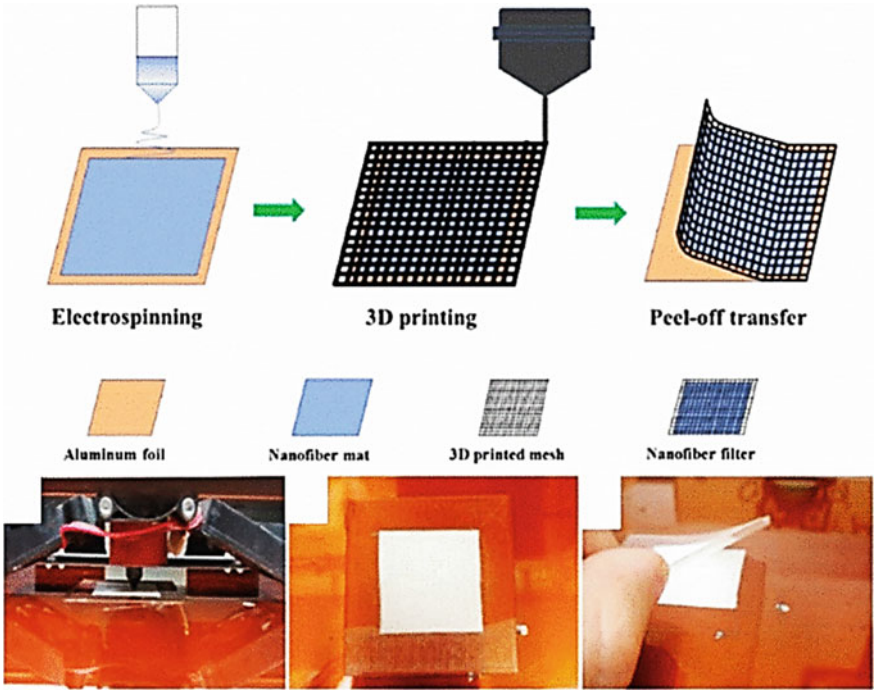


Fig. 22.7 The schematic experimental set-up of the fabrication of mask filter with the combination of 3D printing and electrospinning. Reproduced with permission from Whioce Publishing [60]

become one of the most useful PPE during the outbreak, as stated above. The basic principle of the study is that the nanofibers provide excellent filtration and the 3D printed structure provides support so that the fibers are not damaged. The fibrous side of masks were prepared with a vertical single needle electrospinning setup using polylactic acid (PLA) polymer. For the 3D printing and the electrospinning, they used the identical PLA grade to make a self-reinforced structure. The aluminum foil covered with the nanofiber mat was glued on the printing bed and different layers were printed directly onto the nanofibrous mat. They found that the multiple layer filter have a similar filtration performance as KN95/N95 and FFP2 filters.

As additional applications of electrospun nanofibrous dressings with non-adherent property to the healing tissue and their combination with antimicrobial agents and drugs have been studied for wide variety of wound care management [61]. In a recent study, non-adherent wound dressing was produced by direct electrospinning of vancomycin embedded gelatin onto a gauze [62]. They are easily applied to the composite dressing and on to the burn injury sites of piglets which simulate the pathophysiology of burn wounds in humans. As the healing progressed, the mats were removed from the injured area without leaving any stain, and the antibiotic-loaded dressing accelerated wound healing and re-epithelization. It was observed that ~46 days after the injury, the wound bed showed a better cosmetic appearance [62]. These are particularly useful as medical supplies in combat rucksack. Other biomedical applications include materials for dental implant [63], prosthetics [64], and biomarkers sensitive membranes [65].

22.4.3 Piezoelectric Materials—Tactile Sensing, Energy Harvesting and Biomedical Application

PVDF, as stated earlier, is a high-performance polymer and due to its excellent piezoelectric characteristics, is used for energy harvesting applications. The spectrum of applications requiring decentralized power units ranges from personal health and medicine, military, transport, agriculture and infrastructure, as part of massively distributed sensor network, as shown in Fig. 22.8. PVDF is one of the most used membrane materials and has received a great attention due to its outstanding properties. Properties such as thermal stability, chemical resistance and processability to form membranes make PVDF an ideal material for biomedical applications.

Recently, electrospun nanofibers using PVDF as polymer are being considered for low power energy harvesting devices and applications for convenient technology that would be reliable for future use. Many research groups have developed PVDF-based biopolymer composites for enhancing device performance as well as their reliability toward the next generation devices. These characteristics coupled with conducting nanofibers are considered for system on fiber (SOF) communication. This technology will pave the way for communication, gaming, such as virtual reality and augmented reality, built into the soldier's uniform, a reality. In addition to the above-mentioned

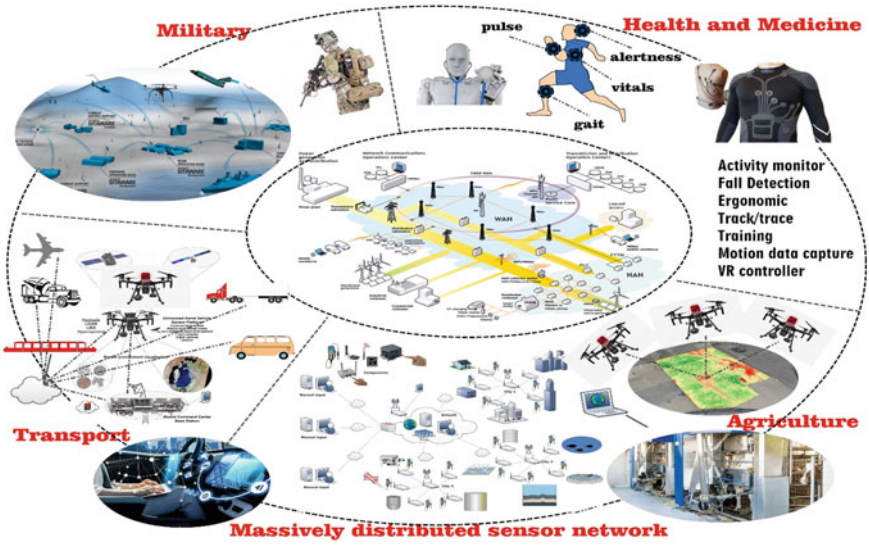


Fig. 22.8 Spectrum of application using decentralized power generation

biomedical applications, there are a few studies conducted on e-textile, tactile and sensor applications using these new generation materials, which are produced using the combination of electrospinning and 3D printing. Rivera and Hudson [66] developed a new type of 3D printer that combines rigid plastic printing with melt electrospinning in a single process which offers new opportunities for fabricating interactive objects and sensors that blend the flexibility, absorbency and softness of produced electrospun textiles with the structure and rigidity of hard plastic for actuation, sensing, and tactile experiences. Potential applications of PVDF as standalone and in a blended configuration demonstrate a variety of biomimetic and minimal invasive medical diagnostic applications. Other applications include infant cardiorespiratory monitoring, pediatric dynamometer, respiratory rate monitor, prostate gland stiffness monitor, detection of articular cartilage softening, catheter position sensing, disposable pressure monitoring system, Parkinson's symptoms and posture monitoring system. Smart textiles or e-textiles are capable of reacting to an external stimulus with an appropriate response and are the subject of much research for diverse set of applications, including and not limited to sports, health and security.

22.4.4 Piezoelectric Devices for Structural Health Monitoring

Electrospun nanofibers have been used in various configurations for enhancing mechanical strength of the mats and reinforcement in composites. A vast majority

of nanofibers for reinforcing purposes are electrospun from thermoplastic polymers, and only a few from thermosetting ones. Nanofibers were also produced by adding carbon nanotubes (CNTs), carbon nanofibers (CNF), tannic acid coated graphene oxide to prepare high performance polymer solutions and fibers produced electrospinning. Nanofibers produced resulting from these processes exhibited excellent thermal stability, flame retardancy, and antibacterial and mechanical properties. In addition, sensors prepared using electrospinning of PVDF and scaffold using 3D printing are now used for structural integrity/health monitoring and risk assessment. Sensors are strategically placed throughout the structure in a sensor network configuration to monitor various parameters. PVDF based sensors, preferably in capacitive mode, produce signal proportional to the displacement and hence real-time monitoring is possible. As shown in Fig. 22.9, this strategy is very commonly used for implementing a damage detection and risk characterization strategy for engineering structures.

While braided fibers are used for textile, use of electrospun nanofibers have been utilized as mechanical reinforcement in resin-based composite laminate materials for impact resistance. This is particularly suitable for uniform of the day (UOD) for soldiers as the outerwear can be made lightweight, breathable and even flame resistance. For battlefield, the nanofibers based composite laminate provide ballistic protection against force or impact. Use of metamaterials provide additional desired capabilities such as camouflaging, optical cloaking and fluorescent tags—for identification to prevent friendly fire in combat theatre.

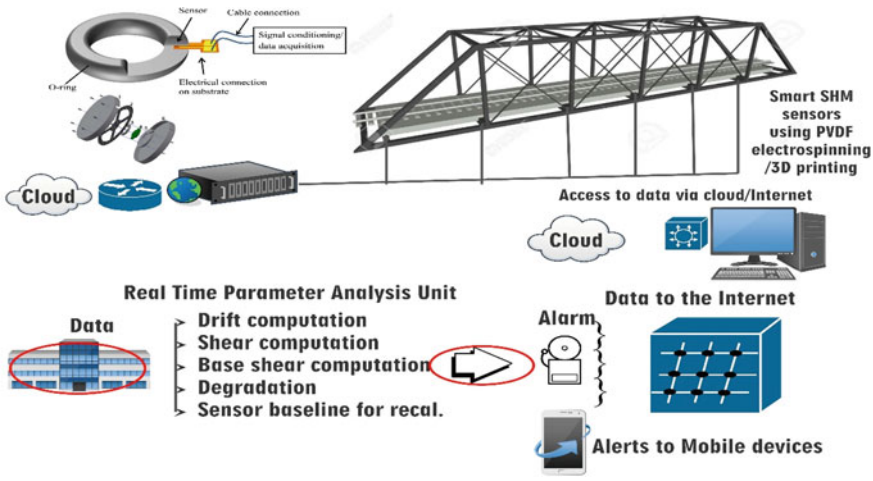


Fig. 22.9 Structural health monitoring using electrospun PVDF nanofibers in 3D printed scaffolds

22.5 Conclusions and Future Applications

The combination of electrospinning and 3D printing is a relatively new and upcoming field of study with unlimited potentials. Researchers continue to work on simple and straightforward methods to successfully combine nanofiber mats with 3D-printed substrates or scaffolds to make functional materials for a variety of applications for rapid prototyping and proof-of-concepts visualizations. The spectrum of applications range from biomedical applications, specialized parts industry for aviation, automobile, defense, water filtration, sensors for structural health monitoring, sport, etc. Tissue engineered scaffolds and wearable textiles are some of the successful examples of these materials. With the new systems being developed, to obtain polymer architectures with 3D printed macro/nano structure from various polymer materials and their composites seems quite possible. Recently, Virginia Tech created a novel process to 3D print rubber to mimic tissue for a human heart model. Virginia Tech is also developing innovative solutions to COVID-19 needs by creating PPE for healthcare providers and developing parts to adapt bilevel positive airway pressure (BiPap) machines to be used as ventilators. During the height of pandemic, a severe shortage of ventilators was experiences and many small businesses produced several different designs of ventilators using 3D printers. As a major medical breakthrough, scientists at Tel Aviv University have "printed" first 3D vascularized engineered heart using a patient's own cells and biological materials. Scientists in regenerative medicine have been successful in printing only simple tissues without blood vessels.

In 2015, a study [67] utilized deoxyribonucleic acid (DNA) as a nucleating agent for the nucleation of electroactive β-phase and alignment of molecular dipoles in PVDF which resulted in a self-poled PVDF film with increased piezoelectricity. PVDF can be blended with copolymers to improve its properties without affecting the compatibility. Since PVDF-trifluoro ethylene (PVDF-TrFE) directly crystallizes into the polar ß-phase and displays higher piezo-electricity as compared to PVDF, polymeric blends of PVDF and PVDF-TrFE have been studies for tactile sensors. In yet another study [68], PVDF based scaffolds were used for the reinforcement of tissues, cell guidance, vascular grafts, ligament and artificial cornea. This is a relatively new paradigm to apply physical stimuli to the cells to achieve not only phenotype but also for other functionalities. Therefore, such smart polymer materials can be developed to apply mechanical and electrical stimuli to certain specific cells, which are subjected to electromechanical stimuli during their functioning. Such studies are very useful to flexible tactile sensors which appear to be the most promising materials for their ultra-sensitivity, high deformability, outstanding chemical resistance, high thermal stability and low permittivity for dynamic tactile sensing in wearable electronics. As stated earlier, an exhaustive review of potential applications using a nexus of electrospinning and 3Dprinting is beyond the scope of this chapter, however, our attempt has been to articulate the viewpoint of conjoining the two processes to project the tremendous potential of this capability. While we promote this concept, our ongoing research is focused on bio-based polymers, use,

reuse, recycle and upcycling of polymers to reduce the environmental footprint of micro/nanoplastics.

Conflict of Interest Statement The authors declare no conflict of interest. Due to commercial interest of this technology, any commercial name or product displayed or described in this chapter is coincidental and in no way, should be treated as an endorsement of that product. The chapter did not require collection of any personal data and hence the Institutional Review Board policy related to involvement of huma subjects is not applicable.

References

1. Vaseashta, A., & Stamatin, I. (2007). Electrospun polymers for controlled release of drugs, vaccine delivery, and system-on-fibers. *Journal of Optoelectronics and Advanced Materials, 9*(6), 1606–1613.
2. Kim, Y. N., Ha, Y.-M., Park, J. E., Kim, Y. O., Jo, J. Y., Han, H., Lee, D. C., Kim, J., & Jung, Y. C. (2021). Flame retardant, antimicrobial, and mechanical properties of multifunctional polyurethane nanofibers containing tannic acid-coated reduced graphene oxide. *Polymer Testing, 93*, 107006.
3. Ding, B., Wang, M., Yu, J., & Sun, G. (2009). Gas sensors based on electrospun nanofibers. *Sensors, 9*(3), 1609–1624.
4. Woo, D. J., Hansen, N. S., Joo, Y. L., & Obendorf, S. K. (2012). Photocatalytic self-detoxification by coaxially electrospun fiber containing titanium dioxide nanoparticles. *Textile Research Journal, 82*(18), 1920–1927.
5. Lee, S. (2009). Developing UV-protective textiles based on electrospun zinc oxide nanocomposite fibers. *Fibers and Polymers, 10*(3), 295–301.
6. Khan, M. Q., Kharaghani, D., Ullah, S., et al. (2018). Self-cleaning properties of electrospun PVA/TiO_2 and PVA/ZnO nanofibers composites. *Nanomaterials, 8*(9), 644.
7. Song, K.,Wu, Q., Qi, Y., & Kärki, T. (2017). Electrospun nanofibers with antimicrobial properties. In M. Afshari (Ed.), *Textiles, electrospun nanofibers* (pp. 551–569). Woodhead Publishing
8. Bölgen, N., Demir, D., & Vaseashta, A. (2015). Nanofibers for the detection of VOCs. In P. Petkov, D. Tsiulyanu, W. Kulisch, & C. Popov (Eds.), *Nanoscience advances in CBRN agents detection, information and energy security. NATO series A*. Springer.
9. Wang, X., Sun, F., Yin, G., Wang, Y., Liu, B., & Dong, M. (2018). Tactile-sensing based on flexible PVDF nanofibers via electrospinning: A review. *Sensors, 18*(2), 330.
10. Yuk, H., Lu, B., Lin, S., et al. (2020). 3D printing of conducting polymers. *Nature Communications, 11*, 1604.
11. Jordahl, J. H., Solorio, L., Sun, H., Ramcharan, S., Teeple, C. B., Haley, H. R., Lee, K. J., Eyster, T. W., Luker, G. D., Krebsbach, P. H., & Lahann, J. (2018). 3D jet writing: Functional microtissues based on tessellated scaffold architectures. *Advanced Materials, 30*(14), 1707196. https://doi.org/10.1002/ADMA.201707196
12. *Intervertebral disc tissue engineering* [12].
13. *Smart scaffolds for abdominal walls* [13].
14. *Bi-layer scaffold for guided bone regeneration* [14].
15. Moon, S., Jones, M. S., Seo, E., Lee, J., Lahann, L., Jordahl, J. H., Lee, K. J., & Lahann, J. (2021). 3D jet writing of mechanically actuated tandem scaffolds. *Science Advances, 7*(16), 5289–5303. https://doi.org/10.1126/SCIADV.ABF5289
16. Quan, H., Zhang, T., Xu, H., Luo, S., Nie, J., & Zhu, X. (2020). Bioactive materials photo-curing 3D printing technique and its challenges. *Bioactive Materials, 5*(1), 110–115. https://doi.org/10.1016/j.bioactmat.2019.12.003

17. Browne, M. P., Redondo, E., & Pumera, M. (2020). *3D printing for electrochemical energy applications*. https://doi.org/10.1021/acs.chemrev.9b00783
18. Hossain, N., Chowdhury, M. A., Shuvho, M. B. A., Kashem, M. A., & Kchaou, M. (2021). 3D-printed objects for multipurpose applications. *Journal of Materials Engineering and Performance, 30*(7), 4756–4767. https://doi.org/10.1007/S11665-021-05664-W
19. Ngo, T. D., Kashani, A., Imbalzano, G., Nguyen, K. T. Q., & Hui, D. (2018). Additive manufacturing (3D printing): A review of materials, methods, applications and challenges. *Composites Part B, Engineering, 143*, 172–196. https://doi.org/10.1016/J.COMPOSITESB.2018.02.012
20. Voet, V. S. D., Schnelting, G. H. M., Xu, J., Loos, K., Folkersma, R., & Jager, J. (2018). Stereolithographic 3D printing with renewable acrylates. *Journal of Visualized Experiments, 2018*(139). https://doi.org/10.3791/58177
21. Tee, Y. L., Peng, C., Pille, P., Leary, M., & Tran, P. (2020). PolyJet 3D printing of composite materials: Experimental and modelling approach. *JOM, 72*(3), 1105–1117. https://doi.org/10.1007/S11837-020-04014-W
22. Shahrubudin, N., Lee, T. C., & Ramlan, R. (2019). An overview on 3D printing technology: Technological, materials, and applications. *Procedia Manufacturing, 35*, 1286–1296. https://doi.org/10.1016/J.PROMFG.2019.06.089
23. Wilms, P., Daffner, K., Kern, C., Gras, S. L., Schutyser, M. A. I., & Kohlus, R. (2021). Formulation engineering of food systems for 3D-printing applications—A review. *Food Research International, 148*, 110585. https://doi.org/10.1016/J.FOODRES.2021.110585
24. Kalkal, A., Kumar, S., Kumar, P., Pradhan, R., Willander, M., Packirisamy, G., Kumar, S., & Malhotra, B. D. (2021). Recent advances in 3D printing technologies for wearable (bio)sensors. *Additive Manufacturing, 46*, 102088. https://doi.org/10.1016/J.ADDMA.2021.102088
25. Mahendiran, B., Muthusamy, S., Sampath, S., Jaisankar, S. N., Popat, K. C., Selvakumar, R., & Krishnakumar, G. S. (2021). Recent trends in natural polysaccharide based bioinks for multiscale 3D printing in tissue regeneration: A review. *International Journal of Biological Macromolecules, 183*, 564–588. https://doi.org/10.1016/J.IJBIOMAC.2021.04.179
26. Li, J., Wu, C., Chu, P. K., & Gelinsky, M. (2020). Materials Science & Engineering R 3D printing of hydrogels: Rational design strategies and emerging biomedical applications. *Materials Science and Engineering R, 140*, 100543. https://doi.org/10.1016/j.mser.2020.100543
27. Tamay, D. G., Dursun Usal, T., Alagoz, A. S., Yucel, D., Hasirci, N., & Hasirci, V. (2019). 3D and 4D printing of polymers for tissue engineering applications. *Frontiers in Bioengineering and Biotechnology, 0*, 164. https://doi.org/10.3389/FBIOE.2019.00164
28. Yang, T., Xie, D., Li, Z., & Zhu, H. (2017). Recent advances in wearable tactile sensors: Materials, sensing mechanisms, and device performance. *Materials Science and Engineering: R: Reports, 115*, 1–37. https://doi.org/10.1016/J.MSER.2017.02.001
29. Vaseashta, A., & Bölgen N. (2017). *4D-printed hydrogel based composite structures by additive processing, presented at ECerS 2017*. Budapest, Hungary.
30. Palwai, S., Batra, A., Kotru, S., & Vaseashta, A. (2022). Electrospun polyvinylidene fluoride nanofiber membranes based flexible capacitive sensors for tactile and biomedical applications. *Surface Engineering and Applied Electrochemistry, 58*(1).
31. Vaseashta, A. (2007). Controlled formation of multiple Taylor cones in electrospinning process. *Applied Physics Letters, 90*, 093115. https://doi.org/10.1063/1.2709958
32. Xue, J., Wu, T., Dai, Y., & Xia, Y. (2019). Electrospinning and electrospun nanofibers: Methods, materials, and applications. *Chemical Reviews, 119*(8), 5298. https://doi.org/10.1021/ACS.CHEMREV.8B00593
33. Moghe, A. K., & Gupta, P. B. S. (2008). Co-axial electrospinning for nanofiber structures: Preparation and applications. *Polymer Reviews, 48*(2), 353–377. https://doi.org/10.1080/15583720802022257
34. Zhao, H., Ma, Y., Sun, D., Ma, W., Yao, J., & Zhang, M. (2019). Preparation and characterization of coaxial electrospinning rhBMP2-loaded nanofiber membranes. *Journal of Nanomaterials*. https://doi.org/10.1155/2019/8106985
35. Ramakrishna, S., Fujihara, K., Teo, W. E., Yong, T., Ma, Z., & Ramaseshan, R. (2006). Electrospun nanofibers: Solving global issues. *Materials Today, 9*(3), 40–50. https://doi.org/10.1016/S1369-7021(06)71389-X

36. Bhardwaj, N., & Kundu, S. C. (2010). Electrospinning: A fascinating fiber fabrication technique. *Biotechnology Advances, 28*(3), 325–347. https://doi.org/10.1016/J.BIOTECHADV.2010.01.004
37. Sameen, D. E., Ahmed, S., Lu, R., Li, R., Dai, J., Qin, W., & Liu, Y. (2021). Electrospun nanofibers food packaging: Trends and applications in food systems. *Critical Reviews in Food Science and Nutrition*. https://doi.org/10.1080/10408398.2021.1899128
38. Khorshidi, S., Solouk, A., Mirzadeh, H., Mazinani, S., Lagaron, J. M., Sharifi, S., & Ramakrishna, S. (2016). A review of key challenges of electrospun scaffolds for tissue-engineering applications. *Journal of Tissue Engineering and Regenerative Medicine, 10*(9), 715–738. https://doi.org/10.1002/TERM.1978
39. Lee, J., Lee, S. Y., Jang, J., Jeong, Y. H., & Cho, D.-W. (2012). Fabrication of patterned nanofibrous mats using direct-write electrospinning. *Langmuir, 28*(18), 7267–7275. https://doi.org/10.1021/LA3009249
40. Abel, S. B., Ballarin, F. M., & Abraham, G. A. (2020). Combination of electrospinning with other techniques for the fabrication of 3D polymeric and composite nanofibrous scaffolds with improved cellular interactions. *Nanotechnology, 31*(17), 172002. https://doi.org/10.1088/1361-6528/AB6AB4
41. Steier, A., Schmieg, B., von Brenndorff, Y. I., Meier, M., Nirschl, H., Franzreb, M., & Lahann, J. (2020). Enzyme scaffolds with hierarchically defined properties via 3D jet writing. *Macromolecular Bioscience, 20*(9), 2000154. https://doi.org/10.1002/MABI.202000154
42. Yu, Y., Hua, S., Yang, M., Fu, Z., Teng, S., Niu, K., Zhao, Q., & Yi, C. (2016). Fabrication and characterization of electrospinning/3D printing bone tissue engineering scaffold. *RSC Advances, 6*(112), 110557–110565. https://doi.org/10.1039/C6RA17718B
43. Vyas, C., Ates, G., Aslan, E., Hart, J., Huang, B., & Bartolo, P. (2020). Three-dimensional printing and electrospinning dual-scale polycaprolactone scaffolds with low-density and oriented fibers to promote cell alignment. *3D Printing and Additive Manufacturing, 7*(3), 105–113. https://doi.org/10.1089/3dp.2019.0091
44. Kozior, T., Trabelsi, M., Mamun, A., Sabantina, L., & Ehrmann, A. (2019). Stabilization of electrospun nanofiber mats used for filters by 3D printing. *Polymers, 11*(10), 1618. https://doi.org/10.3390/POLYM11101618
45. Benaben, P., & Boddaert, X. (2016). Design and development of printed acoustic sensor. *Flexible and Printed Electronics, 1*, 015001.
46. Alomari, A., Batra, A., Aggrawal, M., & Bowen, C. R. (2016). A multi-source energy harvesting utilizing highly efficient ferroelectric PMN-PT single crystal. *Journal of Materials Science*. https://doi.org/10.1007/s10854-016-5073-5
47. Sebald, G., Seveyat, L., Guyomar, D., Lebrun, L., Guiffard, B., & Pruvost, S. (2006). Electrocaloric and pyroelectric properties of $0.75Pb(Mg_{1/3}Nb_{2/3})O_3$–$0.25PbTiO_3$ single crystals. *Journal of Applied Physics, 100*, 124112.
48. Zhang, R., Jiang, B., & Cao, W. (2001). Elastic, piezoelectric, and dielectric properties of multidomain $0.67Pb(Mg_{1/3}Nb_{2/3})O_3$–$0.33PbTiO_3$ single crystals. *Journal of Applied Physics, 7*, 90.
49. Kalimuldina, G., Turdakyn, N., Abay, I., Medeubayev, A., Nurpeissova, A., Adair, D., & Bakenov, Z. (2020). A review of piezoelectric PVDF film by electrospinning and its applications. *Sensors (Basel), 20* (18), 5214. https://doi.org/10.3390/s20185214.PMID:32932744; PMCID:PMC7570857
50. Saxena, P., & Shukla, P. (2021). A comprehensive review on fundamental properties and applications of poly(vinylidene fluoride) (PVDF). *Advanced Composites and Hybrid Materials, 4*, 8–26. https://doi.org/10.1007/s42114-021-00217-0
51. Jun, I., Han, H.-S., Edwards, J. R., & Jeon, H. (2018). Electrospun fibrous scaffolds for tissue engineering: Viewpoints on architecture and fabrication. *International Journal of Molecular Sciences, 19*, 745. https://doi.org/10.3390/IJMS19030745
52. Yang, Z., Song, Z., Nie, X., et al. (2020). A smart scaffold composed of three-dimensional printing and electrospinning techniques and its application in rat abdominal wall defects. *Stem Cell Research and Therapy, 11*, 533. https://doi.org/10.1186/s13287-020-02042-6

53. Maver, T., Smrke, D. M., Kurečič, M., Gradišnik, L., Maver, U., & Kleinschek, K. S. (2018). Combining 3D printing and electrospinning for preparation of pain-relieving wound-dressing materials. *Journal of Sol-Gel Science and Technology, 88*(1), 33–48. https://doi.org/10.1007/S10971-018-4630-1
54. Bölgen, N., & Vaseashta, A. (2016). Nanofibers for tissue engineering and regenerative medicine. In V. Sontea & I. Tiginyanu (Eds.), *3rd International Conference on Nanotechnologies and Biomedical Engineering. IFMBE Proceedings* (Vol. 55). Springer. https://doi.org/10.1007/978-981-287-736-9_77
55. Vaseashta, A. (2018). Loaded electrospun nanofibers: Chemical and biological defense. In J. Bonča & S. Kruchinin (Eds.), *Nanostructured materials for the detection of CBRN. NATO science for peace and security series A: Chemistry and biology*. Springer. https://doi.org/10.1007/978-94-024-1304-5_3
56. Kotta, S., Nair, A., & Alsabeelah, N. (2018). 3D printing technology in drug delivery: Recent progress and application. *Current Pharmaceutical Design, 24*(42), 5039–5048. https://doi.org/10.2174/1381612825666181206123828 PMID: 30520368.
57. Wang, Z., Wang, H., Xiong, J., Li, J., Miao, X., Lan, X., Liu, X., Wang, W., Cai, N., & Tang, Y. (2021). Fabrication and in vitro evaluation of PCL/gelatin hierarchical scaffolds based on melt electrospinning writing and solution electrospinning for bone regeneration. *Materials Science and Engineering C, 128*, 112287. https://doi.org/10.1016/J.MSEC.2021.112287
58. Zhu, M., Tan, J., Liu, L., Tian, J., Li, L., Luo, B., Zhou, C., & Lu, L. (2021). Construction of biomimetic artificial intervertebral disc scaffold via 3D printing and electrospinning. *Materials Science and Engineering C, 128*, 112310. https://doi.org/10.1016/J.MSEC.2021.112310
59. Chen, T., Bakhshi, H., Liu, L., Ji, J., & Agarwal, S. (2018). Combining 3D printing with electrospinning for rapid response and enhanced designability of hydrogel actuators. *Advanced Functional Materials, 28*(19), 1800514. https://doi.org/10.1002/ADFM.201800514
60. He, H., Gao, M., Illés, B., & Molnar, K. (2020). 3D printed and electrospun, transparent, hierarchical polylactic acid mask nanoporous filter. *International Journal of Bioprinting, 6*(4). https://doi.org/10.18063/IJB.V6I4.278
61. Homaeigohar, S., & Boccaccini, A. R. (2020). Antibacterial biohybrid nanofibers for wound dressings. *Acta Biomaterialia, 107*, 25–49.
62. Dhand, C., Venkatesh, M., Barathi, V. A., et al. (2017). Bio-inspired crosslinking and matrix-drug interactions for advanced wound dressings with long-term antimicrobial activity. *Biomaterials, 138*, 153–168.
63. Song, W., Seta, J., Chen, L., et al. (2017). Doxycycline-loaded coaxial nanofiber coating of titanium implants enhances osseointegration and inhibits *Staphylococcus aureus* infection. *Biomedical Materials (Bristol, England), 12*(4), 045008.
64. Chen, L., & Ren, W. (2020). Three-dimensional (3D) and drug-eluting nanofiber coating for prosthetic implants. In B. Li, T. Moriarty, T. Webster, & M. Xing (Eds.), *Racing for the surface* (pp. 91–114). Springer.
65. Mane, P. P., Ambekar, R. S., & Kandasubramanian, B. (2020). Electrospun nanofiber-based cancer sensors: A review. *International Journal of Pharmaceutics, 583*, 119364.
66. Rivera, M. L., & Hudson, S. E. (n.d.). Desktop electrospinning A single extruder 3D printer for producing rigid plastic and electrospun textiles spinning: A single extruder 3D printer for producing rigid plastic and electrospun. In *Proceedings of the 2019 CHI conference on human factors in computing systems*. https://doi.org/10.1145/3290605
67. Tamang, A., Ghosh, S. K., Garain, S., et al. (2015). DNA-assisted β-phase nucleation and alignment of molecular dipoles in PVDF film: A realization of self poled bioinspired flexible polymer nanogenerator for portable electronic devices. *ACS Applied Materials and Interfaces, 7*, 16143.
68. Cheng, Y., Xu, Y., Qian, Y., Chen, X., Ouyang, Y., & Yuan, W. (2020). 3D structured self-powered PVDF/PCL scaffolds for peripheral nerve regeneration. *Nano Energy, 69*, 104411.



Ashok Vaseashta is CEO/CTO and Executive Director for research with the International Clean Water Institute in Virginia, USA. He also serves as a Professor at Riga Technical University, Chaired Professor of Nanotechnology at the Academy of Sciences of Moldova, Academician at Euro-Mediterranean Academy of Arts and Sciences, and a Senior Strategic Research Advisor for several organizations. Inspired by nature and guided by societal necessities, he strives for technological innovations to address the global challenges of the twenty-first century. His research interests include CBRN defense, critical infrastructure safety and security, and environmental sustainability—all using nexus of advanced technological solution platforms. He is a scholar, visionary, strategist, and dedicated futurist providing strategic leadership to promote and advance research initiatives and priorities using data-driven decisions. He received Ph.D. from the Virginia Polytechnic Institute and State University, Blacksburg, VA in 1990 followed by Kobe post-doctoral fellowship. Following his Ph.D., he served as a professor and researcher at Virginia Tech and Marshall University. He also served as the Director of Research at the Institute for Advanced Sciences Convergence and International Clean Water Institute for Norwich University Applied Research Institutes, Vice-Provost (Rector) for Research in South Carolina, Visiting Professor at the 3 Nano-SAE Research Centre, University of Bucharest, Romania and Visiting Scientist at the Helen and Martin Kimmel Center of Nanoscale Science at the Weizmann Institute of Science, Israel. He served the U.S. Department of State in two rotations, as strategic S&T advisor in the Bureau of International Security and Nonproliferation, Office of Weapons of Mass Destruction and Terrorism, and U.S. diplomat. His research interests span foresight, nanotechnology, environmental/ecological science and critical infrastructure safety and security. He is the author/editor of 11 books and has published over 300 articles in scientific journals, book chapters, and conferences. He serves on editorial boards of several international journals and is an active member of various professional organizations.



Didem Demir was born in İstanbul, Turkey, in 1988. She received the B.S. and M.S. degrees in Chemical Engineering from the Fırat University, Turkey, in 2011 and Mersin University, Turkey, in 2014, respectively. She received Ph.D. degree in Chemical Engineering at Mersin University, in 2021. She is working as Assistant Professor at the Chemistry and Chemical Processes Technologies Department of Tarsus University, Mersin, Turkey. Mrs. Demir's proficiency is the development and characterization of biomaterials including gels, nanofibers and micro- and nanoparticles for tissue engineering applications such as tissue regeneration, wound healing and drug release. Her research interests also include the extraction of natural polymers and fabrication of polymeric materials for wastewater treatment. Up to now, she published 22 articles, 6 book chapter and 50 proceedings.



Burcu Sakım was born in Mersin, Turkey in 1994. She graduated from Eskişehir Osmangazi University, Faculty of Engineering and Architecture, Department of Chemical Engineering in 2018. Since 2019, She has been doing her master's degree in Chemical Engineering at Mersin University, Institute of Science. Her research interests are the production of multi-layer tissue scaffolds in tissue engineering, cryogel production by cryogelation method, and nanofiber production technology by electrospinning method.



Müge Aşık was born in Adana in 1995. She received the B.S. degree in chemical engineering from University of Mersin, Mersin, Turkey in 2017 and the M.S. degree in chemical engineering from the University of Mersin, Mersin, Turkey in 2019. She is currently pursuing the Ph.D. degree in chemical engineering at Mersin University, Mersin, Turkey. From 2017 to 2019, she was a researcher with the TUBITAK industry-focused research project about developing the drug nanoformula that supports the immune system in Mersin University and Izmir High Technology Institute. Her research interests include the development of nanoformulations for biomaterials using green and sustainable methods and its applications in tissue engineering and the development innovative applications with electrospinning method for tissue engineering.



Nimet Bölgen received B.S. degree in Chemical Engineering at Ankara University, Turkey in 2002, and M.S. degree in Chemical Engineering at Hacettepe University, Turkey in 2004. She received Ph.D. degree in Bioengineering at Hacettepe University, Turkey in 2008. She was visiting scientist at Sabancı University, Turkey; Lund University, Sweden; Institute of Polymer Science and Technology, Spain; and Keele University, United Kingdom. She has been working at Chemical Engineering Department, Mersin University, Turkey since 2009. She is the author of 13 book chapters, 45 articles, and more than 100 proceedings. Prof. Bölgen's research is focused on the development of biomaterials for tissue engineering and regenerative medicine, drug delivery systems from natural and synthetic polymers, cryogels, and electrospun nanofibers for biomedical applications.

Chapter 23
Integration of Electrospinning and 3D Printing Technology



Zhaoxu Zhang, Wei Zhang, Xiaoli Peng, Xindan Zhang, Yunpeng Wang, Bing Yu, Ming Tian, Liqun Zhang, Jiajia Xue, and Yunqian Dai

Abstract Combining the equally valued electrospinning technology with 3D printing can form specific patterns on electrospun fibers and improve the size defects of 3D printing. 3D printing and electrospinning can be used in turn to prepare multi-layered scaffolds with specific structures, such as building blocks or sandwich structures. Melt electrospinning writing (MEW) technology also be used to prepare 3D scaffold with precise structure and composition controlled. Above all, The 3D scaffold retains the complete 3D structure and mechanical properties of 3D printing, while a porous structure similar to the extracellular matrix (ECM) is provided by the electrospun nanofiber network. It is worth mentioning that the combination of the two methods also supports the addition of active substances such as cells, which provides more possibilities for the remodeling and regeneration of tissues and organs or serves as a new catalyst.

Keywords Electrospinning · 3D printing

23.1 Introduction

Before the advent of electrospinning and 3D printing, people could never have imagined that the imaginations of the past would become a reality in the future. In the early developmental stages of electrospinning and 3D printing, novel application areas had not yet been developed because these new material fabrication processes were not well understood. However, in recent years, as researchers have further explored the mechanism of electrospinning and 3D printing processes, these technologies have broken through many obstacles of original application technologies

Z. Zhang · W. Zhang · X. Zhang · B. Yu · M. Tian · L. Zhang · J. Xue (✉)
State Key Laboratory of Organic-Inorganic Composites, Beijing Laboratory of Biomedical Materials, Beijing University of Chemical Technology, Beijing 100029, P.R. China
e-mail: jiajiaxue@mail.buct.edu.cn

X. Peng · Y. Wang · Y. Dai (✉)
School of Chemistry and Chemical Engineering, Southeast University, Nanjing, Jiangsu 211189, P.R. China
e-mail: daiy@seu.edu.cn

© The Author(s), under exclusive license to Springer Nature Switzerland AG 2022

A. Vaseashta and N. Bölgen (eds.), *Electrospun Nanofibers*,
https://doi.org/10.1007/978-3-030-99958-2_23

and achieved rapid development. Therefore, they gradually enter the public's vision and are widely used in many fields. However, it remains a challenge to integrate these two technologies. On the one hand, with the continuous development of nanotechnology, the application of electrospinning technology has become more and more extensive, and it plays an increasingly important role in tissue engineering scaffolds, drug delivery systems, and other aspects [1]. Therefore, electrospinning has immeasurable prospects. On the other hand, 3D printing has been widely applied in the field of industrial design, digital product modeling, etc. It is worth noting that it also plays an essential role in the medical field. Using 3D printing technology to design human cells, tissues and organs have become a hot topic in current research [2]. It is envisioned that 3D printing technology holds great promise in many fields. Taken together, the integration of electrospinning and 3D printing technology can meet the general trend of technological development.

The preparation of nanofibrous materials by electrospinning technology is one of the most important academic and technological activities in the world of materials science and technology in the last few decades. With its advantages of simple fabrication devices, low cost, a wide variety of spinnable materials, and controllable processes, electrospinning has become one of the main ways to effectively prepare nanofibrous materials. Electrospinning is a special fiber manufacturing process in which a polymer solution or melt is jet spun in a strong electric field. Under the action of the electric field, the droplets at the tip of the needle change from spherical to conical (i.e., "Taylor cone") and are extended from the tip of the cone to obtain fiber filaments. In this way, polymer filaments of nanometer diameter can be produced. A rich variety of nanofibers have been prepared by electrospinning technology, including organic, organic/inorganic composite and inorganic nanofibers. German and the United States started early in this field. After long-term development, companies such as Freudenberg in Germany, Donaldson in the United States have core technologies for preparing commercial electrospun fiber products [3]. However, the research of electrospinning in China is still relatively late, due to the problems of small enterprise-scale, extensive fragmentation, and weak independent R&D ability in developing electrospun fiber products. But recently, China's electrospinning industry has entered a period of great strides in development. And the industrialization of electrospun nanofibrous materials has become an inevitable trend in the development of the industry in our state. There are already applications of electrospinning in environmental treatment, personal protection, biomedical, clean energy, national defense and other fields.

3D printing technology is considered one of the core technologies in the third industrial revolution and one of the representative technologies in the fourth industrial revolution. 3D printing is a kind of rapid prototyping technology, also known as additive manufacturing, which is a kind of technology that constructs objects by printing layer by layer based on digital model files, and using bondable materials such as powdered metal or plastic. 3D printing is usually achieved by using digital technology material printers. It is often applied to make models in fields such as mold making and industrial design, and then gradually used in the direct manufacturing of some products. 3D printing has applications in jewelry, footwear,

industrial design, architecture, engineering and construction, automotive, aerospace, dental and medical industries, education, geographic information systems, civil engineering, firearms, and other fields. Its rapid development has inspired all researchers and has been highly valued by governments of various countries. The United States and Germany are recognized as significant manufacturing countries, and they are in the world's leading position in the field of 3D printing [4]. In 2019, for the first time, the University of California, San Diego used rapid 3D printing technology to create a spinal cord scaffold that mimics the structure of the central nervous system, successfully helping rats regain motor function. Although China started late in 3D printing, it has developed rapidly and aroused great attention. The aviation manufacturing has been at the forefront of the world in 3D printing technology. Many aircraft models have used 3D printed parts, and some of the technologies have reached the world's leading level [5]. In 2020, China's first successful flight of the Long March 5B launch vehicle carried a "3D printer". This was China's first 3D printing experiment in space, and the first international 3D printing experiment of continuous fiber-reinforced composite materials in space.

However, as the research progressed, electrospinning and 3D printing have exposed some shortcomings, respectively. As for electrospinning, this technology is challenging to realize the precise control of the shape and the structure. Besides, the problem of insufficient mechanical properties of the prepared structure has become increasingly prominent [6]. As for 3D printing, some traditional 3D printing technologies have low printing resolution, and the wire size can only reach the millimeter level [7]. Additionally, the surface of the printing products is generally rough, which makes it challenging to achieve the ideal effect. Moreover, some biological products will reduce their biological activity when they pass the high-temperature sintering or melting deposition process of 3D printing so that they cannot play their due role. Researchers began to think about how to combine electrospinning with equally valued 3D printing to change the size defects of 3D printing and expand the electrospun products from a simple two-dimensional structure of membranes to three-dimensional structure to improve the corresponding mechanical properties of the product. Therefore, electrospinning combined with 3D printing have gradually come out of the imagination of researchers and into reality. At the same time, some emerging technologies are starting to be applied.

In 2011, Visser J et al. used a new 3D printing technology-melt electrospinning writing to fabricate a 3D printed cartilage for repairing human tissues [8]. This is a process in which an electrically charged polymer melt forms a jet in an electrostatic field to prepare polymer microfibers. This method helps to provide sites for cell growth, as well as meets the demand of mechanical rigidity required by cells. The resulting structure not only promotes the regeneration of injured tissues, but also promotes the growth of new tissues. This revolutionary 3D printing technology based on electrospinning principle opens a new door for biomedical researchers. Many other examples of 3D printing combined with electrospinning have aroused widespread attention for scholars at home and abroad, becoming a significant focus of current research.

In this review, we begin with a discussion on principle/setup of electrospinning and 3D printing, which can provide an overview of these two straightforward and versatile techniques to readers. Then we concentrate on the most relevant examples to highlight the advances related to the development of electrospinning combined with 3D printing. Next, we discuss the materials for electrospinning and 3D printing as well as the engineering of the materials. Finally, we present a large number of industrialized products as examples to illustrate the industrialization progress of these two technologies. The integration of electrospinning and 3D printing is crucial for the preparation of emerging materials and the development of new applications, making a huge contribution to the progress of industrialization in the country and the world.

23.2 The Principle/Setup of Electrospinning and 3D Printing

23.2.1 The Principle/Setup of Electrospinning

Electrospinning involves an electrohydrodynamic process, during which a liquid droplet is electrified to generate a jet, followed by stretching and elongation to generate fibers [9]. As illustrated in Fig. 23.1a, the device of electrospinning is relatively simple, easy to install and use. The setup includes a high-voltage power supply (DC or AC), a syringe pump, a spinneret (usually a hypodermic needle with a blunt tip) and a conductive collector.

During the process of electrospinning, the polymer solution or melt forms a Taylor cone at the tip of the capillary under the action of electric field force. When the electrostatic repulsion force is greater than the surface tension, the charged jet is ejected from the tip of the Taylor cone. The jet initially extends along a straight line and then experiences violent whipping motion due to bending instability [9]. As the solvent evaporates or the melt cools, the fibers are solidified and are constantly stretched into more acceptable diameters, resulting in deposition of solid fibers on the collecting device. Generally, the process of electrospinning can be divided into four continuous steps including charging of the liquid droplet and formation of Taylor cone, extension of the charged jet in the stable stage, thinning of jet flow and growth of electrical bending instability in the unstable stage, jet coagulation and fiber deposition [10–12].

23.2.1.1 Charging of the Liquid Droplet and Formation of Taylor Cone

During electrospinning, the hollow spinning needle is generally connected to the positive electrode of high voltage, while the receiving plate is connected to the negative electrode and keeps a certain distance with needles. Under the action of

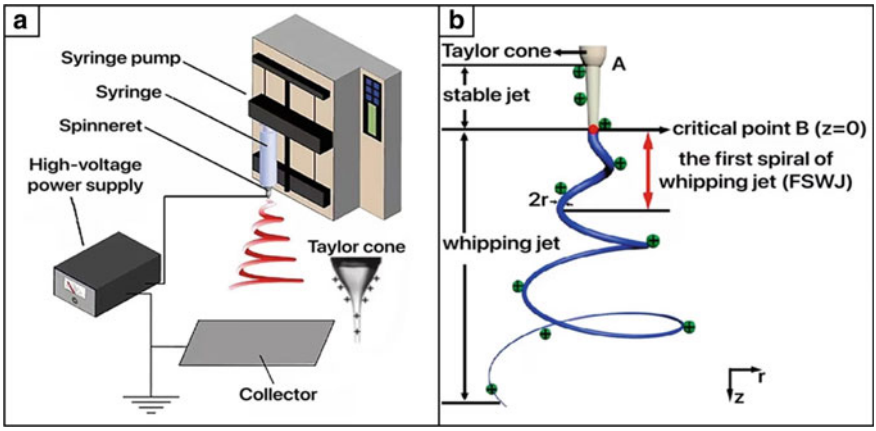


Fig. 23.1 **a** Basic setup for electrospinning. **b** Stable stage and unstable stage in electrospinning. **a** Reprinted with permission from Ref. [13]. Copyright 2017 Accounts of Chemical Research **b** Reprinted with permission from Ref. [14]. Copyright 2021 Elsevier

surface tension, the melt polymer solution presents spherical droplets at the needle. As the voltage increases, the charge with the same polarity as the spinneret will migrate to the surface of the droplet, increasing the droplet's surface charge. As a result, the electrostatic repulsion will be greater than the surface tension, so the droplet on the spinneret surface will be elongated. When the electric field is strong enough at the critical voltage, the electrostatic repulsion can overcome the surface tension and the droplet changes from spherical to conical [15]. In electrospinning, the critical voltage required for the droplet to change into a conical shape is related to the nature of the liquid. When viscous liquid is used in electrospinning, the critical voltage needs to generate stronger electrostatic repulsion to overcome the surface tension and the viscoelastic force of the liquid [9].

23.2.1.2 Extension of Charged Jet in the Stable Stage

During electrospinning, the second stage is that the polymer jet being smoothly stretched and accelerated under the action of electrostatic force, gravity, etc., and the shape of the jet no longer changes with time. As shown in Fig. 23.1b, the charged jet is ejected from the top of the Taylor cone, then accelerated by the electric field, and the jet will be extended in the direction of the electric field as it moves towards the collector [16].

Based on both experimental observations and electrohydrodynamic theories, different models have been developed to describe the behavior of the charged jet. The typical models include the viscoelastic model, thin body model and leaky dielectric model. In the viscoelastic model, a series of the viscoelastic dumbbells is used to

simulate the jet stream [17]. In one study, researchers used a linear Maxwell equation to calculate the 3D trajectory. The calculation results were in agreement with the experimental observations. The thin body model integrates factors such as jet stretch, charge transfer and electric field. The jet is treated as a long, slender object to account for the electrospinning phenomenon [18, 19]. In this case, the electrospinning process only involves whipping rather than splaying. This model is further extended to predict the saturation of whipping amplitude and the diameter of the resultant fibers [20]. The leakage dielectric model considers the effect of nonlinear rheology in the process of jet stretching to describe the jet's motion in electric field [21].

23.2.1.3 Thinning of Jet Flow and Growth of Electrical Bending Instability in the Unstable Stage

The complexity of the electrospinning process is mainly reflected in the unstable stage of the charged jet, which can ultimately determine the diameter and shape of fibers. As illustrated in Fig. 23.1b, the acceleration of the charged jet is gradually attenuated under the effect of surface tension and viscoelastic force after undergoing a short linear motion. When the acceleration drops to zero or a constant, any small fluctuations will destroy the straight movement, which can easily arise instability [22]. In addition, the charged jet will be disturbed by one or more instabilities during its movement [23], depending on the basic parameters such as the surface charge density, radius and jet velocity.

The growth mode of jet instability can be divided into axisymmetric instability and non-axisymmetric instability. Axisymmetric instability includes Rayleigh instability and axisymmetric varicose instability, while non-axisymmetric instability is known as whipping instability. Rayleigh instability is caused by capillary and viscous forces, which may lead to the breakup of the jet into droplets. It is dominated by surface tension and can be suppressed at a strong electric field [9]. Therefore, only in the case of low electric field strength is the effect more obvious. Axisymmetric varicose instability is caused by the force of the surface charge in the tangential electric field, which occurs at a stronger electric field compared with Rayleigh instability. Whipping instability, also known as bending instability, describes long-wave perturbations to the jet as driven by the aerodynamic instability and the lateral electrostatic force in a radial direction relative to the jet, attributing to the electrostatic repulsion among surface charges in a strong electric field [24]. It is found that the main reason why the jet eventually becomes nanofiber is the whipping effect of the jet, which makes the jet continuously stretch and bend forward at a very high frequency [25, 26]. In the electrospinning process, the two unstable modes will compete with each other. The unstable mode with the enormous increase rate of the disturbance amplitude will dominate the jet motion and determine the final shape of the fiber.

23.2.1.4 Jet Coagulation and Fiber Deposition

During the process of elongation, solvent evaporation or melt cooling makes the jet solidify into fibers, which are finally deposited on the collecting device. When the solidification process is slow, the elongation of the charged jet can last for a more extended period of time to generate fibers with a thinner diameter [9]. After deposition, most of the charges on the fibers are quickly dissipated through the grounded collector. However, a measurable amount of residual charges still remain on the surface of the collected fibers due to the low conductivity of most materials [27, 28]. The buildup of residual charges on the collected fibers tends to repel the similarly charged jet, causing a pendulum-like motion for the electrified jet [29]. As a result, the achievable thickness of electrospun fibrous membranes is often restricted by an upper limit of about 0.5–1 mm [30].

23.2.2 The Principle/Setup of 3D Printing

3D printing is a rapid prototyping technology, the principle of which works basically the same as ordinary printers, but the printing materials are somewhat different. The printing materials of ordinary printers are paper and ink, while 3D printing materials contain plastics, ceramics, metals, sand, etc. Based on the digital model, the printing materials in printers can be superimposed layer by layer under the control of the computer, and finally, the blueprint in the computer can be turned into a real object [31].

A complete 3D printing process consists of the following parts. Firstly, establish a 3D digital model through 3D modelling software such as Auto CAD. Then use the professional software equipped with the printer to obtain layer-by-layer cross-sectional data, generating a file format recognizable by the printer (usually an STL format file), and transmit this information to the 3D printer. Next, the 3D printer will control the machine to stack the two-dimensional slices according to the description of the slice data file until a solid object is formed. Finally, after the model is printed, there are usually burrs or rough sections. Meanwhile, post-processing of the model is required, such as curing, peeling, trimming, coloring, etc., in order to complete the production of the required model.

According to the state of the materials used in 3D printing and the differences in fabricating methods, 3D printing technology can be roughly divided into four types, including Fused Deposition Modeling (FDM), Stereo Lithography Apparatus (SLA), Digital Light Processing (DLP) and Three-Dimensional Printing (3DP). A more detailed discussion of these four types is provided in the following subsections.

23.2.2.1 Fused Deposition Modeling (FDM)

As shown in Fig. 23.2a, during the FDM process, the filaments on the spools are fed into the liquefier head by a driver gear and a grooved bearing, then they are extruded above the glass transition temperature. The first desired layer is deposited onto the print bed, which moves downward one-layer thickness for subsequent layer deposition. Such processes will be repeated in the same way until the part is completed [32].

FDM is a widely used 3D printing technology with a simple process and low cost. The materials currently available for this technology are mainly low-melting materials. Different materials have different melting temperatures. However, FDM is only suitable for the production of small and medium-sized model parts, and the structural strength of the forming parts is weak in the direction of thickness. Most importantly, the molding speed and the efficiency of FDM are low. These shortcomings make FDM somewhat limited in its application.

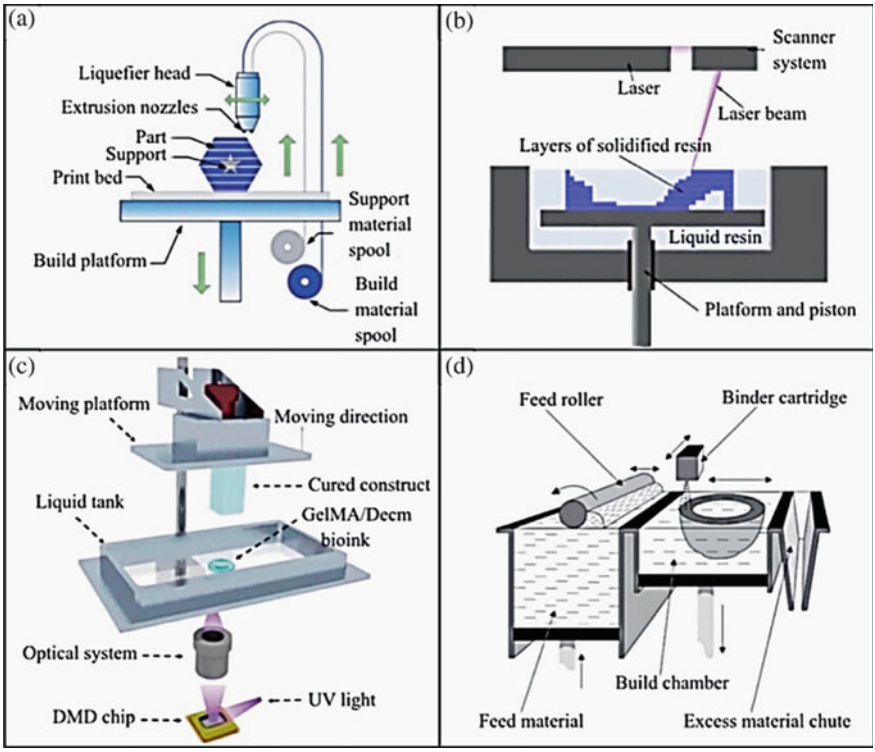


Fig. 23.2 **a** Schematic of FDM process. **b** Schematic of SLA process. **c** Schematic of DLP process. **d** Schematic of 3DP process. **a** Reprinted with permission from Ref. [32]. Copyright 2016 Journal of Composite Materials. **b** Reprinted with permission from Ref. [33]. Copyright 2019 Multimedia Tools and Applications. **c** Reprinted with permission from Ref. [34]. Copyright 2020 Elsevier. **d** Reprinted with permission from Ref. [33]. Copyright 2019 Multimedia Tools and Applications

23.2.2.2 Stereo Lithography Apparatus (SLA)

As shown in Fig. 23.2b, SLA is an additive manufacturing process. An ultraviolet laser is focused on a vat of photopolymer resin material to make it solidified and form a single layer of the desired 3D shape. This process is repeated until the shape is completed [35].

SLA is the first commercial rapid prototyping method that permits to print objects with extremely complicated geometries while preserving the details and the quality simultaneously. The materials available for this technology are photopolymer materials, such as acrylic resin and epoxy resin. The high price of raw materials makes costs one of the major disadvantages of this molding method, making the ordinary use of this technology only affordable to some companies and laboratories. Moreover, the liquid resins are generally toxic and irritating, consequently, some precautions are to be taken in order to work with them using suitable equipment and tools.

23.2.2.3 Digital Light Processing (DLP)

As shown in Fig. 23.2c, DLP uses a digital micromirror device (DMD) to project the cross-sectional graphics of the product onto the surface of the liquid photosensitive resin, so that the irradiated resin can be light-cured layer by layer. The most prominent features of DLP are its fast printing speed and high molding accuracy. DLP can be used to produce relatively delicate parts, such as jewelry and dental molds. However, compared with other large 3D printers, DLP printing technology can't print large items, so most of them are desktop 3D printers.

23.2.2.4 Three-Dimensional Printing (3DP)

During 3DP (Fig. 23.2d), a printed material is sprayed onto the build tray in an ultra-thin layer and then cured with ultraviolet light. After a layer of jet printing and curing been completed, the machine's built-in workbench will drop a forming layer with extreme precision and continue to eject the print material until the entire print is completed [33].

A large variety of materials are applied in 3DP. In theory, any materials that can be made into powders are capable to be formed through this technology, including plastic powders such as ABS and nylon, as well as metal powders, ceramic powders, etc. What's more, this method can simultaneously use two materials with different mechanical characteristics. However, the mechanical properties and the surface quality of the objects manufactured through this technology are not quite perfect, so it is generally only used for conceptual models or handicrafts rather than functional tests.

Although the principles of electrospinning and 3D printing seem to be quite different, their application fields have certain similarities, and both of them have the ability to promote the development of industrialization in the future. However,

electrospinning and 3D printing have their own shortcomings. So how to combine these two technologies so as to achieve complementary advantages is the focus of our research.

23.3 The Integration of Electrospinning and 3D Printing

23.3.1 Near-Field Electrospinning

23.3.1.1 Introduction of Near-Field Electrospinning

For conventional electrospinning, the bending instability of the jet can pose a negative major on the deposition of fibers. During conventional electrospinning, chaotic and irregular fibers will be generated and deposited on the collector. At the same time, the high voltage used in conventional electrospinning raises concerns about safety and energy consumption issues. Later researchers have explored and improved upon traditional electrospinning with a series of attempts, including using magnetic and electric fields to assist in altering the deposition of fibers, increasing the electrical conductivity of the spinning fluid, and applying physical forces such as rotating mechanical shafts. One of the most effective way is to change the spinning distance, that is, near-field electrospinning, during which only altering the spinning distance can effectively reduce the voltage during electrospinning and precisely regulate the deposition of fibers, facilitating fiber patterning and expanding the use of near-field fibers in fields such as tissue engineering, wearable devices, sensors and more.

Near-field electrospinning is based on conventional electrospinning with reduced collection distance and voltage. While combined with 3D printing technology, the adding movable collection platform can achieve straight writing capability to get various shapes of fibers on the collector according to a preset trajectory. When the collection distance is reduced, the instability of the spinning can be controlled, and the fibers can be deposited in a successive phase after the liquid injection, reducing the irregularity of the product and realizing a controllable fabrication of fibers. The resistance generated during the movement of the collecting platform weakens the residual charge on the collector, facilitating the observation of individual fibers and the precise regulation of fiber shapes, resulting in a wide range of 2D and 3D products.

In 2003, Kameoka et al. used a self-prepared scanning silicon tip needle to prepare aligned fibers. They immersed gold on the top surface, and applied a spinning distance of 0.5–1 cm to successfully prepare aligned fibers using PEO as the raw material. This method confirmed the ability to produce aligned fibers in a low voltage mode and under near-field conditions [36]. In 2006, Sun et al. introduced the concept of near-field electrospinning, with a minimum voltage of 600 V and a minimum spinning distance of 500 μm [37]. Fibers between 50 and 500 nm in diameter were produced. The deposition of fibers in a direct, continuous, and controlled manner was achieved.

23.3.1.2 Near-Field Versus Conventional Electrospinning

Near-field electrospinning is an improvement on conventional electrospinning and thus shares many aspects. For instance, the equipment is similar, which consists a high-voltage power supply, syringe, a spinneret, and a collector. Besides, both of them can be used for spinning in solution and the melt state and can be used with dynamic or static collectors. However, near-field and conventional electrospinning are different in the setting of spinning conditions. Conventional electrospinning has a lengthy collection distance of fibers, usually 5–15 cm, at a voltage of 10–20 kV, making it difficult to control the deposition of fibers [38]. With near-field electrospinning, the collection distance of fibers is significantly reduced to 500 μm–5 cm, and the jet is deposited directly in the collector at the edge of the linear section. The voltage of the spinning process is around 10–30 kV for conventional electrospinning, while near-field electrospinning requires less voltage due to the reduced distance, around 0.6–30 kV. The fluid flow rate for near-field electrospinning is also reduced to 0.01–1 mL/h.

In terms of fiber morphology, conventional electrospinning equipment can generate disordered fibers due to the random, unregulated spraying of the liquid. And the spinning liquid has chaotic nature, so it is always challenging to fabricate ordered fibers. On the other hand, near-field electrospinning can generate ordered fibers due to the precise regulation of fibers. It can achieve the regulation of a single fiber, making it easy to produce highly controllable patterned products.

Due to some characteristics of conventional electrospinning such as relatively simple, commercial and mature equipment, batch industrial production can be achieved through conventional electrospinning. Near-field electrospinning adds a movable 2D/3D platform to the electrospinning equipment compared to conventional electrospinning, and most near-field electrospinning requires to use more expensive multi-axis microscopes, which increases the complexity of the equipment. The polymer solution impregnated at the tip of the near-field electrospinning needle limits the production of large batches, and the shorter collection distance limits the stretching and thinning of fibers, which ultimately results in larger diameter fibers and small-scale production. But on the other hand, improved near-field electrospinning has been used to obtain 3D fiber products from non-conductive materials such as glass sheets, polymer-coated glass slides, and hydrogel blocks [38]. In contrast to conventional electrospinning, near-field electrospinning eliminates the need for electrostatic substrates and expands the prospects for near-field electrospinning in tissue engineering. Due to the convenient displacement in the x/y axis of the collector, near-field electrospinning avoids the problems of edge fiber deposition caused by changes in direction during fiber collection during conventional electrospinning, creating smoother edges. Near-field electrospinning technology offers the possibility to meet the demand for precise control of fiber morphology, and therefore has very promising applications in the fields of nano direct writing technology, large-area ordered deposition of nanofibers, high-precision deposition of nanofibers, and microelectronic systems.

23.3.1.3 Modulation of the Near-Field Electrospinning

Similar to conventional electrospinning, near-field electrospinning process can be regulated by adjusting the electrospinning parameters. For near-field electrospinning, the fiber density can be modified by adjusting the displacement parameters of the table and the pattern filling capacity. The concentration of polymer, flow rate of polymer, voltage, and distance from the spinneret to the collector can also be modified to regulate the characteristics of fibers. Next, we will describe the parameters that can be regulated in this process in detail.

Firstly, the spinning solution concentration is one of the adjustable parameters. In 2003, Kameoka et al. investigated the effects of polymer solution and spinning distance on fibers by fabricating PEO fibers through near-field electrospinning [36]. In a concentration gradient of 5–30%, the diameter of the fiber increased with spinning concentration and viscosity, resulting in a gradual increasing in fiber diameter. The concentration of the polymer was kept above a certain value. When the concentration was low, the viscosity of the polymer was not sufficient for the production of continuous fibers, leading to the failure of electrospinning.

Secondly, the flow rate of the spinning fluid is another one of the adjustable parameters. During near-field electrospinning, the fiber diameter increases with the flow rate of the spinning fluid within a certain range. When the polymer flow rate is low, the jet becomes discontinuous beads.

Thirdly, the collection speed is also one of the adjustable parameters. As the collection speed increases, the irregularity of the deposited fibers gradually decreases. Typically, as the collector velocity increases to a certain range, the deposited fibers gradually change from an irregular shape to an aligned one. In one study, as the collection distance decreased from 0.35 m/s to 0.08 m/s, the fibers presented in the form of straight line, waved line, single circle coil, and multi circle coil, respectively [39].

Additionally, the collection distance can also be adjusted. In near-field electrospinning, the fiber morphology can be controlled by the distance between the spinneret and the collector. And the collection distance can be adjusted by computer software, as the distance from the spinneret to the collector increases, the diameter of the fibers decreases. This decreasing of fiber diameter is due to the increased stretching of the fiber. It should be noted that the relationship between collection distance and fiber diameter in near-field electrospinning is contrary to that in traditional electrospinning. In one study of 3D near-field electrospinning, the fiber collection distance increased from 1.6 mm to 2.4 mm, and the fiber diameter decreased from 3.81 to 1.54 μm [40].

Finally, the voltage of electrospinning is adjustable during near-field electrospinning. Similar to conventional electrospinning, in near-field electrospinning, if the spinning voltage is too low while other conditions remain the same, the electric field force on the polymer cannot overcome the surface tension of the droplets, the spinning process cannot occur. As the electric field increases to a critical voltage, the spinning process occurs. When the spinning voltage is too high, the instability of the spinning process increases, the jet whip phenomenon occurs, consequently, the fiber

diameter distribution is more extensive and presents an irregular shape. In particular, for near-field electrospinning, changing the speed of collector displacement and the capacity of drawing the patterns results in changes of fiber density [38].

23.3.1.4 Applications in the Near-Field Electrospinning

By reducing the spinning distance, near-field electrospinning technology reduces the voltage during the spinning process and improves the fibers' controllability, and reduces the energy consumption. The reduced voltage value increases the safety and reliability, which makes near-field eletrospinning a more environmentally friendly and safe way to produce fibers. Owing to the characteristic of precisely regulating the fibers, near-field electrospinning technology gets a broader application in the fields of micro and nano 3D device production, direct-write fiber manufacturing and the field of tissue engineering scaffolds preparation et al.

23.3.1.5 Summary and Future Perspectives On Near-Field Electrospinning

Near-field electrospinning is a promising and versatile fiber manufacturing method, which enhances the ability to precisely control fiber deposition, enabling the manufacture of high-quality products in areas such as high precision devices. Additionally, near-field electrospinning has the potential for scale-up industrial production and high reproducibility of products, which can be developed in some areas in the future, including further exploration of the mechanism of near-field electrospinning to reduce deviations between computer design and the actual production process, commercial promotion of near-field electrospinning technology to manufacture equipment with small space and low production costs. The current scope of application is still relatively concentrated, so we look forward to exploring and expanding more new applications.

23.3.2 Melt Electrospinning

23.3.2.1 Introduction to Melt Electrospinning

The difference between melt electrospinning and conventional electrospinning is that the raw material needs to be in a molten state, accompanied with a higher voltage, higher temperature of the nozzle, and a movable collection device. Therefore, the equipment is relatively complex consisting of a high-pressure generator, a feeder, an extruder, and a fiber collection device. With the aid of a computer platform, the high voltage is loaded onto the nozzle. The polymer in the molten state is continuously

extruded and collected in the movable collection platform at a computer pre-defined deposition position, finally completing the melt electrospinning process.

For melt electrospinning, the viscosity is higher than that of solution electrospinning, so the further linear distance during electrospinning makes it easier to control the jet and achieve fiber deposition in the linear phase of the jet. At the same time, the movement of the collector will avoid the bending state of the melt due to its viscoelasticity and mechanical forces, resulting in a more precise and ordered fibers on the collector. Melt electrospinning is also highly manipulable and can be easily combined with 3D printing to produce 3D products with a higher degree of control over shape and size.

In 2011, using melt electrospinning, Toby D. Brown successfully established a process link between solution electrospinning and direct writing, matching the collector translation speed to the jet velocity to control the deposition position of the fibers. The melt electrospun fibers possessed a moving collection platform for controlled deposition, confirming that melt electrospun fibers can be repeatedly stacked longitudinally and horizontally to obtain PCL microfibers.

23.3.2.2 Melt Electrospinning Versus Conventional Electrospinning

Melt electrospinning can avoid the instability of solvent volatilization and solvent pollution of the environment during solution electrospinning, which contributes to environmental protection while improving spinning efficiency and product performance. Thus, the production process does not require ventilation, which reduces production costs.

Under equivalent collection conditions, melt electrospinning has a higher viscosity and lower electrical conductivity compared to conventional electrospinning during the spinning process of the jet, which brings stability in the linear motion phase of the fibers when deposited and solidified at the designated collection location. The high specific surface area and internal porosity of the fibers prepared by melt electrospinning give them natural advantages as scaffold materials, which can be applied in biomedical (Fig. 23.3).

Due to the presence of the plasticizing system, melt electrospinning technology requires a higher voltage value during the spinning process compared to solution electrospinning, increasing the risk of electrostatic interference. The equipment for melt electrospinning is also relatively more complex and has higher manufacturing costs.

23.3.2.3 Regulation of Melt Electrospinning

In melt electrospinning, melt temperature, fiber collection distance, the movement speed of the collection device, nozzle diameter, feed air pressure, collection speed, and other factors all impact the final shape of the fibers. Matching the collection

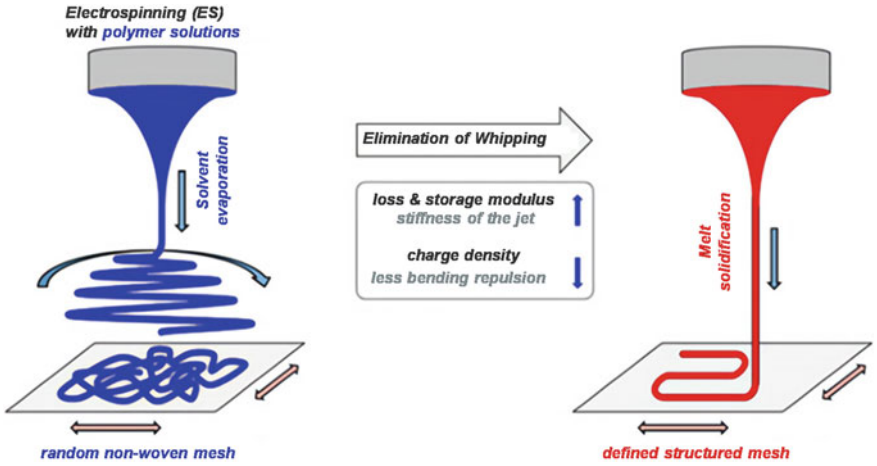


Fig. 23.3 Schematic illustration of melt electrospinning versus conventional electrospinning. Reprinted under the terms and conditions of the Creative Commons CC BY-NC-ND 3.0 License [41]. Copyright 2015 IOP Science

speed with the extrusion speed is the most critical factor. The critical travel speed (CTS) of the collection device is an essential indicator of the fiber condition.

When the movement speed of the collector is faster than the critical speed, the diameter of fibers becomes more acceptable, and one-dimensional products can be generated. However, from a spatial point of view, the mechanical properties of the fibers are reduced at this point, which is not conducive to the manufacture of 3D products. When the collector velocity is less than the jet velocity, the deposition of fibers is shifted forward, the melt electrospinning process is affected, and the fibers show a non-linear fluid pattern or do not function properly. When the two are matched, the fibers are closest to an ordered deposition. Therefore, it is necessary to keep the jet velocity equal to the collection velocity during fiber production through melt electrospinning. In other words, ensuring that s_c (speed of the collector) is approximately equal to s_j (the jet speed) during actual production, a smoother pattern with smoother edges can be obtained when the jet can reach the collector in a straight line (Fig. 23.4) [42]. The velocity of the collection device should change in response to changing conditions, as changes in external conditions such as air pressure can cause the changing of s_j jet velocity during the actual production process. In particular, increasing the speed of the collector when other conditions such as flow rate are constant reduces the diameter of the fibers due to the introduction of a drawing effect.

Fiber collection distance: In the process of melt electrospinning, the collection distance of the fibers should not be too small. Otherwise, the melt cannot be extruded for sufficient time to cure, which will affect its distribution on the collector, thus affecting the morphology and mechanical properties of the fibers. Another effect of the increased melt temperature during the writing process is the fracture of the fibers.

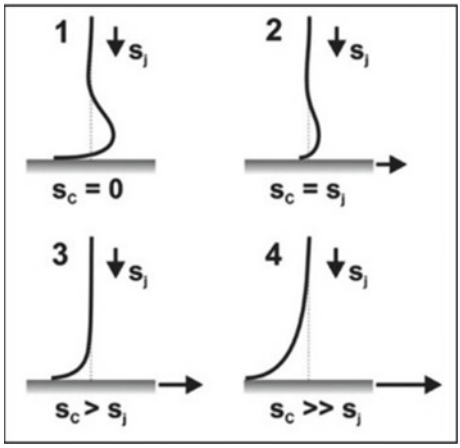


Fig. 23.4 The shape of the fiber jet during melt electrospinning is influenced by the velocity of the collector concerning the jet velocity. Reprinted with permission from Ref. [42]. Copyright 2011 Wiley online library

When the melt temperature rises, the molten fibers do not have sufficient cohesion, resulting in the inability to penetrate the collected fibers, which leads to incomplete of fibers [42].

Melt temperature: Different materials have different melting points, and the processing temperature can be chosen for particular materials. The temperature of the melt has an impact on the final product during the actual preparation process. For the reasons of environment and time, the lower limit of the processing temperature range of the chosen material is preferred, which reduces the heat carried away by the melt during cooling.

As the temperature increases, the viscosity of the melt decreases, improving the melt flow behavior of the extruded polymer. As the melt is extruded from the needle, the decrease in viscosity means that the melt passing through the needle at the same time is subject to less resistance and passes in larger volumes, thus increasing the diameter of the collected fibers. However, when the melt temperature is too high, the fibers do not undergo sufficient solidification and thus show inhomogeneity at the collector (Fig. 23.5).

23.3.2.4 Overview of Melt Electrospinning Applications

Melt electrospinning eliminates the need for solvents in the process, avoiding the impact of solvent residues on product performance and applications, making the spinning process and products more environmentally friendly. What's more, melt electrospinning allows for precise regulation of material in the linear phase. The diameter of fibers can be adjusted by regulating various parameters. Multi-phase structures can also be connected with different structures printed together, giving unlimited product

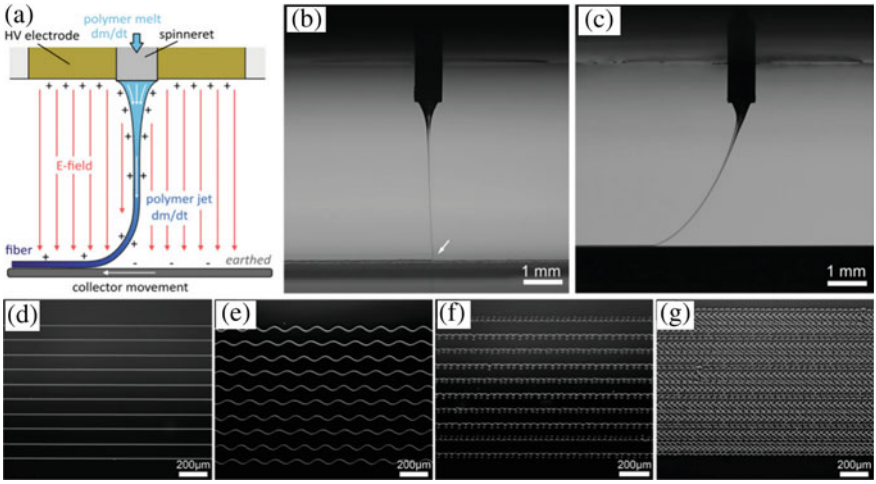


Fig. 23.5 Example of matching the collector velocity to the velocity of the jet for the fibers. In the diagram. **a** Shows fiber collection in equilibrium without the presence of fiber pulses. **b** Shows the PCL written directly on the plate collector at CTS. **c** Shows a series of fibers collected at increasingly lower speeds. **d** Shows the fiber morphology when the collector speed is faster than CTS. **e** Speed at 0.75 CTS. **f** Speed at 0.35 CTS. **g** Speed at 0.10 CTS. Reprinted under the terms and conditions of the Creative Commons CC BY-NC-ND 4.0 License [43]. Copyright 2019 Wiley online library. **a** Reprinted under the terms and conditions of the Creative Commons CC BY-NC-ND 3.0 License [44]. Copyright 2016, The Authors, published by De Gruyter. **b**, **c** Reprinted under the terms and conditions of the Creative Commons CC BY-NC-ND 4.0 License [43]. Copyright 2019 Wiley online library. **d–g** Reproduced under the terms and conditions of the Creative Commons CC BY-NC-ND 3.0 License [44]. Copyright 2016, The Authors, published by De Gruyter

versatility. Materials with different pore sizes can also be prepared [45]. The products prepared by melt electrospinning have a high level of reproducibility. As more and more raw materials are developed to complete the melt electrospinning process, melt electrospinning have a broad future in fabricating biomedical materials, flexible electronic devices, soft robotics et al.

23.3.2.5 Summary and Outlook for Melt Electrospinning

Melt electrospinning has unique advantages in the field of manufacturing due to its solvent-free preparation process and other characteristics. Melt electrospinning is able to create multi-phase complex materials and achieve product diversification, making it a promising application in many fields such as biological scaffold manufacturing. The future development direction of melt electrospinning can be summarized as follows.

- Simulation of the jet stream during spinning with the aid of computer technology to achieve digital precision regulation and enhance the repeatable manufacture of the product.
- Continue to explore diverse materials, explore practical applications of melt electrospun products in more areas through different combinations of shapes.
- Most of the current melt electrospinning printers are obtained by improving on the commercially available devices. In the future, we hope to see more advanced melt electrospinning equipment to expand their commercialization and impact.

23.3.3 Other 3D Printed Electrospinning Technology

In addition to near-field electrospinning and melt electrospinning, other methods that combine electrospinning with 3D printing have also been developed to produce more diversified products and achieve more types of 3D printed electrospun products.

Han et al. prepared a gelatin/poly(lactic-co-glycolic acid) (PLGA) 3D printed scaffold by dissolving gelatin and PLGA with excellent biocompatibility and biodegradability in hexafluoro isopropanol solution using a melt electro-writing printer at room temperature [46]. In this process, the temperature of the substrate was appropriately increased to enable accelerated evaporation of the solvent, resulting in rapid formation of a high-viscosity liquid. The viscosity of the solution can also be regulated by adjusting the ratio of the ink. The fine diameter and large surface area of the gelatin/PLGA 3D printed scaffold allow it to be applied to cartilage injury repair. Chen et al. prepared hyaluronic acid (HA)/polyethylene oxide (PEO) nanofibers through electrospinning, and then the nanofibers were dehydrated, cut, and freeze-dried to obtain short fibers. The obtained short fibers were used as bio-ink for 3D printing. Using freeze-dried and cross-linked short fibers as 3D printing inks, the pore shapes of products can be controlled to obtain 3D scaffolds which can effectively mimic the structure of extracellular matrix (ECM). The scaffold combined with chondrocytes as a tissue-engineered scaffold can achieve satisfactory cartilage regeneration in vivo.

By combining stable jet electrospinning with a removable collector and adjusting the viscoelasticity of the solution, stable fibers can be prepared from nondegradable polymers, what's more, the instabilities of the jet can also be eliminated. Yuan et al. mixed a small amount of high molecular weight PEO in silk protein to form a stable fiber jet during electrospinning and obtained pre-patterned products by the collector's movement (Fig. 23.6) [47]. Finally, they obtained patterned 3D ultrafine fibers, which were proved to be suitable for cell culture.

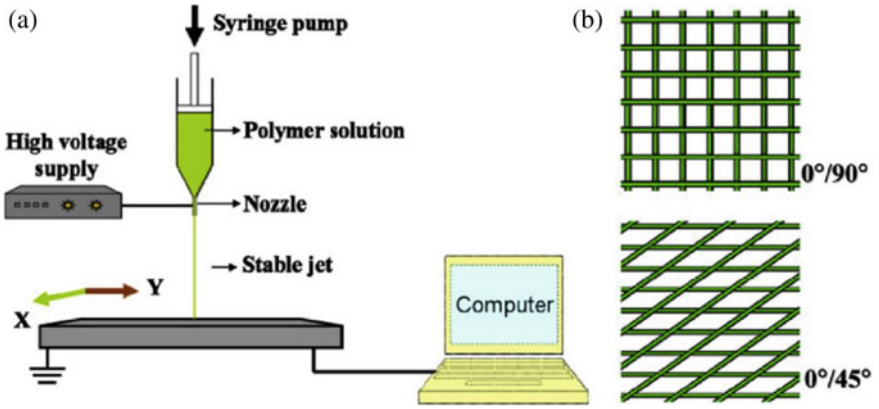


Fig. 23.6 Schematic illustration of the stable jet electrospinning. Reprinted with permission from Ref. [47]. Copyright 2015 IOP Publishing

23.4 Materials for Electrospinning and 3D Printing

A wide selection of materials is available for conventional electrospinning, ranging from small molecule materials to composites and organic polymers. For small molecule materials, they can be used directly for electrospinning as long as they can self-assemble and produce sufficient entanglement. For composites, when sol–gel chemistry is achieved, they can be spun directly into nanofibers. Last but not least, as the most common electrospinning materials, polymers can be directly spun to form fiber products after mixing and dissolving. Many natural and synthetic polymers can be made into electrospun fibers or scaffolds. Natural polymers include collagen, alginates, chitosan, gelatin, etc. While synthetic polymers include polystyrene (PS), polyvinyl chloride (PVC), polycaprolactone (PCL), poly(lactic acid) (PLA), PLLA, etc. [48].

For near-field electrospinning and melt electrospinning, the most commonly used raw materials are still polymers. Of all the conditions that need to be met for a polymer to be used for electrospinning, the molecular weight of the polymer is an important one. When the molecular weight is too low, continuous fibers cannot be generated normally. Besides, the concentration, volatilization, and conductivity of the solution and molten state should also be taken into account. In particular, thermoplastic polymers are often chosen for melt electrospinning, for they have properties that enable better bending and stretching above a specific temperature and can be cured after cooling. Due to these properties, thermoplastic polymers have unique advantages in melt electrospinning. Melt electrospinning technology can prepare scaffolds with high accuracy and good biocompatibility with porosity, but it is difficult to print natural polymer materials [46], which make it inadequate in the actual manufacturing process for the limited choosing of materials. Polymers with low melting point such as PCL shows good thermal stability and melt processing

performance, reducing processing costs and difficulties. Common materials used for melt electrospinning include PCL, polypropylene (PP), PLGA, PLA et al. In practice, functional polymers are often blended with other polymers to obtain the desired spinning solution.

PCL is one of the most widely used materials in the process of 3D printed electrospinning. Precisely, PCL fibrous product own the smallest fiber diameter among the fibers prepared by melt electrospinning from medical-grade polymers as raw materials. In addition, the combined use of multiple materials can improve the performance of each material when used alone. For example, the combination of poly(3-hydroxybutyrate-co-3-hydroxyhexanoate) (PHBH) and PLA can improve the processing performance of PHBH and the mechanical properties of PLA [49]. Alternatively, by mixing PCL with polyethylene glycol (PEG), the viscosity of the PCL melt will be changed and the polarity of the jet can be increased.

23.5 Engineering of the Materials

At present, electrospinning is the most suitable and standard technology for preparing nanofibers, whether polymer materials, inorganic materials, or hybrid materials [50]. Most importantly, electrospinning is the only technology capable of mass-producing continuous nanofiber particles of polymers, metals, and oxides for catalytic applications from various polymers and precursors. Emerging 3D printing technology has become a new component in the development of rich fiber scaffolds due to its powerful ability to precisely control the composition, structure, and shape of the supports [51]. The in-fiber porosity, geometry, structure, composition, and properties of nanofibers and scaffolds can be fabricated to target specific applications by controlling the materials and methods of electrospinning. A variety of nanoparticles can also be incorporated into the nanofibers and scaffolds to bestow new functions. Various physical and chemical methods can be used to decorate nanofibers and scaffolds to incorporate nanoparticles. By manipulating the alignment and patterning, the scaffolds of 3D printing and electrospinning nanofibers can be assembled to control the morphology, alignment, and stacking into ordered arrays or hierarchical structures.

23.5.1 Control of In-Fiber Porosity and Geometry

Previously, 3D scaffolds were manufactured using traditional techniques such as 3D printing [52], gas foams [53], direct electrospinning [54], electrospray [55], and freeze-drying [56]. However, the scaffolds manufactured using these methods do not have fully interconnected holes. It is challenging to control the pore size and porosity of the scaffold. To overcome these bottlenecks, 3D printing technology has been extensively researched. 3D printing is a promising technology for engineering

biomaterials characterized by customizable shapes and fully connected channels. It is commonly used in the design and manufacture of intricate tissue scaffolds such as bones, and electrospinning can control the microstructure of materials. The combination of 3D printing with electrospinning has been widely used in 3D scaffolds [57].

In recent years, it has been found that various polymers based on electrospinning and 3D printing technology have gained extensive attention in biomedical applications. Therefore, it also puts forward higher requirements to the performance of materials. The control of the microstructure of biomaterials, such as the porosity and mechanical properties of the material, has attracted widespread attention. Jacob H et al. used 3D jet writing to make polymer fibers into an open-pore structure. The mechanically stable scaffold structure is formed by controlling the fiber orientation and pore geometry. This study realizes that the spacing of parallel fibers is less than 0.3 nm, and the fiber verticality is less than 1.1 nm. Moreover, the geometry of the 3D scaffold is highly controllable while the consistency is within 5% [58].

Zhi Yang et al. combined 3D printing technology and electrospinning technology to prepare biological scaffolds with macro and microstructures. The study showed that the pore size of the biological scaffold can be controlled at 424.47 ± 58.49 um, and the porosity is around $70.46 \pm 2.48\%$. It successfully provided a new set of intelligent scaffolds for abdominal wall defects and hernia repair [59]. The application scenarios of the composite scaffold can be precisely controlled by adjusting the inner diameter and geometric shape of the composite scaffolds fiber.

23.5.2 Incorporation of Nanoparticles

The incorporation of nanoparticles into scaffolds and electrospinning nanofibers brings additional functionality and enhanced performance. Nanoparticles can be manufactured from materials ranging from metals to metal oxides, carbon, and polymers. There are two main strategies for binding/attaching nanoparticles to scaffolds and nanofibers: (i) direct binding during the process (ii) post-processing of the brackets and spun nanofibers.

For the direct method, nanoparticles are added to the solution for electrospinning and 3D printing. Alternatively, nanoparticles are electro sprayed onto the surface of nanofibers during electrospinning. In another example, Pt nanoparticles are grown in situ on Nb-doped TiO_2 nanofibers by heat treatment of composite nanofibers containing Pt (II) 2, 4-pentlandite (metal precursor) in the air 500 °C. At heating rates of 2 and 10 °C min^{-1}. The sizes of Pt nanoparticles are 3.5 nm and 10 nm, respectively [60]. Nanoparticles with particular morphology can also be synthesized in situ by controlling the heat treatment conditions.

Nanoparticles can also be generated on the surface of scaffolds and nanofibers by surface deposition, in-situ synthesis, or hydrothermal treatment. For example, negatively charged gold nanoparticles and positively charged lysozymes are alternately deposited on negatively charged cellulose nanofibers.

23.5.3 Control of Morphology, Alignment, and Stacking

The combination of electrospinning technology and 3D printing has the potential to simulate the extracellular matrix. They can create scaffolds with stable mechanical strength and control cell behavior by controlling the fiber shape [61], alignment [62], and stacking so that the scaffold prepared by this technology has excellent biocompatibility. Cian Vyas et al. successfully prepared a dual-scale scaffold composed of 3D printed and electrospun PCL fibers (Fig. 23.1). And the microscope can be controlled by combining a neatly arranged low-density electrospinning meshes with 3D printed scaffolds [63]. The structure is well used to regulate cell behavior. At the same time, the study shows it's possible to potentially change the mindset, alignment and stacking of fibers by changing the shape of the 3D printed and adding a third component (such as a conductive material) to the scaffold. It is excellent to design specific structures to control cell behavior. As we all know, the scaffold prepared by the traditional 3D printing technology is not conducive to the profound growth of cells [64]. Using the combination of electrospinning technology and 3D printing technology, electrospun nanofibers introduce micro-nano structures, and the orientation of the fibers can be adjusted to satisfy the depth of growth of the cells. The orientation of the fibers can be adjusted to meet the depth of cell growth by combining electrospinning and 3D printing as well as introducing micro-nano structures. GeunHyung Kim et al. combined a 3D dispensing system and electrospinning process to produce a hierarchical three-dimensional structure composed of micro-sized polymer chains and micro/nanofibers. A three-dimensional structural scaffold composed of vertically arranged and continuous thin nanofiber nets was fabricated [65]. By controlling the orientation of the fibers, a three-dimensional scaffold suitable for cell growth can be prepared. The regulation of fiber morphology, alignment, and stacking of fiber morphology and the structural control of 3D scaffolds will be a research trend in the future, which is one step closer to clinical application. Studying the morphology and arrangement of electrospinning fibers alone can be extended to the combination of 3D printing technology and electrospinning technology. The regulation of fiber microstructure will be an issue that we need to study further (Fig. 23.7).

23.6 Scale-Up Production for Industrial Applications

Traditional 3D printing technology has the advantages of accurate molding and controllable structure. However, due to the limitation of equipment, its minimum processing accuracy must be greater than 200 μm [66]. This scale is unfavorable to cell adhesion and guiding cells to grow to the expected position. The traditional electrospinning technology has a processing precision at hundreds of nanometers. But generally, it commonly processes thin-film products with relatively uniform compositions and structures, similar to a planar structure. Combining the two advantages,

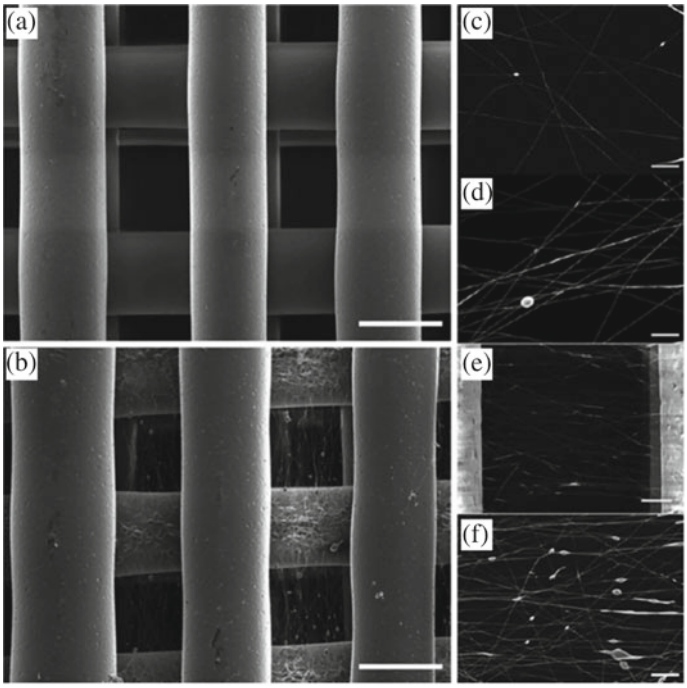


Fig. 23.7 SEM images of the **a** 3D-printed only scaffold and **b** dual-scale scaffold with electrospun (45 s) nanofibers (scale bar = 300 μm). Electrospun mesh density as function of time **c** 15 s, **d** 30 s, **e** 45 s, and **f** 120 s [scale bar = 20 μm, (**e** 50 μm]. Reprinted with permission from Ref. [63]. Copyright 2019 Elsevier

3D printing and electrospinning technology can fulfill the nano-scale microstructure of fibers, content the personalized three-dimensional customization of product components, and complex shapes according to the needs of regeneration and repair of different tissues and organs [67]. The combination of electrospinning technology and 3D printing technology has a wide range of application scenarios in electronics, environment, energy, and biomedicine [68]. However, the technical bottleneck that is tough to scale up manufacturing has dramatically hindered its commercialization process. Therefore, solving various technical problems in the mass manufacturing process and increasing the manufacturing rate of technology-integrated materials are the keys to its commercial application. Many countries (including China, the United States, Japan, South Korea et al.) are working to achieve the industrialized manufacturing goals of this technology in biomedicine.

23.6.1 Basic Research on Scale-Up Production of 3D Printed Electrospinning

The 3D printing scaffold retains the complete 3D structure and mechanical properties of 3D printing, while the electrospun nanofiber network provides a porous structure similar to the extracellular matrix [69, 70]. At the same time, the combination of these two technologies also support the addition of active substances such as cells. The biomedicine provides more possibilities for the remodeling and regeneration of tissues and organs.

23.6.1.1 Bone Tissue Repair or Regeneration

Bone tissue repair or regeneration engineering provides an excellent platform for bone tissue, and bone tissue engineering is an alternative treatment method for damaged bones. Compared with traditional tissue transplantation (including autologous transplantation and allogeneic transplantation), bone tissue engineering technology eliminates the problems of insufficient donors, limited supply, and immune rejection [71]. The three necessary components of bone regeneration engineering are stem cells that can differentiate into bone cells, growth factors that stimulate the behavior of bone-forming cells, and a scaffold that mimics the extracellular matrix [72]. Among various scaffolds, highly porous nanofiber scaffolds are potential candidates for supporting cell functions. The manufacturing firms of bone regeneration scaffolds mainly include electrospun nanofiber scaffolds [65], three-dimensional printing scaffolds, microspheres, nanoparticles, hydrogel [73], and scaffolds prepared by other traditional and emerging methods. Recent studies have shown that improvements based on electrospinning and 3D bioprinting technologies make it possible to change nanofiber's chemical and physical properties to regenerate specific target tissues [74]. Micro and nano structures composed with hierarchical functional scaffold tissue engineering is a crucial goal of the research.

A common bottleneck of electrospun nanofibers for bone regeneration or repair is preparing three-dimensional tissue engineering scaffolds and the weak mechanical properties of the prepared scaffolds, limiting these materials in clinical applications [52]. Electrospun nanofibers begin to be combined with various specific scaffolds to enhance mechanical strength and fracture toughness, regulate degradation behavior and cell behavior. The standard method of combination: in a two-step process, electrospun nanofibers are directly coated on the surface of the 3D printed scaffold, or the fibers are cut into pieces to fill the pore structure of the 3D scaffold, or combined with biological agents, such as collagen and then mixed to prepare 3D printing bio-ink printing stent [75]. The materials prepared by combining the two technologies, the bio-tubular scaffolds for the manufacture of artificial blood vessel grafts, have been reported for the first time. In recent years, Yu et al. have used electrospinning and 3D printing technology to electrospun PCL/gelatin nanofibers [76]. The fibers

are evenly dispersed and filled into the grid of the PCL printed stent to form a three-dimensional composite stent. This study proves that the 3D composite scaffold has excellent mechanical stress, outstanding biocompatibility, good cell migration and proliferation capabilities [77]. Naghieh et al. develop polylactic acid microfibers and a new type of bone tissue engineering scaffold material combined with a gelatin-forsterite fibrous layer. These 3D multi-level hierarchical structures have excellent mechanical strength and biocompatibility in bone tissue engineering applications (Fig. 23.8a) [78]. These first reports show that combining the two technologies can provide the additional advantages of using a single technology and has potential in future research. In addition to the common method of evenly dispersing and filling electrospun nanofibers into the 3D scaffold, some researchers also directly deposit the fibers on the surface of the scaffold. For example, electrospun PCL nanofibers are deposited on the vertical pattern of the PCL line produced by 3D printing (Fig. 23.8b) [65]. A hybrid scaffold composed of delicate chains filled with electrospun fibers is prepared (Fig. 23.8b inset). In a similar study, Park et al. used a hybrid process of direct polymer melt deposition and electrospinning to prepare nanofiber polymer scaffolds to provide favorable cell adhesion and growth conditions. A polycaprolactone/collagen nanofiber matrix is deposited between the three-dimensional structure layers by an electrospinning process (Fig. 23.8c) [79].

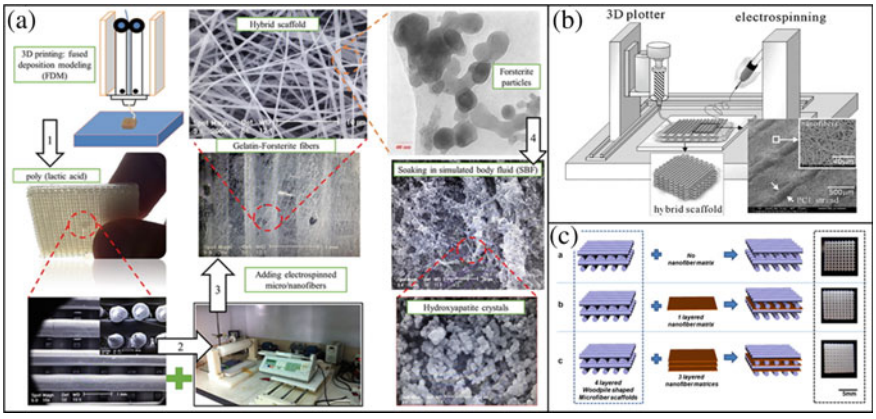


Fig. 23.8 **a** Schematic illustration showing the synthetic steps of hierarchical scaffolds including poly (lactic acid) (PLA) micro struts and nanocomposite gelatin-forsterite fibrous layers and corresponding SEM image. **b** Schematic illustration showing the preparation of 3D nanofiber scaffold by combining 3D printing and electrospinning. The inset shows an SEM image of a hybrid PCL 3D scaffold. **c** Schematic diagrams and photographs of the three types of hybrid scaffolds used in the cell culture experiments. (a) Type I has no nanofiber matrix and only a PCL scaffold as a control specimen. PCL scaffolds combined with (b) a one-layer PCL/collagen nanofiber matrix (type II) and (c) three-layer PCL/collagen nanofiber matrices (type III). **a** Reprinted with permission from Ref. [78]. Copyright 2019 Elsevier. **b** Reprinted with permission from Ref. [65]. Copyright 2008 Macromolecular Rapid Communication. **c** Reprinted with permission from Ref [79]. Copyright 2008 Elsevier

With the continuous innovation of the two technologies, the cartilage regeneration scaffold prepared by Weiming Chen et al. can achieve satisfactory cartilage regeneration in vivo based on the 3D printing electrospinning technology experiment [80]. In this study, one-dimensional (1D) gelatin/polylactic acid-glycolic acid (PLGA) electrospun fibers are processed into inks suitable for 3D printing in the first time. The electrospun fiber ink successfully makes a 3D printing scaffold with a precisely controlled shape and large pores by combining 3D printing and freeze-drying (Fig. 23.3). In addition, the fiber surface morphology is similar to that of the natural extracellular matrix (ECM). So that the 3D printed joint cartilage cells can achieve satisfactory cartilage regeneration in the body. There are more researches on innovative scaffolds prepared by combining three-dimensional printing and electrospinning. The innovative scaffolds prepared by Yang, Z et al. have been successfully tested in rats with abdominal wall defects [59] (Fig. 23.9).

The combination of 3D printing and electrospinning technology in biomedical applications is becoming more and more extensive, leading to expanded production for clinical applications as well as future research targets. The continuous improvement of these primary research methods promotes the mass production of 3D printing and electrospinning to prepare extraordinary skeletons. It provides ideas for the industrial manufacturing of intelligent skeletons.

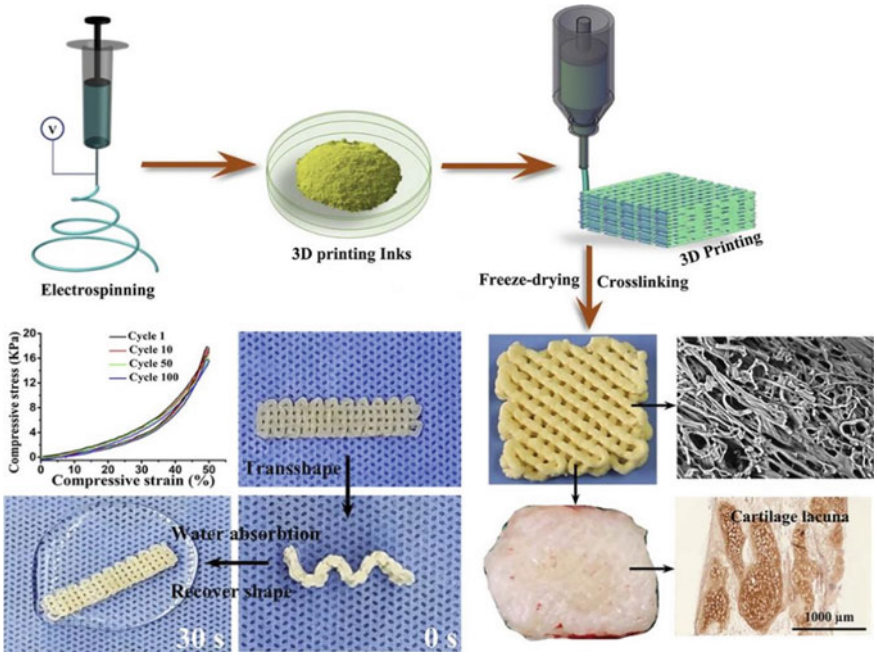


Fig. 23.9 Schematic illustration showing the synthetic steps of 3D-printed fiber-based scaffold for cartilage regeneration. Reprinted with permission from Ref. [80]. Copyright 2019 Elsevier

23.6.2 Current Situation of Scale-Up Manufacturing Equipment for 3D Printing Electrospinning

China's research on medical devices used to guide the regeneration and repair of tissues and organs began in the mid to late 1990s. At present, the development of implantable medical devices in China is mainly focused on structural products (such as skin, bone, tendon et al.). Many products are still in the preclinical and clinical research stages. The gap between developed countries such as Europe and the United States is pronounced. Therefore, although the current implantable medical devices have been extensively studied, there is still a big gap compared with the actual needs of current clinical applications. Implantable medical devices have developed rapidly, with a growth rate of more than 20%. Neomodulus corporation pioneers the use of 3D printing electrospinning technology as the core, combining traditional electrospinning with conventional 3D printing technology and using 3D electrospinning technology to make a gradient layer biopolymer, which makes the two raw materials and structures tightly combined. Physical isolation is achieved in space to meet different tissue and organ regeneration, and repair needs to achieve clinical trials [81]. Dr. Stephan Meskath, a German expert at Neomodulus, constructs a bionic bio-skeleton through a 3D bio-printing production line. The product is currently undergoing trial production process design, and the sample structure design has been finalized.

The combination of 3D printing and electrospinning technology has many applications. But further research is needed to realize industrialized production. Therefore, the following issues may remain to be resolved in the future:

- Batch development and production of equipment combining 3D printing and electrostatic spinning technology;
- In terms of electrospinning technology, using the principle of electrospinning technology to design electrospinning equipment with simple structure and convenient operation, which can be better combined with 3D printing technology;
- The intelligent skeleton prepared by batch electrospinning and 3D printing technology accelerates its clinical application and realizes industrialized production;
- Theoretically, explore the batch 3D printing electrospinning technology, and combine theory and practice with improving the 3D printing electrospinning equipment.

23.7 Concluding Remarks

In this review, a comprehensive overview of electrospinning and 3D printing has been presented, including their principles, methods, materials, and applications. We begin with the discussion of their principles and typical apparatus, and then we introduce the latest progress of electrospinning combined with 3D printing from three aspects, namely near-field electrospinning, melt electrospinning, and other 3D printed electrospinning technologies. What's more, we briefly summarize the characteristics of

materials applied in electrospinning and 3D printing. Next, in order to address the size defects of 3D printing, expand the structure of electrospinning and improve the corresponding mechanical performance of the products, we discuss several engineering methods, such as control of in-fiber porosity, geometry, morphology, alignment, stacking, and incorporation of nanoparticles. In the end, we introduce the scale-up production for industrial applications, conducting an overview of progress in industrialization. With the expansion of the range of available materials and the advancement of preparation technology, electrospinning combined with 3D printing will be more and more widely used, especially in the biomedical field. We can enable the manufacture of higher quality products in areas such as high precision devices by near-field electrospinning and create more complex scaffold materials by melt electrospinning. Taken together, we believe that the wide application of electrospinning combined with 3D printing will bring about revolutionary advances in the preparation and application of new materials.

References

1. Shao, H., Zhang, X. B., LIU, S. S., Ding, Y. F., Xu, J., & Chen, F. Y. (2011). Application and prospect of electrospinning technique. *Guangzhou Chemical Industry*, *39*, 42–43.
2. Yang, X. Y., Zhan, C., Ming, L. I., et al. (2016). Application progress of 3D printing in medical field. *Fudan University Journal of Medical Sciences, 43*(4), 490–494
3. Wang, B., & Ping, H. U. (2007). Development of electrospinning at home and abroad. *Plastics.*
4. Li, X., Mo, H., Li, S. S., et al. (2016). Research progress on 3D printing technology process control problem. *Acta Automatica Sinica, 42*(7), 983–1003.
5. Liu, M., Zhang, K., & Fan, Z. Z. (2013). Application of 3D printing technology in the field of aviation manufacturing. *Equipment Manufacturing Technology*.
6. Chen, W., Chen, S., Morsi, Y., El-Hamshary, H., El-Newhy, M., Fan, C., & Mo, X. (2016). Superabsorbent 3D scaffold based on electrospun nanofibers for cartilage tissue engineering. *ACS applied materials & interfaces*, *8*(37), 24415–24425.
7. Yu, Y., Hua, S., Yang, M., et al. (2016). Fabrication and characterization of electrospinning/3D printing bone tissue engineering scaffold. *RSC Advances*, *6*(112), 110557–110565. 10.1039.C6RA17718B.
8. Visser, J., Melchels, F. P. W., Jeon, J. E., et al. (2015). Reinforcement of hydrogels using three-dimensionally printed microfibres. *Nature Communications, 6*.
9. Xue, J., Wu, T., Dai, Y., et al. (2019). Electrospinning and electrospun nanofibers: Methods, materials, and applications. *Chemical Reviews.*
10. Li, D., & Xia, Y. (2004). Electrospinning of nanofibers: Reinventing the wheel? *Advanced Materials, 16*(14), 1151–1170.
11. Sun, B., Long, Y. Z., Zhang, H. D., et al. (2014). Advances in three-dimensional nanofibrous macrostructures via electrospinning. *Progress in Polymer Science, 39*(5), 862–890.
12. Liao, Y., Loh, C. H., Tian, M., Wang, R., & Fane, A. G. (2018). Progress in electrospun polymeric nanofibrous membranes for water treatment: Fabrication, modification and applications. *Progress in Polymer Science*, *77*, 69–94.
13. Xue, J., Xie, J., Liu, W., et al. (1976). Electrospun nanofibers: New concepts, materials, and applications. *Accounts of Chemical Research, 50*(8), 1976–1987.
14. Lei, S., Xiong, C., Quan, Z., Qin, X., & Yu, J. (2021). Controlled stretching of the first spiral in electrospinning whipping jet via surface charge. *Polymer*, *217*, 123443.
15. Liu, Z. X., Liu, Y., Wang, X., An, Y., Ding, Y. M., & Yang, W. M. (2012). Phenomena analysis of taylor cone, jet whipping and corona in process of electrospinning. *Plastics.*

16. Collins, R. T., Jones, J. J., Harris, M. T., & Basaran, O. A. (2008). Electrohydrodynamic tip streaming and emission of charged drops from liquid cones. *Nature Physics*, *4*(2), 149–154.
17. Reneker, D. H., Yarin, A. L., Fong, H., & Koombhongse, S. (2000). Bending instability of electrically charged liquid jets of polymer solutions in electrospinning. *Journal of Applied Physics*, *87*(9), 4531–4547.
18. Hohman, M. M., Shin, M., Rutledge, G., & Brenner, M. P. (2001). Electrospinning and electrically forced jets. I. Stability theory. *Physics of Fluids, 13*(8), 2201–2220.
19. Hohman, M. M., Shin, M., Rutledge, G., & Brenner, M. P. (2001). Electrospinning and electrically forced jets. II. Applications. *Physics of Fluids*, *13*(8), 2221–2236.
20. Fridrikh, S. V., Jian, H. Y., Brenner, M. P., & Rutledge, G. C. (2003). Controlling the fiber diameter during electrospinning. *Physical Review Letters*, *90*(14), 144502.
21. Feng, J. J. (2003). Stretching of a straight electrically charged viscoelastic jet. *Journal of Non-Newtonian Fluid Mechanics, 116*(1), 55–70.
22. He, J. H., Yue, W., & Zuo, W. W. (2005). Critical length of straight jet in electrospinning. *Polymer, 46*(26), 12637–12640.
23. Saville, D. A. (1970). Electrohydrodynamic stability: Fluid cylinders in longitudinal electric fields. *Physics of Fluids, 13*(12), 2987–2987.
24. Dhr, A., & Aly, B. (2008). Electrospinning jets and polymer nanofibers—science direct. *Polymer, 49*(10), 2387–2425.
25. Shin, Y. M., Hohman, M. M., Brenner, M. P., & Rutledge, G. C. (2001). Experimental characterization of electrospinning: the electrically forced jet and instabilities. *Polymer*, *42*(25), 09955–09967.
26. Shin, Y. M., Hohman, M. M., Brenner, M. P., & Rutledge, G. C. (2001). Electrospinning: A whipping fluid jet generates submicron polymer fibers. *Applied physics letters*, *78*(8), 1149–1151.
27. Catalani, L. H., Collins, G., & Jaffe, M. (2007). Evidence for molecular orientation and residual charge in the electrospinning of poly(butylene terephthalate) nanofibers. *Macromolecules, 40*(5), 1693–1697.
28. Collins, G., Federici, J., Imura, Y., & Catalani, L. H. (2012). Charge generation, charge transport, and residual charge in the electrospinning of polymers: A review of issues and complications. *Journal of Applied Physics*, *111*(4), 044701.
29. Tao, H., Reneker, D. H., & Yarin, A. L. (2008). Pendulum-like motion of straight electrified jets. *Polymer, 49*(8), 2160–2169.
30. Filatov, Y., Budyka, A., & Kirichenko, V. (2008). Electrospinning of Micro- and nanofibers: Fundamentals in separation and filtration processes. *Journal of Engineered Fibers and Fabrics.*
31. Li, Q. A., & Wang, Q. (2013). 3D Printing: A new technology for learning. *Journal of Distance Education.*
32. Ning, F., Cong, W., Hu, Y., & Wang, H. (2017). Additive manufacturing of carbon fiber-reinforced plastic composites using fused deposition modeling: Effects of process parameters on tensile properties. *Journal of Composite Materials*, *51*(4), 451–462
33. Zhou, K., Liao, J., & Zhou, X. (2019). Counterfeiting ancient Chinese Armour using 3D-printing technology. *Multimedia Tools and Applications, 78*(1), 1103–1116.
34. Qmab, C., Ywab, D., Yang, L., et al. (2020). Fabrication of liver microtissue with liver decellularized extracellular matrix (dECM) bioink by digital light processing (DLP) bioprinting—sciencedirect. *Materials Science and Engineering: C, 109.*
35. Roulet, M., Atkins, C., Hugot, E., Lemared, S., Lombardo, S., & Ferrari, M. (2018, May). 3D printing for astronomical mirrors. In *3D Printed Optics and Additive Photonic Manufacturing* (Vol. 10675, p. 1067504). International Society for Optics and Photonics.
36. Kameoka, J., Orth, R., Yang, Y., Czaplewski, D., Mathers, R., Coates, G. W., & Craighead, H. G. (2003). A scanning tip electrospinning source for deposition of oriented nanofibres. *Nanotechnology*, *14*(10), 1124.
37. Sun, D., Chang, C., Li, S., et al. (2006). Near-Field electrospinning. *Nano Letters, 6*(4), 839–842.

38. He, X. X., Zheng, J., Yu, G. F., You, M. H., Yu, M., Ning, X., & Long, Y. Z. (2017). Near-field electrospinning: progress and applications. *The Journal of Physical Chemistry C*, *121*(16), 8663–8678.
39. Zheng, G., Li, W., Wang, X., Wu, D., Sun, D., & Lin, L. (2010). Precision deposition of a nanofibre by near-field electrospinning. *Journal of Physics D: Applied Physics*, *43*(41), 415501.
40. Fattahi, P., Dover, J. T., & Brown, J. L. (2017). 3D Near-Field electrospinning of biomaterial microfibers with potential for blended microfiber-cell-loaded gel composite structures. *Advanced Healthcare Materials, 6*(19), 1700456.
41. Hochleitner, G., Jüngst, T., Brown, T. D., et al. (2015). Additive manufacturing of scaffolds with sub-micron filaments via melt electrospinning writing. *Biofabrication, 7*(3), 035002.
42. Brown, T. D., Dalton, P. D., & Hutmacher, D. W. (2011). Direct writing by way of melt electrospinning. *Advanced Materials, 23*(47), 5651–5657.
43. Robinson, T. M., Hutmacher, D. W., & Dalton, P. D. (2019). The Next Frontier in Melt Electrospinning: Taming the Jet. *Advanced Functional Materials, 29*(44), 1904664.
44. Hochleitner, G., Youssef, A., Hrynevich, A., Haigh, J. N., Jungst, T., Groll, J., & Dalton, P. D. (2016). Fibre pulsing during melt electrospinning writing. *BioNanoMaterials*, *17*(3-4), 159–171.
45. Wunner, F. M., Wille, M. L., Noonan, T. G., Bas, O., Dalton, P. D., De-Juan-Pardo, E. M., & Hutmacher, D. W. (2018). Melt electrospinning writing of highly ordered large volume scaffold architectures. *Advanced Materials*, *30*(20), 1706570.
46. Han, Y., Jia, B., Lian, M., et al. (2021). High-precision, gelatin-based, hybrid, bilayer scaffolds using melt electro-writing to repair cartilage injury. *Bioactive Materials, 6*(7), 2173–2186.
47. Yuan, H., Zhou, Q., Li, B., Bao, M., Lou, X., & Zhang, Y. (2015). Direct printing of patterned three-dimensional ultrafine fibrous scaffolds by stable jet electrospinning for cellular ingrowth. *Biofabrication*, *7*(4), 045004.
48. Jayasinghe, S. N. (2013). Cell electrospinning: A novel tool for functionalising fibres, scaffolds and membranes with living cells and other advanced materials for regenerative biology and medicine. *The Analyst, 138*(8), 2215–2223.
49. Murphy, J. P., Brockway, M. C., Andriolo, J. M., et al. (2018). Fabrication of optically active fiber mats via melt electrospinning. *MRS Communications, 8*(3), 1098–1103.
50. Hosseini, N. S., & Khenoussi, N. (2017). Structuring of electrospun nanofiber mats by 3D printing methods. In *Electrospun Materials for Tissue Engineering and Biomedical Applications* (pp. 73–85). Woodhead Publishing.
51. Chen, T., Bakhshi, H., Liu, L., Ji, J., & Agarwal, S. (2018). Combining 3D printing with electrospinning for rapid response and enhanced designability of hydrogel actuators. *Advanced Functional Materials, 28*(19), 1800514.
52. Chen, W., Chen, S., Morsi, Y., et al. (2016). Superabsorbent 3D scaffold based on electrospun nanofibers for cartilage tissue engineering. *ACS Applied Materials & Interfaces, 8*(37), 24415–24425.
53. Chen, Y., Shafiq, M., Liu, M., et al. (2020). Advanced fabrication for electrospun three-dimensional nanofiber aerogels and scaffolds. *Bioact Mater, 5*(4), 963–979.
54. Gao, Q., Gu, H., Zhao, P., Zhang, C., Cao, M., Fu, J., & He, Y. (2018). Fabrication of electrospun nanofibrous scaffolds with 3D controllable geometric shapes. *Materials & Design*, *157*, 159–169.
55. Yi, B., Zhang, H., Yu, Z., Yuan, H., Wang, X., & Zhang, Y. (2018). Fabrication of high performance silk fibroin fibers via stable jet electrospinning for potential use in anisotropic tissue regeneration. *Journal of Materials Chemistry B*, *6*(23), 3934–3945.
56. Si, Y., Yu, J., Tang, X., et al. (2014). Ultralight nanofibre-assembled cellular aerogels with superelasticity and multifunctionality. *Nature Communications, 5*, 5802.
57. Smith, L. A., & Ma, P. X. (2004). Nano-fibrous scaffolds for tissue engineering. *Colloids and Surfaces. B, Biointerfaces, 39*(3), 125–131.
58. Jordahl, J. H., Solorio, L., Sun, H., et al. (2018). 3D Jet writing: Functional microtissues based on tessellated scaffold architectures. *Advanced Materials, 30*(14), e1707196.

59. Yang, Z., Song, Z., Nie, X., Guo, K., & Gu, Y. (2020). A smart scaffold composed of three-dimensional printing and electrospinning techniques and its application in rat abdominal wall defects. *Stem Cell Research & Therapy*, *11*(1), 1–11.
60. Cavaliere, S., Subianto, S., Chevallier, L., Jones, D. J., & Rozière, J. (2011). Single step elaboration of size-tuned Pt loaded titania nanofibres. *Chemical Communications*, *47*(24), 6834–6836.
61. Denchai, A., Tartarini, D., & Mele, E. (2018). Cellular response to surface morphology: electrospinning and computational modeling. *Front Bioeng Biotechnol, 6*, 155.
62. Wang, K., Liu, L., Xie, J., Shen, L., Tao, J., & Zhu, J. (2018). Facile strategy to generate aligned polymer nanofibers: Effects on cell adhesion. *ACS Applied Materials & Interfaces*, *10*(2), 1566–1574.
63. Cian, V., Gokhan, A., Enes, A., et al. (2020). Three-dimensional printing and electrospinning dual-scale polycaprolactone scaffolds with low-density and oriented fibers to promote cell alignment. *3D Printing and Additive Manufacturing, 7*, 3.
64. Sachlos, E., & Czernuszka, J. T. (2003). Making tissue engineering scaffolds work. Review: the application of solid freeform fabrication technology to the production of tissue engineering scaffolds. *Eur Cell Mater, 5*(29–39), 39–40.
65. Kim, G., Son, J., Park, S., & Kim, W. (2008). Hybrid process for fabricating 3D hierarchical scaffolds combining rapid prototyping and electrospinning. *Macromolecular Rapid Communications*, *29*(19), 1577–1581
66. Kwan, J. G. (2013). Design of electronics for a high-resolution, multi-material, and modular 3D printer.
67. Kang, M. S., Lee, S. H., Park, W. J., Lee, J. E., Kim, B., & Han, D. W. (2020). Advanced techniques for skeletal muscle tissue engineering and regeneration. *Bioengineering*, *7*(3), 99.
68. Chen, S., Li, R., Li, X., & Xie, J. (2018). Electrospinning: An enabling nanotechnology platform for drug delivery and regenerative medicine. *Advanced Drug Delivery Reviews*, *132*, 188–213.
69. Yoshimoto, H., Shin, Y. M., Terai, H., & Vacanti, J. P. (2003). A biodegradable nanofiber scaffold by electrospinning and its potential for bone tissue engineering. *Biomaterials, 24*(12), 2077–2082.
70. Vyas, C., Ates, G., Aslan, E., Hart, J., Huang, B., & Bartolo, P. (2020). Three-dimensional printing and electrospinning dual-scale polycaprolactone scaffolds with low-density and oriented fibers to promote cell alignment. *3D Printing and Additive Manufacturing, 7*(3), 105–113.
71. Liu, X., & Ma, P. X. (2004). Polymeric scaffolds for bone tissue engineering. *Annals of Biomedical Engineering, 32*(3), 477–486.
72. Udomluck, N., Koh, W. G., Lim, D. J., & Park, H. (2019). Recent developments in nanofiber fabrication and modification for bone tissue engineering. *International Journal of Molecular Sciences, 21*(1), 99.
73. Visser, J., Melchels, F. P., Jeon, J. E., et al. (2015). Reinforcement of hydrogels using three-dimensionally printed microfibres. *Nature Communications, 6*, 6933.
74. Vong, M., Speirs, E., Klomkliang, C., Akinwumi, I., Nuansing, W., & Radacsi, N. (2018). Controlled three-dimensional polystyrene micro-and nano-structures fabricated by three-dimensional electrospinning. *RSC Advances*, *8*(28), 15501–15512.
75. Yang, X., Lu, Z., Wu, H., Li, W., Zheng, L., & Zhao, J. (2018). Collagen-alginate as bioink for three-dimensional (3D) cell printing based cartilage tissue engineering. *Materials Science and Engineering: C*, *83*, 195–201.
76. Lee, S. J., Heo, D. N., Park, J. S., et al. (2015). Characterization and preparation of bio-tubular scaffolds for fabricating artificial vascular grafts by combining electrospinning and a 3D printing system. *Physical Chemistry Chemical Physics: PCCP, 17*(5), 2996–2999.
77. Fan, X., & Keynton, R. S. (2019). Fabrication and characterization of biopolymer fibers for 3D oriented microvascular structures. *Journal of Micromechanics and Microengineering, 29*(8).
78. Naghieh, S., Foroozmehr, E., Badrossamay, M., & Kharaziha, M. (2017). Combinational processing of 3D printing and electrospinning of hierarchical poly (lactic acid)/gelatin-forsterite scaffolds as a biocomposite: Mechanical and biological assessment. *Materials & Design*, *133*, 128–135.

79. Park, S. H., Kim, T. G., Kim, H. C., Yang, D. Y., & Park, T. G. (2008). Development of dual scale scaffolds via direct polymer melt deposition and electrospinning for applications in tissue regeneration. *Acta Biomaterialia*, *4*(5), 1198–1207.
80. Chen, W., Xu, Y., Liu, Y., et al. (2019). Three-dimensional printed electrospun fiber-based scaffold for cartilage regeneration. *Materials & Design, 179*, 107886.
81. NEOMODULUS, http://www.Neomodulus.com Trademark-Neo Modulus (Suzhou) Medical Sci-Tech Co., Ltd. (bizapedia.com)



Zhaoxu Zhang was born in Dingzhou, Hebei Province. He received the B.S. degree in Materials Science and Engineering from Beijing University of Chemical technology, Beijing, China, in 2020. He is pursuing the M.S. degree in Materials Science and Engineering at Beijing University of Chemical Technology with Prof. Liqun Zhang. His research interests include materials for bone tissue engineering and near-field electrospinning.



Wei Zhang was born in Heze City, Shandong Province, China in 1999. He received the B.S. degree in Polymer Materials and Engineering from Shandong University of Science and Technology in 2020. He is currently studying for his master's degree in Materials and Chemical Engineering from Beijing University of Chemical Technology. His research interests include the application of elastomer materials in biomedical devices.



Xiaoli Peng was born in Zunyi, Guizhou Province, China. She has been a graduate student at Southeast University in the School of Chemistry and Chemical Engineering since 2020 with Prof. Yunqian Dai. Her current research interests include high performance flexible electromagnetic materials and their applications in wearable devices and systems.



Xindan Zhang was born in 1995 in Jilin City, Jilin Province, majored in polymer materials and engineering at Beijing University of chemical technology with a bachelor's degree and materials science and engineering at Beijing University of chemical technology with a master's degree. She is pursuing the doctorate degree at Beijing University of Chemical Technology with Prof. Jiajia Xue. Her research direction is electrospinning soft tissue repair (skin and spinal cord).



Yunpeng Wang received the B.S. degree in mineral processing engineering from Henan Polytechnic University, Jiaozuo, China, in 2019. He is pursuing the Ph.D. in materials physical and chemistry at Southeast University.His research interests are new nanofibers for clean energy, high efficiency catalysis and environmental applications.



Bing Yu received his Ph.D. in Macromolecular Chemistry and Physics from Shanghai Jiao Tong University in 2015 with Prof. Xuesong Jiang and Prof. Jie Yin. He worked as a postdoctoral fellow in the Prof. Yue Zhao's group at University of Sherbrooke from 2015 to 2017. He is now working as an Associate Professor at the Beijing University of Chemical Technology. His research interests include the design, preparation, and modification of intelligent polymer nanocomposites as well as the investigation of self-healing, shape memory, and self-assembly behavior of polymer materials.



Ming Tian is currently a professor in College of Materials Science and Engineering at Beijing University of Chemical Technology. He received his B.S. degree (1994) from Shenyang University of Chemical Technology, and M. S. degree (1997) in Composites and Ph.D. (2004) in Materials Science from Beijing University of Chemical Technology. In 2006, he worked as visiting scholar in Department of Chemistry at South Dakota School of Mines and Technology, USA. His research focuses on rubber science and technology, polymer blends and composites.



Liqun Zhang obtained his B.Sc. (1990), M.Sc. (1992), and Ph.D. (1995) from Beijing University of Chemical Technology. He has been a professor in College of Materials Science and Engineering at Beijing University of Chemical Technology since 1995. He worked as a visiting scholar at the University of Akron (1990–2000) and then as a postdoctoral fellow at Case Western Reserve University (2000–2001). His research interests include rubber science and engineering, polymer nanocomposites, bio-based and biomedical materials, polymer processing engineering, etc.



Jiajia Xue received her Ph.D. in Materials Science and Engineering from Beijing University of Chemical Technology in 2015 with Prof. Liqun Zhang. She worked as a postdoctoral fellow in the Prof. Younan Xia's group at Georgia Institute of Technology from 2015 to 2019. She is now working as a professor at the Beijing University of Chemical Technology. Her research interests include the fabrication of nanomaterials and scaffolds for tissue engineering and regenerative medicine.



Yunqian Dai was born in Longchang, Sichuan Province, China. She received her Ph.D. from Southeast University in 2011 with Prof. Yueming Sun. She spent two years in Prof. Xia's group as a visiting graduate student from 2008–2010. She has been a full professor at Southeast University in the School of Chemistry and Chemical Engineering since 2019. Her current research interests include electrospun nanofibers and their applications in catalysis, environmental science, and energy technology.

Chapter 24
Electrospun Nanofibers for Industrial and Energy Applications



Narayanan Vimalasruthi, Ganesan Vigneshkumar, Shanmugasundaran Esakkimuthu, Krishnamoorthy Sivakumar, and Thambusamy Stalin

Abstract In today's world, electrostatic fiber spinning is promising and meticulous nanotechnology that produces fine fibers with micro to nano dimensions. The electrospun nanofibers material used in the recent nanoworld has to be modified to improve several qualities. The surface-to-volume ratio, porosity, stability, and usefulness, in particular, allow them to work in industrial domains. Sensors, medication delivery, wound healing, medicines, and the food sector are just a few examples. The input of several criteria for nanofibers and the moderation of electrospinning tools varied. Electrospun materials of various morphologies, forms, structures, and nano sizes are attracted economic interest. Electrospun nanofibers based on cyclodextrin inclusion complexes have extensively developed over the last decade. And there's more testing to be done to improve solubility and optimize the releasing profile. The polymeric electrospun nanofibers encapsulated, cyclodextrin-based inclusion complex (CDs-ICs-P-NF) is the main factor in that field. CDs-ICs-NF (polymer-free complex electrospun nanofibers) are also promising materials for industries. Food and medications have in that. Carbon nanofibers (CNFs) electrospun are a desirable component in the energy sector. Because of their surface areas, pore balance, and reactivity, supercapacitors, batteries, and fuel cells are an example in this area. But there are numerous papers accessible on wound healing and medicine delivery methods. However, few articles are only available in the food industry, pharmaceuticals, and energy conversion. It works in research and development for developments of CDs-ICs-P-NF, CDs-ICs-NF, and CNFs materials and the properties emphasis in this paper's application. Nanofiber's applications are now limited to laboratory-scale production, although technical advancements are intriguing in this regard. Electrospinning is becoming more popular, and it is causing a lot of buzz in the food, pharmaceutical, and energy industries. There's a feature on nanofiber in this review.

N. Vimalasruthi · G. Vigneshkumar · S. Esakkimuthu · T. Stalin (✉)
Department of Industrial Chemistry, Alagappa University, Karaikudi, Tamil Nadu 630003, India
e-mail: stalin.t@alagappauniversity.ac.in

K. Sivakumar (✉)
Department of Chemistry, Faculty of Science, Sri Chandrasekharendra Saraswathi Viswa Mahavidyalaya University (SCSVMV) (Deemed to be University), Enathur, Kanchipuram, Tamil Nadu 631561, India
e-mail: chemshiva@gmail.com; sivakumar.k@kanchiuniv.ac.in

© The Author(s), under exclusive license to Springer Nature Switzerland AG 2022

A. Vaseashta and N. Bölgen (eds.), *Electrospun Nanofibers*,
https://doi.org/10.1007/978-3-030-99958-2_24

Keywords Electrospinning · Carbon nanofibers · Cyclodextrin-based inclusion complex · Energy

24.1 Introduction

The review article summarises recent research on the potential applications of polymeric electrospun nanofibers. To start something using an efficient and versatile electrospinning method that exhibits desirable properties such as high surface to volume ratio, high porosity, high molecular orientation, and, most importantly, 1-D nanoscale features [1]. Tissue engineering [2], biosensors [3], drug-releasing [4], catalysts, energy storage [5], reactors, environmental protection, and other sectors have all used electrospun nanofibers extensively.

Because of their small size, biocompatibility, and low toxicity, functional fibrous materials of food preservatives, effective medication delivery agents, and active energy storage agents are promising. Researchers have recently concentrated on the food business and energy science. These electrospun nanofibres in the inclusion complex with encapsulating polymeric material play a critical function. Electrospun nanofibers and carbon nanofibers are frequently in the fabrication of this material have used.

The number of publications about the nanofibers fabrication of CDs-ICs-P-NF and CDs-ICs-NF has steadily increased over the last five years [6–8]. Most Cyclodextrins (CDs) have improved solubility and stability of the encapsulating agent, resulting in improved food preservation properties at an industrial level [9]. The wide surface area of the interaction material, which is the ability is to manage the releasing variables, is used in the dynamic design of new CDs-ICs-P-NF nanofibers to improve the shelf-life of food goods. CNFs, on the other hand, are essential in the energy industry because of their increased conductivity, modulation pores system, doping capacity, and mechanical strength. Many polymers fabricate the electrospun nanofibers using the electrospinning technique. Including biodegradable synthetic polymers such as Polyvinyl alcohol (PVA) [10], Polyethylene glycol (PEG) [11], Polyvinylpyrrolidone (PVP) [12], Polylactic acid (PLA), Polylactic-co-glycolic acid (PLGA) [13], and Polycaprolactone (PCL) [14]. Because of its high carbon yield and extraordinary mechanical strength, PAN is a polymer for forming CNFs via the carbonization process for energy concepts. Many parameters influence the electrospinning processability of polymers. Solution viscosity, conductivity, useable solvent, and high molecular weight electrospinning techniques are impossible without polymers. At this period, nanosized materials played a significant role in food preservatives. Like food additives, and enhanced the resistivity of meals, beverages, and environments.

Recently, some research groups have focused on two or more polymers blended composite electrospun nanofibers. Such as cellulose acetate/polyester (PE) for wound dressing applications. Polyacrylonitrile (PAN)/Chitosan for the textile industry, PVA/Cellulose acetate for the cosmetic industry applications. PMMA/Polyaniline (PANI) for energy application, PVA/PANI for solar cell and battery applications.

Chitosan/CDs-ICs have become the most popular over the last 20 years[15, 16]. Because CDs are polymeric cyclic oligosaccharides with the ability to form ICs with organic molecules. Reduced volatility, controlled antimicrobial active compound release, and improved thermal stability. Solubility, and bioavailability, a process is known as supramolecular chemistry or host–guest chemistry [17]. Co-precipitation [18], kneading [19], microwave-assisted [20], physical mixing, and freeze-drying to prepare the host molecule of CDs and the guest molecule of the anti-bacterial, anti-oxidant agent. Due to the high surface-to-volume ratio, high porosity, and high mechanical stability, CDs-ICs encapsulated CDs-ICS-P-NF have applications in the last five years. Including the food industry and wound dressing [21–23]. Due to odor and moisture absorbing, anti-oxidant releasing, highly hydrophobic, enhancing anti-bacterial activity, edible, biodegradable, and other properties. Chemistry researchers have developed polymer-free electrospun nanofibers in recent years [24]. It means polymer-free CDs-ICs-NF in functional packaging material. CNFs, the material used in energy conversion systems, store energy in electrostatic charge at the electrode/electrolyte interface and provide high power density. In addition, it has better cyclic stability than other metal oxides [25]. The studies have focused solely on electrospun nanofibers for tissue engineering for the wound healing characteristics is little attention paid to food and energy applications. Because of the controlled release of encapsulating antimicrobial compounds from the nanofibers, care must while using antimicrobial agent-loaded CDs-ICs-NF as a food preservative and packaging material. CDs-ICs-NF has in a variety of fields. Although much research has focused on CDs-ICs enclosing CDs-ICs-P-NF, polymer-free CDs-ICs-NF have emerged in recent decades. Low water solubility, unsustainability, uncontrolled release of the anti-bacterial molecule, and low thermal and mechanical stability are all severe difficulties in the food preservative sector. These problems by introducing supramolecular chemistry principles are solved. Some essential structural and functional properties of ICs to improve the stability, biological activity, and solubility of the antimicrobial molecule in this paper. Furthermore, the surface properties of electrospun nanofibers for control releasing the application. And bio-degradability of electrospun nanofibers for interaction with foods to surface and boosting solubility of CDs-ICs-NF for crusily contact with food and preservation [26]. Simultaneously, researchers are focused on CNF pores, which have a large surface area and high porosity of roughly 709 $m^2\ g^{-1}$ and 0.356 $cm^3\ g^{-1}$, respectively, and may aid in increasing the specific capacitance of supercapacitors [27]. As a result, this review is into three key sections. The first and second sections must examine CDs-ICs-P-NF and polymer-free CDs-ICs-NF, respectively., which have in food and packaging due to their multiple features, including complexation properties. We describe CNFs as an active carbon source for battery and supercapacitor devices. In the third section, thanks to their fibrous physical features. After the evaluation, there are several disagreements about concluding remarks and the future outlook.

24.2 Electrospinning

Electrospinning technology has been the subject of extensive investigation. According to this study, it is a simple, low-cost, and adaptable method. For producing, 1D nanostructure materials with fiber diameters ranging from nanometers to micrometers under a strong electric field. Formhals introduced and described fiber formation through the spinning process in 1934, and Taylor (1969) explained the formation of polymer droplets at the tip of the needle, involving electrostatic interaction with the help of a cone and jet to produce fiber on the collecter, dubbed the "Taylor Cone". Because of the Taylor cone principle, most research focuses on this fiber manufacturing method and various polymer solutions to make types of nanosize fiber for applications.

Polymers are material for electrospinning because they have a molecular weight and enough viscosity to dissolve in a suitable solvent and create nanofibers. Ceramic and metal nanofiber manufacture, on the other hand, is an operation due to their low viscosities and solubility. It is combined with a suitable polymer to form fine nanostructure fibers. Following fiber creation, various treatment procedures followed carbonization, calcination, hydrothermal, and solvent immersion. For activation purposes, depending on the application. The calcination technology in which polymer hydrocarbon nanofibers into carbon nanofibers at high temperatures in an inert atmosphere is for energy applications. This technology uses ceramics and metal blend polymers to create flexible nanofibers in energy storage and energy applications. And, The nanofiber structures on an electrospinning and handling method. We first discuss the principle of electrospinning and the effects of parameters. The appropriate polymers and solvents for electrospinning techniques are discussed here in this relevant. We describe the flexible nanofiber preparation and stabilizable approaches [10, 28].

24.3 Electrostatic Interaction Principle

Electrospinning is an electrostatic technology that uses the interaction between two electrodes and a high-voltage power supply to create nanofibers from a suitable solution. A high-voltage power supply, a spinneret, and a collector make up an electrospinning apparatus. Before beginning the spinning process, the polymer solution is appropriate, placed in a plastic syringe, and the syringe in the electrospinning instrument's syringe setup. A liquid drop of the polymer solution from the needle has a high electrical potential between the spinneret and collector. It is causing the induced electrical charge to cover the droplet solution. The Taylor cone is the conical structure of the droplet that results from the influence of electrical forces. After, the evaporation of water from the solution force causes the surface tension of the polymer solution, which involves stretching and whipping processes and forms thread-like materials. The thread fibers are continually collected on the collector, resulting in

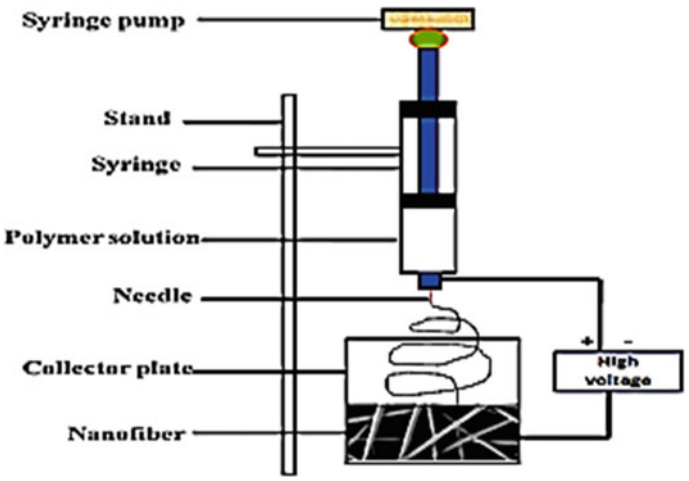


Fig. 24.1 The schematic representation of the electrospinning technique

nanofiber to think sheets. The qualities of nanofibers include a large surface area, porous structure, changeable surface shape, and nanoscale, all of which may be modifying electrospinning parameters electric potential, flow rate, and the distance between capillary and collector. Figure 24.1 shows schematic schematics of the electrospinning process's setup and is the fabrication is highly aligned fibers. Surface tension, viscosity, useable solvent, concentration, molecular weight, and density of polymeric solutions are all factors in nanoscale electrospun nanofibers [29, 30].

24.4 Effect of Parameters on Electrospinning

Morphological analysis was to assess the electrospinning process and the formation of nanofibers. Furthermore, numerous parameters affect the electrospinning process and the creation of nanofibers. Table 24.1 shows electrospinning parameters such as applied voltage, flow rate, needle to collector distance, flow rate, and

Table 24.1 Electrospinning technique-parameters

Solution parameters	Electrospinning parameters	Environmental parameters
Selective solvent Polymer concentration Polymer molecular weight Viscosity Conductivity	Applied electric field Flow rate Needle diameter	Relative humidity Temperature (RT)

needle diameters. Solvent, polymer concentration, viscosity, and conductivity are the solution parameters in this method. Environmental variables like relative humidity and the temperature of the electrospinning setup box in this process. Where, in this method, the parameter has a direct effect on the development of smooth electrospun nanofibers. And the findings have led to a better understanding of electrospinning technology and the fabrication of polymeric nanofibers. In practice, the flow velocity, applied voltage, and solution concentration generate larger nanofibers while the needle to collector distance forms smaller nanofibers. The qualities of nanofibers in terms of shape, size, and structure are all dependent on the solution and spinning parameters [31].

24.4.1 Applied Voltage and Flow Rate

When a voltage to a polymer droplet solution, the Taylor cone effect occurs, making it a parameter in electrospinning. The voltage that is delivered varies based on the polymer. Because we only get beads nanofibers when the applied voltage is low, higher voltage produces beads and fibers with smaller diameters. In this process, the optimizations and the corresponding voltage are crucial. The flow rate, which is affected by the flow of polymer solution to the needle tip, and determined by the geometry of nanofibers, is another critical component. The flow rate of polymers only provides homogeneous beadless fibers because smaller-diameter fibers at lower flow rates and bead fibers at higher flow rates.

24.4.2 Needle to Collector Distance

The distance between the metallic needle and the collector is critical. It affects the deposition and evaporation times of the component in the electrospinning process. In addition, the geometry of the nanofiber varies depending on the polymer. Furthermore, a distance must be maintained when creating homogeneous and smooth fibers. Small yield large-diameter nanofibers, while high produce small-diameter nanofibers; nonetheless, the shape of the fibers is unaffected by the distance effect.

24.4.3 Type and Materials of Collector

Electrospun fibers can be collected using stationary or spinning collectors and their design and the nanofibers by the collector. Flat plates on stationary collectors capture fibers in a random area directly covered by the needle of a polymer syringe. The spinning disc fibers are complete, captured resulting, in a thick fiber process. Furthermore, the velocity of a revolving disc affects the form of the nanofibers. Several materials

such as silver, aluminum, and copper foils are used as collector materials to produce homogeneous and large diameter nanofibers via a moderate and optimized rotation and electrospinning process. Because the fiber is light and quickly broken, the collector materials should be from the substrates.

24.4.4 Solvents

The solvent is one of the most aspects of the electrospinning process. Keep in mind that the polymer must thoroughly dissolve the substance and that the solvent must have a boiling point when choosing a solvent. The soluble solution used in the spinning process generates only smooth fibers with no obstacles. Higher boiling point solvents have a reduced volatile property, which stops the drying process during nanofiber jet flight. The volatile solvents evaporate quickly before involving the Taylor cone process, causing a clotting problem on the needle tip, so be avoided. Furthermore, the polarity nature of solvents produces porous nanofiber. The distinct volatile character of the solvent combined polar and nonpolar solvents form a fiber. Different solvents such as DMF, THF, DMSO, NMP, and Water are formed in this method of nanofiber by electrospinning for the shape fibers due to their variable solubility, conductivity, and dipole moment qualities.

24.4.5 Solution Viscosity and Conductivity

The viscosity of the solution has a significant impact on the stretching charge jet, making it a critical parameter in the electrospinning method. When is low, the applied electrical field and surface tension break down? The polymer chain fragments before they reach the collector, resulting in the creation of beaded fibers. The high viscosity solution also causes clotting on the needle tip, prevents fiber production. As a result, the fine structure nanofibers with the right viscous solution. The viscosity of a fluid is proportional to the diameter of its fibers.

$$\mathrm{df} = k_2 \eta^{\mathrm{n}} \tag{24.1}$$

where k_2 is a constant and n depends on the polymer precursor.

Furthermore, because of high conductivity materials for fiber fabrication, the conductivity of the solution has a significant impact on the Taylor cone formation. The coulomb charge field between the charge of the field surface and the applied electric field in the electrospinning technique. The dielectric charge material has free on the fluid surface. The conductive charge material has adequate charge and can readily create Taylor cones by applying an electric field, resulting in nanofibers with small diameters. Because some polymers lack conductivity in their natural state, salt boost conductivity. The salts increase the charge capacity on the Taylor cone surface,

resulting in a beadless fiber. As a result, the material chosen for electrospinning qualities should have suitable viscosity and conductivity [3, 32].

24.5 Functional Nanofibers

Polymeric nanofibers are important nanomaterials that have gotten a lot of press in the recent two decades [33]. Interfacial polymerization, phase separation, template synthesis, melt bowling, drawing, island-in-sea, gas jet techniques, and electrospinning are some systems used to make them. Electrospinning is the most important of these technologies, having advantages. Regards have simplicity, cost-effectiveness, flexibility, adaptability, and industrial scale-up potential [34]. Because of their low cost, bioavailability, and well-defined chemical and physical properties, synthetic polymers such as PVA, PLA, and PMMA have been used extensively in this method [35]. The majority of the research in this study focuses on the application and manufacture of polymeric nanofibers.

Biocompatible and safe polymers found in nature, Cyclodextrins, chitosan, and proteins, are currently used in the applications. On the other hand, cellulose elastin alginates-based nanofibers have filtration, adsorbent beads, tissue engineering antibacterial, and protective garment membranes in the pharmaceutical, food, and biomedical areas. The features and use of nanofibers and in Fig. 24.2, it is commonly known that electrospinning in Formhals fiber fabrication in the year 1930; utilized in the textile and filtering industries in the nineteenth century. During the 1930s and 1940s, many electrospinning processing techniques considerably aided electrospinning's growth toward commercialization.

Taylor quantitatively modified the electric field of the technique in 1960, and the electrical field cone became known as the "Taylor cone". Martin and Cockshot proposed electrospun fibers for wound dressing applications later in 1974. The rapid development of industrial applications since the 1990s [36, 37]. Electrospun nanofibers have intrinsic advantages, such as a high surface area to volume ratio and the ability to combine materials easily prepared. Fiber deposition onto other surfaces, fiber functionalization, biocompatibility, and bioactivity are advantages. High extensibility (elasticity), high porosity, thermal stability, and good tensile strength are its mechanical qualities. Here, Drug delivery systems, cell culture, electric conductive materials, supercapacitors, batteries, sensors, tissue engineering wound healing, and food preservatives are only available. A few examples of electrospinning's multifunctional capabilities [38, 39].

24.6 Polymer-Based Electrospun Nanofiber

Electrospinning is a physical technique used to create ultrathin nanofibers, and the material selection process is an aspect in influencing nanofiber diameter. The final

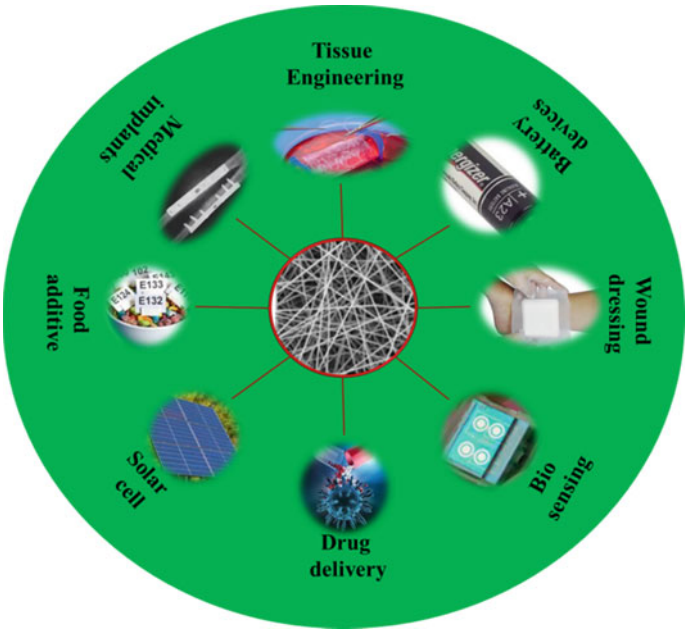


Fig. 24.2 Represent the electrospun nanofiber materials applied in various fields

structure and function of electrospun nanofibers here. Several hundred synthetic polymeric polymers have to fabricate bead-free surface-modified electrospun nanofibers. including polyvinyl alcohol, poly (methyl methacrylate), poly(vinylpyrrolidone), poly(caprolactone), and poly(ethylene oxide). These synthetic polymers are more important because they have high molecular weight. In biomedical uses such as tissue engineering and medication delivery, synthetic materials developed here.

Nanofiber technology has become a very adaptable solution for solving difficulties thanks to its versatility and control properties derived from electrospinning factors such as fiber diameter and porosity. Furthermore, CNFs technology energy conversion devices, such as electrospun PAN or PMMA under decomposition temperature. Acts as an activator in mesopore content, graphitization degree, and conductivity. Table 24.2 shows the many types of polymeric nanofibers utilized in different sectors. Most researchers have discovered that two or more polymers generated electrospun nanofibers for various areas in the last 15 years. They combined three distinct sorts. (1) Natural-natural polymers, (2) natural-synthetic polymers, and (3) synthetic-synthetic polymers. Comparison to single polymer nanofibers, they exhibit modified surface functionalities and size reducibility. The Chitosan/cellulose composite electrospun nanofiber suggested by Duy-Nam Phan et al. is an excellent material for eliminating heavy metal ions.

Table 24.2 Some of the natural and polymers-nanofibers and their applications

Natural and synthetic polymer electrospun nanofiber	Solvent	Thickness of nanofiber	Applied voltage in kV, Feed rate in mL/h, collector distance in cm	Applications	References
Cellulose acetate (16%)	Acetone/DMF/tetrafluoroethylene—(3:1:1)	200–1000 nm	25 4 15	Enhancing bio-compatibility, anti-bacterial activity, anti-viral activity	[40]
Chitosan (8%)	TFA:dicholoromethane (70:30)	<100 nm	15 – 150	Cell culture, anti-microbial agent, and anti-inflammatory agents	[41]
Sodium alignatenanofiber (0.25–2.0%)	Deionized water	131–123 nm	11 0.01 10	Wound dressing, biomedical applications	[42]
Raw silk fibers (0.5%)	Distilled water	450 nm	16 1 8	Various kind of applications	[43]
Tropoelastin (20%)	1,1,1,3,3,3-hexafluoro-2-propanol	–	20 1–3 20	Dermal tissue engineering	[44]
Polyvinyl alcohol (8–12%)	Water	86–100 nm	10–15 – 15	Enhancing water solubility	[45]

(continued)

Table 24.2 (continued)

Natural and synthetic polymer electrospun nanofiber	Solvent	Thickness of nanofiber	Applied voltage in kV, Feed rate in mL/h, collector distance in cm	Applications	References
Polylactic acid (16%)	2,2,2-trifluroethanol	562 ± 210 nm	15 0.6 10	Using as scaffolds for wound dressing	[46]
PANI + camphorsulfonic acid	chloroform	678 ± 54	5 0.6 25	Applied in supercapcitor electrodes	[47]
Alginate (2%) and PVA (10%)	DI water + 2-propanol (4:1)	250 ± 30	30 0.2 10	Drug delivery, wound healing, tissue engineering	[48]
Polylactic acid (10%)	Dichloromethane + 1 mL acetic acid	300–350 nm	–	Anti-HIV drug delivery system	[49]
Polyurethane (0.5%) + hydroxypropyl cellulose (1.2–10%)	DMF	464 ± 24 995 ± 14 1172 ± 10	15 1 15	Potential transdermal drug delivery system	[50]
PANI + gelatin	1,1,1,3,3,3-hexafluoro-2-propanol	100–800 nm	10 – 10	For tissue engineering applications	[51]
PLGA (9–10%) + gelatin (0–1%)	2,2,2-trifluroretanol	342 ± 34 313 ± 69	10 0.5 10	Potential drug delivery system	[52]

(continued)

Table 24.2 (continued)

Natural and synthetic polymer electrospun nanofiber	Solvent	Thickness of nanofiber	Applied voltage in kV, Feed rate in mL/h, collector distance in cm	Applications	References
Chitosan + cellulose acetate (1:1)	TFA + acetic acid (7:3)	331 ± 118 546 ± 91	15–20 0.1–0.8 –	Adsorption property with enhanced mechanical property	[53]
PCL (10%)	N,N-dimethylformamide	200–500 nm	15 0.5 15	Improve endothelial cell spreading and proliferation and to control cell orientation	[54]
Poly(L-lactic acid)co-poly(e-caprolactone) + collagen	1,1,1,3,3,3,-hexafluoro-2-propanol	100–200	12 1.2 12	Potential vascular graft for blood vessel tissue engineering	[55]
Zein + PLA + HPMC	Chloroform + ethanol + acetic acid (40:45:5)	1213 ± 316 1098 ± 235, 718 ± 186	18 1 2	Active food packaging system	[56]
Chitosan + PVA (2% + 2%)	Distilled water + acetic acid	146.03	22 0.6 9 cm	Nanoscale material for fish balls	[57]

24.7 Cyclodextrins (CDs)

Enzymatic breakdown of starch produces chemically and physically stable cyclodextrin macromolecules schematic shown in Fig. 24.3a. They are cyclic oligosaccharides made up of (α-1,4) connected-D-glucopyranose units [58]. Because of CD's nanocavity, a hydrophobic interior, a hydrophilic exterior, and low molecular weight substances. Most researchers believe they are the ideal choice for hosting molecules. The physical, chemical, and biological properties by the encapsulation properties ascribed [59] in Table 24.3 the CDs' varied features.

Guests that can cause ICs include clusters, polymers, surfactants, and antioxidant chemicals. α-Cyclodextrin (six glucose units named cyclohexaamylose), β-Cyclodextrin (seven glucose units named cycloheptaamylose), and γ-Cyclodextrin (eight glucose units named cyclohexaamylose). They are the commercially available cyclodextrins used. Among these β-CD stands for all sectors due to cavity size. Drug inclusion complexation bioavailability, and low cost. Due to hydroxyalkylation, CDs derivatives of Hydroxypropyl-β-cyclodextrin (HP-β-CD), Hydroxypropyl-α-cyclodextrin (HP-α-CD), can hold hydrophobic guests like aromatic chemicals in their cavities [60]. Hence the guest's choice is determined by the cavity's size. Pharmaceuticals, food, chemistry, chromatography, catalysis, biotechnology, agriculture, cosmetics, hygiene, medicine, textiles, and the environment are just a few industries that use it [61].

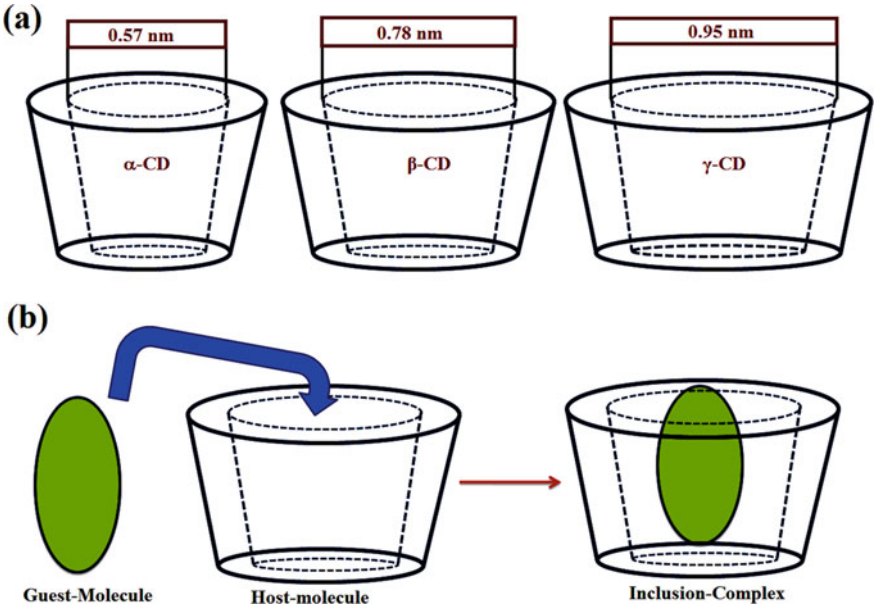


Fig. 24.3 Schematic representation of **a** Structure of cyclodextrins. **b** Formation of inclusion complex

Table 24.3 Physical properties of cyclodextrins

Properties	CDs		
	α-CD	β-CD	γ-CD
No of glucose units	6	7	8
Molecular weight (g/mol)	972	1135	1297
Solubility in water at room temperature	14.5	18.5	23.2
Outer diameter (Å)	14.6	15.3	17.5
Cavity diameter (Å)	4.7–5.3	6.0–6.5	7.5–8.3
Height of tours (Å)	7.8	7.8	7.8
Cavity volume (Å)	174	262	427

24.8 Inclusion Complexes (ICs)

Figure 24.3b shows how the ICs between the host and guest molecules. Host–Guest ICs are a sort of supramolecular structure that is crucial. When pharmacological or biological molecules are partial/or entirely included inside the host. The ICs are forming because the host's hydrophobic cavity allows the guest to have a proper environmental interaction [62]. Non-covalent forces hold two components of a compound together. These driving forces include (1) ionic bonding (predominantly electrostatic), (2) hydrogen bonds, (3) van der Waals forces, and hydrophobic interactions (predominantly dispersive—London forces and -interactions), which differ from covalent and ionic bond interactions [63].

Crown ethers, macrocyclic polyamines, calixarene, cyclophane, cucurbiturils, and CDs are examples of hosts. They contain permanent cavities and may accommodate the guest to form complexes in both the solid and aqueous states. Recently, numerous guest molecules such as medicines, steroids, ionic liquids, dyes, and organic compounds have to transform or improve the properties of guest molecules into the desired or pleasant form [64]. The physical blending method, solvent evaporation, melting method, freeze-drying technique, co-precipitation method, kneading method, and microwave irradiation are all options for making ICs. Because of their higher solubility and dissolution rate ability. It stabilizes active substances during processing, storage, and use is highly regarded in the food and pharmaceutical industries.

24.9 Cyclodextrin Inclusion Complexes Encapsulating Electrospun Nanofiber (CDs-ICs-P-NF)

Making ICs with CDs is a very appealing structural feature. Due to the geometry of the cavity and structural properties [65], the host of CDs and guests of a variety of active molecules can generate ICs. The ICs have to improve the molecular stability,

bioavailability, and solubility of many encapsulating compounds such as medicines, essential oils, phenolic acid, tastes, and fragrances, according to the majority of the studies. CDs in pharmaceuticals, oral medications, cosmetics, and food preservation because of their non-toxicity. Electrospinning is a promising technology for creating fast-dissolving nanofibers. It controlled the drug molecule release behavior and the oral drug delivery systems. And the nanoencapsulation of microbial medicines in this scenario. Furthermore, electrospun nanofibers and CDs-ICs encapsulating electrospun nanofiber CDs-ICs-P-NF have recently been developed. Food preservation, food packing, food odor, and masking are all included in the food sector. Solubility, binding stability, mechanical strength, temperature behavior, active molecule release control, and self-life periods have improved.

However, the antibacterial drugs have undesirable chemical features such as limited water solubility and poor oxidative stability. The antimicrobial drug is evaporated in nature and has physical and thermal stressors. Some research groups focused on this and discovered that the problem might by host–guest inclusion complexation [66]. To parent guest molecules, ICs have also improved thermal stability, solubility, and interesting good bioavailability proc. The functionality, makes them popular in food additives and medication delivery systems. Furthermore, fabricating electrospun nanofibers with integrated circuits is a fascinating research topic. Table 24.4 shows the inclusion complexes variety of host molecules such as CDs with guest molecules such as highly volatile antimicrobial agents such as eugenol, essential oil, gallic acid, ferulic acid, retinol acetate. Vitamins that were incorporated with polymeric electrospun nanofibers using the electrospinning technique. Antibacterial, antifungal, and antimicrobial active chemicals encased in nanofibrous webs have potential utility in food delivery and biotechnology.

24.10 Polymer Free Electrospun Nanofiber (CDs-ICs-NF)

The electrospun nanofiber is a promising material in the polymer-free cyclodextrin inclusion complex. Due it to the increased guest molecule load. Furthermore, compared to CDs-ICs-P-NF, the number of nanofibers in polymer-free CDs-IC nanofibers is substantial. CDs-ICs-P-NF only used 5–25% (w/v) of polymer solution, but polymer-free nanofibers used 120–160% (w/v) of cyclodextrins, resulting in polymer-free CDs-ICs producing several nanofibers with uniform shape. Furthermore, due to the hydrogen bonding in CDs, more than 120% of CDs. They are highly concentrated solutions that form colloidal aggregates. In recent years, some researchers have developed hydroxypropylated-cyclodextrins (HP-CDs). Typically HP-α-CD, HP-β-CD, and HP-γ-CD inclusion complex systems without further addition polymeric matrix. It has many advantages as faster dissolving, higher stability, and, most importantly, CDs are highly water-soluble compared to the polymer matrix. Nanofibers without polymers are in textiles, pharmaceuticals, drug delivery, food, etc. Table 24.5 shows the function of electrospun nanofiber function properties

Table 24.4 Antimicrobial and drug agents combined with supporting polymeric electrospun nanofiber and their functional applications

Guest molecule	Supporting polymer (Solvent)	Thickness of nanofiber	Applied voltage (kV) Feed rate (mL/h) Collection distance (cm)	Applications	References
Thymol	Chitosan [Trifluoroacetic acid/dichloromethane (70:30)]	98.12 ± 35.43 135.94 ± 51.62	22 and 24 0.6 10	Vitamin B stability of fish fillets, a promising approach for food applications	[67]
Angelica essential oil (0–9%)	Gelatin solution [acetic acid (12%)]	330.50 ± 71.60 377.38 ± 74.30	15 0.3 20	Active food packaging	[68]
Hordein	Chitosan [acetic acid (99%)]	0.49 ± 0.30 0.62 ± 0.34	9 1 13	Food grade water resistance	[69]
Essential oil (1–5%)	Chitosan/PCL [formic acid/acedic acid(50:50)]	332.4 ± 138.7 314.0 ± 72.1 295.4 ± 104.2 206.5 ± 96.6	18 *0.1* 15	Antimicrobial food packaging applications	[70]
ε-polylysine	Chitosan [acetic acid (1%)]	100–500	25 0.5 15	Food packaging against salmonella on chicken	[71]
Clove oil	Gelatin [acetic acid (30%)]	274 375	25 0.5 15	*Escherichia coli* O157:H7 biofilms on cucumber	[72]
Asprin	Chitoosan + PEO [citric acid + acetic acid]	–	18 1.5 15	Thermal treatment of controlled drug release	[73]
Pleurocidin	PVA [15% of water]	890–960	15 *0.2* 10	Retain antimicrobial activity of food system applications	[74]

(continued)

Table 24.4 (continued)

Guest molecule	Supporting polymer (Solvent)	Thickness of nanofiber	Applied voltage (kV) Feed rate (mL/h) Collection distance (cm)	Applications	References
Phlorotannin	Alginate/PEO [Distilled water]	100–500	20 0.5 15	Preserve chicken meat from salmonella contaminations	[75]
Alevvera extract	Chitosan + PCL [acetic acid (90%)]	37–104.68	–	Membranes for novel wound dressing	[76]
Essential oil (peppermint oil + chamomile oil)	Gelatin solution [acetic acid + water (22.3)]	330–462	15 0.3 10	Potential edible packaging	[77]
Thymol essential oil	Chitosan + gelatin [ethanol + acetic acid (50:45)]	–	25 – 5	Reduce nitrite in sausages	[78]
Tea extract	PLA [DCM/DMF (7:3)]	–	20 20 15	Active food packaging applications	[79]
Phenolic compound extraction	Chitosan + polyethylene oxide [acedic acid (90%)]	262 ± 32	20 0.2 100	Antibacterial activity of food packaging system	[80]
Green tea extract	Chitosan + PEO [acedic acid (50%)]	–	17–20 0.3–0.5 10	Wound dressing applications	[81]
Pomegranate extract	Chitosan + PEO [acetic acid (2%0]	306 ± 21	20 0.5 15	Meat preservation	[82]
Lemon Murtle essential oil	Cellulose acetate [DMF + DMAc (2:1)]	444–471	15.5 – 10	Active agent with potent and sustainable antimicrobial acitivity	[83]
Thyme	PEO	274	15–20 0.3–0.6 10	Antimicrobial wound dressing	[84]

(continued)

Table 24.4 (continued)

Guest molecule	Supporting polymer (Solvent)	Thickness of nanofiber	Applied voltage (kV) Feed rate (mL/h) Collection distance (cm)	Applications	References
Aspirin	PLA/Raw silk [CaCl2/H2O/EtOH]		22 0.5 18	Drug Release and blood compatibility	[85]

without polymer cyclodextrin inclusion complex. The electrospun nanofiber function properties are used in various fields, as mentioned above said.

24.11 Food Packaging Applications

According to studies, the electrospun nanofiber is have used in the food packaging business. Food packaging materials are have created using electrospun nanofibers of biopolymer-like CDs. In recent years, most researchers have focused on the packaging of foods. Bacterial and fungal infections release of active dietary components contributes to this. The CDs-ICs-NF and CDs-ICs-P-NF for sub-micron to nanoscale size diameter have this introduced to address this issue. Nanofibers have antibacterial, moisture absorbing, antimicrobial, oxygen scavenger, and odor absorbing active packaging systems. Gallic acid, ferulic acid, vanillic acid, caffeic acid, cinnamic acid, and other phenolic compounds have recently been encapsulated in cyclodextrin nanofibers (Host–guest system) for highly anti-microbial qualities and their usage as food preservatives. In addition, the essential oil, food flavor, and food additive loaded cyclodextrin inclusion complex in anti-microbial nanofiber manufacture of controlled releasing behavior and degradation and significantly employed in active food packaging systems. As a result, food goods will be the future focus of electrospinning laboratory scale preparation. It should be the transition to an industrial size.

24.12 Pharmaceutical Applications

In today's world, the pharmaceutical industry is a vital sector, The use of electrospinning to encapsulate antimicrobial agents, pharmaceutical medications. The biologically active substances into electrospun nanofibers have gained in popularity. And these to treat a variety of ailments, including wound healing and anti-cancer cells. The

Table 24.5 Types of CDs-ICs encapsulating polymeric electrospun nanofiber (CDs-ICs-P-NF) and their functional properties and applications

Type of CD (%)	Guest	Supporting polymer (%) [Solvent]	Fiber diameter	Parameters (Voltage *Feed rate* distance)	Potential application	References
α-CD (33%) β-CD (39%) γ-CD (44%)	Eugenol	PVA (12%) [distilleld water]	310–930 270–1140 310–1170	15 1 10	Enhancing thermal stability for food industry	[86]
α-CD (33%) β-CD (39%) γ-CD (44%)	Triclosan	PLA [Choloroform/DMF (9:1)]	– 640 ± 480 940 ± 500	15 1 10	Enhancing anti-bacterial activity	[87]
β-CD (19%)	Quercetin	PAA (7.5%) [aqueous solution]	270 ± 50	15 1 15	Slow releasing of the antimicrobial molecule and high solubility	[88]
β-CD	Curcumin	Almond gum/PVA [ethanol/water (1:3)]	98 ± 18	18 0.125 15	Highly anti-microbial activity, releasing capacity	[89]
γ-CD	α-Tocopherol	PLA (10%) [DCM/DMF (7:3)]	430 ± 170	15 1 10	Active food packaging and food additive	[90]
β-CD	Cinnamaldehyde	PLA (15%) [DCM/DMF (3:1)]	317 ± 234	20 1 15	Anti-microbial	[91]
β-CD	Styrylpyridinium	PVA(50%) [distilled water]	266 ± 65	19 0.3 10	Wound dressing and enhancing mechanical strength	[92]
β-CD	Dexamethasone	PLGA (15%0 [Chloroform/methanol (3:1)]	356 ± 30	15 1.5 14	Dental pulp therapy	[93]
α-CD β-CD	Ciprofloxacin	PCL [DMSO/DCM(35/65)]	–	15 1 18	Controlling releasing behavior	[94]

(continued)

Table 24.5 (continued)

Type of CD (%)	Guest	Supporting polymer (%) [Solvent]	Fiber diameter	Parameters (Voltage *Feed rate* distance)	Potential application	References
α-CD	Pseudorotaxane	PCL [Acetaone (80%)]	–	20 3 30	Enhancing bacterial characteristics and wound dressing	[95]
β-CD	Menthol	PVA (16%0 [Distilled water	–	16 0.3 15	Smoke filtration and flavor retention	[96]
β-CD (30%)	Retinyl acetate	PVA (10%) [Distilled water]	223 ± 49	18 – 20	Decreasing releasing of retinyl acetate and enhancing thermal stability	[97]
γ-CD	Ferulic acid	PVA (16%) [Distilled water]	168 ± 32	15–17 1 10	Increasing thermal stability and releasing capacity	[21]
γ-CD	Quercetin	Zein [ethanol/water (8:2)]	750 ± 310	15 1 10	Enhancing antioxidant activity and antibacterial activity	[98]
β-CD	Cinnamon essential oil	PLA [ethanol/water (9:1)]	320 ± 50	12–16 2–2.4 10–14	Antimicrobial packaging	[99]
Hp-β-CD (10%)	Ciprofloxacin	Gelatin (13%) [Acetic acid/water (7:3)]	90 ± 20	15 1 15	Fast-dissolving drug delivery	[100]
Hp-β-CD	Sulfisoxazole	Hydroxypropyl cellulose [Ethanol]	60 ± 25	16 1 11	Developing drug delivery systems of hydrophobic drugs	[101]

cyclodextrin inclusion complex, on the other hand, has been used. In medical domains because of its solubility, stability, and favorable dissolution profile. The research has focused on the phase solubility analysis of cyclodextrin with drug inclusion complex, with the resulting AL type graph indicating improved solubility and inclusion complex binding strength. Essentially, many pharmaceutical drug molecules have limited physicochemical properties that problems. It can administer the inclusion complex, which has good physical properties. As well as the biological activities are reducing evaporation. Stabilized flavors, reducing odors, and preventing chemical instabilities. A few years later the materials are study group demonstrated. The pharmaceutical medication with cyclodextrin inclusion complex encapsulating electrospun nanofibers. It has excellent qualities for paramecia and the medical industry [26]. The advantages of fibrous materials are structure minimization. The integration of hydrophilic and hydrophobic drugs into the electrospinning process, morphology, high surface to volume ratio, and porosity had. Therefore they chose to move the approach forward in industrial scale-up [39].

24.13 Energy Applications

Because of their larger surface area, interconnected pores structure, lightweight, and mechanical strength, nanofibers are gaining increased interest in energy storage and conversion applications. Template synthesis, chemical vapor deposition, and electrospinning are just a few techniques used to create CNFs. Electrospinning is a particular element because of its instrumental characteristics and environmental safety. Electrospun nanofiber produces polymer solutions is that converted to CNFs. The carbonization process with the help of thermal treatment. One-dimensional carbon nanotubes have virtually the same multifunctionality as multiwalled carbon nanotubes. But they are easier to make, have a lower cost, are more crystallin, have better functionalities, and have more flaws. That is the result of their smooth, porous, hollow, helical. The appropriate architectures these carbon materials have in many domains of energy conversion storage. And is the catalysis, biosensor, adoption, and separation techniques. Many research articles have previously documented the production of CNF-based nanomaterials made from PAN nanofibers for diverse energy applications. Due to surface area considerations and diffusion rates, most articles currently claim that CNFs act as electrode material in supercapacitors. Following that, because of their high specific capacitance, excellent cycle stability, rate capability, and surface changes, heteroatom-doped CNFs are being considered. Table 24.6 shows the many types of CNFs that have different applications.

Table 24.6 Types of CNFs used in various applications

CNF sources	Applications	References
PAN	Lithium-based batteries as an activating electrode material	[102]
PAN/Ni nitrate	Energy storage of batteries and supercapacitors	[102]
PAN/rGO/ACNF	CO_2 adsorption applications	[103]
PAN/gACNFs	HDouble gas adsorption performance	[104]
N/S/Co/PAN	High-performance supercapacitors high-performance	[105]
SiO_2/PAN	Energy storage materials for batteries and supercapacitors	[106]
N/PAN	Sodium-Ion batteries	[107]
PAN/N doped	Using in CO_2 capture	[108]
PAN/PVP	Using as a gas sensor	[109]

24.14 Conclusions

Because of its cost-effectiveness, ease of modification, and flexibility in creating continuous thread-like nanofibers. With the high porosity, surface volume ratio, and small diameter, electrospinning is a versatile process is here. One of the fascinating uses for CDs-ICs-NF, CDs-ICs-P-NF, and CNFs from carbonization thermal treatment is in the food industry and energy storage. So, because of their anti-oxidant and anti-microbial properties, we can develop these materials for food packaging in the future, extending the shelf-life of food products and releasing controlled amounts of an active food additive looking into electrochemical studies for energy storage systems. Food coating, food packaging, food safety, food additives encapsulation, and food sensing are all areas where we can grow the food processing business. Finally, encapsulating bioactive and antibacterial compounds in cyclodextrin nanofibers and cyclodextrin polymeric nanofibers improves. Noteworthy is that nanofiber's solubility, stability, and controllable release method are highly useful for food applications. Furthermore, nanofiber-based CNFs have higher mechanical strength and appropriate porosity, making them an ideal material for energy storage systems such as supercapacitors, batteries, and current devices. Furthermore, due to their barrier properties of solubility, stability, and absorption, some nanofibers are a food coating material. Finally, CDs-ICs-NF, CDs-ICs-P-NF, and CNFs are promising materials from the lab to the factory.

Acknowledgements One of the authors, Vimalasruthi Narayanan gratefully acknowledges the Department of Science and Technology (DST) India, under the scheme of DST-INSPIRE Programme [No. IF 180377] to carry out this work, and Dr. Stalin Thambusamy likes to thank RUSA-Phase 2.0 grant No. F. 24-51/2014-U, Policy (TNMulti-Gen), Dept. of Edn., Govt. of India, Dt. 09.10.2018.

Notes The authors declare no competing financial interest.

References

1. Zhang, C., Li, Y., Wang, P., & Zhang, H. (2020). *Comprehensive Reviews in Food Science and Food Safety, 12536*, 124.
2. Ma, Z., Kotaki, M., Inai, R., & Ramakrishna, S. (2005). *Tissue Engineering, 11*, 1/2.
3. Rodoplu, D., & Mutlu, M. (2012). *Journal of Engineered Fibers and Fabrics, 7*(2), 118–123.
4. Krogstad, E. A., Ramanathan, R., Nhan, C., Kraft, J. C., Blakney, A. K., Cao, S., Ho, R. J. Y., & Woodrow, K. A. (2017). *Biomaterials, 144*, 1–6.
5. Kenry, & Lim, C. T. (2017). Nanofiber technology. *Progress in Polymer Science, 70*, 1–17.
6. Aytac, Z., Kusku, S. I., Durgun, E., & Uyar, T. (2016). *Materials Science and Engineering C, 63*, 231–239.
7. Rezaei, A., & Nasirpour, A. (2018). *International Journal of Food Properties, 21*(1), 1608–1618.
8. Okur, N., Saricam, C., Gocek, I., Kalav, B., & Sahin, U. K. (2019). *Journal of Industrial Textiles, 1–13*.
9. Loftsson, T., & Duchêne, D. (2007). *International Journal of Pharmaceutics, 329*(1–2), 1–11.
10. Kayaci, F., Sen, H. S., Durgun, E., & Uyar, T. (2014). *Food Research International, 62*, 424–431.
11. Zhang, C., Wang, L., Zhai, T., Wang, X., Dan, Y., & Turng, L. S. (2016). *Journal of the Mechanical Behavior of Biomedical Materials, 53*, 403–413.
12. Tonglairoum, P., Chuchote, T., Ngawhirunpat, T., Rojanarata, T., & Opanasopit, P. (2014). *Pharmaceutical Development and Technology, 19*(4), 430–437.
13. Ajallouеian, F., Tavanai, H., Hilborn, J., Donzel-Gargand, O., Leifer, K., Wickham, A., & Arpanaei, A. (2014). *BioMed Research International*, 1–13.
14. Masoumi, S., Amiri, S., & Bahrami, S. H. (2018). *Journal of the Textile Institute, 109*(8), 1044–1053.
15. Kim, H. W., Yu, H. S., & Lee, H. H. (2008). *Journal of Biomedical Materials Research Part A, 87A*(1), 25–32.
16. Somsap, J., Kanjanapongkul, K., Chancharoonpong, C., Supapvanich, S., & Tepsorn, R. (2019). *Current Applied Science and Technology, 19*, 235–247.
17. Kfoury, M., Landy, D., & Fourmentin, S. (2018). A review. *Molecules, 23*(5), 1204.
18. Abarca, R. L., Rodríguez, F. J., Guarda, A., Galotto, M. J., & Bruna, J. E. (2016). *Food Chemistry, 196*, 968–975.
19. Figueiras, A., Carvalho, R. A., Ribeiro, L., Torres-Labandeira, J. J., & Veiga, F. J. B. (2007). *European Journal of Pharmaceutics and Biopharmaceutics, 67*(2), 531–539.
20. Wen, X., Tan, F., Jing, Z., & Liu, Z. (2004). *Journal of Pharmaceutical and Biomedical Analysis, 34*(3), 517–523.
21. Narayanan, V., Mani, M. K., & Thambusamy, S. (2020). *Journal of Molecular Structure*, 128767.
22. Kayaci, F., & Uyar, T. (2012). *Food Chemistry, 133*(3), 641–649.
23. Wu, X., Li, P., Cong, L., Yu, H., Zhang, D., Yue, Y., Xu, H., Xu, K., Zheng, X., Wang, X. (2020). *Colloids and Surfaces A: Physicochemical and Engineering Aspects*, 125378.
24. Celebioglu, A., Kayaci-Senirmak, F., Ipek, S., Durgun, E., & Uyar, T. (2016). *Food and Function, 7*(7), 3141–3153.
25. Nie, G., Zhao, X., Luan, Y., Jiang, J., Kou, Z., Wang, J. (2020). *Nanoscale*, 1–65.
26. Yildiz, Z. I., Kilic, M. E., Durgun, E., & Uyar, T. (2019). *Journal of Agricultural and Food Chemistry, 67*(40), 11066–11076.
27. Tiwari, A. P., Mukhiya, T., Muthurasu, A., Chhetri, K., Lee, M., Dahal, B., Lohani, P. C., & Kim, H. (2021). *Electrochem, 2*, 236–250.
28. Lou, L., Osemwegie, O., & Ramkumar, S. S. (2020). *Industrial and Engineering Chemistry Research, 59*, 5439–5455.
29. Xue, J., Wu, T., Dai, Y., & Xia, Y. (2019). *Chemical Reviews, 119*, 5298–5415.
30. Thenmozhi, S., Dharmaraj, N., Kadirvelu, K., Kim, H. Y. (2017). *Materials Science and Engineering: B Solid-State Materials for Advanced Technology, 217*, 36–48.

31. Haider, A., Haider, S., & Kang, I. K. (2018). *Arabian Journal of Chemistry, 11*, 1165–1188.
32. Heikkilä, P., & Harlin, A. (2008). *European Polymer Journal, 44*(10), 3067–3079.
33. Zhao, Y., Qiu, Y., Wang, H., Chen, Y., Jin, S., & Chen, S. (2016). *International Journal of Polymer Science*, 1–17. Chigome, S., & Torto, N. (2011). *Analytica Chimica Acta, 706*(1), 25–36.
34. Khajavi, R., Abbasipour, M., & Bahador, A. (2016). *Journal of Applied Polymer Science, 133* (3).
35. Zhang, X., Ji, L., Toprakci, O., Liang, Y., & Alcoutlabi, M. (2011). *Polymer Reviews, 51*(3), 239–264.
36. Kriegel, C., Arrechi, A., Kit, K., McClements, D. J., & Weiss, J. (2008). *Critical Reviews in Food Science and Nutrition, 48*(8), 775–797.
37. Wang, X., & Hsiao, B. S. (2016). *Current Opinion in Chemical Engineering, 12*, 62–81.
38. Kumbar, S. G., James, R., Nukavarapu, S. P., & Laurencin, C. T. (2008). *Biomedical Materials, 3*(3), 034002.
39. Ma, Z., Kotaki, M., & Ramakrishna, S. (2005). *Journal of Membrane Science, 265*(1–2), 115–123.
40. Ohkawa, K., Minato, K. I., Kumagai, G., Hayashi, S., & Yamamoto, H. (2006). *Biomacromolecules, 7*(11), 3291–3294.
41. Jeong, S. I., Krebs, M. D., Bonino, C. A., Khan, S. A., & Alsberg, E. (2010). *Macromolecular Bioscience, 10*(8), 934–943.
42. Park, W. H., Jeong, L., Yoo, D. I., & Hudson, S. (2004). *Polymer, 45*(21), 7151–7157.
43. Rnjak-Kovacina, J., Wise, S. G., Li, Z., Maitz, P. K. M., Young, C. J., Wang, Y., & Weiss, A. S. (2011). *Biomaterials, 32*(28), 6729–6736.
44. Park, J.-C., Ito, T., Kim, K.-O, Kim, K.-W., Kim, B.-S., Khil, M.-S., Kim, I.-S. (2010). *Polymer Journal, 42*(3), 273–276.
45. Gómez-Pachón, E. Y., Vera-Graziano, R., & Campos, R. M. (2014). *Materials Science and Engineering, 59*, 012003.
46. Simotwo, S. K., DelRe, C., & Kalra, V. (2013). *ACS Applied Materials and Interfaces, 8*(33), 21261–21269.
47. Stone, S. A., Gosavi, P., Athauda, T. J., & Ozer, R. R. (2013). *Materials Letters, 112*, 32–35.
48. Dev, A., Binulal, N. S., Anitha, A., Nair, S., Furuike, V. T., Tamura, H., & Jayakumar, R. (2010). *Carbohydrate Polymers, 80*(3), 833–838.
49. A. Gencturk, E. Kahraman, S. Güngör, G. Özhan, Y. Özsoy, & A. S. Sarac, *Nanomedicine, and Biotechnology, 45*(3), 655–664.
50. Li, M., Guo, Y., Wei, Y., Macdiarmid, A., & Lelkes, P. (2006). *Biomaterials, 27*(13), 2705–2715.
51. Meng, Z. X., Xu, X. X., Zheng, W., Zhou, H. M., Li, L., Zheng, Y. F., & Lou, X. (2011). *Colloids and Surfaces B: Biointerfaces, 84*(1), 97–102.
52. Phan, D.-N., Lee, H., Huang, B., Mukai, Y., & Kim, I.-S. (2018). *Cellulose, 26*, 1781–1793.
53. Ma, Z., He, W., Yong, T., & Ramakrishna, S. (2005). *Tissue Engineering, 11*(7–8), 1149–1158.
54. He, W., Yong, T., Teo, W. E., Ma, Z., & Ramakrishna, S. (2005). *Tissue Engineering, 11*(9–10), 1574–1588.
55. AmanMohammadi, M., Ramezani, S., Hosseini, H., Mortazavian, A. M., Hosseini, S. M., & Ghorbani, M. (2021). *Food and Bioprocess Technology, 14*(8), 1529–1541.
56. Z. Ceylan. (2018). *Journal of Food Safety*, 12551.
57. Uekama, K., Hirayama, F., & Irie, T. (1998). *Chemical Reviews, 98*(5), 2045–2076.
58. Zhou, J., & Ritter, H. (2010). *Polymer Chemistry, 1*(10), 1552.
59. Marques, H. M. C. (2010). *Flavour and Fragrance Journal, 25*(5), 313–326.
60. Sherje, A. P., Dravyakar, B. R., Kadam, D., & Jadhav, M. (2017). *Carbohydrate Polymers, 173*, 37–49.
61. Anselmi, C., Centini, M., Maggiore, M., Gaggelli, N., Andreassi, M., Buonocore, A., Beretta, G., & Facino, R. M. (2008). *Journal of Pharmaceutical and Biomedical Analysis, 46*(4), 645–662.

62. Jullian, C., Miranda, S., Zapata-Torres, G., Mendizábal, F., & Olea-Azar, C. (2007). *Bioorganic Medicinal Chemistry, 15*(9), 3217–3224.
63. Rasheed, A., Ashok Kumar, C. K., & Sravanthi, V. V. N. S. S. (2008). *Scientia Pharmaceutica, 76*(4), 567–598.
64. Yildiz, Z. I., Celebioglu, A., Kilic, M. E., Durgun, E., & Uyar, T. (2018). *Journal of Food Engineering, 224*, 27–36.
65. Kayaci, F., Umu, O. C. O., Tekinay, T., & Uyar, T. (2013). *Journal of Agricultural and Food Chemistry, 61*(16), 2901–3908.
66. Ceylan, Z., Yaman, M., Sağdıç, O., Karabulut, E., & Yilmaz, M. T. (2018). *LWT, 98*, 162–169.
67. Zhou, Y., Miao, X., Lan, X., Luo, J., Luo, T., Zhong, Z., & Tang, Y. (2020). *Polymers, 12*(2), 299.
68. Guan, X., Li, L., Li, S., Liu, J., Huang, K. (2020). *Food Bioscience*, 100687.
69. Ardekani-Zadeh, A. H., & Hosseini, S. F. (2019). *Carbohydrate Polymers*, 115108.
70. Lin, L., Xue, L., Duraiarasan, S., & Haiying, C. (2018). *Food Packaging and Shelf Life, 17*, 134–141.
71. Cui, H., Bai, M., Rashed, M. M. A., & Lin, L. (2018). *International Journal of Food Microbiology, 266*, 69–78.
72. Xing, G., Shao, L., Du, Y., Tao, H., & Qi, C. (2020). *Cellulose, 28*(2), 961–971.
73. Wang, X., Yue, T., & Lee, T. (2015). *Food Control, 54*, 150–157.
74. Surendhiran, D., Cui, H., & Lin, L. (2019). *Food Packaging and Shelf Life, 21*, 100346.
75. Yin, J., & Xu, L. (2020). *International Journal of Biological Macromolecules, 160*, 352–363.
76. Tang, Y., Zhou, Y., Lan, X., Huang, D., Luo, T., Ji, J., & Wang, W. (2019). *Journal of Agricultural and Food Chemistry, 67*(8), 2227–2234.
77. Vafania, B., Fathi, M., & Soleimanian-Zad, S. (2019). *Food and Bioproducts Processing, 116*, 240–248.
78. Liu, Y., Liang, X., Wang, S., Qin, W., & Zhang, Q. (2018). *Polymers, 10*(5), 561.
79. Kuntzler, S. G., Costa, J. A. V., & de Morais M. G. (2018). *International Journal of Biological Macromolecules, 117*, 800–806.
80. Sadri, M., Arab-Sorkhi, S., Vatani, H., & Bagheri-pebdeni, A. (2015). *Fibers and Polymers, 16*(8), 1742–1750.
81. Surendhiran, D., Li, C., Cui, H., & Lin, L. (2020). *Food Packaging and Shelf Life, 23*, 100439.
82. Han, W., Xie, S., Sun, X., Wang, X., & Yan, Z. (2017). *Fibers and Polymers, 18*(8), 1554–1560.
83. Van Hai, L., Zhai, L., Kim, H. C., Panicker, P. S., Pham, D. H., & Kim, J. (2020). *Nanomaterials, 10*(9), 1752.
84. Beikzadeh, S., Akbarinejad, A., Swift, S., Perera, J., Kilmartin, P. A., & Travas-Sejdic, J. (2020). *Reactive and Functional Polymers, 157*, 104769.
85. Kayaci, F., Ertas, Y., & Uyar, T. (2013). *Journal of Agricultural and Food Chemistry, 61*(34), 8156–8165.
86. Kayaci, F., Umu, O. C. O., Tekinay, T., & Uyar, T. (2013). *Journal of Agricultural and Food Chemistry, 61*(16), 3901–3908.
87. Aytac, Z., Kusku, S. I., Durgun, E., & Uyar, T. (2016). *Food Chemistry, 197*, 864–871.
88. Rezaei, A., & Nasirpour, A. (2019). *BioNanoScience*, 438–445.
89. Aytac, Z., Keskin, N. O. S., Tekinay, T., & Uyar, T. (2017). *Journal of Applied Polymer Science, 134*(21).
90. Liu, Y., Liang, X., Zhang, R., Lan, W., & Qin, W. (2017). *Polymers, 9*(12), 464.
91. Zhou, J., Wang, Q., Lu, H., Zhang, Q., Lv, P., & Wei, Q. (2016). *Fibers and Polymers, 17*(11), 1835–1841.
92. Daghrery, A., Aytac, Z., Dubey, N., Mei, L., Schwendeman, A., & Bottino, M. C. (2020). *Biointerfaces, 191*, 111011.
93. Masoumi, S., Amiri, S., & Bahrami, S. H. (2017). *Journal of the Textile Institute, 109*(8), 1044–1053.
94. Narayanan, G., Aguda, R., Hartman, M., Chung, C.-C., Boy, R., Gupta, B. S., & Tonelli, A. E. (2015). *Polymers (Basel), 17*(1), 271–279.

95. Wu, X., Li, P., Cong, L., Yu, H., Zhang, D., Yue, Y., & Wang, X. (2020). *Colloids and Surfaces A: Physicochemical and Engineering Aspects*, 125378.
96. Lemma, S. M., Scampicchio, M., Mahon, P. J., Sbarski, I., & Wang, J. (2015). *Journal of Agricultural and Food Chemistry, 63*(13), 3481–3488.
97. Aytac, Z., Ipek, S., Durgun, E., & Uyar, T. (2017). *Journal of Materials Science, 53*(2), 1527–1539.
98. Wen, P., Zhu, D.-H., Feng, K., Liu, F.-J., Lou, W.-Y., Li, N., & Wu, H. (2016). *Food Chemistry, 196*, 996–1004.
99. Aytac, Z., Ipek, S., Erol, I., Durgun, E., & Uyar, T. (2019). *Colloids and Surfaces B: Biointerfaces, 178*, 129–136.
100. Aytac, Z., Sen, H., Durgun, E., & Uyar, T. (2015). *Colloids and Surfaces B: Biointerfaces, 128*, 331–338.
101. Li, W., Li, M., Adair, K., Sun, X., & Yu, Y. (2017). *Journal of Materials Chemistry A, 5*, 5355.
102. Nataraj, S. K., Kim, B. H., Yun, J. H., Lee, D. H., Aminabhavi, T. M., & Yang, K. S. (2009). *Synthetic Metals, 162*(2), 75–81.
103. Che Othman, F., Yusof, N., González-Benito, J., Fan, X., Ismail, A. (2020). *Polymers, 12*(9).
104. Che Othman, F., Yusof, N., Ismail, A., Jaafar, J., Wan Salleh, W., Aziz, F. (2020). *AIP Advances, 10*(5), 055117.
105. Dai, Z., Ren, P., Jin, Y., Zhang, H., Ren, F., & Zhang, Q. (2019). *Journal of Power Sources, 437*, 226937.
106. Ji, L., Lin, Z., & Medford, A. J. (2009). *Carbon, 47*(14), 3346–3354.
107. Zhu, J., Chen, C., Lu, Y., Ge, Y., Jiang, H., Fu, K., & Zhang, X. (2015). *Carbon, 94*, 189–195.
108. Li, L., Wang, X., Zhong, J., Qian, X., Song, S., Zhang, Y., & Li, D. (2018). *Industrial and Engineering Chemistry Research, 34*, 11608–11616.
109. Patil, S., Chigome, S., Hägerhäll, C., Torto, N., & Gorton, L. (2013). *Bioresource Technology, 132*, 121–126.



Narayanan Vimalasruthi received her M.Sc. degree in general chemistry from Alagappa University, Karaikudi,Tamil Nadu, India in 2018. She is doing Ph.D. under the guidance of Dr. T. Stalin at Department of Chemistry, Alagappa University. Her research field focuses on the fabrication of electrospun nanofibers based on synthetic polymers for biological applications.



Ganesan Vigneshkumar received his M.Sc. degree in general chemistry from Alagappa University, Karaikudi, Tamil Nadu, India in 2017. Currently, he is working as a Ph.D. Research Scholar under the guidance of Dr. T. Stalin at Department of Chemistry, Alagappa University. His research interests focus on the Electrochemical biosensor.



Shanmugasundaran Esakkimuthu received his M.Sc. degree in general chemistry from Alagappa University, Karaikudi, Tamil Nadu, India in 2018. He is doing Ph.D. under the guidance of Dr. T. Stalin at Department of Chemistry, Alagappa University. His research-based on the preparation and characterization polymer materials by electrospun and electropolymerization technique for organic solar cell application.



Krishnamoorthy Sivakumar Professor in the Department of Chemistry at Sri Chandrasekharendra Saraswathi Viswa Mahavidyalaya (Deemed to be University) [SCSVMV University], Enathur, Kanchipuram-631561, Tamil Nadu, India. He has more than 20 years of experience in teaching and research. He has guided for Ph.D.s., M.Phil. Scholars and M. Sc., Students. He has published 85 research papers. His h-index is 15, and i10 index is 20. He has successfully completed research projects from various funding agencies, like DST, UGC. His current research interest involves the development of chemosensory materials for environmental and biological applications.



Thambusamy Stalin is an Assistant Professor of Chemistry in the Department of Industrial Chemistry at Alagappa University, Tamilnadu, India (From 2009 to date). He received his Ph.D. degree from the Annamalai University, India in 2008. He has more than 15 years of teaching and 20 years of research experience. He has guided for 9 Ph.D.s., 9 M.Phil. Scholars, and 42 M.Sc., Students. Currently, he is guiding 5 Ph.D. Scholars. He has published 63 research papers in SCI journals and presented more than 75 research papers in national and international conferences. He has a very good citation index (1486) for his publications and his present h-index is 24 and i10 index is 45. He has successfully completed and running 5 research projects from various funding agencies, like DST, UGC., He has won awards like YOUNG SCIENTISTAWARD, 2011–2014. DST and RAMAN FELLOWSHIPS for postdoctoral research for Indian scholars in USA, 2017–2018, UGC, Vallal Alagappar Research Recognition Award -2020; Alagappa University, Karaikudi, Tamil Nadu. He is a Life member of the Indian science congress Association, Solid State Chemistry and the Indian society for Radiation and Photochemical Sciences. His current research interest involves the development of chemosensor materials for environmental and biological applications.

Chapter 25
Electrospun Nanofibers for Energy Harvesting



Mina Abbasipour and Ramin Khajavi

Abstract Electrospinning is a versatile and efficient method for the fabrication of polymeric materials in the form of solution and melt into a 3D nanofibrous structure of nanofibers. These fabricated products have shown and proven their high potential in many other fields such as biomedical scaffolds and nanofiltration, but now they are making way to the energy harvesting field due to their high specific surface area, lightweight, flexibility, and ease of fabrication. This chapter provides an overview of triboelectric, piezoelectric, pyroelectric materials, and solar cells that are made by electrospun nanofibers. Details on the materials, underlying physical principles, energy harvester structures, approaches for optimizing the total energy conversion efficiency of energy harvesters are discussed. The effect of the microscopic structure of electrospun nanofibers on energy conversion efficiency is presented. Finally, the future perspectives of electrospun nanofibers for developing the next generation of high-performance energy harvesters are summarized.

Keywords Electrospun nanofibers · Energy harvesting · Piezoelectric · Triboelectric · Pyroelectric · Solar cells

25.1 Introduction

By increasing self-powered devices, new technologies have been required for powering. To provide electricity for these devices, a novel cost-effective and environment-friendly approaches such as solar, wind, mechanical vibrations, or thermal energy have been presented as alternatives to fossil fuels [1]. Wearable electronics have been offered in a wide range of applications such as sensors, healthcare

M. Abbasipour
Department of Textile Engineering, Science and Research Branch, Islamic Azad University, Tehran, Iran

R. Khajavi (✉)
Department of Polymer and Textile Engineering, South Tehran Branch, Islamic Azad University, Tehran, Iran
e-mail: khajavi@azad.ac.ir

© The Author(s), under exclusive license to Springer Nature Switzerland AG 2022

A. Vaseashta and N. Bölgen (eds.), *Electrospun Nanofibers*,
https://doi.org/10.1007/978-3-030-99958-2_25

monitoring, and energy harvesting. Various kinds of components including flexible power systems, sensors, display, and energy storage should be integrated to the system to have a complete flexible electronic device. Fabrication of flexible, low energy-consuming, and battery-free personal electronic devices is required for modern life. Piezoelectric, pyroelectric, triboelectric, solar cells, electrochemical, and electromagnetic are different types of mechanisms that have been suggested for harvesting energy from the ambient for self-powered electronic devices [2].

Nanostructured materials in the form of nanofibers (NFs), nanowires (NWs), nanotubes (CNTs), and nanorods (NRs) have been considered due to physical and chemical characteristics. The unique properties of NFs like high specific area, lightweight, flexibility, and ease of fabrication make them applicable for many purposes. Template-assisted synthesis, chemical vapor deposition (CVD), self-assembly, wet chemical synthesis, and electrospinning are methods for nanofibrous fabrication. Electrospinning is considered a simple, highly efficient, low cost, and highly reproducible method for NFs production among all suggested methods. In addition, electrospun NFs have a high specific area, aspect ratio, and better pore interconnectivity which are suitable for energy harvesting. Moreover, various morphologies and structures of NFs such as core-shell, hollow, porous, and yarn can be achieved by the electrospinning technique [3, 4]. In this chapter, various kinds of energy harvesting such as piezoelectric, pyroelectric, triboelectric nanogenerator, and hybrid nanogenerator based on electrospun nanofibers are presented.

25.2 Piezoelectric Nanogenerators (PNGs)

Piezoelectricity is the ability of materials to convert mechanical stress to electrical energy. Different polymeric and inorganic materials have been introduced to fabricate piezoelectric and pyroelectric nanogenerators. Piezoelectric materials can be classified into organic and inorganic materials [5]. Inorganic piezoelectric materials with wurtzite and perovskite structures have non-central symmetric. When mechanical stress is applied to materials, negative charges, and positive cation form and cause dipole moments and spontaneous polarization. Piezoelectricity has been measured by piezoelectric coefficients (d_{33}, d_{31}, d_{14}) and electrical output.

Nylon, poly(vinylidene fluoride) (PVDF), polyurethane, and polyurea shows piezoelectric properties. Natural polymers (e. g. cellulose, collagen, chitosan, poly(l-lactic acid), and silk) are recognized as bio-PNGs [2]. Electrospinning technique has been suggested for producing both polymeric and inorganic devices [6].

Among all the piezoelectric polymers, PVDF and its copolymers such as poly(vinylidene fluoride-trifluoroethylene) (P(VDF-TrFE)) and poly(vinylidene fluoride)-co-hexafluoropropylene (P(VDF-HFP)) are most widely used polymers for mechanical and thermal energy harvesting. PVDF contains five distinct phases including α (TGTG′), β (TTTT), γ (T_3GT_3G'), δ (polarized) and ε. The β-phase with trans configuration shows the highest piezoelectric and pyroelectric properties rather than other phases. Fourier transform infrared spectroscopy (FTIR), X-ray diffraction

analysis (XRD), and differential scanning calorimetry (DSC) are used to β-phase content determination. Various methods such as mechanical stretching, electrical poling, and filler addition have been applied to increase output voltage [7]. Although, the electrospinning process causes increasing β-phase content of electrospun PVDF nanofibers by applying in-situ mechanical and electrical stretching, the electrospun PVDF nanofibers still show low output voltage. The output voltage and current of polarized electrospun PVDF membrane were 1.5 V and 0.4 μA, respectively. It was found that using high speed rotating drum collector instead of a flat collector causes additional mechanical stretching. In addition to the conventional solution electrospinning, melt and near field electrospinning (NFES) are used for piezoelectric fiber mat production. Low porosity fibers with controlled diameter can be produced with melt electrospinning. Molecular dipoles in fibers are randomly oriented due to the low applied voltage in melt electrospinning. So, additional drawing and poling processes are required for dipole alignment [8]. The bubble-electrospinning technique also used to produce PVDF nanofibers with high piezoelectricity. In bubble electrospinning, a feeding gas is entered to solution for Taylor cone formation and collector plate is placed above the PVDF solution. In this method, the β-phase content is near to 100% by regulating the applied voltage [9]. Shao et al. [10] investigated the effect of electrospinning parameters such as polymer concentration, applied voltage, spinning distance and thickness of nanofiber membrane on β-phase content and energy harvesting properties. The finer aligned PVDF nanofibers showed higher β-phase content and hence higher output voltage. By increasing PVDF solution concentration from 20 to 26% the average fiber diameter changed from 284 to 810 nm. The beaded fibers formed when the polymer concentration is above the entanglement concentration (C_e), and when polymer solution is 2–2.5 times of C_e, uniform fibers formed due to appropriate chain entanglement. The polymer solution with 20% concentration showed higher output voltage (2.3 V) and output current (2.4 μA) as well as β-phase content (85.9%). However, the β-phase content gradually decreased from 85.9 to 82.5%, when polymer concentration increased from 20 to 26%. The average diameter of nanofibers decreased when the spinning distance from 9 to 15 cm. The highest β-phase content (85.9%), output voltage (1.5 V) and output current (1.6 μA) were obtained at the spinning distance 15 cm. In addition, the thickness of PVDF nanofiber membrane has an influence on energy conversion properties. The membrane with a thickness of 70 μA showed a higher output voltage. Chang et al. [11] used a near-field electrospinning technique to produce direct-write piezoelectric PVDF nanofiber. The direct-wrote PVDF nanogenerator generated 5- 30 mV output voltage and 0.5–3 nA. Fang et al. [12] investigated the effect of impact frequency (1, 5, 10 Hz) on the output voltage of PVDF nanofiber membrane. The output voltage reached to 6.3 V Aligned P(VDF-TrFE) nanofibers with 76% β-phase content were fabricated by parallel electrodes. Aligned P(VDF-TrFE) nanofibers showed output voltage and short circuit current of 12 V and 0.15 μA. The mechanically stretched P(VDF-TrFE) at 2 mm s^{-1} showed output voltage of 0.08496 V, which was 266% more than randomly distributed P(VDF-TrFE) nanofibers. These aligned P(VDF-TrFE) nanofibers are twisted to form fibers bundles and then woven as outfit to sense

body movement. Electrospun PVDF nanofiber web produced by disc electrospinning could generate 2.6 V output voltage and 4.5 μA current [12]. Similarly, Fang et al. [13] enhanced mechanical energy harvesting (Voltage = 3 V and current = 5 μA) using the needleless electrospinning method. To further improve piezoelectric properties, electrospun PVDF nanofibers have been impregnated with different inorganic nanofillers including multiwall carbon nanotube (MWCNT), zinc oxide (ZnO), lead zirconate titanate (PZT), barium titanate ($BaTiO_3$), etc. Piezoelectric nanofillers induce β-phase to PVDF. The morphology and filler content influence on piezoelectric and pyroelectric properties. In addition, nanofiller doping improves mechanical and thermal properties. The Aligned platinum (Pt)/PVDF nanofibers were obtained by high-speed rotating drum (2000 rpm) and mechanical properties improved by doping Pt nanoparticles by increasing degree of crystallization (75%). The piezoelectricity of electrospun Pt/PVDF nanofibers was five times higher than neat electrospun PVDF nanofibers. The output voltage of electrospun PVDF nanofibers doped with ZnO nanorods and $BaTiO_3$ nanospheres fillers increased to 12 V under a force of 1.5 N. Alam et al. [14] fabricated PVDF nanofibers doped with ZnO-paper ash to increase output to 4.8 V under 145 Pa wind energy. Parangusan et al. [15] added Co-doped ZnO nanoparticles (2 wt%) into P(VDF-HFP) matrix. The output voltage of 2 wt.% Co-voltage ZnO/P(VDF-HFP) nanofibers increased to 2.8 V compared to neat P(VDF-HFP) (≈120 mV). There is a threshold value for increasing the amount of additives, because the β-phase content does not more than this critical value. Introducing piezoelectric nanofiller into the electrospun PVDF nanofibers gives more chance to increase piezoelectric properties rather than conventional nanofillers. Bairagi and Ali [16] used different percentage of potassium sodium niobate (KNN) (0%, 1%, 3%, and 5%). The 3% amount showed the highest β-phase content (97%), output voltage (17.5 V), and current (0.522 μA) than other concentrations.

There are some other piezoelectric biopolymers such as collagen, gelatin, silk fibroin, cellulose, and chitosan used for mechanical energy harvesting [17, 18]. Sencadas et al. [19] showed that the piezoelectric constant of poly(ε-caprolactone) was equal to 5 ± 2 pm.V^{-1} and output voltage had stability until 16,000 cycles under 1mN force. Inorganic piezoelectric materials have higher piezoelectric properties than organic. Liu et al. [20] synthesized barium zirconate-titanate/barium calcium titanate (BZT-BCT, 650 pV N^{-1}) nanoparticles using electrospinning, calcination and grinding. In this study, P(VDF-TrFE)/BZT-BCT nanofiber composite prepared by different amount of BZT-BCT ranging from 0 to 50%. The nanofiber generator with 40% BZT-BCT content showed the highest output voltage (V_{OC} = 13.01 V) among other percentages. Table 25.1 shows the comparison between piezoelectric properties of electrospun piezoelectric inorganic and organic nanofibers.

Table 25.1 Piezoelectric properties of electrospun piezoelectric inorganic and organic nanofibers

Materials	β-phase content (%)	Piezoelectric coefficient (d_{33}, pC/N)	Output voltage	Output current
Randomly oriented electrospun PVDF [21]	79 ± 3	16.8 ± 1.4	9 mV	30 nA [22]
Aligned electrospun PVDF [21]	88 ± 1	27.4 ± 1.5	19.5 mV	40 nA [23]
PVDF/polyurethane random NFs	–	24.9 [24]	–	–
Aligned electrospun PVDF/CNT [21]	89 ± 2	31.3 ± 2.1	25.5 mV	–
PVDF/MWCNT random NFs [25]	84	35	2 V [26]	–
PVDF/1%(MWCNT-Ag) random NFs [25]	84	54	–	–
PVDF/$BaTiO_3$	91 [27]	48 [28]	1.6 V [29]	100 nA [30]
Core–shell structured PVDF/graphene oxide	88.5 [31]	93.75 [31]	–	–
PVDF/graphene oxide [32]	70	40	–	–
PVDF/carboxylated graphene oxide [32]	79	46	–	–
PVDF/carboxylated graphene oxide [32]	89	63	–	–
BZT-0.5BCT	–	180 [33]	–	–
Electrospun $BaTiO_3$ NFs	–	40 [34]	–	–
Electrospun PZT NFs	–	83.4 [35]	1.63 V [36]	–
Electrospun vanadium doped ZnO NFs	–	121 [37]	–	–
Electrospun P(VDF-HFP)	85.9 [38]	–	120 [39]	30 [40]
Electrospun P(VDF-HFP)/polyaniline/zinc sulphide [39]	55	–	300	1.5 μA

25.3 Piezo-Pyroelectric Hybrid Nanogenerators

Recently, different researchers fabricated flexible hybrid nanogenerator based on piezoelectric and pyroelectric effects [41]. The working principle of piezo-pyroelectric hybrid nanogenerator is shown in (Fig. 25.1) [42]. The output voltage is equal to zero in mechanical stress and thermal gradient absence, due to randomly oscillating of the electric dipoles in respect to aligning axes. In this state, the spontaneous polarization of electric dipoles remains in an equilibrium state [41]. When

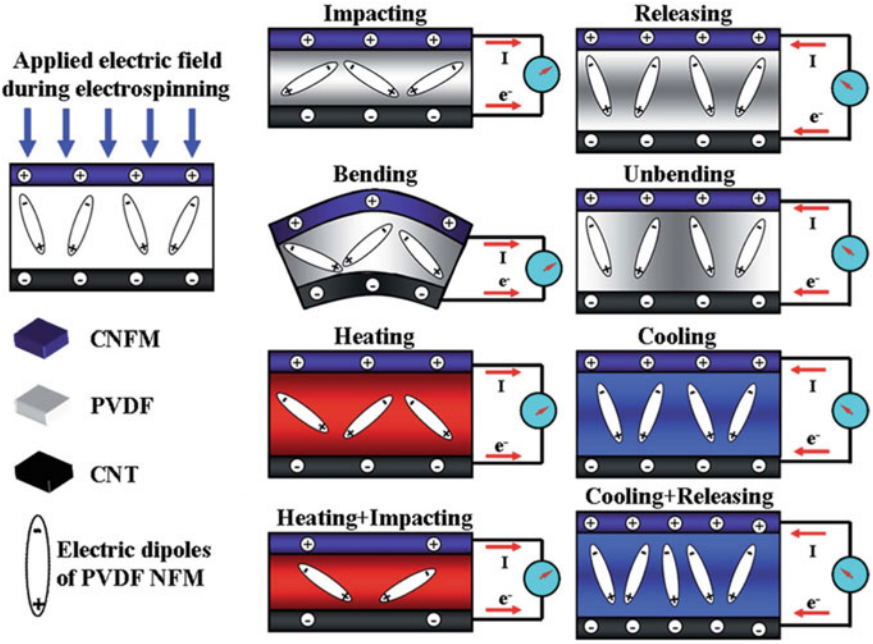


Fig. 25.1 Working mechanism of piezo-pyroelectric nanogenerator [42]

compression stress is applied on the piezo-pyroelectric nanogenerator, the electric dipole moments increase, which leads to a significant increase in the polarization of PVDF and produces a positive output voltage. When the mechanical impact is released, a negative pulse is produced. By applying mechanical stress, the total spontaneous polarization decreases and electrons flow from the bottom electrode to the top electrode and induced charges decrease. On the contrary, when mechanical stress is released, the polarization is recovered an opposite signal is observed [42]. You et al. [42] fabricated a piezo-pyroelectric hybrid nanogenerator based on electrospun PVDF nanofibers. They used CNT coated electrospun thermoplastic polyurethane nanofibers as bottom electrode and electrospun poly(3,4-ethylenedioxythiophene): poly(styrene sulfonate)-polyvinyl pyrrolidone (PEDOT:PSS-PVP) nanofibers as top electrode. When the temperature increased a positive current pulse (20 nA) was observed. Although, the negative current pulse (−16 nA) was produced when the temperature returned to the first temperature.

25.4 Triboelectric Nanogenerators (TENGs)

Triboelectric effect happens when two materials with different surface potential are came into contact and electron charge induce at the interface. When

the surface of two dissimilar materials is in contact, opposite charges form and the relative position of charges change, causes the induced potential difference between electrodes. Different working mechanism of TENGs including vertical contact separation, lateral shear, single electrode, and noncontact are developed by researchers (Fig. 25.2a) [43]. The performance of TENGs is dependent to the surface charge density of used materials. The modification surface morphology, functionalization and thickness of materials influence the surface charge density. Also, applying micro/nanostructure on the surface of materials enhances surface charge density by increasing the contact area on the surface. In comparison to lithography techniques, electrospinning is cost-effective, simple, and scalable for triboelectric materials production with micro/nanostructured. Different polymers such as PVDF and its copolymers, polyacrylonitrile (PAN), poly(vinylalcohol) (PVA), poly(dimethyl siloxane) (PDMS), polyurethane (PU), polyethylene terephthalate

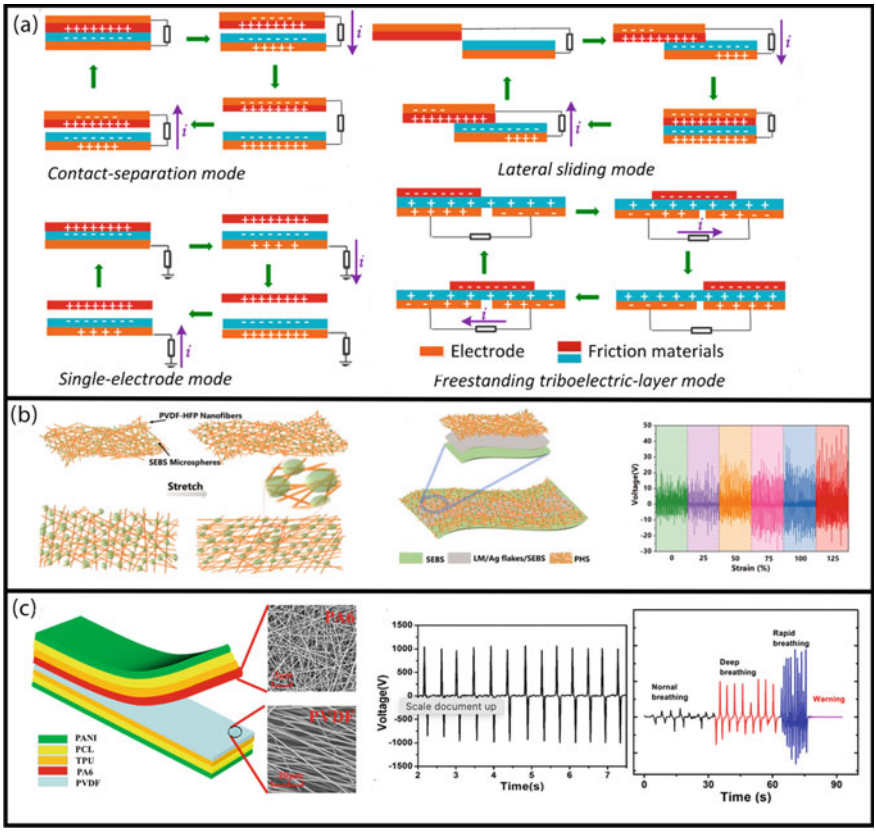


Fig. 25.2 **a** Four working modes of triboelectric effect-based electronics [43], **b** highly stretchable, durable, breathable, and hydrophobic TENG based on electrospun PVDF-HFP nanofibers [52], **c** PCL/PANI TENG structure, output voltage and its usage for health monitoring [53]

(PET), poly(tetrafluoroethylene) (PTFE), poly(methyl methacrylate) (PMMA), polyimide (PI), polyamide 6 (PA 6), silk fibroin, and ethyl cellulose have been used for TENG application [44]. For example, Zhang et al. [45] made bio-inspired (petiole-like) TENG using nano-porous PVDF fibers and the rubber layer as a negative surface. The porosity of PVDF fibers is adjusted by changing PVDF concentration from 10 to 18 wt./v% in dimethyl sulfoxide/acetone mixture. Also, by changing the relative humidity the output voltage was 1.7 and 2.2 times higher than TENG made by smoother nanofibers. The optimized power density and output voltage of petiole-like TENG were 56.9 Wm^{-2} and 2209 V. Kim et al. [46] used electrospun P(VDF-TrFE) nanofibers and Ag NWs to fabricate transparent and wearable single-electrode TENG. This single-electrode TENG had a power density 217 Wm^{-2} and showed mechanical durability until 10,000 cycles. Shaikh et al. [47] used woven TENG from electrospun PVDF nanofibers/MWCNT nanofibers and commercial nylon cloth to harvest mechanical energy from human body movement. The β-phase content of PVDF nanofibers increased by MWCNT addition caused triboelectric performance improvement. For example, 1 wt.% MWCNT increased average peak to peak current output from 4 to 16 nA. Xiong et al. [48] developed a self-recovery TENG from electrospun shape memory polymer nanofibers for water energy harvesting and water temperature sensing. Electrospun nanofibers create microstructures with surface roughness. The surface roughness increased the output voltage and current to ~150–320 V and 2.5–4 $\mu A\ cm^{-2}$, respectively. Cao et al. [49] prepared a self-powered triboelectric sensor from electrospun PVDF nanofibers/Ag nanoparticles for health monitoring. In this study, the electrical output of different electrospun polymer nanofibers membranes such as PET, PAN, PVDF and PU were compared together. In comparison to PAN, PET and PU, PVDF nanofibers showed higher output voltage and current. In other study, TENG was constructed from electrospun PMMA nanofibers and compared the triboelectric output compared to the PMMA film. In this study, electrospun PMMA nanofibers were produced from negative and positive voltage polarities. The surface potential of negative PMMA (1.2 V) was more than positive PMMA (0.6 V) [50]. The TENG assembled with PMMA nanofibers on Al foil and copper substrate was used as counter-electrode. The output voltage and output current under cyclic 0.7 N force at frequency of 2 Hz. Negative PMMA produced more output voltage (5.7 V) and output current (148.7 nA) than positive PMMA (2.9 V, 67.7 nA) under the same condition. Rana et al. [50] functionalized nylon-11 with poly(diallyldimethylammonium chloride) (poly-DADMAC) to fabricate robust and high potential TENG. Electrospun nylon-11/poly-DADMAC composite nanofibrous mat showed excellent durability (>86,000 cycles) at a 12 Hz frequency under 36 kPa. Ultra-stretchable TENG based on thermoplastic PU/rGO/Ag NWs was constructed as high-sensitive and self-powered electronic skin for energy harvesting and tactile sensor by Zhou et al. [51]. This TENG showed high sensitivity (78.4 kPa^{-1}) and a fast response (1.4 ms). In addition, the electronic skin converted biomechanical energy to electricity steadily at a large strain 200%. Li et al. [52] made highly stretchable, durable, breathable and hydrophobic TENG based on electrospun PVDF-HFP nanofibers with output voltage of 85 V. PVDF-HFP nanofibers network was inter-blocked with tyrene-ethylene-butylene-styrene microspheres to increased

stretchability and waterproofness (Fig. 25.2b). Qui et al. [53] used PCL and PANI as electrodes to fabricate gas permeable and adhesive TENG with TENG output of 200 μA and 1000 V. PCL/PANI TENG can be used for health monitoring, and it could light 1000 LED (Fig. 25.2c). Sun et al. [54] Proposed ultralight and flexible TENG based on all electrospun paper containing PAN as separator and carbon paper as electrodes. The output voltage and power density of PAN/carbon TENG were 98.6 V and 184 mW/m^2, respectively. Jiang et al. [55] introduced MXene nanosheet/PVA nanofibers to TENG system to increase power density to 1087.6 mW/m^2. Tayyab et al. [56] increased β-phase to 88% by doping printer ink to PVDF. PVDF/printer ink nanofibers TENG showed power density of 22 Wm^{-2}, which was higher than PVDF nanofibers. Kim and Park [57] optimized the content of Eu in PVDF nanofibers to improve triboelectric properties. The triboelectric power increased from 13 μW cm^{-2} to 26 μW cm^{-2} when the Eu content increased from 0 to 2.7 wt.%. However, the power decreased to 4.9 μW cm^{-2} by further addition of Eu content to 5.3 wt.%.

25.5 Piezoelectric and Triboelectric Nanogenerators (PTNGs)

The main goal of the combination of piezoelectric and triboelectric effects is increasing electrical output. A hybrid piezo-triboelectric generator contains at least one piezoelectric part and a pair of triboelectric layers. Different working mechanisms have been used to fabricate piezo-triboelectric generators. The most used method is contact-separation or press-release of a pair of layers when one of these layers has piezoelectric properties. Special geometry is used for designing this working mechanism (Fig. 25.3a). Recently, an arc-shaped geometry is used to separate layers after loading. Usually, the arc-shaped layer is used as a support layer for the piezoelectric part [58]. When compressive stress is applied to the arc-shaped polymer, leads to bending piezoelectric part and consequently, piezoelectric charge create. In addition, the compressive stress causes physical contact between layers and results in triboelectric charge generation. Yu et al. [59] used PZT nanofibers/PDMS film and Cu film to simultaneously combine piezoelectric and triboelectric effects to detect pulse wave signals such as heart rate in cardiovascular disease. The output voltage of the system was as the sequence of hybrid nanogenerator > TENG > PNG. The P(VDF-TrFE) nanofibers were used to reduce the adhesion of two layers (Fig. 25.3b). Fuh et al. [60] used piezo-triboelectric effects simultaneously by electrospinning PVDF (NFES) on graphene layer as a piezoelectric layer and PET/graphene as a triboelectric layer. By combining piezoelectric and triboelectric systems the output current reached to 300 nA. Zhao et al. [61] fabricated a multifunctional sensor based on piezoresistive, piezo and triboelectric effects from carbonized electrospun PAN and $BaTiO_3$ (Fig. 25.3c). The sensor showed high durability up to 60,000 cycles of bending. $BaTiO_3$ doping on PAN nanofibers improves both piezoelectric and triboelectric effects over 2.4 times. Wu et al. [62] improved piezo-triboelectric properties

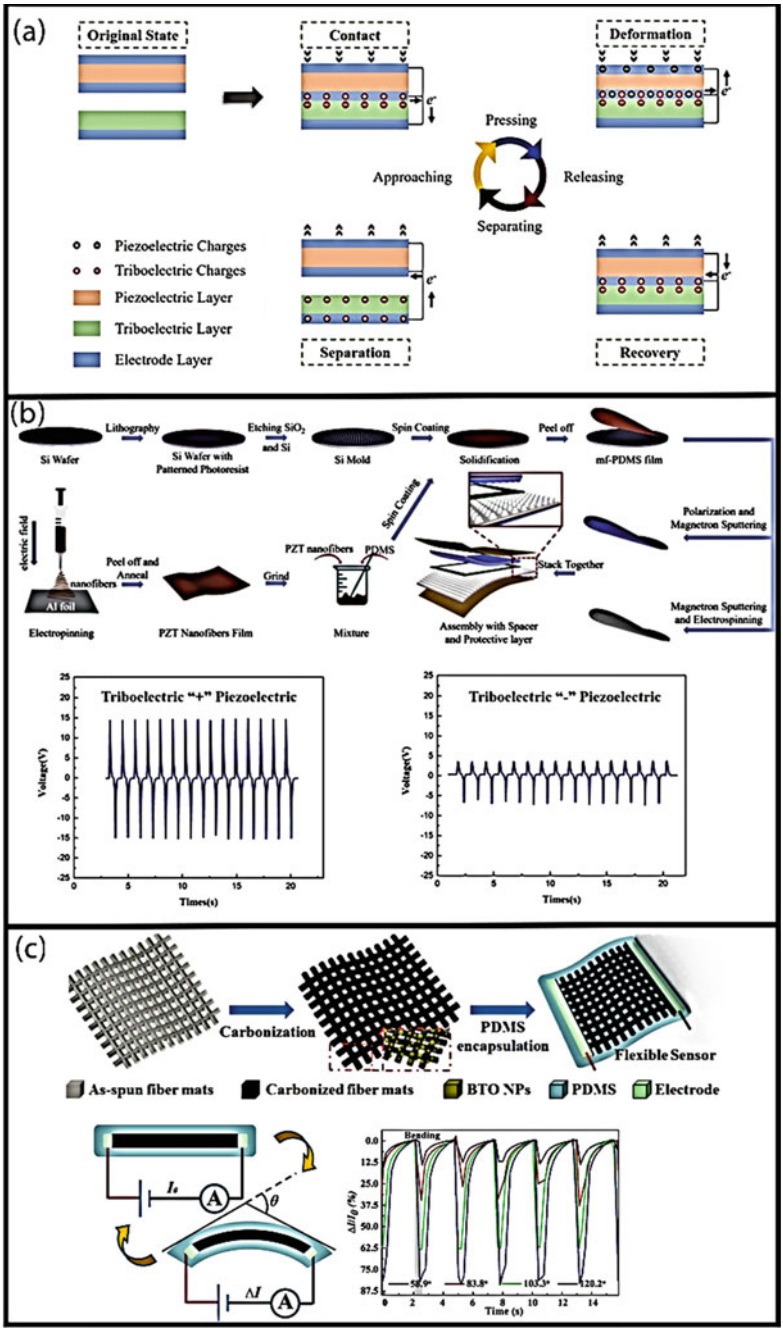


Fig. 25.3 **a** Working mechanism of PTENGs, **b** fabrication process and output voltage of PZT nanofibers/PDMS PTNG [59], **c** fabrication process of PAN/$BaTiO_3$ PTNG and its output current regarding different bending angle [61]

by doping BCZT into PVDF-HFP nanofibers. PVDF-HFP nanofibers/BCZT based PTNG showed 5.5 times higher power density than $BaTiO_3$/PVDF-based PTNG. The output voltage of PVDF-HFP nanofibers/BCZT based PTNG had stability after 1200 cycles. Sahatiya et al. [63] used PVDF nanofibers and grown MoS_2 on cellulose paper for both piezo and triboelectric effects. The strain rate and polarization affected on piezoelectric performance and triboelectric response is dependent on the separation distance and the contact velocity. Song et al. [64] used PVDF/CNT/$BaTiO_3$ nanofibers as piezoelectric parts and PDMS/CNT/graphite film as triboelectric part. The rectified peak average voltage was 166.67 V with a power density of 2.22 Wm^{-2}, which could light 150 LED.

Sun et al. [65] used leaf pattern Ag NWs and PVDF nanofibers to make a transparent piezo-pyro-triboelectric nanogenerator. This hybrid nanogenerator showed output voltage of 55 V and 86 V from mechanical and thermal energy scavenging, respectively. Wang et al. [66] used one structure nanogenerator based on PVDF NWs to fabricate piezo-pyro-triboelectric hybrid nanogenerator. PVDF NWs were produced using the electrospinning method. The current output of the pyroelectric system was ~0.1 μA. However, the current output increased to ~15 μA when the system was hybrid. In addition, the electrical output from the piezo-pyro-triboelectric hybrid nanogenerator was the same as the piezo-triboelectric nanogenerator.

25.6 Conclusion

Stretchability and flexibility are essential for wearable electronics to the comfortable movement of users. PENGs and TENGs based on fibers have required flexibility and stretchability for wearable electronic textiles and can be used as human motion energy harvesting and health monitoring. However, conventional fiber-based PENGs and TENGs have shortcomings such as low electrical output. For overcoming this deficiency, different methods such as nanofiller addition, multilayer structure, and hybrid nanogenerator have been suggested. Therefore, energy conversion and generation in PENGs, TENGs, and hybrid nanogenerators mostly depend on material design and structure.

Electrospinning is a simple, cost-effective, and efficient method for producing fiber-based nanogenrators. Different electrospinning methods such as NFES, multineedle or needle-free electrospinning, emulsion, wet, coaxial, and bubble electrospinning have been used for producing nanogenerators. Although electrospun nanofibers have the ability to use for energy harvesting, they may deform and disrupt after long-term of device use. Therefore, device materials components and structures should be considered in designing of device.

References

1. Xu, Q., Wen, J., & Qin, Y. (2021). Development and outlook of high output piezoelectric nanogenerators. *Nano Energy, 86*, 106080. https://doi.org/10.1016/j.nanoen.2021.106080
2. Mahapatra, S, D., Mohapatra, P. C., Aria, A. I., Christie, G., Mishra, Y. K., Hofmann, S., & Thakur, V. K. (2021). Piezoelectric materials for energy harvesting and sensing applications: Roadmap for future smart materials. *Advanced Science, 8*:2100864. https://doi.org/10.1002/advs.202100864.
3. Khajavi, R., & Abbasipour, M. (2012). Electrospinning as a versatile method for fabricating coreshell, hollow and porous nanofibers. *Scientia Iranica;19*. https://doi.org/10.1016/j.scient.2012.10.037.
4. Abbasipour, M., & Khajavi, R. (2013). Nanofiber bundles and yarns production by electrospinning: A review. *Advances in Polymer Technology, 32*. https://doi.org/10.1002/adv.21363.
5. Fan, F. R., Tang, W., & Wang, Z. L. (2016). Flexible nanogenerators for energy harvesting and self-powered electronics. *Advanced Materials, 28*, 4283–4305. https://doi.org/10.1002/adma.201504299
6. Briscoe, J., & Dunn, S. (2015). Piezoelectric nanogenerators—a review of nanostructured piezoelectric energy harvesters. *Nano Energy, 14*, 15–29.
7. Khajavi, R., & Abbasipour, M. (2016). Piezoelectric PVDF polymeric films and fibers: Polymorphisms, measurements, and applications. https://doi.org/10.1007/978-3-319-26893-4_15.
8. Asai, H., Kikuchi, M., Shimada, N., & Nakane, K. (2017). Effect of melt and solution electrospinning on the formation and structure of poly(vinylidene fluoride) fibres. *RSC Advances, 7*. https://doi.org/10.1039/C7RA01299C.
9. Hernández-Navarro, N., González-González, V., Moreno-Cortez, I. E., Garza-Navarro, M. A. (2016). Electrospun polyvinylidene fluoride nanofibers by bubble electrospinning technique. *Materials Letters, 167*. https://doi.org/10.1016/j.matlet.2015.12.112.
10. Shao, H., Fang, J., Wang, H., & Lin, T. (2015). Effect of electrospinning parameters and polymer concentrations on mechanical-to-electrical energy conversion of randomly-oriented electrospun poly(vinylidene fluoride) nanofiber mats. *RSC Advances, 5*, 14345–14350. https://doi.org/10.1039/C4RA16360E
11. Chang, C., Tran, V. H., Wang, J., Fuh, Y.-K., & Lin, L. (2010). Direct-Write piezoelectric polymeric nanogenerator with high energy conversion efficiency. *Nano Letters, 10*, 726–731. https://doi.org/10.1021/nl9040719
12. Fang, J., Wang, X., & Lin, T. (2011). Electrical power generator from randomly oriented electrospun poly(vinylidene fluoride) nanofibre membranes. *Journal of Materials Chemistry, 21*, 11088–11091. https://doi.org/10.1039/c1jm11445j
13. Fang, J., Niu, H., Wang, H., Wang, X., & Lin, T. (2013). Enhanced mechanical energy harvesting using needleless electrospun poly(vinylidene fluoride) nanofibre webs. *Energy & Environmental Science, 6*, 2196. https://doi.org/10.1039/c3ee24230g
14. Alam, M. M., Ghosh, S. K., Sultana, A., & Mandal, D. (2018). An effective wind energy harvester of paper ash-mediated rapidly synthesized ZnO nanoparticle-interfaced electrospun PVDF fiber. *ACS Sustainable Chemistry & Engineering, 6*:292–299. https://doi.org/10.1021/acssuschemeng.7b02441.
15. Parangusan, H., Ponnamma, D., & Al-Maadeed, M. A. A. (2018). Stretchable electrospun PVDF-HFP/Co-ZnO nanofibers as piezoelectric nanogenerators. *Scientific Reports, 8*, 754.
16. Bairagi, S., & Ali, S. W. (2020). Poly (vinylidine fluoride) (PVDF)/potassium sodium niobate (KNN) nanorods based flexible nanocomposite film: Influence of KNN concentration in the performance of nanogenerator. *Organic Electronics, 78*, 105547. https://doi.org/10.1016/j.orgel.2019.105547
17. Ramadan, K. S., Sameoto, D., & Evoy, S. (2014). A review of piezoelectric polymers as functional materials for electromechanical transducers. *Smart Materials and Structures, 23*, 033001. https://doi.org/10.1088/0964-1726/23/3/033001

18. Ghosh, S. K., & Mandal, D. (2016). Efficient natural piezoelectric nanogenerator: Electricity generation from fish swim bladder. *Nano Energy, 28*, 356–365. https://doi.org/10.1016/j.nanoen.2016.08.030
19. Sencadas, V. (2020). Energy harvesting applications from poly(ε-caprolactone) electrospun membranes. *ACS Applied Polymer Materials, 2*. https://doi.org/10.1021/acsapm.0c00209.
20. Liu, J., Yang, B., Lu, L., Wang, X., Li, X., Chen, X., & Liu, J. (2020). Flexible and lead-free piezoelectric nanogenerator as self-powered sensor based on electrospinning BZT-BCT/P(VDF-TrFE) nanofibers. *Sensors and Actuators A: Physical, 303*. https://doi.org/10.1016/j.sna.2019.111796.
21. Wu, C.-M., Chou, M.-H., & Zeng, W.-Y. (2018). Piezoelectric response of aligned electrospun polyvinylidene fluoride/carbon nanotube nanofibrous membranes. *Nanomaterials, 8*, 420. https://doi.org/10.3390/nano8060420
22. Chang, J., & Lin, L. (2011). Large array electrospun PVDF nanogenerators on a flexible substrate. In *2011 16th International Solid-State Sensors, Actuators and Microsystems Conference* (p. 747–50). IEEE.https://doi.org/10.1109/TRANSDUCERS.2011.5969865
23. Kang, S. B., Won, S. H., Im, M. J., Kim, C. U., Park, W. I., Baik, J. M., & Choi, K. J. (2017). Enhanced piezoresponse of highly aligned electrospun poly (vinylidene fluoride) nanofibers. *Nanotechnology*, *28*(39), 395402. https://doi.org/10.1088/1361-6528/aa7f6b.
24. Guo, H. F., Li, Z. S., Dong, S. W., Chen, W. J., Deng, L., Wang, Y. F., & Ying, D. J. (2012). Piezoelectric PU/PVDF electrospun scaffolds for wound healing applications. *Colloids and Surfaces B: Biointerfaces*, *96*, 29-36.https://doi.org/10.1016/j.colsurfb.2012.03.014
25. Sharma, M., Srinivas, V., Madras, G., & Bose, S. (2016). Outstanding dielectric constant and piezoelectric coefficient in electrospun nanofiber mats of PVDF containing silver decorated multiwall carbon nanotubes: Assessing through piezoresponse force microscopy. *RSC Advances, 6*, 6251–6258. https://doi.org/10.1039/C5RA25671B
26. Eun, J. H., Sung, S. M., Kim, M. S., Choi, B. K., & Lee, J. S. (2021). Effect of MWCNT content on the mechanical and piezoelectric properties of PVDF nanofibers. *Materials & Design, 206*, 109785. https://doi.org/10.1016/j.matdes.2021.109785
27. Jiang, J., Tu, S., Fu, R., Li, J., Hu, F., Yan, B., et al. (2020). Flexible piezoelectric pressure tactile sensor based on electrospun $BaTiO_3$ /Poly(vinylidene fluoride) nanocomposite membrane. *ACS Applied Materials & Interfaces, 12*, 33989–33998. https://doi.org/10.1021/acsami.0c08560
28. Baji, A., Mai, Y.-W., Li, Q., & Liu, Y. (2011). Nanoscale investigation of ferroelectric properties in electrospun barium titanate/polyvinylidene fluoride composite fibers using piezoresponse force microscopy. *Composites Science and Technology, 71*, 1435–1440. https://doi.org/10.1016/j.compscitech.2011.05.017
29. Dashtizad, S., Alizadeh, P., & Yourdkhani, A. (2021). Improving piezoelectric properties of PVDF fibers by compositing with $BaTiO_3$-Ag particles prepared by sol-gel method and photochemical reaction. *Journal of Alloys and Compounds, 883*, 160810. https://doi.org/10.1016/j.jallcom.2021.160810
30. Kim, H., Lee, D., Kim, D., Kong, D., Choi, J., Lee, M., et al. (2018). Dominant role of young's modulus for electric power generation in PVDF–$BaTiO_3$ composite-based piezoelectric nanogenerator. *Nanomaterials, 8*, 777. https://doi.org/10.3390/nano8100777
31. Liu, X., Ma, J., Wu, X., Lin, L., & Wang, X. (2017). Polymeric nanofibers with ultrahigh piezoelectricity *via* self-orientation of nanocrystals. *ACS Nano, 11*, 1901–1910. https://doi.org/10.1021/acsnano.6b07961
32. Gebrekrstos, A., Madras, G., & Bose, S. (2018). Piezoelectric response in electrospun poly(vinylidene fluoride) fibers containing fluoro-doped graphene derivatives. *ACS Omega, 3*, 5317–5326. https://doi.org/10.1021/acsomega.8b00237
33. Jalalian, A., Grishin, A. M., Wang, X. L., Cheng, Z. X., & Dou, S. X. (2014). Large piezoelectric coefficient and ferroelectric nanodomain switching in $Ba(Ti_{0.80}\ Zr_{0.20})O_3$ -0.5$(Ba_{0.70}\ Ca_{0.30})TiO_3$ nanofibers and thin films. *Applied Physics Letters, 104*, 103112. https://doi.org/10.1063/1.4867013.

34. Wang, F., Mai, Y.-W., Wang, D., Ding, R., & Shi, W. (2015). High quality barium titanate nanofibers for flexible piezoelectric device applications. *Sensors and Actuators A: Physical, 233*, 195–201. https://doi.org/10.1016/j.sna.2015.07.002
35. Fan, M., Hui, W., Li, Z., Shen, Z., Li, H., Jiang, A., et al. (2012). Fabrication and piezoresponse of electrospun ultra-fine $Pb(Zr_{0.3}, Ti_{0.7})O_3$ nanofibers. *Microelectronic Engineering, 98*, 371–373. https://doi.org/10.1016/j.mee.2012.07.026.
36. Chen, X., Xu, S., Yao, N., & Shi, Y. (2010). 1.6 V Nanogenerator for mechanical energy harvesting using PZT nanofibers. *Nano Letters, 10*:2133–2137. https://doi.org/10.1021/nl100812k.
37. Chen, Y. Q., Zheng, X. J., & Feng, X. (2010). The fabrication of vanadium-doped ZnO piezoelectric nanofiber by electrospinning. *Nanotechnology, 21*, 055708. https://doi.org/10.1088/0957-4484/21/5/055708
38. Tohluebaji, N., Putson, C., & Muensit, N. (2019). High electromechanical deformation based on structural beta-phase content and electrostrictive properties of electrospun poly(vinylidene fluoride- hexafluoropropylene) nanofibers. *Polymers, 11*, 1817. https://doi.org/10.3390/polym11111817
39. Parangusan, H., Bhadra, J., & Al-Thani, N. (2021). Flexible piezoelectric nanogenerator based on [P(VDF-HFP)]/PANI-ZnS electrospun nanofibers for electrical energy harvesting. *Journal of Materials Science: Materials in Electronics, 32*, 6358–6368. https://doi.org/10.1007/s10854-021-05352-4
40. Tohluebaji, N., Thainiramit, P., Putson, C., & Muensit, N. (2021). Phase and structure behavior vs. electromechanical performance of electrostrictive P(VDF-HFP)/ZnO composite nanofibers. *Polymers, 13*, 2565. https://doi.org/10.3390/polym13152565.
41. Abbasipour, M., Khajavi, R., Yousefi, A. A., Yazdanshenas, M. E., Razaghian, F., & Akbarzadeh, A. (2019). Improving piezoelectric and pyroelectric properties of electrospun PVDF nanofibers using nanofillers for energy harvesting application. *Polymers for Advanced Technologies, 30*, 279–291. https://doi.org/10.1002/pat.4463
42. You, M.-H., Wang, X.-X., Yan, X., Zhang, J., Song, W.-Z., Yu, M., et al. (2018). A self-powered flexible hybrid piezoelectric–pyroelectric nanogenerator based on non-woven nanofiber membranes. *Journal of Materials Chemistry A, 6*. https://doi.org/10.1039/C7TA10175A.
43. Li, C., Cao, R., & Zhang, X. (2018). Breathable materials for triboelectric effect-based wearable electronics. *Applied Sciences, 8*. https://doi.org/10.3390/app8122485.
44. Arica, T. A., Isık, T., Guner, T., Horzum, N., & Demir, M. M. (2021). Advances in electrospun fiber-based flexible nanogenerators for wearable applications. *Macromolecular Materials and Engineering, 306*. https://doi.org/10.1002/mame.202100143.
45. Zhang, J.-H., Li, Y., & Hao, X. (2020). A high-performance triboelectric nanogenerator with improved output stability by construction of biomimetic superhydrophobic nanoporous fibers. *Nanotechnology, 31*. https://doi.org/10.1088/1361-6528/ab72bd.
46. Kim, S.-R., Yoo, J.-H., & Park, J.-W. (2019). Using electrospun AgNW/P(VDF-TrFE) composite nanofibers to create transparent and wearable single-electrode triboelectric nanogenerators for self-powered touch panels. *ACS Applied Materials & Interfaces, 11*. https://doi.org/10.1021/acsami.9b03338.
47. Shaikh, M. O., Huang, Y.-B., Wang, C.-C., & Chuang, C.-H. (2019). Wearable Woven triboelectric nanogenerator utilizing electrospun PVDF nanofibers for mechanical energy harvesting. *Micromachines, 10*. https://doi.org/10.3390/mi10070438.
48. Xiong, J., Luo, H., Gao, D., Zhou, X., Cui, P., Thangavel, G., et al. (2019). Self-restoring, waterproof, tunable microstructural shape memory triboelectric nanogenerator for self-powered water temperature sensor. *Nano Energy, 61*. https://doi.org/10.1016/j.nanoen.2019.04.089.
49. Cao, R., Wang, J., Zhao, S., Yang, W., Yuan, Z., Yin, Y, et al. (2018). Self-powered nanofiber-based screen-print triboelectric sensors for respiratory monitoring. *Nano Research, 11*. https://doi.org/10.1007/s12274-017-1951-2.
50. Busolo, T., Ura, D. P., Kim, S. K., Marzec, M. M., Bernasik, A., Stachewicz, U., et al. Surface potential tailoring of PMMA fibers by electrospinning for enhanced triboelectric performance. *Nano Energy, 57*. https://doi.org/10.1016/j.nanoen.2018.12.037.

51. Zhou, K., Zhao, Y., Sun, X., Yuan, Z., Zheng, G., Dai, K., et al. (2020). Ultra-stretchable triboelectric nanogenerator as high-sensitive and self-powered electronic skins for energy harvesting and tactile sensing. *Nano Energy, 70*. https://doi.org/10.1016/j.nanoen.2020.104546.
52. Li, Y., Xiong, J., Lv, J., Chen, J., Gao, D., Zhang, X., et al. (2020). Mechanically interlocked stretchable nanofibers for multifunctional wearable triboelectric nanogenerator. *Nano Energy, 78*. https://doi.org/10.1016/j.nanoen.2020.105358.
53. Qiu, H.-J., Song, W.-Z., Wang, X.-X., Zhang, J., Fan, Z., Yu, M., et al. (2019). A calibration-free self-powered sensor for vital sign monitoring and finger tap communication based on wearable triboelectric nanogenerator. *Nano Energy, 58*. https://doi.org/10.1016/j.nanoen.2019.01.069.
54. Sun, N., Wen, Z., Zhao, F., Yang, Y., Shao, H., Zhou, C., et al. (2017). All flexible electrospun papers based self-charging power system. *Nano Energy, 38*. https://doi.org/10.1016/j.nanoen.2017.05.048.
55. Jiang, C., Wu, C., Li, X., Yao, Y., Lan, L., Zhao, F., et al. All-electrospun flexible triboelectric nanogenerator based on metallic MXene nanosheets. *Nano Energy, 59*. https://doi.org/10.1016/j.nanoen.2019.02.052.
56. Tayyab, M., Wang, J., Wang, J., Maksutoglu, M., Yu, H., Sun, G., et al. (2020). Enhanced output in polyvinylidene fluoride nanofibers based triboelectric nanogenerator by using printer ink as nano-fillers. *Nano Energy, 77*. https://doi.org/10.1016/j.nanoen.2020.105178.
57. Kim, H.-S., & Park, I.-K. (2018). Enhanced output power from triboelectric nanogenerators based on electrospun Eu-doped polyvinylidene fluoride nanofibers. *Journal of Physics and Chemistry of Solids, 117*. https://doi.org/10.1016/j.jpcs.2018.02.045.
58. Kim, D. W., Lee, J. H., Kim. J. K., & Jeong, U. (2020). Material aspects of triboelectric energy generation and sensors. *NPG Asia Materials, 12*. https://doi.org/10.1038/s41427-019-0176-0.
59. Yu, J., Hou, X., Cui, M., Zhang, S., He, J., Geng, W., et al. (2019). Highly skin-conformal wearable tactile sensor based on piezoelectric-enhanced triboelectric nanogenerator. *Nano Energy, 64*. https://doi.org/10.1016/j.nanoen.2019.103923.
60. Fuh, Y.-K., Li, S.-Ch., Chen, Ch.-Y., & Tsai, Ch.-Y. (2018). A fully packaged self-powered sensor based on near-field electrospun arrays of poly(vinylidene fluoride) nano/micro fibers. *Express Polymer Letters, 12*. https://doi.org/10.3144/expresspolymlett.2018.12.
61. Zhao, G., Zhang, X., Cui, X., Wang, S., Liu, Z., Deng, L., et al. (2018). Piezoelectric polyacrylonitrile nanofiber film-based dual-function self-powered flexible sensor. *ACS Applied Materials & Interfaces, 10*. https://doi.org/10.1021/acsami.8b02564.
62. Wu, Y., Qu, J., Daoud, W. A., Wang, L., & Qi, T. (2019). Flexible composite-nanofiber based piezo-triboelectric nanogenerators for wearable electronics. *Journal of Materials Chemistry A, 7*. https://doi.org/10.1039/C9TA02345C.
63. Sahatiya, P., Kannan, S., & Badhulika, S. (2018). Few layer MoS_2 and in situ poled PVDF nanofibers on low cost paper substrate as high performance piezo-triboelectric hybrid nanogenerator: Energy harvesting from handwriting and human touch. *Applied Materials Today, 13*. https://doi.org/10.1016/j.apmt.2018.08.009.
64. Song, J., Yang, B., Zeng, W., Peng, Z., Lin, S., Li, J., et al. (2018). Highly flexible, large-area, and facile textile-based hybrid nanogenerator with cascaded piezoelectric and triboelectric units for mechanical energy harvesting. *Advanced Materials Technologies, 3*. https://doi.org/10.1002/admt.201800016.
65. Sun, J.-G., Yang, T.-N., Wang, C.-Y., & Chen, L.-J. (2018). A flexible transparent one-structure tribo-piezo-pyroelectric hybrid energy generator based on bio-inspired silver nanowires network for biomechanical energy harvesting and physiological monitoring. *Nano Energy, 48*. https://doi.org/10.1016/j.nanoen.2018.03.071.
66. Wang, S., Wang, Z. L., & Yang, Y. (2016). A one-structure-based hybridized nanogenerator for scavenging mechanical and thermal energies by triboelectric-piezoelectric-pyroelectric effects. *Advanced Materials, 28*. https://doi.org/10.1002/adma.201505684.



Mina Abbasipour is a Ph.D. graduated from Science and Research Branch, Islamic Azad University, Tehran, Iran. She received her B.Sc and M.Sc in fiber and textile chemistry from Yazd University and Yazd Branch, Islamic Azad University, in 2009 and 2011, respectively. Her areas of interest include nanostructures materials, nanofibers fabrication for renewable and sustainable energy harvesting. She published 9 peer-reviewed papers and 2 chapters.



Ramin Khajavi is a full professor in the Department of polymer, textile, and Chemical Engineering at Islamic Azad University-South Tehran Branch. His main research focuses on the development of functional surfaces on polymeric materials, nanofibrous scaffolds (especially medical scaffolds), and nanocomposites. He is interested in smart materials including smart and multi-functional polymers and textiles and stimuli-responsive polymers such as PVDF, especially in their nanofibrous form. He has published over 70 peer-reviewed papers. His H-index is 16.

Chapter 26
Development of Micro/Nano Channels Using Electrospinning for Neural Differentiation of Cells



Zahra Hesari

Abstract Electrospinning has emerged as a simple, flexible, and highly scalable nanotechnology process over recent decades. This technology provides a range of tunable parameters to produce uniquely functionalized nanofiber materials for various applications. Microfluidics or lab-on-a-chip (LOC) is a rapidly developing technology, enabling precise manipulation of small volumes of fluids, leading to the achievement of low-cost and portable systems and presenting high surface–to–volume ratios. Additionally, fast reaction times and ease of automation make microfluidic devices ideal for different applications. Combining the merits of electrospinning and microfluidics provides fascinating approaches in biomedical research. In this chapter, we review the integrated electrospinning and microfluidics systems that have been utilized in the neural differentiation of cells. On the other hand, there is another manner in the combination of electrospinning and microfluidics technologies, which include the incorporation of microfluidic systems in the fabrication of electrospun nanofibers and conversely, application of electrospinning in the production of micro/nano size channels; appropriate for differentiation of stem cells into neurons that are to be discussed in this chapter.

Keywords Electrospinning · Microfluidics · Neural differentiation · Nanofibrous scaffold · Microfluidic spinning

26.1 Introduction: Neural Differentiation of Cells

Nerve injury is a worldwide health problem that significantly influences patients' quality of life alongside a tremendous socioeconomic charge [102]. There are several pathological conditions resulting in neurodegeneration including spinal cord injury (SCI), traumatic brain injury (TBI), and Peripheral nerve injury (PNI), as well as neurological diseases such as Parkinson's, Alzheimer's, and Huntington's diseases

Z. Hesari (✉)
Department of Pharmaceutics, School of Pharmacy, Guilan University of Medical Sciences, Rasht, Iran
e-mail: z.hesari@gmail.com

© The Author(s), under exclusive license to Springer Nature Switzerland AG 2022

A. Vaseashta and N. Bölgen (eds.), *Electrospun Nanofibers*,
https://doi.org/10.1007/978-3-030-99958-2_26

[135]. The Schwann cells producing myelin sheaths around axons provide the potential for spontaneously regeneration and recovery of PNS axon's function after peripheral nerve lesions. Conversely, various factors make CNS regeneration more complicated and ineffective in comparison with the PNS, including specific inhibitory proteins in CNS myelin, glial-scar-associated inhibitory molecules, and slower debris clearance in the CNS [20, 50, 116]. Furthermore, scar formation after injury and unguided axonal regrowth are of multiple factors contributing to imperfect nervous tissue regeneration and restoration [42]. However, multiple investigations have been performed to obtain a dependable and efficient technique to restore of neural defects. Still, there is no complete and satisfactory recovery of the neural lesions [95, 144]. Limitations in regenerative potentials of the nervous system augmented the stem-cell-based neural tissue engineering (NTE), which has shown the excellent capability for nerve regeneration due to the differentiation and self-restoration ability of stem cells [110], including induced pluripotent stem cells (IPSCs), mesenchymal stem cells (MSCs) [39] and neural stem cells (NSCs) [3]. Stem cells merits including guiding axonal regrowth and prevention of scar tissue ingrowth, provide much promise in nerve tissue engineering. Proper scaffolds are supposed to develop a neural guidance platform to bridge gaps in damaged peripheral or central neurons, concomitantly direct axonal sprouting, and regulate neurotrophic factors release and diffusion [134]. A fiber-shaped structure in microscale can act as a physical conduit for axon growth between the nerve gaps and is one of the most typical biomedical components in nerve tissue regeneration [22, 40]. Many synthetic and natural polymers have been studied for use as NTE fiber-shape providing platforms [59]. Among several existing methods in the fabrication of fiber-shaped scaffold structures, electrospinning is a prosperous field.

26.2 Biomedical Applications of Electrospinning (an Overview)

Electrospinning has gained great focus and development in the last two decades due to its versatility for the fabrication of continuous one dimensional polymeric micro to nano-fibers [35]. More than 100 polymers (natural and synthetic) and various inorganic materials have been developed into nanofibers through electrospinning technique [28]. Resulted nanofibers can present several distinct morphological structures, such as core-sheath [101, 107], side-by-side [41, 58] and porous-surface nanofibers [1, 147]. Due to nanofiber's ultra-small diameters, nanofiber mats provide various advantages including an extremely high ratio of surface area to volume, high porosity with excellent pore interconnectivity, capability of several surface functionalization and augmentation of mechanical properties [114]. These prominent characteristics of polymeric electrospun nanofibers suggest them as a prevalent candidate in a wide range of leading applications some of which have reached industrial scale production [85, 114]. Current main application areas include: filtrations [78, 124], affinity

membranes and recovery of metal ions [89, 152], drug delivery systems [72, 88], tissue engineering scaffolds [99, 103, 146],wound healing [51, 56], catalyst and enzyme carriers [14, 96], sensors [83, 77], energy storage [100, 112].

26.2.1 Drug Delivery Systems

Novel drug delivery systems are developed to balance the drug release rate and kinetics, decrease the side effects and toxicity and ameliorate patient compliance by reducing the required dose and administration frequency leading to potentially enhanced therapeutic efficacy of the drugs [151]. In this way, electrospun nanofibers have exhibited many advantages as a potential drug delivery nanocarrier, including easy drug loading implementation, feasibility of higher overall release rate control due to high specific surface area and short diffusion passage length, modulation of drug release with adjustment of nanofiber morphology, porosity and composition and potential simultaneous delivery of diverse therapeutics [85]. Consequently, active pharmaceutical ingredients (API)s in various classes are investigated to be delivered through electrospun nanofibers, including antibiotics and various antibacterial agents, anticancer drugs, protein, DNA, RNA and growth factors [48, 129].

26.2.2 Wound Healing

When someone is wounded as a consequence of burn, cut or trauma, an orchestrated cascade of biochemical and cellular reactions starts to repair the damaged site [94]. Wound healing undergoes a process of regeneration in dermal and epidermal tissues. This process consists of inflammatory, proliferative, remodeling and epithelialization steps. Normally in deep ulcers or full thickness burns, no source of cells remains and body is not capable for self-regeneration [90]. Various dressings from traditional to novels are incorporated to accelerate wound healing, functioning as wound protectant, absorbing exudate body fluid, allowing gas exchange (esp. oxygen), preventing exogenous microbial colonization on wound area [120]. For these aims, an electrospun nanofibrous membrane with high porosity presents some ideal characteristics, including large specific surface area, softness, lightness, safety, and environmental protection [53, 136]. Nanofibers with high porosity can cause the wound to have good permeability, effectively promote wound exudates, and carry on effective absorption to keep the wound in the ideal moist degree. The nanometer fiber membrane pores inside can also effectively protect the wound from bacterial invasion, help wound healing, and prevent decay [45, 61]. Also, for a full-thickness dermal injury, the adhesion and integration of an "artificial dermal layer" consisting of a 3D nanofibrous scaffold with well cultured dermal fibroblasts will considerably assist the re-epithelialization [12, 19].

26.2.3 Tissue Engineering Scaffolds

Trauma, surgical procedures, inflammation and congenital factors are of the most prevalent causes of tissue defects, in which a vast number mainly cannot be self-healed. In order to compensate the tissue defects, transplantation of autologous tissue is executable, but limitations in relevant tissue source exist. On the other hand, allograft tissue transplantation is followed by potential challenges, such as disease transfer and immune system rejection [54, 79].

Tissue engineering, is 'an interdisciplinary field that applies the principles of engineering and life sciences toward the development of biological substitutes that restore, maintain, or improve tissue function or a whole organ' [73]. Successful tissue engineering utilizes scaffold matrices to 3 dimensionally fill or cover the defected tissue, to provide 3D architectonic support and to bear related growth factors and/or cells (especially stem cells) that are capable of forming desired tissues inside the body upon transplantation [46].

As briefly mentioned, an appropriate scaffold requires some essential characteristics [4] such as high porosity, with an appropriate pore size distribution, high surface area, biodegradability with the degradation rate matching the rate of neo-tissue formation (most of the times), capable of forming required 3D structure with the appropriate mechanical properties, being non-toxic and biocompatible to cells, positively interacting with the cells to promote cell adhesion, proliferation, migration, and differentiated cell function [87, 156].

Body tissues are constructed on three-dimensional (3D) networks of nanometer-sized fibers made of various proteins as natural scaffolds [63]. Advantageous characteristics of electro-spun nanofibers mats, including their well-known 3D porous, interconnected structures, relatively large surface areas [76], potential incorporation of biodegradable natural/synthetic materials, provide a class of ideal options to mimic the natural extracellular matrix (ECM) essential for tissue engineering. Electrospun nanofibers are widely utilized in regeneration of almost all tissues, including heart [23, 82], skin [64, 71], bone [49, 81], neurons [5, 36], kidney [26, 153], liver [33, 97] and so on.

26.3 Electrospinning in Neural Differentiation of Cells

To mimic the architecture of the natural extracellular matrix (ECM), is a common approach in tissue engineering. The interplay between neural cells and their surrounding ECM plays a critical role in the regulation of cellular behaviors via influencing cells with biochemical signals and topographical cues [117, 130], resulting in a close imitation of the ECM and a more conducive environment for most aspects of nervous system development and function such as adhesion, survival, migration, proliferation, and differentiation of cells [30, 55, 131]. ECM is constructed of two main components: fibrous proteins and polysaccharides. Hence, nanofibrous

scaffolds have been incorporated broadly as potential tissue engineering platforms. Meantime, based on nanofiber's extremely high surface area-to-volume ratio, this characteristic promotes the release of biochemicals, including drugs, proteins, and nucleic acids [123], which can be delivered via fibers. In addition, the large surface enhances the contact area between cells and the fibers, leading to an increase in chemical uptake by cells. Hence, nanofibrous scaffolds also may be potentially used as drug carrier for chemical therapy [11].

Advances in recent years in nanofiber fabrication using electrospinning techniques, such as direct writing electrospinning [13], fabrication of three-dimensional electrospun scaffolds [16, 80], and integration of electrospinning into 3D printing [15, 92], have provided high promise in the development of biomimetic nanofibrous scaffolds and has promoted many biomedical applications of neural tissue engineering [143]. Typically, it has progressed as a multidisciplinary technology that combines biology, engineering and material science, intending to develop neuroregenerative medicine for transplantation, restoration and 3D in vitro neural models for drug screening [25].

Generally, electrospinning introduces a simple fabrication technique for various materials varying in resources, compositions, and properties. The scaffolds made of electrospun fibers can also serve as a platform to deliver bioactive molecules such as drugs, genes, growth factors, or ECM proteins in the lesion site at a controlled release rate, shifting the inhibitory environment to a permissive one for neural regeneration and functional recovery [7, 27]. In the following sections, electrospun nanofibrous scaffolds made of single or combination polymers or nanofibers containing drugs or biological macromolecules to promote neural cell differentiation, will be reviewed.

26.3.1 Polymeric Nanofibrous Scaffolds

26.3.1.1 Single Polymers

Several studies were performed using various types of polymers (synthetic, natural), solitary or combined with two or more polymers, as the primary material for fabrication of nanofibrous scaffolds, using electrospinning technique. In such studies, mainly polymers are modified in surface or structure using bioactive or chemical molecules. Among the scaffolds using a single polymer, Motamedi et al. utilized polyvinylidene fluoride (PVDF) as the single polymer for nanofibrous scaffold fabrication, optimizing electrospinning parameters such as PVDF solution concentration, applied voltage, tip-to-collector distance, feeding rate, collector speed and the solvent. Results revealed that the optimal parameters were 30 w/v% PVDF concentration, 15 kV applied voltage, 18 cm tip-to-collector distance, 0.5 ml/h feeding rate, 2500 rpm collector speed and *N*,*N*′-dimethylacetamide/acetone as a solvent. The mean fiber diameter of the obtained scaffold was 352.9 ± 24 nm with uniform and aligned morphology. According to neural tissue engineering, the cell viability and morphology of PC-12 cells on the optimum scaffold confirmed the potential of PVDF

nanofibrous scaffold [98]. Poly(L-lactic acid) (PLLA) was also incorporated solitary as nanofibrous scaffold. Fiber diameter range 150–300 nm with random orientation. Cell culture revealed that PLLA nanofibrous scaffold supports neural stem cell (NSC) differentiation and neurites out-growth and promotes NSC adhesion [150]. In Nisbet et al. study, randomly orientated poly(ε-caprolactone) PCL fibrous scaffolds, with an average fiber diameter of 750 nm was modified with ethylene-diamine (ED) to determine if amino functionalization and changes in surface tension of the fibrous scaffolds affected the proliferation and differentiation characteristics of NSCs. Results showed that although surface treatment did not change the differentiation of the NSCs, the modified scaffolds were more hydrophilic, resulting in a significant increase in the number of adhered cells, and increased spreading throughout the entirety of the scaffold. When the NSCs were seeded on the PCL scaffolds, the stem cells differentiated primarily into oligodendrocytes, indicating that electrospun PCL can direct the differentiation of NSCs towards a specific lineage [105]. Furthermore, PLGA [137], gelatin [8], PLLA [149] and PCL [18] are of the most applied polymers in fabrication of nanofibers for neural differentiation.

26.3.1.2 Polymer Combinations

Several studies have merged the advantages of two or more polymers in developing electrospun nanofibrous scaffolds for neural tissue engineering. Based on electrospinning technique, concomitant use of two or more polymers in nanofiber production is readily possible. in this way, four main methods are applied:

- Mixture of polymers in a polymer solution.
- Incorporation of two or more nozzles for each polymer solution.
- Spinning of second polymer solution on primary nanofiber mat.
- Utilizing core-shell nozzles.

Prabhakaran et al. designed a PCL/chitosan nanofibrous scaffold and compared it with PCL and chitosan individual nanofibers. PCL/chitosan surface characteristics proved more hydrophilic than PCL nanofibers and mechanical properties showed that the Young's modulus and strain at break were better than those of the chitosan nanofibers. Also, PCL/chitosan scaffolds showed better cell proliferation than PCL scaffolds and maintained their characteristic cell morphology, spreading bipolar elongations to the nanofibrous substrates [109]. Another combination of PCL/chitosan with additional polypyrrole (PPy) was designed. Various compositions of the PCL/chitosan/PPy polymeric scaffolds were fabricated and analyzed. Similarly, results illustrated that chitosan in the scaffold imposed significant advancement in hydrophilicity. PC12 cell culture studies revealed that the PCL/chitosan/PPy nanofibrous scaffold supports cell attachment, spreading and revealed a significant increase in proliferation up to 356% compared to pure PCL and neurite extension of PC12 [119]. Chitosan also has been combined with various other polymers such as Chitosan/Poly(vinyl alcohol) (PVA) [125], chitosan-aniline oligomer/PVA [6], Chitosan-Gelatin [127], Poly(hydroxybutyrate) /chitosan [66], chitosan/ silk,

chitosan/ collagen, chitosan/agarose, etc. [111]. Several other polymer combinations have been investigated as electrospun nanofibrous scaffolds for neural differentiation of cells, including PCL/gelatin, PCL/collagen, PCL/PLGA [11].

26.3.1.3 Conductive Nanofibrous Scaffolds

Recently, a wide variety of applications have been investigated for conductive nanofiber mats, including sensors, electromagnetic shielding, organic photovoltaics, multifunctional textile surfaces, or biomedicine [10]. Electroactive or conductive biomaterials can guide an electrical stimulus to modulate neuronal activity in neural tissue engineering treatments, pain management, neurological disorders, and regenerative medicine [128]. Suitable precursor cells as well as the necessary biochemical and physical cues are of basic needs to guide neurite extension and tissue development for neural tissue engineering. A prospective scaffold for neural regeneration can be both fibrous and electrically conductive [62].

Various techniques have been incorporated to fabricate conductive nanofibers such as electrospinning from conductive solutions or melts, electrospinning and subsequent calcination of an electroactive substance, conductive coatings and so forth. Electroactive substances used to develop conductive nanofibers are mainly categorized as metals (as salts or nanoparticles), organic nanoparticles and polymers. Polypyrrole (PPy) and Polyaniline (PANI) are of the most applied conductive polymers for spinning of nanofibrous scaffolds [34], which are widely utilized in combination with other polymers, for example, PPy with PCL/PLA to form a core-sheath nanofibers [145], or with chitosan/collagen for probable neural differentiation [154] and also PANI with poly(L-lactic acid-co-ε-caprolactone)/silk fibroin [157] or PANI-PCL nanofibers [31], etc. Iron [32, 159], gold [106], copper [121], silver [74] are of metals that have been incorporated in neural tissue engineering nanofiber mats. Additionally, carbo nanotubes (CNTs) and graphene oxide (GO) are the typical organic nanoparticles, widely incorporated in electrospun mats for neural differentiation due to their impressive conductive properties [36, 115, 122, 128].

26.4 Biomedical Applications of Microfluidics (an Overview)

The term ‘Microfluidics’ refers to the science and technology of processing microscopic volumes of fluids in series of channels and chambers ranging from one to a few hundred microns in size. Microfluidic systems transport volumes of fluid that vary from microliters to femtoliters in channels usually carved on the surface of a polymer, glass, paper, etc. Microfluidics has several features that have attracted users in biology, chemistry, engineering and medicine. It requires only smaller reagent

volumes, shorter reaction times, produces little waste, offers short reaction and analysis times and the possibility of parallel operation, is relatively cheap, and has reduced dimensions compared with other analytical devices. They also hold the promise of integrating an entire laboratory onto a single chip (i.e., lab-on-a-chip) [9].

In addition, microfluidics are able to provide structures with scales comparable to the actual dimensions of single cells, colonies of cells, organoids, etc. These characteristics make microfluidics particularly useful in studying biology and biomedicine [38], including protein analysis [69], DNA sequencing [68], cell sorting and analysis [29], flow cytometric cell counting; and simulation of in vivo tissues by deposition of several advanced layers of supportive molecules within cell culture chambers to evaluate the effect of various 3-dimensional structures on the function of cells [132, 133]. Also, microfluidic chambers have been utilized to investigate the effect of different forces such as laminar flow on the function of endothelial, neural, etc. cells [37, 86], Mimicking blood circulation between various organ-simulating cell culture chambers to test the pharmacokinetics of various agents [126], chambers with cell-based biosensors as transducers to assay the test specimens for the presence of suspected toxins and other agents [91, 118], and single (or near-single cell study of basic cell physiology and cell-cell interactions [75, 141]. For example, after a certain period of time since patients take chemotherapy, cells experience a transient high level of drugs. At the same time point, cells located at different distances to blood vessels experience different concentration gradients of drugs, cytokines, growth factors, etc. Also the mechanical and biochemical interactions between cells and the extracellular matrix or between a sub-population of cells and their neighboring cells change dynamically.

Further complexity exists in the internal structure of tissues. Cells in tissues are not homogeneous but rather organized in a systematic way that remains the normal functions of tissues. The complex biochemical, physical and mechanical structures of the tissue microenvironment ultimately influence cellular decisions like stem cell differentiation of s [158].

Soft lithography is a set of techniques that is frequently used to produce microfluidic systems and is based on etching channels in a thin slab of PDMS polymer that is the most common material used in academic laboratories [24]. The soft lithography techniques present an inexpensive and convenient alternative to previous microfabrication methods based on e-beam writing or laser and photolithography in glass or silicon. The utilization of soft lithography also makes possible the generation of prototype microfluidic systems in short periods of time (typically less than one day) and the production of multiple copies of a device in several hours. Also, other technologies have been utilized for the fabrication of microfluidic chips [140], such as three-Dimensional (3D) printing, laser-based processes and other chemical and mechanical processes, which have been recently reviewed [104].

26.5 Microfluidics in Neural Differentiation of Cells

In recent decades, microfluidic systems have provided great potential in the study of molecular and cellular biology [139]. With its excellent advantages, such as miniaturization, flexible microstructure design, multifunctional integration, accurate microenvironment control, and capacity for automatic sample processing [161] microfluidics offered a new platform to visualize the cell structures' development within a microscale device. In neuroscience, they also confirm precise control of the microenvironment surrounding individual cells, and the delivery of biochemical or physical stimuli in vitro, to study the cellular physiology and the pathophysiology of many congenital and acquired neurodegenerative diseases. Microfluidic systems allow isolation of cells derived from the nervous system, isolation of neurites and synapses, and analysis of single-cell responses to perturbations of their environment [38]. Along with neural physiology and pathophysiology, several microchips have been designed and fabricated to promote neural tissue engineering, guide neural migration and differentiation, and monitoring these processes. Furthermore, the behavior of stem cells and their microenvironment have been discovered through the application of different microfluidic-based stem cell culture and tissue engineering techniques [67]. In addition, The microfluidic system has a patterned and well-organized structure that can be combined with other differentiation techniques to provide optimal conditions for neuronal differentiation of stem cells [43]. The design, fabrication, and general advantages of microfluidic devices hold promise for resolving complicated issues of neuronal development. These high-resolution approaches are poised to contribute new insights into mechanisms for restoring neuronal function and connectivity compromised by injury, stress, and neurodegeneration [93].

Several studies outline recent advances in microfluidic-based applications in neurobiology, with emphasis on neural differentiation of stem cells and various techniques incorporated along with microfluidics for neural differentiation of stem cells in order to regenerate and restore the damaged tissue such as chemical and biological stimulating molecules, electric stimuli, 3D scaffolds, topography and mechanical interventions, micro RNA.

26.6 Electrospinning and Microfluidic Hybrid Systems in Neural Differentiation of Cells

Although microfluidics can be utilized individually for stem cell differentiation, they mainly provide a suitable platform for combining differentiation techniques, as was previously discussed. Among the other types of scaffolds, electrospun nanofibrous membranes have been indicated as a promising stratum to integrate into microfluidic devices [77] due to ease and flexibility in their fabrication process and relatively large specific surface area. However, several polymers have been incorporated as

nanofiber mats in combination with microfluidic systems for neural purposes such as PLGA, collagen, recombinant spider silk protein, graphene oxide, alginate and so on. Nanofibers are combined with microfluidics mainly in one of the following cases:

26.6.1 Electrospun Nanofibers in Attachment with a Microfluidic Chip

Several investigations have revealed that incorporating electrospun fibrous mats into microfluidic chips could be beneficial for neural cell differentiation studies. These researches have evaluated the full potential of electrospun fiber substrates and investigated cellular responses in greater detail in a highly controlled microenvironment.

Additionally, to mimic the extra cellular matrix successfully, one approach is using porous electrospun polymer fiber scaffolds in combination with microfluidic networks which has shown to generate spatially and temporally defined liquid microenvironments efficiently. In this regard, some methods have been innovated; for example, both aligned and random orientation of electrospun fibers were patterned on glass substrates and were irreversibly bonded to microfluidic networks produced in PDMS. Concentration gradients in the fiber-containing channels were characterized experimentally and compared with computational fluid dynamic simulation values. For evaluation of the influence of fiber pads on fluidic properties, velocity and shear stress profiles, as well as vortex formation, were calculated. The capability of the platform for cell attachment and growth was evaluated using a fibroblast cell line. The potential of the system was further studied by a functional investigation of neural stem cell alignment in response to electrospun fiber orientation versus a microfluidic generated chemoattractant gradient of stromal cell-derived factor 1 alpha. Computational fluid dynamics simulations and experimentally determined linear concentration gradients confirmed that the fiber pads do not significantly disturb the laminar flow in the microfluidic channel. It was shown that cells can be seeded in the system under mild flow conditions for at least 24 h, and that cells can be visualized in situ using bright field and fluorescent microscopies. Culture of neural stem cells in microfluidic channels on aligned electro spun fibers were used to study the full potential of the system in combined effects of surface topography and chemical gradients. This platform provides the ability to verify cell outgrowth in response to a chemical gradient under three main substrate configurations: a flat surface, aligned fibers parallel to the gradient, and aligned fibers perpendicular to the surface [138] (Fig. 26.1).

In another study, a hybrid microfluidic system consisting of electrospun PLGA nanofibrous scaffold and a Polydimethylsiloxane (PDMS) microfluidic chip was developed to differentiate of human induced pluripotent stem cells (hiPSCs) into neurons. The neural differentiation of hiPSCs was confirmed using qRT-PCR and immunostaining evaluations. Incorporation of a hybrid microfluidic system for hiPSC

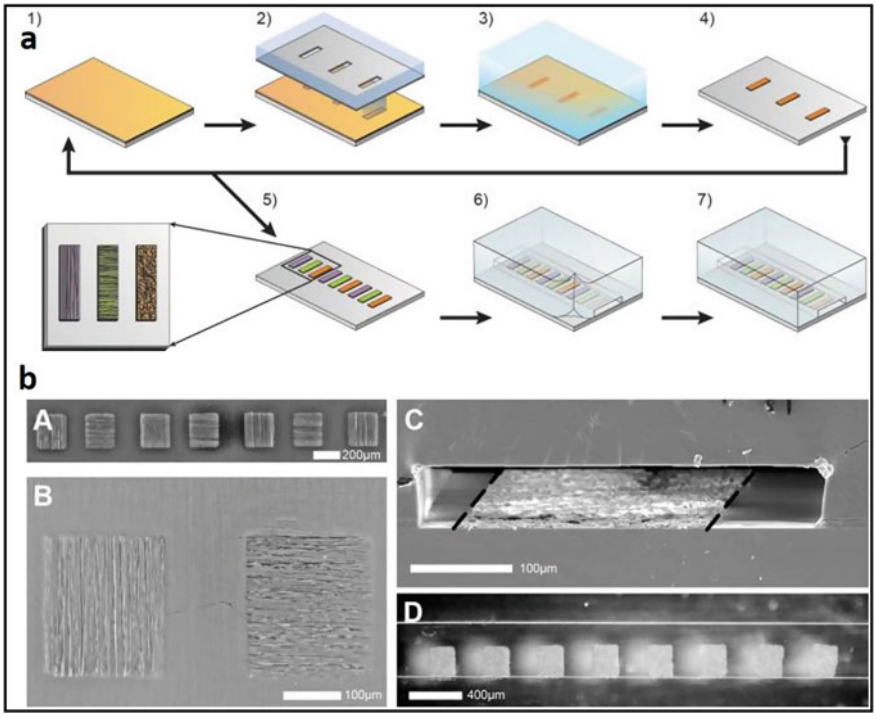


Fig. 26.1 **a** Schematic process steps for integrating spatially and geometrically defined electrospun fibers into PDMS-based microfluidic channels. **b** Scanning electron micrograph of electrospun fiber pads with alternating fiber orientation and light micrograph (top view) of electrospun fiber pads within the microfluidic chip. Reproduced by the permission of AIP Publishing and Copyright Clearance Center

differentiation revealed an increased level of β-tubulin III (a neuron-specific marker) gene expression while the expression of the glial fibrillary acidic protein (GFAP) gene (a classic marker for astrocytes) was decreased. Consequently, the hybrid device was turned to be optimum for neuronal differentiation. For further in vivo evaluation of this hybrid system, the cell-loaded scaffold was implanted in a spinal cord injury (SCI) model of rats (hemi-section) in the acute phase. Results demonstrated that although animals receiving this implant showed higher functional improvement according to Basso, Beattie, and Bresnahan (BBB) score, during 28 days of study, the difference with the control group was statistically insignificant. However, it seems that the result could be significant in a longer period of in vivo functional study. Finally, they concluded that combination of fluidic channels with nanofiber scaffolds provides an excellent microenvironment for neural tissue engineering [44] (Fig. 26.2).

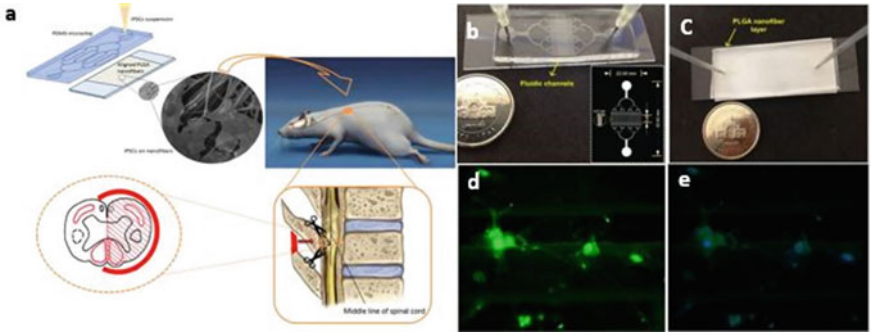


Fig. 26.2 Hybrid microfluidic device. **a** Schematic representation of in vitro and in vivo experiments. **b** PDMS microchip with fluidic channels. **c** The hybrid device consisted of the PDMS chip on top and glass substrate coated with PLGA nanofibers at the bottom. **d** Fluorescent image of the dendritic spines in differentiated hiPSCs, inside the microchannels after 8 days. A neural marker of NSE was utilized. **e** Nuclear co-staining with DAPI [43]

26.6.2 Microfluidic Spinning of Nanofibrous Scaffolds

Micro- or nanofiber-based materials have shown immense applications in biomedicine due to their ability to imitate many aspects of physiological in vivo microenvironment. Therefore, the fabrication of biocompatible and biodegradable micro- or nanofibers is becoming of great focus in biomaterials and tissue engineering. Among the several technologies, electrospinning and microfluidic spinning are the two promising methods to fabricate fibers at micro and nano-scale. In addition to many applications in biomedicine, microfluidics is also a potent tool for fabrication of structural platforms like fibers. It is especially considering that microfluidic spinning can continuously produce uniform microfibers in diameter with high spatiotemporal control [17]. This method has been incorporated for engineering of various organs, including skin and wound healing [2], blood vessel [21], pancreas [60], nerve [57], mussel [47], etc.

For neural differentiation of stem cells using this technique, the main widely incorporated polymer is alginate, which has produced grooved microfibers [57], micro ribbons [65] and hydrogel microfibers [108], yet. The PDMS pre-polymer surface tension was utilized to fabricate the groove patterned and round channels structures in the microfluidic chip to produce grooved microfibers,. As a consequence of using the device, the groove patterned alginate microfiber was successfully produced. Microfibers were continuously fabricated without clogging and there was variation in grooved microfibers diameters in correlation with the flow rate. For testing the usability of cell alignment, fibers were coated with laminin and the neuro-progenitor cells from prenatal rats were cultured on the prepared grooved fibers. Through the immunostaining with neurofilament, the guided growth of neuronal cells on the fiber was confirmed [57].

For fabrication of miroribbons, a method of continuously producing alginate with size-tunable grooved microstructures using a microfluidic system was developed. Raised patterns could be engraved on the surfaces of the flat fibers in the longitudinal direction. Myoblast and neuron cells were cultured on the grooved fibers, and the cell morphology and alignment were evaluated and revealed many neuron cells adhered to the ridges of the grooves and the neurites were projected along the ridges of the grooved fiber. Moreover, clusters of neuron cells were present, and their neurites formed networks along the ridges (Fig. 26.3). Also, the microfluidic spinning technique was utilized to encapsulate adult rat hippocampal stem/ progenitor cells (AHPCs) within alginate-based fibrous hydrogels. The results presented that the 3D environment provided within a hydrogel promotes proliferation and neuronal differentiation of AHPC.

The other polymer utilized for neural differentiation based on the technique mentioned above is PLGA. The synthesis of PLGA fibers was achieved using a PDMS-based microfluidic spinning device in which linear streams of PLGA dissolved in dimethyl sulfoxide (DMSO) were precipitated in a glycerol-containing water solution. Fibers diameters ranged from 20 to 230 μm by tuning the flow rate of PLGA solution from 1 to 50 μL/min along with a sheath flow rate of 250 or 1000 μL/min. The PLGA fibers consisted of a dense outer surface and a highly porous interior. To evaluate the potential of generated PLGA microfibers as nerve guide neural progenitor cells were seeded on the PLGA fibers. Results showed that the neural axons elongated along the PLGA microfibers [52].

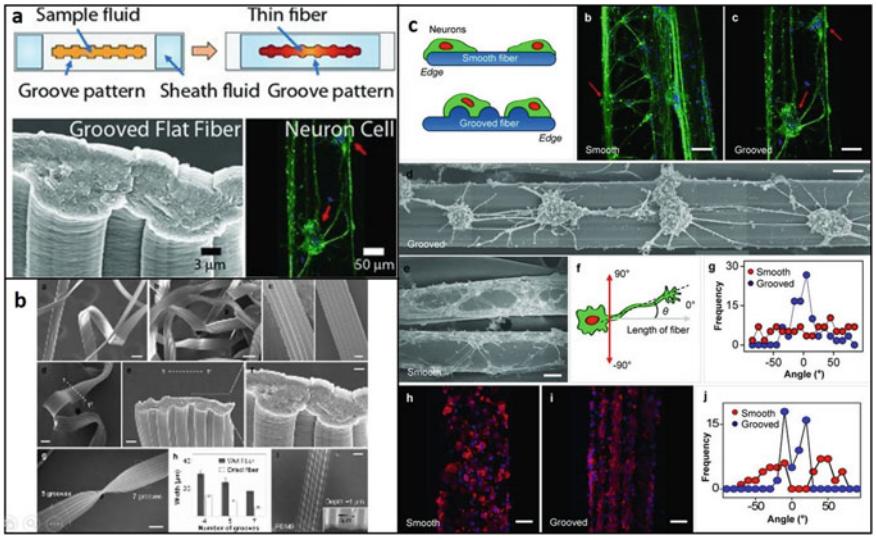


Fig. 26.3 **a** Graphical abstract of a microfluidic chip, microfibers and differentiated neural cells on fiber scaffold. **b** Grooved micro-ribbons with microfluidic spinning. **c** Cell alignment on the micro-grooved flat fibers, SEM and Fluorescence microscopy images of neurons on a smooth flat fiber [65]

Due to the recent widely application of electrically conductive materials as a scaffold for neural differentiation, Qing et al. recently developed microfluidic 3D printing technology for fabrication of 3D graphene oxide (GO) microfibrous scaffolds with adjustable fiber length and diameter and scaffold structure by integrating microfluidic spinning technology with programmable 3D printing system [113].

Also, it should be notably mentioned that the aforementioned studies did not include external voltage on polymer fibers in contrast with some studies that take the advantage of both microfluidic channels and external voltage application. The main advantage of an additional voltage source is reducing fiber diameter from micro to nano scale [160]. Hence we see that the fiber size in above mentioned alginate fibers is in the micrometer range.

26.6.3 Electrospun Fiber Molding for Fabrication of Microfluidic Channels

Microfluidics is a flourishing field of research, known as advantageous for the development of various scientific areas. Soft-lithography based on polydimethylsiloxane (PDMS) stands as the most popular technique for rapid prototyping microfluidic chips due to its lower cost, optical transparency, gas permeability, biocompatibility, etc. Recently, a number of different fabrication techniques have emerged for manufacturing the master mold with micro-channels and microstructures for PDMS replica molding. Thus, investigations are still developing less expensive and more flexible techniques for creating PDMS microfluidic platforms [155].

The emerging 3D printing is a recent production method, that is highly flexible for fabricating fluidic devices with controlled architecture. However, due to its low resolution, utilizing 3D printing method is still limited. Additionally, Electrospinning is the other technique as a straightforward and low-cost one to fabricate fibers with diameters ranging from tens of nanometers to several micrometers [142] as the template to fabricate a master mold for PDMS microfluidic devices to achieve orderly microstructures, without resorting to any means of lithography at all [84].

Several methods have been incorporated for controlling and determining the ES fiber orientations, including employing two parallel electrodes as the fiber collectors, or setting a magnetic field to align magnetic nanoparticle-doped fibers [148]. Rotating wheels and disks are also helpful for obtaining aligned fibers on areas over several square centimeters [70]. The currently higher resolution compared to 3D printing, the lower cost and the more flexibility compared to photolithography, would make electrospinning fiber molding a complement to the current methods for creating microchannel orientations.

In the recent decade, some studies have utilized electrospun fibers for microchannel molding in PDMS to guide cells toward neural differentiation. Various polymers have been utilized for electrospinning such as polycarbonate (PC), polystyrene (PS), and polyvinyl alcohol (PVA), polyvinylidene fluoride (PVDF) as

the template to achieve orderly microstructures for guiding the growth of mammalian neurons. In this study, fibers had aligned orientation and the microgrooves with a width of 1 μm were chosen for neurite extension and guidance. Results demonstrated that the neurons confined within the channels developed neurites along the grooves after 3 days [84].

Another study developed poly(ε-caprolactone) (PCL) fiber master mold-based, PDMS microfluidic channels. PCL fibers were manufactured by a modified spinning technique termed melt-electrospinning direct writing (MEDW). To obtain microscale architectures with a high aspect ratio, multilayer fiber deposition was developed and applied. Hence, the microchannels fabricated by the mentioned approach could provide tunable width and depth. Also, to create either laminar flow or microdroplets, T-shape and cross-channel devices were designed and fabricated [155]. However, cell differentiation studies, were not performed in this study, it seems that mentioned technique provides a promising platform for various tissue engineering applications including neural differentiation. Finally, it seems that electrospinning can serve as a supporting method to produce replica molded fibers in various types of microgrooves and microstructures composed of microchannels on biocompatible PDMS substrates.

26.7 Conclusions

Electrospinning is a popular technology for the fabrication of continuous nanofibers with a simple setup. Nanofibrous scaffolds can serve as powerful tools in tissue regeneration, drug-delivery and high efficiency sensing platforms. In neural differentiation, the fibrous structure (specially aligned fibers) closely resembles the natural environment that cells grow in and provides appropriate physical cues for manipulating cellular functions. It also enables the incorporation of biochemicals to provide a synergistic effect in promoting nerve regeneration. Meanwhile, advances in microfluidics have allowed scientists to unveil many aspects of bio-chemical, topographical or mechanical regulations, especially in the context of stem cells. Miniaturized microfluidic chips provide a more in vivo-like microenvironment for cells with tight spatiotemporal control. The combination of these two technologies has resulted in tremendous merits in various fields of tissue regeneration including neural differentiation. Worth mentioning, the integration of electrospinning with microfluidic technology, has been expanded in three main fields: Electrospun nanofibers in attachment with a microfluidic chip, microfluidic spinning of nanofibrous scaffolds and electrospun fiber molding for fabrication of microfluidic channels. All possess their special merits in promoting the application of microfluidics and electrospinning hybrid systems, especially in neural tissue engineering.

References

1. Abolhasani, M. M., Naebe, M., Hassanpour Amiri, M., Shirvanimoghaddam, K., Anwar, S., Michels, J. J., & Asadi, K. (2020). Hierarchically structured porous piezoelectric polymer nanofibers for energy harvesting. *Advanced Science, 7*(13), 2000517.
2. Ahn, S. Y., Mun, C. H., & Lee, S. H. (2015). Microfluidic spinning of fibrous alginate carrier having highly enhanced drug loading capability and delayed release profile. *RSC Advances, 5*(20), 15172–15181.
3. Akhavan, O., Ghaderi, E., & Shirazian, S. A. (2015). Near infrared laser stimulation of human neural stem cells into neurons on graphene nanomesh semiconductors. *Colloids and Surfaces. B, Biointerfaces, 126*, 313–321.
4. Asadian, M., Chan, K. V., Norouzi, M., Grande, S., Cools, P., Morent, R., & De Geyter, N. (2020). Fabrication and plasma modification of nanofibrous tissue engineering scaffolds. *Nanomaterials, 10*(1), 119.
5. Babaie, A., Bakhshandeh, B., Abedi, A., Mohammadnejad, J., Shabani, I., Ardeshirylajimi, A., Reza Moosavi, S., Amini, J., & Tayebi, L. (2020). Synergistic effects of conductive PVA/PEDOT electrospun scaffolds and electrical stimulation for more effective neural tissue engineering. *European Polymer Journal, 140*, 110051.
6. Bagheri, B., Zarrintaj, P., Samadi, A., Zarrintaj, R., Ganjali, M. R., Saeb, M. R., Mozafari, M., Park, O. O., & Kim, Y. C. (2020). Tissue engineering with electrospun electroresponsive chitosan-aniline oligomer/polyvinyl alcohol. *International Journal of Biological Macromolecules, 147*, 160–169.
7. Bai, Y., He, L., Lou, X., & Quan, D. (2021). *Electrospun bioactive composites for neural tissue engineering applications* (pp. 1–43). Elsevier.
8. Baiguera, S., Del Gaudio, C., Lucatelli, E., Kuevda, E., Boieri, M., Mazzanti, B., Bianco, A., & Macchiarini, P. (2014). Electrospun gelatin scaffolds incorporating rat decellularized brain extracellular matrix for neural tissue engineering. *Biomaterials, 35*(4), 1205–1214.
9. Beebe, D. J., Mensing, G. A., & Walker, G. M. (2002). Physics and applications of microfluidics in biology. *Annual Review of Biomedical Engineering, 4*(1), 261–286.
10. Blachowicz, T., & Ehrmann, A. (2020). Conductive electrospun nanofiber mats. *Materials, 13*(1), 152.
11. Cao, H., Liu, T., & Chew, S. Y. (2009). The application of nanofibrous scaffolds in neural tissue engineering. *Advanced Drug Delivery Reviews, 61*(12), 1055–1064.
12. Chen, H., Lui, Y. S., Tan, Z. W., Lee, J. Y. H., Tan, N. S., & Tan, L. P. (2019). Migration and phenotype control of human dermal fibroblasts by electrospun fibrous substrates. *Advanced healthcare materials, 8*(9), 1801378.
13. Chen, H., Malheiro, A. D. B. F. B., van Blitterswijk, C., Mota, C., Wieringa, P. A., & Moroni, L. (2017). Direct writing electrospinning of scaffolds with multidimensional fiber architecture for hierarchical tissue engineering. *ACS Applied Materials & Interfaces, 9*(44), 38187–38200.
14. Chen, H. Y., Cheng, K. C., Hsu, R. J., Hsieh, C. W., Wang, H. T., & Ting, Y. (2020). Enzymatic degradation of ginkgolic acid by laccase immobilized on novel electrospun nanofiber mat. *Journal of the Science of Food and Agriculture, 100*(6), 2705–2712.
15. Chen, W., Xu, Y., Li, Y., Jia, L., Mo, X., Jiang, G., & Zhou, G. (2020). 3D printing electrospinning fiber-reinforced decellularized extracellular matrix for cartilage regeneration. *Chemical Engineering Journal, 382*, 122986.
16. Chen, Y., Shafiq, M., Liu, M., Morsi, Y., & Mo, X. (2020). Advanced fabrication for electrospun three-dimensional nanofiber aerogels and scaffolds. *Bioactive Materials, 5*(4), 963–979.
17. Cheng, J., Jun, Y., Qin, J., & Lee, S.-H. (2017). Electrospinning versus microfluidic spinning of functional fibers for biomedical applications. *Biomaterials, 114*, 121–143.
18. Chew, S. Y., Mi, R., Hoke, A., & Leong, K. W. (2008). The effect of the alignment of electrospun fibrous scaffolds on Schwann cell maturation. *Biomaterials, 29*(6), 653–661.
19. Chui, C.-Y., Mouthuy, P.-A., & Ye, H. (2018). Direct electrospinning of poly (vinyl butyral) onto human dermal fibroblasts using a portable device. *Biotechnology Letters, 40*(4), 737–744.

20. Curcio, M., & Bradke, F. (2018). Axon regeneration in the central nervous system: Facing the challenges from the inside. *Annual Review of Cell and Developmental Biology, 34*, 495–521.
21. Daniele, M. A., Adams, A. A., Naciri, J., North, S. H., & Ligler, F. S. (2014). Interpenetrating networks based on gelatin methacrylamide and PEG formed using concurrent thiol click chemistries for hydrogel tissue engineering scaffolds. *Biomaterials, 35*(6), 1845–1856.
22. dos Santos, D. M., Correa, D. S., Medeiros, E. S., Oliveira, J. E., & Mattoso, L. H. C. (2020). Advances in functional polymer nanofibers: From spinning fabrication techniques to recent biomedical applications. *ACS Applied Materials & Interfaces, 12*(41), 45673–45701.
23. Du, J., Zhu, T., Yu, H., Zhu, J., Sun, C., Wang, J., Chen, S., Wang, J., & Guo, X. (2018). Potential applications of three-dimensional structure of silk fibroin/poly(ester-urethane) urea nanofibrous scaffold in heart valve tissue engineering. *Applied Surface Science, 447*, 269–278.
24. Duffy, D. C., McDonald, J. C., Schueller, O. J., & Whitesides, G. M. (1998). Rapid prototyping of microfluidic systems in poly (dimethylsiloxane). *Analytical chemistry, 70*(23), 4974–4984.
25. Dvir, T., Timko, B. P., Kohane, D. S., & Langer, R. (2011). Nanotechnological strategies for engineering complex tissues. *Nature nanotechnology, 6*(1), 13–22.
26. Eftekhari, A., Maleki Dizaj, S., Ahmadian, E., Przekora, A., Hosseiniyan Khatibi, S. M., Ardalan, M., Zununi Vahed, S., Valiyeva, M., Mehraliyeva, S., & Khalilov, R. (2021). Application of advanced nanomaterials for kidney failure treatment and regeneration. *Materials, 14*(11), 2939.
27. Faccendini, A., Vigani, B., Rossi, S., Sandri, G., Bonferoni, M. C., Caramella, C. M., & Ferrari, F. (2017). Nanofiber scaffolds as drug delivery systems to bridge spinal cord injury. *Pharmaceuticals, 10*(3), 63.
28. Fang, J., Niu, H., Lin, T., & Wang, X. (2008). Applications of electrospun nanofibers. *Chinese Science Bulletin, 53*(15), 2265.
29. Fu, A. Y., Chou, H.-P., Spence, C., Arnold, F. H., & Quake, S. R. (2002). An integrated microfabricated cell sorter. *Analytical chemistry, 74*(11), 2451–2457.
30. Gao, X., Wang, Y., Chen, J., & Peng, J. (2013). The role of peripheral nerve ECM components in the tissue engineering nerve construction. *Reviews in the Neurosciences, 24*(4), 443–453.
31. Garrudo, F. F. F., Mikael, P. E., Rodrigues, C. A. V., Udangawa, R. W., Paradiso, P., Chapman, C. A., Hoffman, P., Colaço, R., Cabral, J. M. S., Morgado, J., Linhardt, R. J., & Ferreira, F. C. (2021). Polyaniline-polycaprolactone fibers for neural applications: Electroconductivity enhanced by pseudo-doping. *Materials Science and Engineering: C, 120*, 111680.
32. Ghaderinejad, P., Najmoddin, N., Bagher, Z., Saeed, M., Karimi, S., Simorgh, S., & Pezeshki-Modaress, M. (2021). An injectable anisotropic alginate hydrogel containing oriented fibers for nerve tissue engineering. *Chemical Engineering Journal, 420*, 130465.
33. Ghahremanzadeh, F., Alihosseini, F., & Semnani, D. (2021). Investigation and comparison of new galactosylation methods on PCL/chitosan scaffolds for enhanced liver tissue engineering. *International Journal of Biological Macromolecules, 174*, 278–288.
34. Ghasemi-Mobarakeh, L., Prabhakaran, M. P., Morshed, M., Nasr-Esfahani, M. H., Baharvand, H., Kiani, S., Al-Deyab, S. S., & Ramakrishna, S. (2011). Application of conductive polymers, scaffolds and electrical stimulation for nerve tissue engineering. *Journal of tissue engineering and regenerative medicine, 5*(4), e17–e35.
35. Giannitelli, S. M., Costantini, M., Basoli, F., Trombetta, M., & Rainer, A. (2018). Electrospinning and microfluidics: An integrated approach for tissue engineering and cancer. In *Electrofluidodynamic Technologies (EFDTs) for Biomaterials and Medical Devices* (pp. 139–155). Elsevier.
36. Girão, A. F., Sousa, J., Domínguez-Bajo, A., González-Mayorga, A., Bdikin, I., Pujades-Otero, E., Casañ-Pastor, N., Hortigüela, M. J., Otero-Irurueta, G., Completo, A., Serrano, M. C., & Marques, P. A. A. P. (2020). 3D Reduced graphene oxide scaffolds with a combinatorial fibrous-porous architecture for neural tissue engineering. *ACS Applied Materials & Interfaces, 12*(35), 38962–38975.
37. Gray, B. L., Lieu, D. K., Collins, S. D., Smith, R. L., & Barakat, A. I. (2002). Microchannel platform for the study of endothelial cell shape and function. *Biomedical Microdevices, 4*(1), 9–16.

38. Gross, P. G., Kartalov, E. P., Scherer, A., & Weiner, L. P. (2007). Applications of microfluidics for neuronal studies. *Journal of the Neurological Sciences, 252*(2), 135–143.
39. Guo, W., Wang, S., Yu, X., Qiu, J., Li, J., Tang, W., Li, Z., Mou, X., Liu, H., & Wang, Z. (2016). Construction of a 3D rGO–collagen hybrid scaffold for enhancement of the neural differentiation of mesenchymal stem cells. *Nanoscale, 8*(4), 1897–1904.
40. Haider, A., Haider, S., Rao Kummara, M., Kamal, T., Alghyamah, A.-A.A., Jan Iftikhar, F., Bano, B., Khan, N., Amjid Afridi, M., Soo Han, S., Alrahlah, A., & Khan, R. (2020). Advances in the scaffolds fabrication techniques using biocompatible polymers and their biomedical application: A technical and statistical review. *Journal of Saudi Chemical Society, 24*(2), 186–215.
41. He, L., Deng-Guang, Y., Menglong, W., & Tingbao, N. (2021). Nanofabrication of janus fibers through side-by-side electrospinning—A mini review. *Materials Highlights, 2*(1–2), 18–22.
42. Hermanns, S., Klapka, N., Gasis, M., Müller, H. W. (2006). The collagenous wound healing scar in the injured central nervous system inhibits axonal regeneration. In Bähr, M. (Ed.), *Brain Repair*, (pp. 177–190). Boston, MA: Springer US.
43. Hesari, Z., Mottaghitalab, F., Shafiee, A., Soleymani, M., Dinarvand, R., & Atyabia, F. (2019). Application of microfluidic systems for neural differentiation of cells. *Precision Nanomedicine, 2*(4), 370–381.
44. Hesari, Z., Soleimani, M., Atyabi, F., Sharifdini, M., Nadri, S., Warkiani, M. E., Zare, M., & Dinarvand, R. (2016). A hybrid microfluidic system for regulation of neural differentiation in induced pluripotent stem cells. *Journal of Biomedical Materials Research Part A, 104*(6), 1534–1543.
45. Homaeigohar, S., & Boccaccini, A. R. (2020). Antibacterial biohybrid nanofibers for wound dressings. *Acta Biomaterialia, 107*, 25–49.
46. Howard, D., Buttery, L. D., Shakesheff, K. M., & Roberts, S. J. (2008). Tissue engineering: Strategies, stem cells and scaffolds. *Journal of Anatomy, 213*(1), 66–72.
47. Hsiao, A. Y., Okitsu, T., Onoe, H., Kiyosawa, M., Teramae, H., Iwanaga, S., Kazama, T., Matsumoto, T., & Takeuchi, S. (2015). Smooth muscle-like tissue constructs with circumferentially oriented cells formed by the cell fiber technology. *PLoS ONE, 10*(3), e0119010.
48. Hu, X., Liu, S., Zhou, G., Huang, Y., Xie, Z., & Jing, X. (2014). Electrospinning of polymeric nanofibers for drug delivery applications. *Journal of Controlled Release, 185*, 12–21.
49. Huang, B., Aslan, E., Jiang, Z., Daskalakis, E., Jiao, M., Aldalbahi, A., Vyas, C., & Bártolo, P. (2020). Engineered dual-scale poly (ε-caprolactone) scaffolds using 3D printing and rotational electrospinning for bone tissue regeneration. *Additive Manufacturing, 36*, 101452.
50. Huebner, E. A., & Strittmatter, S. M. (2009). Axon regeneration in the peripheral and central nervous systems. *Results and Problems in Cell Differentiation, 48*, 339–351.
51. Hussein, Y., El-Fakharany, E. M., Kamoun, E. A., Loutfy, S. A., Amin, R., Taha, T. H., Salim, S. A., & Amer, M. (2020). Electrospun PVA/hyaluronic acid/L-arginine nanofibers for wound healing applications: Nanofibers optimization and in vitro bioevaluation. *International Journal of Biological Macromolecules, 164*, 667–676.
52. Hwang, C. M., Khademhosseini, A., Park, Y., Sun, K., & Lee, S.-H. (2008). Microfluidic chip-based fabrication of PLGA microfiber scaffolds for tissue engineering. *Langmuir, 24*(13), 6845–6851.
53. Ignatova, M., Rashkov, I., & Manolova, N. (2013). Drug-loaded electrospun materials in wound-dressing applications and in local cancer treatment. *Expert opinion on drug delivery, 10*(4), 469–483.
54. Ito, Y., Hasuda, H., Kamitakahara, M., Ohtsuki, C., Tanihara, M., Kang, I. K., & Kwon, O. H. (2005). A composite of hydroxyapatite with electrospun biodegradable nanofibers as a tissue engineering material. *Journal of Bioscience and Bioengineering, 100*(1), 43–49.
55. Jalili-Firoozinezhad, S., Mirakhori, F., & Baharvand, H. (2015). Nanotissue engineering of neural cells. *Stem Cell Nanoeng, 265*, 265–283.
56. Jeckson, T. A., Neo, Y. P., Sisinthy, S. P., & Gorain, B. (2021). Delivery of therapeutics from layer-by-layer electrospun nanofiber matrix for wound healing: An update. *Journal of Pharmaceutical Sciences, 110*(2), 635–653.

57. Jeong, G. S., & Lee, S.-H. (2014). Microfluidic spinning of grooved microfiber for guided neuronal cell culture using surface tension mediated grooved round channel. *Tissue Engineering and Regenerative Medicine, 11*(4), 291–296.
58. Ji, S.-M., Tiwari, A. P., Oh, H. J., & Kim, H.-Y. (2021). ZnO/Ag nanoparticles incorporated multifunctional parallel side by side nanofibers for air filtration with enhanced removing organic contaminants and antibacterial properties. *Colloids and Surfaces A: Physicochemical and Engineering Aspects, 621*, 126564.
59. Jiang, X., Lim, S. H., Mao, H. Q., & Chew, S. Y. (2010). Current applications and future perspectives of artificial nerve conduits. *Experimental Neurology, 223*(1), 86–101.
60. Jun, Y., Kang, A. R., Lee, J. S., Jeong, G. S., Ju, J., Lee, D. Y., & Lee, S.-H. (2013). 3D co-culturing model of primary pancreatic islets and hepatocytes in hybrid spheroid to overcome pancreatic cell shortage. *Biomaterials, 34*(15), 3784–3794.
61. Juncos Bombin, A. D., Dunne, N. J., & McCarthy, H. O. (2020). Electrospinning of natural polymers for the production of nanofibres for wound healing applications. *Materials Science and Engineering: C, 114*, 110994.
62. Kabiri, M., Soleimani, M., Shabani, I., Futrega, K., Ghaemi, N., Ahvaz, H. H., Elahi, E., & Doran, M. R. (2012). Neural differentiation of mouse embryonic stem cells on conductive nanofiber scaffolds. *Biotechnology Letters, 34*(7), 1357–1365.
63. Kadler, K. E., Holmes, D. F., Trotter, J. A., & Chapman, J. A. (1996). Collagen fibril formation. *Biochemical Journal, 316*(1), 1–11.
64. Kalantary, S., Golbabaei, F., Latifi, M., Shokrgozar, M. A., & Yaseri, M. (2020). Assessment of electrospinning antioxidant nanofibers in skin exposure to oxidative stress. *Journal of Mazandaran University of Medical Sciences, 30*(186), 68–79.
65. Kang, E., Choi, Y. Y., Chae, S. K., Moon, J. H., Chang, J. Y., & Lee, S. H. (2012). Microfluidic spinning of flat alginate fibers with grooves for cell-aligning scaffolds. *Advanced materials, 24*(31), 4271–4277.
66. Karimi, A., Karbasi, S., Razavi, S., & Zargar, E. N. (2018). Poly(hydroxybutyrate)/chitosan aligned electrospun scaffold as a novel substrate for nerve tissue engineering. *Advanced biomedical research, 7*, 44–44.
67. Karimi, M., Bahrami, S., Mirshekari, H., Basri, S. M. M., Nik, A. B., Aref, A. R., Akbari, M., & Hamblin, M. R. (2016). Microfluidic systems for stem cell-based neural tissue engineering. *Lab on a Chip, 16*(14), 2551–2571.
68. Kartalov, E. P., & Quake, S. R. (2004). Microfluidic device reads up to four consecutive base pairs in DNA sequencing-by-synthesis. *Nucleic acids research, 32*(9), 2873–2879.
69. Kartalov, E. P., Zhong, J. F., Scherer, A., Quake, S. R., Taylor, C. R., & French Anderson, W. (2006). High-throughput multi-antigen microfluidic fluorescence immunoassays. *BioTechniques, 40*(1), 85–90.
70. Katta, P., Alessandro, M., Ramsier, R., & Chase, G. (2004). Continuous electrospinning of aligned polymer nanofibers onto a wire drum collector. *Nano letters, 4*(11), 2215–2218.
71. Keirouz, A., Chung, M., Kwon, J., Fortunato, G., & Radacsi, N. (2020). 2D and 3D electrospinning technologies for the fabrication of nanofibrous scaffolds for skin tissue engineering: A review. *Wiley Interdisciplinary Reviews: Nanomedicine and Nanobiotechnology, 12*(4), e1626.
72. Khodadadi, M., Alijani, S., Montazeri, M., Esmaeilizadeh, N., Sadeghi-Soureh, S., & Pilehvar-Soltanahmadi, Y. (2020). Recent advances in electrospun nanofiber-mediated drug delivery strategies for localized cancer chemotherapy. *Journal of Biomedical Materials Research Part A, 108*(7), 1444–1458.
73. Langer, R., & Vacanti, J. P. (1993). Tissue engineering. *Science, 260*(5110), 920–926.
74. Lee, J. M., Moon, J. Y., Kim, T. H., Lee, S. W., Ahrberg, C. D., & Chung, B. G. (2018). Conductive hydrogel/nanowire micropattern-based sensor for neural stem cell differentiation. *Sensors and Actuators B: Chemical, 258*, 1042–1050.
75. Lee, P. J., Hung, P. J., Shaw, R., Jan, L., & Lee, L. P. (2005). Microfluidic application-specific integrated device for monitoring direct cell-cell communication via gap junctions between individual cell pairs. *Applied Physics Letters, 86*(22), 223902.

76. Li, D., & Xia, Y. (2004). Electrospinning of nanofibers: Reinventing the wheel? *Advanced materials, 16*(14), 1151–1170.
77. Li, J., Liu, X., Sun, H., Wang, L., Zhang, J., Huang, X., Deng, L., Xi, J., & Ma, T. (2021). A new type of optical fiber glucose biosensor with enzyme immobilized by electrospinning. *IEEE Sensors Journal*.
78. Li, Z., Song, J., Long, Y., Jia, C., Liu, Z., Li, L., Yang, C., Liu, J., Lin, S., Wang, H., Liu, Y., Fang, M., & Wu, H. (2020). Large-scale blow spinning of heat-resistant nanofibrous air filters. *Nano Research, 13*(3), 861–867.
79. Liao, S., Li, B., Ma, Z., Wei, H., Chan, C., & Ramakrishna, S. (2006). Biomimetic electrospun nanofibers for tissue regeneration. *Biomedical Materials, 1*(3), R45-53.
80. Lin, W., Chen, M., Qu, T., Li, J., & Man, Y. (2020). Three-dimensional electrospun nanofibrous scaffolds for bone tissue engineering. *Journal of Biomedical Materials Research Part B: Applied Biomaterials, 108*(4), 1311–1321.
81. Liu, W., Bi, W., Sun, Y., Wang, L., Yu, X., Cheng, R., Yu, Y., & Cui, W. (2020). Biomimetic organic-inorganic hybrid hydrogel electrospinning periosteum for accelerating bone regeneration. *Materials Science and Engineering: C, 110*, 110670.
82. Liu, X., Kim, B., Loke, Y. H., Mass, P., Olivieri, L., Hibino, N., Fuge, M., & Krieger, A. (2021). Semi-Automatic planning and three-dimensional electrospinning of patient-specific grafts for fontan surgery. *IEEE Transactions on Biomedical Engineering,* 1–1.
83. Liu, Y., Hao, M., Chen, Z., Liu, L., Liu, Y., Yang, W., & Ramakrishna, S. (2020). A review on recent advances in application of electrospun nanofiber materials as biosensors. *Current Opinion in Biomedical Engineering, 13*, 174–189.
84. Liu, Y., Sun, Y., Yan, H., Liu, X., Zhang, W., Wang, Z., & Jiang, X. (2012). Electrospun fiber template for replica molding of microtopographical neural growth guidance. *Small (Weinheim an der Bergstrasse, Germany), 8*(5), 676–681.
85. Lu, P., & Ding, B. (2008). Applications of electrospun fibers. *Recent Patents on Nanotechnology, 2*(3), 169–182.
86. Ma, N., Koelling, K. W., & Chalmers, J. J. (2002). Fabrication and use of a transient contractional flow device to quantify the sensitivity of mammalian and insect cells to hydrodynamic forces. *Biotechnology and bioengineering, 80*(4), 428–437.
87. Ma, P. X. (2004). Scaffolds for tissue fabrication. *Materials today, 7*(5), 30–40.
88. Madhukiran, D. R., Jha, A., Kumar, M., Ajmal, G., Bonde, G. V., & Mishra, B. (2021). Electrospun nanofiber-based drug delivery platform: Advances in diabetic foot ulcer management. *Expert Opinion on Drug Delivery, 18*(1), 25–42.
89. Managheb, M., Zarghami, S., Mohammadi, T., Asadi, A. A., & Sahebi, S. (2021). Enhanced dynamic Cu(II) ion removal using hot-pressed chitosan/poly (vinyl alcohol) electrospun nanofibrous affinity membrane (ENAM). *Process Safety and Environmental Protection, 146*, 329–337.
90. Marler, J. J., Upton, J., Langer, R., & Vacanti, J. P. (1998). Transplantation of cells in matrices for tissue regeneration. *Advanced drug delivery reviews, 33*(1–2), 165–182.
91. Matsubara, Y., Murakami, Y., Kobayashi, M., Morita, Y., & Tamiya, E. (2004). Application of on-chip cell cultures for the detection of allergic response. *Biosensors and Bioelectronics, 19*(7), 741–747.
92. Maver, T., Smrke, D., Kurečič, M., Gradišnik, L., Maver, U., & Kleinschek, K. S. (2018). Combining 3D printing and electrospinning for preparation of pain-relieving wound-dressing materials. *Journal of Sol-Gel Science and Technology, 88*(1), 33–48.
93. Millet, L. J., & Gillette, M. U. (2012). New perspectives on neuronal development via microfluidic environments. *Trends in neurosciences, 35*(12), 752–761.
94. Moeini, A., Pedram, P., Makvandi, P., Malinconico, M., & Gomez d'Ayala, G. (2020). Wound healing and antimicrobial effect of active secondary metabolites in chitosan-based wound dressings: A review. *Carbohydrate Polymers, 233*, 115839.
95. Mohammadi, A., Maleki-Jamshid, A., Sanooghi, D., Milan, P. B., Rahmani, A., Sefat, F., Shahpasand, K., Soleimani, M., Bakhtiari, M., Belali, R., Faghihi, F., Joghataei, M. T., Perry,

G., & Mozafari, M. (2019). Correction to: transplantation of human chorion-derived cholinergic progenitor cells: A novel treatment for neurological disorders. *Molecular neurobiology, 56*(1), 319–320.
96. Mohd Syukri, M. S., Rahman, R. A., Mohamad, Z., Md Illias, R., Nik Mahmood, N. A., & Jaafar, N. R. (2021). Optimization strategy for laccase immobilization on polyethylene terephthalate grafted with maleic anhydride electrospun nanofiber mat. *International Journal of Biological Macromolecules, 166*, 876–883.
97. Montaser, L. M., & Fawzy, S. M. (2020). Innovative patterning of electrospinning fabrication nano scaffolds with cell culturing for liver tissue engineering. Nanoengineering: Fabrication, Properties, Optics, Thin Films, and Devices XVII, International Society for Optics and Photonics.
98. Motamedi, A. S., Mirzadeh, H., Hajiesmaeilbaigi, F., Bagheri-Khoulenjani, S., & Shokrgozar, M. (2017). Effect of electrospinning parameters on morphological properties of PVDF nanofibrous scaffolds. *Progress in Biomaterials, 6*(3), 113–123.
99. Movahedi, M., Asefnejad, A., Rafienia, M., & Khorasani, M. T. (2020). Potential of novel electrospun core-shell structured polyurethane/starch (hyaluronic acid) nanofibers for skin tissue engineering: In vitro and in vivo evaluation. *International Journal of Biological Macromolecules, 146*, 627–637.
100. Mukhiya, T., Tiwari, A. P., Chhetri, K., Kim, T., Dahal, B., Muthurasu, A., & Kim, H. Y. (2021). A metal–organic framework derived cobalt oxide/nitrogen-doped carbon nanotube nanotentacles on electrospun carbon nanofiber for electrochemical energy storage. *Chemical Engineering Journal, 420*, 129679.
101. Najafiasl, M., Osfouri, S., Azin, R., & Zaeri, S. (2020). Alginate-based electrospun core/shell nanofibers containing dexpanthenol: A good candidate for wound dressing. *Journal of Drug Delivery Science and Technology, 57*, 101708.
102. Napoli, I., Noon, L. A., Ribeiro, S., Kerai, A. P., Parrinello, S., Rosenberg, L. H., Collins, M. J., Harrisingh, M. C., White, I. J., Woodhoo, A., & Lloyd, A. C. (2012). A central role for the ERK-signaling pathway in controlling Schwann cell plasticity and peripheral nerve regeneration in vivo. *Neuron, 73*(4), 729–742.
103. Nazarnezhad, S., Baino, F., Kim, H.-W., Webster, T. J., & Kargozar, S. (2020). Electrospun nanofibers for improved angiogenesis: Promises for tissue engineering applications. *Nanomaterials, 10*(8), 1609.
104. Niculescu, A.-G., Chircov, C., Bîrcă, A. C., & Grumezescu, A. M. (2021). Fabrication and applications of microfluidic devices: A review. *International Journal of Molecular Sciences, 22*(4), 2011.
105. Nisbet, D. R., Yu, L. M. Y., Zahir, T., Forsythe, J. S., & Shoichet, M. S. (2008). Characterization of neural stem cells on electrospun poly(ε-caprolactone) submicron scaffolds: Evaluating their potential in neural tissue engineering. *Journal of Biomaterials Science, Polymer Edition, 19*(5), 623–634.
106. Orza, A., Soritau, O., Olenic, L., Diudea, M., Florea, A., Rus Ciuca, D., Mihu, C., Casciano, D., & Biris, A. S. (2011). Electrically conductive gold-coated collagen nanofibers for placental-derived mesenchymal stem cells enhanced differentiation and proliferation. *ACS Nano, 5*(6), 4490–4503.
107. Paimard, G., Shahlaei, M., Moradipour, P., Akbari, H., Jafari, M., & Arkan, E. (2020). An impedimetric immunosensor modified with electrospun core-shell nanofibers for determination of the carcinoma embryonic antigen. *Sensors and Actuators B: Chemical, 311*, 127928.
108. Patel, B. B., McNamara, M. C., Pesquera-Colom, L. S., Kozik, E. M., Okuzonu, J., Hashemi, N. N., & Sakaguchi, D. S. (2020). Recovery of encapsulated adult neural progenitor cells from microfluidic-spun hydrogel fibers enhances proliferation and neuronal differentiation. *ACS Omega, 5*(14), 7910–7918.
109. Prabhakaran, M. P., Venugopal, J. R., Chyan, T. T., Hai, L. B., Chan, C. K., Lim, A. Y., & Ramakrishna, S. (2008). Electrospun biocomposite nanofibrous scaffolds for neural tissue engineering. *Tissue Engineering Part A, 14*(11), 1787–1797.

110. Prabhakaran, M. P., Venugopal, J. R., & Ramakrishna, S. (2009). Mesenchymal stem cell differentiation to neuronal cells on electrospun nanofibrous substrates for nerve tissue engineering. *Biomaterials, 30*(28), 4996–5003.
111. Qasim, S. B., Zafar, M. S., Najeeb, S., Khurshid, Z., Shah, A. H., Husain, S., & Rehman, I. U. (2018). Electrospinning of chitosan-based solutions for tissue engineering and regenerative medicine. *International Journal of Molecular Sciences, 19*(2), 407.
112. Qin, L., Yang, D., Zhang, M., Zhao, T., Luo, Z., & Yu, Z.-Z. (2021). Superelastic and ultralight electrospun carbon nanofiber/MXene hybrid aerogels with anisotropic microchannels for pressure sensing and energy storage. *Journal of Colloid and Interface Science, 589*, 264–274.
113. Qing, H., Ji, Y., Li, W., Zhao, G., Yang, Q., Zhang, X., Luo, Z., Lu, T. J., Jin, G., & Xu, F. (2019). Microfluidic printing of three-dimensional graphene electroactive microfibrous scaffolds. *ACS applied materials & interfaces, 12*(2), 2049–2058.
114. Ramakrishna, S. (2005). An introduction to electrospinning and nanofibers, World scientific.
115. Reddy, S., Xu, X., Guo, T., Zhu, R., He, L., & Ramakrishana, S. (2018). Allotropic carbon (graphene oxide and reduced graphene oxide) based biomaterials for neural regeneration. *Current Opinion in Biomedical Engineering, 6*, 120–129.
116. Reier, P. J., Zholudeva, L. V., & Lane, M. A. (2017). Chapter 25—Axonal degeneration and regeneration in the peripheral and central nervous systems. In P. M. Conn (Ed.), Conn's Translational Neuroscience (pp. 553–575). San Diego: Academic Press.
117. Reilly, G. C., & Engler, A. J. (2010). Intrinsic extracellular matrix properties regulate stem cell differentiation. *Journal of biomechanics, 43*(1), 55–62.
118. Rothert, A., Deo, S. K., Millner, L., Puckett, L. G., Madou, M. J., & Daunert, S. (2005). Whole-cell-reporter-gene-based biosensing systems on a compact disk microfluidics platform. *Analytical biochemistry, 342*(1), 11–19.
119. Sadeghi, A., Moztarzadeh, F., & Aghazadeh Mohandesi, J. (2019). Investigating the effect of chitosan on hydrophilicity and bioactivity of conductive electrospun composite scaffold for neural tissue engineering. *International Journal of Biological Macromolecules, 121*, 625–632.
120. Sarabahi, S. (2012). Recent advances in topical wound care. *Indian Journal of Plastic Surgery, 45*(02), 379–387.
121. Saveh-Shemshaki, N., Bagherzadeh, R., & Latifi, M. (2019). Electrospun metal oxide nanofibrous mat as a transparent conductive layer. *Organic Electronics, 70*, 131–139.
122. Shafiee, A., Kehtari, M., Zarei, Z., Soleimani, M., Varshochian, R., Ahmadi, A., Atyabi, F., & Dinarvand, R. (2021). An in situ hydrogel-forming scaffold loaded by PLGA microspheres containing carbon nanotube as a suitable niche for neural differentiation. *Materials Science and Engineering: C, 120*, 111739.
123. Shahriar, S., Mondal, J., Hasan, M. N., Revuri, V., Lee, D. Y., & Lee, Y.-K. (2019). Electrospinning nanofibers for therapeutics delivery. *Nanomaterials, 9*(4), 532.
124. Shen, H., Zhou, Z., Wang, H., Zhang, M., Han, M., Durkin, D. P., Shuai, D., & Shen, Y. (2021). Development of electrospun nanofibrous filters for controlling coronavirus aerosols. *Environmental Science & Technology Letters.*
125. Shokrgozar, M. A., Mottaghitalab, F., Mottaghitalab, V., & Farokhi, M. (2011). Fabrication of porous chitosan/poly (vinyl alcohol) reinforced single-walled carbon nanotube nanocomposites for neural tissue engineering. *Journal of Biomedical Nanotechnology, 7*(2), 276–284.
126. Sin, A., Chin, K. C., Jamil, M. F., Kostov, Y., Rao, G., & Shuler, M. L. (2004). The design and fabrication of three-chamber microscale cell culture analog devices with integrated dissolved oxygen sensors. *Biotechnology Progress, 20*(1), 338–345.
127. Singh, A., Shiekh, P. A., Das, M., Seppälä, J., & Kumar, A. (2019). Aligned chitosan-gelatin cryogel-filled polyurethane nerve guidance channel for neural tissue engineering: fabrication, characterization, and in vitro evaluation. *Biomacromolecules, 20*(2), 662–673.
128. Steel, E. M., Azar, J.-Y., & Sundararaghavan, H. G. (2020). Electrospun hyaluronic acid-carbon nanotube nanofibers for neural engineering. *Materialia, 9*, 100581.
129. Stojanov, S., & Berlec, A. (2020). Electrospun nanofibers as carriers of microorganisms, stem cells, proteins, and nucleic acids in therapeutic and other applications. *Frontiers in Bioengineering and Biotechnology*, *8*(130).

130. Taipale, J., & Keski-Oja, J. (1997). Growth factors in the extracellular matrix. *The FASEB Journal, 11*(1), 51–59.
131. Talac, R., Friedman, J., Moore, M., Lu, L., Jabbari, E., Windebank, A. J., Currier, B. L., & Yaszemski, M. J. (2004). Animal models of spinal cord injury for evaluation of tissue engineering treatment strategies. *Biomaterials, 25*(9), 1505–1510.
132. Tan, W., & Desai, T. A. (2004). Layer-by-layer microfluidics for biomimetic three-dimensional structures. *Biomaterials, 25*(7–8), 1355–1364.
133. Tan, W., & Desai, T. A. (2005). Microscale multilayer cocultures for biomimetic blood vessels. *Journal of Biomedical Materials Research Part A: An Official Journal of The Society for Biomaterials, The Japanese Society for Biomaterials, and The Australian Society for Biomaterials and the Korean Society for Biomaterials, 72*(2), 146–160.
134. Tang, X., Xue, C., Wang, Y., Ding, F., Yang, Y., & Gu, X. (2012). Bridging peripheral nerve defects with a tissue engineered nerve graft composed of an in vitro cultured nerve equivalent and a silk fibroin-based scaffold. *Biomaterials, 33*(15), 3860–3867.
135. Thompson, D. M., Koppes, A. N., Hardy, J. G., & Schmidt, C. E. (2014). Electrical stimuli in the central nervous system microenvironment. *Annual Review of Biomedical Engineering, 16*, 397–430.
136. Unnithan, A. R., Barakat, N. A., Pichiah, P. T., Gnanasekaran, G., Nirmala, R., Cha, Y.-S., Jung, C.-H., El-Newehy, M., & Kim, H. Y. (2012). Wound-dressing materials with antibacterial activity from electrospun polyurethane–dextran nanofiber mats containing ciprofloxacin HCl. *Carbohydrate Polymers, 90*(4), 1786–1793.
137. Valmikinathan, C. M., Tian, J., Wang, J., & Yu, X. (2008). Novel nanofibrous spiral scaffolds for neural tissue engineering. *Journal of Neural Engineering, 5*(4), 422–432.
138. Wallin, P., Zandén, C., Carlberg, B., Hellström Erkenstam, N., Liu, J., & Gold, J. (2012). A method to integrate patterned electrospun fibers with microfluidic systems to generate complex microenvironments for cell culture applications. *Biomicrofluidics, 6*(2), 024131.
139. Wang, J., Ren, L., Li, L., Liu, W., Zhou, J., Yu, W., Tong, D., & Chen, S. (2009). Microfluidics: A new cosset for neurobiology. *Lab on a Chip, 9*(5), 644–652.
140. Weibel, D. B., & Whitesides, G. M. (2006). Applications of microfluidics in chemical biology. *Current Opinion in Chemical Biology, 10*(6), 584–591.
141. Wheeler, A. R., Throndset, W. R., Whelan, R. J., Leach, A. M., Zare, R. N., Liao, Y. H., Farrell, K., Manger, I. D., & Daridon, A. (2003). Microfluidic device for single-cell analysis. *Analytical Chemistry, 75*(14), 3581–3586.
142. Wiley, B. J., Qin, D., & Xia, Y. (2010). Nanofabrication at high throughput and low cost. *ACS Nano, 4*(7), 3554–3559.
143. Wu, J., Xie, L., Lin, W. Z. Y., & Chen, Q. (2017). Biomimetic nanofibrous scaffolds for neural tissue engineering and drug development. *Drug Discovery Today, 22*(9), 1375–1384.
144. Wu, Y., Wang, L., Guo, B., Shao, Y., & Ma, P. X. (2016). Electroactive biodegradable polyurethane significantly enhanced Schwann cells myelin gene expression and neurotrophin secretion for peripheral nerve tissue engineering. *Biomaterials, 87*, 18–31.
145. Xie, J., MacEwan, M. R., Willerth, S. M., Li, X., Moran, D. W., Sakiyama-Elbert, S. E., & Xia, Y. (2009). Conductive core–sheath nanofibers and their potential application in neural tissue engineering. *Advanced Functional Materials, 19*(14), 2312–2318.
146. Xie, X., Chen, Y., Wang, X., Xu, X., Shen, Y., Khan, A. u. R., Aldalbahi, A., Fetz, A. E., Bowlin, G. L., El-Newehy, M., & Mo, X. (2020). Electrospinning nanofiber scaffolds for soft and hard tissue regeneration. *Journal of Materials Science & Technology 59*, 243–261.
147. Xuan, H., Li, B., Xiong, F., Wu, S., Zhang, Z., Yang, Y., & Yuan, H. (2021). Tailoring nanoporous surface of aligned electrospun poly (L-Lactic Acid) fibers for nerve tissue engineering. *International Journal of Molecular Sciences, 22*(7), 3536.
148. Yang, D., Lu, B., Zhao, Y., & Jiang, X. (2007). Fabrication of aligned fibrous arrays by magnetic electrospinning. *Advanced materials, 19*(21), 3702–3706.
149. Yang, F., Murugan, R., Wang, S., & Ramakrishna, S. (2005). Electrospinning of nano/micro scale poly (L-lactic acid) aligned fibers and their potential in neural tissue engineering. *Biomaterials, 26*(15), 2603–2610.

150. Yang, F., Xu, C. Y., Kotaki, M., Wang, S., & Ramakrishna, S. (2004). Characterization of neural stem cells on electrospun poly(L-lactic acid) nanofibrous scaffold. *Journal of Biomaterials Science, Polymer Edition, 15*(12), 1483–1497.
151. Yih, T. C., & Al-Fandi, M. (2006). Engineered nanoparticles as precise drug delivery systems. *Journal of Cellular Biochemistry, 97*(6), 1184–1190.
152. Yin, X., Zhang, Z., Ma, H., Venkateswaran, S., & Hsiao, B. S. (2020). Ultra-fine electrospun nanofibrous membranes for multicomponent wastewater treatment: Filtration and adsorption. *Separation and Purification Technology, 242*, 116794.
153. Zamani, M., Shakhssalim, N., Ramakrishna, S. Naji, M. (2020). Electrospinning: Application and prospects for urologic tissue engineering. *Frontiers in Bioengineering and Biotechnology, 8*.
154. Zarei, M., Samimi, A., Khorram, M., Abdi, M. M., & Golestaneh, S. I. (2021). Fabrication and characterization of conductive polypyrrole/chitosan/collagen electrospun nanofiber scaffold for tissue engineering application. *International Journal of Biological Macromolecules, 168*, 175–186.
155. Zeng, J., Wang, H., Lin, Y., Zhang, J., Liang, F., Fang, F., Yang, F., Wang, P., Zhu, Z., & Chen, X. (2018). Fabrication of microfluidic channels based on melt-electrospinning direct writing. *Microfluidics and Nanofluidics, 22*(2), 1–10.
156. Zhang, F., & King, M. W. (2020). Biodegradable polymers as the pivotal player in the design of tissue engineering scaffolds. *Advanced Healthcare Materials, 9*(13), 1901358.
157. Zhang, J., Qiu, K., Sun, B., Fang, J., Zhang, K., Ei-Hamshary, H., Al-Deyab, S. S., & Mo, X. (2014). The aligned core–sheath nanofibers with electrical conductivity for neural tissue engineering. *Journal of Materials Chemistry B, 2*(45), 7945–7954.
158. Zhang, Q., & Austin, R. H. (2012). Applications of microfluidics in stem cell biology. *BioNanoScience, 2*(4), 277–286.
159. Zhang, R., Han, S., Liang, L., Chen, Y., Sun, B., Liang, N., Feng, Z., Zhou, H., Sun, C., Liu, H., & Wang, J. (2021). Ultrasonic-driven electrical signal-iron ion synergistic stimulation based on piezotronics induced neural differentiation of mesenchymal stem cells on FeOOH/PVDF nanofibrous hybrid membrane. *Nano Energy, 87*, 106192.
160. Zhang, X., Gao, X., Jiang, L., & Qin, J. (2012). Flexible generation of gradient electrospinning nanofibers using a microfluidic assisted approach. *Langmuir, 28*(26), 10026–10032.
161. Zhao, Y., Demirci, U., Chen, Y., & Chen, P. (2020). Multiscale brain research on a microfluidic chip. *Lab on a Chip, 20*(9), 1531–1543.



Zahra Hesari was born in 1986. Received her Pharm. D. degree from Shahid Beheshti University of Medical Sciences, Tehran, Iran, in 2010 and the Ph.D. of Pharmaceutics from Tehran University of Medical Sciences, Tehran, Iran, in 2016. Since 2016, she has been an Assistant Professor of Pharmaceutics in Guilan University of Medical Sciences, Rasht, Iran. Her research interest includes biocompatible scaffolds for neural tissue engineering, nanofibrous scaffolds, magnetic nanofibers for stem cell differentiation, natural-based nanoparticles for stem cell differentiation, and antimicrobial properties. Dr. Hesari was a recipient of the best researcher and best instructor awards of Guilan University of Medical Sciences in 2020 and best student in Shahid Beheshti University of Medical Sciences in 2010.

Author Index

A
Abbasipour, Mina, 721
Abid, Sharjeel, 519
Aliyeva, Nargiz, 35
Almeida de, Ana Claudia Araujo, 473
Alvarenga, Ana Gabrielle Pires, 473
Angaiah, Subramania, 351
Ashammakhi, Nureddin, 555
Aşık, Müge, 3, 631
Augustine, Robin, 555
Ayala-Zavala, Jesús Fernando, 207
Aytac, Zeynep, 93

B
Ballesteros, Camilo A. S., 297
Başkan, Havva, 183
Beigh, Mushtaq A., 331
Bölgen, Nimet, 3, 631

C
Campa-Siqueiros, Paola I., 207
Castillo-Ortega, Maria M., 207
Chagas, Paulo A. M., 297
Cochrane, Cedric, 417
Correa, Daniel S., 297
Costa, Jorge Alberto Vieira, 451, 473
Costa, Vittor P. V., 297

D
Dai, Yunqian, 657
Demir, Didem, 3, 631
Dziemidowicz, Karolina, 159

E
Ertas, Yavuz Nuri, 555
Esakkimuthu, Shanmugasundaran, 693

G
Gandra, Eliezer Avila, 451
Gayakwad, Pitambar V., 491
Godakanda, V. Umayangana, 159

H
Hameed, Misbah, 519
Hasan, Anwarul, 555
Hesari, Zahra, 737
Hezarkhani, Marjan, 35
He, Zhongchen, 391
Hussain, Tanveer, 519

J
Jafari, Arman, 555
Javed, Sonia, 519

K
Kalva, Sumama Nuthana, 555
Karakaş, Hale, 183
Khajavi, Ramin, 721
Khan, Rumysa Saleem, 331
Khenoussi, Nabyl, 519
Koncar, Vladan, 417
Kondawar, Sanchit S., 491
Kondawar, Subhash B., 491
Krisch, Eniko, 135
Kuntzler, Suelen Goettems, 473

© The Editor(s) (if applicable) and The Author(s), under exclusive license to Springer Nature Switzerland AG 2022

A. Vaseashta and N. Bölgen (eds.), *Electrospun Nanofibers*,
https://doi.org/10.1007/978-3-030-99958-2

L
Lewandowski, Maryline, 391
Li, Song, 555
Liu, Xiao-Fei, 67
Liu, Zhong, 67, 605
Long, Yun-Ze, 67, 605
López-Cervantes, Jaime, 207

M
Madera-Santana, Tomas J., 207
Martins, Albino, 251
Maurya, Dheeraj Kumar, 351
Menceloglu, Yusuf Ziya, 35
Mohamadi, Parian, 417
Mohsenzadeh, Elham, 391, 417
Molnar, Kristof, 135
Morais de, Michele Greque, 451, 473
Mora-López de la, David Servin, 207
Moreira, Juliana Botelho, 451

N
Nazir, Ahsan, 519
Neves, Nuno M., 251

P
Parker, Geoff J. M., 121
Peng, Xiaoli, 657
Puskas, Judit E., 135

R
Ramakrishna, Seeram, 67, 605
Rather, Anjum Hamid, 331
Rault, François, 391
Reis, Rui L., 251

S
Sakım, Burcu, 3, 631
Salaün, Fabien, 391
Saner Okan, Burcu, 35
Santos, Danilo M., 297
Savoji, Houman, 555
Schneider, Rodrigo, 297
Sheikh, Faheem A., 331
Silva de, K. M. Nalin, 159
Silva de, Rohini M., 159
Sivakumar, Krishnamoorthy, 693
Sonwane, Nayana D., 491
Stalin, Thambusamy, 693
Sun, Yueming, 657

T
Tavafoghi, Maryam, 555
Teodoro, Kelcilene B. R., 297
Tian, Ming, 657

V
Vasconcelos, Filipa, 251
Vaseashta, Ashok, 3, 631
Vigneshkumar, Ganesan, 693
Vimalasruthi, Narayanan, 693

W
Wang, Bing-Chang, 605
Wang, Xinzhu, 93
Wang, Yunpeng, 657
Wani, Taha Umair, 331
Wani, Taseen Aamir, 331
Williams, Gareth R., 159

X
Xue, Jiajia, 657

Y
Yu, Bing, 657
Yu, Miao, 67, 605

Z
Zhang, Jun, 67, 605
Zhang, Liqun, 657
Zhang, Wei, 657
Zhang, Xindan, 657
Zhang, Zhaoxu, 657
Zhou, Feng-Lei, 121

Subject Index

A
Active packaging, 17, 451, 452, 454, 457, 463, 477, 480, 710
Additive manufacturing, 83, 93–96, 106, 114, 561, 566, 631, 632, 634, 658, 665
Air filtering, 419, 444
Application areas, 3, 12, 14, 18, 94, 197, 638, 657, 738
Aqueous solubility, 189, 331–333, 340

B
Biomedical applications, 15, 19, 55, 69, 80, 81, 95–97, 114, 123, 125, 135, 151, 183, 184, 198, 217, 221, 222, 224, 268, 269, 282, 283, 558, 559, 575, 631, 642, 643, 646, 647, 649, 677, 682, 702, 738, 741, 743
Biopolymer, 20, 107, 184, 186, 208, 213, 217, 222, 227, 238, 307, 315, 456, 540, 559, 568, 646, 683, 710, 724

C
Carbon nanofibers, 356, 648, 693, 694, 696
Catalysis, 50, 52, 497, 705, 713
Catalyst, 8, 26, 47, 136, 224, 657, 694, 739
Characterization, 14, 55, 135, 146, 191–195, 303, 305, 397, 426, 427, 429, 432, 438, 455, 530, 633, 648
Chitosan, 12, 19, 21, 37, 45, 46, 165, 166, 185–188, 191, 194, 195, 197, 198, 208, 213–217, 223, 227, 253, 269, 272, 302, 312, 313, 316, 421, 423, 424, 459, 460, 462, 463, 475, 482, 536, 537, 541, 558, 569, 675, 694, 695, 700–702, 704, 708, 709, 722, 724, 742, 743
Co-electrohydrodynamic (co-HED), 121, 122
Composites, 11, 23, 52, 67, 107, 110, 112, 211, 219, 237, 310, 359–361, 399, 401, 419, 424, 429, 491, 493, 502, 503, 505, 506, 510, 558, 633, 635, 637, 646, 647, 649, 675
Core/Shell electrospinning, 48, 49, 438
Cyclodextrin-based inclusion complex, 693

D
3D bioprinting, 556, 557, 569, 574, 575, 579–582, 584, 586, 639, 680
Diabetes, 19, 207, 208, 215, 216, 219, 227
Diffusion MRI, 121, 122, 127, 129, 130
3D printing, 71, 561, 562, 569, 571–578, 580, 608, 631, 632, 634–641, 644–649, 657–660, 663–666, 670, 674–684, 741, 750
Drug delivery, 208, 212, 217, 224
Drug release modality, 161–163, 165–168, 186, 189, 277, 279, 310, 334, 336, 342, 343, 537, 556, 565, 568, 586, 638, 708, 710, 739

E
Electrospinning, 3–11, 13–20, 22–24, 26, 27, 35–48, 50–59, 67–87, 93–96, 98–100, 112, 113, 122–125, 130, 135, 137–139, 146–148, 150, 151, 159, 161, 162, 164, 166, 167,

© The Editor(s) (if applicable) and The Author(s), under exclusive license to Springer Nature Switzerland AG 2022

A. Vaseashta and N. Bölgen (eds.), *Electrospun Nanofibers*,
https://doi.org/10.1007/978-3-030-99958-2

169–172, 183–198, 207, 208, 211, 212, 220–222, 224, 227, 251–259, 261, 262, 265, 268, 269, 271–280, 282, 283, 297, 302, 333–337, 341, 343, 351, 355, 357, 359, 362, 363, 366, 368–370, 372–374, 394, 395, 397–402, 405, 417, 420, 421, 424, 425, 427, 432, 434–436, 442–445, 452, 456, 457, 473–475, 479, 481, 482, 493–498, 502–504, 506, 508–510, 535, 536, 538, 539, 544, 555, 557–559, 561–570, 577–580, 661, 662, 666–669, 671, 674–678, 680, 697, 699, 700, 713, 722–724, 731, 737, 738, 741, 743, 750, 751
Electrospun membrane electrolyte, 351, 367
Electrospun nanofibers, 3–5, 10–13, 15–21, 23, 24, 41, 45, 48, 49, 80, 87, 94, 100, 114, 183, 184, 188, 189, 193, 195, 197–199, 207, 208, 211, 212, 214–218, 227, 254, 267, 271, 277, 282, 297, 298, 300, 303, 314, 316, 331, 333, 334, 338, 340–343, 351, 374, 479, 491, 493–495, 503, 535–538, 540, 543, 545, 563, 565, 568, 585, 605, 623, 633, 634, 636, 639, 640, 642, 644, 646–648, 678, 680, 681, 693–695, 697, 698, 700, 701, 707, 710, 713, 721, 722, 728, 731, 737–740, 746, 751
Electrospun systems, 159, 168, 172
Energy, 53, 352, 375, 376, 404, 429, 713, 714
Energy harvesting, 391–393, 396–399, 401–405, 566, 631, 634, 641, 644, 646, 721–724, 728, 731

F

Facemasks, 519, 521–525, 527–529, 531, 534, 538–542, 544, 545
Fibers, 3–10, 12, 13, 15–24, 26, 27, 35–56, 58, 59, 67–82, 84–87, 93–101, 104–114, 121, 122, 124, 125, 127, 128, 130, 135, 138–140, 143–149, 151, 159, 161, 162, 165, 166, 169, 211, 212, 215, 216, 219, 220, 222–225, 227, 252–261, 265, 266, 268–270, 272–276, 279–282, 305, 308, 309, 311, 394, 400, 402, 405, 419, 462, 495, 504, 506, 519, 522, 527, 536, 539–543, 556–566, 610, 611, 614, 616, 620, 622, 637, 638, 640, 646, 648, 657, 660, 662, 663, 666–668, 670, 671, 702, 723, 728, 731, 738, 740, 741, 746–751
Filtration, 22, 528, 530–532, 538, 542, 543
Food safety, 478
Food security, 464
Functional fibers, 135, 414
Functional nanofibers, 14, 700

H

Handheld electrospinning device, 611, 617
Hollow fibers, 40, 265

I

Immobilization, 197, 224
In-Situ electrospinning, 86
Intelligent packaging, 481

J

Janus fibers, 38, 39, 43, 44, 52–55, 58, 59, 162, 260, 262, 266
Jet printing, 665

M

Melt Electrospinning Writing (MEW), 93–102, 106, 107, 109–114, 562, 566, 578, 657
Metal oxides, 362, 364, 365, 497, 506
Micro- and nano-fibers, 5, 184, 222–225, 606, 634, 678
Microfluidics, 262, 263, 737, 743, 745, 750
Microfluidic spinning, 263, 267, 748
Micro/nano textile structure, 91
Multi-axial electrospun structures, 36
Multifunctionality, 50, 52, 58, 713

N

Nanoencapsulation, 473, 474
Nanofibers, 3–26, 36, 43, 45–48, 50, 53–55, 59, 67, 75–80, 93, 94, 137, 139, 151, 166, 168, 169, 183–190, 192, 194–198, 207, 208, 211, 212, 214–220, 222, 223, 227, 233, 235, 237, 254, 256, 259, 261, 262, 270–273, 275–279, 281, 282, 297, 300–302, 304, 308–310, 313, 315, 331, 333–337, 394–402, 404, 405, 417, 418, 420, 422, 427–430, 580, 581, 585, 605, 606, 608, 612–614, 622, 637, 640, 642, 646, 648, 658,

667, 675–677, 679, 681, 694–701, 707, 708, 710, 713, 714, 721–729, 731, 738–743, 748
Nanofibrous scaffold, 11, 16, 185, 233, 234, 270, 272, 282, 566, 634, 739, 741–743, 746, 748, 751
Nanomaterials, 44, 57, 58, 194, 300, 430, 451, 452, 455–457, 460, 462–464, 478, 492, 493, 496, 632–634, 642, 700, 713
Nanotechnology, 14, 58, 183, 184, 207, 331, 451, 452, 455, 456, 462–464, 473, 478, 541, 578, 606, 632, 633, 637, 658, 693, 737
Neural differentiation, 111, 737, 740, 742, 743, 745, 746, 748–751
Nonwovens, 300, 304, 309

P
Phantoms, 121, 122, 126–129
Piezoelectric, 23, 125, 392–395, 397–405, 574, 612, 642, 646, 721–725, 729, 731
Piezoelectricity, 391, 394, 398, 400, 402, 640, 649, 722–724
Polyaniline, 15, 48, 55, 75, 376, 491, 493, 494, 496, 501–503, 505, 506, 509, 694, 725, 743
Polyaspartamide, 135
Polycaprolactone (PCL), 15, 26, 37, 39, 46, 49, 58, 72, 81–84, 96, 97, 100–113, 189, 191–193, 195–197, 208, 215, 218, 220–222, 224, 227–237, 268, 270, 272, 274, 275, 302, 303, 308, 310, 315, 463, 537, 543, 559, 573, 580, 582, 583, 616, 620–623, 642, 670, 675, 676, 678, 681, 704, 743, 751
Polymer carrier, 58, 159, 173
Polymer nanofibers, 14, 261, 300, 395, 396, 430, 505, 701, 728
Polysuccinimide, 135, 136, 146, 151
Polyurethane nanofibers, 420, 426, 430, 432, 440, 442, 726
Poorly soluble drugs, 331, 343
Pressure-driven membranes. *See* 000
Prototyping, jet printing, 632, 642, 649, 658, 663, 665, 750
Pyroelectric, 392, 401, 402, 721, 722, 724–726, 731

R
Regeneration, 101–104, 106, 108, 110, 111, 113, 190, 194–196, 217, 233, 237, 268, 270–272, 274, 275, 283, 300, 303, 312, 537, 556, 558, 566, 624, 634, 642, 657, 659, 674, 679, 680, 682, 683, 738–741, 743, 751

S
Sensor, 8, 10, 14, 15, 22, 23, 53, 55, 263, 315, 355, 391–393, 400, 404, 405, 417, 419, 420, 429, 438, 440–442, 444, 456, 463, 464, 481, 491–493, 496–511, 537, 541, 566, 612, 631, 632, 634, 636, 637, 641, 644, 646–649, 666, 693, 700, 714, 721, 722, 728, 729, 739, 743
Skin injuries, 298, 316, 618
Smart textile, 35, 55, 391–393, 395, 402–405, 647
Solar cells, 355, 392, 622, 638, 721, 722
Solvent-free, 67–69, 71–82, 84–87, 136, 673
Supercapacitors, 15, 351, 352, 354–356, 358, 359, 361–366, 370, 372–375, 404, 405, 693, 695, 700, 713, 714
Surface modification, 14, 16, 143, 270, 273, 302, 335, 373, 430, 584

T
Thermocuring, 67, 69, 75
Tissue engineering, 8, 11, 12, 14–19, 35, 53, 58, 67, 71–73, 77, 81, 82, 93, 94, 96, 101, 106, 107, 114, 137, 146, 151, 163, 168, 171, 183, 184, 186, 194–197, 218, 220, 221, 224, 234, 252, 253, 267, 268, 270–272, 279, 281–283, 355, 429, 536, 537, 540, 555–559, 561, 562, 565–567, 569, 573, 576–580, 582–585, 608, 632, 634, 636–638, 641–643, 658, 666, 667, 680, 681, 694, 695, 700–704, 738–743, 745, 747, 748, 751
Tissue-mimicking, 121, 127, 129
Tissue models, 555
Tissue regeneration, 93, 97, 100, 106, 108, 109, 114, 183, 184, 194, 196, 198, 208, 224, 268, 310, 316, 556, 558, 567, 568, 606, 610, 642, 738, 751
Titanium dioxide, 16, 22, 26, 51, 186, 261, 455

Triboelectric, 392, 397, 403, 721, 722, 726–729, 731

W
Wastewater treatment, 23, 26
Water treatment, 12, 26, 36, 58, 59, 198, 537
Wound dressing, 17–19, 53, 67, 75, 77, 79, 81, 82, 85, 86, 123, 183, 184, 186, 187, 207, 208, 211, 212, 215–218, 221, 222, 224, 227, 267, 277, 282, 297, 299–312, 315, 316, 417, 423, 438, 536, 558, 567, 605
Wound healing, 8, 18, 19, 48, 100, 112, 150, 166, 184, 186, 187, 195, 197, 198, 207–210, 212–214, 216, 217, 221, 223, 227, 273, 276, 279, 298–301, 303, 304, 309, 313–315, 355, 537, 540, 557, 558, 561, 562, 567, 568, 613, 616, 620, 623, 646, 693, 695, 700, 703, 710, 739, 748